

**V. International Symposium on
Column Liquid Chromatography,
Avignon, May 11-15, 1981**

JOURNAL OF

CHROMATOGRAPHY

INTERNATIONAL JOURNAL ON CHROMATOGRAPHY, ELECTROPHORESIS AND RELATED METHODS

EDITOR, Michael Lederer (Switzerland)

ASSOCIATE EDITOR, K. Macek (Prague)

EDITORIAL BOARD

W. A. Aue (Halifax)
V. G. Berezkin (Moscow)
V. Betina (Bratislava)
A. Bevenue (Honolulu, HI)
P. Boulanger (Lille)
A. A. Boulton (Saskatoon)
G. P. Cartoni (Rome)
G. Duyckaerts (Liège)
L. Fishbein (Jefferson, AR)
A. Frigerio (Milan)
C. W. Gehrke (Columbia, MO)
E. Gil-Av (Rehovot)
G. Guiochon (Palaiseau)
I. M. Hais (Hradec Králové)
J. K. Haken (Kensington)
E. Heftmann (Berkeley, CA)
S. Hjertén (Uppsala)
E. C. Horning (Houston, TX)
Cs. Horváth (New Haven, CT)
J. F. K. Huber (Vienna)
A. T. James (Sharnbrook)
J. Janák (Brno)
E. sz. Kováts (Lausanne)
K. A. Kraus (Oak Ridge, TN)
E. Lederer (Gif-sur-Yvette)
A. Liberti (Rome)
H. M. McNair (Blacksburg, VA)
Y. Marcus (Jerusalem)
G. B. Marini-Bettolo (Rome)
Č. Michalec (Prague)
R. Neher (Basel)
G. Nickless (Bristol)
J. Novák (Brno)
N. A. Parris (Wilmington, DE)
P. G. Righetti (Milan)
O. Samuelson (Göteborg)
G.-M. Schwab (Munich)
G. Semenza (Zürich)
L. R. Snyder (Tarrytown, NY)
A. Zlatkis (Houston, TX)

EDITORS, BIBLIOGRAPHY SECTION

K. Macek (Prague), J. Janák (Brno), Z. Deyl (Prague)

COORD. EDITOR, DATA SECTION

J. Gasparič (Hradec Králové)

ELSEVIER SCIENTIFIC PUBLISHING COMPANY
AMSTERDAM

Scope. The *Journal of Chromatography* publishes papers on all aspects of chromatography, electrophoresis and related methods. Contributions consist mainly of research papers dealing with chromatographic theory, instrumental development and their applications. The section *Biomedical Applications*, which is under separate editorship, deals with the following aspects: developments in and applications of chromatographic and electrophoretic techniques related to clinical diagnosis (including the publication of normal values); screening and profiling procedures with special reference to metabolic disorders; results from basic medical research with direct consequences in clinical practice; combinations of chromatographic and electrophoretic methods with other physicochemical techniques such as mass spectrometry. In *Chromatographic Reviews*, reviews on all aspects of chromatography, electrophoresis and related methods are published.

Submission of Papers. Papers in English, French and German may be submitted, in three copies. Manuscripts should be submitted to: The Editor of *Journal of Chromatography*, P.O. Box 681, 1000 AR Amsterdam, The Netherlands, or to: The Editor of *Journal of Chromatography, Biomedical Applications*, P.O. Box 681, 1000 AR Amsterdam, The Netherlands. Reviews are invited or proposed by letter to the Editors and will appear in *Chromatographic Reviews* or *Biomedical Applications*. An outline of the proposed review should first be forwarded to the Editors for preliminary discussion prior to preparation. Submission of an article is understood to imply that the article is original and unpublished and is not being considered for publication elsewhere. For copyright regulations, see below.

Subscription Orders. Subscription orders should be sent to: Elsevier Scientific Publishing Company, P.O. Box 211, 1000 AE Amsterdam, The Netherlands. The *Journal of Chromatography* and the *Biomedical Applications* section can be subscribed to separately.

Publication. The *Journal of Chromatography* (incl. *Biomedical Applications*, *Chromatographic Reviews* and *Cumulative Author and Subject Indexes*, Vols. 201–210 and 211–220) has 24 volumes in 1981. The subscription prices for 1981 are:

J. *Chromatogr.* (incl. *Chromatogr. Rev.* and *Cum. Indexes*) + *Biomed. Appl.* (Vols. 203–226):

Dfl. 3240.00 plus Dfl. 432.00 (postage) (total ca. US\$ 1468.75)

J. *Chromatogr.* (incl. *Chromatogr. Rev.* and *Cum. Indexes*) only (Vols. 203–220):

Dfl. 2556.00 plus Dfl. 324.00 (postage) (total ca. US\$ 1152.00).

Biomed. Appl. only (Vols. 221–226):

Dfl. 852.00 plus Dfl. 108.00 (postage) (total ca. US\$ 384.00).

Journals are automatically sent by air mail to the U.S.A. and Canada at no extra costs, and to Japan, Australia and New Zealand with a small additional postal charge. Back volumes of the *Journal of Chromatography* (Vols. 1 through 202) are available at Dfl. 156.00 (plus postage). Claims for issues not received should be made within three months of publication of the issue. If not, they cannot be honoured free of charge. For customers in the U.S.A. and Canada wishing additional bibliographic information on this and other Elsevier journals, please contact Elsevier/North-Holland Inc., Journal Information Centre, 52 Vanderbilt Avenue, New York, NY 10164. Tel: (212) 867-9040.

Abstracts/Contents Lists published in Analytical Abstracts, Biochemical Abstracts, Biological Abstracts, Chemical Abstracts, Chemical Titles, Current Contents/Physical, Chemical & Earth Sciences, Current Contents/Life Sciences, Index Medicus, and Science Citation Index.

See page 3 of cover for Publication Schedule, Information for Authors, and information on the News Section and Advertisements.

© ELSEVIER SCIENTIFIC PUBLISHING COMPANY — 1981

All rights reserved. No part of this publication may be reproduced, stored in a retrieval system or transmitted in any form or by any means, electronic, mechanical, photocopying, recording or otherwise, without the prior written permission of the publisher, Elsevier Scientific Publishing Company, P.O. Box 330, 1000 AH Amsterdam, The Netherlands.

Submission of an article for publication implies the transfer of the copyright from the author(s) to the publisher and entails the authors' irrevocable and exclusive authorization of the publisher to collect any sums or considerations for copying or reproduction payable by third parties (as mentioned in article 17 paragraph 2 of the Dutch Copyright Act of 1912 and in the Royal Decree of June 20, 1974 (S. 351) pursuant to article 16 b of the Dutch Copyright Act of 1912) and/or to act in or out of Court in connection therewith.

Special regulations for readers in the U.S.A. This journal has been registered with the Copyright Clearance Center, Inc. Consent is given for copying of articles for personal or internal use, or for the personal use of specific clients. This consent is given on the condition that the copier pays through the Center the per-copy fee stated in the code on the first page of each article for copying beyond that permitted by Sections 107 or 108 of the U.S. Copyright Law. The appropriate fee should be forwarded with a copy of the first page of the article to the Copyright Clearance Center, Inc., 21 Congress Street, Salem, MA 01970, U.S.A. If no code appears in an article, the author has not given broad consent to copy and permission to copy must be obtained directly from the author. All articles published prior to 1980 may be copied for a per-copy fee of US\$ 2.25, also payable through the Center. This consent does not extend to other kinds of copying, such as for general distribution, resale, advertising and promotion purposes, or for creating new collective works. Special written permission must be obtained from the publisher for such copying.

Special regulations for authors in the U.S.A. Upon acceptance of an article by the journal, the author(s) will be asked to transfer copyright of the article to the publisher. This transfer will ensure the widest possible dissemination of information under the U.S. Copyright Law.

Printed in The Netherlands

Reagents

MERCK

Gradient elution is your job:

You need: extreme UV-transmittance
You need: absence of interfering peaks
You need:

LiChrosolv®

Cat. 30 Acetonitrile

Cat. 6007 Methanol

Cat. 15333 Water



Acetonitrile

New Specifications

Min % transmission
(1 cm cell v. water)

205 nm	90%
225 nm	98%

Suitability

for gradient elution is tested for each batch
using LiChrosolv® Water.
Therefore both gradient partners
are best correlated to each other
as required for HPLC.

Please ask for our special brochure!

E. Merck, Darmstadt (F. R. Germany)

HPLC- The background story

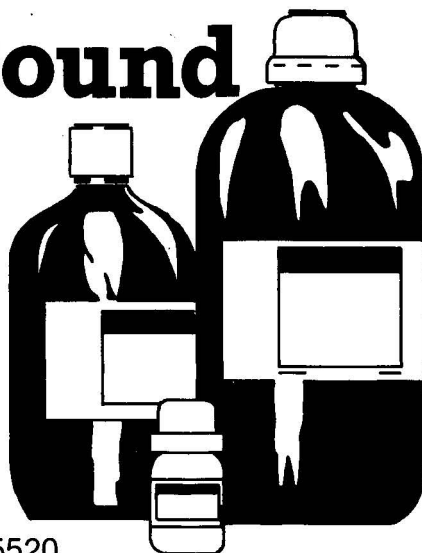
BDH provides the right background for your HPLC investigations. The optical transparency and high purity of the BDH range of solvents and ion pair reagents for liquid chromatography ensure accurate sample analysis. These competitively priced HPLC solvents and reagents are outlined in a free booklet available from



BDH Chemicals Ltd Poole 0202 745520

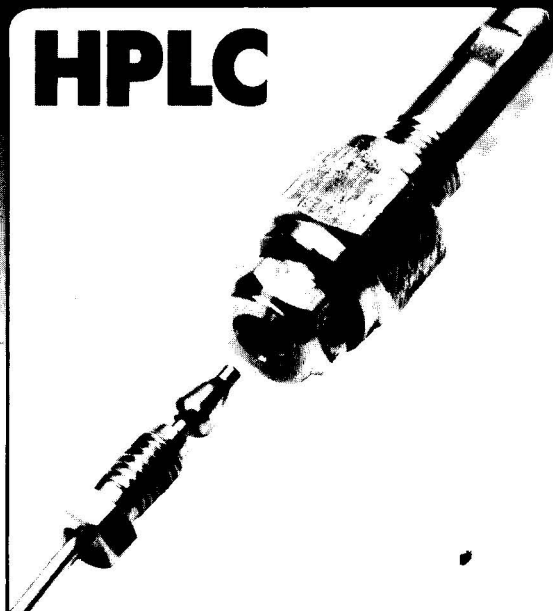


Hopkin & Williams Chadwell Heath 01 590 7700



507

HPLC



Our new HPLC columns are available in stainless steel and polyethylene. Each column is fitted with a 1/4" and 1/16" fitting each end of polyethylene adapter with seal element and 1/16" inner thread.

We supply the new columns packed with NUCLEOSIL® and POLYGOSIL®, as well as empty columns.

Our standard HPLC columns (stainless steel tubing 6 x 4 mm, 1/4" fittings with reducing unions to 1/16") are also available.

Our new HPLC brochure, presenting our entire programme in detail, can be mailed to you on request.

MACHERY-NAGEL GMBH & CO. KG
P.O. Box 307, 5160 Düren, West-Germany
Tel. .. 2421 / 6 10 71 · Telex 08 33 893

MACHERY-NAGEL · DÜREN

MN

546

The Acknowledged
Symbol of Excellence
Since 1959

HPLC Solvents from Burdick & Jackson

Purified to
the exacting
requirements of HPLC,
gas chromatography,
fluorescence and
spectrophotometric
analysis.

Call or write for more information.



**BURDICK & JACKSON
LABORATORIES, INC.**

1953 South Harvey Street
Muskegon, Michigan U.S.A. 49442
(616) 726-3171

Acetone
Acetonitrile
Benzene
Butanol-1
Butanol-2
n-Butyl Acetate
Butyl Chloride
Carbon Tetrachloride
Chlorobenzene
Chloroform
Cyclohexane
Cyclopentane
o-Dichlorobenzene
Diethyl Carbonate
Dimethyl Acetamide
Dimethyl Formamide
Dimethyl Sulfoxide
Dioxane
2-Ethoxyethanol
Ethyl Acetate
Ethyl Ether
Ethylene Dichloride
Heptane
Hexadecane
Hexane
Isobutyl Alcohol
Iso-hexanes
Methanol
2-Methoxyethanol
2-Methoxyethyl Acetate
Methyl t-Butyl Ether
Methyl Ethyl Ketone
Methyl Isoamyl Ketone
Methyl Isobutyl Ketone
Methyl n-Propyl Ketone
Methylene Chloride
N-Methylpyrrolidone
Nonane
Pentane
Petroleum Ether
beta-Phenethylamine
Propanol-1
Propanol-2
Propylene Carbonate
Pyridine
Tetrahydrofuran
Toluene
Trichloroethylene
Trichlorotrifluoroethane
2,2,4-Trimethylpentane
Water for HPLC
o-Xylene

A NEW BOOK SERIES

Chromatographic Methods

W. G. Jennings (USA)

Comparisons of Fused Silica and other Glass Columns in Gas Chromatography

1981, 81 pp., 39 figures and tables, hard cover, \$ 19.00
ISBN 3-7785-0729-X

Abdel Salam Said (Saudi Arabia)

Theory and Mathematics of Chromatography

1981, 210 pp., 44 figures, hard cover, \$ 28.00
ISBN 3-7785-0166-1

W. Bertsch (USA)

W. G. Jennings (USA),

R. E. Kaiser (Germany) (Editors)

Recent Advances in Capillary Gas Chromatography

1981, 592 pp., hard cover, \$ 38.00
ISBN 3-7785-0711-7

G. Schwedt (Germany)

Chromatographic Methods in Inorganic Analysis

1981, 226 pp., 35 figs. and 62 tables, hard cover, \$ 38.00
ISBN 3-7785-0690-0

R. E. Kaiser and E. Oelrich (Germany)

Optimization in HPLC

1981, 278 pp., 108 figs., hard cover, \$ 33.00
ISBN 3-7785-0657-9

W. Bertsch (USA), S. Hara (Japan),
Rudolf E. Kaiser (Germany),
A. Zlatkis (USA)

Instrumental HPTLC

1980, 390 pp., 200 figs., hard cover, \$ 49.00
ISBN 3-7785-0658-7

Dr. Alfred Hüthig Verlag GmbH
Postfach 102869
D-6900 Heidelberg 1

(Address of our New York Office:
611 Broadway, Room 227,
New York, N. Y. 10012)

Order your desk copy of:

CUMULATIVE AUTHOR AND SUBJECT INDEXES OF THE JOURNAL OF CHROMATOGRAPHY

covering Volumes 1-50.

1972 282 pages.

Price: US \$56.00/Dfl. 115.00.

covering Volumes 51-100.

1975 354 pages.

Price: US \$78.00/Dfl. 160.000.

covering Volumes 101-110.

1975 126 pages.

Price: US \$26.75/Dfl. 55.00.

covering Volumes 111-120.

1976 128 pages.

Price: US \$26.75/Dfl. 55.00.

covering Volumes 121-130.

1977 84 pages.

Price: US \$19.50/Dfl. 40.00.

covering Volumes 131-140.

1978 88 pages.

Price: US \$19.50/Dfl. 40.00.

covering Volumes 141-160.

1978 168 pages.

Price: US \$34.25/Dfl. 70.00.

covering Volumes 161-180.

1980 179 pages.

Price: US \$35.00/Dfl. 70.00.

One copy of the Cumulative Author and Subject Index is supplied free of charge to subscribers of the Journal of Chromatography. Additional copies can be purchased.

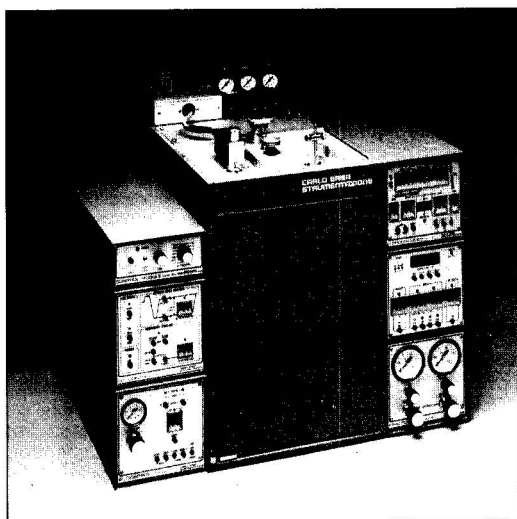
ELSEVIER



P.O. Box 211, Amsterdam.
The Netherlands.

The Dutch guilder price is definitive. US \$ price are subject to exchange rate fluctuations.

High resolution is not enough! High fidelity is also necessary to assess quantitative sample composition.



Unique

Specially cooled, automatic, non-vaporizing septum-less on-column injector allowing true: non-discriminating non-destructive non-contaminating sampling into capillary column. Automatic split-splitless injector.

Innovative

Zero dead volume, true all-glass system. New accurate all-metal pneumatic system. Constant flow/constant pressure option for carrier gas. Ultra-rapid amplifier. Wide range of easily interchangeable detectors.

These are only some of the most advanced features making the

Fractovap 4160 Series the only real answer for true quantitation in capillary gas chromatography.

**CARLO ERBA
STRUMENTAZIONE**

FARMITALIA CARLO ERBA SUBSIDIARY  **MONSIEISON GROUP**

FOUR NEW BOOKS



Order from your bookseller
or directly from

ELSEVIER SCIENTIFIC
PUBLISHING COMPANY
P.O. Box 211,
1000 AE Amsterdam,
The Netherlands

ELSEVIER
NORTH-HOLLAND INC.
52 Vanderbilt Ave.,
New York, NY 10017

Prepaid orders are supplied postfree.

The Dutch guilder price is definitive. US \$ prices
are subject to exchange rate fluctuations.

Electron Capture – Theory and Practice in Chromatography

edited by A. ZLATKIS, Houston, TX, USA, and C. F. POOLE, Detroit, MI, USA
JOURNAL OF CHROMATOGRAPHY LIBRARY – Volume 20

This comprehensive coverage of all aspects of the theory, design, operation and applications of the electron-capture detector in chromatography contains solutions to instrumental and technical problems which can arise during practice. It includes an extensive tabulation of all pertinent data concerning the use of this technique in gas and liquid chromatography. Each chapter has been prepared by experts in their fields and contains in-depth coverage of its topic.

Sept. 1981 viii + 376 pages
Price: US \$76.50/Dfl. 180.00
ISBN 0-444-41954-3

Affinity Chromatography and Related Techniques

edited by T. C. J. GRIBNAU, Oss, J. VISSER, Wageningen, and R. J. F. NIVARD, Nijmegen, The Netherlands

ANALYTICAL CHEMISTRY SYMPOSIA SERIES – Volume 9

The 45 papers in this Proceedings volume cover the theoretical aspects of affinity chromatography, review the preparation and properties of polymeric matrices and methods for ligand immobilization, and illustrate the increasing importance of affinity techniques in industrial and biomedical/diagnostic applications. A wide variety of the applications of organic dyes are included, as well as information on the application of affinity techniques in high-performance liquid chromatography.

Nov. 1981 xviii + 584 pages
Price: US \$83.00/Dfl. 195.00
ISBN 0-444-42031-2

Drugs of Abuse

by L. FISHBEIN, Jefferson, AR, USA

CHROMATOGRAPHY OF ENVIRONMENTAL HAZARDS 4

This is both a practical text and a literature reference source for chromatographic procedures used in the separation, detection and quantification of a spectrum of commonly abused drugs from biological, licit and illicit samples. These procedures are primarily useful in therapeutic monitoring, pharmacokinetic studies, emergency, clinical, forensic and toxicological analyses, and monitoring in drug abuse screening programs. It is the final volume in this series which also covers carcinogens, mutagens and teratogens, metals, gaseous and industrial pollutants, and pesticides.

Oct. 1981 x + 490 pages
Price: US \$95.75/Dfl. 225.00
ISBN 0-444-42024-X

Mass Spectrometry in Biochemistry, Medicine and Environmental Research, 7

Proceedings of the 7th International Symposium on Mass Spectrometry in Biochemistry, Medicine and Environmental Research, Milan, Italy, 16-18 June 1980

edited by A. FRIGERIO, Milan, Italy

ANALYTICAL CHEMISTRY SYMPOSIA SERIES – Volume 7

The main topics covered in the 32 papers presented at this symposium are the applications of mass spectrometric techniques in drug metabolism, metabolism of other substances, the identification and/or quantitation of endogenous compounds, studies involving respiratory gases, and environmental studies. Advances in methodology are also included.

Oct. 1981 x + 360 pages
Price: US \$72.50/Dfl. 170.00
ISBN 0-444-42029-0

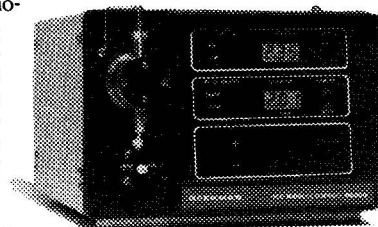
Beckman reinvents the liquid chromatograph.

First as Altex, and now as part of Beckman, we have led the way in HPLC pump technology. Seven years ago we introduced the innovative Model 100, a dual piston, electronic pulse corrected pump—still considered the standard of the industry. This was followed by the cost-effective 110A—the world's first high performance single piston rapid refill pump.

Now, 10,000 pumps later, Beckman introduces the Model 112—with the μ -Flow™ Solvent Delivery System, combining the best of both technologies into the most advanced solvent delivery system available.

The Model 112 was "reinvented" to meet industry needs demanding a liquid chromatograph with precision and accuracy plus trouble-

free operation. Built right into the high-pressure piston chamber is a new μ -Flow™ transducer. Regard-



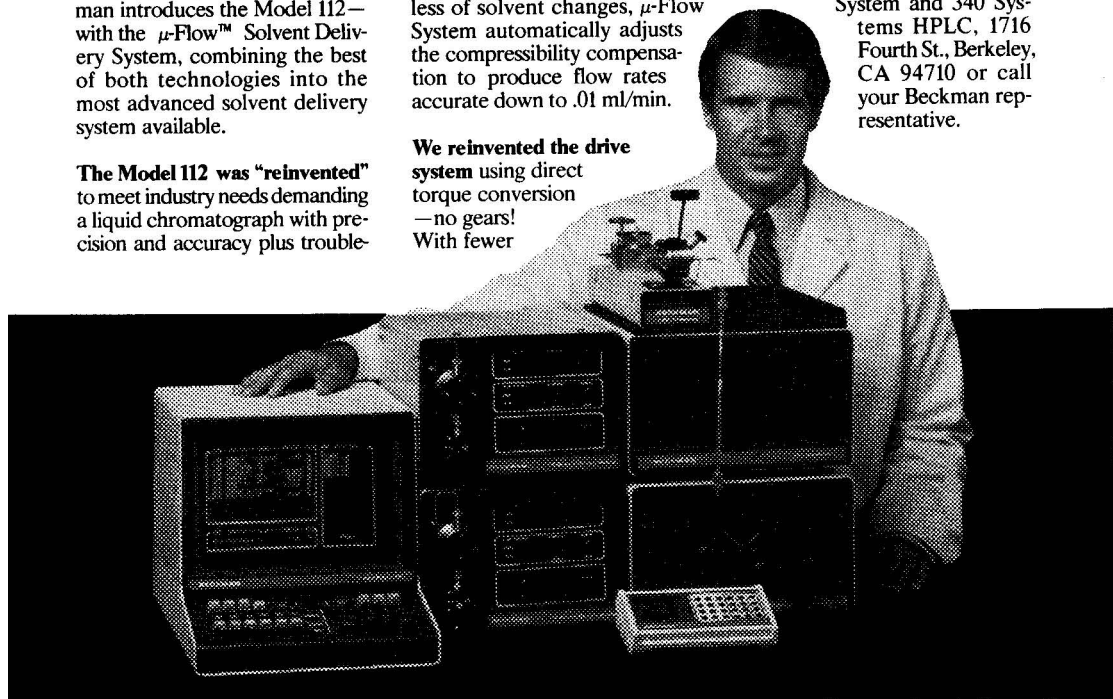
less of solvent changes, μ -Flow System automatically adjusts the compressibility compensation to produce flow rates accurate down to .01 ml/min.

We reinvented the drive system using direct torque conversion—no gears! With fewer

mechanical parts, the 112 provides greater reliability.

Totally new 340 Series utilizing the μ -Flow Solvent Delivery System, is designed for high resolution gradient separations. Combined with the 160-165 Detectors you receive unsurpassed HPLC performance.

Write for brochure #7396 for more information on the Model 112 Solvent Delivery System and 340 Systems HPLC, 1716 Fourth St., Berkeley, CA 94710 or call your Beckman representative.



BECKMAN

ISCO's variable wavelength monitor detects sugars to cytochromes

...and everything in between

Take advantage of variable wavelength detection and ISCO's low price to upgrade your liquid chromatography. Whether you're doing conventional or HPLC, and presently have a complete chromatograph, a system made of components, or are just getting started, an ISCO Model 1840 is the next step for you to consider.

Ten sensitivity ranges from 0.002 to 2.0 AUFS, fast response, and interchangeable flow cells allow you to handle practically any LC application. Several optical and electronic innovations increase the useful deuterium lamp life many times—lamp costs no longer need keep you from putting the whole spectrum in your chromatograph.

You can use this detector with any recorder, but the optional 10 cm built-in recorder is hard to beat for convenience. Another option is the ISCO Peak Separator which can control a fraction collector to put separate peaks in individual tubes.

An ISCO Model 1840 gives you all the advantages of continuously selectable wavelengths for \$2995. And with the built-in recorder and Peak Separator, it's still only \$3795—less expensive than many other variable detectors with the same specifications but without these features. To find out more, send for an ISCO catalog, or phone us toll free at [800] 228-4250 (continental U.S.A. except NE). ISCO, Box 5347, Lincoln, NE 68505.



Instruments with a difference



(use
this card
for more
information
on the
advertisement
pages)

Reader service card

JOURNAL OF

CHROMATOGRAPHY

INTERNATIONAL JOURNAL OF CHROMATOGRAPHY, ELECTROPHORESIS AND RELATED METHODS

I would like to receive, without any obligation, further information
on advertisement nos.:

Name (please print): _____

Position: _____

Address: _____



please use
envelope;
mail as
printed
matter

ELSEVIER SCIENCE PUBLISHERS

advertising department

P.O. BOX 211,

1000 AE AMSTERDAM – THE NETHERLANDS



(use
this card
for more
information
on the
advertisement
pages)

Reader service card

JOURNAL OF

CHROMATOGRAPHY

INTERNATIONAL JOURNAL OF CHROMATOGRAPHY, ELECTROPHORESIS AND RELATED METHODS

I would like to receive, without any obligation, further information
on advertisement nos.:

Name (please print): _____

Position: _____

Address: _____

please use
envelope;
mail as
printed
matter



ELSEVIER SCIENCE PUBLISHERS

advertising department

P.O. BOX 211,

1000 AE AMSTERDAM – THE NETHERLANDS

(use
this card
for more
information
on the
advertisement
pages)

Reader service card



I would like to receive, without any obligation, further information
on advertisement nos.:

Name (please print): _____

Position: _____

Address: _____

please use
envelope;
mail as
printed
matter

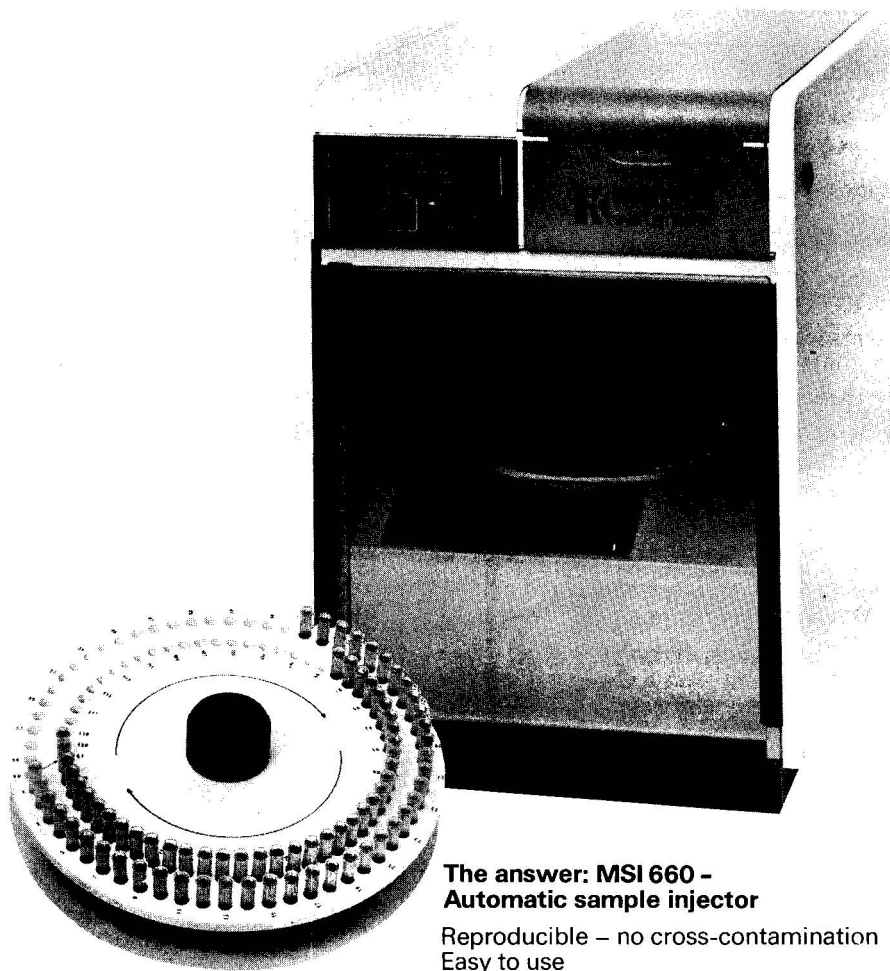
ELSEVIER SCIENCE PUBLISHERS

advertising department

P.O. BOX 211,

1000 AE AMSTERDAM – THE NETHERLANDS

Would you like to reduce your sample wastage?



The answer: MSI 660 - Automatic sample injector

Reproducible – no cross-contamination

Easy to use

No contamination

60 samples (30 or 120 as option)

Positive sample identification

System control using modern technology



KONTRON LTD.
Analytic International
Bernstrasse Süd 169
CH-8048 Zurich, Switzerland

Australia (Sydney) (02) 9383433
Austria (Vienna) (0222) 945646
Belgium (Brussels) (02) 3444900
Canada (Mississauga) (416) 6781151
Denmark (Ballerup) (02) 651666

France (Vélizy) (3) 9469722
Germany (Munich) (08165) 771
Great Britain (St. Albans) (0727) 66222
Italy (Milan) (02) 50721
Japan (Tokyo) (03214) 5371

Netherlands (Maarssen) (03465) 60894
Norway (Oslo) (02) 170390
Spain (Madrid) (01) 7348413
Sweden (Taebby) (08) 7567330
Switzerland (Zurich) (01) 62 92 62

U.S.A.: Kontron Electronics Inc., 630 Price Avenue, Redwood City/California 94063, (415) 3611012

**EXPERIENCE
THE
STATE of the ART
IN**

**ANALYTICAL CHEMISTRY
AND
APPLIED SPECTROSCOPY**



**MARCH 8-13, 1982
ATLANTIC CITY
CONVENTION HALL
NEW JERSEY, U.S.A.**



- OVER 1300 EXHIBITION BOOTHS
- TECHNICAL PROGRAM of 850 PAPERS
- 17 INVITED SYMPOSIA
- SPECIAL SHORT COURSES
- OVER 6000 ROOMS w/i WALKING DISTANCE of CONVENTION HALL
- SPOUSES & EVENING SOCIAL PROGRAMS
- SPECIAL DOMESTIC & EUROPEAN TRAVEL ARRANGEMENTS

for further information
clip & mail coupon below

to: Pittsburgh Conference
437 Donald Rd. dept. J-057
Pittsburgh, Pa. 15235
U.S.A.

name: _____

address: _____



TRAC

TrAC Travel from Europe to the 1982 Pittsburgh Conference

TrAC - Trends in Analytical Chemistry is Elsevier's new monthly which covers the latest trends and developments in analytical chemistry. It is easy to read, informative and affordable to the individual scientist.

TrAC Travel is a low price travel package from Europe to the Pittsburgh Conference and Exhibition on Analytical Chemistry and Applied Spectroscopy, Atlantic City, NJ, U.S.A., March 8-12, 1982.

The package includes:

- airfare from several European cities to and from New York
- transfer by luxury coach to Atlantic City, NJ
- 5 nights accommodation in a first class hotel in Atlantic City
- 1 night accommodation in a first class hotel in New York, and a sight-seeing tour of "The Big Apple"
- portorage, taxes, service charges, guid services and airport assistance

Prices (based on shared double room occupancy) at 1st October, 1981: Bfr. 32627; DM 2,195; Ffr. 4848; Dfl. 1995; £ 523; Sfr. 19.

For further details and a free sample copy of TrAC write now to

TrAC,
Elsevier/North-Holland,
68 Hills Road,
Cambridge,
England CB2 1LA,
(tel. 0223-325961)

TrAC and TrAC Travel



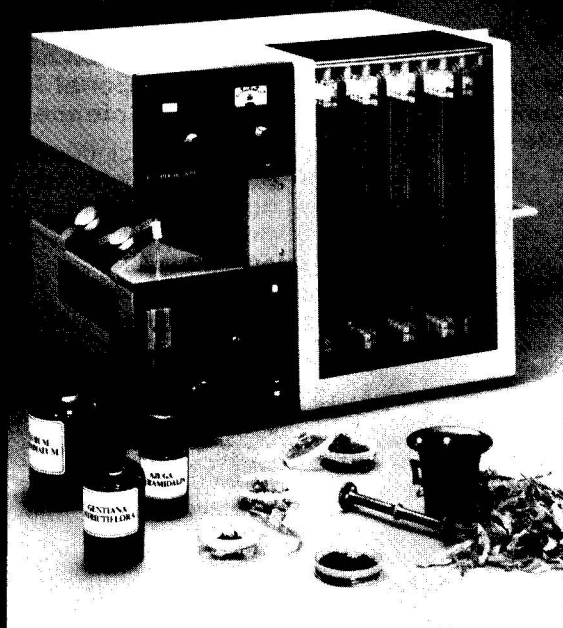
Affordable ways to bring
analytical chemists together

BÜCHI 670 DCC Chromatograph

for
separations and isolations
of
medium to strong polar samples
by
Droplet Countercurrent Chromatography

- Liquid-liquid method
- No solid column packing material
- easy to use
- reproducible separations
- sample quantities up to several grams
- hundred percent sample recovery

Büchi -
advanced laboratory
technique



Büchi
Laboratory-Techniques Ltd.
CH-9230 Flawil
Switzerland
Tel. 071-83 40 83
Telex 77 403

A NEW JOURNAL

Editor-in-chief:

B. DELMON, Louvain-la-Neuve,
Belgium

Editors:

J. A. CUSUMANO, Santa Clara, CA.

L. GUCZI, Budapest, Hungary

D. L. TRIMM, Kensington, Australia

D. A. WHAN, Edinburgh, U.K.

Supported by an international
Editorial Board.

Subscription Information:

1981 Volume 1 (in 6 issues)

\$80.50/173.00 Dutch guilders
including postage

applied catalysis

**Further details and a
free sample copy are
available on request.**

An International Journal Devoted to Catalytic Science and its Applications

The scope includes:

- catalytic phenomena occurring in industrial processes or in processes in the stage of industrial development and in conditions similar to those of industrial processes. Both heterogeneous and homogeneous catalysis are included, together with aspects of industrial enzymatic catalysis;
- scientific aspects of preparation, activation, ageing, poisoning, rejuvenation, regeneration and start up transient effects;
- methods of catalyst characterization when they are both scientific and have potential applications in industry;
- aspects of chemical engineering relevant to the science of catalysis;
- new catalytic reactions of practical interest, and new catalytic routes

A News Brief section, provided by correspondents, contains information gathered from patents, technical journals etc., on new catalytic reactions, catalysts and processes, new methods of catalyst preparation, and on new scientific facts related to the application of catalysis.

Rapid publication will be a special feature



P.O. Box 211
1000 AE Amsterdam
The Netherlands

52 Vanderbilt Ave
New York, N.Y. 10017
U.S.A.

ELSEVIER

The Dutch guilder price is definitive. US \$ prices are subject to exchange rate fluctuations.

How To Comply With The New Copyright Law

Participation in the Copyright Clearance Center (CCC) assures you of legal photocopying at the moment of need.

Libraries everywhere have found the easy way to fill photocopy requests legally and instantly, without the need to seek permissions, from more than 3000 key publications in business, science, humanities and social science. You can:

Fill requests for multiple copies, interlibrary loan (beyond the CONTU guidelines), and reserve desk without fear of copyright infringement.

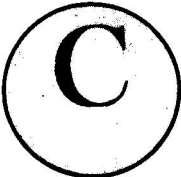
Supply copies from CCC-registered publications simply and easily.

The Copyright Clearance Center is your one-stop place for on-the-spot clearance to photocopy for internal use.

Its flexible reporting system accepts photocopying reports and returns an itemized invoice. You send only one convenient payment. CCC distributes it to the many publishers whose works you need.

And, you need not keep any records, the CCC computer will do it for you. Register now with the CCC and you will never again have to decline a photocopy request or wonder about compliance with the law for any publication participating in the CCC.

To register or for more information, just contact:

	Copyright Clearance Center		
	21 Congress Street Salem, Massachusetts 01970 (617) 744-3350 <small>a not-for-profit corporation</small>		
NAME		TITLE	
ORGANIZATION			
ADDRESS			
CITY		STATE	ZIP
COUNTRY		TELEPHONE	

COLLOIDS AND SURFACES

**AN INTERNATIONAL JOURNAL DEVOTED TO
THE APPLICATIONS AND PRINCIPLES OF
COLLOID AND INTERFACE SCIENCE**

Editor-in-Chief:

P. Somasundaran,
Henry Krumb School of Mines,
Columbia University,
New York, NY 10027, U.S.A.

Regional Editors:

E. D. Goddard,
Union Carbide Corp.,
Tarrytown Technical Center,
Old Saw Mill River Road,
Tarrytown, NY 10591,
U.S.A.

T. W. Healy,

Dept. of Physical Chemistry,
University of Melbourne,
Parkville, Vic. 3052,
Australia

Scope:

COLLOIDS AND SURFACES is an international journal concerned with applications and principles of colloidal and interfacial phenomena. It is designed to encourage publication of basic colloid and surface science and, in particular, its application in engineering and applied science. In addition to research papers, the journal contains notes, brief communications, book reviews and announcements.

Areas, topics and subjects covered include emulsions, foams, aerosols, detergency and wetting, flocculation and dispersion, rheology, cosmetics, paints, foods, paper and pulp, electrokinetic and electrode phenomena, friction and lubrication, thin films, liquid membranes and bilayers, biomaterials and biocolloids, polymer colloids, pharmaceutical and related health sciences, environmental and aquatic systems, water treatment and dewatering, agricultural and soil science, minerals extraction and metallurgy, precipitation and crystal growth and modification.

**Subscription
Information:**

**1981: Volumes 2-3
(in 8 issues) –
US \$182.50/
Dfl. 356.00
including postage.**

The Dutch guilder price is definitive.
US \$ prices are subject to exchange rate
fluctuations.



**P.O. Box 211,
1000 AE Amsterdam,
The Netherlands,**

**52 Vanderbilt Ave,
New York, N.Y. 10017.**

**Free sample copies
will be sent on
request.**

ELSEVIER

Errata

J. Chromatogr., 218 (1981) 123–135

Page 130, 6th line below eqn. A7, " α_1' " should read " α_f ".

Page 135, ref. 9 should be added, as follows: "9 J.C. Maxwell, *A Treatise on Electricity and Magnetism*, Vol. 1, Oxford, 3rd ed., 1904, p. 441."

J. Chromatogr., 218 (1981) 299–326

Page 308, legend to Fig. 5, 3rd line, " , pyridine" should read "c1ccncc1, pyridine".

Page 310, 5th line, "miror" should read "minor".

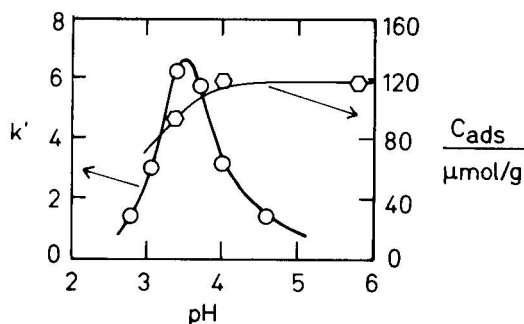
Page 313, 32nd line, "eqn. 7" should read "eqn. 4".

Page 320, Table VIII, mobile phase 26, m value, "0.43" should read "0.69".

Page 326, ref. 5, 2nd line should be deleted.

J. Chromatogr., 218 (1981) 341–354

Page 351, Fig. 11 should be replaced by the figure below.



J. Chromatogr., 218 (1981) 365–393

Page 372, 4th line below eqn. 6, " $h_{il_i,t}$, $h_{il_i,p}$ and $h_{il_i,p}$ " should read

" $h_{il_i,t}$, $h_{il_i,r}$ and $h_{il_i,p}$ ".

Page 372, 11th and 14th lines below eqn. 6, "c" should read "i".

JOURNAL OF CHROMATOGRAPHY

VOL. 218 (1981)

JOURNAL *of* CHROMATOGRAPHY

INTERNATIONAL JOURNAL ON CHROMATOGRAPHY,
ELECTROPHORESIS AND RELATED METHODS

EDITOR

MICHAEL LEDERER (Switzerland)

ASSOCIATE EDITOR

K. MACEK (Prague)

EDITORIAL BOARD

W. A. Aue (Halifax), V. G. Berezkin (Moscow), V. Betina (Bratislava), A. Bevenue (Honolulu, HI), P. Boulanger (Lille), A. A. Boulton (Saskatoon), G. P. Cartoni (Rome), G. Duyckaerts (Liège), L. Fishbein (Jefferson, AR), A. Frigerio (Milan), C. W. Gehrke (Columbia, MO), E. Gil-Av (Rehovot), G. Guiochon (Palaiseau), I. M. Hais (Hradec Králové), J. K. Haken (Kensington), E. Heftmann (Berkeley, CA), S. Hjertén (Uppsala), E. C. Horning (Houston, TX), Cs. Horváth (New Haven, CT), J. F. K. Huber (Vienna), A. T. James (Sharnbrook), J. Janák (Brno), E. sz. Kováts (Lausanne), K. A. Kraus (Oak Ridge, TN), E. Lederer (Gif-sur-Yvette), A. Liberti (Rome), H. M. McNair (Blacksburg, VA), Y. Marcus (Jerusalem), G. B. Marini-Bettolo (Rome), Č. Michalec (Prague), R. Neher (Basel), G. Nickless (Bristol), J. Novák (Brno), N. A. Parris (Wilmington, DE), P. G. Righetti (Milan), O. Samuelson (Göteborg), G.-M. Schwab (Munich), G. Semenza (Zürich), L. R. Snyder (Tarrytown, NY), A. Zlatkis (Houston, TX)

EDITORS, BIBLIOGRAPHY SECTION

K. Macek (Prague), J. Janák (Brno), Z. Deyl (Prague)

COORDINATING EDITOR, DATA SECTION

J. Gasparič (Hradec Králové)



ELSEVIER SCIENTIFIC PUBLISHING COMPANY
AMSTERDAM

J. Chromatogr., Vol. 218 (1981)

© ELSEVIER SCIENTIFIC PUBLISHING COMPANY — 1981

All rights reserved. No part of this publication may be reproduced, stored in a retrieval system or transmitted in any form or by any means, electronic, mechanical, photocopying, recording or otherwise, without the prior written permission of the publisher, Elsevier Scientific Publishing Company, P.O. Box 330, 1000 AH Amsterdam, The Netherlands.

Submission of an article for publication implies the transfer of the copyright from the author(s) to the publisher and entails the authors' irrevocable and exclusive authorization of the publisher to collect any sums or considerations for copying or reproduction payable by third parties (as mentioned in article 17 paragraph 2 of the Dutch Copyright Act of 1912 and in the Royal Decree of June 20, 1974 (S. 351) pursuant to article 16 b of the Dutch Copyright Act of 1912) and/or to act in or out of Court in connection therewith.

Special regulations for readers in the U.S.A. This journal has been registered with the Copyright Clearance Center, Inc. Consent is given for copying of articles for personal or internal use, or for the personal use of specific clients. This consent is given on the condition that the copier pays through the Center the per-copy fee stated in the code on the first page of each article for copying beyond that permitted by Sections 107 or 108 of the U.S. Copyright Law. The appropriate fee should be forwarded with a copy of the first page of the article to the Copyright Clearance Center, Inc., 21 Congress Street, Salem, MA 01970, U.S.A. If no code appears in an article, the author has not given broad consent to copy and permission to copy must be obtained directly from the author. All articles published prior to 1980 may be copied for a per-copy fee of US\$ 2.25, also payable through the Center. This consent does not extend to other kinds of copying, such as for general distribution, resale, advertising and promotion purposes, or for creating new collective works. Special written permission must be obtained from the publisher for such copying.

Special regulations for authors in the U.S.A. Upon acceptance of an article by the journal, the author(s) will be asked to transfer copyright of the article to the publisher. This transfer will ensure the widest possible dissemination of information under the U.S. Copyright Law.

Printed in The Netherlands

SPECIAL VOLUME



**V. INTERNATIONAL SYMPOSIUM
ON COLUMN LIQUID CHROMATOGRAPHY**

Avignon (France), May 11–15, 1981

CONTENTS

FIFTH INTERNATIONAL SYMPOSIUM ON COLUMN LIQUID CHROMATOGRAPHY,
AVIGNON (FRANCE), MAY 11-15, 1981

Foreword by G. Guiochon	XI
<i>Detection problems in liquid chromatography —equipment</i>	
Fluorescence detection of chloroanilines in liquid chromatography using a post-column reaction with fluorescamine. Comparison of reactor types and mixing tees by A. H. M. T. Scholten, U. A. Th. Brinkman and R. W. Frei (Amsterdam, The Netherlands)	3
Thermal lens calorimetry. Application to chromatographic detection by R. A. Leach and J. M. Harris (Salt Lake City, UT, U.S.A.)	15
Middle molecule mass spectrometry (a review) by C. Fenselau, R. Cotter, G. Hansen, T. Chen and D. Heller (Baltimore, MD, U.S.A.)	21
Reversed-phase ion-pair chromatography with UV-absorbing ions in the mobile phase by M. Denkert, L. Hackzell, G. Schill and E. Sjögren (Uppsala, Sweden)	31
Extra-column effects in polarographic <i>versus</i> UV detection in high-performance liquid chromatogra- phy by W. Kutner, J. Dębowski and W. Kemula (Warsaw, Poland)	45
Fluorescence derivatization of tertiary amines with 2-naphthyl chloroformate by G. Gübitz, R. Wintersteiger and A. Hartinger (Graz, Austria)	51
Ion chromatography of inorganic and organic ionic species using refractive index detection by F. A. Buytenhuys (Arnhem, The Netherlands)	57
Separation and determination of phenyl isocyanate-derivatized carbohydrates and sugar alcohols by high-performance liquid chromatography with ultraviolet detection by B. Björkqvist (Espoo, Finland)	65
Limits of the internal standard technique in chromatography by P. Haefelfinger (Basle, Switzerland)	73
Computer-controlled single-pump solvent programmer for high-performance liquid chromatogra- phy by C. Laurent, H. A. H. Billiet, H. C. van Dam and L. de Galan (Delft, The Netherlands)	83
<i>Column types and column technology in liquid chromatography and related techniques</i>	
Dispersion of peaks by short straight open tubes in liquid chromatography systems by J. G. Atwood and M. J. E. Golay (Norwalk, CT, U.S.A.)	97
Effect of radial thermal gradients in elevated temperature high-performance liquid chromatography by S. Abbott, P. Achener, R. Simpson and F. Klink (Walnut Creek, CA, U.S.A.)	123
Microcapillary liquid chromatography in open tubular columns with diameters of 10–50 μm . Poten- tial application to chemical ionization mass spectrometric detection by R. Tijssen, J. P. A. Bleumer, A. L. C. Smit and M. E. van Kreveland (Amsterdam, The Netherlands)	137
Flow characteristics and technology of capillary columns with inner diameters less than 15 μm in liquid chromatography by M. Krejčí, K. Tesařík, M. Rusek and J. Pajurek (Brno, Czechoslovakia)	167

Micro-column high-performance liquid chromatography and flame-based detection principles by V. L. McGuffin and M. Novotný (Bloomington, IN, U.S.A.)	179
Study of the performance of cation-exchange columns in open-tubular microcapillary liquid chromatography by D. Ishii and T. Takeuchi (Nagoya, Japan)	189
Application of ultra-micro high-performance liquid chromatography to trace analysis by T. Takeuchi and D. Ishii (Nagoya, Japan)	199
High-resolution separations based on electrophoresis and electroosmosis by J. W. Jorgenson and K. DeArman Lukacs (Chapel Hill, NC, U.S.A.)	209
Comparison of sedimentation field flow fractionation with chromatographic methods for particulate and high-molecular-weight macromolecular characterizations by W. W. Yau and J. J. Kirkland (Wilmington, DE, U.S.A.)	217
<i>Retention mechanisms</i>	
Development of modern bioaffinity chromatography (a review) by J. Porath (Uppsala, Sweden and Paris, France)	241
Systematic study of ternary solvent behaviour in reversed-phase liquid chromatography by P. J. Schoenmakers, H. A. H. Billiet and L. de Galan (Delft, The Netherlands)	261
High-performance liquid chromatography of organic acids on bare silica by W. J. Th. Brugman, S. Heemstra and J. C. Kraak (Amsterdam, The Netherlands)	285
Theoretical basis for systematic optimization of mobile phase selectivity in liquid-solid chromatography. Solvent-solute localization effects by L. R. Snyder (Tarrytown, NY, U.S.A.) and J. L. Glajch and J. J. Kirkland (Wilmington, DE, U.S.A.)	299
Study on the retention of amines in reversed-phase ion-pair chromatography on bonded phases by R. S. Deelder and J. H. M. van den Berg (Geleen, The Netherlands)	327
Mechanism of zwitterion-pair chromatography. I. Nucleotides by J. H. Knox and J. Jurand (Edinburgh, Great Britain)	341
Mechanism of zwitterion-pair chromatography. II. Ampicilline, lysergic acid, tryptophan and other solutes by J. H. Knox and J. Jurand (Edinburgh, Great Britain)	355
High-performance displacement chromatography by Cs. Horváth, A. Nahum and J. H. Frenz (New Haven, CT, U.S.A.)	365
Chromatographic characterization of silica surfaces by H. Engelhardt and H. Müller (Saarbrücken, G.F.R.)	395
Estimation of aqueous solubilities of organic non-electrolytes using liquid chromatographic retention data by T. L. Hafkenschied and E. Tomlinson (Amsterdam, The Netherlands)	409
Structural effects in enthalpy/entropy compensated and non-compensated behaviour in ion-pair reversed-phase high-performance liquid-solid chromatography by C. M. Riley (Lawrence, KS, U.S.A.) and E. Tomlinson and T. L. Hafkenschied (Amsterdam, The Netherlands)	427
Retention and selectivity characteristics of a non-polar perfluorinated stationary phase for liquid chromatography by H. A. H. Billiet, P. J. Schoenmakers and L. de Galan (Delft, The Netherlands)	443
Separation of proton-donating solutes by liquid chromatography with a strong proton acceptor, tri- <i>n</i> -octylphosphine oxide, in the liquid stationary phase by H. W. Stuurman and K.-G. Wahlund (Uppsala, Sweden)	455

Selectivity and efficiency of separation of isomers of organic acids by clathrate chromatography by W. Kemula, D. Sybilska and J. Lipkowski (Warsaw, Poland)	465
Comparison of dimensions obtained by size-exclusion chromatography and X-ray diffraction of rigid molecules by G. Samay, L. Füzes, F. Cser and G. Bodor (Budapest, Hungary)	473
<i>Applications of liquid chromatography in the analysis of proteins, peptides and amino acids</i>	
Buffer-focusing chromatography using multicomponent electrolyte elution systems by M. T. W. Hearn and D. J. Lyttle (Dunedin, New Zealand)	483
High-performance liquid chromatography of amino acids, peptides and proteins. XXXVI. Organic solvent modifier effects in the separation of unprotected peptides by reversed-phase liquid chromatography by M. T. W. Hearn and B. Grego (Dunedin, New Zealand)	497
Application of 1,1'-carbonyldiimidazole-activated matrices for the purification of proteins. III. The use of 1,1'-carbonyldiimidazole-activated agaroses in the biospecific affinity chromatographic isolation of serum antibodies by M. T. W. Hearn and E. L. Harris (Dunedin, New Zealand) and G. S. Bethel, W. S. Hancock and J. A. Ayers (Palmerston North, New Zealand)	509
Analysis of N-acetyl-N,O,S-permethylated peptides by combined liquid chromatography-mass spec- trometry by T. J. Yu, H. Schwartz, R. W. Giese, B. L. Karger and P. Vouros (Boston, MA, U.S.A.)	519
Assessment and optimization of system parameters in size exclusion separation of proteins on diol- modified silica columns by P. Roumeliotis and K. K. Unger (Mainz, G.F.R.)	535
Ligand-exchange chromatography of racemates. XV. Resolution of α -amino acids on reversed-phase silica gels coated with N-decyl-L-histidine by V. A. Davankov, A. S. Bochkov and Yu. P. Belov (Moscow, U.S.S.R.)	547
Ligand-exchange chromatography of racemates. XVI. Microbore column chromatography of amino acid racemates using N,N,N',N'-tetramethyl-(R)-propanediamine-1,2-copper(II) complexes as chiral additives to the eluent by A. A. Kurganov and V. A. Davankov (Moscow, U.S.S.R.)	559
Comparison of short and ultrashort-chain alkylsilane-bonded silicas for the high-performance liquid chromatography of proteins by hydrophobic interaction methods by E. C. Nice and M. W. Capp (Sutton, Great Britain), N. Cooke (Berkeley, CA, U.S.A.) and M. J. O'Hare (Sutton, Great Britain)	569
Analysis of glycoprotein hormones and other medically important proteins by high-performance gel filtration chromatography by D. H. Calam and J. Davidson (London, Great Britain)	581
High-performance liquid chromatography of ^{125}I -labelled proteins with on-line detection by O. von Stetten and R. Schlett (Blaubeuren, G.F.R.)	591
Improved high-performance liquid chromatographic method for the analysis of insulins and related compounds by G. Szepesi and M. Gazdag (Budapest, Hungary)	597
Separation of large polypeptides by high-performance liquid chromatography by M. Gazdag and G. Szepesi (Budapest, Hungary)	603
<i>Applications of liquid chromatography in the analysis of drugs</i>	
Rapid automated determination of D-penicillamine in plasma and urine by ion-exchange high-per- formance liquid chromatography with electrochemical detection using a gold electrode by F. Kreuzig (Kundl, Austria) and J. Frank (Herisau, Switzerland)	615

Rapid high-performance liquid chromatographic method for the measurement of verapamil and norverapamil in blood plasma or serum by S. C. J. Cole, R. J. Flanagan, A. Johnston and D. W. Holt (London, Great Britain)	621
Automated measurement of catecholamines in urine, plasma and tissue homogenates by high-performance liquid chromatography with fluorometric detection by K. Mori (Kawasaki, Japan)	631
Group-contribution approach to the behaviour of 2-phenylethylamines in reversed-phase high-performance liquid chromatography by R. Gill, S. P. Alexander and A. C. Moffat (Reading, Great Britain)	639
High-performance liquid chromatography of bile pigments: separation and characterization of the urobilinoids by R. V. A. Bull, C. K. Lim and C. H. Gray (Harrow, Great Britain)	647
Isolation and characterization of three new polymyxins in polymyxins B and E by high-performance liquid chromatography by I. Elverdam (Copenhagen, Denmark) and P. Larsen and E. Lund (Hørsholm, Denmark)	653
Determination of 5-hydroxytryptophan, serotonin and 5-hydroxyindoleacetic acid in rat and human brain and biological fluids by reversed-phase high-performance liquid chromatography with electrochemical detection by L. Semerdjian-Rouquier (Bagneux, France), L. Bossi (Paris, France) and B. Scatton (Bagneux, France)	663
Separation of acidic drugs in the $\mu\text{g/ml}$ range in untreated blood plasma by direct injection on liquid chromatographic columns by K.-G. Wahlund (Uppsala, Sweden)	671
<i>Other applications</i>	
High-performance liquid chromatography of flavonoids in barley and hops by I. McMurrough (Dublin, Ireland)	683
Separation and determination of some organic acids and their sodium salts by high-performance liquid chromatography by E. Rajakylä (Kantvik, Finland)	695
Analysis of additives in plastics by high-performance size-exclusion chromatography by M. J. Shepherd and J. Gilbert (Norwich, Great Britain)	703
High-performance liquid chromatographic column switching techniques for rapid hydrocarbon group-type separations by T. V. Alfredson (Walnut Creek, CA, U.S.A.)	715
Thin-layer chromatography as a pilot technique for the optimization of preparative column chromatography by E. Soczewiński and T. Wawrzynowicz (Lublin, Poland)	729
<i>Author Index</i>	733

FOREWORD

The Vth Symposium on Column Liquid Chromatography has been organized jointly by GAMS, the Chromatography Discussion Group of UK, the Arbeitskreis Chromatographie der Fachgruppe Analytische Chemie der Gesellschaft Deutscher Chemiker, the Division of Analytical Chemistry of the French Chemical Society, the Swiss Chemical Society (SCV), the Austrian Chemical Society (VOeV), the Royal Dutch Chemical Society (KNCV) and the Chromatography Forum of the Delaware Valley. It is a pleasure to acknowledge the support of these societies and the excellent cooperation with them.

The success of such a meeting depends mainly on the quality of its scientific program. Thus, I wish to express my gratitude to the many authors who contributed to it and to the members of the Scientific Committee (H. Colin, R. S. Deelder, Cs. Horvath, J. F. K. Huber, K. P. Hupe, B. L. Karger, J. J. Kirkland, J. H. Knox, M. Martin, G. Schill, W. Simon, L. R. Snyder) for having helped me in the difficult task of inviting or selecting and organizing such a large number of excellent contributions.

Thanks are due also the Editor of the *Journal of Chromatography* for his help in publishing these proceedings which contain a large proportion of the papers presented at the meeting.

The success of the Symposium is also largely due to the ability, dedication and kindness of Ms. M. Jacquet who helped me in arranging all the details of the scientific program and the relations with authors, publisher and printers, and of Ms. de Haro, delegate of the Centre des Congrès du Palais des Papes, Avignon, who was responsible for the Social Programme and the solution of the many problems associated with the organization of a large meeting of over 600 scientists. The financial equilibrium of such a symposium could not be achieved without a successful exhibition. I acknowledge the contributions of the companies which were present at the Palais des Papes and the efficient help of Mr. Lauret (Touzart et Matignon, France), Chairman of the Exhibition Committee.

Finally, thanks are due to all the chromatographers who, in spite of their busy schedule and a terrible weather, came to Avignon between May 10 and 15, 1981, participated actively in the meeting and made it so successful.

G. GUIOCHON

DETECTION PROBLEMS IN LIQUID CHROMATOGRAPHY —EQUIPMENT

CHROM. 14,049

FLUORESCENCE DETECTION OF CHLOROANILINES IN LIQUID CHROMATOGRAPHY USING A POST-COLUMN REACTION WITH FLUORESCAMINE

COMPARISON OF REACTOR TYPES AND MIXING TEES

A. H. M. T. SCHOLTEN, U. A. Th. BRINKMAN and R. W. FREI*

Department of Analytical Chemistry, Free University, de Boelelaan 1083, 1081 HV Amsterdam (The Netherlands)

SUMMARY

The fluorescamine (Fluram) reaction for primary amines has been used for the post-column derivatization of three chloroanilines at relatively low pH values. Separation was carried out on a CN-modified bonded phase with acetonitrile–water (pH 3) as the mobile phase. Various types of reactors (tubular, packed-bed and air-segmented) and mixing tees have been studied and compared for their suitability in post-column reactor systems.

Under optimal conditions, detection limits for the derivatized chloroanilines are in the 100-pg range, which is about 10-fold better than with UV detection. The linearity of the calibration graphs is excellent ($r = 0.9999$ – 1.0000) over a concentration range of 2–3 orders of magnitude.

INTRODUCTION

Halogenated anilines, especially chloroanilines, can be released into the environment either directly as industrial effluents or indirectly as breakdown products of phenylcarbamates and phenylurea herbicides, and materials such as paints. Over the years, many papers on the determination of halogenated anilines have been published (see, e.g., refs. 1–4 and the literature cited therein). Here, we call attention to a paper by Sherma and Marzoni⁵, who separated these anilines by thin-layer chromatography and quantitated them by fluorescence detection after spraying with fluorescamine {4-phenylspiro[furan-2(3*H*),1'(3'*H*)-isobenzofuran]-3,3'-dione}. Fluorescamine (Fluram) is a well known reagent for the detection of primary and secondary amino groups^{6,7} in a variety of compounds such as amino acids^{8,9}, polyamines¹⁰, peptides^{11,12}, proteins¹³, cephalosporin¹⁴, phenelzine¹⁵, ampicillin¹⁶ and fluvoxamine and clovoxamine¹⁷. The non-fluorescent reagent reacts with the primary amines to form pyrrolinones which, upon excitation at 390 nm, emit strong fluorescence at 475–500 nm; in the quoted work both pre- and post-column derivatization were used. Several thorough investigations on the selection of suitable conditions for

the reaction between amines and Fluram have been published^{6,13,18-21}. It has been shown that, in general, reaction must take place at pH 7-9 and that in organic solvents the reaction proceeds much more slowly than it does in an aqueous medium. Under non-aqueous conditions, 50 % conversion into the Fluram derivative typically takes from several minutes²¹ to several hours²⁰, compared with seconds in an aqueous solution.

Hydrolysis of Fluram, which takes place parallel to the derivatization reaction, can be a serious interference, particularly for kinetically slow reactions. According to Stein *et al.*²⁰, who studied the use of various aqueous-organic solvent mixtures, the rate of hydrolysis of Fluram increases with increasing pH, and depends strongly on the nature of the organic co-solvent and the buffer selected. The authors also state that the product of hydrolysis is non-fluorescent. According to our observations, however, and also those of Castell *et al.*¹³, a fluorescence signal appears upon hydrolysis. The latter workers suggested two possible hydrolysis reactions, *viz.*, a reversible one, in which merely the lactone ring of Fluram is opened, and one which results in the formation of a yellow (fluorescent) end-product.

In this paper, the separation of three of the more important chloroanilines (3- and 4-chloroaniline and 3,4-dichloroaniline) by high-performance liquid chromatography (HPLC) and their subsequent determination by post-column derivatization with Fluram at relatively low pH values is described. The system has been used to compare the potential of a tubular reactor with that of a packed-bed reactor and a reactor based on the air-segmentation principle. Also, the dependence of band broadening and, thus, system performance, on the construction of mixing tees has been evaluated.

EXPERIMENTAL

Chromatography

The experimental arrangement is shown in Fig. 1. The system consisted of an Altex (Berkeley, CA, U.S.A.) Series 100 pump, a Valco (Houston, TX, U.S.A.) six-port injection valve with a 20- μ l sample loop, a 10 cm \times 4.6 mm I.D. stainless-steel column packed with Polygosil 60-10 CN (Macherey, Nagel & Co., Düren, G.F.R.), a Perkin-Elmer (Norwalk, CT, U.S.A.) LC 55 variable-wavelength UV detector set at 243 nm, a post-column reaction system (see below) and a Perkin-Elmer Model 204A or 3000 fluorescence spectrophotometer with 10-nm slits operated at $\lambda_{\text{ex.}}$ = 398 nm and $\lambda_{\text{em.}}$ = 498 nm. The signals were recorded with Kipp (Delft, The Netherlands) BD-8 recorders.

Post-column reaction system

For reagent addition, a home-made syringe pump with a capacity of 300 ml was used. With this constant-pressure pump a regular and pulse-free reagent stream could be added to the mobile phase, with a pressure limit of about 200 bar. In the air-segmentation experiments, a Technicon (Tarrytown, NY, U.S.A.) AutoAnalyzer pump was installed in the system. Routinely, the reagent stream and mobile phase were mixed in a stainless-steel tee-piece, in which the capillaries (0.25 mm I.D. and 1/16 in. O.D.) made a 120° angle. In order to prevent the formation of tiny air bubbles in this tee-piece, which often occurred, a piece of stainless-steel capillary or Tygon

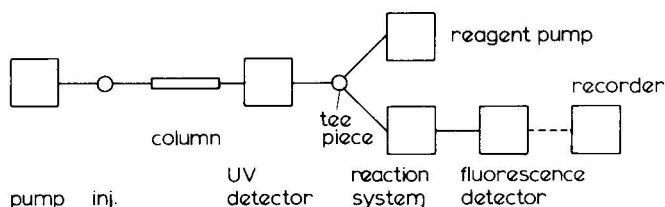


Fig. 1. Instrumental arrangement of the chromatographic system.

tubing, which will give a back-pressure of a few bars, was installed at the outlet of the detector flow-cell. In such cases, the Perkin-Elmer Model 3000 fluorospectrometer had to be used for analysis, as its flow-cell can withstand back-pressures of up to 35 bar.

Three types of reactor were used: (1) the packed-bed reactor consisted of a 10 cm \times 4.6 mm I.D. stainless-steel column packed with 15- μ m glass beads (Euroglas, Delft, The Netherlands); (2) the tubular reactor was a stainless-steel capillary of varying length (6–18 m) and 0.3 mm I.D. with a helix diameter of 3 cm; (3) for the air-segmentation system a 2-m long PTFE capillary purchased from Omnifit (Biolab, Cambridge, Great Britain) of 0.8 mm I.D., 1/16 in. O.D. and a 5-cm helix diameter was used as the reactor. Air was added via a Technicon A-10 glass tee-piece at a flow-rate of 0.6 ml \cdot min⁻¹. A modified²² tee-piece of 1/16 in. I.D. in order to allow insertion of the PTFE capillary was used as a phase separator; 50–80% of the liquid stream passed through the phase separator to the flow cell of the detector.

Reagents

Fluram and 3- and 4-chloroaniline were obtained from Fluka (Buchs, Switzerland) and 3,4-dichloroaniline from Merck (Darmstadt, G.F.R.). Acetonitrile and all other chemicals were of analytical-reagent grade from Merck. Aqueous buffer solutions were prepared using appropriate amounts of sodium acetate and acetic acid; the total acetate concentration was 0.05 *M*.

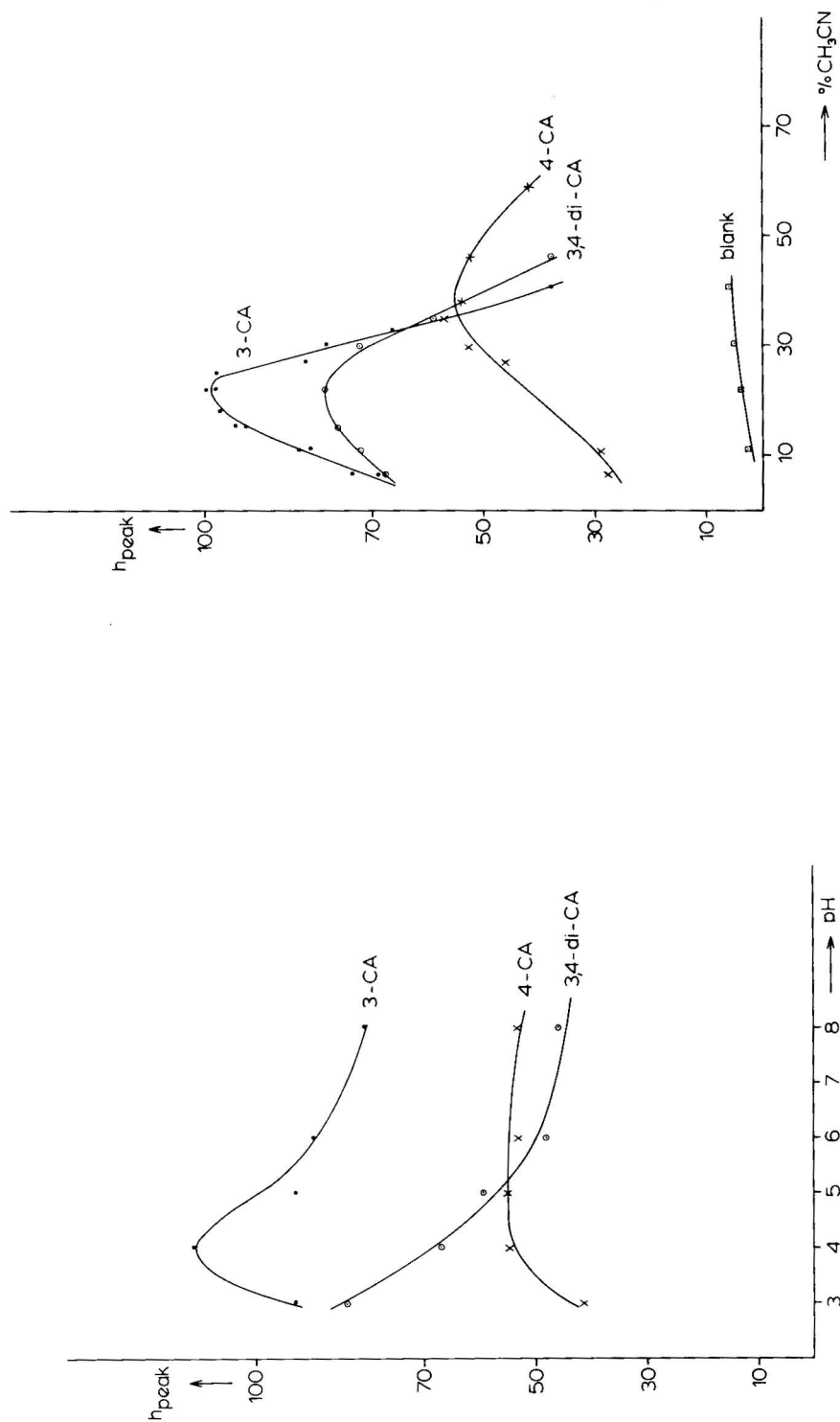
Stock solutions of the anilines were prepared in the mobile phase and kept in the dark. Solutions of Fluram in acetonitrile were degassed in an ultrasonic bath for 10 min. Mobile phases were degassed under vacuum for 2 min.

RESULTS AND DISCUSSION

HPLC conditions

HPLC on chemically bonded stationary phases is often carried out with methanol–water or acetonitrile–water mixtures as the mobile phase. Acetonitrile was preferred as the organic solvent, as methanol (and other alcohols) are known to effect a considerable increase in the time of reaction between Fluram and amino groups because of reversible hydrolysis of Fluram by the alcohol²⁰; consequently, the net fluorescence is low.

Initially, 10- μ m LiChrosorb RP-18 (Merck) was used as the stationary phase. A good separation of 3- and 4-mono- and 3,4-dichloroaniline with capacity ratios (*k'*) of 1–3 was obtained with acetonitrile–0.05 *M* sodium acetate (4:6) as the mobile phase. One should realize, however, that Fluram has to be added to the mobile phase



as a solution in acetonitrile. This implies that the post-column reaction medium contains 50–60% or more of acetonitrile. Such high proportions of organic solvent are known^{12,13} to have a negative effect on the formation of the fluorescent reaction products. This was confirmed in a series of batch experiments (Fig. 2) in which the optimal percentage of acetonitrile was found to vary from 20% for 3,4-di- and 3-chloroaniline to 35% for 4-chloroaniline.

As a consequence of the above, with a flow-rate of $1.0 \text{ ml} \cdot \text{min}^{-1}$ through the HPLC column and even with a reagent flow-rate as low as $0.2 \text{ ml} \cdot \text{min}^{-1}$ (see below) the mobile phase had to consist of an organic–aqueous solvent mixture containing about 95% of water. The use of more polar packing materials such as LiChrosorb RP-2 and Polygosil 60-10 CN as the stationary phase therefore had to be studied. Excessive retention could be avoided only by using the CN-modified bonded phase. Unfortunately, however, at an aqueous phase pH of 5 or higher, the resolution between 3- and 4-chloroaniline was negligible, and a 95:5 mixture of a pH 3 acetate buffer and acetonitrile had to be used to create well resolved peaks. Under these conditions, the capacity ratios were: 3-chloroaniline 1.7, 4-chloroaniline 1.4 and 3,4-dichloroaniline 4.4. The results of a subsequent batch study (10 min reaction time

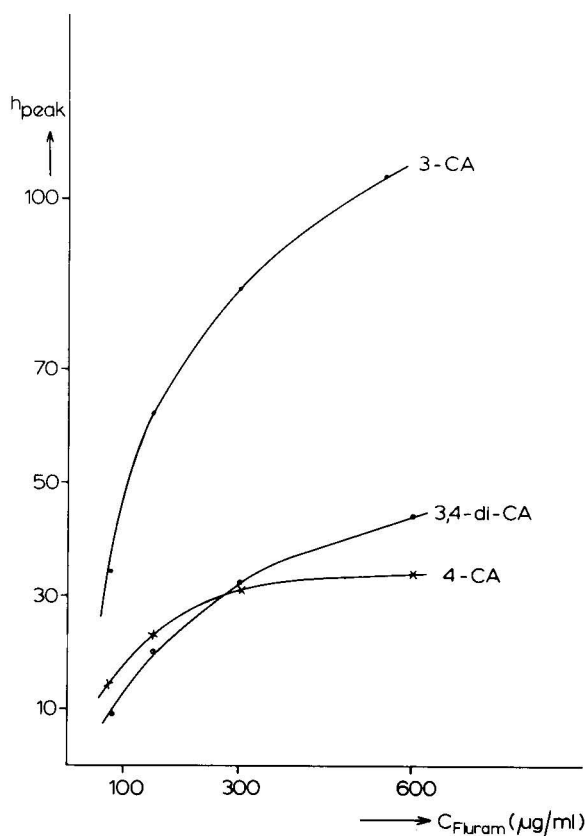


Fig. 4. Influence of Fluram concentration on fluorescence intensity, measured in the dynamic system at pH 3. Reaction time, 60 sec; further conditions and symbols, see text and Fig. 2.

with optimal acetonitrile–acetate conditions) on the influence of pH on fluorescence intensity are shown in Fig. 3. A pH of about 4 is seen to be the best overall choice; however, the decrease in signal intensity observed for 3-mono- and 3,4-dichloroaniline on lowering the pH to 3 certainly is not dramatic.

Fluram concentration and reaction time

Fig. 4 shows the dependence of fluorescence peak height on Fluram concentration, recorded at pH 3 under dynamic conditions. The time of reaction was 60 sec and the composition of the reaction system corresponded to the optimal conditions established in the previous section. For all further work, a concentration of $600 \mu\text{g} \cdot \text{ml}^{-1}$ of Fluram was used; higher concentrations were found to result in precipitation of Fluram and clogging of the capillaries on mixing of the reagent and carrier stream.

The influence of the reaction time on fluorescence yield was studied by using different lengths of capillary, each $6 \text{ m} \times 0.3 \text{ mm}$ I.D. capillary causing a 30-sec residence time in the post-column reactor. An increase in the reaction time from 30 to 60 sec resulted in a 10–40% increase in peak height, the actual percentage depending on the chloroaniline tested. A further increase to 90 sec led to a diminution of the peak heights, although the peak areas still showed an increase. As the resolution was found to deteriorate considerably on increasing the capillary length, a 30-sec residence time was deemed to offer the best compromise as regards band broadening and fluorescence peak height.

Linearity and detection limits

Calibration graphs were constructed using the following conditions: mobile phase, acetonitrile–pH 3 acetate buffer (5:95) at a flow-rate of $1 \text{ ml} \cdot \text{min}^{-1}$; reagent stream, $600 \mu\text{g}$ of Fluram per millilitre of acetonitrile at $0.2 \text{ ml} \cdot \text{min}^{-1}$; reaction time, 30 sec. Over the concentration ranges investigated the linearity was excellent, as is evident from the following data: 3-chloroaniline, $r = 1.0000$ (0.03 – $4.1 \mu\text{g} \cdot \text{ml}^{-1}$); 4-chloroaniline, $r = 0.9999$ (0.1 – $12.7 \mu\text{g} \cdot \text{ml}^{-1}$); 3,4-dichloroaniline, $r = 0.9999$ (0.09 – $11.8 \mu\text{g} \cdot \text{ml}^{-1}$).

The detection limits for the Fluram derivatives of the chloroanilines, calculated for a signal/peak-to-peak noise ratio of 2:1, were 60 pg for 3-chloroaniline and 130 pg for 4-mono- and 3,4-dichloroaniline. The UV detection limits, recorded at 243 nm, were 0.6 ng for the former and 1 ng for the latter two compounds. It should be emphasized that under the experimental conditions used, the fluorescence background signal of hydrolysed Fluram was relatively high. Consequently, especially when working at high sensitivities, a pulse-free pumping system had to be used in order to avoid undue baseline fluctuations.

Reactor design

Comparison of reactors. The work reported so far was carried out with a coiled tubular reactor. On the basis of literature data, it could not be expected that, for the reaction times used (30 sec), a segmented system can compete with a tubular or a packed-bed reactor. Recently, we have calculated²², however, that the use of a segmented instead of a non-segmented system should be beneficial for fast reactions. For example, it was found that with reaction times of over about 8 sec in a capillary of 0.25 mm I.D., and a time of over 19 sec in a $10 \text{ cm} \times 4.6 \text{ mm}$ I.D. reactor packed with

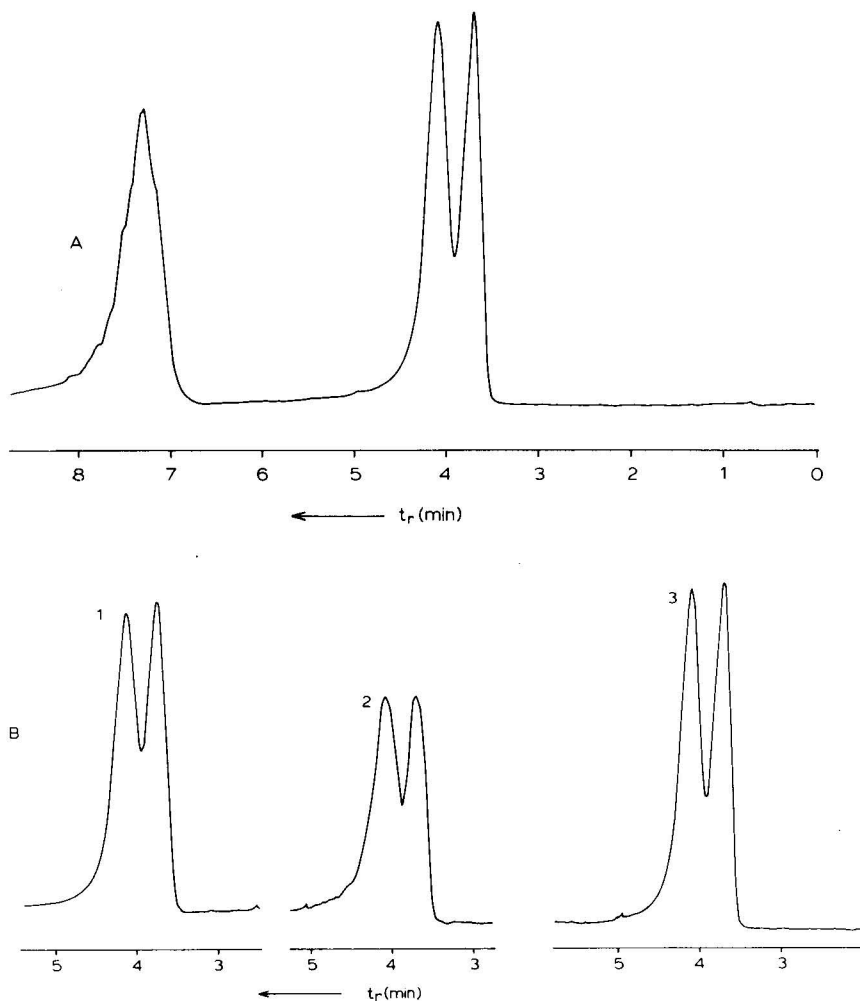


Fig. 5. (A) HPLC trace for air-segmented system. (B) Resolution of peaks due to Fluram derivatives of 3- and 4-chloroaniline: 1, tubular non-segmented reactor; 2, packed-bed reactor; 3, air-segmented reactor. For conditions and explanation, see text and Table I.

15- μm glass beads, a segmented reactor should be preferred. The three types of reactor were therefore compared. Typical chromatograms are shown in Fig. 5. Further results are summarized in Table I; the data on band broadening and resolution are average values from five measurements.

The main conclusion from the data in Table I is that the air-segmented system shows a distinctly smaller total band broadening of $\sigma_{v,\text{tot}}^2 = 8500 \mu\text{l}^2$ compared with the systems in which a coiled tubular or a packed-bed reactor was inserted ($\sigma_{v,\text{tot}}^2 = 18,000 \mu\text{l}^2$). This corresponds to σ_v values of *ca.* 90 and 130 μl , respectively, a difference which is reflected in the considerably improved resolution of the peaks due to 3- and 4-chloroaniline, *viz.*, from 0.69–0.71 to 0.89. It is disappointing that the band broadening for the packed-bed reactor system is as high as that for the tubular

TABLE I

COMPARISON OF PERFORMANCES OF COILED-TUBULAR REACTOR, PACKED-BED REACTOR AND AIR-SEGMENTED SYSTEM

Reactor type	t_r (sec)	ϕ_{cell} ($\mu\text{l} \cdot \text{sec}^{-1}$)	σ_t (sec)	$\sigma_{v,tot}^2$ (μl^2)	R_s
Coiled tubular (1 capillary)	30	18	7.4	18,000	0.71
Packed-bed (15- μm glass beads)	41	18	7.4	18,000	0.69
Air-segmented	38	14.7	6.3	8600	0.89
UV signal	—	16	5.1	6700	1.14

t_r = Retention time; ϕ_{cell} = flow-rate through the flow-cell; R_s = resolution.

reactor system (which is at least partly due to the relative large variance contributions caused by the other parts of the HPLC system). Still, the experimental results agree satisfactorily with calculated band-broadening data ($\sigma_v = 125$, 115 and 100 μl for systems involving the tubular reactor, packed-bed reactor and segmented reactor, respectively). Obviously, also when using a system as complicated as the present post-column reaction system, our previous conclusions hold true, *i.e.*, segmentation is an experimentally sound principle to suppress band broadening even with relatively short reaction times.

Detection limits determined with the air-segmented reaction system were 30–40% better than those obtained with the tubular reactor. Such a relatively minor improvement is to be expected on the basis of the σ_t results quoted in Table I. An attempt to substitute liquid for air segmentation (with *n*-hexane as segmentation liquid) was only partly successful. Peak shapes were much the same in both instances; however, the signal of the Fluram derivative of 3-chloroaniline was seriously reduced, possibly owing to dissolution of the compound in hexane.

Mixing tees. In the literature, information on the proper construction of mixing tees, and especially on the contribution of these devices to band broadening, is rather scarce. A short study was therefore made using three different home-made tee-pieces (for constructional details, see Fig. 6), in which complete mixing was shown to occur by means of an indicator technique. Two further series of experiments were performed. In one, two purely aqueous streams were mixed; in another series, ac-

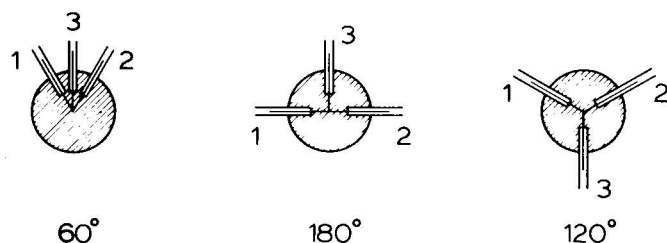


Fig. 6. Home-made stainless-steel tee-pieces tested (diameter, 2 cm). 1 = Eluent stream; 2 = reagent stream; 3 = to detector. Capillaries: 0.25 mm I.D. and 1/16 in. O.D.; channels: 0.25 mm I.D.

TABLE II

DEPENDENCE OF BAND BROADENING ($\sigma_{v,tee}$, μ l) OF VARIOUS TEE-PIECES ON FLOW-RATEConditions: water-water system with 20 μ l of sodium nitrate solution injected in the "eluent" stream; for tee-pieces, see Fig. 6.

Eluent flow-rate, ϕ_1 (ml/min)	Tee-piece	Reagent flow-rate, ϕ_2 (ml/min)			
		0.5	1.0	2.0	3.0
0.5	60°	28	44	66	90
	120°	26	36	65	83
	180°	26	38	64	84
1.0	60°	20	24	41	60
	120°	17	15	37	48
	180°	20	24	42	55
2.0	60°	21	22	31	40
	120°	16	18	26	32
	180°	19	22	31	40
3.0	60°	11	17	22	33
	120°	< 1	4	20	25
	180°	20	24	34	42

etonitrile-water (15:85) mixtures were mixed with pure acetonitrile. Measurements were performed by injecting 20 μ l of a sodium nitrate solution into the pure water and a *p*-aminobenzoic acid solution into the acetonitrile-water stream.

In order to calculate the variance contribution of the tee-piece, $\sigma_{v,tee}^2$, experimentally determined and/or calculated values of the variance contributions for the injector, connective tubing, coupling pieces and detector flow cell were subtracted from the total band broadening of the system, $\sigma_{v,tot}^2$. The results so obtained for the water-water system are shown in Table II. With the acetonitrile-water/acetonitrile system, the $\sigma_{v,tee}^2$ values showed the same trend, but they generally were up to 30 % lower than for the purely aqueous system.

From the data in Table II two main conclusions can be drawn. First, there appears to be little difference in performance between the three geometrical configurations tested. The 120° angle device gives slightly better results; however, one should consider that, for each configuration, only a single tee-piece was tested. Secondly, $\sigma_{v,tee}^2$ is seen to increase with increasing dilution of the mobile phase by the reagent stream (horizontal rows from left to right; vertical columns from bottom to top). This implies that, in practice, the use of a relatively low flow-rate of the reagent stream has to be recommended. As for an interpretation, one should realise that $\sigma_{v,tee}^2$ is made up from contributions due to (1) the dilution which inevitably occurs upon mixing and (2) band broadening inside the tee-piece itself. As regards the dilution effect, it seems reasonable to assume that, if the solute zone emerging from a HPLC column is n -fold diluted [$n = (\phi_1 + \phi_2)/\phi_1$; cf., Table II] by the addition of a reagent stream, the variance due to injection, $\sigma_{v,inj}^2 = V_{inj}^2/4$, will increase n^2 -fold. In other words, the variance contribution due to dilution, $\sigma_{v,dil}^2$, can be written as

$$\sigma_{v,dil}^2 = (n^2 - 1) V_{inj}^2/4 \quad (1)$$

Use of this equation allows the rapid calculation of $\sigma_{v,dil}^2$, and thus also of the actual contribution of the tee-piece, for any set of experimental (V_{inj} ; n) conditions. Using this procedure, we have calculated from the data in Table II that, except with impractical values of n greater than about 4, $\sigma_{v,tee}$ is largely (80–95 %) caused by band broadening inside the tee-piece, with a relatively minor (20–5 %) contribution due to dilution.

CONCLUSION

The potential of a post-column reactor for the fluorescent detection of chloroanilines after their derivatization with Fluram at low pH values (< 5) and short reaction times (30 sec) has been demonstrated. Hydrolysis of Fluram causes a relatively high fluorescence background; for optimal performance a pulseless reagent pump is therefore required. The use of the Fluram reactor instead of direct UV detection of the substituted anilines increases both the sensitivity and selectivity; the latter aspect has been demonstrated in a previous paper^{2,3} on the determination of the phenylurea herbicide diuron in soil samples.

The Fluram reaction has been used to compare three reactor designs, *viz.*, a tubular non-segmented, a tubular (air-)segmented and a packed-bed reactor. Even for the short reaction time mentioned above, the segmented system has been shown to give less band broadening and, thus, higher resolution. As for the miniaturized tee-pieces used in this work, their design does not appear to be very critical. Under normal operating conditions, their contribution to band broadening is mainly due to the tee-piece proper, with a minor contribution from dilution effects.

ACKNOWLEDGEMENTS

We thank Mr. H. Bruins for performing the batch experiments and Dr. H. Poppe of the University of Amsterdam for giving us the possibility of sieving the glass beads. Sandoz Ltd. (Basle, Switzerland) are thanked for partial financial support.

REFERENCES

- 1 G. Fuchsichler, *Thesis*, Technische Universität München, Munich, 1977.
- 2 D. E. Bradway and T. Shafik, *J. Chromatogr. Sci.*, 15 (1977) 322.
- 3 G. Voss, *Deutsche Forschungsgemeinschaft, Rückstandsanalytik von Pflanzenschutzmitteln*, Band II, Verlag Chemie, Weinheim, 1977, p. S6-1.
- 4 K. Ramsteiner, *Deutsche Forschungsgemeinschaft, Rückstandsanalytik von Pflanzenschutzmitteln*, Band II, Verlag Chemie, Weinheim, 1977, p. S6-A-1.
- 5 J. Sherma and G. Marzoni, *Amer. Lab.*, 6 (1974) 21.
- 6 A. M. Felix, V. Toome, S. De Bernardo and M. Weigle, *Arch. Biochem. Biophys.*, 168 (1975) 601.
- 7 H. Nakamura and Z. Tamura, *Anal. Chem.*, 52 (1980) 2087.
- 8 A. M. Felix and G. Tekelsen, *Arch. Biochem. Biophys.*, 157 (1973) 177.
- 9 C. J. Little, J. A. Whatley and A. D. Dale, *J. Chromatogr.*, 171 (1979) 63.
- 10 H. Veening, W. W. Pitt, Jr. and G. Jones, Jr., *J. Chromatogr.*, 90 (1974) 129.
- 11 R. W. Frei, L. Michel and W. Santi, *J. Chromatogr.*, 142 (1977) 261.
- 12 R. W. Frei, L. Michel and W. Santi, *J. Chromatogr.*, 126 (1976) 665.
- 13 J. V. Castell, M. Cervera and R. Marco, *Anal. Biochem.*, 99 (1979) 379.
- 14 E. Crombez, G. van der Weken, W. van den Bossche and P. de Moerloose, *J. Chromatogr.*, 177 (1979) 323.

- 15 B. Caddy and A. H. Stead, *Analyst (London)*, 103 (1978) 937.
- 16 J. Kusnir, V. Adamecova and K. Barna, *Arzneim.-Forsch.*, 28 (1978) 2058.
- 17 G. J. de Jong, *J. Chromatogr.*, 183 (1980) 203.
- 18 S. Udenfriend, S. Stein, P. Böhlen, W. Dairman, W. Leimgeber and M. Weigle, *Science*, 178 (1972) 871.
- 19 S. De Bernardo, M. Weigle, V. Toome, K. Nanhart, W. Leimgeber, P. Böhlen, S. Stein and S. Udenfriend, *Arch. Biochem. Biophys.*, 163 (1974) 390.
- 20 S. Stein, P. Böhlen and S. Udenfriend, *Arch. Biochem. Biophys.*, 163 (1974) 400.
- 21 B. A. Tomkins, V. H. Ostrum and C.-H. Ho, *Anal. Lett.*, 13 (1980) 589.
- 22 A. H. M. T. Scholten, U. A. Th. Brinkman and R. W. Frei, *J. Chromatogr.*, 205 (1981) 229.
- 23 A. H. M. T. Scholten, B. J. de Vos, J. F. Lawrence, U. A. Th. Brinkman and R. W. Frei, *Anal. Lett.*, 13 (1980) 1235.

CHROM. 14,258

THERMAL LENS CALORIMETRY APPLICATION TO CHROMATOGRAPHIC DETECTION

R. A. LEACH and J. M. HARRIS*

Department of Chemistry, University of Utah, Salt Lake City, UT 84112 (U.S.A.)

SUMMARY

The laser-induced thermal lens effect has been applied to the calorimetric detection of absorbing samples having negligible fluorescence quantum yields. A simple but fast method for numerically fitting the thermal lens transient data, during the 0.25-sec period while the sample cools, allows the instrument to serve as a real-time absorbance monitor. Preliminary results, using 190 mW laser power, indicate detection limits of $A_{\min} \approx 1.5 \cdot 10^{-5} \text{ cm}^{-1}$ for a 5-sec response time.

INTRODUCTION

The incorporation of laser sources into spectroscopic detectors for liquid chromatography¹⁻³ has produced improvements in limits of detection. While the most significant advances have been made in fluorescence detection due to the large excitation intensity of the laser, a similar advantage should exist for detecting samples having insignificant fluorescence quantum yields by a calorimetric absorbance measurement using a laser source. This concept was first proposed by Kreuzer⁴ for thermocouple calorimetry and first demonstrated by Oda and Sawada⁵ for laser-induced photoacoustic spectroscopy. In this work, we report the suitability of a related technique, thermal lens calorimetry⁶, for detection of liquid chromatographic eluents.

The thermal lens effect, first reported by Gordon *et al.*⁷, produces a time dependent divergence of a chopped laser beam due to the additional heat deposited in an absorbing sample at the center of a Gaussian laser beam profile, where the intensity is greatest. When the sample is located one confocal length beyond a waist in the beam, the strength of the thermal lens can be determined by the loss of intensity from the center of the beam measured by a detector having its field of view restricted by a pinhole. For a motionless sample, the intensity change is governed by thermal diffusion^{7,8}

$$I_{\text{bc}}(t) = I_{\text{bc}}(0) \left[1 + \frac{\theta}{1 + t_c/2t} + \frac{1}{2} \left(\frac{\theta}{1 + t_c/2t} \right)^2 \right]^{-1} \quad (1)$$

where θ is proportional to the absorbance of the sample, A

$$\begin{aligned}\theta &= -2.303 P (dn/dT) A / \lambda k \\ &= 2.303 EA\end{aligned}\quad (2)$$

where P is the laser power, (dn/dT) is the change in refractive index with temperature, λ is the laser wavelength and k is the thermal conductivity. It is convenient to group the terms which effect sensitivity into a constant, E , which is the enhancement of the linear response portion compared to Beer's law⁶. The time constant, t_c , depends on the radius of the laser beam in the sample, ω

$$t_c = \omega^2 \varrho C_p / 4k \quad (3)$$

where ϱ is the density and C_p is the heat capacity of the sample.

The modification of this theory, to account for the additional heat transport which occurs when the sample is flowing, has been recently studied⁹. For sufficiently slow flow-rates, the effect of mixing within the path of the laser beam can be modeled as a perturbation increase to the effective thermal conductivity. This allows the data to be fit to the thermal diffusion response, which is extremely beneficial in reducing the uncertainty of the measurement⁸, while E and t_c are somewhat smaller due to the increase in the effective value of k .

EXPERIMENTAL

The argon ion laser based, thermal lens calorimeter is shown in Fig. 1. The major construction details for the instrument have been previously published¹⁰. The laser beam, $\lambda = 458$ nm, $P = 190$ mW, is focused by a 33 cm focal length lens, L, through an electronic shutter, S, and an 18- μ l, 1 cm pathlength flow cell, C, obtained from Helma Cells, Inc. The beam propagates along a 5 m folded optical path to a Silicon Detector Corp., photovoltaic detector, D, which is constrained to view the center of the beam profile by a pinhole, P, having an aperture of 2.5 mm radius.

The laser calorimeter flow cell is connected in series directly to the outlet of a Beckman-Altex Model 153 UV-VIS detector equipped with a 470 ± 5 nm wavelength interference filter, which also monitors the eluent from the liquid chromatograph, Beckman-Altex Model 330. The column is ODS on 5- μ m silica support, 25 cm

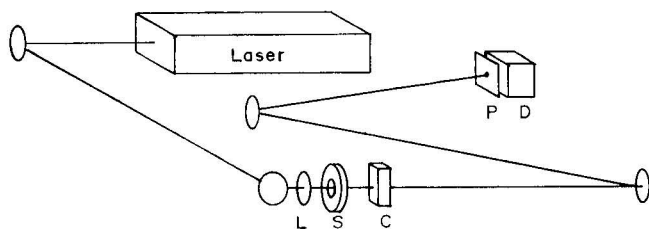


Fig. 1. Thermal lens calorimeter. L = 33 cm focal length lens; S = electronic shutter; C = flow cell; P = pinhole; D = photovoltaic detector.

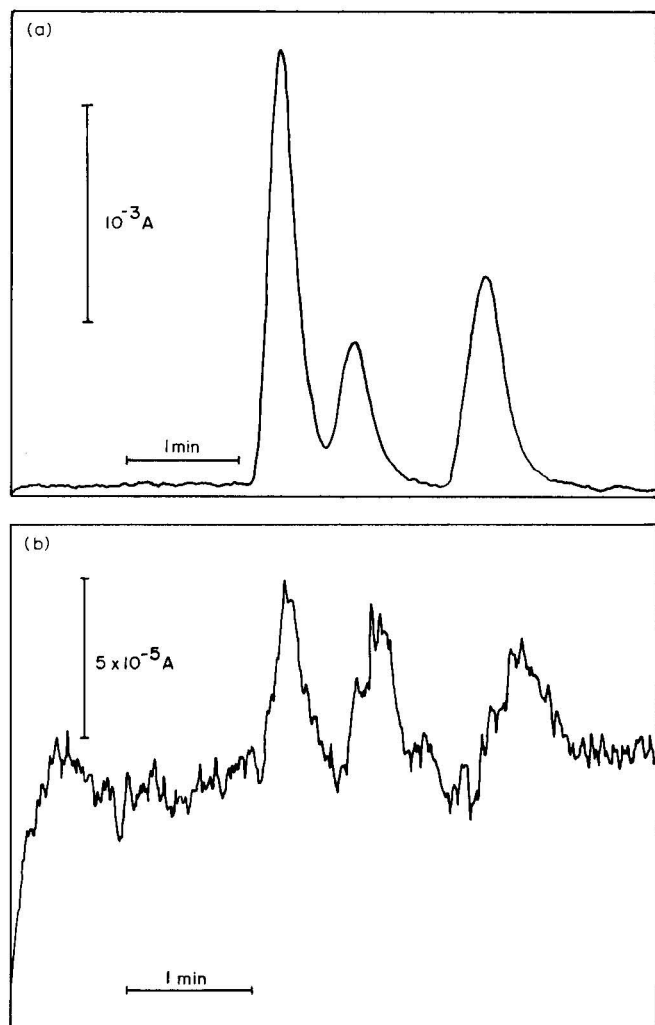


Fig. 2. Nitroaniline isomers detected by thermal lens calorimetry. Order of elution: *para*, *meta* and *ortho*. Amounts injected are: (a), 330, 210, 26 ng; (b), 6.6, 4.2, 0.53 ng. The initial rise on the left (b) is due to the moving average settling from an initial value of $\bar{\theta} = 0$.

$\times 4.6 \text{ mm}$, held at a temperature of 60°C ; the solvent is methanol–water (50:50), pumped at a rate of 1 ml/min . Standard solutions of the positional isomers of nitroaniline were prepared in methanol–water (50:50), and their absorbances at 458 nm are checked spectrophotometrically. Quantitative dilutions of these solutions were combined into mixtures to assess the performance of the instrument.

RESULTS AND DISCUSSION

A major challenge in application of thermal lens calorimetry to detection of transient samples is to have adequately short response time while maintaining the

many advantages⁸ of fitting the data to the kinetic response of eqn. 1. Although the time constant can be measured in advance for a particular beam size, solvent composition and flow-rate, there are still two independent parameters, $I_{bc}(o)$ and θ , which describe a given thermal lens transient. An optimum fitting procedure allows both parameters to be adjusted but requires, for a 100 point transient, about 1 min to converge running an efficient FORTRAN algorithm on a DEC LSI-11 microcomputer.

As a compromise between precision and speed, we choose to assign $I_{bc}(o)$ the value of the first data point in the thermal lens transient. This reduces the fit to a single parameter, θ , but adds a component of noise associated with the short-term fluctuations effecting the value of $I_{bc}(o)$. For an N point transient, each point, $I_{bc}(t > o)$, contributes to the average value of θ after applying a correction term which accounts for the time dependence, obtained by rearranging eqn. 1:

$$\theta = \frac{1}{N-1} \cdot \sum (1 + t_c/2t) \{ [2I_{bc}(o)/I_{bc}(t) - 1]^2 - 1 \} \quad (4)$$

For a 100 point transient, this weighted average can be determined in about 250 msec using the same microcomputer hardware, as above. This speed allows real-time monitoring of the sample absorbance on a sufficiently fast scale for LC detection.

To trade-off unnecessary speed for precision, a digital filter or moving average may be applied to the result of each transient, θ_i . For this study ten experiments were correlated to form an average, $\bar{\theta}_i$, by allowing an individual result, θ_i , only a 10% influence in changing the old value of the average, $\bar{\theta}_{i-1}$:

$$\bar{\theta}_i = 0.9 \bar{\theta}_{i-1} + 0.1 \theta_i \quad (5)$$

At the repetition rate of the experiment, 2.0 Hz, this provides a 5.0 sec response time (10–90%).

In order to determine the time constant, required to implement eqn. 4, and the enhancement, needed for interpreting absorbance information from θ , a solution diluted from stock of known absorbance is pumped through the flow cell using a syringe pump operated at rates which closely bracket the flow-rate for chromatography. For each flow-rate, 100 transients are averaged together and fit⁸ to the three parameters, $I_{bc}(o)$, θ and t_c . For the chromatographic conditions, methanol–water (50:50), 1.0 ml/min, the enhancement, $E = 120$, and time constant, $t_c = 28$ msec, are found by linear interpolation⁹.

These values are then used in a computer routine which gathers 100 point transients of 50 msec duration (2 kHz clock rate), fits the data according to eqns. 4 and 5, and plots $\bar{\theta}_i$, which requires ten transients to settle from the initial value of $\bar{\theta} = 0$. Preliminary results are obtained for the detection of substitutional isomers of nitroaniline, shown in Fig. 2. The peak absorbance values thus measured agree, within the error of measurement, with the values calculated from the known absorbance of the injected sample and the concentration profile of the peak. For the more concentrated runs, agreement was also observed with the commercial optical detector, corrected for the differences in molar absorptivities at the two different wavelengths. The limit of detection, which depends on particular solvent composition and

flow-rate as well as laser power, is determined from the fluctuations in the baseline to be $A_{\min} \approx 1.5 \cdot 10^{-5} \text{ cm}^{-1}$, in this case.

These preliminary results appear promising for future applications of the thermal lens effect to chromatographic detection. Further work to reduce the laser intensity fluctuations, the primary noise source, must be carried out in order to improve the detection capabilities. Since discrete wavelength, continuous wave, gas lasers (*e.g.*, He-Ne, Ar⁺, Kr⁺, CO₂, CO), which have the continuous power and spatial coherence required for thermal lens measurements, are uniquely simple to operate and are relatively inexpensive, their use in routine detection applications is plausible. Although their lack of continuous tunability precludes the generation of spectra, they should be quite suitable for single wavelength detection which could allow, for example, functional group monitoring in the infrared. In addition, detection of post-column reaction products in the near-UV and visible would transfer the specificity of the reaction to a detector which is very sensitive, but otherwise only semi-selective.

ACKNOWLEDGEMENTS

The assistance of S. K. Loh in developing the chromatographic procedure is acknowledged. This material is based upon work supported by the National Science Foundation under Grant CHE79-13177.

REFERENCES

- 1 N. K. Freeman, F. T. Upham and A. A. Windsor, *Anal. Lett.*, 6 (1973) 943.
- 2 G. J. Deibold and R. N. Zare, *Science*, 196 (1977) 1439.
- 3 E. S. Yeung, L. E. Steenhock, S. D. Woodruff and J. C. Kuo, *Anal. Chem.*, 52 (1980) 1399.
- 4 L. B. Kreuzer, *U.S. Pat.*, 4,048,499 (1977).
- 5 S. Oda and T. Sawada, *Anal. Chem.*, 53 (1981) 471.
- 6 J. M. Harris and N. J. Dovichi, *Anal. Chem.*, 52 (1980) 695A.
- 7 J. P. Gordon, R. C. C. Leite, R. S. Moore, S. P. S. Porto and J. R. Whinnery, *J. Appl. Phys.*, 36 (1965) 3.
- 8 N. J. Dovichi and J. M. Harris, *Anal. Chem.*, 53 (1981) 106.
- 9 N. J. Dovichi and J. M. Harris, *Anal. Chem.*, 53 (1981) 689.
- 10 N. J. Dovichi and J. M. Harris, *Anal. Chem.*, 52 (1980) 2338.

CHROM 14,095

MIDDLE MOLECULE MASS SPECTROMETRY (A REVIEW)

CATHERINE FENSELAU, ROBERT COTTER, GORDON HANSEN, TOM CHEN and DAVID HELLER

The Johns Hopkins University School of Medicine, Department of Pharmacology and Experimental Therapeutics, 725 North Wolfe Street, Baltimore, MD 21205 (U.S.A.)

SUMMARY

This paper reviews some recent advances in the application of mass spectrometry to the analysis of middle molecules in the mass range of 1000 to 10,000 daltons, and of very polar molecules (organic salts). The quantitative analysis of components of mixtures will be illustrated, carried out by creating a spectrum which consists primarily of molecular ion species whose relative intensities correspond to the relative molar concentrations of the various components.

In the analyses of heavy and/or polar substances, four components of the mass spectrometer must all be considered: the inlet system, ionization method, ion analyser and ion detector. Reading the spectrum also requires some special considerations, as will be seen later. Among the inlet systems, the direct probe and liquid chromatography (LC) are suitable for middle molecules or for organic salts. Suitable detectors can presently be constructed to detect ions of any size, relying, if necessary, on post acceleration or on smashing the large ions into smaller ones after separation in the analyser. All three of the most commonly used kinds of analyzers (magnetic, quadrupole and time-of-flight) have been shown to transmit ions of masses in excess of 5000 daltons; however, only magnetic analyzers can do so with unit resolution. Currently, the limiting factor in the extension of mass spectrometry (MS) to analysis of middle molecules is ionization. No ionization technique has as yet gained complete acceptance as a reliable, versatile and efficient technique for middle molecules and organic salts.

As a brief history of middle molecule MS, four spectra may be mentioned. In 1966, Fales¹ published the electron impact mass spectrum of a tetrameric phosphazene of molecular weight 3628. The spectrum was obtained using a magnetic analyzer and unit resolution was achieved in the molecular ion region. The spectrum of a set of cluster ions of isopropyl alcohol formed in a high-pressure source and transmitted through a quadrupole analyzer has been measured by Beuhler and Friedman^{2,3}. While the resolution is low, the clusters sixty units apart in mass may be distinguished above 8000 daltons. The spectrum of a mixture of polystyrene polymers of average mass 8500 has been published by Japanese workers⁴. This spectrum was obtained by field desorption with resolution of about 2000 using a toroidal magnetic analyzer. Ions are formed, transmitted, and detected above 10,000 daltons.

The fourth spectrum to be mentioned in this short history is that of an oligodeoxyribonucleotide containing derivatized phosphotriesters. A peak at m/z 6301 corresponds to $(M + Na)^+$ ions and one at 12637 is proposed as a cationized dimer⁵. The spectrum was measured on a time-of-flight analyzer using Cf.252 plasma desorption as the ionization technique. Although the resolution of this analyzer is below 1000, centroids of the broad peaks are calculated by computer and related to average masses⁵.

Thus it seems that ions in the middle mass range can be analyzed by MS. However this kind of work is not yet done routinely, and one of the main reasons is the difficulty of forming ions of heavy or polar, *i.e.* involatile, substances.

Two transformations are required initially for mass spectral analysis. Each molecule must be put into gas phase and each molecule must be ionized. The older ionization techniques for organic samples, electron impact and chemical ionization, require that vaporization precede ionization. Thus they are well suited for coupled gas chromatography-MS.

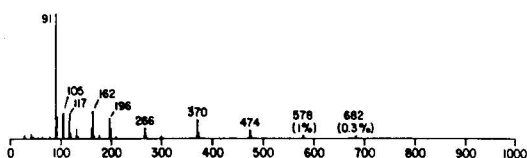
Some inroads have been made into the middle molecule mass range using electron impact or chemical ionization. The spectrum of phosphazene molecular weight 3628 mentioned above provides an early example. A most influential paper from Gif-sur-Yvette⁶ reported not only the molecular weight of the nonapeptide fortuitin, but also electron-impact induced fragmentation which permitted the sequence of the peptide to be deduced. Eventually it was realized that this analysis of fortuitin was made possible because the compound was naturally derivatized. The terminal amine occurred as the amide of a long chain acyl group, and three of the nine amides in the peptide were themselves alkylated. By these means intermolecular hydrogen bonding is sufficiently reduced as to permit the vaporization required for mass spectral analysis. Derivatization has also permitted analysis of important polysaccharides in the middle molecule mass range by electron impact (permethylation)⁷ and chemical ionization⁸.

However, derivatization is not always desirable, and even with derivatization many molecules can not be vaporized without pyrolysis. To paraphrase Fales⁹, the more important a compound is, the less likely it is to produce a molecular ion. Consequently considerable energy has, in recent years, gone into the development of new techniques to produce desorption and ionization of samples in the solid phase. These include field desorption, laser desorption, fast atom bombardment, and fast ion bombardment or plasma desorption. Work will be reviewed here from the Middle Atlantic Mass Spectrometry laboratory (an NSF Regional Instrumentation Facility) in which two of these techniques are evaluated, field desorption and fast atom bombardment (FAB). Emphasis is placed on analysis of middle molecules, organic salts and mixtures.

Fig. 1 (ref. 10) compares the electron impact mass spectrum and the field desorption mass spectrum of a mixture of soluble polystyrene oligomers of average molecular weight 1020, and dramatically makes the point that a solid phase ionization technique enhances the production of molecular ions and reduces pyrolysis. Lattimer *et al.*¹¹ have shown that the relative abundances of molecular ions, produced by careful field desorption of a number of oligomer mixtures of average mass above 1000, can be directly related to the relative molarities of the components of the mixture as measured by vapor pressure osmometry, gel permeation, or LC. In Fig. 2

the distribution measured by high-performance liquid chromatography (HPLC) of oligomers in a polystyrene mixture may be compared with the distribution measured by field desorption. The number average molecular weight was 811 measured by vapor pressure osmometry, 855 by LC, and 928 by field desorption MS¹¹. The molecular ion distribution of a heavier polystyrene mixture is shown in Fig. 3. The number average molecular weight determined by MS was 2900 as compared with 3100 by vapor pressure osmometry¹¹. These mass measurements were made on a Kratos MS-50 mass spectrometer with a special 23K gauss magnet and a Daly detector. Several scans were averaged and corrections were made for the multiplicity of molecular ions resulting from isotope abundances in these heavy hydrocarbons. This approach works best if little fragmentation or pyrolysis occur, and if there is little instrumental discrimination through the mass range.

a. EI 70eV,



b. FD (16mA)

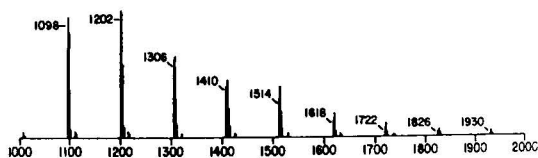
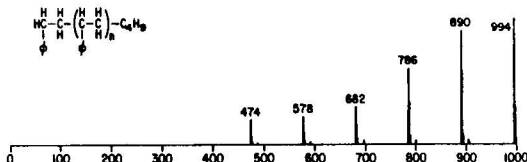


Fig. 1. Electron impact and field desorption mass spectra of a polystyrene mixture of number average mass 1020. (Reprinted with permission from ref. 10, copyright 1979 American Chemical Society.)

Lattimer and Hansen¹² have also shown that polyglycol oligomers (polyethylene glycol, polypropylene glycol and polytetrahydrofuran) can be assessed by field desorption using the high field magnet. In the cases of these more polar polymers abundances of $(M + H)$ or $(M + Na)$ ions were measured.

The need for corrections for multiplicity of molecular ions due to isotope abundances leads to an interesting point. The abundances of molecular species containing ^{13}C become significant in these hydrocarbon middle molecules, and the mass defect of hydrogen (and other atoms) can contribute significantly to the molecular weights observed. Thus while the nominal molecular weight for polystyrene $n = 33$, $C_{276}H_{282}$ is 3594, based on the convention that $C = 12$ daltons and $H = 1$, actually $H = 1.0078$ and $282 \times 1.0078 = 284.2$ daltons. In working with middle molecules we define the monoisotopic mass as the molecular weight calculated from the most abundant isotope of each atom present in the molecule, in this case $C = 12.000$ and $H = 1.0078$. Consequently, the monoisotopic mass for polystyrene $n = 33$ is 3596.2

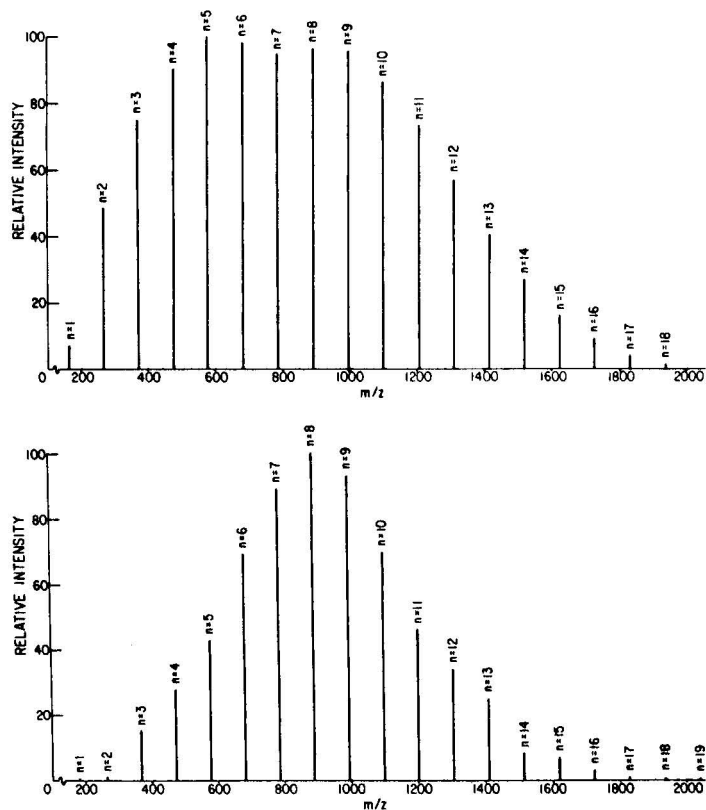


Fig. 2. Distribution of oligomers determined in a polystyrene mixture by field desorption-MS (bottom) and HPLC (top)¹¹.

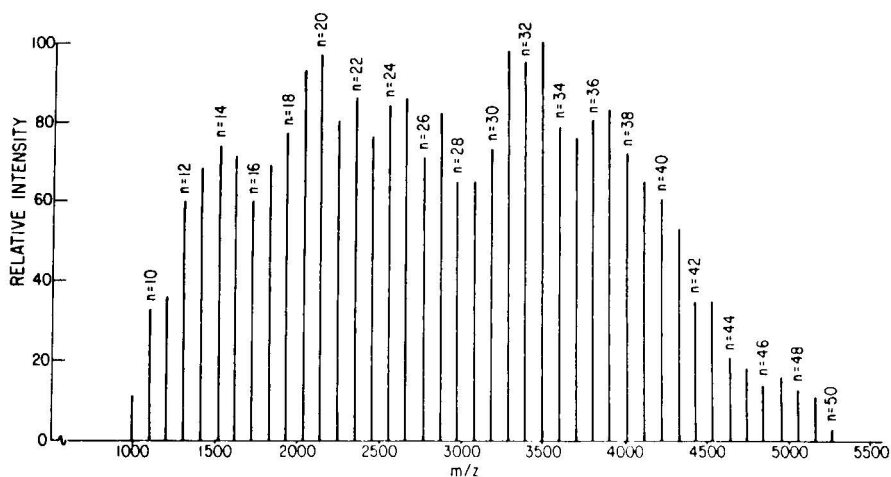
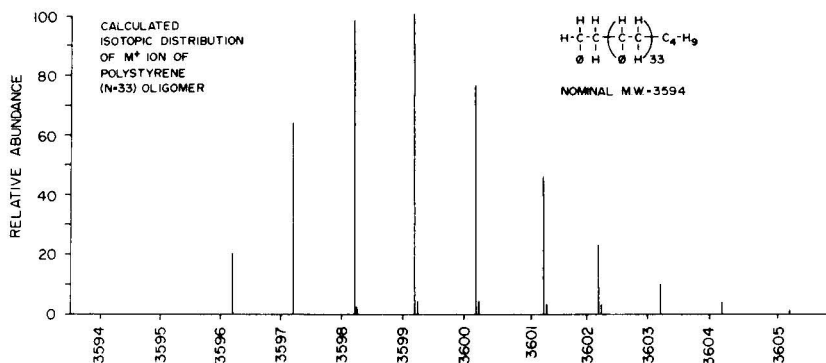


Fig. 3. Distribution of oligomers in a polystyrene mixture of number average mass 2900 determined by field desorption-MS.



daltons. However, this is not the mass of the most abundant molecular ion. The abundance of ^{13}C is about 1.1 % for each atom of carbon in the molecule. If the abundance of monoisotopic ions is set as equal to 100 %, the relative abundance for $^{13}\text{C}_3$, $^{12}\text{C}_{275}$, $\text{H}_{282} = 315$ %, and the most abundant ions (487 %) in the molecular ion group will be $^{13}\text{C}_3$, $^{12}\text{C}_{273}$, H_{282} . The theoretical distribution of the molecular ions for polystyrene $n = 33$ is shown in Fig. 4, generated by computer and including consideration of ^2H abundances as well. The high mass end of the field desorption spectrum of trehalose octapalmitate synthesized in the MAMS laboratory is presented in Fig. 5. Here again the multiplicity of molecular ions is visible and the monoisotopic mass is indicated.

The intermittent nature of the ion flux produced by field desorption and the resultant inadequacies in ion statistics have been remarked by many workers. We illustrate the problem and our solution in Figs. 6 and 7. A single scan of the molecular ion region of polystyrene $n = 33$ is shown in Fig. 6, and a spectrum of this region compiled from 10 scans recorded and added on a multi-channel analyzer is shown in

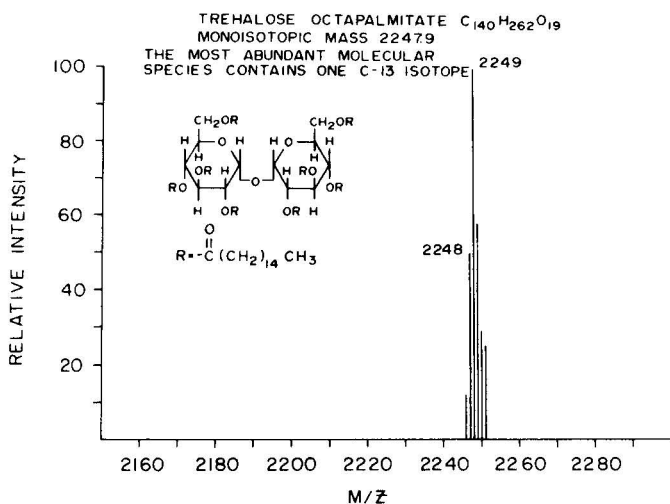


Fig. 7. The signal-to-noise ratio is much improved in the latter, and the relative intensities correspond well to the theoretical distribution in Fig. 4. A similar set of distributions is shown in Fig. 8 for the molecule hexapus synthesized by F. Menger at Emory University. Again the single scan is visibly aberrant, while the averaged spectrum matches the theoretical distribution more closely.

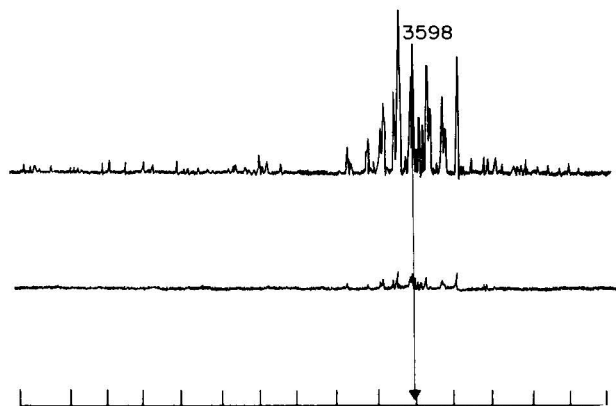


Fig. 6. A single field desorption scan of the molecular ion region of polystyrene $n = 33$. Resolution, *ca.* 4000.

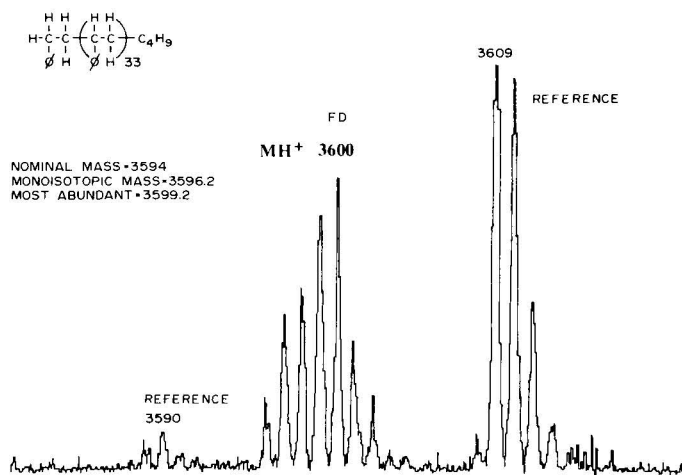


Fig. 7. Spectrum accumulated from 10 scans by multichannel analyzer.

We conclude that field desorption is a useful technique for analysis of some middle molecules. We have found it difficult, however, to obtain accurate molecular ion distributions of some more polar polymers. Thus we are currently evaluating a complementary solid phase ionization technique, called by its developers¹³ Fast Atom Bombardment (FAB). The partial spectra in Fig. 9 and 10 indicate that middle molecules may be analyzed by FAB, as either positive or negative ions. In addition to the molecular ion species presented here, fragment ions are observed in the spectra of both neurotensin and γ -cyclodextrin. It should be pointed out that neurotensin con-

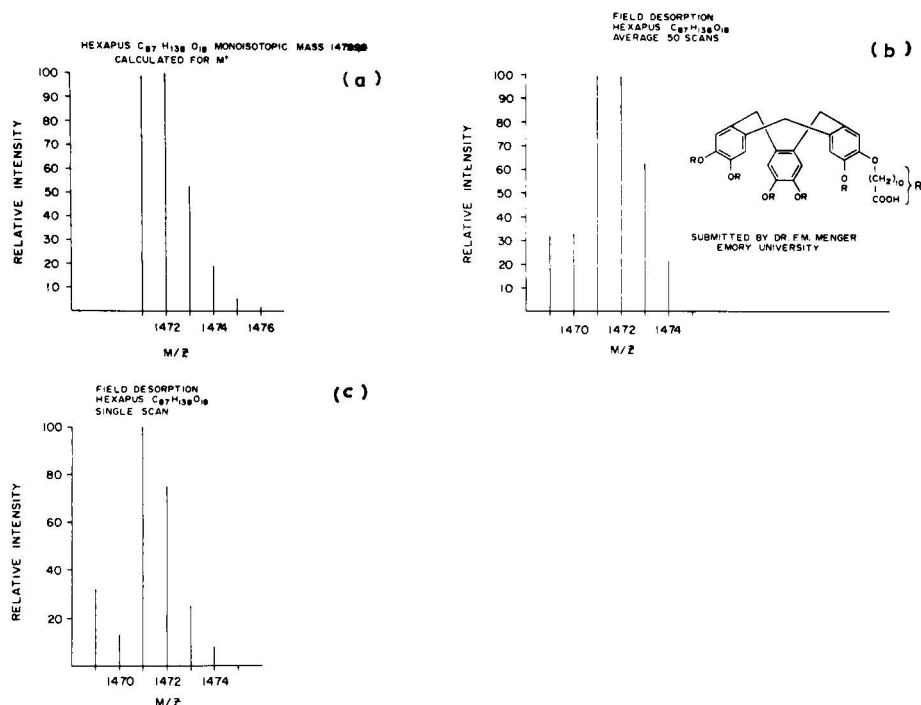


Fig. 8. Partial field desorption spectrum of hexapus, synthesized by F. Menger at Emory University. (a), Calculated; (b), averaged; (c), single scan.

tains two polar arginine residues in addition to one asparagine. FAB exhibits many of the characteristics of thermal desorption^{14,15}, including the fact that preformed ions, *i.e.* organic salts, are readily analyzed. An interesting example is the dimer of guanosine monophosphate crosslinked by the alkylating metabolite of cyclophosphamide, phosphoramidate mustard¹⁶. Isolated by LC, this compound contains two quaternary ammonium cations and two potentially ionized phosphate groups. Yet it is readily

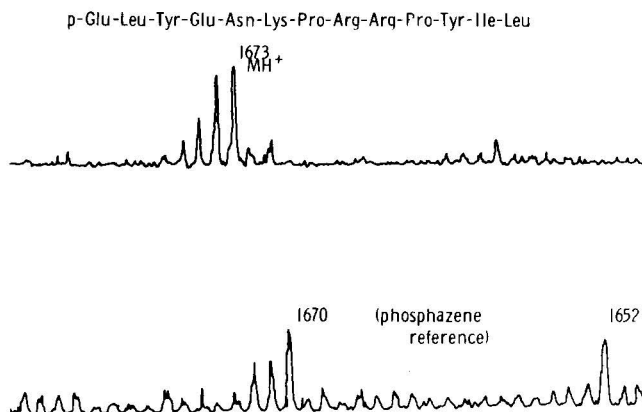


Fig. 9. Molecular ion region of the positive ion FAB mass spectrum of neurotensin.

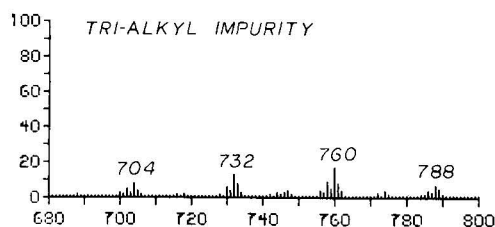
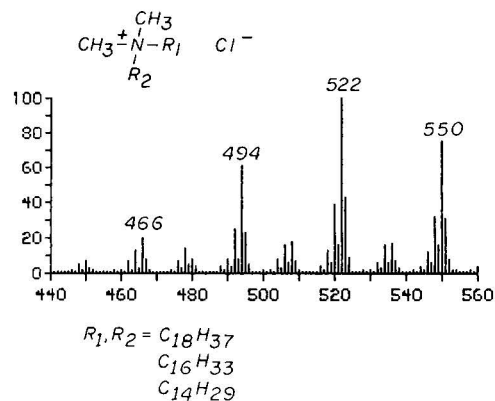


Fig. 12. Molecular ion region of the FAB spectrum of a mixture of surface active quaternary amines¹⁷.

In this case FAB allows a value of 10% to be calculated while HPLC gives a value of 7.7% (ref. 17).

An example of the analysis of biovariability by FAB is presented in Fig. 13, where the array of molecular ion species of bovine sphingomyelin is visible¹⁸. This compound also contains a quaternary ammonium center and a polar phosphate group.

We suggest that FAB as well as field desorption has good potential for the analysis of mixtures based on the principle of generating an array of molecular ion species whose relative abundances correspond to the molarities of different species in the mixture.

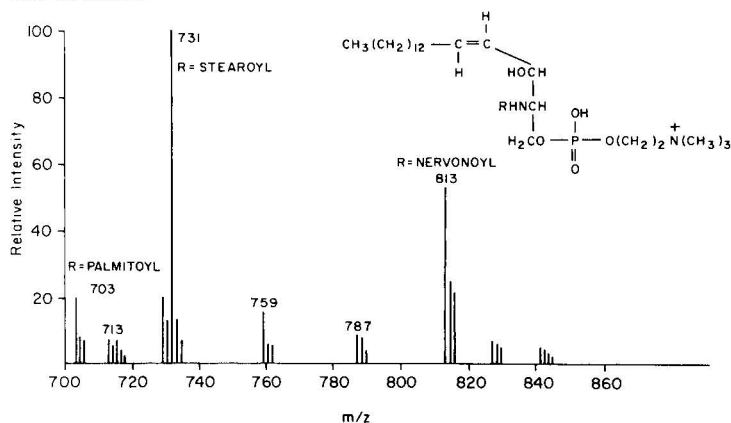


Fig. 13. Molecular ion region of the FAB spectrum of bovine sphingomyelin.

The FAB spectra shown here were measured with the Kratos FAB source on the MS-50 with the 23K gauss magnet.

Advances made in many laboratories in recent years in ionization methods for MS have brought many compounds within analytical reach which cannot be chromatographed in hot gas phase systems. If these compounds are to enjoy the considerable advantage of analysis by combined chromatography-MS, the chromatography must be in the liquid phase.

Among the solid phase ionization techniques proven for polar molecules and/or middle molecules, field desorption is unique in its incompatibility for use in on-line LC-MS. On-line coupling of plasma desorption (fast ion bombardment)¹⁹, secondary ion MS²⁰, laser desorption and FAB are underway in a variety of laboratories. The thermospray method used by Blakeley *et al.*²¹ for on-line LC-MS should be included as a proven technique.

ACKNOWLEDGEMENTS

This research was supported by Grant CHE-78-18396 from the National Science Foundation and was carried out at the Middle Atlantic Mass Spectrometry Laboratory, an NSF Regional Instrumentation Facility.

REFERENCES

- 1 H. Fales, *Anal. Chem.*, 38 (1966) 1058.
- 2 R. J. Beuhler and L. Friedman, private communication.
- 3 R. J. Beuhler and L. Friedman, *Nuclear Instruments Methods*, 170 (1980) 309.
- 4 T. Matsuo, H. Matsuda and I. Katakuse, *Anal. Chem.*, 51 (1979) 1329.
- 5 C. J. McNeal and R. D. MacFarlane, *J. Amer. Chem. Soc.*, 103 (1981) 1609.
- 6 M. Barbier, P. Jolles, E. Vilkas and E. Lederer, *Biochem. Biophys. Res. Commun.*, 18 (1965) 469.
- 7 K.-A. Karlsson, *Biochemistry*, 13 (1974) 3643.
- 8 R. Dougherty, J. D. Roberts, W. W. Binkley, O. S. Chizhov, V. I. Kadentsev and A. A. Solovyov, *J. Org. Chem.*, 39 (1974) 451.
- 9 C. Fenselau, in T. Kuwana (Editor), *Physical Methods in Modern Chemical Analysis*, Vol. 1, Academic Press, 1978, p. 103.
- 10 R. P. Lattimer, D. J. Harmon and K. R. Welch, *Anal. Chem.*, 51 (1979) 1293.
- 11 R. P. Lattimer, D. J. Harmon and G. E. Hansen, *Anal. Chem.*, 52 (1980) 1808.
- 12 R. Lattimer and G. Hansen, *Macromolecules*, 14 (1980) 776.
- 13 M. Barber, R. S. Bordoli, R. D. Sedgwick and A. N. Tyler, *J.C.S. Chem. Comm.*, (1981) 325.
- 14 R. J. Cotter and A. L. Yergey, *J. Amer. Chem. Soc.*, 103 (1981) 1596.
- 15 R. J. Cotter and A. L. Yergey, *Anal. Chem.*, 53 (1981) 1306.
- 16 V. Vu and C. Fenselau, *J. Amer. Chem. Soc.*, in press.
- 17 R. J. Cotter and T. R. Jones, submitted for publication.
- 18 C. Fenselau, T. Chen and Y. Kishimoto, submitted for publication.
- 19 H. Jungclas, H. Danigel and R. Schmidt, *Anal. Chem.*, in press.
- 20 A. Benninghoven, A. Eicke, M. Junack, W. Sichtermann, J. Krizek and H. Peters, *Org. Mass Spectrom.*, 15 (1980) 459.
- 21 C. R. Blakeley, J. J. Carmody and M. L. Vestal, *Anal. Chem.*, 52 (1980) 1636.

CHROM. 14,073

REVERSED-PHASE ION-PAIR CHROMATOGRAPHY WITH UV-ABSORBING IONS IN THE MOBILE PHASE

M. DENKERT, L. HACKZELL, G. SCHILL* and E. SJÖGREN

Department of Analytical Pharmaceutical Chemistry, Biomedical Center, University of Uppsala, Box 574, S-751 23 Uppsala (Sweden)

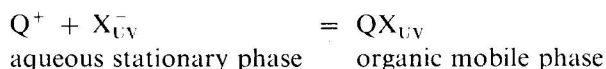
SUMMARY

Reversed-phase systems have been developed that permit the detection and quantification of down to 0.1 nmole of non-UV-absorbing cations and anions using a UV detector. The samples give positive or negative peaks depending on their charge and retention relative to the UV-absorbing ionic component in the mobile phase. The relative detector response has a maximum, which can be considerably more than 100 %, when the sample and the UV-absorbing mobile phase ion have about the same retention. Detection and separation studies on, *e.g.*, sulphonates, sulphates, carboxylates, amino acids, dipéptides and alkylammonium compounds of different degrees of substitution are described.

INTRODUCTION

In ion-pair chromatography it is usual to regulate the retention and separation selectivity for the ionic samples by changing of the nature and the concentration of the counter ion. The counter ion can, however, have a double function in these systems and it can also be used to improve the detection possibilities to a considerable extent. The technique has so far mainly been utilized on photometric detectors, where the ion-pair chromatographic principle offers excellent possibilities of a high detector response even for non-UV-absorbing compounds by using a counter ion of high molar absorptivity at the measuring wavelength.

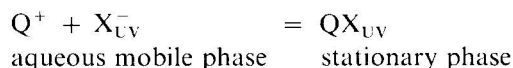
The principle was applied initially to liquid-liquid straight-phase systems, where the connection to ion-pair extraction by the batch technique is striking. The UV-absorbing counter ion (X_{UV}^-) is applied in solution on a hydrophilic solid phase. A non-UV-absorbing sample with the opposite charge (Q^+) will migrate with the organic mobile phase as an ion pair which, owing to the high absorptivity of the counter ion, will have a high UV absorbance:



The technique was first used in low-pressure systems¹⁻⁴ but its usefulness in

high-performance systems has been demonstrated in several recent publications⁵⁻¹⁰.

The ion-pair principle can, however, also be applied in reversed-phase systems with a hydrophobic adsorbent as the stationary phase. The sample is distributed to the adsorbent which, owing to the prerequisite for electroneutrality in the phases, might give rise to changes in the concentration of the UV-absorbing counter ion in the mobile phase. The basic principle can be illustrated by



Parris^{11,12} used diisobutylethoxyethyltrimethylbenzylammonium and aromatic sulphonates as UV-absorbing counter ions in the aqueous mobile phase in chromatographic separations of bile acids and ionic surfactants. Improvements in detection by using UV-absorbing counter ions in reversed-phase systems have also been obtained by Bidlingmeyer and co-workers^{13,14}, with phenethylammonium and cetylpyridinium as counter ions and alkylsulphonates as samples.

Our studies on reversed-phase ion-pair chromatographic systems with a UV-absorbing counter ion in the mobile phase have shown that they can be highly suitable for the detection of non-UV-absorbing anions and cations of widely different kinds. The samples give rise to positive or negative peaks depending on their charge and retention and both positive and negative peaks are well suited for quantification. The response depends basically on the molar absorptivity of the counter ion, but it can be changed by varying the composition of the chromatographic systems and it is even possible to limit the response to certain groups of compounds.

This paper describes studies of the influence of the mobile phase composition on the response for cationic and anionic compounds of different kinds using one cation, 1-phenethyl-2-picolinium, and one anion, naphthalene-2-sulphonate, as UV-absorbing components and a moderately hydrophobic adsorbent, μ Bondapak Phenyl, as stationary phase.

EXPERIMENTAL

Apparatus

The detectors were an LDC UV-III-Monitor and an LDC Spectromonitor III. The pumps were a Gynkotek 600/200 and an Altex 100 A. Rheodyne 70-10 and 71-25 injectors with loop volumes of 25.2 and 15.5 μ l, respectively, were used.

The columns (100 \times 3.2 mm I.D.) were made of stainless steel with a polished inner surface, equipped with modified Swagelok connectors and Altex 250-21 filters.

The pH measurements were made with an Orion Research Model 801 instrument with Ingold Type 401 combined electrode. The spectrophotometric measurements were made with a Zeiss PMQ II Spektralphotometer.

Chemicals and reagents

Sodium naphthalene-2-sulphonate was obtained from Eastman-Kodak (Rochester, NY, U.S.A.) and was recrystallized from water before use. 1-Phenethyl-2-picolinium bromide (Eastman-Kodak) was converted into the hydroxide by use of an

ion exchanger in the hydroxide form and freed from UV-absorbing impurities by repeated extractions with methylene chloride.

All other chemicals were of analytical-reagent grade.

Chromatographic system

μ Bondapak Phenyl (10 μ m) (Waters Assoc., Milford, MA, U.S.A.) was used as packing. The mobile phases were aqueous solutions of naphthalene-2-sulphonate or 1-phenethyl-2-picolinium, which usually also contained buffering compounds or other salts.

Column preparation

The columns were packed by a slurry technique using water-ethanol (58:42) as the suspending medium. They were washed with 200 ml of water-methanol (1:4) before use. Column testing was carried out with water-methanol (2:3) as mobile phase and toluene and mesitylene as retained samples, giving capacity ratios (k') of about 1 and 4 respectively. Columns that gave reduced plate heights of less than 10 were accepted.

Chromatographic technique

The eluent reservoir, injector, column and connecting tubes were thermostated at $25.0 \pm 0.1^\circ\text{C}$ in a water-bath. Detection was effected at 254 nm.

The mobile phase flow-rate was 0.50 ml/min. Equilibrium was obtained after passage of 30–50 ml of mobile phase. No recirculation of mobile phase was used. The samples were injected dissolved in the mobile phase, if not stated otherwise. The volume of mobile phase in the column, V_m , was obtained from the front peak of the chromatogram. Peak areas were determined by planimetry.

RESULTS AND DISCUSSION

The basic reversed-phase chromatographic studies were performed with alkylsulphates, alkylsulphonates, alkylcarboxylates and alkylammonium ions of different degrees of substitution. The only UV-absorbing components were the counter ions, naphthalene-2-sulphonate (NS) or 1-phenethyl-2-picolinium (PEP), and the observed chromatographic peaks were due to changes in the concentration of the counter ions.

Injections of ionized samples in systems of this kind gives rise to two kinds of migrating zones: one for each of the ionized components in the sample and one zone that is typical of the chromatographic system (the system zone). If the sample ion and the UV-absorbing ion have opposite charges, the first peak in the chromatogram is negative, and it can be given by the sample or by the system zone, whichever comes first. The sums of the areas of the positive and the negative peaks are equal. The system peak always has the same capacity ratio, whether it is negative or positive. It is also easy to recognize: injection of mobile phase containing an excess or a deficiency of the counter ion gives a positive or negative peak at the k' of the system peak.

Injection of a sample with the same charge as the UV-absorbing ion in the mobile phase also gives a chromatogram with a sample peak and a system peak, but the direction of the peaks is reversed. The first peak is positive and the second is negative.

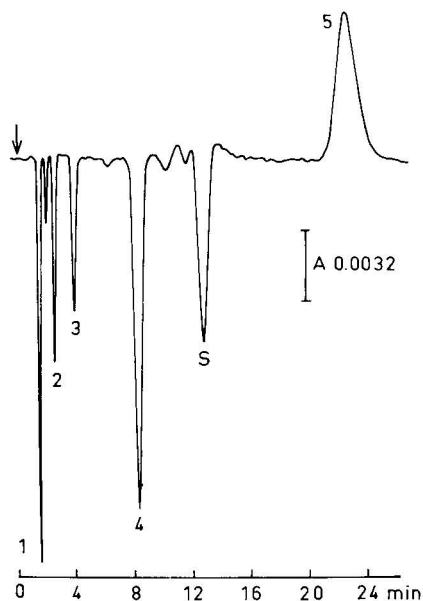


Fig. 1. Carboxylic acids in a system with PEP as UV-absorbing ion. Mobile phase: 1-phenethyl-2-picolinium (PEP), $3 \cdot 10^{-4}$ M in acetate buffer (pH 4.6). Solid phase: μ Bondapak Phenyl. Sample: 1 = acetic acid; 2 = propionic acid; 3 = butyric acid; 4 = valeric acid; 5 = caproic acid (12 nmole of each). S = system peak.

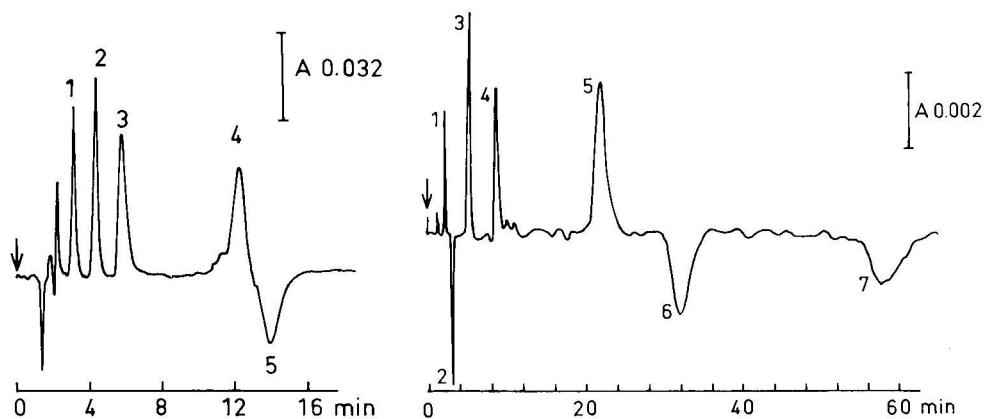


Fig. 2. Quaternary ammonium ions in a system with PEP as UV-absorbing ion. System as in Fig. 1. Sample: 1 = trimethylphenylammonium; 2 = trimethylbenzylammonium; 3 = methyltripropylammonium; 4 = tetrapropylammonium (1.5 nmole of each); 5 = system peak.

Fig. 3. Anionic and cationic compounds with NS as UV-absorbing ion. Mobile phase: naphthalene-2-sulphonate (NS), $4 \cdot 10^{-4}$ M in 0.05 M phosphoric acid. Solid phase: μ Bondapak Phenyl. Sample: 1 = butyl sulphate; 2 = pentylamine; 3 = hexanesulphonate; 4 = system peak; 5 = heptylamine; 6 = octanesulphonate; 7 = octyl sulphate.

It has been verified that the total amount of an injected compound is eluted in the sample peak. The tests were made with compounds with inherent UV absorbance in other wavelength regions than that of the counter ion and measurement of peak areas at the wavelength specific for the sample.

A typical chromatogram is given in Fig. 1, which shows the separation of carboxylates with 1–5 alkyl carbon atoms in a system with the cationic PEP as counter ion. The separation factor is about 3 per alkyl carbon atom. The same system can also be used for quaternary ammonium ions but the number of carbon atoms in this case must be higher, 9–12 (Fig. 2).

Fig. 3 shows the separation of a mixture of anionic and cationic compounds, two alkylamines, two alkylsulphates and two alkylsulphonates, with the anionic NS as the UV-absorbing component. The separation factors in this case are also 2.5–3 per alkyl carbon atom. The direction of the peaks follows the general principle, without exception. The anionic samples give positive peaks when they appear before the sample peak (butyl sulphate, hexanesulphonate) and negative after (octanesulphonate, octyl sulphate). The cations are negative before (pentylamine) and positive after (heptylamine) the system peak.

This NS system has pH 2 and some amino acids and dipeptides have acidities such that they are ionized and can be detected at that pH. Some examples are shown in Figs. 4 and 5.

Substances with inherent UV absorbance should, if possible, be chromatographed in systems where they give positive peaks, as inherent UV absorbance decreases the height of a negative peak. An example is given in Fig. 6. Tyrosine and phenylalanine, with low molar absorptivities, give negative peaks, whereas DOPA, with a considerably higher molar absorptivity, gives a positive peak.

In the above cases, the sample was dissolved in the mobile phase. Dissolution of the sample in water does not seem to affect the sample peak, as demonstrated in Fig. 7. The main difference from the previous systems is that the system peak is strongly

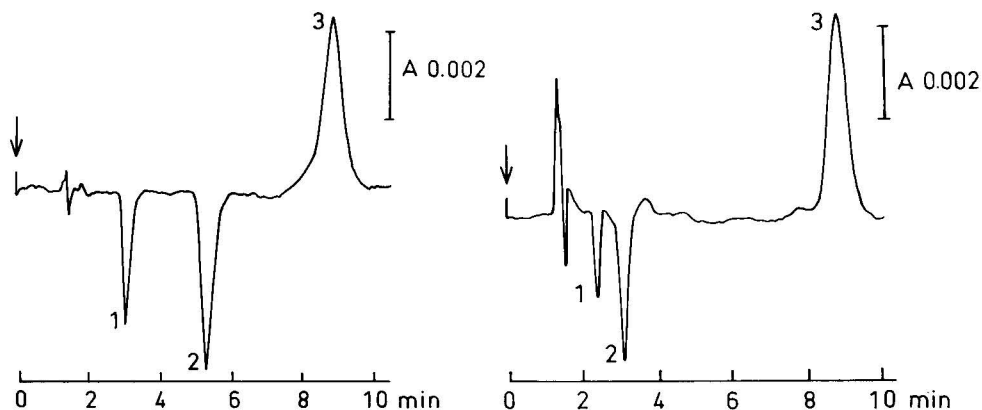


Fig. 4. Amino acids with NS as UV-absorbing ion. System as in Fig. 3. Sample: 1 = norleucine (2 nmole); 2 = phenylalanine (0.8 nmole); 3 = system peak.

Fig. 5. Dipeptides with NS as UV-absorbing ion. System as in Fig. 3. Sample: 1 = leucylserine; 2 = leucylalanine; 3 = system peak.

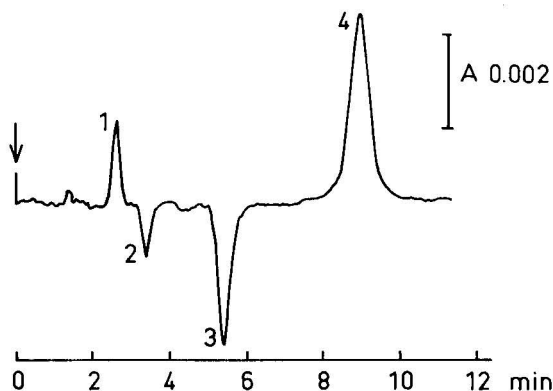


Fig. 6. Amino acids with NS as UV-absorbing ion. System as in Fig. 3. Sample: 1 = DOPA (1.3 nmole); 2 = tyrosine (0.7 nmole); 3 = phenylalanine (0.6 nmole); 4 = system peak.

negative, exactly as when pure water is injected. Some extra front peaks are also obtained.

Retention model

Negative peaks are used for detection purposes in "vacancy chromatography"¹⁵, in which the mobile phase contains a series of detectable compounds at constant concentration. On injection of a sample, negative or positive peaks can be obtained depending on whether the sample contains these components at lower and higher concentration than the mobile phase. Scott *et al.*¹⁶ used this principle for detection of nucleic acid bases separated by cation exchangers.

Šlais and Krejčí¹⁷ used a different technique for the detection of organic sol-

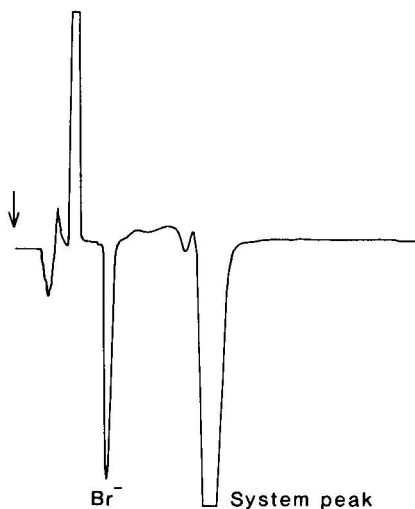


Fig. 7. Sample dissolved in water. Mobile phase: $3 \cdot 10^{-4}$ M 1-phenethyl-2-picolinium in 0.1 M acetic acid. Solid phase: μ Bondapak Phenyl. Sample: bromide.

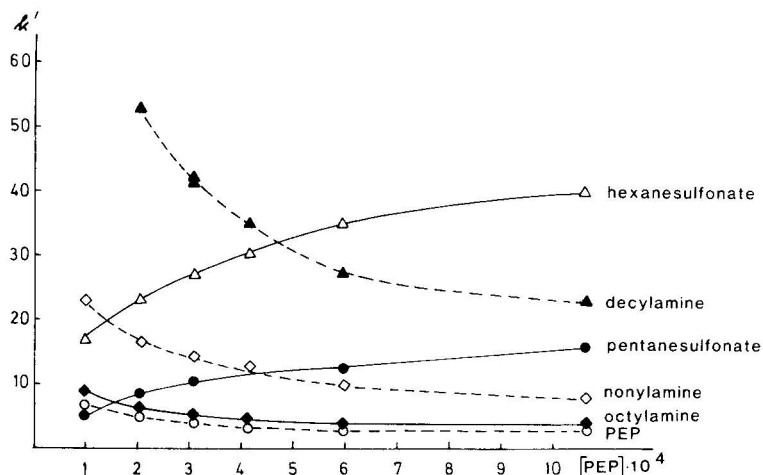


Fig. 8. Retention of anionic and cationic compounds with PEP in mobile phase. Mobile phase: 1-phenethyl-2-picolinium (PEP) in 0.1 *M* acetic acid. Solid phase: μ Bondapak Phenyl.

vents with a refractive index detector after separation on charcoal. Cyclohexane with a low content of diethyl ether was used as the mobile phase and chromatograms were obtained that contained a sample peak and a "system peak" with constant retention. The two peaks had opposite directions. No mechanism for the observed effect was suggested.

Chromatograms with positive and negative peaks are also obtained by gel permeation chromatography of proteins on columns equilibrated with UV-absorbing, low-molecular-weight cofactors. The phenomenon is due to binding between protein and cofactor and binding constants have been calculated from the peak areas¹⁸⁻²⁰.

In the present case, the column is equilibrated with a mobile phase containing a UV-absorbing ion and it is likely that the observed peaks are due to changes in its distribution to the solid phase as an ion pair. The distribution changes can be elucidated to a certain extent by studies of the influence of the composition of the mobile phase on the capacity ratio of samples of different charge.

The relationship between the capacity ratio and the concentration of the UV-absorbing mobile phase component (the counter ion) is demonstrated in Fig. 8. The k' of the counter ion (PEP) and k' of all samples of the same charge decrease with increasing PEP concentration, whereas the retention of samples of opposite charge increases.

Addition of other ions to the mobile phase will also affect the retention. In a system with an anionic UV-absorbing mobile phase component, NS, an increase in the concentration of an ion of opposite charge, tetramethylammonium (TMA^+), increases the retention of the UV-absorbing component, whereas samples of the same charge as the added ion show decreased retention (Fig. 9).

Further illustrations are given in Fig. 10, which shows the influence of the hydrophobicity of the ions that are added to the mobile phase. A change in the cationic component from Na^+ to tetraethylammonium increases the retention of the

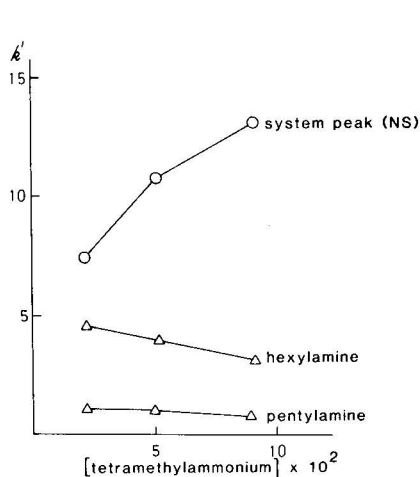


Fig. 9. Retention of cationic compounds with NS and tetramethylammonium in mobile phase. Mobile phase: $4 \cdot 10^{-4}$ M naphthalene-2-sulphonate (NS) and tetramethylammonium in phosphate buffer (pH 2.0). Solid phase: μ Bondapak Phenyl.

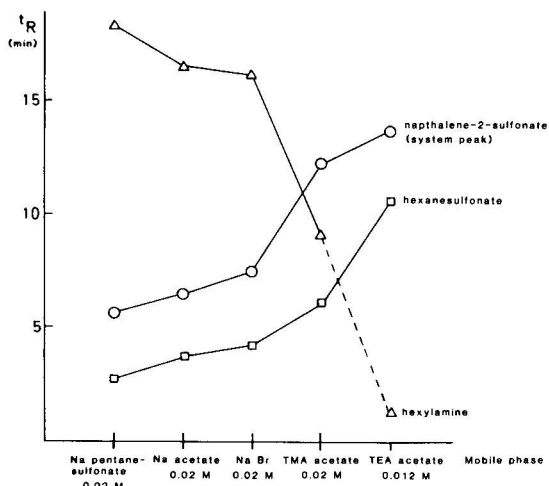


Fig. 10. Retention of cationic and anionic compounds with NS and different cations and anions in mobile phase. Mobile phase: $4 \cdot 10^{-4}$ M naphthalene-2-sulphonate in aqueous salt solutions (pH 5). Solid phase: μ Bondapak Phenyl.

sulphonates considerably whereas the retention of the ammonium ion decreases to such an extent that a sample peak can no longer be observed. A change in the anionic component from acetate to pentanesulphonate has the opposite effect.

The response pattern seem to depend on the presence of ions in the mobile phase besides the UV-absorbing component. A system with $4 \cdot 10^{-4}$ M sodium naphthalene-2-sulphonate in water as the mobile phase only gives a normal response for strongly hydrophobic ions.

These results indicate that the retention of the ionic samples and the UV-absorbing mobile phase ion follows the general rules for reversed-phase ion-pair chromatography with a hydrophobic adsorbent as the stationary phase²¹⁻²³. The UV-absorbing mobile phase component is distributed to the hydrophobic adsorbent as an ion pair with other mobile phase components (cations for NS; anions for PEP). The sample is distributed to the stationary phase as an ion pair with the UV-absorbing ion or with other mobile components of the opposite charge. There is a competition between the ion pairs for the limited capacity of the adsorbent. Measurements of the adsorption of NS from a mobile phase with 0.05 M phosphoric acid as solvent have shown that it follows a Langmuir expression, as indicated by a reciprocal plot of amount adsorbed *versus* mobile phase concentration²¹.

These facts can be summarized in the following expressions for the capacity ratio of a cationic sample, HA^+ , and an anionic sample, Z^- , when the mobile phase contains NS^- (UV-absorbing component), Y^- and Q^+ :

$$\log k'_{HA} = \log K_0 \cdot q + \log (K_{HANS}[NS] + K_{HAY}[Y]) - \log \{1 + [HA] (K_{HANS}[NS] + K_{HAY}[Y]) + [Q] (K_{QNS}[NS] + K_{QY}[Y])\} \quad (1)$$

$$\log k'_Z = \log K_0 \cdot q + \log K_{QZ}[Q] - \log \{1 + [Q] (K_{QZ}[Z] + K_{QNS}[NS] + K_{QY}[Y])\} \quad (2)$$

[NS], [Z], [HA], [Q] and [Y] represent concentrations of the ionic components in the mobile phase in the migrating zone, K_{HANS} , K_{HAY} , K_{QNS} , K_{QZ} and K_{QY} are constants for ion-pair distribution between mobile and stationary phase, K_0 is the capacity of the adsorbent and q the phase ratio in the column²¹⁻²³. It is assumed that the adsorbent has one kind of adsorption site only.

Response

The injection of an ionic sample can be assumed to give rise to changes in the concentrations of all ionic mobile phase components in the injection zone. All of these ions (UV-absorbing ion, other anions and cations) will migrate in separate zones with the mobile phase, which is supplied to the system at constant composition.

The sample usually has a low concentration (about 10^{-4} M) and it will give rise to small changes in the concentrations of the other mobile phase ions. The effect on the capacity ratio, which is controlled by the concentration of these ions, is therefore very limited: an increase in the concentration of a cationic sample ($k' = 16$) from $2 \cdot 10^{-5}$ to $2 \cdot 10^{-4}$ M decreases its retention by about 2% in an NS system similar to that used in Fig. 3. A small change in the concentration of a highly UV-absorbing ion can, however, be measured with high precision with a UV detector, which registers the difference in concentration.

The response pattern in the chromatograms is due to competing distribution processes comprising of binding and displacement of the UV-absorbing ion. A qualitative interpretation can be based on assumptions regarding the distribution changes on application of the sample. An example is given in Table I. The concentration of the UV-absorbing ion in the mobile phase, [NS], changes in the injection zone. This gives rise to a migrating NS-zone beside the sample zone, and the change of [NS] is transferred to the faster of the migrating zones. The change of NS-concentration in the system zone compensates that in the sample zone.

The UV-absorbing ion is usually the only mobile phase component that gives

TABLE I

RESPONSE WITH ANIONIC UV-ABSORBING ION IN MOBILE PHASE

Ions in mobile phase: NS⁻ (UV-absorbing), Y⁻ and Q⁺.

Sample	Capacity ratio	Distribution processes	NS ⁻ peak (system peak)	Sample peak
HA ⁺	$k'_{HA} < k'_{NS}$	Binding of HANS dominates over displacement of QNS	Positive	Negative
	$k'_{HA} > k'_{NS}$		Negative	Positive
Z ⁻	$k'_Z < k'_{NS}$	Displacement of QNS dominates over binding of QZ	Negative	Positive
	$k'_Z > k'_{NS}$		Positive	Negative

TABLE II

OBSERVED MOLAR ABSORPTIVITY (ϵ') OF NAPHTHALENE-2-SULPHONATE

Solvent: water.

Maximum concentration in the range (mol/l $\cdot 10^4$)	$\Delta C \cdot 10^5$ (mol/l)	ΔA	ϵ'
2.41	5.98	0.155	2595
3.70	4.24	0.100	2374
3.91	2.11	0.0494	2341
4.23	3.18	0.0740	2327
5.43	6.04	0.135	2243

an easily observed chromatographic peak. Q^+ and Y^- are often highly hydrophilic with short retentions and give peaks that appear close to the front.

The amount of counter ion in the sample peak can be calculated from the peak area and the molar absorptivity of the ion. The absorbance of the mobile phase at 254 nm ranges between 0.3 and 1.2, depending on the concentration of the UV-absorbing counter ion. The observed molar absorptivity of the counter ions decreases gradually with increasing absorbance in the range $A = 0.1$ – 1.0 , probably owing to stray-light disturbances in the UV detector. The changes obtained with naphthalene-2-sulphonate are demonstrated in Table II, which gives the observed molar absorptivity, $\epsilon' = \Delta A / \Delta C$, in different concentration ranges, where ΔA is the change in absorbance given by a certain change in concentration, ΔC .

The peak heights (positive and negative) correspond under normal chromatographic conditions to an absorbance change of less than 0.05 units. The observed molar absorptivity under these conditions can be considered as almost constant, as seen from Table II, and it can be used in a calculation of the amount of counter ion in a chromatographic peak from the measured peak area.

The response factor, *i.e.*, the amount of counter ion in the peak divided by the

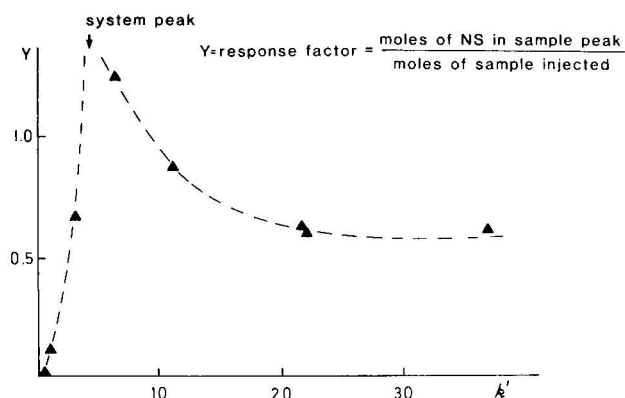


Fig. 11. Response in system with NS as UV-absorbing ion. Mobile phase: $3.7 \cdot 10^{-4}$ M naphthalene-2-sulphonate in 0.01 M phosphoric acid. Solid phase: μ Bondapak Phenyl.

amount of sample injected, is strongly dependent on the capacity ratio of the sample, as illustrated in Fig. 11. The response factor increases with increasing k' , goes through a maximum when the sample and the system peak have about the same retention and levels out at higher k' . The influence of the composition of the system on the response factor at high k' has so far not been elucidated.

Remarkably high response factors are often obtained when the sample and the counter ion have about the same capacity ratio and even response factors higher than 4 have been obtained. The effect seems to be due to interaction between the ions in the two zones.

Optimization of the response factor of a sample can be achieved by changing the mobile phase composition in such a way that the k' values of the sample and system peak coincide. If the sample and the UV-absorbing ion have different charges, an increase in the response factor might be obtained by changing the concentration of the UV-absorbing component, as demonstrated by Fig. 8 and Table III.

TABLE III

RESPONSE FACTORS WITH 1-PHENETHYL-2-PICOLINIUM AS UV-ABSORBING ION

Conditions as in Fig. 8.

$[PEP] \cdot 10^4$ (mol/l)	Response factor		
	<i>Pentanesulphonate</i>	<i>Octylamine</i>	<i>Nonylamine</i>
1.01	1.14	2.16	0.63
2.07	0.95	2.16	0.58
3.08	0.60	1.97	0.60
4.13	0.60	1.75	0.53

Pentanesulphonate and PEP have about the same retention when the PEP concentration is about $1 \cdot 10^{-4}$ M (Fig. 8). The response factor is about 1.1 under these conditions (Table III), but it decreases with increasing PEP concentration and increasing deviation in retention. Octylamine, which has the same charge and also about the same retention as PEP, retains a very high response in the whole concentration range. The more strongly retained nonylamine gives a considerably lower response.

The retention and the response factors can also be regulated by other mobile phase components, as has been demonstrated for hexylamine and hexanesulphonate in Fig. 10 and Table IV. An increase in the size of the cation in the mobile phase has a drastic effect on the response of hexylamine. In the presence of 0.02 M tetramethylammonium the sample peak is close to the system peak (NS) and a response of more than 1.5 is obtained. Addition of tetraethylammonium, on the other hand, will decrease the retention to such an extent that no response at all is obtained.

Quantitation

The relationship between amount injected and peak height has shown good linearity up to 10 nmoles for both positive and negative peaks. The counter ions used

TABLE IV

RESPONSE FACTORS WITH NAPHTHALENE-2-SULPHONATE AS UV-ABSORBING ION

Conditions as in Fig. 10.

Mobile phase	Response factor	
	Hexylamine	Hexanesulphonate
Sodium pentanesulphonate (0.02 M)	0.24	0.05
Sodium acetate (0.02 M)	0.62	0.30
Sodium bromide (0.02 M)	0.60	0.67
Tetramethylammonium acetate (0.02 M)	1.58	0.18
Tetraethylammonium acetate (0.012 M)	—	0.12

in these studies have molar absorptivities between 2300 and 3100 and they permit the quantitation of about 0.1 nmole of a sample with acceptable precision if the conditions are such that the response factor is about 0.5.

The background absorbance of the mobile phase is high, as mentioned above, and the observed changes in absorbance are often only a few parts per thousand. It is obvious that the precision is highly dependent on the quality of the equipment and the stability of the experimental conditions. High-quality pumps with pulseless flow and careful thermostating of the whole system are prerequisites for good precision in quantitation at the lowest levels.

The systems are usually very easy to prepare: a stable baseline is normally obtained within 1 h after the introduction of a new mobile phase. The stability is extremely good: with mobile phases of pH 2–6 it is possible to run the systems for several months without a significant change in their properties.

Studies have so far been performed only with UV-absorbing counter ions and UV detectors. It might also be possible, however, to use fluorescent or electroactive counter ions to obtain higher sensitivity.

REFERENCES

- 1 S. Eksborg and B. A. Persson, *Acta Pharm. Suecica*, 8 (1971) 205.
- 2 S. Eksborg, *Acta Pharm. Suecica*, 12 (1975) 19.
- 3 K. O. Borg and G. Schill, *Acta Pharm. Suecica*, 5 (1968) 323.
- 4 P. O. Lagerström, *Acta Pharm. Suecica*, 12 (1975) 215.
- 5 W. Santi, J. M. Huen and R. W. Frei, *J. Chromatogr.*, 115 (1975) 423.
- 6 J. Crommen, B. Fransson and G. Schill, *J. Chromatogr.*, 142 (1977) 283.
- 7 J. Crommen, *J. Chromatogr.*, 193 (1980) 225.
- 8 J. Crommen, *Thesis*, University of Liège, Liège, 1981.
- 9 L. Hackzell and G. Schill, *Acta Pharm. Suecica*, 18 (1981) in press.
- 10 M. Denkert, L. Hackzell and G. Schill, *Acta Pharm. Suecica*, 18 (1981) in press.
- 11 N. A. Parris, *Anal. Biochem.*, 100 (1979) 260.
- 12 N. A. Parris, *J. Liquid Chromatogr.*, 3(11) (1980) 1743.

- 13 B. A. Bidlingmeyer, S. N. Deming and B. Sachok, *13th International Symposium on Chromatography*, Cannes, 1980.
- 14 B. A. Bidlingmeyer, *J. Chromatogr. Sci.*, 18(10) (1980) 525.
- 15 A. A. Zhukhovitskii and N. M. Turkel'taub, *Dokl. Akad. Nauk SSSR*, 143 (1962) 646.
- 16 R. P. W. Scott, C. G. Scott and P. Kucera, *Anal. Chem.*, 44 (1972) 100.
- 17 K. Šlais and M. Krejčí, *J. Chromatogr.*, 91 (1974) 161.
- 18 J. P. Hummel and W. J. Dreyer, *Biochim. Biophys. Acta*, 63 (1962) 530.
- 19 L. L. Kastenschmidt, J. K. Kastenschmidt and E. Helmreich, *Biochemistry*, 7 (1968) 4543.
- 20 H. G. Baeumert, H. Fasold, F. Keller, M. Halbach and F. Ortanderl, *FEBS Lett.*, 31 (1973) 23.
- 21 A. Tilly Melin, Y. Askemark, K. G. Wahlund and G. Schill, *Anal. Chem.*, 51 (1979) 976.
- 22 A. Tilly Melin, M. Ljungerantz and G. Schill, *J. Chromatogr.*, 185 (1979) 225.
- 23 A. Sokolowski and K.-G. Wahlund, *J. Chromatogr.*, 189 (1980) 299.

CHROM. 14,004

EXTRA-COLUMN EFFECTS IN POLAROGRAPHIC *VERSUS* UV DETECTION IN HIGH-PERFORMANCE LIQUID CHROMATOGRAPHY

W. KUTNER*, J. DĘBOWSKI and W. KEMULA

Institute of Physical Chemistry of the Polish Academy of Sciences, Kasprzaka 44/52, 01-224 Warsaw (Poland)

SUMMARY

A comparison of extra-column effects of chromatographic peaks in high-performance liquid chromatography recorded using a flow-through polarographic detector and a typical UV (254 nm) detector is presented. The diameter of the detection channel of the polarographic detector was 2 mm and the volume of the detection channel of the UV detector was 9.2 μl . When extra-column effects due to injection, tubing and the electronic system were considered, it was found that within experimental error the values of the peak variances are comparable for UV and polarographic detection and equal to $(2.7 \pm 1.0) \cdot 10^3 \mu\text{l}^2$.

INTRODUCTION

One of the most important features of a good detector for high-performance liquid chromatography (HPLC) is a minimal detection volume in order to eliminate broadening of the chromatographic peaks. This extra-column effect of peak broadening, which in practice should not exceed one tenth of the peak volume^{1,2}, becomes important for narrow bands in high-performance size-exclusion chromatography and also when small-volume analytical columns with a diameter of the support particles smaller than 5 μm are used. For integrating detectors in which changes of some physico-chemical bulk property of a flowing liquid is measured, *e.g.*, a UV detector, a decrease in extra-column effects due to the detector may be achieved by making its detection volume smaller. However for non-integrating detectors in which detection is performed from a thin layer of solution directly contacting a sensor, *e.g.*, a wall jet detector, the problem is more complicated. Then, the shape of the detection channel and the hydrodynamics of the mobile phase flow are responsible for peak broadening due to detection. Therefore, it is impossible to predict which of these two types of detectors causes a larger extra-column effect if one simply compares solely the geometrical volumes of the detection channels.

We have mentioned this problem previously^{3,4} and, for polarographic detectors it has also been considered by other workers⁵. For the determination of washing out, *i.e.*, the "active" volume of the detector, a frontal method in a flowing system in the absence of a column was used⁴. In this work we have considered this problem in

detail using methods more relevant to the usual operating conditions in HPLC. A comparison of extra-column effects of a flow-through polarographic detector with those of a commonly used UV (254 nm) detector is presented.

The total variance of a gaussian chromatographic peak expressed in volume units, $\sigma_{v,\text{tot}}^2$, can be presented as a sum of independent variance components^{1,2,6-9} of column $\sigma_{v,\text{col}}^2$, and extra-column, $\sigma_{v,\text{ext}}^2$, effects of peak broadening.

$$\sigma_{v,\text{tot}}^2 = \sigma_{v,\text{col}}^2 + \sigma_{v,\text{ext}}^2 \quad (1)$$

where

$$\sigma_{v,\text{ext}}^2 = \sigma_{v,\text{det}}^2 + \sigma_{v,\text{inj}}^2 + \sigma_{v,\text{tub}}^2 + \sigma_{v,\text{other}}^2 \quad (2)$$

Here $\sigma_{v,\text{det}}^2$, $\sigma_{v,\text{inj}}^2$, $\sigma_{v,\text{tub}}^2$ and $\sigma_{v,\text{other}}^2$ denote, respectively, peak variances due to detection, injection, tubing and other possible factors, *e.g.*, electronic apparatus delay, $\sigma_{v,\text{el}}^2$. The peak variance due to detection can be calculated when other components of eq. 2 are evaluated.

Column peak variance is related to the retention volume, V_R , by the number of theoretical plates, N :

$$N = \left(\frac{V_R}{\sigma_{v,\text{col}}} \right)^2 \quad (3)$$

So, from eqns. 1 and 3 it follows that the dependence of $\sigma_{v,\text{tot}}^2$ on V_R^2 for a mixture of substances with similar diffusion coefficients separated on the column should be linear and, when extrapolated to zero, one could obtain the value of the extra-column effects $\sigma_{v,\text{ext}}^2$.

For the estimation of the values of $\sigma_{v,\text{inj}}^2$, eqn. 4 can be applied:

$$\sigma_{v,\text{inj}}^2 = k V_{\text{inj}}^2 \quad (4)$$

where V_{inj} is the volume of sample injected and k is a constant for the given system. For a plug type of injection $\sigma_{v,\text{inj}}^2$ is independent of flow-rate.

For sufficiently long and narrow straight tubes, the value of $\sigma_{v,\text{tub}}^2$ can be calculated from the dependence^{1,10-15}

$$\sigma_{v,\text{tub}}^2 = \frac{\pi r^4 l f}{24 D} \quad (5)$$

where r and l are the radius and length of the connecting tubing, respectively, f is the mobile phase flow-rate and D is the diffusion coefficient of the substance in the mobile phase. Eqn. 5 holds in the absence of mixing in tubes.

EXPERIMENTAL

The high-performance liquid chromatograph, columns and packings, chromatographic procedure and detectors, *i.e.*, UV (254 nm) with a detection channel of

length 10 mm and diameter 1.08 mm and a polarographic flow-through detector with a detection channel of diameter 2 mm, have been described previously⁴.

Polarographic detection was performed using an LP-7 polarograph and an EZ-7 $y-t$ recorder (Laboratorní Přístroje, Prague, Czechoslovakia). For recording chromatograms with UV detection a TZ 21 $y-t$ recorder (Laboratorní Přístroje) was used. Samples were injected with a Rheodyne Model 7120 injection valve with a 10- μ l sample loop unless stated otherwise. The dropping mercury electrode capillary characteristics in dynamic (flow-through) experiments were $m = 3.005 \text{ mg sec}^{-1}$, $t_1 = 0.9 \text{ sec}$ at $h_{\text{Hg}} = 150 \text{ cm}$ and $E = -1.0 \text{ V}$ vs. Hg pool, and in steady-state experiments for the determination of diffusion coefficients they were $m = 3.56 \text{ mg sec}^{-1}$ and $t_1 = 1.875 \text{ sec}$ at $h_{\text{Hg}} = 50 \text{ cm}$. Current oscillations due to the mercury dropping were eliminated using electronic damping of the polarograph. The time constant of this damping at $1 - 1/e = 0.632$ of full scale of the recorder was 2.2 sec and for UV detection it was 0.5 sec. A Hewlett-Packard Model 9830 A minicomputer was used for linear regression analysis calculations.

Analytical-reagent grade chemicals and doubly distilled water were used for the preparation of solutions. The mobile phase was methanol-1/15 M phosphate buffer (pH 6) (2:3) according to Michaelis. A mixture of substances that were easily detectable by UV and polarographic methods was used to represent model compounds, i.e., *p*-, *m*- and *o*-nitroaniline and β -(5-nitrofuryl-2)acrylic acid.

RESULTS AND DISCUSSION

For the calculation of extra-column effects, high-performance liquid chromatograms of the mixture of model compounds were recorded independently with UV and with polarographic detectors (Fig. 1). It can be seen that nitrate, the ion often used as a marker of column dead volume, V_0 , (peak 1) can be detected by the UV method whereas it is polarographically inactive, and oxygen dissolved in a sample is polarographically active (peak 3) but is UV inactive. The retention volume of potassium nitrate was 2.2 ml, whereas the theoretical value of V_0 for a cylindrical column closely packed with spheres was 1.04 ml. The mean value of the peak asymmetry factor measured at 10% of the peak height^{2,16} was 2.7 for oxygen and 1.7 ± 0.1 for all nitro compounds.

In Fig. 2, the dependence of $\sigma_{v,\text{tot}}^2$ on V_R^2 is plotted for all substances being separated using linear regression analysis at flow-rates of 0.2, 0.5, 1.0 and 2.0 ml min^{-1} . It can be seen that the plots recorded with both UV and polarographic detectors are linear with a mean correlation coefficient for all curves close to 0.999. The value of $\sigma_{v,\text{tot}}^2$ for nitrate and oxygen were not taken into account in this calculation as they deviated markedly from this linear dependence, presumably owing to some other retention mechanism resulting in higher peak asymmetry factor for oxygen and peak splitting for nitrate. The intercepts of the plots in Fig. 2 represent $\sigma_{v,\text{ext}}^2$, with a mean value for both polarographic and UV detection of $2900 \pm 1000 \mu\text{l}^2$ at a significance level of 90%.

For the elucidation of the extra-column effect due to injection, eqn. 4 was tested. Fig. 3 shows the dependence of $\sigma_{v,\text{tot}}^2$ on the square of the injection volume, V_{inj}^2 , for *o*- and *m*-nitroaniline for a flow-rate of 0.2 ml min^{-1} using the UV detector. The mean value of k (eqn. 4) calculated from the slopes of these curves was 1.36,

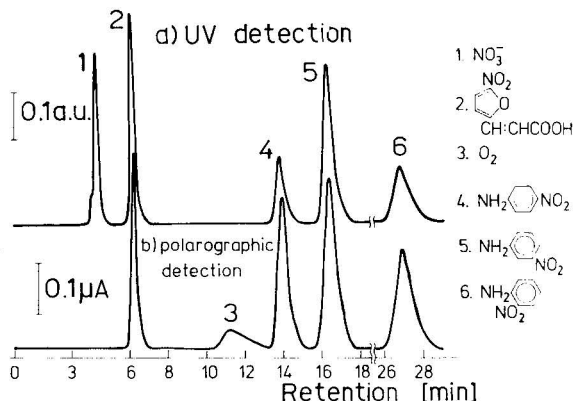


Fig. 1. HPLC traces recorded with (a) a UV (254 nm) detector and (b) a polarographic flow-through detector. Separation conditions: 250×4 mm I.D. column filled with LiChrosorb RP-18 ($10 \mu\text{m}$); mobile phase, methanol-1/15 M phosphate buffer (pH 6) (2:3) according to Michaelis; flow-rate, 0.5 ml min^{-1} ; sample size, $10 \mu\text{l}$; $E = -1.0 \text{ V vs. Hg pool}$. Peaks: 1 = $1 M \text{ KNO}_3$; 2 = $7.5 \cdot 10^{-4} M \beta$ -(5-nitrofuryl-2)acrylic acid; 3 = O_2 ; 4 = $10^{-3} M$ *p*-nitroaniline; 5 = $10^{-3} M$ *m*-nitroaniline; 6 = $10^{-3} M$ *o*-nitroaniline.

which is much higher than $1/12$, the theoretical value for plug-type injection⁶. Hence, for a $10\text{-}\mu\text{l}$ injection volume $\sigma_{v,\text{inj}}^2 = 136 \mu\text{l}^2$.

Extra-column effects originating in the tubing were calculated using eqn. 5. Diffusion coefficients of nitro compounds in the mobile phase were calculated from the polarographic steady-state diffusion limiting currents using the Ilkovič equation.

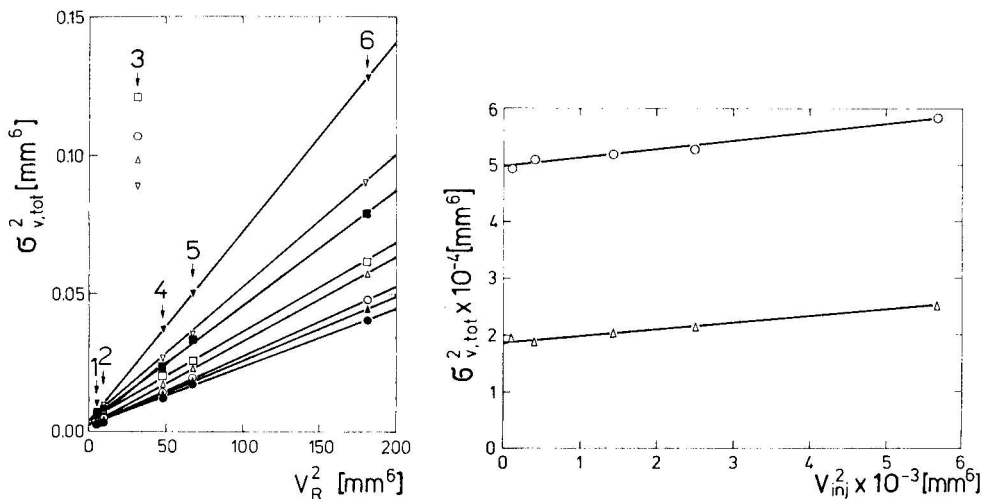


Fig. 2. Dependence of total peak variance, $\sigma_{v,\text{tot}}^2$, on square of retention volume, V_R^2 . Flow-rate: (\circ , \bullet) 0.2 ; (\triangle , \blacktriangle) 0.5 ; (\square , \blacksquare) 1.0 ; (∇ , \blacktriangledown) 2.0 ml min^{-1} . Open symbols represent the polarographic detector and closed symbols the UV detector. Separation conditions as in Fig. 1. Numerals indicate separated compounds as in Fig. 1.

Fig. 3. Dependence of total peak variance, $\sigma_{v,\text{tot}}^2$, on square of sample volume injected, V_{inj}^2 , with UV detection. (\circ) $4 \cdot 10^{-4} M$ *o*-nitroaniline; (\triangle) $7 \cdot 10^{-4} M$ *m*-nitroaniline. Flow-rate, 0.2 ml min^{-1} . Other separation conditions as in Fig. 1.

For *m*-nitroaniline it was $D = 7.05 \cdot 10^{-6} \text{ cm}^2 \text{ sec}^{-1}$ and for other nitro compounds it did not deviate more than 15%. The radius of the connecting stainless-steel capillary tubing was 0.015 cm and its length was 20 cm for both detectors. Hence, the value of $\sigma_{v,\text{tub}}^2$ for a flow-rate of 0.2 ml min^{-1} was close to $60 \mu\text{l}^2$. When the other factors contributing to peak broadening are small enough, $\sigma_{v,\text{det}}^2$ for both the polarographic and UV detector is close to $(2.7 \pm 1.0) \cdot 10^3 \mu\text{l}^2$. This result confirms our previous estimation⁴ and enables one to conclude that regardless of the great differences in the geometrical volumes and shapes of the detection channels of the two detectors, our polarographic flow-through detector causes practically the same peak broadening as the UV detector.

The comparison of $\sigma_{v,\text{det}}^2$ for the two detectors does not require any assumption with regard to the presence or absence of mixing of the sample in the detection channels. In the limiting cases of a non-mixing or ideal mixing behaviour of the detection channel, $\sigma_{v,\text{det}}^2$ may be calculated for integrating detectors from eqn. 5 or taken as V_{det}^2 ^{1,6}, respectively. For our UV (254 nm) detector these values were 84.64 and $61,816 \mu\text{l}^2$, respectively. The deduced value of $\sigma_{v,\text{det}}^2$ of $(2.7 \pm 1.0) \cdot 10^3 \mu\text{l}^2$ indicates that some mixing occurs in both detectors. This was confirmed by the dependence of $\sigma_{v,\text{tot}}^2$ on flow-rate with V_R kept constant. This dependence of the mean slope of $\log \sigma_{v,\text{tot}}^2$ on $\log f$ is close to 0.5 and 0.25 for the UV and polarographic detector, respectively, for *o*-nitroaniline (Fig. 4). For other nitro compounds this slope for the UV detector is also higher than that for the polarographic detector and the values of these slopes do not differ much from those for *o*-nitroaniline. Hence the greater the mobile phase flow-rate, the greater is the extra-column effect caused by the UV detector compared with the polarographic detector.

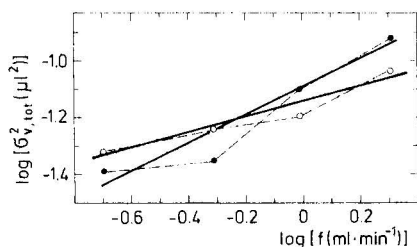


Fig. 4. Dependence of the logarithm of $\sigma_{v,\text{tot}}^2$ on logarithm of flow-rate, f , for *o*-nitroaniline. (●) UV detector; (○) polarographic detector. Separation conditions as in Fig. 1.

ACKNOWLEDGEMENTS

We thank to Dr. Peter Markl of the Institute for Analytical Chemistry, University Vienna, Vienna, Austria, for inspiring suggestions. This work was carried out within research project 03.10 of the Polish Academy of Sciences.

REFERENCES

- 1 M. Martin, C. Eon and G. Guiochon, *J. Chromatogr. Sci.*, 108 (1975) 229.
- 2 J. J. Kirkland, W. W. Yau, H. J. Stoklosa and C. H. Dills, Jr., *J. Chromatogr. Sci.*, 15 (1977) 303.
- 3 W. Kutner, J. Dębowski and W. Kemula, *Polish Pat. Appl.*, No. P 210602, 1978.
- 4 W. Kutner, J. Dębowski and W. Kemula, *J. Chromatogr.*, 191 (1980) 47.

- 5 H. B. Hanekamp, P. Bos, U. A. Th. Brinkman and R. W. Frei, *Z. Anal. Chem.*, 297 (1979) 404.
- 6 J. C. Sternberg, *Advan. Chromatogr.*, 2 (1966) 205.
- 7 J. F. K. Huber, J. A. R. J. Hulsman and C. A. M. Meijers, *J. Chromatogr.*, 62 (1971) 79.
- 8 J. J. Kirkland, in S. G. Perry (Editor), *Gas Chromatography 1972*, Applied Science, Barking, 1973, pp. 39–56.
- 9 B. L. Karger, M. Martin and G. Guiochon, *Anal. Chem.*, 46 (1974) 1640.
- 10 G. Taylor, *Proc. R. Soc. London, Ser. A*, 219 (1953) 186.
- 11 G. I. Taylor, *Proc. R. Soc. London, Ser. A*, 223 (1954) 446.
- 12 R. Aris, *Proc. R. Soc. London, Ser. A*, 235 (1956) 67.
- 13 I. Halász and P. Walking, *Ber. Bunsenges. Phys. Chem.*, 74 (1974) 66.
- 14 J. F. K. Huber, R. van der Linden, E. Ecker and M. Oreans, *J. Chromatogr.*, 83 (1973) 267.
- 15 R. G. Brownlee and J. W. Higgins, *Chromatographia*, 11 (1978) 567.

CHROM. 14,081

FLUORESCENCE DERIVATIZATION OF TERTIARY AMINES WITH 2-NAPHTHYL CHLOROFORMATE

G. GÜBITZ*, R. WINTERSTEIGER and A. HARTINGER

Institut für Pharmazeutische Chemie, Universität Graz, A-8010 Graz (Austria)

SUMMARY

2-Naphthyl chloroformate (NCF) was found to be a suitable fluorescence reagent for the derivatization of drugs containing a tertiary amino group. The tertiary amines undergo dealkylation when heated with NCF, forming fluorescent carbamates. The reaction has been applied to the pre-column derivatization of some anti-histamines.

INTRODUCTION

A great problem in high-performance liquid chromatography (HPLC) is the detection of drugs with low UV absorbance. In such instances it is advantageous to form UV-absorbing or fluorescent derivatives for detection enhancement. Most drugs contain amino groups, and for primary and secondary amines a number of reagents have been described^{1–4}. No satisfactory reactions, however, are known for the derivatization of tertiary amines. On the other hand, many drugs contain a tertiary amino group as the only functional group.

A reaction principle already used in gas chromatography^{5–11} is the reaction of tertiary amines with chloroformates, which undergo dealkylation under suitable conditions, forming carbamates with the resulting secondary amine.

The aim of this work was the development of reagents on this basis for the HPLC analysis of tertiary amines with fluorescence detection.

EXPERIMENTAL

Apparatus

A Perkin-Elmer Series 2 liquid chromatograph and an LC 55 UV detector connected to a Perkin-Elmer MPF 44 fluorimeter were used with a 25- μ l flow-through cell.

Reagents and chemicals

2-Naphthyl chloroformate (NCF) was synthesized according to the literature^{12,13}. The reagents used were potassium carbonate (p.a. grade, anhydrous) and saturated methanolic potassium hydroxide. All solvents were of analytical-reagent grade.

Derivatization procedure

About 10 pmol–5 nmol of the tertiary amine (as the free base) were heated with a 10-fold molar excess of NCF and 10 mg of potassium carbonate in 100 μ l of dry benzene at 100°C for 1 h in a sealed conical vial. After cooling, the excess of the reagent was removed by shaking the reaction mixture with 300 μ l of saturated methanolic potassium hydroxide for 1 min. After phase separation by adding 1 ml of water, an aliquot of the benzene layer was injected into the chromatograph.

Chromatography

The column contained Knauer RP-18 and the following mobile phases were used: I, methanol–water (80:20); II, methanol–water (70:30); and III, methanol–water–tetrahydrofuran (65:30:5).

RESULTS AND DISCUSSION

2-Naphthyl chloroformate can be synthesized easily by reaction of β -naphthol with phosgene^{12,13}. The reagent is sensitive to moisture, but is stable for several months if stored under the cool and dry conditions.

In addition to primary and secondary amines, tertiary amines also form carba-

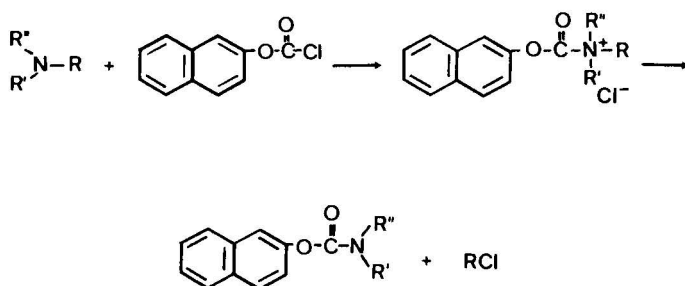


Fig. 1. Scheme of the reaction of NCF with tertiary amines.

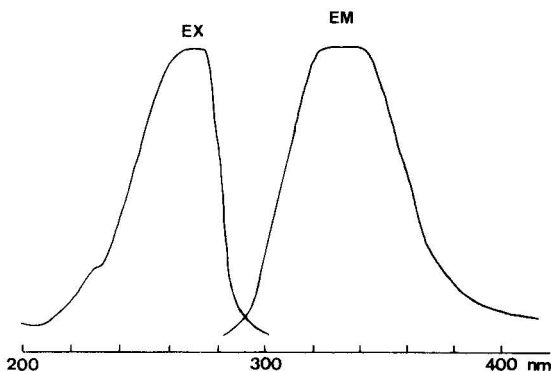


Fig. 2. Fluorescence spectrum of the diphenhydramine derivative in methanol–water (80:20). λ_{max} : excitation, 275 nm; emission, 335 nm.

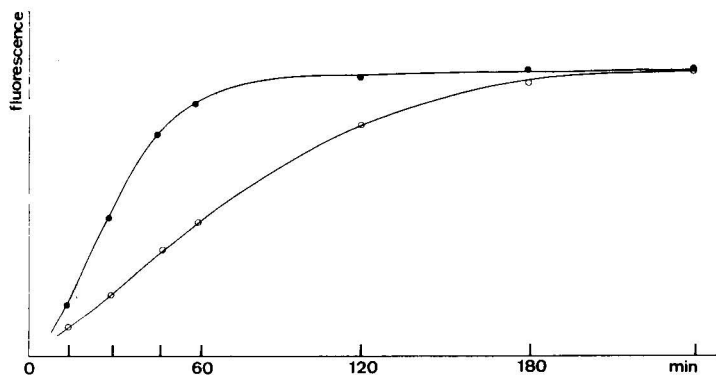


Fig. 3. Kinetics of the reaction of NCF with diphenhydramine. ○, Without catalyst; ●, with K_2CO_3 catalyst.

mates under dealkylation when heated with chloroformates. The scheme of the reaction of NCF with tertiary amines is shown in Fig. 1.

Highly fluorescent carbamates were formed, which showed fluorescence stability for more than 24 h. The fluorescence spectrum showed an excitation maximum at 275 nm and an emission maximum at 335 nm (Fig. 2).

Optimization of the reaction conditions was carried out with the antihistamine diphenhydramine as a model compound. As can be seen from Fig. 3, the use of potassium carbonate as a catalyst permits a higher reaction rate. The excess of the chloroformate can be destroyed by shaking the reaction mixture with alcoholic alkali⁹ followed by the addition of water to obtain a better phase separation.

In addition to methyl groups, ethyl and benzyl groups can also be split off. The reaction is also applicable to N-methyl groups in heterocyclics such as N-methylpiperidine. As far as more complicated compounds are concerned, however, the reaction does not take place homogeneously. For example, by-products were formed during the reaction of mebhydroline, clemizol and antazoline. In comparison with the main

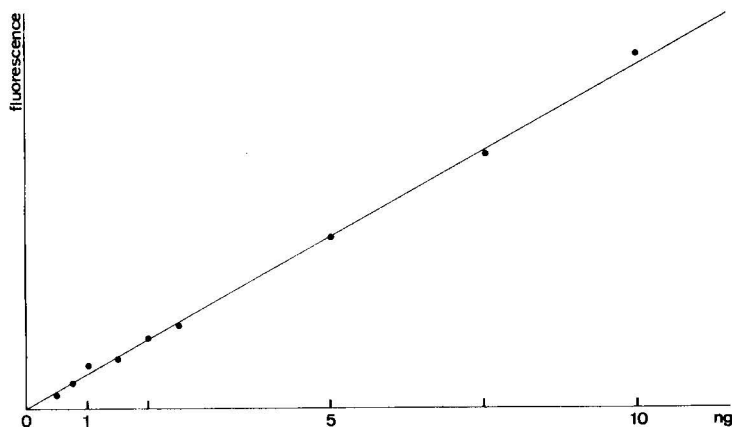


Fig. 4. Calibration graph for diphenhydramine.

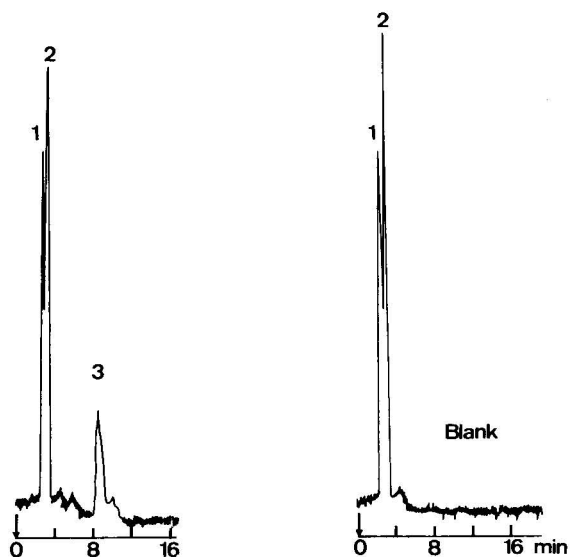


Fig. 5. HPLC of 500 pg diphenhydramine after derivatization with NCF. Column: RP-18, 25×0.4 cm I.D. Mobile phase: methanol-water (80:20). Flow-rate: 2 ml/min. Detection: fluorescence, $\lambda_{\text{ex}} = 275$ nm, $\lambda_{\text{em}} = 335$ nm. 1, 2 = Decomposition products of the reagent; 3 = 500 pg of diphenhydramine.

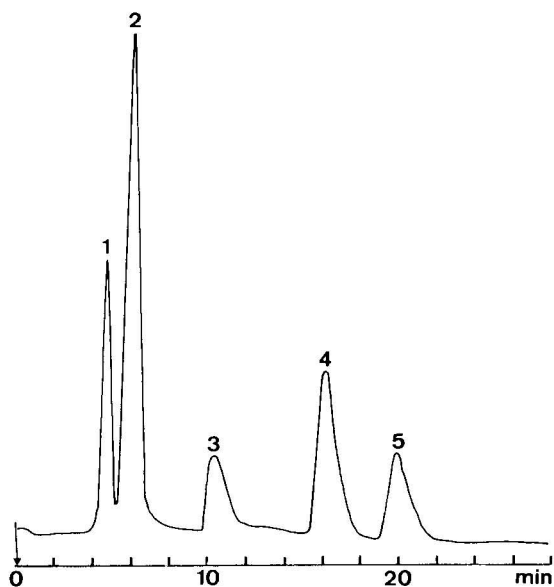
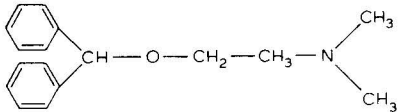
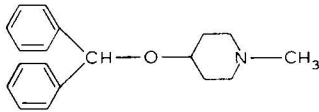
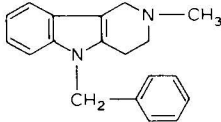
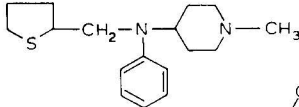
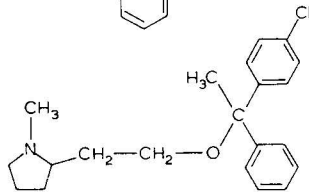
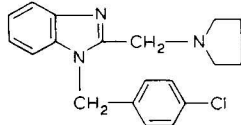
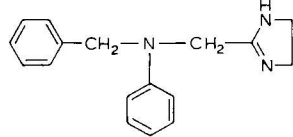


Fig. 6. HPLC separation of antihistamine derivatives. Conditions as in Fig. 5, except mobile phase is methanol-water-tetrahydrofuran (65:30:5). 1, 2 = Decomposition products of the reagent; 3 = diphenylpyraline; 4 = diphenhydramine; 5 = thenalidine.

TABLE I

k' VALUES AND DETECTION LIMITS OF SOME ANTIHISTAMINE DERIVATIVES

Column: RP-18, 25 × 0.4 cm I.D. Mobile phase: methanol-water (70:30). Flow-rate: 2 ml/min. Detection: fluorescence, λ_{ex} = 275 nm, λ_{em} = 335 nm.

Compound	Formula	Detection limit (ng per 20 μ l)	<i>k'</i>
Diphenhydramine		0.5	17.9
Diphenylpyraline		1	16.6
Mebhydroline		5	18.5
Thenalidine		1	20.1
Clemastine		5	19.9
Clemizol		10	19.0
Antazoline		5	17.9

product, however, the by-products amounted to only 1–10%. Quantitative determination is not possible in these instances. It has been found that the reaction also fails with pyridyl-substituted compounds¹⁴.

The absolute yield of the carbamate from diphenhydramine is 81%, estimated

by comparison with a known amount of a synthetic authentic sample. The reaction, however, although not absolutely quantitative, shows good reproducibility. The relative standard deviation determined for 200 ng of diphenhydramine is 1.6% and for 20 ng it is 3% ($n = 9$).

The linearity of the reaction was investigated by preparing calibration graphs for various antihistamines. Linearity was observed over a range of more than one order of magnitude. The correlation coefficients lay between 0.997 and 0.999. A calibration graph for diphenhydramine in the lower nanogram range is shown in Fig. 4.

The capacity ratios (k') and detection limits for some antihistamines are given in Table I. A high sensitivity was observed for diphenhydramine. Fig. 5 shows a chromatogram for 500 pg diphenhydramine after derivatization. The use of a UV detector is also possible, although of course it is much less sensitive.

Fig. 6 shows the separation of a mixture of three antihistamine derivatives.

In addition to the application of the method to antihistamines, it was also applied to examples of other groups of drugs containing tertiary amino groups, such as analgesics, local anaesthetics and psychotropic drugs. The adaption of this method to the determination of drugs in plasma samples is now being examined. Further promising reagents, such as anthrylmethyl chloroformate and fluorenylmethyl chloroformate^{16,17}, are under investigation.

This derivatization procedure has also been applied with good results to thin-layer chromatography with fluorodensitometric evaluation¹⁵.

REFERENCES

- 1 N. Seiler and J. Wiechmann, *Experientia*, 20 (1966) 559.
- 2 M. Roth, *Anal. Chem.*, 43 (1971) 880.
- 3 P. B. Gosh and M. W. Whitehouse, *Biochem. J.*, 108 (1968) 155.
- 4 S. Udenfriend, S. Stein, P. Bohler and W. Dairman, *Science*, 178 (1972) 871.
- 5 P. Hartvig and J. Vessman, *Acta Pharm. Suecica*, 11 (1974) 115.
- 6 P. Hartvig and J. Vessman, *Anal. Lett.*, 7 (1974) 223.
- 7 P. Hartvig, N. O. Ahnfelt and K. E. Karlsson, *Acta Pharm. Suecica*, 13 (1976) 181.
- 8 P. Hartvig, K. E. Karlsson, L. Johansson and C. Lindberg, *J. Chromatogr.*, 121 (1976) 235.
- 9 P. Hartvig and W. Handl, *Anal. Chem.*, 48 (1976) 390.
- 10 P. Hartvig, K. E. Karlsson, C. Lindberg and L. O. Boreus, *Eur. J. Clin. Pharmacol.*, 11 (1977) 65.
- 11 K. E. Karlsson and P. Hartvig, *Acta Pharm. Suecica*, 17 (1980) 249.
- 12 *Ger. Pat.*, 251,805; *Friedländer*, 11 (1912) 82.
- 13 L. C. Raiford and G. O. Inman, *J. Amer. Chem. Soc.*, 56 (1934) 1586.
- 14 L. A. Sternson and A. D. Cooper, *J. Chromatogr.*, 150 (1978) 257.
- 15 G. Gübitz, R. Wintersteiger and A. Hartinger, *Sci. Pharm.*, in preparation.
- 16 L. A. Carpino and G. Y. Han, *J. Org. Chem.*, 37 (1972) 3404.
- 17 H. A. Moye and A. J. Boning, *Anal. Lett.*, B, 12, No. 1 (1979) 25.

CHROM. 14,252

ION CHROMATOGRAPHY OF INORGANIC AND ORGANIC IONIC SPECIES USING REFRACTIVE INDEX DETECTION

F. A. BUYTENHUYIS

Akzo Research Laboratories Arnhem, Corporate Research Department, PO Box 60, 6800 AB Arnhem (The Netherlands)

SUMMARY

Ion chromatography of inorganic and non-UV-absorbing organic species can be monitored with a differential refractive index detector if aromatic counter ions are used. Practical applications show that in this way refractive index (RI) detection can compete with systems for ion chromatography (IC) using electric conductivity detection. IC with RI detection can be carried out with any liquid chromatograph. Hence high efficiency ion-exchange columns can be used.

INTRODUCTION

The analysis of ionic species in aqueous solutions is becoming increasingly important. It is well known that the specificity of ion exchange can be utilized for liquid chromatography of ionic compounds. In high-performance liquid chromatography (HPLC), however, the application of ion-exchange chromatography is limited because of poor detection sensitivity. This is not a problem if the ionic solutes absorb in the UV or visible range, but ion-exchange chromatography of inorganic ions is limited by the lack of sensitivity inherent in universal detectors such as the refractive index and electrical conductivity detectors. Thus, the development of ion-exchange chromatography has not been as rapid as that of other liquid chromatographic techniques such as straight phase adsorption, reversed-phase and size exclusion chromatography.

In 1975 Small *et al.*¹ reported a new chromatographic method using electrical conductometric detection and mentioned ion chromatography (IC). In addition to the separation or analytical column they used a stripper or suppressor column. The stripper column removes the buffer used for the elution of the ionic species from the separation column, which results in a low background activity for the conductivity cell. This principle has been adopted in the ion chromatographs of the Dionex Corporation.

Gjerde and co-workers^{2,3} demonstrated that a suppressor column is not absolutely necessary for ion chromatography with electric conductivity detection. They used an anion exchanger having a low exchange capacity and an eluent having a very low conductivity. In this way the background conductivity is low enough to allow the

separated anions to be detected with a simple conductance detector. Molnár *et al.*⁴ applied a specially designed conductivity detector both with and without a suppressor column, for the separation of anions and cations on C₁₈ columns using secondary equilibria in the mobile phase. For the separation of cations a silicious cation exchanger was used.

Besides ion exchange, some researchers have used ion exclusion for the separation of weak acids. Turkelson and Richards⁵ employed this technique for separation of the acids of the citric acid cycle, and Tanaka *et al.*⁶ described the ion-exclusion behaviour of a large number of strong and weak acids. Bio-Rad Labs. (Richmond, CA, U.S.A.) recently introduced a so-called organic acid analysis column, based on ion exclusion. The use of diluted sulphuric acid as the mobile phase allows UV detection at 210 nm and thus high sensitivity for a variety of weak organic acids. However, ion-exclusion chromatography is not capable of selectivity for the separation of strong acids.

A large number of applications of the Dionex equipment in the fields of process control and environmental research and in the power industry have been reported⁷. From the chromatographic point of view, there are some drawbacks:

(1) the number of injections is restricted by the capacity of the suppressor column

(2) the suppressor column introduces extra band broadening, which results in lower resolution

(3) special equipment is needed for IC

(4) only those buffers can be applied which, after passage through the suppressor column, result in a low electrical background conductivity.

In this paper, a promising mode of IC monitored by a refractive index detector is described. The method allows IC to be carried out with commercially available HPLC equipment. It differs in certain aspects from the IC technique employed by Dionex, and attains a sensitivity similar to that obtained by conductivity detection.

THEORETICAL

In an ion-exchange process, counter ions are removed from the ion exchanger on injection of a sample solution. The excess of the counter ions in the mobile phase results in a "solvent peak" at the unretained place (the elution "volume" of compounds not interacting with the ion exchanger, such as glucose) in the chromatogram. In addition, since there is a dynamic exchange process between the solute and the counter ions, the migration of the solute ions through the column is accompanied by a local deficiency of the buffer ions. If a differential refractive index detector is employed the signal obtained will be the result of these two concentration changes, which are always opposite. The sensitivity is determined by the difference in refractive index between the buffer ions and the solute ions.

If, as usual, inorganic buffers are used for the separation of inorganic ionic species, the sensitivity is very low. Therefore, to increase the sensitivity, buffers with a very high (or very low) refractive index relative to that of the solute have to be used, e.g., an aromatic anion for an anion-exchange process and an aromatic cation for a cation-exchange process.

EXPERIMENTAL

Apparatus

The high-performance liquid chromatograph consisted of a high-pressure pump (Model 6000 A, Waters Assoc.) equipped with a differential refractometer (Waters R 401), a high-pressure sampling valve (Rheodyne RH 7010), a linear potentiometric recorder (Kipp and Zonen BD 8) and a GCA precision thermostat. The latter was used for thermostating in series both the column (via a water-jacket) and the detector.

Three different anion-exchange packings were used in stainless-steel columns Nucleosil SB, 5- and 10- μ m particles, 150 and 250 \times 4.6 mm ((Chrompack, Middelburg, The Netherlands); Partisil 10 SAX, 250 \times 4.6 mm (Whatman), and Zorbax AX, 250 \times 4.6 mm (DuPont). For cation-exchange chromatography use was made of a 250 \times 4.6 mm stainless-steel column packed with Nucleosil 10 SA (Chrompack).

Chemicals

The eluents used were prepared from distilled water and reagent grade chemicals (Baker, Deventer, The Netherlands), and degassed carefully.

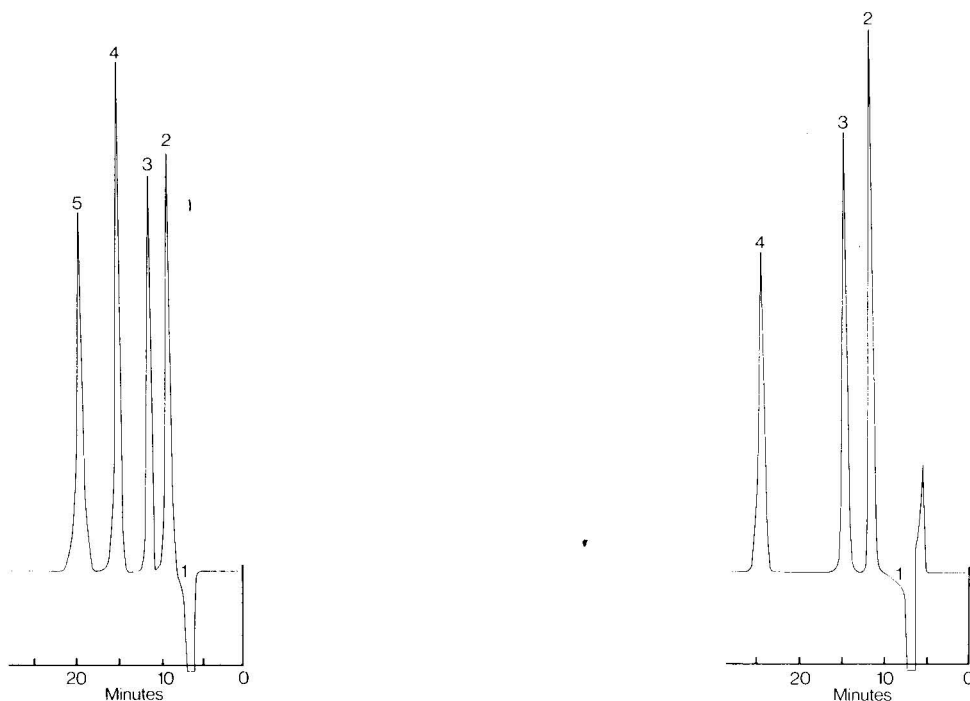


Fig. 1. IC chromatogram of a synthetic mixture of inorganic anions. Column: 250 \times 4.6 mm Nucleosil 10 SB. Mobile phase: 0.03 *M* sodium salicylate, pH 4.0; flow-rate 0.5 ml/min. Sample size: 20 μ l. Detection: RI, attenuation \times 8. Peaks: 1 = solvent effect; 2 = phosphate (20 μ g); 3 = chloride (10 μ g); 4 = nitrate (20 μ g); 5 = sulphate (20 μ g).

Fig. 2. IC chromatogram of halogens. For conditions see Fig. 1. Peaks: 1 = solvent effect; 2 = chloride (14 μ g); 3 = bromide (25 μ g); 4 = iodide (50 μ g).

RESULTS AND DISCUSSION

In Figs. 1 and 2 the separations of some mixtures of inorganic anions are given. A good resolution was obtained by using 0.03 mol/l sodium salicylate, pH 4, as the eluent. Since the decrease in the buffer ion concentration is measured, the corresponding decrease of the refractive index has been plotted along the vertical axis.

The selectivity can be altered by changing the counter ion, *e.g.*, benzoate, *p*-hydroxybenzoate, sulphobenzoate or phthalate, and the pH (see Figs. 3 and 4). Moreover, the selectivity depends on the type of column. The Zorbax AX packing (Du-Pont) has a much higher capacity than the Partisil SAX and the Nucleosil SB material and hence requires stronger eluents.

Organic anions can also be separated, as shown in Fig. 5 for chloroacetates.

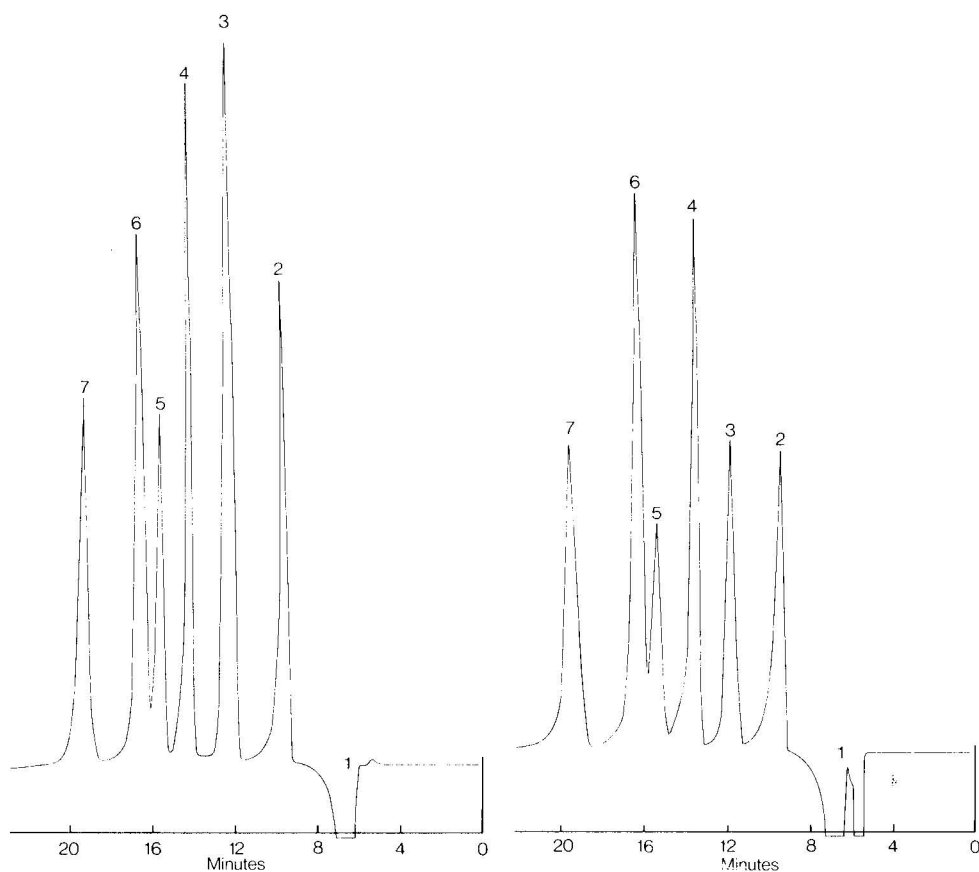


Fig. 3. IC chromatogram of a synthetic mixture. Mobile phase: 0.075 *M* sodium *p*-hydroxybenzoate, pH 5.6. Other conditions as in Fig. 1. Peaks: 1 = solvent effect; 2 = glycolate (20 μ g); 3 = chloride (20 μ g); 4 = nitrite (20 μ g); 5 = chlorate (20 μ g); 6 = nitrate (20 μ g); 7 = sulphate (20 μ g).

Fig. 4. IC chromatogram of a synthetic mixture. Mobile phase: 0.05 *M* potassium biphthalate, pH 3.9. Other conditions as in Fig. 1. Peaks: 1 = solvent effect; 2 = dihydrogen phosphate (25 μ g); 3 = chloride (10 μ g); 4 = nitrite (25 μ g); 5 = bromide (25 μ g); 6 = nitrate (25 μ g); 7 = sulphate (25 μ g).

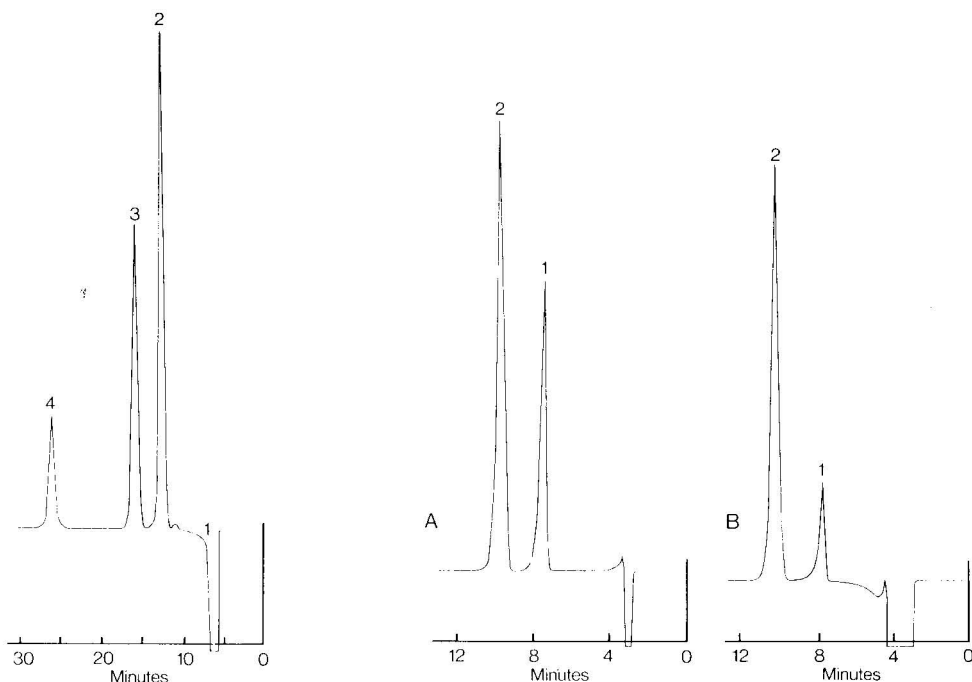


Fig. 5. IC chromatogram of chloroacetates. For conditions see Fig. 1. Peaks: 1 = solvent effect; 2 = monochloroacetate (20 μg); 3 = dichloroacetate (20 μg); 4 = trichloroacetate (20 μg).

Fig. 6. A, IC chromatogram of a synthetic mixture of sodium glycolate (1) and sodium chloride (2). B, IC chromatogram of a water-methanol extract of carboxymethyl-cellulose. Column: 250 \times 4.6 mm Partisil 10 SAX. Mobile phase: 0.035 *M* sodium salicylate, pH 5.0; flow-rate 1 ml/min. Sample size: 20 μl . Detection: RI, attenuation \times 8.

The efficiencies of the separations are in principle better than those obtained with the Dionex system⁷. The absence of a suppressor column and the use of silica based ion exchangers with a mean particle size of 5 or 10 μm result in less peak dispersion.

In Fig. 6A the IC chromatogram of a standard mixture of sodium glycolate and sodium chloride is shown. These two compounds are present in water-methanol extracts of sodium carboxymethyl-cellulose, as is seen in Fig. 6B. Since the efficiency of the carboxymethylation and the degree of substitution can be calculated from the amounts of sodium glycolate and sodium chloride, quantification is important. For these ions a linear relationship between peak area and concentration was established up to an injected amount of 100 μg chloride and 30 μg glycolate; the correlation coefficient was better than 0.9999. The relative standard deviation for the two ions, based on data from six independent measurements, was less than 1% for chloride (at the 20% level) and about 2% for glycolate (at the 5% level).

The sensitivity is reflected in Fig. 7, where the chromatogram of 180 ng nitrate is presented at attenuation position 4 of the Waters R 401 refractive index detector. For this detector the detection limits for some ions are: Cl^- , 20 ng; NO_3^- , 30 ng; SO_4^{2-} , 30 ng; H_2PO_4^- , 50 ng and tetramethylammonium (TMA^+), 50 ng.

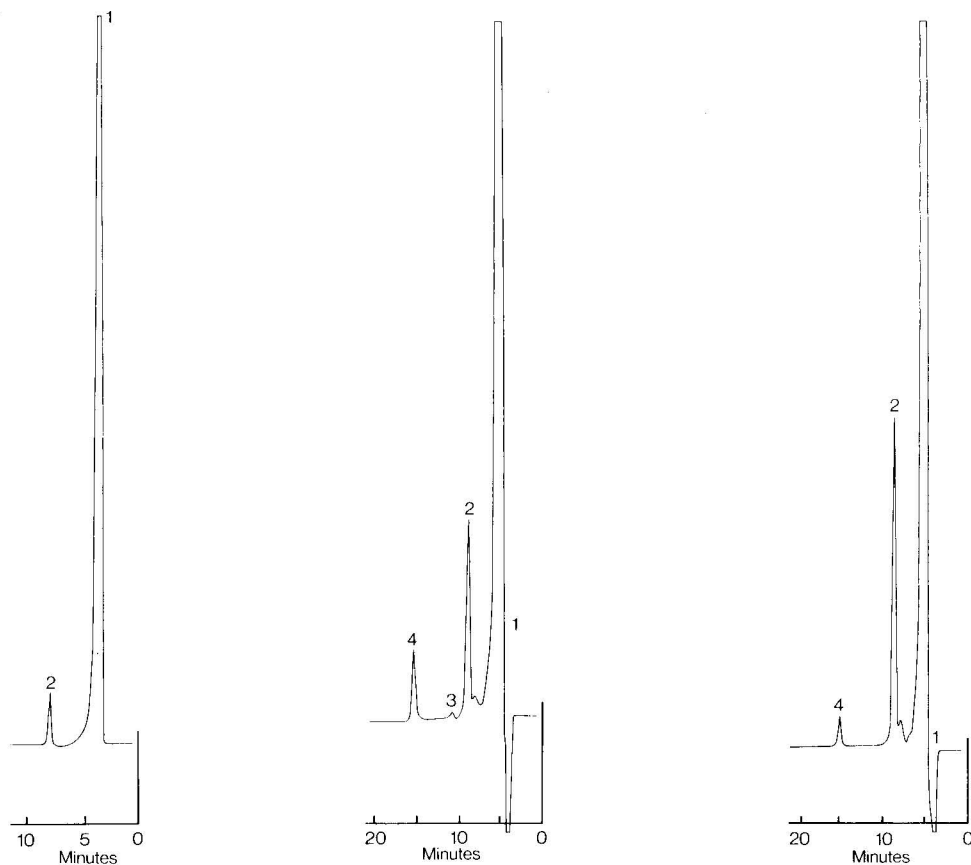


Fig. 7. IC chromatogram of 180 ng nitrate. Column: 150×4.6 Nucleosil 5 SB. Mobile phase: 0.03 *M* sodium salicylate, pH 4.0; flow-rate 0.5 ml/min. Sample size: 20 μ l. Detection: RI, attenuation $\times 4$.

Fig. 8. IC chromatogram of tap-water from Arnhem. Sample size: 100 μ l. Other conditions as in Fig. 7. Peaks: 1 = solvent effect; 2 = chloride; 3 = nitrate; 4 = sulphate.

Fig. 9. IC chromatogram of spring-water from Westervoort. for conditions and peak assignments see Fig. 8.

Figs. 8, 9 and 10 show the chromatograms of 100 μ l tap-water (from Arnhem, The Netherlands), spring-water (Westervoort, The Netherlands) and channel-water (Hengelo, The Netherlands), respectively. Calculations with external standards show that the tap-water contains about 12 mg/l chloride, 10 mg/l sulphate and 300 μ g/l nitrate. It is evident that the sensitivity, which depends to a small extent on the kind of counter ion, can be improved by increasing the concentration of these ions. In this way, less peak dispersion occurs and, accordingly, the peak height increases. On the other hand, it should be borne in mind that the sensitivity decreases with increasing molecular weight (see Figs. 2 and 5).

The sensitivity can also be improved indirectly by concentration methods. The detection limit of sulphate in brine decreased appreciably when the brine solution was first passed through a small amount of a cation exchanger (H^+). The liberated hy-

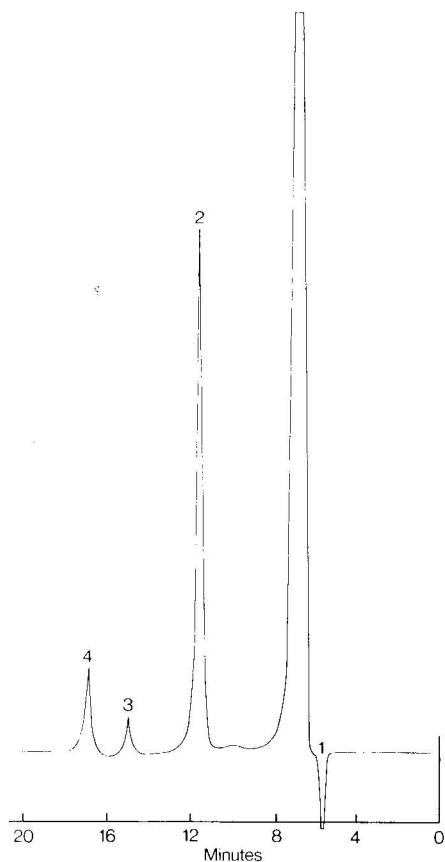


Fig. 10. IC chromatogram of channel-water from Hengelo. Column: Nucleosil 10 SB. Mobile phase: 0.07 *M* sodium *p*-hydroxybenzoate, pH 5.0; flow-rate 0.5 ml/min. Sample size: 20 μ l. Detection: RI, attenuation $\times 8$. Peaks as in Fig. 8.

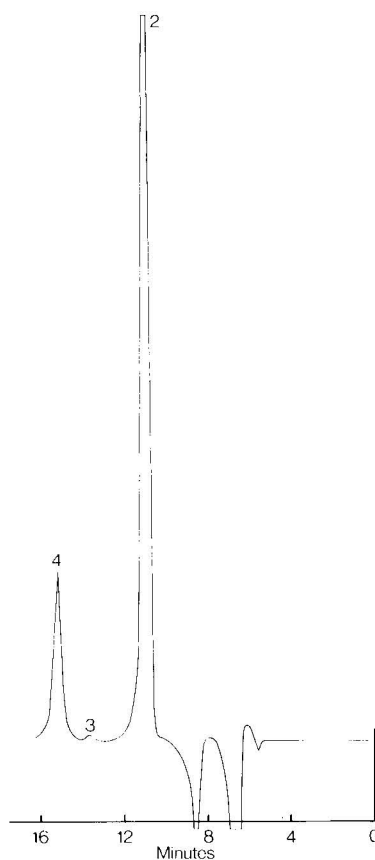


Fig. 11. IC chromatogram of sulphate in brine after cation-exchange treatment. For conditions and peak assignments see Fig. 10.

drochloric acid was evaporated during the concentration of the sulphuric acid, any loss of the latter being prevented by adding one drop of a 0.01 *M* sodium hydroxide solution. A chromatogram representing 200 mg sulphate per kg brine is given in Fig. 11.

For the separation of cations, aromatic cations have to be used as counter ions. With a Nucleosil 10 SA column and trimethylphenylammonium as the counter ion, a baseline separation has been obtained for mono-, di- and triethylamine (Fig. 12).

The advantages of IC with RI detection can be summarized as follows:

no suppressor column is required so that peak dispersion is less, resulting in a better resolution; moreover, no regeneration step has to be included

any ion-exchange material, silica or polystyrene based, can be applied, not only specially prepared low capacity separation columns

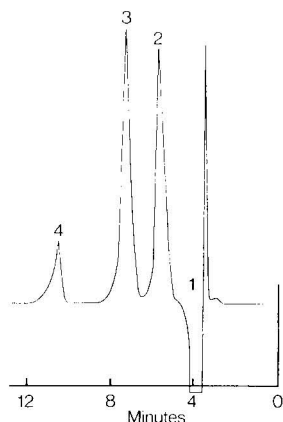


Fig. 12. IC chromatogram of ethylamines. Column: 250×4.6 mm Nucleosil 10 SA. Mobile phase: $0.03 M$ trimethylbenzylammonium formate, pH 3.5; flow-rate 1.0 ml/min. Sample size: $20 \mu\text{l}$. Detection: RI, attenuation $\times 8$. Peaks: 1 = solvent effect; 2 = monoethylamine ($40 \mu\text{g}$); 3 = diethylamine ($60 \mu\text{g}$); 4 = triethylamine ($60 \mu\text{g}$).

no special equipment is needed; the separations can be achieved on any liquid chromatograph equipped with a differential refractometer
the sensitivity is within the nanogram range.

ACKNOWLEDGEMENTS

I wish to thank Mrs. E. E. Hnatiuk-de Rooij and Miss M. Hendriks for their technical assistance and Mr. W. B. M. Holthausen for his help in developing the chloride and glycolate determination in carboxymethyl-cellulose.

REFERENCES

- 1 H. Small, T. S. Stevens and W. C. Bauman, *Anal. Chem.*, 47 (1975) 1801.
- 2 D. T. Gjerde, J. S. Fritz, and G. Schmuckler, *J. Chromatogr.*, 186 (1979) 509.
- 3 D. T. Gjerde and J. S. Fritz, *J. Chromatogr.*, 176 (1979) 199.
- 4 I. Molnár, H. Knauer and D. Wilk, *J. Chromatogr.*, 201 (1980) 225.
- 5 V. T. Turkelson and M. Richards, *Anal. Chem.*, 50 (1978) 1420.
- 6 K. Tanaka, T. Ishizuka and H. Sunahara, *J. Chromatogr.*, 174 (1979) 153.
- 7 *Dionex Application Notes*, Dionex Corporation, 1228 titan Way, Sunnyville, CA, U.S.A., 1978, 1979.

CHROM. 14,041

SEPARATION AND DETERMINATION OF PHENYL ISOCYANATE-DERIVATIZED CARBOHYDRATES AND SUGAR ALCOHOLS BY HIGH-PERFORMANCE LIQUID CHROMATOGRAPHY WITH ULTRAVIOLET DETECTION

BÖRJE BJÖRKQVIST

Kemira Oy, Espoo Research Centre, P.O. Box 44, SF-02271 Espoo 27 (Finland)

SUMMARY

The free hydroxyl groups of saccharides and sugar alcohols react with phenyl isocyanate to yield very stable and strongly UV-absorbing derivatives, which possess good chromatographic properties in a reversed-phase system. UV monitoring at *ca.* 240 nm allows detection down to the 0.5–10 ng level.

Reducing sugars yield a peak for each enantiomer, while non-reducing sugars and sugar alcohols yield a single peak. The chromatograms resemble those obtained by gas-liquid chromatography after silylation.

Oligomers containing eight glucose units have been separated with good resolution by this method. Applications to the separation and determination of sugar alcohols and wood hydrolysates are described.

INTRODUCTION

Underivatized carbohydrates are usually separated and determined by high-performance liquid chromatography (HPLC) using bonded aminophases¹, amino-modifiers on silica² or ion exchangers³ together with a refractive index (RI) detector. This allows detection down to the μg level.

Trimethylsilylation followed by gas chromatography (GC)⁴ results in a detection limit of *ca.* 10 ng of the carbohydrate. A peak for each anomeric form (if present) is obtained. Nachtmann and Budna^{5,6} have described the use of 4-nitrobenzoyl chloride as derivatizing agent for carbohydrates and related compounds. The derivatives are chromatographed in a straight phase system and monitored by UV detection at 260 nm. The anomers are well separated and the detection limit is at the nanogram level for the appropriate carbohydrate.

The use of phenyl isocyanate (PHI) as derivatizing agent for compounds containing active hydrogen atoms, such as alcohols, water and amines, has been described in our previous papers^{7–9}. PHI also reacts with the free hydroxyl groups of carbohydrates and sugar alcohols. The resulting derivatives are very stable and show excellent chromatographic properties in a reversed-phase system. UV-monitoring at 240 nm permits detection down to the nanogram level.

The corresponding chromatograms resemble those of GC following silylation, *i.e.*, reducing sugars give a peak for each enantiomer while non-reducing sugars and sugar alcohols give a single peak. Thus five peaks of derivatized L(+)-arabinose and one peak of derivatized sucrose are obtained. Oligomers containing up to eight glucose units have been separated with good resolution by this method.

EXPERIMENTAL

Apparatus

A Varian 5020 gradient liquid chromatograph (Varian Aerograph, Walnut Creek, CA, U.S.A.) equipped with either a Perkin-Elmer LC-55B or LC-75 variable-wavelength UV-VIS detector (Perkin-Elmer, Oak Brook, IL, U.S.A.), a Goerz-Servogor 541 recorder (Goerz Electro, Vienna, Austria), a Valco loop injector and self-packed Spherisorb 5 ODS columns (125, 160 or 250 \times 4.6 mm I.D.) (Phase Separations, Deeside Industrial Estate, Clwyd, Great Britain) was used for the chromatographic separation and detection of the derivatives. A Hewlett-Packard 3352 Lab Data System (Hewlett-Packard, Karlsruhe, G.F.R.) was used to calculate retention times and peak areas.

Reagents

The eluent was a mixture of acetonitrile (HPLC Grade S; Rathburn Chemicals, Walkerburn, Great Britain) and 0.01 M K_2HPO_4 adjusted to pH 7 with H_3PO_4 in twice distilled water. Phenyl isocyanate (PHI), methanol and pyridine (E. Merck, Darmstadt, G.F.R.) were of analytical grade.

The sugars and sugar alcohols (E. Merck, except for cellobiose, Koch-Light, and maltotriose, Sigma) were of biochemical grade. Commercial oligomers having more than three glucose units could not be found. Caution: use of a fume cupboard is recommended when handling PHI, because it is an eye and respiratory irritant.

Derivatization procedure

Tertiary nitrogen atoms seem to catalyze PHI reactions. Dimethylformamide (DMF) has proven to be an excellent solvent when derivatizing, *e.g.*, aliphatic alcohols and amines^{7,9}, but in this case pyridine was chosen. It has the same catalytic properties but is a better solvent for sugars and sugar alcohols than DMF.

Standards. A 1-ml volume of a standard solution containing about 2 mg sugar per ml of pyridine was pipetted into a 10-ml measuring flask equipped with a short magnetic rod. The flask was placed in a 323°K oil-bath on a heatable magnetic stirrer. A 2-ml volume of PHI was added and the mixture allowed to react for 1 h in the stoppered flask. A 1-ml volume of methanol was added to the cooled flask in order to destroy the excess of PHI. After 5 min the measuring flask was filled to the mark with either pyridine or DMF. Appropriate dilutions were made so that the injected solution usually contained <0.1 mg/ml of each sugar in the calibration solution.

Samples. Aqueous samples containing not more than 1 mg of each sugar to be determined were brought to dryness in a 10-ml test-tube in a rotary evaporator. A short magnetic rod, 1 ml of pyridine and 2 ml PHI were added, the tube was stoppered and treated in the same way as for the standards. The reaction mixture was then transferred into a 10-ml measuring flask and filled to the mark. Solid samples or dry samples in pyridine were directly weighed or pipetted into the measuring flask.

Blanks. It is advisable to prepare a blank in the same way as for the standards in order to check the "purity" of the chromatogram in the carbohydrate region.

Liquid chromatographic separation and quantitation

Derivatized samples and standards dissolved in pyridine or pyridine-DMF and free of particulate matter were injected (1–5 μ l) into the chromatographic system via the Valco loop injector. To avoid tailing of the pyridine peak, it is important to turn the valve back to the load position after *ca.* 5 sec.

The Spherisorb 5 ODS column was at ambient temperature. The eluent, consisting of water and acetonitrile, was pumped (2 ml/min) either isocratically or using different gradients depending on the quality of the compounds to be determined. The peaks were monitored at 240 nm (Fig. 1). It is also important to employ low concentrations of the individual derivatives, usually <0.1 mg/ml as free sugar or sugar alcohol, so that they fall in the relatively narrow linear range.

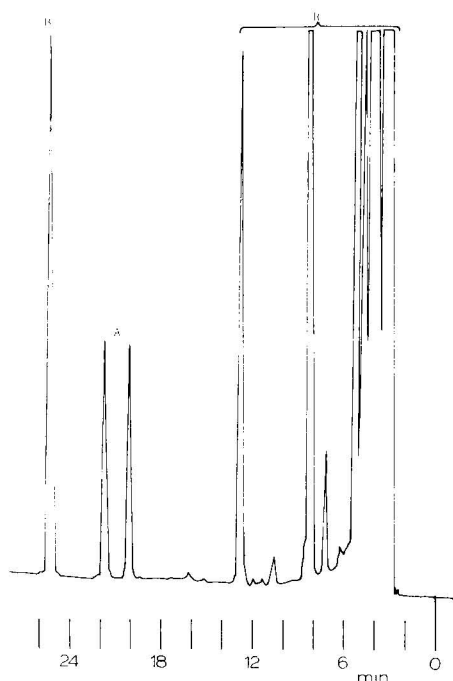


Fig. 1. Chromatogram of derivatized galactose and sorbitol. Column: Spherisorb 5 ODS, 120 \times 4.6 mm I.D. UV detection at 240 nm, 0.05 a.u.f.s. Gradient: 45–80% acetonitrile at 1%/min. Peaks: R = reagents; A = α - and β -galactose; B = sorbitol.

Quantitation was carried out either in the usual way⁸ using, *e.g.*, O-nonyl-N-phenylurethane or derivatized sorbitol as internal standard, or by the method of Nachtmann and Budna⁶ which means that each reacted hydroxy group gives rise to a constant increase of the extinction coefficient. Thus a certain "response factor", *f*, for each known sugar can be calculated using eqns. 1 and 2:

$$C_{\text{sugar}} = \frac{A_{\text{sugar}}}{A_{\text{standard}}} \cdot \frac{C_{\text{standard}}}{f} \quad (1)$$

$$f = \frac{MW_{\text{standard}}}{MW_{\text{sugar}}} \cdot \frac{n(\text{OH})_{\text{sugar}}}{n(\text{OH})_{\text{standard}}} \quad (2)$$

Where C = amount (concentration) reacted, A = peak area, MW = molecular weight and $n(\text{OH})$ = number of hydroxy groups reacted.

In this work sorbitol ($n = 6$) was used as internal standard. The Hewlett-Packard Lab Data System was employed for peak area calculations.

RESULTS AND DISCUSSION

Amount of PHI, reaction time and temperature, destruction of excess of PHI

Alcohols, amines, carboxylic acids and water react with PHI. Therefore a large excess of the derivatizing agent should be used, at least with unknown samples. Water should be removed before derivatization^{8,9}. In contrast to amines and aliphatic alcohols, carbohydrates and sugar alcohols do not react at room temperature. Various temperatures and reaction times were tested but the "smoothest" reaction conditions were found to be 1 h at 323°K; a time of 15 min at 353°K could also be used, at least for non-degradable sugars.

PHI reacts under these conditions with all free hydroxyl groups of the sugar or sugar alcohol. This was shown by infrared and ¹³C nuclear magnetic resonance studies of the crystalline derivative of D(+)-glucose.

The excess of PHI must be destroyed before injection. Otherwise it reacts with water in the column. Methanol was found to be a suitable reagent for this purpose because the corresponding urethane is eluted before the sugar derivatives. It is advisable to cool the reaction vessel before adding methanol.

Standards

Standards were prepared from commercial sugars and sugar alcohols, when available, by the procedure mentioned above. Crystalline derivatives were not prepared except for D(+)-glucose, because they always tend to contain diphenylurea, the reaction product of water and PHI.

Oligomers were prepared from acid-hydrolyzed cellulose. No standards were available and peaks were identified from a comparison of the measured retention times with those of standard pentoses, hexoses and di- and trisaccharides (Figs. 2 and 3). A mass spectrometric study or exclusion chromatography would probably give further confirmation of these "unknown" peaks, but no such work has yet been done.

Note: Fructose decomposes during the derivatization procedure.

Stability of the derivatives

Derivatized standards and samples were stored in solution at room temperature for several days with no noticeable changes in the chromatograms. The urethane bond is not very pH-sensitive.

Liquid chromatography

As mentioned above, reducing sugars yield a peak for each enantiomeric form present. Thus, five peaks of derivatized L(+)-arabinose, three of D(+)-xylose, two of D(+)-glucose, etc., are obtained. This also leads to some degree of overlapping of

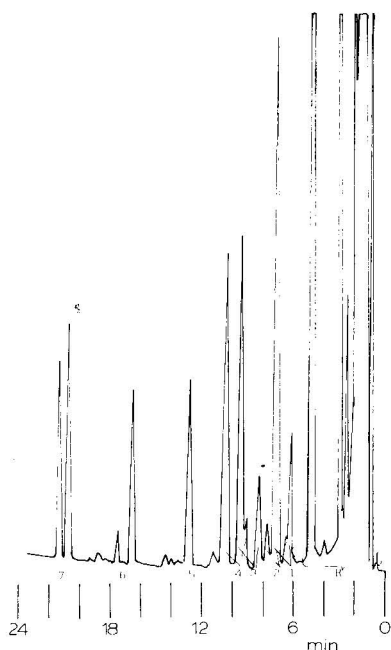


Fig. 2. Chromatogram of mono-, di- and trisaccharides. Column: Spherisorb 5 ODS, 150 \times 4.6 mm I.D. Gradient elution: 55–95% acetonitrile in 25 min. UV detection at 240 nm, 0.08 a.u.f.s. Peaks: R = reagents; 1 = xylose; 2 = arabinose; 3 = glucose; 4 = mannose; 5 = sorbitol (0.03 mg/ml internal standard); 6 = cellobiose; 7 = maltotriose. Injection: 2 μ l, *ca.* 0.06 mg/ml of each saccharide.

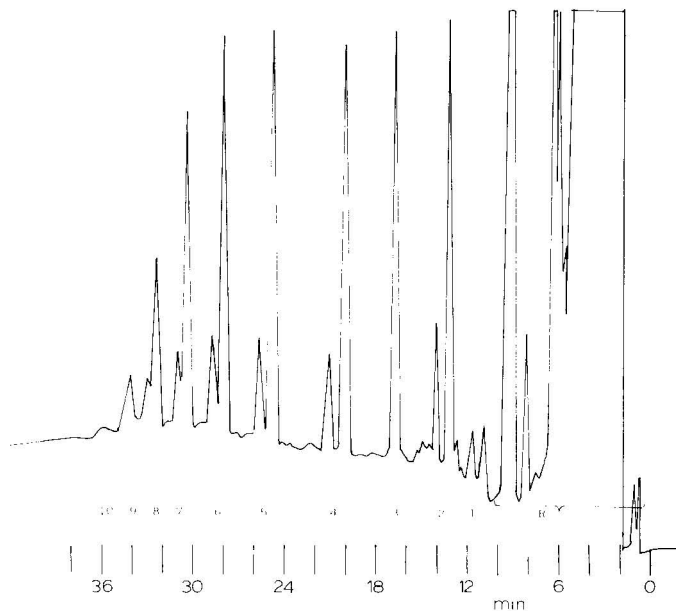


Fig. 3. Chromatogram of cellulose hydrolysate. Conditions as in Fig. 1. Gradient: 55–99% acetonitrile in 30 min. Peaks: R = reagents; 1 = pentoses; 2 = hexoses; 3 = sorbitol (internal standard); 4 = di-; 5 = tri-; 6 = tetra-; 7 = penta-; 8 = hexa-; 9 = hepta-; 10 = octasaccharide.

similar sugars (Fig. 2). The ratio between, *e.g.*, the α - and β -forms, varies depending on the origin of the sample and whether it is dissolved in pyridine before adding PHI. The sugars are eluted in the order of the number of free hydroxyl groups present in the original compound. Thus, pentoses are eluted before hexoses which are eluted before disaccharides, etc.

Non-reducing sugars and sugar alcohols (Fig. 4) yield a single peak as expected.

Linear gradients, starting from at least 45% acetonitrile, were usually employed to elute the compounds. To avoid tailing of pyridine the water was adjusted to *ca.* pH 7.2. Column lengths varied from 12.5 to 25 cm (0.46 cm I.D.), but *ca.* 15 cm packed with 5- μ m ODS particles is sufficient for most purposes. Oligomers containing eight glucose units could be eluted by using this chromatographic system.

Detection and linearity

The derivatives show a very strong UV maximum at *ca.* 240 nm. This enables

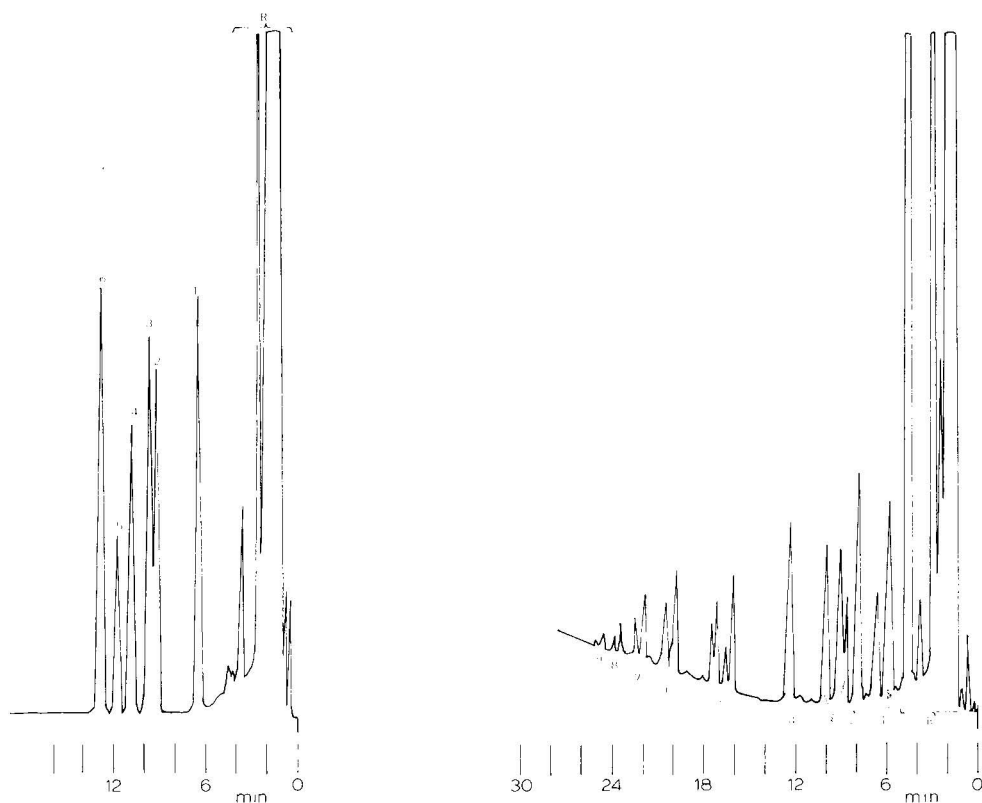


Fig. 4. Chromatogram of sugar alcohols. Conditions as in Fig. 2. Peaks: R = reagents; 1 = erythritol; 2 = arabitol; 3 = xylitol; 4 = rhamnitol; 5 = dulcitol; 6 = sorbitol + mannitol.

Fig. 5. Chromatogram of wood hydrolysate. Conditions as in Fig. 2. Peaks: R = reagents; 1 = xylose; 2 = glucose; 3 = mannose; 4 = sorbitol (internal standard); 5 = di-; 6 = tri-; 7 = tetra-; 8 = penta-; 9 = hexasaccharide.

detection down to the 0.5–10 ng level of the starting compound. A 1-ng amount of sorbitol gave a signal to noise ratio of 1:12.

The derivatization is quantitative, as shown by the reaction of various amounts of D(+) -glucose with PHI.

Derivatized D(–)-sorbitol was used as internal standard. Quantitation was by the usual internal standard method and by use of eqns. 1 and 2. The graphic plot of concentration vs. peak area was shown to be linear in the range 5–1000 ng counted as *e.g.* free glucose. If larger amounts are injected the curve becomes non-linear. This is due to peak broadening and poor resolution because of the relatively high molecular weights of the derivatives. For examples glucose (MW 180) has $MW = 180 + 5 \times 120$ (PHI) = 780 when derivatized. Raising the column temperature to, *e.g.*, 323°K may extend the range of linearity.

Applications

This method has mainly been used to determine the content of mono, di-, tri- and oligomeric sugars in wood hydrolysates (Fig. 5). Since the anomer ratio was not of interest, no attempts were made to keep it constant, not even in the derivatization of standards. Sugar alcohols in various samples have also been determined by this method.

During the evaluation of the method the following sugars and sugar alcohols were derivatized with good results: D(–)-ribose, L(+)-arabinose, D(+)-xylose, L(+)-rhamnose, D(+)-mannose, D(+)-galactose, D(+)-glucose, maltose, lactose, sucrose, D-cellobiose, maltotriose, *meso*-erythritol, D(+)-arabitol, xylitol, dulcitol, rhamnitil, D(–)-sorbitol and mannitol.

REFERENCES

- 1 R. Schwarzenbach, *J. Chromatogr.*, 117 (1976) 206–210.
- 2 K. Aitzetmüller, *J. Chromatogr.*, 156 (1978) 354–358.
- 3 M. R. Ladisch and G. T. Tsao, *J. Chromatogr.*, 166 (1978) 85–100.
- 4 A. E. Pierce, *Silylation of Organic Compounds*, Pierce, Rockford, IL, 1968, pp. 259–331.
- 5 F. Nachtmann, *Z. Anal. Chem.*, 282 (1976) 201–213.
- 6 F. Nachtmann and K. W. Budna, *J. Chromatogr.*, 136 (1977) 279–287.
- 7 B. Björkqvist and H. Toivonen, *J. Chromatogr.*, 153 (1978) 265–270.
- 8 B. Björkqvist and H. Toivonen, *J. Chromatogr.*, 178 (1979) 271–276.
- 9 B. Björkqvist, *J. Chromatogr.*, 204 (1981) 109–114.

CHROM. 14,029

LIMITS OF THE INTERNAL STANDARD TECHNIQUE IN CHROMATOGRAPHY

P. HAEFELFINGER

Biological Pharmaceutical Research Department, F. Hoffmann-La Roche & Co., Ltd., CH-4002 Basle (Switzerland)

SUMMARY

By use of the law of propagation of error it is possible to determine how the internal standard technique affects the reproducibility of a given chromatographic analysis. The usefulness of this procedure is demonstrated with practical examples. Guidelines are provided for the proper application of the internal standard technique in the analysis of drugs in biological materials. It can be shown that, in practice, an external calibration is often advantageous compared to the internal standard technique.

INTRODUCTION

The internal standard technique is widely used in chromatography. In this approach an accurate amount of a known compound is added to the sample solution prior to analysis. Thereby errors in the analytical measurement are often reduced, since any loss of sample is compensated by the loss of an equivalent amount of internal standard. Instead of the absolute value of the peak height (or peak area), the ratio of the peak height of the compound to the peak height of the internal standard is used in calibration and in the evaluation of the unknown samples.

In gas chromatography (GC), where small quantities (often only a few microlitres) are injected onto the column, the internal standard technique considerably improves the reproducibility of determinations. The volumes injected in high-performance liquid chromatography (HPLC) are much higher and yield a better precision of injection. With modern sample injectors, the precision of injection is reported to be 0.3% for partial loop filling and 0.05% for complete loop filling¹. These excellent results were obtained without the use of an internal standard. Therefore the question arises as to whether, in HPLC procedures, the addition of an internal standard is necessary.

Furthermore, some critical remarks have recently been published² about the usefulness of the internal standard technique in the analysis of drugs. In the present paper it will be shown by means of the law of propagation of error how an internal standard can improve or impair the reproducibility of an assay. The application of the formulae is illustrated by experimental data.

THEORETICAL

Law of propagation of error in the internal standard technique

Some simple formulae may be used to get information about the precision of the quantitative evaluation of chromatographic procedures, both with and without an internal standard.

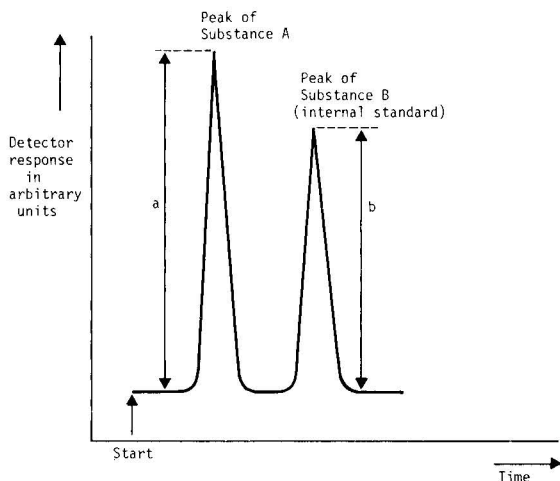


Fig. 1. Chromatogram of a substance A and internal standard B.

In Fig. 1 a chromatogram is shown of two substances. This record could originate from a GC, HPLC or thin-layer chromatographic separation. Peak A is the signal of the substance to be determined and peak B that of the internal standard. The corresponding peak heights (or peak areas) are a and b . If the same sample amount is chromatographed repeatedly, the peak heights show distinct variations. A measure of this variation, corresponding to the precision of the determinations, is the relative standard deviation, also called the coefficient of variation. The following symbols and definitions will be used.

For peak A (substance to be determined) the standard deviation of the peak height a

$$s_a = \sqrt{\frac{\sum_{i=1}^n (a_i - \bar{a})^2}{n - 1}} \quad (1)$$

where n is the number of the individual measurements a_i . The relative standard deviation of a

$$s_{a, \text{rel}} = s_a / \bar{a} \quad (2)$$

where $\bar{a} = \sum_{i=1}^n a_i / n$, the mean of individual values.

For peak B (internal standard) the standard deviation of the peak b

$$s_b = \sqrt{\frac{\sum_i^n (b_i - \bar{b})^2}{n - 1}} \quad (3)$$

where n is the number of the individual measurements b_i . The relative standard deviation of b

$$s_{b,\text{rel}} = s_b/\bar{b} \quad (4)$$

where $\bar{b} = \sum_i^n b_i/n$, the mean of the individual values.

In the internal standard technique the quotient Q_i , rather than the absolute values a_i , is used:

$$Q_i = a_i/b_i$$

For this quotient the standard deviation

$$s_Q = \sqrt{\frac{\sum_i^n (Q_i - \bar{Q})^2}{n - 1}} \quad (5)$$

where n is the number of the individual ratios Q_i , and the relative standard deviation

$$s_{Q,\text{rel}} = s_Q/\bar{Q} \quad (6)$$

where $\bar{Q} = \sum_i^n Q_i/n$. If the internal standard technique improves the precision of a method

$$s_{Q,\text{rel}} < s_{a,\text{rel}} \quad (7)$$

or:

$$s_{Q,\text{rel}}^2 < s_{a,\text{rel}}^2 \quad (7')$$

It is obvious that the relative standard deviation of the quotient, $s_{Q,\text{rel}}$, is related to the relative standard deviations $s_{a,\text{rel}}$ and $s_{b,\text{rel}}$. From the theory of propagation of error^{3,4}

$$s_Q^2 \approx \left(\frac{\bar{a}}{\bar{b}}\right)^2 \left[\left(\frac{s_a}{\bar{a}}\right)^2 + \left(\frac{s_b}{\bar{b}}\right)^2 - 2 \cdot \frac{s_{ab}}{\bar{a}\bar{b}} \right] \quad (8)$$

where $s_{ab} = (1/n - 1) \sum_i^n (a_i - \bar{a})(b_i - \bar{b})$. When \bar{a}/\bar{b} is approximated by \bar{Q} , relation 8 can be transformed to:

$$s_{Q,\text{rel}}^2 \approx s_{a,\text{rel}}^2 + s_{b,\text{rel}}^2 - 2 \cdot \frac{s_{ab}}{s_a s_b} \cdot \frac{s_a}{a} \cdot \frac{s_b}{b} \quad (9)$$

Using the definition^{4,5} of the correlation coefficient $r = s_{ab}/s_a s_b$ one obtains:

$$s_{Q,\text{rel}}^2 \approx s_{a,\text{rel}}^2 + s_{b,\text{rel}}^2 - 2rs_{a,\text{rel}}s_{b,\text{rel}} \quad (10)$$

This approximation approaches equality as $s_{a,\text{rel}}$ and $s_{b,\text{rel}}$ tend to zero. In general, values of less than 10 % are allowable. The approximation for $s_{Q,\text{rel}}^2$ can be substituted in eqns. 7 and 7' respectively

$$s_{a,\text{rel}}^2 + s_{b,\text{rel}}^2 - 2rs_{a,\text{rel}}s_{b,\text{rel}} < s_{a,\text{rel}}^2$$

and rearrangement yields:

$$s_{b,\text{rel}} < 2rs_{a,\text{rel}} \quad (11)$$

Only if this relation holds true will an internal standard procedure improve a particular method.

The correlation coefficient is within the limits⁵ $-1 \leq r \leq +1$. Furthermore $s_{a,\text{rel}}$ and $s_{b,\text{rel}}$ are positive, therefore the relation 10 can only hold true if $r > 0$. This requirement is obvious, since a positive correlation must exist between the peak height of the internal standard and of the analyte.

Some special cases are now discussed.

(1) *Correlation coefficient $r = +1$.* There is a strong linear correlation between the peak heights a and b . Formula 11 yields $s_{b,\text{rel}} < 2s_{a,\text{rel}}$. This means that the precision of a method cannot be improved with an internal standard, even under best correlation, if the relative standard deviation of the internal standard is more than twice the relative standard deviation of the substance to be determined.

(2) *The relative standard deviations of the substance to be determined and of the internal standard are of equal size: $s_{a,\text{rel}} = s_{b,\text{rel}}$.* In this case formula 11 gives $r > 0.5$. Only if the correlation coefficient between a and b is larger than 0.5 will use of the internal standard improve the precision.

(3) *The relative standard deviation of the substance to be determined is twice that of the internal standard.* In this case, use of the internal standard improves the precision of the method, if $r > 0.25$. This finding can be generalized: The smaller $s_{b,\text{rel}}$ is compared to $s_{a,\text{rel}}$, the weaker will be the correlation between a and b .

Practical examples will illustrate the usefulness of formula 11. In all the cases described below, the relative standard deviations are expressed as a percentage.

Practical examples

In many cases the relative standard deviations s_a and s_b are not calculated and only $s_{Q,\text{rel}}$ is evaluated, but the data required to calculate $s_{a,\text{rel}}$ and $s_{b,\text{rel}}$ are available. With the small advanced calculators of today it is possible to get all the parameters needed with minimal effort.

Example 1: HPLC with manual injection and partial loop filling. The same volume (100 μl) of a mixture of the substance to be determined and the internal standard was injected several times and chromatographed. The loop volume was 200

TABLE I

EXAMPLE 1: HPLC WITH MANUAL INJECTION AND PARTIAL LOOP FILLING

Correlation coefficient, $r = +0.949$.

Injection No.	Peak height, a , of substance A (mm)	Peak height, b , of substance B (internal standard) (mm)	Peak height ratio, Q
1	96	98	0.9796
2	101.5	104	0.9760
3	100	103	0.9702
4	100.5	104	0.9663
5	98.5	102	0.9657
6	101	104	0.9712
7	100	102	0.9804
8	97.5	101	0.9653
9	98.5	101.5	0.9704
10	101.5	104.5	0.9713
11	100	104	0.9615
12	101	104.5	0.9665
	$\bar{a} = 99.7$	$\bar{b} = 102.7$	$\bar{Q} = 0.9704$
	$s_{a,rel} = 1.7\%$	$s_{b,rel} = 1.9\%$	$s_{Q,rel} = 0.60\%$

μl . The calculated peak heights are in Table I. To interpret the results the individual relative standard deviations of signals A and B and the correlation coefficient have to be calculated. They are: $s_{a,rel} = 1.7\%$, $s_{b,rel} = 1.9\%$ and $r = +0.949$. Substitution of these values in formula 9 gives an estimation of the relative standard deviation of the ratio: $s_{Q,rel}^2$ (approx.) $\approx 1.7^2 + 1.9^2 - 2 \cdot 0.949 \cdot 1.7 \cdot 1.9$, i.e., $s_{Q,rel}$ (approx.) = 0.61% . This value is in good agreement with the value (0.60%) found directly with formula 6.

In this example the precision of the volume of injection is the limiting factor and the internal standard technique improves the reproducibility, since the relative standard deviation of the substance to be determined ($s_{a,rel} = 1.7\%$) is much larger than $s_{Q,rel}$ (0.60%). This shows that the imprecision due to the variation of the injection volume can largely be eliminated by use of an internal standard. There exists a high correlation between the peak heights a and b ($r = 0.949$), $s_{a,rel}$ and $s_{b,rel}$ are of the same order of magnitude and therefore the internal standard is appropriate (special cases 1 and 2 respectively).

Example 2: as in example 1, but automatic injection with complete loop filling (100 μl). The peak height measurement was done by a data system. The data are summarized in Table II. The following values were calculated: $s_{a,rel} = 0.82\%$, $s_{b,rel} = 0.89\%$ and $r = +0.496$. Formula 9 yields $s_{Q,rel}$ (approx.) $\approx 0.87\%$. This is again in good agreement with the value (0.81%) calculated directly from formula 6.

In contrast to example 1, use of the internal standard does not improve the precision of the method. The reason is that, when $s_{a,rel}$ and $s_{b,rel}$ are of equal magnitude, then the correlation coefficient must be larger than 0.5 for the internal standard to improve the precision of a procedure (special case 2). This example shows that when an automatic sample injector is used in HPLC the precision of the injection

TABLE II

EXAMPLE 2: HPLC, AUTOMATIC INJECTION WITH COMPLETE LOOP FILLING

Correlation coefficient, $r = +0.496$.

Injection No.	Peak height, a , of substance A (arbitrary units)	Peak height, b , of substance B (internal standard) (arbitrary units)	Peak height ratio, Q
1	1696	1771	0.9577
2	1685	1774	0.9498
3	1665	1772	0.9396
4	1648	1737	0.9488
5	1658	1754	0.9453
6	1678	1746	0.9611
7	1672	1727	0.9682
8	1663	1744	0.9536
9	1673	1756	0.9527
10	1677	1749	0.9588
	$\bar{a} = 1672$	$\bar{b} = 1753$	$\bar{Q} = 0.9536$
	$s_{a,rel} = 0.82\%$	$s_{b,rel} = 0.89\%$	$s_{Q,rel} = 0.87\%$

volume is not the limiting factor for the reproducibility and the internal standard brings no evident advantages.

Example 3: HPLC of plasma extracts. Aliquots of plasma, which had been spiked with the substance to be determined, were mixed with the internal standard and extracted. The extracts were injected with an automatic sample injector with

TABLE III

EXAMPLE 3: HPLC OF PLASMA EXTRACTS WITH AUTOMATIC INJECTION AND COMPLETE LOOP FILLING

Correlation coefficient, $r = -0.672$.

Injection No.	Peak height, a , of substance A (mm)	Peak height, b , of substance B (internal standard) (mm)	Peak height ratio, Q
1	114	119	0.9580
2	112	120	0.9333
3	112	120	0.9333
4	112	120	0.9333
5	112	121	0.9256
6	112	123	0.9106
7	110	122	0.9016
8	111	124	0.8952
9	111	124	0.8952
10	111	125	0.8880
11	111	126	0.8801
	$\bar{a} = 111.6$	$\bar{b} = 122.2$	$\bar{Q} = 0.9140$
	$s_{a,rel} = 0.92\%$	$s_{b,rel} = 1.9\%$	$s_{Q,rel} = 2.6\%$

complete loop filling (100 μ l). The peak heights found are summarized in Table III. The following data were calculated: $s_{a,rel} = 0.92\%$, $s_{b,rel} = 1.9\%$ and $r = -0.672$. Formula 9 gives $s_{Q,rel}$ (approx.) $\approx 2.6\%$, which is equal to the value (2.6%) found with formula 6.

In this example, the internal standard procedure considerably impairs the precision of the assay; instead of $s_{a,rel} = 0.92\%$ a precision of $s_{a,rel} = 2.6\%$ is obtained. There are two reasons for this phenomenon. On the one hand $s_{b,rel}$ is more than twice $s_{a,rel}$; as mentioned under special case 1, even with the best correlation ($r = 1$) use of the internal standard cannot improve the precision under these circumstances. On the other hand, there r is negative and therefore there is no correlation between the signals of substances A and B in the chromatogram. The reasons for this finding will be discussed below.

Example 4: GC of plasma extracts. The following example, from the GC determination of a drug, illustrates the general applicability of formula 11. Plasma

TABLE IV

EXAMPLE 4: GC OF PLASMA EXTRACTS WITH AUTOMATIC INJECTION

Correlation coefficient, $r = +0.558$.

Injection No.	Peak area, a , of substance A (arbitrary units)	Peak area, b , of substance B (internal standard) (arbitrary units)	Peak area ratio, Q
1	2109	1338	1.576
2	2056	1356	1.516
3	1970	1272	1.549
4	1937	1285	1.507
5	1757	1285	1.367
6	1984	1315	1.509
7	1943	1294	1.502
8	1884	1332	1.414
9	1942	1308	1.485
	$\bar{a} = 1954$	$\bar{b} = 1309$	$\bar{Q} = 1.492$
	$s_{a,rel} = 5.1\%$	$s_{b,rel} = 2.2\%$	$s_{Q,rel} = 4.3\%$

extracts containing an internal standard were injected with an automatic sample injector and the peak areas measured with a data system. The results are compiled in Table IV. The values calculated were: $s_{a,rel} = 5.1\%$, $s_{b,rel} = 2.2\%$ and $r = +0.558$. From formula 9, $s_{Q,rel} \approx 4.3\%$, the same value as calculated directly from the ratios of Table IV.

The relative standard deviation of the internal standard, $s_{b,rel}$, is considerably smaller than $s_{a,rel}$ and therefore a correlation coefficient of $+0.556$ is sufficient to improve the precision of the procedure with an internal standard.

DISCUSSION

The variations of the injection volume can be overcome by the internal standard technique as demonstrated by example 1. But in many chromatographic assays

the injection volume is not the only source of the methodological variations. The chromatographic systems are often responsible for fluctuations which are independent of the injection volume. In example 3 the relative standard deviation of the internal standard is larger than that of the substance being analysed. The chromatographic conditions, which are not optimal for the internal standard, are one reason for this effect. The peak shape deviates in some cases from the ideal gaussian curve. Possibly, peak area measurement could improve the precision in this case. However, the main point in this example is the variation of the extraction. Even though the internal standard and the substance to be determined are similar compounds, the extraction behaviour is different and is responsible for the higher relative standard deviation. This phenomenon can be often observed in the analysis of drugs in biological materials². The extraction conditions and the chromatographic system could be changed in example 3. However, this is no guarantee that the precision will be improved, since all the conditions described below must be met. In this example, therefore, external standardization provides the best precision. In the analysis of drugs and metabolites in biological materials the precision of the assays is often in the range of 2–5%. In example 3 a relative standard deviation of 0.9% was found for substance A. It is unlikely that the precision would be improved using an internal standard.

Curry and Whelpton² have mentioned several important points which are often overlooked. It is often fallacious to use a second compound as internal standard for checking the extraction, stability or derivatization: "it is naive to expect two compounds (even homologous) to exhibit identical chemistry —be it extraction, derivatization or stability — and there is no reason to suppose the inclusion of an internal standard will inevitably produce a more satisfactory assay. The probability that the internal standard adversely affects the data should even be considered". Example 3 demonstrates that these remarks are well-founded.

Guidelines for application of the internal standard technique in the assay of drugs in biological materials

The following are general requirements of the internal standard:

- (i) It must be completely resolved in the chromatogram from the other known and unknown substances
- (ii) It must be eluted near the peak of interest
- (iii) The peak height (or peak area) of the internal standard must be similar to that of the substance to be determined
- (iv) It must be chemically similar to the substance of interest
- (v) It must be chemically stable

The following points have to be observed in the analysis of drugs in biological materials:

- (i) The internal standard must be added to the biological samples in solution. Whenever possible, aqueous solutions should be used. After addition, the samples must be mixed thoroughly to obtain a uniform distribution of the internal standard
- (ii) If there are extraction steps prior to chromatography, the internal standard should show similar behaviour to the analyte; namely, the partition coefficients should be equal
- (iii) The internal standard should not be a metabolite of the drug of interest

(iv) The internal standard should not interfere with metabolites of the drug or endogenous compounds

Unsuitable approaches are as follows:

(i) Evaporation of an organic solution of the internal standard and addition of the biological sample to the residue followed by mixing is not recommended. It is impossible to guarantee in each case a complete dissolution of the internal standard under these circumstances.

(iii) The addition of an "internal standard" to the extract after extraction prior to chromatography is only of limited value in HPLC, since with modern injectors excellent precision of the injection volume is obtained. The variation of the injection volume is small, compared to the variation of the clean-up steps. An exception is the case where the extract is injected in a volatile solvent. The addition of an "internal standard" can eliminate evaporation losses.

CONCLUSIONS

The aim of this study was to show that the internal standard technique will not inevitably improve the precision of an assay. In every case the relative standard deviation of both the analyte and internal standard should be considered as well as $s_{a,rel}$, according to the law of propagation of error. In this way it is possible to evaluate whether the precision of a method is better with external calibration or with an internal standard. When use of the internal standard gives no improvement or even impairs the precision the critical steps can be found by the decoding method mentioned. If these steps can be improved or eliminated the internal standard technique should be used. If not, it is better to avoid the use of an internal standard, since it is often easier and less time-consuming to look for a suitable external calibration approach. In any case, if an assay for a drug in biological material has been developed with the use of an internal standard, it should be established that this technique does not impair the precision of the method.

ACKNOWLEDGEMENTS

The author wishes to thank Dr. U. Timm for the data of Table IV and Dr. M. Wall for his helpful discussions.

REFERENCES

- 1 *Technical Notes 1*, Rheodyne, Berkeley, CA, Sept. 1979, pp. 4-5.
- 2 S. H. Curry and R. Whelpton, in E. Reid (Editor), *Blood Drugs and Other Analytical Challenges*, Ellis Horwood, Chichester, 1978, pp. 29-41.
- 3 K. Stange and H. J. Henning (Editors), *Formeln und Tabellen der mathematischen Statistik*, Springer, Berlin, Heidelberg, New York, 2nd ed., 1966, p. 225.
- 4 H. H. Ku, *J. Res. Nat. Bur. Stand., Sect. C*, 70 (1966) 263-273.
- 5 *Wissenschaftliche Tabellen*, Documenta Geigy, Basle, 6th ed., 1960, p. 170.10.

CHROM. 14,181

COMPUTER-CONTROLLED SINGLE-PUMP SOLVENT PROGRAMMER FOR HIGH-PERFORMANCE LIQUID CHROMATOGRAPHY

C. LAURENT*, H. A. H. BILLIET, H. C. VAN DAM and L. DE GALAN

Laboratorium voor Analytische Scheikunde, Technische Hogeschool Delft, Jaffalaan 9, 2628 BX Delft (The Netherlands)

SUMMARY

A solvent programmer for high-performance liquid chromatography is described that consists of a dual-piston reciprocating pump equipped with displacement transducers, and two synchronously switching two-way valves connected to the solvent reservoirs. The system is controlled by a PDP 11/03 microcomputer. The software includes correction for solvent compressibility, generation of gradients of widely varying shape and delivery of binary mixtures between 0 and 100%.

INTRODUCTION

The mobile phase is usually a mixture of two or more solvents in high-performance liquid chromatography (HPLC) especially in the reversed-phase mode. If the composition changes during the chromatographic run, we speak of gradient elution chromatography. More commonly, the mobile phase composition varies between chromatographic runs, because different samples require different mobile phases for optimum separation. In either case it is desirable to make mixtures of arbitrary composition from the parent solvents. To this end a variety of solvent programmers has been developed that can be broadly divided into two categories: dual-pump systems with a mixing chamber at the high-pressure side, and single-pump systems with a switching valve at the low-pressure side. In a previous publication¹ the two designs were compared and it was demonstrated that single-pump programmers can provide optimum performance, provided that the distributing valve between the solvent reservoirs is switched synchronously with the stroke of the pump piston. Specifically, it was shown experimentally that a single-pump system using synchronized valve switching rapidly delivers a very stable mixture. On the other hand, the accuracy of the solvent composition was less than desired, with deviations of up to 18% between the imposed composition and the actual output. Also, the system was not tested for gradient elution, because it was manually operated.

In the single-pump system to be described presently the principle of synchronized valve switching is maintained. The pump is interfaced with a microcomputer to provide gradient elution facilities. The problem of obtaining high accuracy is addressed specifically, because other studies in this laboratory have shown that the

composition of the mobile phase is critically important in reversed-phase liquid chromatography (RPLC)^{2,3}. Accurate solvent composition has also been shown to be essential for predictable gradient elution chromatography^{4,5}.

PRINCIPLE OF OPERATION

A single-pump solvent programmer operates on the principle that the composition of the mixture is determined by the periods during which the distributing valve before the pump is open to either of the parent solvents. For example, if the valve is open to either of two solvents for equal periods of time, then the delivered mixture should contain equal fractions of the two solvents (50:50 composition). In our previous publication¹ we showed that this is indeed the case for the overall composition, averaged over a large number of pumping cycles, but not necessarily for each stroke of the pump piston. In fact, if the switching sequence of the valve is unrelated to the pumpstroke, successive strokes may yield quite different mixtures leading to a periodically varying composition. To a certain extent, the problem can be overcome by incorporating a large mixing chamber after the reciprocating pump, but this makes the system rather sluggish.

It has been pointed out that constant delivery by successive pump strokes is easily accomplished when the valve switching is synchronized with the stroke of the moving piston. In our previous design this was realized with an optical encoder that sent a switching command after a predetermined lapse-time during each refill period of the pump. The delivered mixture was indeed very stable: better than 0.2 % of the actual composition. On the other hand, a certain ratio of the two time fractions in one refill period does not produce the same ratio in the binary composition. The reason for this inaccuracy can be explained as follows.

Understandably, pump manufacturers place great emphasis on the constant flow of the solvent during the delivery period of the piston. Dual pistons with partially overlapping delivery periods, as well as acceleration and retardation of the pistons, are used to provide nearly pulse-free delivery. Much less attention is given to the refill stroke of the piston, with the result that the inflow of the solvent is far from uniform during the refill period. As a result, partitioning of the refill period on a time basis does not yield the expected solvent composition. This is illustrated in Fig. 1, where an experimentally measured refill profile is presented, which is clearly not square-wave. Consequently, switching the distributing valve after 70 % of the total refill time has elapsed does not produce a 70:30 mixture, but in this case a 84:16 mixture. It should be noted that this difficulty is inherent to the synchronization principle. If the valve switching is not synchronized to the piston stroke, the switching moment changes from one stroke to another and the deviations average out to zero. This means that the output of non-synchronized systems fluctuates, but on the average accurately represents the value imposed by time partitioning.

The remedy for this problem seems trivial. Once the refill profile is known, it is easy to draw up a conversion table connecting the desired composition to the switching moment during the refill period. In the example of Fig. 1 a desired composition of 70:30 could be obtained by switching the valve after 59 % of the refill period has elapsed. This can easily be programmed into a computer provided that the refill profile of the pump remains unaltered.

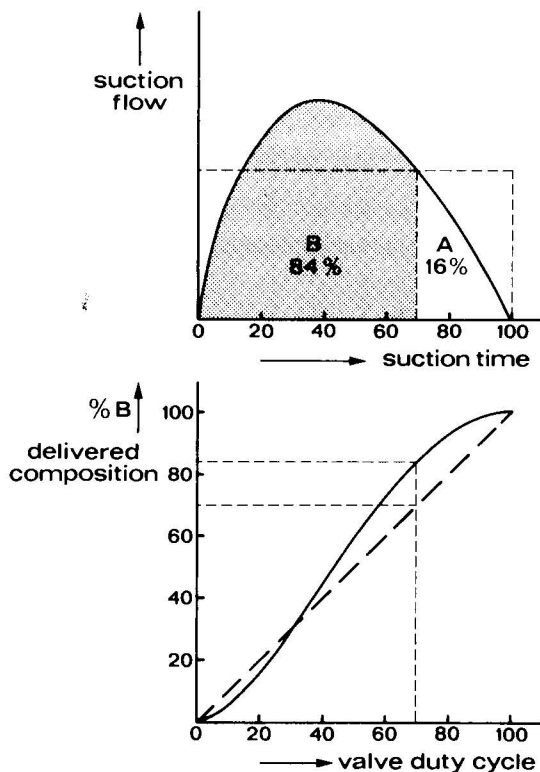


Fig. 1. Inaccuracy of synchronized valve switching based on time partitioning. The lower graph illustrates the non-linear relationship between the delivered binary composition and the fractional periods of the switching valve, if the inlet profile of the reciprocating pump piston is not square-wave as exemplified by the upper graph.

In practice, this condition is not always fulfilled. Certainly, the refill profile varies from one pump to another, requiring calibration for each individual specimen. Also, the refill profile is neither square-wave nor symmetrical, so that the conversion must probably be put in tabular form. More important is the fact that some reciprocating pumps incorporate a pressure feed-back device that again ensures constant-delivery flow independent of column resistance or solvent viscosity. As a result, however, the refill profile of such pumps varies in shape and duration with the pressure after the pump. This makes synchronized valve switching on a time basis quite impossible and, consequently, this principle would lose its general applicability.

It must be realized that the integrated refill profile at the top of Fig. 1 actually represents the non-linear movement of the piston in the pump chamber. Consequently, the switching command to the valve should not be based on the time elapsed since the turning moment of the piston, but on the displacement of the piston since its turning point. In that case, the correct solvent composition will always be delivered, independent of any variation in the speed of the piston either during its refill stroke or during an entire chromatogram. The only condition is that the position of the pump piston is monitored continuously, so that the total length of the piston stroke can be determined and switching commands to the valve can be issued at the appropriate

position. A possible solution will be presented in the next section. Here we note only that it appears to be rather difficult to impose switching commands close to the turning points of the moving piston. Therefore, if the valve is switched only once during each refill stroke, binary mixtures containing only a few percent of one component become rather irreproducible. The precision is significantly enhanced if the valve is switched twice, so that the minor component is bracketed in between the major component. In other words, a switching cycle A/B/A is recommended over a switching cycle A/B. The two switching points should be positioned symmetrically to the midpoint of the piston stroke. The A/B/A switching cycle offers the further advantages of requiring less supervision time from the computer and improved mixing inside the pump chamber. This removes the need for an additional mixing chamber after the pump, so that the solvent delivery system responds rapidly to changes in imposed composition.

CONSTRUCTION

The equipment consists of two Angar Scientific two-way switching valves (368-NO-24-30 Z), and a Pye Unicam LCX-3 dual-piston reciprocating pump equipped with two EMI Labs. SE 373115 displacement transducers. The latter convert the 9-mm stroke of a piston into a voltage varying by about 2 V. The signal from the transducer is sampled every millisecond by a 12-bit analogue-to-digital converter (ADC) and the digitized signal is processed by a DEC Model PDP 11/03 microcomputer supplied with 8 K memory. The configuration is shown in Fig. 2 and will be discussed with reference to Fig. 3, which shows schematically the movement of the two pistons.

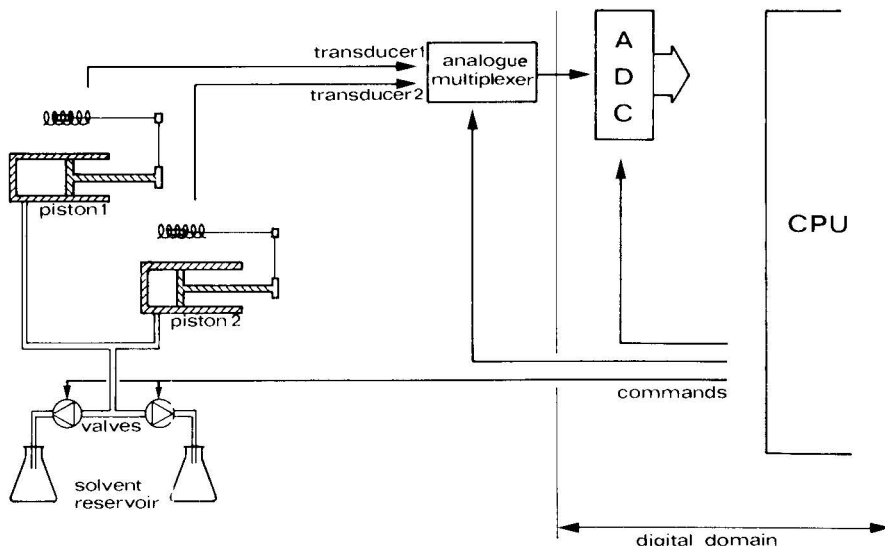


Fig. 2. Schematic picture of the microcomputer controlled single-pump solvent programmer using synchronized valve switching based on position partitioning. Two simultaneously switching two-way valves allow either of two solvents, A or B, to enter the chambers of a dual-piston pump. The position of each piston is detected by a displacement transducer, the digitized signal of which is processed by the microcomputer, indicated in the figure as Central Processing Unit (CPU), to derive the switching commands for the valves.

Let us consider piston 1 just before it ends its delivery stroke. The digitized signal from its displacement transducer is smoothed by a running eight-point averaging routine and the minimum value is stored in the memory. At the end of the refill period the process is repeated to detect the maximum position of piston 1. Because the pistons take more time to deliver the solvent than for refilling there is now a void period, where both pistons 1 and 2 are delivering. This period is used by the computer to calculate the positions of piston 1 where the valve will be ordered to switch from solvent A to B and back again. As discussed in the preceding section, these positions are located symmetrically around the midpoint. Their separation, of course, is determined by the desired composition of the minor component B present with the excess of A. Well before piston 2 reaches the end of its delivery stroke the computer is ready to accept the signals from the displacement transducer of piston 2, whereupon its minimum and maximum position are also stored in the computer memory. In the next void period the computer calculates the switching positions for piston 2.

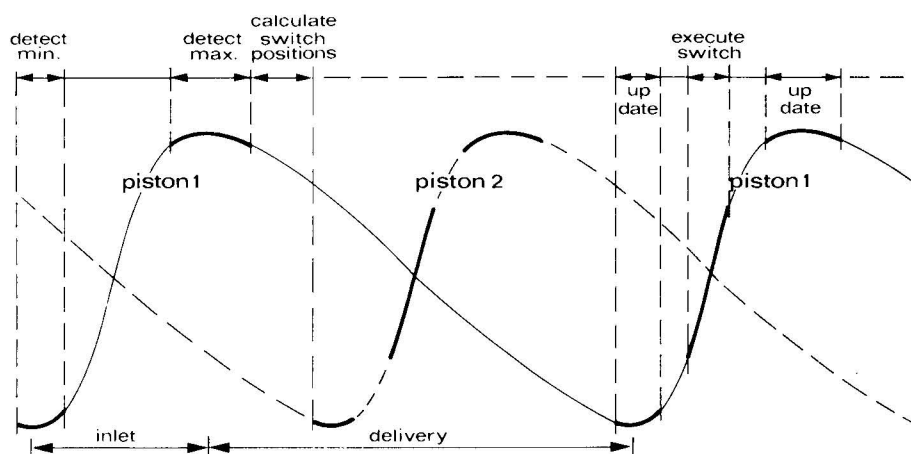


Fig. 3. Sequence of computer operations. The vertical scale represents the transducer signal, indicative of the piston position. Thick line segments represent periods during which the computer supervises the piston movement, thin line segments the void periods reserved for data processing. The sequence of computer operations in the horizontal scale at the top refers to piston 1 and is explained in the text.

Returning to piston 1, the first task of the computer is to update the minimum position of this piston at its turning from delivery to refill. After a brief void period the computer picks up the signal from the displacement transducer of piston 1 again to compare this with the first switching value calculated from the *previous* refill stroke. At the appropriate position a switching command is sent simultaneously to both two-way valves so that component B is allowed to enter the pump chamber. At the second command position the two-way valves are switched back to let solvent A enter the pump chamber again. Once again the computer is momentarily relieved of its supervising task. It then updates the value for the maximum position of piston 1, recalculates the switching positions, returns to piston 2, etc.

The continuous updating of the turning positions of the pistons corrects for drift in the transducer signal, but this drift is small enough to allow extrapolation

from one refill stroke of a piston to the next one. Possible differences between the two pistons are taken into account by using two displacement transducers.

As can be seen in Fig. 3 the total cycle time of a piston is divided into four equal parts. The first quarter is taken up by the refill stroke, the second quarter is free for calculating the switching positions and in the final two quarters these processes are repeated for the other piston. The actual duration of the periods obviously depends upon the imposed flow-rate of the solvent. The present pump is designed for flow-rates up to 10 ml/min, at which rate the piston cycle time is 1200 msec and each quarter takes 300 msec.

Because the transducer signal is sampled every millisecond, the switching points and hence the solvent composition can be determined to better than 1 %. This could be improved by increasing the sampling frequency from the present value of 1 kHz to a few kHz. Obviously, however, the sampling error is already quite insignificant at more common flow-rates of about 2 ml/min.

Similarly, at the highest flow-rate at least 300 msec are available for the computer to calculate the switching positions needed in the next refill stroke. As is clear from Fig. 3, the actual time is even longer if we take into account the two additional void times during each refill stroke. Clearly, 300 msec are abundant for the straightforward calculation of switching positions when the pump is operating in a constant delivery mode, say 30 % B and 70 % A.

In the case of gradient elution the desired solvent composition varies continuously according to an imposed time function. Linear gradients are the most widely used⁶, but in order to test the system more fully, two subroutines that generate more complex gradient shapes have been written in assembler language. The first subroutine permits gradients with the general shape

$$\varphi(t) = \varphi(0) + St^n \quad (1)$$

where $\varphi(t)$ is the volume fraction of solvent B at time t and S the speed of the gradient. The shape of the gradient is determined by the exponent n , which can be selected between 1/9 (convex) through $n = 1$ (linear) and 9 (concave). The second subroutine generates gradients according to

$$\varphi(t) = (1/q) [1 - (1 - q)^{t/t_g}] \quad (2)$$

where t_g is the total gradient time and q has values from 0 (linear gradient) to 0.9 (convex gradient). The shape expressed by eqn. 2 has been proposed by Schoenmakers *et al.*³.

Even at the highest flow-rates the calculation of either gradient did not interfere with the data processing of the transducer signals.

We conclude, therefore, that the proposed system is sufficiently versatile for practical HPLC.

RESULTS AND DISCUSSION

Valve switching

The system described differs in several respects from the design proposed in our previous publication¹. The changes will be discussed first.

The changeover from time partitioning of the refill period to position partitioning of the piston displacement is essential for pumps using pressure feed-back. The feed-back option is designed to ensure constant solvent delivery against variable column pressure. This is realized by adjusting the piston speed at the start of the delivery stroke. As a result, the refill period of the other piston varies, depending on solvent viscosity, column deterioration, etc. Indeed, the calibration curve relating the binary composition to the switching moment is not only non-linear (Fig. 1), but also varies significantly from one solvent to another. By contrast, a similar calibration curve based on piston position is perfectly linear and independent of solvent or of column pressure.

The accurate determination of the total length of the piston stroke is an essential requirement in the present system. Initial attempts to detect the turning points of the pistons by analogue devices failed, because the derivative circuitry is very sensitive to noise in the transducer signal. The use of a microprocessor allows all software functions to be executed in the digital domain. A simple smoothing routine readily overcomes the noise problem and guarantees precise determination of the piston stroke length.

Changing the valve switching routine from A/B to A/B/A improves the mixing of the two solvents inside the pump chamber. It also decreases the period during which the transducer signal must be supervised to execute the valve switching commands. The resulting additional void time can be utilized for composition calculations or other tasks.

Either valve switching routine may be realized by a single three-way valve. However, moderately priced valves take non-negligible time to open or close. In fact, the two lag times are unequal, so that the amount of the interspaced component, B, differs somewhat from its intended value. For example, a typical three-way valve used by us switches in 8 msec to one solvent by applying a 24-V pulse, but takes 43 msec to switch to the other solvent due to a slow spring release. The difference of 35 msec is significant in relation to the total refill time varying between 300 and 3000 msec.

This problem was overcome by replacing the single three-way valve by two symmetrical two-way valves, both of the normally open type. At the start of the refill cycle valve A is open to solvent A and valve B is closed. At the first switching command valve A is closed after 8 msec, whereas valve B is opened only after 43 msec. There is thus a period of 35 msec during which both valves are closed. At the second switching command the situation is reversed: valve B closes rapidly and valve A opens more slowly, again leaving a period of 35 msec with both valves closed. This arrangement gave satisfactory results. A 50:50 mixture could be produced by either sequence A/B/A or B/A/B, *provided no chromatographic column is connected*.

Compressibility correction

With a chromatographic column present the delivered binary composition differs systematically from the imposed composition, as shown in Fig. 4a. Apparently, when operating against column pressure, the contribution of the interspaced minor component is larger than anticipated on the basis of the switching commands. The deviation is proportional to the concentration of the minor component, being larger for more compressible solvents, and increases with the pressure exerted by the pump during delivery.

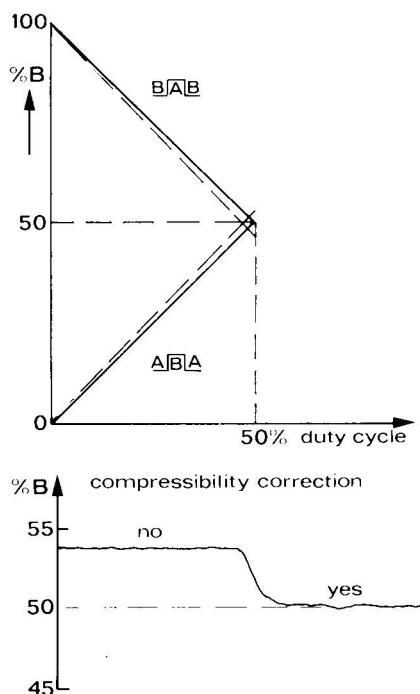


Fig. 4. Influence of the compressibility correction upon the delivered composition. a, Binary composition of a mixture of water (A) and 0.1 % acetone in water (B) as a function of the fractional separation between the two switching positions of the valves; the pump is operating against a pressure of 15 MPa. — — —, Without compressibility correction; - - - -, with compressibility correction after eqn. 4; the same straight lines are observed when the pump is operating at 100 kPa, *i.e.*, without a chromatographic column. b, Generation of a mixture of 50 % methanol and 50 % water against a pressure of 30 MPa, without and with correction for solvent compressibility.

The obvious explanation is that the true refill stroke experienced by the piston is less than derived from the turning positions of the piston. The influences of solvent compressibility and back pressure seem to indicate that the pump piston upon retracting from its delivery stroke does not start to refill the pump chamber immediately. Rather, the release of the pressure induces some back flow of solvent through the outlet valve of the pump chamber. Also, the decompression of the dead volume in the pump chamber and the connection tubes to the outlet and inlet valves will reduce the actual refill stroke length.

The latter effect can easily be expressed mathematically as

$$L^* = L - l \beta P \quad (3)$$

where L^* is the true refill displacement, L is the stroke length derived from the turning points of the piston, l is the equivalent length of the pump dead volume, β is the compressibility of the liquid in the pump chamber and P is the pressure. With this correction the separation between the two positions for the switching commands to the distributing valves becomes

$$D = \varphi L^* = \varphi L (1 - l \beta P/L) \quad (4)$$

where φ is the desired volume fraction of the minor component. Experimentally, the correction factor varies from about 1% for pure water to 3% for pure methanol at 15 MPa. This is in the ratio of the compressibilities of the two solvents. Quantitatively, however, the correction expressed by eqn. 4 can only be reconciled if l/L is taken to be as large as 3. Although the dead volume of the pump is certainly less than the volume of the pump chamber (100 μ l), it appears that eqn. 4 approximately corrects for both solvent compressibility and back-flush through the closing outlet valves (Fig. 4a).

The correction expressed by eqn. 4 can readily be incorporated in the computer program even for mixed solvents, provided that we know the compressibility of mixtures of variable composition. Unfortunately, such information is not available. However, crude interpolation between data for pure liquids appears to yield acceptable results. With the compressibility correction, the calibration curve becomes very accurate, as shown in Fig. 4a. This is also confirmed by the recorder trace of methanol-water (50:50) with and without the correction (Fig. 4b).

Performance

Fig. 5 shows a stepwise and linear variation of a binary mixture of water and methanol. Perfectly linear gradients have been obtained for flow-rates up to 4 ml/min. When the correction for compressibility is applied the accuracy of the delivered binary mixture is better than 1% and over a period of several hours no drift in the composition is noticeable. When the pressure filter of 1.5 ml supplied with the pump is removed, the response of the system to a stepwise variation takes only 0.71 ml, which compares favourably to existing commercial solvent programmers¹.

On the other hand, removal of the pressure filter gave rise to small rapid fluctuations in the delivered binary composition, synchronous to the piston movement (Fig. 6a). The amplitude of the oscillations is proportional to the concentration of the

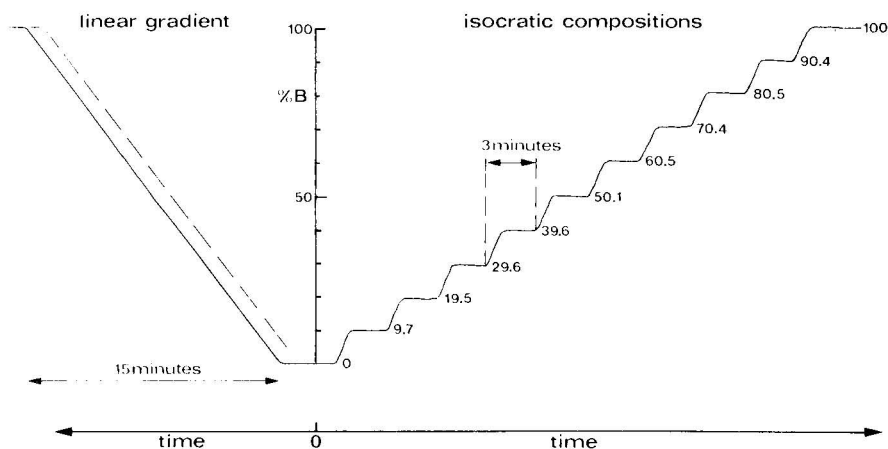


Fig. 5. Generation of linear gradient (left) and isocratic mixtures (right) against 15 MPa with compressibility correction. Flow-rate: 1 ml/min. The dashed line shows the imposed gradient and the solid curve represents the delivered gradient measured at the top of the chromatographic column. Isocratic compositions are varied in steps of 10%, and the numbers represent the experimentally obtained binary compositions.

minor component and rarely exceeds 0.1 %. Apparently, the effect is due to a slight mismatch of the two transducer units. As is clear from Fig. 6b, it is readily overcome by including the pressure filter, which acts as a mixing chamber, but obviously this lengthens the response time of the system.

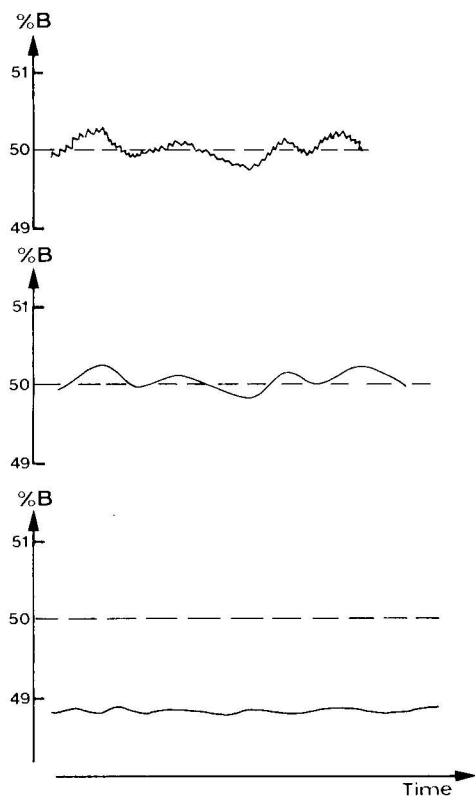


Fig. 6. Stability of the delivered composition intended to be 50 % methanol and 50 % water (worst case). a, Without pressure filter; b, with pressure filter added to the pump; c, with strong analogue filtering of the transducer signals.

Unfortunately, the displacement transducers used in our system produce a rather noisy signal. Consequently, the location of the turning points of the pistons and the switching commands becomes somewhat imprecise. Therefore, the stability of the delivered binary composition is less than aimed for. Under scale expansion, slow (1 min) variations with amplitude up to 0.3 % can be observed (Fig. 6b), which cannot be removed with the pressure filter. When the output of the transducer is passed through an analogue filter before it is fed into the ADC, the solvent composition becomes more stable (Fig. 6c), but also inaccurate because the analogue filter retards the detection of the turning points of the pistons too much. (For improved performance, see Note added in proof.)

Finally, the system was tested under true chromatographic conditions by subjecting a sample with six solutes to eight consecutive isocratic and gradient elution runs. Under isocratic conditions (acetonitrile-water, 35:65) the average standard

deviation of the solute retention times was 0.4 %. When a mixture of the mobile phase was pumped continuously no improvement in precision was observed. Under gradient elution conditions (15 min from pure water to pure methanol), the solute retention times showed a standard deviation of 0.4 % or less.

CONCLUSIONS

The equipment described has been used to demonstrate that a single-pump solvent programmer can be constructed that fulfils all current needs of HPLC. The programmer provides a rapid response and yields binary mixtures that are stable and accurate to within 1 %. With improved displacement transducers the specifications could be improved to better than 0.1 %. This is considered to be adequate for current chromatographic requirements.

It should be emphasized that the present design is largely dictated by the features of the dual-piston reciprocating pump available to us. Specifically, the pressure feed-back option necessitates the use of displacement transducers. For other pumps this need not be true. For example, pumps operating at constant motor speed could be instructed on the basis of time partitioning provided that the non-uniform inlet profile (Fig. 1) is taken into account by the computer software. Alternatively, the presently employed linear displacement transducer can be replaced by more sophisticated revolution encoders coupled directly to the rotating shaft that drives the pump pistons.

Whatever solution is adopted, the present investigation has shown that single-pump solvent programmers can be highly competitive for liquid chromatographic practice.

ACKNOWLEDGEMENTS

The present study could not have been undertaken without the continuing support of Pye Unicam Ltd. Helpful discussions with Dr. M. Hewins, a grant to one of the authors (C.L.), the loan of the pump and the permission to report the results of this investigation are gratefully acknowledged. Stimulating discussions and welcome suggestions have been received from Dr. P. J. Schoenmakers.

NOTE ADDED IN PROOF

After completion of the manuscript, the low frequency noise of the transducer signal has been significantly reduced by:

- (i) Using separate power supplies for both displacement transducers.
- (ii) Maximizing the transducer sensitivity with an increased impedance (20 kOhm).

As a result, the stability of the delivered binary composition has been improved from 0.3 % (Fig. 6b) to 0.1 %.

REFERENCES

- 1 H. A. H. Billiet, P. D. M. Keehnen and L. de Galan, *J. Chromatogr.*, 185 (1979) 515.
- 2 P. J. Schoenmakers, H. A. H. Billiet, R. Tijssen and L. de Galan, *J. Chromatogr.*, 149 (1978) 519.
- 3 P. J. Schoenmakers, H. A. H. Billiet and L. de Galan, *J. Chromatogr.*, 185 (1979) 179.
- 4 L. R. Snyder, in Cs. Horváth (Editor), *High Performance Liquid Chromatography—Advances and Perspectives*, Vol. 1, Academic Press, New York, 1980, pp. 207–316.
- 5 P. J. Schoenmakers, H. A. H. Billiet and L. de Galan, *J. Chromatogr.*, 205 (1981) 13.
- 6 L. R. Snyder, J. W. Dolan and J. R. Gant, *J. Chromatogr.*, 165 (1979) 3.

COLUMN TYPES AND COLUMN TECHNOLOGY IN LIQUID CHROMATOGRAPHY AND RELATED TECHNIQUES

CHROM. 14,090

DISPERSION OF PEAKS BY SHORT STRAIGHT OPEN TUBES IN LIQUID CHROMATOGRAPHY SYSTEMS

JOHN G. ATWOOD* and MARCEL J. E. GOLAY

The Perkin-Elmer Corporation, Main Avenue, Norwalk, CT 06856 (U.S.A.)

SUMMARY

The theory of spreading of a sample peak in a long straight open tube is known. However, when the tube becomes shorter than 30 theoretical plates, the eluted peak becomes non-gaussian and the theory for long tubes does not apply. This is the case for connecting tubes, injection loops and detector flow cells in liquid chromatographic (LC) systems. In earlier work, we studied the theory of this case using a computer model combining Poiseuille flow with diffusion, obtaining unexpected results about how samples wash out of short tubes. This work extends that study to obtain the peak shapes and bandwidths eluted from straight open tubes ranging from 0.01 to 30 plates in length.

An empirical expression was found for peak width which fits the results of the computer model to within 4% over this entire range. Below 3 plates, the normalized peak width is approximated by a constant times the inverse fourth root of normalized tube length in plates. It becomes as small as a quarter of the value predicted by the long tube theory for 0.01 plates. Experimental measurements on short tubes agree approximately with the computer model when diffusion is the only cause of radial mixing. An expression was derived which determines whether a tube is sufficiently straight so that secondary flow is unimportant compared with diffusion as a cause of radial mixing. Measurements on curved tubes are consistent with the expression. The conditions under which measurements of peak spreading in an open tube can be used to obtain the diffusivity of an LC sample are discussed.

A consequence of these results is that LC systems can be designed with substantially less bandwidth contribution from extra-column components than would be predicted using the long tube theory. Another consequence is that variances contributed by consecutive segments of short open tubes are not additive unless there is complete radial mixing at the connections between segments.

INTRODUCTION

The theory of dispersion of a sample peak injected into Poiseuille flow in a long straight tube is well known from the works of Taylor¹ and Golay². When the tube is long there is ample time for radial diffusion to average each sample molecule's forward progress over the parabolic velocity distribution in the tube. The eluted peaks

are gaussian in shape and the theory is in excellent agreement with experiments.

However, when the tube is short, or the diffusivity of the sample is low, or the flow-rate is high enough so that there is insufficient time for velocity averaging, the peak eluted from a small injection becomes markedly non-gaussian, and the theory for long tubes does not apply. This typically occurs for the connecting tubes, injection loops, and detector flow cells of liquid chromatography (LC) systems.

Gill and Ananthakrishnan³ solved the convective-diffusion equations in a short tube and found that the peaks at the end of the tube may have double maximums. Golay and Atwood⁴ studied this early phase of dispersion of the sample using a computer model combining diffusion and Poiseuille flow in an open tube with no retention. It was found that for the conditions typically encountered in LC systems, the shape of the peak eluted from the tube as a function of time depended only on the normalized length of the tube in theoretical plates, treating the tube as an open tubular column with zero retention². The bandwidth of the eluted peak was proportional to tube volume, and when normalized by tube volume depended only on the normalized tube length in plates. It was found, surprisingly, that the washing out of the sample in the slowly moving layer near the tube wall occurred as a hump at the rear of an otherwise rectangular distribution along the length of the tube. This hump was shown by the computer model to cause a peculiar doubly curved shape in the peaks eluted from tubes shorter than 30 theoretical plates. Computer-calculated shapes of six peaks from tubes ranging from 30 down to 0.1 theoretical plates in normalized length were published, but no analysis of their bandwidths or variances was presented. Maycock *et al.*⁵ solved the shape of peaks from tubes in the same range of normalized lengths by an entirely different numerical method and obtained results in general agreement.

This paper extends the earlier work as follows. Because some LC components such as detector flow cells may typically be as little as 0.01 theoretical plates in normalized length, the computer model was revised so that the calculation could be extended to tubes as short as this. Bandwidth and other properties of the peak shapes were calculated, and the way these properties vary with normalized length of the tube was studied. The purpose was to characterize these highly non-gaussian peaks so that more accurate estimates could be made of the bandwidth contributions of the components that produce them.

It was found that as the tube becomes longer than 3 plates, the normalized peak bandwidth, expressed as standard deviation, σ , divided by the tube volume, V_1 becomes asymptotic to the inverse square root of normalized tube length as predicted by the theory for long tubes^{1,2}. But as the tube becomes shorter than 3 plates, the normalized peak bandwidth becomes significantly smaller than predicted by the long tube theory. At 0.01 plates it is only one fourth as large.

A consequence of this result is that it appears possible to design LC components that make significantly less contribution to extra-column bandwidth than would be predicted using the long tube theory only.

Another consequence of the result is that the variances contributed by consecutive segments of short open tubes are not additive unless there is complete radial mixing at the connection between the segments.

Several experiments are described which tend to verify the correctness of the computed results, yet show the limits of their applicability. The principal limitation is

that in the theory for laminar flow in straight tubes, diffusion is the only cause of radial mixing. Therefore, any experiments to be governed by such a theory must be free of the radial mixing effects of secondary flow such as is caused by curved tubing paths or abrupt changes in cross section. It was found necessary in the experiments to keep tubes surprisingly straight to get results in agreement with the theory, except at very low flow-rates. A simple expression was derived from the work of Golay⁶ which determines in advance whether a tube is sufficiently straight so that secondary flow is unimportant compared with diffusion as a cause of radial mixing. Measurements of peak dispersion made in a curved tube are consistent with this expression. Many other predictions of the theory remain to be tested experimentally, however.

THEORY

A straight open tube can be treated as an open tubular column without retention². It has an optimum velocity at which the height of a theoretical plate is minimum. Multiplying the expression for the optimum velocity by the area of the tube's cross-section gives the corresponding optimum flow-rate, F_{opt} as

$$F_{\text{opt}} = \sqrt{48} \pi D r_0 \quad (1)$$

where D is diffusivity of the sample in the mobile phase and r_0 is the inside radius of the tube. For a typical sample with $D = 10^{-5}$ cm²/sec in a tube with 0.009 cm radius, $F_{\text{opt}} \approx 2 \cdot 10^{-6}$ cm³/sec, or roughly 10^{-4} ml/min. Thus, the flow-rates in typical LC systems are of the order of 1000 to 10,000 times the optimum flow-rates in the connecting tubes. Even for detector cells with 0.025 cm radius, $F_{\text{opt}} \approx 3 \cdot 10^{-4}$ ml/min, so that a flow-rate of 10 μ l/min, as is typically used with microbore columns⁸ is about 30 times F_{opt} . Under these conditions, except for a brief instant at the start, convection due to Poiseuille flow is always far more important than longitudinal diffusion as the cause of axial dispersion of the sample and we may use only the dynamic diffusion term of the expression for plate height, h , in the tube. Expressed in terms of flow-rate, F , it is

$$h = F/24 \pi D \quad (2)$$

Using this expression we can determine the number of theoretical plates, n , in a tube of length L :

$$n = L/h = 24 \pi DL/F \quad (3)$$

For long tubes where $n > 30$, the shape of the eluted peak is very close to gaussian, and its variance, σ^2 , is the familiar

$$\sigma^2 = V_T^2/n \quad (4)$$

where V_T is the volume of the tube, and the standard deviation is expressed in units of volume.

Ref. 4 shows that as n decreases below about 30, the eluted peak becomes

increasingly non-gaussian and the assumptions under which eqn. 4 is derived become less and less true. It is then necessary to compute the shape of the eluted peak from a numerical computer model.

It is sufficient for typical LC systems to compute the eluted peak shape for each tube length at only one flow-rate. Referring to Figs. 6 and 8 of ref. 4, and noting that $F/F_{\text{opt}} = v_0/v_{\text{opt}}$ (where v_0 and v_{opt} are the average flow velocity and the optimum flow velocity, respectively) it is clear that the variance and skewness of the sample distribution inside the tube are almost independent of flow-rate when $F/F_{\text{opt}} \geq 30$, even when the average flow has traveled only 0.015 theoretical plates. This is the earliest event observable in this computer model. It is a single iteration. Thus, it is justifiable to use peak shapes calculated for $F/F_{\text{opt}} = 100$ as reasonably representative for all flow-rates such that $F/F_{\text{opt}} \geq 30$, the range of interest for short tubes in LC systems.

THE NUMERICAL COMPUTER MODEL

The model used to calculate the peak shapes is described in detail in ref. 4. Briefly, it divides the tube into volume elements consisting of 20 concentric rings at equal increments of radius and slices at equal increments of length along the tube. Poiseuille flow is simulated by advancing the sample in each volume element along the tube according to the velocity at that radius. Diffusion is simulated by redistributing part of the sample in each volume element to the elements adjacent to it. One cycle of simulated flow followed by simulated diffusion is defined as one iteration and corresponds to the time unit in the model. Sample injection is simulated by starting with an initial sample in all the rings of the first slice of the tube. Thousands of iterations over tens of thousands of volume elements simulate the combination of Poiseuille flow with diffusion which disperses the sample in the tube. The model can be asked to describe the distribution of sample along the tube after a certain time, or the sample content in all the rings of a certain slice as a function of time, or the rate of elution of sample from a tube of a certain length as a function of time.

After a sufficient number of iterations, the sample is smoothly distributed over a large number of volume elements, and the model can be expected to simulate the physical process with very great accuracy. However, it can be seen by referring to Fig. 5 of ref. 4 that for $F/F_{\text{opt}} = 100$, it takes only 3 iterations for the sample to reach the end of a tube 0.1 plates long, and the computed distribution of sample still shows substantial effects from the discreteness of the model.

Therefore, to study peak shapes eluted from tubes as short as 0.01 theoretical plate, it was necessary to modify the computer model to give it a finer grid in space and time. This was done by changing the number rings into which the tube was subdivided from 20 to 50. This raised the iterations per theoretical plate from 66.67 to 416.67. In the 50-ring model, the sample reaches the end of a tube 0.01 plates long at the second iteration.

Both models become increasingly accurate after several iterations because the width of the features being measured becomes larger than a few slices. These conditions, however, do not apply for the initial onset and rapid drop at the start of peaks where $n \leq 0.3$ plates. The accuracy of computer-calculated properties such as width at half height and retention volume at the peak maximum are thus visibly affected by the coarseness of the grid of the models. Fortunately, for these limiting cases, reliable

simple theory of dispersion by Poiseuille flow without diffusion indicates the correct limiting values.

In this work, data for normalized tube lengths of 0.3–30 plates were calculated using the 20-ring model of ref. 5. For normalized tube lengths from 0.1 to 0.01 plates the 50-ring model described above was used. For a normalized tube length of 0.1 plate, the two models agreed as to standard deviation of the eluted peak to within 1.5%. This small discrepancy is believed to be caused in part by the fact that at 0.1 plate, the 20-ring model's accuracy is slightly affected by having an insufficient number of iterations at the onset of the peak to average out the discreteness of the model.⁵

The calculated peak shapes were processed by another program which determined the location of the peak maximum, the location of the centroid, the standard deviation, and the minimum width containing 95% of the peak's area. Since this program was designed to process relatively noisy experimental data, its accuracy in calculating standard deviation of the computed peaks is estimated to be about 0.5%.

COMPUTED RESULTS

Elution peak shapes

Elution is the average concentration of sample in the fluid leaving the end of a tube as a function of time, after a very narrow injection uniformly across the entrance to the tube. It is the signal that would be seen by a detector with very small volume that mixes together the fluid from all parts of the end of the tube and responds to the instantaneous concentration that results.

Fig. 1 shows the peak shapes eluted from tubes from 0.01 to 30 plates in length.

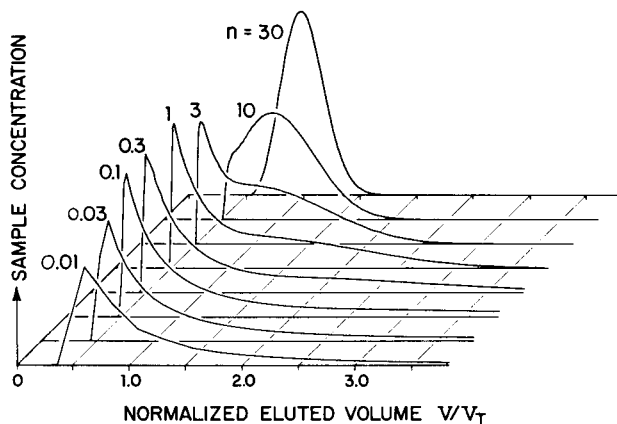


Fig. 1. Elution peak shapes as a function of normalized tube length, n , in plates. Eluted sample concentrations from numerical computer model are normalized to represent injections of a small, constant sample mass into tubes of constant volume V_T and plotted *versus* normalized eluted volume V/V_T . When $n < 0.3$ plates, the true peak shape has an almost instantaneous onset and peak maximum at $V/V_T = 0.5$. Sloping onsets and angularity of the computed curves for these values of n are caused by coarseness of the model for very early events. Transition from the short-tube peak shape to gaussian peaks for long tubes as n increases can be seen to occur by the development of a hump which moves in from the tail to a normalized retention volume of 1.0, where it grows and narrows to become the main peak.

Sample concentration in arbitrary units is plotted *versus* normalized eluted volume, V/V_T , where V is the volume eluted since the time of injection. Each peak computed by the model is normalized by dividing its abscissa scale by the length of the tube in theoretical plates. Thus, each curve represents elution from a tube of unit volume. Each ordinate scale is adjusted so that all curves have the same area. Thus the curves simulate an experiment in which a sample of fixed mass and very small volume is injected into a tube of fixed volume whose length in theoretical plates is varied by changing the flow-rate or sample diffusivity.

When $n < 0.3$, the Poiseuille velocity profile should result in each peak having a very abrupt onset at $V/V_T = 0.5$, followed by a hyperbolic decay proportional to $(V/V_T)^{-2}$ in the early stages. The results show this only approximately. The sloping onset for the shortest tubes is attributable to the aforementioned coarseness of the model grid for the earliest stages of dispersion.

As shown in ref. 4, the hyperbolic tail of each peak is truncated by combined radial diffusion and velocity shear. This sweeps the sample at the walls ahead as a "hump" of concentration which accelerates until it catches up with the average flow in the tube. This hump can be seen in the curves of Fig. 1 moving in from near $V/V_T = 8$ when $n = 0.01$ toward $V/V_T = 2$ at $n = 0.3$. Finally, for $n \geq 3$, the hump becomes the main peak at $V/V_T = 1.0$. The onset peak at $V/V_T = 0.5$ finally disappears at $n = 30$ as diffusion destroys the sharp front on the axis of the tube and the eluted peak approaches a gaussian shape. For $n \geq 30$ the longitudinal sample distributions at all radii in the tube are close to being gaussian, with the distribution on axis leading the distribution at the wall by 3 theoretical plates, and the eluted peaks are very close to gaussian.

Table I gives quantitative data on the persistence of the tails on elution peaks from short tubes. The first four columns give the number of tube volumes that must be eluted before the concentration drops below 10, 1 and 0.1 % of its peak value, as a function of normalized tube length, n .

TABLE I
LENGTHS OF TAILS OF ELUTION AND SLICE CONTENT PEAKS IN TERMS OF NORMALIZED ELUTED VOLUMES, V/V_T TO ATTAIN CONCENTRATIONS LESS THAN 10, 1 AND 0.1 % OF PEAK CONCENTRATION

Normalized tube length, plates	Elution peaks			Slice content peaks		
	V/V_T for these percents of peak concentration:			V/V_T for these percents of peak concentration:		
	10	1	0.1	10	1	0.1
0.01	2.1	8.6	15.4	9.4	16.5	22.6
0.03	1.9	7.5	10.9	7.2	11.1	13.8
0.10	1.7	5.8	7.5	5.4	7.5	8.8
0.30	2.3	4.6	—*	4.2	5.5	—*
1.0	2.4	3.4	—	3.1	3.9	—
3.0	2.1	2.7	—	2.4	2.9	—
10	1.7	2.1	—	1.8	2.3	—
30	1.4	1.6	—	1.4	1.6	—

* Data not available from peaks computed with the 20-ring model.

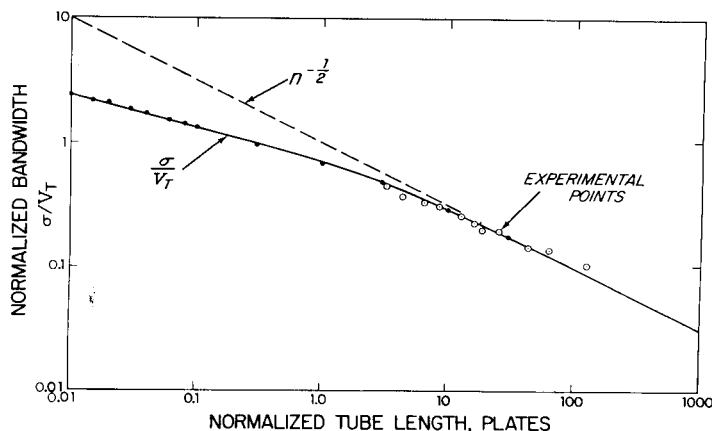


Fig. 2. Elution bandwidth *versus* tube length on log-log scales. Normalized standard deviation σ/V_T *versus* normalized tube length n in plates for the peak eluted from a straight open tube. Solid dots are values from the numerical computer model. The solid line is from eqn. 5. Open circles are means of measurements on a straight stainless-steel tube (366 cm \times 0.41 mm I.D.) where flow-rate was varied from 4.2 to 0.105 ml/min to vary the normalized tube length. Sample was sodium benzoate in water at room temperature. Broken line shows extension of $n^{-1/2}$ asymptote which applies for $n > 30$.

Elution bandwidth

Fig. 2 shows a log-log plot of the normalized standard deviation, σ/V_T , of eluted peaks *vs.* tube length in plates. It shows that for $n > 3$ plates, σ/V_T is asymptotic to $n^{-1/2}$, in expected agreement with the theory for long tubes. For $n < 3$ plates, σ/V_T has a continually decreasing slope indicating that it is approximately proportional to $n^{-1/4}$. It can be seen that when $n < 10$, significant errors in calculation of σ result if the long-tube formula is used.

Table II gives some properties of the computed peak shapes for 13 different normalized tube lengths. The second column gives the normalized standard deviation, σ/V_T . An empirical expression was found that closely approximates these computed values down to $n = 0.01$ plates. It is

$$\sigma/V_T \approx n^{-1/2} (1 + 3/n)^{-1/4}, \quad n \geq 0.01 \quad (5)$$

The third column of Table II gives the ratio of this approximate expression to the computed σ/V_T . It shows that the maximum error of the approximation is 3.8%. Thus, for many purposes, eqn. 5 has adequate accuracy within its range down to $n = 0.01$. The empirical character of this equation must be emphasized: theoretical considerations indicate that for indefinitely decreasing values of n , σ/V_T approaches a constant times $n^{-1/6}$.

To measure the true σ of non-gaussian peaks in experimental work involves substantial computation. Therefore it is of interest to see how the commonly used simpler methods of estimating σ perform for the particular non-gaussian shapes which occur for $n = 30$. One such measure is width at half height, $W_{1/2}$, which equals 2.355σ for a gaussian peak. The fourth column of Table II gives the ratio $W_{1/2}/2.355 \sigma$. A similar measure also used is width at 0.6067 of peak height, $W_{0.6}$ which equals 2σ

TABLE II

PROPERTIES OF THE PEAK SHAPE ELUTED FROM A SHORT STRAIGHT TUBE AS A FUNCTION OF TUBE LENGTH IN THEORETICAL PLATES

Normalized tube length in plates, n	Normalized standard deviation from computer, σ/V_T	Ratio of approximate formula to normalized standard deviation from computer, $n^{-1/2} (1 + 3/n)^{1/4} / (\sigma/V_T)$	Ratios of other bandwidth measures to standard deviation			
			Width at half height, $W_{1/2}/2.355\sigma$	Width at 0.6066 of height $W_{0.6}/2\sigma$	Width containing 0.9546 of peak area $W_{0.95}/4\sigma$	Normalized centroid, V_c/V_T
0.010	2.453	0.980	0.0849	0.0696	0.772	2.016
0.015	2.176	0.997	0.0838	0.0752	0.797	1.914
0.020	2.009	0.971	0.0857	0.0776	0.802	1.853
0.030	1.846	0.986	0.0812	0.0682	0.790	1.824
0.040	1.702	0.995	0.0804	0.0666	0.788	1.757
0.060	1.522	1.004	0.0772	0.0646	0.789	1.677
0.080	1.418	1.001	0.0849	0.0765	0.787	1.639
0.10	1.332	0.994	0.0846	0.0707	0.786	1.597
0.30	0.965	1.038	0.121	0.108	0.785	1.387
1.0	0.688	1.029	0.148	0.127	0.767	1.259
3.0	0.480	1.011	0.338	0.221	0.810	1.134
10.0	0.297	0.997	1.18	1.21	0.898	1.034
30.0	0.179	0.997	1.05	1.05	0.978	1.011

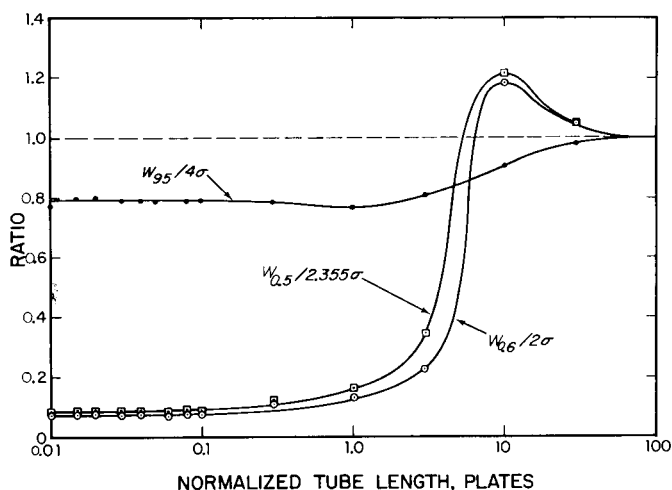


Fig. 3. Accuracy of commonly used measures of bandwidth in determining the standard deviation of peaks eluted from a straight tube. W_{95} is bandwidth containing 95.46% of peak area. $W_{0.5}$ and $W_{0.6}$ are widths at half and 0.606 of maximum height, respectively. Each measure is divided by its value in terms of the standard deviation, σ , for a gaussian peak. These ratios are plotted *versus* normalized tube length on a log scale. Values are from the numerical computer model.

for a gaussian peak. The fifth column gives $W_{0.6}/2\sigma$. A third measure is "base width", W_{95} , the minimum width containing 0.9546 of the peak area. Though harder to measure than $W_{1/2}$ and $W_{0.6}$, it is easier to measure than true σ , especially when the peak is recorded on a system which can integrate peak area. It equals 4σ for a gaussian peak. The sixth column gives $W_{95}/4\sigma$. Fig. 3 shows these three ratios plotted vs. tube length in plates.

These results show that $W_{1/2}$ and $W_{0.6}$ give reasonable values down to $n = 10$ plates, but for shorter tubes become an extremely unreliable measure of σ . Below 0.3 plates, when the early part of the peak has adopted its sharp onset and hyperbolic decay, both measures again assume a fixed ratio with the true σ .

For $n = 0.1$ plates, these ratios are

$$W_{1/2} \approx \sigma/12 \quad (6)$$

and

$$W_{0.6} \approx \sigma/14 \quad (7)$$

W_{95} varies much less with n than the others. For $n \leq 0.3$ plates,

$$W_{95} \approx 0.79\sigma \quad (8)$$

and for $n \leq 4$ plates, eqn. 8 is still accurate to 3%.

Peak location and centroid

It is common to estimate the "dead" volume of a tube or column by measuring

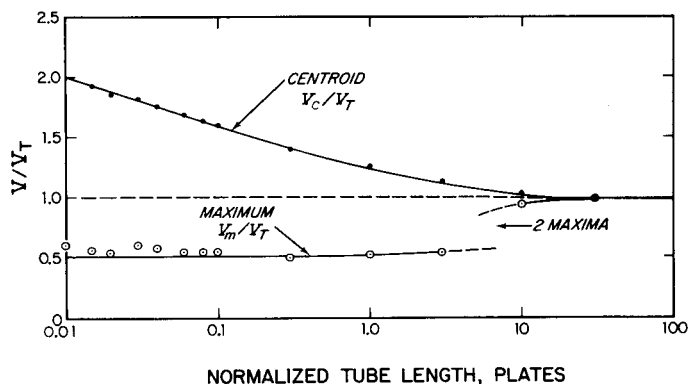


Fig. 4. Retention volume of the centroid V_c and the maximum V_m of elution peaks from the numerical computer model of a straight tube *versus* tube length. Normalized retention volumes V_c/V_T and V_m/V_T are plotted *versus* normalized tube length, n , in plates on a log scale. Above 10 plates, both curves are asymptotic to 1.0. For lower plates, the centroid becomes increasingly delayed owing to the tail caused by slow moving sample near the wall. The peak has two maxima between about 3 to 10 plates. For shorter tubes the correct theoretical maximum is extremely close to the onset at $V/V_T = 0.5$. Values above 0.5 for $0.01 \leq n \leq 0.1$ plates show errors caused by the coarseness of the model for early events.

the delay between injection into it and elution of a peak from it at a known flow-rate. This method implies an assumption that there has been sufficient velocity averaging so that the injected peak has traveled at the average flow-rate in the tube. In straight open tubes where $n < 30$ plates, this condition is not true. Fig. 4 is a plot of the normalized retention volumes of the eluted peak's maximum V_m/V_T and its centroid, V_c/V_T as a function of tube length in plates. Data for the centroid are in the seventh column of Table II.

Above a length of 10 plates, the eluted peak has a single maximum near V_T . Between 10 and 3 plates, the peak has two maxima, one near V_T and one near $V_T/2$. Below 3 plates, the location of the maximum approaches $V_T/2$ very closely, as expected by the simple theory. That the computed values of V_m below 0.1 plates lie slightly above $V/V_T = 0.5$ can be ascribed entirely to the aforementioned coarseness of the model for the very earliest events.

The centroid on the other hand, is predominately determined by the center and long tail of the peak, which are more accurately computed than the peak maximum, even for the shortest tube. Fig. 4 shows that for $n < 10$, the centroid of the eluted peak becomes delayed to far beyond $V/V_T = 1$. For a tube 0.01 plates long, a large error will be made by estimating its volume to be equal to the retention volume of the eluted peak. The estimate will be a factor of 2 low if the peak maximum is used, and a factor of 2 high if the centroid is used as the measure of retention.

Slice content peaks

Some detectors respond to the total sample content of a slice across the tube, regardless of the radial location or longitudinal velocity of the sample within the slice. An example is a fluorescence detector whose beam crosses a transparent segment of the tube, and responds to concentration of the sample.

Fig. 5 shows the peak shapes seen by detectors that respond to slice content in

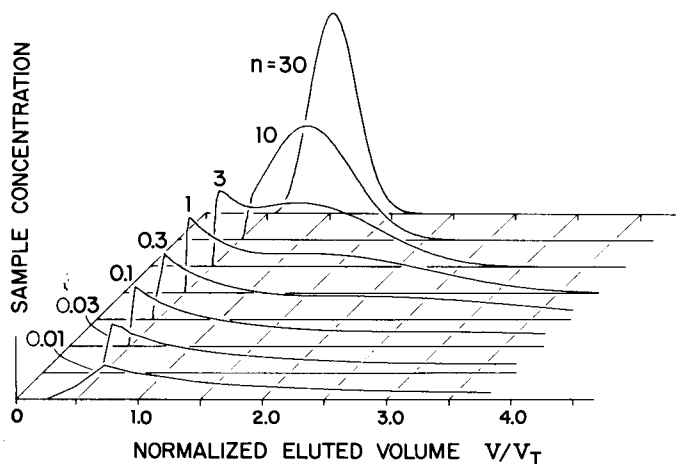


Fig. 5. Slice content peak shapes as a function of normalized tube length, n , in plates. Computed average sample concentration in the last slice of the tube is plotted *versus* normalized retention volume. Normalizations are the same as for the elution peaks of Fig. 1. Slice content peaks are broader and show a more pronounced development of the transition hump than the corresponding elution peaks because relatively greater weight is given to the slowly moving sample near the tube wall where the hump develops.

the slice at the end of the tube for tubes from 0.01 to 30 plates in length. The abscissa scales are normalized in the same way as for the elution curves of Fig. 1 to represent tubes of constant volume. The ordinate scales are set to simulate the same mass of sample injection for all peaks.

Just as for elution curves, the slice content curves for $n < 3$ plates should all rise abruptly to a peak at $V/V_T = 0.5$. But unlike elution curves, they should then decline with a hyperbolic form $(V/V_T)^{-1}$ until the passage of the hump. Except for

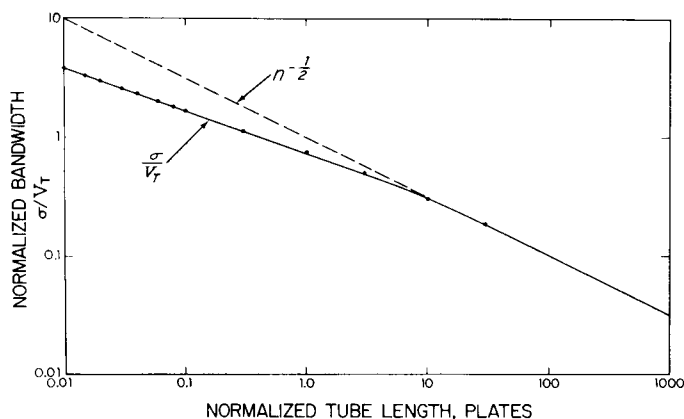


Fig. 6. Slice content bandwidth *versus* tube length on log-log scales. Normalized standard deviation σ/V_T *versus* normalized tube length n in plates for the peak seen by a slice content detector at the output end of the tube. Solid dots are values from the numerical computer model. Broken line shows extension of $n^{1/2}$ asymptote which applies for $n > 30$.

TABLE III
PROPERTIES OF THE SLICE CONTENT SIGNAL AT THE END OF A SHORT STRAIGHT TUBE AS A FUNCTION OF NORMALIZED TUBE LENGTH IN THEORETICAL PLATES

Normalized tube length in plates, n	Normalized standard deviation from computer, σ/V_T	Ratio of approximate formula to normalized standard deviation from computer, $n^2 (1 + 8/n)^{-1/2} / (\sigma/V_T)$	Ratios of other bandwidth measures to standard deviation			
			Width at half height, $W_{1/2}/2.355\sigma$	Width at 0.6066 of height, $W_{0.6}/2\sigma$	Width containing 0.9546 of peak area, $W_{0.95}/4\sigma$	Normalized centroid, V_d/V_T
0.010	3.864	0.996	0.119	0.0930	0.788	4.470
0.015	3.264	1.020	0.0936	0.0676	0.785	3.927
0.020	2.921	1.028	0.0945	0.0711	0.784	3.640
0.030	2.570	1.010	0.111	0.0856	0.784	3.217
0.040	2.306	1.016	0.120	0.0965	0.785	3.112
0.060	1.992	1.018	0.134	0.106	0.784	2.808
0.080	1.814	1.008	0.139	0.112	0.785	2.645
0.10	1.674	1.008	0.148	0.116	0.787	2.504
0.30	1.131	1.005	0.220	0.174	0.804	1.956
1.0	0.748	0.977	0.727	0.243	0.815	1.547
3.0	0.499	0.959	1.114	1.18	0.845	1.273
10.0	0.302	0.960	1.156	1.13	0.921	1.027
30.0	0.178	0.989	1.05	1.04	0.982	1.033

sloped onsets for the shortest tubes, the computed curves show this form. Their tails are higher and longer than the $(V/V_1)^{-2}$ tails of the elution curves. In slice content peaks, sample near the wall is weighted equally with sample near the axis of the tube, in spite of its slower velocity. Since the sample hump that terminates the tail is largely at the wall in the early stages, its passage in slice content peaks is much more pronounced than in the corresponding elution peaks. Table I shows that the persistence of slice content peaks is always greater than for elution peaks for the same tube, and much greater for very short tubes.

Fig. 6 shows plots of normalized standard deviation σ/V_T versus tube length in plates. As for elution, the normalized standard deviation of slice content peaks is also asymptotic to $n^{-1/2}$ for large n , but is approximately proportional to $n^{-0.38}$ for $0.01 < n < 0.3$ plates.

Table III gives computed values for σ/V_T , $W_{1/2}/2.355\sigma$, $W_{0.6}/2\sigma$, $W_{95}/4\sigma$ and V_c/V_T . These results show that for slice content peaks, $W_{1/2}$ and $W_{0.6}$ are also poor measures of bandwidth, while W_{95} bears nearly the same ratio to true σ as it does for elution peaks. For slice content peaks, the centroid is delayed more than twice as much as for elution peaks.

An approximate empirical formula for σ/V_T for slice content peaks is

$$\sigma/V_T \approx n^{-1/2} (1 + 8/n)^{-1/7}, \quad n \geq 0.01 \quad (9)$$

Over the range $n \geq 0.01$ it agrees with computed results to within 4.1 %, as shown in Table III. As for eqn. 5 eqn. 9 is completely empirical, and there is no justification for extending it to values of n below 0.01.

Curved tubes and inertial mixing

If a tube is not perfectly straight, smooth, and of uniform cross section, then at high flow-rates, an inertial flow may develop in it. This may cause radial mixing in addition to that caused by diffusion alone. If this additional radial mixing is significant compared to that caused by diffusion, then the straight tube theory will not apply. In LC systems this occurs while the Reynolds number is still too small for true turbulence, and both the main and secondary flows are laminar.

Since the radial mixing effect of inertial flow generally increases rapidly with increasing flow-rate, while the mixing effect of diffusion alone does not, we can expect there to be a transition flow-rate, F_{trans} , at which the inertial mixing effect becomes significant compared to diffusion.

When the tube is coiled into a helicoidal path, the centrifugal force on the faster flowing fluid on the tube's axis causes it to drift radially outward from the center of the curved path. This gives rise to a secondary flow superposed on the Poiseuille flow which divides it into two kidney-shaped counter-rotating circulations in the plane normal to the tube's axis. Under these conditions, the secondary flow will cause a decrease in the plate height, and at the transition flow-rate, the fractional plate height reduction will be proportional to the fourth power of the main flow-rate, as determined by Golay⁶. Using his eqn. 35 for the diffusion constant, k :

$$k = D + \frac{v_0^2 r_0^2}{48D} (1 - 18.43\sigma^2) \quad (10)$$

this fractional decrease is given by his term $18.43\sigma^2$, wherein, from his eqn. 23 σ designates the dimensionless quantity

$$\sigma = \frac{\varrho v_0^2 r_0^3}{525 D \mu r_1} = \frac{\varrho F^2}{525 \pi^2 D \mu r_0 r_1} \quad (11)$$

where r_1 is the radius of its helicoidal path, μ is the mobile phase's viscosity and ϱ its density. Defining the transition point as that at which σ has the value 0.1, for which we would have an 18% decrease in plate height, we derive the transition flow-rate as

$$F_{\text{trans}} = (518 r_1 r_0 D \mu / \varrho)^{1/2} \quad (12)$$

The same relationship can be derived from Tijssen⁷ (Table I, eqn. 1) by setting his $D_r/D_m = 1.1843$ and solving for flow-rate. The coefficient resulting within the parentheses is 491, which is in substantial agreement with eqn. 12.

It is worth noting that with any likely tube curvature in an LC system, the transition flow-rate, F_{trans} , will be much less than the flow-rate at which turbulence will occur which is for a Reynolds number of the order of 2000, *i.e.*, for a flow-rate given by

$$F_{\text{turb}} \approx 1000 \pi \mu r_0 / \varrho \quad (13)$$

Setting $F_{\text{trans}} = F_{\text{turb}}$, we determine for r_1 :

$$r_1 \approx \frac{(1000 \pi)^2}{518} \left(\frac{\mu}{\varrho D} \right) r_0 \quad (14)$$

For the dimensionless ratio $\mu/\varrho D$, the lowest reasonable value in LC mobile phases is about 10^2 , so we obtain

$$r_1 \approx 2 \cdot 10^6 r_0 \quad (15)$$

Even for a very small tube with $r_0 = 0.05$ mm, the radius of curvature r_1 would be about 100 m. For all such tubes less straight than this, as flow-rate is increased, transition flow would occur at a lower flow-rate than turbulence.

In the case of the continuously curved tube, the inertial mixing occurs uniformly throughout the length of the tube, as does diffusion mixing. However, significant inertial mixing can also occur at single locations in a tube, such as sharp bends, step changes in diameter, or internal projections which partially block the cross section of the tube.

The mixing effect of features such as these will also increase rapidly with the flow-rate so that when they are present, a transition flow-rate will exist beyond which experimentally determined plate heights may be markedly lower than predicted by the straight tube theory.

EXPERIMENTAL AND RESULTS

Measurements on a straight tube

The peak shapes and bandwidths eluted from a straight tube of fixed length were measured over a wide range of flow-rates. In this way the normalized length of the tube was varied by varying the flow-rate only.

A 366 cm \times 1/16 in. O.D. \times 0.38 mm (0.015 in.) I.D. stainless-steel tube was fastened to a groove in a long wood beam so that it was maintained straight within about 5 mm over its entire length. Samples were injected into the tube using a Rheodyne Model 7120 valve with an injection loop modified to deliver 6 μ l, and connected to the straight tube with about 10 cm of 0.18 mm I.D. tube and an SSI (State College, PA, U.S.A.) low dead-volume union. The peaks eluted from the tube were measured by a specially made 3 \times 1 mm I.D. UV flow cell, with a volume of about 2.6 μ l, connected to the straight tube by about 25 cm of 0.18 mm tube and 2 SSI unions. The cell was mounted in a Perkin-Elmer Model LC-55 UV detector set at 254 nm. Output peaks were recorded on a strip chart recorder. The mobile phase was deionized water pumped by a Perkin-Elmer Series 2 pump. Flow-rates were measured by timing collection of effluent in a graduated cylinder. The samples injected were 0.1 or 0.2% sodium benzoate in water. At each of 11 flow-rates, from 0.105 to 4.16 ml/min, at least two injections were recorded. Recorded peaks were digitized on a Bendix Datagrid (Fairfield, CT, U.S.A.) and processed to obtain bandwidth measures by the same program used to process peaks generated by the computer model described above.

The length of the tube was chosen so that at the three lowest flow-rates used, 0.105, 0.21 and 0.31 ml/min, its normalized length was over 30 plates, and the eluted peaks were nearly gaussian. This made it possible to measure the tube volume accurately by measuring the retention volume V_c of the centroid of the eluted peak. Also it permitted a determination of the actual sample diffusivity by measuring the peak spreading in the tube under conditions where the long tube theory of eqns. 3 and 4 applied. Knowledge of the diffusivity was necessary to determine n , the normalized tube length in plates, at higher flow-rates where n cannot be determined directly from the peaks themselves because of their extreme departure from gaussian shape.

First, the instrumental contribution to retention volume, V_i , and standard deviation σ_i were determined by replacing the 366-cm tube with a short segment of 0.18 mm I.D. tube having negligible volume contribution, and recording the output peaks at the same flow-rates. At the three lowest flow-rates, the instrumental retention volume V_i varied little and averaged 42 μ l. With the 366-cm tube in place, the average difference between the total retention volume V_c and the instrumental retention volume V_i measured at the three lowest flow-rates gave a value of tube volume V_T of 485 μ l. This corresponds to an inside diameter of 0.41 mm, 8% above the nominal for the tube. This value for V_T was used in normalizing all measurements on the 366-cm tube.

To determine sample diffusivity, two measurements of σ corrected for instrumental contribution σ_i were made at each of the three lowest flow-rates used. From each of these σ measurements, a plate height, h , in the tube was calculated, using eqn. 4 to calculate n in eqn. 3. The results are shown in Table IV.

From eqn. 2, under conditions where the long tube theory applies, and S is the

TABLE IV

MEASURED PLATE HEIGHT VS. FLOW-RATE FOR 366-cm STRAIGHT TUBE

Sample was 0.1% sodium benzoate in water at 24°C. These data were used to determine the diffusivity of sodium benzoate to be $8.1 \cdot 10^{-6} \text{ cm}^2/\text{sec}$.

Flow-rate, F (ml/min)	Plate height, h (cm)	
	First run	Second run
0.105	4.3	3.3
0.21	7.6	6.1
0.31	7.1	7.7

slope of the straight line which passes through the origin and relates plate height to flow-rate:

$$D = 1/24 \pi S \quad (16)$$

A least squares best fit straight line passing through the origin was fitted to the data of Table IV and its slope was determined. From eqn. 16, D was found to be $8.1 \cdot 10^{-6} \text{ cm}^2/\text{sec}$. This value of diffusivity was used in analyzing all experiments with sodium benzoate sample in water mobile phase. As a check on its reasonableness, it may be compared with the value of $9 \cdot 10^{-6} \text{ cm}^2/\text{sec}$ for toluene, a molecule of similar size, in water at 20°C given by Bristow⁹.

Using the measured value of D and eqn. 3, n was found for each flow-rate. The measured σ at each flow-rate was normalized by the measured tube volume, V_T . The results are plotted on Fig. 2, to compare them with the values predicted by the computer model.

Measurement of transition flow in a curved tube

The 366-cm tube described above was removed from its straight wooden support and coiled into a circle of radius $R = 56 \text{ cm}$. Eluted peaks were recorded at 6 flow-rates from 0.105 to 4.16 ml/min and their standard deviations were measured. Fig. 7 shows a plot of the normalized measured standard deviations vs. flow-rate. Also shown for comparison are the theoretical values for this tube calculated using the measured V_T , D and F in eqn. 3 to obtain n , then using the approximate formula of eqn. 5 to calculate σ/V_T .

It can be seen that at and below about 0.5 ml/min, the measured bandwidth agrees well with the straight tube theory, but above this flow-rate it becomes lower. At 4 ml/min, it is half that predicted for a straight tube. The calculated transition flow-rate for this tube using eqn. 12 is $F_{\text{trans}} = 0.38 \text{ ml/min}$.

Fig. 8 shows comparison of the peak shapes at the same flow-rate for the straight tube and the same tube curved to 56 cm radius. The effect of curving the tube is to delay and slope the sharp onset of the typical short-tube peaks, truncate the tail and make the profile much more gaussian. Ref. 4 showed that in short tubes the sharp onset is caused by sample on the tube axis while the tail is from sample at the wall, so these changes in peak shape indicate that radial mixing has occurred.

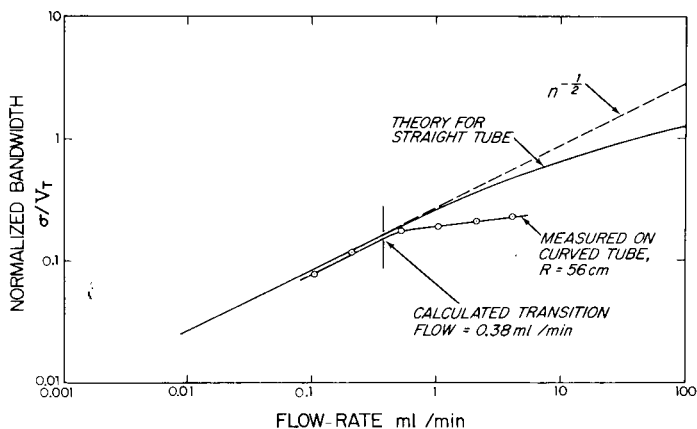


Fig. 7. Bandwidth *versus* flow-rate for a curved tube on log-log scales. Normalized bandwidth σ/V_t *versus* flow-rate for a tube 366 cm long with sodium benzoate sample in water mobile phase at room temperature. Solid curve is calculated from eqn. 5 for the tube when straight. Broken line is extension of asymptote applicable when $n > 30$. Circles are measurements made when the tube was curved into a circular path with radius 56 cm. Arrow indicates the transition flow-rate above which theory for straight tubes does not apply, calculated from eqn. 12.

In another experiment the 366-cm tube was folded into a "hairpin" shape with a 180° bend of 10 cm radius between two straight segments 167 cm long. In this shape, the tube's bandwidth obeyed straight tube theory up to a flow-rate of about 0.7 ml/min, but departed at higher flow-rates with bandwidth only 0.6 of that for the straight tube at 2.08 ml/min.

Measurements on a fluorescence flow cell

To study the applicability of the computer model to very short tubes, measurements were made on an experimental flow cell for a fluorescence LC detector. The flow cell consisted of a cylindrical fused-silica tube (8×1.5 mm I.D.). At each end of

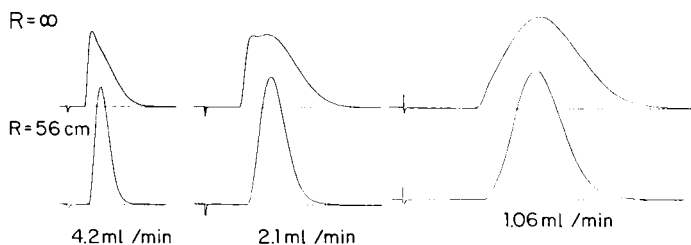


Fig. 8. Effect of curved path on eluted peak shape. Measured peak shapes eluted from a stainless-steel tube ($366 \text{ cm} \times 0.38 \text{ mm I.D.}$) at three flow-rates. For upper curve of each pair (marked $R = \infty$), the tube was straight. For lower curve, the same tube was coiled in a circular path of radius $R = 56 \text{ cm}$. Sample was sodium benzoate in water at room temperature. These peak shapes for the curved case are from among the runs averaged to obtain the three corresponding experimental points plotted in Fig. 7. Though the radius of the curved path was about 1700 times the radius of the tube, curvature reduced the standard deviation of the eluted peak more than a factor of 2 at 4.2 ml/min. Repeated curving and straightening of the same tube showed that these peak shapes and bandwidth effects were quite reproducible.

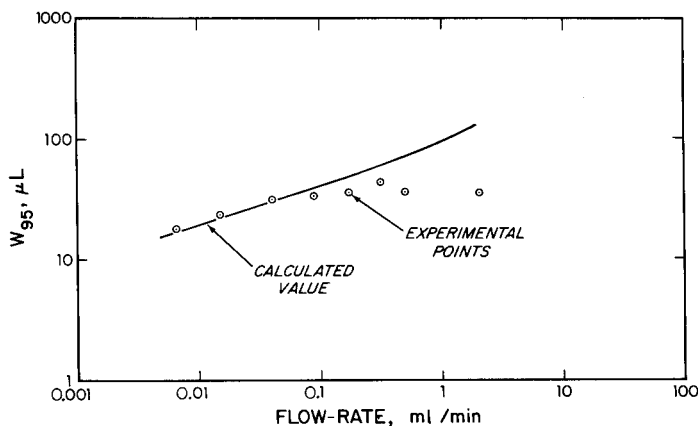


Fig. 9. Bandwidth of a fluorescence flow cell *versus* flow-rate. Measured bandwidth containing 95% of the peak area, W_{95} , is plotted *versus* flow-rate on log-log scales. The cell had 1.5 mm I.D. and was 8.5 mm long. The excitation and fluorescence beams intersected at a focus 4.3 mm from the cell entrance. Sample inlet was axially via a 0.38 mm diameter tube and a conical transition piece of 90° included angle. Cell volume from inlet to beam focus was 7.5 μ L. Sample was naphthalene in isopropanol. Calculated curve is from eqn. 9 and assumed the cell acted as a slice content detector. Bandwidth lower than calculated at high flow-rates may be evidence of inertial mixing at the junction of the inlet tube and cell entrance.

this silica tube, an entrance or exit tube of 0.38 mm I.D. connected to it coaxially with a conical transition piece of 90° included angle. The optical excitation and fluorescence beams crossed at the center of the cell. Their images were about 1.5 mm high and 1.5 mm wide, effectively filling the cross-section of the cell.

The mobile phase was isopropanol. The sample was naphthalene at 0.5 to 2 μ g/ml in isopropanol. The experimental fluorimeter was set for 280 nm excitation and 340 nm fluorescence with 10 nm spectral slit width in both beams. Pumps used were a Perkin-Elmer Series 2 for flow-rates from 2 to 0.2 ml/min, and a specially modified version of the same pump with smaller piston and stroke below 0.2 ml/min. A Valco injection valve with 0.5- μ L loop was connected to the detector with 10.5 cm of nominal 0.007 in. stainless-steel tubing and an SSI union. Measurements were made at 8 flow-rates from 0.0065 to 2.0 ml/min. Three to five injections were recorded at each flow-rate on a Bascom Turner recorder. The integrating feature of the recorder was used to determine W_{95} , the bandwidth containing 95.46% of the peak area. The results are shown in Fig. 9.

The theoretical bandwidth of the detector was calculated as follows. The cell was treated as a tube 1.5 mm in diameter with a uniform injection over its input end, and a slice content detector 4.25 mm from the input. Its tube volume was calculated to be 7.5 μ L. The diffusivity of naphthalene in isopropanol was estimated to be $4.1 \cdot 10^{-6}$ cm²/sec by multiplying published values in methanol and benzene⁹ by the ratios of the viscosities of those solvents to the viscosity of isopropanol. The normalized length at each flow-rate was calculated using eqn. 3. It ranged from 1.21 plates at 0.0065 ml/min to 0.0039 plates at 2 ml/min. At 0.01, 0.1 and 1 ml/min, the σ for the cell was calculated using eqn. 9 for slice content detectors, and corrected for the error of this expression by interpolation from column 3 of table III. Then W_{95} was calculated by multiplying by the tabulated ratio $W_{95}/4\sigma$ from column 6. Similar calcu-

lation of the elution bandwidth of the connecting tubes show that their contribution should range from a W_{95} of about $2\ \mu\text{l}$ at $0.01\ \text{ml/min}$ to about $4\ \mu\text{l}$ at $1\ \text{ml/min}$ even if they were straight, which they were not. The contribution of the $0.5\text{-}\mu\text{l}$ injection value was previously measured and found insignificant. Therefore their contributions were ignored. The calculated results are plotted on Fig. 6 for comparison with the measured values.

Measurements on tubes of varying length at fixed flow-rate

Four different straight lengths of a nominal $0.007\ \text{in.}$ I.D. stainless-steel tube were connected between the injection valve and the detector of an LC instrument system and the bandwidth contribution of the instrument and of each length of tubing were determined.

The instrument consisted of a Perkin-Elmer Series 2 pump, a Valco injection valve with $0.5\text{-}\mu\text{l}$ loop, a Perkin-Elmer Model LC-75 UV detector with flow cell ($3 \times 1\ \text{mm}$ I.D.) with a volume of about $2.6\ \mu\text{l}$, but slightly different design than that described in the previous experiment.

First a 100-cm straight length of 0.007-in. tube was put in place, several injections were made, and the detector signal was recorded. Then, a 25-cm length was cut from this tube, leaving $75\ \text{cm}$ of the original tube. A new ferrule was mounted on it and the 75-cm piece was reconnected in place and more injections were made. This process was repeated leaving 50- , then 25-cm lengths of tubing in place. For each length of tubing, three to five injections were recorded. The flow-rate was measured to be $0.5\ \text{ml/min}$.

Data were processed as follows. First, the actual volume of each length of tube was determined as shown in Table V. It was assumed that each 25-cm segment of tube had the same unknown volume, V_{25} , and that the instrument alone contributed a fixed volume with centroid V_1 in all the measurements. It was also assumed that the centroid of the instrumental contribution V_1 and of the peak eluted from each tube, V_c , added to give the measured centroid in each experiment. The mean measured centroid is given in the third column of Table V with 90% confidence limits calculated from the measured standard deviations and Student's t factor¹⁰.

From Fig. 4, the ratio of V_c to V_1 for each tube was determined. Using it, an equation relating measured centroid, instrumental centroid, and tube volume was written as shown in the fifth column of Table V. Three independent solutions from the four equations gave mean values of $25.9\ \mu\text{l}$ for V_1 and $7.56\ \mu\text{l}$ for V_{25} . The volume of each tube was taken to be the appropriate multiple of V_{25} . They correspond to an inside diameter of $0.196\ \text{mm}$ ($0.0077\ \text{in.}$), 10% larger than nominal.

The mean variance measured for each tube length is shown in the fourth column of Table VI, with 90% confidence limits calculated from the standard deviation of the measurements and Student's t factor. It was assumed that each mean variance was the sum of the fixed instrumental variance σ_1^2 plus the variance of the tube. Using the measured tube volumes and eqn. 5 the variance of each tube was calculated as shown in the sixth column of Table VI. The instrumental variance was determined as the single value which when added to the four calculated tube variances gave the least squares best fit to the four measured mean variances. This instrumental variance was $66.3\ \mu\text{l}^2$. The difference between it and each measured total variance was taken as the variance of each tube from measurements. This is compared in column 5

TABLE V

DETERMINATION OF TUBE VOLUMES FROM MEASUREMENTS

Change in measured centroid with change of tube length is corrected by delay ratio V_e/V_T for centroid of short tubes. V_1 is the centroid volume of the instrument alone, assumed to be fixed. V_{2s} is the true volume of a 2.5 cm segment of the tube, assumed to be uniform for all lengths of tube. Tube volume is the average of 3 independent determinations from the four equations. Average value for V_1 is 25.9 μ l.

Tube length (cm)	Normalized length in plates (n)	Measured centroid of instrument plus tube, with 90% confidence limits (μ l)	Delay ratio of centroid to tube volume, V_e/V_T from Fig. 4	Equation relating measured centroid to instrumental centroids and tube volume	Tube volume, V_1 determined from simultaneous equations (μ l)
100	7.34	57.6 ± 1.5	1.04	$57.6 = V_1 + 1.04 (4V_{2s})$	30.2
75	5.50	50.0 ± 0.6	1.07	$50.0 = V_1 + 1.07 (3V_{2s})$	22.7
50	3.67	42.2 ± 0.7	1.11	$42.2 = V_1 + 1.11 (2V_{2s})$	15.1
25	1.835	35.1 ± 0.6	1.17	$35.1 = V_1 + 1.17 (1V_{2s})$	7.56

TABLE VI

COMPARISON OF MEASURED AND THEORETICAL BANDWIDTHS FOR FOUR SHORT TUBES

Four different lengths of nominal 0.007-in. diameter straight tube measured in a UV instrument system with an estimated instrumental variance of $66.3 \mu\text{l}^2$. Sample is sodium benzoate in water mobile phase at room temperature.

Tube length, (cm)	Calculated normalized length in plates (n)	Tube volume from centroid measurements, V_T (μl)	Measured variance of tube plus instrument, with 90% confidence limits (μl^2)	Variance of tube		Standard deviation of tube	
				From measurements, σ^2 (μl^2)	Theoretical, from eqn. 5, σ^2 (μl^2)	From measurements, σ (μl)	Theoretical, from eqn. 5, σ (μl)
100	7.34	30.2	163.8 ± 26.2	97.5	104.7	9.9	10.2
75	5.50	22.7	146.0 ± 5.1	79.6	75.4	8.9	8.7
50	3.67	15.1	119.9 ± 13.3	53.6	46.1	7.3	6.8
25	1.84	7.6	81.2 ± 2.2	14.9	19.1	3.9	4.4

TABLE VII

BANDWIDTH OF TUBES JOINED BY UNIONS

A total length of 100 cm of nominal 0.007-in. tube divided into segments joined by unions, and measured in a U instrument system with an estimated instrumental variance of $66.3 \mu^2$. Sample was sodium benzoate in water mobil phase at room temperature.

Length of tube segments joined by unions (cm)	Measured variance of joined tubes plus instrument, with 90% confidence limits (μ^2)	Variance of joined tubes		Standard deviation of joined tubes	
		From measurements (μ^2)	Theoretical from col. 6, Table V (μ^2)	From measurements (μ)	Theoretical from col. 4, this table (μ)
100	164.8 ± 26.2	98.5	104.7	9.9	10.2
75, 25	153.0 ± 15.9	88.7	94.5	9.4	9.7
50, 25, 25	150.0 ± 4.7	83.5	84.2	9.1	9.2
25, 25, 25, 25	138.8 ± 1.7	72.5	76.4	8.5	8.7

of Table VI. Standard deviations of the tubes from measurement and theory are the square roots of these variances shown in columns seven and eight.

Measurements on coupled tubes

The effect of breaking a single straight tube into an assembly of shorter segments coupled with unions was studied as follows. During the performance of the previously described experiment on tubes of varying length, after each 25-cm segment was cut from the initially 100-cm tube, it was joined again to that tube with an SSI union, together with all other 25-cm segments previously cut off, so that the overall length was still 100 cm. Several injections were made and peaks were recorded. All conditions were otherwise the same as in the previous experiment. This resulted in measurements on 100 cm of tube in these four configurations: one piece, 100 cm; one piece 75 cm, one piece 25 cm and one union; one piece 50 cm, two pieces 25 cm and two unions; four pieces 25 cm and three unions. The means of variances measured on each configuration, with 90% confidence limits are shown in the second column of Table VII.

The variance of each tube configuration was determined by subtracting from the mean total variance the $66.3 \mu^2$ instrumental variance determined in the previously described experiment with tubes of varying length. The results are shown in the third column of Table VII. In the fourth column the theoretical variance for each configuration is given. It was calculated by adding the theoretical variances of the appropriate components previously calculated and given in the sixth column of Table VI, and ignoring the contribution of the unions. For example, the theoretical variance for the combination of 50-, 25- and 25-cm pieces is the sum of the calculated variance for the 50-cm tube plus twice the calculated variance of the 25-cm tube from Table VI. The corresponding standard deviations from measurement and theory are compared in the fifth and sixth column of Table I.

DISCUSSION

Applicability of the results for straight tubes

In the experiments on the 366-cm tube, its normalized length ranged from 126 down to about 3 plates. Though the predicted doubly curved peak shapes were observed in the transition region near 10 plates, this is an insufficient range of n to show conclusively that the experimental results agree with the results of the computer model. However, the good agreement of the measurements on the fluorescence detector with the predictions for low flow-rates suggests that the results of the computer model apply to very short tubes. Long tube theory applied to the fluorescence cell would predict a minimum bandwidth contribution 2.5 times greater than observed at 0.1 ml/min.

We speculate that the measured bandwidths of the fluorescence cell which are much lower than predicted at high flow-rates are caused by an inertial mixing effect at the junction of the 0.38 mm diameter lead-in tube and the 1.5 mm diameter cell. Rough calculations show that at 0.1 ml/min, the kinetic energy of the liquid leaving the lead-in tube is more than adequate to sustain a toroidal secondary circulation in the initial part of the cell. This circulation may extend 1 or 2 tube diameters into the cell. Since the cell's length from entrance to detector beam is less than 3 tube diameters, such an inertial mixing process could be expected to substantially reduce its bandwidth. Just as for other inertial mixing effects, it should exhibit a transition flow-rate. If this is true, the experimental data suggest that the transition flow-rate is of the order of 0.05 ml/min in this case.

Curved tubes

Measurements on the curved 366-cm tube confirm the applicability of the transition flow eqn. 12. No effort was made in this work to study quantitatively the bandwidth of curved tubes at higher than the transition flow-rate.

Significant findings are the surprising sensitivity of bandwidth of connecting tubes to slight curvature, and that a single bend functions as a localized mixing feature at flow-rates common in LC systems. These results mean that in practical LC systems so much of the tubing is operated above its transition flow-rate that its contribution to extra-column bandwidth is generally much less than straight tube theory would predict, except at the very low flow-rates used with microbore columns⁸.

Additivity of variances

A uniform tube can contribute a variance proportional to its length if and only if the variance of any segment of the tube obeys eqn. 4, the long-tube case. In the results of the computer model for short tubes where $n < 30$ the variance departs increasingly from eqn. 4. Therefore, according to the model the variances of successive short segments of a tube do not add.

The results of the experiment with four tubes of different length reported in Tables V and VI, are consistent with the results of the computer model, but they may not be proof of the non-additivity of variances because, within the errors of the assumptions and measurement, other interpretations may be possible. But this experiment established reasonable values for the tube volumes and the instrumental

variance used in the parallel experiment on the effect of unions on the bandwidth of 1 m of tube reported in Table VII. In this parallel experiment, it was clearly shown that the sum of the measured variances of separate segments of tube joined by unions is less than the measured variance of the same segments when in one continuous piece. This is in agreement with the computer model's results for short tubes.

An explanation of the bandwidth-reducing effect of unions is as follows. A necessary condition for variances of successive components in a flow path to add is that the concentration of sample entering and leaving each component must be describable by a single-valued function of time. This is not the case for short segments of open tube smoothly joined together to form a continuous piece. Sample injected on the axis of a short segment is eluted close to the axis. Sample injected near the wall is eluted much later, near the wall. Even in a very long straight tube, when a sample is injected uniformly and simultaneously over the entrance to the tube, it emerges at the end with the sample distribution on the axis leading the distribution at the wall by 3 theoretical plates. Because of this, the variance of a segment which is connected as a continuation of the tube will be additive to the variance of the original tube only if the normalized length of the continuation is much greater than 3 plates. Then the spread of 3 plates between axis and wall as the sample enters the continuation will be negligible compared to the spreading effect of the continuation segment itself.

If the second segment is added not as a continuation of the first tube, but is coupled to it with a union, the union may act as a localized mixing feature which thoroughly mixes sample from the axis and the walls of the first segment of tube and redistributes it uniformly over the entrance to the following segment, without adding significant spreading of its own. Any such localized mixing component causes a transfer of sample from one segment to the next which is describable by a single-valued function of time. Therefore, variances of tube segments joined by such mixing components should add, no matter what the normalized length of the segments.

The experimental results of Table VII show that the measured total variances of the tubes segmented by unions approximately equalled the sum of the variances of their separate segments. This is consistent with the assumption that at 0.5 ml/min, each union functioned as a localized mixing component.

Within the errors of measurement, there was no evidence that the unions contributed variance that was significant compared to the variance contribution of a 25-cm segment of the tube. Since the nominal volume of the through hole in these unions was of the order of 0.2 μ l, this is a reasonable result.

It is very likely that most of the radial mixing process in the union is inertial, caused by step changes in cross section or by misalignment. Hence there is probably a transition flow-rate below which the union becomes relatively ineffective as a mixing component. Therefore, one can speculate that in systems used with microbore columns with much lower flow-rates and instrumental bandwidth, the variance contribution of such unions may be higher, their mixing effectiveness lower, and their contribution to instrumental bandwidth no longer negligible.

An ideal column end fitting should also function as a radial mixing component. At the input, it should mix sample from the axis and the wall of a small-bore connecting tube and distribute the resultant fluid uniformly and simultaneously across the top of the column without adding significant variance. At the output of the column, it should perform a corresponding transfer of sample mixture from axis and wall of the

column uniformly and simultaneously cross the entrance to the connecting tube.

Ideal end fittings could have an important effect in joining together a set of packed columns that share a defect which permits samples to travel at a different velocity on axis than at the wall, especially if these columns are short compared to the length that permits radial dispersion to redistribute sample uniformly over the cross-section. The variances of the peaks eluted from these columns should add if they are coupled in series with ideal column fittings and short connecting tubes of negligible bandwidth contribution. But if the columns are coupled in series by removing the end fittings and butting their ends in drilled out unions, it can be expected, for the same reasons as for short open tubes, that their variances should not add, and that the variance of the combination should be greater than the sum of the variances measured on separate segments between column end fittings. Golay¹¹ proposed mixing devices similar to a pair of ideal end fittings, but internal to the column for large preparative gas chromatographic columns.

Use of a long straight tube to determine diffusivities

When the diffusivity of an LC sample in a particular mobile phase is not known, a convenient method to determine it is to use an LC instrument system to measure the spreading of the sample peak injected into a long straight tube between injection valve and detector. The method should be accurate if precautions are taken against mixing effects other than diffusion, and the tube is long enough so that the long-tube theory applies. These conditions are assured if the measured plate height in the tube is accurately proportional to flow-rate over at least a 2 to 1 range of flow-rates.

To achieve this the tube must be smooth and in a single piece, and straight enough so that F_{trans} calculated using eqn. 12 is substantially larger than the largest flow-rate at which measurements will be made. It must be long enough so that at the highest flow-rate and for the diffusivity being measured, its normalized length is greater than 30 plates. This will generally require physically separating the injection valve from the detector so that they can be connected to the opposite ends of the long tube with short connections. Naturally, the eluted peaks from the tube should have variances at least an order of magnitude greater than that of the instrumental system alone, so that no significant error is caused by correcting for the instrumental volume and variance. This can be measured by replacing the long tube with a very short tube of small diameter having negligible volume and variance contribution.

Axially illuminated absorbance flow cells

The results presented in this paper do not apply directly to axially illuminated flow cells such as are typical in Ultraviolet absorbance detectors. In these cells the sample is injected at one end of the cell and remains fully in the beam until it reaches the other end. The detector signal is thus neither an elution curve nor a slice content curve. Instead, it is the initial amount of sample injected into the tube minus the integral of the elution curve from a short tube of the same length and volume as the cell. Curves for axially illuminated cells and their moments can be derived from the results of the computer model reported here by additional data processing. These results will be reported in another paper.

ACKNOWLEDGEMENTS

The computer numerical models were programmed by Harold Jackson. The programs to analyze results were written by Duncan Harris. The experimental data were taken and reduced by Jane Goldstein. The authors are grateful to these co-workers for their skillful contributions, and to Mrs. Goldstein for conceiving the experiment on the effect of unions.

REFERENCES

- 1 G. Taylor, *Proc. Roy. Soc. A*, 255 (1956) 67.
- 2 M. J. E. Golay, in V. J. Coates, H. J. Noebels and I. S. Fagerson (Editors), *Gas Chromatography 1957, (Lansing Symposium)*, Academic Press, New York, 1958, p. 1.
- 3 W. N. Gill and V. Ananthakrishnan, *AIChE J.*, 13 (1967) 801.
- 4 M. J. E. Golay and J. G. Atwood, *J. Chromatogr.*, 186 (1979) 353.
- 5 K. P. Maycock, J. M. Tarbell and J. L. Douda, *Separ. Sci. Technol.*, 15(6) (1980) 1285-1296.
- 6 M. J. E. Golay, *J. Chromatogr.*, 196 (1980) 349.
- 7 R. Tijssen, *Separ. Sci. Technol.*, 13 (1978) 681.
- 8 R. P. W. Scott and P. Kucera, *J. Chromatogr.*, 169 (1979) 51.
- 9 P. A. Bristow, *Liquid Chromatography in Practice*, hctp, Wilmslow, 1976, p. 250.
- 10 E. L. Bauer, *A Statistical Manual for Chemists*, Academic Press, New York, 2nd ed., 1971, p. 16.
- 11 M. J. E. Golay, in H. J. Noebels, R. F. Wall and N. Brenner (Editors), *Gas Chromatography*, Academic Press, New York, 1961, p. 11.

CHROM. 14,230

EFFECT OF RADIAL THERMAL GRADIENTS IN ELEVATED TEMPERATURE HIGH-PERFORMANCE LIQUID CHROMATOGRAPHY

S. ABBOTT*, P. ACHENER, R. SIMPSON and F. KLINK

Varian Associates Instrument Group, Walnut Creek Division, 2700 Mitchell Drive, P.O. Box 9016, Walnut Creek, CA 94598 (U.S.A.)

SUMMARY

The advent of highly efficient columns in high-performance liquid chromatography (HPLC) requires careful design of extra-column components such as injectors, coupling tubing and detectors in order to minimize peak dispersion. A dispersion effect which has not been treated in detail in the chromatographic literature is that of a radial thermal gradient at the column inlet generated by an imbalance between the inlet fluid and column temperature. The significance of this effect and a means to reduce it in elevated temperature HPLC is demonstrated in this report.

INTRODUCTION

A potential limit to achieving the separation efficiency inherent to an high-performance liquid chromatographic (HPLC) column is the variance due to a mismatch of the temperature of the mobile phase entering the column and the column temperature. Typical HPLC solvents and packings such as silica and polystyrene are poor thermal conductors relative to stainless steel. Thus, the fluid segment entering the wall region of the column will come to the column set temperature before the fluid segment entering the center of the column. The resultant radial thermal gradient translates into a radial retention gradient and hence into solute band broadening.

THEORETICAL

A detailed theoretical treatment of a radial thermal gradient in a column, generated by a mismatch of inlet fluid and column temperatures is given in Appendix I. The radial thermal gradient, $T_{\text{center}} - T_{\text{wall}}$, should be dependent on the difference between the inlet fluid and column temperature, the flow-rate and column bore and should be essentially independent of the mobile phase, the particle size of the packing and the solute.

The theoretical treatment of Appendix I predicts that radial thermal gradients can be minimized by reducing the column bore (decreases with the second power of the column bore) and by heating the mobile phase to the column temperature prior to the column inlet. The success of the latter procedure is demonstrated later in this report.

The variance due to the presence of a radial thermal gradient in an HPLC column is a complex function of several factors. Since the temperature at the column center will be lower than that at the walls, the center fluid will have a higher viscosity, η , and thus center molecules will not only experience a higher capacity factor, k' , but a lower flow velocity, u , and different eddy diffusion and mass transfer plate heights than do wall molecules. These radial effects should lead to increased peak dispersion.

The degree to which a centrally injected solute band diffuses out towards the column walls during its migration through the column will determine the degree to which it "sees" the radial thermal gradient. A centrally injected sample slug and a smaller particle size¹ packing should decrease outward diffusion of the solute band and thus reduce the variance observed for a given radial thermal gradient.

One should also note that frictional heating of the mobile phase produces a radial thermal gradient opposite in direction to that of the inlet fluid/column temperature mismatch. The magnitude of this effect has been shown by Halasz *et al.*² to increase linearly with operating pressure.

Factors which determine the degree to which a radial thermal variance affects chromatographic performance are the column plate height and column length. Since radial thermal gradient and column plate heights are additive, the effect of a given radial thermal gradient variance on chromatographic performance will increase as column plate height is reduced. The fraction of the column in which the radial thermal gradient is significant increases as column length decreases. The theoretical treatment of Appendix I predicts that the radial thermal gradient is significant over the initial 1.5–2.5 cm of a typical column. Thus, use of shorter columns such as 5–10 cm should increase the effects of radial thermal variances over those seen with 15–30 cm columns.

EXPERIMENTAL

Chromatography was performed using a Varian Model 5060 liquid chromatograph and a Varian UV-50 variable-wavelength detector having an 8- μ l flow cell and selectable time constants of 2, 1, 0.5 sec. Injections (2 μ l) were made using a six-port Valco sample injection valve with a 10- μ l loop. The 13% C moderate loading C₁₈ reversed-phase columns used were Varian MicroPak MCH-10 (4 \times 300 mm) and MicroPak MCH-5 (4 \times 150 mm). The inlet mobile phase was pre-heated between the injector and column, using an aluminum bar in which two slots were milled, to hold a 10-cm loop of 0.23 mm I.D., 316 stainless-steel tubing. The bar was placed in the A side of the Model 5060 column heater, and connected via a 5 cm \times 0.23 mm I.D. tube to the analytical column in the B side of the heater. The 5-cm connector was insulated with a short piece of refrigeration tubing.

RESULTS AND DISCUSSION

Radial thermal gradients in reversed-phase chromatography (RPC) of non-polar solutes

The chromatographic consequences of a radial thermal gradient are shown in the experimental plate height–temperature data of Fig. 1, obtained on 4 \times 300 mm MCH-10 (10- μ m C₁₈) and 4 \times 150 mm MCH-5 (5- μ m C₁₈) columns. Data was taken

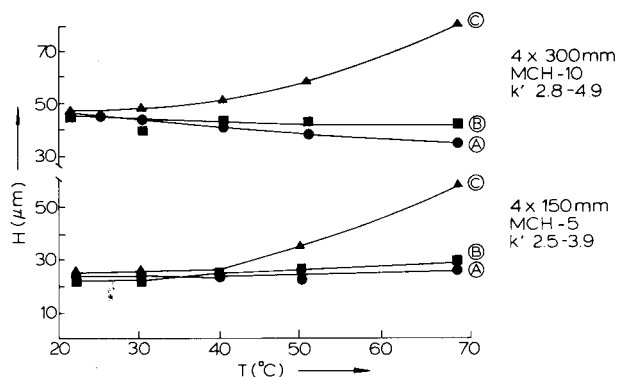


Fig. 1. RPC of anthracene. Temperature dependence of plate height: A, theoretical prediction (see Appendix III). B, experimental data, with inlet mobile phase heated to column T with preheater loop; C, experimental data, without pre-heating of inlet mobile phase. Lower section is data for 4×150 mm MicroPak MCH-5. Upper section is data for 4×300 mm MicroPak MCH-10. Mobile phase: 70% acetonitrile in water; flow-rate 1 ml/min.

with and without heating of the mobile phase to the column temperature prior to the column inlet. The "pre-heating" was achieved simply by fixing a 10-cm loop of 0.23 mm I.D. tubing in an aluminum bar which was placed in one compartment of the Model 5060 dual column heater. Calculation of the tubing length necessary to pre-heat the mobile phase to a given temperature at a given flow-rate, is described in Appendix II. The heated loop was connected to the column, located in the second compartment of the column heater, via a 5×0.23 cm tubing length which was insulated with a short piece of refrigeration tubing.

The 10- μ m C_{18} traces of Fig. 1 represent a theoretical prediction of $H(T)$, as described in Appendix III (Trace A); experimental $H(T)$ data, using pre-heated mobile phase (Trace B); and experimental $H(T)$ data, without pre-heating of the mobile phase (Trace C).

The experimental data demonstrate the efficacy of the pre-heater loop in that its experimental $H(T)$ curve matches the theoretical $H(T)$ curve up to 50°C, the

TABLE I

RADIAL THERMAL GRADIENT PLATE HEIGHT CONTRIBUTIONS

Non-polar solute: anthracene. Mobile phase: 70% acetonitrile in water; flow-rate 1 ml/min. Column: MicroPak MCH-10 (10- μ m C_{18}), 4×300 mm.

Plate height term	Contribution (μ m)	
	30°C (k' 4.9)	50°C (k' 3.7)
Column	47	42
H_T , radial thermal gradient (uncorrected)	4.8	14.9
Pre-heater loop for elimination of H_T^*	0.41	0.46

* Theoretical estimate based on treatment of ref. 3.

normal operating range of silica-based HPLC columns. The deviation between curves B and C at $T > 50^\circ\text{C}$ may indicate increased radial diffusion of the solute band rather than a radial thermal gradient effect. The reduction in plate height with temperature is due to dominance of the eddy diffusion and mobile phase diffusion terms which are proportional to $D_m^{-0.33}$ and $D_m^{-1.0}$ respectively, where the mobile phase diffusion coefficient, D_m , is proportional to T/η (η = viscosity).

Curve C, representing $H(T)$ without the pre-heater loop demonstrates the consequences of a radial thermal gradient. The plate height increase is significant above $\approx 25^\circ\text{C}$. The difference between the B and C curves can be taken to be the radial thermal gradient plate height, H_T . The data of Table I shows that at 30°C and 50°C , the thermal term H_T is highly significant. These experimental values are compared to theoretical estimates of variance due to laminar flow through the pre-heater loop (based on treatment of ref. 3).

The data of Fig. 1 suggests that optimum operation of the $10\text{-}\mu\text{m}$ column for RPC of non-polar compounds would be at a temperature $\approx 10^\circ\text{C}$ above ambient in order to control column T and thus optimize retention reproducibility, and obtain $\approx 10\%$ lower plate height. Higher temperature does not significantly reduce the plate height. Thus, $30\text{--}40^\circ\text{C}$ operation with a pre-heated mobile phase is recommended for $10\text{-}\mu\text{m}$ RPC of non-polar compounds.

The $5\text{-}\mu\text{m}$ C_{18} traces of Fig. 1 again demonstrate the efficacy of the pre-heater loop in that its experimental curve matches the theoretical prediction of $H(T)$. The relatively flat H versus T curve was predicted due to the fact that in reducing particle size to $5\text{ }\mu\text{m}$, the mobile phase diffusion term loses relative significance and the eddy diffusion and longitudinal terms, which are proportional to $D_m^{-0.33}$ and $D_m^{+1.0}$ gain significance.

The C curve of the $5\text{-}\mu\text{m}$ data indicates that up to 40°C , the thermal plate height H_T is relatively small ($\approx 1.5\text{ }\mu\text{m}$). This may be due to increased frictional heating of the mobile phase, which could balance the inlet fluid/column temperature thermal gradient and to the reduced degree of solute diffusion to the walls with the $5\text{-}\mu\text{m}$ particle bed. The $5\text{ }\mu\text{m}$, 15 cm column operated at $\approx 2.6\times$ the pressure of the $10\text{ }\mu\text{m}$, 30 cm column and thus should have a 2.6 fold greater degree of frictional heating.

The H_T term (B minus C curves) becomes significant above 40°C , presumably due to the simultaneous decrease in frictional heating due to reduced operating pres-

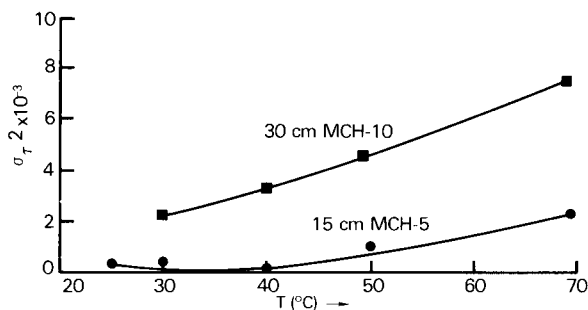


Fig. 2. Variance due to radial thermal gradient, σ_T^2 , as function of temperature for $4 \times 150\text{ mm}$ MicroPak MCH-5 and $4 \times 300\text{ mm}$ MicroPak MCH-10 columns. Details as in Fig. 1. Note: in absence of secondary effects, σ_T^2 would be equivalent for the columns.

TABLE II

RADIAL THERMAL GRADIENT PLATE HEIGHT CONTRIBUTIONS

Conditions as in Table I, except for MicroPak MCH-5 (5- μm C₁₈), 4 \times 150 mm.

Plate height term	Contribution (μm)	
	30°C (k' 3.7)	50°C (k' 2.9)
Column	20	20
H_T , radial thermal gradient (uncorrected)	1.5	11.5
Pre-heater loop for elimination of H_T *	1.3	1.3

* Theoretical estimate based on treatment of ref. 3.

sure, the increase in solute band diffusion to the walls due to increased D_m and the increasing radial thermal gradient. However, the 5- μm H_T values are still significantly less than one would predict in the absence of the secondary effects of frictional heating and reduced radial diffusion. This fact is shown clearly in Fig. 2, a plot of radial thermal gradient variance, σ^2_T , versus temperature for the 10- μm and 5- μm RPC columns. The σ^2_T values for the 5- μm column are 5–10 fold lower than those of the 10- μm column in the 25–50°C operating range.

The data of Table II indicates that heating of the 5- μm column will not significantly reduce plate height, and that operation slightly above ambient (25–30°C) with a pre-heated mobile phase, in order to optimize retention reproducibility (due to column T control) is optimum. The pre-heater loop can be reduced to less than 5 cm for this low T operation.

Radial thermal gradients in reversed-phase chromatography of ionic compounds

Reversed-phase plate heights of ionic solutes are significantly larger than those observed for non-polar solutes. The increased plate height of an ionic compound is

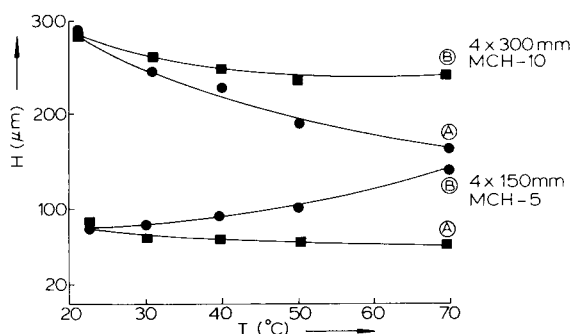


Fig. 3. RPC of quinidine. Temperature dependence of plate height: A, experimental data, with inlet mobile phase heated to column T with pre-heater loop. B, experimental data, without pre-heating of inlet mobile phase. Mobile phase: 90% aqueous KH_2PO_4 buffer (0.02 M , pH 2), 10% acetonitrile, 0.02 M in tetramethylammonium chloride (competing base); flow-rate 1 ml/min.

presumably due to slower mass transfer in the stationary and/or mobile phase. These processes are dependent on the first power of the diffusion coefficient. Thus, the plate height of an ionic solute such as the base quinidine should decrease more rapidly with an increase in column temperature than does that of a non-polar solute such as anthracene. This effect is shown in the experimental data of Fig. 3. Again, one notes that the use of a pre-heated mobile phase provides a significant reduction in observed plate height.

The data of Fig. 3 suggests that optimum ionic RPC operation should be at $\approx 35\text{--}50^\circ\text{C}$ to reduce plate height by 20–40% for 10- μm and 10–20% for 5- μm columns. Higher temperatures can result in a significant reduction in column life due to increased rate of silica dissolution by aqueous RPC buffers. As is the case for non-polar solutes, mobile phase pre-heating is recommended for elevated temperature RPC of ionic solutes.

CONCLUSIONS

An imbalance between the inlet fluid temperature and the column temperature should generate a radial thermal gradient in the initial 1.5–2.5 cm of a 4 mm I.D. reversed-phase column. Peak dispersion in RPC due to a radial thermal gradient has been shown to be significant for 4 mm \times 15–30 cm columns and has been shown to be greater for the case of 10- μm particles than for 5- μm particles. The latter observation may be due to the action of secondary effects such as frictional heating, which creates a radial thermal gradient opposite in direction to that generated by an inlet fluid/column temperature imbalance; and reduced radial diffusion of a centrally injected slug outwards to the walls with the smaller particles.

The use of a short "pre-heater" loop of 0.23 mm I.D. tubing in the column thermal block has been demonstrated to be effective in reducing the radial thermal gradient effect. A theoretical treatment of temperature gradients in packed columns (Appendix I) indicates an exponential decrease in the radial thermal gradient as column bore decreases, predicting that this dispersion effect should be significantly reduced with future microbore (*e.g.*, 1 mm I.D.) packed columns.

APPENDIX I

Theoretical treatment of temperature gradients in packed columns

The mechanism of heat transfer in packed cylinders has been studied, both experimentally and theoretically, by a number of investigators. One of the most successful analyses was developed by Singer and Wilhelm⁴ who obtained an analytical solution and applied it to the data of Leva⁵, Leva and Grummer⁶ and others. The result of these authors for the temperature distribution in a cylindrical geometry is

$$\frac{\theta_r}{\theta_o} = \sum_1^x \frac{2}{\beta_n J_1(\beta_n)} \cdot J_0\left(\beta_n \frac{r}{R}\right) \cdot \exp(-4\beta_n^2 E_n z/D) \quad (\text{A1})$$

where

$\theta_f = t_w - t_f = (\text{wall temperature}) - (\text{fluid temperature along the column}), ^\circ\text{C}$
 $\theta_o = t_w - t_o = (\text{wall temperature}) - (\text{entrance temperature of fluid}), ^\circ\text{C}$
 J_o and J_1 = Bessel functions of zero and first order respectively
 β_n = n th root of $J_o(\beta)$
 $R = D/2$ = inner radius of tube, cm
 r = radius in the cylindrical coordinate system, cm
 z = axial coordinate

$$E_n = \left[\frac{1}{(\text{Pe})_o \frac{K_f}{K_{e,s}} + S_n} + \frac{\sigma}{(\text{Pe})_o} + \frac{1}{(\text{Pe})_{e,0}} \right] \frac{D_p}{D} \quad (\text{A2})$$

where

$(\text{Pe})_o$ = a reduced Peclet number = $U_o D_p / \alpha_f$
 $(\text{Pe})_{e,0}$ = a reduced and modified Peclet number = $U_o D_p / E$
 U_o = superficial velocity that would exist if the tube were empty, cm/sec
 D_p = particle diameter, cm
 α_f = thermal diffusivity of the fluid, cm^2/sec
 ε = eddy diffusivity, cm^2/sec
 σ = void fraction between particles
 S_n = a dimensionless quantity which can be shown to be negligible in the cases of interest in the present study
 $K_{e,s}$ = an equivalent thermal conductivity for the combined fluid and the solid particles, $\text{cal}/\text{cm} \cdot \text{sec} \cdot ^\circ\text{C}$
 K_f = (true) thermal conductivity of the fluid, $\text{cal}/\text{cm} \cdot \text{sec} \cdot ^\circ\text{C}$

then E_n reduces to:

$$E = \left[\frac{K_{e,s}}{(\text{Pe})_o K_f} + \frac{\sigma}{(\text{Pe})_o} + \frac{1}{(\text{Pe})_{e,0}} \right] \frac{D_p}{D} \quad (\text{A3})$$

Inserting numerical values for β_n and J_1 in eqn. A1 gives the following equation for the temperature distribution:

$$\begin{aligned}
 \frac{\theta_f}{\theta_o} = & 1.602 J_o \left(2.405 \frac{r}{R} \right) e^{-23.13 E r/D} - 1.065 J_o \left(5.52 \frac{r}{R} \right) e^{-121.9 E r/D} + \\
 & + 0.851 J_o \left(8.65 \frac{r}{R} \right) e^{-299.5 E r/D} - 0.730 J_o \left(11.79 \frac{r}{R} \right) e^{-566 E r/D} + \dots \quad (\text{A4})
 \end{aligned}$$

To apply this equation, the dimensionless parameter E must be first evaluated and this requires that $K_{e,s}$, the equivalent thermal conductivity of the combined liquid and solid particles be calculated. Maxwell⁹ derived an equation which described the thermal conductivity of a mixture of two phases of properties K_c (continuous) and K_d (discontinuous)

$$K = K_c \left[\frac{K_d + 2K_c - 2\chi_d (K_c - K_d)}{K_d + 2K_c + \chi_d (K_c - K_d)} \right] \quad (\text{A5})$$

where χ_d is the concentration of the discontinuous material. Substituting our previous notations, $K_c = K_f$ for the fluid, $K_d = K_s$ for the solid particles and $\chi_d = 1 - \sigma$, eqn. A5 can be written:

$$K_{e,s} = K_f \left[\frac{3K_s - 2\sigma (K_s - K_f)}{3K_f + \sigma (K_s - K_f)} \right] \quad (\text{A6})$$

Inserting this expression in eqn. A3 and replacing $(\text{Pe})_o$ and $(\text{Pe})_{e,o}$ by their values gives the simplified equation:

$$E = \left\{ \alpha_f \left[\frac{3K_s - 2\sigma (K_s - K_f)}{3K_f + \sigma (K_s - K_f)} \right] + \sigma \alpha_f + \varepsilon \right\} \frac{1}{U_o D} \quad (\text{A7})$$

It is noted that the particle diameter, D_p , has dropped out which is due to the fact that the dimensionless parameter S_n was neglected in eqn. A2.

For the case of water flowing at 1 ml/min into a packed column, one can evaluate E by substitution of the following thermal properties: $K_f = 1.43 \times 10^{-3}$ cal/cm · sec · °C; ρ (density of fluid) = 1.0 g/ml; C_p (specific heat of fluid) = 1.0 cal/g · °C; $\alpha_f = K_f / \rho C_p = 1.43 \times 10^{-3}$ cm²/sec; thermal conductivity of fused silica, $K_s = 3.70 \times 10^{-3}$ cal/cm · sec · °C; $\sigma = 0.53$; $U_o = Q/A = (1/60) \times 4/(0.4)^2 = 0.133$ cm/sec (Q = flow-rate; A = cross-sectional area of tube); $\varepsilon = 1.5 \times 10^{-5}$ cm²/sec. Inserting the above values in eqn. A7 yields:

$$E = (2.26 \times 10^{-3} + 7.58 \times 10^{-4} + 1.5 \times 10^{-5}) / 0.133 \times 0.4 \quad (\text{A8})$$

$$= 0.0570$$

The first term in eqn. A8, which involves the equivalent thermal conductivity, is seen to be predominant. Using the above value for E the temperature profile of the fluid at the entrance of the column was calculated for $r/R = 0, 0.25, 0.5$ and 0.75 assuming a constant wall temperature $t_w = 40^\circ\text{C}$ and an inlet fluid temperature of 25°C . The resulting temperature profile is shown plotted in Fig. A1. It is seen that it takes about 1.5 cm for the fluid temperature to come to equilibrium with the wall temperature.

The data of Fig. A1 was replotted in Fig. A2 to show the radial temperature gradients at different distances χ from the entrance.

TABLE A1

THERMAL PROPERTIES OF COMMON HPLC SOLVENTS

Solvent	K_f (cal/cm · sec · °C)	ρ (g/ml)	C_p (cal/g · °C)	α_f (cm ² /sec)
Hexane	3.29×10^{-4}	0.659	0.542	9.21×10^{-4}
Methanol	4.83×10^{-4}	0.787	0.608	1.01×10^{-3}
Dichloromethane	2.91×10^{-4}	1.317	0.284	7.77×10^{-4}

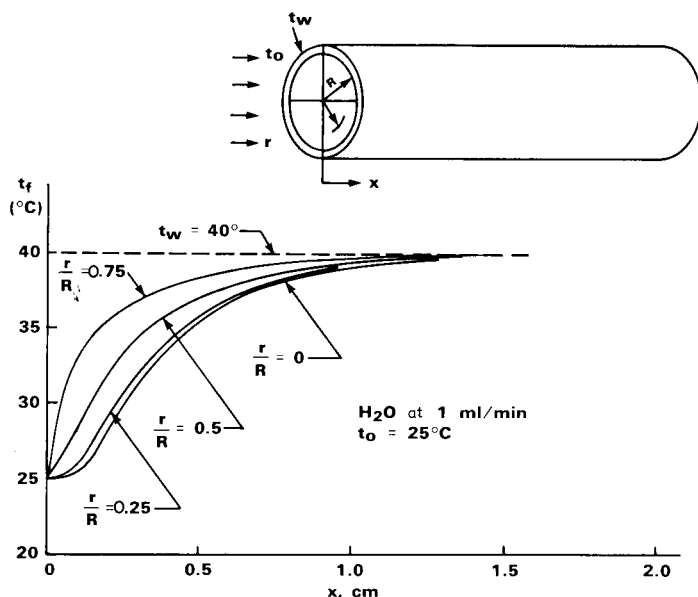


Fig. A1. Theoretically predicted radial thermal gradient in packed silica column. χ = Axial coordinate; r = radial coordinate; R = inner radius of column; t_o = inlet fluid temperature = 25°C ; t_w = wall temperature = 40°C ; t_f = temperature of fluid in column at given (r, χ) coordinates. Mobile phase: water; flow-rate 1 ml/min.

It is of interest to examine the manner in which other solvents behave in comparison with water. Table A1 gives the values of the properties that were used for that purpose.

The resulting values for E are given below for hexane

$$E = (2.499 \times 10^{-3} + 4.88 \times 10^{-4} + 1.5 \times 10^{-5}) / 0.133 \times 0.4 = 0.0564$$

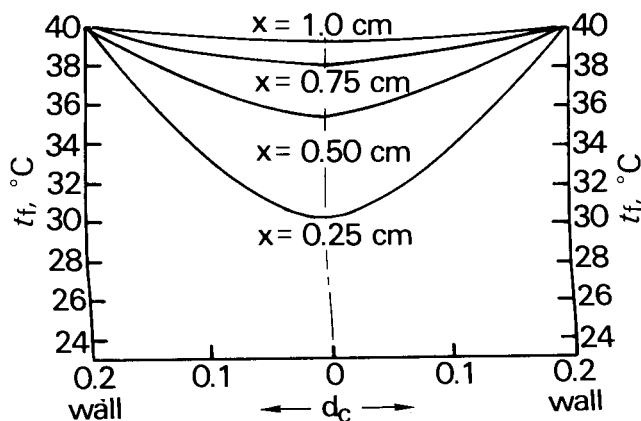


Fig. A2. Radial thermal profiles at different points along column length. χ . d_c = Column diameter; $t_o = 25^{\circ}\text{C}$; $t_w = 40^{\circ}\text{C}$. Mobile phase as in Fig. A1.

for methanol

$$E = (2.463 \times 10^{-3} + 5.35 \times 10^{-4} + 1.5 \times 10^{-5})/0.133 \times 0.4 \\ = 0.0566$$

and for dichloromethane

$$E = (2.171 \times 10^{-3} + 4.12 \times 10^{-4} + 1.5 \times 10^{-5})/0.133 \times 0.4 \\ = 0.0488$$

It is interesting to note that even though there are significant differences between the properties of water and those of the other solvents there is but a slight difference in the resulting values of E which determines how fast the fluid will heat up. This is due to the fact that the dominant factor in E is the first term which is controlled to a large extent by the thermal conductivities of the solid silica particles.

APPENDIX II

Heating of a fluid inside a narrow bore tube with constant wall temperature

The solution of this problem is of interest for the determination of the length of tubing required to pre-heat the mobile phase to a given temperature prior to entering the column. The problem will be solved using the dimensionless approach developed by Kays and London⁷ for compact heat exchangers. The assumption will be made that the tubing is in good thermal contact with a heater block and that the inner wall of the tube is thus at constant temperature. It is first necessary to determine the heat transfer coefficient across the laminar layer. An empirical correlation due to Hausen⁸ is applicable to the case of laminar flow in a circular tube with constant wall temperature

$$\text{Nu} = 3.65 + \frac{0.0668 (d/l) \text{RePr}}{1 + 0.04 [(d/l) \text{RePr}]^{2/3}} \quad (\text{A9})$$

where

$\text{Nu} = hd/K$ = average Nusselt number over the length l , dimensionless

h = heat transfer coefficient, $\text{cal/cm}^2 \cdot \text{sec} \cdot ^\circ\text{C}$

d = inside tube diameter, cm

K = thermal conductivity of fluid, $\text{cal/cm} \cdot \text{sec} \cdot ^\circ\text{C}$

$$\text{Re} = 4Q\rho/\pi d\eta = \text{Reynolds number} \quad (\text{A10})$$

$$\text{Pr} = \eta C_p/K = \text{Prandtl number} \quad (\text{A11})$$

Q = flow-rate, ml/sec

ρ = fluid density, g/ml

η = fluid dynamic viscosity, poise

C_p = fluid specific heat, $\text{cal/g} \cdot ^\circ\text{C}$

Once the heat transfer coefficient has been determined, the number of heat transfer units, Ntu , can be calculated. This is a non-dimensional expression of the "heat transfer size" of the exchanger and is given by

$$\text{Ntu} = Ah/C_m \quad (\text{A12})$$

where

A = heat transfer area, cm^2

$$C_m = Q\rho C_p = \text{fluid capacity rate, cal/sec} \cdot ^\circ\text{C} \quad (\text{A13})$$

Finally, the heat transfer effectiveness, ε , is calculated from which the temperature of the fluid at any point along the tube can be deduced. For a constant wall temperature the relation between Ntu and ε is

$$\varepsilon = 1 - e^{-\text{Ntu}} \quad (\text{A14})$$

and furthermore

$$\varepsilon = (t_2 - t_1)/(t_w - t_1) \quad (\text{A15})$$

where

t_1 = entrance fluid temperature, $^\circ\text{C}$

t_2 = fluid temperature at distance l from entrance, $^\circ\text{C}$

t_w = wall temperature, $^\circ\text{C}$

The first HPLC system to consider is that of hexane flow since hexane, having a low thermal conductivity and low thermal diffusivity, can be expected to be more slowly heated than aqueous solvents and thus constitutes a worst case example. Assume a flow-rate of 1 ml/min inside a stainless steel tube having an internal diameter of 0.23 mm. Hexane physical properties are: $C_p = 0.542 \text{ cal/g} \cdot ^\circ\text{C}$; $\rho = 0.659 \text{ g/ml}$; $\eta = 0.00313 \text{ poise}$; $K = 3.29 \times 10^{-4} \text{ cal/cm} \cdot \text{sec} \cdot ^\circ\text{C}$; $\text{Re} = 194$; $\text{Pr} = 5.16$. Using these values the Nusselt number and heat transfer coefficient are then calculated for various lengths of tubing and the corresponding number of heat transfer units, heat transfer effectiveness and temperatures are determined. For instance at $l = 5 \text{ cm}$: $(d/l) \cdot \text{Re} \cdot \text{Pr} = 4.60$; $\text{Nu} = 3.65 + 3.93$; $h = 0.056 \text{ cal/cm}^2 \cdot \text{sec} \cdot ^\circ\text{C}$; $C_m = 5.95 \times 10^{-3} \text{ cal/sec} \cdot ^\circ\text{C}$; $A = \pi dl = 0.361 \text{ cm}^2$; $\text{Ntu} = 3.40$; $\varepsilon = 0.966$.

The fluid temperature can now be calculated for any desired fluid inlet and wall temperature. Taking for example $t_1 = 20^\circ\text{C}$ and $t_w = 70^\circ\text{C}$ the fluid temperature at $l = 5 \text{ cm}$ can be calculated from eqn. A15:

$$t_2 = t_1 + \varepsilon(t_w - t_1) = 68.3^\circ\text{C}$$

Similar calculations have been carried out for different points along the tube and for wall temperatures of 30°C and 50°C . The results are shown plotted in Fig. A3A.

Another set of temperature profiles was calculated for hexane at a flow-rate of 2 ml/min and these data are shown plotted in Fig. A3B. It can be seen that in the worst case, that of hexane flow at 2 ml/min and a wall temperature of 70°C , a length of tubing of 12 cm is sufficient to raise the fluid temperature to within 1°C of the final temperature.

For comparison purposes, the heating behavior of water under the conditions

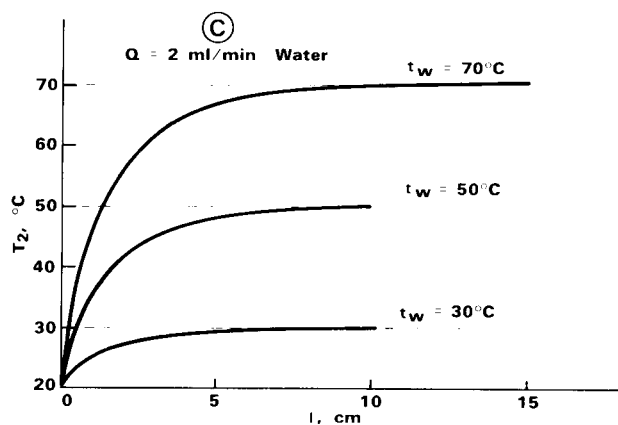
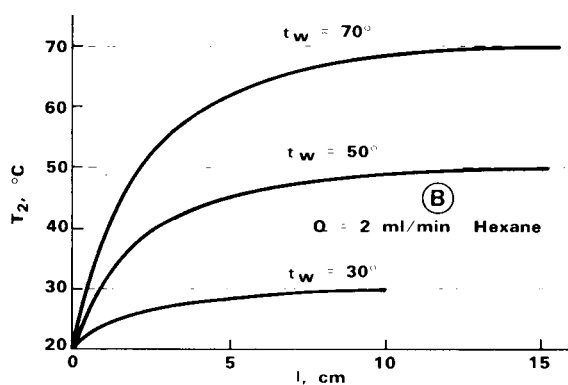
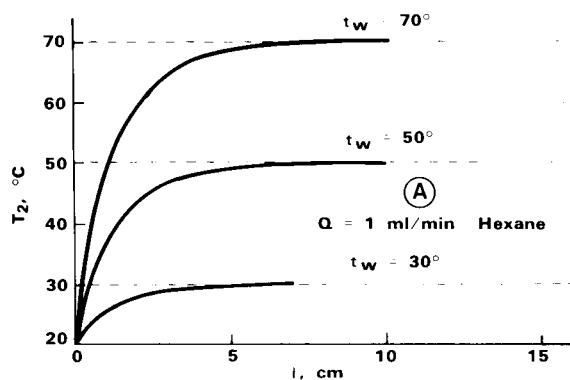


Fig. A3. Fluid temperature t_2 , at a distance l from the tube inlet for a narrow bore tube, inside heater block. t_w = Wall temperature = heater block temperature. Inlet fluid $t = 20^\circ\text{C}$. Mobile phases: 1 ml/min hexane (A); 2 ml/min hexane (B); 2 ml/min water (C).

previously described for hexane has been estimated using the following average properties: $C_p = 1.0 \text{ cal/g} \cdot ^\circ\text{C}$; $\rho = 1.0 \text{ g/ml}$; $\eta = 0.01 \text{ poise}$; $K = 1.43 \times 10^{-3} \text{ cal/cm} \cdot \text{sec} \cdot ^\circ\text{C}$. The calculated profiles for water at 2 ml/min are shown plotted in Fig. A3C. It can be seen that in the worst case, that of $t_w = 70^\circ\text{C}$, a length of only 7.5 cm of tubing is required to raise the fluid temperature to within 1°C of the final temperature.

APPENDIX III

Theoretical estimate of $H(T)$ for RPC of anthracene

The theoretical values of Fig. A1 were obtained using the Knox equation

$$h = Av^{0.33} + (B/v) + Cv \quad (\text{A16})$$

where

h = reduced plate height = H/D_p

v = reduced velocity = ud_p/D_m

A = eddy diffusion constant

B = longitudinal diffusion constant

C = mass transfer term constant

For example, the $h(v)$ plot of the columns studied was approximated by the Knox equation using values of 1.23, 2.8 and 0.04 for the A , B , C parameters of the $10\text{-}\mu\text{m}$ column.

The diffusion coefficient D_m was estimated by assuming $D_m \approx 1 \times 10^{-5} \text{ cm}^2/\text{sec}$ for anthracene at 20°C in the mobile phase (70% acetonitrile–30% water) and the relationship:

$$D_m \propto \frac{T}{\eta} \quad (\text{from Wilke–Chang equation, } T \text{ in } ^\circ\text{K, } \eta \text{ in poise})$$

The relative viscosity at each temperature was obtained from the experimental data of column pressure as $f(T)$. Thus, one calculates $D_m(T)$ and by insertion into eqn. A16 derives $H(T)$ for the experimental condition of $u = 0.25 \text{ cm/sec}$ (1 ml/min on $4 \times 300 \text{ mm}$ column).

REFERENCES

- 1 J. H. Knox, G. R. Laird and P. A. Raven, *J. Chromatogr.*, 122 (1976) 129.
- 2 I. Halász, R. Endeke and J. Asshauer, *J. Chromatogr.*, 112 (1975) 37.
- 3 M. Martin, C. Eon and G. Guiochon, *J. Chromatogr.*, 108 (1975) 229.
- 4 E. Singer and R. H. Wilhelm, *Chem. Eng. Progr.*, 46 (1950) 343.
- 5 M. Leva, *Ind. Eng. Chem.*, 39 (1947) 857.
- 6 M. Leva and M. Grummer, *Ind. Eng. Chem.*, 46 (1948) 415.
- 7 W. Kays and A. L. London, *Compact Heat Exchangers*, McGraw-Hill, New York, 2nd ed., 1964.
- 8 H. Hausen, *Verfahrenstechnik, Beih. Z. Ver. deut-Ing.*, 4 (1943) 91.
- 9 J.C. Maxwell, *A Treatise on Electricity and Magnetism*. Vol.1, 3rd ed., 1904, p. 441

NY 4.2.25

CHROM. 14,142

MICROCAPILLARY LIQUID CHROMATOGRAPHY IN OPEN TUBULAR COLUMNS WITH DIAMETERS OF 10–50 μm

POTENTIAL APPLICATION TO CHEMICAL IONIZATION MASS SPECTROMETRIC DETECTION

R. THJESSEN*, J. P. A. BLEUMER, A. L. C. SMIT and M. E. VAN KREVELD

Koninklijke/Shell-Laboratorium (Shell Research B.V.), Amsterdam (The Netherlands)

SUMMARY

The theoretical separation efficiency of open microcapillary liquid chromatography (LC) columns, including peak-broadening effects resulting from interphase resistance to mass transfer, has been considered and an expression is derived for the plate height caused by interphase resistance.

The use of such columns with internal diameters down to 10 μm is explored for LC separations. The columns were prepared from soft glass tubing and coated with polar and non-polar stationary phases. Several applications in straight phase as well as reversed-phase systems demonstrate the high separation speed (up to 50 effective plates per second). Relatively wide (30–50 μm) and short (1–5 m) columns allow rapid analyses within minutes. Smaller (10–30 μm) and longer (5–25 m) columns yield extremely high plate numbers (up to $5 \cdot 10^6$), permitting very difficult separations in a reasonable time (2–5 h). The required pressure never exceeds the generally accepted value of 400 bar. Preliminary results obtained with fused silica columns are discussed.

Split-injection and addition of make-up mobile phase through the (UV) detector have been applied. In order to avoid undesirable dilution of the sample zones by the make-up liquid, the microcapillaries were directly coupled to a mass spectrometer (in the chemical ionization mode). This technique has yielded promising results.

INTRODUCTION

Gas chromatography (GC) with capillary columns is a well-accepted method for gas analysis. This technique is becoming increasingly popular, as open tubular or capillary columns (with tube diameters of about 0.25 mm) offer more separation power than classical packed columns. In principle, the same applies to liquid chromatography (LC), but, in view of the much slower diffusion in liquids, much smaller column diameters are required (of the order of 10–50 μm)¹. The practical difficulties accompanying this microcapillary LC technique have prevented its successful application until very recently. Apart from the work done in our laboratory, studies of microcapillary LC in columns with diameters down to about 30 μm have recently

been reported²⁻⁷. In the present work we describe the results obtained in columns with diameters down to 10 μm .

In earlier work we tried to enhance radial diffusion in open tubular columns by introduction of secondary flow effects⁸⁻¹⁰, which turned out to be successful in GC and in flow injection analysis (FIA) but not in LC. Here the only way to obtain satisfactory results is to apply drastic miniaturization.

EXPERIMENTAL

Apparatus

Apart from the columns and their connections, only commercially available LC apparatus was used. The main pump was a Perkin-Elmer Series 2 liquid chromatography pump, a dual pump capable of delivering 60 ml/min at pressures up to 4000 p.s.i. A Tracor 950 pump, suitable for low flow-rates (< 1 ml/min), was used for delivering "make-up" or scavenger liquid to the detector. A Waters U6K injector was employed.

The main detectors used were UV absorption detectors, of three types: fixed wavelength (254 nm), Waters Model 440; variable wavelength, Jasco Uvidec 100-II; variable wavelength, Spectra-Physics SP 8400. For all three detectors it was necessary to reduce dead volumes by circumventing the inlet connecting tubes. The most simple way to achieve this is by using the detector cell outlet as the inlet, which can be done with the Waters and the SP detectors without any problems. The result is that the column exit actually protrudes into the measuring cell, thus minimizing dead volumes to the cell volume itself. With the Jasco detector some modifications were required to reach the same goal.

In this way the total dead volumes in the detectors were reduced to the order of 2–8 μl . This, however, is still too large^{1,7} for direct application of the detectors in microcapillary LC, where mobile phase flow-rates through the column of 1–10 $\mu\text{l}/\text{min}$ are common. When such flow-rates enter the detector cell the time constant will be about 1 min, far too large for the detection of peaks which are only a few tens of seconds wide, at most. Reduction of cell volumes to around 1 μl has recently been described^{7,11}, but even so scavenger ("make-up") liquid has to be added to the detector in order to reduce the time constant and peak broadening to acceptable levels. Using specially made T-pieces, each tailored to suit the particular column O.D., we added 0.3–1 ml/min of make-up liquid to the column effluent (just before it entered the detector cell) in order to eliminate most of the peak broadening in the detector. The Jasco detector, although having the lowest cell volume, required a flow-rate of about 1 ml/min, probably due to an unfavourable cell geometry.

The addition of make-up liquid to the column effluent has the major drawback that sample concentrations are diluted by at least a factor of 100. An alternative method of detection which avoids this dilution problem is chemical ionization mass spectrometry (CIMS), using the mobile phase as the ionizing reagent gas. As the column exit can be positioned directly into the ion source via a slightly modified hollow sample probe, no make-up liquid is necessary, thus ensuring far lower detection limits than are possible with UV detectors. A Finnigan 4000 mass spectrometer was used in this work.

Sample introduction

The split injection method was employed to introduce samples into the microcapillary LC columns. Specially made splitting T-pieces were connected to the outlet of the Waters U6K injector, carefully avoiding any additional dead volumes. The inside diameter of each T-piece was adapted to the outside diameter of the particular column used, such that the dead volume inside the splitter was minimized. Nonetheless, splitting ratios of 1:100 to 1:5000 had to be applied to avoid peak broadening from injection. The relatively large split flow (up to 30 ml/min) was recirculated to the mobile phase vessel, except for a short moment during injection, when this flow was directed to waste.

Injection with the U6K turned out to be most efficient when the injector was switched into the injection position only for a very short time (say 0.2–1 sec). Switching back into the "load" position ensures that the rear ends of sample zones are cut off. When this technique was used, especially the earlier peaks in the chromatograms were much more symmetrical and narrower than those found when the injector remains in the injection mode until the next injection.

Injection of samples, either pure or dissolved in some solvent, invariably leads to increased peak widths, especially for the earlier peaks. Obviously, mixing of the sample with the mobile phase requires a finite time, which may affect the efficiency of separations. Therefore samples were dissolved in the mobile phase.

Columns

With the aid of a modified Shimadzu GDM1 Glass Drawing Machine, soft-glass (AR) microcapillaries with internal diameters in the range of 10–100 μm (lengths up to 50 m) were drawn from either standard 6×0.3 mm glass tubing (different manufacturers) or thermometer glass capillaries. The fragile microcapillaries obtained in this way required very careful handling and mounting on a supporting frame onto which both splitting and make-up T-pieces were fastened. The ends of the columns were glued into these T-pieces using epoxy type resins; such connections can easily withstand pressures up to 600 bar. The low-pressure T-piece connection to the column exit can also be effected with a graphite ferrule.

With samples of high molecular weight ($\text{MW} > 250$) and using a mass spectrometer as the detector, enhanced transfer of the column effluent into the ion source is found when a liquid jet is produced at the column outlet. As for packed LC columns¹², this requires that the column effluent should leave the column exit through a very narrow orifice of about 1–5 μm . This can be effected by melting the soft-glass column end and drawing out rapidly. Thus, a conically shaped tip is obtained as the column exit, which is polished to the required opening of a few μm (microscopic inspection).

Recently S.G.E. (Australia) kindly supplied us with fused silica microcapillaries with internal diameters in the range 7–40 μm . Manual handling of these flexible columns is so convenient that no supporting frame is needed.

Coating of the columns

As in capillary GC, it has been possible to coat the inner wall of the column with a thin layer of some polar stationary liquid phase, using the dynamic coating technique¹³. As the shear forces in LC with a liquid mobile phase are appreciably

greater than in GC with a gaseous mobile phase, the shear stability of film coatings has to be enhanced by some surface-roughening technique. We used a modified alkaline etching technique for the soft-glass column wall, originally proposed by Mohnke and Saffert¹⁴. Under somewhat milder conditions than proposed by these authors, *viz.*, 0.5–1.5 *N* KOH at 100°C for 15–30 min, we produced a very thin but highly adsorptive siliceous layer on the column wall. Nota *et al.*¹⁵ and recently Tesářík and co-workers^{16,17} have described analogous procedures.

This porous and active layer can be used either as an adsorptive stationary phase or supplied with a liquid phase by the dynamic coating technique; even the possibility of attaching a chemically bonded phase for reversed-phase LC has to be considered. The latter has been shown to be feasible^{2,3,7}, but in this work we only applied physically adhering coatings.

We also tried to attach a porous adsorptive layer to the column wall, as described by Schwartz and co-workers^{18–20} and Cramers *et al.*²¹ for GC capillaries. Recently Hibi *et al.*²² applied the method to LC capillaries. In this method submicron silica particles are deposited onto the column wall from a stabilized suspension of the aerogel Cab-O-Sil (Cabot Corp., Boston, MA, U.S.A.) in water, again using the dynamic coating procedure. Like etched glass surfaces, Cab-O-Sil coatings can be used either as a stationary adsorbent or subsequently coated with a liquid phase.

For straight-phase LC we used oxydipropionitrile (ODPN) as the stationary liquid on both types of roughened and activated glass surfaces. The mobile phase was isooctane saturated with ODPN. For reversed-phase LC we first determined which non-polar materials were stable against aqueous mobile phases without droplet formation after some time. Using microscope slides we found that many silicon liquid phases (OV-101, SE-30, silicone oils) produced neat layers at first, but when immersed in aqueous mobile phases these layers disintegrated into separate droplets, even if the mobile phases contained a surfactant to reduce surface tension. Only very viscous greases like Apiezon L, M or N were stable for long periods of time. Therefore, for reversed-phase separations we coated the microcapillaries with Apiezon L.

We did not succeed in achieving any stable physically adhering coating on the fused silica columns. Probably, chemical bonding is to be preferred here as the coating technique; examples have been described for GC^{23–25} and recently also in LC⁷.

Data handling

Signals from the UV detectors were stored in digital form on a cassette tape, such that each peak was described by at least 100 data points. From these data the first statistical moment, μ_1 , and the second central moment (variance), μ_2 , were carefully obtained and used to calculate the plate height, H , from:

$$H = L \mu_2 / \mu_1^2 \quad (1)$$

As has been discussed^{26,27}, the commonly used plate height in chromatography, $H = L(\sigma_r/t_R)^2$, may differ appreciably from the moment-based plate height of eqn. 1 for asymmetrical peaks. The mobile phase linear velocity, u , is obtained from the residence time, μ_1 , of non-retained solutes:

$$u = L / \mu_1 \quad (2)$$

THEORETICAL

Dispersion and separation speed

According to the theory of Golay²⁸ for capillary chromatography in straight open tubular columns, the axial dispersion in terms of plate height, neglecting axial molecular diffusion, is given by:

$$H = (C_M + C_S)u \quad (3)$$

The convective dispersion term, C_M , represents the combined effect of velocity profile, radial diffusion and partitioning between mobile and stationary phase

$$C_M = \frac{1 + 6k + 11k^2}{(1 + k)^2} \cdot \frac{R^2}{24 D_M} \quad (4)$$

and the stationary phase term, C_S , represents the slowness of mass transfer by diffusion in the liquid phase film:

$$C_S = \frac{2}{3} \cdot \frac{k}{(1 + k)^2} \cdot \frac{\delta^2}{D_S} \quad (5)$$

For sufficiently thin films ($\delta \ll 1 \mu\text{m}$), C_S has values of 10^{-4} sec or less, which are small in comparison with the C_M term, values of which are in the range of 10^{-2} – 10^{-3} sec. Therefore C_S is negligible and eqn. 3 reduces to:

$$H = C_M u = \frac{1 + 6k + 11k^2}{(1 + k)^2} \cdot \frac{R^2 u}{24 D_M} \quad (6)$$

When comparing experimental plate heights reported in the literature (mainly GC) with the predicted values according to eqn. 6, one invariably finds that the theory underestimates the experimentally observed peak broadening. An obvious reason for this is the additional peak broadening in extra-column parts of the apparatus (injector, detector, connections)²⁶. Even in carefully designed apparatus, however, observed plate heights are not in agreement with eqn. 6^{9,29}.

Several attempts have been made to correct the Golay equation for slow inter-phase mass transfer. Most notable are the theories by Aris^{30,31}, Khan³² and Pethö³³, where an additional C term in the plate height equation has been introduced, which contains a mass transfer coefficient, k_M . This coefficient describes the mass flux in the mobile phase perpendicular to the phase boundary, *i.e.*, the mass flux that is transferred between the two phases. The plate height equation in all three theories is:

$$H = C_M u + C_i u = \frac{1 + 6k + 11k^2}{(1 + k)^2} \cdot \frac{R^2 u}{24 D_M} + \left(\frac{k}{1 + k} \right)^2 \cdot \frac{Ru}{k_M} \quad (7)$$

The physical meaning of k_M and its magnitude are still a matter of debate, however²⁹⁻³⁴.

On the basis of the analogy between heat and mass transfer and using relations

given by Giddings' non-equilibrium theory for chromatographic dispersion³⁴, we have been able to find (see Appendix) an approximate expression for k_M which leads to a simple relationship between C_i and C_M :

$$C_i = kC_M/(1 + k) \quad (8)$$

Eqn. 8 is not exact, but gives an impression of the magnitude of the interphase resistance effect. Combining eqns. 7 and 8 leads to:

$$H = \frac{1 + 2k}{1 + k} \cdot C_M u = \frac{(1 + 2k)(1 + 6k + 11k^2)}{(1 + k)^3} \cdot \frac{R^2 u}{24 D_M} \quad (9)$$

Eqn. 9 shows that observed plate heights can indeed be well in excess of the Golay estimation, depending upon the capacity factor k up to a factor of 2. In this work we investigate whether eqn. 9 is able to describe relative peak broadening in straight microcapillary columns for LC.

Eqn. 9 can be used to find an expression for the speed of separation in micro-

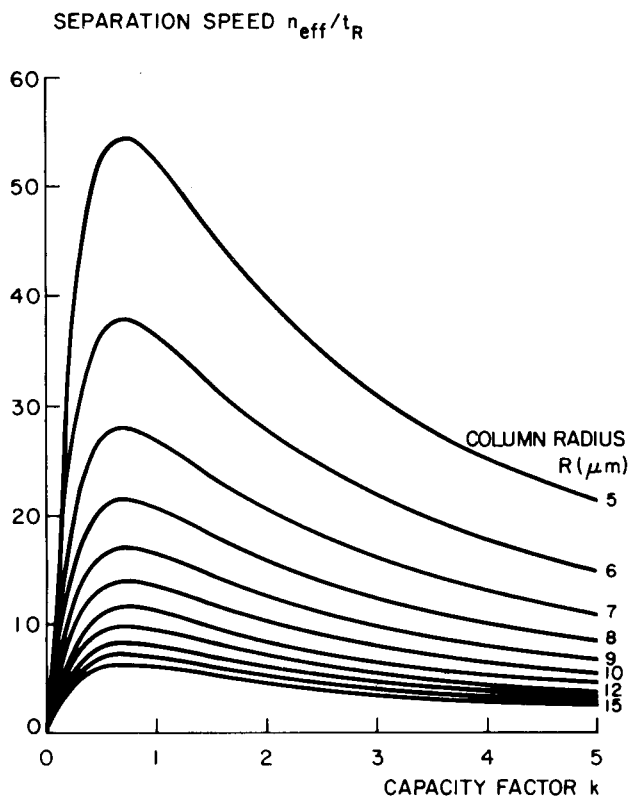


Fig. 1. Separation speed in microcapillary liquid chromatography according to eqn. 10, as a function of relative retention. The diffusion coefficient in eqn. 10 has been taken as $2.94 \cdot 10^{-5}$ cm²/sec (aniline in isooctane).

capillary LC in terms of the number of effective plates generated per unit time. As $H = L/n$, $u = L/t_M$, $t_R = t_M (1 + k)$ and $n_{\text{eff}} = n/(1 + k)^2$, we find that

$$\frac{n_{\text{eff}}}{t_R} = \frac{24 D_M}{R^2} \cdot \frac{k^2}{(1 + 2k)(1 + 6k + 11k^2)} \quad (10)$$

which is plotted as a function of k in Fig. 1, for different column radii, R . Differentiation of eqn. 10 with respect to k shows that the maximum separation speed is obtained at $k = 0.72$; this value is somewhat lower than in packed LC columns, where the optimum is found in the range $k = 2-4$ ³⁵. Fig. 1 clearly shows this maximum: values of more than five effective plates per second, which are of practical interest, can only be obtained in very narrow capillaries with diameters less than 30 μm . As the separation speed is inversely proportional to the square of the column diameter (eqn. 10), high separation speeds can be expected, especially in columns of diameter 10 μm or less. Fig. 1 shows that, e.g., at $k = 1$ a 10- μm microcapillary yields about 50 effective plates per sec, which is much more than can be obtained with modern packed high-performance liquid chromatography (HPLC) columns, even with the smallest (2–5 μm) particles.

The high separation speed of microcapillary columns can be exploited in two ways: for rapid analyses of not too difficult separations (e.g., 10^3 effective plates are available in about 20 sec); or for a very high separation efficiency in the case of very difficult separations, at the cost of longer analysis times (of the order of ≥ 1 h). For instance, in 1 h a 10- μm column at $k = 1$ yields $2 \cdot 10^5$ effective plates (i.e., $7 \cdot 10^5$ theoretical plates). The number of plates obtained may be well above 10^6 , which indicates that very difficult separations which cannot be carried out in packed columns can potentially be performed.

An estimation of the pressure drop required for the operation of microcapillary columns can be based on the Poiseuille equation

$$u = R^2 \Delta p / 8 \eta L \quad (11)$$

where the high permeability ($R^2/8$) of open tubular columns is an important advantage. The linear velocity, u , in eqn. 11 equals L/t_M or $L(1 + k)/t_R$, where t_R is the retention time required to obtain n_{eff} effective plates from eqn. 10; eliminating t_R from eqns. 10 and 11 yields:

$$\Delta p = \frac{192 L^2}{R^4} \cdot \frac{\eta D_M}{n_{\text{eff}}} \cdot \frac{k^2 (1 + k)}{(1 + 2k)(1 + 6k + 11k^2)} \quad (12)$$

For the near-optimum case $k = 1$, the pressure drop has been plotted in Fig. 2 as a function of the number of effective plates, n_{eff} , generated, for different column lengths, L , and for two retention times ($t_R = 1$ min and 1 h). For example, a 10 m \times 20 μm column yields $3 \cdot 10^4$ effective plates in 1 h, requiring a pressure drop of only 22 bar. The same performance can be obtained in 1 min also in a 1 m \times 2.5 μm column, requiring some 800 bar as the inlet pressure. Although Tesařik *et al.*³⁶ claimed to have prepared columns with such small diameters (down to 3 μm), it seems questionable whether these columns can be operated in an efficient way in view of the extra-column broadening. With respect to more practical column diameters of 10 μm or more, Fig.

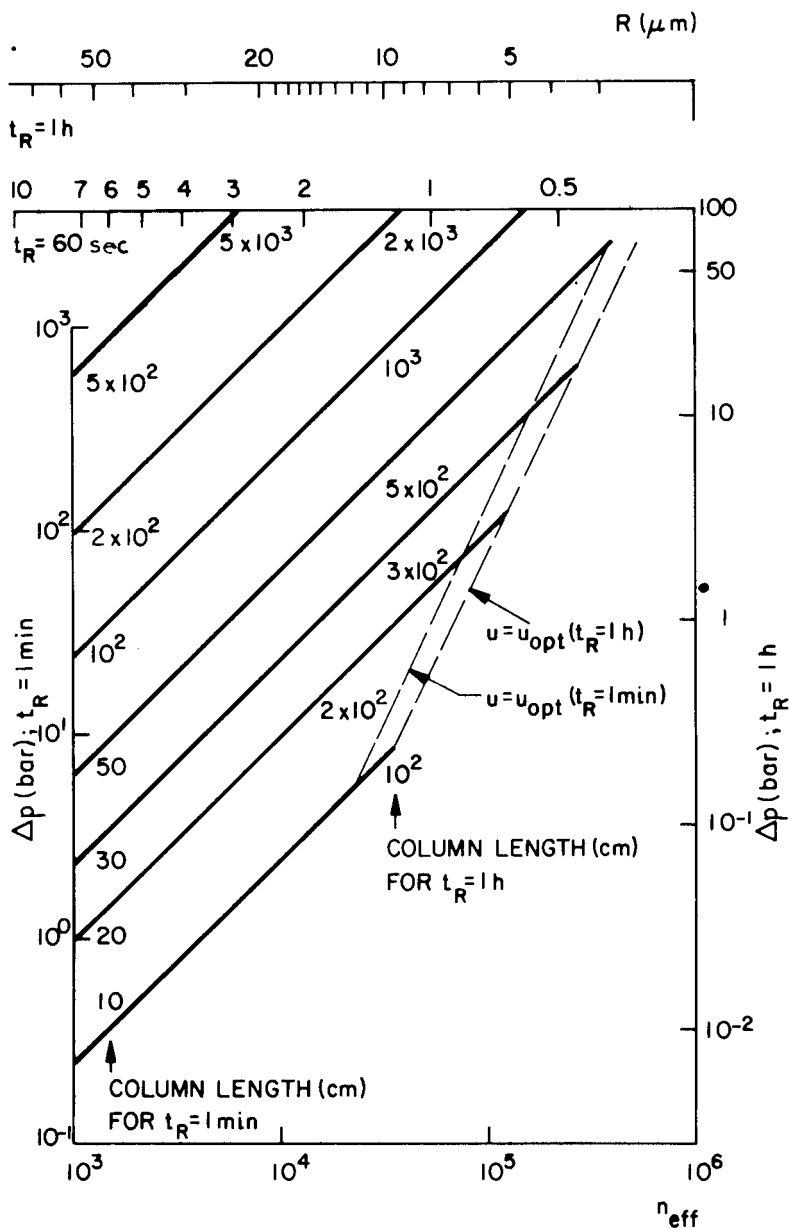


Fig. 2. Operational parameters for microcapillary LC for analysis times of 1 min and 1 h. $k = 1$; $D_M = 2 \cdot 10^{-5} \text{ cm}^2/\text{sec}$; $\eta = 5 \cdot 10^{-3} \text{ P}$.

2 reveals that easy separations with several thousand effective plates can be performed within 1 min in columns of about 3 m in length, applying an inlet pressure of 300–600 bar. The required pressure sharply drops with decreasing column length (*cf.*, eqn. 12: Δp is proportional to L^2): a 1-m column can be operated at the same performance as a 3-m column, but requires a tenth of the pressure.

The scope for optimization towards ever shorter columns is limited, however, for two reasons. First, the extra-column broadening should not become the major source of peak broadening, and secondly the length should be chosen such that the velocity $u = L/t_M$ does not drop below the chromatographic "optimum" velocity where axial diffusion becomes an important source of peak broadening ($H = 2 D_M/u = B/u$). As the optimum velocity is given^{1,13,34} by $u_{opt} = (B/C)^{1/2}$, we find with $C = C_i + C_M = (1 + 2k) C_M/(1 + k)$ that:

$$u_{opt} = \frac{D_M}{R} \left[\frac{48 (1 + k)^3}{(1 + 6k + 11k^2)(1 + 2k)} \right]^{1/2} \quad (13a)$$

For $u \geq u_{opt}$ with $u = L/t_M = L(1 + k)/t_R$ we obtain:

$$L \geq \frac{D_M t_R}{R} \left[\frac{48 (1 + k)}{(1 + 6k + 11k^2)(1 + 2k)} \right]^{1/2} \quad (13b)$$

In the near-optimum case where $k = 1$, and for $R = 10 \mu\text{m}$ and $t \leq 10 \text{ h}$, we have $L \geq 10 \text{ m}$, for example. For $t = 1 \text{ h}$ and $t = 1 \text{ min}$ the dashed lines in Fig. 2 indicate the condition set by eqn. 13b, in the case where $k = 1$.

From Fig. 2 it may be concluded that rapid analysis by microcapillary LC should be performed in short ($L < 3 \text{ m}$) and very narrow columns ($R < 10 \mu\text{m}$). On the other hand, very difficult separation problems can be handled by wider ($R = 10\text{--}20 \mu\text{m}$) and longer ($L = 2\text{--}20 \text{ m}$) columns. In neither case are the required inlet pressures unacceptable.

Direct LC-MS coupling with jet formation

As stated above, the residence time and peak broadening in the commonly used LC detectors, with cell volumes in the range of $1\text{--}10 \mu\text{l}$, should be kept within acceptable limits by the use of a scavenger liquid flow of the order of 1 ml/min . This flow causes dilution by a factor of $100\text{--}1000$, such that only major components of sample mixtures can be detected (contents $> 0.01 \%$).

A detector which avoids this severe dilution by accepting column effluent flows up to $20 \mu\text{l/min}$ is the mass spectrometer, when used in the chemical ionization (CI) mode. In fact, direct microcapillary LC flows of this magnitude ensure a nearly ideal compatibility with the requirement of ion source pressures of about $0.2\text{--}1 \text{ Torr}$ for the CI process.

Interfacing of LC effluents from packed columns with MS in the CI mode has recently been studied intensively^{12,37,38}. The main conclusion was that sufficiently rapid and effective vaporization of the column effluent can be obtained only by using additional vaporization techniques such as rapid heating³⁹, electrospraying⁴⁰, laser irradiation^{38,41,42} or jet formation¹². Especially for samples of high molecular weight (> 250), for high concentrations and for thermally unstable or solid materials, where blocking of the microcapillary column exit can be envisaged, it is worthwhile to consider the liquid jet formation technique in connection with (soft-glass) microcapillary LC. A liquid jet created at the column exit avoids deposition of sample material there by ejecting the whole of the column effluent rapidly into the ion source. For packed HPLC columns this jet interface has already shown promise¹² (with per-

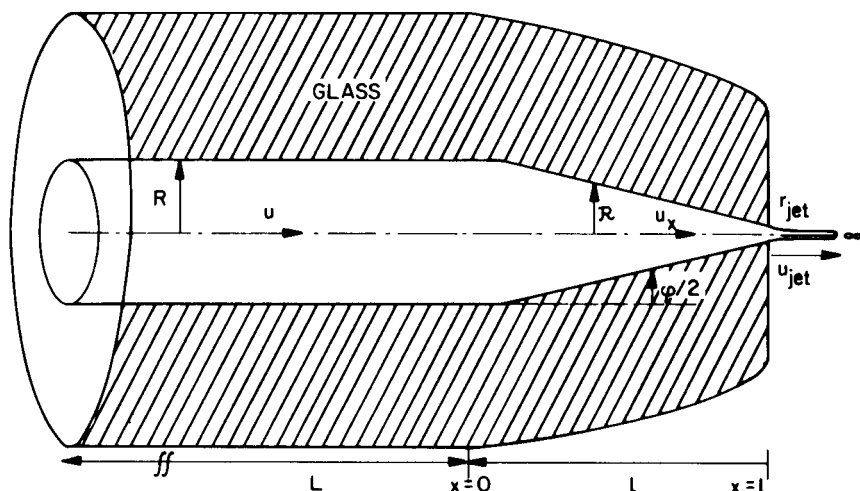


Fig. 3. Schematic representation of the liquid jet forming tip at the column exit.

forated membranes at the column outlet and an orifice of about 2–5 μm). Small diameters of that magnitude are necessary to create the high liquid velocities for jet formation.

Notably with soft-glass microcapillaries, it is possible (although tedious) to produce a conical tip at the column exit with an outlet diameter near the required value of 1 μm . Fig. 3 shows a schematic representation. In practice, the tip length, l , is typically 3 mm, and from this we can calculate the pressures needed for jet formation, on the basis of the viscous dissipation within the conical tip.

According to the literature^{43,44}, liquid jet formation occurs only above a certain critical liquid velocity in the orifice:

$$u_{\text{jet}} \geq 2 (\gamma/\rho)^{\frac{1}{2}} r_{\text{jet}}^{-\frac{1}{2}} \quad (14)$$

For most liquids $(\gamma/\rho)^{\frac{1}{2}}$ lies in the range 4–10 $\text{dyne} \cdot \text{cm}^2 \cdot \text{g}^{-1}$, and for estimating purposes eqn. 14 can be written as:

$$u_{\text{jet}} = 10 r_{\text{jet}}^{-\frac{1}{2}} \quad (15)$$

For orifice radii smaller than 25 μm this implies very high velocities, in excess of 200 cm/sec, increasing with decreasing diameter. These velocities are too high for chromatographic purposes and so it will never be possible to reach the ideal situation where the column itself constitutes the jet forming channel. Hence, jet formation in combination with chromatographic separation implies that $r_{\text{jet}} \ll R$ in order to obtain sufficiently low column velocities for efficient separation as well as sufficiently high jet velocities.

As the flow-rate is the same in the column and in the jet, we have, with eqn. 15:

$$u R^2 = u_{\text{jet}} r_{\text{jet}}^2 = 10 r_{\text{jet}}^{3/4} \quad (16)$$

At position x , where the local radius, \mathcal{R} , of the conical tip may be approximated by the linear relation

$$\mathcal{R} = R \left[1 - \frac{x}{l} \left(1 - \frac{r_{\text{jet}}}{R} \right) \right] \quad (17)$$

(i.e., $\mathcal{R} = R$ at $x = 0$ and $\mathcal{R} = r_{\text{jet}}$ at $x = l$), the continuity of flow requires that:

$$u R^2 = u_x \mathcal{R}^2 \quad (18)$$

The average velocity, u_x , at location x is now obtained from the Poiseuille equation as⁴⁵

$$u_x = -(\partial p / \partial x) (\mathcal{R}^2 / 8 \eta) \quad (19)$$

i.e., the pressure gradient in the tip, taking eqn. 18 into account, is given by:

$$-(\partial p / \partial x) = 8 \eta u R^2 / \mathcal{R}^4 \quad (20)$$

If this is integrated over the tip length, l , using eqn. 17 for \mathcal{R} , we obtain the pressure drop, $\Delta p_l = p(x = 0) - p(x = l)$, as:

$$\Delta p_l = \frac{8}{3} \cdot \frac{\eta u l R}{r_{\text{jet}}^3} \left[1 + \frac{r_{\text{jet}}}{R} + \left(\frac{r_{\text{jet}}}{R} \right)^2 \right] \quad (21)$$

In eqn. 21 the terms in (r_{jet}/R) can be neglected with respect to the term 1 between brackets, as $r_{\text{jet}} \ll R$. With the jet formation condition eqn. 16, we then find from eqn. 21:

$$\Delta p_l = \frac{80}{3} \cdot \frac{\eta l}{r_{\text{jet}}^{3/2} R} \quad (22)$$

As a typical example, Δp_l for a 2- μm orifice at the end of a column of diameter 20 μm and a tip length, l , of 3 mm amounts to 80 bar. Such a high pressure differs considerably from the low pressures needed for pin hole jets in very thin membranes as discussed by Arpino *et al.*¹² for packed HPLC columns. The reason is that, in our case of a finite tip length, viscous dissipation dominates over kinetic energy losses, i.e., the Poiseuille equation rather than the Bernoulli equation is valid.

The total pressure drop over the column of length, L (Δp_L after eqn. 11) and the jet forming tip of length, l (Δp_l after eqn. 22) now amounts to:

$$\Delta p = \frac{80 \eta}{R^{5/2}} \left[\frac{l}{3} \left(\frac{R}{r_{\text{jet}}} \right)^{3/2} + L \left(\frac{r_{\text{jet}}}{R} \right)^{3/2} \right] \quad (23)$$

In Fig. 4, Δp has been plotted as a function of r_{jet} for a specified column radius $R = 16 \mu\text{m}$ and various column lengths, L . It is seen that the minimum pressure drop can be obtained for a rather narrow range of jet radii (between 1 and 2 μm) only. The

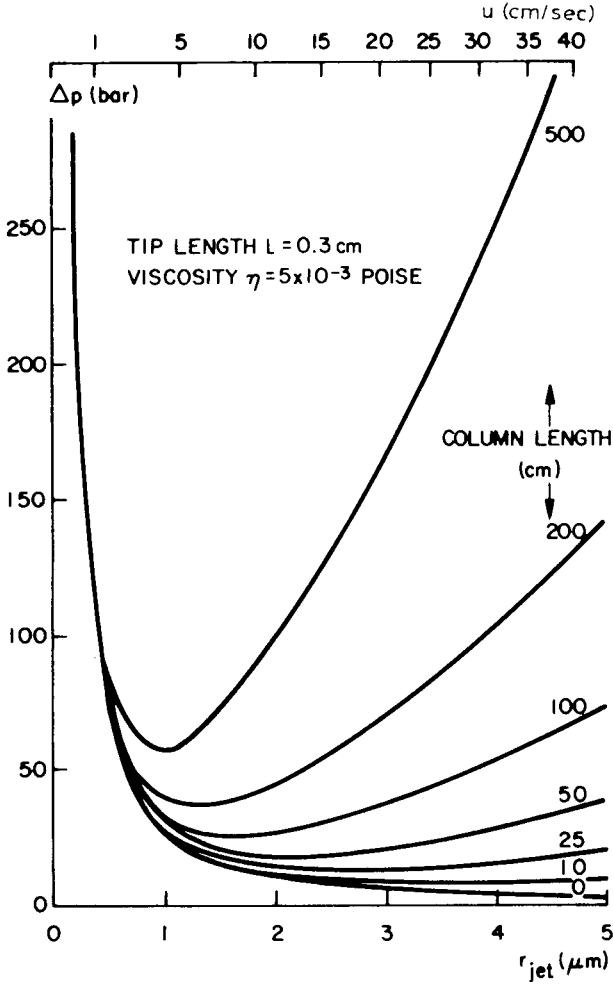


Fig. 4. Pressure drop in a microcapillary column (diameter $32 \mu m$) with jet formation, as a function of the jet radius.

minimum pressure drop and accompanying jet radius are obtained from eqn. 23 by differentiation with respect to r_{jet} :

$$\Delta p_{min} = \frac{1}{R^{5/2}} \cdot \left(\frac{L}{3} \right)^{1/2} \quad (24)$$

$$r_{jet, opt} = R \left(\frac{L}{3} \right)^{1/3} \quad (25)$$

From this it follows that not too small column radii, R , should be used to keep Δp_{min} within reasonable limits. As a typical example, for $R = 10 \mu m$, $L = 1$ m and $l = 0.3$ cm, we obtain $\Delta p_{min} = 100$ bar and $r_{jet, opt} = 1 \mu m$.

Now, the column radius, R , and length, L , are chosen such that a sufficient number of effective plates, n_{eff} , can be generated (eqn. 10 and Fig. 2). For the near-optimum case of $k = 1$ we obtain from eqn. 16 with $u = L/t_M = L(1 + k)/t_R = 2L/t_R$:

$$2L(R^2/t_R) = 10r^{3/2} \quad (26)$$

From eqn. 10 with $k = 1$ and $D_M = 2 \cdot 10^{-5} \text{ cm}^2/\text{sec}$ the ratio R^2/t_R in eqn. 26 can be derived:

$$R^2/t_R = 10^{-5}/n_{\text{eff}} \quad (27)$$

So, combining eqns. 26 and 27 yields the required length for a microcapillary column which produces n_{eff} effective plates and forms a liquid jet as well:

$$L = 5 \times 10^5 \cdot n_{\text{eff}} \cdot r^{3/2} \quad (k = 1) \quad (28)$$

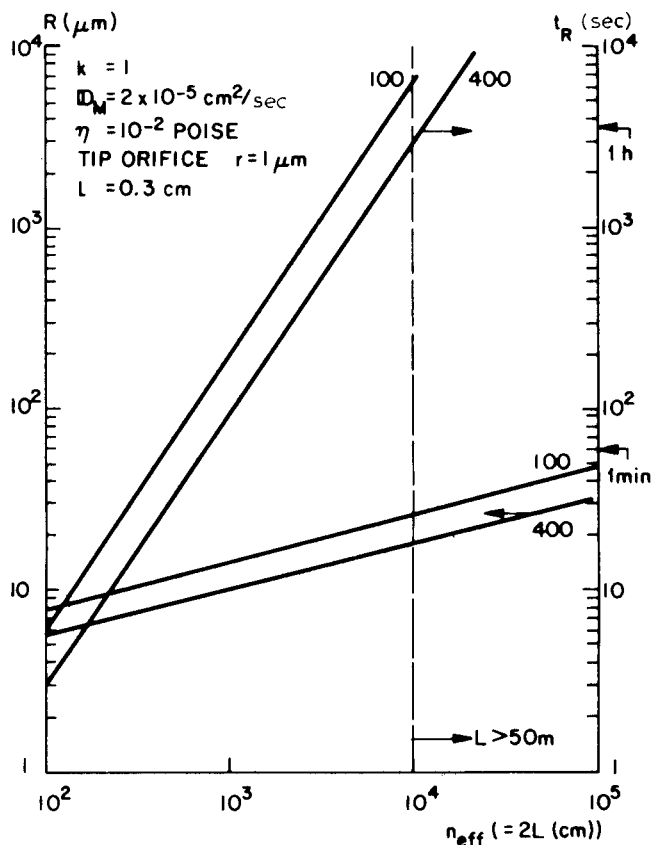


Fig. 5. Operating parameters for microcapillary LC with liquid jet formation. The data on the lines indicate the maximum allowable pressures (bar).

A standard jet radius of 1 μm then implies that:

$$L = \frac{1}{2} n_{\text{eff}} (r_{\text{jet}} = 1 \mu\text{m}, k = 1) \quad (28a)$$

As eqn. 16 results in $u = 10^{-5}/R^2$ for $r_{\text{jet}} = 1 \mu\text{m}$, the required column radius, R , that produces $n_{\text{eff}} = 2 L$ effective plates from the Poiseuille equation for u , provided that Δp_L dominates over Δp_l (*i.e.*, r_{jet} is slightly larger than $r_{\text{jet,opt}}$; *cf.*, Fig. 4):

$$R = (4 \eta \cdot n_{\text{eff}} / \Delta p_L \cdot 10^{-5})^{\frac{1}{4}} \quad (29)$$

For an allowed pressure drop $\Delta p_L = 400$ bar, eqn. 29 yields approximately $R^4 = 10^{-15} \cdot n_{\text{eff}}$, *i.e.*, with eqn. 27:

$$t_R = 3 \cdot 10^{-3} \cdot n_{\text{eff}}^{3/2} \quad (30)$$

The required operating parameters R , L and t_R are plotted in Fig. 5 as a function of the required separation efficiency n_{eff} for $\Delta p_L = 400$ and 100 bar.

Lengths in excess of about 50 m are not practical, which implies that the microcapillary LC-MS combination with jet interfacing will at most yield about 10^4 effective plates (in about 1 h), a very useful number, although less than with conventional detection (*cf.*, Fig. 2).

RESULTS AND DISCUSSION

UV-detection and non-retained solutes

Non-retained solutes were used to obtain the amount of extra-column broadening resulting from injection, column connections and detection. Ideally, peak broadening only occurs in the column itself by convective dispersion, producing plate heights which are expected to follow the predictions of the well-established theories of Taylor⁴⁶⁻⁴⁸, Aris^{30,31} and Golay (for $k = 0$)²⁸. From eqn. 3 with $k = 0$ it is seen that plate height depends on velocity as:

$$H = R^2 u / 24 D_M \quad (31)$$

We measured H vs. u relationships for columns with diameters ranging from 100 to 10 μm and found little deviation from the theoretical relation eqn. 31, provided that make-up flows were in the range of 0.3–1 ml/min and splitting ratios well below 1:50. The most sensitive test for extra-column broadening is to measure plate heights in columns of very small diameters, where column broadening is only slight. Fig. 6 shows the H - u curve we obtained from two of the smallest columns available at present, a soft-glass column (diameter 14 μm) and a fused silica column with a diameter of 10 μm (diameters obtained from microscopic measurement).

The peak shapes are nearly symmetrical, but the resulting plate heights deviate from the theoretical prediction, the more so for smaller make-up flows. With these smaller flows a distinct tailing occurs, accompanied by an increase in plate height. This is shown in Fig. 7.

The additional broadening observed for the best detector (Waters) can be

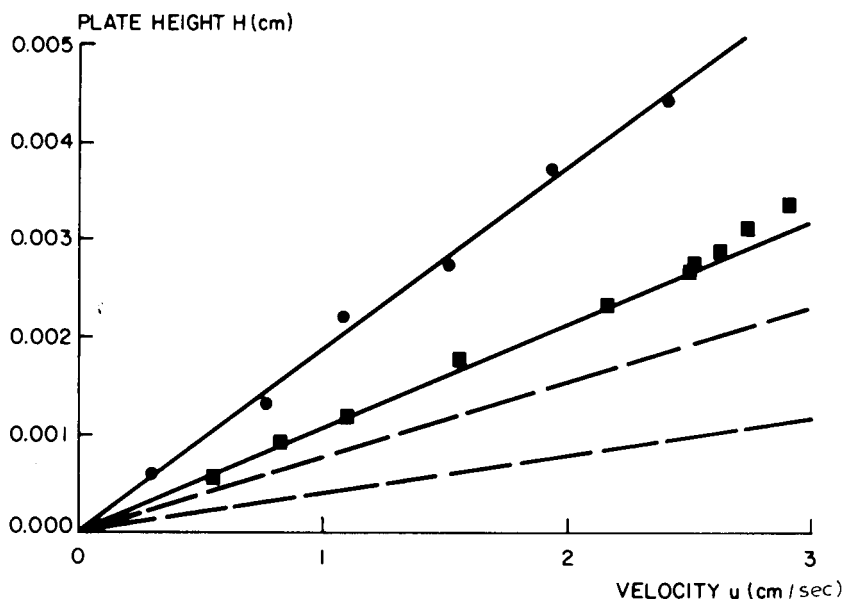


Fig. 6. Plate height vs. velocity for a non-retained solute in microcapillaries with diameters of $10\ \mu\text{m}$ ($L = 291\ \text{cm}$; ■) and $14\ \mu\text{m}$ ($L = 472\ \text{cm}$; ●) using UV detection. Solute: toluene. Mobile phase: isooctane. Detector: Waters 440 at 254 nm, with make-up flow of 1.3 ml/min. The dashed lines represent the theoretical predictions.

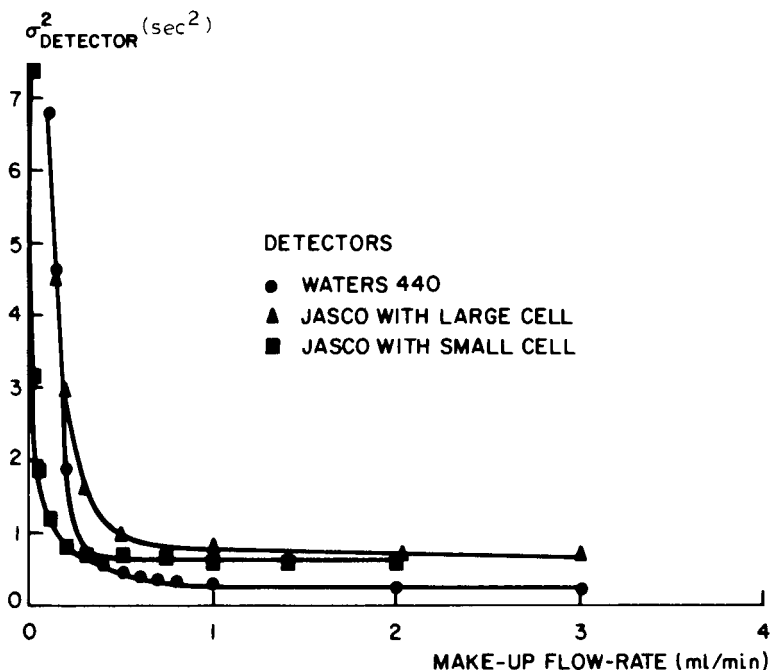


Fig. 7. Extra-column broadening in UV detectors as a function of the make-up flow-rate. Solute: toluene ($k = 0$). Mobile phase: isooctane, $u = 3\ \text{cm/sec}$. Column: $R = 13.5\ \mu\text{m}$, $L = 325\ \text{cm}$. The theoretical column variance ($R^2 t_R / 24 D_M$) = $0.32\ \text{sec}^2$ has been subtracted from measured variances.

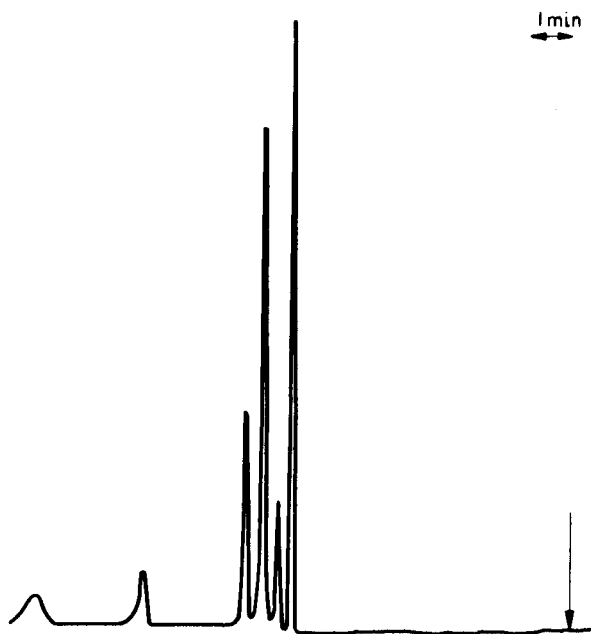


Fig. 8. Typical separation of polar aromatic compounds by microcapillary LSC. Column: etched soft glass, 355 cm \times 32 μ m. Mobile phase: isooctane. Detector: Waters UV, 254 nm, 0.01 a.u.f.s.; make-up flow 0.3 ml/min. Solutes (in order of elution): toluene; Sudan yellow; 2-ethylanthraquinone; 1,4-naphthoquinone; benzoquinone; *p*-aminoazobenzene.

characterized as the dispersion from an ideally mixed dead volume of 8 μ l at a make-up flow-rate of 1 ml/min, which corresponds well with the detector cell volume. Recently, it has been shown¹¹ how this cell volume can be diminished.

UV-detection and adsorption microcapillary LSC

As described in the Experimental, alkaline etching of soft glass produces a

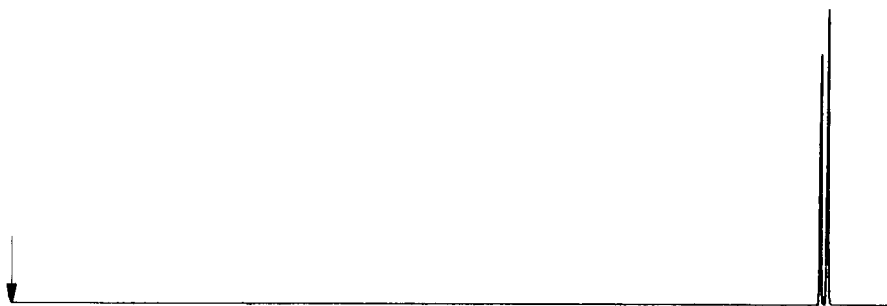


Fig. 9. Generation of very large plate numbers with microcapillary LC. Column: etched soft glass, 27.5 m \times 32 μ m. $u = u_{opt} = 0.12$ cm/sec, $n = 2.8 \cdot 10^6$ (!), $H = 9.8$ μ m. Mobile phase: isooctane. Detector: Waters UV (254 nm, 0.01 a.u.f.s.). Solutes: toluene and *N*-propylaniline (relative retention 1.009). Analysis time: 6.5 h.

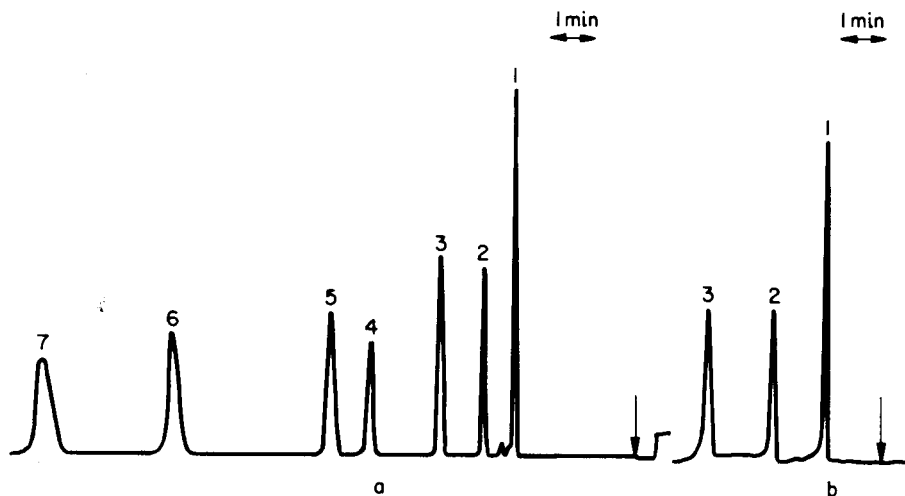


Fig. 10. Separation of aromatic compounds in a microcapillary (a) and a packed column (b). Columns: a, 325 cm \times 27 μ m; b, 10 cm Partisil 5 (particle size 5 μ m). Stationary phase in both cases: ODPN. Mobile phase: isooctane (in b 1% methanol is added to reduce tailing); flow-rate 1 ml/min. Detection: UV absorption at 212 nm. Solutes: 1 = toluene; 2 = benzophenone; 3 = benzonitrile; 4 = *o*-toluidine; 5 = *m*-toluidine; 6 = aniline; 7 = benzyl alcohol.

highly adsorptive siliceous layer on the inner wall of the column, which layer can be used as the stationary phase.

Using isooctane as the mobile phase, saturated with water to suppress tailing, very useful chromatograms were obtained, examples of which are shown in Figs. 8 and 9. Fig. 9 demonstrates how several millions of plates were obtained in a separation in an etched 32- μ m microcapillary column by using velocities near the optimum. The rather long time (6.5 h) required in this particular case may be drastically reduced by using smaller diameter columns. A 10- μ m column of the same length would produce even more plates ($9 \cdot 10^6$) in less time (2 h), operating at 80 bar only.

The present result illustrates the potential application of microcapillary LC to extremely difficult separations of closely related compounds, requiring separation

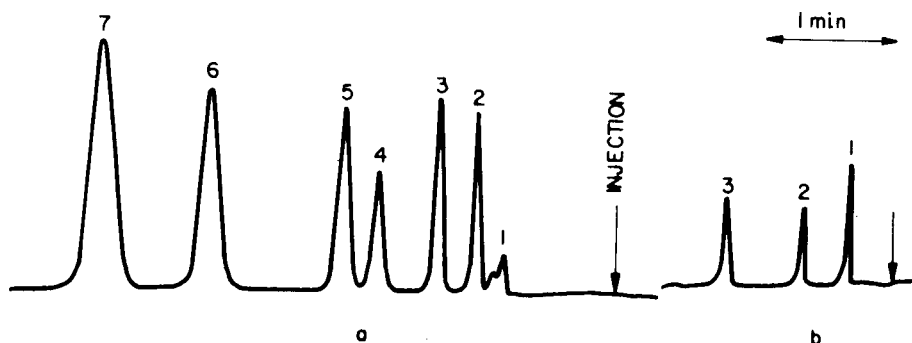


Fig. 11. Separation of aromatic compounds in a microcapillary (a) and a packed column (b). Conditions as in Fig. 10 except that velocity in b was 4 ml/min.

efficiencies of several million plates, which cannot be obtained with packed HPLC columns.

UV-detection and straight phase microcapillary LLC

Etched and Cab-O-Sil-treated microcapillaries could easily be coated by the dynamic coating technique with a polar stationary liquid phase like ODPN. Using isooctane (saturated with ODPN) as the mobile phase, these columns were stable for long operating periods (months).

Figs. 10–13 show separations of different samples at different velocities, illustrating that microcapillary LC can be used either as a rapid separation technique or as a more time-consuming but very efficient technique for more difficult separations. The presence of a small amount of ODPN in the mobile phase prohibited the use of a mass spectrometer as the detector, as this would lead to rapid contamination of the ion source.

UV-detection and reversed-phase microcapillary LLC

Reversed-phase LC in microcapillary columns has been achieved by coating etched capillaries with the non-polar phase Apiezon L. With methanol–water as the mobile phase, a $1\text{ m} \times 32\text{ }\mu\text{m}$ column readily separated aromatic compounds within several minutes. When the retention time of the last peak is chosen to be about 20 min, as in the lower trace of Fig. 14, a comparison can be made with a separation of aromatics recently published by Yang⁷. This author used a chemically bonded ODS phase in a $2\text{ m} \times 30\text{ }\mu\text{m}$ fused-silica column. The present separation compares very

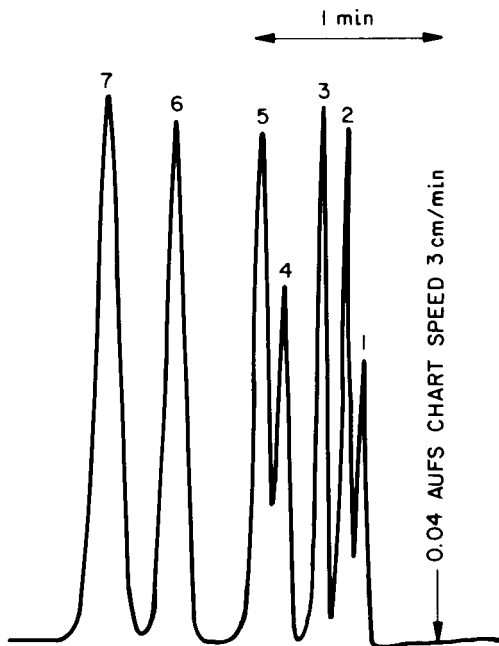


Fig. 12. Rapid separation of aromatic compounds in a microcapillary column. Conditions as in Fig. 10 except for velocity.

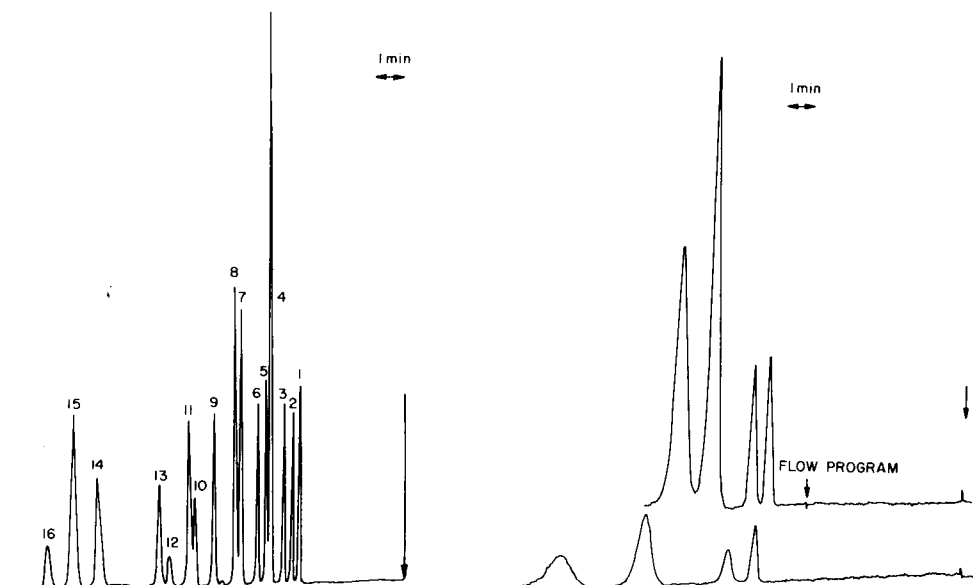


Fig. 13. Microcapillary LC separation of aromatic compounds by straight phase partitioning. Analysis time: 13 min. Inlet pressure: 200 bar. Separation speed: 16 effective plates per sec (last peak), in accordance with eqn. 10. Column: $R = 6 \mu\text{m}$, $L = 4.95 \text{ m}$, etched soft glass, coated with ODPN as the stationary phase. Mobile phase: isooctane (saturated with ODPN at 23°C). Detector: UV absorption at 212 nm, 0.04 a.u.f.s.; make-up mobile phase 0.4 ml/min. Solutes: 1 = diisooheptyl phthalate; 2 = dibutyl phthalate; 3 = dipropyl phthalate; 4 = 2,4,5-trimethylaniline; 5 = N-methylaniline; 6 = diethyl phthalate; 7 = *o*-chloroaniline; 8 = 2,3-dimethylaniline; 9 = *o*-toluidine; 10 = *p*-toluidine; 11 = *m*-toluidine; 12 = benzoquinone; 13 = dimethyl phthalate; 14 = aniline; 15 = *m*-chloroaniline; 16 = *p*-chloroaniline.

Fig. 14. Separation of polynuclear aromatic compounds by reversed-phase microcapillary LC. Upper trace: programmed flow (after 6 min increase of flow at the rate of 27%/min). Lower trace: constant flow. Column: 108 cm \times 32 μm I.D. Stationary phase: Apiezon L. Mobile phase: methanol-water (75:25). Detector: UV absorption at 254 nm, 0.01 a.u.f.s. Solutes (from right to left): benzene; naphthalene; anthracene and pyrene.

favourably with the cited work, as is evident from the plate numbers obtained for the pyrene peak [$n = 1600$ ($n_{\text{eff}} = 400$) on our 1-m column vs. $n = 200$ ($n_{\text{eff}} = 90$) in the 2-m (!) ODS column] as well as from the peak shapes (symmetrical on our column, see Fig. 14; several tailing peaks on the ODS column).

The same separation can be used to illustrate the profitable use of flow programming, provided that the chromatogram is not too crowded. By increasing the mobile phase flow-rate through the column during the analysis (or alternatively only during the elution of a peak), peak heights are appreciably enhanced, as is seen from the upper and lower traces in Fig. 14.

Direct coupling of microcapillary LC with MS detection

For samples of low molecular weight ($\text{MW} < 250$) the direct inlet of column effluent from unmodified microcapillary columns is very well suited for practical qualitative as well as quantitative analysis. An example which illustrates this is the reversed-phase separation of polynuclear aromatics (PNAs), as discussed in the

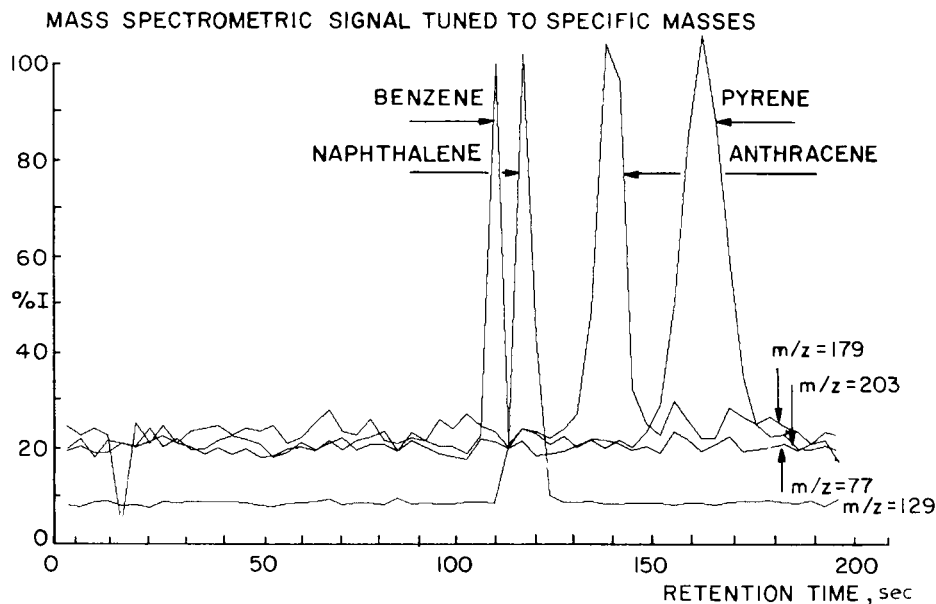


Fig. 15. Chromatogram showing the superimposed signals of four specific masses for polynuclear aromatics separated by reversed-phase microcapillary LC. (Benzene in CI-MS behaves differently from other PNAs and is detected at $m/z = MW - 1$.) Peak heights (in counts): benzene, 383; naphthalene, 2939; anthracene, 158; pyrene, 539. Sample concentrations: 10^{-2} g/ml. Flow-rate: 2 μ l/min. Splitting ratio: 1:5000. Each peak contains 10 ng of the compound.

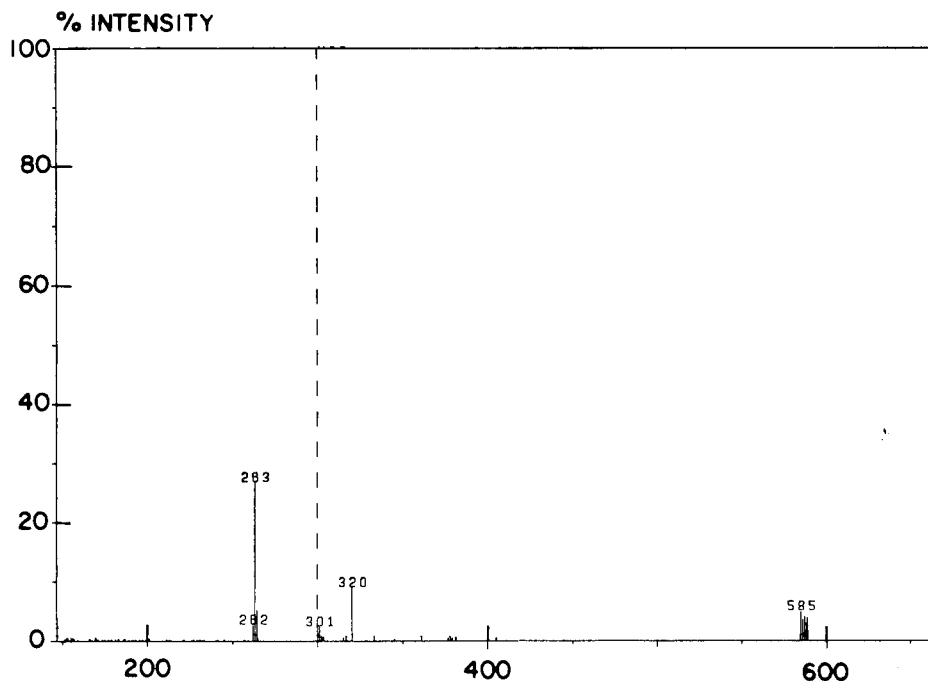


Fig. 16. CI mass spectrum of triphenylphosphinitungsten pentacarbonyl as obtained by microcapillary liquid jet introduction.

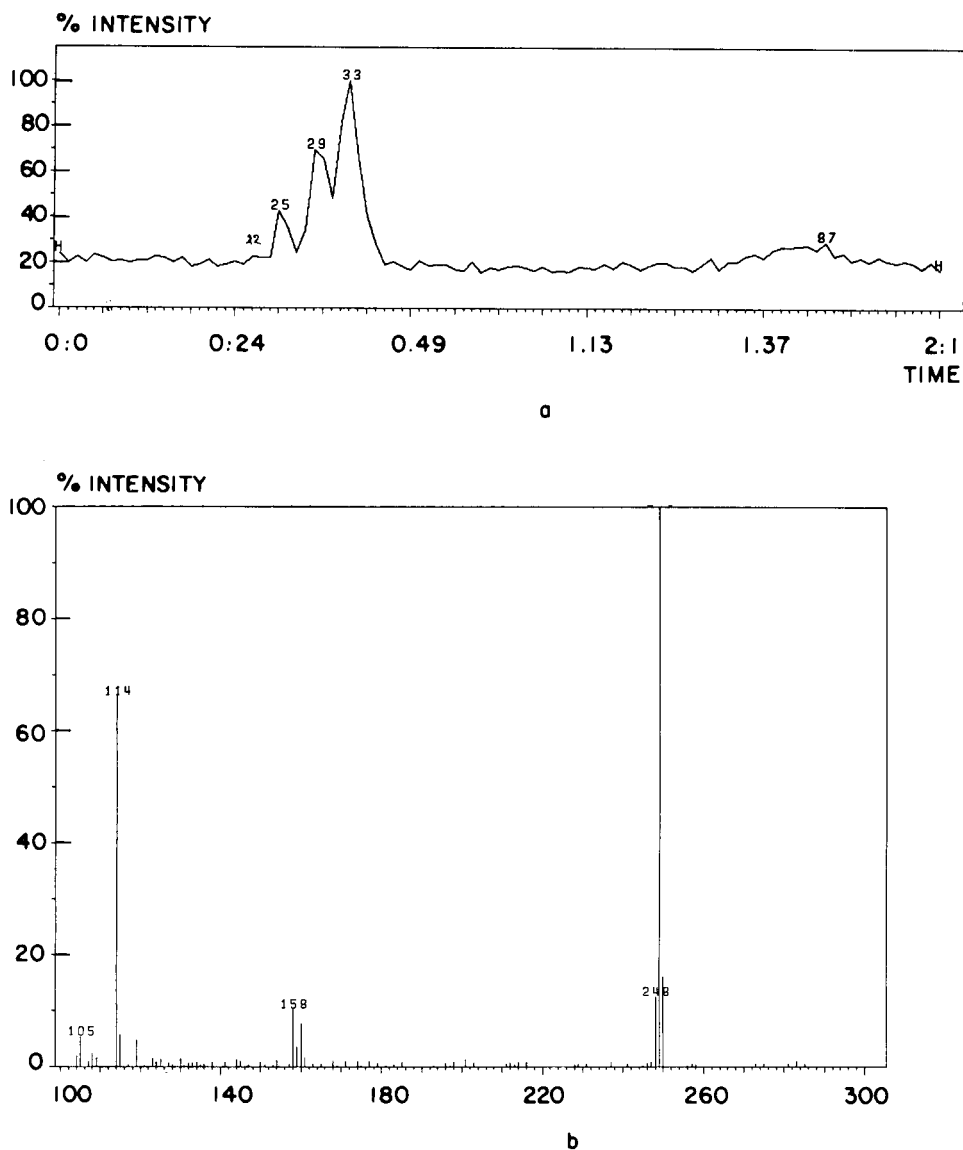


Fig. 17. Chromatogram obtained by microcapillary LC-MS with jet formation. a, Solutes: toluene (scan 22); Sudan yellow (scan 25); 2-ethylanthraquinone (scan 29); 1,4-naphthoquinone (scan 33) and *p*-aminoazobenzene (scan 87). Column: 322 cm \times 32 μ m, r_{jet} = 2.5 μ m, etched glass. Mobile phase: isooctane. b. Mass spectrum accompanying the Sudan yellow peak.

above paragraph, using Apiezon L as the stationary phase. This separation was performed on a 4.5 m \times 32 μ m column within 3 min, as is shown by Fig. 15. The peak shapes are quite symmetrical and the peak widths do not differ much from those obtained by UV detection. Samples of about 100 pg can still be detected, far smaller than with UV detectors.

For concentrated samples of high molecular weights ($MW > 250$), irregular peak shapes as well as fluctuating ion source pressures are observed, however, indicating deposition and discontinuous evaporation of sample near the column outlet. Liquid jet formation could be realized by providing a conical tip with $r_{jet} = 2.5 \mu m$ at the end of a $322 \text{ cm} \times 32 \mu m$ etched glass microcapillary. In this case, samples of high molecular weight could be introduced into the ion source without difficulty; symmetrical peaks were recorded and good CI spectra obtained, *e.g.*, for heavy hydrocarbons (squalane; $MW = 422$), undecane benzene sulphonic acid ($MW = 312$), sucrose ($MW = 342$), and Lubad J (4,4'-methylenebis-*tert.*-butylphenol; $MW = 424$).

Thermally unstable compounds such as triphenylphosphine tungsten pentacarbonyl ($MW = 584$) and volatile solids such as Ionol (2,6-di-*tert.*-butyl-*p*-cresol; $MW = 220$), notoriously problematic when other introduction techniques (*e.g.*, moving belt) are used, are flawlessly introduced into the ion source by the jet interface technique and yield good CI spectra, see Fig. 16. Fig. 17 shows an example of a rapid separation in this etched column with liquid jet formation, and an accompanying CI mass spectrum.

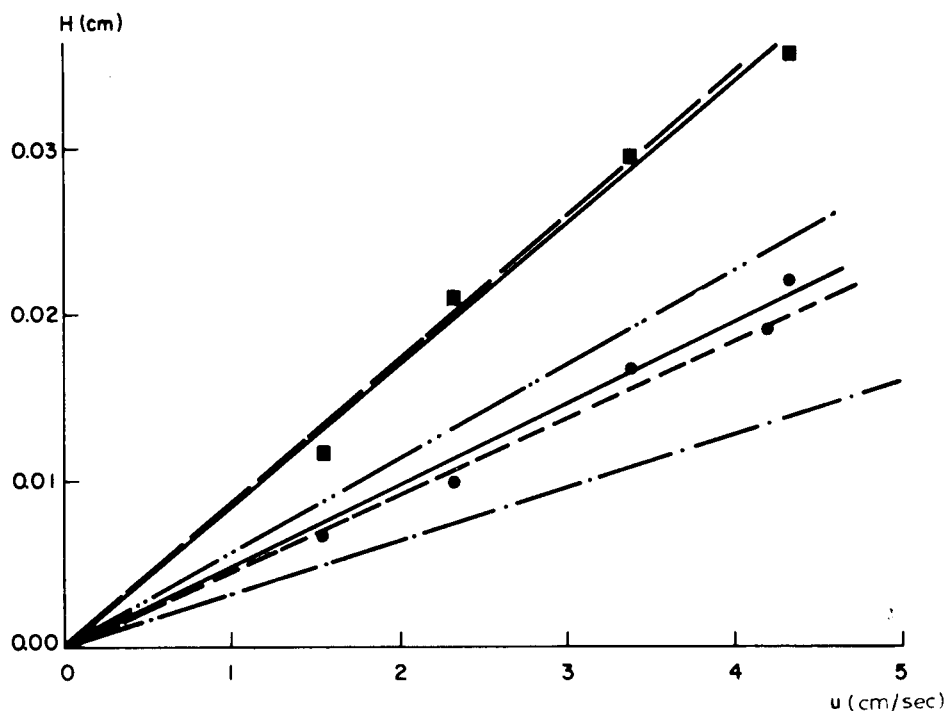


Fig. 18. Plate height vs. velocity for retained solutes in microcapillary LLC. Column: $472 \text{ cm} \times 14 \mu m$, etched and coated with ODPN. Mobile phase: isooctane. Detector: Waters UV (254 nm) with make-up flow of 1.3 ml/min. \bullet , *o*-Toluidine, $k = 0.80$, $D_M = 2.53 \times 10^{-5} \text{ cm}^2/\text{sec}$; \blacksquare , dimethyl phthalate, $k = 1.30$, $D_M = 1.88 \times 10^{-5} \text{ cm}^2/\text{sec}$. ---, Golay theory for $k = 0.80$; - - - -, Golay theory for $k = 1.30$; ———, present theory for $k = 0.80$; ———, present theory for $k = 1.30$. In view of the non-linear partitioning isotherms, plate heights were determined from moments extrapolated to zero concentration.

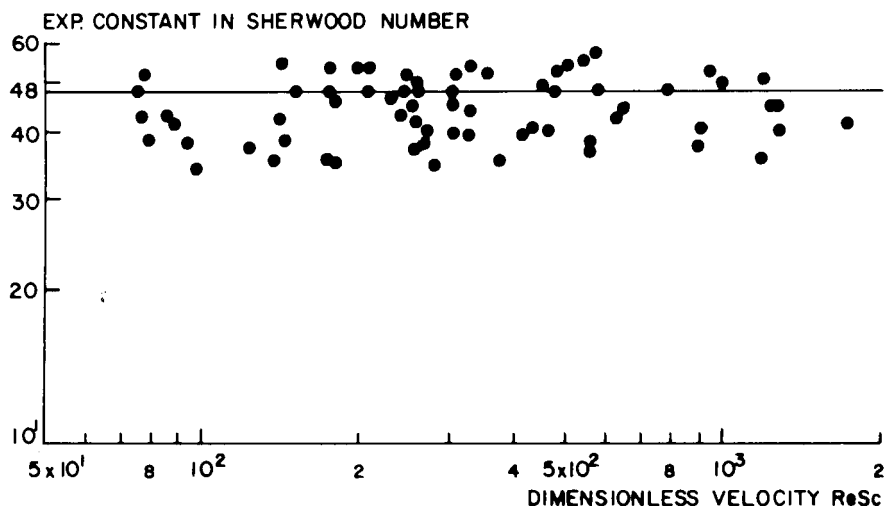


Fig. 19. Interphase resistance to mass transfer in microcapillary LC columns with diameters in the range of 11–100 μm . Capacity factors: 0.07–3.7. Velocities: 0.2–5 cm/sec. Adsorption as well as partitioning.

Separation speed and axial dispersion

Notwithstanding careful avoidance of extra-column broadening effects, and even after correction for these effects (by subtracting moments²⁶), we observe that the experimental plate heights are invariably larger than those predicted by the Golay equation, up to a factor of about 2. A typical illustration of this can be seen in Fig. 18.

In the Theoretical we suggested that the additional broadening may originate from interphase resistance effects analogous to the resistance to heat transfer in tubular heat exchangers. If this is correct, the experimentally obtained coefficient k_M , which describes the additional broadening, should be in accordance with the approximation given in the Appendix (eqn. A7).

In other words, if we plot the experimentally observed k_M in the dimensionless form of the Sherwood constant, given in the Appendix, as a function of (dimensionless) velocity ($ReSc$) under different experimental parameters (R , k , phase system), the theoretical value of 48 should be approached independently of the experimental parameters mentioned. Fig. 19 shows the resulting plot and it is observed that a tendency to approach the theoretical value of 48 is indeed present for column diameters in the range of 11–100 μm , for capacity factors in the range of 0.07–3.7, for velocities in the range of 0.2–5 cm/sec and for adsorption (etched glass and Cab-O-Sil) as well as partitioning (ODPN).

The spread observed around the value of 48 can largely be attributed to errors in the determination of the moments²⁶ as well as of the column diameters. In anticipation of more precise experiments and a more exact theoretical background for the mass transfer coefficient, on which we are working at present, we conclude that our approach of including interphase resistance in chromatographic dispersion is sound. At least it is clear that the mass transfer coefficient model for interphase resistance is able to describe the observed axial dispersion, which deviates from the Golay prediction by a factor between 1 and 2 in our experiments.

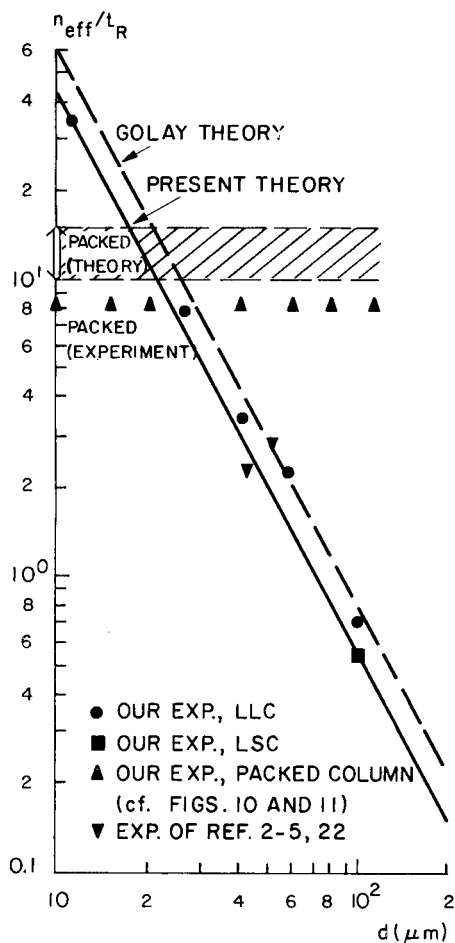


Fig. 20. Separation speed of microcapillary LC columns as a function of the column diameter. Retained solutes with capacity factors 0.6–0.9. The theoretical zone for the packed column is based on work by Snyder³⁵.

Although our theory is somewhat more conservative than Golay's, this does not imply that the technique of microcapillary LC will have less favourable prospects. This is illustrated by the separations shown, and is further supported by the observed separation speeds.

Fig. 20 shows the dependence of experimental separation speed on column diameter; it is clear that our theory describes these results very well. Evidently, columns with diameters of less than 30 μm will have the greatest future, as the separation speeds obtained are well above those of packed HPLC columns.

CONCLUSIONS

- (1) It has been shown experimentally that microcapillary columns for liquid

chromatography with diameters of 10–50 μm can be prepared and coated with polar as well as non-polar stationary phases. Both LSC (adsorption) and LLC (partitioning in straight- and reversed-phase modes) have proved to be of practical interest.

(2) The separation performance of a column of 30 μm I.D. compares very well with that of modern packed HPLC columns (5- μm particles) and yields about five effective plates per second as the separation speed. Smaller diameter columns have been found to have a much higher speed of separation, *e.g.*, 50 effective plates per sec for a 10- μm column.

(3) In small diameter (10–30 μm I.D.) and long (5–25 m) microcapillary columns operated at the optimum velocity, extremely high separation efficiencies (up to about 10^7 plates) can be obtained within a few hours, which is still reasonable. Very difficult separations can thus be performed.

(4) Avoidance of extra-column peak broadening is a major problem in microcapillary LC. Especially detection with (UV-absorption) flow-through cells (relatively large volumes, 1–10 μl , and non-ideal cell geometry) requires the application of a scavenger liquid flow to reduce peak broadening. This make-up liquid flow amounts to 0.3–1 ml/min and causes dilution of the column effluent by a factor of 100–1000, such that only the main components can be detected.

(5) When a mass spectrometer is used as the detector and is operated in the chemical ionization mode, direct inlet of the total column effluent ($< 10 \mu\text{l/min}$) is possible. The dilution problem is absent, which implies that trace components can be determined (qualitatively and quantitatively) down to pg levels. Compounds of low molecular weight ($\text{MW} < 200$) can be separated and introduced; higher molecular weights require an additional transfer technique. Liquid jet formation at the column exit, under chromatographically still attractive velocity conditions, has been found to be of practical interest.

(6) The observed peak broadening, carefully corrected for extra-column effects, cannot be interpreted with the common Golay theory of capillary chromatography. Experimental plate heights are a factor of 1–2 larger than those predicted by that theory. By introducing interphase mass transfer in analogy with heat transfer to a solid pipe wall in tubular heat exchangers, we have expressed the additional peak broadening in terms of a mass transfer coefficient, using expressions from the theories of Aris, Khan, Pethö and Giddings. It is concluded that the observed peak broadening can be adequately described by a sum of convective dispersion (Golay) and interphase mass transfer effects.

APPENDIX

Estimation of the axial dispersion from interphase resistance to mass transfer

Golay's theory for peak broadening in open tubular columns for chromatography is based on a solution to the mass balance equations which are coupled to each other by the condition of equilibrium in the partitioning of solute molecules between the two phases. Upon removing this equilibrium condition and allowing for a resistance to interphase mass transfer to be described by linear kinetics with a transfer coefficient, k_M , several other theories^{30–33} yield an additional C term for peak broadening, which we call the interphase term, C_i :

$$H = (C_M + C_S + C_i)u \quad (A1)$$

C_M and C_S are the same as in the Golay theory (eqns. 4 and 5), while C_i in all three theories is expressed as:

$$C_i = \frac{R}{k_M} \cdot \left(\frac{k}{1+k} \right)^2 \quad (A2)$$

So far, a conclusive model for k_M has not been presented and we propose that k_M be found from the analogy of the mass transfer problem with the well-known solution to the heat transfer problem in tubular heat exchangers^{49,50}. Earlier, Wong *et al.*²⁹ proposed the same, but they took an unrealistic extreme value for k_M , not recognizing the important dependency of k_M on the partition ratio, k . This will be illustrated in the following approximate derivation, where use is made of the results obtained by Giddings³⁴ in his non-equilibrium theory.

The mass transfer coefficient, k_M , is defined as the proportionality constant between the mass flux, ϕ_i'' , at the phase boundary and the driving force for that flux (*i.e.*, concentration difference) in the mobile phase:

$$\phi_i'' = k_M (c_i - c_{\text{bulk}}) \quad (A3)$$

By continuity, this flux at the interface i equals those in both phases

$$\phi_i'' = \phi_M'' = \phi_S'' \quad (A4)$$

where both ϕ_M'' and ϕ_S'' can be expressed as diffusional fluxes by Fick's first law. Using the appropriate expressions in the non-equilibrium theory³⁴ for ϕ_M'' and ϕ_S'' , from eqn. A4 we arrive at an expression for k_M :

$$k_M = \frac{u R}{2} \cdot \frac{k}{1+k} \cdot \frac{\hat{\partial} \bar{c}_M}{\partial z} / (c_{M,i} - c_{M,\text{bulk}}) \quad (A5)$$

In all dispersion theories^{9,28-34}, concentration differences in a cross-section of the column are so small that $c_{M,i}$ may be replaced by the average concentration \bar{c}_M in eqn. A5.

The concentration difference $(\bar{c}_M - c_{M,\text{bulk}})$ plays an important rôle in Giddings' non-equilibrium theory³⁴ as total plate height is determined by this difference:

$$H = 2 (\bar{c}_M - c_{M,\text{bulk}}) \left/ \left(\frac{\partial \bar{c}_M}{\partial z} \right) \right. \quad (A6)$$

We know already that $H = Cu$, where $C \approx C_M$ according to Golay, *i.e.*, from eqns. A5 and A6:

$$k_M \approx \frac{R}{C_M} \cdot \frac{k}{1+k} \quad (A7)$$

Hence, when k_M is substituted in eqn. A2:

$$C_i \approx k C_M / (1 + k) \quad (\text{A8})$$

The dimensionless Sherwood number $Sh = 2 R k_M / D_M$ and we find from eqn. A7 and eqn. 4 for C_M that

$$Sh = \frac{2}{D_M} \cdot \frac{R^2}{C_M} \cdot \frac{k}{1 + k} = 48 \cdot \frac{k (1 + k)}{(1 + 6k + 11k^2)} \quad (\text{A9})$$

i.e., the Sherwood number is a constant, which we will call the Sherwood constant (with the theoretical value of 48), times a function that depends on the retention, k . For infinite retention, $k \rightarrow \infty$ and $Sh = 48/11$, which is exactly the result reported for heat transfer⁴⁹ as well as for mass transfer⁵⁰ in tubes.

To test the usefulness of the present approximation for k_M we plotted

$$\frac{2 R^2 u}{D_M (H_{\text{exp}} - C_M u)} \cdot \frac{(1 + 6k + 11k^2) k}{(1 + k)^3}$$

as a function of dimensionless velocity $ReSc = 2 u R / D_M$ in Fig. 19. The figure shows that the theoretical value of 48 is approached. Although the present derivation of eqns. A7–A9 is only approximate, these equations seem to describe experimentally observed dispersion data quite well. A more exact derivation of mass transfer effects is under study.

NOMENCLATURE

B	$2 D_M$, plate height term (cm ² /sec) for axial diffusion
c	Concentration (mole/cm ³)
c_M	Concentration of solute in the mobile phase (mole/cm ³)
c_S	Concentration of solute in the stationary phase (mole/cm ³)
\bar{c}	Average concentration
c_{bulk}	Mean cup concentration, $(1/u) \cdot \int c(r) \cdot u(r) r \, dr \, d\phi$
C	H/u , plate height term (sec)
C_i	H/u , plate height term (sec) for interphase resistance
C_M	H/u , plate height term (sec) for convective dispersion in the mobile phase
C_S	H/u , plate height term (sec) for diffusion in the stationary phase
D_M	Diffusion coefficient (cm ² /sec) in the mobile phase
D_S	Diffusion coefficient (cm ² /sec) in the stationary phase
H	Plate height (cm), $L \mu_2 / \mu_1^2 \approx L (\sigma_i / t_R)^2$
k	Capacity factor, $(t_R - t_M) / t_M$
k_M	Mass transfer coefficient (cm/sec)
L	Column length (cm)
l	Length (cm) of the conical jet tip
MW	Molecular weight
n	Number of plates, L/H
n_{eff}	Effective number of plates, $n (k / (1 + k))^2$

Δp	Pressure drop (bar)
r	Radial coordinate
R	Column radius $R = \text{I.D.}/2$ (cm)
ReSc	Dimensionless velocity, $2 u R/D_M$
\mathcal{R}	Radius (cm) in the jet tip
Sh	Dimensionless Sherwood number, $2 R k_M/D_M$
t_M	Retention time (sec) of a non-retained solute = residence time of the mobile phase
t_R	Retention time (sec) of a retained solute, $t_M (1 + k)$
u	Average linear velocity (cm/sec), $L/\mu_1 \approx L/t_M$
z	longitudinal coordinate along the column (cm)
γ	Surface tension (dyne/cm)
δ	Film thickness (cm) of the stationary phase
η	Dynamic viscosity (poise)
μ_1	First time moment (sec), $(1/c_0) \cdot \int c(t) \cdot t \, dt \approx t_R$
μ_2	Second central moment (sec ²), $(1/c_0) \cdot \int c(t - \mu_1) \cdot t^2 \, dt \approx \sigma_t^2$
ϱ	Density (g/cm ³)
σ_t^2	Variance (sec ²) of symmetrical peaks
ϕ	Angle
ϕ''	Mass flux (mol/cm ² · sec)

ACKNOWLEDGEMENTS

The authors wish to thank Ms. A. van Dam for her collaboration in developing the LC–MS coupling technique. They are also indebted to Mr. E. F. Dawes of S.G.E. (Australia), who kindly supplied fused silica microcapillaries.

REFERENCES*

- 1 J. H. Knox and M. T. Gilbert, *J. Chromatogr.*, 186 (1979) 405.
- 2 T. Tsuda, K. Hibi, T. Nakanishi, T. Takeuchi and D. Ishii, *J. Chromatogr.*, 158 (1978) 227.
- 3 K. Hibi, T. Tsuda, T. Takeuchi, T. Nakanishi and D. Ishii, *J. Chromatogr.*, 175 (1979) 105.
- 4 D. Ishii, T. Tsuda and T. Takeuchi, *J. Chromatogr.*, 185 (1979) 73.
- 5 K. Hibi, D. Ishii, I. Fujishima, T. Takeuchi and T. Nakanishi, *J. High Resolut. Chromatogr. Chromatogr. Commun.*, 1 (1978) 21.
- 6 T. Tsuda and M. Novotny, *Anal. Chem.*, 50 (1978) 632.
- 7 F. J. Yang, *J. High Resolut. Chromatogr. Chromatogr. Commun.*, 3 (1980) 589.
- 8 R. Tijssen, *Separ. Sci. Technol.*, 13 (1978) 681.
- 9 R. Tijssen, *Axial Dispersion in Helically Coiled Open Columns for Chromatography*; Ph.D. Thesis, University of Technology, Delft, 1979.
- 10 R. Tijssen, *Anal. Chim. Acta*, 114 (1980) 71.
- 11 J. Hermansson, *Chromatographia*, 13 (1980) 741.
- 12 P. J. Arpino, P. Krien, S. Vajta and G. Devant, *J. Chromatogr.*, 203 (1981) 117.
- 13 L. S. Etire, *Open Tubular Columns in Gas Chromatography*, Plenum, New York, 1965.
- 14 M. Mohnke and W. Saffert, in M. van Swaay (Editor), *Gas Chromatography 1962*, Butterworths, London, 1962, p. 216.

* *Editor's Note:* A paper by T. Tsuda, K. Tsuboi and G. Nakagawa, *J. Chromatogr.*, 214 (1981) 283, received on May 18th, 1981 gives the same conclusions as this paper; Tsuda *et al.* give results with a 20- μm I.D. column. See also M. Krejčí, K. Tesařík, M. Rusek and J. Pajurek, *J. Chromatogr.*, 218 (1981) 167. *Editor J. Chromatogr.*

- 15 G. Nota, G. Marino, V. Buonocore and A. Ballio, *J. Chromatogr.*, 46 (1970) 103.
- 16 M. Krejčí, K. Tesařík and J. Pajurek, *J. Chromatogr.*, 191 (1980) 17.
- 17 K. Tesařík, *J. Chromatogr.*, 191 (1980) 25.
- 18 R. D. Schwartz, D. J. Brasseaux and R. G. Mathews, *Anal. Chem.*, 38 (1966) 303.
- 19 R. D. Schwartz, D. J. Brasseaux and G. R. Shoemaker, *Anal. Chem.*, 35 (1963) 496.
- 20 R. G. Mathews, J. Torres and R. D. Schwartz, *J. Chromatogr.*, 186 (1979) 183.
- 21 C. A. Cramers, E. A. Vermeer and J. J. Franken, *Chromatographia*, 10 (1977) 412.
- 22 K. Hibi, D. Ishii and T. Tsuda, *J. Chromatogr.*, 189 (1980) 179.
- 23 S. R. Lipsky, W. J. McMurray, M. Hernandez, J. E. Purcell and K. A. Billeb, *J. Chromatogr. Sci.*, 18 (1980) 1.
- 24 G. Schomburg, H. Hulsman and H. Behlau, *Chromatographia*, 13 (1980) 321.
- 25 W. Jennings, *J. High Resolut. Chromatogr. Chromatogr. Commun.*, 3 (1980) 601.
- 26 J. E. Sternberg, *Advan. Chromatogr.*, 2 (1966) 205.
- 27 O. Grubner, *Advan. Chromatogr.*, 6 (1968) 173.
- 28 M. J. E. Golay, in D. H. Desty (Editor), *Gas Chromatography 1958*, Butterworths, London, 1958, p. 36.
- 29 A. K. Wong, B. J. McCoy and R. G. Carbonell, *J. Chromatogr.*, 129 (1976) 1.
- 30 R. Aris, *Proc. R. Soc. London, Ser. A*, 235 (1956) 67.
- 31 R. Aris, *Proc. R. Soc. London, Ser. A*, 252 (1959) 538.
- 32 M. A. Khan, in M. van Swaay (Editor), *Gas Chromatography 1962*, Butterworths, London, 1962, p. 3.
- 33 A. Pethö, in E. Leibnitz and H. G. Struppe (Editors), *Handbuch der Gas Chromatographie*, Geest & Portig, Leipzig, 1966, p. 70.
- 34 J. C. Giddings, *Dynamics of Chromatography*, Marcel Dekker, New York, 1965.
- 35 L. R. Snyder and J. J. Kirkland, *Introduction to Modern Liquid Chromatography*, Wiley, New York, 2nd ed., 1979.
- 36 K. Tesařík, M. Krejčí, M. Rusek, J. Pajurek and K. Slais, *4th International Symposium on Capillary Chromatography, Hindelang, May, 1981*.
- 37 P. J. Arpino and G. Guiochon, *Anal. Chem.*, 51 (1979) 682A.
- 38 W. H. McFadden, *J. Chromatogr. Sci.*, 18 (1980) 97-115.
- 39 C. R. Blakley, J. J. Carmody and M. L. Vestal, *Anal. Chem.*, 52 (1980) 1636.
- 40 M. Dole, H. L. Cox and J. Gieniec, *Advan. Chem. Ser.*, 125 (1971) 73.
- 41 C. R. Blakley, M. J. McAdams and M. L. Vestal, *J. Chromatogr.*, 158 (1978) 261.
- 42 E. R. Lory and F. W. McLafferty, *Advan. Mass Spectrom.*, 8 (1980) 954.
- 43 L. Kuhn and R. A. Myers, *Sci. Amer.*, 240 (1979) 120.
- 44 N. R. Lindblad and J. M. Schneider, *J. Sci. Instr.*, 42 (1965) 635.
- 45 W. J. Beek and K. M. K. Muttzall, *Transport Phenomena*, Wiley, London, 1975.
- 46 G. I. Taylor, *Proc. R. Soc. London, Ser. A*, 219 (1953) 186.
- 47 G. I. Taylor, *Proc. R. Soc. London, Ser. A*, 223 (1954) 446.
- 48 G. I. Taylor, *Proc. R. Soc. London, Ser. A*, 225 (1954) 473.
- 49 J. D. Parker, J. H. Boggs and E. F. Blick, *Introduction to Fluid Mechanics and Heat Transfer*, Addison-Wesley, Reading, 1969, p. 190.
- 50 A. H. P. Skelland, *Diffusional Mass Transfer*, Wiley, New York, 1974, p. 142.

CHROM. 14,143

FLOW CHARACTERISTICS AND TECHNOLOGY OF CAPILLARY COLUMNS WITH INNER DIAMETERS LESS THAN 15 μm IN LIQUID CHROMATOGRAPHY

M. KREJČÍ*, K. TESÁŘÍK, M. RUSEK and J. PAJUREK

Institute of Analytical Chemistry, Czechoslovak Academy of Sciences, Brno 61142 (Czechoslovakia)

SUMMARY

The flow characteristics of capillary columns at flow-rates up to 10^{-5} $\mu\text{l}/\text{sec}$ have been studied experimentally as a function of the column diameter and of the pressure drop. Theoretical conclusions based on the Poiseuille equation and band broadening for unadsorbed solutes have been tested.

The preparation of glass capillary columns is described, and the rôle of the glass melting temperature is discussed. The inner diameters (5–34 μm) of the columns were measured both by microscopy and hydrodynamically. The maximum difference between the two measurements was 2.8 μm , but in most cases it did not exceed 1.5 μm . The modified flame-ionization detector was used.

INTRODUCTION

The development of liquid chromatography in capillary columns has led to the use of columns with very small diameters on the grounds of efficiency and the time required for analysis^{1–4}. However, scepticism as to whether such usage can be justified has arisen because of the untried technology for the preparation of capillary columns with diameters, $d_c < 15$ μm , and the lack of suitable sampling and detection methods. The present paper describes an attempt to solve some of these problems.

We have examined experimentally some of the significant parameters in capillary liquid chromatography, such as the dependences of the dead time, number of theoretical plates and the pressure drop on the diameter of the column. In addition, hydrodynamic values are used to compare the diameters of capillary columns with diameters at discrete points determined with the aid of a microscope in order to evaluate the homogeneity of the capillary column throughout its length.

Previous studies^{5–17} have made use of open tubular capillary columns, usually with diameters from 50 to 30 μm . The liquid–liquid system has most often been used, although adsorption and even ion-exchange liquid chromatography have been employed¹⁸. Attention was therefore concentrated upon columns with diameters less than 30 μm and on the liquid–liquid system.

THEORETICAL

In order to study the influence of the diameter of the capillary column on some chromatographic parameters, we started from a relationship derived from the Poiseuille equation

$$t_m = \varphi \eta L^2 / d_c^2 \Delta p \quad (1)$$

where φ is the column resistance parameter ($= 32$ for capillary columns), η is the viscosity of the mobile phase, L is the column length, d_c is the column diameter, Δp is the pressure drop in the column and t_m is the dead retention time.

The dead retention time and thus also the analysis time increase for a given capacity ratio, k , with decreasing column diameter, provided the other parameters in eqn. 1 remain constant. However, if the optimum velocity of the mobile phase, u_{opt} , is employed, which corresponds to the minimum height equivalent to a theoretical plate for an unadsorbed solute, H_{min}

$$H_{min} = 2\sqrt{BC_m} \quad u_{opt} = \sqrt{B/C_m} \quad (2)$$

where the coefficient of longitudinal diffusion $B = 2 D_m$ and the coefficient of the mass transfer in the mobile phase

$$C_m = \frac{1 + 6k + 11k^2}{1 + k^2} \cdot \frac{d_c^2}{96 D_m}$$

the corresponding retention time for an unadsorbed solute can be expressed as

$$t_m^* = L d_c / 13.9 D_m \quad (3)$$

where D_m is the diffusion coefficient of the solute in the mobile phase. Under these conditions (u_{opt} and constant L and D_m), the dead retention time decreases with decreasing diameter of the capillary column. For high column efficiency, it is necessary that extra column contributions to the height equivalent to a theoretical plate are negligible.

For the total time constant of the detector, t_d , the following conditions must be satisfied

$$t_d \leq t_m / 2\sqrt{N} \quad (4a)$$

$$t_d \leq (Lh)^{1/2} d_c^{3/2} / 2 D_m v \quad (4b)$$

where N is the number of theoretical plates, h is the reduced height equivalent to a theoretical plate ($= H/d_c$) and v is the reduced velocity of the mobile phase ($= u d_c / D_m$). At the optimum velocity of the mobile phase, relationship 4a can be expressed as:

$$t_d^* \leq \frac{t_m^*}{2} \sqrt{\frac{0.29 d_c}{L}} = \frac{1}{51.6} \cdot \frac{\sqrt{L} d_c^{3/2}}{D_m} \quad (5)$$

Requirement of the time constant of the detector diminishes, *i.e.*, even a higher value of the detector time constant can be admitted (according to eqn. 4 or 5) under the assumption that N decreases or d_c increases. For instance, when $L = 1\text{ m}$, $D_m = 1 \cdot 10^{-9}\text{ m}^2/\text{sec}$ and $d_c = 5\text{ }\mu\text{m}$, $t_d = 0.22\text{ sec}$, while when $d_c = 10\text{ }\mu\text{m}$, $t_d = 0.62\text{ sec}$. By substituting real values into relationship 4 or 5, the values of t_d obtained are so small that the technical requirements of the design of the classical detection methods such as spectrophotometry, fluorometry, refractometry, etc., are immediately obvious. All these methods, based on the measurement of a change in an analytical property, require that the cuvettes employed have lengths of 0.01–0.1 mm and diameters equal to the column diameter. These requirements are unrealizable. Still less realizable therefore are any connections between the column and the detector.

For the reasons mentioned above, we consider transport detectors as promising. In such detectors the solute is transported quickly from the column outlet into the detection system where it gains a velocity substantially higher than the velocity of the mobile phase in the column. Examples are mass spectrometric detectors, flame ionization detectors¹⁹ and their modifications and electrochemical detectors.

EXPERIMENTAL AND RESULTS

Drawing of capillaries

Glass can be applied to advantage in the preparation of capillaries of this type, owing to the properties described previously^{12,20}. Capillaries are drawn in the device described by Desty *et al.*²¹. The diameters required can be drawn in a single or double run. The former procedure is commonly used for capillaries with larger inner diameters. It is necessary that the initial glass tube has dimensions about $8 \times 0.3\text{ mm}$ in order for a suitable outer diameter (0.7–0.8 mm) to be obtained with an orifice of 30 μm or less. The latter procedure makes it possible to prepare a suitable capillary without the use of a thick glass tube²². A capillary of 0.95 mm O.D. is first drawn from a commonly available $7 \times 1\text{ mm}$ tube and is then inserted into another $7 \times 1\text{ mm}$ tube. Both tubes are then drawn into a capillary of 0.7–0.8 mm O.D. The inner diameter of this composite capillary corresponds to the dimension that is required.

The temperature of the oven in the drawing device is decisive for either procedure. The start of drawing is dependent on the melting temperature of the glass and, dynamic equilibrium in the oven having been reached, the dimensions of the capillary are controlled by the following relationship

$$d_{c1}/d_{c2} = \sqrt{c_1}/\sqrt{c_2}$$

where d_{c1} and d_{c2} are the diameters of the tube and the capillary, respectively, and c_1 and c_2 the velocities of the tube feeding and the capillary drawing from the oven, respectively. If the temperature increases and the glass is overheated, the capillary closes inside and the inner diameter is thus diminished. An increase of about 30°K (above the drawing temperature at which the relationship $d_{c1}/d_{c2} = \sqrt{c_1}/\sqrt{c_2}$ is valid) will result in a solid glass rod. The effect of temperature on capillary narrowing is shown in Tables I and II and Fig. 1.

The temperature range in which capillaries having the required diameters can be drawn is 20–30°K (Fig. 2) and is, of course, different for each kind of glass.

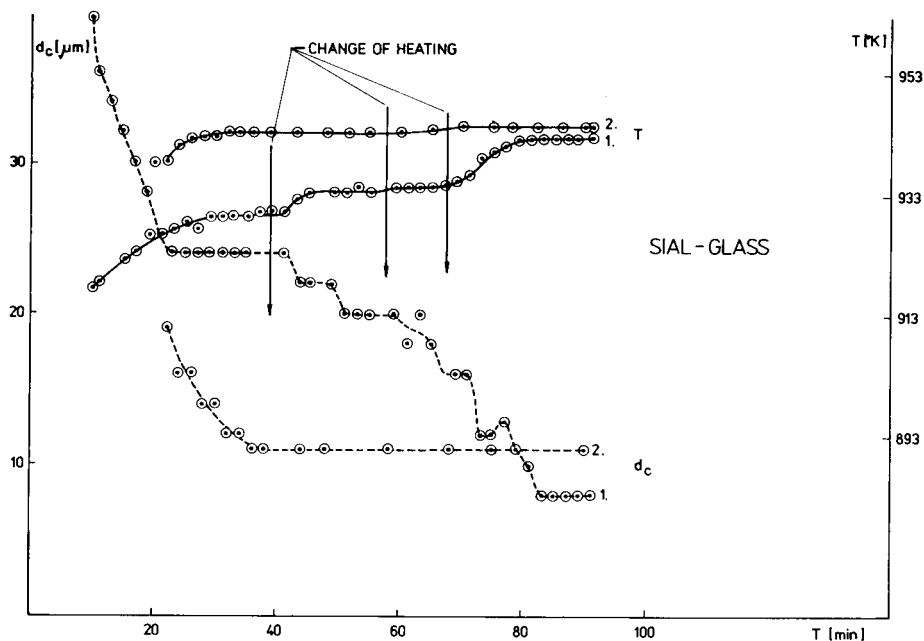


Fig. 1. Dependence of temperature and column diameter on time. 1, Changes of d_c as a function of temperature changes i ; 2, constancy of d_c at constant oven temperature.

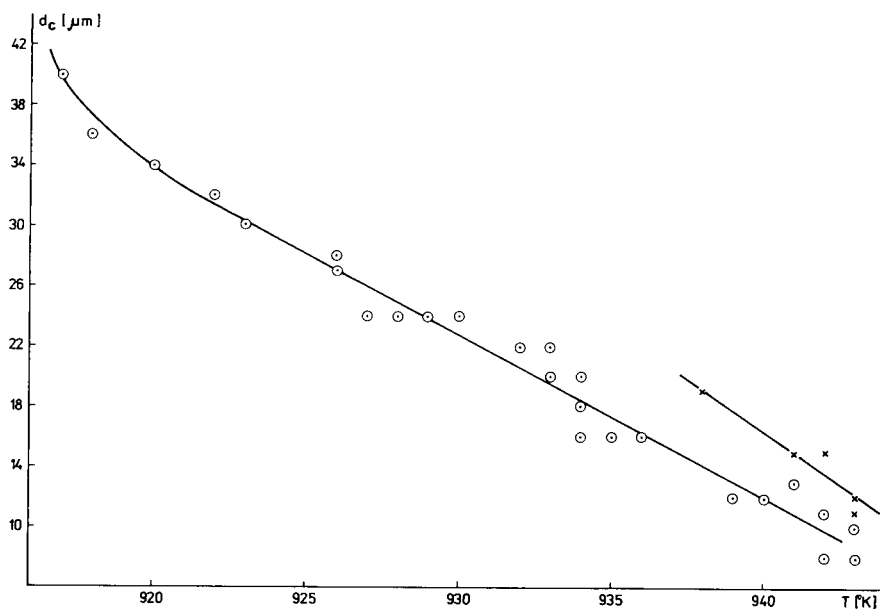


Fig. 2. Dependence of column diameter on temperature. Capillary A (\odot); capillary B (\times).

TABLE I

DEPENDENCE OF THE CAPILLARY DIAMETER ON THE TEMPERATURE OF THE OVEN IN THE DRAWING DEVICE

Time (min)	Temperature (°K)	d_c (μm)	Time (min)	Temperature (°K)	d_c (μm)
10	917	40	51	933	20
11	918	36	53	934	20
13	920	34	55	933	20
15	922	32	59	934	20
17	923	30	61	934	18
19	926	28	63	934	20
21	926	25	65	934	18
23	927	24	67	934	16
25	928	24	69	935	16
27	927	24	71	936	16
29	929	24	73	939	12
31	929	24	75	940	12
33	929	24	77	941	13
35	929	24	79	942	11
37	930	24	81	943	10
39	930	24	83	942	8
41	930	24	85	943	8
43	932	22	87	943	8
45	933	22	89	943	8
49	933	22			

Modification of the internal surface

Etching of the internal surface of a glass capillary can be performed in the gaseous phase with hydrogen chloride, hydrogen fluoride, methyl trifluorochloroethyl ether, etc., or in the liquid phase with acidic or basic reagents. The procedures for the gaseous phase are less exacting since relatively low pressures, about 1–2 MPa, of an inert gas are sufficient for filling the capillary and activating its surface. In order to fill the capillaries with liquids, the operating pressures must be increased to 10–15 MPa and the probability of capillary blocking during filling or washing is greater.

The device for capillary filling with gases, vapours or liquids should have a

TABLE II

DEPENDENCE OF CAPILLARY DIAMETER ON THE OVEN TEMPERATURE AT CONSTANT OPERATING CONDITIONS

Time (min)	Temperature (°K)	d_c (μm)	Time (min)	Temperature (°K)	d_c (μm)
22	938	19	34	943	12
24	941	16	36	943	11
26	942	16	38	943	11
28	942	14	48	943	11
30	942	14	75	944	11
32	943	12	90	944	11

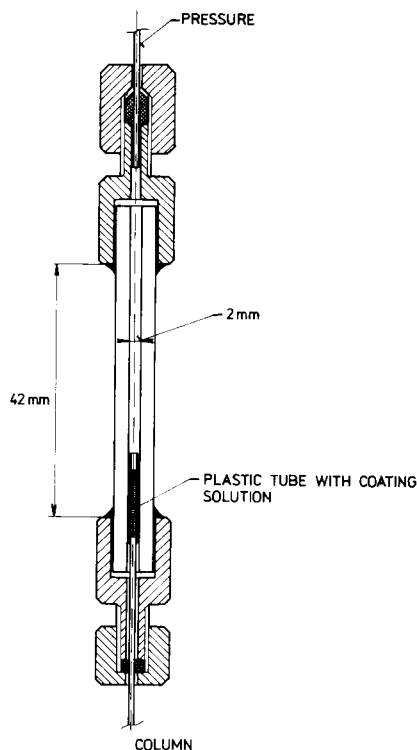


Fig. 3. Device for coating capillaries under pressure.

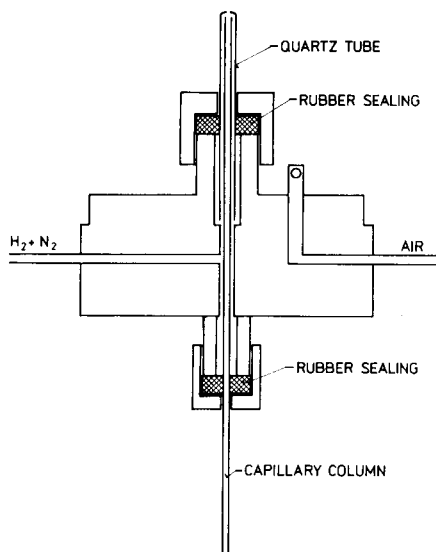


Fig. 4. Diagram of the burner of the flame ionization detector.

small working volume with respect to the small volume of the capillaries (up to $10 \mu\text{l}$) and should be able to withstand even higher operating pressures. To fill the capillary with a liquid, a short polyethylene capillary (Fig. 3), containing a measured volume of the liquid is placed at the inlet of the glass capillary in a glass pressure tank. The pressure is increased and the liquid is forced into the capillary. The velocity of the liquid forced into the capillary is observed from the decrease in level in the polyethylene capillary. This capillary serves as a pressureless transparent reservoir of the liquid. The passage of the liquid is observed at the outlet of the glass capillary to which another thin polyethylene capillary is connected. The liquid can thus be collected in the latter capillary and forced out with gas pressure.

The concentration of the solution, velocity of filling and operating pressure are determined by the inner diameter of the capillary. The internal surface of the capillary diminishes linearly with decreasing diameter, while the volume of the liquid or the vapour in the capillary decreases with the square of the diameter. This decrease may be compensated by increasing the concentration or repeating the process until a regular stationary phase film or adsorption layer on the capillary wall is obtained.

Detection technique

A special burner was designed for liquid chromatography capillary columns, which was used in flame ionization and in alkali flame ionization detectors. The

burner (Fig. 4) consists of a quartz tube into which one tip of the capillary column is inserted. The column outlet is thus washed with a hydrogen–nitrogen mixture (50:50 v/v). The temperature of the end of the column can be varied from room temperature up to ca. 1000° K, depending on the type of burner and the distance from the flame. Under suitable conditions, the velocity of transfer into the detector is identical for solutes with boiling points within the range 350–600° K.

The flame ionization detector was of a common design with electrometric amplifiers, Vibron Model 33C (Electronic Instruments, Richmond, Great Britain) and one manufactured by Laboratory Instruments (Prague, Czechoslovakia). The alkali flame ionization detector in dual arrangement^{23,24} was operated with the same electrometric amplifiers.

The flame ionization detector can also be used with such mobile phases for which the detector provides a response. If the detector response to solute i , $R_i^{\text{H}_2\text{O}}$, with water as the mobile phase is employed as a standard, then the detector response, R_i , to a mobile phase containing one detectable component b (e.g., methanol) is determined by

$$R_i = R_i^{\text{H}_2\text{O}} \left(1 - \frac{\sum C_b^{\text{eff}} y_b}{\sum C_i^{\text{eff}}} \right) \quad (6)$$

where C^{eff} is the effective number of carbon atoms of component b or solute i and y_b is the molar fraction of component b in water. The detector response thus decreases as the value of the fraction at the right-hand side of eqn. 6 increases; likewise, in gas chromatography it decreases with the increasing tension of the stationary phase leaving the column for the detector²⁵. A negative response is obtained in the case when $\sum C_i^{\text{eff}} < \sum C_b^{\text{eff}} y_b$. The ionization efficiency of the flame ionization detector used was 0.02 C/mole for isopropanol in water + 5% methanol as mobile phase. The detector efficiencies for other solutes were similar.

The alkali flame ionization detector extends substantially the application range²⁶ of this detection principle in capillary liquid chromatography. For instance, a hydrocarbon mobile phase can be employed for halogen and phosphorus containing compounds. Sufficient sensitivity of detection of these substances is ensured by the high selectivity of the detector response.

A spectrophotometric detection using a scavenger liquid¹² was also used to measure retention time. A Variscan flow-through cuvette (volume 8 μl ; Varian, Palo Alto, CA, U.S.A.) was washed with a mobile liquid with a ratio of mobile phase flow-rate from the capillary column to scavenger liquid flow-rate of 1:500–10,000 in such a way that the chromatogram obtained from measurements in the capillary column was not affected by the cell volume.

Hydraulic measurements of the column diameter

The homogeneity of the diameter of the capillary column throughout its length was checked for several columns by breaking the column and measuring with the aid of a microscope. The common procedure of determining the diameter at the beginning and at the end of the column was not considered sufficient when investigating a new method of preparation of glass columns.

Eqn. 1 was used to calculate the diameter of the capillary column. The dead retention time, t_m (sec), the length of the capillary column, L (m), and the pressure at

TABLE III

DIAMETERS OF CAPILLARY COLUMNS MEASURED BY MICROSCOPY AND CALCULATED ACCORDING TO EQN. 1

Column No.	d_c (μm)		$\pm \sigma$ (μm^2)	$\pm \sigma_{rel}$ (%)	L (m)	Mobile phase
	Microscope	Calculated				
1	5	4.8	0.13	2.70	1.00	Water + 2% methanol
2	8-9	8.0	0.17	2.12	2.20	Isopropanol
3	8-9	7.3	0.38	5.20	2.20	Water + 5% methanol
4	8-9	7.7	0.23	2.98	2.20	Water + 5% methanol
5	8-9	8.6	0.31	3.63	1.65	Cyclohexane
6	8	8.5	0.12	1.47	2.70	Cyclohexane
7	13	11.4	0.49	4.36	1.40	Methanol
8	13	13.7	0.68	5.97	1.60	Methanol
9	13	11.3	0.32	2.83	2.06	Cyclohexane
9a	6-8	13.7	0.37	2.71	2.05	Cyclohexane
10	15	16.3	0.34	2.08	3.60	Water
11	17	16.9	1.24	7.30	2.05	Cyclohexane
12	17	17.1	1.73	10.10	1.96	Cyclohexane
13	34	37.6	11.77	31.31	2.00	Cyclohexane

the column inlet, ΔP (MPa), were measured experimentally. The following values were assumed: $\varphi = 32$; viscosities ($\text{N} \cdot \text{sec}/\text{m}^2$) at 295.7°K , $\eta_{\text{H}_2\text{O}} = 0.0942$, $\eta_{\text{MeOH}} = 0.0548$, $\eta_{\text{C}_6\text{H}_{14}} = 0.0306$, $\eta_{\text{i-PrOH}} = 0.195$ and $\eta_{\text{cyclohexane}} = 0.0710$. Table III shows the satisfactory agreement between the diameter at the beginning of the column determined by microscopy and the diameter calculated by using eqn. 1. Each d_c value was calculated as the average of measurements performed at up to ten different mobile phase flow-rates (at ten different pressures at the column inlet). The standard deviation of an individual measurement was on the average 3.6%. These measurements were also performed at various points of the same column and for selected columns with different mobile phases. The values of the standard deviation were in the range 6-8%.

In some instances, particularly for capillary columns with diameters $d_c < 15 \mu\text{m}$, anomalies in the mobile phase flow-rate were observed in the course of measure-

TABLE IV

CHANGE IN d_c DETERMINED ACCORDING TO EQN. 1 IN THE COURSE OF THE MEASUREMENT $L = 2.5 \text{ m.}$

d_c (μm)		$\pm \sigma$ (μm)	$\pm \sigma_{rel}$ (%)
microscope	calculated		
6-7	5.7	0.194	3.4
6-7	6.3	0.154	2.5
6-7	6.9	0.111	1.6

ment. The rapid response of the flame ionization detector made it possible to measure not only the overall change in the flow-rate, appearing as a change in t_m , at a constant pressure, but also an instantaneous change in the flow-rate, appearing as a periodic decrease almost to zero followed by its re-establishment. In some instances, the mobile phase flow-rate ceased, as described earlier¹²; in the majority of instances, however, a pressure of up to 16 MPa was not sufficient to renew the flow-rate.

Table IV shows an example of the change in flow-rate and thus also the change in the value of d_c calculated for a column with a diameter of $d_c = 6\text{--}7 \mu\text{m}$ (microscopy). The height equivalent to a theoretical plate was measured simultaneously with the parameters required for the calculation of d_c . The dependence of the reduced values is shown in Fig. 5. Boundary values, marked on this graph as 5 and $9 \mu\text{m}$, were measured independently in other columns. The column described in Table IV and Fig. 5 became blocked after the injection of about 80 samples of isopropanol. At first, the flow-rate could be re-established temporarily by an increased pressure; ultimately, at a pressure of 30 MPa and at 80°C , the column remained blocked. Blocking of the inlet or outlet of the column was circumvented by gradual removal of sections at the column ends. It is assumed that the observed phenomenon is associated with the presence of surface active substances in the binary mobile phase.

Measurement of the efficiency of capillary columns

The dependence of the reduced height equivalent to a theoretical plate, h , on the reduced velocity, v , for an unadsorbed solute (isopropanol) in columns with diameters $d_c = 15, 14, 9$ and $5 \mu\text{m}$ is presented in Fig. 6. Columns of diameter $d_c = 9 \mu\text{m}$ or larger exhibit dependences which deviate significantly from the theoretical dependence, the values of h being about four-fold greater than expected. However, the theoretical values are approached at the curve minimum and at low reduced velocities. The column of diameter $5 \mu\text{m}$ exhibits even great deviations although it was studied under identical conditions. In this case, the values of the reduced plate height approach the theoretical ones at low reduced velocities, but in the region of the minimum and at higher linear velocities the difference between the experimental and theoretical values of h increases rapidly. The main reason for this phenomenon would

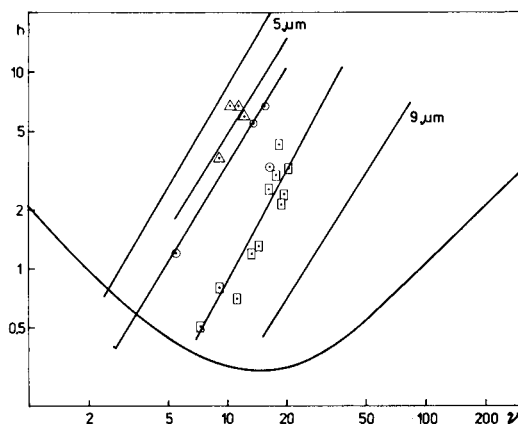


Fig. 5. Dependence of the reduced height equivalent to a theoretical plate, h , on the reduced velocity, v , for a column with $d_c = 6\text{--}7 \mu\text{m}$. Apparent diameter: $\approx 5.7 \mu\text{m}$ (Δ); $\approx 6.3 \mu\text{m}$ (\circ); $\approx 6.9 \mu\text{m}$ (\square).

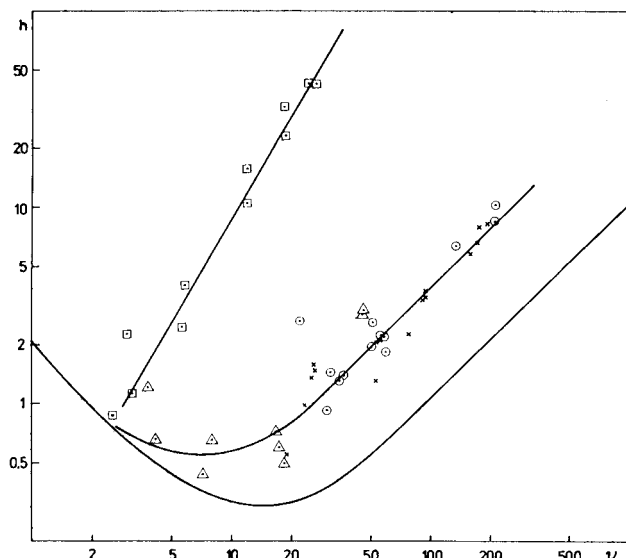


Fig. 6. Dependence of h on ν for the columns with $d_c = 15 \mu\text{m}$ (\circ), $14 \mu\text{m}$ (\times), $9 \mu\text{m}$ (\triangle) and $5 \mu\text{m}$ (\square).

seem to be that the demands placed on the detection mode are so great that they are not satisfied by the given arrangement.

The dependence of the detection time, t_d , calculated according to eqn. 4b, on the difference between the theoretical and experimental reduced plate heights is presented in Fig. 7. This shows that a column with $d_c = 5 \mu\text{m}$ requires t_d to be of the order of seconds, which could not be achieved with our flame ionization detector, not only with respect to the electronics but also probably because of the speed of the solute transfer into the detection system. However, the detector is suitable for columns with larger diameters, where the required value of t_d is larger.

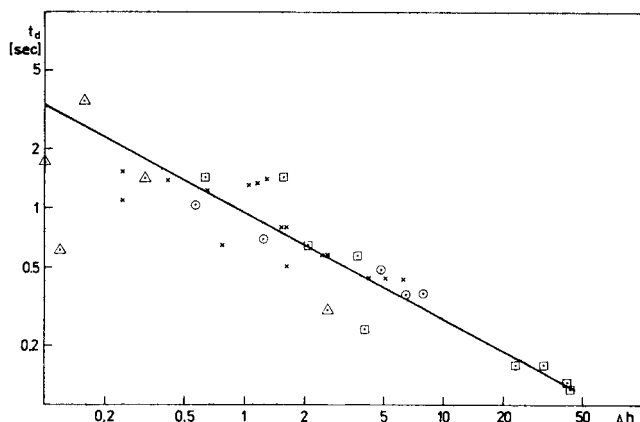


Fig. 7. Dependence of detection time, t_d (according to eqn. 4), on the difference between the theoretical and experimental values of the reduced height equivalent to a theoretical plate, Δh . Other conditions as in Fig. 6.

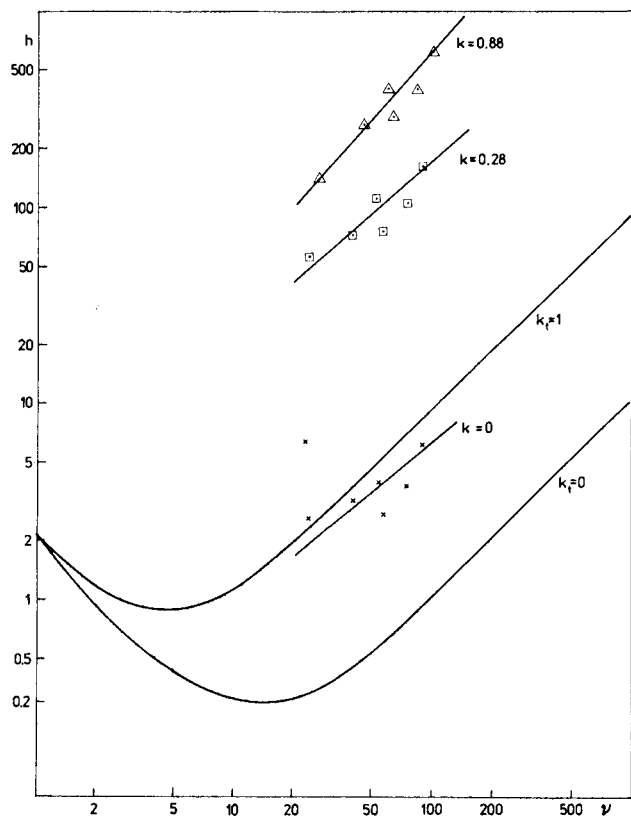


Fig. 8. Dependence of h vs. v for *o*-nitrobenzaldehyde ($k = 0$), *m*-cresol ($k = 0.28$) and β -naphthol ($k = 0.88$). Column: $3 \text{ m} \times 25 \mu\text{m}$ I.D., coated with 1,2,3-tris(cyanoethoxy)propane. Mobile phase: cyclohexanone saturated with 1,2,3-tris(cyanoethoxy)propane. UV detection at 220 nm. Theoretical values of k_i were calculated for thickness of the stationary phase, $d_i = 1 \mu\text{m}$, $D_m = 1.2 \cdot 10^{-9} \text{ m}^2/\text{sec}$ and diffusion coefficient of the solute into the stationary phase, $D_s = 1.4 \cdot 10^{11} \text{ m}^2/\text{sec}$.

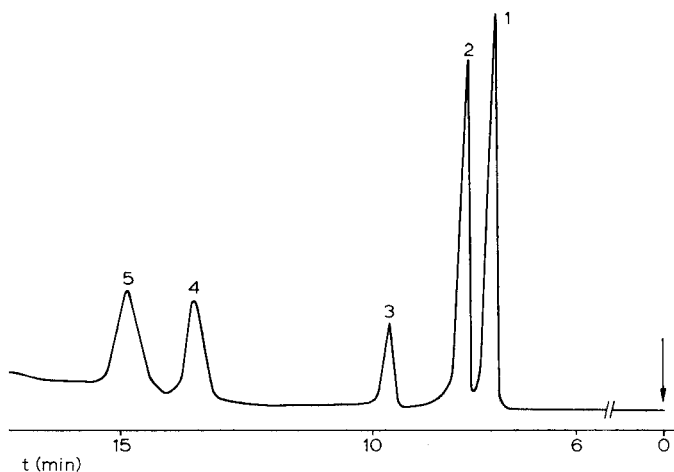


Fig. 9. Example of a chromatogram with flame ionization detection. Column: $3 \text{ m} \times 14 \mu\text{m}$ I.D. Stationary liquid: OV-101. Mobile phase: water. Solutes: 1 = triethylene glycol; 2 = *m*-cresol; 3 = 2,4-dimethylphenol; 4 = 2-methyl-4-ethylphenol; 5 = 2-isopropylphenol.

To evaluate the effect of retention on column efficiency, a glass capillary with $d_c = 25 \mu\text{m}$ was coated with 1,2,3-tris(cyanoethoxy)propane (Lachema, Brno, Czechoslovakia). The coating procedure and the detection were described earlier¹². The results are shown in Fig. 8. The column efficiency is significantly lower and expected, and is ascribed to non-homogeneities in the film thickness; for the solutes used, non-ideal behaviour in both the mobile and stationary phases cannot be excluded.

CONCLUSIONS

The possibility of preparing columns of $5 \mu\text{m}$ diameter or larger has been demonstrated. Column diameters determined with the aid of a microscope and by flow-rate measurements were in good agreement. Anomalies in the flow-rate were found for columns with small diameters, caused probably by surface active substances present in the capillary. Conditions for application of a flame ionization detector have been suggested. A typical separation is shown in Fig. 9.

REFERENCES*

- 1 J. H. Knox and M. T. Gilbert, *J. Chromatogr.*, 186 (1979) 405.
- 2 J. H. Knox, *J. Chromatogr. Sci.*, 18 (1980) 453.
- 3 G. Guiochon, *J. Chromatogr.*, 185 (1979) 3.
- 4 G. Guiochon, *Anal. Chem.*, 52 (1980) 2002.
- 5 T. Tsuda and M. Novotný, *Anal. Chem.*, 50 (1978) 632.
- 6 K. Hibi, D. Ishii, I. Fujishima, T. Takeuchi and T. Nakanishi, *J. High Resolut. Chromatogr. Chromatogr. Commun.*, 1 (1978) 21.
- 7 T. Tsuda, K. Hibi, T. Nakanishi, T. Takeuchi and D. Ishii, *J. Chromatogr.*, 158 (1978) 227.
- 8 K. Hibi, T. Tsuda, T. Takeuchi, T. Nakanishi and D. Ishii, *J. Chromatogr.*, 175 (1979) 105.
- 9 I. Ishii, T. Tsuda and T. Takeuchi, *J. Chromatogr.*, 185 (1979) 73.
- 10 D. Ishii, T. Tsuda, K. Hibi, T. Takeuchi and T. Nakanishi, *J. High Resolut. Chromatogr. Chromatogr. Commun.*, 2 (1979) 371.
- 11 T. Takeuchi, K. Matsuoka, Y. Watanabe and D. Ishii, *J. Chromatogr.*, 192 (1980) 127.
- 12 M. Krejčí, K. Tesařík and J. Pajurek, *J. Chromatogr.*, 191 (1980) 17.
- 13 T. Tsuda and G. Nakagawa, *J. Chromatogr.*, 199 (1980) 249.
- 14 K. Hibi, D. Ishii and T. Tsuda, *J. Chromatogr.*, 189 (1980) 179.
- 15 C. Dewaele and M. Verzele, *J. High Resolut. Chromatogr. Chromatogr. Commun.*, 1 (1978) 174.
- 16 F. J. Yang, *J. High Resolut. Chromatogr. Chromatogr. Commun.*, 3 (1980) 589.
- 17 F. J. Yang, *J. High Resolut. Chromatogr. Chromatogr. Commun.*, 4 (1981) 83.
- 18 D. Ishii and T. Takeuchi, *J. Chromatogr. Sci.*, 18 (1980) 462.
- 19 M. Krejčí and M. Rusek, *Coll. Czech. Chem. Commun.*, in press.
- 20 K. Tesařík, *J. Chromatogr.*, 191 (1980) 25.
- 21 D. H. Desty, J. N. Haresnape and B. H. F. Whyman, *Anal. Chem.*, 32 (1960) 302.
- 22 K. Tesařík and K. Šlais, *Technology of Preparation of Glass Capillary Columns with I.D. 2–30 μm* (in Czech), VZ 68, Institute of Analytical Chemistry, Czechoslovak Academy of Sciences, Brno, 1980.
- 23 B. Chundela, M. Krejčí and M. Rusek, *Deut. Z. Gesamt. Gerichtl. Med.*, 63 (1968) 154.
- 24 A. Carmen, *Anal. Chem.*, 36 (1964) 1416.
- 25 J. Novák, J. Gelbičová-Růžicková, S. Wičar and J. Janák, *Anal. Chem.*, 43 (1971) 1996.
- 26 M. Krejčí and M. Dressler, *Chromatogr. Rev.*, 13 (1970) 1.

* *Editor's Note:* Work on narrow capillaries was also presented simultaneously by R. Tijssen, J. P. A. Bleumer and M. E. van Krevel, *J. Chromatogr.*, 218 (1981) 135, and by T. Tsuda, K. Tsuboi and G. Nakagawa, *J. Chromatogr.*, 214 (1981) 283. *Editor J. Chromatogr.*

CHROM. 13,996

MICRO-COLUMN HIGH-PERFORMANCE LIQUID CHROMATOGRAPHY AND FLAME-BASED DETECTION PRINCIPLES

V. L. McGUFFIN and M. NOVOTNÝ*

Department of Chemistry, Indiana University, Bloomington, IN 47405 (U.S.A.)

SUMMARY

Novel detectors are described for micro-column high-performance liquid chromatography; they are based on the well-known principles of flame photometric and thermionic detection. These devices exhibit good selectivity and sensitivity for organophosphorus compounds in both aqueous and selected organic solvents. The extremely small volume of these flame-based detectors and their enhanced response at low flow-rates make them particularly attractive for capillary-column high-performance liquid chromatography.

INTRODUCTION

Miniaturized high-performance liquid chromatography (HPLC) systems are rapidly gaining recognition in modern separation science because of their very high efficiency and reduced consumption of sample and solvent. In recent communications, Guiochon¹ and Knox and Gilbert² discussed the theoretical and practical potential of such systems with optimistic conclusions, yet both papers emphasized the necessity for low-volume, sensitive detectors in order to realize the full potential of capillary-column technology.

Conventional concentration-sensitive detectors, such as UV absorbance³, fluorescence⁴, and electrochemical⁵ devices, have been modified to incorporate low-volume (*ca.* 0.1 μ l) flow-cells. Although such devices are adequate at the current stage of column development, the consequences of further cell-volume reduction become immediately apparent. It will be necessary in the future to develop certain detection and ancillary techniques that are inherently well suited to the unique conditions of micro-column HPLC. Among such techniques, direct-interface micro-liquid chromatography–mass spectrometry (LC–MS) has recently been demonstrated^{6,7} and shows promise in its application to complex samples of limited volatility. Similarly, direct-interface Fourier-transform IR spectroscopy should be feasible, and will greatly facilitate solute identification. In addition, detectors based on a transport system or flame should also benefit greatly from the reduced flow-rates characteristic of micro-columns.

Flame-based detection has been largely unsuccessful in conventional HPLC because the large volume of solvent disrupts the delicate balance of chemical and

physical processes that occur in the flame. Chemical interference severely limits the range of compatible mobile phases. In addition, the introduction of combustible organic solvents changes the temperature and fuel-to-oxidant ratio of the flame, thus influencing detector response and restricting the use of gradient elution. Despite the inherent incompatibility of these methods, there have been several attempts to use flame-based detection in conventional HPLC.

Julin *et al.*⁸ described a flame photometric detector (FPD) in which the HPLC effluent was pneumatically nebulized, and a fraction (25 %) was aspirated into a cool, hydrogen-rich diffusion flame. Phosphorus and sulfur compounds were selectively detected by monitoring the optical emission of the HPO (526 nm) and S₂ (384 nm) species. Under favorable conditions, this device was capable of sensing $2 \cdot 10^{-5}$ g/l of phosphorus, and $2 \cdot 10^{-4}$ g/l of sulfur. Organic solvents severely quenched emission from the chemiluminescent species, so that applications of this detector were limited to purely aqueous systems. Chester^{9,10} later developed an inverted-flame FPD for conventional HPLC in which interference by many organic solvents, metal ions and buffers was minimized. However, the detection limits obtained with this modified FPD were not significantly improved; $1 \cdot 10^{-5}$ g/l of phosphorus could be detected with continuous sample introduction.

Flame ionization¹¹ and thermionic^{12,13} detectors have been utilized in HPLC with a transport system for solvent evaporation before analysis. Such devices permit the use of a wide range of solvent systems and of gradient elution, but the sensitivity and stability are frequently inadequate for routine applications. The transport system introduces a significant amount of band dispersion and limits the linear dynamic range of the detector. The volatility of lower-molecular-weight solutes may further limit the accuracy of quantitative measurements.

In contrast to conventional HPLC columns, micro-columns (and capillary columns in particular) are very well suited to selective flame-based detection. The reduced flow-rate of solvent, typically 1 μ l/min for open-tubular or packed capillary columns, may be directly introduced with minimal disruption of the flame.

A novel flame-based detector has been developed and characterized, in which the total capillary-column effluent is concentrically nebulized and aspirated directly into a hydrogen-air diffusion flame. Solutes are then selectively detected using either optical emission or secondary ionization phenomena. This preliminary report illustrates the performance and potential of these versatile new detectors, which are believed to be the predecessors of other useful flame-based devices for micro-column liquid chromatography.

EXPERIMENTAL

Flame photometric detector

The flame base and housing are shown schematically in Fig. 1 and have been described previously¹⁴.

Hydrogen (55 ml/min) and nitrogen (90 ml/min), a non-combustible nebulizing gas, are pre-mixed in a baffle and flow through a stainless-steel flame jet (0.76 mm I.D.). Purified air (75 ml/min) is supplied to the fuel-rich flame by diffusion through a fritted metal disk. A glass capillary (50 μ m I.D., 0.6 mm O.D., and 10 cm in length) is inserted through the baffle, burner base and flame jet, and extends approximately 1

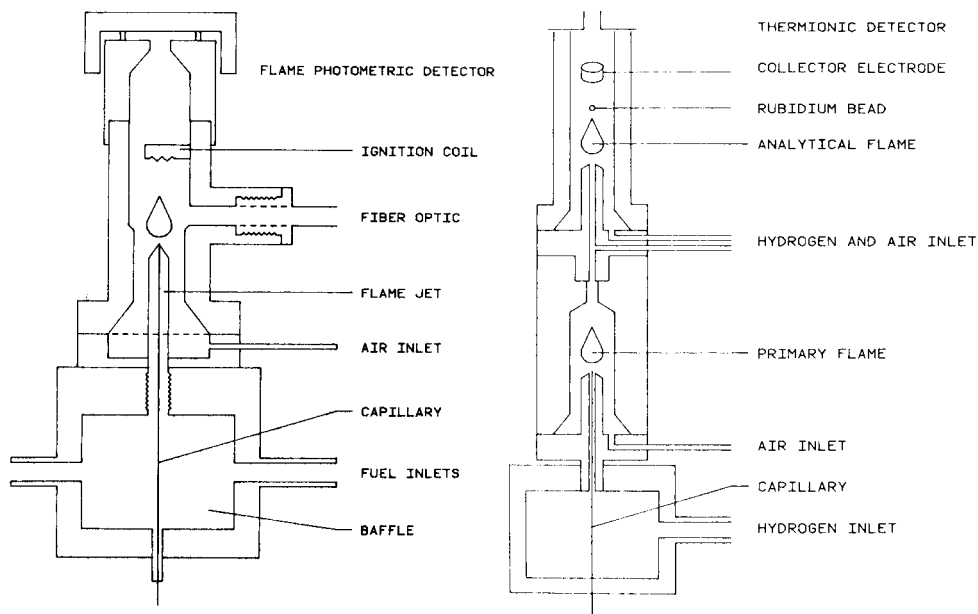


Fig. 1. Schematic diagram of the flame photometric detector for capillary-column HPLC.

Fig. 2. Schematic diagram of the dual-flame thermionic detector for capillary-column HPLC.

mm above the top of the flame jet. The other end of this capillary is connected to the HPLC micro-column with shrinkable PTFE tubing. The total column effluent is nebulized by the concentric flow of gases over the orifice of the capillary.

A fiber-optics probe is fixed in the wall of the housing, and views the cooler central region of the diffusion flame. The emission from the chemiluminescent species is then measured with an interference filter (530 nm, FWHM 14 nm) and photomultiplier tube (Hamamatsu Corp., Model R-372). The electrical signal from the photomultiplier is amplified by a picoammeter (RCA, Model WV-511A) and filtered to remove high-frequency noise; the output is then displayed on a strip-chart recorder (Shimadzu, Model R-101).

Thermionic detector

A schematic diagram of the dual-flame thermionic detector for micro-column HPLC is shown in Fig. 2. The baffle and lower burner base are similar to those described for the FPD. The lower flame housing is constructed of aluminum and includes an ignition coil and a thermocouple to monitor flame conditions.

Hydrogen (60–70 ml/min) and nitrogen (90 ml/min) are pre-mixed in the baffle, and nebulize the micro-column effluent at the glass-capillary orifice; purified air (140 ml/min) is supplied to the flame by diffusion through a fritted metal disk. Organic solutes and solvents are decomposed in the lower primary flame; the combustion products are combined with additional fuel (50–65 ml/min of hydrogen) and are swept into the analytical flame, which is also supplied with air by diffusion (280 ml/min). The analytical flame is not allowed to ignite and burn freely; the best response is obtained when combustion is carefully controlled in the region near the

alkali bead. If the upper flame should accidentally ignite, a large increase in background ion current is observed.

The alkali bead (rubidium nitrate), fabricated according to the procedure of Lubkowitz *et al.*¹⁵, is positioned 1–2 mm directly above the analytical flame jet. This bead is electrically heated by a controlled-current source (Perkin-Elmer). The cylindrical collector electrode is polarized to 200 V by a high-voltage power supply (Keithley, Model 244), and the upper flame jet is grounded to minimize solvent background. The ion current is amplified by using an electrometer (Perkin-Elmer), filtered to remove high-frequency noise and then displayed on a strip-chart recorder (Linear, Model 355).

Liquid chromatograph

A syringe pump (Varian, Model 8500) was utilized in this investigation to minimize fluctuations in pressure and flow-rate, which were expected to significantly affect the mass-sensitive FPD and the thermionic detector.

Packed micro-capillary HPLC columns were prepared as described previously¹⁴; octylsilane and octadecylsilane bonded phases were utilized in this investigation. Samples (0.2 μ l) were injected directly on to the column as described by Hirata and Novotný⁴.

A variable-wavelength UV detector (Jasco Uvidec 100-II), with modified flow-cell (*ca.* 0.1 μ l), was used for comparison of response and dead volume with those of the flame-based detectors.

Reagents

Trimethyl phosphate, a model solute used to characterize the flame-based detectors, was obtained from Aldrich.

Organophosphorus pesticide standards were of "qualitative grade", and were purchased from Anspec. Cygon [O,O-dimethyl-S-(N-methylcarbamoylmethyl) phosphorothioate; 98 % purity], DDVP (2,2-dichlorovinyl phosphate; 93 % purity), ethion [O,O,O',O'-tetraethyl-S,S'-methylenebis(phosphorothioate); 95 % purity], guthion [O,O-dimethyl-S-(4-oxo-1,2,3-benzotriazin-3(4H)-ylmethyl) phosphorothioate; 99 % purity], malathion [O,O-dimethyl-S-(dicarbethoxyethyl)dithiophosphate, 95 % purity] and zolone [O,O-diethyl-S-(6-chloro-2-oxybenzoxazolin-3-ylmethyl)phosphorodithioate; 98 % purity] were used as standards in this investigation.

"Nanograde" methanol was purchased from Mallinckrodt; water was deionized, distilled, and finally redistilled from alkaline permanganate.

RESULTS AND DISCUSSION

Flame photometric detector

The FPD was nominally optimized in the phosphorus mode by independently varying the hydrogen, nitrogen and air flow-rates to obtain the maximum signal-to-noise ratio. The temperature of the central portion of the flame under optimum conditions was 400–450°C (measured with a thermocouple), when water was aspirated at 1 μ l/min. The optimum fuel-to-oxidant ratio was 3.7, which is comparable with that of the gas chromatographic detector of this type¹⁶. These results confirmed the work of Dagnall *et al.*¹⁷: the HPO species is formed most efficiently in a cool, highly reducing flame.

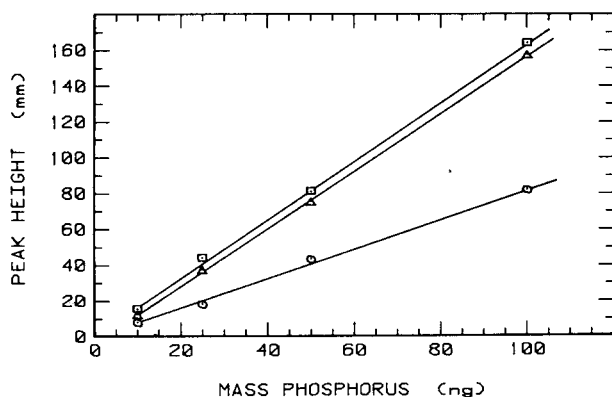


Fig. 3. Linearity of the flame photometric detector as a function of mobile phase composition. Column: 10-m octylsilane micro-column. Mobile phase: ○, pure water; □, 10% aqueous methanol; △, 25% aqueous methanol. Solute: trimethyl phosphate.

The effect of selected organic solvents on phosphorus emission was studied using trimethyl phosphate as a model solute. Methanol, ethanol, acetone and acetonitrile were added to the aqueous mobile phase in concentrations ranging from 0 to 50%. For moderate concentrations of alcohol or acetone, a slight enhancement in emission intensity was observed. As shown in Fig. 3, a twofold enhancement was achieved when 10% aqueous methanol was used as mobile phase. Methanol could be tolerated in concentrations up to 50% with no loss in signal intensity; however, the flame background was substantially increased. Similarly, ethanol and acetone provided small increases in analytical sensitivity, and could be tolerated in concentrations up to 40%. In contrast, acetonitrile severely quenched phosphorus emission and increased background noise even at very low concentrations (1–5%). Similar results were reported by Chester^{9,10} in an investigation of solvent effects on the inverted-flame FPD in conventional HPLC.

The increase in emission intensity in the presence of alcohols and acetone does not indicate that quenching of the type described by Julin *et al.*⁸ and Dagnall *et al.*¹⁷ does not occur in this detector. It merely suggests that vast improvement in other areas may overshadow any slight decrease in emission due to chemical quenching in the flame. The signal enhancement is most probably due to changes in the physical properties of the HPLC effluent, such as surface tension, viscosity, volatility and combustibility, which result in improved nebulization and desolvation.

The flame-based detector was able to accept in excess of 20 $\mu\text{l}/\text{min}$ of 10–25% aqueous methanol without extinction of the flame or production of luminous soot. The best response was obtained at flow-rates less than 5 $\mu\text{l}/\text{min}$, which is typical of open-tubular and packed capillary HPLC columns.

The detection limits were determined according to the method of McGuffin and Novotny¹⁴, with trimethyl phosphate as a model solute under non-retained conditions. The minimum detectable quantity was 2.0 ± 0.1 ng of phosphorus at a signal-to-noise (RMS) ratio of 5 (99.5% confidence level). This corresponds to a mass flux of 71 ± 3 pg/sec at the maximum of the Gaussian peak.

The linear range of this detector was determined for mobile phases containing

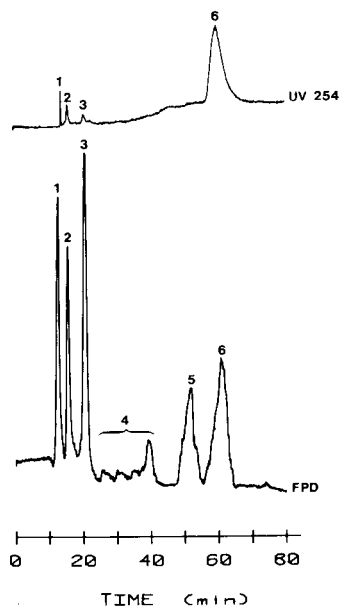


Fig. 4. Chromatogram of organophosphorus pesticides using the FPD. Column: 10-m octylsilane micro-column. Mobile phase: 42% aqueous methanol (50 atm). Peaks: 1 = solvent front; 2 = cygon (80 ng of phosphorus); 3 = DDVP (280 ng of phosphorus); 4 = phosphorus-containing impurities; 5 = malathion (230 ng of phosphorus); 6 = guthion (200 ng of phosphorus). UV detector range: 0.02.

pure water, 10% aqueous methanol and 25% aqueous methanol. The results summarized in Fig. 3 indicate that response is linear for all three solvent systems from the detection limit to at least 100 ng of phosphorus.

To illustrate the potential of the FPD, a mixture of four structurally diverse organophosphorus pesticides was separated on a short reversed-phase micro-column. The response of the FPD was compared with UV detection at 254 nm; the sensitivity of the UV detector was adjusted to give approximately the same signal-to-noise ratio as the FPD for the last peak (guthion). As shown in Fig. 4, the FPD exhibited good sensitivity and selectivity for all pesticides, and additionally revealed the presence of three phosphorus-containing impurities in the pesticide standards. In general, flame photometric detection was superior to UV detection whenever the molar absorptivity (ϵ) of the phosphorus-containing solute was less than 500 to 800 l/mol·cm at the wavelength of interest.

Although this investigation has been limited to the determination of organophosphorus compounds, flame-emission detection may also be utilized for sulfur, nitrogen, boron, and some organometallic species.

Thermionic detector

The dual-flame thermionic detector spatially separates the analytical measurement process from the fundamental flame processes, such as nebulization and desolvation. For this reason, higher concentrations of organic modifiers may be added to the mobile phase with less matrix interference. The thermionic detector has been

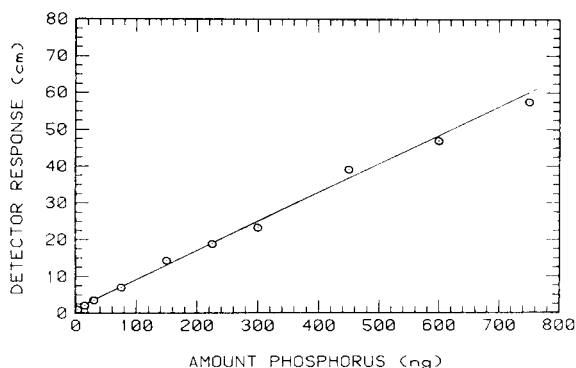


Fig. 5. Linearity of thermionic detector. Column: 10-m octylsilane micro-column. Mobile phase: methanol. Solute: trimethyl phosphate.

utilized with mobile phases containing 75 to 100% aqueous methanol; gradient elution is also feasible with minimal baseline drift. In addition, pump pulsations seem to have little, if any, effect on the detector response.

Although the device has not as yet been optimized, the sensitivity seems quite good. From preliminary experiments, the detection limit appears to be at least one, and possibly two, orders of magnitude less than that of the FPD. An injected quantity of 2 ng of phosphorus was clearly visible above the background noise [signal-to-noise (RMS) ratio > 30].

The linear dynamic range of the thermionic detector was investigated using

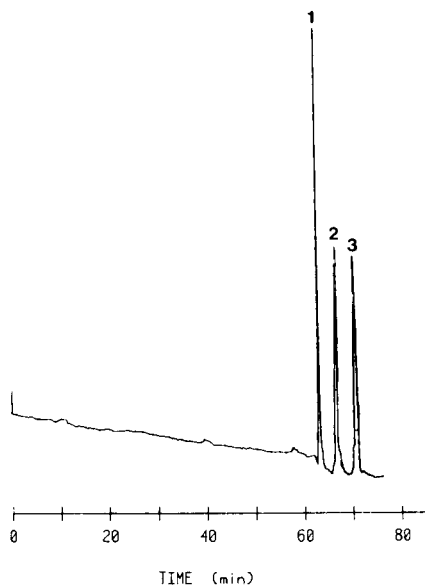


Fig. 6. Chromatogram of organophosphorus pesticides using thermionic detection. Column: 27-m octadecylsilane micro-column. Mobile phase: 85% aqueous methanol (120 atm). Peaks: 1 = guthion (97 ng of phosphorus); 2 = zolone (87 ng of phosphorus); 3 = ethion (130 ng of phosphorus). Detector range: 16×1 .

trimethyl phosphate as a model solute and methanol as mobile phase. As shown in Fig. 5, the device was linear from 2 ng up to at least 750 ng of phosphorus injected.

To demonstrate the potential of the thermionic detector, several of the more strongly retained organophosphorus pesticides were chromatographed on an octadecylsilane capillary column, with 85% aqueous methanol as mobile phase. The high sensitivity and low background noise characteristic of the dual-flame thermionic detector are illustrated in Fig. 6; guthion, zolone and ethion were easily detected in amounts ranging from 87 to 130 ng of phosphorus.

In these preliminary investigations, the thermionic detector has been utilized primarily for the determination of organophosphorus compounds; however, selectivity has also been demonstrated for some nitrogen-containing compounds, such as caffeine and pyrazine.

CONCLUSION

A novel flame-based detector has been developed, which benefits highly from the reduced flow-rates of capillary HPLC columns. The total micro-column effluent is nebulized and aspirated directly into a hydrogen-air diffusion flame. Solutes may then be selectively detected by their characteristic optical emission or secondary-ionization phenomena.

The total-consumption burner utilized in this investigation provides efficient use of the small samples and low flow-rates associated with capillary column HPLC. In addition, it ensures that a representative fraction of the effluent reaches the flame; thus, no pre-concentration of volatile solutes or solvents occurs, as it might with separate, heated nebulizer chambers. Another advantage is the very small dead volume of this design; the end of the capillary column may be inserted directly into the flame. Although this investigation has been limited to packed capillaries, the detectors should also be compatible with open-tubular columns, provided that chemically bonded stationary phases are utilized.

The FPD and the thermionic detector exhibit high selectivity and good sensitivity for organophosphorus compounds. Moreover, the detectors permit the use of a wide range of organic mobile-phase concentrations; thus, sufficient variety is available to design chromatographic systems that will accomplish useful separations.

The selective detection of nitrogen-containing compounds will be the desirable extension of this research. Potential applications include the determination of nitrogen-containing drugs and their metabolites in physiological fluids, the detection of polynuclear heteroaromatic compounds in energy-related samples, and the determination of alkaloids in plant material. A more thorough characterization and optimization of the thermionic detector will be necessary before routine application is possible.

ACKNOWLEDGEMENT

This research was supported by the National Institute of Health, Grant No. PHS R01 GM 24349.

REFERENCES

- 1 G. Guiochon, *J. Chromatogr.*, 185 (1979) 3.
- 2 J. H. Knox and M. T. Gilbert, *J. Chromatogr.*, 186 (1979) 405.
- 3 Y. Hirata, M. Novotny, T. Tsuda and D. Ishii, *Anal. Chem.*, 51 (1979) 1807.
- 4 Y. Hirata and M. Novotný, *J. Chromatogr.*, 186 (1979) 521.
- 5 Y. Hirata, P. T. Lin, M. Novotný and R. M. Wightman, *J. Chromatogr.*, 181 (1980) 287.
- 6 J. D. Henion and G. A. Maylin, *Biomed. Mass Spectrom.*, 7 (1980) 115.
- 7 J. D. Henion, *J. Chromatogr. Sci.*, 19 (1981) 57.
- 8 B. G. Julin, H. W. Vandeborn and J. J. Kirkland, *J. Chromatogr.*, 112 (1975) 443.
- 9 T. L. Chester, *Anal. Chem.*, 52 (1980) 638.
- 10 T. L. Chester, *Anal. Chem.*, 52 (1980) 1621.
- 11 R. P. W. Scott, *Liquid Chromatography Detectors*, Elsevier Scientific Publishing Co., New York, 1977.
- 12 K. Šlais and M. Krejčí, *J. Chromatogr.*, 91 (1974) 181.
- 13 B. J. Compton and W. C. Purdy, *J. Chromatogr.*, 169 (1979) 39.
- 14 V. L. McGuffin and M. Novotny, *Anal. Chem.*, 53 (1981) 947.
- 15 J. A. Lubkowitz, B. P. Semonian, J. Galobardes and L. B. Rogers, *Anal. Chem.*, 50 (1978) 673.
- 16 S. S. Brody and J. E. Chaney, *J. Gas Chromatogr.*, 4 (1966) 42.
- 17 R. M. Dagnall, K. C. Thompson and T. S. West, *Analyst (London)*, 93 (1968) 72.

CHROM. 14,043

STUDY OF THE PERFORMANCE OF CATION-EXCHANGE COLUMNS IN OPEN-TUBULAR MICROCAPILLARY LIQUID CHROMATOGRAPHY

DAIDO ISHII* and TOYOHIDE TAKEUCHI

Department of Applied Chemistry, Faculty of Engineering, Nagoya University, Chikusa-ku, Nagoya-shi 464 (Japan)

SUMMARY

Aromatic and aliphatic cation-exchange columns have been prepared for open-tubular microcapillary liquid chromatography. The performance of these columns was evaluated by using a UV spectrophotometer as the detector and nucleosides as samples. The dependence of solute retention on the pH and salt concentration of the mobile phase or column temperature was examined. A difference in selectivity between aromatic and aliphatic cation-exchange columns was observed, and is ascribed to the difference in matrices. The ion-exchange capacity per unit column length was about $2 \cdot 10^{-8}$ equiv./m.

INTRODUCTION

During the last five years a number of studies of the use of small-bore columns in high-performance liquid chromatography (HPLC) have been published. The consumption of both solvents and packing was found to be reduced and the low flow-rates facilitated the direct combination to a mass spectrometer.

Open-tubular microcapillary columns have also been observed to have higher efficiencies in terms of theoretical plate numbers compared with conventional HPLC columns. We have prepared various types of open-tubular microcapillary columns and examined their chromatographic performances: columns physically coated with silicone grease¹, β,β' -oxydipropionitrile² and polyethylene glycols²; solid columns^{3,4}; chemically bonded octadecylsilane columns^{5,6} and polystyrene columns⁷. Good results were obtained on the various columns and the applicability of the columns was substantiated. The results were also supported theoretically by Knox and co-workers^{8,9}.

The theoretical plate height (H or HETP) was determined from the equation proposed by Golay¹⁰

$$H = \frac{2D_m}{u} + \frac{(11k'^2 + 6k' + 1) d_c^2}{96 (1 + k')^2 D_m} \cdot u + \frac{2k' d^2}{3 (1 + k')^2 D_s} \cdot u \quad (1)$$

where D_m and D_s are the diffusion coefficients of a solute in the mobile and the

stationary phase, u is the linear velocity of the mobile phase, k' is the capacity factor, d_c is the column diameter and d is the thickness (or depth) of the stationary phase, respectively. Eqn. 1 indicates that d_c and d should be minimized in order to attain a low H value. Since the contribution of the first term in eqn. 1 (a longitudinal diffusion term) is usually small, the desired chromatographic system is one which results in large D_m and D_s values.

We have found² that the contribution of the mass transfer resistance in the mobile phase (the second term in eqn. 1) to H was predominant for physically coated columns of 30–60 μm I.D. Thus, the stationary phase can be considered to exist as a thin layer having low resistance to mass transfer.

The above results encouraged us to develop narrower-bore and/or longer columns which can generate larger numbers of theoretical plates. However, it is difficult to prepare columns having such dimensions, especially chemically bonded columns.

Recently, a preparation technique for chemically bonded stationary phase has been developed and chemically bonded octadecylsilane (ODS) columns (5–20 m \times 30–50 μm I.D.) were prepared⁶. The conditions, such as temperature of pre-treatment with an alkaline solution, reaction temperature and time and diluents of silane reagents, were examined in detail. The reactions between silane reagents and silanol groups were promoted by heating for longer than 4 h at 150°C. In the case of the above ODS columns, the contribution of mass transfer resistance in the mobile phase was predominant. Thus, it is expected that narrower-bore columns can be prepared.

This method can be applied to the preparation of various kinds of stationary phases, and we now describe the preparation of chemically bonded cation-exchange columns. Both aromatic and aliphatic cation-exchange columns have been prepared and some parameters which affect solute retention have been examined. The use of aliphatic cation-exchange columns in HPLC has previously been reported^{11,12}.

EXPERIMENTAL

The reagents were purchased from Wako (Osaka, Japan), unless noted otherwise.

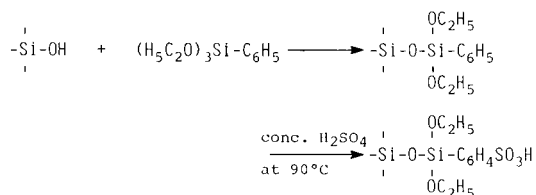
A liquid chromatograph was assembled from a micro feeder (Azumadenki Kogyo, Tokyo, Japan) and a gas-tight syringe as a pump, a UV spectrophotometer UVIDEC-100 (Japan Spectroscopic, Tokyo, Japan) with a modified flow cell and a home-made column oven comprising an asbestos board equipped with a heater and a fan. The temperature was adjusted by a slide rheostat which altered the applied voltage.

Soda-lime glass capillary tubing (30–60 μm I.D.) was prepared with a glass drawing machine, as described previously², and treated with a 1 *N* sodium hydroxide aqueous solution at 20–50°C for 2 days. Subsequent to pre-treatment, the capillary tubings were washed with pure methanol or hydrochloric acid or with a mixture of these compounds and then dried in a stream of helium at 120°C for 5 h. The capillary was filled with a toluene solution of phenyltriethoxysilane or 2-mercaptoethyltriethoxysilane (Tokyo Chemical Industry, Tokyo, Japan) and the reaction was promoted at elevated temperature (*ca.* 140°C). Alternatively, the capillary was coated with a 20% (v/v) phenyltriethoxysilane solution in dichloromethane by the dynamic coating method, as previously reported^{1,2,5}. Solvents employed were dried on a column

packed with 4-Å molecular sieves (8–12 mesh; Yoneyama Yakuhin kogyo, Osaka, Japan). Ion-exchange groups were introduced into the capillaries by treatment with concentrated sulphuric acid at 90°C for 4 h (for phenylsilyl groups) or with 1 *N* sulphuric acid containing 2% (w/w) potassium permanganate at room temperature (for 2-mercaptoethylsilyl groups). After the reaction, the columns were washed with deionized water in the former case and with 0.1 *M* oxalic acid and deionized water in the latter case.

Reaction models are given in Fig. 1. Silane reagents are shown as reacting mono-functionally with silanol groups, but in practice, some reagents react bi-functionally.

(A) Aromatic cation-exchange column



(B) Aliphatic cation-exchange column

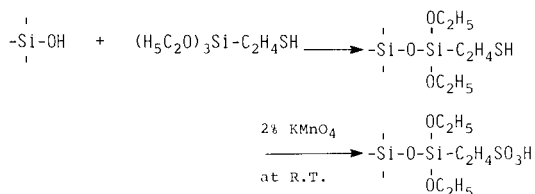


Fig. 1. Reaction models for cation-exchange columns.

A support coated open-tubular column was also prepared in order to compare the properties of the chemically bonded stationary phases with commercially available packings, *e.g.*, Shodex 125S (sodium polystyrene sulphonate, 12.5 μm ; Showa Denko K.K., Tokyo, Japan). A soda-lime capillary, which had previously been treated with an alkaline solution, was filled with an aqueous suspension of the packing material (ground to particles less than 1 μm). It was then heated at a rate of 4°C/min from 30 to 130°C before being kept at 130°C overnight. Finally, the capillary was washed with deionized water.

Ion-exchange capacities were measured by the following method. A sodium chloride solution (0.1 *M*, 50–100 μl) was passed through the prepared cation-exchange column (H^+) converting it completely into the sodium form. The effluent contained hydrochloric acid in an amount equivalent to the capacity of the column, which was then determined by titration with sodium hydroxide solution (10^{-3} *M*).

The performance of cation-exchange columns was estimated by employing nucleosides (Kohjin, Tokyo, Japan) as test samples and formic acid–ammonium formate as the mobile phase. The pH of the mobile phase was adjusted with formic acid.

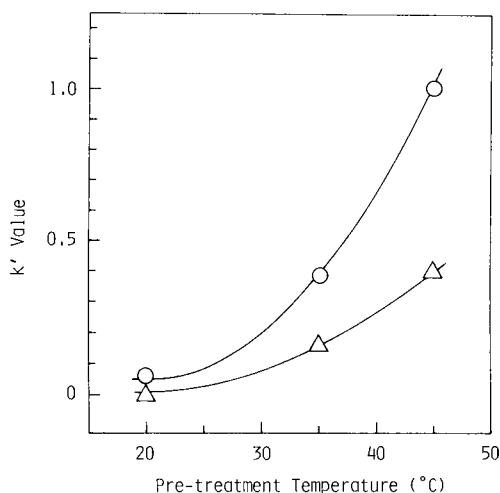


Fig. 2. Effect of pre-treatment temperature on retention for phenylsilane column. Stationary phase: phenylsilane, reacted for 15 h at 170°C. Mobile phase: acetonitrile–water (2:8 v/v). Samples: Δ , naphthalene; \circ , biphenyl.

RESULTS AND DISCUSSION

The treatment of soda-lime glass capillaries with a 1 *N* sodium hydroxide aqueous solution effectively increases their surface areas. Fig. 2 shows the effect of pre-treatment temperature on solutes retention for a phenylsilane column. In this case, a 20% silane solution in dichloromethane was coated by the dynamic coating method, as described earlier⁵. The retention of solutes increases with increasing pre-treatment temperature, *i.e.*, more phenylsilyl groups are introduced on the glass surface at higher temperatures.

Tables I and II show the variations of solute retention with sulphonation for the aromatic and aliphatic cation-exchange columns, respectively. On both cation-exchange columns, retention of aromatic hydrocarbons decreased after sulphonation, while that of nucleosides increased. This is ascribed to the decrease of hydrophobicity, which results in the introduction of ion-exchange groups. Nucleosides were

TABLE I

VARIATION OF SOLUTE RETENTION WITH SULPHONATION ON THE AROMATIC CATION-EXCHANGE COLUMN

Mobile phase	Solute	k'	
		$-C_6H_5$	$C_6H_4SO_3H$
Acetonitrile–water (3:7)	Biphenyl	0.35	0
	Pyrene	0.69	0
$2 \cdot 10^{-3}$ M	Uridine	0	0
Ammonium formate, pH 2.7	Guanosine	0	0.06
	Adenosine	0.08	0.46
	Cytidine	0.19	0.43

TABLE II

VARIATION OF SOLUTE RETENTION WITH SULPHONATION ON THE ALIPHATIC CATION-EXCHANGE COLUMN

Mobile phase	Solute	k'	
		$-C_2H_4SH$	$-C_2H_4SO_3H$
Acetonitrile-water (2:8 v/v)	Biphenyl	0.25	—
	Pyrene	0.80	0.18
1×10^{-3} M Ammonium formate, pH = 3.4	Uridine	0	0
	Guanosine	0.03	0.06
	Adenosine	0.26	0.93
	Cytidine	0.19	0.98

retained on phenylsilane and 2-mercaptoethylsilane columns, leading to a difference in selectivity between the aromatic and aliphatic cation-exchange columns.

In ion-exchange HPLC, solute retention depends on various parameters such as the pH and the ionic strength of the mobile phase, concentration of organic solvent, column temperature, etc. Fig. 3A and 3B illustrates the influence of pH of the mobile phase on solute retention for support coated and chemically bonded aromatic cation-exchange columns, respectively. Similar pH dependences were observed, confirming that the chemically bonded columns possessed ion-exchange properties. The k' values and elution order of adenosine and cytidine were sensitive to pH, while the retention of guanosine increased gradually with decreasing pH. However, uridine was not retained. Four nucleosides could be separated at low pH (*e.g.*, 2.2).

Fig. 3C illustrates the dependence of solute retention on pH of the mobile phase for the aliphatic cation-exchange column. The behaviour of adenosine and cytidine was different from that on the aromatic cation-exchange columns. The two

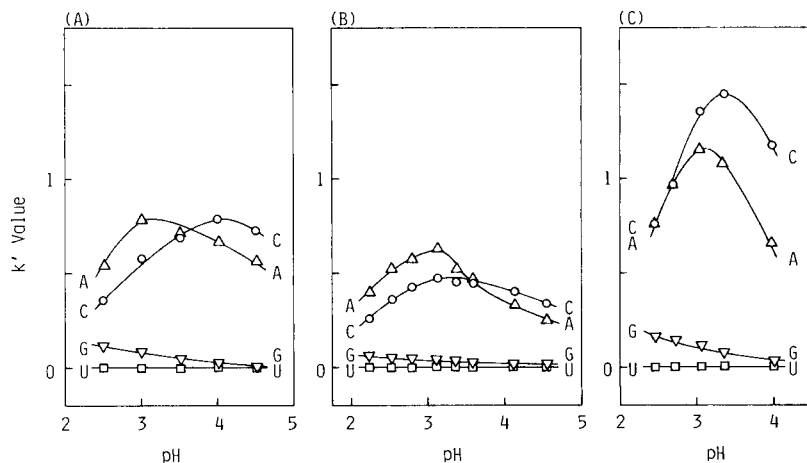


Fig. 3. k' values as a function of pH of the mobile phase. Columns: A, coated with Shodex HC-125S R- SO_3Na ; B, chemically bonded aromatic column, $-C_6H_4SO_3H$; C, chemically bonded aliphatic column, $-C_2H_4SO_3H$. Mobile phases: ammonium formate, 5×10^{-3} M (A) or 2×10^{-3} M (B and C). Sample: U = uridine; G = guanosine; C = cytidine; A = adenosine.

nucleosides could not be separated at low pH (less than 3), but they could be separated at pH *ca.* 3.5. This difference in selectivity between the two kinds of stationary phases may be due to difference in the matrices.

Fig. 4 shows the effect of the concentration of a salt on the retention of cytidine. The smaller the salt concentration the larger is the k' value obtained, which is consistent with the results of conventional ion-exchange chromatography.

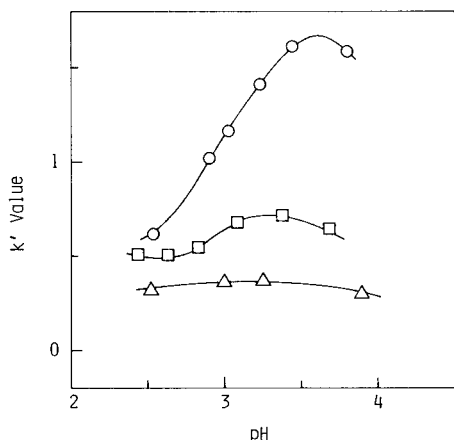


Fig. 4. k' value of cytidine as a function of the pH and ionic strength of the mobile phase on the aliphatic cation-exchange column (5.3 m \times 52 μ m I.D.). Mobile phases: ammonium formate, $1 \cdot 10^{-3} M$ (\circ), $5 \cdot 10^{-3} M$ (\square), $1 \cdot 10^{-2} M$ (\triangle). The pH was adjusted with formic acid.

Typical chromatograms obtained with chemically bonded cation-exchange capillary columns are shown in Fig. 5. Operating conditions were selected according to the above observations. Four nucleosides are satisfactorily separated on both columns. The peak shapes are symmetrical on the aliphatic cation-exchange column, but slight tailing is observed on the aromatic cation-exchange column.

The diffusion coefficients of solutes in the mobile phases employed in ion-exchange chromatography are small. Thus, it is preferable to operate at higher temperatures. In general, the column temperature affects both the column efficiency and solute retention. Fig. 6 shows the effect of column temperature on both parameters. For the non-retained solute (uridine), theoretical plate numbers increased with increasing temperature, whereas those for cytidine decreased at 75°C. The chromatographic peaks observed at higher temperature had pronounced leading edges for retained solutes, resulting in poor efficiency. The k' value of cytidine decreased with increasing column temperature and plots of k' value on a logarithm scale against reciprocal of absolute temperature were linear.

Baseline separation of nucleosides was achieved at 43°C, as shown in Fig. 7.

Eqn. 1 indicates that a lower H value can be attained with a smaller-bore capillary column. Fig. 8 shows the relationship between linear velocity, u , and HETP obtained with columns of different bores. Lower H values and lower slopes of the plots are observed for the smaller-bore column, in agreement with the preceding discussion.

The ion-exchange capacity is a significant characteristic of ion-exchange chro-

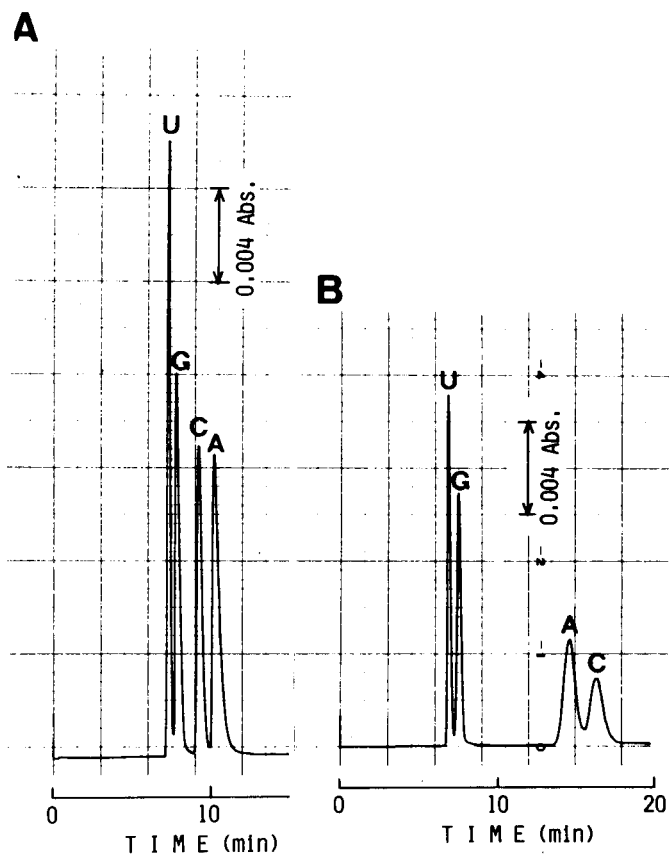


Fig. 5. Separations of nucleosides on cation-exchange columns at room temperature (*ca.* 20°C). Columns: A, 5.2 m \times 44 μ m I.D., $-\text{C}_6\text{H}_4\text{SO}_3\text{H}$; B, 5.3 m \times 52 μ m I.D., $-\text{C}_2\text{H}_4\text{SO}_3\text{H}$. Mobile phases: ammonium formate, $2 \cdot 10^{-3}$ M, pH 2.2 (A); $1 \cdot 10^{-3}$ M, pH 3.4 (B). Flow-rate: 1.1 μ l/min (A); 1.7 μ l/min (B). Sample: 12 ng uridine; 12 ng guanosine; 13 ng cytidine; 11 ng adenosine. Wavelength of UV detection: 260 nm.

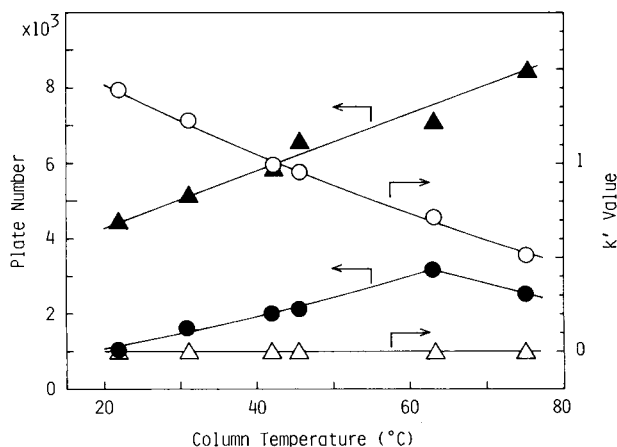


Fig. 6. Effect of column temperature on column efficiency and retention of nucleosides. Column: 5.1 m \times 46 μ m I.D., aliphatic cation-exchange. Mobile phase: $1 \cdot 10^{-3}$ M ammonium formate, pH 3.4; flow-rate 1.7 μ l/min. Samples: \triangle , \blacktriangle , uridine; \circ , \bullet , cytidine.

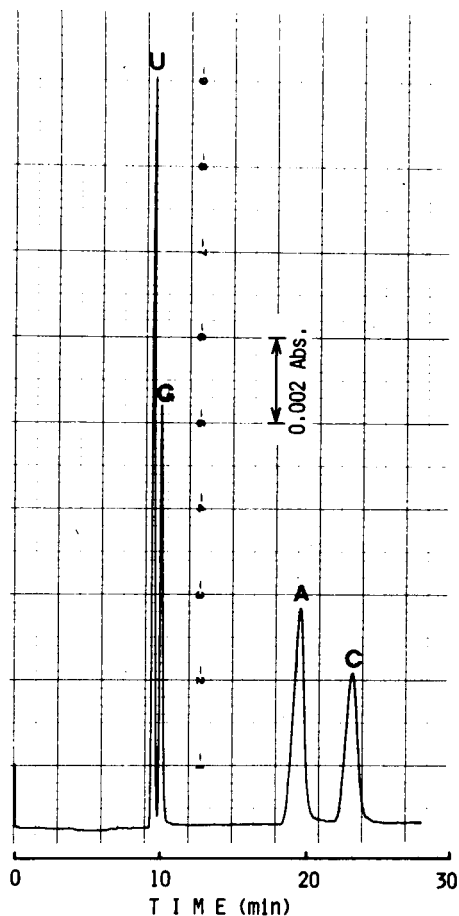


Fig. 7. Separation of nucleosides at 43°C, on the aliphatic cation-exchange column (6.0 m \times 39 μ m I.D.). Mobile phase: $2 \cdot 10^{-3}$ M ammonium formate, pH 3.4; flow-rate 0.83 μ l/min. Sample: 6.9 ng uridine; 6.8 ng guanosine; 6.2 ng adenosine; 9.0 ng cytidine; eluted in that order. Wavelength of UV detection: 260 nm.

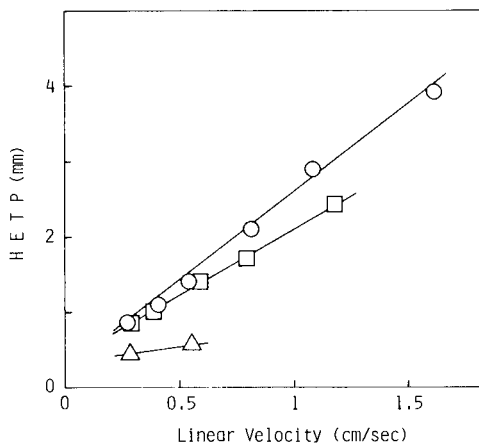


Fig. 8. Relationship between linear velocity and HETP. Columns ($-C_2H_4SO_3H$): O, 4.2 m \times 47 μ m I.D.; □, 6.0 m \times 39 μ m I.D.; Δ, 5.8 m \times 33 μ m I.D. Sample: cytidine; k' 1.5 (O), 1.2 (□), 1.2 (Δ).

matography. Commercial ion-exchangers possess 2–5000 μ equiv./g of ion-exchange capacity, depending upon the porosity and type of matrix. The cation-exchange capacities of some capillary columns prepared in this work are shown in Table III: $1 \cdot 10^{-8}$ – $2 \cdot 10^{-8}$ equiv./m of cation-exchange capacity is obtained. For the second column the total cation-exchange capacity of $7.2 \cdot 10^{-8}$ equiv. corresponds to the number of sulphonic groups, $4.3 \cdot 10^{16}$, and the density of ion-exchange groups is calculated to be $7.3 \cdot 10^{15}$ groups per cm^2 when the glass surface is assumed to be bare (or smooth). Since it is accepted that there are $4 \cdot 10^{14}$ – $8 \cdot 10^{14}$ silanol groups per cm^2 on silica gel, at most $4 \cdot 10^{14}$ – $8 \cdot 10^{14}$ ion-exchange groups can be introduced of surface per cm^2 .

The above results indicate that the second capillary column in Table III

TALBE III

CATION-EXCHANGE CAPACITIES

Capillaries were treated with 1 *N* sodium hydroxide aqueous solution for 2 days.

Pre-treatment temperature (°C)	Stationary phase	I.D. (μm)	Length (m)	Volume (μl)	Ion-exchange capacity		
					Total (equiv.)	Per unit volume (equiv./μl)	Per unit length (equiv./m)
35	-C ₆ H ₄ SO ₃ H	60	5.35	15.1	8.0×10^{-8}	5.3×10^{-9}	1.5×10^{-8}
50	-C ₂ H ₄ SO ₃ H	45	4.18	6.6	7.2×10^{-8}	1.1×10^{-8}	1.7×10^{-8}
48	-C ₂ H ₄ SO ₃ H	39	6.02	7.2	6.6×10^{-8}	9.2×10^{-9}	1.1×10^{-8}

possesses a larger surface area than that of bare glass, due to the pre-treatment with an alkaline solution: the surface area increased by a factor of at least 9–18 upon treatment with a 1 *N* sodium hydroxide aqueous solution for 2 days at 50°C.

CONCLUSION

Cation-exchange capillary columns prepared in this work showed similar characteristics to conventional ion-exchange columns. A difference in selectivity between aromatic and aliphatic cation-exchange columns was observed, which would serve to improve resolution. Operation at higher temperatures gave better results.

REFERENCES

- 1 K. Hibi, D. Ishii, I. Fujishima, T. Takeuchi and T. Nakanishi, *J. High Resolut. Chromatogr. Commun.*, 1 (1978) 21.
- 2 K. Hibi, T. Tsuda, T. Takeuchi, T. Nakanishi and D. Ishii, *J. Chromatogr.*, 175 (1979) 105.
- 3 D. Ishii, T. Tsuda and T. Takeuchi, *J. Chromatogr.*, 185 (1979) 73.
- 4 K. Hibi, D. Ishii and T. Tsuda, *J. Chromatogr.*, 189 (1980) 179.
- 5 T. Tsuda, K. Hibi, T. Nakanishi, T. Takeuchi and D. Ishii, *J. Chromatogr.*, 158 (1978) 227.
- 6 D. Ishii and T. Takeuchi, *International Symposium on Capillary Chromatography, May 3–7, 1981, Hindelang*.
- 7 T. Takeuchi, K. Matsuoka, Y. Watanabe and D. Ishii, *J. Chromatogr.*, 192 (1980) 127.
- 8 J. H. Knox and M. T. Gilbert, *J. Chromatogr.*, 186 (1979) 405.
- 9 J. H. Knox, *J. Chromatogr. Sci.*, 18 (1980) 453.
- 10 M. J. E. Golay, in D. H. Desty (Editor), *Gas Chromatography 1958*, Butterworths, London, 1958, p. 36.
- 11 B. B. Wheales, *J. Chromatogr.*, 177 (1979) 263.
- 12 B. B. Wheales, *J. Chromatogr.*, 187 (1980) 65.

CHROM. 14,070

APPLICATION OF ULTRA-MICRO HIGH-PERFORMANCE LIQUID CHROMATOGRAPHY TO TRACE ANALYSIS

TOYOHIDE TAKEUCHI* and DAIDO ISHII

Department of Applied Chemistry, Faculty of Engineering, Nagoya University, Chikusa-ku, Nagoya-shi 464 (Japan)

SUMMARY

A pre-column concentration technique in ultra-micro high-performance liquid chromatography has been developed and applied to trace analysis. The micro pre-columns are composed of PTFE tubing ($3\text{--}12 \times 0.1\text{--}0.2$ mm I.D.) packed with commercially available materials. Components in water or samples are collected in a micro pre-column and then separated on ultra-micro packed columns (*ca.* $10\text{ cm} \times 0.12$ mm I.D.). Polynuclear aromatic hydrocarbons, phthalates and corticosteroids can be separated on these columns, in spite of the small dimensions. Phthalates in water and corticosteroids in serum have been determined by this technique.

INTRODUCTION

The use of micro-bore columns in high-performance liquid chromatography (HPLC) has several advantages: (1) consumption of the mobile phase, which is sometimes toxic, is low; (2) the amounts of packing materials can be reduced; (3) the amounts of sample required for analysis are small, which is especially favourable *in vivo*; (4) the low flow-rate of the mobile phase facilitates the direct combination of a liquid chromatograph with a mass spectrometer.

Ishii and co-workers have developed micro-HPLC¹ and examined various modes of chromatography with columns of $3\text{--}20\text{ cm} \times 0.5$ mm I.D.^{2–7}. The internal volume of these columns was one-hundredth that of conventional HPLC columns. Since solute band broadening in a micro-HPLC column is small, solutes can be detected sensitively.

We have recently developed ultra-micro-HPLC and examined the parameters which affect the column efficiency⁸. Pyrex glass columns gave the highest efficiencies and satisfactory separations of aromatic hydrocarbons were obtained with columns of $3\text{--}10\text{ cm} \times 0.12$ mm I.D. The dimensions of columns employed in ultra-micro-HPLC are about one-tenth of those of micro-HPLC and one-thousandth of those of conventional HPLC. The sensitivity increased by a factor of ten compared with that in micro-HPLC and the consumption of the mobile phase could be markedly reduced.

In ultra-micro-HPLC the amounts of sample injected should be as small as

possible (around $0.02\ \mu\text{l}$). Thus, the pre-treatment of a sample prior to injection is indispensable in the case of the analysis of constituents existing in dilute solutions.

The micro pre-column method was useful for the analysis of samples *in vivo*, as previously reported⁴. The pre-columns were composed of PTFE tubing (1–3 cm \times 0.5 mm I.D.). The samples were first placed on the micro pre-column and then required solutes eluted by a mobile phase. The solutes were then loaded onto a separation column.

We now describe the use of the micro pre-column method in ultra-micro-HPLC, and the application of this technique to trace analysis.

EXPERIMENTAL

The apparatus employed was nearly the same as described previously⁸. Pyrex glass tubing was selected as the column material since a pyrex glass column gave the highest efficiency of all the materials examined.

The micro pre-column was composed of PTFE tubing (0.1–0.2 mm I.D.) packed with commercially available packings. After the concentration step, the pre-column was connected to a separation column by stainless-steel tubing (3–5 \times 0.13 mm I.D.), as shown in Fig. 1. For the analysis of corticosteroids, the pre-column was freed from water using an Hitachi rotary oil vacuum pump (Hitachi, Tokyo, Japan).

Both separation and collection columns were packed with commercially available packing materials: silica ODS SC-01 (5 μm ; Japan Spectroscopic, Hachioji-shi, Japan); Develosil ODS (3, 5 and 10 μm ; Nomura Chemical, Setoshi, Japan); porous polymer Hitachi GEL No. 3011 (12 μm , Hitachi) and Nucleosil NH₂ (10 μm). The preparation of these micro-bore columns was as described previously⁸.

The sample solution was passed into a pre-column by one of two methods: (1) manual feeding using a gas-tight syringe (1 ml) or (2) feeding via a glass pipe (*ca.* 0.3 mm I.D.) and nitrogen pressure (*ca.* 20 atm). The gas-tight syringe and glass pipe were carefully washed with organic solvents and distilled water prior to use, otherwise solutes were sometimes adsorbed on the vessel walls. For a micro pre-column (5 \times 0.2 mm I.D.) packed with 10- μm materials, 5–20 min were required to pass 1 ml of an aqueous solution. The performance of the pre-columns was examined with polynuclear aromatic hydrocarbons and phthalates as samples.

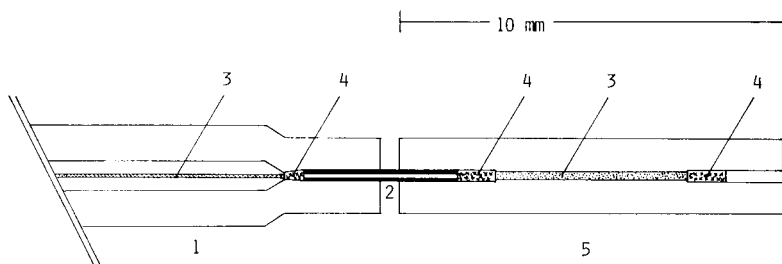


Fig. 1. Schematic diagram of a micro pre-column and the inlet of a separation column. 1 = Separation column; 2 = stainless-steel tubing (3–5 \times 0.13 mm I.D.); 3 = packing; 4 = quartz wool; 5 = micro pre-column.

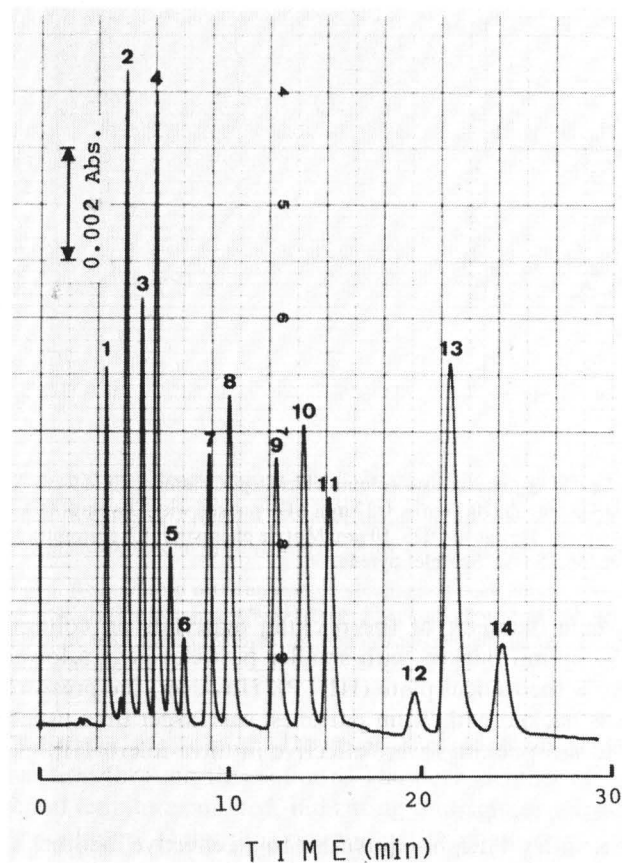


Fig. 2. Separation of aromatic hydrocarbons on an ultra-micro column (10.1 cm \times 0.12 mm I.D. Pyrex glass capillary) packed with silica ODS SC-01. Mobile phase: acetonitrile-water (65:35); flow-rate 0.83 μ l/min. Sample: 1 = 130 ng benzene; 2 = 11 ng naphthalene; 3 = 2.4 ng biphenyl; 4 = 3.4 ng fluorene; 5 = 0.6 ng phenanthrene; 6 = 0.4 ng anthracene; 7 = 3.4 ng fluoranthene; 8 = 3.4 ng pyrene; 9 = 3.4 ng *p*-terphenyl; 10 = 1.0 ng chrysene; 11 = 1.3 ng 9-phenylanthracene; 12 = 1.0 ng perylene; 13 = 4.1 ng 1,3,5-triphenylbenzene; 14 = 1.1 ng 3,4-benzopyrene. Wavelength of UV detection: 254 nm.

All reagents were purchased from Wako (Osaka, Japan) or Tokyo Chemical Industry (Tokyo, Japan). Horse serum was filtered through a membrane filter (0.45 μ m) prior to use.

RESULTS AND DISCUSSION

Performance of ultra-micro columns

Despite the fact that the internal volume of an ultra-micro column (10 cm \times 0.12 mm I.D.) is only about 1 μ l, sufficient separability is observed. Fig. 2 illustrates the separation of polynuclear aromatic hydrocarbons. Solute amounts less than 1 ng can be detected since there is little spreading through the column; solute band broadening is only 0.3–1.5 μ l.

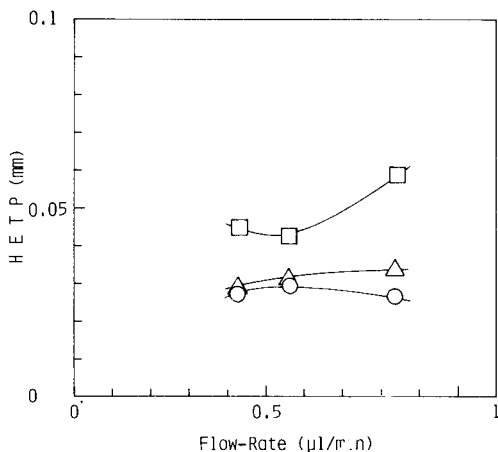


Fig. 3. Influence of particle diameter of packing materials on column efficiency. Columns: ○, 4.9 cm × 0.12 mm I.D., packed with Develosil ODS, 3 μm; △, 10.1 cm × 0.12 mm I.D., packed with Develosil ODS, 5 μm; □, 10.1 cm × 0.12 mm I.D., packed with Develosil ODS, 10 μm. Mobile phases: ○, □, acetonitrile–water (60:40 v/v); △, acetonitrile–water (65:35 v/v). Sample: pyrene.

The influence of the particle diameter of the packing materials on column efficiency is shown in Fig. 3. A column packed with smaller particles gave a lower value of the height equivalent to a theoretical plate (HETP). However, the pressure drop over the column, which was packed with 3-μm particles, was larger than usual. Thus, columns packed with 5–10 μm packings were effective in ultra-micro-HPLC.

Examination of the micro pre-column method

The effect of pre-column length on height equivalent to an effective theoretical plate (HEETP) was examined using SC-01 as the packing for both the separation and collection columns. Fig. 4 shows that a slightly lower HEETP value was observed for

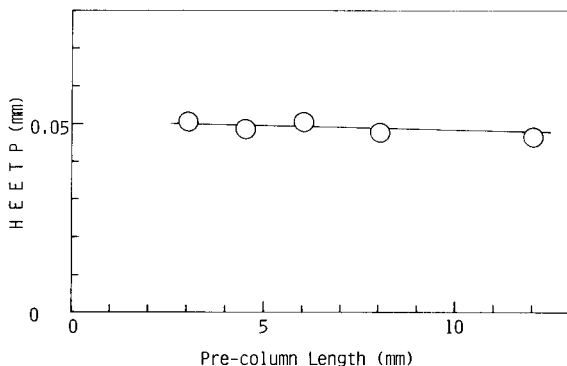


Fig. 4. Effect of pre-column length on column efficiency. Column: 10.1 cm × 0.12 mm I.D. packed with SC-01. Pre-column: 0.15 mm I.D., packed with SC-01. Mobile phase: acetonitrile–water (65:35); flow-rate 0.83 μl/min. Sample: 58 ppb anthracene in distilled water; volume 10 μl. Wavelength of UV detection: 254 nm.

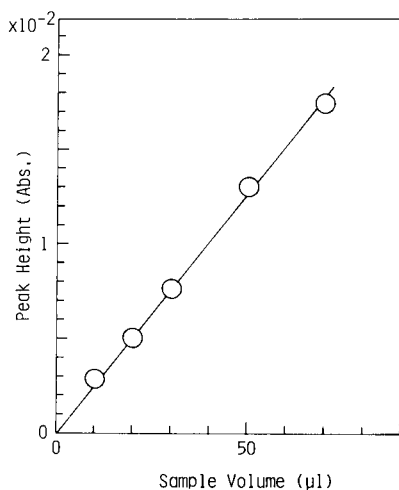


Fig. 5. Relationship between sample volume and peak height. Pre-column: 4×0.15 mm I.D. Sample: 42 ppb phenanthrene in distilled water. Other operating conditions as in Fig. 4.

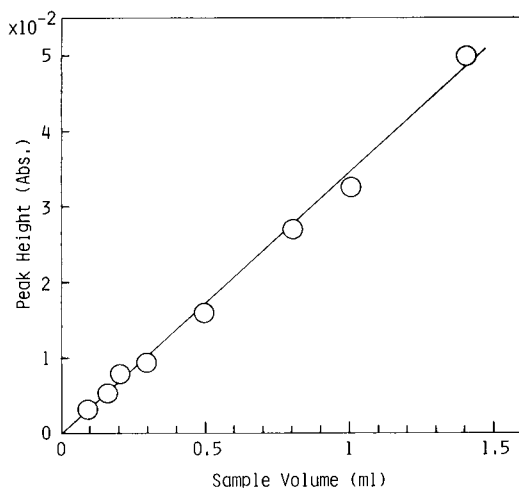


Fig. 6. Relationship between sample volume and peak height. Column: 10.1 cm \times 0.12 mm I.D., packed with SC-01. Pre-column: 4×0.15 mm I.D., packed with SC-01. Mobile phase: acetonitrile-water (65:35); flow-rate 0.83 μ l/min. Sample: 20 ppb diisopropyl phthalate in distilled water. Wavelength of UV detection: 230 nm.

the longer pre-column. However, too much time was required to pass an aqueous solution through this column. The peak heights of solutes were similar for the different lengths examined, indicating that solutes were collected completely in a micro pre-column. Thus, pre-columns with dimensions of 4–6 \times 0.1–0.2 mm I.D. were selected for the following studies; the internal volume was 0.03–0.19 μ l.

Fig. 5 shows the relationship between sample volume and peak height, which is linear in the range 10–70 μ l. A linear relation was also observed in the range 0.1–1.4 ml, Fig. 6. In the former case 0.42–2.9 ng phenanthrene and in the latter case 2–28 ng diisopropyl phthalate were collected, respectively. In addition, similar HEETP values were obtained, independent of sample volume.

Fig. 7 shows the relationship between sample concentration and peak height, which is linear in the range 0.02–0.88 ppm. The samples were prepared in acetonitrile–water (20:80). The effect of sample concentration on the column efficiency was negligible, as illustrated in Fig. 7. A linear relationship between sample concentration and peak height was obtained at low concentrations (1–20 ppb*), Fig. 8.

For dilute sample solutions, the problem of adsorption of solutes on the vessel walls is serious. Ogan *et al.*⁹ found that adsorption could be reduced by treating glass walls with dimethyldichlorosilane. In contrast, we found that addition of 1 ppm of ethylene glycol to a sample solution was sufficient to reduce adsorption of phthalates.

The non-zero intercept in Fig. 8 indicates that di-*n*-butyl phthalate is present as an impurity in distilled water and/or ethylene glycol. Unfortunately, di-*n*-butyl

* Throughout this article, the American billion (10^9) is meant.

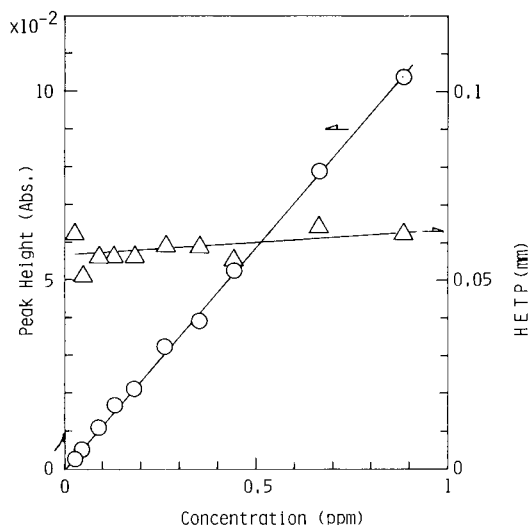


Fig. 7. Dependence of peak height and column efficiency on sample concentration. Sample: phenanthrene in acetonitrile–water (20:80); volume 15 μ l. Other operating conditions as in Fig. 4.

phthalate and diisobutyl phthalate have the same retention in the reversed-phase system employed. Ishida *et al.*¹⁰ reported that di-*n*-butyl phthalate was present as an impurity in water and various organic solvents. The content of di-*n*-butyl phthalate was determined, assuming the absence of diisobutyl phthalate, to be *ca.* 3 ppb in distilled water containing 1 ppm ethylene glycol.

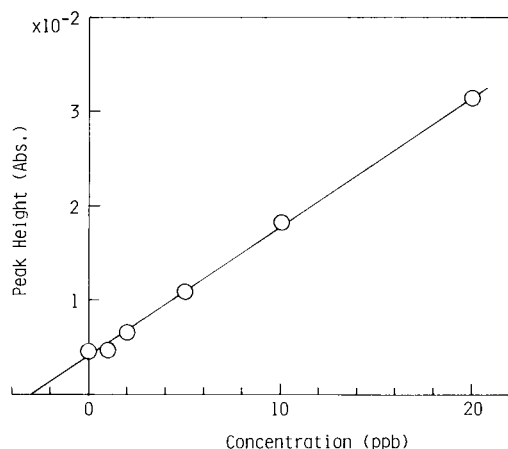


Fig. 8. Relationship between sample concentration and peak height. Column: 9.9 cm \times 0.12 mm I.D., packed with SC-01. Pre-column: 5–6 \times 0.15 mm I.D., packed with SC-01. Mobile phase: acetonitrile–water (65:35); flow-rate 0.83 μ l/min. Sample: di-*n*-butyl phthalate in distilled water containing 1 ppm ethylene glycol; volume 1 ml. Wavelength of UV detection, 230 nm.

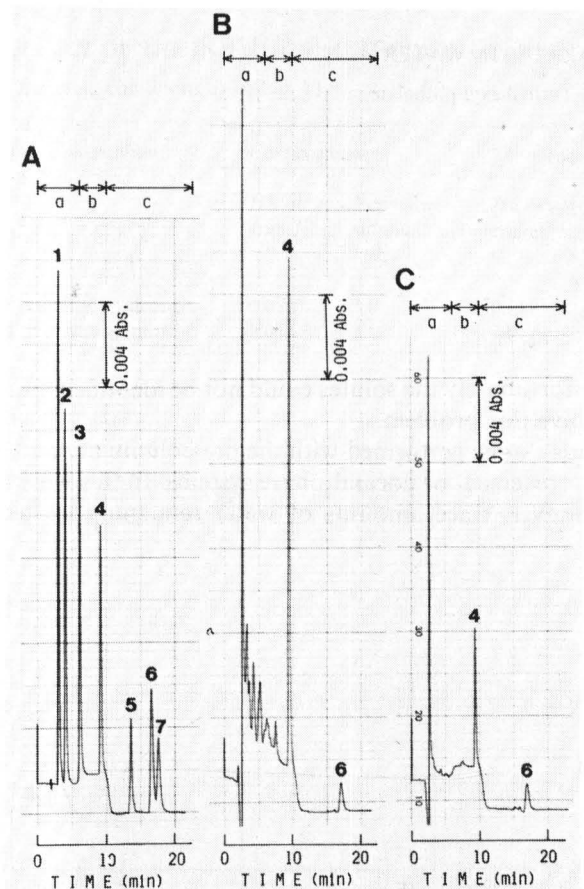


Fig. 9. Analysis of phthalates in water. Column: 10.2 cm \times 0.12 mm I.D., packed with SC-01. Pre-column: 5 \times 0.19 mm I.D., packed with Develosil ODS (10 μ m). Mobile phases: acetonitrile-water (55:45) (a); (65:35) (b); (90:10) (c); flow-rate 0.83 μ l/min. Samples: A, 1 = 9.9 ng dimethyl; 2 = 9.8 ng diethyl; 3 = 9.8 ng diisopropyl; 4 = 9.8 ng di-*n*-butyl; 5 = 6.6 ng diheptyl; 6 = 7.3 ng di-2-ethylhexyl; 7 = 8.3 ng dinonyl phthalate; B, deionized water, 200 μ l; C, tap-water, 400 μ l. Wavelength of UV detection: 235 nm.

Application to trace analysis

The pre-column method was applied to the analysis of phthalates in water. Fig. 9A shows the stepwise gradient separation of standard mixtures of phthalates. Gradient elution was performed as follows. Prior to a chromatographic run, different proportions of mobile phases were stored in a fused silica glass capillary tubing (0.25 mm I.D.) in the order as indicated in Fig. 9 and then forwarded onto the separation column via the injection part by feeding the third solution (c) from a pump. A sample solution was sucked in the top of the mobile phase manually.

Fig. 9B and C shows the analysis of phthalates in deionized and tap-water using the pre-column method, respectively. Solutes were identified from their retention times and the amounts of di-*n*-butyl and di-2-ethylhexyl phthalate were determined from standard samples. The results are given in Table I.

Fig. 10 shows the analysis of drained water from a sewage treatment plant. A

TABLE I

ANALYTICAL RESULTS FOR PHTHALATES IN WATER

DBP = di-*n*-butyl phthalate; DEHP = di-2-ethylhexyl phthalate.

Sample	Concentration (ppb)	
	DBP	DEHP
Deionized water	101	8.4
Tap-water	14	4.0
Distilled water	1.5	2.8

number of peaks were detected. Unfortunately the solutes could not be identified, but use of a mass spectrometer may solve this problem.

The analysis of corticosteroids can be performed with the pre-column method, as previously reported⁴, using either reversed- or normal-phase systems. In this work, the latter mode was adopted. However, trace amounts of water remaining in the

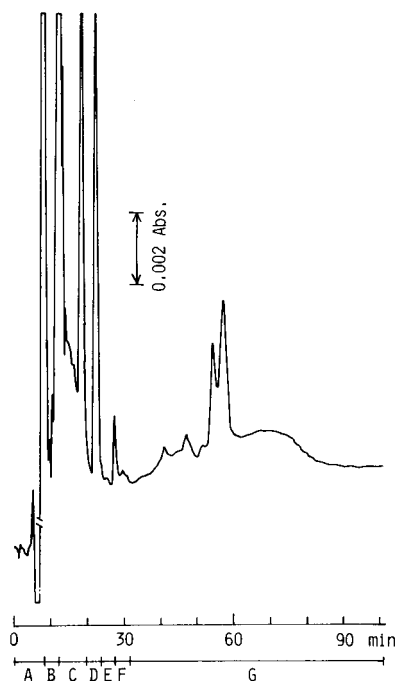


Fig. 10. Analysis of drained water from a sewage treatment plant. Column: 10.0 cm \times 0.12 mm I.D., packed with SC-01. Pre-column: 4 \times 0.2 mm I.D., packed with SC-01. Mobile phases: acetonitrile-water (3:7) (A); (4:6) (B); (5:5) (C); (6:4) (D); (7:3) (E); (8:2) (F); (9:1) (G). Sample: drained water, 100 μ l. Flow-rate: 0.42 μ l/min. Wavelength of UV detection: 220 nm.

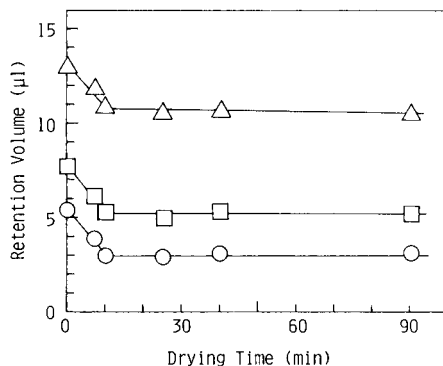


Fig. 11. Influence of drying time on solute retention. Column: 10.1 cm \times 0.12 mm I.D., packed with Nucleosil NH₂. Pre-column: 4-6 \times 0.19 mm I.D., packed with Hitachi GEL No. 3011. Mobile phase: dichloromethane saturated with water-methanol (98.5:1.5); flow-rate 0.83 μ l/min. Samples: \circ , cortisone; \square , cortisone; \triangle , cortisol.

TABLE II

EFFECT OF THE INJECTION METHOD ON COLUMN EFFICIENCY

Operating conditions as in Fig. 11.

Injection method	Corticosterone		Cortisone		Cortisol	
	HETP (mm)	Retention volume (μl)	HETP (mm)	Retention volume (μl)	HETP (mm)	Retention volume (μl)
On-column injection	0.086	3.0	0.11	5.0	0.12	10.5
Pre-column injection	0.074	3.1	0.077	5.3	0.090	10.6

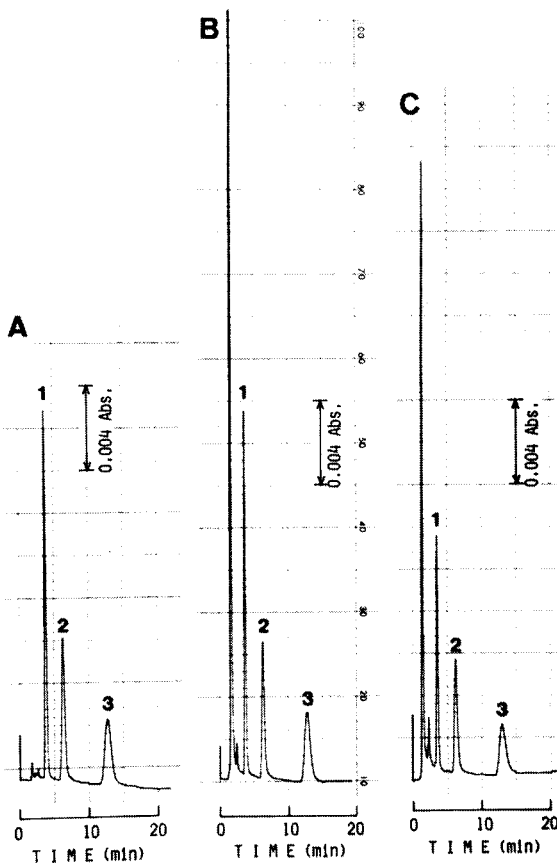


Fig. 12. Analysis of corticosteroids. Conditions as in Fig. 11. Samples: A, 0.024 μl dichloromethane solution containing 0.019 % (w/w) corticosterone (1), 0.017 % cortisone (2) and 0.016 % cortisol (3); B, 500 μl of aqueous solution containing 12 ppb corticosterone, 11 ppb cortisone and 9.9 ppb cortisol; C, 16 μl of horse serum in 144 μl distilled water. Wavelength of UV detection, 240 nm.

collection column affect the separation of solutes. Thus, after a concentration step, the micro pre-column was dried *in vacuo* by using a rotary oil pump.

Fig. 11 shows the influence of drying time on the retention of corticosteroids. Drying for longer than 10 min gave constant solute retention.

Table II shows the effect of the injection method on column efficiency. Despite the fact that the extra-column dead volume for the pre-column injection is larger than for the on-column injection, lower HETP values are observed with the former method. This indicates that collected solutes are removed from the collection column in a narrower band by the mobile phase and loaded onto the separation column quantitatively.

Separations of standard mixtures of corticosteroids are shown in Fig. 12A and B, with on-column injection and pre-column injection, respectively. Fig. 12C shows the analysis of corticosteroids in horse serum, which was diluted in distilled water ten times after filtration. In previous work⁴, certain components interfered with the determination of corticosterone; here this problem was absent. This difference seems to be due to the difference in packing materials: silica gel (used previously) and silica-NH₂. In 1 ml of horse serum 0.24 μ g corticosterone, 0.28 μ g cortisone and 0.23 μ g cortisol were present.

CONCLUSION

The pre-column method developed in this work is useful for the analysis of constituents in natural water and *in vivo*. In combination with mass spectrometry, this technique has great potential.

REFERENCES

- 1 D. Ishii, K. Asai, K. Hibi, T. Jonokuchi and M. Nagaya, *J. Chromatogr.*, 144 (1977) 157.
- 2 D. Ishii, K. Hibi, K. Asai and T. Jonokuchi, *J. Chromatogr.*, 151 (1978) 147.
- 3 D. Ishii, K. Hibi, K. Asai and M. Nagaya, *J. Chromatogr.*, 152 (1978) 341.
- 4 D. Ishii, K. Hibi, K. Asai, M. Nagaya, K. Mochizuki and Y. Mochida, *J. Chromatogr.*, 156 (1978) 173.
- 5 D. Ishii, A. Hirose and I. Horiuchi, *J. Radioanal. Chem.*, 45 (1978) 7.
- 6 D. Ishii, A. Hirose, K. Hibi and Y. Iwasaki, *J. Chromatogr.*, 157 (1978) 43.
- 7 D. Ishii, A. Hirose and Y. Iwasaki, *J. Radioanal. Chem.*, 46 (1978) 41.
- 8 T. Takeuchi and D. Ishii, *J. Chromatogr.*, 190 (1980) 150.
- 9 K. Ogan, E. Katz and W. Slavin, *J. Chromatogr. Sci.*, 16 (1978) 517.
- 10 M. Ishida, K. Suyama and S. Adachi, *J. Chromatogr.*, 189 (1980) 421.

CHROM. 14,178

HIGH-RESOLUTION SEPARATIONS BASED ON ELECTROPHORESIS AND ELECTROOSMOSIS

JAMES W. JORGENSEN* and KRYNN DeARMAN LUKACS

Department of Chemistry, University of North Carolina, Chapel Hill, NC 27514 (U.S.A.)

SUMMARY

The related electrokinetic effects of electrophoresis and electroosmosis may be used to achieve high resolution separations. An "instrumental" version of zone electrophoresis carried out in 75 μm I.D. glass capillaries is described. This technique demonstrates excellent resolution of charged substances in a short time. Using virtually the same apparatus, reversed-phase chromatography is performed with electroosmotic pumping of an acetonitrile mobile phase. This technique also produces separations with excellent efficiency. Very low values of reduced plate height are found, which suggests that column packing irregularities are less important when electroosmotic flow is used instead of flow generated by pressure.

INTRODUCTION

Electrophoresis and electroosmosis are related electrokinetic effects. Electrophoresis is the familiar phenomenon of migration of charged particles in solution in an electric field gradient. The velocity of migration, v_{ep} , is given by:

$$v_{ep} = \mu_{ep} E \quad (1)$$

where μ_{ep} is the electrophoretic mobility and E the electric field gradient. The related phenomenon of electroosmosis is perhaps a little less familiar. If charged particles are held stationary (as, for instance, silica particles packed tightly in a tube), then in the presence of an applied electric field, instead of the particles migrating through the liquid, the liquid migrates or flows through the bed of particles. The velocity of this electroosmotic flow, v_{eo} , is given by:

$$v_{eo} = \mu_{eo} E \quad (2)$$

where μ_{eo} is the coefficient of electroosmotic flow. In 1952 Mould and Synge^{1,2} first demonstrated the use of electroosmotic flow in a thin-layer chromatographic system for the separation of polysaccharides in collodion membrane strips. This method of generating flow was applied to both thin-layer and column chromatographic systems in 1974 by Pretorius *et al.*³. In their column work, these authors reported only on

their results with unretained solutes. Their initial data on column efficiency were promising, and electroosmotic flow appeared to offer some interesting possibilities from a chromatographic point of view.

The purpose of this paper is to describe two forms of high-efficiency separations based on these two electrokinetic effects. First we will consider zone electrophoresis in open tubes, and second, chromatography in packed columns with flow generated by electroosmosis. The equipment used in the two separation systems is essentially the same. However, for the sake of clarity, the topics will be treated in two separate sections.

ZONE ELECTROPHORESIS IN OPEN TUBES

Theory

Zone electrophoresis is fundamentally a simple process of migration of zones of charged substances in an electric field. Certainly molecular diffusion contributes to some of the broadening of an initially narrow zone. However, it is by no means the only cause, and in most cases it is actually a fairly insignificant contributor to zone broadening. The real situation is generally more complex. Heat is generated uniformly throughout the separation medium by the passage of electric current, but is only removed at the edges of the medium. The inevitable result is a temperature gradient within the medium, and associated with this, a density gradient⁴. Some means must be used to suppress convective flows associated with density gradients or else zone broadening will result. The most common approach is to perform zone electrophoresis in a gel. Although gels solve the problem of convection, they introduce new zone-broadening phenomena such as eddy migration and adsorptive interactions between solutes and gel⁴. A more sophisticated solution to the problem of convection which circumvents the difficulties associated with gels is the free zone electrophoresis technique developed by Hjertén⁵. In this method, stabilization is achieved by the continuous rotation of the electrophoresis tube about its longitudinal axis. Another approach is the group of methods known as continuous-flow deviation electrophoresis. This ingenious group of techniques uses flow in "serpentine" or "helical" paths to combat convection, and has been reviewed by Kolin⁶. A still simpler approach involves the use of capillary tubes as the separation chamber, as described by Mikkers *et al.*⁷. The walls of a tube act with the liquid's viscosity to counteract flow. As the tube diameter is decreased this stabilizing "wall effect" is enhanced.

Although these various approaches are effective ways to minimize convection they do not eliminate the temperature gradient. Since electrophoretic mobility increases at an approximate rate of 2% per °C (ref. 4), solute molecules in the hotter interior of the medium will migrate faster than solute at the cooler edges, resulting in significant spreading of the zones. According to Wieme⁴, when electrophoresis is performed in tubes of circular cross-section the magnitude of the temperature difference from the center to the wall of the tube is proportional to the square of the tube diameter. Thus a reduction in tube diameter will result in a significant decrease in temperature differences across the tube. Even with tubes of very small diameter some temperature gradient will persist, and thus some zone broadening should result owing to the temperature dependence of migration velocity. However, if the tube diameter is

small enough, the solute molecules will be able to diffuse back and forth across the tube's diameter many times during their migration down the length of the tube. In this way they randomize their occupancy of the tube's cross-section, which tends to average-out any radially dependent velocity differences. This will tend to minimize the importance of any remaining temperature gradient.

If zone electrophoresis were carried out in an open tube of small diameter, a situation may develop where zone broadening occurs predominantly by molecular diffusion. If electrophoresis is carried out in tubes, substances could be introduced at one end and would migrate under the influence of the electric field to the far end. At the far end they could be detected as they migrated past a detection device. This would yield a plot of solute concentration as a function of time, which is called an electropherogram. The migration velocity, v_{ep} , was given by eqn. 1. This equation may be rewritten as:

$$v_{ep} = \mu_{ep} E = \mu_{ep} V/L \quad (3)$$

where V is the voltage applied across the length, L , of the tube. The time, t , that a solute takes to migrate the entire length of the tube is given by:

$$t = \frac{L}{v_{ep}} = \frac{L^2}{\mu_{ep} V} \quad (4)$$

Diffusion will be occurring during this time. If an initially infinitely thin zone is allowed to diffuse for a time, t , the spatial variance, σ_L^2 , of the zone will be:

$$\sigma_L^2 = 2Dt = \frac{2DL^2}{\mu_{ep} V} \quad (5)$$

where D is the diffusion coefficient of the solute. We can express the separation efficiency of an electrophoretic system in terms of the number of theoretical plates, as suggested by Giddings⁸. The number of theoretical plates, N , is defined as:

$$N = \frac{L^2}{\sigma_L^2} \quad (6)$$

and by substituting eqn. 5 into eqn. 6,

$$N = \frac{\mu_{ep} V}{2D} \quad (7)$$

This simple result suggests that the most direct approach to high separation efficiencies in zone electrophoresis is the use of very high voltages. Interestingly, as long as heat dissipation is adequate, tube length plays no direct role in separation efficiency. If very high voltages are applied to narrow-bore capillary tubes, high separation efficiencies should be obtained.

Experimental

Glass capillary tubes were drawn from Pyrex borosilicate glass to an I.D. of 75 μm , an O.D. of 550 μm , and a length of 1 m, using a Shimadzu (Kyoto, Japan) GDM-1B glass-drawing machine. These tubes were filled with a $5 \cdot 10^{-2}$ M phosphate buffer (pH 7) as the electrophoresis medium. A Megavolt (Hackensack, NJ, U.S.A.) Model RDC-30-10 high-voltage d.c. power supply, delivering from 0 to +30 kV, provided the electric field for electrophoresis. Accidental contact with the high-voltage end of the system was prevented with an interlock mechanism. The high-voltage end was encased in a plexiglass box, and opening this box automatically shut off the high voltage. Graphite electrodes were used to connect the power supply to the buffer reservoirs located at each end of the capillary. Samples were introduced at the positive (high-voltage) end and the detector was located at the negative (ground) end of the system. Samples were introduced into the capillary by replacing the buffer reservoir with a sample container. A brief application of high voltage caused the migration of a small amount of sample into the tube. The buffer reservoir was then replaced, voltage applied, and electrophoresis proceeded. The detector used was a home-made on-column fluorescence detector. This device permitted the sensitive detection of solutes while still in the capillary and thus avoided extracolumn zone broadening. However, only fluorescent solutes were detectable. Details of the design of this detector will be published. In all instances, 30 kV potential was applied to the system, and the current measured under these circumstances was $1 \cdot 10^{-4}$ A.

Results and discussion

Fig. 1 is an electropherogram of a series of *n*-alkylamines labeled with fluorescamine (note the truncated time axis). Each amine derivative differs from its neighbor by only one methylene unit and yet all are well resolved. Each addition of a methylene

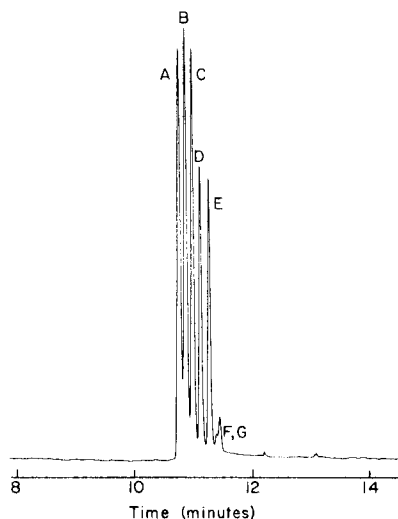


Fig. 1. Electropherogram of *n*-alkylamines as fluorescamine derivatives. Peaks: A = octyl; B = heptyl; C = hexyl; D = pentyl; E = butyl; F = unknown impurity; G = propyl. Approximately 7 pmoles of each derivative, except for propylamine.

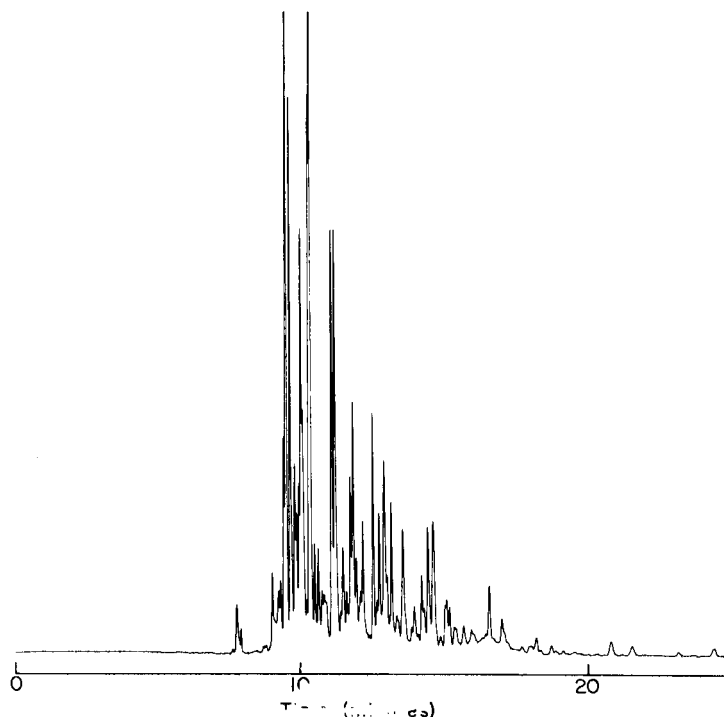


Fig. 2. Electropherogram of fluorescamine labeled peptides obtained from a tryptic digest of chicken ovalbumin.

unit represents roughly a 4% increase in molecular mass or a 1% increase in molecular diameter of the derivative. This is an indication of the very high efficiency of this electrophoresis system. An interesting aspect of this separation is that all these derivatives are negative ions and yet migrate toward the negative electrode. This apparent paradox is explained by the fact that the buffer is undergoing a very strong electroosmotic flow, and is carrying the negative ions with it toward the negative electrode. The solute ions are migrating against this flow, but are eventually carried by it to the detector. This also explains why the larger amine derivatives appear at the detector first. The larger derivatives have lower mobilities, and thus are less effective in migrating against the electroosmotic flow. Electroosmotic flow modifies the equations describing the separation process somewhat. However, owing to the flat flow profile of electroosmotic flow^{3,9}, the basic linear dependence of separation efficiency on applied voltage remains correct¹⁰. Electroosmotic flow is an advantage in this system in that it permits analysis of both positive and negative ions in a single run. Fig. 2 is an electropherogram of fluorescamine labeled peptides. The peptides were obtained from a tryptic digest of heat-denatured chicken ovalbumin¹¹. Both very high resolution and speed of analysis are evident in this separation of a complex mixture.

The potential of this technique for yielding rapid and efficient separations has been clearly demonstrated. However, fluorescence detection is rather limiting, and a wider range of detection devices will be desirable. The possibilities for protein analysis

are particularly promising, and continuing development in this direction will be pursued.

ELECTROSMOTIC FLOW IN CHROMATOGRAPHY

Theory

As previously mentioned, electroosmosis is the flow of liquid through a porous medium under the influence of an applied electric field. This phenomenon was well reviewed by Pretorius *et al.*³, as well as in standard texts¹². The flow velocity was given in a simple form by eqn. 2. An extended form gives the flow velocity as:

$$v_{eo} = \left[\frac{\epsilon \zeta}{4\pi\eta} \right] E \quad (8)$$

where ϵ is the dielectric constant and η the viscosity of the solvent, and ζ is the zeta potential of the liquid-solid interface³. One interesting aspect of electroosmotic flow is that unlike other forms of flow it generates a flat flow profile^{3,9}. In a chromatographic system this should result in a lower resistance to mass transfer in the mobile phase. Perhaps a more important facet of electroosmosis is that, according to eqn. 8, the velocity of flow is independent of the geometry and size of the channels in the packing. This means that, in a packed column, flow should be uniform across the column regardless of packing irregularities. Lower values of the height equivalent of a theoretical plate (HETP) should thus be obtained with electroosmotic flow than with other forms of flow. Indeed this was found to be the case for unretained solutes by Pretorius *et al.*³. The purpose of this investigation was to study the performance of electroosmotic flow in realistic chromatographic systems.

Experimental

A straight length of Pyrex glass tube was drawn to an I.D. of 170 μm , an O.D. of 650 μm , and a length of 68 cm on a glass-drawing machine (Shimadzu GDM-1B). This column was to be packed with a 10 μm packing, and thus the column end had to be "plugged" with a porous plug. To accomplish this, *ca.* 5 mm of one end of the tube was filled with Permaphase ODS pellicular packing (DuPont, Wilmington, DE, U.S.A.) of *ca.* 30- μm diameter. This end was then heated in a flame, sintering the pellicular packing into the end of the tube and forming a porous plug. Partisil-10 ODS-2 (Whatman, Clifton, NJ, U.S.A.), a 10- μm reversed-phase packing, was then pumped at 1000 p.s.i.g. as an acetonitrile slurry into the column in a "down-flow" manner. This was continued until the column appeared fully packed. The acetonitrile was then forced from the column with gas pressure, and the remaining end "sealed" by sintering another 5-mm plug of pellicular packing in this end. Once sealed, the column was again filled with acetonitrile and was ready for use. This column was operated in essentially the same manner as described for the electrophoresis. Samples were introduced to the column by replacing a solvent reservoir with sample and applying voltage briefly. Flow of solvent was in the direction of the negative electrode. The on-column fluorescence detector was again used to detect solutes. The distance from the column inlet to the detector was 58 cm, which represents the portion of the column available for separation prior to detection.

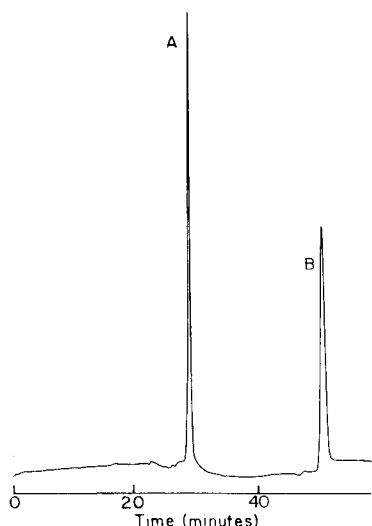


Fig. 3. Chromatogram obtained with electroosmotic flow. Peaks: A = 9-methylanthracene; B = perylene.

Results and discussion

With acetonitrile as the mobile phase, and with 30 kV applied across the column, a current of *ca.* 50 nA was observed. Fig. 3 shows a chromatogram of 9-methylanthracene and perylene obtained in this system. The efficiency for 9-methylanthracene is 31,000 theoretical plates while for perylene it is 23,000 theoretical plates. These efficiencies are relatively good although retention times are long. The values of the HETP for the two peaks are 19 μm and 25 μm , respectively. This leads to values for the reduced plate heights of 1.9 and 2.5, respectively. In view of the crude methods and low pressure used in packing this column, these plate heights are quite good¹³. Current theories of column packing would predict that this column is poorly packed, and should give mediocre performance. However, if the flow is uniform and independent of packing irregularities, as predicted by the theory of electroosmotic flow, then these good results are to be expected.

Our experience in using electroosmotic flow in a chromatographic system has been that the method is a bit difficult and inconvenient to work with. Certainly part of this is due to the novelty of this approach to chromatography. However, electroosmosis lacks the direct and simple control over mobile phase flow that we are accustomed to with conventional pumping systems. The performance of these columns appears to offer a modest improvement over conventional flow, but may not justify the increased difficulty in working with electroosmotic flow.

The possibility that packing irregularities cause little peak broadening is interesting. One might infer from this that a narrow particle size distribution is also not essential to good performance when electroosmotic flow is used. An ideal application of electroosmotic flow may be in large diameter preparative-scale columns. The low power dissipation of 1.5 mW for our column indicates that columns of several centimeters inside diameter could be operated without overheating problems. The great expense of high-performance small-particle packing virtually precludes their use in

columns of large volume. Also, application of the necessary high pressure to large diameter tubes is potentially dangerous, although not an insurmountable problem. Furthermore, uniform packing of a large diameter column may prove difficult. If small-particle packings with a broader size distribution were used, the expense of the packing would drop dramatically, and if packing irregularities are less significant, column packing would be less of a problem. It appears that preparative-scale separations may be the area of most potential impact for electroosmotic flow in chromatography.

ACKNOWLEDGEMENT

Support for this work was provided by the Petroleum Research Fund of the American Chemical Society and the University Research Council of the University of North Carolina.

REFERENCES

- 1 D. L. Mould and R. L. M. Synge, *Analyst (London)*, 77 (1952) 964.
- 2 D. L. Mould and R. L. M. Synge, *Biochem. J.*, 58 (1954) 571.
- 3 V. Pretorius, B. J. Hopkins and J. D. Schieke, *J. Chromatogr.*, 99 (1974) 23.
- 4 R. J. Wieme, in E. Heftmann (Editor), *Chromatography — A Laboratory Handbook of Chromatographic and Electrophoretic Methods*, Van Nostrand Reinhold, New York, 3rd ed., 1975, Ch. 10.
- 5 S. Hjertén, *Chromatogr. Rev.*, 9 (1967) 122.
- 6 A. Kolin, in Z. Deyl (Editor), *Electrophoresis — A Survey of Techniques and Applications, Part A: Techniques*, Elsevier, Amsterdam, 1979, Ch. 12.
- 7 F. E. P. Mikkers, F. M. Everaerts and Th. P. E. M. Verheggen, *J. Chromatogr.*, 169 (1979) 11.
- 8 J. C. Giddings, *Separ. Sci.*, 4 (1969) 181.
- 9 C. L. Rice and R. Whitehead, *J. Phys. Chem.*, 69 (1965) 4017.
- 10 J. W. Jorgenson and K. D. Lukacs, *Anal. Chem.*, 53 (1981) 1298.
- 11 R. W. Canfield, *J. Biol. Chem.*, 238 (1963) 2691.
- 12 A. W. Adamson, *Physical Chemistry of Surfaces*, Wiley-Interscience, New York, 3rd ed., 1976, Ch. 4.
- 13 L. R. Snyder and J. J. Kirkland, *Introduction to Modern Liquid Chromatography*, Wiley-Interscience, New York, 2nd ed., 1979, Ch. 5.

CHROM. 14,093

COMPARISON OF SEDIMENTATION FIELD FLOW FRACTIONATION WITH CHROMATOGRAPHIC METHODS FOR PARTICULATE AND HIGH-MOLECULAR-WEIGHT MACROMOLECULAR CHARACTERIZATIONS

W. W. YAU* and J. J. KIRKLAND

Central Research and Development Department, E. I. Du Pont de Nemours and Company, Experimental Station, Wilmington, DE 19898 (U.S.A.)

SUMMARY

Quantitative particle size and molecular weight determinations by time-delayed exponential force-field sedimentation field flow fractionation (TDE-SFFF) can currently be carried out in 15–20 min using automated apparatus with force fields of up to 50,000 gravities. New resolution parameters provide a common basis for comparing the ability of the commonly used separation methods for particle size analyses. These parameters show that TDE-SFFF has a 5–10 fold and 10–50 fold greater specific resolution than size-exclusion chromatography (SEC) and packed column or capillary hydrodynamic chromatography (HDC), respectively. Because of high resolving power and other characteristics, TDE-SFFF provides superior accuracy in particle size distribution analyses relative to these other separation methods, as confirmed by direct comparisons with typical literature data for a range of particulate samples. TDE-SFFF also has similar advantages over conventional non-chromatographic methods. For example, SFFF exhibits approximately the same resolving power as disc centrifugation but a much wider dynamic range of particle diameter separation in a single analysis.

SFFF provides higher separation resolution than SEC and HDC because of intrinsic differences in retention mechanisms. These latter chromatographic methods separate species by size-exclusion effects —peaks elute prior to the mobile phase solvent —therefore, HDC and SEC are basically limited by available fractionation volume. On the other hand, SFFF exhibits true retention like the affinity liquid chromatography (LC) methods —peaks elute after the unretained mobile phase solvent. In contrast to SEC and HDC, but like LC, TDE-SFFF has the potential for very high peak capacity.

INTRODUCTION

There is growing interest in high-resolution separation methods for characterizing colloidal particles and macromolecular suspensions. Recently, the unique analytical capabilities of sedimentation field flow fractionation (SFFF) have been demonstrated for such materials^{1–4}. A new SFFF technique with a time-delayed

exponential force-field decay (TDE-SFFF) has many advantages over constant-field (CF) SFFF for particle size or mass distribution analyses⁵⁻⁷. This new approach permits accurate quantitative analyses in the ≤ 0.01 – $1\ \mu\text{m}$ range in a few minutes.

In addition to TDE-SFFF, other separation methods such as hydrodynamic chromatography (HDC), size-exclusion chromatography (SEC) and disc centrifugation have also been used for characterizing colloidal particles and macromolecular suspensions of $\leq 1\ \mu\text{m}$. Electron or optical microscopy can be applied to particles in the 0.01 – $10\ \mu\text{m}$ range, but this approach is tedious and often imprecise. Other separation methods such as the Coulter counter are commonly used for particles of $\geq 1\ \mu\text{m}$.

Unfortunately, direct comparison of the capabilities of these various methods has not previously been attempted. Such a comparison is needed so that potential users might have the information needed to decide which method would be best for a particular analytical goal. Important features of any particle size analytical method should include the total particle size separation dynamic range achievable in a single experiment, separation resolution or the ability to discriminate between particle sizes, analysis time, convenience and the applicability to various particle types. Unfortunately, two of the most important features, particle size dynamic range and resolution, previously have not been evaluated for the various methods.

The resolution capability inherent in a separation method measures the quality of the separation or the quality of the particle size information obtainable in the optimum size range. High resolution is a prerequisite to accurate and precise particle size analyses⁵. Recently there has been particular interest in methods such as HDC, SEC and disc centrifugation for the < 0.1 – $1\ \mu\text{m}$ particle range. Until now there has been a lack of a common basis for comparing the resolutions of the various particle size analysis methods.

In this paper we propose new specific resolution expressions to serve as a common basis for objectively comparing the resolving power of these most commonly used separation methods for particle analysis. The useful separation range and the dynamic range of some of these methods are also documented. Finally, a descriptive separation performance parameter has been developed that defines the peak capacity of each method. Typical examples of published separations have been utilized to compare the important performance features of some of the separation methods. Comparative data from some conventional non-separation particle size analytical techniques also are included.

COMMONALITY IN RESOLUTION

The extent of separation for two species can be described by the well-known chromatographic resolution expression⁸:

$$R_s = \frac{\Delta V_R}{4\sigma} \quad (1)$$

where, ΔV_R is the difference in peak retention volumes for the individual species and σ is the peak standard deviation in retention volume units resulting from instrumental band broadening. The resolution value R_s provides a measure of the fidelity of the information in terms of the discriminating power (ΔV_R) as modulated by the un-

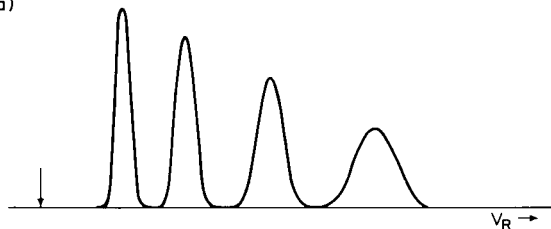
certainties (σ) in the analytical information. This resolution expression can be applied to many types of analytical information, as well as to chromatographic results. However, the general resolution expression can provide specific information about the resolving power of particle size separation methods only when these resolution values can be normalized in terms of particle size differences. This situation is further complicated by the fact that the dependence of ΔV_R and σ on particle size varies greatly from one particle size analytical method to the other. Thus, the direct use of common R_s values to compare different separation methods is not practical and a more basic resolution parameter is needed.

In previous studies of SEC⁹ and SFFF⁵ we described the use of the specific resolution factor to provide a general description of resolving power through reduced parameters. In the case of particle size analysis, a variety of particle retention and band broadening mechanisms are involved, and an exact resolution parameter that can serve all separation methods equally well does not appear to be feasible. However, we show here that the specific resolution parameter can satisfactorily describe the capability of many separation methods. Approximations are necessary in this comparison since the specific resolution values are not strictly independent of particle mass M and particle diameter d_p . However, errors due to these approximations appear to be small, and the large differences in the resolution which exist between some methods are clearly demonstrated. Thus the proposed semi-quantitative resolution concepts provide for the first time a reasonable comparison of different separation methods on the same scale.

We have considered the resolution of two general forms of particle size separations. In Fig. 1a, for Case I peak band broadening increases with peak retention and is

$$\text{BAND BROADENING: } \sigma = V_R / \sqrt{N}$$

(a)



$$\text{RETENTION: } V_R = V_0 + aM^b = V_0 + a'd_p^{3b}$$

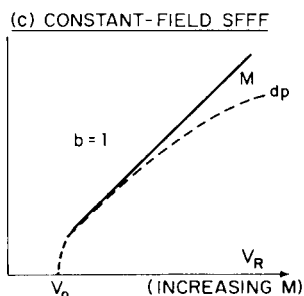
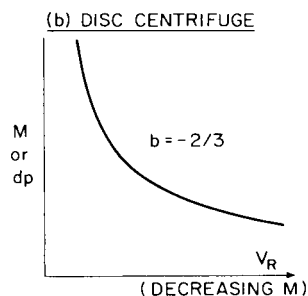


Fig. 1. General forms of particle size separation —Case I.

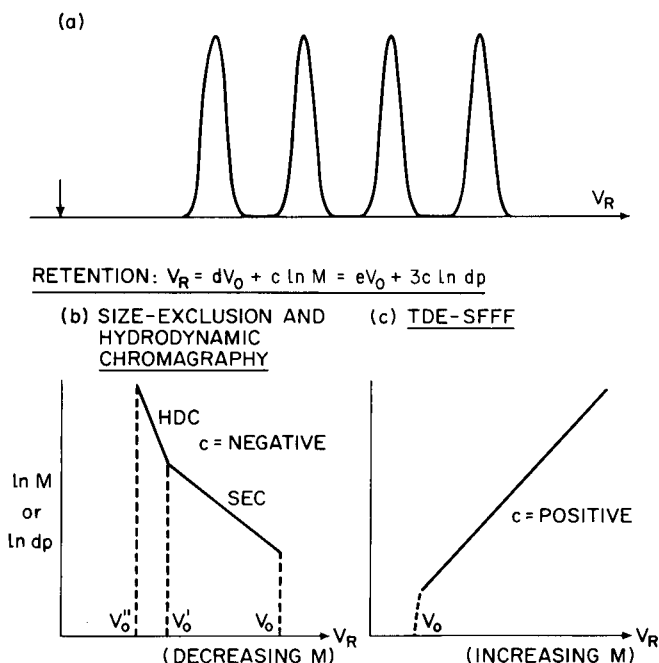
BAND BROADENING: $\sigma = \text{CONSTANT}$ 

Fig. 2. General forms of particle size separation — Case II.

described by $\sigma = V_R / \sqrt{N}$, where plate count N remains constant. For case II band broadening is independent of peak retention and peaks exhibit a constant σ , as in Fig. 2a. For Cases I and II the dependence of retention volume V_R on particle mass M and particle diameter d_p is considered as:

Case I:

$$V_R = V_0 + aM^b \approx V_0 + a'd_p^{3b} \quad (2)$$

Case II:

$$V_R = dV_0 + c \cdot \ln M = eV_0 + 3c \cdot \ln d_p \quad (3)$$

where, $M \propto d_p^3$ for spherical particles, V_0 is retention volume for an unretained solvent peak, and a , b , c , d , and e are numerical constants. While actual band broadening and particle retention for particular separation methods may deviate somewhat from Cases I and II, there usually is a sufficient resemblance to identify the separation method of interest with one of these cases. For example, the general non-linear retention relationship expressed by eqn. 2 approximately describes disc centrifugation (Fig. 1b), where $V_0 = 0$ and $b = -2/3$, and CF-SFFF with $b = 1$ (Fig. 1c). Both of these separation methods have peak dispersion characteristics similar to that described by Case I. SEC, both column chromatography and HDC, and TDE-SFFF identify with Case II (Figs. 2b and 2c and eqn. 3). The logarithmic separation depicted

by eqn. 3 describes HDC and SEC with a negative value for the constant c , as illustrated in Fig. 2b. Data from TDE-SFFF demonstrate a positive c value, as depicted in Fig. 2c.

The band broadening and retention characteristics of Cases I and II (Figs. 1 and 2) approximate most of the typical separations commonly encountered in particle size analyses. Therefore, these two cases have been used in this work as a basis for developing a comparison of various particle size analysis methods.

Case I (retention of eqn. 2; constant N)

To develop the resolution relationship for Case I, eqn. 2 is combined with eqn. 1 to yield:

$$R_s = \frac{a \Delta M^b}{4V_R/\sqrt{N}} \quad (4)$$

For significantly retained peaks, and small ΔM differences, $V_R \approx aM^b$ and $\Delta M^b \approx (bM^{b-1}) \Delta M$. Therefore, R_s may be defined in terms of particle mass M as:

$$R_s \approx \frac{(a|b| M^{b-1}) \Delta M}{4aM^b/\sqrt{N}} \cong \left(\frac{|b|\sqrt{N}}{4} \right) \left(\frac{\Delta M}{M} \right) \quad (5a)$$

or for particle diameter d_p :

$$R_s \approx \left(\frac{|b|\sqrt{N}}{4} \right) \left(\frac{3d_p^2 \Delta d_p}{d_p^3} \right) \cong \left(\frac{3|b|\sqrt{N}}{4} \right) \left(\frac{\Delta d_p}{d_p} \right) \quad (5b)$$

where ΔM and Δd_p are the particle mass or diameter differences, respectively, for a pair of species of interest. (Note that the absolute value $|b|$ is used in these expressions.)

To provide a general measure of separating power, it is appropriate to define a specific resolution factor, $R_{s,(1+x)}$, which in terms of particle mass M , may be expressed as:

$$R_{s,(1+x)} = xR_s \left/ \left(\frac{\Delta M}{M} \right) \right. \quad (6a)$$

and for particle diameter d_p :

$$R_{s,(1+x)} = xR_s \left/ \left(\frac{\Delta d_p}{d_p} \right) \right. \quad (6b)$$

where, x is the fractional particle mass or diameter differences for a pair of species of interest. For example, a particle diameter resolution of $R_{s,1.2} = 1$ describes a separation method that can distinguish a 20% difference in particle diameter with a resolution of unity. This definition of particle resolution will become clearer in later discussions.

The specific resolution parameter is very similar in form to that previously developed for SEC⁹. For the Case I type separations presently under consideration, we can also show for particle mass:

$$R_{s,(1+x)} = \frac{|b| \sqrt{Nx}}{4} \quad (7a)$$

and for particle diameter:

$$R_{s,(1+x)} = \frac{3|b| \sqrt{Nx}}{4} \quad (7b)$$

It should be noted that eqns. 7a and 7b are approximate expressions that are valid for small particle size differences (small x values). The exact specific resolution expressions derived in the Appendix should be used to calculate specific resolution values for large particle size differences.

Case II (retention of eqn. 3; constant σ)

In a manner equivalent to that described for Case I, specific resolution factors can be developed for Case II for small particle size differences. By combining eqn. 3 with eqn. 1, we can define R_s in terms of particle mass M as:

$$R_s = \frac{\Delta V_R}{4\sigma} \approx \frac{|c| \Delta \ln M}{4\sigma} \approx \frac{|c|}{4\sigma} \left(\frac{\Delta M}{M} \right) \quad (8a)$$

and in terms of particle diameter d_p :

$$R_s = \left(\frac{|c|}{4\sigma} \right) \frac{3d_p^2 \Delta d_p}{d_p^3} \cong \frac{3|c|}{4\sigma} \left(\frac{\Delta d_p}{d_p} \right) \quad (8b)$$

(Note that the absolute value $|c|$ is used in these resolution expressions.) The specific resolution factors $R_{s,(1+x)}$ for Case II can now be defined. For particle mass:

$$R_{s,(1+x)} = \frac{|c|x}{4\sigma} \quad (9a)$$

and for particle diameter:

$$R_{s,(1+x)} = \frac{3|c|x}{4\sigma} \quad (9b)$$

Eqns. 9a and 9b are approximate expressions that are only valid for small particle size differences (small x values). Exact specific resolution relationships are developed in the Appendix.

It is important to note that in eqns. 5 and 8, resolution R_s is directly proportional to $\Delta M/M$ or $\Delta d_p/d_p$, the fractional difference in particle mass or particle diame-

ter, respectively. Because of this unique result, we now can expect the specific resolution $R_{s,(1+x)}$ to compare adequately the resolving power capability of each of the various forms of particle size separations discussed for both cases above. This specific resolution factor generally is used to describe the performance of a particular method, independent of sample polydispersity. However, monodispersed standards typically are used for evaluating the specific resolution values of particular separation methods.

Discrimination capacity

Based on the $R_{s,(1+x)}$ concept, another resolution parameter¹⁰ termed the particle mass or particle diameter discrimination capacity X_M or X_{d_p} is defined. X_M and X_{d_p} values describe the minimum fractional differences in M or in d_p that a particular method can separate with a resolution of unity. Stated otherwise, X_M and X_{d_p} values are simply the required x values to satisfy eqn. 6 by setting $R_{s,(1+x)} = 1$. For example, a X_{d_p} value of 0.2 means that a particular method can discriminate a pair of species with a 20% or larger difference in particle diameter with resolution of unity or more.

The discrimination capacity relationship takes the form:

$$X_M = \left(\frac{\Delta M}{M} \right) / R_s \quad (10a)$$

and

$$X_{d_p} = \left(\frac{\Delta d_p}{d_p} \right) / R_s \quad (10b)$$

For Case I separations, eqn. 10 becomes:

$$X_M = \frac{4}{|b| \sqrt{N}} \quad (11a)$$

or

$$X_{d_p} = \frac{4}{3|b| \sqrt{N}} \quad (11b)$$

and for Case II separations:

$$X_M = \frac{4\sigma}{|c|} \quad (12a)$$

or

$$X_{d_p} = \frac{4\sigma}{3|c|} \quad (12b)$$

Peak capacity

Another useful resolution parameter in particle separations is the peak capacity of the method¹¹. For particle size or mass separations we propose the parameter N_{\max} to describe the maximum number of fully resolved ($R_s = 1$) peaks that can be obtained within the dynamic range of a separation method. This peak capacity parameter is based on the discrimination capacity X_M or X_{d_p} of the method in relation to the dynamic range DR_M or DR_{d_p} for the same method. Based on the definition of the discrimination capacity (eqns. 10a and 10b), the particle mass or diameter ratio of the resolved species is defined by $(1 + X_M)$ or $(1 + X_{d_p})$. The number of pairs of these resolved species that can fit into the available dynamic range is specified by:

$$(1 + X_M)^{N_{\max}} = DR_M$$

or

$$(1 + X_{d_p})^{N_{\max}} = DR_{d_p} \quad (13a)$$

Then by rearranging:

$$N_{\max} = \frac{\ln DR_M}{\ln (1 + X_M)} = \frac{\ln DR_{d_p}}{\ln (1 + X_{d_p})} \quad (13b)$$

where DR_M and DR_{d_p} are the dynamic ranges of a separation expressed in terms of the ratio of the largest to the smallest particles separable in a single experiment for either particle mass M or particle diameter d_p . For example, for a method having a discrimination capacity X_{d_p} of 0.5 (minimum fractional difference in particle diameter that can be clearly discerned), the particle diameter ratio corresponds to $(1 + X_{d_p}) =$

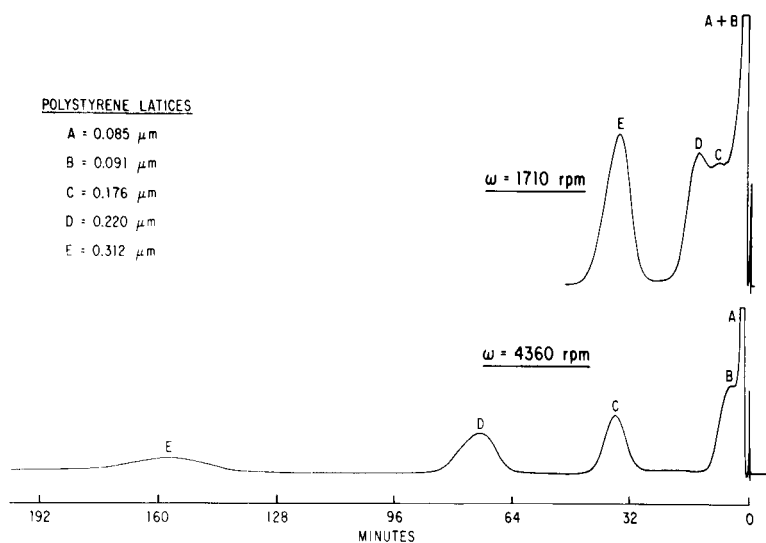
TABLE I
SPECIFIC PARTICLE DIAMETER RESOLUTION EXPRESSIONS

Method	Specific resolution*, $R_{s,1+x}$	Discrimination capacity**, X_{d_p}
CF-SFFF	$\frac{3x\sqrt{N}}{4}$	$\frac{4}{3\sqrt{N}}$
Exponential SFFF	$\frac{3\tau Fx}{4\sigma}$	$\frac{4\sigma}{3\tau F}$
HDC, SEC	$\frac{3x}{4\sigma D_2}$	$\frac{4\sigma D_2}{3}$
Disc centrifugation	$\frac{x\sqrt{N}}{2}$	$\frac{2}{\sqrt{N}}$

* For molecular weight, $R_{s,(1+x)(\text{mass})} = 1/3 R_{s,(1+x)d_p}$.

** For molecular weight, $X_M = 3X_{d_p}$.

(a)



(b)

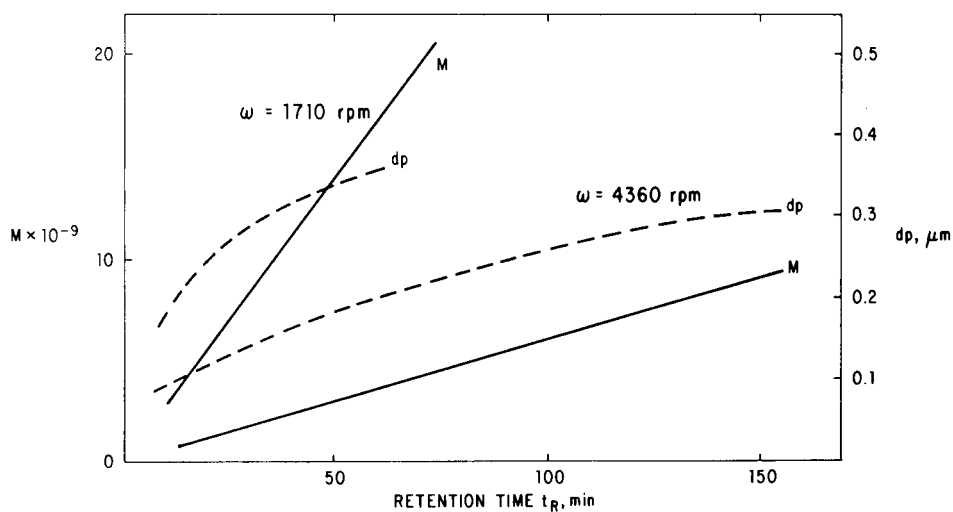


Fig. 3. CF-SFFF data; effect of rotor speed. (a) Fractogram; (b) calibration. Channel, $57 \times 2.54 \times 0.0254$ cm; mobile phase, 0.1% FL-70; flow-rate, $2.0 \text{ cm}^3/\text{min}$; relaxation, 10.0 min at $\omega_0 = 10,000 \text{ rpm}$; sample, $25 \mu\text{l}$ of 0.1% 0.085 μm , 0.09% 0.091 μm ; 0.04% each of 0.176-, 0.220-, 0.312- μm PS latex standards; detector, UV, 300 nm; temperature, 22°C. (Taken from ref. 5.)

TABLE II
PERFORMANCE OF VARIOUS SEPARATION METHODS IN PARTICLE SIZE ANALYSIS

Method	Reference	Polystyrene standards (μm)*	Dynamic range ($DR_{d,p}$)	Specific resolution ($R_{s,1,2}$)	Discrimination capacity ($X_{d,p}$)	Peak capacity (N_{max})
CF-SFFF (1710 rpm)	5	0.085–0.312	2	1.5	0.13	5.7
(4360 rpm)	5	0.085–0.312	2	1.6–2.3	0.13–0.09	5.7–8.0
TDE-(Exponential)-SFFF (3.0 ml/min)	5	0.091–0.481	6	1.2	0.17	11.4
(1.5 ml/min)	5	0.091–0.481	6	0.89	0.22	9.0
Disc centrifugation	13	0.5–1.01	2	1.2–1.4	0.17–0.14	4.4–5.3
Packed-Column HDC	14	0.038–0.176	5	0.10	1.9	1.5
Capillary HDC	15	1.0–10.0	50	0.055	3.7	2.6
SEC	19	0.085–0.183	3	0.26	0.76	1.9

* Diameter of polystyrene latex standards in representative samples selected for comparison.

1.5. In this case, for a dynamic range $DR_{d_p} = 10$, peak capacity $N_{max.} = 5.7$ as calculated by eqn. 13b ($N_{max.} = \ln 10 / \ln 1.5 = 5.7$).

Working equations for specific separation methods

Specific particle diameter resolution expressions for SFFF, HDC, SEC and disc centrifugation are summarized in Table I. These relationships have been based on: $b = 1$ for CF-SFFF, $b = -2/3$ for disc centrifugation, $c = \tau \cdot F$ for TDE-SFFF and $c = -1/D_2$ for SEC and HDC, where τ is SFFF exponential-decay time constant (min)⁵, F is the volumetric flow-rate (cm³/min) and D_2 = molecular weight calibration curve constant (ml⁻¹)¹².

RESULTS

Data taken from the literature have been used to develop comparative information in Table II on the dynamic range DR_{d_p} , the specific resolution of $R_{s,1,2}$, the discrimination capacity X_{d_p} , and the peak capacity $N_{max.}$ of several separation methods used for particle size analysis. These comparative values are based on polystyrene latex standards of approximately the same particle size range and separation times of no more than one hour. The highly discriminating $R_{s,1,2}$ value was arbitrarily selected to enable a critical comparison of the high-resolution methods, SFFF and disc centrifugation.

CF-SFFF

The CF-SFFF fractograms shown in Fig. 3a were taken from ref. 5 and analysed in the following manner. At a rotor speed of $\omega = 1710$ rpm the retained 0.312 μ m polystyrene (PS) latex peak exhibits a plate number $N = 103$ for the separation. The specific resolution $R_{s,1,2}$ is calculated by eqn. 7b as 1.5 for this run. Since SFFF separations do not exhibit a constant plate number as a function of retention volume¹⁶, the calculated plate number of the higher force field separation at 4360 rpm increases from 112 to 243 then to 313 for PS peaks C, D and E, respectively. This result causes a $R_{s,1,2}$ value increase of 1.59 to 2.34 to 2.65, respectively. The last peak elutes at about 2.5 h and is not tabulated in the Table II summary because it exceeds our arbitrary comparison guideline of limiting separation times to about one hour. The dynamic range of the separations in Fig. 3a is estimated to be about 2 in particle diameter. This means that in a one-hour analysis with CF-SFFF, the range in particle diameter covered by the separation would be no more than two-fold difference in diameter. This is a very narrow dynamic range and is the inherent disadvantage of CF-SFFF for the analysis of samples with wide particle size distributions.

The calibration plot in Fig. 3b shows the expected linear relationship between particle mass (molecular weight) and retention time, and a non-linear (cubic power) dependence on particle diameter⁵. Increase of force field decreases the slope of the calibration plot, leading to an increase in resolution at the expense of reduced dynamic range for the separation.

TDE-(exponential)-SFFF

The TDE-SFFF separations in Fig. 4a (from ref. 5) performed at two different flow-rates were similarly evaluated in terms of performance. The peaks for $F = 3.0$

and 1.5 cm³/min runs exhibited average σ values of 1.8 and 1.2 ml, respectively ($\tau = 4.76$ min). It should be noted that the results tabulated for TDE-SFFF in Table II are based on a 20-min separation; much higher performance is expected for an one hour analysis. Note also that resolution improves with increasing flow-rate. This result is in keeping with the fact that higher resolution occurs at a higher force field in SFFF. Higher flow-rates in TDE-SFFF cause all particles to elute at a higher force field with resultant higher resolution⁵.

Fig. 4b shows the predicted log-linear TDE-SFFF calibration relationship between the logarithm of particle diameter and retention time⁵. As expected, flow-rate variation changes the range of particle separation but has only a small effect on resolution.

Based on the data in Table II, it is apparent that the dynamic range and peak capacity of TDE-SFFF are significantly larger than those of CF-SFFF. For TDE-SFFF, the dynamic range and peak capacity have been improved with only a slight degradation of values for the specific resolution $R_{s,1,2}$ and discrimination capacity $X_{d,p}$, relative to CF-SFFF. However, on balance, TDE-SFFF is much superior for carrying out particle size analysis. Band broadening corrections are negligible in SFFF and generally are not required in data handling for accurate particle size analyses⁵.

Disc centrifugation

The values in Table II for the performance of the disc centrifugation method are calculated from the separation in Fig. 5a (taken from ref. 13). The disc centrifugation method exhibits high resolution but a narrow dynamic range, much like CF-

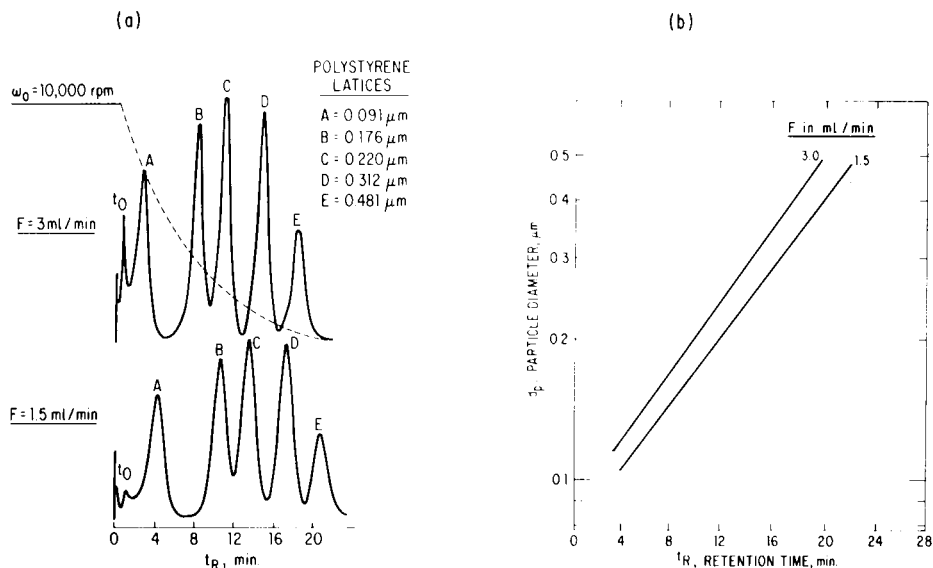


Fig. 4. Exponential field-programmed SFFF data; effect of flow-rate. 10- μ l of polystyrene standards: 0.09% 0.091 μ m; 0.04% ea. of 0.176-, 0.220- and 0.312- μ m; 0.05% 0.481 μ m; detector, UV, 254 nm; 0.1% FL-70 mobile phase; channel, $57 \times 2.54 \times 0.0125$ cm; flow-rate, 3.0 and 1.5 cm³/min; initial rotor speed, 10,000 rpm; decay time constant τ , 4.76 min.

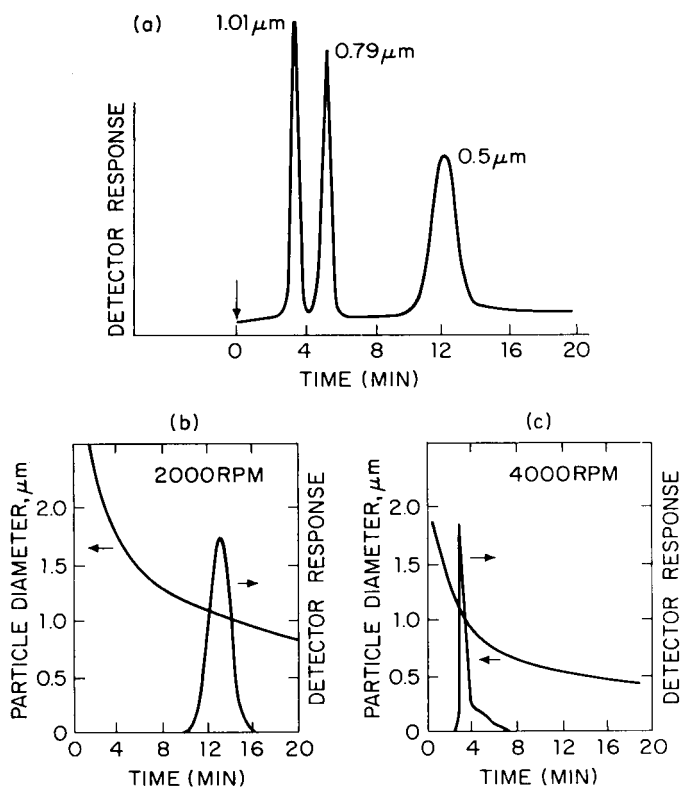


Fig. 5. Disc centrifugation data. 0.5 ml of polystyrene latex mixture dispersion. (a) Separation pattern. Effect of rotor speed on separation: (b) 2000 rpm, (c) 4000 rpm. (Taken from ref. 13.)

SFFF. From the retention characteristics shown in Fig. 5b, the dynamic range of disc centrifugation can be estimated as only about 2, regardless of the field strength used for the separation. As a matter of fact, as shown in Fig. 5c, if the field is too high, the separation range is significantly shifted so that resolution now is seriously degraded. While programming the field strength during analysis would increase the dynamic range of disc centrifugation, such facilities are not currently available in commercial instruments.

Clearly, disc centrifugation exhibits excellent specific resolution, discrimination capacity, and peak capacity, but its dynamic range is relatively small – roughly comparable to CF-SFFF. This limited dynamic range places severe restrictions on the utility of disc centrifugation as a general method for particle size analysis. Also, the high level of operator skill needed with this technique curtails its application.

Disc centrifugation can be used to measure larger particle sizes, up to about 5 μm , compared to about 1 μm for SFFF. Therefore, these methods are somewhat complementary in providing useful data on particles. Because SFFF separates particles according to effective mass while disc centrifugation separates according to sedimentation velocity or particle cross-sectional area, some information regarding particles shape also can be deduced by using both techniques. The Sedigraph is

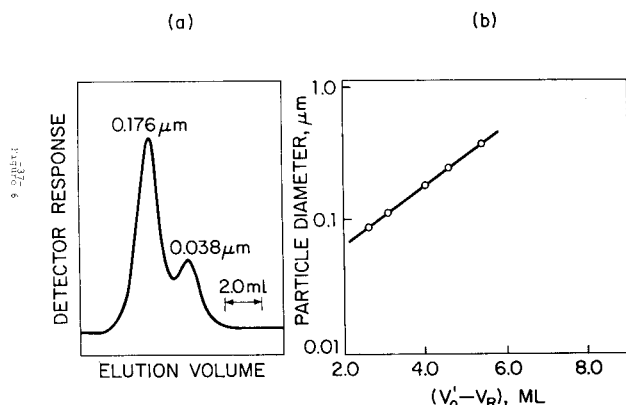


Fig. 6. Column hydrodynamic chromatographic data. (a) Chromatogram; (b) calibration. Polystyrene latices; columns, three 110×0.9 cm of non-porous styrene-divinylbenzene beads, $20 \mu\text{m}$; mobile phase, 1.29 mM sodium dihexylsulfosuccinate; detector, UV. (Taken from ref. 14.)

another sedimentation velocity technique for particle size analysis, but is generally applicable only to larger particles.

Packed-column hydrodynamic chromatography (Col-HDC)

The typical HDC chromatogram shown in Fig. 6a (from ref. 14) exhibits a σ value of 0.68 ml and a D_2 value of 2.11 ml^{-1} . The calibration curve in Fig. 6b indicates a dynamic range of about 5 for Col-HDC. The tabulated data in Table II show that Col-HDC has a much poorer specific resolution, discrimination capacity, and peak capacity than any of the previously discussed methods, but a fairly wide dynamic range is available.

Capillary hydrodynamic chromatography (Cap-HDC)

From the Cap-HDC chromatogram shown in Fig. 7a (from ref. 15), a peak σ value of 4.95 ml , a D_2 value of 0.55 ml^{-1} and a (σD_2) value of 2.7 is calculated. The calibration curve in Fig. 7b shows an effective separation range of $1 \mu\text{m}$ to about $50 \mu\text{m}$, indicating a dynamic range of 50. Based on these values, the performance of Cap-

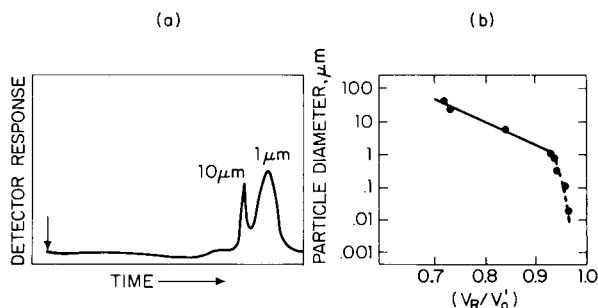


Fig. 7. Capillary hydrodynamic chromatographic data. (a) Chromatogram; (b) calibration. Polystyrene latices; column, $200 \text{ ft.} \times 0.015 \text{ in. I.D.}$; mobile phase, methanol. (Taken from ref. 15.)

HDC was calculated and listed in Table II. This method shows poorer resolution and discrimination capacity than Col-HDC, but a significantly wider dynamic range. However, Cap-HDC clearly is much inferior to all of the other separation techniques in terms of specific resolution, discrimination capacity and peak capacity.

The dynamic range of 50 for Cap-HDC as shown in Fig. 7b seems to be unrealistically large. This reported dynamic range is based on a peak retention volume which elutes 30% earlier than that of the marker peak, that is, $V_R/V'_0 = 0.7$ as indicated in Fig. 7b. However, it has been predicted by theory¹⁶ that the earliest possible elution is limited to a volume of only 15% prior to peak elution volume of the total permeating marker peak, V'_0 . If indeed the smaller available volume for separation predicted by theory is more typical, Cap-HDC exhibits a smaller dynamic range and an even poorer performance than suggested by data in ref. 15.

Unfortunately, both Col- and Cap-HDC suffer from problems of potential column pluggage and poor solute recovery. In both methods, quantitative particle size distribution calculations are difficult and relatively imprecise because of the necessity for making very large corrections for instrumental peak broadening. In many instances HDC also suffers from undesirable effects as result of changes in solute concentration, flow-rate and mobile phase composition.

Size-exclusion chromatography

The use of SEC for particle size separations has been reported in several publications¹⁷⁻¹⁹. Published data on polystyrene standards again can be used¹⁹ for comparing the performance of SEC with the various other separation methods. The two chromatograms in Fig. 8a indicate a σD_2 value of about 0.57 for PS standards. The SEC particle size calibration curves shown in Fig. 8b indicate that SEC has a dynamic range DR_{u_p} of about 3 for materials of this type. Calculations with these data provide the resolution performance information summarized in Table II. SEC compares poorly with SFFF and disc centrifugation, but is generally superior to HDC in most areas.

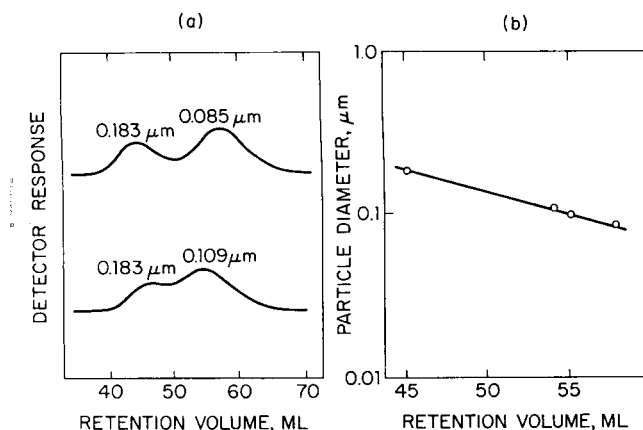


Fig. 8. Size-exclusion chromatographic data. (a) Chromatograms; (b) calibration. Columns: two 2 ft. \times 0.35 in., 3000 Å CPG; mobile phase, water with 1 g/l of Aerosol OT and NaNO_3 ; flow-rate, 0.78 ml/min. (Taken from ref. 19.)

Particle size analyses with SEC sometime suffer from column pluggage and poor solute recovery. Also, since the permeation process in SEC requires that solute particles encounter much of an internal porous surface of the column packings, particle size analyses can be complicated by surface adsorption effects¹⁸. Data handling techniques for SEC also are somewhat complicated, because of significant corrections for peak broadening which must be applied. However, this compares favorably with the extensive peak broadening corrections required for particle size analyses by HDC.

MECHANISTIC VIEW OF RESOLUTION IN SEPARATIONS

The much higher resolution of SFFF documented in Table II compared to SEC and HDC is the result of basic differences in retention mechanisms. SFFF is similar to most liquid chromatography (LC) methods in that all solute particles elute after the unretained solvent peak. In this retentive mode, both LC and SFFF have essentially unlimited retention volumes available for separating sample components. On the other hand, the retention volumes available to SEC and HDC are very limited. Retention in these methods is the result of wall-exclusion effects that cause all solute particles to elute prior to the solvent peak. For SEC, separation is confined within the available pore volume of the column packing, that is, between the interparticle (or total exclusion) volume V'_0 and the total permeation volume V_0 as shown in Fig. 9a.

The HDC effect occurs only in the interstitial volume between the column packing particles. Relative to SEC, an even smaller volume is available for separation in HDC, as illustrated in Fig. 9b. The HDC effect is superimposed on SEC retention

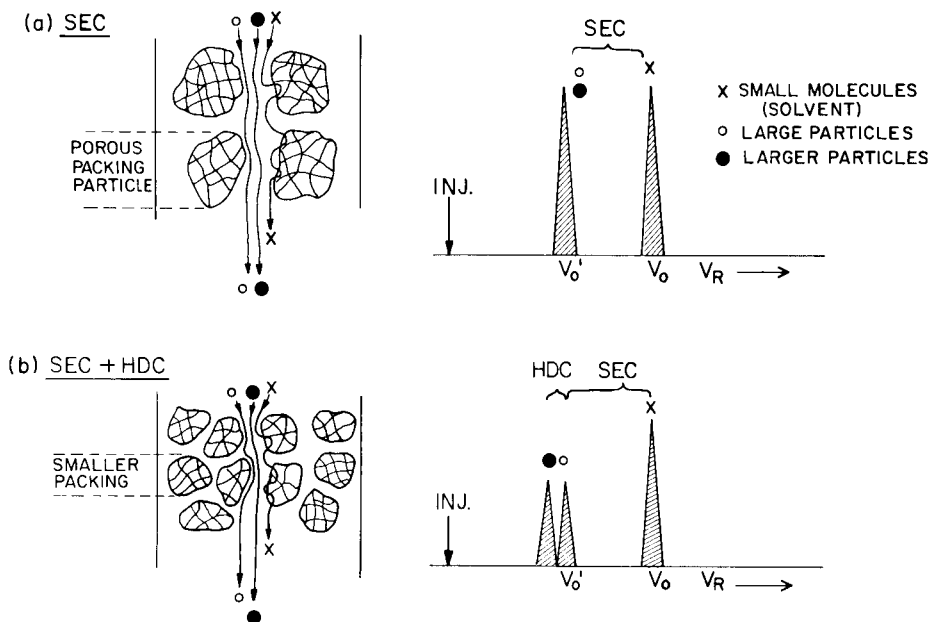


Fig. 9. Comparison of column hydrodynamic and size-exclusion chromatography.

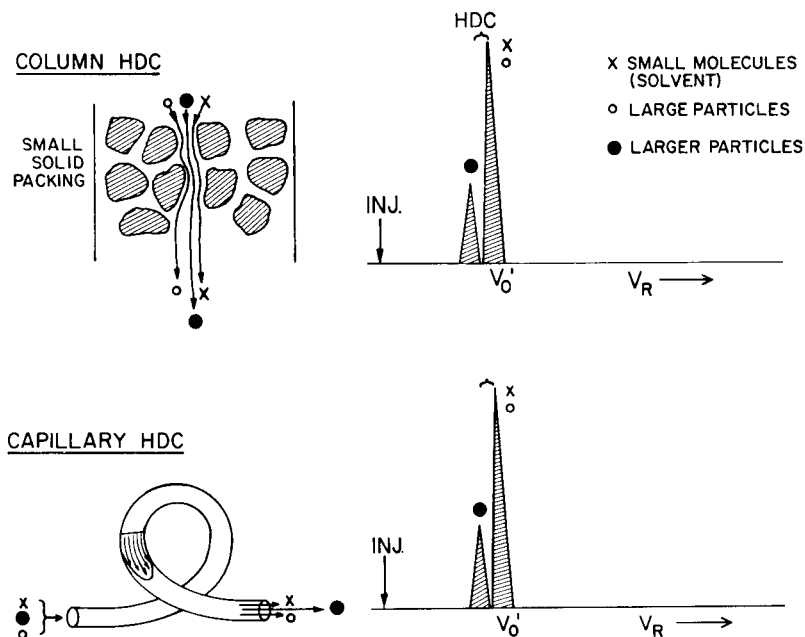


Fig. 10. Comparison of column and capillary hydrodynamic chromatography.

and is only significant when small packing particles are used. In Fig. 10 the elution characteristics of both packed column and capillary HDC are illustrated. A non-porous packing is shown here, but the HDC effect occurs in packed column of both porous and non-porous packing particles. Note that in these methods, just as in SEC, large solute particles elute prior to the mobile phase peak. In both packed-column and capillary HDC the available volume for separation is very small. Only about 15% of the void volume between the column packing particles (*i.e.*, interstitial space) is available for separation. This represents an inherent limitation in the available elution volume range and is directly responsible for the poor resolution of HDC.

On the other hand, SFFF exhibits retention more like LC, with peaks eluting well after the unretained solvent peak. Because of this retentive feature, SFFF has the potential for a very large peak capacity. Fig. 11 illustrates the retention characteristics of SFFF compared to HDC. SFFF is in essence a flow-enhanced equilibrium sedimentation separation. Under an equilibrium sedimentation condition, poorly resolved solute layers are separated by the mobile phase flow which has a laminar (parabolic) velocity profile. With the aid of this flow profile, peaks are highly resolved in SFFF just as in the sedimentation velocity techniques. However, as suggested by the data in Table II, SFFF can have a much higher dynamic range than other methods. In contrast to that found in HDC and SEC, open SFFF channels are expected to be relatively free from pluggage and surface effects.

OTHER PARTICLE SIZE ANALYSIS METHODS

It is also generally feasible to apply the same performance criteria described

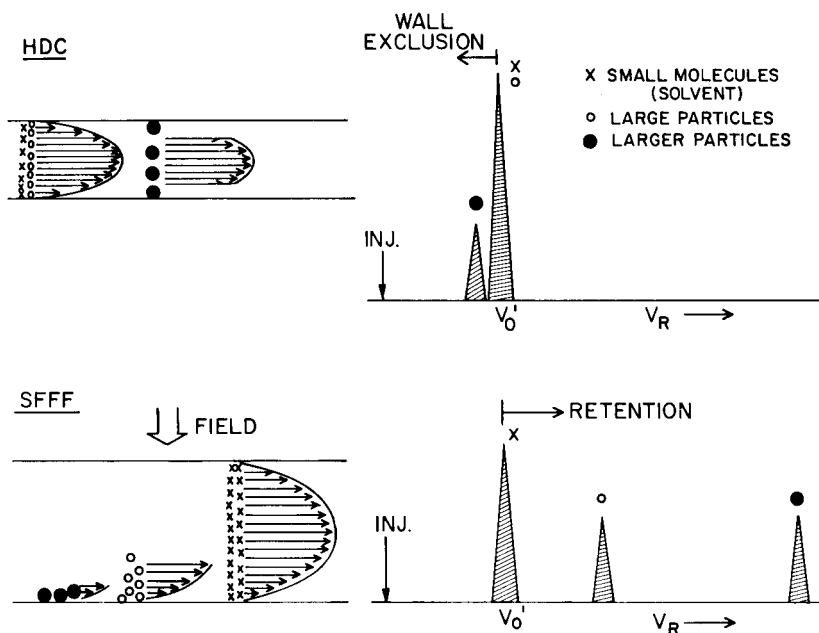


Fig. 11. Comparison of hydrodynamic chromatography and sedimentation field flow fractionation.

above to non-separation particle size analytical methods such as transmission electron microscopy (TEM) and quasi-elastic laser light scattering (LLS) techniques. For example, the Coulter counter is commonly used for determining the size of larger particles, and a typical result is shown in Fig. 12 (taken from ref. 20). In this case, two particle populations with about a seven-fold difference in size are completely resolved. This roughly corresponds to a specific resolution $R_{s,1,2}$ value of 0.04 and a discrimination capacity $X_{d,p}$ value of 5.5, indicating the relatively poor resolution capability of this method. It should be noted that this calculation could be somewhat in error since it

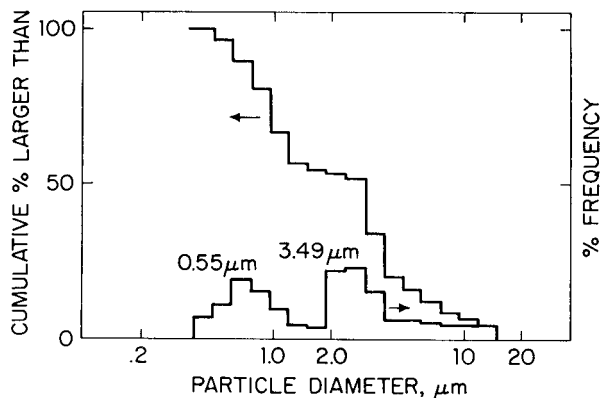


Fig. 12. Coulter counter particle size data. Polystyrene latex standards. (Taken from ref. 20.)

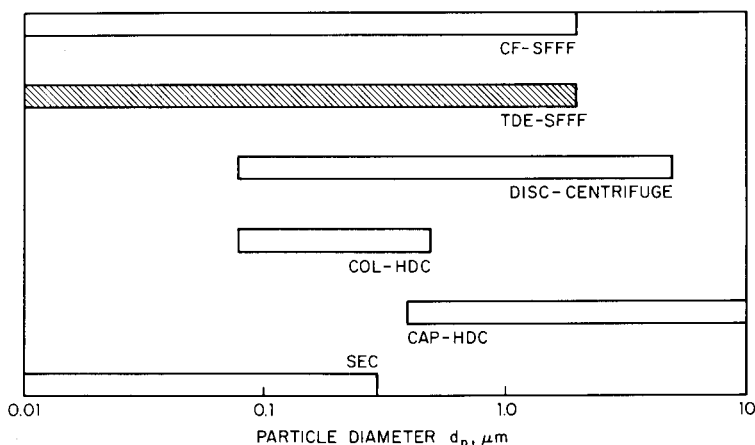


Fig. 13. Accessible particle size range of separation methods.

assumes that the latex particles of each population measured are monodispersed. Nevertheless, it is clear that the resolution of this method is inferior to the other particle size analytical methods listed in Table II. This result suggests that the performance criteria described in this paper can be used for particle size distribution methods other than those based on separations.

Quasi-elastic LLS has been used as a method for rapidly measuring the average size of particles²¹. A computer curve-fitting approach to prepare particle size distribution histograms also has been proposed in an attempt to extract particle size distribution information from the frequency distribution data obtained from light scattering²¹. Unfortunately, the specific resolution of this method is poor. However with the latest techniques, a bimodal distribution has been resolved with a rather poor specific resolution $R_{s,1,2}$ value of 0.3. Also, in this method problems of non-unique solutions sometime occur in the attempt to extract true particle size distributions. The LLS method also suffers from the effect of solute particle concentration dependence and the effect of the angular dependence of the scattered light on particle sizes.

CONCLUSIONS

As illustrated by typical literature data plotted in Fig. 13, SFFF shows a larger total separation range than any of the other separation methods for particle size analysis. However, the more important feature is the range of particle sizes which can be separated in a single experiment, since this feature largely dominates the practical utility of the analytical method. The dynamic range DR_{d_p} of the particle size methods in a single optimum separation is given in Fig. 14a. While Cap-HDC potentially has a wider dynamic range than the other methods, this range is only available for larger particles and at very low resolution.

Fig. 14b has plots of comparative $R_{s,1,2}$ values for the various methods. ($R_{s,1,2}$ distinguishes a 20% difference in particle diameter with a resolution of unity.) SFFF shows approximately equivalent values compared to disc centrifugation, and these methods are highly superior to the others in this regard. For example, TDE-SFFF

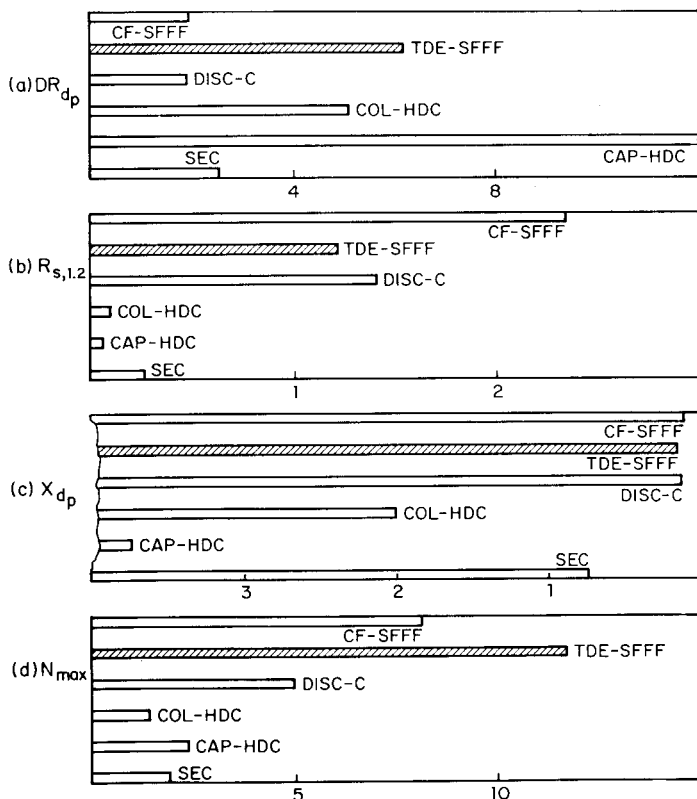


Fig. 14. Comparative resolution performance parameters. (a) Dynamic range, (b) specific resolution, (c) discrimination factor, (d) peak capacity.

shows $R_{s,1,2}$ values which are about 5 times that of SEC and about 11 times that of Col-HDC.

As shown in Fig. 14c, SFFF and disc centrifugation are about equivalent in discrimination capacity X_{dp} , the lower limit in fractional particle diameter difference that can be discerned by a particular method with a resolution of unity. In terms of X_{dp} values, SEC and Col-HDC are significantly less effective, followed by Cap-HDC which is very poor in this regard.

TDE-SFFF clearly is shown in Fig. 14d to have a distinct superiority in peak capacity N_{max} , the maximum number of resolved peaks that can fit into the dynamic range of a particular separation. This is an important advantage since it represents the range of particle sizes which can be characterized in a single experiment. Less effective in this regard are CF-SFFF, disc centrifugation, Cap-HDC, SEC and Col-HDC, in that order.

Since numerical values are sometimes difficult to picture, the specific resolutions of the various methods are compared schematically in Fig. 15 for the particle size methods at two specific resolution levels, $R_{s,1,2}$ and $R_{s,3,0}$ (the latter calculated from the exact specific resolution expressions in the Appendix.) At $R_{s,1,2}$, SFFF and disc centrifugation effectively resolves two particles with a 20% difference in diameter; however, no resolution is evident with the other methods. For a three-fold particle size difference at $R_{s,3,0}$, little or no resolution still is characteristic of the HDC

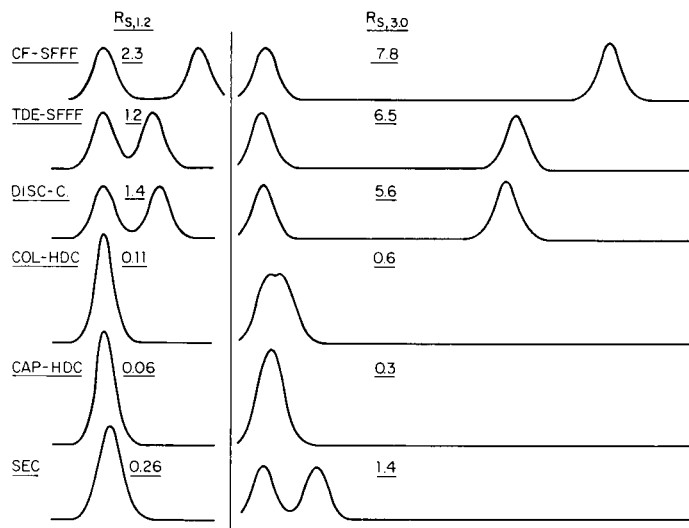


Fig. 15. Comparative resolving power of different separation methods. Left, for $R_{s,1,2}$; right, for $R_{s,3,0}$.

methods and SEC now resolves the two particles. However, TDE-SFFF and disc centrifugation now show enormous resolution for these materials, with CF-SFFF being the most effective.

Clearly, TDE-SFFF is a powerful method for particle size analysis since it possesses a combination of desirable properties, a wide total particle size range, a wide dynamic range for a single experiment, a large specific resolution, a good discrimination factor, and a large peak capacity.

ACKNOWLEDGEMENT

We very much appreciate the critical comments made on this manuscript by D. D. Bly.

APPENDIX

EXACT SPECIFIC RESOLUTION EXPRESSIONS

Case 1 (see Fig. 1 and text)

$$\begin{aligned}
 R_s &= \frac{V_{R_2} - V_{R_1}}{2(V_{R_2} + V_{R_1})\sqrt{N}} \cong \frac{aM_2^b - aM_1^b}{2(aM_2^b + aM_1^b)/\sqrt{N}} \\
 &= \frac{\sqrt{N}}{2} \left(\frac{M_2^b - M_1^b}{M_2^b + M_1^b} \right) = \frac{\sqrt{N}}{2} \left[\frac{(M_2/M_1)^b - 1}{(M_2/M_1)^b + 1} \right]
 \end{aligned}$$

For particle mass:

$$R_{s,X} = \frac{\sqrt{N}}{2} \left[\frac{X^{|b|} - 1}{X^{|b|} + 1} \right] \quad (1a)$$

For particle diameter:

$$R_{s,X} = \frac{N}{2} \frac{X^{3|b|} - 1}{X^{3|b|} + 1} \quad (\text{Ib})$$

where X is ratio of particle masses or particle diameters for a pair of reference particle species. For example, an $R_{s,3}$ value for particle diameter separation describes the expected resolution for a pair of particles with a three-fold difference in particle diameter.

Case II (see Fig. 2 and text)

For particle mass:

$$R_{s,X} = \frac{|c|}{4\sigma} \frac{\Delta \ln M}{\ln X} = \frac{|c|}{4\sigma} \ln X \quad (\text{IIa})$$

For particle diameter:

$$R_{s,X} = \frac{3|c| \cdot \ln X}{4\sigma} \quad (\text{IIb})$$

REFERENCES

- 1 F. J. F. Yang, M. N. Myers and J. C. Giddings, *Anal. Chem.*, 46 (1974) 1924.
- 2 J. C. Giddings, L. K. Smith and M. N. Myers, *Anal. Chem.*, 48 (1976) 1587.
- 3 F. J. F. Yang, M. N. Myers and J. C. Giddings, *J. Colloid Interface Sci.*, 60 (1977) 574.
- 4 J. J. Kirkland, W. W. Yau, W. A. Doerner and J. W. Grant, *Anal. Chem.*, 52 (1980) 1944.
- 5 W. W. Yau and J. J. Kirkland, *Sep. Sci. Technol.*, 1981, in press.
- 6 J. J. Kirkland, S. W. Rementer and W. W. Yau, *Anal. Chem.*, 1981, in press.
- 7 J. J. Kirkland, W. W. Yau and F. C. Szoka, *Science*, 1981, in press.
- 8 W. W. Yau, J. J. Kirkland and D. D. Bly, *Modern Size-Exclusion Chromatography*, Wiley, New York, 1979, Ch. 4.
- 9 W. W. Yau, J. J. Kirkland, D. D. Bly and H. J. Stoklosa, *J. Chromatogr.*, 125 (1976) 219.
- 10 E. Pfannkock, K. C. Lu, F. E. Regnier and H. G. Barth, *J. Chromatogr. Sci.*, 18 (1980) 430.
- 11 J. C. Giddings, *Anal. Chem.*, 39 (1967) 1027.
- 12 W. W. Yau, J. J. Kirkland and D. D. Bly, *Modern Size-Exclusion Chromatography*, Wiley, New York, 1979, Ch. 9.
- 13 T. Provder and R. M. Holsworth, *Preprints, 172nd American Chemical Society Meeting, San Francisco*, 32 (2) (1976) 150.
- 14 A. J. McHugh, D. J. Nagy and C. A. Silebi, in T. Provder (Editor), *Size-Exclusion Chromatography (GPC)*, A.C.S. Sym. Ser. 138, Washington, DC, 1980.
- 15 R. J. Noel, K. M. Gooding, F. E. Regnier, D. M. Ball, C. Orr and M. E. Mullins, *J. Chromatogr.*, 166 (1978) 373.
- 16 C. Orr, Jr., in M. J. Groves (Editor), *Particle Size Analysis*, Heyden, London, 1978, p. 92.
- 17 H. Coll, G. R. Fague and K. A. Robillard, *Exclusion Chromatography of Colloidal Dispersions*, unpublished results, 1975.
- 18 J. J. Kirkland, *J. Chromatogr.*, 185 (1979) 273.
- 19 A. Husain, A. E. Hamielec and J. Vlachopoulos, in T. Provder (Editor), *Size-Exclusion Chromatography (GPC)*, A.C.S. Symposium Series 138, Washington, DC, 1980.
- 20 E. A. Collins, J. A. Davidson and C. A. Daniels, *J. Paint Technol.*, 47 (1975) 35.

RETENTION MECHANISMS

CHROM. 14,089

DEVELOPMENT OF MODERN BIOAFFINITY CHROMATOGRAPHY (A REVIEW)

JERKER PORATH*

Institute of Biochemistry, University of Uppsala, Uppsala (Sweden) and U.E.R. de Biochimie, Université Pierre et Marie Curie, Paris (France)

SUMMARY

The principles of bioaffinity chromatography are presented and illustrated by some applications. The practicability of bioaffinity chromatography depends very much on the solid support (matrix) and the methods chosen for covalent attachment of the ligands that serve as adsorption centres. Some of the significant developments in this area that led to a breakthrough in modern bioaffinity chromatography and the technical developments that ensued are discussed. Future developments are considered.

INTRODUCTION

Several centuries ago a skilful university professor was reputed to be omniscient regarding the accumulated scientific facts and truths of his time. From a Chair in Natural Science he could advance through law and medicine to a position as professor in theology or even to become a bishop. How times have changed! Now we are hardly able to master completely a narrow sector of a specified branch of science.

Consider chromatography, for example, a limited area of separation science which in itself is only a minor division of chemistry. Nobody can keep pace with the output of papers in chromatography, and if one is rash enough to try, there will be no spare time left for one's own research. High-performance liquid chromatography (HPLC) and affinity chromatography are two rapidly developing branches and most participants in this Symposium are experts in HPLC. This is the background, I suppose, for the invitation to me to present a survey of affinity chromatography at this session. I shall outline the main concepts and the scope of bioaffinity chromatography, and shall take the liberty of exemplifying applications by frequent reference to contributions made by my co-workers and myself. This will undoubtedly make my presentation personally biased but perhaps also more authoritative. Those who wish to delve deeper into the subject may consult excellent books¹⁻³ or collections of published lectures in symposia books and review articles⁴⁻⁷.

* Permanent address: Institute of Biochemistry, Biomedical Center, Box 576, S-751 23 Uppsala, Sweden.

GENERAL PRINCIPLES AND POTENTIAL APPLICATION AREAS

Objections have been raised to the term "affinity chromatography" as encompassing a broader area than was originally intended. In this review I shall cover *bioaffinity* chromatography in the restricted sense that the adsorbents used consist of inert solid supports to which naturally occurring substances or closely related compounds of high selectivity have been introduced by covalent coupling to act as adsorption centres. The interactions involved in the adsorption process are usually similar or identical to interactions that occur in nature.

It is indeed true that bioaffinity chromatography in its various forms can be extremely effective and extraordinarily selective. What makes the "new" technique so fascinating is the fact that it takes advantage of nature's own ways of selectively joining, separating and regulating its elements of matter: to form molecular complexes and aggregates of lower or higher order, be it a simple enzyme-inhibitor complex, complicated multienzyme units, antigen-antibody complexes, hormone-receptor complexes or other membrane components or viruses. Indeed, by its nature, biospecific affinity chromatography offers not only means for the rapid and effective isolation of desired biomolecules but also for the study of molecular interactions.

Biologically functioning complexes are formed under the influence of familiar molecular forces and interactions that are systematized under the terms ionic bonds, hydrophobic interactions, hydrogen bonding, Van der Waal's forces, London dispersion forces, dipole-dipole interactions, charge-transfer interactions, etc. Some of these interactions, which take place in aqueous media, often in or at the phase boundaries, are not so well understood. Although there is nothing mysterious about biospecificity it is a concept with blurred or ill-defined boundaries.

Affinity chromatography implies the use of affinity adsorbents, although sometimes the term is used also for the affinity elution of non-specifically adsorbed substances. A chosen matrix substance (matrix substance forms the solid macroreticular network) of natural origin may itself specifically adsorb substances from biological extracts or exudates. For example, polysaccharide-based gels may in rare instances adsorb lectins with affinity for monosaccharide units of the matrix. Usually the affinity adsorbent is prepared by covalently coupling one of the complex-forming partners to the matrix. The covalently immobilized substance is called a "ligand" or adsorption centre and its soluble complement a "ligate". The ligand-ligate complex is an "adsorption complex" (Figs. 1, 4 and 8).

The anchoring of the ligand molecule to the matrix reduces its freedom to interact with the ligate. To counteract this effect, a spacer arm may be introduced between the matrix and the ligand. An important fact that was not recognized in the early days is that the spacer arm should not impart any adverse properties to the adsorbent. For example, it should not act as an adsorption centre itself. In addition, the coupling reaction may result in an immobilized derivative of lower or even negligible biospecificity (meaning the ability to form a specific complex as in free solution).

In its most schematic form, the adsorption-desorption of the ligate may be described by the law of mass action applied to the reaction



where L is the ligand and I the ligate. The upper limit (presumably) of the distribution

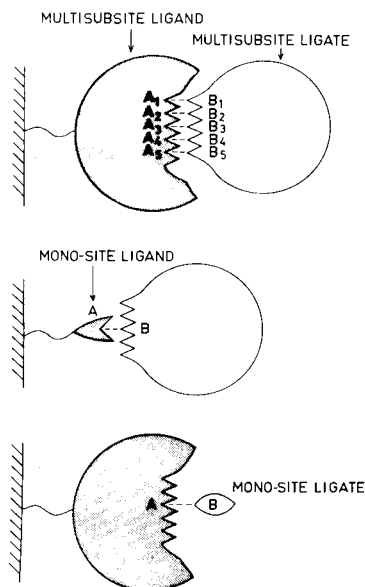


Fig. 1. Schematic representation of the principle of bioaffinity chromatography. An adsorption complex is formed between an insoluble, matrix-bound ligand and a solute (the ligate). Biospecific adsorption occurs as the sum total of many cooperating (unit) interactions within a region of high complementarity (indicated by five interaction sites in the upper figure). Monosite ligands and ligates (if they indeed exist in a strict sense) are likely to form weak, less specific complexes.

constant is the affinity or association constant, K , for L and l in free solution. When $K > 10^5 \text{ M}^{-1}$ the ligand concentration in the solid phase may be kept low and still permit good chromatographic performance. K for an enzyme-inhibitor or -substrate complex is usually in the range 10^4 – 10^8 M^{-1} and the same is true for many antigen-antibody systems.

Usually the adsorption involves multipoint interactions, and the law of mass action in its simple form gives only a very crude account of the thermodynamics of the complex formation and dissociation. Theories on affinity chromatography based on mass action-governed equilibria do not deviate from those of ordinary chromatography. In fact, no theory has been advanced that is uniquely adapted for bioaffinity chromatography. Such a theory should describe chromatographic behaviour in terms of molecular interaction parameters, which means that in addition to all of the complexities encountered in describing molecular interactions of polymers in solution the restrictions caused by the matrix should also be included. It is especially important to clarify, at least in a semiquantitative way, the importance of water. Water plays a fundamental role as a mediator in the ligand-ligate and ligate-matrix interaction.

Yon⁸ introduced the concept "unit interactions" to describe individually weak non-covalent bonds acting to form the complex and to adsorb the ligate to non-specific sites in the adsorbent. Unit interaction, although not possible to define strictly, is a useful descriptive term to account for multipoint adsorption. A protein is adsorbed to a cellulosic-type ion exchanger primarily (in certain pH ranges, perhaps exclusively) by one type of unit interaction, namely, by formation of ionic bonds (perhaps ion exclusion caused by electrostatic repulsion should also be considered as

a kind of unit interaction?). In "pure" amphiphilic agarose adsorbents protein adsorption occurs almost exclusively by unit interactions that are hydrophobic in character.

The same kinds of unit interactions operate in biospecific and non-specific adsorption. However, biospecific adsorption occurs as a result of numerous cooperative unit interactions with localized, close-fitting surface regions on complex-forming biomolecules. In other words, biospecificity depends on the complementarity between the ligand and the ligate molecules with respect to surface geometry and spatial distribution of binding sites within the contact areas. Small deviations from the natural structures of the binding sites occasionally strengthen but usually weaken the adsorption. Attenuation of the interaction by appropriate derivatization may sometimes be recommended to facilitate mild and complete desorption.

In bioaffinity chromatography we exploit some of nature's own information channels. Proteins provide an almost unlimited array of molecular structures. Complementary adaptation to almost any conceivable substance, be it natural or artificial, has therefore been possible. Nature makes use of such adaptative interactions between proteins, enzyme cofactors, nucleic acids, carbohydrates, etc., in catalytically governed reactions and in its molecular signal systems and regulatory devices.

Bioaffinity chromatography may be used as an *in vitro* method to discover unknown biological interactions. For example, a suspected cancerogen may be coupled to agarose and allowed to make contact with liver extract to discover possible interference with liver proteins. Bioaffinity chromatography can also serve to screen biological extracts for the presence of promoters or inhibitors of vital functions, *e.g.*, hormones, nerve impulse transmitters, antihumoral factors and antibiotics.

Adsorbents may be designed that are capable of sensing individual species of very closely related substances. An antibody directed toward a particular unique antigen may thus be singled out from a mixture containing thousands of "sister molecules", all so closely similar in their molecular characteristics that only a biological recognition system can distinguish the substance of interest from the "impurities".

Biospecific hybridization, used in phylogenetic studies and "genetic engineering", depends on base pairing between complementary nucleotide sequences. In fact, such interactions are the background for the functioning of nucleic acids as biological information molecules. Hybridization may be used for affinity chromatographic fractionation of nucleic acids and their degradation products. Complications may be encountered due to complex formation among the nucleotides present together in the liquid phase.

To give some further insight into the potential of bioaffinity chromatography I shall borrow an example from the work of D. E. Koshland and co-workers in which the "induced fit hypothesis" is used to enlighten the complicated key interactions in chemotaxis^{9,10}. Fig. 2 is a schematic representation of how interactions are thought to occur. The small-sized substances, in the concentration gradient in which the bacteria move, interact directly with a membrane protein (as with aspartic acid) or indirectly (as with carbohydrates) by formation of ternary adsorption complexes in which a protein serves to link a substance of small molecular size to another protein. The figure also indicates induced long-distance conformational changes that may be transmitted through the membrane, 30–40 Å or more away from the surface to the

interior of the cell, with the result that carboxylic groups become internally exposed and can react with cytoplasmic proteins. Such changes are suggested to occur in "domino" fashion where amino acid residues slide from one side to the other. This mechanism illustrates how nature makes use of affinity adsorption. Koshland and co-workers used immunoprecipitation to elucidate some of the interactions, but it is easy to visualize how adsorbents carrying the appropriate ligands may be used to isolate free or membrane fragment-bound proteins. In terms of our nomenclature the inter-linking protein may be considered either as a secondary ligand or a primary ligate and we have a "sandwich-type" adsorbate of another kind than that to be discussed later.

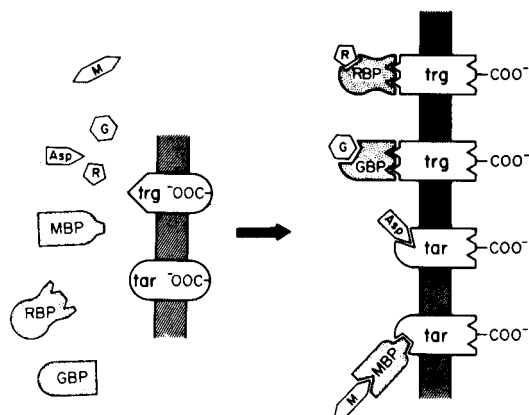


Fig. 2. Hypothetical scheme for induced conformational changes that are involved in the mechanism of bacterial chemotaxis according to Koshland *et al.* It illustrates a system of naturally occurring very complicated ligand-ligate interactions. Methyl-accepting chemotaxis proteins (MCP), coded by the genes *tar* and *trg*, are located in the bacterial membrane. Upon ligand binding the proteins change conformation. As a result, carboxylic groups are exposed on the inner side of the membrane and can interact with cytoplasmic methyltransferase. Aspartic acid binds directly to the primary receptor protein in the membrane while the low-molecular-size solutes galactose, ribose and maltose bind indirectly to the transmembrane proteins via periplasmic solute-binding proteins denoted by GBP, RBP and MBP, respectively. Reproduced by permission of the authors [E. A. Wang and D. E. Koshland, Jr., *Proc. Nat. Acad. Sci. U.S.A.*, 77 (1980) 7157].

DEVELOPMENT OF MODERN BIOAFFINITY CHROMATOGRAPHIC METHODS

Sometimes it is said that chromatography was never discovered, as chromatographic processes occur in the earth's crust when minerals are formed and deposited. If we take this attitude towards the concept of chromatography, we may also maintain that bioaffinity chromatography indeed occurs on a macroscale in nature, *e.g.*, when humus and other debris from rotting plants, microbes or animals filter down through the soil. In the laboratory, occasional attempts have been made to use bioaffinity chromatography during more than half a century before the breakthrough at the end of the 1960s. Those interested in the early contributions in the field should consult our review¹¹ and other books¹⁻³.

The introduction of Sephadex and agarose as supporting media and cyanogen bromide as a coupling agent were contributions that paved the way for the advent of modern bioaffinity chromatography. The methods involved were first briefly de-

scribed in 1967¹² and 1968¹³ and later, together with my co-workers, in more detail^{14,15}.

The term "affinity chromatography" was coined in 1968¹⁶ with the intention of covering a "new" form of chromatography based on biological recognition. This paper by Cuatrecasas *et al.* signalled an immediate breakthrough for affinity separation techniques. Suddenly, all kinds of short cuts to the isolation of biomaterials seemed to be opened. I should point out, however, that our research in Uppsala, which was aimed at the conversion of the molecular sieves Sephadex and Sepharose to a variety of derivatives that could be useful as biospecific adsorbents and for the immobilization of proteins, was a prerequisite for the classical paper of Cuatrecasas *et al.*¹⁶.

The biotin-avidin complex was chosen early as a suitable model for developmental work¹². It also stimulated me to develop charge-transfer chromatography in aqueous solvent systems, a topic that will not be discussed here. The association constant is very large, which makes adsorption extremely efficient but renders elution difficult. The adsorption and desorption of [¹⁴C]biotin went smoothly with quantitative recovery. The reverse procedure, *i.e.*, with biotin as ligand, was a disappointment. We could concentrate avidin directly from diluted hen's eggwhite and obtained in a single-step operation more than a 10,000-fold purification. However, the yield was low and, worse, the adsorption capacity decreased rapidly upon each exposure. The gel thus became useless after two or three adsorption-desorption cycles. The low yield was due to unintended ionic adsorption. The adsorbent had been prepared by coupling avidin to isothiocyanato-Sephadex, which in turn originated from amino-Sephadex. There was thus an excess of free amino groups. This example convinced me that removal of non-specific adsorption centres was an obligatory condition for the preparation of adsorbents of the extreme specificity desired. The fact that cross-linked dextran with a low matrix content is too soft forced me to abandon Sephadex in favour of agarose as a supporting matrix¹⁵. Even with the technical improvements made shortly thereafter, the biotin-avidin model was not easily managed; Cuatrecasas *et al.*¹⁶ used 6 *M* guanidinium chloride to accomplish desorption.

The state of the art at the end of 1967 was described in a paper in *Nature*¹³, from which I cite, "Particularly interesting, however, are the specific adsorbents that can be synthesized by binding adsorption active substances to "Sephadex" or agarose. Substances present in trace amounts in tissue extracts or biological fluids might be purified ten thousand times or more in a single step by specific adsorption. For this reason specific adsorbents, especially immunosorbents, based on cellulose, polystyrene, polyamino acids and other polymers have been prepared in many laboratories. Desorption, however, is a bottle-neck problem. Unsatisfactory desorption may depend on several factors, one of the most important being the presence of fixed charged groups in the polymer used for the preparation of the adsorbents. In my opinion, therefore, "Sephadex" and agarose, particularly the latter, are superior base materials for specific adsorbents... Activation of the carbohydrate with cyanogen bromide in alkali followed by treatment with proteins (amino acids, peptides and so on) in alkaline, neutral or slightly acidic solution will result in coupling of the solute, via its amino group(s), to "Sephadex", agarose or any other carbohydrate. The yields are high under optimum conditions." I have also taken the next example of early applications from the same paper.

Partially deacetylated blood group substance A was covalently coupled to a gel of 2% swollen agarose. A 30-ml volume of human plasma was introduced into the bed of the bioadsorbent which in volume (1×10 cm) was smaller than the sample. The anti-A-isoagglutinin [immunoglobulin(s)], together with some other proteins, were adsorbed on to the column. Most of the non-specifically adsorbed proteins were removed by decreasing the pH from 7.4 to 5.0. Further lowering of the pH to 3.5 caused the desorption of isoagglutinin. The protein concentration was too low to determine by spectrophotometric measurements, but calculation indicated a purification factor in excess of 25,000. The chromatogram is shown in Fig. 3. A more detailed account of our early work may be found in refs. 17 and 18.

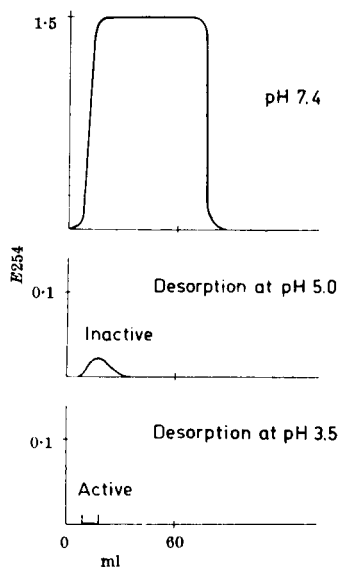
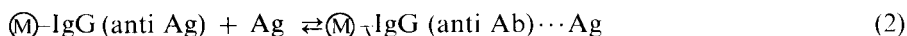


Fig. 3. Isoagglutinin A purification. Human plasma (30 ml) was subjected to bioaffinity chromatography on a column (1×10 cm) of agarose with blood group substance A as ligand. The purification was estimated to be well over 25,000-fold. This experiment was carried out together with T. Kristiansen and L. Sundberg. J. Porath, *Nature (London)*, 218 (1968) 837.

Immunoaffinity chromatography, as just exemplified by the purification of haemagglutinin, deserves some discussion to indicate its potentialities. I shall confine myself to simple complex formation between an antigen (Ag) and immunoglobulin (IgG). The IgG molecule consists of a pair of identical short peptide chains and a pair of identical long chains. The four chains are interconnected so as to give two identical combining sites for the antigen. In other words, the antibody is divalent with respect to the antigen. It is possible to evoke antibodies, in humans or any other mammal, against almost any foreign biopolymer (in the natural state or a derivative, such as a protein to which a low-molecular-weight substance has been coupled as a "hapten").

If an antibody, IgG (anti Ag), *i.e.*, directed toward the antigen, Ag, is coupled to an insoluble carrier, an adsorbent is obtained that can specifically adsorb Ag:



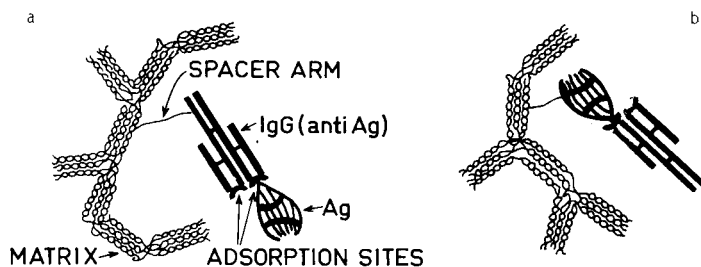
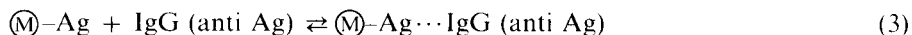


Fig. 4. Schematic representation of the adsorption of (a) antigen, Ag, to its immobilized antibody, Ig (anti Ag) and (b) antibody to immobilized antigen.

The adsorption is shown schematically in Fig. 4a.

It is possible, of course, to attach the antigen (or part of an antigen) to the matrix and thus to obtain an antibody-selective adsorbent, as in the experiment referred to in Fig. 3 and represented schematically in Fig. 4b, according to the reaction:



It is also possible to make antibodies directed toward the whole IgG class of antibodies, for example, anti-human IgG. Such an antibody can thus in turn be coupled to the antigen-antibody complex to form a ternary adsorption complex—a "sandwich complex" (Fig. 5a). The formation of such complexes is utilized in certain types of immunoassays.

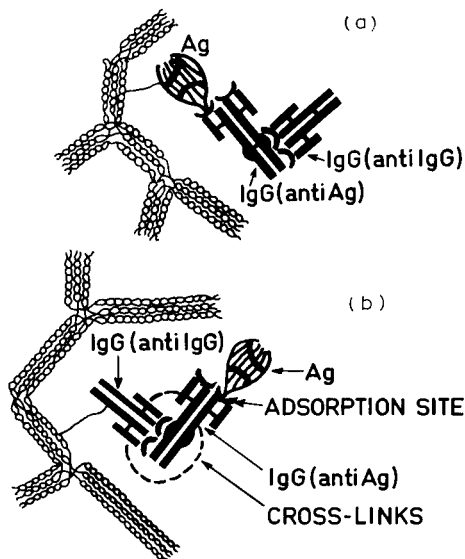


Fig. 5. Schematic representation of the sandwich-type adsorption of (a) immunoglobulin, IgG (anti Ag) against the antigen (Ag) followed by adsorption of antibody to the whole class of immunoglobulin IgG and (b) specific adsorption of antigen (Ag) to a complex ligand formed by covalent fixation of IgG (anti IgG) and subsequent binding of an antibody against antigen. The composite ligand may be cross-linked to prevent elution of IgG (anti Ag).

The flexibility in the use of immunoabsorption methods is perhaps even more apparent if we reverse the order of coupling and anchor IgG (anti IgG) to the matrix (Fig. 5b). We have now prepared an adsorbent directed against Ag but different in nature from that indicated in Fig. 4a.

IgG (anti IgG) may be replaced by Protein A from *Staphylococcus aureus*. Protein A is thus a specific ligand for the class of IgG immunoglobulins¹⁹. It is commercially available under the trade name Protein A-Sepharose CL-4B (Pharmacia, Uppsala, Sweden) as a ready-to-use adsorbent.

Sandwich systems of various kinds are useful for more than the fractionation and isolation of desired substances. For example, multienzyme systems and proteins composed of many subunits may be coupled to the matrix with attachment points in only one or a limited number of the polypeptide chains. The multicomponent system, thus immobilized, is packed to form a bed. Buffers and solvents are passed through the column. Dissociation may be followed by identifying the eluted components. The residual ligands may then be used to study reconstitution of the original complex. Such operations may be regarded as a particular form of bioaffinity chromatography. A useful survey of immunoaffinity methods was given by Ruoslahti²⁰.

We realize now that bioaffinity chromatography is closely related to enzyme immobilization, to hybridization methods with one of the nucleic acid partners adsorbed on to paper or other solid supports and to immunoassay techniques with granular gels. The last technique was first introduced by us prior to the cyanogen bromide method²¹.

Anti IgG-agarose is a group-specific adsorbent binding all kinds of antibodies belonging to the class IgG. Group-specific adsorbents are very useful. The affinity of lectins for carbohydrates has recently been extensively exploited by means of affinity chromatography. Lectins are proteins, often found in plants, which are characterized by their abilities to bind specified hexoses and hexosamines. They also form complexes with many polymers and other derivatives containing hexose or hexosamine residues (glucosides, oligo- and polysaccharides, glycopeptides, glycoproteins and glycolipids). Lectins are therefore effective tools for the isolation of biologically important polymolecular complexes and particles such as viruses, bacteria, whole plant and animal cells and cell fragments.

Agrawal and Goldstein²² in 1967 were the first to isolate a lectin by affinity chromatography, followed not much later by another lectin purification in our laboratory²³. In both cases, the plant extract was passed through a bed of Sephadex and the adsorbed lectin was eluted by including glucose in the buffer. Concanavalin A and a lectin from *Vicia cracca*, respectively, were thus isolated in single-step procedures. It is worth pointing out that the matrix itself exhibits the affinity for the lectin ligate. In the same manner, agarose may be used to "fish out" certain galactose-specific lectins. However, when the affinity requires terminal galactose units it may be advisable to hydrolyse the gel partially or preferably to couple galactose or lactose to the gel. In this way, Ersson *et al.*²⁴ increased the adsorption capacity of agarose gel for *Crotalaria juncea* lectin (Fig. 6).

The converse procedures with coupled lectin as a specific adsorbent for glycoproteins were first published in 1970 by Lloyd²⁵ and independently by Aspberg and myself²⁶.

Many viruses carry binding sites for lectins. In our laboratory Kristiansen has

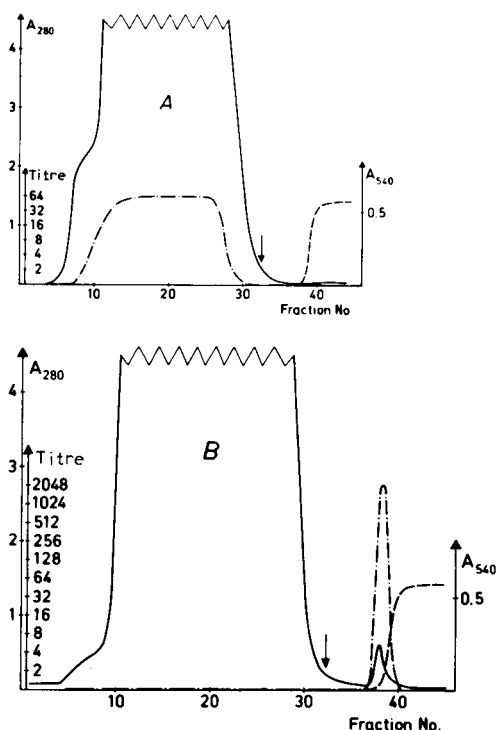


Fig. 6. Bioaffinity chromatography of sunn hemp seed extract. The lectin forms a complex with terminal galactose units. Partially hydrolysed and cross-linked Sepharose 6B is therefore an excellent adsorbent for the lectin (B), whereas untreated gel is not (A). Samples of 40 ml of extract were applied to each column (1.9×10 cm) in 0.05 M sodium phosphate buffer (pH 7.5) containing 1 M sodium chloride (to suppress protein-protein interactions in the solution). After washing, the lectin was eluted biospecifically with 0.1 M lactose included in the buffer. Lactose at that high concentration competes effectively with the galactose residues in the gel. Duration of the experiment: 8 h (at 4°C). ———, $A_{280\text{ nm}}$ ("protein"); - - - - -, haemagglutinin titre; - - - - -, $A_{540\text{ nm}}$ (sugar). B. Ersson, K. Aspberg and J. Porath, *Biochim. Biophys. Acta*, 310 (1972) 446.

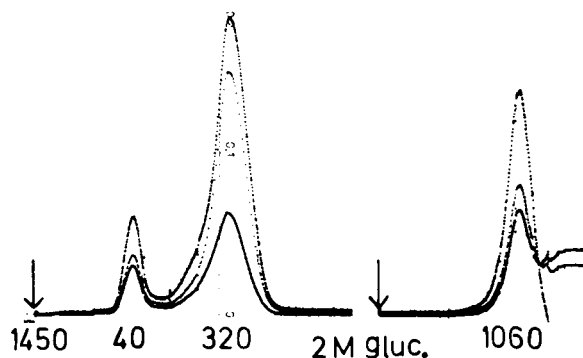


Fig. 7. Bioaffinity chromatography of influenza virus on *Vicia ervilia* lectin-Sepharose 2B. Column volume: 50 ml. Amount of immobilized lectin: 50 mg. The sample (5 ml) was applied at the point indicated by the left-hand arrow and 2 M glucose was then included in the buffer for biospecific affinity elution (right-hand arrow). The numbers refer to haemagglutination titres. The solid lines indicate concentration of solute. With author's permission. T. Kristiansen, *Protides Biol. Fluids*, 23 (1976) 663.

purified whole influenza virus on *Vicia ervilia* lectin Sepharose (Fig. 7). The same column was used more than 20 times with recoveries up to 100%²⁷. Kristiansen and co-workers have also prepared vaccines by lectin affinity chromatography. The virus and its glycoprotein split products adsorb more strongly to concanavalin A-Sepharose than to the *Vicia ervilia* lectin adsorbent, but the yield is much lower. Too strong an interaction is thus a disadvantage, a statement which is true generally in bioaffinity chromatography.

To illustrate the principle as applied to the formation of an enzyme-inhibitor complex, I have selected our isolation of human carbonic anhydrase (Fig. 8). Carbonic anhydrase is the enzyme that catalyses the hydration of carbon dioxide. Simple as this reaction is, it plays a key role in cellular respiration. The enzyme structure has been elucidated by Nyman and collaborators in Gothenburg (primary structure) and by Strandberg, Kannan and their associates in Uppsala (secondary and tertiary structure).

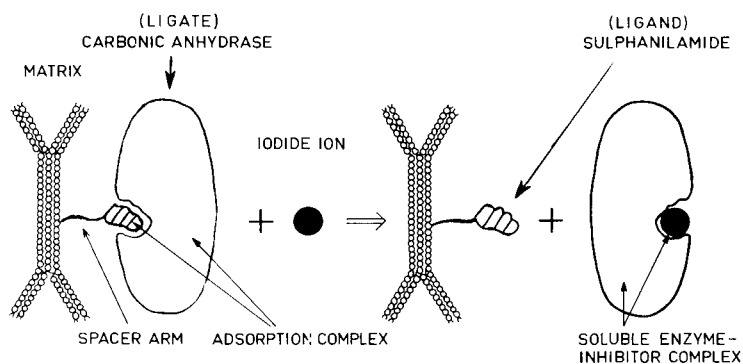


Fig. 8. The principle of using an inhibitor ligand for specific adsorption of an enzyme (carbonic anhydrase) and another inhibitor (iodide ion) for specific desorption. The binding site is often located at an indented region ("cleft" or "cavity") at the protein surface.

The molecule consists of a single peptide chain of 259 amino acid residues folded so as to create a catalytically active site in a 15 Å deep cavity. The cavity has the form of a cone, half the surface of which is hydrophobic and the other half hydrophilic. A zinc atom is located at the bottom of the groove. Inhibitors penetrate into the groove and block the site by replacing water liganded to the zinc. The active site has been mapped in detail. Fig. 9 shows a spacefilling model with the active site in a deep groove²⁸. Halide ions are stronger inhibitors the larger are the ions²⁹. Certain sulphonamides are also strong inhibitors. The binding is reversible. This extensive knowledge of the structure and properties of the enzyme was used by us to design procedures for its isolation³⁰.

Carbonic anhydrase exists in two forms (isoenzymes) in human erythrocytes. The problem is to eliminate all other proteins, including haemoglobin, except the desired enzyme. To this end the cells are first burst by an osmotic shock and the lysed cells are centrifuged to remove the membranes. The clear, strongly red-coloured solution is drained into a bed of Sephadex or Sepharose to which sulphanilamide has been coupled. A chromatogram from such an experiment is shown in Fig. 10. The chromatogram was developed by passage of buffer through the bed followed by the

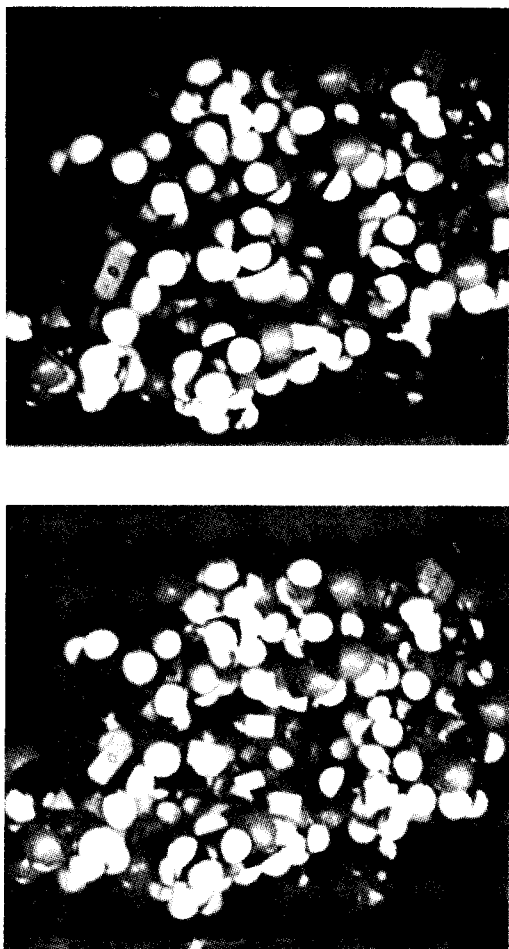


Fig. 9. Packing model of the active site of human carbonic anhydrase C and the same site (cavity) partially occupied by a sulphonamide inhibitor (indicated by the arrows). I. Vaara (1974), *Thesis*, Uppsala University, Uppsala, Sweden. With the author's permission.

same buffer to which sodium iodide had been added. The iodide displaced the sulphonamide from the active site and mobilized the carbonic anhydrase B isoenzyme, leaving the type C enzyme still adsorbed. By exchanging iodide for cyanate the C isoenzyme was easily eluted. Both the B and C isozymes were recovered in pure form and in quantitative yield. The purification factors were of the order of 200 and 4000, respectively.

A very slight modification of the active site may change the adsorption behaviour profoundly. Fig. 11 shows the separation of human carbonic anhydrase B from its monocarboxymethylated derivative.

Sulphanilamide is a "general ligand" for carbonic anhydrase and inhibits the enzyme from any organism. For example, the carbonic anhydrase from the bacterium *Neisseria sicca* can also be isolated from a crude extract by chromatography on

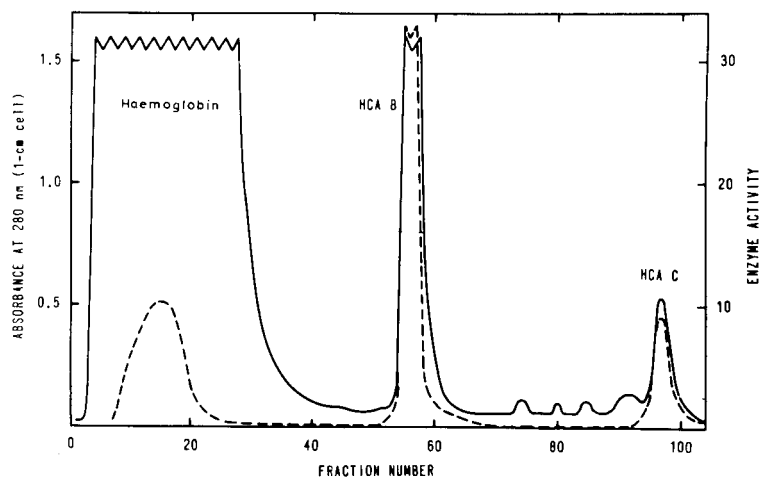


Fig. 10. Chromatogram showing isolation of two human carbonic anhydrase isoenzymes in a haemolysate of erythrocytes (red blood corpuscles). A 25-ml volume of haemolysate was applied to a column (total volume 47 ml) of sulphanilamide-Sephadex G-150 with 0.1 M Tris-sulphate as equilibrating buffer. The isoenzymes were separated by including first 0.1 M sodium iodide and then 0.01 M KOCN in the buffer. Protein concentration, —; enzyme activity, ----. S. O. Falkbring, P. O. Göthe, P. O. Nyman, L. Sundberg and J. Porath, *FEBS Lett.*, 24 (1972) 229.

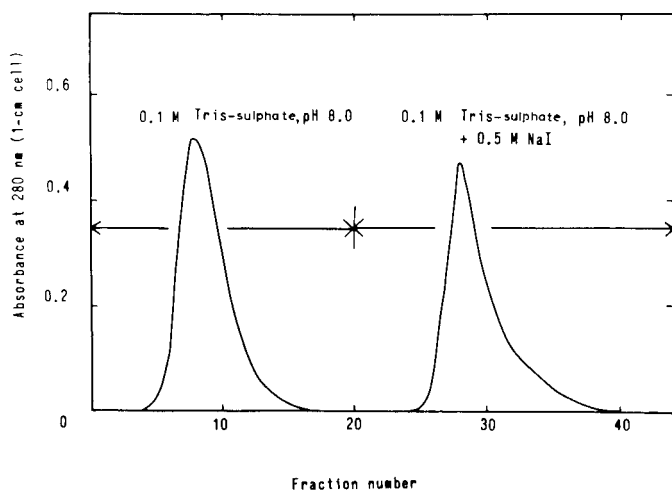


Fig. 11. Chromatogram showing the separation of human carbonic anhydrase B from its derivative in which a histidine side-chain in the active site region has been carboxymethylated. The derivatization reaction was interrupted halfway before completion. The modified protein is not retarded and the native protein requires a competing inhibitor for desorption. In molecular weight the protein and its derivative differ by only about 0.2%. The separation is even more remarkable, however, considering that the outer parts of the surface area are identical for the two molecular species. The separation is almost complete. Adsorbent and reference as in Fig. 10.

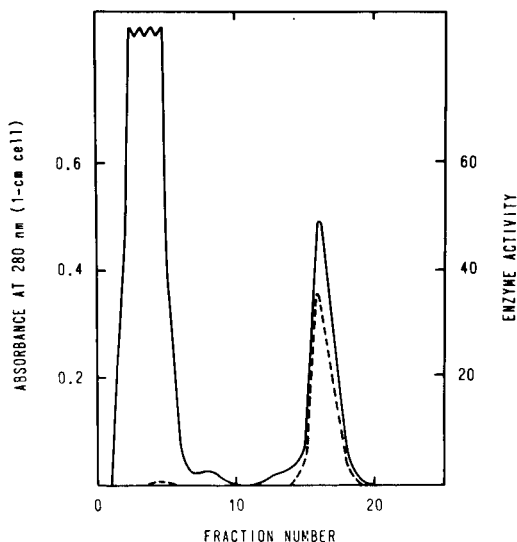


Fig. 12. Chromatogram showing isolation of bacterial carbonic anhydrase on the same adsorbent as in Figs. 10 and 11. The crude extract of *Neisseria sicca* was applied to a 10×1.2 cm I.D. column. Flow-rate, 18 ml/h; fraction volume, 3 ml. Equilibrating buffer, 0.1 M Tris-sulphate, pH 7.5; displacer, 0.01 M KOCN in the equilibrating buffer. Enzyme activity, - - - - -; protein concentration, ———. Reference as in Fig. 10.

sulphanilamide-Sephadex (Fig. 12). The bacterial and human enzymes resemble each other in their inhibition properties and therefore presumably also in their active site.

TECHNICAL ASPECTS

The bioaffinity principle is attractive, simple and almost self-evident. Why, then, did it take so long before affinity chromatography became a routine method in biochemists' laboratories? The reason is trivial: no suitable matrix substance had been found. The introduction of cyanogen bromide as a coupling agent was also of significant importance. Agarose is superior to Sephadex and, according to my experience, also to other matrix media, including polyacrylamide. It is not ideal but has been gradually improved. Many of its assumed weak points seem to have been deliberately exaggerated to favour other products. For example, it has been claimed or insinuated that agarose, being of natural origin, will be microbially degraded. In fact, agarose is attacked by very few organisms³¹ and when cross-linked the gel appears to be resistant even to isolated agarases. Another weakness often pointed out is mechanical instability. Certainly granules of agarose are elastic and will be damaged by harsh treatment. However, the gels are considerably strengthened by cross-linking with agents of suitable length³², but admittedly, even such gels cannot resist the pressures used for HPLC. Are such high pressures necessary or desirable?; possibly for very rapid analysis, but in many instances batch procedures may be preferable and less expensive, as for example for serial immunoassays as practiced in hospitals.

A new type of agar/agarose gel has recently been prepared in my laboratory,

on the basis of our old ideas (Fig. 13). Particles or macromolecules that can be dissolved under conditions that leave agarose gel untouched are included in agarose beads of low matrix concentration. The water is displaced by washing the gel with a suitable organic solvent, *e.g.*, methanol. Upon evaporation of the solvent the gel beads shrink but retain their shape. The gel is then cross-linked in a medium in which the shrunken gel does not swell. The included particles, *e.g.*, silica or protein molecules, are then dissolved out to leave a spongy gel. Such a gel combines the advantages of mechanical strength with high permeability and efficient ligate–ligand interaction.

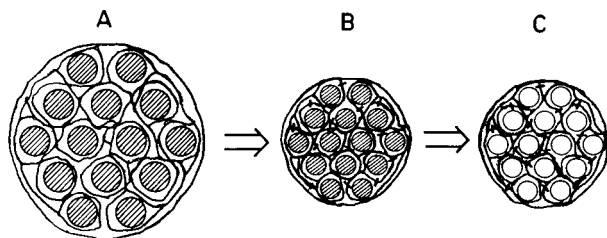


Fig. 13. Schematic representation of how a strong, highly permeable agarose gel may be produced. Small particles or large molecules are included in a gel matrix. The gel is contracted (see text) and cross-linked. The included material is dissolved, leaving "imprints" in the gel (unpublished work).

Porous ceramics and silica gels seem to be the matrix material of choice when extreme mechanical stability is needed. However, non-specific adsorption must be minimized, or preferably eliminated completely, so that protein yields exceeding 99% can be attained. Glyceropropylsilylation, as suggested by Regnier and Noel³³, seems to be promising.

The gels formed by agar and agarose are, owing to their open structure and inner stabilization due to arrangement of the polysaccharide chains into dense bundles of helices, very suitable as starting materials for biopolymer adsorbents. Interestingly, agarose adsorbs proteins and nucleic acids at high salt concentrations. The weak hydrophobicity is presumably due to the ether structure of the anhydrogalactose residues. In my opinion, the adsorption caused by bound water acts as a screen which keeps the solutes away from the matrix and thus provides the biopolymer with a mild environment.

If affinity binding is very weak, the cooperative effect of non-specific ligands may perhaps be an advantage. However, when devising coupling methods we have tried to avoid the introduction of extra adsorption centres that may lower the specificity and complicate desorption. Selection of simple methods has been another guiding principle. Additional demands are that the covalent ligand–matrix linkage should be stable, the coupling yield should be high and the ligand not unduly damaged.

The cyanogen bromide method, which has been criticized as not fulfilling the demand of giving completely stable coupling, is still the most popular method for preparing affinity adsorbents. I prefer oxirane coupling with halohydrins, bis- or trisoxiranes³⁴ and divinylsulphone³⁵. Oxiranes give extremely stable ether, thioether or amine linkages, the drawback being the slow and/or incomplete reactions at low alkalinity. Divinylsulphone and quinone coupling³⁶ have not yet been optimized. As

we would stray too far from the main theme if we go deeper into this subject, I shall instead refer to reviews^{1-7,34}.

Detailed studies aimed at revealing the role of the spacer arm have been carried out by Cuatrecasas *et al.*¹⁶, Lowe³⁷ and O'Carra *et al.*³⁸. The early belief that the spacer arm serves only to reduce steric hindrance received a hard blow when β -galactosidase was observed to adsorb to a "mock affinity" gel with non-ionic spacer arms but without affinity ligands³⁸. The desirability of using hydrophilic non-ionic spacer arms is now generally agreed upon. Such spacer arms of extreme length can be obtained by coupling butanediol bisglycidyl ether to the gel and then converting the terminal oxirane into a sulphydryl group followed by repeated coupling with the same bisglycidyl ether under more mildly alkaline conditions. The hydrophilic spacer arm will then contain 25 atoms with a terminal oxirane group (unpublished work).

If the affinity binding is very strong, desorption may become a serious problem, as was discussed for the biotin-avidin case. Drastic elution procedures may be necessary. For example, in order to dissociate antigen-antibody adsorption complexes extreme pH or chaotropic ions of high concentrations may be tried. There is a considerable risk of damage to the ligate, the ligand or both. Morgan *et al.*³⁹ devised a very mild procedure in which the ligate is eluted electrophoretically by application of an electric field across the gel. Excellent yields were claimed.

Few large-scale applications have been published so far. At the Biochemical Separation Centre in Uppsala Ersson and Brink are routinely processing hundreds of litres of plant extracts for the isolation of lectins on affinity columns with a volume of *ca.* 1 l.

To improve the separation power of bioaffinity methods further we should strive for higher chemical selectivity rather than for increased plate numbers. The distribution is almost always one-sided, *i.e.*, the ligate is found quantitatively in one

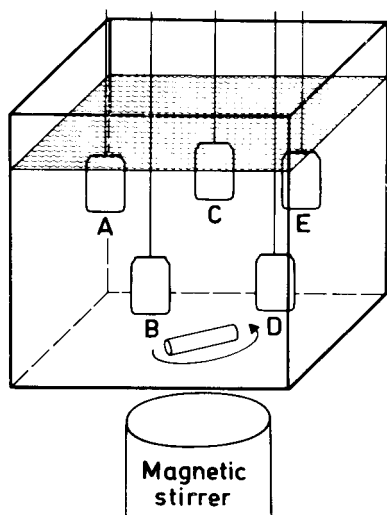


Fig. 14. The "tea bag" procedure for simultaneous adsorption of many solutes. Each nylon net bag is filled with different granular adsorbents and immersed in the solution or suspension containing the desired substances. The bags are removed after equilibrium has been attained and placed in funnels that fit the bags, and elution is executed with suitable displacers.

of the phases: in solution or adsorbed. Isocratic elution is seldom practicable in bioaffinity chromatography, which means that bed procedures are used more for convenience than of necessity. At the extremes, where very small or large volumes are to be handled, batch procedures are more appropriate. Extraction from a solution only 1 μ l or less in volume may be easier by means of a single particle or a slip of paper with covalently bound ligand followed by washing. For large amounts, when many substances are to be isolated, the "tea bag" principle¹¹ can be used (Fig. 14). Industrial application may require fluidized bed techniques.

"Magnetogels" with permanent magnets, usually iron oxide particles, in the gel may be included to facilitate collection of the gel from the suspension⁴⁰, but the risk of extra adsorption and other adverse effects should not be neglected.

RECENT DEVELOPMENTS AND FUTURE PROSPECTS

Hydrophobic interaction, charge-transfer and metal-chelate adsorption chromatography as applied to biological materials are all closely related to the topic of this review, but I shall not discuss them here. Covalent chromatography may also be included among the affinity methods that are in a phase of rapid development. Chromatography is thus joined to solid-phase synthesis, carrier-bound drugs and the use of immobilized enzymes as tools in biotechnology. The synthesis of ligands of high stereoselectivity is in an initial stage of development. Polymer-attached crown ethers and other ion-selective substances should be mentioned, as well as adsorbents for resolving racemic mixtures. In the end we may perhaps synthesize extremely selective adsorbents suitable for fractionation work in organic solvents.

Chryobiology seems to have enormous potentialities and will no doubt be even more exploited in the future. Relevant to my subject is the pioneering work carried out by Douzou and Balny^{41,42}, who have begun to perform subzero bioaffinity chromatography. Denaturation is retarded upon lowering the temperature and ceases almost completely well below zero. Isolation may then take place in hydroorganic solvents. A new field of application opens up, wherein it might be possible, for example, to isolate enzyme-substrate complexes which at ordinary temperatures exist with half-lives of the order of milli- or microseconds.

An increasing demand for extremely selective methods for the isolation and analysis of highly complex natural, reconstituted or semi-synthetic biologically functioning entities including cells and modified cells can be anticipated. For such purposes chromatography is likely to be replaced by other methods. Batch procedures based on biospecific adsorption have often been used in the past. The elegant nylon fibre method of Edelman *et al.*⁴³ should be mentioned. Liquid-liquid extraction with polymer phase systems as introduced by Albertsson⁴⁴ is another attractive technique of great potential. High selectivity in the extraction can be obtained by including polymeric bioaffinity carriers in the system ("bioaffinity partition"). The conversion of such methods into bioaffinity partition chromatography is a challenging task, perhaps not entirely hopeless if only a suitable support can be found. In any case, accumulated knowledge from the developmental work aimed at the refinement of bioaffinity chromatography will also serve to improve the related methods mentioned.

CONCLUDING REFLECTIONS ON THE ART OF SEPARATION

When enjoying a masterpiece of painting we usually think of the painter but never give a thought to the inventor of the paint; when we listen to a symphony we never give a thought to those who made music possible, the instrument makers. Artists are more likely to be recognized than the artisans, who used to be anonymous. Yet art could never have come into existence without invented tools. We may expand the analogy to other fields, to science and technology. The increase in our knowledge of the structure and function of living matter on the molecular level that we have witnessed during the last 25 years would hardly have been possible without the introduction and refinement of physical and chemical methods for the fractionation of biological material down to its molecular entities. This simple fact is seldom appreciated by those who receive the credit for progress in molecular biology.

The points I have just made will perhaps be interpreted in terms like the cook's appraisal of his own food. This is not my intention. In a world of diminishing understanding and support of research, especially in natural sciences, and, as a consequence of that attitude, the harder struggle for financial backing and personal recognition, it becomes necessary that we who devote our time and labour to the art of fractionation, advertise our achievements and struggle for a better general understanding of the key role of our specialities, and by doing so, contribute to the further advance of other more illustrious branches of natural science.

Separation science, especially as applied to biology in the form of affinity methods, offers thrilling adventures and challenging strategic problems often closely associated with biologically highly significant and important phenomena. In addition, separation science is justified in itself, being a branch of "scheikunde" (the Dutch name for chemistry).

REFERENCES

- 1 C. R. Lowe and P. D. G. Dean. *Affinity Chromatography*, Wiley, Chichester, 1974.
- 2 J. Turková, *Affinity Chromatography*, Journal of Chromatography Library, Vol. 12, Elsevier, Amsterdam, 1978.
- 3 C. R. Lowe, *An Introduction to Affinity Chromatography*, in T. S. Work and E. Work (Editors), *Laboratory Techniques in Biochemistry and Molecular Biology*, Vol. 7, Part II, North-Holland, Amsterdam, 1979.
- 4 B. Jacoby and M. Wilchek (Editors), *Methods in Enzymology*, Vol. 34, *Affinity Techniques*, Academic Press, New York, 1974.
- 5 R. Epton (Editor), *Chromatography of Synthetic and Biological Polymers*, Vol. 2, *Hydrophobic, Ion-Exchange and Affinity Methods*, Published for The Chemical Society Macromolecular Group by Ellis Horwood, Chichester, 1978.
- 6 O. M. Hoffmann-Ostenhof, F. Breitenbach, F. Koller, D. Kraft and O. Scheiner (Editors), *Affinity Chromatography*, Pergamon Press, Oxford, New York, 1978.
- 7 J. M. Egly (Editor), *Chromatographie d'Affinité et Interaction Moléculaire*, Les éditions de l'Institut National de la Santé et de la Recherche Médicale (available from INSERM, Paris), Paris, 1979.
- 8 R. J. Yon, Ref. 7, p. 109.
- 9 D. E. Koshland, Jr., *TIBS*, (1980) 297.
- 10 E. A. Wang and D. E. Koshland, Jr., *Proc. Nat. Acad. Sci. U.S.*, 77 (1980) 7157.
- 11 J. Porath and L. Sundberg, in M. L. Hair (Editor), *The Chemistry of Biosurfaces*, Vol. II, Marcel Dekker, New York, 1979, pp. 633-661.
- 12 J. Porath, in J. Killander (Editor), *Nobel Symposium 3, Gamma Globulins*, Almquist and Wiksell, Stockholm; Wiley, New York, 1967, p. 287.

- 13 J. Porath, *Nature (London)*, 218 (1968) 834.
- 14 R. Axén, J. Porath and S. Ernback, *Nature (London)*, 214 (1967) 1302.
- 15 J. Porath, R. Axén and S. Ernback, *Nature (London)*, 215 (1967) 1491.
- 16 P. M. Cuatrecasas, M. Wilchek and C. B. Anfinsen, *Proc. Nat. Acad. Sci. U.S.*, 61 (1968) 636.
- 17 T. Kristiansen, L. Sundberg and J. Porath, *Biochim. Biophys. Acta*, 184 (1969) 93.
- 18 T. Kristiansen, *Biochim. Biophys. Acta*, 263 (1974) 567.
- 19 H. Hjelm, K. Hjelm and J. Sjöqvist, *FEBS Lett.*, 28 (1972) 73.
- 20 E. Ruoslahti (Editor), *Immunsorbents in Protein Purification*, University Park Press, Baltimore, 1976.
- 21 L. Wide and J. Porath, *Biochim. Biophys. Acta*, 130 (1966) 257.
- 22 B. B. L. Agrawal and I. J. Goldstein, *Biochim. Biophys. Acta*, 147 (1967) 262.
- 23 K. Aspberg, H. Holmén and J. Porath, *Biochim. Biophys. Acta*, 160 (1968) 116.
- 24 B. Ersson, K. Aspberg and J. Porath, *Biochim. Biophys. Acta*, 310 (1973) 446.
- 25 K. O. Lloyd, *Arch. Biochem. Biophys.*, 137 (1970) 460.
- 26 K. Aspberg and J. Porath, *Acta Chem. Scand.*, 24 (1970) 1839.
- 27 T. Kristiansen, *Protides Biol. Fluids*, 23 (1976) 663.
- 28 I. Vaara, *The Molecular Structure of Human Carbonic Anhydrase, Form C and Inhibitor Complexes*, Dissertation; *Acta Univ. Upsaliensis*, 1974, Uppsala, Sweden.
- 29 K. K. Kannan, in R. Srinivasan (Editor), *Biomolecular Structure, Conformation, Function and Evolution*, Vol. I, Pergamon Press, Oxford, 1980, p. 165.
- 30 S. O. Falkbring, P. O. Göthe, P. O. Nyman, L. Sundberg and J. Porath, *FEBS Lett.*, 24 (1972) 229.
- 31 M. Malmqvist, *Acta Univ. Upsaliensis*, 1977, 406, Uppsala, Sweden (Dissertation).
- 32 J. Porath, T. Låås and J.-C. Janson, *J. Chromatogr.*, 103 (1975) 49.
- 33 F. E. Regnier and R. Noel, *J. Chromatogr. Sci.*, 14 (1976) 316.
- 34 L. Sundberg and J. Porath, *J. Chromatogr.*, 90 (1974) 87.
- 35 J. Porath and R. Axén, in K. Mosbach (Editor), *Methods in Enzymology*, Vol. 44, *Immobilized Enzymes*, Academic Press, New York, 1976.
- 36 J. Brandt, L. O. Andersson and J. Porath, *Biochim. Biophys. Acta*, 386 (1975) 196.
- 37 C. R. Lowe, *Eur. J. Biochem.*, 73 (1977) 265.
- 38 P. O'Carra, S. Barry and T. Griffin, *Methods Enzymol.*, 34 (1974) 108.
- 39 M. R. A. Morgan, P. J. Brown, M. J. Leyland and P. D. G. Dean, *FEBS Lett.*, 87 (1978) 239.
- 40 K. Mosbach and L. Andersson, *Nature (London)*, 270 (1977) 259.
- 41 P. Douzou and C. Balny, *Advan. Protein Chem.*, 32 (1978) 77.
- 42 C. Balny and P. Douzou, *Ref. 7*, p. 99.
- 43 G. M. Edelman, U. Rutishauer and C. F. Millette, *Proc. Nat. Acad. Sci. U.S.*, 68 (1971) 2153.
- 44 P. A. Albertsson, *Partition of Cell Particles and Macromolecules*, Almquist and Wiksell, Stockholm. 2nd ed., 1971.

CHROM. 14,222

SYSTEMATIC STUDY OF TERNARY SOLVENT BEHAVIOUR IN REVERSED-PHASE LIQUID CHROMATOGRAPHY*

PETER J. SCHOENMAKERS*, HUGO A. H. BILLIET and LEO DE GALAN

Laboratorium voor Analytische Scheikunde, Technische Hogeschool Delft, Jaffalaan 9, 2628 BX Delft (The Netherlands)

SUMMARY

An extensive experimental survey of the retention behaviour of 32 solutes in the system methanol–tetrahydrofuran–water and 49 solutes in the system methanol–acetonitrile–water is presented. The retention data are fitted to a second order six-parameter equation, describing the capacity factor as a function of mobile phase composition. Iso-elutotropic lines, *i.e.*, lines that connect solvents of equal elutotropic strength, are constructed in the ternary diagrams for the two systems and compared with theoretical lines, predicted from solubility parameter theory. Specific effects are defined as variations in retention for a particular solute, using solvents of equal elutotropic strength. Such effects appear to be larger between different binary mixtures than within the ternary triangle. Ternary solvents thus provide a smooth transition between two limiting binary mixtures.

INTRODUCTION

Phase systems in liquid chromatography can be evaluated using three characteristics:

(i) Retention which is determined by the polarity of the solute, relative to that of the mobile and stationary phases, and by the absolute difference between the polarities of the two phases.

(ii) The latter factor also determines the selectivity of the system, *i.e.*, its general separation power. Therefore, in general, the selectivity of the system cannot be increased without at the same time increasing retention. For example, in reversed-phase liquid chromatography (RPLC), the addition of more water to the mobile phase usually results in an increase of both retention and selectivity¹.

(iii) The specificity of the system, *i.e.*, its increased separation power for certain pairs of solutes, which arises from specific interactions between the solute molecules and those of the chromatographic phases. Unlike retention and selectivity, specificity is hard to predict for LC phase systems.

In RPLC we use a single stationary phase of low polarity for many different

* Part of the Ph.D. Thesis of P.J.S.

samples. By using binary mixtures, the polarity of the mobile phase can be increased continuously until, for a given sample, retention reaches a practical upper limit. This mobile phase will lead to the highest possible selectivity. Different binary mobile phases can be prepared with the same polarity, *e.g.*, a mixture of 60% (v/v) methanol and 40% water has the same polarity as acetonitrile–water (47:53) or tetrahydrofuran (THF)–water (37:63)². Such binary mobile phases of equal polarity can be shown to produce considerable specific effects³. There is, however, a very small number of organic modifiers that can be used in such binary mixtures with water. Many more mobile phases of the same polarity can be used, if we include ternary mixtures. For example, the 60% methanol and the 47% acetonitrile solvents can be mixed in any arbitrary ratio to yield an infinite number of possible ternary mobile phases. Hence, ternary mobile phases greatly increase our flexibility to search for optimum specificity.

In recent years, many practical examples of the advantageous use of ternary mobile phases in RPLC have been published (*e.g.*, refs. 4–8). Also, the combination of water with three organic modifiers has been shown to be of practical use⁸.

The first systematic investigation of ternary mobile phases was performed by Bakalyar *et al.*⁴. They compared seven ternary mixtures containing 50% (v/v) water, 40% methanol and 10% of a second organic modifier. The binary mixture of 50% methanol and 50% water was used as a reference. At first sight the specific effects they reported appear to be striking, but they are obscured by considerable differences in retention between the different mobile phases. Indeed, the specific effects largely vanish when we normalize the retention data in such a way that the same average retention is obtained as for the reference mixture. The remaining differences are much smaller, and give a better insight into the specificity of the different systems. Nevertheless, it is true that even such minor differences can be exploited in practice.

A more recent systematic study of the behaviour of ternary and quaternary mixtures of water, methanol, THF and acetonitrile was reported by Glajch *et al.*⁸. They describe procedures to search for optimal multicomponent mobile phases.

In this paper we report a systematic study of the retention behaviour of two ternary mobile phase systems (methanol–acetonitrile–water and methanol–THF–water). We varied the composition of all constituents from zero to 100%. The data are used to define ternary compositions of equal polarity and to analyse specific separation effects.

THEORETICAL

Retention in RPLC using ternary mobile phases

In previous work we have used the solubility parameter concept to establish the general shape of the relationship between the capacity factor and the binary mobile phase composition⁹. Moreover, this concept yields good estimates of the compositions of different binary solvents that lead to equal retentions². Therefore, we feel encouraged to use it in a similar way for ternary systems.

In LC, the capacity factor can be expressed in terms of activity coefficients¹⁰

$$k_i = \frac{\gamma_{i,m}}{\gamma_{i,s}} \cdot \frac{n_s}{n_m} \quad (1)$$

where $\gamma_{i,m}$ and $\gamma_{i,s}$ are the activity coefficients of the solute i in the mobile and stationary phase, respectively, and n_s and n_m are the number of moles of the two phases present in the column. Eqn. 1 is based on the pure liquid solute as the standard state for both phases.

We described elsewhere² how the activity coefficients can be expressed in terms of total solubility parameters. If we neglect entropy effects (*cf.*, ref. 2), we find

$$RT \ln \gamma_{i,f} = v_i (\delta_i - \delta_f)^2 \quad (2)$$

where R is the gas constant ($1.9865 \text{ cal K}^{-1} \text{ mole}^{-1}$), T is the absolute temperature ($^{\circ}\text{K}$), $\gamma_{i,f}$ is the activity coefficient of solute i in phase f , v_i is the molar volume of the solute ($\text{cm}^3 \text{ mole}^{-1}$) and δ is the solubility parameter ($\text{cal}^{1/2} \text{ cm}^{-3/2}$)*. Combination of eqns. 1 and 2 now results in:

$$\ln k_i = \frac{v_i}{RT} [(\delta_i - \delta_m)^2 - (\delta_i - \delta_s)^2] + \ln \frac{n_s}{n_m} \quad (3)$$

As before⁹, we will assume that the solubility parameter of a mixture can be found from that of its constituents as

$$\delta_{\text{mix}} = \sum_{j=1}^N \varphi_j \delta_j \quad (4)$$

for a mixture of N constituents, each with volume fraction φ_j and solubility parameter δ_j . Since, of course, $\sum_{j=1}^N \varphi_j = 1$, eqn. 4 can be written for a ternary mixture as:

$$\delta_{\text{mix}} = \varphi_1 \delta_1 + \varphi_2 \delta_2 + (1 - \varphi_1 - \varphi_2) \delta_3 \quad (5)$$

From now on we will assign the subscript 1 to methanol and 3 to water. The subscript 2 will then refer to the second organic modifier (acetonitrile or THF).

Substitution of eqn. 5 into eqn. 3 yields

$$\ln k_i = \frac{v_i}{RT} \{[\delta_i - \varphi_1 \delta_1 - \varphi_2 \delta_2 - (1 - \varphi_1 - \varphi_2) \delta_3]^2 - (\delta_i - \delta_s)^2\} + \ln \frac{n_s}{n_m}$$

and after rearrangement:

$$\begin{aligned} \ln k_i = \frac{v_i}{RT} & \cdot [\varphi_1^2 (\delta_1 - \delta_3)^2 + \varphi_2^2 (\delta_2 - \delta_3)^2 + \\ & + 2 \varphi_1 (\delta_i - \delta_3)(\delta_3 - \delta_1) + 2 \varphi_2 (\delta_i - \delta_3) \times \\ & \times (\delta_3 - \delta_2) + (\delta_3 - \delta_i)^2 - (\delta_s - \delta_i)^2 + \\ & + 2 \varphi_1 \varphi_2 (\delta_3 - \delta_1)(\delta_3 - \delta_2)] + \ln \frac{n_s}{n_m} \end{aligned} \quad (7)$$

* Historically (*cf.*, ref. 10) the solubility parameter is expressed in $\text{cal}^{1/2} \text{ cm}^{-3/2}$. The conversion to S.I. units reads: $1 \text{ cal}^{1/2} \text{ cm}^{-3/2} = 2.05 \text{ MPa}^{1/2}$.

This equation describes the dependence of the capacity factor on the composition of the mobile phase. It is of the form

$$\ln k = A_1 \varphi_1^2 + A_2 \varphi_2^2 + B_1 \varphi_1 + B_2 \varphi_2 + C + D \varphi_1 \varphi_2 \quad (8)$$

with:

$$A_1 = \frac{v_i}{RT} \cdot (\delta_1 - \delta_3)^2 \quad (9)$$

$$A_2 = \frac{v_i}{RT} \cdot (\delta_2 - \delta_3)^2 \quad (10)$$

$$B_1 = \frac{2v_i}{RT} \cdot (\delta_i - \delta_3)(\delta_3 - \delta_1) \quad (11)$$

$$B_2 = \frac{2v_i}{RT} \cdot (\delta_i - \delta_3)(\delta_3 - \delta_2) \quad (12)$$

$$C = \frac{v_i}{RT} \cdot [(\delta_3 - \delta_i)^2 - (\delta_s - \delta_i)^2] + \ln \frac{n_s}{n_m} \quad (13)$$

$$D = \frac{2v_i}{RT} \cdot (\delta_3 - \delta_2)(\delta_3 - \delta_1) = 2\sqrt{A_1 A_2} \quad (14)$$

Eqn. 8 expresses a non-linear dependence of the logarithm of the capacity factor on the two volume fractions of organic modifier. A representative example of its behaviour is shown in Fig. 1. The composition of the ternary mobile phase is represented by the usual equilateral triangle in the horizontal plane at the base. The capacity factor is plotted vertically on a logarithmic scale. The surface described by eqn. 8 is curved, but otherwise quite smooth. Local maxima or minima, discontinuities or asymptotes cannot be observed.

In binary mobile phase systems, the generally non-linear relationship between $\ln k$ and composition can be approximated by a straight line over a limited range of k values ($1 < k < 10$)¹. It should be noted, however, that it does not appear to be feasible to approximate the surface described by eqn. 8 by a plane over a wide range of ternary compositions.

If we consider the values of the solubility parameters of the different mobile phase constituents, some further predictions can be made. The respective δ values are given in Table I. Using these values we expect A_2 to be much larger than A_1 , and, of course, both are positive. Since the solubility parameter of the solute will be of the order of $10 \text{ cal}^{1/2} \text{ cm}^{-3/2}$, B_1 and B_2 are expected to be strongly negative, again with the absolute value of B_2 larger than that of B_1 . The value of D is the geometric mean of that of A_1 and A_2 and is thus expected to be positive. Finally, C is, strictly speaking, equal to $\ln k_w$, the logarithm of the capacity factor of the solute in pure water. The parameters for *o*-cresol in the methanol-THF-water system that were used to construct Fig. 1 follow these guidelines.

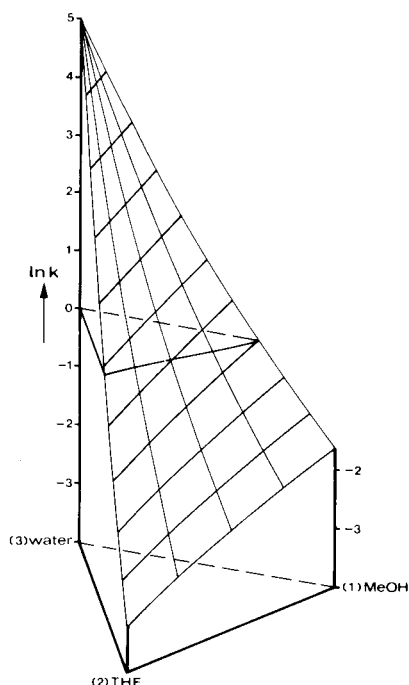


Fig. 1. Dependence of the capacity factor on mobile phase composition, for *o*-cresol in the system methanol (MeOH)-THF-water. The curved surface obeys eqn. 8 with coefficients from Table II.

For each solute the experimental retention data have been fitted to eqn. 8, yielding a set of coefficients (A_1 through D) for a particular solute in each mobile phase system.

We preferred the six-parameter linear equation given by eqn. 8 over a five-parameter non-linear version, in which $D = 2\sqrt{A_1 A_2}$, because it yielded a closer fit in the regression analysis. One reason for this may be found in the factor n_s/n_m . It may be argued that n_s/n_m varies with the composition of the mobile phase. With decreasing water content, n_s probably increases due to solvation (see, *e.g.*, refs. 11 and 12). Even without this effect, n_m is bound to decrease, due to the increase in the molar volume of

TABLE I

SOLUBILITY PARAMETERS FOR THE SOLVENTS USED IN THE PRESENT STUDY

Data taken from ref. 10.

Mobile phase component	Subscript	Solubility parameter ($\text{cal}^{1/2} \text{cm}^{-3/2}$)
Methanol	1	15.85
Tetrahydrofuran (THF)	2	9.88
Acetonitrile		13.14
Water	3	25.52

the mobile phase from water ($v = 18 \text{ cm}^3 \text{ mole}^{-1}$) to methanol (40), acetonitrile (52) or THF (81). The latter effect can be mathematically accounted for, by introducing the logarithm of the molar volume of the mobile phase into eqn. 8. In doing so, however, we did not find a significant improvement in the regression analysis. Therefore, we decided to treat (n_s/n_m) as a constant, which means that its variation with mobile phase composition is included in the coefficients A_1 through D in eqn. 8.

Iso-elutropic diagrams

As stated before, ternary systems in high-performance liquid chromatography (HPLC) offer the possibility to exploit specific effects. For certain solute pairs, the relative retention can be increased considerably, while retention itself remains roughly constant. Theoretically (eqn. 3), different mobile phases will lead to the same retention times if their polarities (solubility parameters) are equal.

Let us consider a sample for which a chromatogram has been obtained in a binary mixture of water and methanol, the volume fraction of the latter being φ_M^* . We will refer to this mobile phase as the (binary) reference. Let us assume that the reference chromatogram shows reasonable retention times, but insufficient separation. Eqn. 4 shows that a ternary phase expected to yield roughly the same retention times obeys:

$$\delta^* = \varphi_M^* \delta_1 + (1 - \varphi_M^*) \delta_3 = \varphi_1 \delta_1 + \varphi_2 \delta_2 + (1 - \varphi_1 - \varphi_2) \delta_3 \quad (15)$$

$$\varphi_2 = (\varphi_M^* - \varphi_1) (\delta_1 - \delta_3) / (\delta_2 - \delta_3) \quad (16)$$

Here δ^* is the polarity of the binary reference mixture. As usual, subscript 1 refers to methanol and subscript 3 to water. According to eqn. 16 all ternary mixtures of water, methanol and a second organic modifier that possess a given polarity follow a straight line between two limiting binary compositions. This is illustrated in Fig. 2a. If $\varphi_1 = \varphi_M^*$, φ_2 becomes zero and eqn. 16 defines the reference binary composition of methanol and water. If $\varphi_1 = 0$, a binary mixture of water and the second organic modifier results. The straight line connecting the two binary compositions will be called a (theoretical) iso-elutropic line. Empirical iso-elutropic lines can be constructed from experimental data collected for a large number of solutes. The procedure is illustrated in Fig. 2b. Let us consider a ternary mobile phase of composition P (25 % methanol, 25 % THF, 50 % water).

The solute dimethyl phthalate shows a capacity factor of 0.8 in this solvent. The same capacity factor is observed with a binary mixture of 70 % methanol and 30 % water. Consequently, for dimethyl phthalate the iso-elutropic line through binary reference composition $\varphi_M^* = 0.7$ passes through P . Other solutes eluted with the ternary composition P not only show different capacity factors, but also yield slightly different binary reference compositions φ_M^* . If, as is the case in practice, the variation in φ_M^* is small, we can take the average reference composition of a large number of solutes and assign this value to the ternary composition P . As shown in Fig. 2b, this average turns out to be 0.63. The same procedure can be applied to other ternary compositions and each of them can be assigned a particular reference value. The data thus obtained are shown in Fig. 2b for a few compositions. Linear interpolation along straight composition lines through the top of the composition triangle then yields the

ternary composition P' , for which $\varphi_M^* = 0.7$. Finally, all the mixtures that yield the same reference value can be connected to form an (empirical) iso-elutotropic curve. The example in Fig. 2 shows the difference between the theoretical prediction (eqn. 16) and the empirical curve. Theory predicts a straight line running from $\varphi_M^* = 0.7$ to $\varphi_{THF} = 0.43$. The empirical curve is slightly concave and intersects the opposite side at $\varphi_{THF} = 0.44$.

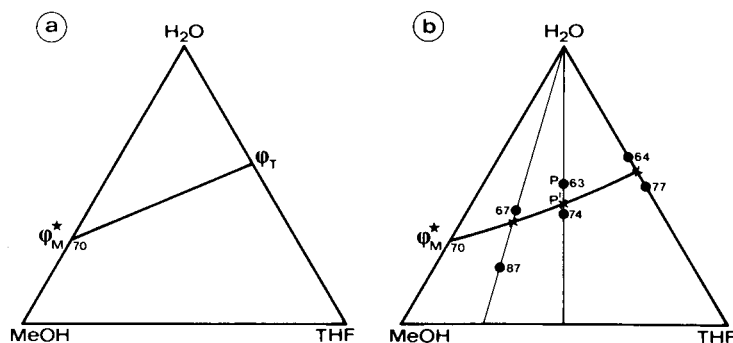


Fig. 2. Illustration of the construction of iso-elutotropic lines. a, Theoretical; the straight line from 70% methanol to 43% THF is calculated from eqn. 16. b, Experimental: the numbers at each composition (indicated by a black dot) represent the corresponding reference binary methanol–water composition (in % methanol) averaged over a large number of solutes. The solid, curved line connects interpolated points of equal elutotropic strength.

The approach outlined here resembles the one used previously for relating different binary compositions³.

EXPERIMENTAL

The instrumentation used was the same as described before¹, except that a Varian Model 8050 autosampler was used for some of the measurements. Mobile phases were mixed from individually measured volumes of methanol, THF (both from J. T. Baker, Phillipsburg, NJ, U.S.A.), acetonitrile (E. Merck, Darmstadt, G.F.R.) and water (carefully treated as described before¹). Columns (30 cm × 4.6 mm I.D.) were home-packed with Nucleosil 10-RP18 from Macherey, Nagel & Co. (Düren, G.F.R.).

The flow-rate was set at 1.5 ml min⁻¹ and was measured at regular intervals. All measured retention times were corrected for variations in the flow-rate and for the residence time outside the column.

For these columns at this flow-rate we chose a uniform hold-up time of $t_0 = 125$ sec. Although there are indications that the hold-up volume of an RPLC column varies with mobile phase composition^{12,13}, there seems to be no valid experimental method for its accurate determination. The two methods that give the most realistic results in binary methanol–water systems¹³ cannot be used in the present ternary systems.

The injection of large amounts of inorganic salts leads to solvent demixing. The linearization of a plot of $\ln k$ vs. carbon number for homologous series yields unrealistic results because the Martin rule cannot be applied with mobile phases rich in

acetonitrile or THF¹⁴. The use of $^2\text{H}_2\text{O}$ (deuterium oxide) as a t_0 -marker, which has recently been studied extensively¹², also has serious disadvantages.

The exchange of deuterium with hydrogen atoms in water, methanol and even residual silanols might cause a problem¹⁵. Moreover, the necessary assumption that water is not absorbed into the stationary phase clearly does not hold over the whole composition range. Therefore, we decided to use a uniform, realistic t_0 value. The consequences of this decision are limited, because the conclusions drawn in this paper apply equally well to gross retention times as to capacity factors.

The present study includes 32 solutes in the system methanol (1)–tetrahydrofuran (2)–water (3) and 49 solutes in the system methanol (1)–acetonitrile (2)–water (3). These two sets of solutes are listed in Tables II and III, respectively. They were used in the highest purity available and diluted in the corresponding mobile phases, if necessary enriched with organic modifier.

The compositions of the two systems that were included in the measurements are indicated in Fig. 3. For each composition solute retention times were measured, up to a maximum value of about 1.5 h ($k \approx 40$), for practical reasons.

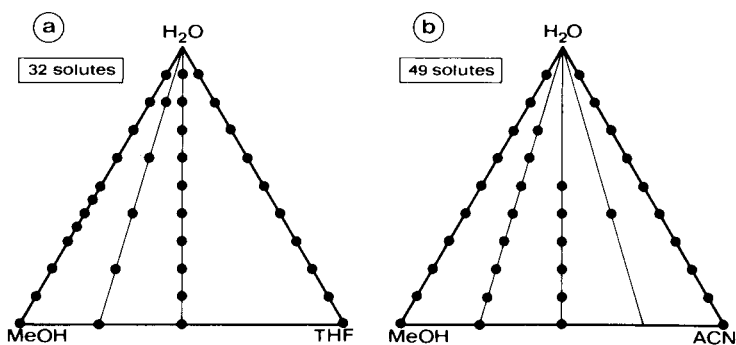


Fig. 3. Overview of the mobile phase compositions used in the present study. ACN = Acetonitrile.

RESULTS AND DISCUSSION

The basic retention data (capacity factors) are given in Appendix I for the methanol–THF–water system and in Appendix II for the methanol–acetonitrile–water system.

For all solutes the experimental retention data were fitted to eqn. 8. The resulting coefficients for each solute are given in Table II for the methanol (1)–THF (2)–water (3) system and in Table III for the system methanol (1)–acetonitrile (2)–water (3). The total number of datapoints, N , for each solute is also listed in the tables. The coefficients follow reasonably well the general behaviour discussed in Theoretical. The values of A_1 and A_2 are usually positive and the values of A_2 are much larger than those of A_1 . However, some A_1 values are negative. As expected, all B values are strongly negative, with the absolute value of B_2 being larger than that of B_1 . C is, of course, positive, but the two C values for a solute that appears in both tables are not exactly the same. The values of D are usually positive, but larger than the geometric mean of A_1 and A_2 . Considering the approximate character of eqns. 9–14 after omitting entropy and phase ratio terms, these results are not discouraging.

The last column in Tables II and III shows the average error between the model (eqn. 8) and the experimental data points. Note that the absolute deviations in $\ln k$ are approximately the same as the relative deviations in k . The average deviation for all data points is 13% for the THF-containing system and 12% for the system with acetonitrile.

Closer examination of the data reveals that moderate capacity factors ($k < 10$) are described consistently better (deviations less than 10%) than large capacity factors ($k > 10$). This is due to the fact that a fixed C term was adopted. In reality, different ternary systems (compare Tables II and III) and different binary systems^{1,9} yield different values of C for the same solute.

As a result, the average deviation between the model (eqn. 8) and the larger values observed in water-rich solvents is 20% for the THF system and 18% for the

TABLE II

RETENTION BEHAVIOUR OF 32 SOLUTES IN THE SYSTEM METHANOL-THF-WATER

Coefficients according to eqn. 8. N = Number of data points included in the regression analysis; a.d. = average deviation between the experimental value for $\ln k$ and the calculated value from eqn. 8, for all data points.

No.	Solute	A_1	A_2	B_1	B_2	C	D	N	a.d.
1	Acetophenone	0.25	4.66	-5.54	-11.27	3.89	3.90	35	0.16
2	Anethole	-2.44	3.51	-4.51	-12.68	6.47	-0.05	22	0.09
3	Aniline	0.09	1.10	-4.91	-6.54	2.90	2.20	31	0.18
4	Anisole	0.44	4.94	-7.02	-12.88	5.51	4.79	30	0.12
5	Anthracene	-2.53	4.17	-4.72	-14.34	7.38	0.06	18	0.07
6	Benzaldehyde	0.10	2.92	-4.97	-9.12	3.39	2.42	35	0.12
7	Benzene	-0.51	2.08	-5.17	-9.15	4.70	1.20	30	0.07
8	Benzonitrile	1.08	3.39	-6.69	-10.35	4.00	4.00	36	0.12
9	Benzophenone	0.37	6.21	-8.28	-16.07	6.91	5.19	27	0.15
10	Benzyl alcohol	0.71	4.40	-5.37	-10.43	2.96	4.69	36	0.16
11	Biphenyl	-2.60	4.08	-4.99	-13.92	7.15	0.28	22	0.09
12	Chlorobenzene	0.28	5.21	-7.82	-14.25	6.70	4.99	27	0.08
13	<i>o</i> -Cresol	1.68	2.94	-8.27	-11.13	4.97	5.22	32	0.10
14	Diethyl phthalate	0.05	6.11	-7.37	-15.08	5.84	4.90	30	0.17
15	<i>N,N</i> -Dimethylaniline	2.30	8.13	-9.90	-16.59	7.04	10.73	25	0.23
16	2,4-Dimethylphenol	1.89	4.52	-9.40	-13.82	6.13	6.67	30	0.07
17	Dimethyl phthalate	0.75	5.93	-6.75	-13.31	4.27	5.23	34	0.18
18	<i>m</i> -Dinitrobenzene	0.06	-0.79	-5.92	-6.98	4.26	-0.05	31	0.11
19	Diphenyl ether	-2.16	4.05	-5.68	-14.00	7.20	0.86	22	0.08
20	Ethylbenzene	-1.70	3.30	-5.33	-11.99	6.42	0.78	23	0.06
21	<i>N</i> -Methylaniline	0.92	5.01	-7.52	-12.04	5.19	6.69	26	0.21
22	Naphthalene	-3.28	6.23	-4.10	-15.64	7.10	-0.21	22	0.27
23	<i>p</i> -Nitroacetophenone	1.17	2.17	-7.09	-9.91	4.41	3.57	33	0.07
24	<i>o</i> -Nitroaniline	2.21	3.00	-8.56	-10.99	4.70	6.45	32	0.11
25	Nitrobenzene	1.03	3.22	-7.23	-10.92	4.86	4.14	32	0.05
26	<i>m</i> -Nitrophenol	1.04	1.16	-7.47	-9.35	4.54	3.21	32	0.19
27	Phenol	1.48	0.99	-6.79	-7.85	3.47	2.86	36	0.09
28	1-Phenylethanol	0.19	4.25	-5.51	-10.78	3.65	3.65	35	0.11
29	2-Phenylethanol	0.25	5.27	-5.63	-12.03	3.69	4.55	35	0.11
30	3-Phenylpropanol	1.59	7.52	-8.33	-15.91	5.33	8.58	33	0.16
31	Quinoline	0.74	9.47	-6.15	-15.56	4.60	8.25	26	0.26
32	Toluene	-0.18	4.16	-6.80	-12.58	6.23	3.25	26	0.07

acetonitrile system. Somewhat surprisingly, such large deviations are not observed for very small capacity factors ($k < 1$). Measurement errors and the assumption of a uniform hold-up time, which would predominantly affect the smallest capacity factors, appear to be of little significance.

Iso-elutotropic lines

Following the procedure outlined in Theoretical, iso-elutotropic lines of constant solvent strength have been constructed for both ternary systems. Theoretically predicted and empirical lines are presented in Figs. 4 and 5. A good agreement is observed, except for the very strong solvents, which are of limited practical value. This suggests that eqn. 16 offers a good first order approximation of iso-elutotropic lines in other ternary systems.

As expected from Fig. 1, the iso-elutotropic lines show a very regular behaviour. Significant maxima or minima are absent, not only for the averaged curves in Figs. 4 and 5, but also for iso-elutotropic lines referring to individual solutes. This indicates that ternary mixtures provide a smooth transition from one binary solvent to another.

Specific effects

Each iso-elutotropic line in Figs. 4 and 5 offers a guideline to the elution of a given sample with different mobile phases, but with roughly constant retention. Since, however, the iso-elutotropic line represents the average over a large number of solutes, minor variations in retention should be expected for individual solutes. We will refer to these variations as specific effects.

When we gradually replace the methanol in a binary methanol–water mixture by THF (*i.e.*, move to the right along one of the iso-elutotropic lines in Fig. 4), some solutes will move forward in the chromatogram and will be eluted more quickly than with the binary reference mixture. Obviously, such solutes show a specific preference to THF over methanol. On the other hand, other solutes interact more favourably with methanol, and hence are comparatively retarded when methanol is replaced by THF.

Fig. 6 illustrates the specific effects that can occur in ternary systems. It shows a series of chromatograms taken along the curve for $\varphi_M^* = 0.5$ in the methanol–THF–water system. The upper chromatogram shows that in methanol–water (50:50) the sample is eluted in 20 min, but that the first two solutes coincide. When we elute the sample with the corresponding binary mixture of THF–water (32:68), the total analysis time indeed remains approximately the same, but the separation is again incomplete. However, the solute pair that coincides in methanol–water (benzyl alcohol and phenol) is different from the unresolved couple in THF–water (phenol and 3-phenylpropanol). Moreover, the sequence of the last bands eluted has reversed in going from methanol–water to THF–water. This reversal originates from the specific acceleration of 2,4-dimethylphenol and the specific retardation of diethyl phthalate. The third solute, benzene, is hardly affected by the changing composition.

Such changes as observed between the top and bottom chromatograms of Fig. 6 form a strong argument in favour of ternary mobile phase systems.

The second chromatogram from the top in Fig. 6 shows the elution with a ternary mixture, in which only a small amount of THF (10%) is present. Not un-

TABLE III

RETENTION BEHAVIOUR OF 49 SOLUTES IN THE SYSTEM METHANOL-ACETONITRILE-WATER

Details as in Table II.

No.	Solute	A_1	A_2	B_1	B_2	C	D	N	$a.d.$
1	Acetophenone	1.07	5.37	- 7.80	-11.45	4.83	7.77	33	0.11
2	Anisole	2.13	5.10	- 9.06	-11.97	5.82	6.79	30	0.12
3	Benzaldehyde	-0.18	3.64	- 6.08	- 9.55	4.38	6.62	34	0.18
4	Benzene	2.31	4.19	- 8.66	-10.82	5.56	5.42	29	0.14
5	Benzonitrile	2.67	4.43	- 9.24	-10.81	4.90	7.87	32	0.08
6	Benzophenone	1.68	5.59	-10.15	-13.85	7.39	6.81	26	0.12
7	Benzyl alcohol	0.47	5.43	- 6.09	-10.38	3.32	8.09	34	0.09
8	Biphenyl	0.00	4.15	- 8.60	-12.78	7.97	3.02	24	0.13
9	<i>n</i> -Butylbenzene	-1.43	3.78	- 7.46	-12.46	8.39	1.10	23	0.12
10	<i>p</i> -Chlorobenzaldehyde	0.59	-0.16	- 5.52	- 5.09	3.78	3.37	26	0.33
11	Chlorobenzene	1.73	5.78	- 9.75	-13.56	7.05	6.96	27	0.13
12	<i>p</i> -Chlorophenol	1.88	6.71	- 9.26	-13.75	5.60	9.58	32	0.10
13	<i>p</i> -Chlorotoluene	0.08	4.12	- 7.96	-11.80	7.08	3.28	25	0.10
14	<i>o</i> -Cresol	2.04	5.47	- 8.56	-11.79	4.80	8.35	33	0.09
15	<i>o</i> -Dichlorobenzene	-0.31	3.09	- 6.85	-10.13	6.43	1.94	25	0.12
16	Diethyl phthalate	2.85	7.21	-11.87	-15.79	7.47	10.10	29	0.14
17	Dimethyl phthalate	2.58	5.94	-10.06	-13.07	5.59	9.72	31	0.14
18	<i>m</i> -Dinitrobenzene	1.71	3.25	- 8.44	-10.14	5.12	5.52	31	0.10
19	<i>o</i> -Dinitrobenzene	2.50	3.93	- 9.96	-11.41	5.57	7.41	31	0.10
20	<i>p</i> -Dinitrobenzene	1.71	2.57	- 8.48	- 9.36	4.92	5.35	32	0.09
21	2,4-Dinitrotoluene	1.77	3.90	- 9.41	-11.77	6.18	5.84	29	0.11
22	2,6-Dinitrotoluene	2.33	4.70	-10.30	-12.72	6.40	7.23	28	0.11
23	3,4-Dinitrotoluene	3.07	5.32	-11.59	-13.65	6.75	9.07	30	0.11
24	Diphenyl ether	0.25	4.58	- 9.22	-13.48	8.16	3.84	24	0.12
25	Ethylbenzene	-0.76	2.69	- 6.18	- 9.35	6.15	0.65	22	0.12
26	<i>m</i> -Fluoronitrobenzene	1.41	3.94	- 8.27	-10.83	5.50	5.44	30	0.09
27	<i>o</i> -Fluoronitrobenzene	1.77	4.21	- 8.67	-11.04	5.31	6.45	31	0.11
28	<i>p</i> -Fluoronitrobenzene	2.10	3.88	- 9.06	-10.81	5.42	6.51	30	0.11
29	<i>p</i> -Fluorophenol	0.70	4.61	- 7.04	-10.51	3.95	7.90	35	0.11
30	<i>p</i> -Hydroxybenzaldehyde	1.55	7.07	- 7.54	-12.32	3.47	11.59	36	0.12
31	<i>p</i> -Methoxybenzaldehyde	0.49	4.23	- 6.74	-10.29	4.57	6.82	28	0.08
32	<i>p</i> -Methylbenzaldehyde	0.08	4.20	- 7.05	-10.66	5.18	7.39	29	0.14
33	Methyl benzoate	2.87	6.62	-10.27	-13.84	6.26	9.16	29	0.15
34	Naphthalene	0.36	3.91	- 8.01	-11.53	6.91	3.39	25	0.11
35	<i>p</i> -Nitroacetophenone	2.18	4.39	- 8.97	-11.11	5.13	7.27	32	0.12
36	<i>p</i> -Nitrobenzaldehyde	-0.18	2.06	- 6.48	- 8.42	4.38	6.64	32	0.20
37	<i>p</i> -Nitrilobenzaldehyde	-0.63	2.77	- 6.14	- 8.78	3.97	7.69	34	0.23
38	Nitrobenzene	2.18	4.17	- 8.88	-10.90	5.34	6.59	31	0.09
39	<i>m</i> -Nitrophenol	1.57	5.69	- 8.16	-11.96	4.62	8.56	35	0.11
40	<i>o</i> -Nitrophenol	1.44	4.46	- 7.46	-10.25	4.64	5.47	33	0.13
41	<i>p</i> -Nitrophenol	1.98	5.17	- 8.43	-11.64	4.50	8.65	35	0.12
42	Phenol	0.92	3.82	- 6.38	- 9.02	3.30	6.80	36	0.09
43	2-Phenylethanol	0.61	6.69	- 6.68	-12.02	4.09	8.39	35	0.10
44	<i>p</i> -Phenylphenol	2.83	8.63	-12.21	-17.68	7.91	11.56	28	0.12
45	3-Phenylpropanol	1.53	8.26	- 8.82	-14.72	5.49	10.16	37	0.09
46	<i>n</i> -Propylbenzene	-1.04	2.37	- 6.61	- 9.97	7.02	0.29	25	0.13
47	Toluene	-0.91	3.40	- 8.12	-10.83	6.30	3.97	28	0.14
48	α,α,α -Trichlorotoluene	0.09	5.46	- 9.72	-14.77	8.80	5.20	18	0.09
49	2,4-Dimethylphenol	1.95	6.75	- 9.46	-13.89	5.93	9.17	31	0.11

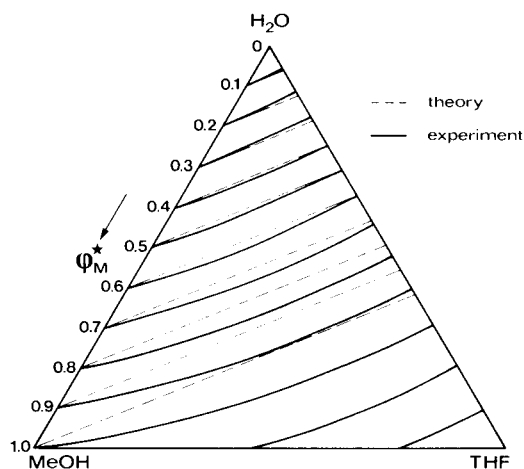


Fig. 4. Iso-elutotropic diagram for the system methanol-THF-water. Theoretical and experimental curves are constructed as shown in Fig. 2, for reference methanol-water compositions at 10% intervals.

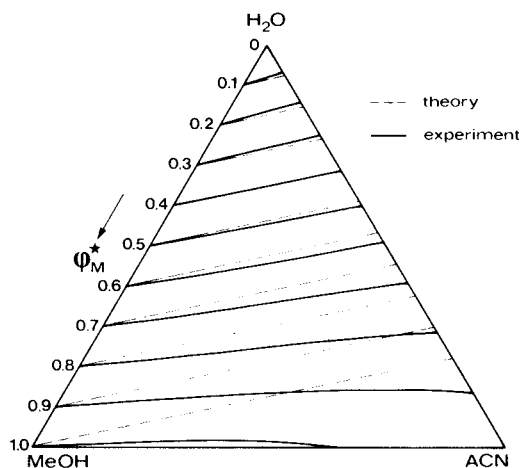


Fig. 5. Iso-elutotropic diagram as in Fig. 4 for the system methanol-acetonitrile-water.

expectedly, the three early peaks are now well separated. However, the three later bands merge into a single peak. This is not surprising, considering the top and bottom chromatograms. The third chromatogram from the top shows the excellent separation that can be obtained by applying the appropriate ternary composition to this particular sample.

We can define the specificity of a mobile phase with respect to a binary mixture of methanol and water for a solute i as:

$$S_i = \ln k_{i,M}^*/k_i \quad (17)$$

Here k_i is the capacity factor of i in the mobile phase, while $k_{i,M}^*$ is the capacity factor in the binary reference solvent. Defined in this way, zero specificity ($S_i = 0$) results if

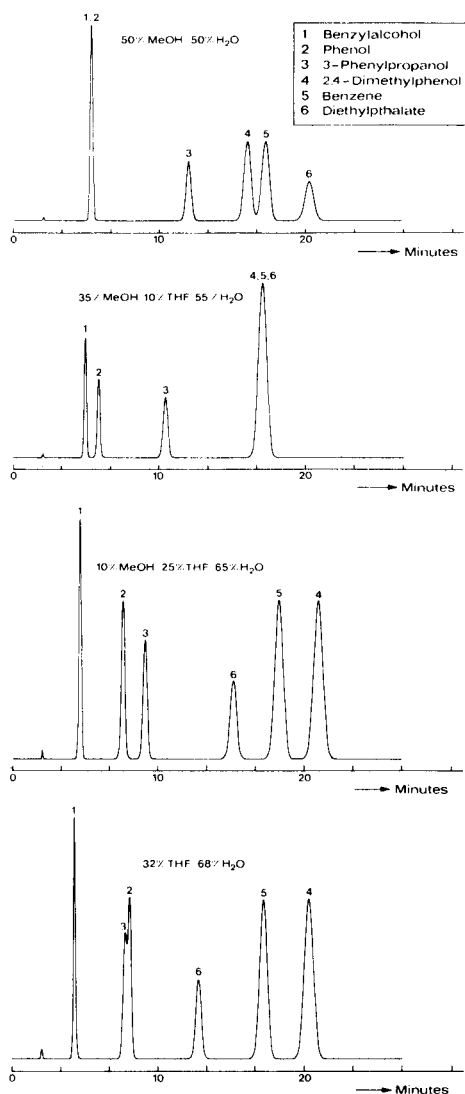


Fig. 6. Chromatograms illustrating the specific effects occurring in some iso-elutotropic mixtures of methanol, THF and water. Retention data taken from Table II. Mobile phase compositions follow the experimental iso-elutotropic curve for $\varphi_M^* = 0.5$ in Fig. 4.

the capacity factor remains unaltered when a binary methanol–water mixture is replaced by another solvent of equal elutotropic strength. Positive S values indicate a specific acceleration of the solute i . A very high S value is found when the solute is essentially non-retained in the eluent chosen. Negative S values signify a specific retardation of the solute relative to its behaviour in methanol–water.

As an example, Fig. 7 shows the specificities of the mobile phases used in the chromatograms of Fig. 6 towards each of the six solutes, as a function of the decreasing methanol content of the solvent. Two additional horizontal axes have been drawn

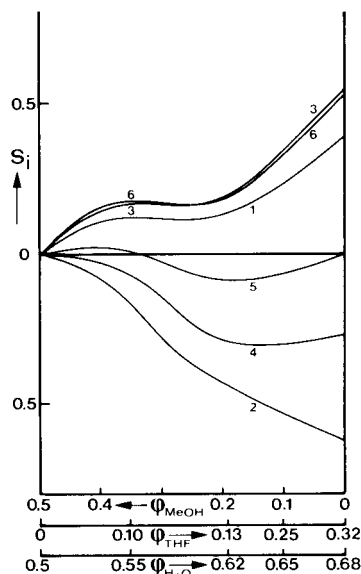


Fig. 7. Specificity according to eqn. 17 in ternary mobile phases containing methanol, THF and water, for the six solutes shown in Fig. 6. The mobile phase composition follows the experimental iso-elutotropic line for $\phi_M^* = 0.5$ in Fig. 4.

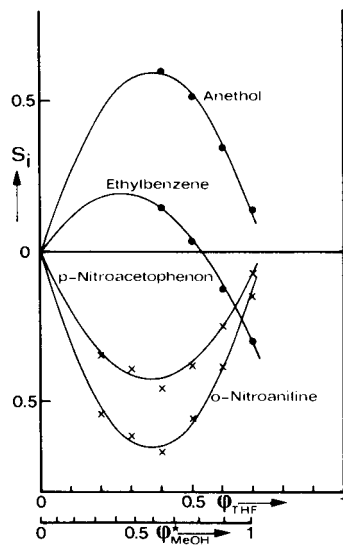


Fig. 8. Specificity for four solutes as a function of THF content in binary mixtures with water. The (non-linear) scale at the bottom indicates the composition of the corresponding reference methanol–water mixture.

to indicate the volume fractions of THF and water, respectively. Note that both of these axes are slightly non-linear.

Obviously, all curves in Fig. 7 start at $S = 0$ for the binary reference composition of methanol–water (50:50). With decreasing amount of methanol and increasing amount of THF the positive specific effects for benzyl alcohol, 3-phenylpropanol and diethyl phthalate become clear, whereas phenol and 2,4-dimethylphenol show negative specificity. Benzene shows approximately zero specificity along this particular iso-elutotropic line. Fig. 7 suggests that the specificity changes quite regularly when methanol is gradually replaced by another organic modifier. This appears to be a general rule for all solutes. A binary solvent almost always shows a more pronounced specific effect relative to methanol–water than the intermediate ternary solvents of the same elutropic strength. Indeed, in Fig. 6, phenol is separated from its neighbours because the specific effect of a ternary mixture of methanol, THF and water is smaller than that of a binary mixture containing only THF and water.

It should be noted that the specificity curves in Fig. 7 correspond to one particular iso-elutotropic line, the one for $\phi_M^* = 0.5$ in Fig. 4. Hence, a large number of specificity curves can be constructed for each solute. However, we can simplify the discussion, if it is realized that the specificity of ternary mixtures is intermediate between those of the limiting binary mixtures. Therefore, a classification of the specific effects in binary mixtures is indicative of the behaviour of ternary systems. We can now construct specificity curves that cover the entire binary composition range, and hence a wide range of retention times. Some examples are shown in Fig. 8, where

the specificity of THF–water mixtures towards four solutes is presented. Each point represents the specificity of a particular mixture of THF and water, relative to the corresponding binary methanol–water reference mixture. For example, the points at $\varphi_{\text{THF}} = 0.4$ indicate the specificity relative to a binary mixture of 65% methanol and 35% water ($\varphi_{\text{M}}^* = 0.65$). Note that binary mixtures containing more than 70% THF have a solvent strength larger than that of 100% methanol. For the solutes included in the present study, such very strong solvents are of little interest. When such solvents are required for very hydrophobic solutes, binary mixtures of water and THF can be taken as a reference instead of methanol–water mixtures.

Naturally, all curves start at $S = 0$ for $\varphi_2 = 0$, which point refers to pure water. Two typical shapes can be observed, one with a minimum and one with a maximum. Only occasionally (*e.g.*, benzene in THF–water) the S vs. φ curve shows no extrema. An equation for the specificity as a function of binary mobile phase composition can be derived from eqns. 8 and 16. If we substitute the appropriate compositions in eqn. 8, *i.e.*, $\varphi_1 = 0$ to find $k_{i,2}$ and $\varphi_1 = \varphi_{\text{M}}^*$, $\varphi_2 = 0$ to find $k_{i,\text{M}}^*$, we obtain:

$$\begin{aligned} S_i &= \ln k_{i,\text{M}}^* - \ln k_{i,2} \\ &= A_1 (\varphi_{\text{M}}^*)^2 - A_2 \varphi_2^2 + B_1 \varphi_{\text{M}}^* - B_2 \varphi_2 \end{aligned} \quad (18)$$

Moreover, for the binary mixture of the second modifier and water, we can substitute $\varphi_1 = 0$ in eqn. 16 and hence

$$\varphi_2 = \varphi_{\text{M}}^* \left(\frac{\delta_1 - \delta_3}{\delta_2 - \delta_3} \right) = \frac{\varphi_{\text{M}}^*}{\lambda} \quad (19)$$

where λ is the constant ratio of solubility parameter differences. Combination of eqns. 18 and 19 now yields:

$$\begin{aligned} S &= \varphi_2^2 (A_1 \lambda^2 - A_2) + \varphi_2 (B_1 \lambda - B_2) \\ &= P \varphi_2^2 + Q \varphi_2 \end{aligned} \quad (20)$$

The solid lines drawn in Fig. 8 represent the quadratic curves according to eqn. 20. The P and Q values for the individual solutes are found from regression analysis on the experimental data for S and are represented in Fig. 9 for the THF–water system and in Fig. 10 for the acetonitrile–water system. The numbers in these two figures refer to the solutes as they occur in Tables II and III. Solute that experience positive specificities can be found in the upper left corner, while the retarded solutes are situated at the bottom right.

The correlation between the P and Q values is remarkable. In fact, almost all solutes fall close to the line $P = -Q$ included in Figs. 9 and 10. If we now substitute $P = -Q$ into eqn. 20, we find that the specificity S is zero for $\varphi_2 = 1$. This leads to the conclusion that solvents rich in either acetonitrile or THF show very little specific effect in comparison to methanol–water mixtures. If specific effects occur they are most pronounced in mixtures containing moderate amounts of water (40–70%).

From Figs. 9 and 10 it appears that the specific effects in THF–water mixtures are larger than those in acetonitrile–water mixtures. Note that Figs. 9 and 10 differ in scale by a factor of 2. Several groups of solutes can be identified. In the THF–water system, large hydrophobic solutes appear to be specifically accelerated, *e.g.*, naphthalene (22), biphenyl (11), anthracene (5), diphenyl ether (19) and ethylbenzene (20). Note that quinoline (31) behaves similarly to naphthalene, despite the introduction of a heterogeneous nitrogen atom. Phenolic compounds, such as phenol (27), *o*-cresol (13) and 2,4-dimethylphenol (16), and nitro compounds, such as *m*-nitrophenol (26), *m*-dinitrobenzene (18), *o*-nitroaniline (24), *p*-nitroacetophenone (23) and nitrobenzene (25), are specifically retarded. The specificities for aliphatic alcohols [benzyl alcohol (10), 1-phenylethanol (28), 3-phenylpropanol (30) and 2-phenylethanol (29)] are slightly positive, in sharp contrast to the large negative effects observed with phenolic hydroxy groups. Esters (14, 17), ketones (1, 9), ethers (4) and aldehydes (6) show small specific effects. In acetonitrile–water mixtures, a large positive specificity is observed for aliphatic alcohols (solutes 45, 43 and 7). Again, phenolic solutes (14, 42 and 49) behave differently, with only slight positive effects. Substituted phenols (40, 41, 39, 29, 12, 44) all behave similarly. Nitro compounds all show negative specificities. The specific effects seems to be larger for dinitro compounds (20, 19, 23, 18, 22, 21) than for molecules containing only one nitro group (28, 38, 27, 26). The specific effects are small for non-polar compounds, esters, ethers and ketones. The behaviour of the various *para*-substituted benzaldehydes is somewhat puzzling. The specific effects are small for most of these compounds (3, 32, 31, 37, 36). However, *p*-hydroxybenzaldehyde (30) shows a large acceleration, while *p*-chlorobenzaldehyde (10) is greatly retarded.

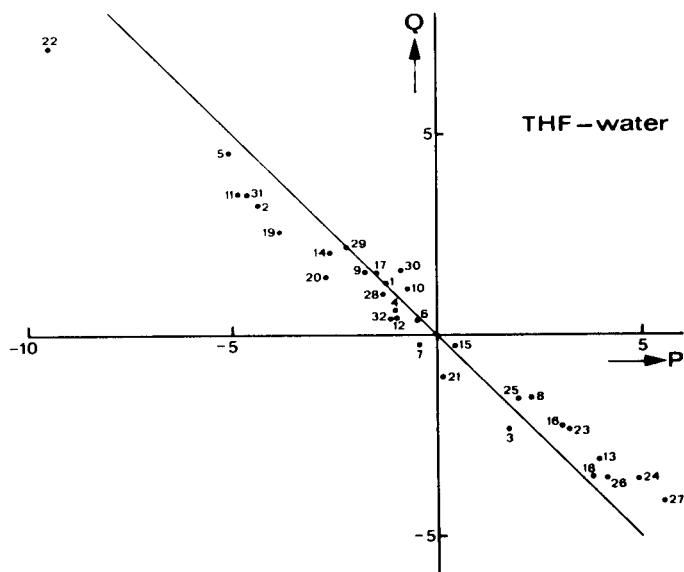


Fig. 9. Coefficients describing the specificity in the system THF–water (eqn. 20). Numbers refer to solutes listed in Table II. A positive Q value indicates specific acceleration in THF–water in comparison to methanol–water. A negative Q value indicates specific retardation of a solute. The straight line represent $Q = -P$.

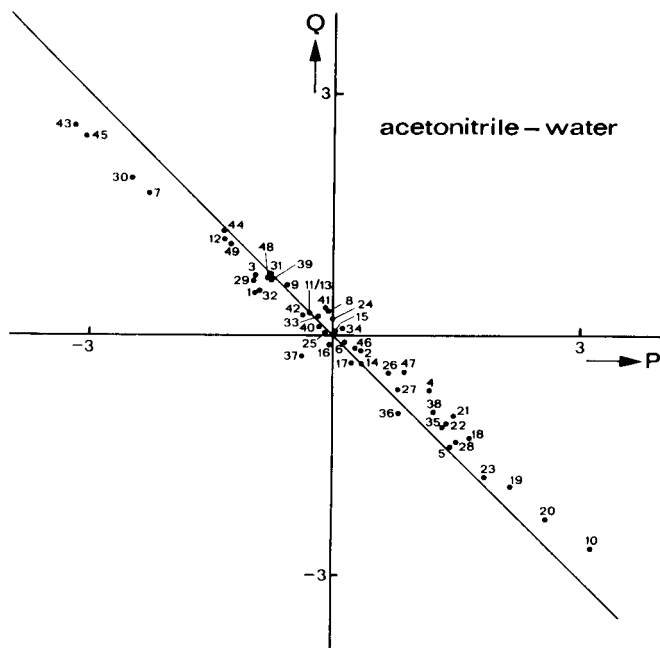


Fig. 10. As Fig. 9, but for the system acetonitrile-water. Solute identification numbers refer to Table III.

Table IV gives a summary of the specific effects encountered in the two binary systems classified according to functional groups. Slight effects are indicated by square brackets.

TABLE IV

SUMMARY OF SPECIFIC EFFECTS IN BINARY MIXTURES OF THF-WATER AND ACETONITRILE-WATER FOR VARIOUS SUBSTITUENTS

Specific effect	THF	Acetonitrile
Retardation	Phenolic OH	
	NO ₂	NO ₂
	NH ₂	CN
	CN	
Acceleration		Aliphatic OH
	CH ₃	[Phenolic OH]
	CH ₂	[CH ₃ ; CH ₂]
	Phenyl	[Phenyl]
		[Cl]
Negligible	Ketones	
	Esters	Ketones
	Aliphatic OH	Esters
	Ethers	Ethers
	Secondary and ternary amines	

CONCLUSIONS

The retention of a wide variety of solutes in the ternary systems methanol–THF–water and methanol–acetonitrile–water can be described by a regular but non-linear three-dimensional surface. A quadratic equation relates the logarithm of the capacity factor to the volume fractions of the two organic modifiers.

Retention data on a large number of solutes can be used to construct iso-elutotropic lines, that connect mixtures of equal solvent strength within the ternary triangle. All the mixtures on such a line will yield roughly the same retention times for

APPENDIX I

EXPERIMENTAL CAPACITY FACTORS IN THE SYSTEM METHANOL–THF–WATER

No.	Solute	ϕ_{MeOH}	0.10	0.20	0.30	0.40	0.50	0.55	0.60	0.65
		ϕ_{THF}	0	0	0	0	0	0	0	0
		ϕ_{water}	0.90	0.80	0.70	0.60	0.50	0.45	0.40	0.35
1	Acetophenone	—	—	32.54	13.82	6.94	4.37	2.49	1.78	1.29
2	Anethole	—	—	—	—	—	—	—	22.38	13.28
3	Aniline	—	—	6.27	3.64	2.71	1.48	1.19	0.96	0.70
4	Anisole	—	—	—	—	38.84	9.02	5.42	3.97	2.71
5	Anthracene	—	—	—	—	—	—	—	—	—
6	Benzaldehyde	—	—	13.01	9.08	5.06	3.63	2.02	1.45	1.10
7	Benzene	—	—	—	21.76	13.86	8.40	6.12	4.17	2.94
8	Benzonitrile	41.40	20.61	9.90	5.14	2.83	2.00	1.44	1.02	1.02
9	Benzophenone	—	—	—	—	27.40	14.78	9.14	5.28	5.28
10	Benzyl alcohol	16.99	8.47	4.52	2.78	2.22	1.18	0.90	0.69	0.69
11	Biphenyl	—	—	—	—	—	—	—	30.68	17.96
12	Chlorobenzene	—	—	—	—	19.70	13.42	8.34	5.41	5.41
13	<i>o</i> -Cresol	—	22.83	12.80	6.44	3.96	2.50	1.73	1.26	1.26
14	Diethyl phthalate	—	—	—	34.76	13.58	6.92	4.26	2.70	2.70
15	<i>N,N</i> -Dimethylaniline	—	—	—	—	—	11.96	8.12	5.48	5.48
16	2,4-Dimethylphenol	—	—	29.00	14.47	7.26	5.15	3.24	2.14	2.14
17	Dimethyl phthalate	—	—	22.38	8.45	4.04	2.25	1.64	1.06	1.06
18	<i>m</i> -Dinitrobenzene	—	14.60	10.95	6.58	4.82	2.81	2.00	1.48	1.48
19	Diphenyl ether	—	—	—	—	—	—	24.78	14.70	14.70
20	Ethylbenzene	—	—	—	—	—	23.48	14.41	9.35	9.35
21	<i>N</i> -Methylaniline	—	—	—	—	4.92	4.18	2.84	1.98	1.98
22	Naphthalene	—	—	—	—	—	—	—	37.88	37.88
23	<i>p</i> -Nitroacetophenone	—	20.82	13.08	6.83	3.70	2.48	1.74	1.29	1.29
24	<i>o</i> -Nitroaniline	—	13.22	9.63	5.42	2.86	1.96	1.40	1.05	1.05
25	Nitrobenzene	—	27.70	15.64	8.72	5.33	3.48	2.54	1.74	1.74
26	<i>m</i> -Nitrophenol	31.80	16.37	9.30	5.04	2.94	1.98	1.38	0.98	0.98
27	Phenol	13.40	7.66	4.61	2.76	1.64	1.22	0.95	0.66	0.66
28	1-Phenylethanol	—	19.92	9.90	5.21	2.84	1.95	1.40	1.03	1.03
29	2-Phenylethanol	—	18.57	9.15	4.97	3.09	1.95	1.39	1.02	1.02
30	3-Phenylpropanol	—	51.56	23.00	11.03	6.27	3.48	2.35	1.64	1.64
31	Quinoline	—	—	—	—	9.08	5.78	3.64	2.37	2.37
32	Toluene	—	—	—	—	19.10	12.58	8.10	5.51	5.51

a given sample. However, mixtures of equal solvent strength will show variations in retention for certain solutes. These variations can be referred to as specific effects.

The specificity of ternary systems along one iso-elutotropic line appears to vary quite regularly, and therefore can be expected to lie in between those of the limiting binary mixtures, at each end of the corresponding iso-elutotropic line. Hence, some predictions as to the specific effects taking place in ternary mixtures can be made, if the specific effects in the limiting binaries can be classified. A sensible classification of specific effects can be obtained for binary mixtures of THF and water and acetonitrile and water, relative to binary methanol–water mixtures.

0.70	0.80	0.90	1.00	0.30	0.45	0.60	0.75	0.05	0.10	0.15	0.20	0.25	0.30	0.35
0	0	0	0	0.10	0.15	0.20	0.25	0.05	0.10	0.15	0.20	0.25	0.30	0.35
0.30	0.20	0.10	0	0.60	0.40	0.20	0	0.90	0.80	0.70	0.60	0.50	0.40	0.30
<hr/>														
0.98	0.57	0.40	0.26	2.98	0.86	0.34	0.22	16.92	8.44	4.22	2.03	1.10	0.63	0.36
8.43	3.31	1.71	0.55	—	7.22	1.39	0.31	—	—	—	—	9.03	3.95	1.58
0.54	0.33	0.25	0.18	2.68	0.88	0.34	0.17	—	—	—	—	2.21	1.22	0.58
2.03	1.07	0.69	0.35	8.86	2.02	0.66	0.26	—	—	13.48	6.03	2.93	1.59	0.78
—	—	3.70	0.94	—	14.36	2.27	0.45	—	—	—	—	16.84	6.08	2.24
0.84	0.50	0.38	0.24	2.46	1.07	0.33	0.18	13.27	7.21	3.83	1.94	1.14	0.57	0.38
2.20	1.15	0.74	0.36	—	2.38	0.76	0.28	45.62	—	15.68	7.23	3.46	1.88	0.96
0.80	0.43	0.32	0.21	3.12	0.78	0.30	0.18	16.60	9.59	4.88	2.38	1.20	0.67	0.37
3.44	1.37	0.81	0.35	22.76	2.63	0.58	0.22	—	—	—	10.76	3.79	1.68	0.78
0.53	0.35	0.26	0.18	1.62	0.72	0.34	0.18	6.81	3.84	2.14	1.09	0.66	0.39	0.22
11.14	4.03	1.94	0.57	—	9.22	1.61	0.32	—	—	—	—	13.26	4.68	1.88
3.79	1.64	0.98	0.40	24.73	3.96	0.99	0.31	—	—	—	14.85	5.71	2.90	1.22
0.94	0.50	0.35	0.20	6.77	2.04	0.36	0.18	—	—	11.09	4.66	2.04	1.09	0.54
1.79	0.76	0.46	0.22	8.25	1.90	0.34	0.16	—	—	12.92	4.38	1.92	0.87	0.46
3.64	1.62	0.98	0.44	14.36	3.54	0.93	0.98	—	—	—	11.52	6.91	3.78	1.62
1.58	0.73	0.47	0.24	11.73	1.98	0.51	0.22	—	—	20.58	7.53	3.06	1.43	0.69
0.78	0.42	0.30	0.19	2.58	0.60	0.24	0.13	27.79	9.82	3.80	1.56	0.79	0.45	0.26
1.10	0.58	0.39	0.20	7.09	1.65	0.40	0.17	—	—	12.66	6.07	2.80	1.44	0.70
8.95	3.20	1.54	0.47	—	7.90	1.42	0.30	—	—	—	—	11.93	4.57	1.74
6.30	2.64	1.42	0.50	—	6.16	1.40	0.35	—	—	—	—	9.31	4.13	1.82
1.36	0.67	0.45	0.26	6.20	1.86	0.58	0.31	—	—	—	—	4.49	2.30	1.13
24.44	8.18	1.43	0.52	—	5.53	1.22	0.33	—	—	—	21.80	7.14	3.13	1.40
0.96	0.52	0.37	0.22	4.35	1.07	0.39	0.18	—	13.79	7.32	3.46	1.77	0.98	0.48
0.79	0.44	0.32	0.20	5.13	1.57	0.34	0.14	—	—	9.19	3.92	1.70	0.85	0.45
1.30	0.68	0.48	0.26	6.68	1.59	0.48	0.20	—	—	10.80	4.85	2.30	1.18	0.62
0.74	0.42	0.29	0.18	6.68	1.99	0.34	0.12	—	—	14.55	5.72	2.32	1.02	0.50
0.53	0.30	0.25	0.17	2.91	0.79	0.28	0.14	14.84	9.46	4.74	2.40	1.21	0.66	0.34
0.78	0.45	0.31	0.20	3.04	0.78	0.32	0.17	15.76	6.92	3.47	1.92	0.98	0.59	0.33
0.78	0.42	0.31	0.20	2.69	0.74	0.26	0.14	14.20	6.97	3.38	1.65	0.83	0.49	0.29
1.18	0.57	0.38	0.22	5.70	1.64	0.32	0.40	—	17.37	7.11	2.90	1.29	0.69	0.34
1.74	0.89	0.62	0.41	—	1.00	0.37	0.65	—	—	—	—	1.54	0.78	0.51
3.93	1.85	1.08	0.44	—	4.02	1.08	0.32	—	—	—	13.98	5.83	2.98	1.36

(Continued on p. 280)

APPENDIX I (continued)

Solute No.

ϕ_{MeOH}	0.40	0.45	0.50	0	0	0	0	0	0	0	0	0	0
ϕ_{THF}	0.40	0.45	0.50	0.10	0.20	0.30	0.40	0.50	0.60	0.70	0.80	0.90	1.00
ϕ_{water}	0.20	0.10	0	0.90	0.80	0.70	0.60	0.50	0.40	0.30	0.20	0.10	0
1	0.24	0.15	0.10	12.60	5.66	2.61	1.26	0.70	0.38	0.21	0.12	0.08	0.06
2	0.76	0.36	0.18	—	—	—	7.13	2.71	1.20	0.53	0.25	0.14	0.06
3	0.34	0.15	0.11	7.79	5.09	3.66	1.64	0.80	0.58	0.26	0.12	0.08	0.17
4	0.46	0.26	0.15	—	21.12	7.78	3.05	1.46	0.75	0.39	0.21	0.13	0.07
5	0.99	0.43	0.18	—	—	—	9.97	3.38	1.33	0.55	0.25	0.13	0.06
6	0.25	0.16	0.11	10.18	5.33	2.70	1.31	0.76	0.43	0.23	0.11	0.09	0.06
7	0.55	0.30	0.18	—	—	10.04	3.80	1.86	0.98	0.50	0.27	0.18	0.09
8	0.24	0.14	0.09	14.01	8.01	3.74	1.61	0.82	0.45	0.22	0.10	0.08	0.05
9	0.40	0.21	0.11	—	—	13.87	3.86	1.62	0.74	0.33	0.16	0.08	0.04
10	0.14	0.08	0.09	5.02	2.64	1.40	0.72	0.42	0.22	0.10	0.06	0.06	0.05
11	0.85	0.38	0.18	—	—	—	9.22	3.29	1.34	0.58	0.27	0.14	0.06
12	0.65	0.33	0.18	—	—	19.47	5.21	2.30	1.08	0.53	0.28	0.17	0.08
13	0.30	0.16	0.09	—	18.79	7.16	2.45	1.09	0.53	0.24	0.10	0.07	0.05
14	0.25	0.14	0.09	—	20.97	6.15	2.14	1.02	0.50	0.22	0.10	0.06	0.03
15	0.71	0.34	—	—	—	14.58	6.06	2.44	1.31	0.60	0.27	0.17	0.38
16	0.35	0.17	0.10	—	—	10.86	3.16	1.39	0.64	0.26	0.14	0.07	0.04
17	0.15	0.10	0.07	16.55	5.64	2.22	0.98	0.52	0.28	0.13	0.09	0.06	0.03
18	0.37	0.18	0.08	—	—	9.81	3.63	1.58	0.71	0.32	0.14	0.08	0.03
19	0.78	0.34	0.15	—	—	—	9.32	3.26	1.34	0.58	0.26	0.13	0.06
20	0.89	0.42	0.19	—	—	—	8.42	3.39	1.53	0.71	0.36	0.21	0.09
21	0.48	0.23	—	—	14.59	8.17	3.86	1.61	0.99	0.42	0.18	0.10	0.34
22	0.70	0.34	0.18	—	—	26.30	6.23	2.51	1.13	0.53	0.26	0.16	0.07
23	0.27	0.14	0.10	—	11.93	5.28	2.14	1.05	0.54	0.24	0.11	0.07	0.03
24	0.25	0.14	0.17	—	16.02	5.78	1.98	0.91	0.43	0.20	0.10	0.06	0.04
25	0.35	0.19	0.12	—	16.86	6.96	2.55	1.20	0.60	0.30	0.16	0.10	0.06
26	0.26	0.12	0.07	—	—	8.63	2.49	1.02	0.45	0.18	0.06	0.06	0.04
27	0.22	0.12	0.07	13.43	7.72	3.72	1.53	0.78	0.38	0.19	0.10	0.06	0.04
28	0.21	0.12	0.08	9.59	6.02	2.22	1.06	0.58	0.32	0.17	0.11	0.06	0.06
29	0.18	0.10	0.07	9.60	4.57	1.88	0.86	0.42	0.23	0.11	0.06	0.06	0.05
30	0.22	0.10	0.06	—	9.66	3.38	1.18	0.58	0.30	0.13	0.06	0.06	0.05
31	0.26	0.17	—	15.37	6.46	2.78	0.99	0.48	0.40	0.19	0.12	0.10	0.37
32	0.72	0.37	0.19	—	—	18.50	5.75	2.60	1.25	0.61	0.34	0.20	0.10

APPENDIX II

EXPERIMENTAL CAPACITY FACTORS IN THE SYSTEM METHANOL-ACETONITRILE-WATER

No.	Solute								
	ϕ_{MeOH}	0.10	0.20	0.30	0.40	0.50	0.60	0.70	0.80
	ϕ_{ACN}	0	0	0	0	0	0	0	0
	ϕ_{water}	0.90	0.80	0.70	0.60	0.50	0.40	0.30	0.20
1	Acetophenone	—	—	14.18	6.66	3.31	1.90	0.90	0.48
2	Anisole	—	—	—	12.78	6.66	3.66	1.68	0.90
3	Benzaldehyde	—	24.33	9.51	4.89	2.58	1.62	0.78	0.46
4	Benzene	—	—	—	11.54	6.53	3.70	1.71	0.91
5	Benzonitrile	—	—	10.60	5.26	2.73	1.55	0.74	0.42
6	Benzophenone	—	—	—	—	22.01	8.04	2.91	1.28
7	Benzyl alcohol	—	10.47	4.50	2.54	1.43	0.89	0.48	0.27
8	Biphenyl	—	—	—	—	—	25.87	7.52	2.78
9	<i>n</i> -Butylbenzene	—	—	—	—	—	45.65	11.67	4.10
10	<i>p</i> -Chlorobenzaldehyde	—	—	7.54	3.39	1.67	1.48	0.90	0.72
11	Chlorobenzene	—	—	—	—	15.42	7.62	2.87	1.33
12	<i>p</i> -Chlorophenol	—	—	18.51	9.24	4.38	2.34	0.98	0.54
13	<i>p</i> -Chlorotoluene	—	—	—	—	—	14.56	4.85	1.99
14	<i>o</i> -Cresol	—	—	10.93	5.57	2.94	1.67	0.78	0.44
15	<i>o</i> -Dichlorobenzene	—	—	—	—	—	14.04	4.58	1.94
16	Diethyl phthalate	—	—	—	31.52	10.54	4.74	1.59	0.73
17	Dimethyl phthalate	—	—	22.30	8.15	3.34	1.78	0.74	0.40
18	<i>m</i> -Dinitrobenzene	—	—	13.15	7.27	3.97	2.38	1.12	0.60
19	<i>o</i> -Dinitrobenzene	—	—	15.15	7.22	3.71	2.03	0.86	0.43
20	<i>p</i> -Dinitrobenzene	—	—	10.49	5.97	3.04	1.82	0.87	0.47
21	2,4-Dinitrotoluene	—	—	—	15.42	7.14	4.02	1.61	0.82
22	2,6-Dinitrotoluene	—	—	—	14.73	6.97	3.53	1.42	0.72
23	3,4-Dinitrotoluene	—	—	—	14.33	6.28	3.09	1.19	0.58
24	Diphenyl ether	—	—	—	—	—	23.52	6.45	2.32
25	Ethylbenzene	—	—	—	—	—	12.23	4.43	1.89
26	<i>m</i> -Fluoronitrobenzene	—	—	—	11.07	5.81	3.53	1.49	0.77
27	<i>o</i> -Fluoronitrobenzene	—	—	16.01	8.28	4.35	2.49	1.11	0.58
28	<i>p</i> -Fluoronitrobenzene	—	—	15.76	8.54	4.32	2.48	1.14	0.66
29	<i>p</i> -Fluorophenol	—	13.26	6.41	3.50	1.89	1.10	0.53	0.27
30	<i>p</i> -Hydroxybenzaldehyde	17.58	7.92	3.77	1.94	0.99	0.58	0.32	0.20
31	<i>p</i> -Methoxybenzaldehyde	—	—	15.27	7.10	—	1.90	0.87	0.51
32	<i>p</i> -Methylbenzaldehyde	—	—	—	10.61	5.07	2.01	1.26	0.74
33	Methyl benzoate	—	—	—	15.35	6.83	3.58	1.50	0.82
34	Naphthalene	—	—	—	—	—	13.31	4.54	1.96
35	<i>p</i> -Nitroacetophenone	—	—	14.31	6.81	3.41	1.98	0.91	0.48
36	<i>p</i> -Nitrobenzaldehyde	—	17.39	8.06	4.00	2.17	1.33	0.61	0.35
37	<i>p</i> -Nitrilobenzaldehyde	—	12.24	5.16	2.66	1.34	0.86	0.40	0.22
38	Nitrobenzene	—	—	17.44	8.78	4.62	2.72	1.26	0.67
39	<i>m</i> -Nitrophenol	—	19.18	9.42	5.00	2.65	1.48	0.71	0.38
40	<i>o</i> -Nitrophenol	—	—	14.49	7.78	4.10	2.38	1.14	0.63
41	<i>p</i> -Nitrophenol	—	17.06	8.62	4.43	2.28	1.34	0.62	0.35
42	Phenol	12.72	7.72	4.25	2.50	1.39	0.94	0.46	0.26
43	2-Phenylethanol	—	18.30	8.84	4.62	2.34	1.36	0.65	0.37
44	<i>p</i> -Phenylphenol	—	—	—	—	15.71	5.57	2.07	0.90
45	3-Phenylpropanol	—	—	21.02	9.25	4.32	2.22	0.97	0.52
46	<i>n</i> -Propylbenzene	—	—	—	—	—	24.06	7.29	2.74
47	Toluene	—	—	—	—	14.22	7.30	2.91	1.42
48	Trichlorotoluene	—	—	—	—	—	24.74	6.93	2.55
49	2,4-Dimethylphenol	—	—	—	12.63	5.87	3.06	1.23	0.62

(Continued on p. 282)

APPENDIX II (continued)

<i>Solute No.</i>														
ϕ_{MeOH}	0.90	1.00	0.15	0.225	0.30	0.375	0.45	0.525	0.60	0.675	0.75	0.25	0.30	0.35
ϕ_{ACN}	0	0	0.05	0.075	0.10	0.125	0.15	0.175	0.20	0.225	0.25	0.25	0.30	0.35
ϕ_{water}	0.10	0	0.80	0.70	0.60	0.50	0.40	0.30	0.20	0.10	0	0.50	0.40	0.30
1	0.36	0.10	27.78	12.10	6.66	2.54	1.33	0.83	0.59	0.38	0.26	1.70	1.03	0.81
2	0.68	0.28	—	27.84	11.75	4.74	2.14	1.26	0.84	0.48	0.28	2.53	1.66	1.26
3	0.33	0.20	—	27.29	13.11	4.80	2.25	1.27	0.81	0.49	0.27	2.65	1.66	1.27
4	1.14	0.41	—	—	15.12	4.87	2.20	1.34	0.93	0.45	0.29	3.03	1.76	1.32
5	0.31	0.18	22.30	11.77	5.38	2.24	1.19	0.78	0.58	0.31	0.23	1.62	1.01	0.78
6	0.76	0.33	—	—	—	12.91	4.23	2.06	1.12	0.57	0.32	6.94	3.22	2.14
7	0.14	0.11	7.65	4.57	2.48	1.25	0.74	0.53	0.46	0.25	0.19	0.85	0.58	0.48
8	1.40	0.50	—	—	—	—	9.76	4.25	1.96	0.82	0.40	16.79	6.69	4.04
9	1.98	0.57	—	—	—	—	17.75	7.18	3.09	1.06	0.49	31.32	12.07	6.50
10	—	0.49	—	—	—	11.90	4.17	2.15	1.30	—	0.32	5.65	3.21	2.22
11	0.86	0.34	—	—	33.14	9.90	4.03	2.01	1.19	—	0.34	4.92	2.89	2.02
12	0.32	0.15	—	20.90	8.38	2.94	1.49	1.00	0.61	0.34	0.21	1.68	1.10	0.82
13	1.09	0.42	—	—	—	18.88	6.98	3.14	1.69	0.70	0.38	10.17	4.70	3.02
14	0.31	0.18	21.88	11.77	5.59	2.18	1.18	0.74	0.51	0.31	0.21	1.46	0.94	0.71
15	1.16	0.44	—	—	—	14.26	6.17	3.13	1.66	0.75	0.39	8.40	4.58	2.99
16	0.50	0.19	—	—	25.86	5.00	2.70	1.30	0.77	0.41	0.23	4.34	2.12	1.39
17	0.27	0.15	—	17.01	7.69	1.93	1.29	0.86	0.58	0.32	0.20	1.61	1.03	0.77
18	0.38	0.17	—	17.36	8.17	2.88	1.54	0.93	0.65	0.31	0.21	2.19	1.26	0.92
19	0.32	0.12	—	17.13	8.05	2.86	1.39	0.81	0.52	0.27	0.18	2.16	1.17	0.81
20	0.31	0.13	—	15.16	6.84	2.84	1.39	0.86	0.55	0.28	0.20	2.07	1.20	0.88
21	0.50	0.19	—	—	14.61	5.37	2.22	1.24	0.75	0.35	0.22	3.46	1.77	1.22
22	0.43	0.18	—	—	14.58	4.31	2.10	1.14	0.75	0.34	0.21	3.38	1.69	1.15
23	0.34	0.14	—	36.26	11.11	3.98	2.02	1.03	0.63	0.35	0.21	3.22	1.66	1.10
24	1.18	0.41	—	—	—	—	9.38	3.96	1.78	0.70	0.37	15.64	6.29	3.71
25	1.14	0.40	—	—	—	12.98	6.02	—	1.50	0.70	0.37	9.42	4.30	2.76
26	0.54	0.22	—	20.10	11.32	4.42	2.05	1.33	0.78	0.41	0.25	2.84	1.56	1.15
27	0.38	0.18	—	20.78	8.88	3.45	1.58	0.97	0.68	—	0.22	1.95	1.29	0.94
28	0.38	0.18	—	20.68	8.94	3.56	1.65	0.94	0.70	—	0.22	2.09	1.39	1.02
29	0.18	0.07	12.10	7.45	3.50	1.66	0.93	0.57	0.47	0.27	0.19	0.97	0.67	0.54
30	0.17	0.06	7.37	3.38	1.87	0.91	0.58	0.42	0.36	0.22	0.18	0.66	0.45	0.38
31	0.36	0.22	—	—	—	3.65	2.18	1.18	0.79	0.39	0.29	2.86	1.62	—
32	0.18	0.25	—	—	—	6.43	3.44	1.78	1.11	0.54	0.32	5.01	2.48	2.07
33	0.64	0.28	—	31.64	13.62	3.73	2.00	1.14	0.82	—	0.29	2.53	1.60	1.22
34	1.13	0.44	—	—	—	17.20	5.70	3.27	1.49	0.72	0.38	9.09	4.19	2.76
35	0.34	0.18	—	16.45	7.30	2.22	1.26	0.81	0.60	0.34	0.21	1.70	1.10	0.82
36	0.23	0.11	—	—	17.18	5.85	2.34	1.36	0.89	0.44	0.25	3.12	1.92	1.38
37	0.22	0.05	—	24.97	10.71	2.71	1.73	0.98	0.70	0.34	0.24	2.38	1.31	0.98
38	0.46	0.23	—	17.70	8.73	3.14	1.70	0.99	0.70	0.40	0.26	2.42	1.42	1.04
39	0.26	0.14	19.22	11.73	4.74	1.90	1.08	0.72	0.47	0.26	0.19	1.39	0.83	0.63
40	0.50	0.21	15.54	12.75	5.87	1.91	1.42	0.87	0.63	0.34	0.25	1.99	1.21	0.90
41	0.27	0.13	23.88	8.08	3.94	1.30	0.98	0.58	0.49	0.25	0.18	1.26	0.78	0.58
42	0.19	0.11	8.30	5.03	2.59	1.21	0.78	0.51	0.41	0.26	0.18	0.97	0.62	0.49
43	0.25	0.14	17.11	7.71	4.12	1.79	1.04	0.72	0.53	0.30	0.21	1.05	0.74	0.58
44	0.57	0.20	—	—	27.14	7.07	3.44	1.45	0.81	0.42	0.24	4.67	2.14	1.40
45	0.33	0.16	—	16.64	8.22	2.98	1.42	0.86	0.64	0.31	0.22	1.77	1.04	0.77
46	1.38	0.48	—	—	—	16.94	9.88	4.54	2.07	0.86	0.41	16.75	7.18	4.23
47	0.86	0.36	—	—	24.98	9.25	3.73	2.00	1.22	0.57	0.34	5.30	2.81	1.95
48	1.38	0.43	—	—	—	—	—	—	2.02	0.87	—	—	—	—
49	0.40	0.19	—	26.72	10.92	4.00	1.75	0.99	0.65	0.50	0.25	2.34	1.34	0.98

0.40	0.45	0.50	0.15	0	0	0	0	0	0	0	0	0	0
0.40	0.45	0.50	0.45	0.10	0.20	0.30	0.40	0.50	0.60	0.70	0.80	0.90	1.00
0.20	0.10	0	0.40	0.90	0.80	0.70	0.60	0.50	0.40	0.30	0.20	0.10	0
0.57	0.40	0.30	1.26	—	13.58	6.32	2.95	1.78	1.03	0.66	0.44	0.31	0.25
0.80	0.51	0.34	2.10	—	—	14.10	5.89	3.34	1.78	1.04	0.66	0.42	0.30
0.81	0.52	0.34	1.14	28.68	10.25	5.72	2.74	1.68	1.00	0.65	0.42	0.30	0.22
0.83	0.53	0.36	2.16	—	—	13.94	6.26	3.51	1.90	1.14	0.70	0.45	0.30
0.53	0.37	0.25	1.17	—	—	7.46	3.38	1.97	1.11	0.70	0.42	0.28	0.21
1.15	0.65	0.39	4.51	—	—	—	15.02	6.69	3.09	1.74	0.94	0.56	0.36
0.36	0.29	0.23	0.49	8.85	3.72	1.99	1.06	0.67	0.46	0.32	0.22	0.18	—
1.92	0.94	0.50	9.59	—	—	—	36.28	14.34	5.79	2.98	1.54	0.82	0.46
2.86	1.24	0.61	14.94	—	—	—	—	24.31	9.55	4.66	2.37	1.25	0.68
1.23	0.70	0.42	1.43	—	24.22	8.57	3.11	—	—	0.99	0.62	0.40	0.31
1.16	0.68	0.42	3.69	—	—	33.67	11.82	5.88	2.94	1.67	0.98	0.59	0.41
0.53	0.36	0.27	1.10	—	19.78	8.22	3.22	1.69	0.92	0.54	0.30	0.22	0.25
1.56	0.82	0.47	6.17	—	—	—	21.38	9.78	4.46	2.35	1.36	0.78	0.50
0.49	0.34	0.26	0.95	—	11.82	5.76	2.74	1.48	0.82	0.51	0.31	0.22	0.22
1.60	0.88	0.50	5.94	—	—	—	19.94	9.25	4.30	2.29	1.38	0.80	0.50
0.79	0.47	0.28	2.54	—	—	28.14	8.89	4.22	2.02	1.09	0.64	0.39	0.27
0.52	0.34	0.24	1.74	—	21.15	8.42	3.41	1.88	1.03	—	0.39	0.25	0.18
0.57	0.36	0.22	1.69	—	—	11.34	4.66	2.51	1.29	0.71	0.39	0.23	0.17
0.50	0.32	0.21	1.41	—	—	13.43	4.94	2.48	1.22	0.68	0.36	0.22	0.14
0.54	0.34	0.21	1.66	—	22.02	11.42	4.86	2.58	1.30	0.71	0.38	0.22	0.16
0.70	0.41	0.24	2.47	—	—	21.86	7.73	3.62	1.70	0.91	0.52	0.28	0.16
0.66	0.39	0.23	1.98	—	—	22.13	7.88	—	1.74	0.91	0.49	0.27	0.18
0.62	0.38	0.22	2.18	—	—	25.47	8.07	3.66	1.73	0.88	0.49	0.27	0.19
1.73	0.83	0.43	8.30	—	—	—	35.34	13.70	5.49	2.66	1.40	0.74	0.42
1.48	0.79	0.46	5.66	—	—	—	19.58	8.90	4.14	—	—	1.10	0.49
0.70	0.43	0.29	2.06	—	—	14.20	5.97	3.07	1.60	0.94	0.54	0.31	0.24
0.60	0.38	0.26	1.66	—	22.96	11.43	4.78	2.53	1.33	0.76	0.45	0.27	0.21
0.65	0.42	0.26	1.77	—	—	12.85	5.26	2.85	1.51	0.84	0.50	0.30	0.20
0.38	0.27	0.22	0.65	15.93	7.60	3.77	1.74	1.03	0.59	0.34	0.20	0.14	0.16
0.29	0.25	0.21	0.40	8.18	3.04	1.60	0.79	0.50	0.30	0.19	0.11	0.10	0.25
0.77	0.50	0.30	1.15	—	13.98	6.30	2.80	1.68	0.96	0.60	0.40	0.28	0.22
1.06	0.63	0.40	0.90	—	24.11	10.94	4.78	2.51	1.43	0.86	0.57	0.38	0.27
0.77	0.50	0.34	1.90	—	—	13.34	5.34	2.89	1.62	0.97	0.62	0.42	0.32
1.46	0.81	0.47	6.18	—	—	—	19.89	8.63	4.05	2.22	1.22	0.70	0.46
0.54	0.35	0.24	1.79	—	19.20	8.80	3.77	2.06	1.12	0.67	0.39	0.24	0.19
0.81	0.48	0.30	1.22	—	23.26	6.48	3.15	1.82	1.00	0.58	0.34	0.22	0.18
0.63	0.41	0.26	0.75	22.62	7.94	4.53	2.25	1.37	0.70	0.47	0.30	0.19	0.14
0.67	0.43	0.30	1.71	—	—	11.32	5.06	2.78	1.47	0.84	0.52	0.33	0.22
0.42	0.30	0.24	0.94	27.57	11.48	5.10	2.21	1.24	0.66	0.38	0.22	0.14	0.27
0.58	0.39	0.28	1.45	—	16.38	8.28	3.74	2.10	1.17	0.73	0.44	0.29	0.38
0.38	0.27	0.22	0.72	23.03	9.09	4.15	2.95	1.08	0.58	0.33	0.19	0.13	0.17
0.37	0.28	0.22	0.56	10.16	4.90	2.70	1.45	0.89	0.52	0.34	0.21	0.15	0.17
0.42	0.32	0.26	0.68	12.86	6.73	3.20	1.49	0.90	0.54	0.36	0.29	0.22	0.31
0.78	0.46	0.30	2.66	—	—	31.76	8.26	3.52	1.61	0.88	0.49	0.30	0.32
0.51	0.36	0.26	0.98	—	15.26	6.11	2.42	1.34	0.80	0.50	0.35	0.29	0.40
2.05	0.99	0.53	9.45	—	—	—	36.18	14.45	6.26	3.17	1.74	0.94	0.52
1.14	0.67	0.42	3.70	—	—	30.67	11.31	5.76	2.80	1.66	0.98	0.60	0.22
2.06	0.97	0.54	9.55	—	—	—	40.03	15.68	6.44	3.29	1.72	0.91	0.55
0.62	0.39	0.29	1.45	—	25.84	10.63	4.20	2.30	1.18	0.70	0.43	0.29	0.30

ACKNOWLEDGEMENT

The assistance of ir. Anton Drouen in constructing some of the figures in this publication is gratefully acknowledged.

REFERENCES

- 1 P. J. Schoenmakers, H. A. H. Billiet and L. de Galan, *J. Chromatogr.*, 185 (1979) 179.
- 2 P. J. Schoenmakers, H. A. H. Billiet and L. de Galan, *Anal. Chem.*, submitted for publication.
- 3 P. J. Schoenmakers, H. A. H. Billiet and L. de Galan, *J. Chromatogr.*, 205 (1981) 13.
- 4 S. R. Bakalyar, R. McIlwrick and E. Roggendorf, *J. Chromatogr.*, 142 (1977) 353.
- 5 N. Tanaka, H. Goodell and B. L. Karger, *J. Chromatogr.*, 158 (1978) 233.
- 6 R. Spatz and E. Roggendorf, *Z. Anal. Chem.*, 299 (1979) 267.
- 7 E. Roggendorf and R. Spatz, *J. Chromatogr.*, 204 (1981) 263.
- 8 J. L. Glajch, J. J. Kirkland, K. M. Squire and J. M. Minor, *J. Chromatogr.*, 199 (1980) 57.
- 9 P. J. Schoenmakers, H. A. H. Billiet, R. Tijssen and L. de Galan, *J. Chromatogr.*, 149 (1978) 519.
- 10 R. Tijssen, H. A. H. Billiet and P. J. Schoenmakers, *J. Chromatogr.*, 122 (1976) 185.
- 11 R. P. W. Scott and P. Kucera, *J. Chromatogr.*, 142 (1977) 213.
- 12 R. M. McCormick and B. L. Karger, *Anal. Chem.*, 52 (1980) 2249.
- 13 G. E. Berendsen, P. J. Schoenmakers, L. de Galan, Gy. Vigh, Z. Varga-Puchony and J. Inczédy, *J. Liq. Chromatogr.*, 3 (1980) 1669.
- 14 P. J. Schoenmakers *et al.*, to be published.
- 15 E. H. Slaats, *Ph. D. Thesis*, University of Amsterdam, Amsterdam, 1980.

CHROM. 14,097

HIGH-PERFORMANCE LIQUID CHROMATOGRAPHY OF ORGANIC ACIDS ON BARE SILICA

W. J. Th. BRUGMAN, S. HEEMSTRA and J. C. KRAAK

Laboratory for Analytical Chemistry, University of Amsterdam, Nieuwe Achtergracht 166, Amsterdam (The Netherlands)

SUMMARY

Unmodified silica gel in combination with mixtures of dichloromethane, methanol, buffer and water as the mobile phase was investigated as a phase system for the separation of aromatic acids by high-performance liquid chromatography. The influence of parameters such as the amounts of methanol and water and of the type, concentration and pH of the buffer in the mobile phase was systematically investigated. For many mobile phase compositions the composition of the adsorbed layer on the silica gel was also determined. The results show that the distribution process in these phase systems is very complex. However, these phase systems are efficient and applicable to the separation of carboxylic and even sulphonic acids. This is demonstrated with a number of separations of test mixtures and the analysis of additives in foods.

INTRODUCTION

Since the introduction of chemically modified silica gels in high-performance liquid chromatography (HPLC), interest in applying unmodified silica gel as an adsorbent for the separation of very polar substances, such as acids, has diminished considerably. It is doubtful whether this reduction in interest is justified nowadays, particularly if one considers the contribution that bare silica made to the popularity of thin-layer chromatography (TLC) for the separation of a great variety of substances, including acids, in recent decades^{1–5}.

In almost all TLC systems applied to the separation of organic acids the developing liquid consists of an apolar solvent acting as a diluent for a very polar solvent component, such as an alcohol, and further contains a considerable amount of an organic acid, such as acetic or formic acid, and in some instances a small amount of water. The results from these TLC experiments were adapted to compose mobile phases for the separation of carboxylic and sulphonic acids on bare silica by HPLC. Thus, diethyl ether–*n*-propanol–aqueous acetic acid was found useful for the separation of oxypurines⁶ and dichloromethane–methanol–aqueous ammonium formate buffer was used for the rapid separation of nucleic acids⁷. Aromatic carboxylic and sulphonic acids could be well separated on bare silica by using *n*-butanol–etha-

nol-aqueous sodium acetate as the mobile phase⁸. In one study the possibility of chromatographing amino acids and sulphonic acids on bare silica with an aqueous mobile phase has been reported⁹. Recently, it was demonstrated that the pre-treatment of bare silica with a crystalline salt or acid allows tailing-free separations of a variety of aromatic carboxylic acids with mixtures of *n*-hexane and diethyl ether as the mobile phase¹⁰.

All of these studies have clearly shown the potential of bare silica gel for the separation of organic acids. However, in most instances very little attention was given to the possibility of varying the retention via the mobile phase composition. In this paper we report the results of an extensive and systematic investigation on the retention behaviour of aromatic carboxylic acids on bare silica with dichloromethane-methanol-acetate buffer mixtures containing small amounts of water as the mobile phase.

It is shown that many parameters can be used to vary the retention and that the mobile phase composition has to fulfil certain requirements in order to be able to chromatograph carboxylic and sulphonic acids under optimal conditions. Various examples of the applicability of unmodified silica gel are demonstrated.

EXPERIMENTAL

Apparatus

The HPLC experiments were carried out with a Hupe-Bush 1010A liquid chromatograph (Hewlett-Packard, Avondale, PA, U.S.A.) equipped with a Rheodyne 7120 high-pressure sampling valve fitted with a 20- μ l sample loop and a Pye-Unicom UV-LC variable-wavelength UV detector. The columns (250 \times 4.6 mm I.D.) were made of 316 stainless steel. All measurements were performed at ambient temperature.

The gas chromatographic (GC) experiments were performed with a Packard-Becker 427 gas chromatograph equipped with a thermal conductivity detector (TCD). The column (1 m \times 4 mm I.D.) was made of copper and was filled with Porapak Q (100–120 mesh) (Waters Assoc., Milford, MA, U.S.A.).

Materials

All chemicals and solvents were of analytical-reagent grade from commercial sources and were used as delivered. The sulphonic acids were kindly donated by Professor H. Cerfontain, University of Amsterdam. The silica gel used in HPLC was Hypersil, mean particle size 5 μ m (Shandon, London, Great Britain).

Procedures

The HPLC columns were packed according to the procedure recommended by the supplier of the silica (Shandon). When changing the eluent the columns were washed successively with 25 ml of absolute ethanol, and 100 ml of dichloromethane and then equilibrated with the mobile phase until constant retention of the solutes was achieved. In all experiments toluene was used as the non-retarded solute.

In order to determine the composition of the adsorbed phase on the silica gel after each set of experiments, the column was washed with 25 ml of absolute ethanol. To the collected ethanol fraction 5 ml of ethyl acetate were added (as an internal

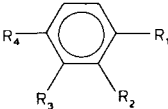
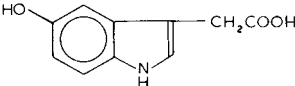
standard) and this mixture was then analysed by GC on a Porapak column using helium as the carrier gas at a flow-rate of 50 ml/min at 180°C. This gives the total amount of water, methanol and dichloromethane present in the column. The amount of mobile phase components adsorbed can then be calculated from the composition of this mixture, the mobile phase composition and from the mobile phase volume (V_m) which was determined from t_{R0} and the flow-rate. The volume of the adsorbed liquid phase (V_s) was determined from the void volume (V_l) of the column ($V_s = V_l - V_m$), which was determined by equilibrating the column with pure dichloromethane and determining the dichloromethane content after its elution with ethanol and GC analysis. The results agreed with those obtained according to ref. 11.

RESULTS AND DISCUSSION

Table I shows the structures of the carboxylic acids selected to study the retention behaviour on bare silica. The dependence of the capacity ratio (k') of these acids on the amounts of methanol and water and on the type, concentration and pH of the buffer present in the mobile phase was systematically investigated. The effect of the mobile phase composition on the peak shape and column efficiency was also studied.

In order to obtain some more insight into the distribution process, the composition of the adsorbed phase on the silica gel was determined as described under Experimental.

TABLE I
STRUCTURES OF THE ACIDS

						
Name	Abbreviation	R_1	R_2	R_3	R_4	pK_a
4-Hydroxybenzoic acid	4HB	COOH	H	H	OH	4.67
3-Hydroxybenzoic acid	3HB	COOH	H	OH	H	4.30
4-Hydroxycinnamic acid	4HC	CH=CHCOOH	H	H	OH	4.64
4-Aminobenzoic acid	4AB	COOH	H	H	NH ₂	4.68
Homovanillic acid	HVA	CH ₂ COOH	H	H	OH	4.41
Hippuric acid	HA	CONHCH ₂ COOH	H	H	H	—
2-Hydroxyphenylacetic acid	2HP	CH ₂ COOH	OH	H	H	—
5-Hydroxyindole-3-acetic acid	5HIA					—

Retention behaviour

Influence of water. The influence of water on k' is shown in Fig. 1; k' for each acid increases significantly with increasing water content and for some solutes it reaches a constant value in the region of 1–2.6% (v/v) of water. However, for hippuric acid (HA) and 5-hydroxyindoleacetic acid (5HIA) k' increases with increasing water content up to 1% and then gradually decreases again up to 2.6% of water.

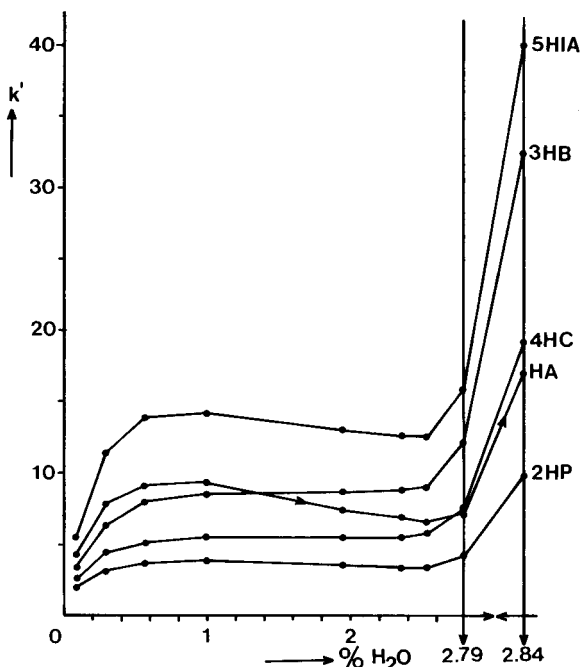


Fig. 1. Dependence of the capacity ratio (k') on the water content of the mobile phase. Mobile phase composition: dichloromethane-methanol (8:2) + 0.01 M acetic acid (HAc) + 0.01 M potassium acetate (KAc) + 0–2.84% (v/v) of water. Solutes: for abbreviations see Table I.

On increasing the water content from 2.6 to 2.79% (which is very close to the saturation point), a significant increase in k' for all solutes is observed. When the mobile phase is saturated with water (corresponding to 2.84% of water) k' for all solutes increases by a factor of about 2.5.

In order to obtain insight into the distribution process occurring in this phase system, the possible modification of the surface of the silica gel, by preferential adsorption of mobile phase components, was measured. Fig. 2 shows the amounts of methanol, water, dichloromethane and potassium acetate (obtained by evaporation of the collected ethanol fraction) adsorbed on the surface of the silica gel as a function of the water content of the mobile phase.

Comparison of Figs. 1 and 2 shows that there is no clear relationship between the variation of k' and the composition of the adsorbed layer up to 2.6% of water in the mobile phase. However, the significant increases in k' at 2.79 and 2.84% coincide very well with the steep increase in the adsorbed layer owing to partial (2.79%) and complete (2.84%) pore filling with a co-existing, relatively water-rich liquid phase¹². The results in Figs. 1 and 2 suggest a complex mixed distribution process. The variation of the amount of adsorbed potassium acetate (KAc) as function of the water content indicates a similar effect. Also, the change in the selectivity factors with increasing water content might be an indication of the occurrence of a mixed distribution process.

Influence of methanol. The influence of methanol on k' , other variables remain-

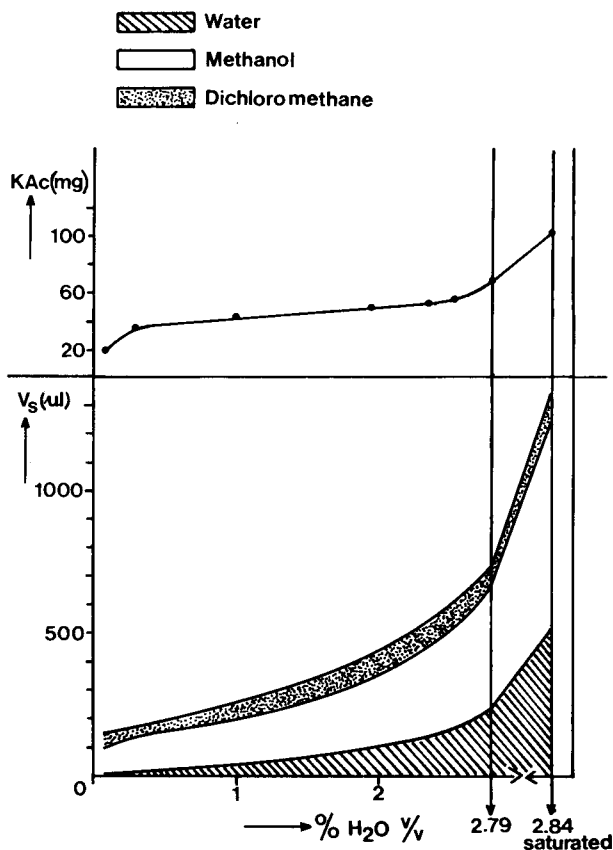


Fig. 2. Amount of adsorbed mobile phase components as a function of the water content of the mobile phase. Conditions as in Fig. 1. V_s = volume of the adsorbed liquid phase.

ing constant, is shown in Fig. 3. In contrast to water (see Fig. 1), methanol acts as a strong moderator and its concentration can be used to adjust the order and degree of retention over a wide range. As can be seen from Fig. 3, the graph of $\log k'$ versus \log [methanol] is approximately linear for most acids in the region 15–40% of methanol, as is commonly found in adsorption systems¹³. For some solutes a deviation occurs at 10% of methanol, which might be attributed to significant pore filling as at lower methanol contents the actual amount of added water (0.6%) comes closer to the saturation point. For two acids (HA and HVA), significantly different behaviour of k' with respect to methanol content compared with the other acids is found. The graph of $\log k'$ versus \log [methanol] is curved and shows a significantly different slope compared with the other acids.

Fig. 3 shows that the methanol content of the mobile phase is a valuable parameter for adjusting the degree and in some instances even the order of retention.

Influence of buffer concentration. The influence of the buffer concentration on k' , with other parameters constant and keeping the ratio of HAc and KAc constant, is shown in Fig. 4. If no buffer is present in the mobile phase all acids are only slightly retained. However, after the addition of only $5 \cdot 10^{-4}$ M of buffer a considerable

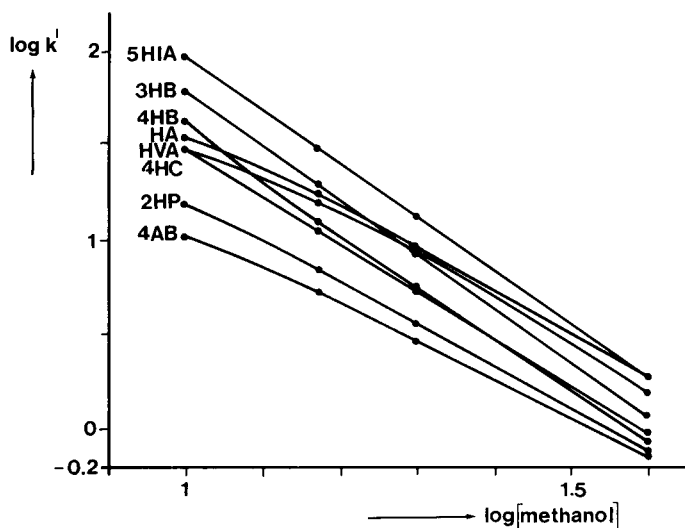


Fig. 3. Dependence of the capacity ratio on the methanol content of the mobile phase. Mobile phase composition: dichloromethane + 10–40% (v/v) methanol + 0.01 *M* HAc + 0.01 *M* KAc + 0.6% (v/v) H₂O.

increase in k' for all acids occurs. A further increase in the buffer concentration causes a small increase in k' up to 10^{-3} *M*, and from this point the k' values of the acids decrease again, with different slopes, up to about $2 \cdot 10^{-2}$ *M* of buffer. At very high buffer concentrations the k' values of all acids increase again. The last effect can be attributed to significant pore filling as the mobile phase comes closer to the water

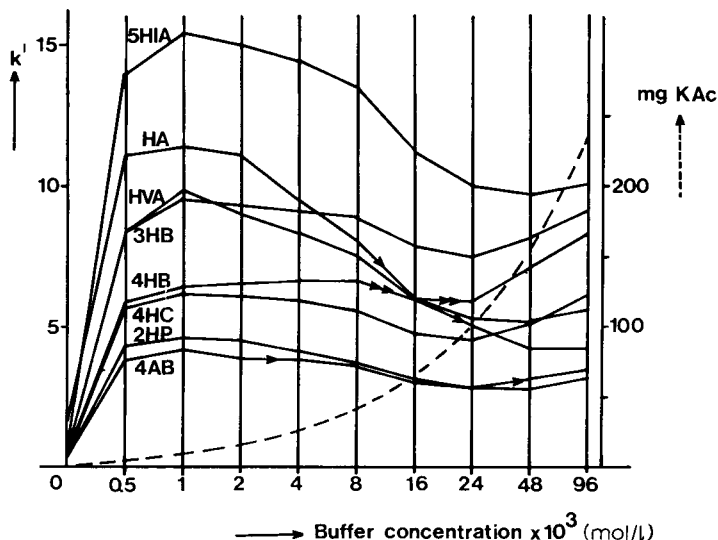


Fig. 4. Dependence of the capacity ratio on the buffer concentration in the mobile phase at a constant HAc/KAc ratio. Mobile phase composition: dichloromethane–methanol (8:2) + 2% (v/v) water + 0–0.1 *M* HAc + 0–0.1 *M* KAc.

saturation point as a result of the high salt concentration (*i.e.*, the water saturation level is about 2.4% at 10^{-1} M of buffer). The significant increase in k' when only a small amount of buffer is added to the mobile phase leads to the conclusion that the solute has to be present in the mobile phase in an ionized form (possibly as an ion pair associated with potassium ions) in order to be transferred to the stationary phase. It can be seen from Fig. 4 that a buffer concentration of about 10^{-3} M is needed in order to create the adsorptive environment for the solutes. However, at a buffer concentration of 10^{-3} M k' decreases again, possibly owing to a competitive effect of KAc. The difference in the slope of this decrease for the acids might be attributed to the relative magnitude of the different distribution processes occurring.

Neglecting any speculation about the distribution process, Fig. 4 clearly shows that significant changes in the degree and order of retention can be introduced by variation of the buffer concentration.

Influence of pH of the buffer. The influence of the ratio of the amount of HAc and KAc added (for simplicity expressed in terms of the pH that an aqueous solution with the same concentrations would have) on k' was measured from 0.1 M HAc to 0.02 M KAc, and is shown in Fig. 5. It can be seen that the pH has a large influence on k' . At low pH (pure HAc) the solutes are almost unretained, indicating again that the acids in their undissociated form (and thus also HAc) show little affinity for the silica in combination with the selected mobile phase composition. Certainly the retention of the acids will increase with decreasing methanol content.

On changing the ratio of HAc and KAc in favour of the latter (increasing pH) k' starts to increase considerably and tends to level off at higher pH. The behaviour of k' as a function of pH coincides well with the degree of dissociation of weak acids in

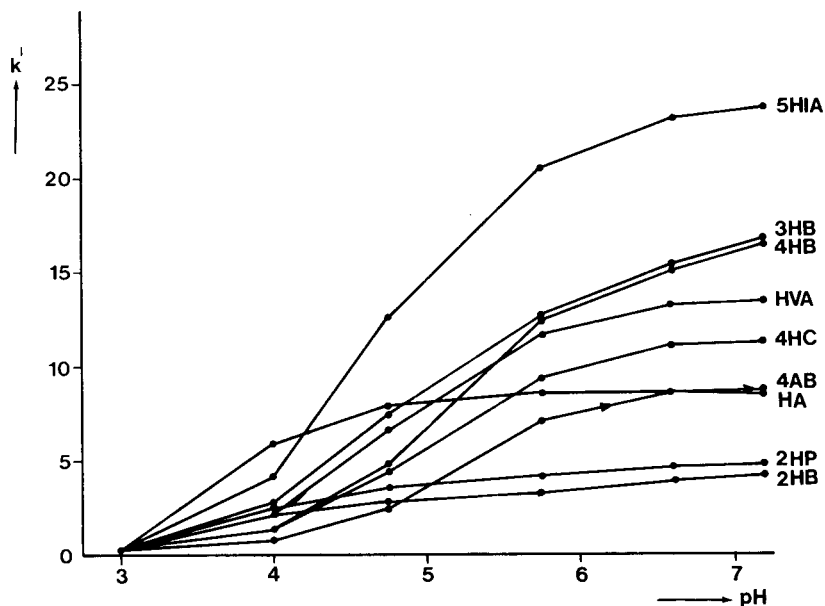


Fig. 5. Influence of the ratio of HAc and KAc (pH) in the mobile phase on the capacity ratio. Mobile phase composition: dichloromethane-methanol (8:2) + 1% (v/v) water + 0.02 M KAc and various amounts of HAc. Solutes: see Table I; 2HB = 2-hydroxybenzoic acid.

aqueous systems with pH and shows that the distribution coefficient, leaving the distribution process as unexplained, is roughly proportional to the term $(1 + [\text{H}^+]/K_a)^{-1}$. From Table I and Fig. 5 it can be seen that there is no clear correlation between the pK_a of the acids and their k' values.

Whether the pH effect occurs in the mobile and/or stationary phase is not yet clear. It seems that the effect is mainly due to the pH change of the mobile phase, as the amount of KAc adsorbed on the silica (and therefore probably the pH of the adsorbed layer) was found to be constant in the pH range 4–7. However, to understand the pH effect it is necessary to know precisely the pH of the adsorbed layer. So far attempts in our laboratory to measure the pH of the adsorbed layer have failed.

As a parameter for adjusting the retention, the ratio of HAc and KAc (the pH) seems to be one of the most effective.

Influence of the type of buffer. The effect of the cationic and anionic part of the buffer on k' was investigated with mobile phases containing a buffer composed of acetic acid (HAc) and potassium, sodium, ammonium and lithium acetate (KAc, NaAc, NH_4Ac , LiAc) and from potassium formate, acetate, propionate and chloroacetate and their corresponding acids. The results of these measurements are shown in Figs. 6 and 7.

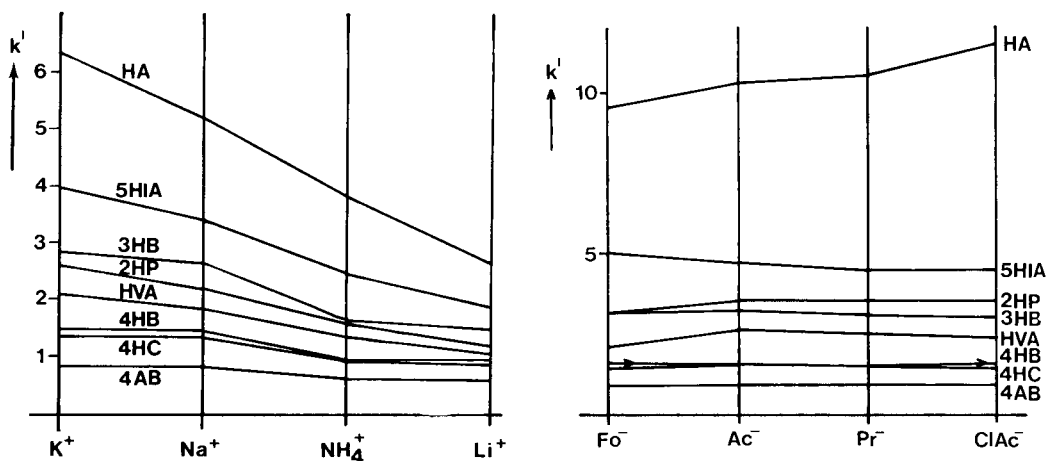


Fig. 6. Effect of the nature of the cationic part of the buffer on the capacity ratio. Mobile phase composition: dichloromethane-methanol (8:2) + 2% (v/v) water + 0.05 M HAc + 0.01 M KAc, NaAc, NH_4Ac or LiAc. pH = 4.05.

Fig. 7. Effect of the nature of the anionic part of the buffer on the capacity ratio. Mobile phase composition as in Fig. 5; the buffer was composed of formic acid/potassium formate; HAc/KAc; propionic acid/potassium propionate (Pr^-); chloroacetic acid/potassium chloroacetate (ClAc^-).

As can be seen from Fig. 6, the type of the cationic part of the buffer has a significant effect on the retention. The degree of retention decreases in the order $\text{K}^+ > \text{Na}^+ > \text{NH}_4^+ > \text{Li}^+$ and the amount of adsorbed salts decreases in the order $\text{K}^+ > \text{Na}^+ > \text{Li}^+$ (NH_4^+ could not be determined). This result does not indicate a competition effect, but more to a pH effect on the surface of the silica due to the adsorption of different amounts of acetate with varying types of cation. The type of the anionic part of the buffer seems to have only a small effect on k' , as can be seen

from Fig. 7. However, in some instances "fine tuning" of the selectivity can be introduced by varying the type of the anionic part of the buffer, as can be seen from Fig. 7.

Column performance

Apart from the influence of the various parameters on k' , their effect on the peak shape and column efficiency was also studied. In order to determine whether the column efficiency decreases with the investigated phase systems, all freshly packed columns were first tested with pure dichloromethane as eluent and 4,4-dinitrodiphenyl ($k' \approx 0.3$) and acetophenone ($k' \approx 1.5$) as solutes. The plate numbers of the columns tested under these conditions ranged between 11,000 and 13,000 for a 25-cm column at a linear velocity of 2.5 mm/sec. This plate number decreased to 6000–7000 when using dichloromethane–methanol–buffer mixtures as the mobile phase and acids as the solutes.

Most of the variables seem to have only a small effect on the column efficiency. However, some restrictions apply with certain mobile phase compositions. Serious leading was noticed when mobile phases were used that contain less than $4 \cdot 10^{-3} M$ of KAc or of which the pH is lower than 3.0. Further, the water content must not be too low in order to obtain reproducible retention (e.g., with 20% of methanol the water content must be $>0.5\%$). On the other hand, maximal column efficiency (7000 plates) was found with eluents of higher pH (ca. 7) and of high KAc concentrations (ca. $2 \cdot 10^{-2} M$) and with eluents with a water content near the saturation point or saturated with water.

The columns used in this study were used for several months with a great variety of eluents without any significant change in column characteristics. However, the performance of columns exposed to an eluent of high pH (8.8) for a longer period showed a large decrease in column efficiency (from 7000 to 3000) and a change in retention characteristics.

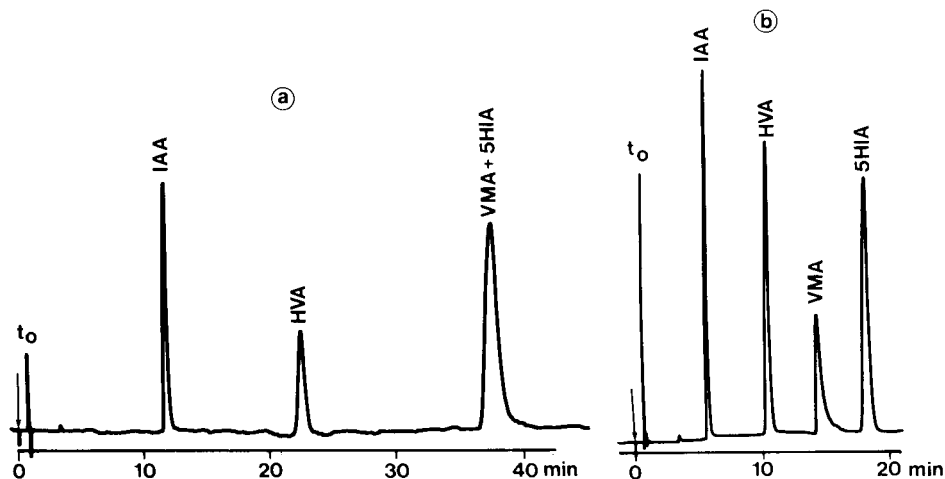


Fig. 8. Effect of the addition of 18-crown-6 to the mobile phase on the retention of some carboxylic acids. Stationary phase: silica. Mobile phase: (a) dichloromethane–methanol (8:2) + 0.01 M KAc, saturated with water; (b) dichloromethane–methanol (8:2) + 0.02 M KAc + 0.01 M 18-crown-6, saturated with water. Solutes: t_0 = toluene; indole-3-acetic acid (IAA); homovanillic acid (HVA); vanilmandelic acid (VMA); 5-hydroxyindole-3-acetic acid (5HIA).

Of about 40 carboxylic acids chromatographed so far with many phase systems, only a few acids showed bad peak shapes (broad and tailing) in all phase systems investigated. These are the acids that are able to form intramolecular hydrogen bonds such as the substituted mandelic acids and salicylic acid. However, promising results for these types of acids were obtained with water-saturated mobile phases and by the addition of a crown ether to the mobile phase¹⁴. The applicability of partition systems for carboxylic acids was demonstrated previously¹⁵.

Fig. 8 shows the effect of the addition of 18-crown-6 to the mobile phase on the retention of some carboxylic acids of biomedical interest. Significant changes in the degree and order of retention can be introduced by adding 18-crown-6. Investigations of the favourable effects of crown ethers on the retention of acids are being continued.

Practical utility

The results obtained so far indicate that bare silica is applicable to the separation of carboxylic acids. With respect to efficiency, selectivity and stability bare silica can compete with alkyl-modified silica gels and is often a useful supplement. Moreover, bare silica is a relatively cheap and stable material compared with alkyl-modified silicas, which makes it attractive as a column support for preparative liquid chromatography, and also because of the ease of removing the organic solvent after collection of the sample.

The applicability of bare silica for the separation of a variety of acids is demonstrated in Figs. 9–12. Fig. 9 shows the rapid separation of a test mixture of

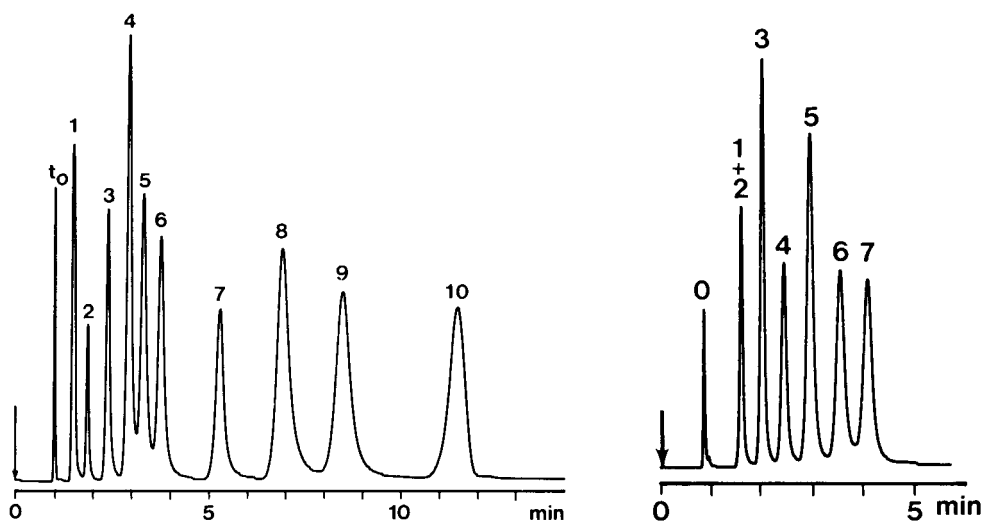


Fig. 9. Separation of a test mixture of aromatic carboxylic acids. Stationary phase: silica. Mobile phase: dichloromethane-methanol (8:2) + 2% (v/v) water + 0.1 M HAc + 0.01 M KAc ("pH" = 3.75). Solutes: t_0 = toluene; 1 = 3,4-dimethoxybenzoic acid; 2 = benzoic acid; 3 = 4-hydroxybenzoic acid; 4 = 3-aminobenzoic acid; 5 = 4-hydroxyphenylacetic acid; 6 = 3-hydroxybenzoic acid; 7 = 3,4-furandicarboxylic acid; 8 = nicotinic acid; 9 = hippuric acid; 10 = 4-aminohippuric acid.

Fig. 10. Rapid separation of closely related cinnamic acids. Conditions as in Fig. 8, except 0.1 M HAc + 0.02 M KAc ("pH" = 4.0). Solutes: 1 = toluene; 2 = 2-methoxycinnamic acid; 3 = cinnamic acid; 4 = 4-hydroxy-3-methoxycinnamic acid; 5 = 4-hydroxycinnamic acid; 6 = 2-hydroxycinnamic acid; 7 = 3-hydroxycinnamic acid.

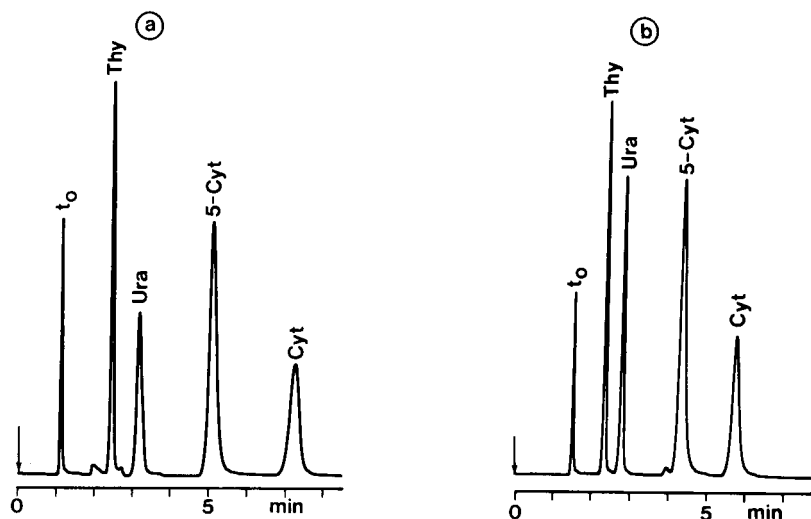


Fig. 11. Rapid separation of nucleobases. Mobile phase composition: (a) dichloromethane-methanol (8:2) + 1% (v/v) water + 0.2 *M* HAc + 0.02 *M* KAc (pH = 4.75); (b) dichloromethane-methanol (8:2) + 2% (v/v) water + 0.1 *M* HAc + 0.01 *M* KAc (pH = 3.75). Solutes: t_0 = toluene; Thy = thymine; Ura = uracil; 5-Cyt = 5-methylcytosine; Cyt = cytosine.

aromatic carboxylic acids of different classes and Fig. 10 shows the separation of closely related cinnamic acids. The developed phase system can also be applied to the efficient separation of a number of nucleobases, as can be seen from Fig. 11. Even aromatic sulphonic acids can be chromatographed on bare silica, as is demonstrated in Fig. 12.

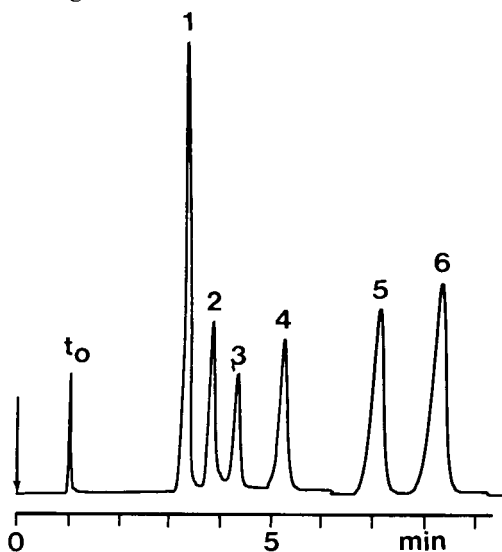


Fig. 12. Rapid separation of aromatic sulphonic acids. Mobile phase composition as in Fig. 11b. Solutes: t_0 = toluene; 1 = anthraquinone-2-sulphonic acid; 2 = benzosuberone-4-sulphonic acid; 3 = indane-4-sulphonic acid; 4 = benzenesulphonic acid; 5 = 1-naphthol-5-sulphonic acid; 6 = 6-hydroxynaphthalene-2-sulphonic acid.

Another advantage of bare silica is the possibility of injecting directly extracts of, for instance, foodstuffs, as is demonstrated in Fig. 13, which shows the analysis of benzoic and sorbic acids extracted with dichloromethane from rye bread and fruit juice.

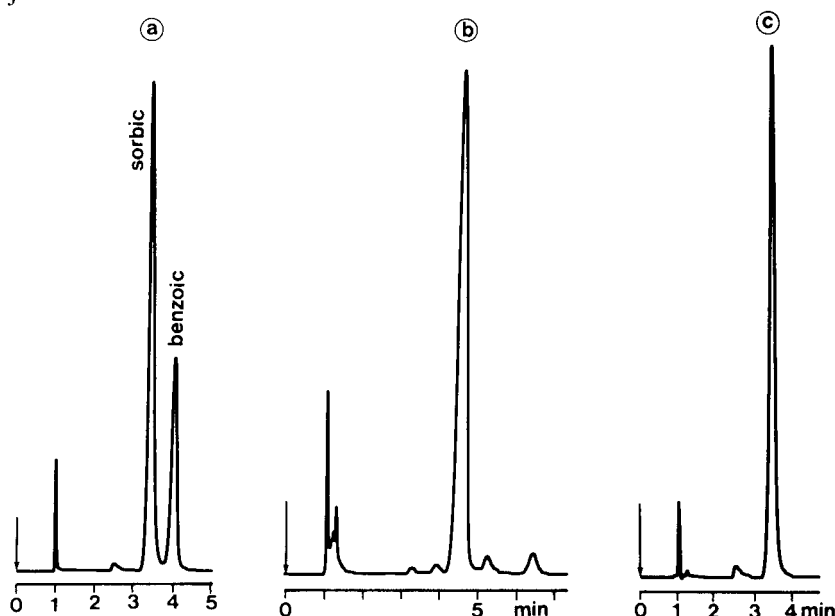


Fig. 13. Analysis of benzoic acid and sorbic acids extracted from foodstuffs and from fruit juice. Mobile phase composition: dichloromethane-methanol (8:2) + 2.3% (v/v) water + 0.01 *M* HAc + 0.01 *M* KAc (pH = 4.75). (a) Separation of sorbic and benzoic acids; (b) benzoic acid in fruit juice; (c) sorbic acid in rye bread.

CONCLUSIONS

Bare silica in combination with mixtures of dichloromethane-methanol-acetate buffer as the mobile phase are very useful for the chromatography of carboxylic and even sulphonic acids. It seems to be necessary to add at least a small amount of water and acetate buffer in order to obtain symmetrical peaks and to retain the acids. Of the available parameters, the ratio of HAc and KAc (the pH) seems to be the most useful for adjusting the retention.

With the available data it is too speculative to postulate the distribution process that occurs. However, a complex mixed distribution process seems the most obvious process.

Future experiments in our laboratory will be devoted to the effect of the type of organic components of the eluent and of the effect of crown ethers on the retention of acids, and further attempts will be made to determine the magnitude of the various separate distribution processes.

ACKNOWLEDGEMENT

The authors thank Dr. H. Poppe for stimulating discussions during the preparation of the manuscript.

REFERENCES

- 1 E. Lederer and M. Lederer, *Chromatography*, Elsevier, Amsterdam, 2nd ed., 1957.
- 2 E. Stahl, *Dünnschicht-Chromatographie*, Springer, Berlin, 1967.
- 3 K. Hiller, *Pharmazie*, 20 (1965) 353.
- 4 S. J. Pinella, A. D. Fako and G. Schwartzman, *J. Ass. Offic. Agr. Chem.*, 49 (1966) 829.
- 5 S. Miyazaki, J. Suhara and T. Kobayashi, *J. Chromatogr.*, 39 (1969) 88.
- 6 E. H. Pfadenhauer, *J. Chromatogr.*, 81 (1973) 85.
- 7 J. E. Evans, H. Tieckelmann, E. W. Naylor and R. Guthrie, *J. Chromatogr.*, 163 (1979) 29.
- 8 U. Streule and A. van Wattenwyl, *Chromatographia*, 12 (1979) 25.
- 9 J. Crommen, *J. Chromatogr.*, 186 (1979) 705.
- 10 R. Schwarzenbach, *J. Chromatogr.*, 202 (1980) 397.
- 11 E. H. Slaats, J. C. Kraak, W. J. T. Brugman and H. Poppe, *J. Chromatogr.*, 149 (1978) 255.
- 12 J. F. K. Huber, J. C. Kraak and H. Veening, *Anal. Chem.*, 44 (1972) 1554.
- 13 L. R. Snyder, *Principles of Adsorption Chromatography*, Marcel Dekker, New York, 1968.
- 14 W. J. T. Brugman and J. C. Kraak, *J. Chromatogr.*, 205 (1981) 170.
- 15 B.-A. Persson and B. L. Karger, *J. Chromatogr. Sci.*, 12 (1974) 521.

CHROM. 14,226

THEORETICAL BASIS FOR SYSTEMATIC OPTIMIZATION OF MOBILE PHASE SELECTIVITY IN LIQUID-SOLID CHROMATOGRAPHY

SOLVENT-SOLUTE LOCALIZATION EFFECTS

L. R. SNYDER*

Technicon Instruments Corp., Tarrytown, NY 10591 (U.S.A.)

and

J. L. GLAJCH and J. J. KIRKLAND

E. I. Du Pont de Nemours & Company, Central Research & Development Department, Experimental Station, Wilmington, DE 19898 (U.S.A.)

SUMMARY

The optimization of retention in liquid-solid chromatography (LSC) is explored in the present paper. Previously it was shown possible to calculate solvent strength (ϵ^0 values) for multi-component mobile phases, and specifically for quaternary solvent mixtures A-B-C-D. With ϵ^0 held optimum and constant for a particular sample, the composition of A-B-C-D can be further varied for optimization of separation factors α (solvent selectivity) for various solute-pairs in the sample of interest. The selection of optimum pure solvents A-D for this purpose and the systematic variation in the proportions of these solvents for optimum separation are approached here in terms of a fundamental description of how solvent selectivity arises in LSC. In this paper we discuss two major contributions to solvent selectivity: solvent/solute localization and solvent-specific localization. In a later paper we apply these findings for the development of a systematic approach to the optimization of retention in LSC separation.

INTRODUCTION

Optimization in liquid chromatography (LC) refers to the selection of experimental conditions for adequate separation and acceptable elapsed time per sample. Most optimization strategies are based on eqn. 1 for resolution, R_s ¹:

$$R_s = \frac{1}{4} \cdot (\alpha - 1) \cdot \sqrt{N} \cdot [k'/(1 + k')] \quad (1)$$

Here, α is the separation factor (k_X/k_Y), N is the plate number of the separation system (column or bed) and k' is the average capacity factor for bands X and Y (k_X

and k_V). It is customary to separately optimize the terms α , N and k' of eqn. 1 for a given separation. The optimization of N in column chromatography (so-called high-performance liquid chromatography, HPLC) is now on a sound theoretical basis¹⁻⁵, which allows calculations of preferred conditions for the best compromise between large N and short separation time, t . The optimization of retention (k' and α) is less well understood, and is usually approached more empirically.

Strategies for retention optimization in LC fall into one of three groups:

(1) empirical (trial-and-error) approaches guided by experience and whatever theory is available¹

(2) statistical-design or computer-search routines which allow intelligent guesses for successive trial-and-error changes in conditions⁶⁻⁸

(3) development of an overall theory of retention as a function of separation conditions; this would then allow the development of optimization schemes based on preselection of a small number of well-chosen LC systems, followed by interpolation to an optimum system for a given sample.

Several LC variables are discontinuous in nature (*e.g.*, selection of mobile phase solvents A, B, C, ..., choice of a particular adsorbent, etc.) so that only the third approach above offers the possibility of absolute optimization, *i.e.*, choosing conditions that provide the best possible separation of a given sample.

In this paper we consider the third approach to optimizing LC separation. Earlier papers^{5,9} have illustrated how optimization in this fashion might proceed, based on partial theories of retention for reversed-phase LC. However, adequately complete theories of retention—particularly as regards sample α values—have not yet been presented for any of the LC methods. Here we examine one particular LC method: liquid-solid (adsorption) chromatography (LSC). Retention for LSC is better understood at present than for the remaining LC methods¹⁰⁻¹⁴; LSC therefore offers a better opportunity for exploring the possibility of the third approach to optimization. Aside from being of value in its own right, optimization in LSC may offer guidance for a similar approach to the other LC methods.

A PRACTICAL SUMMARY OF THE PRESENT PAPER

A general approach to optimizing retention in LSC is as follows:

(1) determine the best solvent strength ϵ^0 of the mobile phase for optimum k' values ($0.5 \leq k' \leq 20$) of the given sample; this is done by varying the composition (% v/v B) of a mobile phase A-B which consists of a weak solvent A and a strong solvent B.

(2) while holding ϵ^0 constant, further vary conditions for an optimum spacing of sample bands within the chromatogram (maximum α values); this can be done in various ways: (a) vary the mobile phase composition by substituting other strong solvents (C, D, ...) for solvent B (Ch. 9 of ref. 1); (b) vary the adsorbent chosen as column packing; silica is the usual first choice, but alumina offers different selectivity for some samples¹⁰; (c) vary the temperature of the column; often temperature has no significant effect on α values; however, exceptions have been noted¹⁵; (d) take advantage of special chemical effects via change in mobile phase pH or the use of complexing agents (*e.g.*, silver ion for olefins); this approach is limited to samples that are acidic or basic, and/or can undergo complexation. In this paper we consider only the

theory of LSC solvent strength as a function of mobile phase composition (1, above), and the variation in α values as a result of change in mobile phase composition (2a). This will in turn allow a major improvement in our ability to develop final LSC methods with a minimum of experimental effort. Further improvement in this approach (options 2b–d above) can best be attempted after we achieve a good understanding of steps 1 and 2a. An optimization scheme based on steps 1 and 2a is presented in a later paper¹⁶.

Once a mobile phase composition (A–B) has been found that has the optimum ϵ^0 value for the sample of interest, we need to be able to calculate other mobile phase compositions (A–C, A–D, ...) that give the same value of ϵ^0 . These new mobile phases will then allow us to vary separation selectivity for improved resolution. It has been found elsewhere^{9,17–19} that mobile phases containing more than two solvents (*e.g.*, A–B–C) are required for the maximum exploitation of selectivity in reversed-phase LC, when the sample contains several components (this is not the case for a two-component sample). This is true of LSC as well. Therefore, a general theory is needed for the calculation of ϵ^0 for any multi-component mobile phase. In practice, ternary and quaternary-solvent mobile phases will be used. Previous papers^{13,14} have shown that it is possible to calculate the strength of multicomponent mobile phases in LSC with adequate precision.

Changes in α which result from a change in the mobile phase composition are presumably due to various physico-chemical phenomena that affect sample retention. These changes in α are very much affected by the particular sample (mixture of solutes) selected for study, and there are an almost unlimited number of possible mobile phase compositions from which to choose. Consequently, the empirical study of mobile phase selectivity will be quite complex, and there is little hope that the results obtained will apply to all possible samples. On the other hand, there are a much smaller number of these discrete physico-chemical effects that can contribute significantly to sample α values. If we can identify these effects and relate them to mobile phase composition in a way that is independent of the nature of the sample to be separated, we can bypass much of the potential difficulty in understanding and using mobile phase selectivity.

Several of these physico-chemical effects have already been identified in LSC systems^{10,11}:

- solvent/solute localization
- solvent strength
- hydrogen-bonding in the stationary phase
- hydrogen-bonding in the mobile phase

In this paper we examine solvent–solute localization. At this time we believe that their contribution to sample α values is generally more important than are hydrogen-bonding effects. Later papers will discuss hydrogen-bonding and its exploitation in a total-optimization scheme for LSC. Table I summarizes such an approach.

Solvent strength and mobile phase composition

Preceding papers^{13,14} have described a general model of solvent strength in LSC for the case of mobile phases that contain two to four solvent components. This model is based upon a displacement mechanism of solute retention in LSC. Thus, for adsorption of a solute X from a mobile phase B, it is assumed that one molecule of X

TABLE I

RETENTION OPTIMIZATION IN LSC: CLASSIFICATION OF A TOTAL APPROACH

hex = Hexane; MC = methylene chloride; MTBE = methyl *tert.*-butyl ether; ACN = acetonitrile; TEA = triethylamine; M = methanol.

Effect		Solvent variables	
1	Optimize solvent strength in terms of k'	A-B	hex-MC
2a	Optimize selectivity in terms of polar solvents (B, C, B-C, etc.) selected for the mobile phase		
	Optimize solvent/solute localization (value of m)	A-B-C	hex-MC-MTBE
	Optimize solvent-specific localization	A-B-C-D	hex-MC-MTBE-ACN
	Fine-tune solvent strength	A-B-C-D	vary N_A
	Create solvent-solute hydrogen-bonding in stationary phase		
	Use proton-acceptor (basic) solvent	A-B-C-E	hex-MC-MTBE-TEA
	Use proton-donor (acidic) solvent	Less effective	
	Create solvent-solute hydrogen-bonding in mobile phase		
	Use proton-donor (acidic) solvent	A-B-C-F	hex-MC-MTBE-M
	Use proton-acceptor (basic) solvent	Less effective	
2b	Optimize column packing (adsorbent type)	Silica, alumina; repeat steps 1 and 2a*	
2c	Optimize separation temperature	After step 2a**	
2d	Optimize pH, add complexing agents	After 2a***	

* Solvent strength and selectivity must be reoptimized when adsorbent is changed.

** Increase N_A to compensate for lower k' at higher temperatures; maintain other N values in same ratio (e.g., N_C/N_B constant).

*** Do not change N_A , N_B , etc.

in the mobile phase (X_n) displaces some number, n , of solvent molecules B from the stationary phase (B_a)



to give a molecule of adsorbed X (X_a) and n molecules of B in the mobile phase (B_n). The effect of solvent strength, ϵ^0 , on sample retention is then given as

$$\log (k_1/k_2) = \alpha' A_s (\epsilon_2 - \epsilon_1) \quad (3)$$

where for a given solute X, k_1 and k_2 refer to k' values for mobile phases 1 and 2, ϵ_1 and ϵ_2 refer to solvent strength (ϵ^0) values for mobile phases 1 and 2, α' is an adsorbent activity parameter and A_s refers to the cross-sectional area of the molecule X. Values of ϵ^0 for multicomponent mobile phases can be related to the mole fractions, N_i , of each solvent component i in the mobile phase, and to the ϵ^0 values (ϵ_i) of each pure solvent i . For so-called "localizing" solvents j (see next section), the value of ϵ_j varies with the mole fraction, θ_j , of j in the stationary phase. The stationary phase is assumed to consist of a monolayer of adsorbed solvent molecules. Values of ϵ_j are relatively constant ($\epsilon_j = \epsilon'$) at low values of θ_j , but ϵ_j decreases as θ_j approaches a

value of 0.75 (toward a lower limiting value ϵ'' for $\theta_j > 0.9$). The condition $\theta_j \approx 0.75$ corresponds to the approximate completion of a "localized" layer of solvent molecules j in the stationary phase. Further filling of the monolayer by j ($\theta_j > 0.75$) corresponds to adsorption of non-localized j molecules. The treatment of refs. 13, 14 yields values of θ_i for all mobile phase components i . The next section suggests that solvent selectivity is also dependent upon values of θ_i for different mobile phase components i .

Fig. 1a plots experimental values of ϵ^0 vs. values calculated according to ref. 13, for 98 different binary-solvent mobile phase compositions and 22 different strong solvents (B, C, ...). Similarly, Fig. 1b plots data calculated according to ref. 14 for mobile phases consisting of ternary and quaternary-solvent mixtures. The experimental data are taken from the review¹³ as well as from ref. 14 and the present paper. These data suggest that the procedures of refs. 13, 14 allow the prediction of ϵ^0 in LSC within ± 0.02 units. This is adequate for selecting optimum-strength mobile phase compositions, since resolution, R_s , is not a sensitive function of k' , when $k' > 1$.

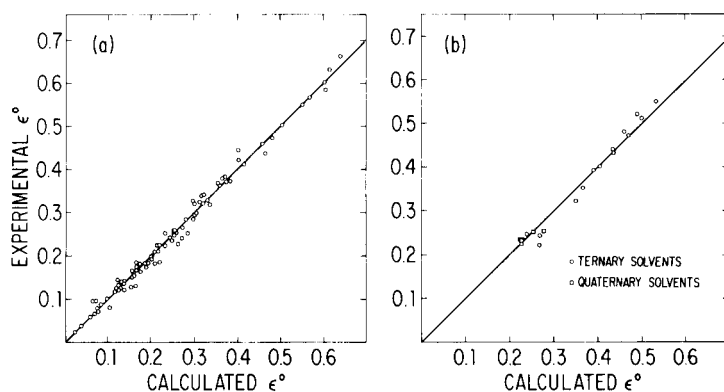


Fig. 1. Comparison of experimental solvent strength values for multi-component mobile phases with calculated values as in refs. 13, 14 for alumina and silica as adsorbents. a, Binary-solvent mobile phases 13; b, mobile phases containing three (○) or four (□) solvents (from ref. 14 and present study).

Solvent selectivity: solvent/solute localization

This selectivity effect has been discussed previously^{12,20}, but not developed to the degree required for optimization as in a later paper¹⁶. Localization refers to the direct interaction of the most polar substituent group, k , in a molecule of solute or solvent with a corresponding polar adsorption site which forms part of the adsorbent surface. Localization of a polar solvent molecule, C, is illustrated in Fig. 2a–d. In the case of silica as adsorbent, the polar surface sites are silanols ($\equiv \text{Si}-\text{OH}$), as illustrated in Fig. 2a for a side view of the silica surface. These silanol groups are shown as asterisks in Fig. 2b from an overhead view of the silica surface; they are randomly distributed across the surface, which accords with the current belief that porous silicas are non-crystalline¹⁰. Adsorbing solvent molecules C are shown in Fig. 2c, d as discs, with the polar group k centered on one face of the disc (this assumed molecular shape is arbitrary). Fig. 2c shows a side view of the adsorbed monolayer of solvent C, with two of the three C molecules (i), shown centered over adsorbent sites,

i.e., these molecules (i) are adsorbed with localization. The third molecule of C in Fig. 2c (ii) cannot assume the optimum configuration required for localization and is therefore delocalized. Fig. 2d shows an overhead view of the monolayer of adsorbed solvent C. Molecules of delocalized C are shown as broken curves, while localized molecules are shown as full circles. Delocalization can be the result of either (a) imperfect alignment of the solvent group *k* with a surface site (ii in Fig. 2c, iia in Fig. 2d), or (b) crowding of adsorbed C by adjacent molecules in the monolayer (iib in Fig. 2d, *i.e.*, steric hindrance to adsorption). Localized molecules (i) are held much more strongly to the adsorbent surface than are delocalized molecules (ii).

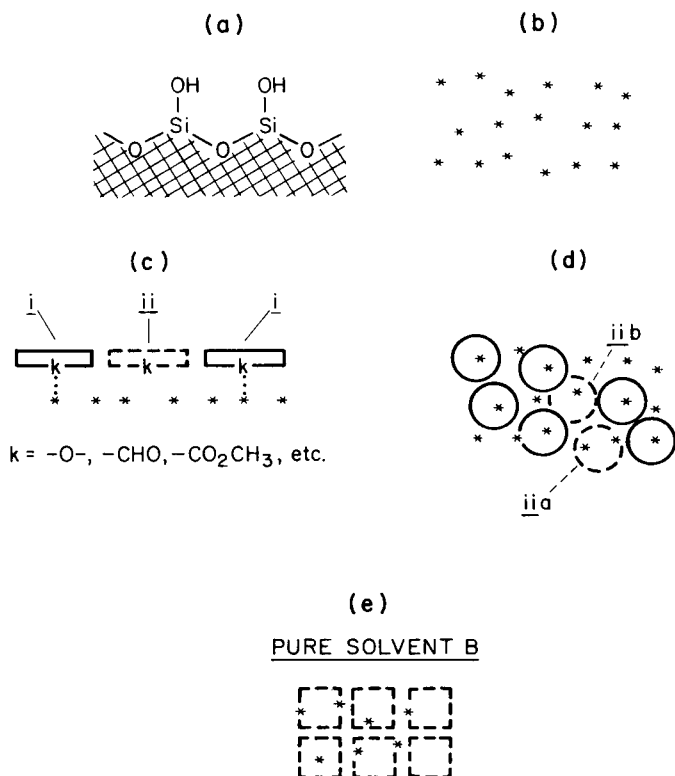


Fig. 2. Visualization of adsorbed solvent monolayer on silica, showing the localization of a polar solvent C. a, Side view of silica surface, showing silanol groups; b, overhead view of silica surface, with silanols shown as *; c, side view of monolayer of adsorbed solvent molecules C, with polar solvent-group *k* shown; d, overhead view of solvent monolayer in c; e, overhead view of adsorbed monolayer of solvent B (non-localizing). See text.

When a molecule of solute or solvent possesses no strongly polar group *k*, there is no reason for that molecule to prefer a specific position or configuration within the adsorbed monolayer, *i.e.*, all molecules will be delocalized. This is illustrated for a less polar solvent molecule, B, in Fig. 2e, where molecules of B in the adsorbed monolayer are shown as squares. Since all molecules of B are delocalized, they are shown as broken squares with no tendency toward centering of the molecule with respect to surface sites (*vs.* Fig. 2d for the localizing solvent C). Polar groups *k* which can cause

the localization of either solvent or solute molecules include such substituents as $-O-$ (ether), $-COR$ (ketone), $-CO_2R$ (ester), $-NR_2$ (amine) and other functional groups of similar polarity. Non-localizing solvents B are less polar compounds such as chloroform, dichloromethane, benzene and RCl , RBr or RI (monohaloalkanes). Localizing solvents C include ethers, esters, nitriles and alcohols.

In LSC separation, moderately polar solvents B and/or polar solvents C are generally used in admixture with a non-polar solvent A such as hexane, heptane or isooctane. Fig. 3 shows the resulting arrangement of adsorbed solvent molecules within the monolayer, for the solvent system A-B (Fig. 3a) and A-C (Fig. 3b). Adsorbed molecules A are shown as broken (*i.e.*, delocalized) triangles. The adsorption of a solute molecule X (localizing) or Y (non-localizing) from the mobile phase A-B is illustrated in Fig. 3c. In either case, because B is non-localizing, the adsorbing solute molecule displaces a non-localized molecule of B (or A). In the case of the adsorption of X or Y from a mobile phase A-C that is localized (Fig. 3d), X adsorbs with localization and must therefore displace a preadsorbed molecule of localized C. Because Y is non-localizing, it adsorbs by displacing a non-localized molecule of A (or C). If we assume that X and Y have the same k' values ($\alpha = 1$) in the system A-B (Fig. 3c), then the k' value of X must be less than that of Y ($\alpha \neq 1$) in the system A-C (Fig. 3d). The reason is that the free energy required to displace a solvent molecule in Fig. 3c is the same for both X and Y, because for each solute the displaced solvent molecule (A or B) is delocalized. In Fig. 3d, however, solute X (but not Y) must displace a localized molecule of C during adsorption, and the energy required for this will be greater than for displacement of a delocalized molecule of C (or A) by an adsorbing molecule of Y.

As a result of solvent/solute localization, a change from a localizing mobile phase (A-C) to a non-localizing mobile phase (A-B) can create large differences in solvent selectivity and the α values of various solute-pairs. The effect is limited to solutes which show some degree of localization, and is therefore more pronounced for more polar samples and the stronger mobile phases that are required for their optimum separation.

A quantitative model: binary-solvent mobile phases. In the general case, both solutes and solvents will exhibit varying tendencies toward localization, rather than being characterizable as simply "localizing" or "non-localizing". Thus, the effects of solute/solvent localization will increase with increasing tendencies toward localization of solute and solvent (*i.e.*, increase in polarity of the localizing group k in each molecule). The effect of solvent localization will also be more pronounced for higher mole fractions, N_C , of the localizing solvent in the mobile phase A-C, as illustrated in Fig. 4. Here, for a lower value of N_C and a resulting value of $\theta_C = 0.5$, a molecule of X can adsorb with localization by displacing a delocalized molecule of A. However, for a higher value of N_C , such that $\theta_C = 0.75$, localized adsorption of X requires displacement of a localized molecule of C. The reason is that with increase in θ_C from zero to 0.75, all adsorbing molecules C can localize onto the surface; when θ_C exceeds a value of 0.75, additional molecules of C adsorb without localization¹³. Therefore, the effect of solvent localization on selectivity will increase in magnitude with increase in N_C and θ_C , until $\theta_C \geq 0.75$.

Eqn. 3 already recognizes the localization of the solvent and solute. Thus, localization of the solvent leads to a predictable change in the value of ϵ^0 (ref. 13, 14),

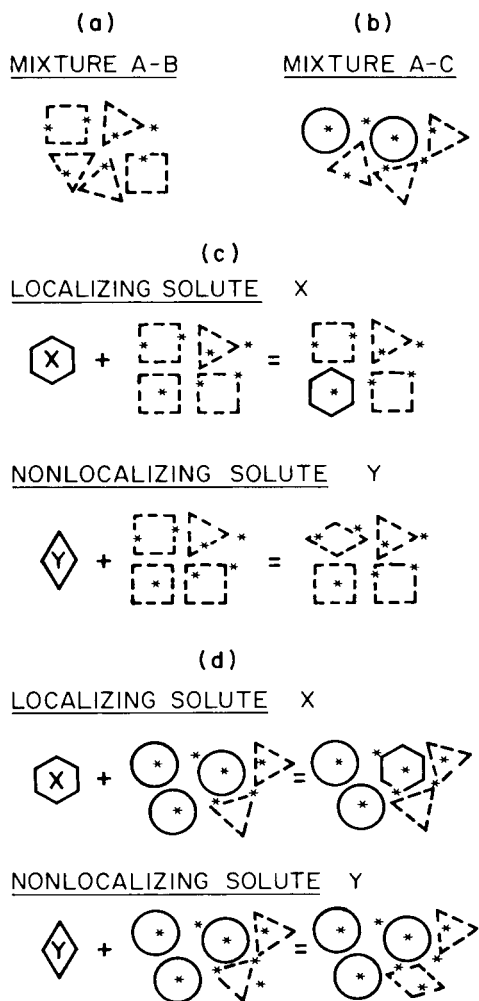


Fig. 3. Visualization of adsorption of localizing solute X and non-localizing solute Y from mobile phases A-B (non-localizing) and A-C (localizing); overhead view in each case. a, Solvent monolayer A-B (non-localizing); b, solvent monolayer A-C (localizing); c, adsorption of X and Y from mobile phase A-B (with displacement of adsorbed solvent molecule); d, adsorption of X and Y from mobile phase A-C (with displacement of solvent molecule). See text.

while localization of the solute leads to a change in its apparent A_s value (silica as adsorbent¹⁰). However, eqn. 3 does not take into account the *interaction* of these two effects as in Fig. 3c, d. Therefore, for the case of polar (*i.e.*, localizing) solutes and solvents, a term Δ_1 must be added to eqn. 3:

$$\log (k_1/k_2) = \alpha' A_s (\epsilon_2 - \epsilon_1) + \Delta_1 \quad (4)$$

The term Δ_1 corrects eqn. 3 for the interaction of solute and solvent localization, and its effect on k' . From our discussion of Fig. 3 (see also ref. 20), it is clear that Δ_1

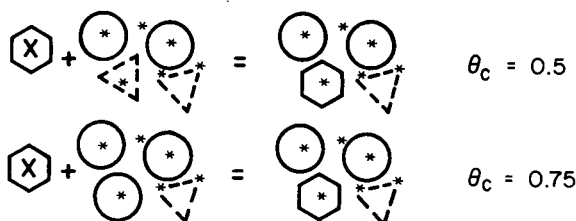


Fig. 4. Visualization of adsorption of solute X from localizing mobile phase A-C. Effect of surface coverage, θ_c , on solvent molecule displaced by X.

should depend upon both the nature of the solute (X) and the mobile phase (i); Δ_1 will become larger for increasing localization of both X and i . We therefore expect that Δ_1 will be a function of parameters Δ_x (solute) and m_i (mobile phase); Δ_x measures the relative localization of X, and m_i increases with both the degree of localization of some mobile phase solvent j and with its relative coverage of the adsorbent surface (θ_j). A linear-free-energy relationship between Δ_1 and the parameters Δ_x and m_i is expected, because Δ_1 is a free-energy term which is the result of the *interaction* of effects produced by solute localization and solvent localization; such a linear-free-energy relationship was verified experimentally^{20,*}

$$\Delta_1 = -\Delta_x m_i \quad (5)$$

Because solute/solvent localization leads to decreased retention of the solute, the term Δ_1 is negative.

The expected increase of Δ_x with increasing localization of X has been observed²⁰. Thus, solute localization increases with the polarity or adsorption energy, Q_k^0 , of the most strongly adsorbing group k in the solute molecule, and Δ_x is found to increase with Q_k^0 .

The solvent selectivity parameter, m , of eqn. 5 is of primary interest in terms of controlling separation. Thus, the sample components in a given LSC separation (and values of Δ_x for those solutes) are fixed, but we can vary mobile phase composition so as to change m and sample α values. As described in a following section, values of m can be related to mobile phase composition as follows. For the case of a mobile phase A- j , where the weak solvent A cannot localize and the strong solvent j can, the value of m is determined by the polarity of pure j (m^0) and by the mole fraction, θ_j , of j in the adsorbed monolayer

$$m = m^0 f(\theta_j) \quad (6)$$

where $f(\theta_j)$ varies from zero for $\theta_j = 0$ to one for $\theta_j = 1$. Eqn. 6 is tested in Fig. 5a, where values of (m/m^0) are plotted vs. θ_j (data of ref. 20 for alumina) for several polar solvents. For a total of 35 mobile phases listed in Table II, it is found that m is predicted by eqn. 6 with an accuracy of ± 0.07 units (1 S.D.), for $-0.29 \leq m \leq 1.16$. The function $f(\theta_j)$ vs. θ_j used in this calculation is shown as the solid curve in Fig. 5a, b, and is listed in Table III. This function was determined as a best fit to the data of Fig. 5.

* Eqn. 5 is expressed in ref. 20 as $\Delta = \Delta^0 m$; we have changed the terminology here (see Glossary).

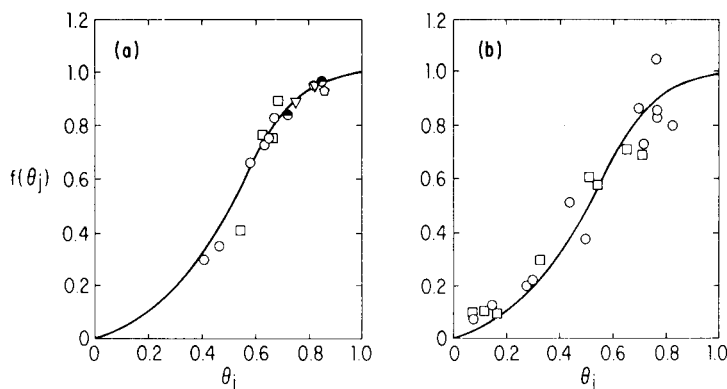


Fig. 5. Verification of eqn. 6 for dependence of solvent-selectivity function, m , on surface coverage, θ_j , by a localizing solvent j . a, Constancy of $m/m^0 = f(\theta_j)$ vs. θ_j for different solvents C and mobile phases A–C (alumina, data of Table II). \circ , Solvent j is acetonitrile; \bullet , pyridine; \square , acetone; ∇ , tetrahydrofuran; \ominus , ethyl acetate (see Table II). b, Dependence of $f(\theta_j)$ on θ_j for multi-component mobile phases and silica (data of this study and ref. 14, see Table V). \circ , Solvent j is MTBE; \square , acetonitrile. Solid curve in each case (a, b) is the function taken from Table III.

As expected, the solvent parameter m^0 increases with the adsorption energy Q_k^0 of the most polar solvent group k . Thus, as discussed in a later section, m^0 is 0.6 or larger for solvents with $Q_k^0 > 3.5$. For solvents with $Q_k^0 < 1.8$, m^0 is less than 0.4. Therefore, more polar solvents j with large values of m^0 (and ϵ^0) can provide larger values of Δ_1 and greater solvent selectivity variation. With such solvents, eqns. 5, 6 allow us to vary Δ_1 in continuous fashion over wide limits, by varying m via change in the concentration of j (N_j).

Consider next two solutes X and Y, with α referring to k_X/k_Y . Assume two mobile phases 1 and 2 which have equal strengths ($\epsilon_1 = \epsilon_2$), let α_1 and α_2 refer to α values in each mobile phase, and let m_1 and m_2 refer to their solvent selectivity (m) values. Further assume that the solvent selectivity m_2 for mobile phase 2 is equal to zero. From eqns. 4, 5 we can write

$$\log \alpha_1 = \log \alpha_2 + (\Delta_Y - \Delta_X) m_1$$

or

$$\log \alpha = C_1 + C_2 m \quad (7)$$

The constants C_1 and C_2 are now defined by the particular pair of solutes (X, Y) selected. Eqn. 7 is tested for representative data from ref. 20 in Fig. 6. The agreement of experimental data with the best fit of eqn. 7 in these plots is ± 0.05 – 0.06 log units (1 S.D.), for a range in $\log \alpha$ of -0.2 to $+0.5$. Other solute-pairs from ref. 20 show comparable agreement with eqn. 7.

A quantitative model: mobile phases containing more than two solvents. Assume a mobile phase composed of solvents A, B, C, ..., where A is non-localizing ($m^0 = 0$) and solvents B, C, ... exhibit increasing localization—and therefore increasing values of m^0 . The coverage of adsorption sites, with localization of the solvent molecule, can be pictured as proceeding in steps: initial adsorption of the strongest solvent j until its equilibrium surface coverage θ_j is attained, then adsorption of the next strongest

TABLE II

ANALYSIS OF SOLVENT-SELECTIVITY PARAMETER, m , FOR DATA FROM REF. 20

Alumina as adsorbent, binary-solvent mobile phases. Solvent A is pentane.

Mobile phase A-B (% v/v)	m^*		θ_B^{**}	m^0	Q_k^0
	Exptl.	Calc.			
1 Acetonitrile				1.31	5.0
0.1	0.39	0.45	0.31		
0.14	0.46	0.57	0.47		
0.3	0.87	0.85	0.59		
0.4	0.95	0.91	0.64		
0.6	0.98	0.94	0.66		
0.7	1.09	1.04	0.68		
2 Pyridine				1.22	4.8
2	1.16	1.14	0.83		
5	1.14	1.17	0.87		
3 Acetone				1.02	5.0
0.2	0.42	0.58	0.55		
0.4	0.79	0.74	0.64		
0.6	0.77	0.80	0.67		
0.8	0.91	0.83	0.70		
4 Tetrahydrofuran				0.82	3.5
2	0.73	0.72	0.76		
5	0.77	0.77	0.84		
5 Triethylamine				0.82	4.4
5	0.77	0.77	0.83		
6 Ethyl acetate				0.77	5.0
1	0.65	0.65	0.73		
4	0.72	0.72	0.85		
7 Diethyl ether				0.62	3.5
2	0.32	0.26	0.47		
5	0.55	0.47	0.63		
9	0.47	0.53	0.73		
23	0.43	0.58	0.85		
8 1,2-Dichloroethane				0.35	1.8
15	0.33	0.33	0.85		
9 Chloroform				0.34	0.7
15	0.23	0.30	0.76		
30	0.41	0.33	0.90		
10 Dichloromethane				0.29	0.8
13	0.25	0.25	0.73		
23	0.26	0.27	0.85		
35	0.33	0.28	0.93		
60	0.22	0.29	0.97		
100	0.30	0.29	1.00		
11 Ethyl sulfide				0.29	2.6
8	0.18	0.20	0.62		
15	0.27	0.25	0.76		
12 Chlorobenzene				0.12	0.3
30	0.12	0.12	0.91		
13 Bromoethane				0.08	2.0
40	0.08	0.08	0.87		

(Continued on p. 310)

TABLE II (continued)

Mobile phase A-B (% v/v)		m^*		θ_B^{**}	m^0	Q_k^0
		Exptl.	Calc.			
14	2-Chloropropane				0.02	1.8
	35	0.02	0.02	0.79		
	60	0.02	0.02	0.91		
15	Perchloroethylene				0.03	0.3
	100	0.03	0.03	1.00		
16	Carbon tetrachloride				-0.09	0.3
	50	-0.08	-0.08	0.78		
17	Benzene				-0.15	0.3
	15	-0.04	-0.13	0.72		
	28	-0.02	-0.14	0.86		
	50	-0.25	-0.15	0.95		
	80	-0.29	-0.15	0.99		
18	Toluene				-0.16	0.3
	30	-0.15	-0.15	0.90		

* Data of ref. 20; calculated values from eqn. 6.

** Calculated as described^{1,3}.

solvent i until a surface coverage equal to $(\theta_i + \theta_j)$ is reached, and so on until completion of adsorption of the weakest solvent A so that $\Sigma\theta = 1$ (completed monolayer of solvent). At some point during the successive adsorption of weaker solvents (j, i, h, \dots) a value of $\Sigma\theta = 0.75$ will be reached, beyond which localization of later solvents is not possible, and their contribution to m will be minor (Fig. 5).

Based on the foregoing discussion, we can infer that m for a four-solvent mobile phase A-B-C-D will be given as:

$$m = m_D^0 f(\theta_D) + m_C^0 [f(\theta_C + \theta_D) - f(\theta_D)] + m_B^0 [f(\theta_B + \theta_C + \theta_D) - f(\theta_C + \theta_D)] \quad (8)$$

For a three-solvent mobile phase A-B-C, eqn. 8 can be used with θ_D and $f(\theta_D)$ set equal to zero. In eqn. 8, m_B^0 , m_C^0 and m_D^0 ref to values of m^0 for solvents B, C and D; $f(\theta_C + \theta_D)$ refers to the value of $f(\theta_j)$ for $\theta_j = (\theta_C + \theta_D)$; $f(\theta_B + \theta_C + \theta_D)$ refers to the

TABLE III

VALUES OF THE SOLVENT-LOCALIZATION FUNCTION, $f(\theta_j)$, FROM EQN. 6 VS. THE FRACTIONAL COVERAGE, θ_j , OF THE ADSORBENT SURFACE BY LOCALIZING SOLVENT j (SEE FIG. 5)

θ_j	$f(\theta_j)$	θ_j	$f(\theta_j)$
0.0	0.00	0.6	0.68
0.1	0.04	0.7	0.83
0.2	0.11	0.8	0.92
0.3	0.20	0.9	0.97
0.4	0.32	1.0	1.00
0.5	0.47		

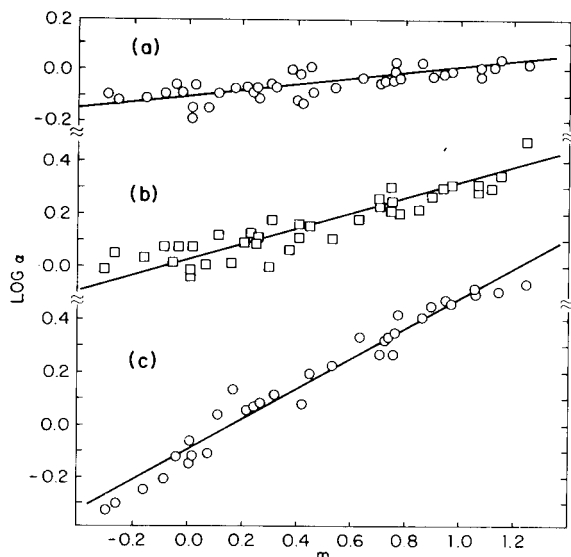


Fig. 6. Variation of $\log \alpha$ values with m , and verification of eqn. 7; data for binary-solvent mobile phases and alumina²⁰. a, X = 1-naphthaldehyde, Y = 1-cyanonaphthalene; b, X = 1-nitronaphthalene, Y = 1,7-dimethoxynaphthalene; c, X = 1,5-dinitronaphthalene, Y = 1-acetylnaphthalene.

value of $f(\theta_j)$ for $\theta_j = (\theta_B + \theta_C + \theta_D)$. In a later section we will see that eqn. 8 provides calculated values of m that agree well with experimental values for both ternary-solvent and quaternary-solvent mobile phases.

The applicability of eqn. 7, which describes α as a function of m , is illustrated in Fig. 7 for silica as adsorbent and several mobile phases which consist of ternary- and quaternary-solvent formulations. Representative plots for three different solute-pairs are shown, based on experimental data from ref. 14 and the present study. The scatter of the data points in Fig. 7 around the best fit to eqn. 7 (± 0.05 log units, 1 S.D.) is comparable to that for the plots in Fig. 6 for binary-solvent mobile phases and alumina. There are eighteen different polar solvents j represented in Fig. 6, and four such solvents in Fig. 7.

Based on the foregoing discussion, we can now select a pair of polar solvents (B and C) with different values of m_B^0 and m_C^0 . These can be blended with a non-polar solvent A in ternary formulations to allow the continuous and independent variation of both ϵ^0 and m for the mobile phase. This then allows the simultaneous optimization of both solvent strength and solvent selectivity (based on solvent/solute localization) as described in ref. 16.

Solvent selectivity vs. mobile phase composition: solvent-specific solvent/solute localization

Eqn. 7 allows us to predict values of α for given solute-pairs as a function of the mobile-phase m value, once we know the values of C_1 and C_2 for that solute-pair. However, although the correlations of Fig. 6 confirm the importance of m in determining solvent selectivity, there is still significant scatter of experimental data around these plots (± 0.05 – 0.06 log units, 1 S.D.). Consequently, two mobile phases

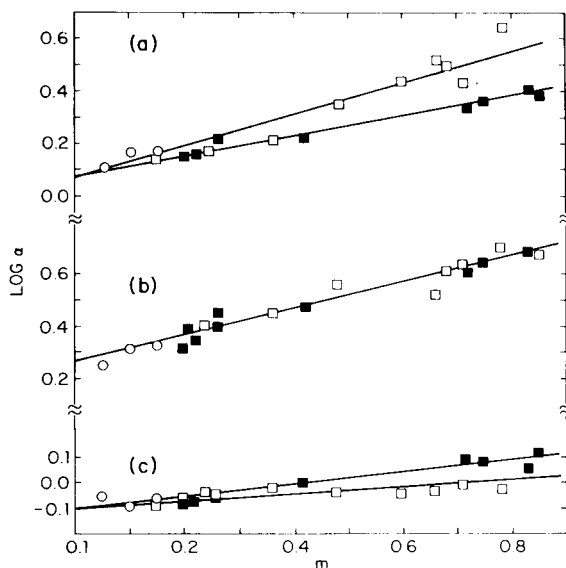


Fig. 7. Variation of $\log \alpha$ values with m ; data for multi-component mobile phases and silica (this study and ref. 14). a, X = 1-nitronaphthalene, Y = 2-methoxynaphthalene; b, X = 1,5-dinitronaphthalene, Y = 1,2-dimethoxynaphthalene; c, X = methyl 1-naphthoate, Y = 2-naphthaldehyde. \circ , Solvent j is chloroform or dichloromethane; \square , solvent j is MTBE; \blacksquare , solvent j is acetonitrile.

which have the same value of m can still exhibit somewhat different selectivities toward different solute-pairs. Thus, once we have optimized selectivity in terms of choosing the best mobile phase m value, the use of different mobile phases of similar m value may lead to further improvement in selectivity. It is therefore of interest to explore the basis of these deviations from eqn. 7 so that we can use them to practical advantage.

Deviations from eqn. 7 of the type discussed above suggest similar deviations from eqn. 4. This additional selectivity effect—which we will call *solvent-specific solvent/solute localization* (see below)—requires the addition of a further term (Δ_2) to eqn. 4:

$$\log(k_1/k_2) = \alpha' A_s (\varepsilon_2 - \varepsilon_1) + \Delta_1 + \Delta_2 \quad (4a)$$

We have found that Δ_2 is a function of both the mobile phase composition and of the two solutes (X, Y) used to measure α .

Deviations from eqn. 4 (non-zero values of Δ_2) were found in ref. 20 and the present study to occur for sample-solvent combinations that do not include proton-donor compounds. Therefore, hydrogen-bonding in the stationary or mobile phase can be ruled out as a possible cause of this effect. An alternative explanation is provided by the solvent/solute localization model *per se*. So far we have considered the degree of localization of solute and solvent molecules (values of Δ_X and m_i), but have ignored the molecular details of the configuration of adsorbed solute and solvent molecules; that is, how do localized molecules of solvent or solute “fit” into the monolayer in relationship to surrounding molecules and to the adjacent silanol group

of the silica surface? Differences in configuration between solvent and solute molecules would be expected to lead to differences in the net adsorption energy of the solute, which translate into a further contribution to α (i.e., Δ_2).

The configuration of localized molecules within the adsorbed monolayer is probably a function of the nature of the bonding between silanol groups and adsorbed molecules. A later section in fact suggests that the relative basicity of the solvent is a major factor in determining the magnitude of Δ_2 as a function of mobile phase composition. This in turn leads to a criterion for selecting two localizing solvents C and D, such that maximum differences in Δ_2 (and in solvent selectivity) can be achieved: the two solvents should have different relative basicities as defined by the selectivity triangle²³. Thus, solvent C can be a less basic solvent from group VI of ref. 23, such as acetonitrile or ethyl acetate. The second solvent D should then be selected from solvent groups I or III; e.g., tetrahydrofuran, methyl *tert.*-butyl ether, triethylamine, etc. The weakly localizing, moderately polar solvent B is ideally a solvent such as dichloromethane, with a small m^0 value. In this way, by varying the proportions of B, C and D in the mobile phase, ϵ^0 can be held constant while values of α are continuously varied over wide limits through change in both solvent/solute localization (value of m) and solvent-specific localization (Δ_2); see ref. 16.

The above hypothesis for solvent-specific localization suggests that the molecular structures of the localizing solutes (X, Y) and solvent C will *together* determine the values of Δ_2 in eqn. 4a. This in turn implies that eqn. 4 (which ignores Δ_2) should be more accurate when m is varied by changing the concentration of a strongly localizing solvent C (in a mixture A-B-C, where B is weakly localizing), rather than by changing to another localizing solvent D*. That is, for a given solvent C and solute X, the value of Δ_2 will remain constant while N_C is varied. This conjecture is tested in Fig. 7 for several solute-pairs from the present study and ref. 14. In the case of each solute-pair in Fig. 7, data for the two strongly localizing solvents used (methyl *tert.*-butyl ether, MTBE, and acetonitrile) are differentiated in these plots (\square , MTBE; \blacksquare , acetonitrile). It is clear that separate straight-line plots for each of these latter two solvents are generally better fit by eqn. 7 (± 0.02 log units, 1 S.D.) than are the composite plots (± 0.05 log units) for each solute-pair. This is expected in terms of the above discussion. That is, significant change in Δ_2 and consequent failure of eqn. 4 (with larger S.D.s) should occur when changing the localizing solvent C, rather than when the concentration of C in the mobile phase is simply varied. The form of the experimental plots of Fig. 7 suggests that C_2 in eqn. 7 is only approximately independent of the localizing solvent j in the mobile phase. Thus, for maximum accuracy, C_2 in eqn. 7 will be a function of the localizing solvent j in the mobile phase A- j (or A-B- j).

EXPERIMENTAL

All measurements were done on a DuPont Model 850 liquid chromatograph (DuPont, Wilmington, DE, U.S.A.) equipped with a Model 870 pump, a UV absorbance detector operated at 254 nm and a Model 845 refractive index detector. Samples were introduced with a Model 725 Micromeritics Auto-Sampler (Micromeritics,

* Note that the somewhat scattered plots of Fig. 6 are based on a number of different localized solvents (Table II), with differing values of Δ_2 .

TABLE IV

EXPERIMENTAL DATA FOR THREE-SOLVENT AND FOUR-SOLVENT MOBILE PHASES WITH SILICA AS ADSORBENT

Solutes are substituted naphthalenes; see Experimental for details. N_A = Mole fraction of hexane; N_B = mole fraction of dichloromethane; N_C = mole fraction of MTBE; N_D = mole fraction of acetonitrile.

Solute	A_S	Mobile phase*														25	26
		14	15	16	17	18	19	20	21	22	23	24					
$N_A =$	0.881	0.849	0.818	0.958	0.870	0.686	0.565	0.555	0.553	0.680	0.710	0.7675	0.920				
$N_B =$	0.096	0.094	0.092	—	0.100	0.300	0.4305	0.442	0.440	0.310	0.280	0.2200	0.048				
$N_C =$	—	—	—	0.042	—	—	—	—	—	0.006	—	0.0125	0.0156				
$N_D =$	0.023	0.057	0.090	—	0.030	0.014	0.0045	0.003	0.007	0.005	0.010	—	0.0164				
										</							

* Data for mobile phases 1-13 in ref. 14.

** Calculated according to ref. 14, eqn. 15 with $\alpha = 0.57$.

*** Calculated according to ref. 14, Appendix I, assumes ϵ^0 (hexane) = 0.00; ϵ^0 (CH_2Cl_2) = 0.30; ϵ' (MTBE) = 0.87, ϵ'' (MTBE) = 0.58; ϵ' (ACN) = 0.9, ϵ'' (ACN) = 0.4.

Norcross, GA, U.S.A.) using a 25- μ l sampling loop. A 15 \times 0.46 cm column packed with Zorbax-SIL chromatographic packing was used for all studies.

All solvents were distilled-in-glass grade (Burdick & Jackson Labs., Muskegon, MI, U.S.A.) except *n*-hexane, which was Spectrograde (Phillips Petroleum Co., Bartlesville, OK, U.S.A.). The mobile phases were 50% water-saturated using the procedure described in ref. 1. The solvents were all degassed individually, and then mixed before the water-saturation procedure. The substituted naphthalenes were dissolved in hexane.

All retention measurements and k' calculations were carried out with a PDP-10 computer system²². Other calculations were performed on a PDP-11/60 minicomputer (Digital Equipment, Maynard, MA, U.S.A.) programmed in FORTRAN. The t_0 measurements for accurate determination of k' were done by injecting a sample aliquot of the mobile phase which had already passed through the column, but which had been diluted slightly with hexane. This had the effect of injecting a sample which was slightly weaker than the mobile phase into the system. Both short- and long-term reproducibility measurements of k' values were shown to have a standard deviation of less than 2%. The k' data for the mobile phases with silica as adsorbent discussed in this paper are shown in Table IV.

RESULTS AND DISCUSSION

Solvent/solute localization

Binary-solvent mobile phases and alumina. The study of ref. 20 examines solvent/solute localization for alumina as adsorbent in considerable detail. The retention of 20 different solutes was studied in 44 different binary-solvent mobile phases A–B, involving 20 different polar solvents B. The m values found²⁰ are summarized in Table II. The measurement of these m values and the verification of eqn. 5 for these LSC systems is further described in ref. 20.

Best values of m^0 for each B solvent of ref. 20 were derived in the present study, along with the function $f(\theta_j)$ of eqn. 6. Values of m^0 are given in Table II; $f(\theta_j)$ is plotted in Fig. 5 and listed in Table III. Table II also provides values of m calculated from eqn. 6, using the m^0 values of Table II plus values of $f(\theta_j)$ from Table III. These experimental and calculated values of m agree within ± 0.07 units (1 S.D.), for $-0.29 \leq m \leq 1.16$.

Values of m^0 correlate roughly with Q_k^0 for the solvent as required by theory. Thus solvents 1–9 of Table II have $Q_k^0 > 3$, and their m^0 values are greater than 0.6. Solvents 10–20 of Table II have $Q_k^0 < 2$, and their m^0 values are less than 0.4. An exact correlation of m^0 vs. Q_k^0 is not observed, possibly because of secondary effects of the type involved in solvent-specific localization.

The shape of the $f(\theta_j)$ vs. θ_j curve in Fig. 5 is reasonable in terms of theory. Thus, we expect m/m^0 to increase only slowly with increase in θ_j , until completion of a localized solvent layer at $\theta_j = 0.75$ is approached. The reason is that prior to completion of the localized solvent layer, a localizing solute molecule can adsorb with displacement of a non-localized solvent molecule. Under these conditions, solvent/solute localization effects are less important in affecting solute α values. However, as θ_j approaches and exceeds a value of 0.75, a rapid increase in m/m^0 is expected. The ratio m/m^0 should then level out at a value of ≈ 1 for $\theta_j > 0.75$.

TABLE V
VALUES OF SOLVENT-SELECTIVITY PARAMETER, m , FOR MULTI-COMPONENT MOBILE PHASES AND SILICA
Data from ref. 16 and present study.

Mobile phase	Composition (mole fractions)			Surface coverage, θ^*			m				
	Hexane	Chloroform	Dichloromethane	MTBE	ACN	Chloroform	Dichloromethane	MTBE	ACN	Exptl.	Calc.**
1	0.422	—	0.578	—	—	—	0.87	—	—	0.09	0.10
2	0.248	0.752	—	—	—	0.94	—	—	—	0.05	0.10
3	0.956	—	—	0.044	—	—	—	0.77	—	0.81	0.74
4	0.7165	—	0.270	0.0135	—	—	0.38	0.44	—	0.44	0.36
5	0.5875	0.399	—	0.0135	—	0.39	—	0.50	—	0.32	0.44
6	0.331	0.399	0.270	—	—	0.49	0.43	—	—	0.16	0.10
7	0.502	0.286	0.204	0.008	—	0.30	0.28	0.30	—	0.24	0.24
8	0.574	0.244	0.176	0.0064	—	0.29	0.27	0.28	—	0.24	0.22
9	0.474	0.053	0.470	0.0017	—	0.06	0.73	0.08	—	0.15	0.13
10	0.542	0.053	0.402	0.0033	—	0.06	0.64	0.15	—	0.20	0.15
11	0.841	0.0713	0.0488	0.0389	—	0.06	0.06	0.72	—	0.60	0.71
12	0.978	—	—	0.022	—	—	—	0.70	—	0.71	0.68
13	0.913	—	—	0.087	—	—	—	0.83	—	0.66	0.77
14	0.881	—	0.096	—	0.023	—	0.15	—	0.51	0.75	0.62
15	0.849	—	0.094	—	0.057	—	0.11	—	0.66	0.85	0.93
16	0.818	—	0.092	—	0.090	—	0.09	—	0.71	0.83	1.02
17	0.958	—	—	0.042	—	—	—	0.77	—	0.68	0.73
18	0.870	—	0.100	—	0.030	—	0.14	—	0.55	0.68	0.72
19	0.686	—	0.300	—	0.014	—	0.44	—	0.33	0.43	0.35
20	0.565	—	0.4305	—	0.0045	—	0.67	—	0.12	0.17	0.15
21	0.555	—	0.442	—	0.003	—	0.70	—	0.08	0.16	0.13
22	0.553	—	0.440	—	0.007	—	0.68	—	0.17	0.21	0.19
23	0.680	—	0.310	0.006	0.005	—	0.47	0.16	0.15	0.34	0.28
24	0.710	—	0.280	—	0.010	—	0.45	—	0.27	0.33	0.26
25	0.7675	—	0.220	0.0125	—	—	0.34	0.44	—	0.37	0.37
26	0.920	—	0.048	0.0156	0.0164	—	0.07	0.32	0.32	0.69	0.70

* Calculated as in ref. 14.

** Eqn. 6 or 8, see text. m^0 values are: chloroform, 0.10; dichloromethane, 0.10; MTBE, 0.82; acetonitrile, 1.19.

Ternary and quaternary-solvent mobile phases and silica. Table V summarizes m values for several multicomponent mobile phases and silica as adsorbent. The approach used in ref. 20 to determine values of Δ_1 cannot be used for silica as adsorbent, because the reference hydrocarbon solutes (for which $\Delta_1 = 0$) have very small k' values on silica, when $\varepsilon^0 \gg 0$. We therefore used eqn. 7 to extract values of m from the data of ref. 14 and the present study. Since the product $C_2 m$ of eqn. 7 is obtained from plots such as those of Fig. 6, the ratio of C_2 to m is arbitrary. We have chosen a value of this ratio such that m^0 values for silica and alumina are of similar size for the same solvents. The detailed procedure used by us to obtain m values in this study is given in Appendix I.

The agreement of present data with eqn. 7 is illustrated in Fig. 7 for representative solute-pairs. Eqn. 7 calculates values of $\log \alpha$ for silica and multi-component mobile phases with an accuracy of ± 0.05 units (1 S.D.)*, which is comparable to that found for alumina and binary-solvent mobile phases.

Values of m for multi-component mobile phases. Calculated values of m from eqn. 8 are compared with experimental values in Table V, for silica as adsorbent. The agreement of these two sets of values (± 0.08 , 1 S.D.) is comparable to that found in Table II (± 0.07) for alumina and binary-solvent mobile phases. For ternary-solvent or quaternary-solvent mobile phases with only a single strongly-localizing solvent D, the term $[m - m_D^0 f(\theta_D)]$ of eqn. 8 is small, so that accurate values of $f(\theta_D)$ can be calculated from eqn. 8 for each value of m . Resulting values of $f(\theta_D)$ for different localizing solvents D are plotted in Fig. 5b with the solid curve from Table III superimposed. Thus, the general relationship of $f(\theta_j)$ vs. θ_j from Table III applies for both alumina and silica as adsorbents, and for binary-, ternary- and quaternary-solvent mobile phases. This in conjunction with the similar plots of Figs. 6 and 7 (eqn. 7) for these various systems suggests that solvent/solute localization occurs in essentially the same manner in these various LSC systems. This similarity of effects and their quantitative adherence to a small number of simple mathematical relationships (eqns. 6, 7) serves as additional evidence for the correctness of the present model and of the displacement mechanism (eqn. 2) on which it is based.

The calculation of m for any mixture of solvents is described in Appendix II.

Solvent-specific localization

Binary-solvent mobile phases and alumina. Values of Δ_1 for the mobile phases of Table II were reported²⁰ for nine standard solutes that do not include proton-donor compounds (compounds I–IX of Table III²⁰). These Δ_1 values were determined experimentally, using eqn. 4 and assuming that $\Delta_2 = 0$. In fact, the values of Δ_1 reported²⁰ are actually equal to $(\Delta_1 + \Delta_2)$. We will refer to these latter values as "apparent Δ_1 values" equal to Δ'_1 . These Δ'_1 values can be used to further analyze the rôle of the solvent in affecting solvent-specific selectivity.

Consider first the case where Δ_2 is in fact zero, and solvent-specific localization is unimportant. Further assume two different mobile phases p and q, with values of m equal to m_p and m_q . From eqn. 5 we then have

$$(\Delta'_1)_p = (m_p/m_q)(\Delta'_1)_q \quad (9)$$

* A single (average) value of C_2 is used for all solvents j in Fig. 7, corresponding to fitting data for each solute-pair to a *single* curve (rather than two curves as in Fig. 7).

where $(\Delta'_1)_p$ and $(\Delta'_1)_q$ are apparent Δ_1 values for mobile phases p and q, and a given solute X. If we now plot values of $(\Delta'_1)_p$ vs. $(\Delta'_1)_q$ for different solutes, all points should fall on a straight line, according to eqn. 9. Similarly, if a least squares correlation is carried out, a correlation coefficient, r , near unity should be obtained.

The situation is altogether different if values of Δ_2 for either mobile phase p or q are not zero. In this case, different solutes experience varying degrees of localization, depending on the polar solvent C or D which forms part of the mobile phase. That is, values of k' and α (Fig. 7a, c) depend upon the exact solvent (C or D) used in the mobile phase, as well as on the m value of that mobile phase. Therefore, we should be able to determine the relative importance of solvent-specific localization among different mobile phases studied in ref. 20, by carrying out correlations of apparent Δ_1 values among different pairs of mobile phases, according to eqn. 9. Those mobile phase-pairs exhibiting r values near unity can be presumed to be relatively free of solvent-specific localization, while poor correlation and smaller values of r must be associated with the presence of relatively large Δ_2 values for one or both mobile phases. *Furthermore, maximum differences in solvent selectivity among mobile phases of similar strength and m value should likewise occur for mobile-phase pairs that exhibit poor correlation* (see related discussion²³).

Correlations of Δ'_1 values from ref. 20 were carried out among various pairs of mobile phases, according to eqn. 9. Since a high degree of correlation is expected for mobile phases containing the same polar solvent (C or D), the mobile phases chosen were binaries A–C where the solvent C was different in each mobile phase*. Furthermore, only relatively polar solvents C (large m^0 values) were tested. The results of these correlations are summarized in Table VI. It is seen that the first four solvents of Table VI (nitromethane, acetonitrile, acetone and ethyl acetate) show excellent correlations with each other ($0.98 \leq r \leq 0.99$) implying an absence of solvent-specific localization for these mobile phases. The last five solvents of Table VI (dimethyl sulfoxide, triethylamine, tetrahydrofuran, diethyl ether and pyridine) show poorer correlation with the first four solvents ($0.87 \leq r \leq 0.97$), and not much better correlation within this group of five solvents ($0.91 \leq r \leq 0.97$). Therefore, it appears that solvent-specific localization is most important for mobile phases containing one of these latter five solvents.

The ranking of various polar solvents in Table VI according to solvent-specific localization effects closely parallels the classification of solvents in ref. 23 according to the relative importance of hydrogen-bonding vs. dipole-interaction tendencies. Thus, the first four solvents of Table VI show little solvent-specific localization, and all belong to selectivity groups VI or VII of ref. 23. These latter solvent-groups (VI, VII) are characterized by strong dipole interactions and lesser proton-donor or acceptor strength. The last five solvents of Table VI show significant solvent-specific localization, and belong to groups I or III of ref. 23. The latter selectivity groups (I, III) comprise solvents that are good proton-acceptors, but show little proton-donor strength or dipole-interaction. Since both alumina and silica behave as acidic adsorbents^{10,24}, this suggests that solvent-specific localization occurs mainly for solvents that strongly hydrogen-bond to the adsorbent surface. This is confirmed in the

* Several mobile phase compositions were reported²⁰ for each C solvent; e.g., 2, 5, 9 and 23% (v/v) diethyl ether–pentane. In these cases, values of Δ'_1 were averaged for each C solvent and a given solute-pair.

TABLE VI

MAXIMALLY DIFFERENT SOLVENTS IN TERMS OF SOLVENT-SPECIFIC LOCALIZATION

Correlation, r , of solvent selectivity among different solvent pairs (i - j) from study of ref. 20 for alumina as adsorbent in terms of eqn. 9.

Solvent i	Solvent j								
	NM	ACN	ACT	EA	DMSO	TEA	THF	EE	PYR
Nitromethane (NM)	1.00	0.98	0.99	0.98	0.97	0.93	0.92	0.92	0.90
Acetonitrile (ACN)	0.98	1.00	0.98	0.98	0.96	0.96	0.90	0.90	0.87
Acetone (ACT)	0.99	0.98	1.00	0.99	0.96	0.94	0.94	0.95	0.92
Ethyl acetate (EA)	0.98	0.98	0.99	1.00	0.97	0.95	0.96	0.96	0.94
Dimethyl sulfoxide (DMSO)	0.97	0.96	0.96	0.97	1.00	0.96	0.97	0.90	0.94
Triethylamine (TEA)	0.93	0.96	0.94	0.95	0.96	1.00	0.92	0.89	0.91
Tetrahydrofuran (THF)	0.92	0.90	0.94	0.96	0.97	0.92	1.00	0.93	0.97
Diethyl ether (EE)	0.92	0.90	0.95	0.96	0.90	0.89	0.93	1.00	0.94
Pyridine (PYR)	0.90	0.87	0.92	0.94	0.94	0.91	0.97	0.94	1.00

next section for silica, where large values of Δ_2 (and poor correlation) are observed for the solvents MTBE (group I) vs. acetonitrile (group VI).

Maximum differences in solvent selectivity as a result of solvent-specific localization are predicted for solvent-pairs with small r values in Table VI. Pyridine-acetonitrile has the poorest correlation of these solvents ($r = 0.87$), but pyridine is not a suitable solvent for LC with photometric detection. Diethyl ether-acetonitrile and tetrahydrofuran-acetonitrile have correlations that are almost as poor ($r = 0.90$), and appear to be suitable solvents (C, D) for use in an optimization scheme based on maximizing differences in localization selectivity. Since MTBE should be quite similar to diethyl ether in terms of solvent selectivity, and is better suited for routine application in LSC¹, we recommend the use of MTBE and acetonitrile as optimum localizing solvents C and D. Because of the poor correlation among the last five solvents of Table VI, we anticipate that additional solvent selectivity is achievable by using more than one of these solvents, *i.e.*, use of additional solvents E, F, ... in a retention-optimization scheme for LSC.

Multi-solvent mobile phases and silica. We have seen in this paper and in ref. 20 that solvent/solute localization effects are similar for silica and alumina, and for mobile phases that contain two, three or four solvent components. We might therefore infer that solvent-specific localization effects are also similar for these various LSC systems. Limited data from the present study suggest that this is the case. We should therefore expect to see significant differences in selectivity between mobile phases A-B-C (hexane-dichloromethane-MTBE) and A-B-D (hexane-dichloromethane-acetonitrile) on the basis of Table VI and the related discussion in a preceding section. Using the solute-pairs defined in Table VII, this premise is confirmed in Table VIII.

The seven solvent systems shown in Table VIII were selected for use in a systematic optimization scheme¹⁶. Their compositions are selected to provide roughly equal changes in selectivity within a "selectivity triangle". We refer to them as "selectivity-spaced" mobile phases. These mobile phases are believed to cover the range of

TABLE VII

SOLUTE-PAIRS USED FOR CALCULATION OF m VIA EQN. i-1

Solute-pair	X	Y	C_1	C_2	
				MTBE	ACN
A	1-Nitro	2-Methoxy	0.08	0.56	0.36
B	1-Nitro	1,2-Dimethoxy	-0.21	0.76	0.53
C	1,5-Dinitro	1,2-Dimethoxy	0.25	0.56	0.50
D	1,5-Dinitro	1-Formyl	-0.06	0.30	0.53
E	2-Methoxycarbonyl	1-Formyl	0.06	0.00	0.13
F	1-Methoxycarbonyl	2-Methoxycarbonyl	0.01	0.03	0.07
G	1-Methoxycarbonyl	2-Formyl	-0.06	0.03	0.20
H	1-Cyanomethyl	2-Formyl	-0.04	0.50	0.50
I	1-Cyanomethyl	1-Acetyl	-0.15	0.56	0.59
J	2-Acetyl	1-Acetyl	0.13	0.00	-0.03

possible α values, for mobile phases of $\epsilon^0 = 0.22$, and exclusion of proton-donor solvents and solutes (*i.e.*, localization-selectivity effects only). Of interest in the present discussion are the mobile phase groupings (a) 5, 23 and 19 and (b) 17, 26 and 18. The first group has m constant at 0.37 ± 0.06 while for the second group m is 0.68 ± 0.01 . Within each of these two groups, the localizing-solvent concentration varies from pure MTBE (5, 17) to pure acetonitrile (19, 18), with an intermediate composition that is roughly 50% of each (23, 26).

The relative importance of various contributions to selectivity can be evaluated from these data. First, for a change in m from 0.1 (mobile phase 1 of Table VIII) to 0.7 (either 17 or 18), we can calculate the change in $\log \alpha$ for a given solute-pair, *e.g.*,

TABLE VIII

SEPARATION FACTORS, $\log \alpha$, FOR STANDARD SOLUTE-PAIRS OF TABLE VII AND SEVEN "SELECTIVITY-SPACED" MOBILE PHASES OF PRESENT STUDY AND REF. 14

For identification of mobile phases see Table V. C = MTBE; D = ACN.

Solute-pair	Mobile phase	1	5	23	19	17	26	18	0.69 m_{25}
	m	0.09	0.32	0.37	0.43	0.68	0.69	0.68	
	$N_C/(N_C + N_D)$	-*	1.00	0.45	0.00	1.00	0.49	0.00	
A		0.17	0.21	0.18	0.23	0.44	0.31	0.32	
B		-0.12	-0.03	-0.05	0.03	0.21	0.16	0.17	
C		0.31	0.45	0.43	0.47	0.57	0.58	0.60	
D		-0.08	0.08	0.06	0.13	0.18	0.23	0.29	
E		0.06	0.06	0.08	0.13	0.06	0.15	0.12	
F		0.00	0.03	0.04	0.02	0.04	0.05	0.09	
G		-0.09	-0.02	0.00	0.01	-0.02	0.07	0.04	
H		0.01	0.13	0.17	0.18	0.35	0.33	0.28	
I		-0.11	0.05	0.07	0.12	0.31	0.27	0.26	
J		0.15	0.11	0.14	0.14	0.13	0.13	0.11	

* No MTBE or acetonitrile present in mobile phase.

solute-pair A, 0.32 units for 17 and 0.16 units for 18. We can then average these changes in $\log \alpha$ for all ten solute-pairs and mobile phases 17 and 18 (twenty values): equal 0.21 log units. Since the localizing solvent (MTBE or acetonitrile) is not changed during each of these comparisons of the effect of m , the average change in $\log \alpha$ (0.21 units) is due only to solvent/solute localization (Δ_1 effect).

Second, with m held constant (mobile phase 17 vs. 18), we can compare $\log \alpha$ values for a given solute-pair and MTBE vs. acetonitrile as localizing solvent. For solute-pair A and m equal 0.7, the difference in $\log \alpha$ values is 0.16 units. The average change in $\log \alpha$ values for all ten solute-pairs is 0.07 units, and this corresponds to the relative contribution of solvent-specific localization (Δ_2 effect) to mobile phase selectivity for the systems of Table VIII.

Finally, consider the agreement of experimental values of $\log \alpha$ for mobile phases 17 and 18 with values calculated from eqn. 7 using values of C_1 and C_2 from Table VII. The average difference between experimental and calculated $\log \alpha$ values is 0.02 units. The latter value comprises other selectivity contributions plus the effects of experimental imprecision in measured values of $\log \alpha$. Imprecision contributes about 0.01 log unit, so that other selectivity contributions must be small.

Similar calculations of these various selectivity contributions can be made for alumina using the data of ref. 20. For the same solute-pairs, but substituting the solvent ethyl acetate for acetonitrile, we obtain the data summarized below:

Selectivity	alumina	silica
Δ_1 (av.)	0.09	0.21
Δ_2 (av.)	0.05	0.07
residual (av.)	—	0.02

The overall conclusions appear as follows. Mobile-phase selectivity is similar for both adsorbents, but more important for silica. Solvent/solute localization, Δ_1 , is significantly more important than solvent-specific localization, Δ_2 , in affecting selectivity. Other contributions to selectivity are minor.

Returning to Table VIII, it is of interest to examine the $\log \alpha$ values of various solute-pairs for the mobile phases which have $N_C/(N_C + N_D) \approx 0.5$. These are roughly intermediate in value between the corresponding $\log \alpha$ values (m constant) for $N_C/(N_C + N_D) = 0$ and 1. That is, to a first approximation these $\log \alpha$ values for $N_C/(N_C + N_D) = 0.5$ can be calculated from eqn. 7, using a value of C_2 that is the average of C_2 values (Table VII) for MTBE and acetonitrile. However, the latter relationship is sufficiently imprecise (S.D. = ± 0.03 log units) to suggest that a simple linear interpolation of $\log \alpha$ values between $N_C/(N_C + N_D) = 0$ and 1 is not recommended.

Solvent strength and solvent-solute localization. We have seen that the value of m for the mobile phase can be varied while solvent strength ϵ^0 is held constant. However, the maximum possible value of m increases with increasing ϵ^0 . This is illustrated in Fig. 8 for alumina as adsorbent. In Fig. 8, we plot m vs. ϵ^0 for different solvents B as N_B is varied. The resulting plots are experimentally indistinguishable for solvents B of similar polarity, i.e., where the pure solvents have similar ϵ^0 values. Therefore, each plot in Fig. 8 is for a group of similar B solvents, e.g., group IV is for $\epsilon^0 = 0.38$ (diethyl ether); group VI is for solvents with ϵ^0 values greater than 0.56

(acetonitrile, nitromethane, etc.). For localizing B solvents, which comprise groups IV, V and VI in Fig. 8, there are two characteristic features of these plots. At low ϵ^0 values (small values of N_B), all B solvents give about the same value of m for a given value of ϵ^0 . However, at higher values of ϵ^0 for the mobile phase, the less polar solvents (e.g., group IV) approach a limiting value of m beyond which no increase in N_B or ϵ^0 will give greater solvent-selectivity.

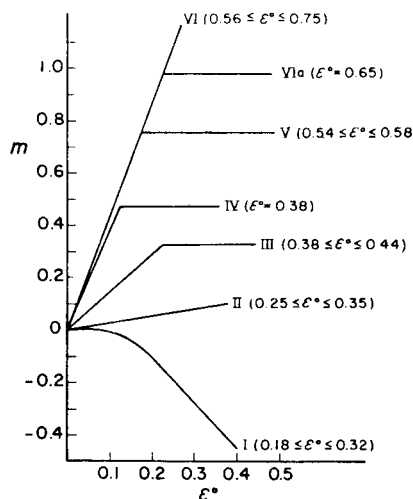


Fig. 8. Dependence of mobile phase m values on solvent strength for binary-solvent mobile phases and alumina; different plots (I, II, ...) refer to different groups of B solvents. From ref. 20.

— The practical significance of the plots of Fig. 8 is as follows. First, for a given value of mobile phase strength ϵ^0 , there is a maximum possible value of m . This value increases with ϵ^0 so that larger m values are possible for the separation of more polar samples which require larger ϵ^0 values for optimum k' values. In the case of MTBE-hexane, the maximum value of m is almost reached for 2% (v/v) MTBE and $\epsilon^0 = 0.22$ ($m = 0.75 = 90\%$ of m^0 for MTBE). For stronger mobile phases ($\epsilon^0 > 0.22$), it is possible to increase m significantly ($m > 0.8$), but only by substituting a more polar solvent for MTBE. On this basis, it is tempting to select the most polar solvents possible for the solvents C and D used to control localization selectivity in LSC separation. However, for weaker mobile phases this will mean very small concentrations of these solvents, which may be experimentally inconvenient in some applications.

CONCLUSIONS

In this paper we have further examined the nature of solvent selectivity in LSC separation. It has been confirmed that localization of solvent and solute molecules can lead to large changes in the α values of different solute-pairs. Detailed mathematical relationships have been derived to describe this dependence of sample separation sequence on mobile phase composition. These equations have been verified by numer-

ous data for alumina and silica as adsorbents, with mobile phases containing two to four solvent components.

We also describe the basis for an overall optimization strategy in LSC separation, as summarized in Table I. A later paper¹⁶ describes the reduction of this scheme to practice using a computer-optimization program. Another paper²⁵ will offer a simplified version of retention-optimization for use without detailed calculations or access to a computer.

We propose that sample retention be varied for maximum resolution using a four-solvent mobile phase A-B-C-D. Each of these four solvents A-D is selected for its ability to contribute in a unique and independent way to optimum retention. The optimum solvent strength, ϵ^0 , for the sample of interest is first established empirically (as in ref. 1) using a binary-solvent mobile phase A-B. Compositions A-B-C-D of equivalent strength, for optimum separation, are then calculated. The solvent A will be a saturated hydrocarbon such as hexane or isooctane. Variation of its concentration allows ϵ^0 to be held constant, while the proportions of B, C and D are varied for change in separation selectivity.

Solvent B should be a weakly localizing compound (small value of m^0) such as methylene chloride. Varying the proportions of B vs. (C + D) allows change in the relative localization (m value) of the mobile phase. This in turn allows continuous variation in solvent/solute localization over wide limits, which generally results in substantial changes in the α values of various solute-pairs within the sample. An acceptable spacing of solute bands within the chromatogram can often be achieved by simple variation of the mobile phase m value.

The localizing solvents C and D are chosen for their differing contributions to solvent-specific localization. Each solvent will have a large value of m^0 , which means that C and D will be relatively polar solvents. Solvent C should be relatively basic (e.g., an ether such as MTBE), while D should be strongly dipolar (e.g., acetonitrile). Varying the concentration ratio of C and D (N_C/N_D) results in a further change in α values. The possible variation of α with change in N_C/N_D is about 1/3 as great as for variation of the total concentration of C plus D ($N_C + N_D$). Therefore, N_C/N_D should be varied only after the optimum value of ($N_C + N_D$) has been determined. Additional solvent selectivity can be achieved by exploring other basic solvents in place of C (solvents from groups I or III of ref. 20).

APPENDIX I

Derivation of m values for mobile phases used with silica as adsorbent

The various mobile phases reported here and in ref. 14 were characterized as to their m values as follows. First, the procedure described²⁰ for alumina as adsorbent could not be used. The latter approach is based on k' values for reference aromatic-hydrocarbon solutes, but with silica these compounds have generally small k' values whenever ϵ^0 exceeds about 0.1. Therefore, a different procedure was used here.

For the various reference solutes of Table IV and ref. 14 we can select adjacent solute-pairs and determine their α values for various mobile phases. We selected ten such pairs as summarized in Table VIII. The solutes 1- and 2-naphthol were excluded because of possible hydrogen-bonding effects that would complicate the interpre-

tation of Δ_1 values and related values of m . For a given mobile phase i , we can sum the values of $\log \alpha_i$ for the ten solute-pairs A–J of Table VIII to give:

$$\begin{aligned}\sum_{i=1}^{10} \log \alpha_i &= \sum_{i=1}^{10} C_1 + m_i \sum_{i=1}^{10} C_2 \\ &= D_1 + D_2 m_i\end{aligned}\tag{i-1}$$

The values of D_1 and D_2 are functions only of the ten solute-pairs selected (Table VIII), and moreover their absolute values are arbitrary. We arbitrarily define $D_1 = 0$ and $D_2 = 3.3$, so that:

$$m_i = 0.3 \sum_{i=1}^{10} \log \alpha_i\tag{i-2}$$

As example, consider mobile phase 8 of ref. 14. The values of $\log \alpha_i$ for solute-pairs A–J are: 0.17, -0.07 , 0.40, 0.03, 0.06, 0.02, -0.04 , 0.10, 0.00, 0.13, and their sum is 0.80. The value of m is then $0.3 \times 0.80 = 0.24$. The present convention of assigning $D_1 = 0$ and $D_2 = 3.3$ gives m^0 values for silica which are similar in magnitude to values for alumina.

Values of m for other mobile phases can be calculated from eqn. 7, using average values of C_1 and C_2 for any of the solute-pairs of Table VIII. However, it is seen that the complication of solvent-specific effects and varying values of Δ_2 can be minimized by selecting solute-pairs which have similar (relatively large) values of C_2 for both MTBE and acetonitrile (*e.g.*, solute-pairs C, H, I of Table VIII).

APPENDIX II

Examples of the calculation of m for different mobile phases

Binary solvent mobile phase. Consider mobile phase 17 of Table V, MTBE–hexane (A–B) with $N_B = 0.042$. The value of θ_B (or θ_j) for the polar solvent MTBE is calculated as 0.77 (refs. 13, 14). The value of $f(\theta_j)$ from Table III is then 0.89. From eqn. 6, with $m^0 = 0.82$, we then have $m = 0.89 \times 0.82 = 0.73$. The experimental value determined as in Appendix I is 0.68.

Ternary solvent mobile phase. Consider mobile phase 5 of Table V, MTBE–chloroform–hexane (C–B–A) with $N_C = 0.0135$ and $N_B = 0.399$. The values of θ are calculated as in ref. 14; $\theta_B = 0.39$, $\theta_C = 0.50$. Eqn. 8 is now used to calculate m , with $m^0 = 0.10$ for chloroform ($= m_B^0$) and $m^0 = 0.82$ for MTBE ($= m_C^0$). Note that θ_D and $f(\theta_D)$ are zero.

First, determine the function $f(\theta_C + \theta_D) = f(\theta_C) = 0.47$ (Table III). Similarly, $f(\theta_B + \theta_C + \theta_D) = f(0.89) = 0.97$. Now inserting these values into eqn. 8.

$$\begin{aligned}m &= 0 + 0.82 (0.47 - 0) + 0.10 (0.97 - 0.47) \\ &= 0.44\end{aligned}$$

The experimental value was 0.36 determined in Appendix I.

Quaternary solvent mobile phase. Consider mobile phase 23 of Table V, acetonitrile–MTBE–dichloromethane–hexane (D–C–B–A). Values of θ for each polar solvent (B–D) are given in Table V determined according to the procedure of ref. 14. The value of m^0 are 0.10 (B), 0.82 (C) and 1.19 (D). These data with Table III allow solution for m in terms of eqn. 8:

$$m = 1.19 \times 0.075 + 0.82 \times (0.21 - 0.075) + 0.10 (0.96 - 0.21) \\ = 0.28$$

The experimental value was 0.37.

GLOSSARY

A, B, C, D	refers to specific solvents comprising the mobile phase; see Table I
A_s	the cross-sectional area of a solute molecule as required on the adsorbent surface during adsorption; one unit is equal to 0.08 nm ²
B_a, B_n	a solvent molecule B in the adsorbed (a) or non-sorbed (n) phase
C_1, C_2	constants in eqn. 9; C_2 varies with the localizing solvent j in the mobile phase, as shown in Table VII
D_1, D_2	constants in eqn. i-1
$f(\theta_B), f(\theta_j)$	a solvent-localization function (Table III) which varies with the fractional coverage θ of the adsorbent surface by a localizing solvent B or j ; eqns. 6, 8
i, j	solvent components of a mobile phase; j is always a localizing solvent
k'	solute capacity factor, equal to fraction of solute molecules in stationary phase divided by fraction in mobile phase
k_X, k_Y	values of k' for solutes X and Y in a given LC system
k_1, k_2	value of k' for a solute X in mobile phases 1 and 2; eqn. 3
m^0	solvent-localization parameter for pure solvent; e.g., $m^0 = 0.1, 0.1, 0.82$ and 1.19 for dichloromethane, chloroform, MTBE and acetonitrile (silica); see Table II for alumina
m_B^0, m_C^0, m_D^0	values of m^0 for solvents B, C and D
MTBE	methyl <i>tert.</i> -butyl ether
n	number of solvent molecules B displaced by an adsorbing solute molecule X; eqn. 2
\bar{N}	column plate number
N_A, N_B, N_C, N_D	mole fraction of solvents A, B, etc., in mobile phase
m	mobile-phase-localization parameter
m_i	value of m for mobile phase i ; eqn. 5
m_1, m_2	values of m for mobile phases 1 and 2; eqn. 7
Q_k^0	dimensionless free energy of adsorption ($\Delta G/RT$) for a substituent group k on a solute molecule; k is normally the most polar or strongly-adsorbing group in the molecule
r	correlation coefficient for least-squares regression analysis, as of eqn. 9 in Table VI

R_s	resolution function, equal to difference in retention times for two solute bands, divided by average band width
X_a, X_n	a solute molecule X in the adsorbed (a) or non-sorbed (n) phase
α	separation factor for two solutes X and Y; equal to k_x/k_y
α_1, α_2	value of α for mobile phases 1 and 2; eqn. 7
α'	adsorbent activity function; eqn. 3
Δ_x, Δ_y	solute localization parameters for solutes X and Y; eqns. 5, 7
Δ_1	contribution to k' from solvent/solute localization (eqn. 4); difference in $\log k'$ values for two mobile phases 1 and 2 when $\varepsilon_1 = \varepsilon_2$
Δ_2	contribution to k' from solvent-specific localization; eqn. 4a
Δ'	equal to $\Delta_1 + \Delta_2$ for a particular mobile phase (relative to a mobile phase with $\Delta' = 0$)
Δ'_p, Δ'_q	values of Δ' for mobile phases p and q, or localizing solvents P and Q; eqn. 9
ε^0	solvent strength parameter; eqn. 3; also, values of ε^0 for pure solvents A, B, C, etc.
$\varepsilon_i, \varepsilon_j$	values of ε^0 for pure solvents i and j
$\varepsilon_1, \varepsilon_2$	values of ε^0 for mobile phases 1 and 2
$\varepsilon', \varepsilon''$	value of ε^0 for localizing solvent j with $\theta_j = 0$ or 1, respectively; see discussion in refs. 13, 14

REFERENCES

- 1 L. R. Snyder and J. J. Kirkland, *Introduction to Modern Liquid Chromatography*, Wiley-Interscience, New York, 2nd ed., 1979, Chs. 2, 5.
- 2 L. R. Snyder, *J. Chromatogr. Sci.*, 15 (1978) 441.
- 3 G. Guiochon, *J. Chromatogr.*, 185 (1979) 3.
- 4 G. Guiochon, in C. Horvath (Editor), *High-performance Liquid Chromatography: Advances and Perspectives*, Academic Press, New York, 1980, p.1.
- 5 J. R. Gant, J. W. Dolan and L. R. Snyder, *J. Chromatogr.*, 185 (1979) 153.
- 6 S. L. Morgan and S. N. Deming, *Sep. Purif. Methods*, 5 (1976) 333.
- 7 R. J. Laub, J. H. Purnell and P. S. Williams, *J. Chromatogr.*, 134 (1977) 249.
- 8 V. Svoboda, *J. Chromatogr.*, 201 (1980) 241.
- 9 J. L. Glajch, J. J. Kirkland, K. M. Squire and J. M. Minor, *J. Chromatogr.*, 199 (1980) 57.
- 10 L. R. Snyder, *Principles of Adsorption Chromatography*, Marcel Dekker, New York, 1968.
- 11 L. R. Snyder, *Anal. Chem.*, 46 (1974) 1384.
- 12 L. R. Snyder and H. Poppe, *J. Chromatogr.*, 184 (1980) 363.
- 13 L. R. Snyder and J. L. Glajch, *J. Chromatogr.*, 214 (1981) 1.
- 14 J. L. Glajch and L. R. Snyder, *J. Chromatogr.*, 214 (1981) 21.
- 15 L. R. Snyder and J. J. Kirkland, *Introduction to Modern Liquid Chromatography*, Wiley-Interscience, New York, 2nd ed., 1979, Fig. 9, 15b.
- 16 J. L. Glajch, J. J. Kirkland and L. R. Snyder, *J. Chromatogr.*, submitted for publication.
- 17 A. Waksmundzki and J. K. Rozylo, *J. Chromatogr.*, 49 (1970) 313.
- 18 N. Tanaka, H. Goodell and B. L. Karger, *J. Chromatogr.*, 158 (1978) 233.
- 19 J. G. Stewart and P. A. Williams, *J. Chromatogr.*, 198 (1980) 489.
- 20 L. R. Snyder, *J. Chromatogr.*, 63 (1971) 15.
- 21 T. Dale and W. E. Court, *Chromatographia*, 13 (1980) 24.
- 22 J. S. Fok and E. A. Abrahamson, *Am. Lab., Fairfield, Conn.*, 7 (6) (1975) 63.
- 23 L. R. Snyder, *J. Chromatogr. Sci.*, 16 (1978) 223.
- 24 B. L. Karger, L. R. Snyder and C. Eon, *Anal. Chem.*, 50 (1978) 2126.
- 25 J. L. Glajch, J. J. Kirkland and L. R. Snyder, *Anal. Chem.*, in preparation.

CHROM. 14,257

STUDY ON THE RETENTION OF AMINES IN REVERSED-PHASE ION-PAIR CHROMATOGRAPHY ON BONDED PHASES

R. S. DEELDER* and J. H. M. VAN DEN BERG

DSM Research, P.O. Box 18, 6160 MD Geleen (The Netherlands)

SUMMARY

The retention behaviour of a series of amines was investigated in phase systems consisting of an alkyl-modified silica as column packing material and an aqueous buffer or buffer-propanol mixtures containing low concentrations of alkylsulphonates as the mobile phase. The adsorption of the alkylsulphonates on the surface of the column packing material was studied by measuring adsorption isotherms. The amphiphilic ions form monomolecular films at the support-eluent interface. Charged electrical double layers are formed, with the sulphonate ions constituting the surface charge and the counter ions forming a diffuse layer in the eluent phase. The adsorption can be described by a Langmuirian equilibrium in which allowance is made for the electrical contributions to the adsorption energy. The retention of amines can be described by an ion-exchange process, *i.e.*, the protonated amines exchange with the counter ions concentrated near the charged surface. The molar ion-exchange selectivity constants were found to depend on the density of the ionized monolayer.

INTRODUCTION

It is common knowledge that the retention of ionized compounds in reversed-phase liquid chromatography is strongly enhanced by the addition of a suitable amphiphilic ion such as a long chain quaternary ammonium compound, an alkylsulphate or alkylsulphonate to the aqueous mobile phase. Johansson *et al.*¹ have investigated the influence of the addition of 1-octanesulphate to the mobile phase on the retention of protonated amines in a reversed-phase liquid-liquid partition system.

Increased retention due to the presence of amphiphilic ions in the eluent is also observed for alkyl-modified silica without any liquid bulk coating. Haney and co-workers²⁻⁴ and Knox and co-workers^{5,6} have pioneered this technique, which is commonly referred to as paired-ion chromatography⁴, soap chromatography⁶, dynamic solvent generated ion-exchange chromatography⁷ or hetaeric chromatography⁸. As for this technique, Kissinger⁹ and Kraak and co-workers^{7,10} demonstrated the strong adsorption of amphiphilic ions on the hydrophobic column packing material, and recent results are indicative of a relation between the adsorption of the amphiphilic ion and the capacity factors of ionized solutes as predicted by simple ion exchange models¹⁰⁻¹².

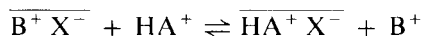
The adsorption of amphiphilic ions at the interface between water and non-aqueous phases has been the subject of a great many studies (*e.g.*, refs. 13 and 14). The interaction between the adsorbed amphiphilic ions and the aqueous phase is strongly influenced by the charge at the interface resulting from the adsorption. The main objective of the present study was further to elucidate the retention mechanism of ionized solutes on alkyl-modified silica in the presence of amphiphilic ions. To that purpose, we have investigated the formation of charged films of these ions at the surface of reversed-phase packing materials, and examined the relation between the adsorption and selectivity. Particular attention was paid to the reliability of the retention data.

THEORETICAL

The ion-exchange model

Detailed discussions of the ion-exchange model for "paired-ion" chromatography can be found elsewhere^{10-12,15}. We confine ourselves to recalling some simplified basic equations.

Amines which are present in the eluent as cations HA^+ are considered to exchange with the counter ions B^+ at the ion-exchange sites formed by the alkylsulphonate X^- , which is adsorbed on the hydrophobic surface:



The bar denotes the "complex" site-solute at the surface. This equilibrium can be described by the molecular selectivity constant for ion exchange

$$K_e = \frac{[\overline{\text{HA}^+ \text{X}^-}][\text{B}^+]}{[\overline{\text{B}^+ \text{X}^-}][\text{HA}^+]} \quad (1)$$

where $[\text{B}^+]$ and $[\text{HA}^+]$ are the concentrations of the species B^+ and HA^+ in the aqueous bulk solutions, and $[\overline{\text{HA}^+ \text{X}^-}]$ and $[\overline{\text{B}^+ \text{X}^-}]$ denote the surface concentrations of the respective complexes (mol/g).

For a partition process based on ion exchange the partition coefficient, K , of a protonated amine may be written as:

$$K = \frac{[\overline{\text{HA}^+ \text{X}^-}]}{[\text{HA}^+]} = K_e \frac{[\overline{\text{B}^+ \text{X}^-}]}{[\text{B}^+]}$$

Now we find for the capacity factor, k' ,

$$k' = q K_e \frac{[\overline{\text{B}^+ \text{X}^-}]}{[\text{B}^+]} \quad (2)$$

where q is the phase ratio, which can be calculated from the amount of packing material in the column and the liquid hold up.

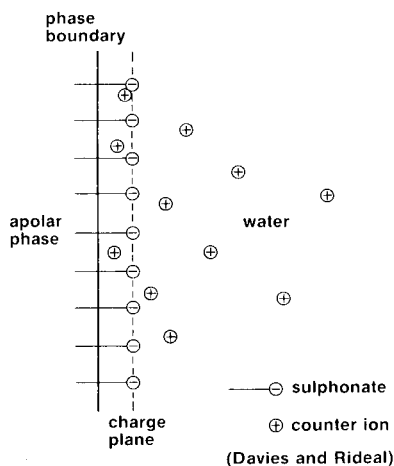


Fig. 1. Hydrocarbon chain ions at a liquid interface.

Model of the double layer

Amphiphilic ions such as long-chain alkylsulphonates are known to be readily adsorbed at the interface between two immiscible liquids of greatly different polarity, *e.g.*, octane and water. A model of the ionized monolayer formed is shown in Fig. 1. It is analogous to that proposed by Haydon and Taylor^{16,17} and Davies and Rideal¹⁴. The adsorbed amphiphilic ions are oriented such that the ionic headgroups are situated in the aqueous phase and the apolar alkyl chains in the hydrocarbon phase. The ionic headgroups will project some distance into the aqueous phase. The adsorbed ions are referred to as potential-determining ions, since they are responsible for a potential difference, ψ_0 , between the plane of the ionic headgroups (charge plane) and the bulk solution. The concentration of electrical charge near the phase boundary brings about a non-random distribution of other ions in the aqueous solution. Ions of opposite charge (counter ions) are attracted towards the fixed charges at the charge plane. It is generally accepted that the counter ions may penetrate into the zone between the charge plane and the phase boundary^{16,17}. On the other hand, ions of like charge (co-ions) are repelled from the surface region.

The methods for estimating the potential ψ_0 as a function of the amount of detergent adsorbed have been reviewed (*e.g.*, ref. 13, 14, 18). In the present study we used a simplified method due to Van den Tempel¹⁹. In this model it is assumed that, for the counter ions, two zones may be distinguished. A proportion of the counter ions is contained, together with the ionic headgroups, in a layer situated in the immediate neighbourhood of the interface. This layer, which is commonly referred to as the Stern layer, has a depth of only several times 10^{-8} cm. It is assumed to have a uniform potential ψ_0 with respect to the homogeneous bulk solution. The remaining counter ions are located in the diffuse Gouy layer and neutralize the net charge of the Stern layer.

The charge, σ_1 , of the counter ions located in the Stern layer is calculated from a simplified Langmuir–Stern equation

$$\sigma_1 = N_1 zF [1 + (1/x_s) \exp(zF\psi_0/RT)]^{-1} \quad (3)$$

where N_1 is the number of available sites in 1 cm^2 of the Stern layer, x is the mole fraction of the counter ions of valence z in the homogeneous bulk solution, F is Faraday's number, R the gas constant and T the temperature. The number of sites in the Stern layer, N_1 , may be estimated as 10^{15} if the depth of this layer is taken as $3 \cdot 10^{-8} \text{ cm}$. The charge σ_2 of the diffuse Gouy layer is given by

$$\sigma_2 = \left(\frac{\epsilon \epsilon_0 R T C}{125} \right)^{\frac{1}{2}} \sinh \left(\frac{z F \psi_0}{R T} \right) \quad (4)$$

where ϵ is the dielectric constant of the medium, ϵ_0 is the permittivity constant and C is the counter ion concentration in the bulk solution. The condition for electric neutrality of the whole double layer systems is:

$$\sigma_1 + \sigma_2 = \sigma \quad (5)$$

where σ is the charge associated with the adsorbed amphiphilic ions. Thus, the potential ψ_0 can be calculated as a function of the adsorbed amount of the detergent, σ , and the counter ion concentration (C and x_s).

This model comprises some drastic simplifications compared with more recent and more elaborate models. Moreover, it is essentially derived for flat surfaces and neglects geometrical complications such as curved interfaces. Recently, Cantwell and Puon²⁰ used a model derived from the Stern–Gouy–Chapman theory for describing the adsorption of aromatic ammonium compounds on Amberlite XAD-2. In this model it is assumed that counter ions are completely excluded from the region between the ionic headgroups of the detergent and the phase boundary. It is not realistic for ionized layers of adsorbed detergents^{14,16,17}.

EXPERIMENTAL

Apparatus

Separations were carried out on a Spectra-Physics Type 3500 liquid chromatograph equipped with a Model 770 variable-wavelength UV photometer; catecholamines were detected at 220 nm. All columns ($15 \text{ cm} \times 4.6 \text{ mm I.D.} \times 6.35 \text{ mm O.D.}$) were of precision-bore stainless-steel tubing, thermostatted to within 0.1°C by water-jackets connected to a water-bath. The eluent was thermostatted before the injection valve by means of a heat-exchanger consisting of 1 m of stainless-steel tubing (0.051 cm I.D.). High-pressure sampling valves (Rheodyne Type 70-10) equipped with $20\text{-}\mu\text{l}$ sample loops were used for sample injection. A Waters Type R401 refractive index detector was used for monitoring breakthrough curves.

Chemicals

Quartz-distilled water and analytical-grade solvents were used for all experiments. Catecholamines were obtained from Aldrich and Serva: NADR = noradrenaline; ADR = adrenaline; DOP = dopamine; OCT = octopamine and TYR = tyramine. The sodium salts of 1-octanesulphonic acid and 1-dodecanesulphonic acid (zur Tensid-analyse) were purchased from E. Merck (Darmstadt, G.F.R.). The purity of the surfactants was verified by surface tension measurements: the curve of surface

tension against surfactant concentration showed no minimum^{21,22}. Buffers were prepared from Titrisol solutions of sodium hydroxide and orthophosphoric acid (E. Merck). The sodium concentration in the aqueous phosphate buffers was 0.01 or 0.05 *M*. Mixed organic aqueous eluents were prepared from known volumes of 1-propanol and aqueous phosphate buffers.

The reversed-phase packing material was prepared from *n*-octadecyldimethylmonochlorosilane and 10- μ m SI-100 silica (E. Merck)²³; the carbon content was 17.6%. The specific surface area was determined by the BET method as 180 m² g⁻¹. This packing material is coded as C₁₈.

Procedures

The columns were packed by a balanced-density slurry technique with 1,1,2,2-tetrabromoethane–tetrachloromethane–dioxane (36:32:32) as the suspension medium and at pressures of about 50 MPa. The columns were washed successively with 100 cm³ each of 2,2,4-trimethylpentane, dichloromethane, 1-propanol and water before the mobile phase was applied.

The capacity factor, k'_i , for a component *i* was determined from its retention volume, V_{Ri} , and the hold-up of the column, V_{RO} . The hold-up of the column and the amount of adsorbed 1-propanol, V_s , were determined as follows. The column, which had previously been filled with the eluent, was rinsed with about 45 cm³ dimethylformamide. The eluate was collected in a 50-cm³ calibrated flask and diluted to 50 cm³. The water content of the collected eluate was determined by Karl Fischer titration, and the amount of 1-propanol by gas chromatography. The composition of the eluent was determined in the same way. From these data V_{RO} as well as V_s can be calculated. The repeatability of this procedure was found to be better than 1% (rel.) for both V_{RO} and V_s .

Adsorption isotherms were calculated from breakthrough curves²⁴. At the beginning of the experiment the column was equilibrated with the eluent but without the sulphonate. Then the eluent containing a known concentration of the detergent was fed to the column and the breakthrough volume was measured with the refractive index detector. By using a series of eluents with increasing sulphonate concentrations the adsorption isotherm could be constructed. Generally, the increase of the surface excess concentration of the sulphonate, $\Delta\Gamma_2^v(n)$, resulting from a stepwise change from concentration $C_2(n-1)$ to $C_2(n)$ with $C_2(n) > C_2(n-1)$ can be calculated from²⁵

$$\Delta\Gamma_2^v = \frac{[V_B(n) - V_1][C_2(n) - C_2(n-1)]}{mS} \quad (6)$$

where $V_B(n)$ represents the corresponding breakthrough volume. V_1 is the difference between the volume of the empty column and the volume of the packing material, *m* the mass of the adsorbent and *S* its specific surface area. Its value was determined by filling the column with the aqueous buffer, rinsing it with dimethylformamide and determining the water content of the collected eluate. The surface excess $\Gamma_2^v(n)$ corresponding to the bulk concentration of the sulphonate, $C_2(n)$, is obtained by adding up the successive $\Delta\Gamma_2^v(n)$ values. In the present study we identify the surface excess Γ_2^v with the amount of detergent ion, n_s , adsorbed on unit surface area¹⁹. If no excess

of inert electrolyte is present, Γ_2^v will not correspond exactly with n_s , because of the deficiency of soap anions in the diffuse part of the double layer. This deficiency amounts to only a few percent of n_s , however¹⁸⁻²⁰.

RESULTS AND DISCUSSION

Adsorption of 1-propanol

Adsorption of non-electrolytes from binary mixtures at a homogeneous surface can often be described by the Langmuir equation

$$A_0/(A - A_0) = x e^{-\Delta G/RT} \quad (7)$$

where A is the area (\AA^2) occupied by the adsorbed molecule at the interface, A_0 the limiting value of A at monolayer coverage, x the mole fraction of the solute in the bulk solution and ΔG the free energy of adsorption. This equation can easily be transformed into the more familiar form:

$$\frac{1}{n_s} = \frac{1}{Kx} + \frac{1}{n_{s,0}} \quad (8)$$

Here n_s is the number of molecules of solute adsorbed at the interface per unit of surface area (cm^{-2}), $n_{s,0}$ is the limiting value of n at monolayer coverage and K is a constant.

We measured the adsorption of 1-propanol from an aqueous phosphate buffer (pH 3.00, 0.01 M Na^+) on the reversed-phase packing material. A plot of the data according to eqn. 8 yielded $1/n_{s,0} = 22 \text{ \AA}^2$ for the limiting area per molecule, A_0 , which corresponds very well with the value of 20 \AA^2 found by surface tension measurements for alcohols at the water-decane interface¹⁶. In the latter case, the low limiting area is adduced as proof that the molecules are oriented perpendicularly to the inter-

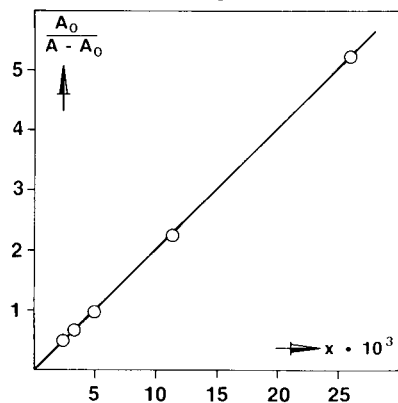


Fig. 2. Adsorption isotherm (eqn. 7) for the adsorption of 1-propanol from an aqueous phosphate buffer (0.01 M Na^+ , pH = 3.00) at 40°C on C_{18} silica.

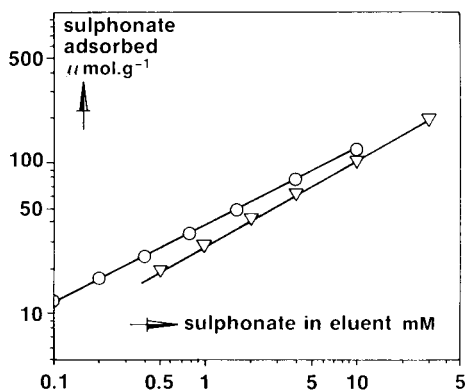


Fig. 3. Adsorption isotherms (Freundlich plots) of sodium 1-octanesulphonate on C_{18} silica at 40°C. Eluents: \circ , phosphate buffer (0.05 M Na^+ , pH 3.00); ∇ , phosphate buffer (0.01 M Na^+ , pH 3.00) + 2% (v/v) 1-propanol.

face. Fig. 2 shows the plot of the adsorption data according to eqn. 7 for $A_0 = 22 \text{ \AA}^2$. From the slope we find $-\Delta G = 12.9 \text{ kJ mol}^{-1}$, which is in good agreement with the value of 13.4 kJ mol^{-1} reported for the adsorption of 1-propanol at the water-decane interface¹⁶.

Adsorption of alkylsulphonates

Fig. 3 shows the adsorption isotherms for sodium 1-octanesulphonate from an aqueous phosphate buffer and a phosphate buffer containing a low concentration of 1-propanol, respectively. In accordance with earlier findings^{11,12}, these isotherms are well fitted by a Freundlich equation

$$n_s = aC^b \quad (9)$$

where C is the detergent concentration in the bulk solution. The error made by assuming $n_s = \Gamma_2^v$ for the adsorption of the sulphonates may be estimated as follows. From the experimental data on the exclusion of inorganic anions from reversed-phase columns "loaded" with anionic detergents²⁶ it may be concluded that the external void volume of the columns is almost completely accessible to anions. If the detergent is completely excluded from the internal void volume, *i.e.*, the pore system of the column packing material, V_1 in eqn. 6 should be replaced by V_e , the external void volume of the column. For the columns used we found $V_1 = 1.6\text{--}1.7 \text{ cm}^3$, depending on the mobile phase composition, and $V_e = 1.1\text{--}1.2 \text{ cm}^3$. Since the breakthrough volumes, V_B , usually exceeded 10 cm^3 , the error in n_s will be 5% at most.

The use of the Freundlich equation for describing the adsorption of ionic detergents on reversed-phase packing materials is merely empirical and has no theoretical background^{11,12}. The adsorption of amphiphilic ions at the interface between water and an apolar hydrocarbon can also be described by a Langmuirian form of the adsorption isotherm, *e.g.*, eqn. 7 (refs. 14, 16, 27). The free energy of adsorption, ΔG , represents the work done by one mole of the surfactant ion on adsorption. This work may be divided into two parts: the work of transfer of the molecules from the aqueous bulk phase to the surface, ΔG_0 ; and the work done against the electrical potential at the surface, ΔG_{el} . Therefore we may write:

$$\Delta G = \Delta G_0 + \Delta G_{el} \quad (10)$$

For the present study ΔG_0 is assumed to be constant. This simplification is justified by experimental data²⁷. Further, the electrical work, ΔG_{el} , done by a univalent ion is given by

$$\Delta G_{el} = N \int_0^{\psi_0} z e d\psi = z F \psi_0 \quad (11)$$

where e is the elementary charge and N is Avogadro's number.

The validity of the modified Langmuir isotherm for describing the adsorption of ionic detergents on reversed-phase packing materials was checked in two ways. First, we consider the case that $A \gg A_0$. Now eqn. 7 can be written as follows:

$$A_0/A = x e^{-\Delta G/RT} \quad (12)$$

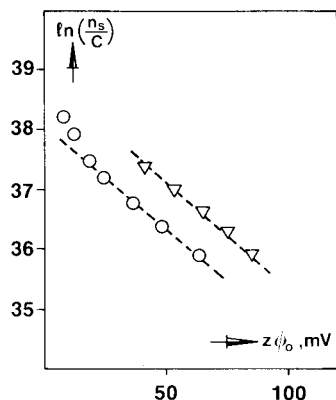


Fig. 4. Test of eqn. 13 for the adsorption of sodium 1-octanesulphonate on C_{18} silica at 40°C . Eluents as in Fig. 3.

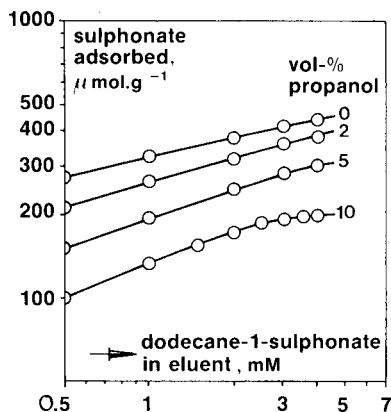


Fig. 5. Adsorption isotherms (Freundlich plots) of sodium 1-dodecanesulphonate on C_{18} silica from phosphate buffer (0.01 M Na^+ , pH 3.00) containing various amounts of added 1-propanol. Temperature: 40°C .

For low concentrations of the detergent ion in water the mole fraction x can be replaced by $C/55.5$. With $A = 10^{16}/n_s$ we find by combining eqns. 10–12

$$\ln \frac{n_s}{C} = \alpha - \frac{ZF\psi_0}{RT} \quad (13)$$

where $\alpha = \ln(1.8 \times 10^{14} RT/A_0 \Delta G_0)$. In Fig. 4 $\ln(n_s/C)$ is plotted as a function of ψ_0 for the adsorption data from Fig. 3. The lines have the theoretical slope $-F/RT$, and ψ_0 is calculated by eqns. 3–5. At low values of ψ_0 , deviations from the straight line are observed, which may result from the very low surface coverage, $n \approx 5 \cdot 10^{12} \text{ cm}^{-2}$.

As a second test for the validity of eqns. 7, 9 and 11 we used the adsorption data for a strongly adsorbed detergent. Fig. 5 shows the adsorption isotherms for sodium 1-dodecanesulphonate from an aqueous phosphate buffer and mixtures of phosphate buffer and increasing amounts of 1-propanol. For the neat aqueous buffer and for mixtures containing low propanol concentrations the isotherms approximately obey the Freundlich equation. As the surface coverage is rather high, the approximation of the adsorption by eqn. 12 cannot be applied. The general equation for adsorption of amphiphilic ions is

$$\frac{A_0}{A - A_0} \exp\left(\frac{zF\psi_0}{RT}\right) = x \exp\left(-\frac{\Delta G_0}{RT}\right) \quad (14)$$

A plot of the left-hand side of this expression vs. x should yield a straight line from the slope of which ΔG_0 can be calculated. This expression, however, can be verified only when a value for A_0 is available. It has been deduced from surface-tension measurements that a constant area per molecule adsorbed at the air–water or hydrocarbon–water interface is obtained when the bulk surfactant concentration is at the critical micelle concentration, CMC^{28,29}. For linear alkylsulphonates, values of $50\text{--}55 \text{ \AA}^2$

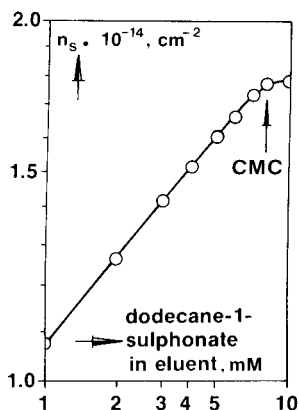


Fig. 6. Saturation adsorption of sodium 1-dodecanesulphonate from phosphate buffer (0.01 M Na^+ , pH 3.00) on C_{18} silica at $40^\circ C$.

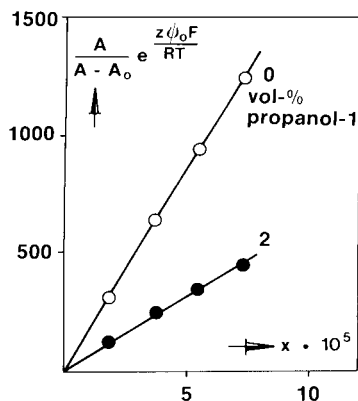


Fig. 7. Test of eqn. 14 for the adsorption of sodium 1-dodecanesulphonate on C_{18} silica from phosphate buffer (0.01 M Na^+ , pH 3.00) at $40^\circ C$.

have been reported for A_0 . Fig. 6 shows the adsorption isotherm for sodium 1-dodecanesulphonate from an aqueous phosphate buffer. At low concentrations the adsorption isotherm obeys a Freundlich equation. When the surfactant concentration approaches the CMC, the adsorption isotherm flattens and tends to a limiting value for n , which corresponds to a limiting area, A_0 , of approximately 55 \AA^2 per ion adsorbed. Flattening of adsorption isotherms near the CMC has also been observed for the adsorption of alkylsulphonates on Graphon³⁰.

Now, we may estimate ΔG_0 by means of eqn. 14 from the adsorption data in Fig. 5 and the calculated ψ_0 values for the eluents containing 0 and 2% 1-propanol assuming $A_0 = 55 \text{ \AA}^2$. Fig. 7 shows plots according to eqn. 14 for these eluents.

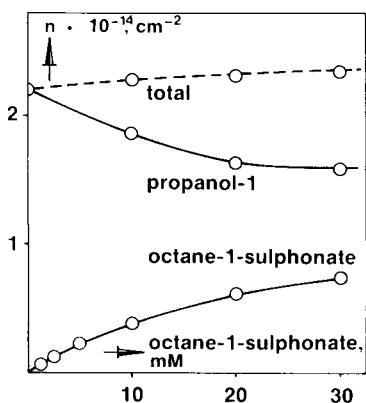


Fig. 8. Simultaneous adsorption of 1-propanol and sodium 1-octanesulphonate on C_{18} silica from phosphate buffer (0.01 M Na^+ , pH 3.00) + 2% (v/v) 1-propanol. Temperature: $40^\circ C$.

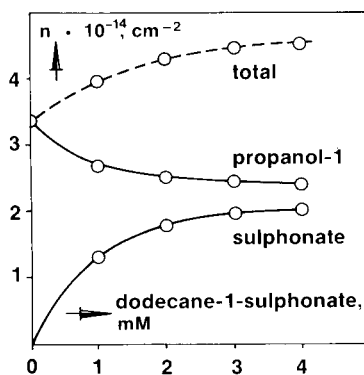


Fig. 9. Simultaneous adsorption of 1-propanol and sodium 1-dodecanesulphonate on C_{18} silica from phosphate buffer (0.01 M Na^+ , pH 3.00) + 10% (v/v) 1-propanol. Temperature: $40^\circ C$.

Straight lines are obtained for both eluents and from the slopes we calculated ΔG_o . For the adsorption of sodium 1-dodecanesulphonate from an aqueous phosphate buffer we find $-\Delta G_o = 43 \text{ kJ mol}^{-1}$. A value of 46 kJ mol^{-1} has been reported for the adsorption of the corresponding alkylsulphate at the water-petroleum ether interface¹⁶. The value of $-\Delta G_o$ decreases upon addition of propanol. For the eluent with 2% propanol we find $-\Delta G_o = 41 \text{ kJ mol}^{-1}$. Apparently, the detergent displaces propanol from the surface. The influence of the adsorption of alkylsulphonates on the amount of propanol adsorbed is illustrated in Figs. 8 and 9. The coverage of the surface increases upon adsorption of the detergent, the amount of propanol displaced being only a fraction of the detergent adsorbed.

Since we had no value for A_o in the eluents containing high propanol concentrations we could not check the validity of eqn. 14 for these cases. At first sight it is surprising that the adsorption of the sulphonates can be described by the modified Langmuir isotherm (see eqn. 8) as well as by a Freundlich isotherm (see eqn. 9). However, in a number of cases¹⁴, the values for ψ_o obtained by solving eqns. 3–5 are well fitted by the following empirical relation

$$\psi_o = \beta + \gamma \ln n_s \quad (15)$$

where β and γ are constants. Combining eqns. 13 and 15 we find, after some rearrangements

$$n_s = a C^b$$

which is equivalent to the empirical Freundlich equation.

Retention behaviour of amines

Fig. 10 shows the k' values for some catecholamines on C_{18} reversed-phase packing material as a function of the 1-octanesulphonate concentration in an

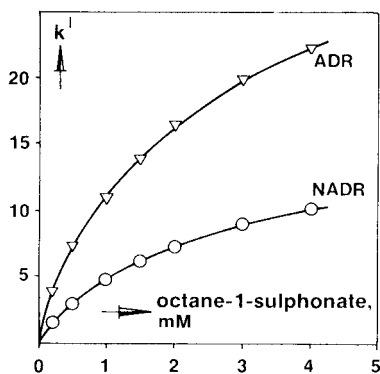


Fig. 10. Capacity factors of catecholamines as a function of sodium 1-octanesulphonate concentration. Column packing: C_{18} silica. Eluent: phosphate buffer, 0.05 M Na^+ , pH 3.00. Temperature: 40°C .

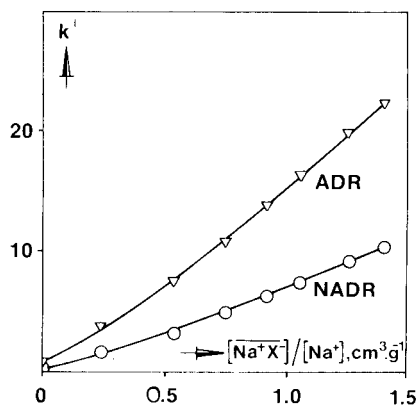


Fig. 11. Capacity factors from Fig. 10 plotted according to eqn. 2.

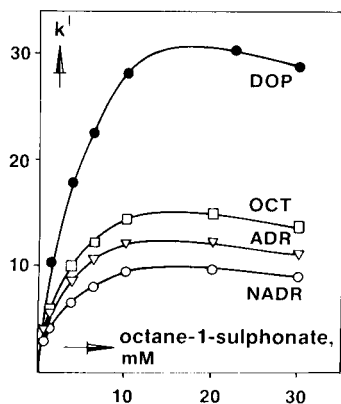


Fig. 12. Capacity factors of catecholamines as a function of sodium 1-octanesulphonate concentration. Column packing: C_{18} silica. Eluent: phosphate buffer, 0.01 M Na^+ , pH 3.00, 2% (v/v) 1-propanol. Temperature: 40°C .

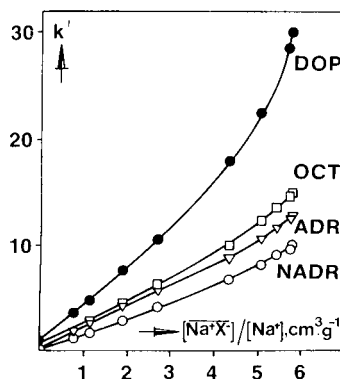


Fig. 13. Capacity factors from Fig. 12 plotted according to eqn. 2.

aqueous phosphate buffer. Fig. 11 shows the dependence of the capacity factors on $[\text{Na}^+ \text{X}^-]/[\text{Na}^+]$. Although at first sight a fairly good linear dependence is observed according to eqn. 2, the plots show a slight but significant curvature. Close examination of earlier data also indicates a non-linear dependence^{11,31}. It turns out that K_e , as calculated from eqn. 2, increases with increasing coverage of the surface by the amphiphilic ion, $[\text{Na}^+ \text{X}^-]$. Plots of k' against sulphonate concentration for eluents containing propanol are given in Fig. 12. These plots show the characteristic maxima for k' ^{8,11,12}. It seems most unlikely that these maxima arise from micelle formation, since the CMCs in the eluents are about 0.1 M and 0.012 M for 1-octanesulphonate and 1-dodecanesulphonate, respectively. A striking feature is the reversal of the elution order of ADR and NADR shown in Fig. 14, which is incompatible with the

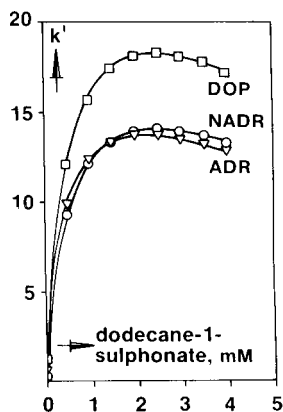


Fig. 14. Capacity factors of catecholamines as a function of sodium 1-dodecanesulphonate concentration. Column packing: C_{18} silica. Eluent: phosphate buffer, 0.01 M Na^+ , pH 3.0, 10% (v/v) 1-propanol. Temperature: 40°C .

simple linear relationship expressed by eqn. 2. Deviations from the linear behaviour are also observed for octylsulphonate as the amphiphilic ion, see Fig. 13. These results confirm earlier findings for eluents containing propanol¹¹.

In the simple model of the double layer used in this study we assumed that the counter ions neutralize the ionized groups of the adsorbed detergent in two ways. A fraction of the counter ions is found in the Stern layer, the remainder being located in the diffuse Gouy layer. The latter ions are retained by non-specific, electrostatic forces and there is no selectivity. Therefore, we may write for the species HA^+ and B^+ (ref. 32)

$$\frac{n_{\text{HA}^+}}{n_{\text{B}^+}} = \frac{[\text{HA}^+]}{[\text{B}^+]} \quad (16)$$

where n_i is the number of counter ions of species i in the diffuse layer. Selectivity will result from specific interactions in the Stern layer between the ionic species and the primary surface charge. The surface densities of the ions concerned in both the Stern and Gouy layers are denoted by $[\overline{\text{HAX}}]$ and $[\overline{\text{BX}}]$, respectively, and the fractions retained in the Stern layer by the combination of electrostatic and specific interactions by α_{HAX} and α_{BX} . Now we may write:

$$\frac{n_{\text{HA}^+}}{n_{\text{B}^+}} = \frac{1 - \alpha_{\text{HAX}}}{1 - \alpha_{\text{BX}}} \cdot \frac{[\overline{\text{HA}^+ \text{X}^-}]}{[\overline{\text{B}^+ \text{X}^-}]} \quad (17)$$

Combination of eqns. 16 and 17 gives:

$$K_e = \frac{[\overline{\text{HAX}}][\text{B}^+]}{[\overline{\text{BX}}][\text{HA}^+]} = \frac{1 - \alpha_{\text{BX}}}{1 - \alpha_{\text{HAX}}} \quad (18)$$

This equation relates the selectivity constant for ion exchange and the specific interactions between, on the one hand, the ions B^+ and HA^+ and, on the other, the charged surface.

Actually, the Stern–Langmuir equation (eqn. 3) as used by Van den Tempel for calculating the number of counter ions in the Stern layer accounts for electrostatic interactions only, neglecting any “specific” or “chemical” interaction. These interactions may be expressed through an additional energy term in the exponent of the Stern–Langmuir equation¹⁸

$$\sigma_1 = N_1 zF \{1 + (1/x_s) \exp [(zF\psi_o + \phi)/RT]\}^{-1}$$

where ϕ is the specific adsorption energy of the ions.

The results of the present study indicate that the simplified eqn. 3 holds for the adsorption of alkylsulphonates in the presence of sodium as the counter ion. This suggests that for sodium the specific interactions are relatively minor compared with the purely electrostatic interactions, *i.e.*, $\phi \ll zF\psi_o$. On the other hand, the results of the study on the retention of amines indicate a strong specific interaction between the sample ions HA^+ and the charged interface. As for the counter ions, the value of α_{BX}

can be calculated from eqns. 3–5 since $\alpha_{\text{BX}} = \sigma_1/(\sigma_1 + \sigma_2)$. For the diluted buffers and the detergent concentrations used in this study a typical value for α_{BX} is about 0.5. As indicated earlier, the value for K_e is 10. Then, we find from eqn. 18 that $\alpha_{\text{HAX}} = 0.95$. This result indicates a strong specific interaction in the Stern layer.

At present, however, no theoretical or experimental method allows for the estimation of the specific adsorption energy, ϕ , for the sample ions. Levine *et al.*³³ have predicted that for simple ions the specific adsorption energy will increase with the charge density of the monolayer. This theoretical result seems to be confirmed by experimental data³⁴. The increase of the specific adsorption energy with increasing surface concentration of the amphiphilic ion may account for the dependence of K_e on the surface concentration of the sulphonate shown in Fig. 11. However, more quantitative information about the specific adsorption energy, ϕ , is required for a better understanding of the retention of ionic compounds on surfaces covered by ionic detergents.

REFERENCES

- 1 I. M. Johansson, K.-G. Wahlund and G. Schill, *J. Chromatogr.*, 149 (1978) 281.
- 2 D. P. Wittmer, N. O. Nuessle and W. G. Haney, Jr., *Anal. Chem.*, 47 (1975) 1422.
- 3 S. P. Sood, L. E. Sartori, D. P. Wittmer and W. G. Haney, Jr., *Anal. Chem.*, 48 (1976) 796.
- 4 W. G. Haney, Jr. and D. P. Wittmer, *U.S. Pat.* 4,042,327 (1977).
- 5 J. H. Knox and G. R. Laird, *J. Chromatogr.*, 122 (1976) 17.
- 6 J. H. Knox and J. Jurand, *J. Chromatogr.*, 125 (1976) 89.
- 7 J. C. Kraak, K. M. Jonker and J. F. K. Huber, *J. Chromatogr.*, 142 (1977) 671.
- 8 Cs. Horváth, W. Melander, I. Molnár and P. Molnár, *Anal. Chem.*, 49 (1977) 2295.
- 9 P. T. Kissinger, *Anal. Chem.*, 49 (1977) 883.
- 10 J. P. Crombeen, J. C. Kraak and H. Poppe, *J. Chromatogr.*, 167 (1978) 219.
- 11 R. S. Deelder, H. A. J. Linssen, A. P. Konijnendijk and J. L. M. van de Venne, *J. Chromatogr.*, 185 (1979) 241.
- 12 J. H. Knox and R. A. Hartwick, *J. Chromatogr.*, 204 (1981) 3.
- 13 A. W. Adamson, *Physical Chemistry of Surfaces*, Wiley, New York, 3rd ed., 1976, Ch. 2–4.
- 14 J. T. Davies and E. K. Rideal, *Interfacial Phenomena*, Academic Press, New York, 1961, Ch. 4.
- 15 C. P. Terweij-Groen, S. Heemstra and J. C. Kraak, *J. Chromatogr.*, 161 (1978) 69.
- 16 D. A. Haydon and F. H. Taylor, *Philos. Trans. R. Soc. London, Ser. A*, 252 (1960) 225.
- 17 D. A. Haydon, *Recent Progr. Surface Sci.*, 1 (1964) 94.
- 18 D. C. Grahame, *Chem. Rev.*, 41 (1947) 441.
- 19 M. van den Tempel, *Rec. Trav. Chim. Pays-Bas*, 72 (1953) 419.
- 20 F. F. Cantwell and S. Puon, *Anal. Chem.*, 51 (1979) 623.
- 21 G. Nilsson, *J. Phys. Chem.*, 61 (1957) 1135.
- 22 S. J. Rehfeld, *J. Phys. Chem.*, 71 (1967) 738.
- 23 H. Hemetsberger, P. Behrensmeyer, J. Henning and H. Ricken, *Chromatographia*, 12 (1979) 71.
- 24 J. F. K. Huber and R. G. Gerritse, *J. Chromatogr.*, 58 (1971) 137.
- 25 E. H. Slaats, W. Markowski, J. Fekete and H. Poppe, *J. Chromatogr.*, 207 (1981) 299.
- 26 J. A. Graham and L. B. Rodgers, *J. Chromatogr. Sci.*, 18 (1980) 614.
- 27 F. Tokiwa and K. Ohki, *J. Colloid Interface Sci.*, 26 (1968) 545.
- 28 F. van Voorst Vader, *Trans. Faraday Soc.*, 56 (1960) 1067.
- 29 S. J. Renfeld, *J. Colloid Interface Sci.*, 31 (1969) 46.
- 30 F. G. Greenwood, G. D. Parfitt, N. H. Picton and D. G. Wharton, in W. J. Webber and E. Matijevic (Editors), *Adsorption from Aqueous Solutions*, Advances in Chemistry Series No. 79, American Chemical Society, Washington, DC, 1968.
- 31 J. L. M. van de Venne, *Thesis*, Eindhoven University of Technology, Eindhoven, 1979.
- 32 M. Plaisance and L. Ter-Minassian-Saraga, *J. Colloid Interface Sci.*, 59 (1977) 133.
- 33 S. Levine, J. Mingins and G. M. Bell, *J. Phys. Chem.*, 67 (1963) 2095.
- 34 M. Plaisance and L. Ter-Minassian-Saraga, *J. Colloid Interface Sci.*, 38 (1972) 489.

CHROM. 14,071

MECHANISM OF ZWITTERION-PAIR CHROMATOGRAPHY

I. NUCLEOTIDES

JOHN H. KNOX* and JADWIGA JURAND

Department of Chemistry, University of Edinburgh, West Mains Road, Edinburgh EH9 3JJ (Great Britain)

SUMMARY

The basis of retention of zwitterionic solutes in reversed-phase liquid chromatography in the presence of zwitterionic pairing agents has been studied using long-chain amino acids (11-aminoundecanoic acid, C11AA and 12-aminododecanoic acid, C12AA), a tripeptide (L-leucyl-L-leucyl-L-Leucine, LLL), and a long-chain diamine (1,10-diaminodecane, C10DA). The adsorption has been determined for each pairing agent under the conditions used for chromatography to show up any correlation between retention and surface concentration of the pairing agents. Eluents were water-methanol (88:12) or water-dimethylformamide (90:10) buffered with acetic acid-acetate, or phosphoric acid-phosphate in the pH range 3–7. The most characteristic feature of zwitterion-pair chromatography is the existence of maxima in retention of zwitterionic solutes at pH where both solute and pairing agent exist as zwitterions. With C11AA and C12AA as pairing agents this occurs at pH of 4.4 and with LLL as pairing agent at pH of 3.5. The peak in retention is most noticeable when the ionic strength of the buffer is small (in the millimolar-range). The pH behaviour of retention in the presence of zwitterionic pairing agents is in striking contrast to that in the presence of C10DA which not only provides much reduced retention when present at the same surface concentration of amino groups, but shows no marked dependence on pH.

It is concluded that zwitterionic pairing agents provide a new mode of retention for zwitterionic solutes, namely the formation in the stationary phase of quadrupolar ion pairs between the zwitterionic forms of the solute and pairing agent when an appropriate pH is employed.

Illustrative separations of mono-, di- and triphosphate nucleotides, and of selected monophosphate nucleotides are shown.

INTRODUCTION

In a previous paper¹ we demonstrated that excellent separations of nucleotides could be achieved on a reversed-phase silica gel (ODS Hypersil[®]) with predominantly aqueous eluents containing millimolar concentrations of zwitterionic pairing agents (11-aminoundecanoic acid, C11AA and 12-aminododecanoic acid, C12AA) when,

without the added pairing agent, little or no retention could be observed. The separations achieved by this method showed excellent plate efficiency, selectivity and flexibility. The term "zwitterion-pair chromatography" was coined for this form of ion-pair chromatography in which both the solute and the pairing agent could exist as zwitterions, but it was not clear from the preliminary work whether or not retention depended upon the formation of quadrupolar ion-pairs or the more conventional dipolar ion-pairs. However, it was observed that while adsorption of C11AA varied somewhat with pH, the variation of column capacity ratio, k' , was much more dramatic with the greatest retention occurring at about pH 4.2 where there was near maximal overlap of the zwitterionic forms of the pairing agent and the nucleotides. Somewhat similar results had been obtained in connection with the chromatography of tetracyclines in the presence of ethylene diamine tetraacetate (EDTA)² when the idea of zwitterion-pairing was first suggested.

Undoubtedly if genuine quadrupolar ion pairing occurred it should be associated with retention maxima at pH values around those where maximum overlap of the zwitterionic forms of the solutes and pairing agents exists. However, such maxima could also arise from interactions of oppositely charged forms of the solute and pairing agent if the range of overlap of the zwitterionic forms was small. It was the purpose of this work to see whether the expected maxima could be clearly observed and, if so, to distinguish between the two possible explanations of the enhanced retention brought about by addition of the zwitterionic pairing agents. Since it had previously been shown by several groups³⁻⁵ that there exists a strong correlation between retention and concentration of adsorbed pairing agent we have determined the adsorption isotherms for the pairing agents used in this study over a wide range of conditions to be certain that major changes in retention were not simply due to changes in the concentration of adsorbed pairing agent. We have also measured the degree of retention over the pH range 3-7 under a variety of conditions of ionic strength.

With dilute buffers, maxima in retention have been found at pH of 4-4.2 with C11AA and C12AA, and at pH of 3.5 with L-leucyl-L-leucyl-L-leucine (LLL) as zwitterionic pairing agents. The maxima are most marked with buffers of lowest ionic strength. When 1,10-diaminodecane (C10DA) is used as pairing agent no maxima are observed and the overall retention in the region of pH 4 is very much less than with C11AA added to give the same surface concentration of amino groups. The results provide strong evidence for the formation of quadrupolar ion pairs being the main cause of the enhanced retention produced by the amino acids as pairing agents.

EXPERIMENTAL

Adsorption isotherms were determined by the breakthrough method previously reported¹ using a refractive index monitor (Optilab Multiref Model 902, Vallingby, Sweden) coupled to the chromatographic column which was supplied with eluent by a membrane microdosing pump (Model 1515; Orlita, Giessen, G.F.R.). The whole equipment downstream of the pump was thermostatted by circulating water at 25°C, and was additionally mounted within an air-box likewise thermostatted at 25°C.

Liquid chromatography was carried out using a thermostatted photometer-

column-oven unit maintained at 25°C (Shandon Southern Products, Runcorn, Great Britain). The column was supplied with eluent by a single piston reciprocating pump (Model 110; Altex, Berkeley, CA, U.S.A.). Samples were introduced by a Rheodyne injection valve (Model 7120; Rheodyne, Berkeley, CA, U.S.A.). Columns were 5 mm bore and 100 or 125 mm long (Shandon Southern Products) and were packed with ODS Hypersil (Shandon Southern Products) using isopropanol as the slurry liquid and a pressure of 400 bar. The isopropanol-slurry was followed by 200 ml hexane before conditioning the column with methanol and finally eluent.

Eluents were water-methanol (88:12) or water-dimethylformamide (90:10). The pH was adjusted within the range 3–7 by addition of phosphate buffer mixture (KH_2PO_4 – Na_2PO_4 – H_3PO_4), acetate buffer mixture (NaCH_3COO – CH_3COOH), pure acetic acid, or pure phosphoric acid. Methanol was HPLC grade (Rathburn Chemicals, Walkerburn, Great Britain). Dimethylformamide was AnalaR Reagent (BDH, Poole, Great Britain). C11AA, C12AA and C10DA were obtained from Aldrich (Gillingham, Great Britain). Nucleotides were obtained from BDH Biochemicals or from Sigma (Poole, Great Britain)

RESULTS AND DISCUSSION

Adsorption isotherms

Recent investigations of the mechanism of ion-pair chromatography using monopolar long-chain pairing agents^{3–5} have established that the degree of retention of monopolar solutes can be closely correlated with the surface concentration of the adsorbed pairing agent. Thus, for a given pairing agent and eluent, the column capacity ratio, k' , is almost exactly proportional to the surface concentration, C_{ads} , of

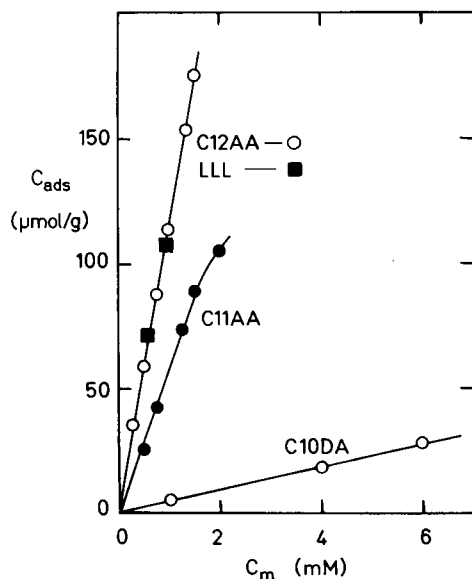


Fig. 1. Adsorption isotherms for C12AA, LLL, C11AA and C10DA. Column packing, ODS Hypersil. Eluent, water-methanol (88:12) containing 75 mM phosphate buffer at pH 5.8.

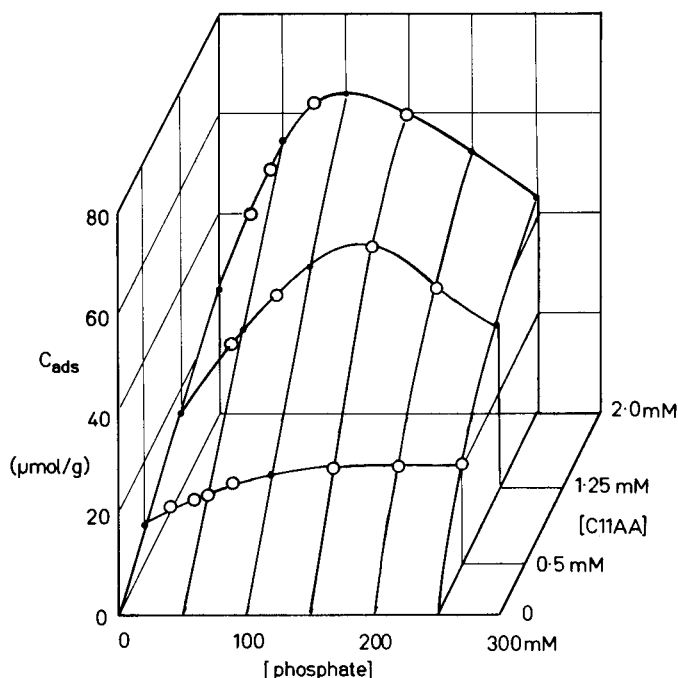


Fig. 2. Adsorption isotherms for C11AA at different phosphate buffer concentrations. Column packing, ODS Hypersil. Eluent, water–dimethylformamide (90:10) containing phosphate buffer at pH 5.35.

the pairing agent up to the point when micelle formation begins in the eluent. At this point or just before it multiple ion clusters form in the eluent and the retention may become constant or even begin to fall while C_{ads} continues to increase. In our previous study¹ somewhat similar results were reported for the retention of nucleotides in the presence of added C11AA. It has also been noted^{4,5} that with a series of homologous pairing agents, while the adsorption coefficients differ greatly, the degree of retention for a given surface concentration is relatively little dependent upon the chain length of the pairing agent. With these results in mind we considered it essential to determine the adsorption isotherms of the various pairing agents used in this study over the range of eluent compositions used.

Fig. 1 shows the adsorption isotherms on ODS Hypersil for the four pairing agents, C12AA, LLL, C11AA and C10DA using a standard eluent of water–methanol (88:12) containing 75 mM phosphate buffer pH 5.8. The isotherms are linear over the range studied. Surface concentrations, C_{ads} , ranged up to 180 $\mu\text{mol/g}$ for the most strongly adsorbed C12AA. C12AA and LLL are twice as strongly adsorbed as C11AA, and C11AA is about twelve times as strongly adsorbed as C10DA under the same conditions. Since the surface area of Hypersil before bonding is about 170 m^2/g (ref. 6), the surface concentrations based upon the original area ranged up to about 1 $\mu\text{mol}/\text{m}^2$. This compares with a concentration of bonded groups of about 2.5 $\mu\text{mol}/\text{m}^2$. Typical concentrations used in the chromatographic experiments were from 35–90 $\mu\text{mol/g}$ or 0.2–0.5 $\mu\text{mol}/\text{m}^2$. In comparing k' values using C11AA and

C10DA the eluent concentrations of the pairing agents were chosen so as to provide about the same concentrations of amino groups, namely about $40 \mu\text{mol/g}$.

Fig. 2 shows three dimensional isotherms for C11AA adsorbed from water-dimethylformamide (90:10) for different concentrations of phosphate buffer up to 250 mM with pH 5.3. At low buffer concentrations the isotherms are linear up to a concentration of pairing agent in eluent, C_m , of 2 mM , but when the phosphate concentration exceeds about 100 mM the isotherms become increasingly curved towards the C_m axis. At low eluent concentrations of C11AA, increase in the phosphate buffer concentration causes a gradual increase in C_{ads} , but at higher concentrations of C11AA, C_{ads} passes through a maximum. The maximum occurs at lower buffer concentrations the higher is C_m . In the chromatographic experiments described below the concentrations of C11AA and buffer were held below 2 mM and 100 mM respectively where the isotherms are linear and C_{ads} increases smoothly with buffer concentration.

Fig. 3 shows how pH affects the adsorption of C11AA from the standard eluent containing 75 mM phosphate buffer. For any pH between 3 and 7 the isotherms are more or less linear, but there is a flat maximum in the dependence of C_{ads} upon pH at pH 4–4.5. Data from Fig. 1 for pH 5.8 and from Fig. 4 for 0.75 mM C11AA are included in Fig. 3. For C10DA C_{ads} at an eluent concentration of 4 mM was found to be $19 \mu\text{mol/g}$ independent of pH in the range 5–7 (see Fig. 5).

The results on the adsorption of C11AA, C12AA and C10DA may be summarised as follows:

- (1) Addition of CH_2 to the chain of C11AA increase its adsorption by a factor of about two.
- (2) Replacement of CH_2NH_2 in C11AA by COOH to give C10DA reduces adsorption by a factor of twelve.

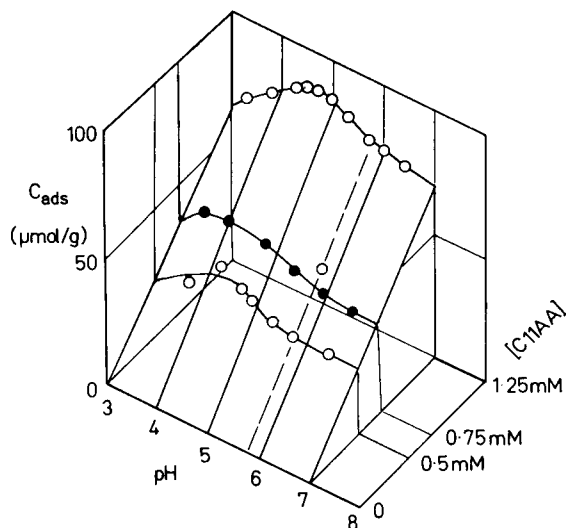


Fig. 3. Adsorption isotherms for C11AA at different pH. Column packing, ODS Hypersil. Eluent, water-methanol (88:12) containing 75 mM phosphate buffer.

(3) The adsorption isotherms of the three pairing agents are essentially linear in the chromatographically useful range.

(4) Addition of phosphate buffer increases C_{ads} slightly when the concentration of C11AA is low. At higher concentrations of C11AA in eluent a maximum in C_{ads} is found as phosphate concentration increases.

(5) pH has only a slight effect on C_{ads} for C11AA adsorbed from 75 mM phosphate buffer. A flat maximum is observed at pH 4-4.5.

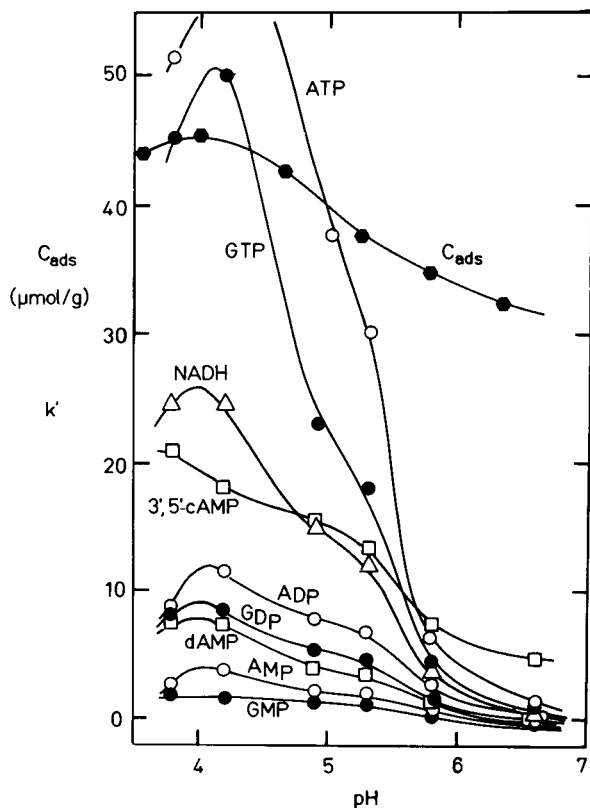


Fig. 4. Dependence of k' of nucleotides and of C_{ads} for C11AA upon pH. Column packing, ODS Hypersil. Eluent, water-methanol (88:12) containing 75 mM phosphate buffer and 0.75 mM C11AA as pairing agent.

(6) C11AA is about twice as strongly adsorbed from water-methanol (88:12) as from water-dimethylformamide (90:10).

(7) Although no quantitative experiments were carried out on the effect of temperature, it was observed that the amount of pairing agent adsorbed decreased with increase of temperature. Accordingly thermostating of the system was essential for reproducible results. In an independent study on the adsorption of cetylpyridinium by ODS Hypersil⁷, an enthalpy of adsorption of -32 kJ/mol was observed corresponding to a temperature coefficient of about 5% per degree.

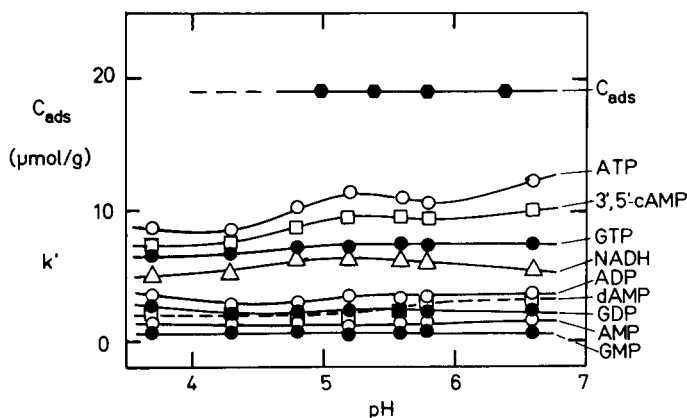


Fig. 5. As for Fig. 4 but with 4 mM C10DA as pairing agent.

Dependence of retention upon pH, C11AA and C10DA

Figs. 4 and 5 compare the effects of pH upon retention of nucleotides when using C11AA and C10DA as pairing agents and standard eluent containing 75 mM phosphate. The concentrations of pairing agents, 0.75 mM for C11AA and 4 mM for C10DA were chosen to give approximately the same surface concentrations of $-\text{NH}_3^+$ groups. The effect of pH upon k' for the two pairing agents may be seen to be completely different. With C10DA (Fig. 5) a fall in pH from 7 to 3 causes a slight overall decline in retention while the surface concentration of C10DA remains constant at 19 $\mu\text{mol/g}$ (giving 38 $\mu\text{mol/g}$ of amino groups). By contrast, with C11AA as pairing agent (Fig. 4), there is a massive increase in k' as the pH is reduced from 7 to

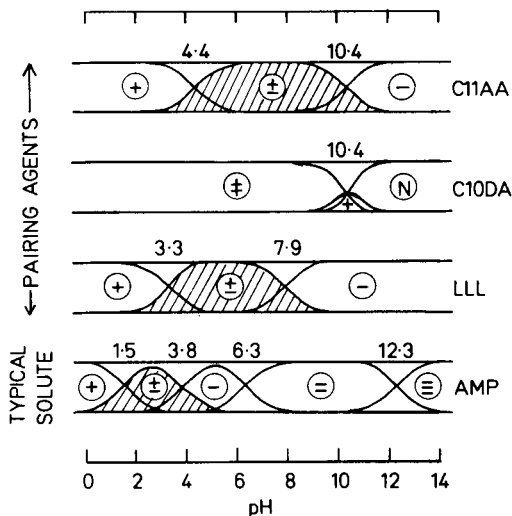


Fig. 6. Ionisation diagrams showing the fractions of different ionic forms as a function of pH for pairing agents, C11AA, C12AA, C10DA and LLL, and for a typical solute, AMP. Note that higher phosphates have additional primary phosphate ionisations at pH around 1.5–2.

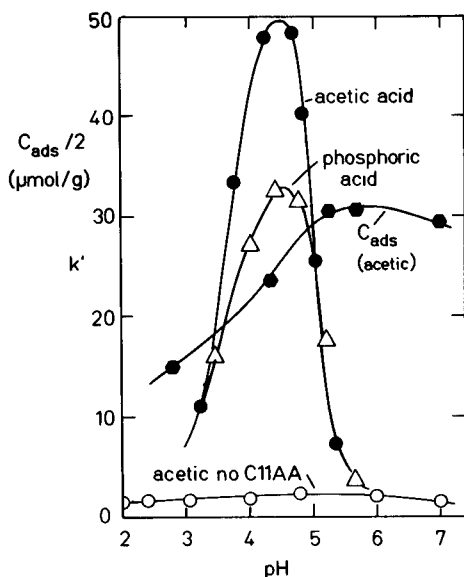


Fig. 7. Dependence of k' for AMP upon pH, with pH adjusted by pure acetic acid or pure phosphoric acid, and dependence of C_{ads} for C11AA upon pH. Column packing, ODS Hypersil. Eluent, water-methanol (88:12) containing 1.25 mM C11AA.

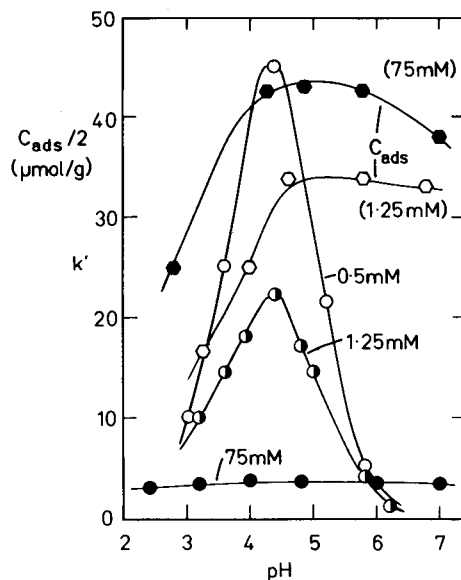


Fig. 8. Dependence of k' for AMP upon pH, with pH adjusted by acetate buffers of different strengths (marked on lines), and dependence of C_{ads} for C11AA upon pH for low and high buffer strengths. Other conditions as for Fig. 7.

about 4.2, and there is evidence for a maximum in k' of several of the nucleotides at about pH 4.2. Over the pH range 3–7 the surface concentration of C11AA changes by only about 40%, while k' values change by up to 50-fold. Evidently the small change in C_{ads} does not in any way account for the massive changes in k' values. Again comparing Figs. 4 and 5 it is noted that at pH around 7 retention with C11AA is only a fraction of that with C10DA, but is many times greater at pH 4.2. Finally a weak maximum (Fig. 5) or bulge (Fig. 4) in the k' -dependence is observed at pH 5.3 for both pairing agents which is superimposed upon the general trends.

Over the entire pH range, as shown for the ionisation diagrams given in Fig. 6, the amino groups of C11AA and C10DA are fully ionised (pK_a 10.4). Likewise the primary phosphate groups of the nucleotides are fully ionised at any pH over 3 ($pK_a < 2$). Thus the strength of the interactions of the amino groups with the phosphate groups must remain constant over the pH range 3–7. This is in agreement with the absence of any strong variation of k' with pH when using C10DA as pairing agent. The slight fall in k' as pH is reduced may be due to the onset of a repulsive interaction between the positive N atoms of the nucleotides (pK_a in range 3–4) and the amino groups of C10DA as pH is reduced.

The strong increase in k' when using C11AA as pH is reduced from 7 to 4.2 can only be due to an increasing interaction between the partially ionised carboxyl group of C11AA (pK_a 4.4) and the partially ionised nitrogen of the nucleotides (pK_a 3–4). These interactions which will appear relatively weak when averaged over all mole-

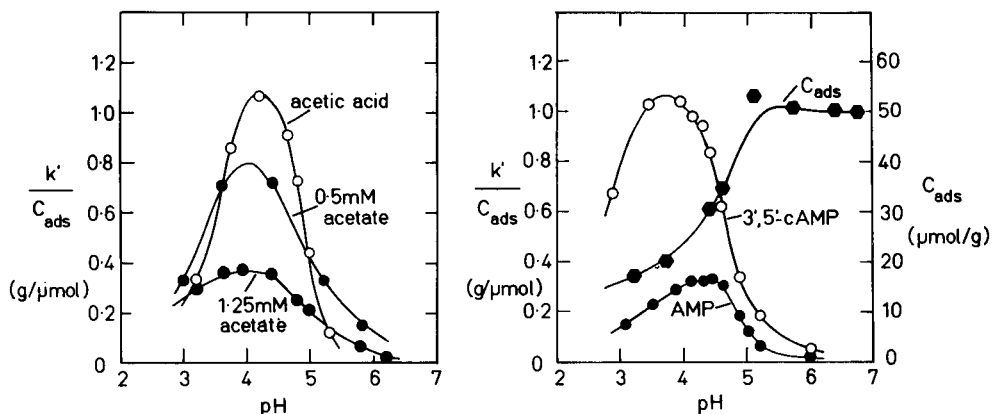


Fig. 9. Dependence of k'/C_{ads} upon pH for AMP. Data and conditions as for Figs. 7 and 8.

Fig. 10. Dependence of k'/C_{ads} upon pH for AMP and 3',5'-cyclic AMP with C12AA as pairing agent, and dependence of C_{ads} for C12AA upon pH. Column packing, ODS Hypersil. Eluent, water-dimethylformamide (90:10) containing 1.0 mM C12AA. pH adjusted by acetic acid.

cules will nevertheless reinforce the strong interactions of the phosphate groups and the ionised amino groups of C11AA which remain unchanged over the pH range. The weak interactions will, however, vary over the pH range due to the variation in the degrees of ionisation of the two species and should be a maximum at a pH which is midway between the pK_a values of the two weakly interacting groups, that is at a pH of about 4.1 (taking pK_a for the nucleotide as 3.8, the value for adenosine phosphates). This predicted value for maximal retention agrees gratifyingly with the observed value of 4.2. When the pH is reduced below 4.2 the decreasing degree of ionisation of the carboxyl group of C11AA more than compensates for the increasing ionisation of the nitrogen of the nucleotides, and k' begins to fall.

The prime interaction which brings about the strong retention on addition of C11AA when the pH is about 4.2 must therefore be due to a quadrupolar interaction of the zwitterionic forms of the nucleotide and the pairing amino acid.

The low retention of the nucleotides in the presence of C11AA at high pH when compared to the retention in the presence of C10DA is most likely due to the increased repulsive interaction between the carboxyl group of the amino acid and the phosphate groups of the nucleotides. This is especially notable for the nucleotides containing secondary phosphate groups with their pK_a of around 6.3. It is notable that 3',5'-cyclic AMP which has no secondary phosphate group is much less affected than the other nucleotides.

Dependence of retention upon pH and ionic strength: C11AA, C12AA and LLL

It is well established in ion-exchange and in ion-pair chromatography that a reduction in the ionic strength of the eluent increases retention by reducing the competition for charged sites in the stationary phase⁸. In order to provide maximum scope for zwitterion pairing and so for the exhibition of a maximum in retention as pH is varied, the retention of selected nucleotides in eluents of very low ionic strength was investigated. With the present group and with standard eluents containing low buffer concentrations it proved impossible to elute di- and triphosphate nucleotides

with reasonable k' values, and therefore only the monophosphates AMP and 3',5'-cyclic AMP were used for the experiments now described.

Fig. 7 shows the dependence of k' for AMP upon pH in the presence of C11AA with pH adjustment by (i) pure acetic acid, and (ii) pure phosphoric acid, and without addition of C11AA with pH adjustment by pure acetic acid. The isotherm for C11AA in the presence of acetic acid is shown. The k' values for AMP in the presence of C11AA show strong maxima at pH of around 4.4. The adsorption of C11AA, however, falls quite steeply as the pH is reduced below about 5.2. This decrease is proportionately less marked with higher concentrations of buffer (see Fig. 8) and then occurs at slightly lower pH. The fall in C_{ads} with decrease of pH is presumably due to the decreasing ionisation of the carboxyl group and the development of a net positive charge by C11AA. There is only slight retention of AMP in the absence of C11AA.

Fig. 8 shows corresponding curves when the pH is adjusted by acetate buffers of various strengths from 0.5 to 75 mM. With the weak buffers strong maxima in k' as a function of pH are observed but even with buffer concentrations as low as 1.25 mM the maximum retention is reduced by a factor of two compared to that with no buffer present. Increase of buffer concentration to 75 mM increases the adsorption of C11AA significantly but greatly reduces the retention of AMP at pH 4.5. Evidently the zwitterion-pairing effect is extremely sensitive to the presence of other ions in the eluent.

At pH below 5 the adsorption of C11AA decreases significantly especially with buffers of low ionic strength. In order to allow for this change in C_{ads} , the data from Figs. 7 and 8 where acetic acid and acetate were used have been replotted in Fig. 9 after dividing the k' values by the concentration of adsorbed C11AA. The normalised curves so obtained confirm that the maxima are not associated with changes in C_{ads} . The maxima in the normalised curves now occur at pH in the range 4.0–4.2 with the maximum being sharpest when pure acetic acid is used to adjust pH. The pH for the maximum is now almost exactly that predicted, that is midway between the pK_a of the nucleotides (3.8) and of the carboxylic acid group (4.4), and corresponds to maximal overlap of the zwitterionic forms of AMP and C11AA.

Fig. 10 shows similar data for C12AA as pairing agent and water–dimethylformamide (90:10) as eluent, again normalised to unit surface concentration of pairing agent. Retention is significantly lower as is expected when dimethylformamide is used as organic modifier, but the maximum in retention is still relatively sharp and occurs at pH 4.2 with AMP and at pH 3.7 for 3',5'-cyclic AMP. Again 3',5'-cyclic AMP behaves somewhat differently from the other nucleotides.

Fig. 11 shows results obtained with the tripeptide LLL. With AMP and LLL the range of zwitterion overlap is greater than with C11AA and AMP (see Fig. 6) since the first ionisation of the peptide occurs at pH 3.3 instead of 4.4. The position of the peak retention now occurs at pH 3.5, again midway between the relevant pK_a values of the nucleotide (3.8) and the pairing agent (3.3). Retention of AMP in the presence of 1.0 mM LLL is much less than in the presence of a similar concentration of C11AA in spite of the stronger adsorption of LLL. This may be due to the unfavourable stereochemistry of the interaction of LLL and the nucleotide.

The following conclusions may be drawn from the results of the last two sections.

- (1) Retention of nucleotides in the presence of C10DA is little dependent upon

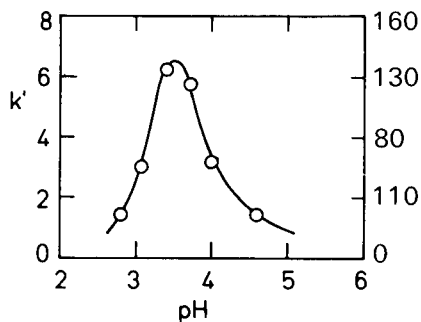


Fig. 11. Dependence of k' for AMP upon pH with LLL as pairing agent, and dependence of C'_{ads} for LLL upon pH. Column packing, ODS Hypersil. Eluent, water-methanol (88:12) containing 0.5 *mM* phosphate buffer and 1.0 *mM* LLL.

pH. Retention in presence of C11AA changes greatly with pH showing maximum retention at pH 4.2.

(2) Buffer strength greatly affects retention: k' decreases greatly as ionic strength increases up to 75 *mM* and the effect is already noticeable with an ionic strength of 1.25 *mM*.

(3) In eluents of low ionic strength the maximum in k' as a function of pH is most pronounced.

(4) The maximum retention as a function of pH occurs at a pH which is midway between the pK_a values for formation of zwitterionic forms of the pairing agent and the nucleotide. This occurs at pH 4.2 for C11AA-AMP and C12AA-AMP, and at pH 3.5 for LLL-AMP. The predicted pH-values are 4.1, 4.1 and 3.5 respectively.

(5) The occurrence of maxima in k' as a function of pH is independent of buffer concentration, nature of buffering system, nature of pairing agent and nature of solute within the limits of this study.

Examples of separations

Separations of nucleotides in the past have normally been carried out by ion-exchange chromatography (for references see ref. 1). The results are generally poor in terms of plate efficiency, and gradient elution is required to separate mono- from di- from triphosphates. As shown previously¹ addition of C11AA allows reversed-phase separations of the three groups to be carried out in an isocratic separation with high plate efficiency. Fig. 12 shows such a separation using optimal conditions. At pH 5.4 there is good resolution of the three groups from one another but fairly small retention of the monophosphates. C10DA instead of C11AA at the same surface concentration gives much poorer separation of these compounds as seen from Fig. 13. Selectivity and peak shape are both poor. In this respect C10DA differs from cetyltrimethylammonium used successfully by Gilbert⁹ for nucleotide separations. The reason for the poor peak shape with C10DA, particularly for ATP is not clear. If the asymmetry arose from a non-linear partition isotherm for ATP, the position of the peak maximum would be expected to depend upon sample size. The comparison of the broken with the full line in Fig. 13 shows that this is not the case. Conventional chromatographic theory would then argue that the broadness of the peak must arise

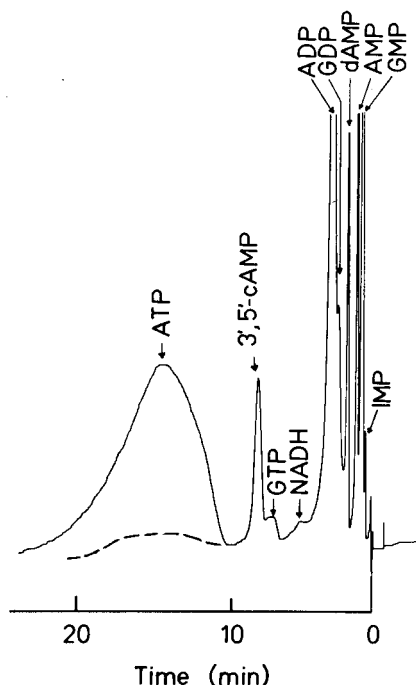
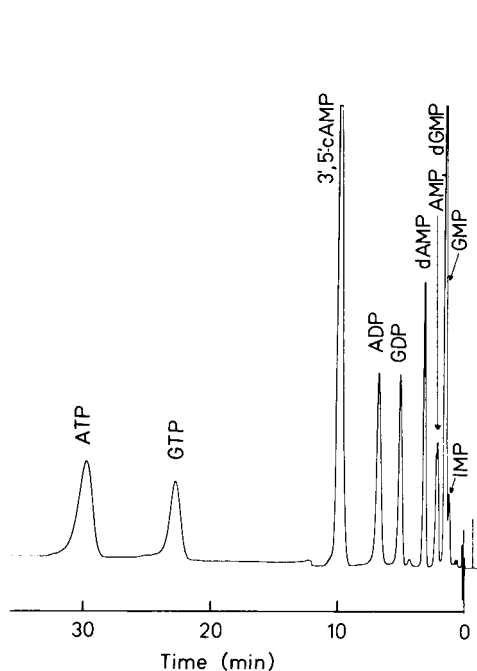


Fig. 12. Separation of mono-, di-, and triphosphate nucleotides using C11AA as pairing agent. Column packing, ODS Hypersil. Eluent, water-methanol (88:12) containing 75 mM phosphate buffer (pH 5.45) and 1.0 mM C11AA. Column 100 \times 5 mm I.D. Flow-rate, 1.2 ml/min. Detector, UV at 254 nm.

Fig. 13. Separation of nucleotides using C10DA as pairing agent. Packing, column and eluent as Fig. 12 except pH 4.25 and 4.5 mM C10DA used as pairing agent.

from slow equilibration of ATP between the mobile and stationary phases, but there seems no obvious reason why this should be the case with C10DA and not with the other pairing agents which have been used.

Although C11AA provides excellent separations of the mono-, di-, and triphosphates, it has proved difficult to resolve a large range of monophosphates, even when the k' values are increased by change in pH and buffer concentration. For this group LLL gives very good selectivity as shown in Fig. 14. IMP and GMP now elute after AMP whereas with C11AA they elute before. The relative retention of the deoxy- to unreduced monophosphates remains roughly the same at about 1.3–1.5. Unfortunately with LLL, IMP and GMP are no longer resolved. To obtain complete resolution of the chosen group of nucleotides it is necessary to use a mixture of the two pairing agents, which breakthrough experiments show are independently adsorbed. Optimal results with such a mixture are shown in Fig. 15. The separations in Figs. 12, 14 and 15 show excellent plate efficiencies of between 3000 and 5000 for 125-mm columns.

Evidently variation of the nature and concentration of the pairing agent, and of the pH and ionic strength of the buffer, provide great flexibility in the control of retention and selectivity so that the method should be readily adaptable to any specific problem.

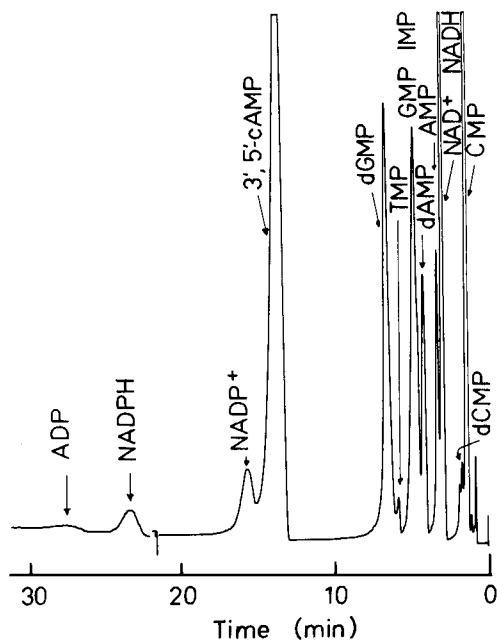


Fig. 14. Separation of mainly monophosphate nucleotides using LLL as pairing agent. Column packing, ODS Hypersil. Eluent, water-methanol (88:12) containing 2.3 mM phosphate buffer (pH 3.3) and 1.0 mM LLL. Column 125 \times 5 mm I.D. Other conditions as in Fig. 12.

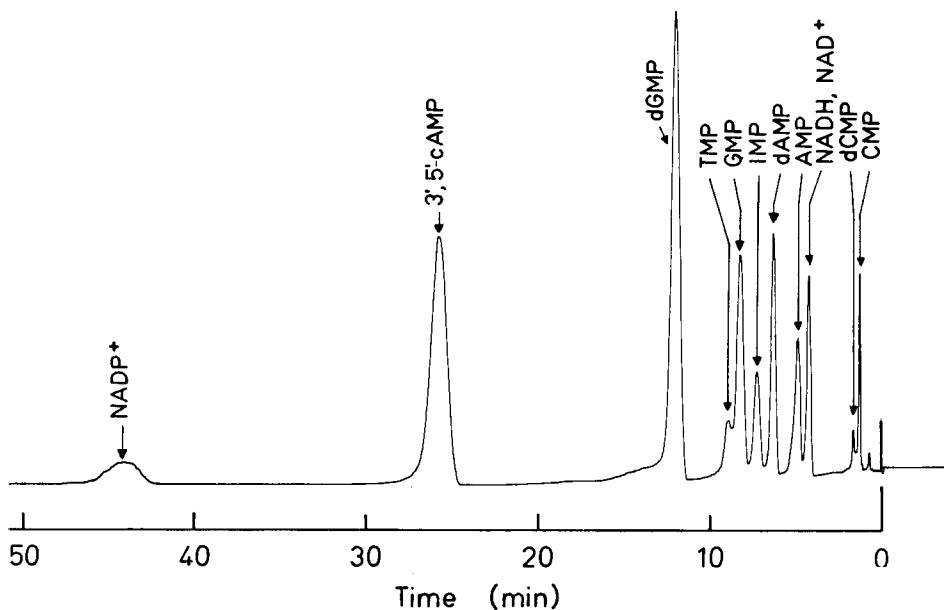


Fig. 15. As for Fig. 14 except 1.0 mM C11AA and 1.0 mM LLL used as mixed pairing agent.

CONCLUSIONS

The experiments described above, we believe, provide compelling evidence that under the correct conditions of pH zwitterionic solutes can interact strongly with zwitterionic pairing agents by the formation of quadrupolar ion pairs in reversed-phase HPLC systems. This new form of ion-pair chromatography offers great flexibility in the control of retention and selectivity by adjustment of the nature and concentration of the pairing agent, by control of pH and of buffer concentration. Thus it is possible to tune the conditions to separate nucleotides according to the number of phosphate groups, or to separate individual nucleotides with the same number of phosphate groups. Because formation of quadrupolar ion pairs involves the formation of two strong interactions between the solute and the pairing agent, it should be possible to exploit zwitterion-pair methods in the resolution of enantiomers by using an optically active zwitterion-pairing agent.

ACKNOWLEDGEMENT

The authors wish to record their thanks to the Science Research Council of Great Britain for their generous support of this work.

NOTE ADDED IN PROOF

Separation of enantiomers by this method has now been achieved and will be reported shortly (*J. Chromatogr.*, in press).

REFERENCES

- 1 J. H. Knox and J. Jurand, *J. Chromatogr.*, 203 (1981) 85.
- 2 J. H. Knox and J. Jurand, *J. Chromatogr.*, 186 (1979) 763.
- 3 C. P. Terweij-Groen, S. Heemstra and J. C. Kraak, *J. Chromatogr.*, 161 (1978) 69.
- 4 R. S. Deelder, H. A. J. Linssen, A. P. Konijnendijk and J. L. M. van de Venne, *J. Chromatogr.*, 185 (1979) 241.
- 5 J. H. Knox and R. A. Hartwick, *J. Chromatogr.*, 204 (1981) 3.
- 6 *Manufacturers Information*, Shandon Southern Products, Runcorn, Cheshire, Great Britain, 1980.
- 7 J. Oliver, Edinburgh University, Edinburgh, unpublished results, 1980.
- 8 J. H. Knox (Editor), *High-Performance Liquid Chromatography*, Edinburgh University Press, Edinburgh, Great Britain, 2nd ed., 1979.
- 9 M. T. Gilbert, in A. M. Lawson, C. K. Lim and W. Richmond (Editors), *Current Developments in The Clinical Applications of HPLC, GC and MS*, Academic Press, London, New York, Toronto, Sydney, S.F., 1980, pp. 19-33.

CHROM. 14,072

MECHANISM OF ZWITTERION-PAIR CHROMATOGRAPHY

II. AMPICILLINE, LYSERGIC ACID, TRYPTOPHAN AND OTHER SOLUTES

JOHN H. KNOX* and JADWIGA JURAND

Department of Chemistry, University of Edinburgh, West Mains Road, Edinburgh EH9 3JJ (Great Britain)

SUMMARY

The dependence upon pH of the column capacity ratio for the zwitterionic solutes ampicilline (zwitterionic from pH 2.5–7.3), lysergic acid (3.3–7.8) and L-tryptophan (2.3–9.3) has been determined on ODS Hypersil® using 1.25 mM acetate and 75 mM phosphate buffers with and without the addition of 1.25 mM 11-aminoundecanoic acid (C11AA) (4.4–10.0). Enhancement of retention is observed within the range of zwitterion overlap with maximum enhancement being observed at pH values corresponding to maximum zwitterion overlap. Outside the region of zwitterion overlap addition of C11AA either has no effect or causes a reduction in retention.

It is concluded that the enhanced retention within the region of zwitterion overlap arises from the formation of quadrupolar ion pairs, whereas the rejection outside this region arises from repulsive interactions of the like-charged forms of the solute and pairing species. The rejection mechanism is confirmed for simple amines and is exploited to provide a useful separation of cimetidine and metiamide. Addition of C11AA enhances the retention of some acids and provides a good separation of the urinary acids, vanilmandelic acid, 5-hydroxy-3-indoleacetic acid and homovanillic acid.

The results provide strong confirmatory evidence for the formation of quadrupolar ion pairs at an appropriate pH in zwitterion-pair chromatography

INTRODUCTION

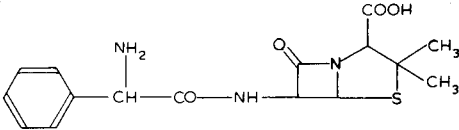
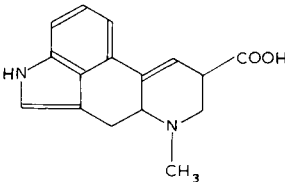
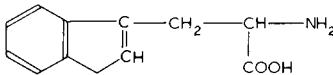
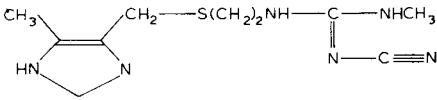

In Part I of this study¹ the thermodynamic basis of zwitterion-pair chromatography was established with nucleotides as model solutes and with 11-aminoundecanoic acid (C11AA) and L-leucyl-L-leucyl-L-leucine (LLL) as ion-pairing agents. The study on the mechanism of this form of ion-pair chromatography followed our earlier report on the separation of nucleotides with C11AA as pairing agent². The concept of zwitterion-pair chromatography had arisen previously in connection with the role of ethylenediaminetetraacetic acid (EDTA) in the separation of tetracyclines³.

The major conclusions derived from this work were: (i) that k' increased with the adsorbed concentration of zwitterion-pairing agent; (ii) that as pH was changed

k' showed maximum value at pH of 4.0–4.2 with C11AA as pairing agent and 3.5 with LLL as pairing agent, these pH values being coincident with maximum overlap of zwitterionic forms; (iii) that as the ionic strength of the buffering salt mixture increased, the zwitterion-pairing effect of pairing agent was gradually suppressed.

While nucleotides are of great biochemical interest, they are not ideal test solutes for examining the thermodynamic basis of zwitterion-pair chromatography because of their complex ionisation patterns, and because of the small range of pH within which both the nucleotides and C11AA or LLL possess significant proportions of molecules in the zwitterionic form. In the present study with C11AA we have therefore sought solutes which will provide a greater range of zwitterion-pair overlap,

TABLE I
SOLUTES AND PAIRING AGENTS

Substance and formula	pK_a	Charge*
Ampicilline	+ 2.5 ± 7.3	—
		
Lysergic acid	+ 3.3 ± 7.8	—
		
Tryptophan	+ 2.3 ± 9.3	—
		
Cimetidine	+ 2 + 6.8 N 12	—
		
Metiamide	As cimetidine	
[as cimetidine]-NH-C-NHCH ₃ 		
11-Aminoundecanoic acid (C11AA) NH ₂ (CH ₂) ₁₀ COOH	+ 4.4 ± 10.0	—

* The symbols +, ±, N and — refer to the charges on the molecules for the appropriate pH ranges: ± indicates a zwitterion, N indicates a neutral species with no charged centres.

and where the pH for maximal overlap would be significantly different from the value provided by the nucleotides. The substances examined comprise three amino acids, ampicilline, lysergic acid and tryptophan, and two bases, cimetidine and metiamide. Their pK_a values, formulae and ionic charges as a function of pH are listed in Table I. Some simple organic acids and bases have also been briefly examined.

The results again show that maximum enhancement of retention on the addition of the zwitterionic-pairing agent C11AA occurs at a pH corresponding to maximum overlap of the zwitterionic forms of the solute and pairing agent. They further support our contention that the enhancement of retention arising from addition of a zwitterionic-pairing agent is due to the formation of quadrupolar ion pairs in the stationary hydrocarbon phase.

EXPERIMENTAL

The chromatographic equipment and column packing procedure have been described previously¹. ODS Hypersil (Shandon Southern Products, Runcorn, Great Britain) was used throughout as column packing material.

Methanol was HPLC grade solvent (Rathburn Chemicals, Walkerburn, Great Britain). C11AA was obtained from Aldrich (Gillingham, Great Britain); ampicilline was BP Pharmaceutical preparation; D-lysergic acid and L-tryptophan were obtained from Sigma (Poole, Great Britain); cimetidine, metiamide and cimetidine sulphoxide were obtained from Smith, Kline & French Labs. (Welwyn Garden City, Great Britain); 5-hydroxy-3-indoleacetic acid (5HIAA) was obtained from Koch-Light Labs. (Colnbrook, Great Britain); homovanillic acid (HVA) and vanilmandelic acid (VMA) were obtained from Hoffmann-La Roche (Basle, Switzerland).

RESULTS AND DISCUSSION

Zwitterionic solutes

The dependence of k' upon pH for the three solutes, ampicilline, lysergic acid and tryptophan is shown in Figs. 1 (ampicilline) and 2 (lysergic acid and tryptophan). A single concentration of C11AA, *viz.* 1.25 mM, and the same basic eluent, *viz.* water-methanol (88:12) has been used throughout. Two different buffers have been used to adjust pH, a weak acetate buffer of ionic strength 1.25 mM, and a stronger phosphate buffer of ionic strength 75 mM. In each figure the range of zwitterion overlap for the solute and pairing agent is shown either by an ionisation diagram or by a horizontal bracket; the ends of the bracket correspond to the pK_a values given in Table I; the central arrow within the bracket corresponds to the pH for maximum zwitterion overlap.

In Figs. 1 and 2 it is noted that with the weak buffer the k' values for ampicilline and lysergic acid in the presence of C11AA show maxima at or close to the position of maximum overlap. These maxima are not attributable to any similar change in the amount of C11AA adsorbed (C_{ads}) as is clearly seen by comparison of the curves for k' with those for C_{ads} taken from ref. 1.

Comparing k' values with and without added C11AA it is seen that within the main part of the region of zwitterion-overlap retention is enhanced by addition of C11AA, but outside this region retention is reduced. Thus C11AA, when not acting

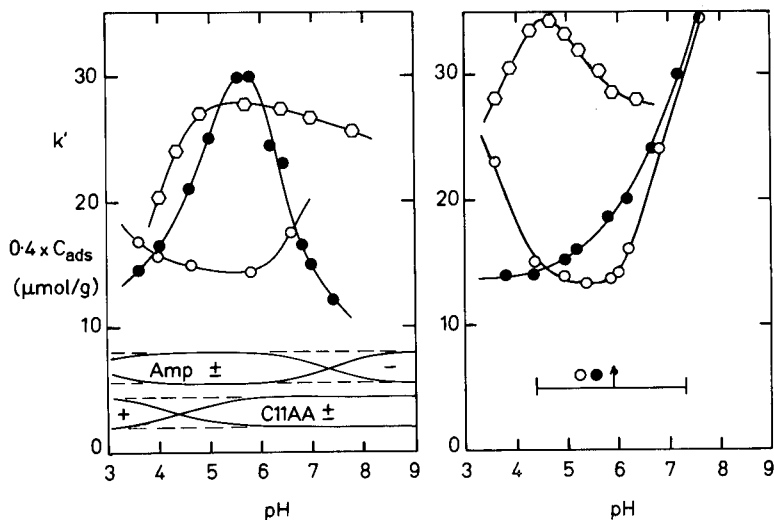


Fig. 1. Dependence of capacity ratio, k' , of ampicilline and of concentration of adsorbed C11AA, C_{ads} , upon pH. Column, 100×5 mm I.D. Packing, $5 \mu\text{m}$ ODS Hypersil. Eluent, water-methanol (88:12) containing 1.25 mM acetate buffer (left hand side) or 75 mM phosphate buffer (right hand side). ●, k' for ampicilline with 1.25 mM C11AA added; ○, k' for ampicilline with C11AA absent; ○, C_{ads} for C11AA. The horizontal bar, indicates the range of zwitterion-pair overlap.

as a zwitterion-pair agent, has the effect of rejecting a charged or dipolar species.

When the stronger 75 mM phosphate buffer is used, retention of ampicilline and lysergic acid in the absence of C11AA is strongly dependent upon pH. Minimum retention occurs at a pH which corresponds closely to the isoelectric point of the solute (4.9 for ampicilline, 5.5 for lysergic acid). The strongly increased retention as the pH moves away from the isoelectric point presumably arises from ion pairing of

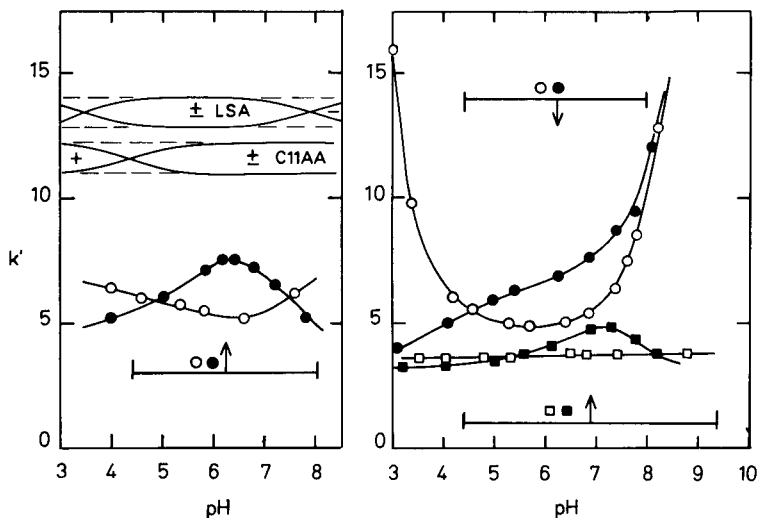


Fig. 2. As for Fig. 1 but for lysergic acid (●, ○) and L-tryptophan (75 mM buffer only) (■, □) as solutes. Filled symbols refer to eluent containing 1.25 mM C11AA; open symbols refer to eluent without C11AA.

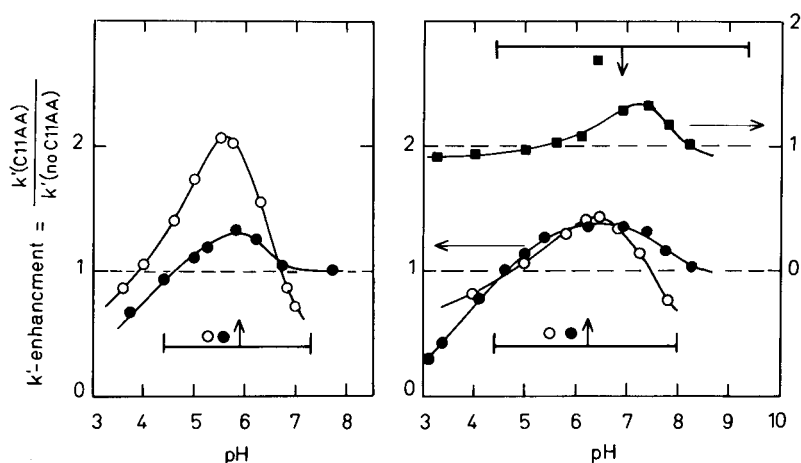


Fig. 3. Dependence of enhancement of retention upon pH when C11AA added to eluent: left, ampicilline; right, L-tryptophan (\square) and lysergic acid (\circ): open symbols refer to 1.25 mM acetate buffer, filled symbols refer to 75 mM phosphate buffer.

the positively or negatively charged forms of the solutes with buffer ions. It should in passing be noted that at pH above 6 the peaks for ampicilline in the absence of C11AA became very wide; and ampicilline cannot therefore be effectively chromatographed with the buffer alone in this pH region.

On addition of C11AA retention is enhanced within the region of zwitterion overlap, but at lower pH (when C11AA is positively charged) rejection occurs. At higher pH (solutes negatively charged) the k' values tend toward those obtained when C11AA is absent.

For tryptophan retention with 75 mM phosphate buffer in the absence of C11AA is by contrast independent of pH. On addition of C11AA, k' shows a maximum at pH 7.2, very close to the pH for maximum zwitterion overlap of 6.9.

In Fig. 3 the enhancement of retention, that is the ratio of k' in the presence of C11AA to k' without C11AA, is plotted against pH for the weak and strong buffers.

TABLE II

pH VALUES FOR MAXIMUM ENHANCEMENT OF RETENTION USING C11AA

Solute	pH for maximum enhancement of retention		pH for maximum zwitterion overlap
	1.25 mM phosphate	75 mM phosphate	
Adenosine monophosphate	4.0	4.4	4.1
Ampicilline	5.5	5.8	5.9
Lysergic acid	6.4	6.6	6.3
Tryptophan	—	7.2	6.9

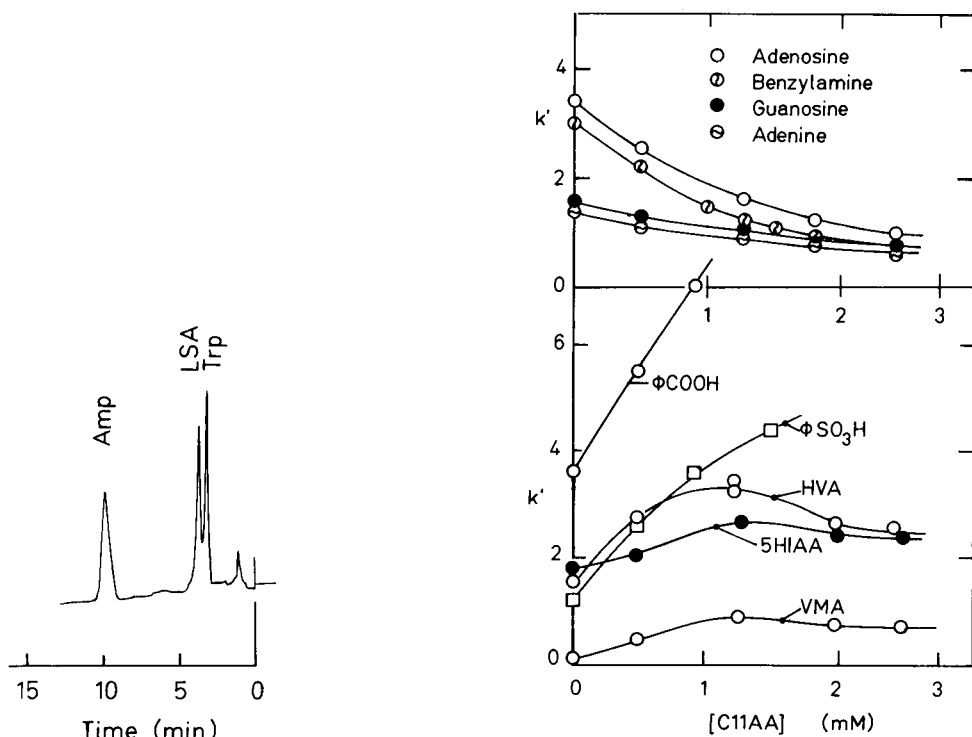


Fig. 4. Representative separation of L-tryptophan, lysergic acid and ampicilline. Conditions as for Fig. 1 with 75 mM phosphate buffer, pH 3. Detection, UV 254 nm.

Fig. 5. Dependence of k' for bases (upper) and acids (lower) upon concentration of C11AA in eluent. Conditions as Fig. 1 with 75 mM phosphate buffer, pH 5.8.

For ampicilline the enhancement is much greater with the weak buffer and rejection (giving an enhancement ratio below unity) occurs on both wings. On the other hand, with the strong buffer while a peak in k' still occurs, it is much lower and the maximum is relatively flat. Whereas rejection occurs at low pH, C11AA tends to have zero effect at high pH. These results are similar to those previously found with AMP¹. That is the maxima in k' were much more pronounced with the weaker buffer solutions. For lysergic acid the maximum in the dependence of enhancement upon pH are comparable for the two buffers although the maximum is sharper for the weaker buffer. Again rejection is noted on both wings with the weaker buffer but only at low pH with the stronger buffer. With tryptophan the results with the strong buffer are similar to those with the other two zwitterionic solutes.

The pH for maximum enhancement of retention are compared in Table II with the pH for maximum zwitterion overlap. The table includes the data for adenosine monophosphate (AMP) from ref. 1. The pH for maximum enhancement of retention is about 0.2–0.4 units higher when using 75 mM buffers than when using weak buffers, but in all cases these pH values are very close to those for maximal zwitterion overlap. The values now cover approximately three pH units.

Fig. 4 shows a representative chromatogram of the three zwitterionic solutes

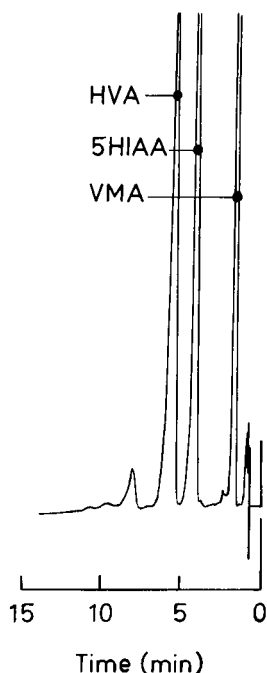


Fig. 6. Representative separation of urinary acids, VMA, 5HIAA and HVA. Conditions as Fig. 5 with 1.25 mM C11AA. Detection, UV 254 nm.

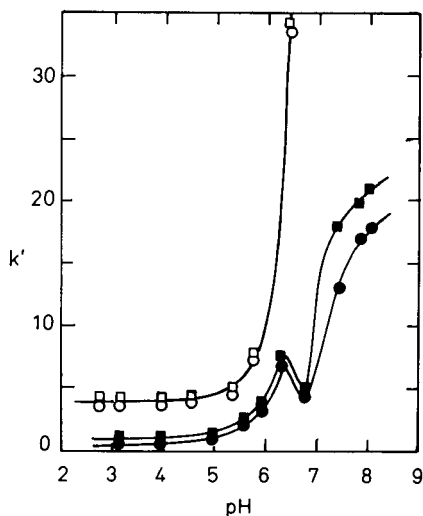


Fig. 7. Dependence of k' upon pH for metiamide (O) and cimetidine (□). Column and packing as for Fig. 1. Eluent: filled symbols, water-methanol (88:12) containing 75 mM phosphate buffer and 1.25 mM C11AA; open symbols, same but with no C11AA present.

and indicates the good plate efficiency which can be obtained. The new data obtained with ampicilline, lysergic acid and tryptophan provide further strong support for the view that a zwitterionic-pairing agent enhances the retention of zwitterionic solutes by the formation of quadrupolar ion pairs in the stationary phase.

Simple acids and bases

The phenomenon of rejection of ionized solutes by C11AA outside the range of zwitterion overlap appears to arise from like charge repulsion when both the pairing agent and the solute can exist with the same charge. We have examined this effect briefly with simple acids and bases at pH 5.8 using 75 mM phosphate buffer and the standard eluent of water-methanol (88:12). Fig. 5 shows that while benzylamine and some nucleic acid bases and nucleosides are rejected by addition of C11AA, retention of acids is either enhanced (benzoic and benzenesulphonic) or behaves indecisively (5HIAA, VMA and HVA). These results are broadly consistent with those found with the zwitterionic solutes in 75 mM buffer in that at low pH when the solutes and C11AA tended to be positively charged the solute was rejected while at high pH when the solutes and C11AA showed negative charge the effect of C11AA appeared to be minimal.

The marked difference between the behaviours of acids and bases in presence

of C11AA as pairing agent can only be understood as a result of higher polarity of NH_2^+ group as compared to COO^- group. The isoelectric point of C11AA lies around pH 7.4 and 7.6. Therefore C11AA can with respect to acidic compounds act as weak cationic pairing agent. This was proved, when k' versus pH dependence curve was studied for benzoic acid in eluents with dilute acetate buffer. The retention of benzoic acid was enhanced above pH 4.2 (the $\text{p}K_a$ of benzoic acid) and reduced below pH 3.6.

Example of good separation of the key urinary acids: 5H1AA, HVA and VMA with C11AA is shown in Fig. 6.

Cimetidine and metiamide

The phenomenon of rejection of amines by addition of C11AA has proved useful in the liquid chromatography of the antihistamine drugs cimetidine and metiamide which cannot be separated using phosphate buffer alone. When 1.25 mM C11AA is added to the eluent the retention of the amines at all pH is much reduced as shown in Fig. 7. Without added C11AA retention remains unchanged between pH 3 and 5.5 then increases dramatically starting from pH 5.8 as the pH approaches the $\text{p}K_a$ value of 6.8 corresponding to the formation of neutral form of the drug. The extent of the increase is suppressed in the presence of C11AA and a small maximum

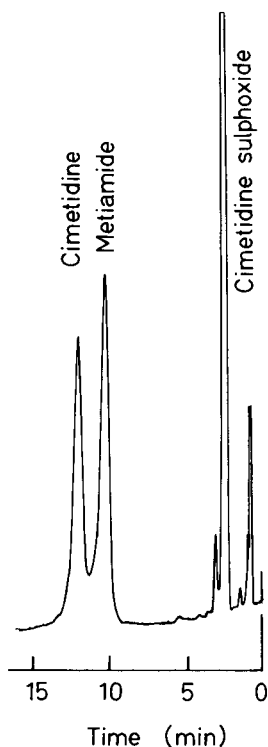


Fig. 8. Representative separation of cimetidine sulphoxide, metiamide and cimetidine. Eluent as for Fig. 7. pH, 7.4 containing 1.25 mM C11AA. Detection, UV 254 nm.

occurs at pH 6.2, which is not well understood. This enables chromatography to be carried out at a higher pH allowing separation of the two drugs to be achieved with reasonable k' values between pH 7.4 and 8. In clinical practice it is important to be able to assay both cimetidine and its main metabolite the sulphoxide. Fig. 8 shows that this separation, previously achieved by normal-phase chromatography^{4,5}, can readily be achieved using C11AA and 75 mM phosphate buffer.

CONCLUSIONS

The results obtained on the pH dependence of the retention of the zwitterionic solutes ampicilline, lysergic acid and tryptophan on a reversed-phase packing material in the presence of C11AA are described. Addition of millimolar concentration of C11AA cause a marked enhancement of retention in the pH range where both the solute and the pairing agent exist predominantly as zwitterions, and the pH for maximum enhancement of retention coincides within a fraction of a pH unit with the pH for maximum zwitterion overlap. The maxima are particularly sharp when weak buffers are used to adjust the pH. These results add further strong support to our contention made in previous papers^{1,2} that enhanced retention caused by a zwitterionic-pairing agent arises from the formation of quadrupolar ion pairs.

ACKNOWLEDGEMENT

The authors wish to record their thanks to the Science Research Council of Great Britain for their generous support of this work.

REFERENCES

- 1 J. H. Knox and J. Jurand, *J. Chromatogr.*, 218 (1981) 341.
- 2 J. H. Knox and J. Jurand, *J. Chromatogr.*, 203 (1981) 85.
- 3 J. H. Knox and J. Jurand, *J. Chromatogr.*, 186 (1979) 763.
- 4 W. C. Randolph, V. L. Osborne, S. S. Walkenstein and A. P. Intoccia, *J. Pharm. Sci.*, 66 (1977) 1148.
- 5 R. M. Lee and P. M. Osborne, *J. Chromatogr.*, 146 (1978) 354.

CHROM. 14,001

HIGH-PERFORMANCE DISPLACEMENT CHROMATOGRAPHY

CSABA HORVÁTH*, AVI NAHUM and JOHN H. FRENZ

Department of Chemical Engineering, Yale University, New Haven, CT 06520 (U.S.A.)

SUMMARY

The potential of the displacement mode of liquid chromatography for preparative-scale separations has been investigated by using microparticulate packed columns and instrumentation typically employed in analytical high-performance liquid chromatography (HPLC). Although the physico-chemical basis of the technique has long been established, its development was handicapped by lack of efficient chromatographic systems and suitable tools to monitor column effluent and gather data required for analysis and design of the displacement chromatographic process and for selection of suitable displacers. The availability of novel solid stationary phases with adequate properties to facilitate rapid sorption kinetics, the possibility of monitoring the effluent of the "fractionator" liquid chromatograph by an auxiliary "analyzer" unit as well as the relatively easy evaluation of appropriate adsorption isotherms by using the HPLC equipment, however, provide a basis to advance the displacement mode of liquid chromatography for preparative separations with analytical columns. After a brief review of the principles of the technique the dual chromatographic system used in the experiments for fractionation and analysis is described. Expressions for the efficiency of separation are given and factors affecting the development of the "displacement train" containing the separated feed components are enumerated. The interplay between the nature and concentration of displacer, the column length, amount of feed, flow-rate as well as the nature and concentration of the components of the mixture to be fractionated is discussed qualitatively. Fractionation of mixtures containing phenolic compounds or adenosine and inosine on columns packed with octadecyl-silica bonded phases (reversed-phase chromatography) is used to exemplify the effect of the operating conditions on the efficacy of the separation. The results are related to the adsorption isotherms of the substances that were measured by frontal analysis and found to follow the Langmuir model. The results suggest that upon accumulation of a sufficient amount of data on adsorptivities in chromatographic systems of interest high-performance displacement chromatography offers a promising approach to the use of ubiquitous HPLC equipment for preparative-scale separations with analytical columns.

INTRODUCTION

Displacement of one sample component by another during the development of a chromatogram in liquid column chromatography was a characteristic feature of the technique prior to the wide acceptance of partition chromatography and the use of linear elution development. The first classification of the different modes of chromatography as frontal, displacement and elution development was made by Tiselius¹. He, as well as Claesson², investigated displacement chromatography with regard to the physico-chemical basis of the separation process with emphasis on potential analytical applications. Therefore, the technique has most commonly been referred to as displacement analysis ("Verdrängungsanalyse" in German) in the literature. The success of Martin and co-workers³⁻⁵ with partition chromatography in the linear elution mode, however, overshadowed further development of displacement chromatography in analytical separations although some of its features are —mainly unwittingly— used in preparative-scale chromatography.

Recent developments in high-performance liquid chromatography (HPLC) with respect to column engineering and instrumentation have prompted us to explore the potential of liquid chromatography in the displacement mode for preparative-scale separations with columns and precision instruments that are presently used in analytical work. Generally, separation of relatively large amounts of material is handicapped in linear elution chromatography by poor utilization of the stationary and mobile phases because of the low permissible elute concentrations. Furthermore the equipment and the column are only partially occupied by the bands of sample components that travel with different velocities. The inevitable dilution process associated with elution chromatography also hampers product recovery from the effluent.

In contradistinction the feed components in displacement chromatography are separated into adjacent square-wave zones having rather high concentrations and traveling at the same velocity. This difference between the elution and displacement modes of chromatography and its implications for preparative scale separation were already fully appreciated by Tiselius and Hagdahl⁶ although the technique has enjoyed popularity neither in analytical nor in preparative chromatography. With the highly efficient columns and precision instrumentation presently available, however, the above features of displacement chromatography offer an opportunity to carry out preparative-scale separations with analytical columns in HPLC.

THEORETICAL

Principles of displacement chromatography

In this mode of chromatography the column packed with a solid adsorbent is first equilibrated with a carrier solvent (mobile phase) that has a low affinity to the stationary phase. Then the feed solution containing the mixture dissolved in the carrier is introduced so that its components are adsorbed in the inlet section of the column.

Subsequently the solution of a displacer substance that has stronger affinity to the stationary phase than any of the feed components is pumped into the column. Provided the column is sufficiently long, the components of the feed arrange them-

selves upon the action of the displacer front moving down the column into a "displacement train" of adjoining square wave concentration pulses of the pure substances, all moving with the same velocity. A displacement diagram is illustrated in Fig. 1. As will be shown later the solute concentrations in the zones are much higher than in linear elution chromatography under comparable conditions⁷.

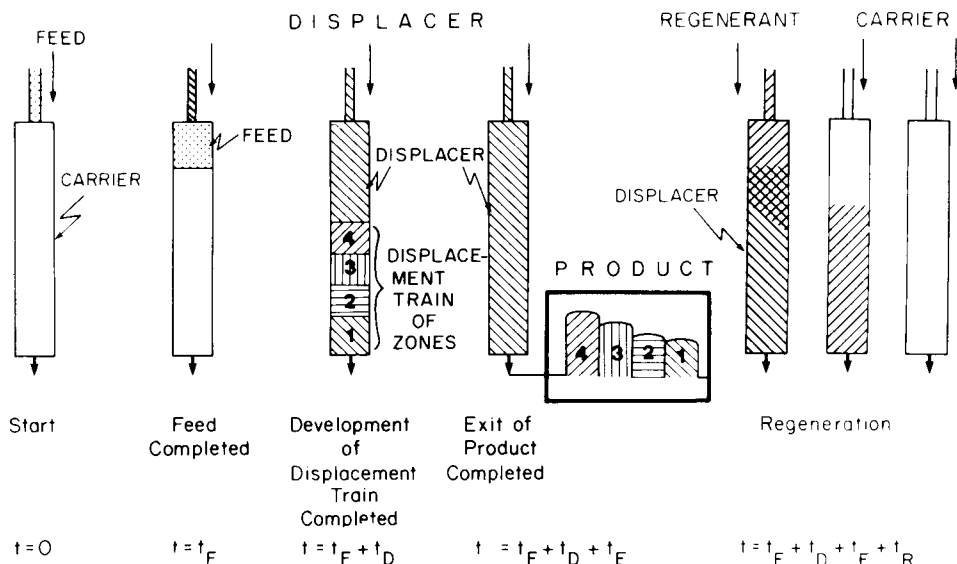


Fig. 1. Stages of operation in displacement chromatography. Initially the column is equilibrated with the carrier. The mixture to be separated is fed into the column and thereafter the displacer solution is introduced. As the displacer front moves down the column the displacer train containing adjacent zones of the separated feed components is developed. After the product zones egress the column it is regenerated by removing the displacer and re-equilibrating with the carrier. The time requirement for the individual steps are as follows: t_F , feed time; t_D , development time of displacement train; t_E , exit time of product; t_R = time of column regeneration.

Fig. 1 shows the sequence of operational steps in displacement chromatography. The process is aimed at obtaining a fully developed displacement train so that the feed components are completely separated and emerge at relatively high concentrations in the effluent at the column outlet where they can be collected as individual fractions. Separation by displacement development is monitored by analyzing the column effluent by a suitable technique. The employment of an "analyzer" HPLC unit as an auxiliary to the "fractionator" liquid chromatograph is probably the most convenient. However, thin-layer chromatography or another analytical device such as one or more selective detectors can be used.

During the introduction of the feed mixture at the top of the column the components saturate the stationary phase and frontal chromatography occurs. The displacer must have greater affinity to the stationary phase than any component of the mixture and the concentration of displacer solution is critical in determining the time and column length required for the development of the displacement train. The velocity of the displacer front moving down the column depends on the adsorptivity

and concentration of the displacer and determines the velocity of the displacement train. The sequence of the individual components from the column outlet toward the displacer front corresponds to increasing affinity of the species for the stationary phase. Thus, in Fig. 1 components 1 and 4 are the most weakly and most strongly adsorbed components, respectively.

After the last component of the feed mixture leaves the column, the displacer has to be removed and the column has to be reequilibrated with the carrier. The need for column regeneration, an operational step that does not contribute directly to separation, is an undesirable feature of the technique.

Upon full development of the displacement train the separation is completed, therefore, further residence in the column does not improve separation. The properties of the fully developed displacement train have a simple relation to the appropriate isotherms of the feed components and the displacer as well as to the concentration of the latter and will be discussed below. On the other hand, a sufficiently general description of the transient part of the process associated with the development of the displacement train in the column has been found mathematically intractable⁸. Consequently we shall restrict ourselves to a qualitative discussion of the effect of various physico-chemical and operational parameters on the transient demixing process that plays a major role in determining the speed and efficiency of separation in displacement chromatography.

Properties of fully developed displacement train

If the column is sufficiently long, successive displacement of the feed components by the displacer and by each other as they move down the column results in a fully developed displacement train. It consists of adjacent square-wave concentration pulses of the individual feed components in the order of increasing affinity to the stationary phase as depicted in Fig. 2. Unlike in elution chromatography where peaks travel at different velocities, at the final stage of displacement development all components move with the same velocity as determined by the adsorption isotherm and concentration of the displacer that "drives" the displacement train. This condition is conveniently termed *isotachic* from $\tau\acute{\alpha}\chi\omicron\sigma\varsigma$, the Greek word for speed.

The velocity of a concentration step, u_i , of species i from mobile phase concentration to C_i , in a chromatographic column is given by

$$u_i = \frac{u_0}{1 + [\Phi q_i/C_i]} \quad (1)$$

where u_0 is the carrier velocity, Φ is the phase ratio in the column and q_i is the amount of solute i adsorbed by unit volume of stationary phase in equilibrium with a mobile phase having solute concentration C_i . As seen in Fig. 2, q_i/C_i is the chord to the isotherm at concentration C_i and determines the species velocities according to eqn. 1. Therefore equality of the velocities of the zones in the fully developed displacement train, which can be considered a series of truncated concentration steps rising from zero to C_i , means that the chords of the isotherms of the displacer and the feed components present in the displacement train fall on the same straight line termed the operating or, occasionally, speed line⁹. This is shown in Fig. 2 and can be expressed by the following relationships:

$$u_D = u_1 = u_2 = \dots = u_i \dots = u_n \quad (2a)$$

$$\frac{q_D}{C_D} = \frac{q_1}{C_1} = \frac{q_2}{C_2} = \dots = \frac{q_i}{C_i} = \dots = \frac{q_n}{C_n} \quad (2b)$$

where the subscript D refers to the displacer. From Fig. 2 and eqn. 2b it follows that the concentrations of fully developed zones of the components are determined by the intersections of the individual adsorption isotherms with the operating line. Thus the solute concentration in each zone moving in the fully developed displacement train is

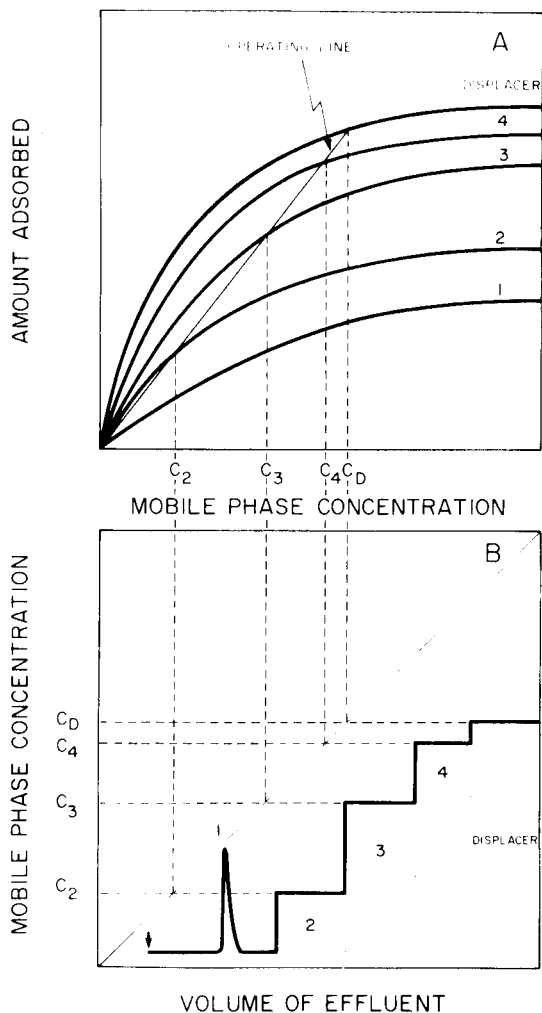


Fig. 2. Graphical representation of the isotherms of the feed components and the operating line (A) as well as the corresponding fully developed displacement train (B). Concentrations of the component zones, determined by the intersections of the operating line and the adsorption isotherms of the components are projected from A to B with the aid of a 45° line. The isotherm of the first component lies below the operating line at all concentrations, hence it elutes from the column.

determined both by the speed line and the isotherm, therefore the height of the zone is characteristic for that solute. On the other hand, conservation of mass requires that the length of each zone be proportional to the amount of solute because concentration is expected to be uniform throughout the zone, with the exception of the boundaries. These features of displacement chromatography were considered very attractive for analytical separation as measurements of zone height and length offer simple means for identification and quantitative determination of the individual components, respectively. Fig. 2 also illustrates that zone heights must increase with retention as the operating line intersects the isotherm at higher and higher concentrations. It also follows that when the concentration in the feed is smaller than this characteristic concentration for a component it will become more concentrated in the course of displacement chromatography.

The requirement for complete displacement development to occur is that the isotherms be convex and the operating line drawn as the chord of the displacer isotherm intersect the isotherms of all feed components. If the affinity of a substance to the stationary phase is so low that its isotherm lies below the operating line, that component will elute as a "peak" as also illustrated in Fig. 2. Adsorbents used as stationary phases in HPLC frequently yield isotherms that can be approximated by the Langmuir model for most substances. Therefore, our description is restricted to chromatographic systems in which Langmuir isotherms prevail and, as a further constraint, the isotherms do not intersect each other.

Factors affecting displacement development

The goal in displacement chromatography is to develop adjacent concentration zones of the components with sharp boundaries in the shortest possible time and with the highest possible load for a particular chromatographic system. High efficiency columns packed with microparticulate stationary phases having mean particle diameter in the range from 3 to 10 μm and appropriate accessories are available today to construct a liquid chromatograph for displacement development and minimize the deleterious effects on the separation process of axial dispersion¹⁰ that plagued early efforts in this field¹¹. Furthermore, adsorbents employed in HPLC as stationary phases exhibit a relatively homogeneous surface. As a result, not only are the adsorption isotherms expected to be nearly Langmuirian but also the sorption kinetics are believed to be sufficiently rapid to obtain favorable dynamic behavior.

It has already been mentioned that successful displacement chromatography calls for conditions under which the isotherms of the components are concave downwards such as those of the Langmuir type. The requirement arises from the need for self-sharpening boundaries to develop the square wave pattern and accomplish the separation of the mixture with a minimum of cross-contamination of the individual components. With such isotherms, if they do not intersect each other, that is, they have similar shape, the corresponding boundaries are self-sharpening. As such conditions occur in a given chromatographic system with solutes having similar chemical structure, displacement chromatography appears to be most effective for the separation of closely related compounds such as homologues.

On the other hand, the time or column length required for full development of the displacement train decreases with increasing difference in the affinities of two consecutive components to the stationary phase, *i.e.*, with increasing potency of the

stronger binding component to displace the weaker adsorbing component from the surface. Therefore the more the competitive isotherm of the latter is suppressed in the presence of the former, the faster can a sharp boundary develop between the zones. Thus, the efficacy of boundary sharpening in displacement chromatography increases with the difference in the adsorptivity of two components. Of course, the effect is enhanced if the stronger retarded species is present at higher concentrations.

Langmuir isotherms are described by the equation

$$q = \frac{b_i K_i C}{1 + K_i C} \quad (3)$$

where q is the amount of surface bound solute per unit amount of sorbent, b_i is the saturation concentration at the surface and K_i is the binding constant of the solute to the sorbent.

It can be shown easily¹² that when the competitive isotherms of the feed components remain Langmuirian in the presence of the other components the criterion for displacement chromatography is expressed by the inequality

$$b_1 K_1 < b_2 K_2 < \dots < b_i K_i < \dots < b_D K_D \quad (4)$$

where subscript D refers to the displacer and the numbers increase with the magnitude of retention. In view of the above discussion the development of the displacement train is facilitated by large absolute and relative values of $b_i K_i$. As can be inferred from the definition of the operating line in Fig. 2 a sufficiently high displacer concentration is also required to accomplish rapid displacement development.

Efficacy of separation

In preparative work the amount of product recovered per unit time and the cost involved ultimately determine the efficiency of the chromatographic separation. In view of the various steps involved in displacement development as shown in Fig. 1, the definition of an overall efficiency measure would include a wide range of system parameters and operational variables. The goal of this section is more modest, we wish to measure the degree of separation and sample purity on the basis of the displacement diagram, in a way similar to that given by Partridge and Westall¹³.

Fig. 3 illustrates a typical displacement diagram as obtained by measuring separately the concentrations of the individual components in the product stream. It is seen that the zones overlap somewhat and the fraction of the components present in the mixed boundary region cannot be recovered in pure form. In other words, the purity of the product decreases with the fraction of that component lost to the overlapping boundary region, and the efficiency of separation increases with the sharpness of the boundaries that determine the recovery of product in pure form.

As shown in Fig. 3, the front and rear boundaries of the i th component are contaminated by the $(i - 1)$ th and $(i + 1)$ th components, respectively. The lengths of the plateau region and the height of zone i are given by $l_{i,p}$ and h_i , respectively. The lengths of the corresponding mixed front and rear boundaries are $l_{i,f}$ and $l_{i,r}$, thus, the total zone length of component i , $l_{i,tot}$, is given by

$$l_{i,tot} = l_{i,f} + l_{i,p} + l_{i,r} \quad (5)$$

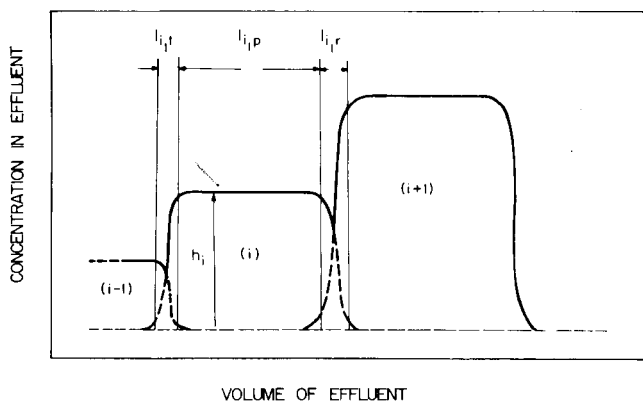


Fig. 3. Diagrammatical representation of zone overlap in the displacement train.

The fraction of the i th component that can be recovered in pure form in the product stream, P_i , is given by

$$P_i = \frac{m_{i,\text{out}} - m_{i,f} - m_{i,r}}{m_{i,\text{out}}} \quad (6)$$

where $m_{i,\text{out}}$ is the total amount of the i th component in the effluent, and $m_{i,f}$ and $m_{i,r}$ are the amounts of the i th component present in the overlapping regions in the front and rear boundaries, respectively. In Fig. 3 quantities $m_{i,f}$, $m_{i,r}$ and $(m_{i,\text{out}} - m_{i,f} - m_{i,r})$ are represented by areas $h_i l_{i,t}$, $h_i l_{i,r}$ and $h_i l_{i,p}$, respectively. It is also indicated that in the fully displacement train the extent of overlap for adjacent zones is expected to be nearly equal.

According to eqn. 6 when $m_{i,\text{tot}} = m_{i,f} + m_{i,r}$ the purity is zero because the solute zone consists solely of the two boundaries, i.e., $l_{i,p} = 0$. In other words, if the amount of component i in the feed is sufficiently small it resides solely in the boundary regions and the zone takes the form of a peak as depicted in Fig. 4A. Upon increasing the amount of i in the feed $m_{i,\text{tot}}$ becomes greater than the sum of $m_{i,f} + m_{i,r}$ and a plateau region of constant concentration is formed *vide* Figs. 4B and 4C. The length of the plateau region as well as the purity of the product increase with the amount of component i as illustrated in Figs. 4B and 4C. As a result, upon increasing the amount of that component in the feed, its purity increases as shown by the values of the purity parameter in Figs. 4A to 4B as long as the displacement train is fully developed and the lengths of mixed boundaries remain invariant.

For the case of displacement chromatography of homologous substances when difficulties in product analysis make it impossible to construct a displacement diagram another graphical construction can be used to illustrate the separation effectiveness. Product fractions are chromatographed by using the analyzer, and the peak heights, h_n and h_{n+1} , of the n th and $(n + 1)$ th members of the homologous series are

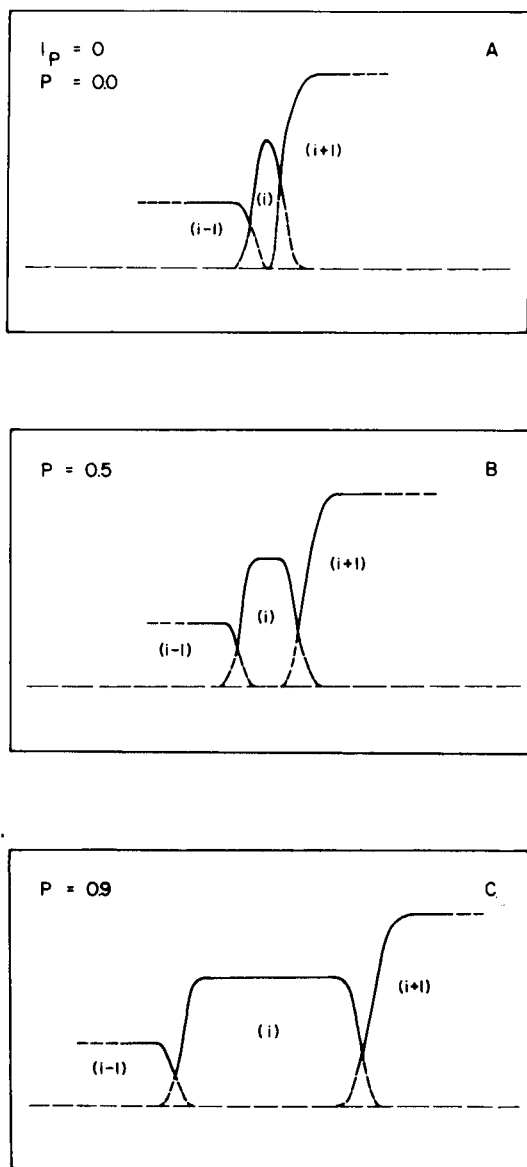


Fig. 4. Schematic illustration of the effect of increasing the amount of component i in the feed on the shape of its zone and the purity.

measured. The sharpness of the boundary between the two zones is measured by the volume dependence of the G function defined by

$$G = \frac{h_n - h_{n+1}}{\alpha h_n + \beta h_{n+1}} \quad (7)$$

with

$$\alpha = 1, \beta = 0 \text{ for } h_n > h_{n+1} \quad (8)$$

and

$$\alpha = 0, \beta = 1 \text{ for } h_n < h_{n+1} \quad (9)$$

Evidently the value of G is $+1$ or -1 when the fraction contains only the pure species n or $n + 1$, respectively, and $G = 0$ when the concentrations of both components are the same in that fraction. As discussed later the G function was used to study the effect of operational conditions on displacement separation of polyethylene glycol oligomers.

EXPERIMENTAL

Materials

Phenol, 2- and 4-hydroxyphenylacetic acids, and 3,4-dihydroxyphenylacetic acid were purchased from Aldrich (Milwaukee, WI, U.S.A.), adenosine, inosine and L-phenylalanine from Sigma (St. Louis, MO, U.S.A.), resorcinol from Baker (Phillipsburg, NJ, U.S.A.), catechol from Matheson, Coleman & Bell (Norwood, OH, U.S.A.), *n*-butanol and methanol were HPLC grade from Fisher Scientific (Fair Lawn, NJ, U.S.A.), *n*-propanol was obtained from Mallinckrodt Chemical Works (St. Louis, MO, U.S.A.) and acetonitrile and isopropanol were "distilled in glass" from Burdick & Jackson Labs. (Muskegon, MI, U.S.A.). Distilled water was prepared with a Barnstead distilling unit.

Commercial 10- μ m Partisil ODS-2 (Whatman, Clifton, NJ, U.S.A.) and 5- μ m Zorbax ODS (DuPont, Wilmington, DE, U.S.A.), columns as well as home-made columns packed with 10- μ m LiChrosorb RP-18 (Merck, Cincinnati, OH, U.S.A.) and 5- μ m Spherisorb (Phase Sep, Hauppauge, NY, U.S.A.) treated with octadecyldimethylchlorosilane (Petrarch Systems, Levittown, PA, U.S.A.) were used for fractionation by displacement chromatography. Columns were 250 \times 4.6 mm but a 500 \times 4.6 mm column packed with octadecyl-Spherisorb was also used. In analytical HPLC a 10- μ m Partisil C₈ column (250 \times 4.6 mm) from Whatman and a home-made 5- μ m octadecyl-Spherisorb column (150 \times 4.6 mm) were used.

Instruments

Fractionator liquid chromatograph. A modified Model 601 liquid chromatograph (Perkin-Elmer, Norwalk, CT, U.S.A.) was used for separations by displacement chromatography. The two syringe pumps of the instrument were individually connected to the feed loading system as shown schematically in Fig. 5. Pump A, which delivered the carrier solvent and the regenerant to the column before and after a chromatographic run respectively, was connected to a Rheodyne (Berkeley, CA, U.S.A.) Model 7030 switching valve. Pump B, which delivered the displacer, was connected to the Rheodyne Model 7010 feed introduction valve, which in turn was

connected to the switching valve. Drain valves (Scientific Systems, State College, PA, U.S.A.) were connected to each line upstream of the feed loading system. The feed valve was fitted with a loop of the appropriate size made from a length of 1 mm I.D. \times 1/16 in. O.D. 316 stainless-steel tubing. The volume of the feed loop varied in the range from 0.5 to 6 ml. Connections to the switching valve were arranged in such a way that in one position pump A was connected to the column and flow from pump B was interrupted, and *vice versa* for the other position. The column effluent was monitored by a Perkin-Elmer Model LC-55 variable-wavelength detector and was collected with a Model 7000 fraction collector (LKB, Rockville, MD, U.S.A.). The detector signal was recorded on a Perkin-Elmer Model 123 strip-chart recorder.

Analyzer. The analytical chromatograph was assembled from a Model 725 automatic injector (Micromeritics, Norcross, GA, U.S.A.), a Model 1220 liquid chromatograph and a Model LC-65T variable wavelength detector, both from Perkin-Elmer, and a Model Elektronik 194 (Honeywell, Ft. Washington, PA, U.S.A.) strip chart recorder.

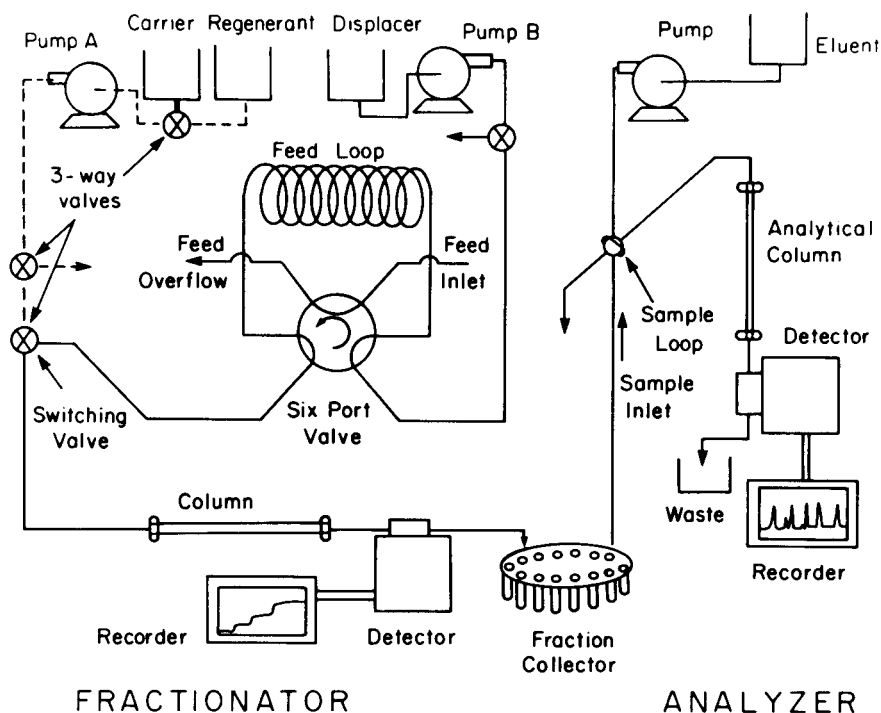


Fig. 5. Diagram of the dual liquid chromatographic system. Preparative-scale displacement chromatography is performed by the "fractionator" and the concentration of the components in the product stream present in the fraction collector is determined by the "analyzer" HPLC unit.

Procedures

Measurement of adsorption isotherms. Frontal analysis by characteristic

point¹⁴ was used to estimate the adsorption of various solutes from water at 25°C. The injector valve of the liquid chromatograph was fitted with a 6-ml sampling loop prepared from a 764 cm long, No. 316 stainless-steel tubing having 1.0 mm I.D. and 1/16 in. O.D. First the sampling valve was connected directly to the detector and about 5 ml of sample solutions at five different concentrations were successively pumped through the flow cell in order to calibrate the detector at one or two appropriate wavelengths. Thereafter a 6 cm long, No. 316 stainless-steel column (4.6 mm I.D., 1/4 in. O.D.) packed with the stationary phase of interest was installed and washed with isopropanol, methanol and exhaustively with water. At a water flow-rate of 0.5 ml/min the introduction of the sample solution began and was marked on the recorder chart paper. After the detector response reached a plateau on the chromatogram, sample introduction was terminated by returning the sampling valve to its original position and this point was marked on the chromatogram. Subsequently the pumping of water continued until the recorder pen returned to baseline. The diffuse rear portion of the chromatogram obtained with the "square-wave" concentration input was used to evaluate the isotherm. For known system dead volume, flow-rate and chart speed, retention times particular to certain solute concentrations in the effluent, $t_R(C)$, were calculated from the recorder trace and the calibration data. The isotherm was evaluated from $t_R(C)$ by using the following equation

$$t_R(C) = t_0 + (t_{sv} - t_0) \frac{dq}{dC} \quad (10)$$

where t_0 is the hold-up time of an unadsorbed solute in the column, t_{sv} is the residence time corresponding to the superficial (empty tube) velocity and q the amount of solute adsorbed by unit volume of the stationary phase. Thus, dq/dC is the slope of the isotherm at the characteristic mobile phase concentration. Evaluating dq/dC over the experimental range of $t_R(C)$ and integrating, we obtain q as a function of the concentration, *i.e.*, the adsorption isotherm of the solute. Due to the inaccuracy associated with the measurement of $t_R(C)$ at $C = 0$, that is, when the recorder pen returns to baseline, the boundary condition required for integration is given by frontal analysis¹⁴ of the self-sharpening front boundary of the chromatogram. From this method of analysis, the amount of solute adsorbed onto the stationary phase at the concentration corresponding to the plateau of the chromatogram, $q_{\max.}$, is given by

$$q_{\max.} = (t_F - t_0) FC_{\max.} \quad (11)$$

where t_F is the breakthrough time of the sharp front, and F is the flow-rate.

Evaluation of the parameters

Assuming that the dependence of the adsorbed solute on the concentration in solution follows the Langmuirian model linear regression analysis was performed by using eqn. 3 in the rearranged form as follows

$$\frac{1}{q} = \frac{1}{bK} \frac{1}{C} + \frac{1}{b} \quad (12)$$

Correlation coefficients greater than 0.99 indicated an adequate fit.

Fractionation

The flow sheet of the two liquid chromatographs, the fractionator and analyzer, is depicted in Fig. 5 in which the main components of the system are labelled. The fractionation of the feed by displacement chromatography is carried out in the fractionator and the column effluent is collected as discrete fractions that were sampled and analyzed by the other HPLC unit operated in the elution mode.

To begin a displacement run, the switching valve was turned so that pump A delivered the carrier to the column at the desired flow-rate, with the drain valve closed. The feed introduction valve was turned to the load position and the loop filled with the feed solution. Pump B was then started at the same flow-rate setting as pump A and the feed valve was turned to pressurize the feed up to the column inlet pressure. When the pressure on the B side of the system equalled that on the A side, the switching valve was turned so that the feed, followed by the displacer, entered the column. The feed valve was returned to its original position after the desired volume of feed was introduced and the displacer solution flowed into the column. The progress of the run was monitored by the detector at an appropriate wavelength setting determined in advance. Following the run, pump A was started pumping the regenerant solvent, and when its pressure equalled that of the system the switching valve was returned to its original position for regeneration of the displacer-saturated column. Following the regenerant the column was perfused with the carrier solvent, delivered to the column by pump A, and the system was ready for another run.

Analysis of fractions

The concentration of the product in each of the fractions obtained from the displacement development run was determined by using the internal standard technique. The peak heights of the feed components injected in a solution of either phenylalanine or phenol were divided by the height of the internal standard peak, and this ratio was correlated with the known concentration of the feed component. Aliquots of each fraction were then diluted with the internal standard solution, and the retention times and peak height ratios measured in order to determine the presence and concentration of feed components in the fraction. The mobile phase for the analysis of the phenyl acetic acid derivatives was 50 mM phosphate buffer, pH 2.12, containing 10% (v/v) acetonitrile and for the dihydroxybenzenes an aqueous solution of 1% triethylamine phosphate, pH 3.0, containing 25% (v/v) methanol was used.

RESULTS AND DISCUSSION

Adsorption isotherms on octadecyl-silica

As seen in Fig. 6 the shape of the isotherms of hydroxyphenylacetic acids resemble the rectangular hyperbolas characteristic for Langmuir isotherms, *cf.* eqn. 3. Similar observations were made also with other aromatic substances upon investigating their adsorption properties from aqueous solutions on hydrocarbonaceous silica-bonded phases. Table I shows the parameters obtained by fitting experimental data to eqn. 3 from isotherm measurement by frontal analysis on the different kinds of octadecyl-silica columns. The product of the saturation concentration, b , and the binding constant, K , is expected to be proportional to the retention (capacity) factor of the solute in linear elution chromatography on the same column when the eluent

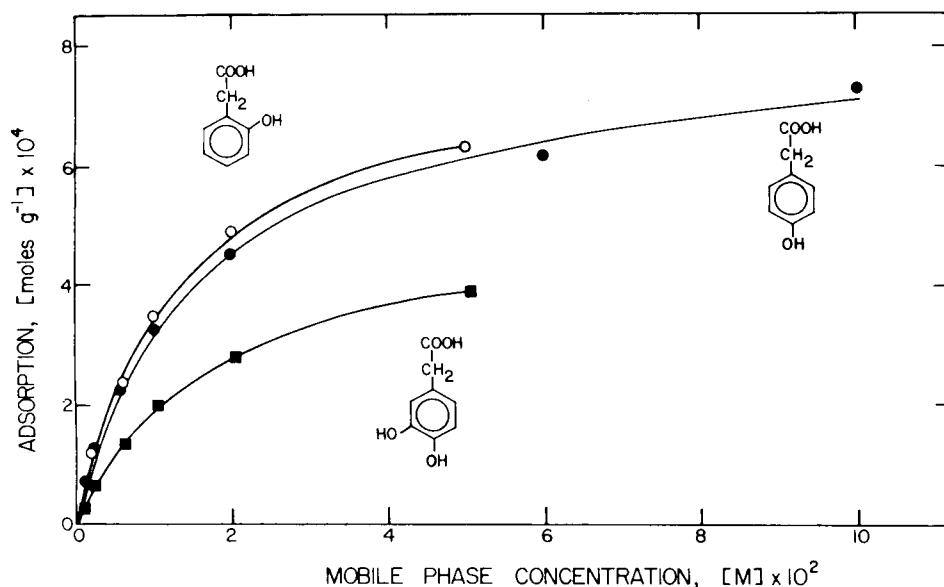


Fig. 6. Adsorption isotherms as measured by the frontal analysis of 3,4-dihydroxyphenyl (■), 2-hydroxyphenyl (○) and 4-hydroxyphenyl (●) acetic acids on 10- μ m Partisil ODS-2 from 0.1 *M* phosphate buffer, pH 2.12, at 25 $^{\circ}$ C. Solid lines were drawn from values calculated by linear least square analysis of the data points to the Langmuir isotherm according to eqn. 12.

composition is the same as that of the carrier used in the determination of the isotherm. The proportionality factor is the phase ratio of the column and therefore, the analysis of a series of Langmuir isotherms and the corresponding chromatographic retention factors may be used to evaluate the phase ratio of the column.

TABLE I

PARAMETERS OF LANGMUIR ISOTHERMS FOR ADSORPTION ON OCTADECYLSILICA FROM WATER

The isotherms were evaluated by frontal analysis and the parameters from eqn. 3.

	h^{***} (mol/g $\times 10^4$)	K^{***} (M^{-1})	bK (ml/g)
Resorcinol*	3.297	19.20	6.33
Catechol*	7.228	10.15	7.33
3,4-Dihydroxyphenyl acetic acid**	5.068	63.41	32.1
4-Hydroxyphenyl acetic acid**	7.804	74.00	57.7
2-Hydroxyphenyl acetic acid**	7.972	76.62	61.1

* Column: Spherisorb ODS; carrier: water.

** Column: Partisil ODS-2; carrier: 0.1 *M* phosphate buffer, pH 2.12.

*** See eqn. 3.

Present development in displacement chromatography with bonded phases have been encouraging as the isotherms that we investigated so far were of the concave downwards type, *i.e.* suitable to meet the requirement for displacement chromatography. Nonetheless, further knowledge of the isotherms will be required for the design of the fractionation system without a great deal of trial and error that may be associated with the selection of a suitable displacer and its concentration. It is hoped that further studies on the relationship between chemical structure and the parameters of the isotherm will facilitate the prediction of isotherms from structural increments of the solute molecules¹⁵⁻¹⁷.

Displacement diagrams

Concentration profiles of the individual feed components in the effluent of the fractionator column are depicted on displacement diagrams such as those shown in Figs. 7 and 8. Fractions of column effluent were analyzed by HPLC in order to determine accurately the concentrations of both components in the mixed boundary region. On the other hand, when the effluent of the fractionator is monitored by a flow-through detector that cannot distinguish between the two species, a displace-

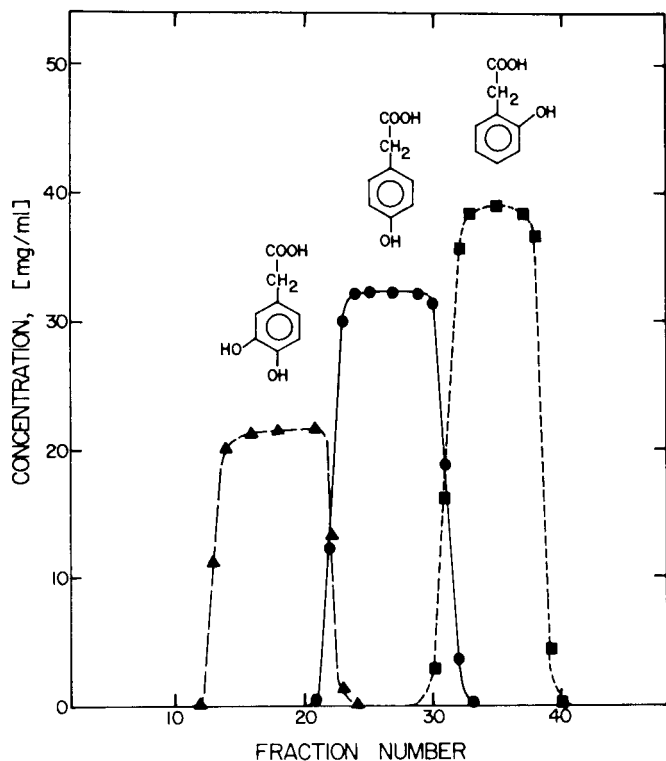


Fig. 7. Separation of hydroxyphenylacetic acids by displacement chromatography on Partisil ODS-2 column (250 × 4.6 mm). The carrier was 0.1 *M* phosphate buffer, pH 2.12, and the displacer was *n*-butanol at a concentration of 0.87 *M*. Flow-rate and temperature were 0.05 ml/min and 25°C, respectively. The feed had a volume of 1.5 ml and contained 30, 35 and 45 mg of 3,4-dihydroxy-, 4-hydroxy and 2-hydroxyphenylacetic acids, respectively. Fraction size was 0.15 ml and fraction number 40 marks an effluent volume of 12 ml.

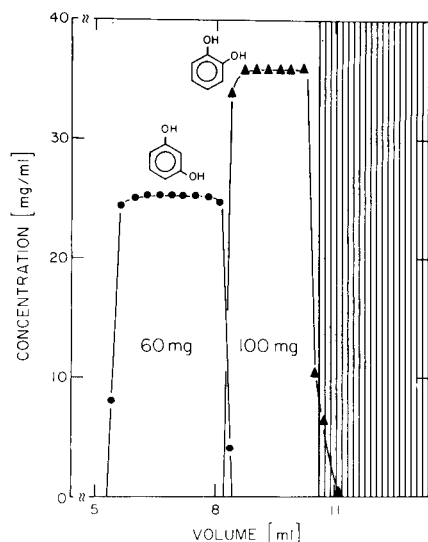


Fig. 8. Displacement separation of resorcinol (●) and catechol (▲), with water as carrier and 0.8 *M* *n*-propanol in water as the displacer. The flow-rate was 0.15 ml/min and the feed contained 60 mg of resorcinol and 100 mg of catechol dissolved in 1.0 ml of water. The purity, *P*, of resorcinol and catechol fractions in the product was 0.97 and 0.94, respectively. The column was packed with 5- μ m octadecyl-Spherisorb and its dimensions were 500 \times 4.6 mm. The displacer is indicated by the shaded region.

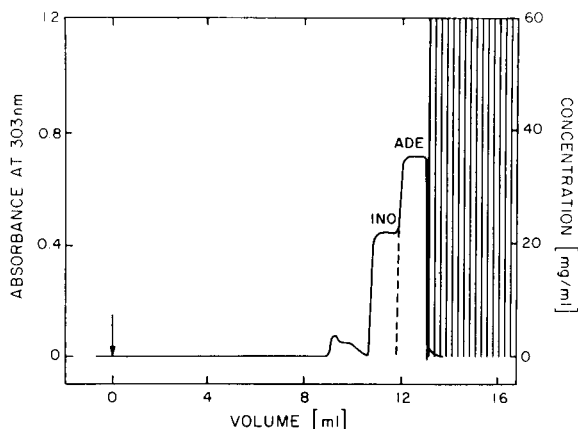


Fig. 9. Displacement chromatogram of adenosine and inosine obtained by monitoring the fractionator effluent. The displacer was 0.66 *M* *n*-butanol in 0.01 *M* phosphate buffer, pH 3.5 and the temperature was 22°C. The flow-rate was 0.20 ml/min and the feed contained 24 mg of each component in 1.5 ml of the neat aqueous phosphate buffer used as the carrier. The purity, *P*, of the adenosine and inosine fractions in the product was 0.92 and 0.83, respectively. The dimensions of the 10- μ m LiChrosorb RP-18 column were 250 \times 4.6 mm. The displacer is indicated by the shaded region.

ment chromatogram is obtained that depicts only the contour of the concentration profiles as shown in Fig. 9. In fact, the employment of an "analyzer" liquid chromatograph to monitor the concentrations of all components in the effluent of the fractionator column greatly facilitate not only the assessment of the purity of the product but also examination of the course of the displacer process and its optimization. Thin-layer chromatography has also been found to be suitable for this purpose but due to its superior accuracy, convenience and speed the analysis of the fractions was carried out in this study by using HPLC only.

The analyzer liquid chromatograph acts as a selective detector, and it can be used to determine zone boundaries accurately, a feat which is impossible by using only the trace from the fractionator detector alone. All separations depicted above are believed to reflect fully developed displacement trains although the boundaries between the zones are not completely sharp due to the effect of axial dispersion.

Purity of the product

Parameter P. That fraction of a component that is recovered in pure form has been defined as its purity, *P*, according to eqn. 6. This parameter has been used to quantitatively measure the efficiency of separation as shown in Tables II and III.

TABLE II

THE VARIATION OF PURITY WITH OPERATING CONDITIONS FOR THE SEPARATION OF PHENOLIC COMPOUNDS

The carrier was a 0.1 *M* phosphate buffer, pH 2.12, and the column was a 10- μ m Partisil ODS-2 (250 \times 4.6 mm).

Purity, <i>P</i>			Displacer	Feed (mg)	Flow-rate (ml/min)
3,4-Dihydroxy- phenyl acetic acid	4-Hydroxy- phenyl acetic acid	2-Hydroxy- phenyl acetic acid			
0.95	0.83	0.73	0.87 <i>M</i> <i>n</i> -butanol	110	0.05
0.87	0.71		0.64 <i>M</i> phenol	52.5	0.30
0.84	0.84		0.74 <i>M</i> phenol	75	0.05
0.86	0.84		0.74 <i>M</i> phenol	75	0.15
0.87	0.80		0.74 <i>M</i> phenol	75	0.50

Some of the figure captions also contain *P* values in order to quantify the degree of separation shown by the displacement diagram.

It is seen that for separations which are considered good the value of *P* is higher than 0.9, that is, after removing the contaminated boundary regions of a given zone more than 90% of the component is obtained in pure form. From the definition of *P* it follows that its value increases with the amount of component when the width of the mixed region remains constant. Such a situation may arise when the displacement train is already isotachic with the largest feed under investigation. The first emerging component of the displacement train is expected to yield a relatively high

TABLE III

THE EFFECT OF OPERATING CONDITIONS ON THE MAGNITUDE OF THE PURITY, *P*, DEFINED BY EQN. 6, OF INOSINE AND ADENOSINE

The carrier was 0.1 *M* phosphate buffer, pH 3.5, and the displacer contained 0.66 *M* *n*-butanol. The 10- μ m LiChrosorb RP-18 column (250 \times 4.6 mm) was maintained at 22°C.

Purity, <i>P</i>		Feed		Flow-rate (ml/min)
Inosine	Adenosine	Volume (ml)	Amount (mg)	
0.76	0.86	1.5	25	0.05
0.74	0.84	1.5	25	0.15
0.53	0.61	1.5	25	0.50
0.83	0.92	1.5	48	0.20
0.73	0.85	4.5	48	0.20
0.47	0.54	6.0	48	0.20

value of P because it does not contain a contaminated front boundary. Despite its shortcomings the purity parameter can conveniently be used to express the effect of changing operating conditions on the efficacy of separation as it is shown in Tables II and III.

G Function. For measuring the degree of separation of homologous series the G function has been defined in eqns. 7-9. Fig. 10 shows a late of the G function

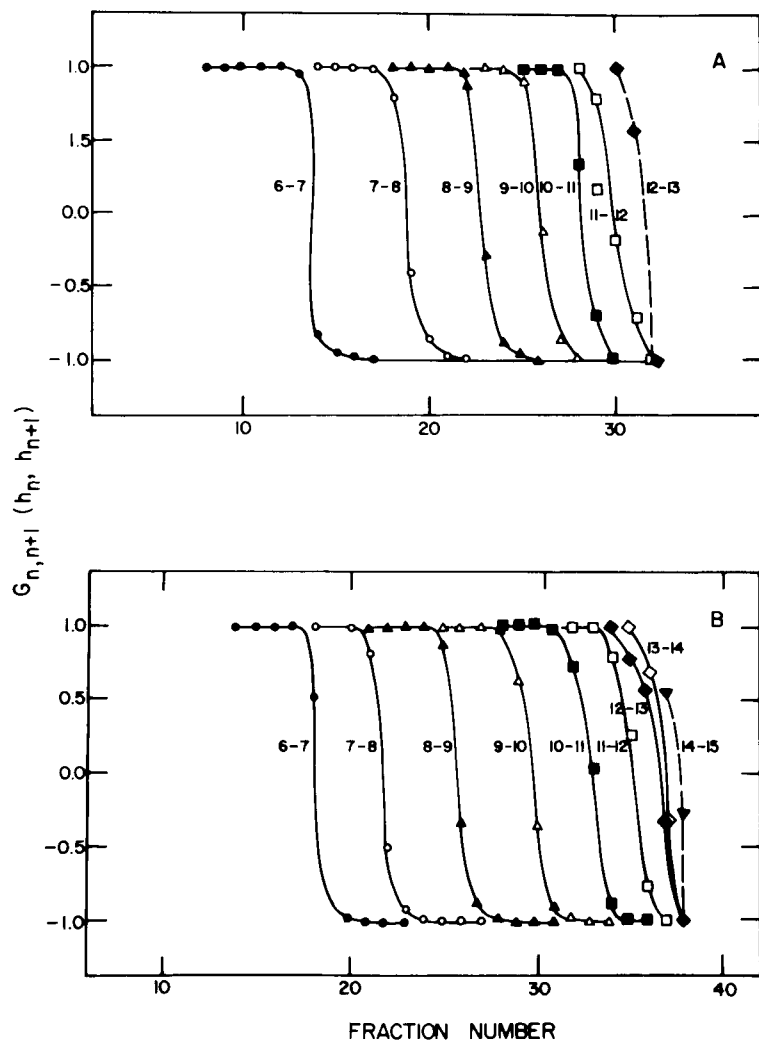


Fig. 10. Illustration of the displacement separation of Carbowax 400 by plotting the G function, eqn. 7 vs. fraction number of the effluent. The numbers at each curve indicate the number of ethylene glycol units, n and $n + 1$, in the two oligomers present in the fractions. The flow-rate and fraction volume were 0.15 ml/min and 0.15 ml, respectively. The column temperature was 22°C and the displacer was 0.66 M n -butanol in the carrier. A, The carrier was 10% (v/v) acetonitrile in water and the feed was 45 mg of Carbowax 400. At fraction number 30, 11.0 ml of column effluent was collected. B, The carrier was 5% (v/v) acetonitrile in water, the feed was 90 mg of Carbowax 400. Fraction number 40 marks 12.3 ml of column effluent.

against the number of fractions in the case of displacement chromatography of ethylene glycol oligomers. The G function denotes the degree of separation of adjacent zones in the displacement train containing n and $n + 1$ ethylene glycol units. The flat portions of the S-shaped curves, in which $G_{n,n+1}$ has a value of $+1$ or -1 , denotes the fractions in which only one of the two oligomers is present, whereas the curved portion indicates the mixed boundary between adjacent zones in the effluent. For instance, in Fig. 10A, heptaethylene glycol appears mixed with hexaethylene glycol in fractions 15–17, and is mixed with octaethylene glycol in fractions 18–21.

The lower homologs were obtained in pure form as depicted in Fig. 10A, but the separation of the larger molecules was less complete, as indicated by the absence of flat portions of the curves corresponding to the 11-, 12- and 13-unit homologues. However, a decrease in the organic modifier content of the carrier results in an increase in the molecular weight of homologues which can be recovered in pure form as shown in Fig. 10B, and also allows the column to accommodate a larger feed. The greater adsorptivity of the feed components as well as the displacer in the presence of the more polar carrier permits the recovery of fractions containing pure nonaethylene glycol as illustrated in Fig. 10B in contrast with the insufficient separation obtained with water lean carrier and depicted in Fig. 10A.

Effect of operational parameters. With presently available microparticulate columns, accurate flow control and precision instrumentation, the ease of separation by displacement chromatography is largely affected by thermodynamic factors such as the shape of isotherms, relative adsorptivity of the components as manifested by the competitive isotherms, solubility, as well as the relative concentration of the components in the feed. Although the fundamental relationships between most of these factors has long been established^{18,19} no analytical expressions could be developed due to the mathematical complexity of the non-linear differential equations underlying the model.

From the practical point of view optimization of the process is tantamount to selection of conditions that yield the most rapid transient period for a full development of the displacement train, *i.e.*, that require the shortest column length to bring about a given separation.

The need for the displacer solution increases the number of variables within the system, compared to elution chromatography. Furthermore, the necessity of achieving the isotachic state before optimal separation is obtained requires that the variables have some minimum value such that the sample resides in the column long enough to attain this state. In order to examine the effect of changes in the variables, the feed concentration and volume, column length, mobile phase flow-rate, displacer and species concentrations were varied. Changes in the variables were made concomitantly as well as individually in order to determine their interdependence.

Flow-rate. Fig. 11 illustrates the effect of flow-rate on the separation of adenosine and inosine by displacement chromatography. It is seen and can be verified by the pertinent values of the purity parameter P that the efficacy of the separation even at the relatively low load of the column is strongly dependent on the flow-rate. Efficiency increases with decreasing flow-rate and as a result P_{Ado} increases from 0.61 to 0.86 upon a respective decrease of the flow-rate from 0.50 to 0.05 ml/min. This behavior is attributed to an increase in the time available for development of the displacement train in the column upon reducing the flow velocity. The purity of the

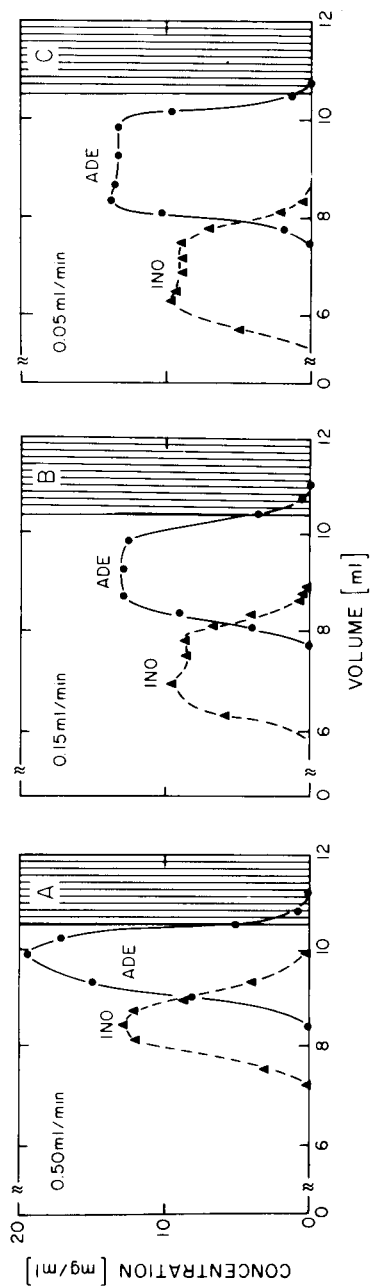


Fig. 11. Effect of flow-rate on the displacement separation of inosine (\blacktriangle) and adenosine (\bullet). Flow-rates: A, 0.05; B, 0.15; C, 0.50 ml/min. The displacer was 0.66 *M* *n*-butanol in 0.10 *M* phosphate buffer, pH 3.5. The feed solution contained 10 and 15 mg of inosine and adenosine, respectively, and the column was a 250×4.6 mm 10- μ m LiChrosorb RP-18. The purities of the products are given in Table III.

product increases with decreasing flow-rate in this manner only up to a point, however. Decreasing the flow-rate below that value at which the displacement is fully developed induces no further effect on any characteristics of the displacement train. This fact is illustrated by the purity values of the last three entries in Table II. The constancy of the P values with changing flow-rate — while all other conditions were kept constant — indicates that the displacement was fully developed at a flow-rate of 0.5 ml/min, and no further benefits in purity were obtained from the longer column residence times achieved by decreasing the flow-rate to 0.15 or 0.05 ml/min.

Feed: Amount. When the column is overloaded in displacement chromatography no full development can take place for two reasons. First, the length of time required to separate the feed components is longer, so a larger column or slower flow rate may be required to achieve separation. It is because an increase in the amount of feed can extend the development time that is defined in Fig. 1. The second quite obvious reason why feed overloading can prevent full development is that the column length may be insufficient to accommodate the length of the fully developed displacement train, so that full development would require a longer column.

Fig. 12 illustrates the effect of column overload that manifests itself in incompletely developed concentration zones having shapes different from the "square wave" form encountered under ideal conditions in displacement chromatography. In the three cases shown, the column was overloaded in different ways and to a different extent with the first and second components, 3,4-dihydroxyphenylacetic acid and 4-hydroxyphenylacetic acid respectively. It is noted that in other experiments, quasi isotachic conditions were obtained in displacement chromatography under operating conditions identical to those given in Fig. 12 when the feed contained 15 and 37.5 mg of 3,4-dihydroxyphenylacetic acid and 4-hydroxyphenylacetic acid, respectively.

As seen in Fig. 12A the zone of the less retarded component, the amount of which in the feed is relatively low, is substantially separated from the band of the more strongly adsorbed component, 4-hydroxyphenylacetic acid. It shows a nearly developed band and the estimated plateau concentration of the zone is close to that predicted from the isotherm and obtained in other runs performed under the same conditions but with reduced load.

The progressive degeneration of the displacement train on increasing the sample load is illustrated by change in the shape of the zone of the more retained 4-hydroxyphenylacetic acid. When the amount of the second component is doubled the band is much broader as shown in Fig. 12B and the residence time in the column is insufficient to attain isotachic conditions. Finally, it is seen in Fig. 12C that when the amount of 3,4-dihydroxyphenylacetic acid is also doubled in the feed, the shape of the 4-hydroxyphenylacetic acid zone further degenerates. The observed zone shapes are in agreement with the expectations. As the less retained component is present in the zone of the other at relatively high concentrations, the isotherm of the first is suppressed to such an extent that its velocity increases and consequently the band width increases.

Volume. In Figs. 9, 13A and 13B three displacement diagrams for adenosine and inosine are shown under identical feed loads and chromatographic conditions but with feed volumes of 1.5, 4.5 and 6.0 ml, respectively. Whereas at the smallest feed volume a fully developed displacement diagram is obtained as shown in Fig. 9, at a larger feed volume a frontal zone is observed for inosine as seen in Fig. 13A. The

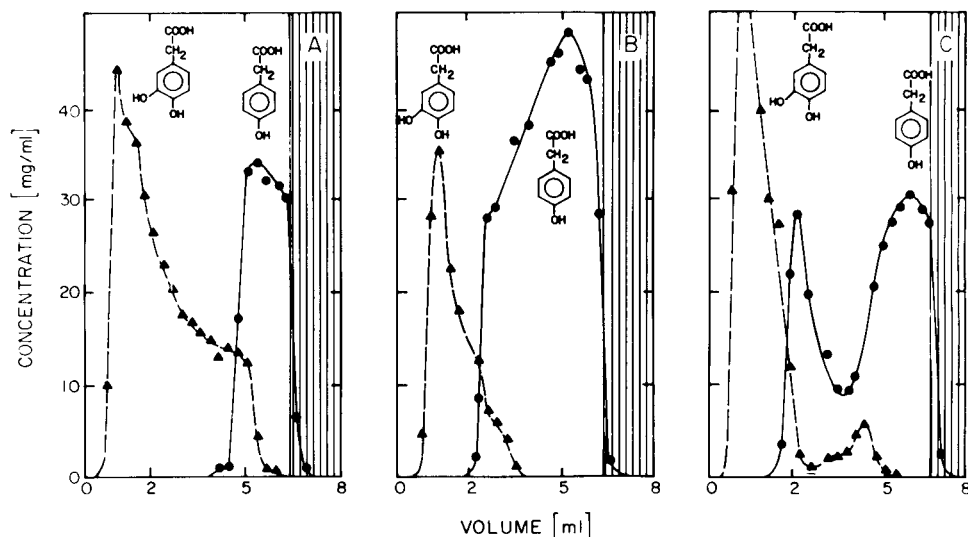


Fig. 12. Effect of feed size on the separation of 3,4-dihydroxyphenylacetic acid (▲) and 4-hydroxyphenylacetic acid (●) by displacement chromatography. The displacer was 0.64 *M* phenol in 0.10 *M* phosphate buffer, pH 2.12, and the temperature was 25°C. The mobile phase flow-rate was 0.3 ml/min. The respective amounts of 3,4-dihydroxyphenylacetic acid and 4-hydroxyphenylacetic acid in the feed were: A, 114 and 57 mg; B, 57 and 114 mg; C, 114 and 114 mg. The column was a 250 × 4.6 mm 10- μ m Partisil ODS-2.

degree of separation declines as well, as seen from the purity values listed in Table III. The displacement diagram obtained with a feed volume of 6.0 ml and shown in Fig. 13B exhibits further deterioration of the separation as seen from the low purity values calculated for this case and the irregular zone shapes as shown in the figure.

The feed volume effect noted here is a manifestation of the mixed frontal and displacement chromatography mechanisms which occur at the beginning of every displacement run. Frontal chromatography takes place when a solution of constant composition is introduced as a step function feed into the column. The feed stage of displacement chromatography is essentially a frontal chromatographic process, only the step function is truncated when the displacer is fed to the column. Therefore, the larger the feed volume, the more advanced this frontal chromatographic development is, and at some limiting value of the feed volume the first feed components emerge from the column before the displacer enters, and essentially a type of frontal chromatography is performed. A mixed mechanism is always operative at the beginning of any displacement run, but with a column long enough, the process of displacement development becomes dominant and prevails until the isotachic stage is reached.

In practice the limits on feed volume are important when the solubility of the feed components in the carrier is low. Therefore, at fixed feed volume the amount of sample that can be separated in a single chromatographic run is limited, among other factors, the solubility of the sample components in the carrier used for the preparation of the feed solution.

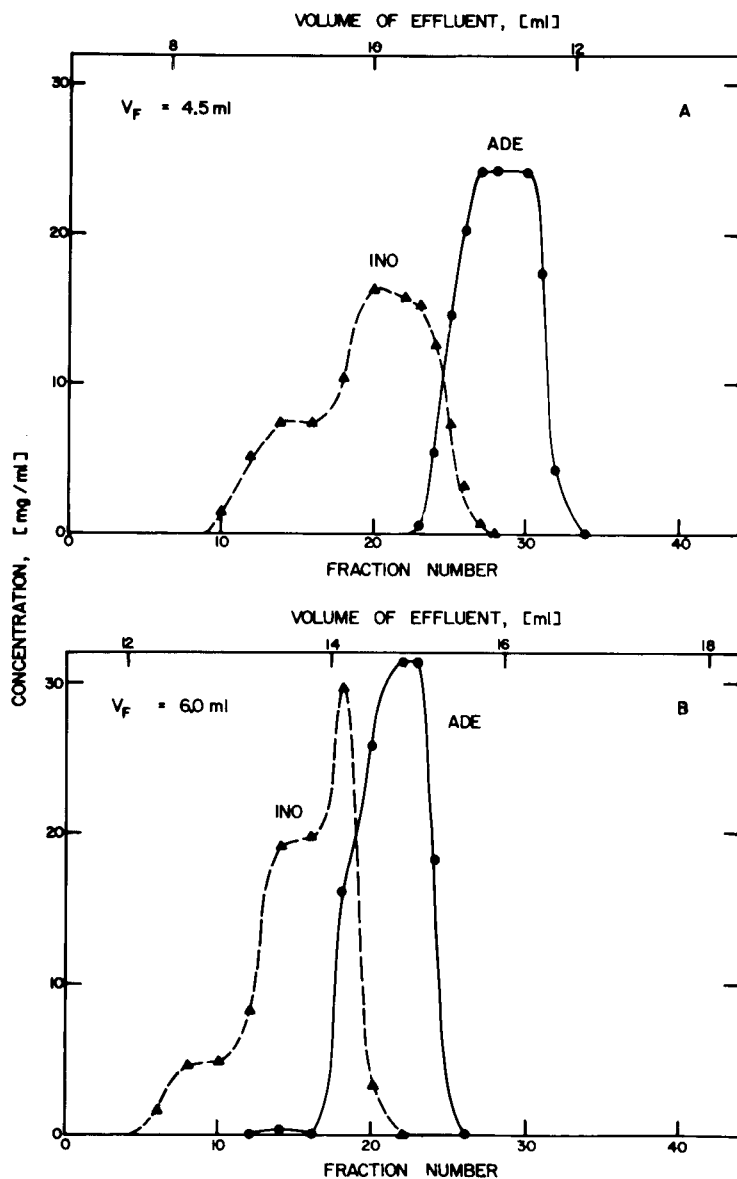


Fig. 13. Effect of feed volume on the separations of fixed amounts of adenosine (●) and inosine (▲) by displacement chromatography. The chromatographic conditions were as specified in Fig. 8. The feed volumes were A, 4.5 ml and B, 6.0 ml.

Column length

Fig. 14A shows the results of fractionation of the two phenolic compounds under conditions identical to those in Fig. 8, except the column was 25 cm instead of 50 cm. It is evident from the figure that with the shorter column the displacement is not completely developed, whereas isotachic conditions were approached with the

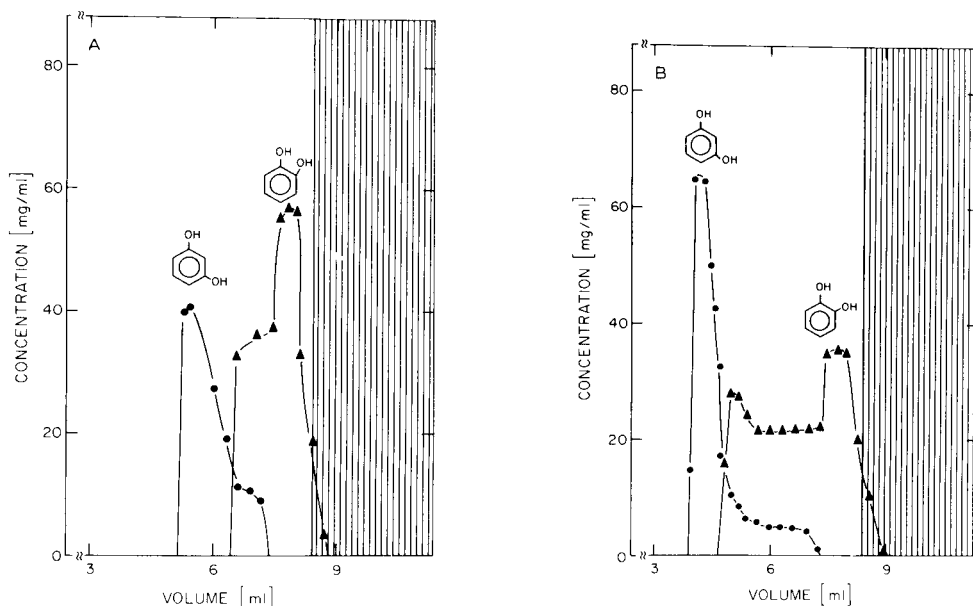


Fig. 14. Effect of flow-rate on the separation of phenolic compounds by displacement chromatography with a 250×4.6 mm I.D. $5\text{-}\mu\text{m}$ octadecyl-Spherisorb column. The flow-rate was 0.15 ml/min in A and 0.075 ml/min in B, whereas other conditions were the same as those in Fig. 8.

longer column. As pointed out above, the column length is a critical parameter that must have some minimum value under a given set of operating conditions. In Fig. 1 a hypothetical dissection of the column during the stages of displacement development was indicated, and the three parts required for the minimum column length given as the feed length, the development length and the length of the fully developed displacement train. The column length when it is minimum consists of length increments necessary for these three stages. The incomplete separation depicted in Fig. 14A demonstrates that the 25 cm long column is not long enough to accommodate the three constituent lengths. The result obtained with the 25 cm long column are representative to those that occur half-way down in the 50 cm long column that just encompasses the length of the three stages or is even longer than necessary.

Decreasing the flow velocity does not decrease the minimum column length by a proportionate amount, as one might expect on a residence-time basis, as shown in Fig. 14B. There the fractionation was run in the 25 cm at a flow-rate of 0.075 ml/min, *i.e.*, half the value in both Figs. 8 and 14A. The chromatogram appears to be nearer to fully developed, but again the isotachic state has not been reached, even though the residence time of the feed in the column was the same as in Fig. 8. The reason for this is that decreasing the flow-rate increases the development time for the train, and so effectively increases the development length within the column, but it has no effect on the length occupied by the fully developed train. The length of the isotachic train is determined by the amount of feed and the concentrations of the isotachic zones, and so is unaffected by the velocity of the carrier. Therefore, changes in the column length are not fully compensated by proportionate changes in flow velocity that primarily effects the length of the feed and development zones in the column.

The discussion of Fig. 12 pointed out similar constraints on column length. There the feed loading was increased and it was argued that this had the effect of increasing both the development time required for the separation and the length of the column required to accommodate the isotachic train. The net effect of an increase in feed loading is, therefore, that a longer column is required for complete separation. This conclusion can be contrasted to the practice in preparative chromatography in the elution mode, where the diameter of the column has to be increased in order to accommodate a larger feed, and still maintain pulse-shaped peaks.

Concentrations at full displacement development

According to eqn. 2b the concentrations of the individual components in the isotachic displacement train are given by the intersection of their isotherms with the appropriate chord of the displacer isotherm.

In order to test the theoretical predictions we compared plateau concentrations of the zones in the displacement diagrams such as those depicted in Figs. 7 and 8 to the values obtained from the isotherms described in Table I. Both kinds of data are listed in Table IV. It is seen that a reasonably good agreement exists between the concentrations obtained from displacement development and those predicted from the isotherms for different displacer strengths, *i.e.*, speed lines. The results strongly suggest that under the experimental conditions employed here the displacer train was fully developed, *i.e.*, the limiting isotachic condition was closely approached. This conclusion is also supported by the observation that the width of the mixed boundary regions between the zones was approximately the same, a feature that is characteristic for full displacement development.

TABLE IV

COMPARISON OF THE CONCENTRATIONS AT PLATEAU IN DISPLACEMENT CHROMATOGRAPHY OF PHENOLIC COMPOUNDS ON OCTADECYLSILICA BY USING ALKYL ALCOHOLS AS DISPLACER TO VALUES CALCULATED FROM THE ISOTHERMS OF THE SUBSTANCES EVALUATED FROM INDEPENDENT MEASUREMENTS

<i>Component</i>	<i>Plateau concentrations (mg/ml)</i>	
	<i>Experimental</i>	<i>Predicted</i>
Resorcinol	25*	21*
Catechol	36*	39*
3,4-Dihydroxyphenyl acetic acid	20**, 21***	22**, 23***
4-Hydroxyphenyl acetic acid	32**, 33***	31**, 34***
2-Hydroxyphenyl acetic acid	38***	35***

* 0.8 *M* *n*-propanol.

** 0.76 *M* *n*-butanol

*** 0.87 *M* *n*-butanol.

Advantages of relatively narrow-bore columns

Preliminary results suggest that in the displacement mode the column diameter can be smaller by at least one order of magnitude than in the elution mode to obtain

the same throughput. The actual factor, of course, depends on the particular chromatographic system employed even if all requirements for complete displacement are fulfilled.

The use of small diameter columns is associated with a number of advantages²⁰. From the operational point of view, the narrowness of the inside diameter relaxes the stringent requirements such as thick wall and bulky connections for operating the column at high inlet pressures. Then the use of small particles having 3- to 5- μm diameter for high efficiency column packing is facilitated. Moreover, the regeneration step can be expedited by using high flow velocities. Uniform radial and flow temperature profiles are essential in attenuating axial dispersion. In narrow-bore columns the occurrence of deleterious temperature non-uniformities is greatly reduced even when heat associated with adsorption and desorption at the high solute concentrations employed in displacement chromatography is significant. Concomitantly fingering and other flow instabilities arising from density and viscosity differences are expected to play a lesser role when the column inner diameter is reduced. Furthermore, the significance of channeling and other packing non-uniformities in determining axial dispersion may decrease with column diameter with the exception of "a wall effect" which generally increases to some limit. Low solvent consumption associated with the use of narrow bore columns has obvious felicitous economical and environmental effects and the compactness of column and instrumentation afforded by employing narrow-bore columns may also be a preferred feature.

Comparison of elution and displacement chromatography

A number of features facilitate analysis by using the linear elution mode of chromatography, including that it yields Gaussian or quasi-Gaussian peaks, the relationship between the migration velocity and thermodynamic equilibrium constant is simple and the role of transport and kinetic phenomena in determining band spreading is well understood. The wide popularity of the technique in analytical separations is most likely due to the relative simplicity of operation and the ease of detection of distinct concentration pulses. In addition its detailed theoretical framework has also contributed to the almost exclusive use of elution chromatography.

The key features of displacement chromatography were clearly recognized even before the rapid development of elution chromatography commenced with the introduction of partition chromatography and the plate height theory. Yet difficulties associated with the detection of the individual sample components, the surface heterogeneity of the adsorbents and the excessive band spreading in columns available at that time thwarted displacement chromatography's becoming an accepted analytical method. Although displacement may occur in the practice of preparative chromatography with overloaded columns, analytical applications involving the conscientious employment of displacement development with a judiciously chosen displacer²¹ or other means such as temperature²² have been largely confined to the scientific literature.

On the other hand, the results of this work suggest that fully developed displacement chromatography may be eminently suitable to carry out preparative scale chromatography with columns packed with microparticulate stationary phases, the use of which is prohibited in large diameter columns because of mechanical problems associated with operation at high column inlet pressures. The method is further

recommended for its characteristic recovery of the products at concentrations significantly higher than obtained in elution chromatography, accompanied by the concomitant economic and environmental benefits of relatively low solvent consumption. In fact, both the stationary and mobile phases as well as the equipment are better utilized in the displacement than in the elution mode of chromatography. As a consequence, the amount of pure product per unit column volume should be greater in displacement chromatography than in linear elution chromatography. Nevertheless the need to regenerate the column by removing the displacer is a significant disadvantage of displacement development in comparison to isocratic elution, although it may vanish if gradient elution is required to carry out a preparative separation. In any case the regeneration of the column is associated with a general cleaning of the system and removal of contaminants that otherwise may accumulate.

Usually zone boundaries are not perfectly sharp in displacement chromatography even when columns are used that are highly efficient in terms of low axial dispersion. Therefore in the recovery of products the boundary regions of the zones are preferentially collected separately and rechromatographed directly without concentrating.

An important difference between elution and displacement chromatography is that an increase in sample size in the former usually mandates an increase in column diameter in order to maintain the efficiency of separation constant, whereas in displacement chromatography the increase in both the diameter and length of column can be used very efficiently to increase throughput.

Selection of the column, carrier and displacer

All results to illustrate displacement chromatography presented in this report were obtained by reversed-phase chromatography using silica-bonded hydrocarbonaceous sorbents and a neat aqueous or a water-rich hydro-organic carrier. The main reason for this was our interest in studying the potential of such bonded phases for displacement chromatography as far as the isotherm shape and column loading capacity are concerned. It should be noted that the use of charcoal²³, ion-exchange resins²⁴ and silica gel²⁵ for displacement chromatography is well documented in the literature but to our best knowledge the employment of bonded phases for such purposes has not yet been described. Other results from our laboratory (to be published) have shown that columns packed with microparticulate silica gel also yield very good results in displacement chromatography when a less polar solvent is used as the carrier. On the other hand, the use of aqueous carriers as described in this study facilitated a strong binding of the feed components as well as that of the displacer to the hydrocarbonaceous stationary phase.

Lack of data on adsorption isotherms is the major impediment to optimization of displacement chromatography because it precludes the *a priori* determination of the nature and concentration of a suitable displacer. Therefore, the selection of the displacer by trial and error appears to be inevitable unless the isotherms of the potential displacers and preferably those of the feed components as well are known. The following guidelines may be useful in choosing the displacer. It should: (i) be adsorbed more strongly from the carrier onto the stationary phase than any of the feed components; (ii) not complex with any of the components; (iii) be inert to the stationary phase; (iv) be readily removed from the column by a suitable regenerant; (v) be highly soluble in the carrier; and (vi) be non-hazardous and inexpensive.

CONCLUSIONS

In displacement chromatography a certain amount of the feed mixture is first adsorbed at the inlet section of the column and thereafter the solution of a suitable displacer that binds more strongly to the adsorbent than any of the feed components is introduced in a continuous fashion. As the displacer front moves down the column the feed components gradually become separated as more strongly sorbed substances displace weakly sorbed components from the surface of the adsorbent. Finally a "displacement train" containing square-wave concentration zones of the individual components is developed in which each zone moves with the same velocity. Successful separation by displacement chromatography largely depends upon the sharpness of the boundaries between the adjacent zones. Therefore the requirements for high efficiency columns are very exacting, however, they can be met by columns presently available.

Indeed the potential of the HPLC columns and instrumentation used in analytical work can be exploited for preparative scale separations by using the displacement mode of chromatography, as illustrated by the separation of binary mixtures, for higher system productivity and product concentration in the effluent than generally encountered in elution chromatography. Knowledge of pertinent adsorption isotherms and solubilities of the feed components and potential displacers greatly facilitates the selection of operating conditions on the basis of the theory describing the properties of the fully developed displacement train and a qualitative understanding of the factors involved in the transient development process leading to separation. In agreement with recent findings²⁶, results presented here indicate that with a packed microparticulate column having the usual length of 25 cm and inside diameter of 0.4 to 0.5 cm binary mixtures containing 50 to 100 mg of each component mentioned above can readily be separated by displacement chromatography within one hour. This mode of chromatography may also be the method of choice in micropreparative separations of precious substances with narrow bore (I.D. ≤ 1 mm) columns. Furthermore, its potential in special analytical applications such as liquid chromatography-mass spectrometry may also warrant serious consideration.

ACKNOWLEDGEMENTS

Thanks are due to M. Lederer for invaluable advice and discussions on displacement chromatography. This work was supported by Grant Nos. GM 20993 and CA 21948 from the National Institute for General Medical Sciences and the National Cancer Institute, U.S. Public Health Services, Department of Health and Human Services.

REFERENCES

1. A. Tiselius, *Ark. Kem., Mineral. Geol.*, 16A (1943) 1.
2. S. Claesson, *Ark. Kem., Mineral. Geol.*, 23A (1947) 1.
3. A. J. P. Martin and R. L. M. Synge, *Biochem. J.*, 35 (1941) 1358.
4. A. T. James and A. J. P. Martin, *Biochem. J.*, 50 (1952) 679.
5. G. A. Howard and A. J. P. Martin, *Biochem. J.*, 46 (1950) 532.
6. A. Tiselius and L. Hagdahl, *Acta Chem. Scand.*, 3 (1950) 394.

- 7 G. Schay, *Theoretische Grundlagen der Gaschromatographie*, Deutscher Verlag der Wissenschaften, Berlin, 1960, pp. 133–139.
- 8 F. Helfferich and G. Klein, *Multicomponent Chromatography*, Marcel Dekker, New York, 1970, pp. 225–254.
- 9 L. Hagdahl, in E. Heftmann (Editor), *Chromatography*, Rheinhold, New York, 1961, p. 71.
- 10 Cs. Horváth and H.-J. Lin, *J. Chromatogr.*, 126 (1976) 401.
- 11 S. Claesson, *Ann. N.Y. Acad. Sci.*, 49 (1948) 183.
- 12 L. Hagdahl, R. J. P. Williams and A. Tiselius, *Ark. Kem., Mineral. Geol.*, 4 (1952) 1932.
- 13 S. M. Partridge and R. G. Westall, *Biochem. J.*, 44 (1949) 418.
- 14 J. R. Conder and C. L. Young, *Physico-Chemical Measurement by Gas Chromatography*, Wiley, Chichester, 1979.
- 15 W. Melander, B.-K. Chen and Cs. Horváth, *J. Chromatogr.*, 185 (1979) 99.
- 16 Cs. Horváth, W. Melander and I. Molnár, *J. Chromatogr.*, 125 (1976) 129.
- 17 G. Belfort, *Environ. Sci. Technol.*, 14 (1980) 1037.
- 18 D. DeVault, *J. Amer. Chem. Soc.*, 65 (1943) 532.
- 19 H. Thomas, *Ann. N.Y. Acad. Sci.*, 49 (1948) 161.
- 20 Cs. Horváth, *Methods Biochem. Anal.*, 21 (1973) 79.
- 21 E. A. Peterson, *Anal. Biochem.*, 90 (1978) 767.
- 22 C. M. A. Badger, J. A. Harris, K. F. Scott, M. J. Walker and C. S. G. Phillips, *J. Chromatogr.*, 126 (1976) 11.
- 23 L. Hagdahl and R. T. Holman, *J. Amer. Chem. Soc.*, 72 (1950) 701.
- 24 S. M. Partridge and R. C. Brimby, *Biochem. J.*, 51 (1952) 628.
- 25 D. L. Carrier and A. J. Raymond, *J. Chromatogr. Sci.*, 11 (1973) 625.
- 26 H. Kalász and Cs. Horváth, *J. Chromatogr.*, 215 (1981) 295.

CHROM. 14,074

CHROMATOGRAPHIC CHARACTERIZATION OF SILICA SURFACES

HEINZ ENGELHARDT* and HARTMUT MÜLLER

Angewandte Physikalische Chemie, Universität des Saarlandes, Saarbrücken (G.F.R.)

SUMMARY

Columns packed with silica differ not only in their phase ratio, specific surface area per unit column volume and volume of mobile phase, but also in the pH of the silica surface. The influence of this surface pH on the separation of solutes with basic or acidic groups in dichloromethane as eluent is demonstrated. Of the commercially available silicas the irregular ones are, as expected, neutral or weakly acidic, whereas the spherical ones are either acidic ($\text{pH} \approx 4$) or basic ($\text{pH} \approx 9$). It is shown that the pH of the silica can easily be adjusted in order to achieve the required and optimal selectivity. These properties contribute to the selectivities of chemically bonded stationary phases based on silica.

INTRODUCTION

In chromatography, silica is the most widely used stationary phase, as a polar phase in classical liquid chromatography and as carrier for chemically bonded stationary phases, *e.g.*, for reversed-phase systems. It is commonly accepted¹⁻⁵ that its chromatographic properties depend on its specific surface area, its specific pore volume, its average pore diameter and the concentration of silanol groups per unit surface area. Because silica is a colloidal system, changes in absolute and relative retention have been traced to alterations in its chemical surface properties, sometimes called its "history"⁵. Silicas for high-performance liquid chromatography (HPLC) are sold under a variety of trade names, such as LiChrosorb, LiChrospher, Nucleosil, Partisil, Porasil, Spherisorb, Spherosil and Zorbax. They are prepared by different procedures, starting from sodium silicates, silicon tetrachloride, silicic acid esters, etc.^{3,4}. The physical properties of these silicas are similar, especially if the specific surface areas per unit column volume are compared⁶. The column efficiencies obtainable have been the main aim in comparing the different brands to evaluate the relative advantages and disadvantages of spherical *versus* irregular particles^{7,8}. Column efficiency is mainly affected by the average particle diameter and its distribution, and only partially by differences in physical properties such as surface area and pore diameter.

Comparing several silicas with specific surface areas between 8 and 400 m²/g and average particle diameters between 6 and 50 μm for adequate resolution, peak capacity and time of analysis, Scott⁹ demonstrated that to a first approximation the

retention of test solutes increases with increasing surface area. No explanation was given for the observed deviations from this rule. From the results, it was concluded that for optimal chromatographic conditions at least four different silicas with surface areas of *ca.* 15, 75, 150 and 300–400 m²/g should be available.

Huber and Eisenbeiss¹⁰ demonstrated, for several silicas with specific surface areas spanning more than two orders of magnitude, that the capacity ratios (k') depend solely on the specific surface area, whereas the selectivity is fairly constant. Of course, in this comparison the k' values had been standardized for differences in the phase ratios in the different columns. In adsorption chromatography the phase ratio correlating k' and the "adsorption coefficient" is determined by the specific surface area (O_{spe} , m²/g), the packing density (ρ , g/cm³) of the stationary phase and the fraction of mobile phase, ϵ_r , in the column. On the other hand, the selectivity, α , for the separation of adjacent pairs of the homologous series of *m*-phenylenes, *e.g.*, for *m*-sexi- and *m*-quinquephenylene, increases from 2.5 to 3.4 when the specific surface area decreases from 280 to 8 m²/g. This may be caused by differences in the "adsorption coefficient" due to changes in the silanol concentration or in the chemical nature of the surface.

The chemical nature of the silica surface influences the retention of hydrocarbons, nitro compounds and ethers in non-polar eluents^{9,10}, it affects the peak shape and solute retention of medium-polar compounds in non-polar to medium-polar eluents and certainly influences the preparation and properties of chemically bonded phases. Therefore, in this work we have attempted to characterize the surface properties of some commercially available silicas by measuring the retention of non-polar to polar solutes in a non-polar eluent.

EXPERIMENTAL

Chromatographic conditions

A liquid chromatograph consisting of an M6000A pump (Waters Assoc., Milford, MA, U.S.A.), a Rheodyne 7125 sampling valve (Kontron, Munich, G.F.R.) and a 254-nm UV detector (home-built) were used. To equilibrate and to control the water content of the eluent dichloromethane, a moisture control system (MCS)¹¹ was used as an eluent reservoir. To maintain a water concentration of 100 ppm the funnel of the MCS was filled with 300 g of alumina (Woelm Pharma, Eschwege, G.F.R.) coated with 1% (w/w) of water. This is sufficient to equilibrate up to 500 ml of dichloromethane. The temperature of the MCS, of the eluent and of the column was maintained at 25 ± 0.1 °C by a water thermostat (Haake, Karlsruhe, G.F.R.). The eluent was first equilibrated by recycling through the MCS. The columns had been equilibrated with the eluent for 14–16 h at a flow-rate of 2 cm³/min, which was used also during chromatography. Stainless-steel columns¹² (25 × 0.41 cm I.D.) were packed as described earlier¹³. The volumes of the empty columns were determined volumetrically. The packing density was measured gravimetrically after unpacking the column and evaporation of the eluent. The samples (mono- and bifunctional benzene derivatives) were taken from the laboratory stock and, if necessary, distilled before use. Always 1 μ l of each 1% solution was injected.

Materials

The following silica stationary phases were studied: Hypersil (Shandon, Frankfurt/Main, G.F.R.), LiChrosorb, LiChrospher (Merck, Darmstadt, G.F.R.), Nucleosil (Machery, Nagel & Co., Düren, G.F.R.), Porasil (Waters), Spherisorb (Phase Separations, Queensferry, Great Britain) and Zorbax (DuPont, Bad Nauheim, G.F.R.). A home-made silica (H 80-10) was also used. If available, materials with a particle diameters of 10 μm were used.

Physical characterization

The specific surface areas were determined by nitrogen adsorption using an Arcameter II (Fa. Ströhlein Labortechnik, Stuttgart, G.F.R.) applying the "single-point differential method" according to Haul and Dümbsen^{14,15} (DIN 66132). The silicas were dried in stream of nitrogen at 130° C for 24 h.

Pore volumes and average pore diameters were determined by exclusion chromatography¹⁶ using polystyrene standards between $2.6 \cdot 10^6$ and 600 daltons. The volume of the eluent within the column (V_M) was defined by the elution volume of benzene, and the interstitial volume (V_Z) from the elution volume of the $2.6 \cdot 10^6$ dalton polystyrene standard. From these volumes and that of the empty column (V_K) the total porosity ϵ_T (V_M/V_K) and the interstitial porosity ϵ_Z (V_Z/V_K) were calculated. In Table I the physical properties and columns parameters of some of the silicas are summarized.

The pH values of the silicas were determined in 1% (w/w) suspensions in doubly distilled water with a glass electrode (EA 121) and a Metrohm E 536 potentiograph (Metrohm, Herisau, Switzerland)¹⁷.

RESULTS AND DISCUSSION

Normalization of capacity ratios

The k' values depend on the polarity of the sample and of the eluent and, of course, on the properties of the stationary phase. The k' values are proportional to the adsorption coefficient and to the phase ratio. If identical samples and eluents are used and the k' values are standardized for differences in the phase ratio, the "adsorption coefficient", K^* , thus obtained should depend only on the surface properties of

TABLE I
PHYSICAL PROPERTIES OF THE SILICA USED

Silica	Specific surface area (m^2/g)	Average pore diameter (nm)	Specific pore volume (cm^3/g)	Column porosities		Packing density (g/cm^3)
				ϵ_T	ϵ_Z	
Hypersil	170	11.5	0.7	0.78	0.43	0.53
LiChrosorb Si 100	320	11.1	1.2	0.83	0.41	0.34
Porasil	350	10.0	1.1	0.88	0.46	0.37
Spherisorb	190	8.1	0.6	0.77	0.43	0.61
Zorbax BPSil	300	5.6	0.5	0.71	0.42	0.60
H 80-10	450	7.5	1.1	0.84	0.45	0.37

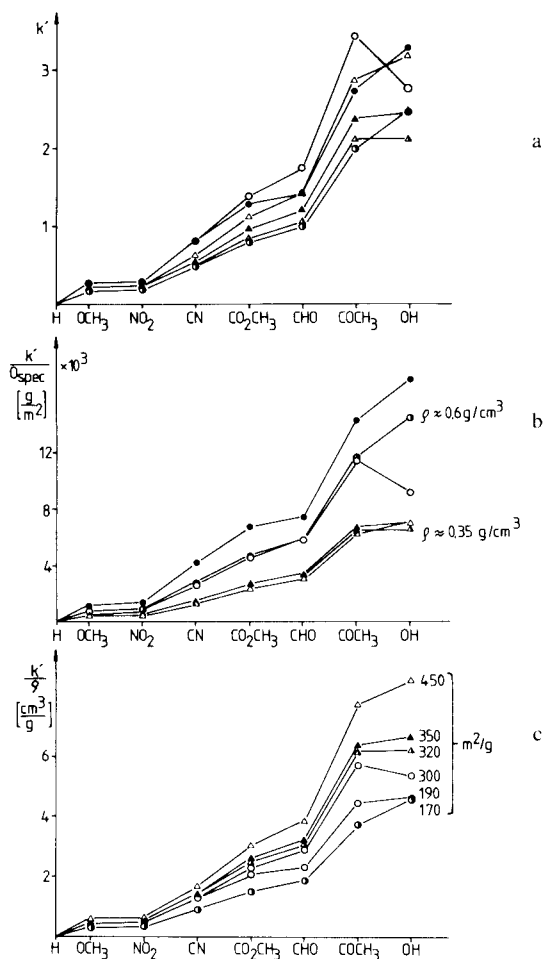


Fig. 1. Normalization of retention parameter. (a) Measured k' values; (b) k' normalized for differences in specific surface areas; (c) k' normalized for packing density differences. Stationary phases: Hypersil (●); LiChrosorb Si 100 (▲); Porasil (▲); Spherisorb (●); Zorbax (○); H 80-10 (△). Columns: 25 cm × 4.1 mm I.D. Eluent: Dichloromethane containing 100 ppm of water. Flow-rate: 2 cm³/min. Samples: Benzene, anisole, nitrobenzene, benzonitrile, methyl benzoate, benzaldehyde, acetophenone, phenol.

the stationary phases. In adsorption chromatography usually the specific surface area is taken as the volume of the stationary phase.

This standardization procedure is demonstrated in Fig. 1. The k' values of benzene derivatives as obtained with the different silica columns are shown in Fig. 1a. The k' values increase with increasing sample polarity, as expected, and no comparison of the different silicas is possible, because their order changes from solute to solute. The normalization for the differences in specific surface area is demonstrated in Fig. 1b. The retention values are much higher with the spherical than with the irregular silicas, owing to the larger packing densities of the spherical materials (larger surface area per unit column volume). If the k' values are normalized for

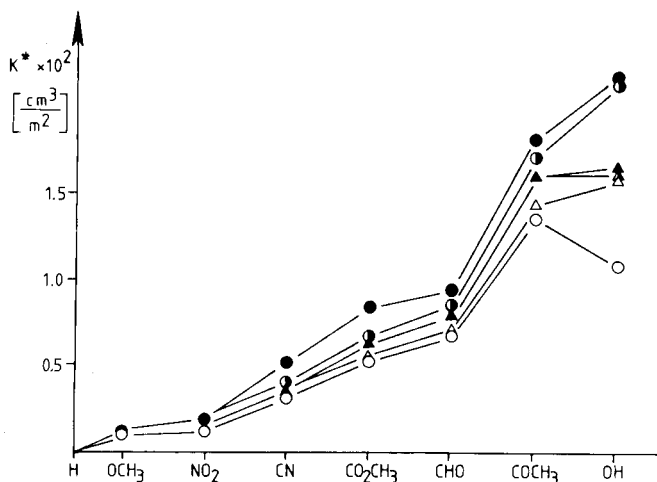


Fig. 2. Adsorption coefficient, K^* , for neutral and acidic solutes on different silicas. Conditions as in Fig. 1.

differences in packing density, as shown in Fig. 1c, they increase with increasing surface area. This is another indication that specific values (usually given per gram) are less important in chromatography because retention depends only on the values per unit column volume. Therefore, the k' values have to be normalized for the specific surface areas and for the packing densities. Table I shows that the packed columns differ also in their total porosities, v_T , *i.e.*, the volume of mobile phase per unit column volume. For these reasons in this paper the "adsorption coefficient", K^* (cm^3/m^2), was calculated according to

$$K^* = k' \cdot \frac{\epsilon_T}{O_{\text{spec}} \cdot \rho}$$

to compare the retention behaviour of the solutes on the different silica columns¹⁰.

In Fig. 2 these K^* values are plotted for different samples on the different silicas. If the surface properties of the silicas were to be identical, an identical sorption mechanism should result in a single line. For slightly retained solutes such as anisole and nitrobenzene this may be partly true, but for more polar solutes large variations in K^* reflect the differences in the surface nature of the silicas. The K^* values are very divergent with the most polar component in this series, *e.g.*, phenol.

Surprisingly large changes in K^* are observed if basic or other nitrogen-containing solutes are separated on different silicas, as shown in Fig. 3. The order of elution of the anilines on the silicas is not a function of their basicity or their hydrogen bonding capabilities. From Zorbax columns these components could not be eluted in a reasonable time ($k' < 20$) with the standard conditions applied. This different behaviour of Zorbax to all the other silicas cannot be explained solely by differences in the surface concentration of the weakly acidic silanol groups⁴.

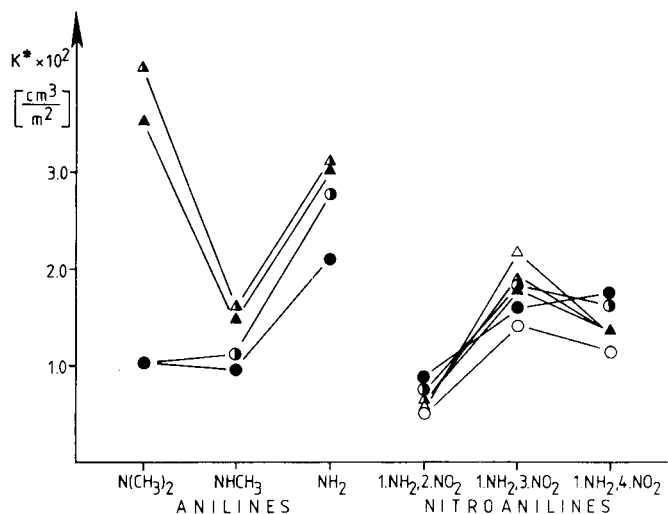


Fig. 3. Adsorption coefficient, K^* , for basic solutes. Conditions as in Fig. 1. Solutes: N,N-dimethylaniline, N-methylaniline, aniline and isomeric nitroanilines.

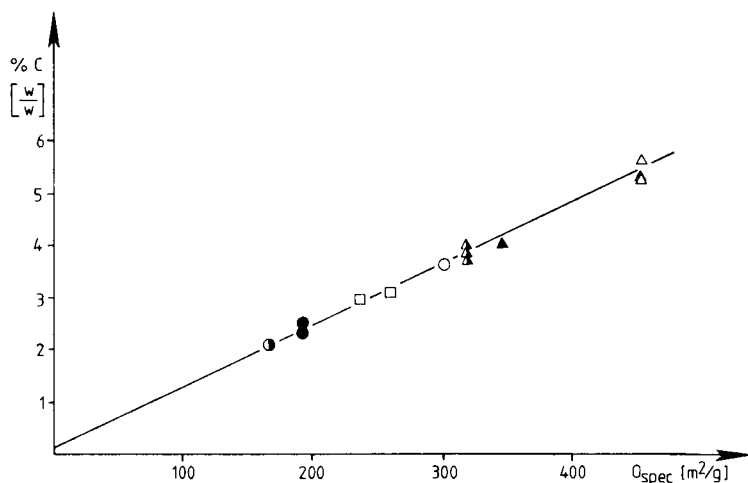


Fig. 4. Specific surface area and carbon content after silanization. Silanizing agent: trimethylchlorosilane. Silicas as in Fig. 1.

Surface properties

Retention on silica should depend on the surface concentration of the silanol groups. Because the silicas used here are prepared in different ways^{3,4}, we first tried to trace the selectivities demonstrated in Figs. 2 and 3 to differences in surface silanol concentrations. The total amount of surface silanols can be calculated from the total amount of water lost at 1000°C¹⁸ minus the amount of physisorbed water, determined from the same silica at the same time by Karl-Fischer titration¹⁹. Despite the large differences in their specific surface areas for LiChrosorb Si 100 and Spherisorb, values between 8.9 and 8.6 $\mu\text{mol}/\text{m}^2$ were obtained by this method. On average, $8.7 \pm$

TABLE II

pH VALUES OF DIFFERENT SILICAS MEASURED IN A 1% (w/w) AQUEOUS SUSPENSION

<i>Silica</i>	<i>pH</i>	<i>Regular (R) or irregular (I)</i>
Zorbax BPSil	3.9	R
LiChrospher Si 100	5.3	R
Nucleosil 100-7	5.7	R
H 80-10 (home-made)	6.5	I
LiChrosorb Si 100	7.0	I
Porasil	7.2	I
Partisil 10	7.5	I
LiChrosorb Si 60	7.8	I
Polygosil 60-5	8.0	I
Spherosil XOA 400	8.1	R
Hypersil	9.0	R
LiChrospher Si 1000	9.2	R
Spherisorb S 10 W	9.5	R
LiChrospher Si 500	9.9	R

0.2 $\mu\text{mol}/\text{m}^2$ had been determined for all the silicas with widely differing specific surface areas. These values are in good agreement with those given in the literature^{4,20}.

When a silica surface is modified with chlorosilanes, only the accessible silanol groups should react. Differences in this silanol concentration should result in different carbon contents per unit surface area of the chemically modified phases²¹. To prevent problems with reactivity and accessibility, trimethylchlorosilane was used as a silanizing agent. Fig. 4 shows that the relationship between carbon content and specific surface area is linear. The achievable surface concentration of the trimethylsilyl group was independent of the silica at $3.7 \pm 0.2 \mu\text{mol}/\text{m}^2$. These values cannot explain the differences in the chromatographic properties of the silicas.

The large differences in the elution behaviour of the anilines led us to compare the pH values of the different silicas in aqueous suspensions¹⁷. It is expected that the surface of pure silica should be weakly acidic owing to the $\text{p}K_a$ value of 9.8 for orthosilicic acid⁴. A suspension of silica in neutral de-salted water should give a pH value of about 5 (ref. 3). Surprisingly, the pH values of the silicas measured in a 1% (w/w) suspension in neutral doubly distilled water deviated greatly from this value. In Table II some of the commercially available silicas are listed in order of increasing pH value. Irregular silicas seem to have the expected pH values between 6 and 7, whereas the specially prepared spherical silicas for HPLC are either acidic or basic.

It should be added that the pH values depend on the concentration of neutral salts in the suspension. Generally, addition of a neutral salt leads to a decrease in the pH of the suspension, owing to an exchange of hydrogen ions of the silanols against the cations of the added salt forced by the law of mass action. On adding sodium chloride to obtain a 20% (w/w) solution, the pH of the LiChrosorb Si 100 suspension decreased from 7.0 to 4.5 and that of Spherisorb from 9.4 to 6.0, whereas that of Zorbax decreased only from 3.9 to 3.3.

pH and chromatographic retention

These pH values, of course, cannot be related to the pH of the silica used in a chromatographic column with a non-polar eluent. However, it can be demonstrated that the pH value measured in aqueous suspension can be correlated with the retention behaviour of polar and non-polar solutes. Fig. 5 shows the separation of anilines and *m*-nitroanilines on a "basic" (Hypersil) (Fig. 5a) and on a "neutral" (Porasil) (Fig. 5b) silica. With the "neutral" silica the strongest base, N,N-dimethylaniline, is eluted last, whereas on the "basic" Hypersil it is eluted as the first of the anilines. The

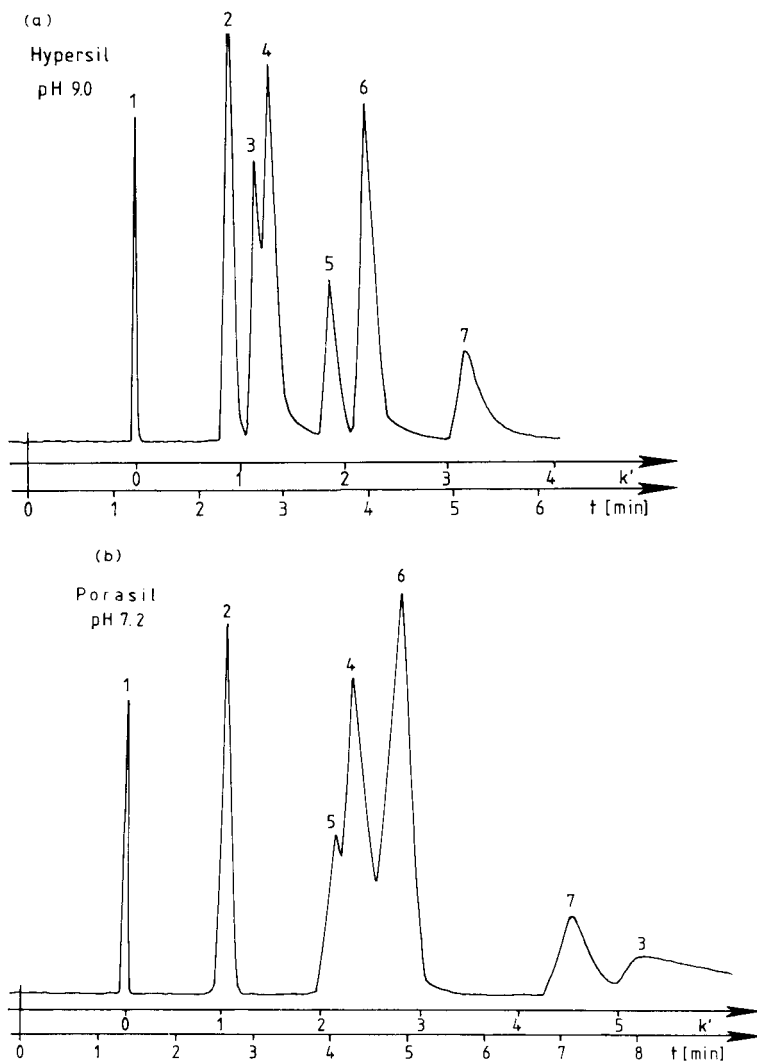


Fig. 5. Separation of basic compounds on "basic" and "neutral" silica. Chromatographic conditions as in Fig. 1. Stationary phases: (a) Hypersil and (b) Porasil. Solutes: 1 = benzene; 2 = *o*-nitroaniline; 3 = N,N-dimethylaniline; 4 = N-methylaniline; 5 = *p*-nitroaniline; 6 = *m*-nitroaniline; 7 = aniline.

efficiency and the symmetry of the peaks also increase with increasing pH of the silica surface. The relative retentions of the nitroanilines also change as a function of the "neutral" or "basic" silica surface. From "acidic" silicas ($\text{pH} < 6.5$) the anilines cannot be eluted as measurable peaks within a reasonable time.

The influence of the pH of the silicas on the separation of acidic compounds is demonstrated in Fig. 6. Phenol is eluted as a very symmetrical peak from the "acidic" Zorbax column (Fig. 6b), whereas it is eluted with severe tailing from the "basic" Spherisorb column (Fig. 6a). The absolute and relative retentions of the neutral phenyl alcohols are also influenced by the pH of the silicas.

It seems that the selectivity for the separation of aromatic hydrocarbons with

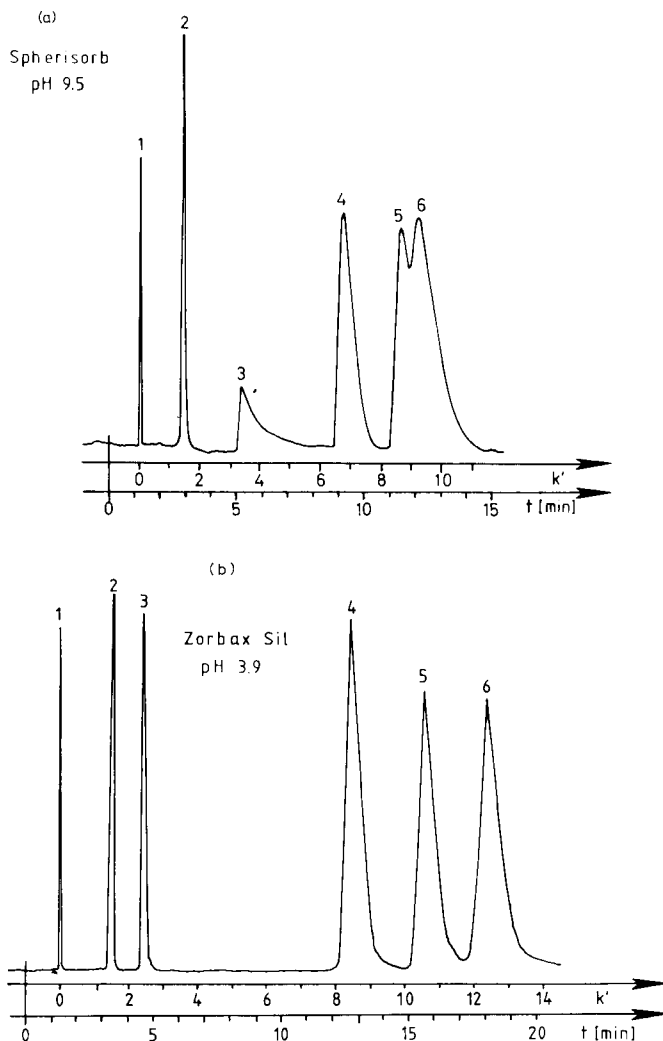


Fig. 6. Separation of neutral and acidic compounds on "basic" and "acidic" silica. Chromatographic conditions as in Fig. 1. Stationary phases: (a) Spherisorb and (b) Zorbax. Solutes: 1 = benzene; 2 = benzaldehyde; 3 = phenol; 4 = benzyl alcohol; 5 = 2-phenylethanol; 6 = 3-phenylpropanol-1.

n-heptane as eluent is also affected by the surface pH. This may explain the increase in the selectivity when changing from a large surface area silica (LiChrospher Si 100) to one with a smaller surface area (LiChrospher Si 4000)¹⁰.

Acid- and base-treated silicas

To confirm these experimental results the pHs of different silicas were adjusted to high values by titration with 0.1 *N* sodium hydroxide in an aqueous suspension containing 20% (w/w) sodium chloride²². To obtain acidic surfaces, 10 g of silica were treated three or four times with 200 ml of 1 *N* hydrochloric acid. These materials were washed with distilled water until the pH of the washings was neutral. After drying they were packed as usual and their chromatographic properties determined. The basic treatment leads to a smaller specific surface area and to a larger average pore diameter if a pH of 8.5 is exceeded. By this treatment the surface area of LiChrosorb Si 100 decreased from 320 to 240 m²/g and its pore diameter increased from 11 to 13 nm if treated at a pH of *ca.* 9.

The alteration of the chromatographic selectivity for the separation of nitrogen compounds is demonstrated in Fig. 7 for basic-treated silicas. The higher the pH of the initially neutral silica was increased, the smaller the *k'* values of the anilines became and the more symmetrical their elution curves. It should be noted that the elution order approaches that on the Hypersil column (Fig. 5a) if the pH of the treated silica exceeds 9.

The initially basic Spherisorb was adjusted to a pH of 6.5. The separation of phenols and phenyl alcohols with this material is shown in Fig. 8. By comparing the elution profile of phenol here with that on the starting material (Fig. 6a), the improvement obtained is remarkable. As mentioned before, the selectivity for the separation of the phenyl alcohols is also improved. After the acid treatment of this initially basic material the anilines can no longer be eluted.

Similar changes in the selectivity of silica on treating silicas with acidic or basic buffer solutions were described by Schwarzenbach^{23,24}. It would not be surprising if the selectivity achieved with such systems were to be different from those obtained with titrated silicas. By coating silicas with buffers the surface is also covered with the anionic counter ions, which also may contribute to stationary phase selectivity. Of course, adding acids or bases to the eluent can also help in adjusting the selectivity.

Characterization of packed columns

From the above it is evident that one should know which kind of silica has been used in preparing a column, if acidic or basic solutes have to be separated. When anilines and other basic nitrogen compounds cannot be eluted from a column, it follows that it was packed with acidic silica. If phenol is eluted with more tailing than for neutral compounds, the surface of the silica may be neutral or basic. In this case, acid washing of the packed column may improve the elution profile of phenol and other acidic compounds. An analogous basic treatment of a packed column, however, is impossible and in this case one should use another type of silica.

The relative retentions of *p*- and *o*-nitroaniline are hardly affected by the pH of the stationary phase, and in our work were between 2.0 and 2.2, whereas the α values for *m*- and *p*- and also for *m*- and *o*-nitroaniline show a more pronounced dependence on the pH of the silicas. It seems possible to use these selectivities for surface charac-

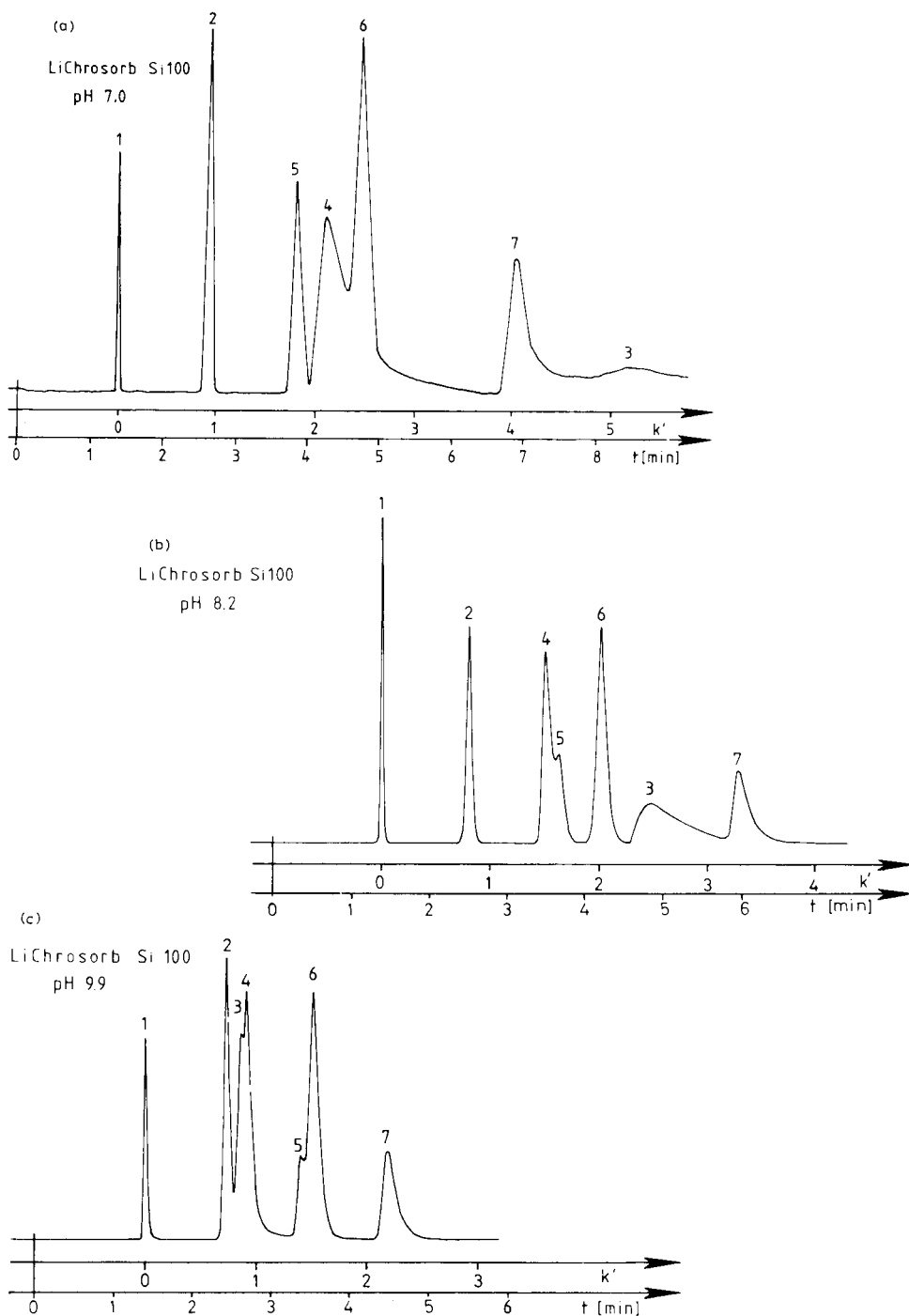


Fig. 7. Separation of basic solutes on basic-treated silica. Conditions and solutes as in Fig. 5. Stationary phases: LiChrosorb Si 100, (a) untreated, (b) pH adjusted to 8.2, (c) pH adjusted to 9.9.

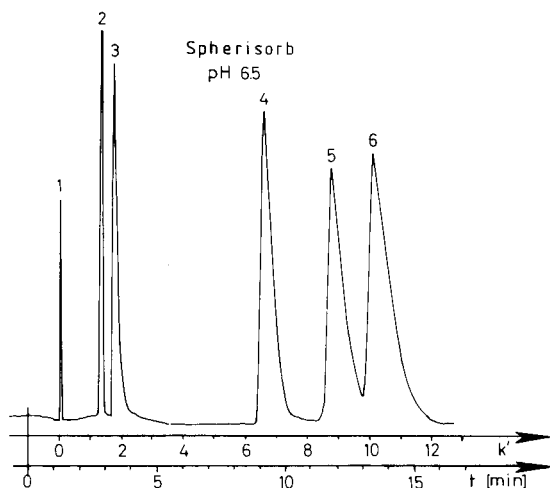


Fig. 8. Separation of neutral and acidic compounds on an acid-treated "basic" silica. Conditions and solutes as in Fig. 6. Stationary phase: Spherisorb, pH adjusted to 6.5.

terization; however, this needs further investigation with more and different silica samples.

CONCLUSION

The different commercially available silicas differ in their physical properties such as specific surface area, specific pore volume and average pore diameter, and the columns contain different amounts of stationary and mobile phase per unit column volume. If the retention parameters are normalized for this, distinct selectivities of the different silicas are still noticeable. Not only silicas with the expected neutral surface reaction but also acidic and basic silicas are commercially available, but this information is usually not stated on the labels as has been the custom for alumina preparations^{25,26}.

For the separation of neutral substances the efficiencies and selectivities obtainable with these different silicas may be optimal, reproducible and sufficient. However, if polar samples have to be separated the surface characteristics may influence peak retention, peak shape and efficiency. Hence "acidic silicas" may prove to be more efficient with neutral and acidic solutes than with basic, nitrogen-containing samples. The opposite, of course, may be true for "basic silicas" and the separation of basic or neutral samples. The classical and usually neutral silicas are in between these extremes. Owing to slight changes in their apparent pH around 7, these silicas may prove better for acidic or for basic solutes. Because of these problems there is no ideal silica for the separation of both acidic and basic samples. It is difficult to determine these characteristics with pre-packed columns. Therefore, it is recommended that the manufacturers should state at least the pH of their silicas.

It seems evident that these properties of the silicas also influence the properties of bonded phases prepared from them. In these cases, where aqueous eluents have to

be used, the acidity or basicity of the starting carrier material is also a contributory determinant.

ACKNOWLEDGEMENT

Financial support of this work by the Deutsche Forschungsgemeinschaft, Bonn-Bad Godesberg, is gratefully appreciated.

REFERENCES

- 1 L. R. Snyder, *Principles of Adsorption Chromatography*, Marcel Dekker, New York, 1968.
- 2 H. Engelhardt, *High Performance Liquid Chromatography*, Springer, New York, Heidelberg, Berlin, 1979.
- 3 K. K. Unger, *Porous Silica*, Elsevier, Amsterdam, 1979.
- 4 R. K. Iler, *The Chemistry of Silica*, Wiley-Interscience, New York, 1979.
- 5 H. Engelhardt, in Cs. Horváth (Editor), *High Performance Liquid Chromatography, Advances and Perspectives*, Vol. 2, Academic Press, New York, 1980, pp. 57-111.
- 6 R. Ohmacht and I. Halász, *Chromatographia*, 14 (1981) 155.
- 7 K. K. Unger, W. Messer and K. F. Krebs, *J. Chromatogr.*, 149 (1978) 1.
- 8 R. Ohmacht and I. Halász, *Chromatographia*, 14 (1981) 216.
- 9 R. P. W. Scott, *J. Chromatogr. Sci.*, 12 (1974) 473.
- 10 J. F. K. Huber and F. Eisenbeiss, *J. Chromatogr.*, 149 (1978) 127.
- 11 W. Böhme and H. Engelhardt, *J. Chromatogr.*, 133 (1977) 67.
- 12 J. Asshauer and I. Halász, *J. Chromatogr. Sci.*, 12 (1974) 139.
- 13 H. Elgass, H. Engelhardt and I. Halász, *Z. Anal. Chem.*, 294 (1979) 97.
- 14 R. Haul and G. Dümbgen, *Chem.-Ing. Techn.*, 32 (1960) 349.
- 15 R. Haul and G. Dümbgen, *Chem.-Ing. Techn.*, 35 (1963) 586.
- 16 I. Halász and K. Martin, *Angew. Chem.*, 90 (1978) 954.
- 17 DIN 53200, Beuth Verlag, Berlin, 1978.
- 18 DIN 55921, Beuth Verlag, Berlin, 1980.
- 19 W. Noll, K. Damm and R. Fauss, *Kolloid Z.*, 169 (1960) 18.
- 20 H. P. Boehm, *Advan. Catal.*, 16 (1966) 226.
- 21 H. Schmidt, *Ph.D. Thesis*, Saarbrücken, 1978.
- 22 G. W. Sears, Jr., *Anal. Chem.*, 28 (1956) 1981.
- 23 R. Schwarzenbach, *J. Liq. Chromatogr.*, 2 (1979) 205.
- 24 R. Schwarzenbach, *J. Chromatogr.*, 202 (1980) 397.
- 25 G. Hesse, I. Daniel and G. Wohleben, *Angew. Chem.*, 64 (1952) 103.
- 26 H. Böhme, H. J. Bohn and J. Roehr, *Arch. Pharm.*, 299 (1966) 282.

CHROM. 14,098

ESTIMATION OF AQUEOUS SOLUBILITIES OF ORGANIC NON-ELECTROLYTES USING LIQUID CHROMATOGRAPHIC RETENTION DATA

T. L. HAFKENSCHIED and E. TOMLINSON*

Subfaculty of Pharmacy, University of Amsterdam, Plantage Muidergracht 24, 1018 TV Amsterdam (The Netherlands)

SUMMARY

The use of reversed-phase liquid chromatographic retention parameters in a modified Hildebrand–Scott equation to describe the aqueous solubilities of non-electrolyte liquids and solids has been studied. The results indicate that, for 32 model solutes of various characters, a semiempirical relationship between aqueous solubility, a theoretical capacity factor obtained by extrapolation of retention data in simple binary systems to a pure aqueous eluent and a function of solute melting points and entropies of fusion can be used to give good estimates of aqueous solubilities. Relationships are given between extrapolated capacity factors and liquid–liquid distribution coefficients or smoothed surface areas. It is suggested that the assumptions and intricacies often needed to calculate the last two parameters make the chromatographic parameter an appropriate candidate for describing solute non-ideality and for use in the modified Hildebrand–Scott equation.

INTRODUCTION

Aqueous solubility has long been recognised as a key factor in pharmaceuticals and chemistry. The phenomenology of drug delivery, transport and distribution, the prediction of chemical environmental effects and development of analytical methods, etc., are dependent *inter alia* upon knowledge of aqueous solubilities. Aqueous solubilities are also of thermodynamic interest since they give information on the nature of non-ideal solutions.

The assessment of solubility can be extremely difficult, particularly for poorly soluble compounds. This may be due to very low equilibration rates, compound instability, the effect of impurities on solubility and (during a drug development programme) lack of sufficient compound or of a specific analytical technique. Discrepancies in reported solubilities are striking, for example Tulp and Hutzinger¹ have found that the aqueous solubility of DDT is between 0.2 and 1000 ppb (10^9). Thus there is a need to be able to make either *a priori* predictions of solubilities in simple and mixed systems or to form reliable estimates using readily obtainable parameters. A number of approaches^{2–7} to this problem have been made, with frequent use being made of semiempirical relationships between solubility and physicochemical properties.

Yalkowsky-Valvani equation

For a solid, taking as a good approximation that the latent heat of fusion, ΔH_f , is independent of temperature, and that the difference in heat capacities of the crystalline and molten forms of the solid is small, it can be shown^{8,9} that the temperature variation of the mole fraction ideal solubility of a pure solid (A_s), $X_{A_s}^i$, is described by

$$\ln X_{A_s}^i = \frac{\Delta H_f}{R} \cdot \left(\frac{1}{T_m} - \frac{1}{T} \right) \quad (1)$$

where T_m and T are the melting point and temperature at which pure solid is in equilibrium with the solution of mole fraction X . For a liquid solute (A_l) the Gibbs free energy excess function, $G_{A_l}^E$, is

$$G_{A_l}^E = RT \ln \gamma_{A_l} = (G_{A_l} - G_{A_l}^i) \quad (2)$$

where γ is the activity coefficient. Thus, it follows that

$$\log X_{A_l} = \log X_{A_l}^i - \log \gamma_{A_l} \quad (3)$$

and, using a mole fraction scale:

$$\log X_{A_l} = -\log \gamma_{A_l} \quad (4)$$

Since the entropy of fusion, ΔS_f , at T_m is given by $\Delta H_f/T_m$, eqns. 1 and 4 can be combined to give:

$$\log X_{A_s} = \frac{\Delta S_f}{2.3 R} \cdot \left(\frac{T_m - T}{T} \right) - \log \gamma_A \quad (5)$$

Eqn. 5 is similar to that derived by Yalkowsky and Valvani^{10,11} using a phenomenological approach without invoking excess functions; from this relationship it is apparent that the estimation of aqueous solubilities of a solid requires knowledge of a term reflecting solid-solid interactions, and one describing solute-solvent and solute-solute interactions. Yalkowsky and Valvani¹⁰ have suggested that, as ΔS_f is often constant, the first term be described by some function of T_m ; and that, since most compounds of pharmaceutical (*sic*) interest have solubility parameters which do not differ greatly from that of octan-1-ol, then the second term in eqn. 5 can be approximated by the water-octan-1-ol liquid-liquid distribution coefficient¹², K_d (by implying that the solute activity coefficients in this oil are unity). This gives

$$\log X_A = -K \log K_{dA} - K' T_{m_A} - K'' \quad (6)$$

which may be regarded as the Yalkowsky-Valvani equation¹⁰. Although this approach has been used by others¹³, problems arise with the use of this K_d scale; in practice, it is extremely difficult to determine $\log K_d$ values greater than 4, solutes need to be pure and stable and there is a high solute consumption. If one resorts to calculation of K_d via a group or fragmental constant approach¹⁴, problems arise with

complicated structures¹⁵ and neighbourhood effects; also the data banks available are unable to predict K_d in mixed solvents (as would be the intention for estimating solute solubilities in the presence of a cosolvent).

The high precision afforded by modern liquid chromatography has prompted the use of this technique for estimating various physicochemical properties of small organic molecules. These include distribution coefficients^{15-17*}, ionization constants^{18,19}, complex formation constants²⁰, diffusion coefficients²¹ and critical micelle concentrations²². It has been demonstrated¹⁷ that the use of reversed-phase high-performance liquid chromatographic (HPLC) retention parameters is suitable for indicating solute chemical potentials in polar solvents, and it appeared useful therefore to attempt to use the Yalkowsky-Valvani model to extend the applicability of HPLC to estimations of aqueous solubilities. Our findings are now described.

EXPERIMENTAL

Materials

Model solutes used were (Table I) benzene and mono- and 1,4-disubstituted benzenes (functional groups CH_3 , Cl , NO_2 , OH , NH_2 and COOH), naphthalene, azulene, anthracene, phenanthrene and isopropyl derivatives (with the above functional groups). These were of synthetic or analytical grade and were obtained from E. Merck (Darmstadt, G.F.R.), Fluka (Buchs, Switzerland), BDH (Poole, Great Britain), ICN Pharmaceuticals (Plainview, NY, U.S.A.) and Aldrich (Milwaukee, WI, U.S.A.). The stationary phase was Hypersil ODS (5 μm) (Shandon, Astmoor, Great Britain). Mobile phases were made up by volume using methanol (analytical grade; J. T. Baker, Phillipsburgh, NJ, U.S.A.) and either (i) water, once distilled from an all-glass still, (ii) 10 mM aqueous phosphate buffer (pH 2.15; ionic strength 0.01 M) or (iii) 2.5 mM aqueous hexadecyltrimethylammonium bromide solution (to give a final eluent concentration not exceeding 0.75 mM). Hexadecyltrimethylammonium bromide (HTAB) was of analytical grade (E. Merck).

Instruments and columns

Chromatographic equipment consisted of an Altex 110A single piston pump (Altex, Berkeley, CA, U.S.A.) with additional dampening, a Model 7125 injection valve (Rheodyne, Berkeley, CA, U.S.A.) and Waters 440 UV absorbance and R401 refractive index detectors (Waterx Assoc., Milford, MA, U.S.A.) arranged in tandem. Peak recording was achieved with a Kipp BD 41 flat-bed potentiometric recorder (Kipp & Zn., Delft, The Netherlands). The eluent reservoir and the column were kept at $20.00 \pm 0.01^\circ\text{C}$ by immersion in a Hetotherm 02PT 623 thermostat water-bath (Heto, Birkerød, Denmark). The eluent reached the injection valve via a 1-ml coil immersed in the water-bath.

Procedures

Columns (100 \times 3 mm and 50 \times 4.6 mm) were of stainless steel (316), and were packed using a slurry of stationary phase (3%, w/v) in carbon tetrachloride-methanol (95:5, v/v), with methanol as packing liquid. Solutes were dissolved in the

* To date, 33 studies have been reported; these references will enable such studies to be identified.

eluent and retention times measured using a Model 310 microsplit stop watch (Heuer, Bienne, Switzerland), with corrections being made for dead volumes of connections. The capacity factor, k , was calculated from $(t \cdot t_0^{-1} - 1)$, where t and t_0 are the corrected solute retention time and the retention time of eluent slightly enriched with water. All k values were calculated from the mean of at least four t values, and had coefficients of variance of less than 0.5%.

Where necessary, aqueous solubility determinations were carried out by shaking/ultrasonication (at 20°C) a supersaturated solution until equilibration, followed by ultracentrifugation, filtration and sampling.

Multiple linear regressions were carried out using a standard computer program.

RESULTS AND DISCUSSION

Using a fixed column and eluent at a given flow and temperature, the retention of a solute in the case of pure solvophobic chromatography is dependent upon the solvation of the solute²³, *i.e.*

$$\kappa = \text{constant} + \left(\frac{\Delta G_e + \Delta G_i}{2.3 RT} \right) \quad (7)$$

where κ is the logarithmic form of k ; the free energy of solvation is given by the excess free energy, G^E , and is the sum of the free energies required to create a cavity in the eluent for the solute, ΔG_e , and that gained due to interactive forces upon placing the solute in the eluent, ΔG_i . The excess free energy arising from placing a solute in the eluent is thus a measure of the deviation from ideal behaviour, such that $G^E = 0$ if the solute is "equivalent" to the eluent. Since²⁴

$$G_A^E = RT \ln \gamma_{A_e} \quad (8)$$

where subscript *e* refers to eluent, and for which it is assumed²³ that stationary phase activity is constant, then the use of water as the eluent, combined with the knowledge that²⁵

$$\ln \gamma_{A_e} = (A/RT) x_w^2 \quad (9)$$

where A is a constant for a given system (accounting for solute-solute, solute-solvent and solvent-solvent interactions) and x_w is the mole fraction of water in a saturated solution, results in an approximately constant value of $\ln \gamma_{A_e}$ if x_w approaches unity. Thus, at low solubility ($x_w \approx 1$), this gives (after combination of eqns. 7, 8 and 9), κ_A in a purely aqueous eluent, κ_{wA} , as a measure of $\log \gamma_A$ in a saturated solution, *viz.*:

$$\log \gamma_{A_{\text{saturated}}} = \kappa_A - \text{constant} \quad (10)$$

For poorly soluble solutes the use of water as eluent in a reversed-phase LC system is made untenable by excessive retention and insufficient detector sensitivity. However, we can approach a value for the capacity ratio in water using extrapolation

techniques. One such method is to relate k to the organic modifier volume fraction, φ , in the eluent, as has been formalized by²⁶

$$\kappa = \kappa_w + B\varphi \quad (11)$$

where κ_w refers to the logarithmic form of the solute capacity factor in pure water.

In this study we have examined the retention of 32 aliphatic and aromatic organic solutes in a reversed-phase mode (see Experimental) using three different eluents, *i.e.*, water-methanol, aqueous buffer (pH 2.15)-methanol and aqueous hexadecylammonium bromide-methanol, using a volume fraction of organic modifier of 0.3–0.90. The data obtained have been analysed using linear regression analysis, and the results are given in Table I for all eluents examined. It can be seen that eqn. 11 well describes retention of the studied volume fraction range, with correlation coefficients being in only one case less than 0.999. For some solutes, deviations from linearity occurred at high volume fractions; here, the resulting low retentions can lead to large inaccuracies in determining k . Moreover, the buffering capacity of the eluent for some carboxylic acids may be too low in this study (methanol increases eluent pH at $\varphi > 0.75$, *ref.* 27). In these cases regression analysis was restricted to the linear portion of the κ *versus* φ plot.

For ionizable solutes, buffered eluents were used to obtain κ_w values, with the addition of buffer to the eluent being tested for other non-ionizable reference solutes (Table I). Thus, for eight reference solutes, the presence of buffer had none or negligible effect on either B or κ_w , which justifies (i) the use of buffering to obtain κ_w for non-ionized solutes and (ii) the inclusion of data from a buffered and a non-buffered system in the same data set.

Recently it has been suggested²⁸ that silanol groups at the surface of reversed stationary phases may be responsible for departure from the retention behaviour expected on the basis of solvophobic theory²³. Being cognisant of this, we have added a silanol-masking compound (hexadecyltrimethylammonium bromide) to the eluents for three solutes expected to be silanophilic²⁹, and the results obtained are also given in Table I. Apart from expected ion-pair effects where appropriate, HTAB affected the retention of the reference compounds only very slightly at volume fractions of organic modifier less than 0.6. Apart from the solutes given in Table I, retention was studied for 4-aminophenol, 1,4-diaminobenzene, 2-aminopropane and trimethylamine. These solutes either did not have proper solvophobic retention (exclusion phenomena, irregular peak shape) or decomposed before or during chromatography.

Using Hypersil ODS and aqueous methanol eluents for the compounds studied, the value of B from the κ *versus* φ relationships (eqn. 11) ranges from -1.4 to -5.2 , and has an approximate rank order with the intercept (κ_w) values. This is shown in Fig. 1, which may be described by

$$\kappa_w = -1.18 B - 1.54 \quad (n = 32, r = 0.930) \quad (12)$$

where n and r are the number of solutes and the correlation coefficient respectively. The variation in B is contrary to the comment of Snyder *et al.*²⁶ that B is constant for any one stationary phase-eluent system, but is consistent with other findings, *e.g.*, *refs.* 17, 30, 31, that eluent changes alter hydrophobic and polar groups selectivity, and

	NH ₂ COOH				3.77	2.48	4	0.9990	2.17	1.05	5	0.9994
Cl	Cl	4.03	3.33	5	0.9998							
	NO ₂	3.31	2.44	4	0.9999							
	OH	3.33	2.21	5	0.9998							
	NH ₂	2.93	1.80	5	0.9992							
	COOH				3.86	2.70	4	0.9996				
NO ₂	NO ₂	2.87	1.72	5	0.9998							
	OH	3.09	1.77	5	0.9998							
	NH ₂	2.77	1.31	5	0.9993							
	COOH				3.27	1.99	4	0.9999				
OH	OH	2.33	0.29	5	1.000							
	COOH				3.01	1.20	4	0.9990				
H ₂	COOH				2.35	0.55	4	0.9999				
Naphthalene		4.07	3.32	5	0.9996							
Phenanthrene		5.06	4.42	4	0.9993							
Anthrane		5.20	4.58	4	0.9992							
CH ₃ · CH(R ³)CH ₃												
R ³ =	OH	1.37	0.18	4	0.9980	1.35	0.17	4	0.9998			
	NO ₂	1.98	0.90	4	0.9990	1.94	0.88	4	0.9999			
	Cl	2.70	1.92	4	0.9990	2.78	1.95	4	0.9980			
	COOH				2.16	0.95	4	0.9990				

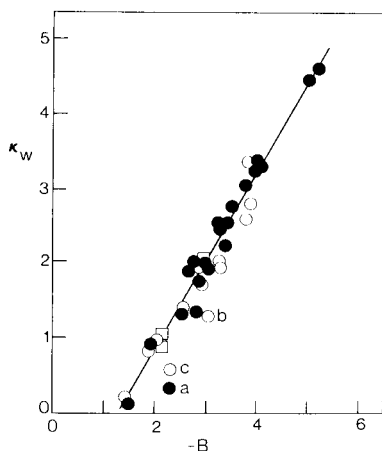


Fig. 1. Relationship between extrapolated log capacity factor, κ_w , and B derived using eqn. 11 for 32 non-electrolytes in a reversed-phase HPLC system. Eluents: ●, water methanol; ○, buffer methanol; □, aqueous HTAB solution methanol. The straight line is the regression line according to eqn. 12. a = *p*-Hydroxyphenol; b = *p*-hydroxybenzoic acid; c = *p*-aminobenzoic acid.

thus appears to reflect not only solvent strength²⁶ but also specific interactions between solutes, stationary phase and eluent¹⁵. Finally, from Table I, it can be seen that, since the relationships given by eqn. 11 are linear over a fairly wide range of volume fractions of organic modifier, there is no need to introduce a parabolic function, *i.e.*, ϕ^2 , as has been suggested³².

Estimation of aqueous solubilities of liquids

Table II gives the physicochemical data used in this study which comprises entropies of fusion (calculated from enthalpies of fusion^{33,34}), melting points^{33,34}, measured water-octan-1-ol distribution coefficients^{14,35} and aqueous solubilities (this study and ref. 36). The validity of introducing a liquid chromatographic retention term in the Hildebrand-Scott equation (eqn. 5) can be tested first by regressing solubility data from Table II for solutes that are liquids at 20°C with κ_w values obtained using eqn. 11, since the term $\Delta S_f/R [T_m - T/T]$ does not play a rôle. This results in:

$$-\log X_w = 0.54 + 1.34 \kappa_w \quad (n = 11, r = 0.959) \quad (13)$$

For the eleven liquids studied, both propan-2-ol and isobutyric acid are too soluble in water to obey the assumption that $\ln \gamma_{A_w}$ (eqn. 9) is constant, since x_w deviates significantly from unity. (For isobutyric acid this deviation is 3.9% and for propan-2-ol 100%.) Regression of the data without these two compounds gives (Fig. 2):

$$-\log X_w = 1.37 + 1.01 \kappa_w \quad (n = 9, r = 0.993) \quad (14)$$

The excellent correlation coefficient obtained and the fact that the coefficient of κ_w approximates to unity is in accord with theory (eqn. 10), and appears to validate the

TABLE II

PHYSICOCHEMICAL PROPERTIES OF MODEL SOLUTES

ΔS_f = Entropy of fusion^{33,34}; T_m = melting point^{33,34}; X_w = observed aqueous mole fraction solubility^{10,36}; SSA = smoothed surface area³⁸; K_d = observed water-octan-1-ol distribution coefficient^{14,35}.

Compound		ΔS_f (J/K·mol)	T_m (°C)	$-\log X_w$	K_w^*	SSA (Å ²)	$\log K_d$	
							obs.	calc.**
$R^1 \cdot C_6H_4 \cdot R^2$								
H	H	***	***	3.36	2.05	89.7	2.13	2.07
	CH ₃	***	***	4.00	2.59	107.0	2.74	2.61
	Cl	***	***	4.10	2.71	109.6	2.84	2.81
	NO ₂	***	***	3.51	1.91		1.87	1.79
	OH	35.9	40.9	1.77	1.35		1.48	1.51
	NH ₂	***	***	2.17	0.86		0.90	0.97
	COOH	43.8	122.4	3.29	1.92		1.87	1.86
CH ₃	CH ₃	***	***	4.54	3.19	124.2	3.15	3.09
	Cl	***	***	4.82 §	3.32	126.8	3.33	3.33
	NO ₂	50.2	54.5	4.13	2.48		2.39	2.31
	OH	40.2	34.8	2.44	1.91		1.94	2.03
	NH ₂	56.5	43.7	2.79	1.05		1.39	1.49
	COOH	51.9	182	4.29	2.48		2.27	2.39
Cl	Cl	56.1	53.1	5.00	3.35	129.5	3.39	3.57
	NO ₂	49.0	85.6	4.59 §	2.44		2.40	2.55
	OH	46.4	43.5	2.73	2.23		2.39	2.27
	NH ₂	57.7	72.5	3.41 §	1.80		1.83	1.73
	COOH	62.8	243	5.26	2.70		2.65	2.85
NO ₂	NO ₂	62.8	174	4.12	1.73		1.48	1.53
	OH	54.4	115	3.33	1.75		1.91	1.25
	NH ₂	50.2	149	4.12	1.31		1.39	0.71
	COOH	72.0	242	4.80	1.99		1.89	1.61
OH	OH	61.1	174	1.91	0.29		0.55	0.97
	COOH	51.1	215	2.98	1.20		1.58	1.32
NH ₂	COOH	45.6	189	2.96	0.55		0.68	0.79
Naphthalene		53.1	80.2	5.37	3.32	128.7	3.37	3.37
Phenanthrene		49.0	96.3	6.73	4.42	165.0	4.46	4.67
Anthracene		60.2	216.5	8.04	4.58	167.6	4.45	4.67
$CH_3 \cdot CH(R^3)CH_3$								
R ³ =	OH	***	***	0	0.18		0.05	-0.01
	NO ₂	***	***	2.36 §	0.89		0.87	0.62
	Cl	***	***	3.18	1.93		1.90	1.70
	COOH	***	***	1.41	0.95		0.82	0.64

* Mean values from Table I.

** Using hydrophobic fragment constants¹⁴.

*** Liquid at room temperature.

§ Determined in this study.

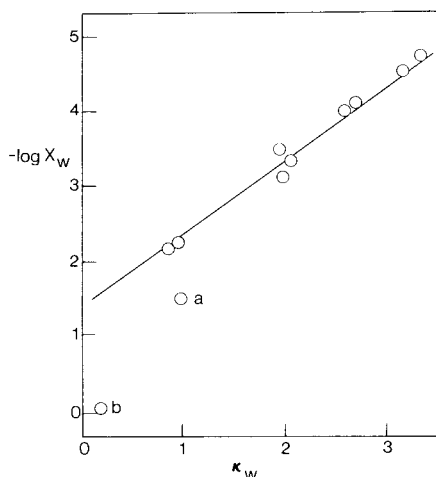


Fig. 2. Estimation of aqueous solubilities of liquids (at 20°C) from mean extrapolated log capacity factors, κ_w , using the general form of eqn. 13. The straight line is the regression line according to eqn. 14. Isobutyric acid (a) and propan-2-ol (b) are outliers since they do not obey the assumption given by eqn. 9.

substitution of $\log \gamma_A$ in eqn. 5 by $(\kappa_w - \text{constant})$. (Eqn. 14 implies that the product of κ_w and $\log X_w$ is constant for liquids, and so any structural modification that increases κ_w without altering the liquid state will result in an equivalent decrease in aqueous solubility.)

Estimation of aqueous solubilities of solids

Using the physicochemical constants given in Table II and the extrapolated κ_w values, the complete data set available for solids ($n = 21$) and for solids and liquids ($n = 32$) has been fitted by multiple linear regression to functions of κ_w and $\Delta S_f(T_m - 20)$, and (eqn. 6) κ_w and $(T_m - 20)$. These analyses gave

$$-\log X_w = 1.28 \kappa_w + 0.0073 (T_m - 20) + 0.42 \quad (15)$$

$(n = 21, R = 0.924, F = 55.4)$

$$-\log X_w = 1.27 \kappa_w + 0.0070 (T_m - 20) + 0.60 \quad (16)$$

$(n = 32, R = 0.956, F = 159.3)$

$$-\log X_w = 1.24 \kappa_w + 1.23 \times 10^{-4} \Delta S_f(T_m - 20) + 0.55 \quad (17)$$

$(n = 21, R = 0.924, F = 55.4)$

$$-\log X_w = 1.26 \kappa_w + 1.15 \times 10^{-4} \Delta S_f(T_m - 20) + 0.65 \quad (18)$$

$(n = 32, R = 0.955, F = 155.5)$

where R and F are the multiple correlation coefficient and the variance ratio. These results show that the aqueous solubilities for both liquids and solids can be estimated by use of the same semiempirical relationship, and that for this data set, the results are not improved by introduction of the ΔS_f term. This is in accord with previous suggestions¹⁰ that the variation in ΔS_f can be neglected. Yalkowsky and Valvani¹⁰ have shown that the ideal aqueous solubility of various classes of molecules can be calculated using the approximation

TABLE III

ESTIMATED AQUEOUS SOLUBILITIES USING HPLC RETENTION DATA TO DESCRIBE NON-IDEALITY

Compound		Estimated aqueous solubility ($-\log X_w$)	
		According to eqn. 16	According to eqn. 18
$R^1 \cdot C_6H_4 \cdot R^2$			
R^1	R^2		
H	H	3.20	3.24
	CH ₃	3.88	3.92
	Cl	4.04	4.07
	NO ₂	3.02	3.06
	OH	2.46	2.44
	NH ₂	1.69	1.74
	COOH	3.74	3.59
CH ₃	CH ₃	4.64	4.67
	Cl	4.81	4.84
	NO ₂	3.91	3.98
	OH	3.12	3.13
	NH ₂	2.12	2.13
	COOH	4.87	4.74
Cl	Cl	5.08	5.09
	NO ₂	4.14	4.08
	OH	3.59	3.59
	NH ₂	3.25	3.27
	COOH	5.58	5.66
NO ₂	NO ₂	3.87	3.94
	OH	3.48	3.45
	NH ₂	3.16	3.08
	COOH	4.67	5.00
OH	OH	2.04	2.10
	COOH	3.48	3.31
NH ₂	COOH	2.47	2.23
Naphthalene		5.23	5.20
Phenanthrene		6.74	6.65
Anthracene		7.78	7.78
$CH_3 \cdot CH(R^3)CH_3$			
$R^3 =$	OH	0.83	0.88
	NO ₂	1.73	1.77
	Cl	3.05	3.08
	COOH	1.80	1.85

$$-\log X_{A_s}^i = 0.01 (T_m - 25) \quad (19)$$

for rigid non-spherical molecules, and

$$-\log X_{A_s}^i = [0.01 + 0.0018 (n - 5)] (T_m - 25) \quad (20)$$

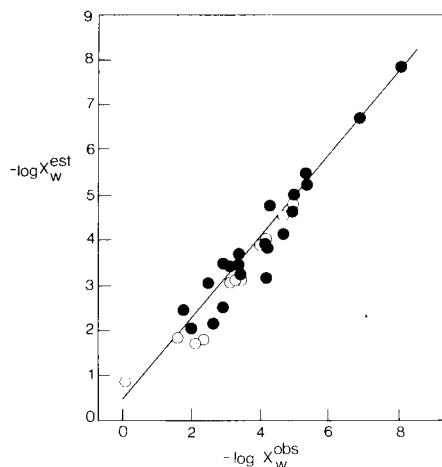


Fig. 3. Relationship between observed mole fraction aqueous solubilities for liquids (open points) and solids and solubilities estimated using the coefficients of eqn. 16.

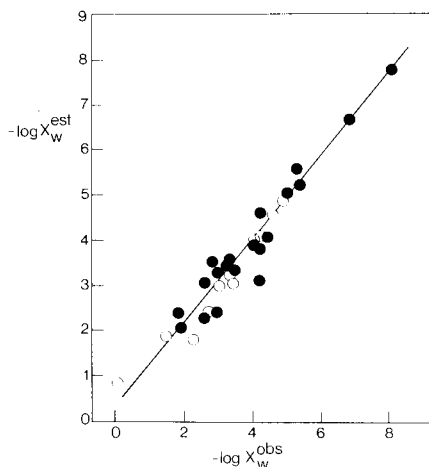


Fig. 4. Relationship between observed mole fraction aqueous solubilities for liquids (open points) and solids and solubilities estimated using the coefficients of eqn. 18.

for partially flexible molecules, where n is the number of carbon and/or heteroatoms in a solute sidechain, and where measurements are at 20 °C.

The good correlation found in this study using the approximations has prompted us to analyse the available data set with respect to structural groupings. Accordingly, eqns. 21–28 give the multiple linear regression analyses for four groupings according to the general forms of eqns. 16 and 18.

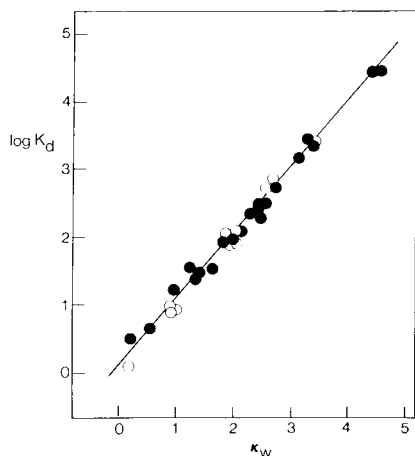


Fig. 5. Relationship between log extrapolated capacity factors, κ_w , according to eqn. 11 (Table II) and observed water-octan-1-ol distribution coefficients (Table II). The straight line is the regression line for all solutes according to eqn. 30. Key as in Fig. 3.

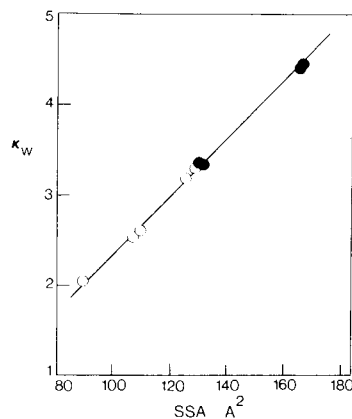


Fig. 6. Correlation between solute smoothed surface area, SSA^{38} , and κ_w . The straight line is the regression line according to eqn. 33. Key as in Fig. 3.

(i) Compounds with CH₃, Cl and NO₂ groups:

$$-\log X_w = 1.10 \kappa_w + 0.0085 (T_m - 20) + 1.18 \quad (21)$$

$$(n = 15, R = 0.989, F = 290.6)$$

$$-\log X_w = 1.13 \kappa_w + 1.37 \times 10^{-4} \Delta S_f (T_m - 20) + 1.14 \quad (22)$$

$$(n = 15, R = 0.986, F = 227.3)$$

(ii) Compounds with OH groups:

$$-\log X_w = 1.22 \kappa_w + 0.0093 (T_m - 20) - 0.07 \quad (23)$$

$$(n = 7, R = 0.956, F = 26.5)$$

$$-\log X_w = 1.29 \kappa_w + 1.71 \times 10^{-4} \Delta S_f (T_m - 20) - 0.14 \quad (24)$$

$$(n = 7, R = 0.968, F = 37.2)$$

(iii) Compounds with CO₂H groups:

$$-\log X_w = 1.28 \kappa_w + 0.0097 (T_m - 20) - 0.03 \quad (25)$$

$$(n = 5, R = 0.926, F = 9.02)$$

$$-\log X_w = 1.19 \kappa_w + 1.21 \times 10^{-4} \Delta S_f (T_m - 20) + 0.37 \quad (26)$$

$$(n = 5, R = 0.988, F = 61.4)$$

(iv) Compounds with NH₂ groups:

$$-\log X_w = 0.53 \kappa_w + 0.0127 (T_m - 20) + 1.80 \quad (27)$$

$$(n = 4, R = 0.988, F = 40.9)$$

$$-\log X_w = 0.40 \kappa_w + 2.63 \times 10^{-4} \Delta S_f (T_m - 20) + 1.91 \quad (28)$$

$$(n = 4, R = 0.991, F = 54.8)$$

From the variance ratios for these equations it is seen that the use of the melting point approximation is not always appropriate for closely related groups of compounds, and we conclude that further work is required to determine the validity of the approximation.

Table III gives the estimated aqueous solubilities found using eqns. 16 and 18, and Figs. 3 and 4 are plots of observed (Table II) and estimated aqueous solubilities (of liquids and solids) found using these relationships. It can be seen that use of the $(T_m - 20)$ or the $\Delta S_f(T_m - 20)$ term combined with κ_w gives estimates of aqueous solubilities ranging from reasonable to excellent, with better correlation being obtained for the more insoluble compounds. The study of compounds with even lower solubilities than those examined here should enable better estimates of the coefficients of eqn. 18, so that the equation can be used predictively.

Since, for the compounds studied, an excellent relationship (Fig. 5 and eqns. 9 and 30) is found between extrapolated κ_w values and experimentally measured water-octan-1-ol distribution coefficients, K_d (Table II)

$$\log K_d = -0.09 + 1.05 \kappa_w \quad (n = 11, r = 0.997) \quad (29)$$

$$\log K_d = -0.06 + 1.02 \kappa_w \quad (n = 32, r = 0.991) \quad (30)$$

where $n = 11$ refers to liquids only, it should follow that the use of K_d in estimating solubilities should give results comparable to those obtained with κ_w . Eqns. 31 and 32 show this to be the case:

$$-\log X_w = 1.29 \log K_d + 0.0071 (T_m - 20) + 0.50 \quad (31)$$

$(n = 32, R = 0.951, F = 141.9)$

$$-\log X_w = 1.29 \log K_d + 1.19 \times 10^{-4} \Delta S_f(T_m - 20) + 0.55 \quad (32)$$

$(n = 32, R = 0.952, F = 145.1)$

As discussed above (Introduction), liquid-liquid distribution coefficients are notoriously difficult to determine over a wide range, and use is often made of estimation procedures. Using a hydrophobic fragment approach and standard computational procedures¹⁴, we have calculated K_d for some of the solutes studied here (Table II), and then used these values in multiple regression analysis of the data according to the general form of eqn. 18. For all compounds we obtain a R value of 0.930, $F = 96.0$, which compares with a value of 0.955, $F = 155.5$, by using κ_w values. Similarly, Yalkowsky and Morozowich (Table 14, ref. 36) found that use of calculated K_d values for complicated drug structures gives poor agreement ($n = 7$, $r = 0.825$) between observed solubilities and those estimated according to eqn. 6. Here lies the advantage in using liquid chromatography, since the experimentally accessible κ_w scale is far greater than that¹⁷ for K_d and the ease and precision of determination obviates the need for calculations of K_d using approximation procedures. (It can be shown that, using reversed-phase LC to obtain κ_w values, aqueous solubilities on a log mole fraction scale of -1 to -11 can readily be accessed.)

Several relationships have been established between K_d ³⁷⁻³⁹, aqueous solubility^{10,40-42}, and some geometrical properties of molecules such as cavity surface area and relative surface area. From eqns. 18, 29 and 30, similar relationships should be expected between κ_w and such properties. Using the smoothed surface area (SSA) (Table II) recently calculated by Bultsma³⁸, which accounts only for exposed surfaces, we find (Fig. 6):

$$\kappa_w = 0.031 \text{ SSA} - 0.79 \quad (n = 9, r = 0.999) \quad (33)$$

The excellent fit of the data by this relationship is in accord with the use of solvophobic theory²³ for describing solute retention in reversed-phase liquid chromatographic systems²⁰, and further justifies our previous use of eqns. 7 and 8. As for calculation of K_d ¹⁴, SSA computations appear to be somewhat complicated for drug structures.

CONCLUSIONS

Locke⁴³ has described as "adequate" a relationship between relative retention data and the aqueous solubilities of nine aromatic fused ring molecules. In the present study the correlation between κ_w and $\log X_w$ is very poor ($n = 32$, $r = 0.452$); the variance between observed and estimated values of $\log X_w$ is only reduced to *ca.* 9% when the $\Delta S_f(T_m - 20)$ or $(T_m - 20)$ approximations are added.

This study has used theoretical and experimental findings to show that the use

TABLE IV
GROUP CONTRIBUTION TERMS, τ_w^X ACCORDING TO EQN. 34

R	X					
	CH ₃	Cl	NO ₂	OH	NH ₂	COOH
H	0.54	0.66	-0.14	-0.70	-1.19	-0.13
CH ₃	0.60	0.73	-0.11	-0.68	-1.54	-0.11
Cl	0.61	0.64	-0.27	-0.48	-0.91	-0.01
NO ₂	0.57	0.53	-0.18	-0.16	-0.60	-0.08
OH	0.56	0.88	0.40	-1.06		-0.15
NH ₂	0.19	0.94	0.45			-0.31
COOH	0.56	0.78	-0.07	-0.72	-1.37	
Mean τ_w	0.52	0.74	0.03	-0.63	-1.12	-0.11
Standard deviation	0.14	0.14	0.29	0.29	0.37	0.13

of reversed-phase retention data in the Hildebrand-Scott equation is justified both for solids and liquid non-electrolytes, although, as recognised by others³⁶, effects such as polymorphism and solid-solid phase interactions can perturb the approach.

Although we have measured κ_w for the non-benzenoid azulene, its aqueous solubility is unknown. Since its κ_w and T_m values are 3.17 and 100°C, using the coefficients of eqn. 16 we predict $\log X_w$ to be -5.19. It will be interesting to learn of the observed value at some future time.

The mono and 1,4-disubstituted benzenes studied (Table I) provide us with a data set from which estimation of functional group contributions to κ_w can be made, with five, six or seven independent estimates being possible (Table IV). Defining an extrapolated group contribution term, τ_w , as¹⁷

$$\tau_w^X = \kappa_{w_j} - \kappa_{w_i} \quad (34)$$

where j and i are solutes having substituents X and R and only R, respectively, it is found that

$$\tau_w^X = 0.93 \pi + 0.07 \quad (n = 6, r = 0.986) \quad (35)$$

where π is a hydrophobic group constant¹⁴ obtained from water-octan-1-ol distribution coefficients (Table II). Tentatively, it is suggested that the use of τ_w values can be used to estimate liquid-liquid distribution (eqn. 30), aqueous solubilities (eqn. 18) and, in conjunction with equations of the form 12, solute retention using binary eluents.

The success of this use of liquid chromatographic retention data to help estimate aqueous solubilities has encouraged us to develop further this approach, and we are currently examining environmental effects (*i.e.*, temperature and ionic

strength) and the effects of co-solvents and co-solutes on the viability of the approach to predict the solubility of drug molecules.

A preliminary report of this work has been made⁴⁴.

ACKNOWLEDGEMENTS

We acknowledge initial discussions with Dr. J. C. Kraak, University of Amsterdam, technical assistance from F. Smedes and computational assistance from P. C. van Krimpen. The interest shown by Dr. S. H. Yalkowsky in this work has been encouraging to us.

REFERENCES

- 1 M. Th. M. Tulp and O. Hutzinger, *Chemosphere*, No. 10 (1978) 849.
- 2 F. Weimer and J. M. Prausnitz, *Hydrocarbon Process.*, 44 (1965) 237.
- 3 C. M. Hansen, *Ind. Eng. Chem., Prod. Res. Develop.*, 8 (1969) 2.
- 4 C. Tsonopoulos and J. M. Prausnitz, *Ind. Eng. Chem., Fundam.*, 10 (1971) 593.
- 5 P. J. Leinonen and D. Mackay, *Can. J. Chem. Eng.*, 51 (1973) 230.
- 6 R. A. Pierotti, *Chem. Rev.*, 76 (1976) 717.
- 7 T. Higuchi, F. M. Shih, T. Kimura and J. H. Rytting, *J. Pharm. Sci.*, 68 (1979) 1267.
- 8 J. Hildebrand and R. L. Scott, *The Solubility of Non-electrolytes*, Reinhold, New York, 1950.
- 9 W. J. Moore, *Physical Chemistry*, Longman, London, 5th ed., 1972, p. 249.
- 10 S. H. Yalkowsky and S. C. Valvani, *J. Chem. Eng. Data*, 24 (1979) 127.
- 11 S. H. Yalkowsky and S. C. Valvani, *J. Pharm. Sci.*, 69 (1980) 912.
- 12 C. Hansch and F. Helmer, *J. Polym. Sci.*, 6 (1968) 3295.
- 13 N. A. Armstrong, K. C. James and C. K. Wong, *J. Pharm. Pharmacol.*, 31 (1979) 627.
- 14 R. F. Rekker, *The Hydrophobic Fragmental Constant*, Elsevier, Amsterdam, 1977.
- 15 T. Braumann and L. H. Grimme, *J. Chromatogr.*, 206 (1981) 7.
- 16 R. Shaw, M. Rivetna and W. H. Elliott, *J. Chromatogr.*, 202 (1980) 347.
- 17 E. Tomlinson, H. Poppe and J. C. Kraak, *Int. J. Pharmaceutics*, 7 (1981) 225.
- 18 D. Palalikit and J. H. Block, *Anal. Chem.*, 52 (1980) 624.
- 19 C. M. Riley, E. Tomlinson and T. M. Jefferies, in A. M. Lawson, C. K. Lim and W. Richmond (Editors), *Current Developments in the Clinical Applications of HPLC, GC and MS*, Academic Press, London, 1980, Ch. 3, p. 35.
- 20 Cs. Horváth, W. Melander, I. Molnár and P. Molnár, *Anal. Chem.*, 49 (1977) 2295.
- 21 W. A. Wakeham, *J. Chem. Soc., Farad. Trans.*, (1981) in press.
- 22 J. A. Graham and L. B. Rogers, *J. Chromatogr. Sci.*, 18 (1980) 614.
- 23 Cs. Horváth, W. Melander and I. Molnár, *J. Chromatogr.*, 125 (1976) 129.
- 24 J. Novák, in Z. Deyl, K. Macek and J. Janák (Editors), *Liquid Column Chromatography - A Survey of Modern Techniques and Applications*, Elsevier, Amsterdam, Oxford, New York, 1975, p. 45.
- 25 K. Denbigh, *The Principles of Chemical Equilibrium*, Cambridge University Press, Cambridge, 1971, p. 432.
- 26 L. R. Snyder, J. W. Dolan and J. R. Gant, *J. Chromatogr.*, 165 (1979) 3.
- 27 S. H. Unger and T. F. Feuerman, *J. Chromatogr.*, 176 (1979) 426.
- 28 W. R. Melander, J. Stoveken and Cs. Horváth, *J. Chromatogr.*, 199 (1980) 35.
- 29 A. Nahum and Cs. Horváth, *J. Chromatogr.*, 203 (1981) 53.
- 30 N. Tanaka, H. Goodell and B. L. Karger, *J. Chromatogr.*, 158 (1978) 233.
- 31 C. M. Riley, E. Tomlinson and T. M. Jefferies, *J. Chromatogr.*, 185 (1979) 197.
- 32 P. J. Schoenmakers, H. A. H. Billiet and L. de Galan, *J. Chromatogr.*, 185 (1979) 179.
- 33 R. C. Weast (Editor), *Handbook of Chemistry and Physics*, CRC Press, Cleveland, OH, 60th ed., 1979/1980.
- 34 E. Martin, S. H. Yalkowsky and J. E. Wells, *J. Pharm. Sci.*, 68 (1979) 4273.
- 35 C. Hansch and A. Leo, *Substituent Constants for Correlation Analysis in Chemistry and Biology*, Wiley, New York, 1979.

- 36 S. H. Yalkowsky and W. Morozowich, in E. J. Ariens (Editor), *Drug Design*, Vol. IX, Academic Press, New York, 1980, pp. 122-183.
- 37 M. J. Harris, T. Higuchi and J. H. Rytting, *J. Phys. Chem.*, 77 (1973) 2694.
- 38 T. Bultsma, *Eur. J. Med. Chem.*, 15 (1980) 371.
- 39 R. Kühne, K. Bocek, P. Scharfenberg and R. Franke, *Eur. J. Med. Chem.*, 16 (1980) 7.
- 40 R. B. Hermann, *J. Phys. Chem.*, 76 (1972) 2754.
- 41 G. L. Amidon, S. H. Yalkowsky and S. Leung, *J. Pharm. Sci.*, 63 (1974) 1858.
- 42 S. C. Valvani, S. H. Yalkowsky and G. L. Amidon, *J. Phys. Chem.*, 80 (1976) 829.
- 43 D. C. Locke, *J. Chromatogr. Sci.*, 12 (1974) 433.
- 44 T. L. Hafkenschield and E. Tomlinson, *Int. J. Pharmaceutics*, 8 (1981) 331.

CHROM. 14,251

STRUCTURAL EFFECTS IN ENTHALPY/ENTROPY COMPENSATED AND NON-COMPENSATED BEHAVIOUR IN ION-PAIR REVERSED-PHASE HIGH-PERFORMANCE LIQUID-SOLID CHROMATOGRAPHY

C. M. RILEY

Department of Pharmaceutical Chemistry, University of Kansas, Lawrence, KS (U.S.A.)

and

E. TOMLINSON* and T. L. HAFKENSCHIED

Subfaculty of Pharmacy, University of Amsterdam, Plantage Muidergracht 24, 1018 TV Amsterdam (The Netherlands)

SUMMARY

This contribution describes a number of linear enthalpy/entropy compensations found with various ion-pair reversed-phase high-performance liquid-solid chromatographic (RP-HPLSC) arrangements. Similar plots for these systems and for those described by non-ion-pair arrangements can be described, and analysis of these compensations in functional group terms indicates that differences in compensation plots are probably due to differences in phase ratios. Time and hydrophobic normalisation, and other extrathermodynamic approaches have been employed to study the effect of organic modifier on phase selectivity in ion-pair systems. The observation of a concomitant behavioural effect by temperature and eluent composition on retention of solutes in such systems has been analysed according to previously described models and it is demonstrated that for ion-pair RP-HPLC there exists a structurally dependent non-compensated residue for the enthalpy of retention. It is suggested that these residues are responsible for observed perturbations in a general enthalpy/entropy compensation relationship for RP-HPLSC.

INTRODUCTION

Linear enthalpy/entropy compensation in liquid chromatographic systems has been reported in a number of recent studies^{1–8}. Some findings^{2,5,7,8} suggest that in reversed-phase high-performance liquid chromatography (RP-HPLC) a single compensation relationship can be used to describe retention of various solutes with a variety of eluents and stationary phases. Theory^{2,9,10} suggests that a similar mechanism of retention (*i.e.*, solvophobic chromatography⁹) can be operating in these systems. Previously⁵ we have demonstrated that linear enthalpy/entropy compensation can occur in ion-pair RP-HPLC using surfactants as pairing ions, although it has been suggested¹¹ that such regular behaviour will generally not be observed for ion-pair systems. A subsequent finding that in our systems changes in temperature and/or

eluent type and composition have the same regular effect on retention, has led us to analyse our results in terms of the extrathermodynamic approach developed recently by Melander *et al.*⁴ for considering those concomitant (*sic*) effects found in LC caused by environmental factors. Further, by employing simple linear free-energy relationships we describe in this present contribution the effect of such behaviour with respect to solute structure.

EXPERIMENTAL

Materials

Benzoic acid, monosubstituted benzoic and phthalic acids ($X = 2,3,4\text{-Cl}$; $2,3,4\text{-NH}_2$; $2,3,4\text{-NO}_2$; $2,3,4\text{-OH}$ and $2,3,4\text{-CH}_3$), phenylacetic acid, cinnamic acid, tyrosine and 3,4-dihydroxyphenylalanine were of at least reagent grade and were obtained from BDH (Poole, Great Britain) and Fisons (Loughborough, Great Britain). 12-dien-Zn(II) was prepared¹² from zinc sulphate and dodecyldiethylenetriamine (Kodak, Liverpool, Great Britain). Alkylbenzyltrimethylammonium chlorides (ABDAC) were as described previously⁵, and sodium dodecyl sulphate (SDDS) was of "biochemical" grade (BDH). Water was double-distilled from an all glass still. All other chemicals were of AnalaR grade (Fisons), except for methanol, acetonitrile, propan-2-ol and tetrahydrofuran which were of HPLC grade (Rathburn, Peebles, Great Britain).

Packing materials used were Spherisorb S5 ODS (Phase Separations, Queensferry, Great Britain) and Hypersil SAS and ODS (Shandon Southern, Runcorn, Great Britain).

Procedures

Using a custom built HPLC apparatus described previously⁵, temperature and mobile phase effects were studied by immersion of the column in a thermostatically controlled ($\pm 0.1^\circ\text{C}$) water-bath. Column packing and preparation, and measurement procedures were as described before⁵. Capacity factors, k , are the means of at least three separate determinations, and were calculated from $[(t/t_0) - 1]$, where t was solute retention time and t_0 the retention time of water enriched mobile phase.

Simple and multiple linear regressions were carried out using standard computer programs.

RESULTS AND DISCUSSION

Thermodynamics

The dependence of solute capacity factors, k , on temperature in a reversed-phase LC system may be given by¹

$$\kappa = -\frac{\Delta H}{2.3RT} + \frac{\Delta S}{2.3R} + \frac{\log \psi}{2.3} \quad (1)$$

where κ is the logarithmic form of the capacity factor and ψ is the phase ratio. Thus the enthalpy change, ΔH , can be assessed from a plot of κ versus T^{-1} , which will be linear

if ΔH is constant. The entropy change, ΔS , can be determined only if ψ is known. Fig. 1 gives some representative Van 't Hoff plots obtained in the present study with various solutes, pairing ions, eluents and stationary phases. In all cases regular¹¹ behaviour is found with an increase in temperature causing a decrease in both retention and selectivity over the studied temperature range. Table I gives the found enthalpies of retention and results are seen to be consistent with a previous finding⁵ that generally with ion-pair systems higher values are found compared with those measured in non-ion-pair LC.

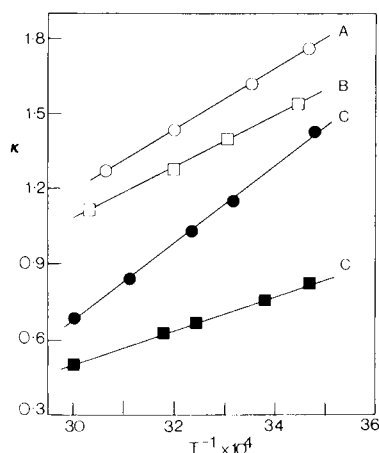


Fig. 1. Van 't Hoff plots for various solutes in a number of ion-pair HPLC arrangements. Key: A, B and C are tyrosine, 4-toluic acid and benzoic acid, respectively; closed squares, open squares, closed circles and open circles are respectively the phase systems 1-4 given in Table I.

Extrathermodynamics

(i) Linear enthalpy/entropy compensation

Physicochemical processes occurring in aqueous environments are often characterised by linear enthalpy/entropy compensation^{10,13}. Lefler and Grunwald¹⁰ have argued that to identify a single unique mechanism for a series of solutes if ΔH and ΔS are approximated as being constant then $\delta\Delta H$ should be simply proportional to $\delta\Delta S$ [where δ denotes a change caused in the thermodynamic parameter by either a medium effect, or, as for the present study, by a change in solute(s) structure(s)]. Using recommended coordinates^{14,15} such compensation effects in reversed-phase LC are well described² by

$$\kappa_T = -(\Delta H/2.3R) \cdot (1/T - 1/\beta) - \Delta G_p/2.3R\beta + \log \psi/2.3 \quad (2)$$

where β is the enthalpy/entropy proportionality factor¹⁰, and which has units of absolute temperature. Such an extrathermodynamic relationship can be described^{5,8} in terms of functional group contributions by

$$\tau_T = -[\Delta(\Delta H)/2.3R] \cdot (1/T - 1/\beta) - \Delta(\Delta G_p)/2.3R\beta \quad (3)$$

TABLE I
 ENTHALPIES OF RETENTION OF SIMPLE SOLUTES IN VARIOUS ION-PAIR RP-HPLC ARRANGEMENTS
 $-\Delta H$ values are in kJ mol^{-1} ; $\kappa = \log$ capacity factor at 40 °C (interpolated values from Van 't Hoff plots).

Solute	Phase system	1	2	3	4
Benzoic acid 4-Aminobenzoic acid 4-Toluic acid 2-Phthalic acid 3-Phthalic acid 4-Phthalic acid	Stationary Modifier	Hypersil SAS	Hypersil SAS	Spherisorb ODS*	Hypersil ODS
	Pairing ion	Acetonitrile, $\phi = 0.25$ C14BDAC, $1 \cdot 10^{-3} \text{ mol dm}^{-3}$	Acetonitrile, $\phi = 0.25$ 12-dien-Zn(II), $(1 \cdot 10^{-3} \text{ mol dm}^{-3})$	Acetonitrile, $\phi = 0.20$ C13BDAC $(5 \cdot 10^{-4} \text{ mol dm}^{-3})$	Propan-2-ol, $\phi = 0.02$ (a), 0.04 (b) SDDS, $2.5 \cdot 10^{-4} \text{ mol dm}^{-3}$ (i), $5 \cdot 10^{-4} \text{ mol dm}^{-3}$ (ii)
	$-\Delta H$	16.5	18.1	34.5	(i) (ii)
	κ	0.70	0.90	κ	κ
				$-\Delta H$	$-\Delta H$
Tyrosine				1.04	
		10.0 20.6 17.0 21.6 15.8	14.2 21.3 28.9 27.8 23.3	20.5 40.1 1.36	(a) 16.3 (b) 15.1
3,4-Dihydroxy-phenylalanine					(a) 20.7 (b) 23.2
					(a) 18.5 (b) 16.8

* From ref. 5, where values for other substituted benzoic and cinnamic acids may be found.

where

$$\tau = \kappa_j - \kappa_i \quad (4)$$

and i and j refer to solutes differing by a functional group. Fig. 2 shows enthalpy/entropy plots according to eqn. 2 (ΔH - ΔG coordinates) for a number of ion-pair and non-ion-pair RP-HPLC systems determined here and elsewhere^{5,8}. The remarkable feature of these plots is that apart from the 12-dien-Zn(II) system all arrangements show (according to theory^{10,14,15}), linear enthalpy/entropy compensation behaviour. Similar slopes can be described for all these systems, although each plot is discrete from the others. If these displacements are due to differences in phase volume ratio then use of eqn. 3 to analyse the data in terms of group contributions should give similar slope and intercept coefficients for all systems. Eqns. 5-9 (Table II) comprise such an analysis, and indeed show both that slope coefficients are similar, and that in all cases intercept values (τ ordinate) approximate to zero. Although using 12-dien-Zn(II) as pairing ion these coefficients approximate to these found (Table II) in other RP systems, the very poor correlations coefficient suggest that here irregular¹¹ non-solvophobic behaviour is occurring.

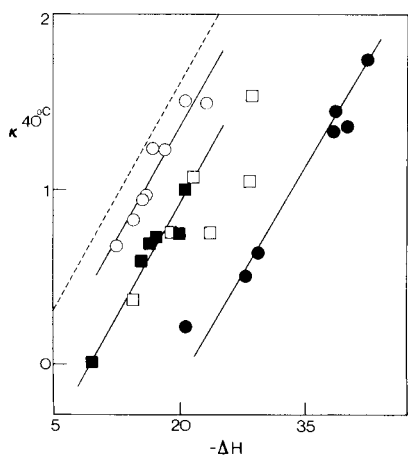


Fig. 2. Relationships between log capacity factor, κ , and enthalpies of retention, ΔH (kJ mol^{-1}), in ion-pair and non-ion-pair HPLC arrangements. Key: the dashed line is the regression line for a non-ion-pair system⁸ using alkylsilicas as stationary phases (Table II), and data points are as for Fig. 1.

(ii) Linear free-energy relationships

Although Schoenmakers *et al.*¹⁶ have theorised that the capacity ratio of a solute will vary quadratically with the volume fraction of organic modifier, ϕ , in a binary mixture eluent, it is often found that over a reasonably wide ϕ range that solute retention can be described by a linear function¹⁷ of volume fraction; which can be given by

$$\kappa = \kappa_w + B\phi \quad (10)$$

where subscript w indicates on capacity value extrapolated to 100% aqueous eluent

TABLE II
FUNCTIONAL GROUP ENTHALPY/ENTROPY COMPENSATION RELATIONSHIPS ACCORDING TO EQN. 3

All data refer to an analytical temperature of 40°C and where necessary have been recalculated from the original measurements. n = Number of data points; r = correlation coefficient.

Solutes	Phase system	Slope coefficient	Intercept coefficient	n	r	Eqn.	Ref.
3-, 4-Monosubstituted benzoic and phthalic acids	Hypersil SAS; acetonitrile-acetate buffer ($\phi = 0.25$); $1 \cdot 10^{-3}$ mol dm $^{-3}$ C14BDAC pairing ion	-7.5	-0.11	5	0.922	5	This study
3-, 4-Monosubstituted benzoic and phthalic acids	Hypersil SAS; acetonitrile-acetate buffer ($\phi = 0.25$); $1 \cdot 10^{-3}$ mol dm $^{-3}$ 12-dien-Zn(II) pairing ion	-7.2	-0.17	5	0.834	6	This study
3-, 4-Monosubstituted benzoic acids	Spherisorb ODS; acetonitrile-phosphate buffer ($\phi = 0.20$); $5 \cdot 10^{-4}$ mol dm $^{-3}$ C13BDAC pairing ion	-6.8	0.04	7	0.976	7	5
3-, 4-Monosubstituted alkylbenzoates	LiChrosorb alkylsilicas; methanol-water ($\phi = 0.60-0.80$)	-7.7	0.02	28	0.934	8	8
2-, 3-, 4-Monosubstituted alkyl benzoates	LiChrosorb alkylsilicas; methanol-water ($\phi = 0.60-0.80$)	-9.1	0.03	40	0.949	9	8

and B is the slope coefficient. The effects of increasing the concentrations of four organic modifiers, *i.e.*, methanol acetonitrile, propan-2-ol and tetrahydrofuran, on the retention of a number of substituted benzoic acids in their ionized form as ion pairs, using a constant low concentration of alkylbenzyltrimethylammonium chloride as pairing ion and Hypersil ODS as stationary phase are given by eqns. 11–68 (see Table III), using eqn. 10 as the analytical function. For all relationships the correlation between κ and ϕ was significant at the $\alpha = 0.001$ level, save with polar functions studied with tetrahydrofuran as modifier. In only one case (eqn. 55, Table III), could the introduction of a quadratic term¹⁶ improve the correlation significantly. In all cases solute retention decreases (negative slope coefficients) with modifier. The values of κ_w and B are dependent upon substituent character, with values of B reflecting not only the effect of the organic modifier type on solute retention but also solute–solute and solute (ion-pair)–solvent interactions. Hence these coefficients may be taken to be a measure of the average solvation number of the formed ion pair in the solvent¹⁸, with highest values of B being obtained with organic modifiers having the greatest extracting ability for the solute ion pairs. Based on benzoic acid behaviour these extracting abilities are given by: propan-2-ol (-10.9) > tetrahydrofuran (-9.3) > acetonitrile (-7.9) > methanol (-4.7). Clearly such values could form the basis of an elutropic series for solvents used in ion-pair reversed-phase high-performance liquid–solid chromatography (RP-HPLSC).

To examine the effect of solute structure on the coefficients of eqn. 10, it is convenient to introduce two group contribution terms, *viz.*

$$\tau_w = \kappa_{w_j} - \kappa_{w_i} \quad (69)$$

and

$$\Delta B = B_j - B_i \quad (70)$$

such that by combining eqns. 4, 10, 69 and 70 it follows that:

$$\tau = (\Delta B) \phi + \tau_w \quad (71)$$

These terms can now be related to other extrathermodynamic terms used to describe functional group physicochemical properties, and since retention in these systems can be regarded^{5,9} as being controlled by both electrostatic and solvophobic forces, these two chromatographic terms have been correlated using regression analysis to group hydrophobicity and electronic parameters, *viz.*

(1) *Slope coefficient term, ΔB*

(a) *Methanol*

$$\Delta B = 1.1\pi - 0.36 \quad n = 10, r = 0.922 \quad (72)$$

$$\Delta B = 0.098\pi - 0.56\sigma - 0.22 \quad n = 10, R = 0.965 \quad (73)$$

(b) *Propan-2-ol*

$$\Delta B = -2.98\pi - 0.51 \quad n = 8, r = 0.901 \quad (74)$$

$$\Delta B = -2.62\pi - 1.39\sigma - 0.22 \quad n = 8, R = 0.951 \quad (75)$$

TABLE III

RELATIONSHIPS BETWEEN κ AND ORGANIC MODIFIER VOLUME FRACTION ACCORDING TO EQN. 10

Chromatographic details: stationary phase, Hypersil ODS; mobile phase modifier, tetradecylbenzylidimethylammonium chloride ($5 \cdot 10^{-4}$ mol dm $^{-3}$); pH 7.5 ($2.5 \cdot 10^{-2}$ mol dm $^{-3}$ K $_2$ HPO $_4$); 30°C.

Benzoic acid ring substituent	Methanol				Propan-2-ol				Acetonitrile				Tetrahydrofuran			
	-B	κ_w	τ_w	Eqn.	-B	κ_w	τ_w	Eqn.	-B	κ_w	τ_w	Eqn.	-B	κ_w	τ_w	Eqn.
H	4.74	2.94		(11)	10.9	3.39		(26)	7.94	2.80		(39)	9.29	2.96		(54)
2-NH $_2$	3.21	1.43	-1.51	(12)	6.2	1.43	-1.84	(27)	4.54	1.24	-1.56	(40)	6.46	1.44	-1.52	(55)
3-NH $_2$	3.84	1.84	-1.10	(13)	8.1	2.10	-1.19	(28)	5.55	1.67	-1.13	(41)	7.36	1.92	-1.04	(56)
2-NH $_2$	5.22	3.10	0.16	(14)	11.2	3.38	-0.01	(29)	8.18	2.88	0.08	(42)	9.73	3.08	0.12	(57)
4-OH	4.22	2.20	-0.74	(15)	9.18	2.45	-0.94	(30)	5.27	1.58	-1.22	(43)	7.39	2.12	-0.84	(58)
3-OH	5.03	2.82	-0.12	(16)	11.2	3.20	-0.19	(31)	7.18	2.34	-0.46	(44)	7.71	2.93	-0.03	(59)
4-NO $_2$	5.38	3.44	0.50	(17)	12.9	4.16	0.67	(32)	8.62	3.36	0.56	(45)	15.3	5.19	2.23	(60)
3-NO $_2$	5.51	3.53	0.59	(18)	13.0	4.16	0.67	(33)	9.07	3.48	0.68	(46)	17.4	5.73	2.87	(61)
2-NO $_2$	4.53	2.75	-0.19	(19)	10.6	3.10	-0.29	(34)	7.26	2.64	-0.16	(47)	8.94	2.77	-0.19	(62)
4-CH $_3$	5.35	3.53	0.59	(20)	12.3	4.05	0.66	(35)	9.38	3.49	0.69	(48)	14.9	4.74	0.78	(63)
3-CH $_3$	5.48	3.63	0.69	(21)	12.3	4.04	0.65	(36)	9.93	3.66	0.86	(49)	14.7	4.67	0.71	(64)
2-CH $_3$	4.71	3.02	0.06	(22)	10.2	3.19	-0.20	(37)	7.89	2.79	-0.01	(50)	8.60	2.73	-0.23	(65)
4-Cl	6.11	4.14	1.20	(23)					10.6	4.10	1.30	(51)	13.0	4.54	1.60	(66)
3-Cl	6.00	4.10	1.16	(24)					10.4	4.08	1.28	(52)	13.1	4.55	1.61	(67)
2-Cl	4.74	2.85	-0.09	(25)	10.5	3.29	-0.10	(38)	8.67	3.06	0.26	(53)	9.03	2.85	-0.11	(68)

(c) Acetonitrile

$$\Delta B = -1.80\pi - 0.68 \quad n = 10, r = 0.901 \quad (76)$$

$$\Delta B = -1.74\pi - 0.28\sigma - 0.63 \quad n = 10, R = 0.811 \quad (77)$$

(d) Tetrahydrofuran

$$\Delta B = -4.15\pi - 2.50 \quad n = 10, r = 0.800 \quad (78)$$

$$\Delta B = -3.45\pi - 2.83\sigma - 2.17 \quad n = 10, R = 0.877 \quad (79)$$

where n refers to the number of (3- and 4-substituted) solutes and where R is the multiple correlation coefficient, and π and σ are the Hansch water/octan-1-ol group hydrophobicity constant¹⁹ and the Hammett group electronic term²⁰ respectively. For the alcoholic organic modifiers the slope coefficient is seen to be controlled primarily by hydrophobic effects, although there is a significant electronic contribution (eqns. 73 and 75). For acetonitrile and tetrahydrofuran the dependency of the slope coefficient on substituent hydrophobicity is reduced, presumably due to specific solvation effects, and the fact that ion pairs retain some polarity²¹.

(2) *The intercept term, τ_w .* The suggestion has been made²²⁻²⁴ that the intercept value of eqns. 10 and 71 may be used as hydrophobicity parameters *per se* for use in, for example, drug design models and the estimation of bulk phase liquid-liquid distribution coefficients. Elsewhere²⁵ we have demonstrated that for non-ion-pair chromatography such a suggestion is tenable, and it is thus of interest to examine its validity for ion-pair arrangements. Thus:

(a) Methanol

$$\tau_w = 1.13\pi + 0.23 \quad n = 10, r = 0.951 \quad (80)$$

$$\tau_w = 1.04\pi + 0.51\sigma + 0.21 \quad n = 10, R = 0.990 \quad (81)$$

(b) Propan-2-ol

$$\tau_w = 1.33\pi + 0.16 \quad n = 8, r = 0.945 \quad (82)$$

$$\tau_w = 1.20\pi + 0.51\sigma + 0.06 \quad n = 8, R = 0.976 \quad (83)$$

(c) Acetonitrile

$$\tau_w = 1.32\pi + 0.21 \quad n = 10, r = 0.912 \quad (84)$$

$$\tau_w = 1.22\pi + 0.40\sigma + 0.13 \quad n = 10, R = 0.928 \quad (85)$$

(d) Tetrahydrofuran

$$\tau_w = 1.60\pi + 0.86 \quad n = 10, r = 0.889 \quad (86)$$

$$\tau_w = 1.38\pi + 0.14\sigma + 0.27 \quad n = 10, R = 0.939 \quad (87)$$

These relationships between τ_w and π are not as significant as those found²⁵ for non-ion-pair systems, although the higher correlations found using methanol and propan-2-ol indicate they are the most suitable organic modifier for obtaining such hydrophobicity indices for ionisable solutes. The correlations are significantly improved in all cases by the introduction of the electronic term, suggesting both solvation effects and a possible contribution of surface silanol groups²⁶ to retention.

(iii) *Time and hydrophobicity normalisation*

To compare functional group selectivity with different organic modifiers it is useful to use an organic solvent normalisation approach^{27,28}. For the solutes and functions given in Table III, time normalisation can be made by choosing concentrations of organic modifiers which result in the same retention of a reference solute (benzoic acid), using methanol ($\phi = 0.50$). Differences in selectivities (group values) can be then obtained using eqn. 88

$$\tau_m = C\tau^* + D \quad (88)$$

which relates substituent values obtained using methanol, τ_m , to those obtained, τ^* , in "equivalent" mobile phases containing the other modifiers (where C and D are constants). Similarly for solutes we may write:

$$\kappa_m = E\kappa^* + F \quad (89)$$

Regression and correlation coefficients obtained using the systems described in Table III are given by eqns. 90–92:

$$\text{acetonitrile:} \quad \kappa_m = 1.03 \kappa^* - 0.09 \quad n = 15, r = 0.980 \quad (90)$$

$$\text{tetrahydrofuran:} \quad \kappa_m = 0.85 \kappa^* + 0.07 \quad n = 15, r = 0.921 \quad (91)$$

$$\text{propan-2-ol:} \quad \kappa_m = 0.99 \kappa^* - 0.01 \quad n = 15, r = 0.992 \quad (92)$$

It may be seen (Figs. 3a–3c) that although propan-2-ol behaves similarly to methanol, the relationships for other modifiers are perturbed by the effect of polar functions (NO_2 , NH_2 and OH), which are displaced significantly from the reference line of slope unity. However (Table IV), hydrophobic group values are shown to be organic modifier independent. These results may be explained within the context of solvophobic theory⁹, which for functional groups can be given by

$$\tau = \Delta K_1 + K_2 \Delta(\Delta[\text{HA}]) \quad (93)$$

where ΔK_1 is related to the free energy of interaction of the functional group with the mobile phase due to van der Waal's interactions, K_2 is a constant related to the surface tension, γ , of the mobile phase and $\Delta(\Delta[\text{HA}])$ is the change in hydrocarbonaceous surface contact between solute and stationary phase caused by the substituent, and is approximately equal to the hydrocarbonaceous surface area of the group⁹. Polar selectivity is influenced by both terms in eqn. 93, and hydrophobic selectivity is dominated by the second term, which may be given by $f_\gamma \cdot \Delta(\Delta[\text{HA}])$ since the surface tension is⁹ proportional to K_2 .

For two mobile phases we can show that

$$\tau^a - \tau^b = -\Delta K_1^a + \Delta K_1^b + f_\gamma^a \Delta(\Delta[\text{HA}]) - f_\gamma^b \Delta(\Delta[\text{HA}]) \quad (94)$$

where superscripts a and b refer to the two mobile phases. If γ^a equals γ^b then the hydrophobic content of the selectivity is normalized²⁷, such that now

$$\tau^a - \tau^b = \Delta K_1^b - \Delta K_1^a \quad (95)$$

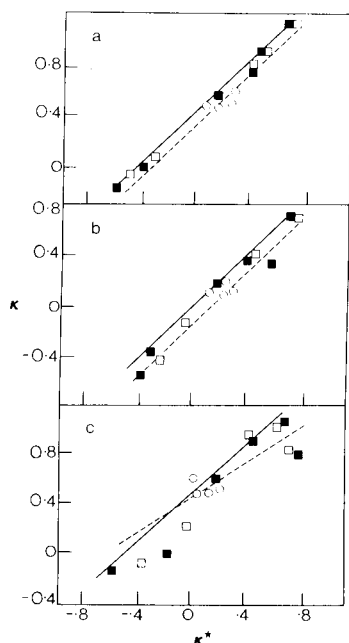


Fig. 3. Time normalised retention plots, showing the relationships between capacity factors of benzoic acids in eluents containing methanol ($\phi = 0.50$), or (κ^*) "equivalent" amounts of (a) propan-2-ol ($\phi = 0.255$), (b) acetonitrile ($\phi = 0.275$) and (c) tetrahydrofuran ($\phi = 0.265$). The solid lines indicate a slope of unity and the dashed lines are regression lines according to eqns. 90-92. Key: 2-, 3- and 4-substituted solutes are open circles, open squares and closed squares, respectively.

and where for time and hydrophobic normalisation conditions:

$$\tau^a - \tau^b = \kappa_i^a - \kappa_i^b \quad (96)$$

Since Table IV gives hydrophobic group selectivity to be independent of modifier then this means that benzoic acid, as the ion pair, is behaving as a purely hydrophobic solute and that the hydrophobic contribution (eqn. 93) is normalised such that differences in mobile phase selectivities are only due to different solute-solvent interactions and will be restricted to polar functions. The perturbations of the relationships embodied in eqns. 78 and 79 are more apparent (Fig. 3) at lower equivalent organic

TABLE IV

HYDROPHOBIC GROUP VALUES WITH DIFFERENT ORGANIC MODIFIERS UNDER TIME NORMALIZATION CONDITIONS (FIG. 3), ACCORDING TO EQN. 88

Organic modifier		$\tau_{CH_3}^*$	τ_{Cl}^*
Type	Concentration, ϕ		
Methanol	0.500	0.30	0.53
Propan-2-ol	0.255	0.31	0.54
Acetonitrile	0.275	0.31	0.57
Tetrahydrofuran	0.265	0.28	0.57

TABLE V

CAPACITY FACTORS FOR SUBSTITUTED BENZOIC ACIDS UNDER IDENTICAL CONDITIONS USING EQUIVALENT CONCENTRATIONS OF PROPAN-2-OL ($\phi = 0.20$) AND TETRAHYDROFURAN ($\phi = 20$)

Benzoic acid substituent	Capacity factor	
	Propan-2-ol	Tetrahydrofuran
4-NH ₂	1.4	1.9
3-NH ₂	2.5	4.1
4-OH	3.1	6.2
3-OH	10.6	10.6
2-NO ₂	10.6	9.1
2-NH ₂	15.0	21.7
H	18.2	18.2

modifier concentrations where there is greater retention of the polar substituted benzoic acids. This effect is demonstrated by Table V which gives the retention of some polar substituted benzoic acids in equivalent mobile phases containing propan-2-ol and tetrahydrofuran. Although these two phase systems produce the same retention for the reference compound (benzoic acid), significant changes in selectivity and retention order are observed. These results indicate that if solute polarity is different, then separations may be improved by changing to an equivalent organic modifier (Fig. 4), containing a different functional group.

(iv) *Eluent and temperature concomitant behaviour*

Figs. 1 and 2, Table II and eqns. 72–79 indicate that the ion-pair systems studied here show regular¹¹ behaviour with respect to both temperature and eluent composition. This can be further appreciated by examination of Fig. 5, where, for example, a decrease in retention and selectivity with increased temperature can be compensated for by a decrease in organic modifier concentration. In terms of solute

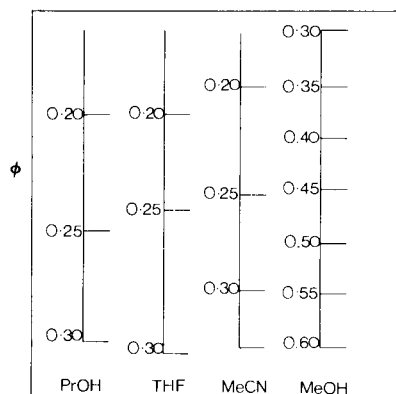


Fig. 4. Equivalent concentrations of eluent modifiers based on benzoic acid retention using ion-pair HPLC systems given in Table III. ProOH = Propan-2-ol; THF = tetrahydrofuran; MeCN = acetonitrile; MeOH = methanol.

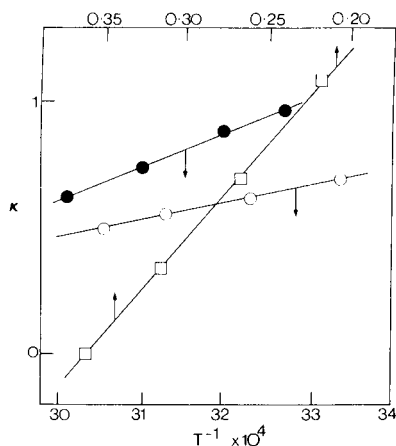


Fig. 5. Interrelationships between the effects of temperature (circles) at two different acetonitrile volume functions (closed \square = 0.20; open \square = 0.25), and the effect of acetonitrile concentration (squares), at 30°C on the capacity factor of benzoic acid using ion-pair HPLC phase systems 1 and 3 (Table I).

structure it should therefore follow that the functional group terms of eqn. 71 are correlated with the group enthalpic contributions found for similar chromatographic arrangements. This is investigated by comparing the data for the enthalpies of retention obtained⁵ using an aqueous acetonitrile eluent ($\phi = 0.20$) and Spherisorb ODS as stationary phase, and group terms obtained in this present study (Table III) using Hypersil ODS. Thus for 3- and 4-monosubstituted benzoic acid using ABDACs as pairing ions:

$$\Delta(\Delta B) = 26.8 \times 10^{-5} \Delta(\Delta H) - 0.03 \quad n = 6, r = 0.977 \quad (97)$$

$$\tau_w = 13.6 \times 10^{-5} \Delta(\Delta H) + 0.06 \quad n = 6, r = 0.984 \quad (98)$$

Considering the different stationary phases used and the precision in obtaining $\Delta(\Delta H)$ values these may be regarded as good correlations (*cf.*, Table II), and illustrate a concomitant effect in ion-pair RP-HPLC for temperature and organic modifier.

The dependence of κ on both solvent composition and temperature for RP systems can be analysed⁴ to show whether ΔH is comprised of both a compensated, ΔH_c , and a non-compensated, ΔH_{nc} , portion at $\phi = 0$, *i.e.*

$$\Delta H(\phi) = \Delta H_{nc}(0) + \Delta H_c(0) \cdot f(\phi) \quad (99)$$

such that

$$\ln k = \frac{-\Delta H_c(0) \cdot f(\phi) - \Delta H_{nc}(0)}{RT} + \frac{\Delta H_c(0)[f(\phi) - 1]}{R\beta} + \frac{\Delta S(0)}{R} + \ln \psi \quad (100)$$

and where when $f(\phi) = 1 + \chi\phi$ (where χ is a constant, *i.e.*, eqn. 10 holds), then the dependence is given by⁴

$$\ln k = A_1\phi(1 + \beta/T) + A_2/T + A_3 \quad (101)$$

TABLE VI

MULTIPLE REGRESSION COEFFICIENTS ACCORDING TO EQN. 101 FOR ION-PAIR SYSTEMS GIVEN IN TABLE III USING ACETONITRILE ($\phi = 0.25$) AS ORGANIC MODIFIER AND BENZOIC ACIDS AS SOLUTES

Solute	A_1	A_2	A_3	A_2/A_1
H	27.2	1799	4.47	66.1
4-NH ₂	9.2	1058	2.88	115.0
3-OH	21.1	1546	3.88	73.2
4-OH	14.3	1428	4.05	99.9
4-NO ₂	33.8	2008	4.49	59.4
4-CH ₃	37.3	2087	4.72	56.0
4-Cl	41.3	2233	6.26	54.1
2-NH ₂	30.2	1919	5.05	63.5
2-Cl	34.1	2118	3.09	62.1
2-CH ₃	20.0	1323	2.74	66.2
2-NO ₂	20.2	1464	3.04	72.5

where the meanings of A_1 – A_3 are model dependent (Table I, ref. 4). Taking β for our systems as 525°K (which can be calculated from ref. 5 using eqn. 3), the data from Table III of this study have been analysed in terms of eqn. 101 at 30°C and at a ϕ value of 0.25, using multiple regression analysis. The multiple regression coefficients obtained are given in Table VI. Since the relationship between A_1 and A_2 may be given by

$$A_2 = 34.2A_1 + 835 \quad n = 7, r = 0.990 \quad (102)$$

and the ratio A_2/A_1 is not constant (Table VI), this indicates⁴ that for these ion-pair systems the enthalpy change upon retention is not exclusively compensated by ΔS and that A_1 , A_2 and A_3 are given by $[\chi\Delta H_c(0)/2.2R\beta]$, $[-\Delta H_c(0) + \Delta H_{nc}(0)]/2.3R$ and $\Delta S(0)/2.3R + \ln \psi/2.3$ respectively. Since⁴

$$A_2 = \Delta H_{nc}(0)/2.3R - \beta A_1/\chi \quad (103)$$

analysis of our data (Table VI) gives for 3- and 4-monosubstituted benzoic acids a non-compensated enthalpy change residue of 15.4 kJ mol⁻¹ (which compares with 15.9 kJ mol⁻¹ found⁴ for alkylbenzenes in a non-ion-pair RP system); and for 2-substituted benzoic acids a residue of 7.6 kJ mol⁻¹. The finding of this structurally dependent non-compensated residue appears to explain our previous findings (Table II) that *ortho* substituents perturb the general relationship between τ and $\Delta(\Delta H)$, and may be a significant result⁴ in elucidating retention mechanisms in reversed-phase liquid chromatography.

For non-ion-pair RP systems A_1 , A_2 and A_3 are found⁴ to be linearly related to the carbon number of the side chain of some *n*-alkylbenzene solutes, which, from Table II and previous discussion (eqns. 3 and 90), suggests that linear free-energy relationships exist for the present ion-pair systems between these regression terms and a solute hydrophobicity term. Fig. 6 shows this to be the case with excellent agree-

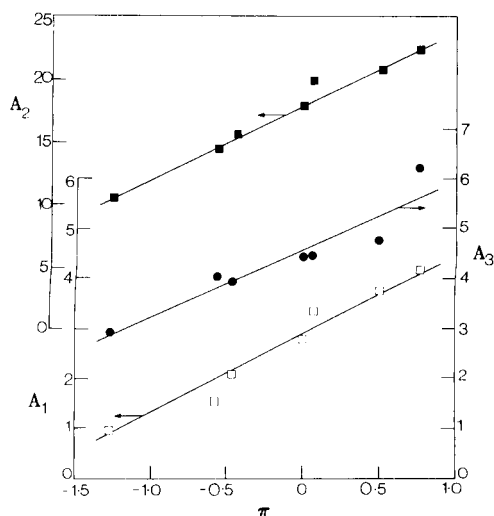


Fig. 6. Dependencies of multiple regression coefficients $A_1 \times 10^{-1}$, $A_2 \times 10^{-2}$ and A_3 from eqn. 101 on solute hydrophobicities as given by the Hansch π term¹⁹. Drawn lines are regression lines according to eqns. 104-106.

ment being found between the Hansch π term and A_2 , the enthalpy dominated coefficient. For 3- and 4-substituted solutes we may formalise the relationships given in Fig. 6 by:

$$A_1 = 16.1\pi + 28.1 \quad n = 7, r = 0.959 \quad (104)$$

$$A_2 = 5.63 \times 10^2 \pi + 1.80 \times 10^3 \quad n = 7, r = 0.991 \quad (105)$$

$$A_3 = 1.30\pi + 4.58 \quad n = 7, r = 0.923 \quad (106)$$

These data confirm the findings given in Table II which show enthalpy/entropy compensation effects determined in ΔH - ΔG coordinates. Further, eqn. 106 shows that there is a markedly reduced correlation between the entropy dominated term of eqn. 100, *i.e.*, A_3 , and π .

CONCLUSIONS

(1) Solute structure effects on retention behaviour in various ion-pair HPLC arrangements can be well described using extrathermodynamic approaches. It is found that similar solute enthalpy/entropy linear compensations are demonstrated by various ion-pair and non-ion-pair systems, and that, in accord with solvophobic theory⁹, analysis of these compensations in functional group terms, shows that differences in found compensation plots are probably due to the phase ratios of the various studied systems.

(2) Time and hydrophobic normalisation can be used for ion-pair LC to indicate differences in phase selectivities, and it is found that although methanol and propan-2-ol behave similarly, acetonitrile and tetrahydrofuran can have very different selectivities, indicating specific solvation effects.

(3) These solvation effects are seen to perturb the relationships described between functional group hydrophobicities and terms accounting for group retention behaviour with respect to changes in eluent type and composition.

(4) Finally, combining findings from this study (Table III) with our previous results⁵ we have been able to determine whether the enthalpies of retention in ion-pair RP-HPLC are totally compensated by ΔS . This is demonstrated to be not the case, with, for 3- and 4-monosubstituted solutes a non-compensated residue of 15.4 kJ mol⁻¹ (which is similar to that found⁴ for non-ion-pair systems), and a value of 7.6 kJ mol⁻¹ for 2-substituted solutes. These findings are suggested as a possible explanation of reported perturbations⁵ in a general τ/Δ (ΔH) relationship found using *ortho*-substituted compounds.

ACKNOWLEDGEMENTS

Part of this work was carried out in the School of Pharmacy and Pharmacology, University of Bath. The valued assistance of Dr. T. M. Jefferies and the award of a Science Research Council/ICI C.A.S.E. studentship to C.M.R. are most gratefully acknowledged.

REFERENCES

- 1 H. Colin and G. Guiochon, *J. Chromatogr.*, 158 (1978) 183.
- 2 W. Melander, D. E. Campbell and Cs. Horváth, *J. Chromatogr.*, 158 (1978) 215.
- 3 H. Colin, J. C. Diez-Masa, G. Guiochon, T. Czajkowska and I. Miedziak, *J. Chromatogr.*, 167 (1978) 41.
- 4 W. R. Melander, B.-K. Chen and Cs. Horváth, *J. Chromatogr.*, 185 (1979) 99.
- 5 C. M. Riley, E. Tomlinson and T. M. Jefferies, *J. Chromatogr.*, 185 (1979) 197.
- 6 J. Chmielowiec and H. Sawatzky, *J. Chromatogr. Sci.*, 17 (1979) 245.
- 7 Gy. Vigh and Z. Varga-Puchony, *J. Chromatogr.*, 196 (1980) 1.
- 8 E. Tomlinson, H. Poppe and J. C. Kraak, *Int. J. Pharmaceutics*, 7 (1981) 225.
- 9 Cs. Horváth, W. Melander and I. Molnár, *J. Chromatogr.*, 125 (1976) 129.
- 10 J. E. Leffler and E. Grunwald, *Rates and Equilibria of Organic Reactions*, Wiley, New York, 1963, pp. 128-314.
- 11 L. R. Snyder, *J. Chromatogr.*, 179 (1979) 167.
- 12 N. H. C. Cooke, R. L. Viavattene, R. Eksteen, W. S. Wong, G. Davies and B. L. Karger, *J. Chromatogr.*, 149 (1978) 391.
- 13 R. Lumry and S. Rajender, *Biopolymers*, 9 (1970) 1125.
- 14 R. R. Krug, W. G. Hunter and G. A. Grieger, *J. Phys. Chem.*, 80 (1976) 2335.
- 15 R. R. Krug, W. G. Hunter and R. A. Grieger, *J. Phys. Chem.*, 80 (1976) 2341.
- 16 P. J. Schoenmakers, H. A. H. Billiet and L. de Galan, *J. Chromatogr.*, 185 (1979) 179.
- 17 L. R. Snyder, J. W. Dolan and J. R. Gant, *J. Chromatogr.*, 165 (1979) 3.
- 18 T. Higuchi, A. Michaelis, T. Tan and H. Hurwitz, *Anal. Chem.*, 39 (1967) 974.
- 19 J. Iwasa, T. Fujita and C. Hansch, *J. Med. Chem.*, 8 (1965) 150.
- 20 L. P. Hammett, *Physical Organic Chemistry*, McGraw-Hill, New York, 1940.
- 21 T. Higuchi, A. Michaelis and J. H. Rytting, *Anal. Chem.*, 43 (1971) 142.
- 22 I. E. Bush, *Methods Biochem. Anal.*, 13 (1965) 357.
- 23 E. Tomlinson, *J. Chromatogr.*, 113 (1975) 1.
- 24 T. Yamana, A. Tsuji, E. Miamoto and O. Kubo, *J. Pharm. Sci.*, 66 (1977) 747.
- 25 T. L. Hafkenscheid and E. Tomlinson, *J. Chromatogr.*, 218 (1981) 409.
- 26 W. Melander, J. Stoveken and Cs. Horváth, *J. Chromatogr.*, 199 (1980) 35.
- 27 B. L. Karger, J. R. Gant, A. Hartkopf and P. H. Weiner, *J. Chromatogr.*, 128 (1976) 65.
- 28 N. Tanaka, H. Goodell and B. L. Karger, *J. Chromatogr.*, 158 (1978) 233.

CHROM. 14,214

RETENTION AND SELECTIVITY CHARACTERISTICS OF A NON-POLAR PERFLUORINATED STATIONARY PHASE FOR LIQUID CHROMATOGRAPHY

HUGO A. H. BILLIET*, PETER J. SCHOENMAKERS and LEO DE GALAN

Gebouw voor Analytische Scheikunde, Technische Hogeschool Delft, Jaffalaan 9, 2628 BX Delft (The Netherlands)

SUMMARY

An experimental study has been made of the chromatographic characteristics of a perfluorinated chemically bonded stationary phase for reversed-phase liquid chromatography. It is demonstrated from the retention data that the perfluorinated material behaves as a less polar stationary phase than an octadecyl (RP-18) material. The gain in selectivity, however, is obscured by large specific effects towards both fluorinated solutes and certain classes of compounds not containing fluorine atoms. The specific fluorine–fluorine interaction can also occur in the mobile phase, when 2,2,2-trifluoroethanol is used as an organic modifier.

INTRODUCTION

In reversed-phase liquid chromatography (RPLC), a non-polar stationary phase is combined with a polar mobile phase. Most often, a chemically bonded hydrocarbon-type material is used. A high concentration of alkyl groups on a silica surface yields a non-polar stationary phase. Different alkyl chain lengths can be used and their mutual differences have been studied^{1,2}. Moderately polar materials can be obtained by chemical bonding of alkylsilanes containing a functional group in the ω -position³. Such materials can be used for special separations, e.g., the application of amino-type stationary phases for the analysis of sugars⁴. Also, stationary phases equipped with diol and cyano groups can occasionally be used advantageously^{5,6}. However, materials with branched chains⁷, alkenes³ and phenyl groups^{8,9} appear to be of limited interest in chromatographic practice.

Recently, we reported on the synthesis of highly fluorinated stationary phases for liquid chromatography¹⁰. These phases appeared to show a remarkably specific fluorine–fluorine interaction. Solutes containing fluorine atoms could be specifically retarded relative to the hydrogen-containing molecular analogues. Moreover, we have suggested elsewhere¹¹ that the extremely low polarity of the perfluorinated stationary phases could result in a higher overall selectivity, if these phases were used for common reversed-phase separations.

This paper describes a more detailed study of the chromatographic properties

of perfluorinated phases. Both specific effects and the general separation power will be considered. Mobile phases containing trifluoroethanol as the organic modifier are used to investigate the occurrence of specific fluorine-fluorine interactions.

THEORETICAL

Retention and selectivity

Elsewhere¹¹, we have discussed a simple model from which different LC phase systems can be evaluated and mutually compared. This model is based on the concept of polarity, and expressed in terms of the solubility parameter, δ . The resulting expression for the capacity factor, k , is

$$\ln k_i = (v_i/RT) (\delta_m + \delta_s - 2\delta_i) (\delta_m - \delta_s) + \ln (n_s/n_m) \quad (1)$$

in which v_i = molar volume ($\text{cm}^3 \text{ mole}^{-1}$) of the solute, R = gas constant ($= 1.9865 \text{ cal K}^{-1} \text{ mole}^{-1}$), T = absolute temperature (K), δ = solubility parameter ($\text{cal}^{1/2} \text{ cm}^{-3/2}$), n = the number of moles present in the column and the subscripts refer to solute (i), mobile (m) and stationary (s) phase.

Two conclusions can readily be drawn from this equation:

(1) Reasonable retention times can be obtained if the polarity (solubility parameter) of the solute is roughly intermediate between those of the two chromatographic phases, *i.e.*:

$$\delta_i \approx \frac{1}{2} (\delta_m + \delta_s) \quad (2)$$

(2) The general selectivity, ∇ , of the chromatographic phase system can be defined as the absolute difference between the polarities of the two phases:

$$\nabla = |\delta_m - \delta_s| \quad (3)$$

∇ determines the separation power of the system towards a pair of solutes with equal molar volumes and a given difference in polarity.

Eqns. 2 and 3 give us the key to the development and operation of LC phase systems. In current high-performance liquid chromatography (HPLC), hydrocarbonaceous stationary phases are favoured, the polarity of which can be approximated by the common value for alkanes: $\delta = 7 \text{ cal}^{1/2} \text{ cm}^{-3/2}$. Adequate general selectivity can then only be obtained with mobile phases of higher polarity, which means that (by definition) we are working with a reversed-phase system (RPLC). The maximum mobile phase polarity is obtained with pure water ($\delta = 25.5$; *cf.*, ref. 16) as the eluent. By using appropriate binary mixtures as mobile phase, all values of δ_m between 7 and 25.5 can be realized and hence, according to eqn. 2, all solutes with polarities between 7 and 16.25 can be eluted from a conventional RPLC column with reasonable retention times. The lower the solubility parameter of the solute, however, the lower that of the mobile phase should be, and hence, with $\delta_s = \text{constant} = 7$, the lower the selectivity of the chromatographic system becomes (*cf.*, eqn. 3).

Perfluorinated hydrocarbons are materials of extremely low polarity, even lower than that of alkanes¹². A value of $\delta = 5$ can be taken as an estimate of their solubility parameter. Hence, a stationary phase containing perfluorinated carbon

chains instead of the conventional alkyl groups can be expected to behave as one of extremely low polarity. If the mobile phase polarity is kept constant, replacement of the conventional RP column ($\delta_s \approx 7$) by a perfluorinated RPF column ($\delta_s \approx 5$) will lead to a decrease in retention. This can easily be seen by differentiation of $\ln k$ (eqn. 1) with respect to δ_s :

$$\partial \ln k / \partial \delta_s = (2v_i/RT) (\delta_i - \delta_s) \quad (1a)$$

Hence, $\ln k$ will decrease with decreasing δ_s , as long as $\delta_i > \delta_s$. This, of course, will always be true in reversed-phase liquid chromatography, and has been observed in practice¹⁰. The familiar remedy is to increase the water content (and hence the polarity) of the mobile phase. This can also be explained in terms of eqn. 2. If the polarity of the stationary phase is decreased, an increase of the mobile phase polarity is needed to fulfil eqn. 2 or, in other words, to maintain optimal retention times.

If we now look at eqn. 3, we see that the combination of a decrease in δ_s and an increase in δ_m should lead to an increase in selectivity in RPLC. Hence, perfluorinated stationary phases might prove to be superior in RPLC.

Iso-elutotropic systems

Previously, we introduced the term iso-elutotropic for mobile phases of different composition that yield (on the average) equal retention times on a given RPLC stationary phase¹³. For example, on RP-18, aqueous solvents containing 36% acetonitrile (ACN) or 33% tetrahydrofuran (THF) are mutually iso-elutotropic, and also with a reference mixture of 50% methanol in water. As a result, the elutotropic strength of such mixtures can be expressed as the volume fraction of the corresponding binary mixture of methanol in water, ϕ_M^* .

When another stationary phase is used the retention will change. However, this effect can be nullified by adapting the mobile phase composition. Let us consider the capacity factor of $k = 5.1$ obtained for chlorobenzene in a binary mixture of 50% methanol and 50% water ($\phi_M^* = 0.5$) on a (reference) RP-18 column. Using a RPF-10 perfluorinated stationary phase, the same retention is obtained with a mobile phase of 34% methanol and 66% water ($\phi_M^* = 0.34$). The value of ϕ_M^* that corresponds to $\phi_M^* = 0.50$ will be different for different solutes. However, if the variations in ϕ_M^* are small, we can take the average over a large number of solutes, ϕ_M^* . The RPLC systems RP-18/methanol (ϕ_M^*)–water and RPF-10/methanol (ϕ_M^*)–water can then be referred to as iso-elutotropic systems. An arbitrary solute is then expected to yield similar capacity factors in both systems.

The specific effect

Since the mobile phase compositions of iso-elutotropic systems are defined as an average over a large number of solutes, few solutes will actually show identical retention times. When a reference RP-18 system is replaced by an iso-elutotropic RPF system, some solutes will be specifically retarded by the stationary phase, while others will be more rapidly eluted. These variations in retention for solutes eluted from iso-elutotropic systems will be referred to as specific effects or specificity¹⁴.

Quantitatively, we can define the specificity for solute i eluted in a particular system relative to the iso-elutotropic system RP-18/methanol–water as

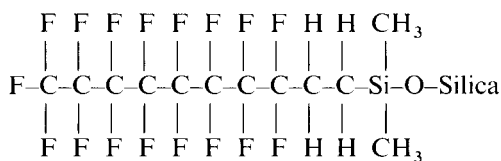
$$S_i = \ln k_i - \ln k_i^* \quad (4)$$

where k_i^* is the capacity factor in the reference system and k_i is the capacity factor in the phase system under consideration. It should be noted that this definition complements the one used to define specific effects induced by the application of different mobile phases¹⁴. Eqn. 4 leads to a positive specificity when a solute is specifically retarded by an RPF stationary phase.

In our first investigation into the behaviour of perfluorinated stationary phases we observed a remarkable positive specificity for molecules containing fluorine atoms. In this paper, we study in more detail the specific effects shown by the RPF column, using a variety of fluorinated solutes, as well as solutes containing other functional groups.

EXPERIMENTAL

The synthesis of the RPF-10 stationary phase has been described by Berendsen *et al.*¹⁰. The starting material 1H, 1H, 2H-perfluorodecene-(1) was purchased from Riedel-de Haën (Seelze-Hannover, G.F.R.) (Code no. 61016). Berendsen *et al.* reported a yield of 60% for the synthesis of the corresponding heptadecafluorodecyl(dimethyl)chlorosilane, *i.e.*, 0.6 moles of silane were obtained from each mole of the starting material. Using a slightly more laborious approach, we have succeeded in obtaining a yield of 80%. The structure of the bonded phase is:



The chromatographic apparatus consisted of a Waters M 6000 pump, a Waters M 440 single-wavelength absorbance detector and a Varian 8050 autosampler equipped with a pneumatic Valco injector. RP-18 columns (300 × 4.6 mm) were packed with a Shandon HPLC packing pump (Cat. no. 628 × 51). The RPF-10 column was packed according to the procedure described in ref. 10. The extremely low polarity of the perfluorocarbon bonded phase has consequences for its wetting properties. To maintain optimum column performance at low modifier content, a pressure restrictor must be included after the detector (or column). Methanol (J. T. Baker, Phillipsburgh, NJ, U.S.A.) and 2,2,2-trifluoroethanol (Aldrich-Europe, Beerse, Belgium) mixed with water were used as mobile phases. The flow-rate was set at 1.5 ml/min and was measured at regular intervals. All measured retention times were corrected for variations in the flow-rate and for the residence time outside the column. For both columns, we assumed a uniform t_0 value of 125 sec (at 1.50 ml/min) (*cf.*, the discussion in ref. 14). All solutes were of the highest purity available and diluted with methanol.

RESULTS AND DISCUSSION

Retention data for nineteen solutes were obtained on two columns, one filled

TABLE I

SUMMARY OF RETENTION DATA OBTAINED ON THE REFERENCE RP-18 AND ON THE PERFLUORINATED RPF-10 COLUMN

The values of $\ln k_0$ and S were obtained from eqn. 5; standard deviations are those from the straight line of eqn. 5 for capacity factors between 1 and 10.

<i>Solute</i>	<i>RP-18</i>			<i>RPF-10</i>		
	$\ln k_0$	S	<i>S.D. 1-10</i>	$\ln k_0$	S	<i>S.D. 1-10</i>
Acetophenone	4.54	6.68	0.01	3.95	6.79	0.08
Benzene	4.87	6.05	0.01	3.23	4.90	0.04
Chlorobenzene	6.38	7.53	0.01	4.60	6.69	0.03
<i>o</i> -Difluorobenzene	5.68	7.15	0.02	4.53	6.43	0.03
Dimethyl phthalate	5.24	7.96	0.01	4.73	8.23	0.03
2,4-Dinitrofluorobenzene	4.08	5.85	0.01	3.27	5.72	0.02
Phenol	3.31	5.96	0.01	2.01	5.37	0.01
Fluorobenzene	5.23	6.58	0.01	3.82	5.59	0.02
<i>p</i> -Fluorophenol	3.82	6.42	0.01	2.57	5.63	0.01
<i>o</i> -Fluoronitrobenzene	4.60	5.79	0.05	3.67	5.99	0.02
<i>m</i> -Fluoronitrobenzene	4.94	6.39	0.01	3.83	5.62	0.01
<i>p</i> -Fluoronitrobenzene	4.51	6.11	0.01	3.85	5.96	0.02
Hexafluorobenzene	6.77	7.76	0.06	6.86	7.71	0.01
Nitrobenzene	4.57	6.05	0.01	3.58	5.73	0.02
<i>p</i> -Nitrophenol	4.00	6.30	0.00	2.78	5.94	0.01
Pentafluorobenzene	6.65	8.07	0.01	6.28	7.49	0.01
1,2,4-Trifluorobenzene	5.67	7.20	0.02	4.96	6.79	0.02
α,α,α -Trifluorotoluene	7.25	8.79	0.01	6.53	8.59	0.03
Toluene	6.15	7.19	0.01	4.43	6.27	0.01

with RP-18 reference material and the other with the RPF-10 perfluorinated stationary phase, using mixtures of methanol and water at 10% composition intervals as the mobile phase. In Table I these data are presented in a condensed form, using a linear equation to relate $\ln k$ with mobile phase composition, ϕ :

$$\ln k = \ln k_0 - S\phi \quad (5)$$

The validity of this equation is limited to capacity factors between 1 and 10 (ref. 15). The parameters $\ln k_0$ and S were obtained from least squares approximation of the generally convex $\ln k$ vs. ϕ curve by a straight line over this particular interval. This procedure has been described before¹⁵. Together with the parameters $\ln k_0$ and S , Table I gives the standard deviation of $\ln k$ from the straight line for k values between 1 and 10. Note that a standard deviation of 0.01 for $\ln k$ corresponds to a deviation of 1% in k , so that it can be concluded that eqn. 5 describes retention within a few percent.

It is seen from Table I that the values obtained for $\ln k_0$ on the RPF-10 column are considerably smaller than those obtained with RP-18. This illustrates that, with the same mobile phase, retention will be weaker on the RPF-10 material. This is in agreement with the prediction from simplified solubility parameter theory that a decrease in δ_s will result in a decrease in retention (*cf.*, eqn. 1a). To compensate

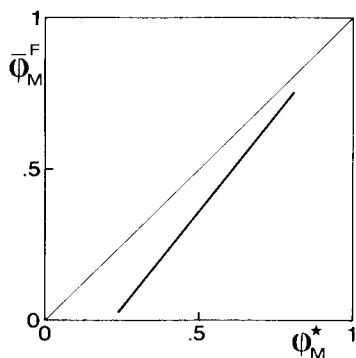


Fig. 1. Iso-elutotropic compositions of methanol-water mixtures on the RPF-10 column, as a function of the methanol-water composition on the reference RP-18 column. Compositions estimated from data on the nineteen solutes listed in Table I.

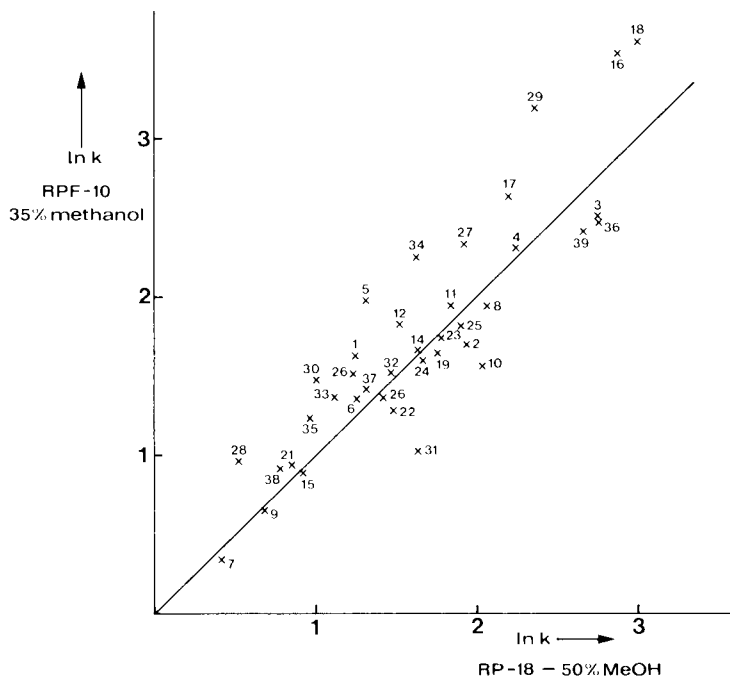


Fig. 2. Logarithmic plot of the capacity factors obtained on the RPF-10 column using a methanol-water (35:65) mobile phase vs. the capacity factors on the iso-elutotropic reference RP-18 system with a methanol-water (50:50) mobile phase. The straight line represents $\ln k_F = \ln k_{18}^*$. Deviations from this line are defined as specific effects (specificity) of the RPF-10 column. Solute: 1-19, as in Table I; 20 = *p*-nitroacetophenone; 21 = 2-phenylethanol; 22 = *p*-chlorophenol; 23 = 2,4-dimethylphenol; 24 = 2,3-dimethylphenol; 25 = anisole; 26 = *o*-nitrophenol; 27 = methyl benzoate; 28 = *p*-chlorobenzaldehyde; 29 = dimethyl phthalate; 30 = benzonitrile; 31 = *p*-methylbenzaldehyde; 32 = 3-phenylpropanol; 33 = *p*-dinitrobenzene; 34 = 3,4-dinitrotoluene; 35 = benzaldehyde; 36 = *p*-phenylphenol; 37 = *o*-dinitrobenzene; 38 = *p*-nitrobenzaldehyde; 39 = 2,5-dimethylphenol.

for this effect, more polar mobile phases should be used with the RPF-10 column than with the RP-18 one.

The correspondence is expressed by the thick solid line in Fig. 1. In order to elute a solute from the RPF-10 column with the same capacity factor as observed on the RP-18 column, a mobile phase must be used that contains less methanol and, hence, more water. Consequently, the RPF-10 material behaves as an even less polar stationary phase, and hence shows less affinity towards the average solute than the common hydrocarbon material.

This effect is definitely due to the fluorination, and not to the shorter chain length of the RPF-10 material (10 rather than 18), as becomes obvious from the following two considerations. First, for the small solutes used in the present study, retention does not increase markedly when the chain length of the hydrocarbon stationary phases is increased from 10 to 18¹. Secondly, an earlier comparison¹⁰ between RPF-10 and a decyl (RP-10) bonded stationary phase confirms the lower polarity of the former.

Having determined the mobile phase composition that allows a fair comparison between RPF-10 and RP-18, we will examine the prediction of improved selectivity provided by the former column. We compared the capacity factors for 38 solutes, obtained with a mixture of 35% methanol and 65% water on the RPF-10 column ($\ln k_F$) with those obtained in the iso-elutotropic system (*cf.*, Fig. 1) applying a methanol-water (50:50) mixture and an RP-18 column ($\ln k_{18}$). The results are shown in Fig. 2. A systematic increase in selectivity on the RPF-10 column would be manifested by a $\ln k_F$ vs. $\ln k_{18}$ plot with a slope of larger than unity. Least squares analysis of the data in Fig. 2 yields a straight line, expressed by $\ln k_F = -0.3 + 1.3 \ln k_{18}$. Hence, the slope of the line is indeed greater than unity. In this case the intercept must be negative because the two systems are iso-elutotropic. However, the scatter of the data points about the line is such that the correlation coefficient is only 0.77. Therefore, we conclude that although the RPF-10 appears to provide a slight gain in selectivity this is overshadowed by large specific effects.

According to eqn. 4, specific effects are defined as deviations from the line $\ln k_F = \ln k_{18}$ in Fig. 2. Solutes that fall above this line show a specific retardation, when RPF-10 is substituted for RP-18. Such solutes can be said to undergo a specific interaction with the RPF-10 phase. Previously, we have observed such a specific interaction between the fluorinated stationary phase and fluorinated solute molecules¹⁰. This observation is confirmed by the data in Fig. 2, *e.g.*, solutes 16 and 18. However, specific effects are not limited to fluorinated solutes. Dimethyl phthalate (5) and diethyl phthalate (29) are good examples of solutes that show a similar specific retardation on RPF-10.

A clear illustration of the specific effects occurring in the RPF-10 system is provided by the chromatograms in Fig. 3. These chromatograms have been constructed using the experimental retention times from Fig. 2. Eight non-fluorinated solutes were used, and although the overall analysis time remains approximately the same in the two chromatograms (as is expected for iso-elutotropic systems), the specific effects are striking. The upper chromatogram corresponds to a methanol-water (50:50) mobile phase on the RP-18 column. The solutes are numbered in order of appearance and are listed in Table II, together with the logarithms of their capacity factors. The lower chromatogram in Fig. 3 shows the elution of the same mixture on the

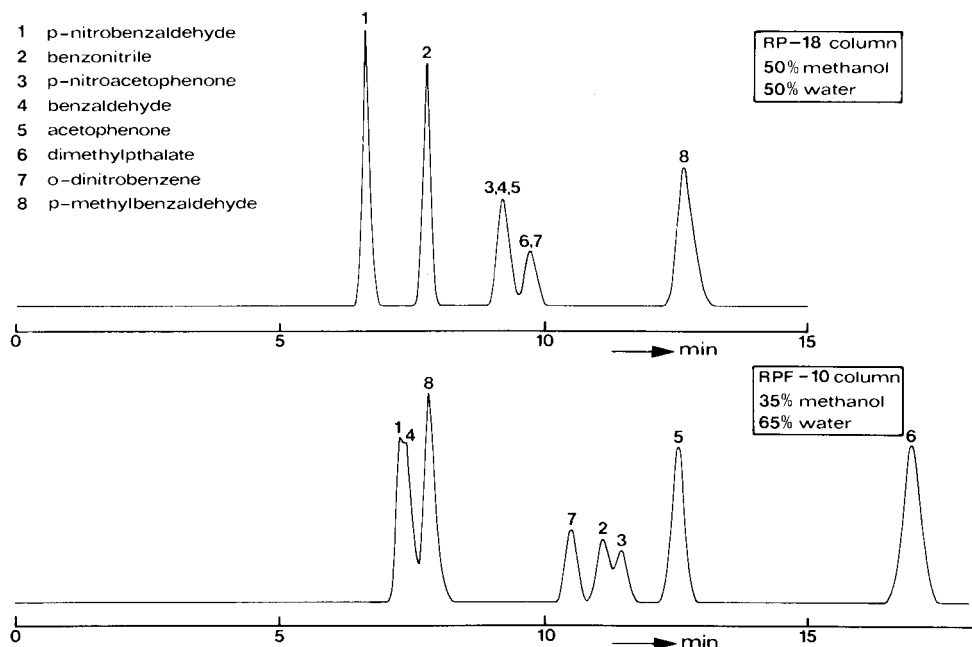


Fig. 3. Chromatograms illustrating the specific effects observed on an RPF-10 column for non-fluorinated solutes. Retention data taken from Fig. 2. Column: 30 cm \times 4.6 mm I.D. Flow-rate: 1.5 ml/min.

iso-elutropic RPF-10 system with a methanol-water (35:65) mobile phase. The appropriate retention data are also shown in Table II. The last column in this table gives the specificities for the present mixture of eight solutes according to eqn. 4. The values for S_i demonstrate once more the large specific effects that can be observed for non-fluorinated molecules. Dimethyl phthalate shows an almost two-fold increase in retention on the RPF-10 column, while the opposite is true for *p*-methylbenzaldehyde. Of course, the fluorinated chains at the silica surface should not be held responsible for all the observed specific effects. Since the content of water and that of methanol in the mobile phase are changed when RPF-10 is substituted for RP-18, the specific effects

TABLE II

RETENTION AND SPECIFICITY FOR THE SOLUTES IN FIG. 3

Peak no.	Solute	$\ln k_{18}$ 50% MeOH	$\ln k_F$ 35% MeOH	S_i
1	<i>p</i> -Nitrobenzaldehyde	0.77	0.92	0.14
2	Benzonitrile	1.00	1.47	0.47
3	<i>p</i> -Nitroacetophenone	1.23	1.51	0.28
4	Benzaldehyde	1.23	0.95	-0.28
5	Acetophenone	1.24	1.62	0.37
6	Dimethyl phthalate	1.30	1.97	0.67
7	<i>o</i> -Dinitrobenzene	1.31	1.40	0.09
8	<i>p</i> -Methylbenzaldehyde	1.62	1.02	-0.61

may also be caused by interactions with water or methanol. For example, the specific retardation of acetophenone and dimethyl phthalate on the RPF-10 system could easily be explained by assuming a specific interaction between methanol and the carbonyl groups of these solute molecules.

To elucidate further the nature of the specific effects observed for both fluorinated and non-fluorinated molecules, we used a fluorinated mobile phase, 2,2,2-trifluoroethanol (TFE), as the organic modifier in binary mixtures with water. If the specific effects are indeed due to specific interactions with fluorine, through the very low dispersive interaction observed for perfluorinated molecules (*cf.*, ref. 11), then we may expect a fluorinated mobile phase to lead to a specific acceleration of fluorinated molecules relative to their hydrocarbon analogues.

TABLE III

RETENTION AND SPECIFICITY OBSERVED WITH 2,2,2-TRIFLUOROETHANOL (TFE) IN THE MOBILE PHASE

Solute	23% TFE		40% TFE		50% TFE	
	$\ln k_i$	S_i	$\ln k_i$	S_i	$\ln k_i$	S_i
Benzene	3.01	-0.16	1.77	-0.42	1.30	-0.37
Fluorobenzene	3.20	-0.16	1.75	-0.35	1.23	-0.30
<i>o</i> -Difluorobenzene	3.25	-0.07	1.74	-0.21	1.19	-0.16
1,2,4-Trifluorobenzene	3.23	-0.08	1.64	0.16	1.06	-0.09
Pentafluorobenzene	3.56	0.62	1.71	0.27	1.08	0.30
Hexafluorobenzene	3.77	0.32	1.80	0.52	1.15	0.57
Dimethyl phthalate	3.72	-1.13	1.70	-1.10	1.04	-0.92
Acetophenone	3.27	-0.99	1.56	-0.93	0.97	-0.77
<i>p</i> -Fluoronitrobenzene	2.73	-0.30	1.06	-0.12	0.42	0.11
<i>m</i> -Fluoronitrobenzene	2.86	-0.05	1.17	0.04	0.65	0.12
<i>o</i> -Fluoronitrobenzene	2.62	-0.05	0.98	0.26	0.44	0.39
Toluene	4.01	0.06	2.37	-0.36	1.85	-0.39
Chlorobenzene	4.14	0.11	2.49	-0.45	1.99	-0.53
2,4-Dinitrofluorobenzene	1.66	0.37	0.14	0.55	-0.36	0.64
Nitrobenzene	2.92	0.39	1.30	0.26	0.77	-0.14
α,α,α -Trifluorotoluene	4.36	0.40	2.32	-0.12	1.70	-0.17
Phenol	0.42	0.74	-0.35	0.29	-0.64	0.25
<i>p</i> -Fluorophenol	0.42	1.13	-0.47	0.60	-0.77	0.53
<i>p</i> -Nitrophenol	0.27	1.53	-0.82	1.17	-1.14	1.11
Reference composition (% MeOH):	35		58		65	

The nineteen solutes of Table I were eluted with three different binary mixtures of TFE and water, containing 23, 40 and 50% TFE, respectively. For each of these mobile phases we can calculate the composition of the binary methanol-water mixture that can be used as the iso-elutotropic reference system. These compositions are shown at the bottom of Table III. In this case, specificity should be defined as

$$S_i = \ln k_i^* - \ln k_i \quad (6)$$

because this results in a positive specificity when the specific interaction between solute and mobile phase causes a specific acceleration.

The observed retention data, together with the calculated specificities from eqn. 6, are presented in Table III. The S_i values show that large specific effects are observed, again for fluorinated as well as for non-fluorinated solutes. Remarkably, the highest specificities are observed, not for the highly fluorinated benzenes, but for phenol and two substituted phenols. The occurrence of such strong specific effects leads to an (average) reference methanol–water composition, such that benzene derivatives with a low degree of fluorination do not show positive specificities. However, the effect of fluorination can be seen in the series benzene, monofluorobenzene, trifluorobenzene, pentafluorobenzene and hexafluorobenzene. Since the specificities increase in this order a positive specific effect is observed for fluorine, which could be interpreted as a specific fluorine–fluorine interaction.

However, the esters (*e.g.*, dimethyl phthalate) and ketones (*e.g.*, acetophenone) that showed large positive specificities on the RF-10 column now show large negative S_i values. Hence, the underlying specific interactions do not originate from the introduction of fluorine atoms in the system. Rather, these observations should be

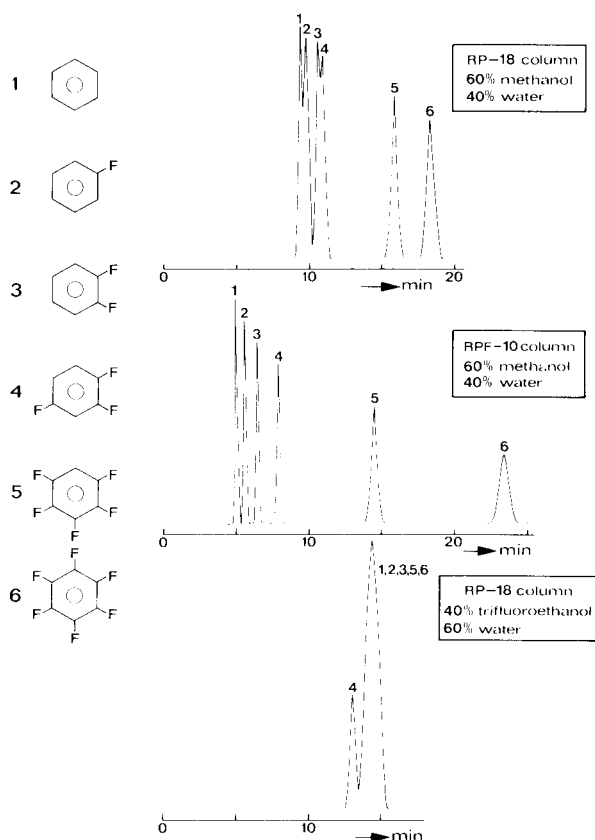


Fig. 4. Chromatograms illustrating the effects of specific fluorine fluorine interactions in both the stationary and the mobile phase. Chromatograms constructed using experimental retention data. Other details as in Fig. 3.

ascribed to the change in mobile phase composition, when RP-18 is substituted by RPF-10, or methanol by TFE.

The exploitation of the large specific effects observed with TFE in practical RPLC will, of course, be restricted by the high cost of TFE.

The specific effects observed for fluorinated solutes, both on the RPF-10 stationary phase and with the TFE mobile phase, enable us to manipulate the separation of fluorinated molecules. This is demonstrated by the three chromatograms in Fig. 4. In the upper chromatogram, we show the separation that can be obtained for benzene and five fluorinated benzenes, all with different numbers of fluorine atoms, in a conventional RPLC system, applying an RP-18 column and a methanol–water (60:40) mobile phase. The separation is poor for two solute pairs: benzene and fluorobenzene (peaks 1 and 2), and *o*-difluorobenzene and 1,2,4-trifluorobenzene (peaks 3 and 4). The second chromatogram shows how the separation can be enhanced by substituting RPF-10 for RP-18. The mobile phase used is the same as for the upper chromatogram. Hence, the two systems are not iso-elutotropic. The overall retention time, however, remains largely unaltered, due to the specific retardation of the fluorinated solutes. The separation is excellent. The final chromatogram underlines our control of specific fluorine–fluorine interactions. With a mobile phase of 2,2,2-trifluoroethanol–water (40:60) on an RP-18 column, the separation deteriorates quite remarkably. Somewhat surprisingly, trifluorobenzene is eluted first, but all other solutes overlap to give a single peak.

Hence, the RPF-10 column has considerable advantages for the separation of solutes with different degrees of fluorination, while a fluorinated mobile phase shows the opposite behaviour. This is borne out by practical RPLC separation problems; an application of RPF-10 for the separation of some herbicides was studied previously¹⁰, and we are at present investigating the application of RPF-10 to the separation of some fluorine-containing drugs.

CONCLUSIONS

The RPF-10 stationary phase behaves as a material of extremely low polarity, relative to the non-polar RP-18. The observed differences in behaviour between these phases are strictly due to the change in polarity, and not to the shorter chain length of the RPF-10 phase. The low polarity of the RPF-10 material results in a decrease in retention time, provided that the mobile phase is kept constant. Alternatively, the same retention is obtained if the water content of the mobile phase is increased, thus creating iso-elutotropic phase systems.

When these iso-elutotropic systems are compared, the general selectivity of the RPF-10 system is expected to be larger than that of the RP-18 system. Although this might be true in practice, the gain in selectivity is overshadowed by large specific effects.

Such effects occur not only for fluorinated solutes, but also for several non-fluorinated classes of compounds, *e.g.*, esters and ketones. The specificities shown by the RPF-10 column lead to astonishing effects on the separation of simple organic mixtures, even if no fluorine atoms are present in the solutes.

The specific effect towards fluorine can be reversed, if fluorine atoms are introduced in the mobile phase, rather than in the stationary phase. It is shown that

fluorine-fluorine interactions can be controlled, either to enhance the separation of fluorinated molecules on an RPF-10 system, or to suppress separation by using TFE in the mobile phase.

The RPF-10 material provides an intriguing stationary phase for RPLC, with many possible applications to the separation of fluorinated as well as non-fluorinated solutes.

REFERENCES

- 1 G. E. Berendsen and L. de Galan, *J. Chromatogr.*, 196 (1980) 21.
- 2 H. Hemetsberger, P. Behrensmeier, J. Henning and R. Ricken, *Chromatographia*, 12 (1979) 71.
- 3 G. E. Berendsen, K. A. Pikaart and L. de Galan, *J. Liquid Chromatogr.*, 3 (1980) 1437.
- 4 H. Binder, *J. Chromatogr.*, 189 (1980) 414.
- 5 R. E. Majors, *J. Chromatogr. Sci.*, 18 (1980) 488.
- 6 L. R. Snyder and J. J. Kirkland, *Introduction to Modern Liquid Chromatography*, Wiley, New York, 2nd ed., 1979, pp. 305, 758.
- 7 V. Rehák and E. Smolková, *J. Chromatogr.*, 191 (1980) 71.
- 8 G. E. Berendsen and L. de Galan, *J. Liquid Chromatogr.*, 1 (1978) 403.
- 9 G. E. Berendsen, K. A. Pikaart and L. de Galan, in G. L. Hawk (Editor), *Biological/Biomedical Applications of Liquid Chromatography IV*, Marcel Dekker, New York, 1981.
- 10 G. E. Berendsen, K. A. Pikaart, L. de Galan and C. Olieman, *Anal. Chem.*, 52 (1980) 199.
- 11 P. J. Schoenmakers, H. A. H. Billiet and L. de Galan, *Anal. Chem.*, submitted for publication.
- 12 J. H. Hildebrand, J. M. Prausnitz and R. L. Scott, *Regular and Related Solutions*, Van Nostrand-Reinhold, New York, 1970, p. 214.
- 13 P. J. Schoenmakers, H. A. H. Billiet and L. de Galan, *J. Chromatogr.*, 205 (1981) 13.
- 14 P. J. Schoenmakers, H. A. H. Billiet and L. de Galan, *J. Chromatogr.*, 218 (1981) 261.
- 15 P. J. Schoenmakers, H. A. H. Billiet and L. de Galan, *J. Chromatogr.*, 185 (1979) 179.
- 16 R. Tijssen, H. A. H. Billiet and P. J. Schoenmakers, *J. Chromatogr.*, 122 (1976) 185.

CHROM. 14,067

SEPARATION OF PROTON-DONATING SOLUTES BY LIQUID CHROMATOGRAPHY WITH A STRONG PROTON ACCEPTOR, TRI-*n*-OCTYLPHOSPHINE OXIDE, IN THE LIQUID STATIONARY PHASE

H. W. STUURMAN* and K.-G. WAHLUND

Department of Analytical Pharmaceutical Chemistry, Biomedical Center, University of Uppsala, Box 574, S-751 23 Uppsala (Sweden)

SUMMARY

Proton-donating solutes, such as aromatic and aliphatic carboxylic acids, are separated in a reversed-phase liquid-liquid chromatographic system with a stationary phase consisting of tri-*n*-octylphosphine oxide (TOPO) in *n*-decane. The retention is based on the formation of a complex between the sample and TOPO, the stoichiometry depending on the number of proton-donating groups in the sample. The retention and separation selectivity are governed by the pH of the mobile phase and the concentration of TOPO in the stationary phase. The latter can be regulated by the addition of competing proton donors to the mobile phase. An example of the separation of several aromatic carboxylic acids and phenol by gradient elution is given.

INTRODUCTION

Reversed-phase liquid-liquid chromatography offers interesting possibilities for the separation of hydrophilic organic acids when a strong proton acceptor such as tri-*n*-octylphosphine oxide (TOPO) is added to the liquid stationary phase. A retention model and some results obtained with such systems have been given in a previous paper¹.

The system contains a solution of TOPO in *n*-decane as stationary phase, coated on a microparticulate support. The mobile phase is an aqueous buffer solution. The concentration of free TOPO in the organic stationary phase determines the retention and the separation selectivity. The concentration can be varied by changing the stationary phase¹, but a more convenient way is to add a competing proton-donating solute to the mobile phase. This makes it possible to perform, *e.g.*, gradient elution to separate both hydrophobic and hydrophilic samples, and also protolytes of different acidity.

The aim of this study was to elucidate the regulation of the retaining properties of the system by changing the composition of the mobile phase.

EXPERIMENTAL

Apparatus

The pump was a Model 110A solvent metering pump (Altex, Berkeley, CA, U.S.A.), equipped with a pulse damper and a pressure transducer (Touzart et Matignon, Vitry, France). A Valco CV-6-UHPa-N60 injection valve (Valco, Houston, TX, U.S.A.) with a 30.6- μ l loop was used for injection of the samples. The UV detectors (LDC, Riviera Beach, FL, U.S.A.) were a UV III Monitor Model 1203, wavelength 254 nm, with a cell volume of 10 μ l, and a Spectromonitor III Model 1204, with a variable wavelength and a cell volume of 12 μ l. The time constant of both detectors was set to 0.5 sec.

The columns (150 \times 4.6 mm I.D.) were made of stainless steel with a polished inner surface, equipped with modified Swagelok connectors and Altex stainless-steel frits (2 μ m). The volume of the empty columns, V_0 , was 2.46 ml as measured volumetrically.

A HETO waterbath (Birkerød, Denmark) Type 02 PT 923 was used to thermostat the system.

For the preparation of the columns a Haskel (Burbank, CA, U.S.A.) air-driven fluid pump, Type DST-150A was used.

Chemicals and reagents

TOPO (for extraction analysis) was obtained from E. Merck (Darmstadt, G.F.R.) and *n*-decane (for synthesis grade) (99 %) and *n*-valeric acid (p.a. grade) were obtained from Schuchardt (Hohenbrunn, G.F.R.).

All other substances were of analytical or reagent grade and were used without further purification.

Column preparation

The support material, LiChrosorb RP-8, mean particle diameter (d_p) 7 μ m, research sample KE 5679, was kindly supplied by E. Merck. It was packed upwards into the column by a slurry packing technique at a pressure of 37.5 MPa, using cyclohexane, isopropanol or mixtures of these with *n*-hexane as suspending liquid (1.3 g of support in 10–20 ml of liquid). After packing, the filling was washed with *n*-hexane (100–200 ml upwards and 100–150 ml downwards), and tested with 0.5 % (v/v) *n*-butanol in *n*-hexane as eluent. Toluene, 1,4-dinitrobenzene and 2,3,5-trimethylphenol were used as test solutes. In this study columns were used that had a reduced plate height ($h = H/d_p$) of less than 7 at a flow rate of 1 mm/sec and asymmetry factors (measured at 10 % of the peak height) between 0.85 and 1.6.

Coating technique

After testing, the column was washed with *n*-hexane. The stationary phase (*n*-decane with varying amounts of TOPO) was applied on the support by the pumping method, as described previously¹.

Chromatographic technique

The reservoir and the column were immersed in the water-bath at 25.0 C.

The mobile phases were aqueous buffer solutions of different pH, ionic

strength 0.1, if not stated otherwise. The mobile and stationary phases were usually not equilibrated with each other.

The volume of the mobile phase, V_m , was determined from the hold-up volume of sodium nitrate or water, after subtraction of the dead volume. The dead volume was determined by measuring the elution volume with the injector directly connected to the detector at a flow-rate of 0.08 ml/min. It was largely due to the volume of the connecting tubings and the heat exchanger in the detector and corresponded to 127 μ l with the Model 1203 detector and 110 μ l with the Model 1204 detector, *i.e.*, *ca.* 10% of V_m .

The porosity, ϵ_m , was calculated from the equation

$$\epsilon_m = V_m/V_0 \quad (1)$$

RESULTS AND DISCUSSION

Choice of support and diluent

The proton-accepting properties of the complexing agent TOPO are best utilized if TOPO is dissolved in an organic solvent which has a very low proton-donating tendency. To obtain good stability the support material should be better wetted by the stationary liquid than by the mobile liquid, *i.e.*, it should be hydrophobic². A totally porous silica support derivatized with octyl chains (LiChrosorb RP-8) was used in these studies.

Several organic solvents were tested as diluents for TOPO. A chloroform coating stripped off very rapidly. *n*-Dodecane and *n*-hexadecane required very long equilibration times, and *n*-hexane showed some instability (stripping). *n*-Decane, showing good stability and a not too long equilibration time, was chosen as diluent in these studies.

Stability and reproducibility of n-decane/TOPO-coated columns

The stability of the *n*-decane-coated columns was studied for periods of 2

TABLE I

STABILITY OF COATED COLUMNS

Stationary phase: 0.1 M TOPO in *n*-decane on LiChrosorb RP-8. Mobile phases: days 7–24, phosphate buffer solutions (pH 1.8), containing 0.0025 M valeric acid; days 24–55, formate buffer solution (pH 3.9). Formate buffer solution (pH 3.9) was used as the mobile phase for all measurements of k' .

Solute	k'		
	Day 7	Day 24	Day 55
Phenol	42.9	38.7	37.0
Benzoic acid	53.4	48.1	44.5
3-Hydroxybenzoic acid	39.0	33.7	32.2
3-Hydroxy-4-methoxybenzoic acid	5.45	4.88	4.63
4-Hydroxyphenylacetic acid	4.50	4.01	3.76
5-Hydroxyindole-3-acetic acid	1.91	1.76	1.69

months at most. The retention decreased by less than 1% per day under conditions that implied frequent changes of the composition of the mobile phase (Table I). As the capacity ratios change by nearly the same factor in spite of differences in the stoichiometry of the complexes¹, the decrease in k' cannot be due to a change in the TOPO concentration. A change in the volume of the stationary phase, V_s , seems to be more plausible, but no significant changes in the porosity could be observed.

Changes in the pH of the mobile phase and pre-saturation of the mobile phase with stationary phase had no significant influence on the stability, probably owing to the very low solubility of the organic phase in the mobile phase.

With the pumping technique, the porosity reached a value of 0.425–0.430 (15 columns), which indicates that the pores of the support are almost completely filled². The pore filling is obviously highly reproducible.

On three columns prepared in the same way, the retention of solutes with a capacity ratio between 4 and 40 could be reproduced to within 15%.

Regulation of the retention

The capacity factor of a proton-donating solute HX in the liquid–liquid system with the strong proton acceptor TOPO in the stationary phase can be expressed by

$$k'_{\text{HX}} = \frac{V_s}{V_m} \cdot \frac{K_{D(\text{HX})} \cdot K_{\text{HXTOPOn}} \cdot [\text{TOPO}]^n}{1 + K'_{a(\text{HX})} \cdot (a_{\text{H}^+})^{-1}} \quad (2)$$

where the subscript m refers to the mobile phase; concentrations in the stationary liquid phase are given without a subscript; $K_{D(\text{HX})} = [\text{HX}]/[\text{HX}]_m$ is the distribution constant and $K_{\text{HXTOPOn}} = [\text{HXTOPOn}]/[\text{HX}] \cdot [\text{TOPO}]^n$ is the formation constant between the solute and TOPO.

A demonstration of the effect of the number of proton-donating groups in the solute (n) is given in Figs. 1 and 2. With 0.15 M TOPO in the stationary phase, mandelic acid and its 3-hydroxy derivative are not separated (Fig. 1). According to eqn. 2 the separation factor of these compounds will change with the TOPO concentration, because the n values are different. On decreasing the TOPO concentration to 0.10 M , 3-hydroxymandelic acid ($n = 2$) becomes less retained than mandelic acid ($n = 1$), giving a good separation (Fig. 2). The separation factor between 3-hydroxymandelic acid and 3,4-dihydroxymandelic acid remains almost constant, indicating that n is the same for these compounds. 3,4-Dihydroxymandelic acid has three proton-donating groups but the second phenolic hydroxy group might be occupied by internal hydrogen bonding.

Retention with formate buffer solutions

The retention of phenol ($\text{p}K'_a = 9.9$) should be independent of the composition of the mobile phase at a pH lower than 8 (see eqn. 2). Constant capacity factors at pH 2–7 were obtained with phosphate buffer solutions and sodium perchlorate solution as mobile phases, but with a formate buffer solution the retention at pH 4 was *ca.* 25% lower (Table II). This effect might be due to complex formation between formic acid (HFO) and TOPO in the stationary phase. The concentration of free TOPO, $[\text{TOPO}]_f$, in the formate system decreases:

$$[\text{TOPO}]_f = C_{\text{TOPO}} - n[\text{HFO} \cdot \text{TOPO}]_n \quad (3)$$

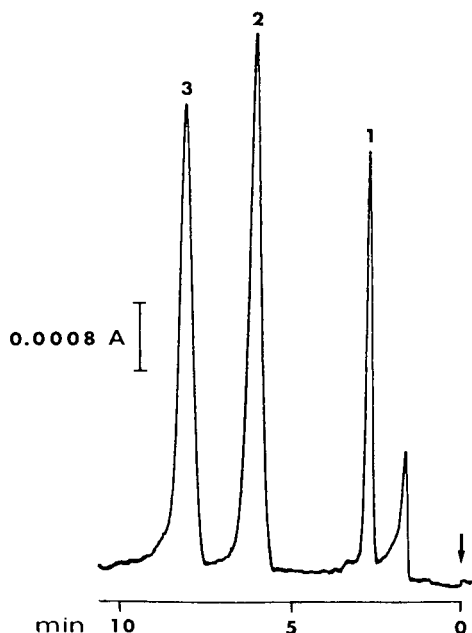
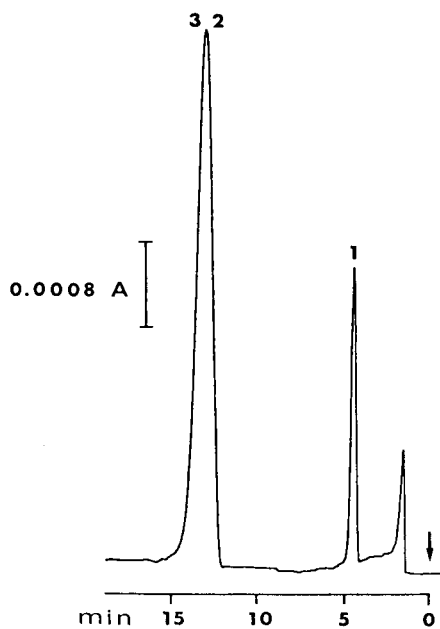


Fig. 1. Separation of mandelic acid derivatives. Stationary phase: 0.15 *M* TOPO in *n*-decane. Mobile phase: phosphate buffer solution (pH 1.8); 0.8 ml/min. Detection wavelength: 254 nm. Solutes: 1 = 3,4-dihydroxymandelic acid; 2 = 3-hydroxymandelic acid; 3 = mandelic acid.

Fig. 2. Separation of mandelic acid derivatives. Stationary phase: 0.10 *M* TOPO in *n*-decane. Mobile phase, detection wavelength and solutes as in Fig. 1.

where C_{TOPO} is the total concentration of TOPO.

If we assume that phenol (ph) and formic acid have $n = 1$, and that the complex formation between TOPO and perchlorate is negligible, the following relationship is obtained between the capacity factors in perchlorate solution, $k'_{\text{ph(p)}}$, and in formate buffer solution, $k'_{\text{ph(f)}}$, (cf., eqn. 2):

$$\frac{k'_{\text{ph(p)}}}{k'_{\text{ph(f)}}} = \frac{C_{\text{TOPO}}}{[\text{TOPO}]_{\text{f}}} \quad (4)$$

TABLE II

INFLUENCE OF MOBILE PHASE COMPOSITION ON RETENTION

C_{TOPO} (<i>M</i>)	k'_{phenol}		k' ratio	$K_{\text{D(HFo)}} \cdot K_{\text{HFO/TOPO}}$
	0.1 <i>M</i> <i>NaClO</i> ₄	Formate pH 4		
0.075	39.1	30.6	1.28	6.37
0.100	57.0	45.0	1.28	6.38
0.150	104.7	81.4	1.29	6.56

V_s/V_m and C_{TOPO} have to be kept constant. The ratios $k'_{\text{ph(p)}}/k'_{\text{ph(f)}}$ are presented in Table II.

The ratio is independent of the total concentration of TOPO, which supports the assumption of $n = 1$ for formic acid. Phenol almost had the same retention with 0.1 M sodium perchlorate solution and with phosphate buffer solutions at pH 2, 3, 6 and 7, which indicates that the concentration of free TOPO was not influenced by phosphoric acid, phosphates or perchlorate. Sekine and co-workers^{3,4} have made the same observations in batch experiments with similar systems.

The distribution of formic acid to the stationary phase is governed by $K_{D(\text{HFO})} \cdot K_{\text{HFO} \cdot \text{TOPO}}$, defined by

$$K_{D(\text{HFO})} \cdot K_{\text{HFO} \cdot \text{TOPO}} = \frac{[\text{HFO} \cdot \text{TOPO}]}{[\text{TOPO}] \cdot [\text{HFO}]_m} \quad (5)$$

An expression that allows the calculation of this constant can be obtained from eqn. 3:

$$K_{D(\text{HFO})} \cdot K_{\text{HFO} \cdot \text{TOPO}} = \left(\frac{C_{\text{TOPO}}}{[\text{TOPO}]_f} - 1 \right) \cdot \frac{1}{[\text{HFO}]_m} \quad (6)$$

The concentration of formic acid in the mobile phase can be calculated from the pH of the mobile phase and the K'_a value of formic acid. The values of $K_{D(\text{HFO})} \times K_{\text{HFO} \cdot \text{TOPO}}$ calculated according to eqn. 6 are given in Table II.

Regulation of the concentration of free TOPO

Eqn. 6 can be transformed into a general expression for the concentration of free TOPO when a competing monobasic acid HY is added to the mobile phase:

$$[\text{TOPO}] = C_{\text{TOPO}} \left\{ 1 + K_{D(\text{HY})} \cdot K_{\text{HY} \cdot \text{TOPO}} \cdot \left[\frac{C_{\text{HY}_m}}{1 + K'_{a(\text{HY})} \cdot (a_{\text{H}^+})^{-1}} \right] \right\}^{-1} \quad (7)$$

This equation shows that the concentration of free TOPO at a given C_{TOPO} depends on the properties of the competing acid HY, expressed by the product of the distribution constant and the complex formation constant, $K_{D(\text{HY})} \cdot K_{\text{HY} \cdot \text{TOPO}}$, and by the acid dissociation constant, $K'_{a(\text{HY})}$. The concentration of free TOPO can be regulated by the total concentration of the competitor in the mobile phase, C_{HY_m} , and the pH of the mobile phase.

Eqn. 7 can be used to calculate the amount of competing acid that is needed to obtain a given suppression of [TOPO]. If, for example, a reduction by 90% is required, then the product $K_{D(\text{HY})} \cdot K_{\text{HY} \cdot \text{TOPO}} \cdot C_{\text{HY}_m}$ has to be 9, if HY is undissociated at the pH of the mobile phase [$K'_{a(\text{HY})}/a_{\text{H}^+} \ll 1$].

From a practical point of view, it is favourable if the competing acid has a low detector response. A number of aliphatic organic acids were tested. They have a λ_{max} at ca. 210 nm, whereas the samples, aromatic acids, were detected at 254 nm. The study was made at pH 1.85 where all competing acids, except formic acid, are undissociated. Their complexing ability can be determined by chromatography. According to eqn. 2, $K_{D(\text{HY})} \cdot K_{\text{HY} \cdot \text{TOPO}}$ is proportional to k'_{HY} , and can be calculated if V_s/V_m , [TOPO], n and $\text{p}K'_{a(\text{HY})}$ are known.

TABLE III
RETENTION OF ALIPHATIC ACIDS

Stationary phase: 0.1 *M* TOPO in *n*-decane. Mobile phase: phosphate buffer solution (pH 1.85), ionic strength 0.1. $V_s/V_m = 0.7$.

Acid	k'	$K_{D(HY)} \cdot K_{HYTOPO}$
Formic	0.43	6.2
Acetic	0.38	5.4
Propionic	1.77	25.2
Butyric	7.3	103
Valeric	30.5	433

The capacity factors of some hydrophilic aliphatic acids, intended as competing acids, are given in Table III, together with the calculated $K_{D(HY)} \cdot K_{HYTOPO}$ values; n was taken as equal to unity. It can be seen that, with the exception of formic acid, $K_{D(HY)} \cdot K_{HYTOPO}$ increases with increasing number of carbon atoms in the molecule ($\Delta \log k' = 0.63$ per CH_2 group). At the same time however, the solubility of the acids in water decreases, and the product $K_{D(HY)} \cdot K_{HYTOPO} \cdot C_{HY, m, \max}$ (cf., eqn. 7) is virtually constant for the more hydrophobic acids, which means that the maximal suppression of free TOPO cannot be increased by increasing the number of carbon atoms in the competitor.

In the following experiment we used *n*-valeric acid as competitor. A concentration of 0.0025 *M* in the mobile phase was sufficient to decrease the concentration of free TOPO by 50%.

Regulation of retention by competition

A number of samples were chromatographed with different concentrations of valeric acid in the mobile phase. The retention of the sample is described by eqn. 2. When the concentration of free TOPO is regulated by the addition of a competing acid HY, $[\text{TOPO}]$ can be calculated from eqn. 7. $K_{D(HY)} \cdot K_{HYTOPO}$ for valeric acid was taken from Table III. A linear relationship was obtained between $\log k'_{HX}$ and \log

TABLE IV
REGULATION OF RETENTION BY COMPETITION

$C_{\text{TOPO}} = 0.1$ *M*. Mobile phase: phosphate buffer solution (pH 1.85). Competitor: *n*-valeric acid, 0–0.0025 *M*. $V_s/V_m = 0.7$. Evaluation methods: logarithmic form of eqn. 2 (\log) and non-linear regression using eqn. 8 (non-lin).

Solute	$\log K_{D(HY)} \cdot K_{HYTOPO}$		Number of TOPO molecules in complex (<i>n</i>)			k'_0
	Log	Non-lin	Log	Non-lin	Expected	
Mandelic acid	1.95	2.05	1.2	1.3	1	0.3
Phenol	2.91	2.99	1.0	1.1	1	3.8
3-Hydroxy-4-methoxybenzoic acid	2.75	3.00	1.5	1.8	2	1.0
3-Hydroxybenzoic acid	4.06	4.21	1.8	2.0	2	4.4

[TOPO], which is in accordance with eqn. 2 (*cf.*, ref. 1). The constants n and $\log K_{D(\text{HX})} \cdot K_{\text{HXTOPOn}}$, which can be calculated from the slope and the intercept of the line, are presented in Table IV.

The agreement between these values and the previously published constants (Table I in ref. 1) is not satisfactory. There are a number of possible reasons for these deviations. It is assumed that retention of the sample is zero in the absence of TOPO, *i.e.*, the sample is not retained by the support and the magnitude of the distribution constant $K_{D(\text{HX})}$ is negligible in comparison with $K_{D(\text{HX})} \cdot K_{\text{HXTOPOn}} \cdot [\text{TOPO}]^n$. Batch experiments have shown that this condition is fulfilled for 3-hydroxybenzoic acid in the [TOPO] range used chromatographically. However, it was found that all samples are retained on the column even in the absence of TOPO, indicating that adsorption to some surface is taking place. Further details about this side-effect will be given in a forthcoming paper. A slight modification of eqn. 2 will describe the retention better:

$$k'_{\text{HX}} = k'_0 + \left[\frac{V_s}{V_m} \cdot \frac{K_{D(\text{HX})} \cdot K_{\text{HXTOPOn}}}{1 + K'_{a(\text{HX})} \cdot (a_{\text{H}^+})^{-1}} \right] \cdot [\text{TOPO}]^n \quad (8)$$

where k'_0 represents the retention of the sample in absence of TOPO. The constants k'_0 , n and $K_{D(\text{HX})} \cdot K_{\text{HXTOPOn}}$ cannot be evaluated by simple linear or logarithmic plots, and a non-linear curve-fitting procedure using eqn. 8 was applied to the data (*cf.*, ref. 5). The constants found are presented in Table IV.

The data from ref. 1 should be treated in the same way in order to make comparison possible, but the constants evaluated in this way are very uncertain owing, for example, to the fact that different columns had to be used. A further

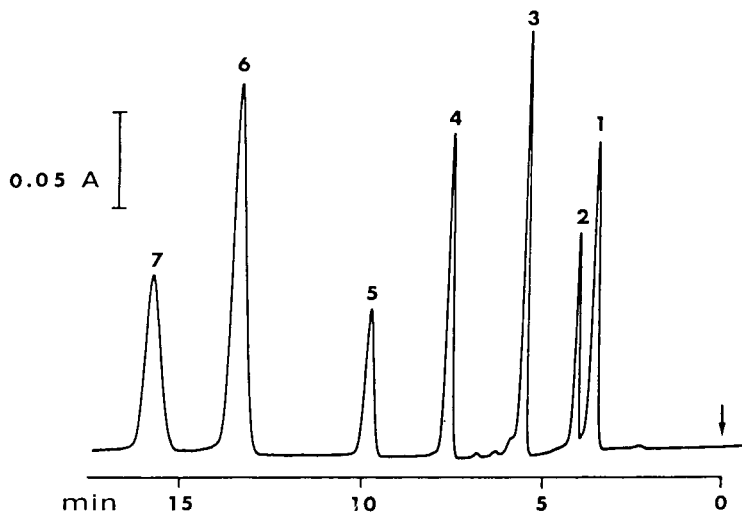


Fig. 3. Separation of some aromatic acids by gradient elution. Stationary phase: 0.165 *M* TOPO in *n*-decane. Mobile phase: step gradient from phosphate buffer solution of pH 1.9 (0–4 min) to acetate buffer solution of pH 2.9 (4–20 min); 0.6 ml/min. Detection wavelength: 270 nm. Solutes: 1 = 4-hydroxy-3-methoxymandelic acid; 2 = 3,4-dihydroxymandelic acid; 3 = 4-hydroxyphenylacetic acid; 4 = 4-hydroxybenzoic acid; 5 = phenylacetic acid; 6 = phenol; 7 = benzoic acid.

discussion on the differences between the values of n and $K_{D(HX)} \cdot K_{HXTOPO_n}$ will be given in a forthcoming paper. In the meantime, we can conclude that addition of a competing acid to the mobile phase can be used to regulate the retention and the selectivity of proton-donating samples.

Gradient elution

The regulation of the retaining properties of the system by the composition of the mobile phase can be easily utilized for gradient elution. An example is given in Fig. 3. The first two solutes, 4-hydroxy-3-methoxymandelic acid and 3,4-dihydroxymandelic acid, are so hydrophilic that they can be separated in the phase system only if the stationary phase contains a high concentration of free TOPO and if the pH of the mobile phase is low. Under these conditions phenol has a very high capacity factor. An increase in the pH of the mobile phase to 7 does not influence the retention, owing to its pK'_a value of 9.9. Only a decrease in [TOPO] will greatly reduce the retention of phenol. This was done by changing to an acetate buffer solution as the mobile phase. Under these conditions a high separation factor between benzoic acid and 4-hydroxybenzoic acid is also obtained.

ACKNOWLEDGEMENTS

We are very grateful to Professor Göran Schill for his interest in this work and for valuable discussions on the manuscript. A travel grant from the C. D. Carlssons Foundation (Swedish Academy of Pharmaceutical Sciences) to one of us (H.W.S.), which made it possible to present this work at the 5th International Symposium on Column Liquid Chromatography, Avignon, May 1981, is gratefully acknowledged.

REFERENCES

- 1 H. W. Stuurman, K.-G. Wahlund and G. Schill, *J. Chromatogr.*, **204** (1981) 43.
- 2 J. C. Giddings, *Dynamics of Chromatography*, Part I, Marcel Dekker, New York, 1965.
- 3 M. Niitsu and T. Sekine, *J. Inorg. Nucl. Chem.*, **38** (1976) 1053.
- 4 S. Kusakabe and T. Sekine, *Bull. Chem. Soc. Jap.*, **53** (1980) 1759.
- 5 M. Schröder-Nielsen, *Acta Pharm. Suecica*, **13** (1976) 439.

CHROM. 14,045

SELECTIVITY AND EFFICIENCY OF SEPARATION OF ISOMERS OF ORGANIC ACIDS BY CLATHRATE CHROMATOGRAPHY

W. KEMULA, D. SYBILSKA* and J. LIPKOWSKI

Institute of Physical Chemistry, Polish Academy of Sciences, 44/52 Kasprzaka, 01-224 Warsaw (Poland)

SUMMARY

Chromatographic separations of *o*-, *m*- and *p*-nitrobenzoic acids, *o*-, *m*- and *p*-nitrocinnamic acids and α - and β -naphthoic acids were studied as a function of pH of the mobile phase in the range 5.2-9.0 and using the β -Ni(NCS)₂(4-methylpyridine)₄ clathrate as the solid stationary phase. The experimental distribution coefficients (k) were combined with dissociation constants (K_a) and pH values in order to evaluate the coefficient of distribution of undissociated acid molecules (k'), which is otherwise unobtainable because the solid phase is unstable at pH < 5.2.

The selectivity observed follows the order typically observed for the β -phase: $k_p > k_m > k_o$ for disubstituted benzene derivatives, $k_\beta > k_\alpha$ for monosubstituted naphthalenes and $k_{trans} > k_{cis}$ for ethylene derivatives.

Despite the relatively low efficiency observed in separations of the acids, good separations of isomers were attained owing to high selectivity of the clathration.

INTRODUCTION

The use of β -Ni(NCS)₂(4-MePy)₄* clathrates as stationary phases to separate mixtures of different types of isomers in chromatographic systems with polar mobile phases has been demonstrated with numerous examples¹. The compounds to be separated can have different functional groups, provided that they do not destroy the host complex, *e.g.*, strongly acidic or alkaline media decompose the Ni(NCS)₂(4-MePy)₄ complex.

It seemed interesting to investigate whether the high selectivity of clathration towards mixtures of isomers² could be used for chromatographic separations of isomers of organic acids. We therefore investigated the practical pH limits for using β -Ni(NCS)₂(4-MePy)₄ clathrate sorbents in liquid chromatographic separations of dissociating compounds and studied the retention mechanism, *e.g.*, in order to establish whether the β -clathrate absorbs molecules only or also ionic species.

Systematic studies on liquid chromatographic separations of *o*-, *m*- and *p*-nitrobenzoic acids, *o*-, *m*- and *p*-nitrocinnamic acids and α - and β -naphthoic acids were performed with the pH of the mobile phase varying from 5.2 to 9.0.

* 4-MePy = 4-methylpyridine.

EXPERIMENTAL

Reagents

The substances to be separated and the solvents were of analytical-reagent grade and their physical constants agreed with those reported in the literature. 4-Methylpyridine contained 0.3% of 3-methylpyridine but did not contain 2,5-dimethylpyridine in amounts detectable by gas chromatography.

Apparatus

The chromatographic experiments were carried out using the Kemula chromatographic apparatus³. Diffusion currents for the reduction of nitro compounds eluted from the chromatographic column were recorded using an LP-7 polarograph (Laboratorní Přístroje, Prague, Czechoslovakia) at a constant potential of -0.9 V against the mercury pool anode.

Naphthoic acids were detected by a.c. polarography in an assembly identical with that applied for the detection of methylnaphthalenes⁴ using a Radelkis universal OH-105 polarograph at a constant potential of -0.6 V against the mercury pool anode.

Procedure

The sorbent was prepared from the clathrate $\beta\text{-Ni}(\text{NCS})_2(4\text{-MePy})_4 \cdot (4\text{-MePy})_{0.7}$ by the method described elsewhere⁵.

The aqueous methanol (30–70%) mobile phase solutions contained ammonium thiocyanate (0.1–0.2 mole/dm³), 4-methylpyridine (0.1–1.0 mole/dm³) and a suitable amount of mandelic or acetic acid for pH control.

Samples of 5–50 μl of solutions containing $5 \cdot 10^{-3}$ – $2 \cdot 10^{-2}$ mole/dm³ of the compounds to be analysed were injected with a Hamilton microsyringe. The mobile phase was not deaerated and the elution flow-rate was 8.0 cm³/h.

RESULTS AND DISCUSSION

The experimental k' values indicated that the practical lower pH limit for chromatography on $\beta\text{-Ni}(\text{NCS})_2(4\text{-MePy})_4$ is 5.2. This result was obtained by studying the retention of non-dissociating dinitrobenzenes. From the data in Table I one can draw the conclusion that the lower pH limit of chromatographic activity of the system studied is not related to the molecular stability of the host complex but rather to the stability of the $\beta\text{-Ni}(\text{NCS})_2(4\text{-MePy})_4 \cdot \text{G}$ clathrate crystalline phase (G = guest molecule). This structure is stable when filled with the guest component, which, in the case under consideration, consists of 4-methylpyridine and added methanol. Simple calculations of the molar percentage of non-protonated 4-methylpyridine in the mobile phases (a), (b) and (c) in Table I ($\text{p}K_a$ of 4-methylpyridine = 6.02) give *ca.* 0.035 *M* in (a) and *ca.* 0.14 *M* in (b). The concentration of 4-methylpyridine in the mobile phase necessary to make the $\text{Ni}(\text{NCS})_2(4\text{-MePy})_4$ chromatographically active has been reported as *ca.* 0.04 *M*⁵. It seems clear that protonated 4-methylpyridine may not be clathrated or form ion pairs (*e.g.*, with CH_3COO^-).

Fig. 1 illustrates the dependence of the equilibrium distribution coefficients (k) of *o*-, *m*- and *p*-nitrobenzoic and *trans-o*-, *-m*- and *-p*-nitrocinnamic acids on the pH of

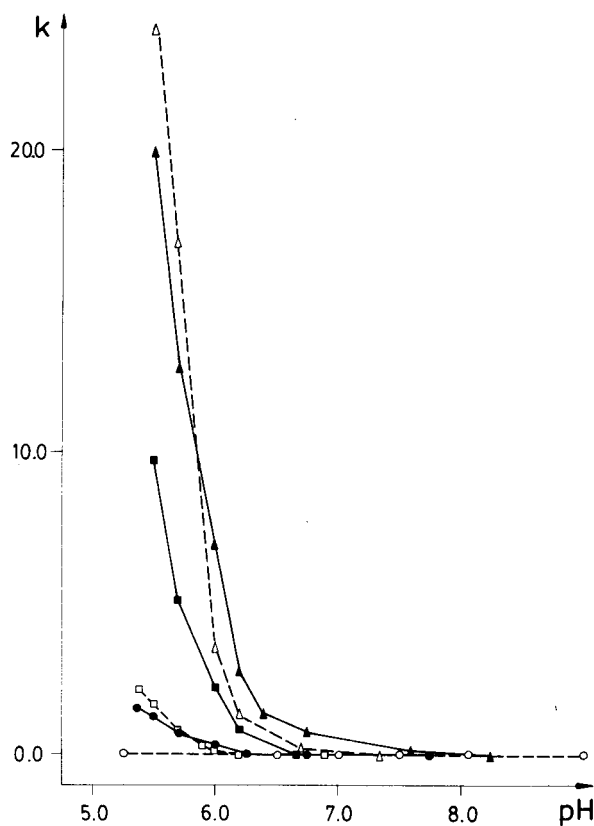


Fig. 1. Plot of distribution coefficients (k) of *o*- (○), *m*- (□) and *p*-nitrobenzoic acid (△) and *o*- (●), *m*- (■) and *p*-nitrocinnamic acid (▲) (in the *trans* configuration) versus pH of the mobile phase. Mobile phase: 0.1 *M* NH_4SCN -0.2 *M* 4-MePy in 30% aqueous methanol. The pH of the solutions were adjusted by the adding acetic acid.

the mobile phase. It is clear that at $\text{pH} > \text{p}K_a + 2$ (corresponding to practically complete dissociation) the distribution coefficients are zero. In other words, clathrate sorbents are able to absorb molecular rather than ionic species and, as in extraction or adsorption reversed-phase chromatography, with a decrease in pH an increase in the distribution coefficients is observed. By using the known equation^{6,7}

$$k' = k (1 + 10^{\text{pH} - \text{p}K_a})$$

the distribution coefficients of the undissociated part of the acids (k') can be calculated (Table II). The high values obtained for this quantity, compared with the k values of non-dissociating dinitrobenzenes (measured under the same experimental conditions), should be mentioned.

The use of mandelic instead of acetic acid (as the pH controlling agent) results in a slight decrease in the measured k values of the acids but the pH dependences of k are strictly analogous.

TABLE I
DEPENDENCE OF CAPACITY FACTORS (k') OF DINITROBENZENES (DNB) ON THE TOTAL 4-METHYLPYRIDINE CONCENTRATION IN THE MOBILE PHASE, THE pH BEING KEPT CONSTANT AT 5.2

Mobile phase: 0.1 M NH_4SCN -4-MePy in 30% aqueous methanol; the pH was kept constant at 5.2 by addition of suitable amount of acetic acid. Column dimensions: 35×5 mm I.D.

Mobile phase	Total concentration of 4-MePy in the mobile phase (mole dm^{-3})	k'			Solid stationary phase
		<i>o</i> -DNB	<i>m</i> -DNB	<i>p</i> -DNB	
a	≤ 0.21	0.0	0.0	0.0	Inactive $\alpha\text{-Ni}(\text{NCS})_2(4\text{-MePy})_4$
b	0.84	1.4	2.7	10.5	Active sorbent $\beta\text{-Ni}(\text{NCS})_2(4\text{-MePy})_4 \cdot \text{G}$
c	≥ 0.84	$0 < k' < 1.4$	$0 < k' < 2.7$	$0 < k' < 10.5$	Active sorbent $\beta\text{-Ni}(\text{NCS})_2(4\text{-MePy})_4 \cdot \text{G}$

TABLE II

DISTRIBUTION COEFFICIENTS (k) CALCULATED FOR UNDISSOCIATED ACID MOLECULES, EXPERIMENTAL DISTRIBUTION COEFFICIENTS ($k^{5.5}$) TAKEN AT pH 5.5 AND DISSOCIATION CONSTANTS (GIVEN AS pK_a) OF NITROBENZOIC (NB) AND NITROCINNAMIC (NC) ACIDS AND $k^{5.5}$ OF DINITROBENZENES (DNB)

Mobile phase and column dimensions as in Fig. 1.

Compound	pK_a	$k^{5.5}$	k
<i>o</i> -NB	2.17	0.0	
<i>m</i> -NB	3.49	1.7	175
<i>p</i> -NB	3.43	24.0	2845
<i>o</i> -NC	4.15	1.3	30
<i>m</i> -NC	4.12	9.8	245
<i>p</i> -NC	4.05	20.0	585
<i>o</i> -DNB	—	6.0	—
<i>m</i> -DNB	—	11.0	—
<i>p</i> -DNB	—	42.0	—

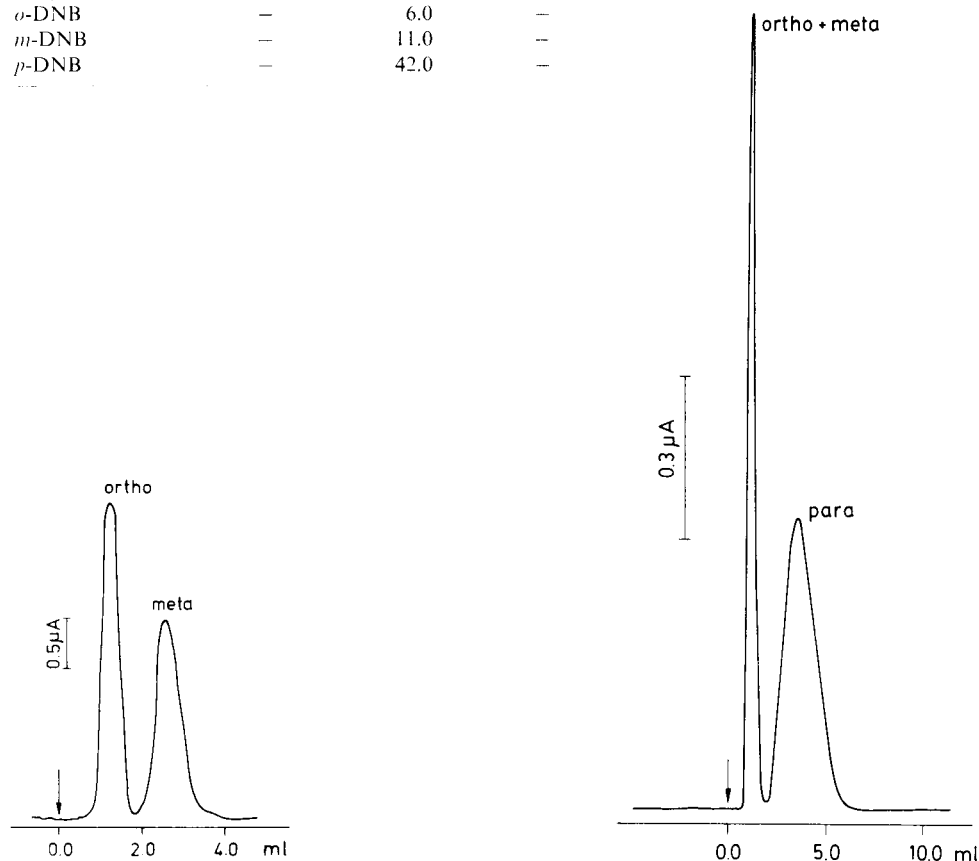


Fig. 2. Elution curves for *o*-, *m*- and *p*-nitrobenzoic acid using different mobile phases. (a) 0.2 *M* NH_4SCN –0.3 *M* 4-MePy, 0.28 *M* CH_3COOH in the 40% aqueous methanol (pH 5.25), with column dimensions, 28 \times 6 mm I.D.; under the conditions of the experiment V_{max} (retention volume) of *p*-nitrobenzoic acid is greater than 20 ml. (b) 0.1 *M* NH_4SCN , 0.84 *M* 4-MePy, 0.56 *M* CH_3COOH in the 30% aqueous methanol; column dimensions, 30 \times 5 mm I.D.

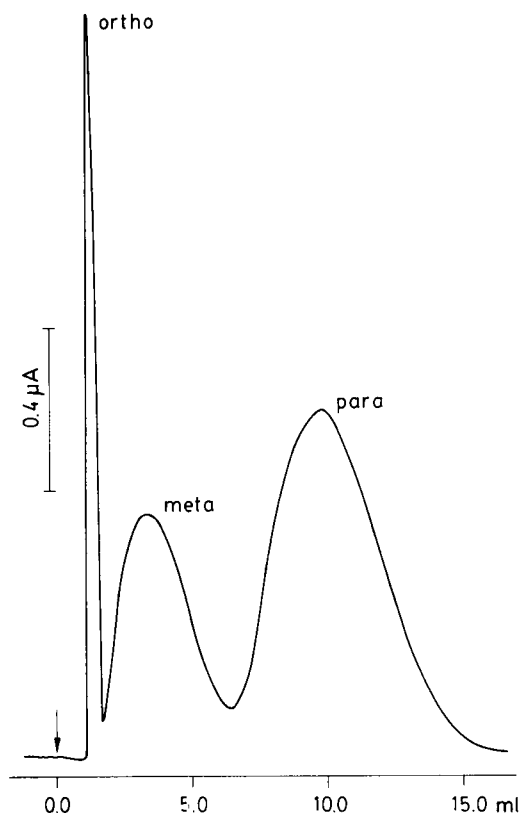


Fig. 3. Elution curve for *o*-, *m*- and *p*-nitrocinnamic acid in the *trans* configuration with 0.1 *M* NH_4SCN –0.84 *M* 4-MePy–0.56 *M* CH_3COOH in 30% aqueous methanol (pH 5.5) as the mobile phase; column dimensions, 65 \times 5 mm I.D.

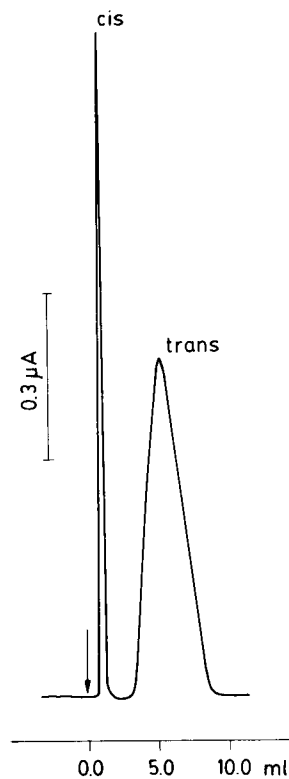


Fig. 4. Elution of *cis*- and *trans*-*p*-nitrocinnamic acids with 0.1 *M* NH_4SCN –0.84 *M* 4-MePy–0.56 *M* CH_3COOH in 30% aqueous methanol as the mobile phase (pH 5.5); column dimensions, 32 \times 5 mm I.D.

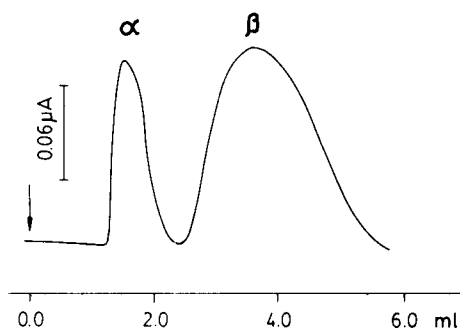


Fig. 5. Elution of α - and β -naphthoic acids with 0.1 *M* NH_4SCN –0.42 *M* 4-MePy–0.14 *M* CH_3COOH in 50% aqueous methanol (pH 5.8) as the mobile phase; column dimensions, 5.7 \times 5 mm I.D. A.c. polarographic detection.

Figs. 2–5 show the separations of *o*-, *m*- and *p*-nitrobenzoic, *o*-, *m*- and *p*-nitrocinnamic, *cis*- and *trans*-*p*-nitrocinnamic and α - and β -naphthoic acids.

As a consequence of the fact that β -Ni(NCS)₂ (4-MePy)₄ · G is able to absorb molecules but not to exchange ions, the selectivity observed (Figs. 2–5) follows the rules previously reported for this solid phase. Thus *o*-, *m*- and *p*-nitrobenzoic and nitrocinnamic acids show $k_p > k_m > k_o$, similarly to dinitrobenzene isomers⁸, $k_\beta > k_\alpha$ for naphthoic acids, which is analogous to the results obtained for the separation of nitronaphthalenes⁹, and $k_{trans} > k_{cis}$ for *p*-nitrocinnamic acid, which is similar to the result for the selective clathration of azobenzenes¹⁰.

As can be seen in Figs. 2–5, the elution curves of the organic acids have diffuse maxima and efficient separations are due to the high selectivity of the clathration and not to the efficiency of the columns.

REFERENCES

- 1 D. Sybilska, *Proceedings of the VIth International Symposium on Chromatography and Electrophoresis*, Presses Académiques Européennes, Brussels, 1971, pp. 212–221.
- 2 W. Kemula, D. Sybilska, J. Lipkowski and K. Duszczek, *J. Chromatogr.*, 204 (1981), 23–28.
- 3 W. Kemula, in L. Zuman and I. M. Kolthoff (Editors), *Progress in Polarography*, Wiley-Interscience, New York, 1962, p. 397.
- 4 W. Kemula, B. Behr, K. Chlebicka and D. Sybilska, *Rocz. Chem.*, 39 (1965) 1315.
- 5 W. Kemula, D. Sybilska, J. Lipkowski and K. Duszczek, *Polish J. Chem.*, 54 (1980) 317–324.
- 6 W. Kemula and H. Buchowski, *J. Phys. Chem.*, 63 (1959) 155–159.
- 7 E. Soczewiński, *Advan. Chromatogr.*, 5 (1968) 3.
- 8 J. Lipkowski, M. Pawlowska and D. Sybilska, *J. Chromatogr.*, 176 (1979) 43–53.
- 9 W. Kemula, D. Sybilska and K. Duszczek, *Microchem. J.*, 11 (1966) 296.
- 10 W. Kemula, Z. Borkowska and D. Sybilska, *Monatsh. Chem.*, 103 (1972) 860–866.

CHROM. 14,022

COMPARISON OF DIMENSIONS OBTAINED BY SIZE-EXCLUSION CHROMATOGRAPHY AND X-RAY DIFFRACTION OF RIGID MOLECULES

G. SAMAY*, L. FÜZES, F. CSER and G. BODOR

Research Institute for the Plastics Industry, Pf. 89, H-1950 Budapest (Hungary)

SUMMARY

Homo- and copolymers of monomers having vinyl groups with large, rigid side chains were investigated by size-exclusion chromatography and small-angle X-ray diffractometry in the solid state. The distributions of the molecular dimensions in dilute solutions and the distributions of the inhomogeneities of electron density in solid materials showed many similarities, and on the basis of these findings some conclusions are drawn concerning the molecular structure in the solid state and in dilute solutions, and also on the nature of the separation mechanism in size-exclusion chromatography.

INTRODUCTION

Size-exclusion is said to occur in gel permeation chromatography (GPC) when dissolved macromolecules are excluded from the pores of the packing beads according to their molecular size. Separations on rigid gels showing no adsorption characteristics have been assumed to be based on this mechanism, as have theoretical considerations concerning the separation mechanism of GPC. Also, different recommended "universal calibrations" have been based on the hydrodynamical dimensions of the dissolved macromolecules using hypothetical hydrodynamic equations for macromolecular solutions^{1,2}. Nevertheless, the only evidence of the validity of these methods was that the calibrating points for different materials fell on the same curve.

In the present study we have determined the average dimensions and also the distribution of the hydrodynamic sizes of dissolved macromolecules via size-exclusion chromatography, and compared these values to the sizes of the local inhomogeneities of electron density in the bulk material. The polymers comprised vinyl chains having long, rigid side groups, therefore no significant expansion was expected upon dissolution in an organic solvent. On the basis of the comparison of the data obtained by the two methods, some conclusions can be drawn on the reliability of the methods and on the solution properties of these rigid macromolecules.

EXPERIMENTAL

Three types of polymers were tested: phenyl-, methoxy-, ethoxy-, propoxy- and butoxyphenyl esters of *p*-acryloyloxybenzoic acid (FAB, MFAB, EFAB, PFAB and

BFAB respectively); copolymers of cholesterylvinyl succinate and *p*-methoxy-*p*'-acryloyloxy-azoxybenzene (CVS/MAAB) of different molar ratios; copolymers of *N*-acryloylpiperidine and cholesteryl acrylate of different molar ratios (AP/CA). The preparations of the materials were described elsewhere^{3,4}.

Two GPC systems were used for the determination of the distribution of molecular sizes in solutions. A Waters GPC-200 apparatus, equipped with five Styragel columns of nominal porosity $3 \cdot 10^4$, 10^4 , $3 \cdot 10^3$, 10^3 and 10^2 nm, respectively, was employed for the FAB samples at 130°C with 1,2,4-trichlorobenzene as solvent. The other instrument was home-made, and employed 10^4 , 10^3 and $3 \cdot 10^2$ nm Styragel columns with tetrahydrofuran as solvent at ambient temperature. The sample concentration was 5 g/l in each case, and 2 ml of each sample solution were injected.

Figs. 1 and 2 show Benoit's universal calibration for the high-temperature and room-temperature GPC systems respectively. In the case of the high-temperature system the curves were obtained by running narrow fractions of polyethylene, polypropylene, poly(propylene oxide) and polystyrene of known molecular mass, while at ambient temperature poly(vinyl chloride) and homo- and equimolar copolymers of styrene and ethyl, *n*-butyl and *n*-octyl methacrylate were used. The intrinsic viscosities of the fractions were measured in an Ubbelohde-type capillary viscometer under conditions pertinent to the GPC measurements. The characterization of the calibrating fractions has been given elsewhere⁵.

The distribution and average sizes of the inhomogeneities in electron density of the solid materials were computed from the course of the intensity curve of diffracted

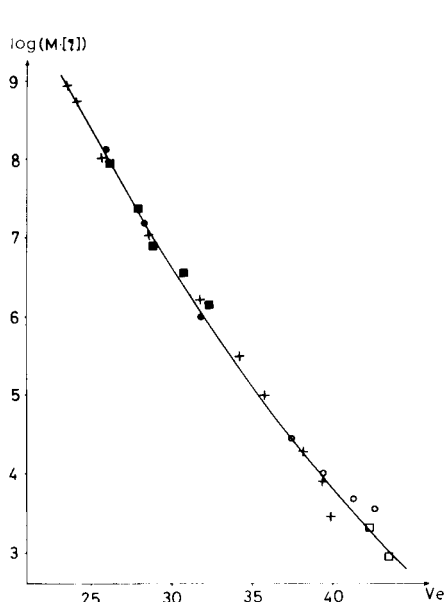


Fig. 1. Universal calibration for high-temperature measurements. Symbols: +, polystyrene; ■, polyethylene; ●, polypropylene; ○, poly(propylene oxide); □, *n*-paraffin.

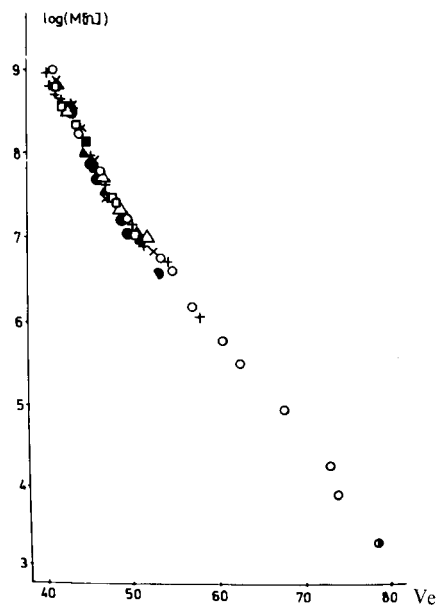


Fig. 2. Universal calibration for low-temperature measurements. Symbols: ○, polystyrene; △, poly(vinyl chloride); □, poly(ethyl methacrylate); ●, poly(butyl methacrylate); ▲, poly(octyl methacrylate); +, styrene-ethyl methacrylate copolymer; ×, styrene-butyl methacrylate copolymer; ■, styrene-octyl methacrylate copolymer; ⊙, squalane.

X-rays in the vicinity of the incident beam. The diffractograms were recorded by a Rigaku-Denki low-angle diffractometer, using pellets of 2 cm in diameter and 0.7–1.5 mm in thickness. Nickel-filtered Cu-K radiation was applied.

THEORETICAL

According to the Flory-Fox equation, used in Benoit's calibration

$$\langle R_0^2 \rangle^{3/2} \alpha^3 = [\eta] \cdot M / \varphi = 10^{F(V)} / \varphi \quad (1)$$

where $[\eta]$ is the intrinsic viscosity in cm^3/g , M is the molecular mass, φ is Flory's universal constant having a magnitude of $2.5 \cdot 10^{23}$ (ref. 6), $F(V)$ is the universal calibration curve according to Benoit, R_0 is the unperturbed radius of gyration of the dissolved molecules and α is the linear expansion coefficient. Thus, $\langle R_0^2 \rangle^{3/2} \alpha^3$ gives the hydrodynamic volume of the molecules. For the hydrodynamic radius of gyration:

$$\langle R^2 \rangle^{1/2} = \alpha \cdot \langle R_0^2 \rangle^{1/2} = [10^{F(V)} / \varphi]^{1/3} \quad (2)$$

The chromatogram—the concentration of the eluted solvent as a function of the elution volume—can be transformed into molecular size distribution using

$$\log \langle R^2 \rangle^{1/2} = F(V)/3 = F'(V) \quad (3)$$

for each point of the elution volume scale, having a chromatogram, $C(V)$

$$w[\langle R^2 \rangle^{1/2}] = \frac{C(V)}{d[F'(V)]/d[\langle R^2 \rangle^{1/2}]} \quad (4)$$

where $w[\langle R^2 \rangle^{1/2}]$ is the distribution of molecular sizes according to mass. Using N equidistant points of the chromatogram, having heights C_i , the average dimensions for the number average are

$$R_n = \sum_i C_i \cdot \langle R_i^2 \rangle^{-1} / \sum_i C_i \cdot \langle R_i^2 \rangle^{-3/2} \quad (5)$$

for the mass average

$$R_m = \sum_i C_i \cdot \langle R_i^2 \rangle^{1/2} / \sum_i C_i \quad (6)$$

and for the most probable dimensions:

$$\langle R^2 \rangle^{1/2} = [\sum_i C_i \cdot \langle R_i^2 \rangle^{1/2} / \sum_i C_i \cdot \langle R_i^2 \rangle^{3/2}]^{2/3} \quad (7)$$

The X-ray intensity data vs. scattering angle functions (scattering curve) reflect the dimensions of the electron-density inhomogeneities in the irradiated material.

According to Guinier and Fornet⁷, the part of the scattering curve in the vicinity of the direct beam can be replaced by a Gaussian curve, *i.e.*, the logarithm of the intensity *vs.* the square of the scattering angle gives a straight line. The slope of this straight line is proportional to the radius of gyration of the inhomogeneities

$$\log I_\theta = \log I_0 - (16\pi^2/3\lambda^2) R_g^2 \theta^2 \quad (8)$$

where θ is the scattering angle, I_θ and I_0 are the intensities of the scattered radiation at angles θ and 0 respectively, λ is the wavelength of the irradiation and R_g is the radius of gyration of the inhomogeneities.

The rough scattering curves were smoothed using nine points for calculation of each smoothed value. The same procedure was employed for the background-scattering, determined from the intensity with the sample not in the scattering position. The difference between these curves were then plotted as described above.

The method of Brill *et al.*⁸ makes it possible to determine the diameters of spherical particles or equivalent spheres, if the scattering curve is known. Accordingly, for the $\varrho(d)$ distribution of dimensions

$$\varrho(d) = Ad^{-2} \int [h^4 \cdot I(h) - C] \psi(h, d) dh \quad (9)$$

where h is a parameter of the reciprocal lattice, related to the scattering angle by $h = (4/\lambda) \cdot \sin \theta/2$, $I(h)$ is the intensity function, A is a normalizing parameter and $C = \lim_{h \rightarrow 0} [h^4 I(h)]$. For the function $\psi(h, d)$:

$$\psi(h, d) = (1 - 8\bar{h}^2 \bar{d}^2 \cos hd) - [4 - 8\bar{h}^2 \bar{d}^2 (\sin hd)/hd]$$

The rough scattering curves were first smoothed and corrected for the background as described above, and then corrected for the finite beam-width with the help of the slit-correction described by Kratky *et al.*⁹.

RESULTS AND DISCUSSION

Fig. 3 shows the distribution functions for the gyration radii of two CVS/MAAB systems obtained from GPC measurements in tetrahydrofuran at room temperature, *i.e.*, these distributions reflect the situation in dilute solution. The electron-density inhomogeneities obtained from the small-angle X-ray scattering data by using eqn. 9 are illustrated in Fig. 4. Comparison of the two figures shows that the two methods yield dimensions of similar order. The region of the distributions shown is the same in both figures, and also the bimodal character in case 2 is seen for both distribution types.

In Fig. 5 the distributions are given for the AP/CA copolymer systems obtained by GPC at room temperature in tetrahydrofuran, while Fig. 6 shows the distribution of the electron-density fluctuation calculated from the X-ray distribution for this series. The character and the region of the distribution curves in these figures exhibit many similarities and suggest that the two methods give similar information.

It is worth comparing the numerical values of the average dimensions. In Fig. 7

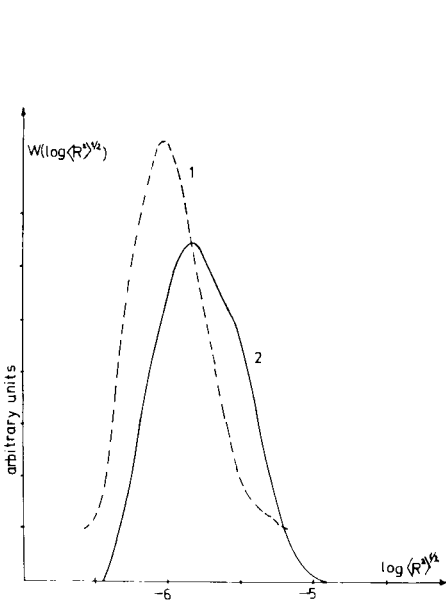


Fig. 3. Hydrodynamic size distribution for CVS/MAAB copolymers.

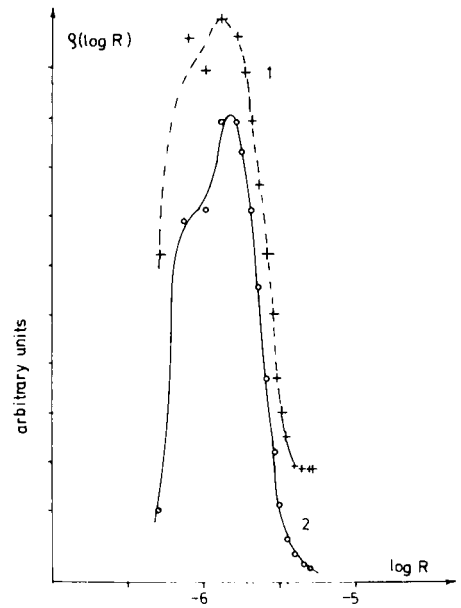


Fig. 4. Distribution of electron-density inhomogeneities in CVS/MAAB copolymers.

the size distributions are shown for FAB polymers, obtained by GPC at elevated temperature. The Guinier plots for these materials are given in Fig. 8, and the calculated average sizes are listed in Table I. From Fig. 8 it is seen that the extrapolation

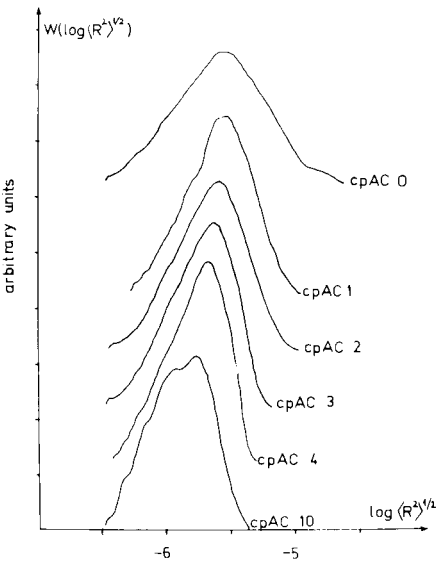


Fig. 5. Hydrodynamic size distribution for AP/CA copolymers.

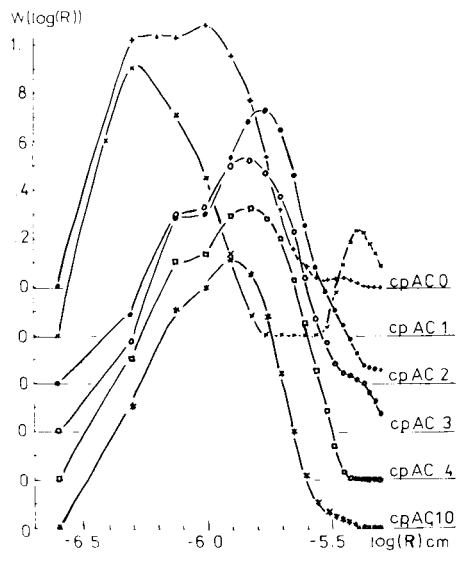


Fig. 6. Distribution of electron-density inhomogeneities in AP/CA copolymers.

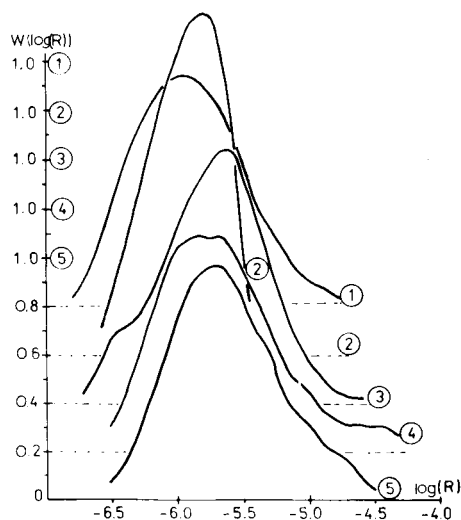


Fig. 7. Hydrodynamic size distributions for FAB polymers.

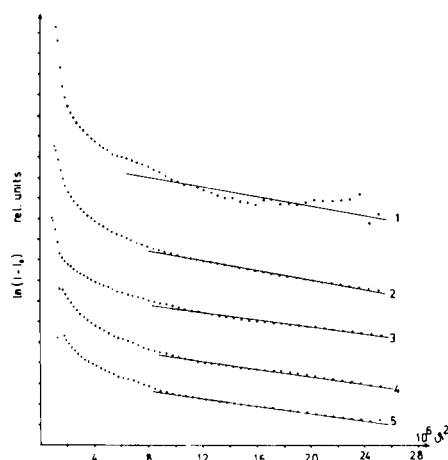


Fig. 8. Guinier plots for FAB polymers.

was done from the asymptote of the scattering curve. Similar extrapolation is often used in studies of the light scattering of dilute polymer solutions¹⁰ and yields $\langle R^2 \rangle^{1/2}$. In this work the $\langle R^2 \rangle^{1/2}$ values obtained by X-ray scattering and by exclusion chromatography are of similar magnitudes.

It can be concluded that the results obtained by small-angle X-ray scattering of the solid materials and by the chromatographic method applied to dilute solutions reflect similar physical properties. Therefore, it seems very probable that the X-ray scattering in these cases yields the dimensions of the individual molecules, which are similar to those in dilute solutions.

Some consideration must be made on the assumptions used in the calculations. The use of the universal calibration of Benoit is based on the hydrodynamical behaviour of random coil molecules in dilute solutions. The validity of this calibration has been confirmed for rod-like molecules¹¹ and for polyelectrolytes¹². Thus, it can

TABLE I

DIMENSIONS (IN nm) MEASURED FOR *p*-ALKOXYPHENYL *p*-ACRYLOYLOXYBENZOATE POLYMERS

SAXS = Small-angle X-ray scattering.

Alkyl group	GPC			SAXS
	$\langle R^2 \rangle^{1/2}$	R_m	R_n	R_g
H	3.78	18.7	3.13	6.6
Methoxy	5.37	13.2	4.58	6.8
Ethoxy	4.37	26.3	3.46	6.4
Propoxy	6.14	46.9	5.13	6.5
Butoxy	6.64	38.9	5.41	6.1

be assumed that, also for the present rigid molecules, chromatography occurs according to the radius of gyration.

The small-angle X-ray scattering method was tried also for dilute solutions, *i.e.*, assuming no interference of the beams reflected by different inhomogeneities and spherical particles. The bulk samples were prepared by precipitation from dilute solutions. Because of the rigidity of the molecules, interpenetration of the particles during precipitation is unlikely, *i.e.*, there are individual macromolecular aggregates in the bulk having the dimensions of the single molecules. Since the molecules have large rigid side groups, the number of conformational variations is small; solvent molecules cannot penetrate into the inner volume of the cylindrical molecules, thus the dimensions of the bulk molecules are similar to those of the dissolved particles.

As regards the possible interference of the reflected beams, Kratky *et al.*⁹ showed that when interference occurs there is a plateau in the innermost region of the scattering curve. In this case the extrapolation can be done only in the region outside the plateau. We did not record any plateau, and the extrapolation was not performed in the region where such plateaux are usually found. It must be emphasized that, both in X-ray scattering and chromatography, spherical particles are assumed, and quasi-dimensions are obtained.

Taking into consideration the above problems and the fact that the calculations were executed for three independent series with fifteen samples, it seems very probable that GPC yields the same dimensions as does X-ray diffraction of the solid materials. This means that the parameter obtained from separation, is the molecular dimension, which in our case was equal to the dimension of the molecular aggregates in the solid material. Therefore, the size exclusion expression is valid also in case of very rigid macromolecules.

REFERENCES

- 1 Z. Grubisic-Gallot, P. Rempp and H. Benoit, *J. Polym. Sci., Polym. Lett. Ed.*, 5 (1967) 753.
- 2 H. Coll and R. L. Prusinowsky, *J. Polym. Sci., Polym. Lett. Ed.*, 5 (1967) 1153.
- 3 Gy. Hardy, F. Cser. K. Nyitrai, G. Samay and A. Kalló, *J. Cryst. Growth*, 48 (1980) 191.
- 4 F. Cser. K. Nyitrai, G. Samay, G. Bodor and Gy. Hardy, *Structure Investigations on Mesomorphic Copolymers, IUPAC Symposium on Macromolecular Chemistry, Mainz, 1979*, Preprints, Vol. II, p. 939.
- 5 G. Samay, M. Kubin and J. Podesva, *Angew. Makromol. Chem.*, 72 (1978) 185.
- 6 M. Kurata and W. H. Stockmayer, *Fortschr. Hochpolym. Forsch.*, 3 (1963) 196.
- 7 A. Guinier and F. Fournet, *Small-angle Scattering of X-rays*, Wiley, New York, 1955, pp. 116-120.
- 8 O. L. Brill, C. G. Weil and P. W. Schmidt, *J. Colloid Interface Sci.*, 27 (1968) 479.
- 9 O. Kratky, G. Porod and L. Kahovec, *Z. Electrochem.*, 55 (1951) 53.
- 10 M. B. Huglin (Editor), *Light Scattering from Polymer Solutions*, Academic Press, London, New York, 1972, pp. 348-349.
- 11 J. V. Dawkins and M. Hemming, *Polymer*, 16 (1975) 554.
- 12 A. L. Spatorico and G. L. Beyer, *J. Appl. Polym. Sci.*, 19 (1975) 2933.

APPLICATIONS OF LIQUID CHROMATOGRAPHY IN THE ANALYSIS OF PROTEINS, PEPTIDES AND AMINO ACIDS

CHROM. 14,075

BUFFER-FOCUSING CHROMATOGRAPHY USING MULTICOMPONENT ELECTROLYTE ELUTION SYSTEMS

MILTON T. W. HEARN** and DAVID J. LYTTLE

MRC Immunopathology Research Unit, University of Otago Medical School, P.O. Box 913, Dunedin (New Zealand)

SUMMARY

Procedures for the generation of internal pH gradients on columns of ion-exchange resins using multicomponent eluent systems of defined chemical composition, comprised of common amphoteric and non-amphoteric buffers, are described. The influence of buffer concentration, pH and resin characteristics on pH gradient formation have been examined. The physicochemical basis of the pH gradient formation under these chromatographic conditions has been discussed in terms of dissociation theory for polyelectrolytes which highlights the similarity with the formation of natural pH gradients by buffer electrofocusing procedures. Applications of this chromatographic technique for the separation of proteins are described.

INTRODUCTION

Ion-exchange chromatography has proved to be a versatile technique for the fractionation of peptides, proteins and other ionogenic biological molecules. Ion exchangers based on derivatised cellulosic resins have gained very wide acceptance particularly for the separation of protein mixtures due to their relatively high sample capacities compared to other types of resins and the ease of elution of the adsorbed proteins using step-wise or differential gradients of ionic strength and/or pH. Two approaches are feasible for the formation of pH gradients used in ion-exchange separations. The most widely used method employs a mixing device to progressively change the pH of the initial buffer by dilution with a second buffer of different pH, the mixer effluent being continuously introduced onto the column. In, for example, an anion-exchange separation, proteins are applied to the column, which has been equilibrated to an initially high pH, and eluted with a descending gradient formed from a buffer of lower pH. The pH gradient formed by this method has conventionally been considered to be an "externally" generated pH gradient. In this elution mode, a protein component will remain adsorbed to the resin until the pH of the incoming buffer is slightly below the pI of that protein.

* Present address: St Vincent's School of Medical Research, Victoria Parade, Melbourne, Victoria 3065, Australia.

It is also possible to form a pH gradient directly on a column of a suitable ion-exchange resin. In this case, the resin, previously equilibrated to a certain pH, is eluted with a buffer of fixed composition but at a different initial pH. The formation of this type of pH gradient, which can be described as "internally" generated, will depend on the dissociation equilibria established between the hydrated, or partially hydrated, ionised buffer components and charged groups on the resin. If mobile phases based on multicomponent polyelectrolyte buffer systems are used, internally generated pH gradients will form because some buffer components preferentially migrate more rapidly than others down the ion-exchange column. As a consequence, these types of pH gradients will be particularly responsive to changes in the chemical composition and buffer capacities of both the eluent and the ion exchanger. Several studies have shown¹⁻⁵ that solutions of random mixtures of proprietary carrier ampholytes such as the Ampholines or Pharmalytes can be effectively used to form internally generated pH gradients on ion-exchange resins. Selective elution of proteins under mild desorption conditions at pH values proximal to the solutes' pI values is one of the desirable features of this chromatographic ampholyte titration technique. In addition, with the proprietary polyamino-polycarboxylic ampholytes, it is possible to produce focusing effects in the ion-exchange chromatographic separation of proteins similar to the effects observed with isoelectric focusing methods.

In recent publications⁶⁻¹¹ from this and other laboratories, methods for electrofocusing in granulated polysaccharide gels and polyacrylamide gels have been described using multicomponent systems of defined chemical composition comprised of common amphoteric and non-amphoteric buffers, to generate the required natural pH gradient. Depending on the choice of the component reagents and the pH of the terminating anolyte and catholyte, linear or cascade-step pH gradients can be formed. Under these electrophoretic conditions, proteins focus to sharp boundaries which have relative positions in accord with their intrinsic pI values. The present paper reports an investigation on the characteristics of pH gradients internally generated on ion-exchange resins using a multicomponent buffer system, previously shown to generate a stable pH gradient over the range pH 3-10 under electrofocusing conditions. The application of this technique to the fractionation of protein mixtures is also described.

EXPERIMENTAL

Materials

The ion exchangers DEAE-Sephadex A-25, QAE-Sephadex A-25 and CM-Sephadex A-25 were obtained from Pharmacia (Uppsala, Sweden), DEAE-cellulose type A17 was from Phoenix (Nelson, New Zealand) and TETA-cellulose was a gift from Dr. J. Ayers, Massey University, Palmerston North, New Zealand. The small ion capacities of these gels were stated by the manufacturer to be 3.5, 3.0, 4.5, 1.0 and 1.8 mequiv./g, respectively. The buffers used in the preparation of the wide pH range eluent system were obtained from Sigma (St. Louis, MO, U.S.A.). A 20 mM stock solution of this multicomponent buffer system was prepared as described previously^{5,6} for use with electrofocusing procedures and can be stored at 4°C for at least six months. This buffer system is also available ready for use from Pierce (Rockford, IL, U.S.A.) as part of their Buffalyte range of electrofocusing reagents (Buffalyte WR

3–10). Human serum albumin, sperm whale myoglobin, bovine serum albumin, bovine haemoglobin, lysozyme, transferrin and catalase were commercial samples from Sigma. Antisera against serum and other proteins were either raised in this laboratory or purchased from Behringwerke (Marburg, G.F.R.).

Chromatographic equipment and procedures

The ion-exchange resins were precycled as recommended by the manufacturer and then equilibrated to the initial buffer condition which was generally 5 mM $\text{Na}_2\text{HPO}_4\text{--NaOH}$, pH 9.5, or 5 mM Tris--HCl , pH 9.8. Columns were slurry packed using about one part of equilibrated, swollen gel to one part of equilibration buffer and the bed stabilised by eluting with *ca.* 50 column volumes of the initial buffer. Flow-rates were controlled with Multiperpex pumps (LKB, Bromma, Sweden) and column eluents were collected with a LKB Ultrarac 7000 fraction collector. The pH of the collected fractions was measured with a combination glass electrode on a Radiometer PHM64 pH meter. Protein samples were applied to the equilibrated ion exchangers in the initial buffer and subsequently eluted with a solution of the multi-component buffer system at an appropriate concentration and pH. Proteins not eluted under these conditions were recovered by elution with a gradient of 1 M NaCl in the final eluting buffer. Proteins in the column effluents and concentrates were detected by their UV extinction 254 and 280 nm on a Uvicord III monitor and by the Bradford assay¹². Analysis of specific proteins was carried out by standard immunodiffusion, immunoelectrophoresis or SDS–polyacrylamide gel procedures.

RESULTS AND DISCUSSION

As a solution containing ampholytes of defined chemical composition passes through an ion-exchange column each buffer component will exhibit a different affinity for the ion exchanger. This will result in a continuous sequence of dynamic replacement events of bound zones of buffer counter-ions by new buffer ions entering the column. Individual buffer components will selectively migrate through the column according to their ionisation state, weakly bound buffer components being progressively displaced by buffer components with higher affinities for the resin. Due to the buffering action of the ion exchanger, a continuous change in the pH of the mobile phase will thus occur as it moves down the column until a limiting pH value is reached, the slope of the pH gradient so formed being controlled by the buffering capacity of the ion-exchange resin and the eluent. By considering the ion-exchange column to be made up of n -sections of an interactive stationary phase which exhibits a range of apparent pK values, the physicochemical basis for the continuous readjustment of the pH and composition of each aliquot of the mobile phase as it passes down the column can be evaluated in terms of the various dissociation equilibria established by the participating ionised and unionised species. According to the detailed theoretical studies of Sluyterman and Elgersma³, the pH at any point in an ion-exchange column eluted with an amphoteric buffer of low ionic strength can be given by

$$\text{pH}_i = \frac{\text{pH}_{m,i} + \frac{a_s}{a_m} \text{pH}_{s,i}}{1 + \frac{a_s}{a_m}} \quad (1)$$

where pH_m and pH_s are the pH values of the mobile phase and the stationary phase and a_m and a_s are the buffer capacities per unit of column length of the mobile phase and the stationary phase, respectively. Furthermore, if the pH difference between two adjacent column sections, i and j , is ΔpH , then the pH change, ΔpH_j , in the section j caused by advancing the mobile phase over this section can be expressed by

$$\Delta\text{pH}_j = -\frac{\Delta\text{pH}}{1 + \frac{a_s}{a_m}} \quad (2)$$

The rate of advance of an individual buffer component, B_1 , down the column under conditions of ideal linear chromatography can be given by¹³

$$\left(\frac{dc'}{dt}\right)_{B_1} \cdot \left(1 + K_{B_1} \frac{A_s}{A_m}\right) = \mu \left(\frac{dc'}{dx}\right)_{B_1} \quad (3)$$

where $(dc'/dt)_{B_1}$ is the change in the buffer component, B_1 concentration in the initial aliquot of the mobile phase as it passes through a controlled section of ion exchangers, of dimensions x , K_{B_1} is the equilibrium distribution constant ($= c_{s,B_1}/c_{m,B_1}$), A_s and A_m are the cross-sectional areas of the stationary and the mobile phases respectively, and μ is the linear flow velocity. If we assume that the charge, Q , on the buffer component confined within a zone a distance x along a column is proportional to pI-pH for ampholytes and pK-pH for monopoles, then the equilibrium distribution constant can be evaluated for each buffer component from

$$\ln K = -\frac{dQ}{d\text{pH}} \cdot \frac{d\text{pH}}{dx} \cdot \chi \cdot x \quad (4)$$

where χ is the appropriate normalised Donnan coefficient and $dQ/d\text{pH}$ is the buffering capacity term. Provided the participating chemical equilibria are rapid relative to the transport processes, the effects of radial and longitudinal temperature gradients can be omitted from eqn. 4. In addition, conditions of electroneutrality will prevail. Under these conditions, the $K \cdot A_s/A_m$ term in eqn. 3 can be related to the buffer capacity per unit volume of the ion-exchange resin, a_e , and the eluent, a_b , respectively and the velocity of the pH gradient can be given by

$$\left(\frac{dx}{dt}\right)_{\text{pH}} = \left(\frac{dx}{dt}\right)_m \left(\frac{1}{\frac{A_s}{A_m} \cdot \frac{a_e}{a_b} + \frac{a_e}{a_b} + \frac{A_s}{A_m} + 1} \right) \quad (5)$$

At all times the pH of the column effluent will be equal to the pH of the last section of the column, whilst the instant the first aliquot of the multicomponent buffer system emerges from the column outlet the complete pH gradient can be considered to be present in the column.

Proteins passing through an ion-exchange column in an internally generated pH gradient will be subjected to the same selective migration effects as the buffer components. The rate of advance of a protein or similar biological polyelectrolyte will

be identical to the rate of advance of a buffer component of the same pI and charge characteristics. In practice, proteins will be confined to zones by buffer components of lower and higher pI/pK values. The migration of each protein will thus be controlled by its ionisation state relative to the adjacent sections of the ion-exchange resin and be bounded by mobile phase aliquots with pH values slightly higher and slightly lower than the pI of the protein. These processes will result in a converging zone for each protein which will be emerged from the column at a pH value near to its pI value.

The selective migration of individual buffer components on ion-exchange supports bears some similarity to the separation of amphoteric buffers under electrofocusing conditions. In the latter technique, buffer ampholytes are initially distributed throughout the support, but during the electrolysis individual components migrate and accumulate in zones corresponding to their isoelectric points. As a consequence of its buffering capacity, each focused ampholyte generates a pH gradient upon the immediate vicinity in the support medium, with the pH gradient increasing monotonously from anode to cathode. The pH gradient stability in these systems is dependent on the buffer capacity, dQ/dpH , of each ampholyte. Furthermore, the velocity of pH gradient formation under electrofocusing conditions is also a function of the buffering capacity, and particularly the relative concentrations and flux mobilities of the different buffer species.

In common with pH gradients formed by electrofocusing methods, shallow pH gradients, *i.e.* when the $\Delta pH/\Delta x$ term in eqn. 4 involves small incremental pH charges per unit column length, internally generated on ion-exchange resins will favour higher resolution in the separation of protein mixtures. According to the outlined theoretical considerations, for any given ion-exchange column, the slope of the internally generated pH gradient will depend on the concentration, composition and pH of the eluent buffer system. For different types of ion-exchange resins, eluted with a common multicomponent buffer system under the same conditions, the pH gradient shape will depend on the buffer capacity per unit volume of the ion exchanger, *i.e.* the pH and surface coverage of charged groups of the resin. These conclusions were verified with a variety of experiments using the wide range buffer system, Buffalytes WR 3-10, and different ion-exchange resins. Typical results from these experiments are summarised below.

Effect of concentration of buffer eluent

The influence of buffer concentration on the pH gradient shape was evaluated using the various resins, packed into columns of the same dimensions. In typical experiments, columns (12×1.6 cm) containing the pre-equilibrated DEAE-cellulose type A17 resin (pH 9.8) were eluted with aqueous solutions containing 1, 2, 5, 10 and 20 mM of the multicomponent buffer system, Buffalyte WR 3-10. The plots of the column effluent pH *versus* elution volume are shown in Figs. 1 and 2. These results clearly demonstrate the synergistic dependence of pH gradient slope on the concentration of the buffer species in the eluent. During the early part of pH gradient formation, most of the buffer species will be bound to the anion exchanger. As an increasing number of the ionic groups on the resin are titrated, more buffer species will move through the column, initially the most basic component followed by the other components in order of decreasing basicity. This movement of buffer species with concomitant internal pH gradient formation, results in a progressive increase in

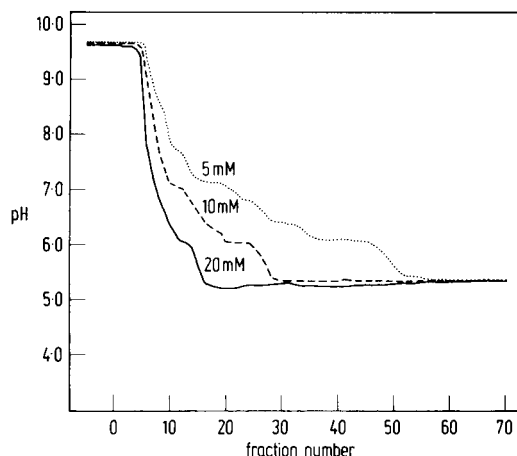


Fig. 1. pH gradient profiles formed with the multicomponent buffer system, Buffalyte WR 3-10, on a DEAE-cellulose column as a function of buffer concentrations. Column dimensions, 12×1.6 cm; flow-rate, 45 ml/h; resin pH 9.8; buffer eluent pH 5.3.

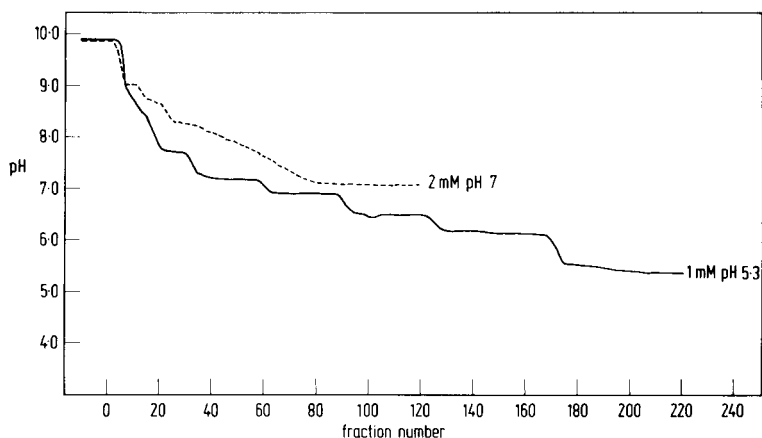


Fig. 2. pH gradient profiles formed with the multicomponent buffer system, Buffalyte WR 3-10, on a DEAE-cellulose column as a function of buffer concentration and pH. Column dimensions and flow-rate as in Fig. 1.

ionic strength throughout the elution. Compared to conventional elution conditions, the ionic strengths and buffer concentrations employed in these experiments are low relative to the total capacity of the ion exchanger. It is worth recalling that low buffer concentrations and large Donnan potentials will favour resolution with ion-exchange separations under buffer focusing elution conditions. Because of practical limitations with very shallow pH gradients which will lead to large dilution factors, a compromise between buffer concentration, pH gradient slope and resolution must be achieved. With the ion exchangers examined in this study, buffer concentrations in the range of 2.5–5 mM (*i.e.* *ca.* 0.0005–0.001 mmol/pH unit/ml eluent) were found to provide convenient pH gradients (in terms of analysis time, elution volume and resolution) with columns containing 20–300 ml swollen resin. Furthermore, an acceptable com-

promise between resolution and solute dilution can be achieved when the total gradient volume was less than or equal to *ca.* 10 bed volumes. It is noteworthy that the internal pH gradients formed by this procedure with the Buffalyte WR 3-10 system show cascade pH steps at very low buffer concentrations. Similar pH gradient effects have been observed⁷ in electrofocusing experiments with related buffer systems. For preparative separations of a particular protein, a pH plateau near the region of *pI* of interest will be advantageous provided it creates a large difference in ionisation between adjacent protein zones. Furthermore, linear pH gradients are not essential with preparative loadings of proteins since it is unlikely that all protein zones will concomitantly migrate at their theoretical narrowest band width. With minor modification of the buffer compositions, it is possible to generate linear internal pH gradients at buffer concentration levels below 1 mM.

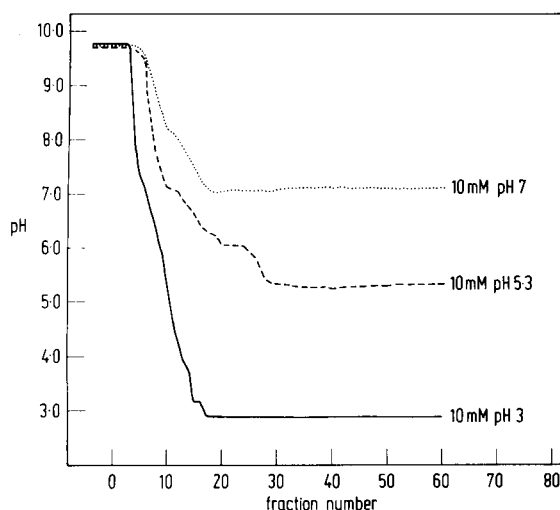


Fig. 3. Influence of buffer eluent pH on the internally generated pH gradients formed on a DEAE-cellulose column with the 10 mM buffer system eluent. Column dimensions and flow-rates as in Fig. 1.

Effect of the pH of the buffer eluent

According to theory, the terminating pH value of an internally generated pH gradient should be identical to the pH of the buffer eluent. Shown in Fig. 3 are the plots of the column effluent pH *versus* elution volume using the 10 mM buffer eluent at its intrinsic pH (pH 5.3) and at pH 7.0 and pH 3.0. In these experiments, DEAE-cellulose column of identical bed dimensions were first equilibrated to pH 9.8 and then eluted with the buffer system adjusted to the appropriate pH. As is evident from these experiments, and from comparisons with the data shown in Figs. 1 and 2, the slope of the pH gradient is affected by changes in buffer concentrations but in each case the terminating pH value of the column effluent ultimately reaches the limit set by the pH of the eluent. The choice of the eluent pH used with this, or other, buffer systems can thus be dictated in preparative protein separations by the operational isoelectric point range of the sample. Since the majority of proteins have isoelectric

points¹⁴ which encompass the range pH 4–7.5, an eluent at pH 4 or below would be required for most applications. When the eluent pH is higher than the *pI* value of a particular protein in a mixture, then that protein will not elute from an anion exchanger. For example, with the Buffalyte WR 3–10 (pH 3.0) eluent, serum proteins including albumin, eluted near to their respective *pI* values with good sample recoveries. However, with the same system but at pH 5.5, albumin and other proteins with isoelectric point values below 5.5 could not be eluted without a salt gradient or an eluent pH change.

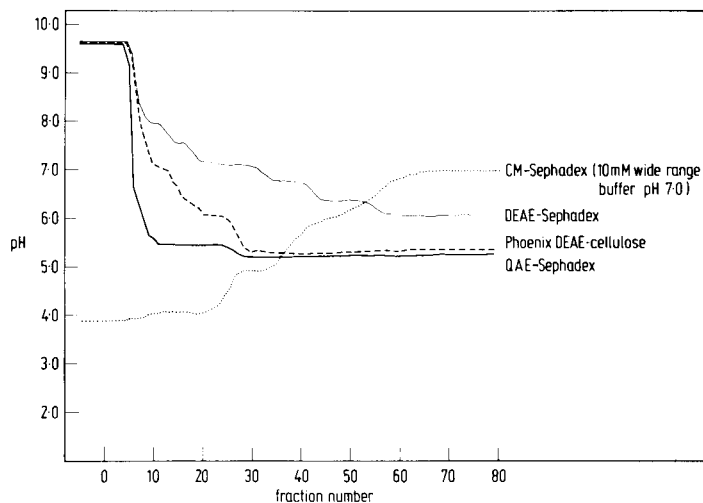


Fig. 4. Plots of the pH gradients formed on the anion exchangers DEAE-Sephadex, DEAE-cellulose and QAE-Sephadex using the 10 mM multicomponent buffer system. The resins were initially equilibrated to pH 9.8 and eluted with the same volume (500 ml) of the buffer system at pH 5.3. Also shown is the plot of the pH gradient formed on the cation exchanger, CM-Sephadex equilibrated to pH 4.0 and eluted with the 10 mM multicomponent buffer system adjusted to pH 7.0.

Effect of the buffering capacity of ion-exchange supports

In Fig. 4 are shown plots of the pH gradients formed with four different ion-exchange resins, packed into columns of identical bed dimensions, using as a common eluent the 10 mM multicomponent buffer system. As anticipated from a comparison of the reported properties of the various resins, the shape of the pH gradient is dependent on the charge functionality and buffering capacity of the ion exchanger. Many commercial cellulose anion exchangers show acceptable buffering capacities only over the range of *ca.* pH 6.5–10.0. To be effective in buffer focusing chromatographic experiments, the ion exchanger should exhibit an extended titration curve, which ideally should cover the range pH 3.0–11.0, and a uniform buffer capacity across this range. Furthermore, the resin should exhibit large penetration constants with macroglobulins, *i.e.* the fraction of the internal surface area available to both high- and low-molecular-weight species is comparable, and have a high surface coverage of charged groups. To meet these requirements, large-pore high-capacity ion-exchange resins are needed. Several recently described resins, for example the cross-

linked, fully porous Sepharose 6B PBE ion exchangers, appear to satisfy most of these criteria.

With anion-exchange resins, the charge on the resin increases as the column pH decreases during the buffer elution. It is thus essential to select the initial pH condition for the sorbent such that the most basic protein in the sample is weakly adsorbed. Typically this pH value was chosen to be *ca.* 0.5 pH units above the *pI* value of the most basic protein. For cation exchangers, the opposite effects apply and a resin pH below the *pI* value of the most acidic protein must be chosen. With two resins of similar charge functionality but different buffering capacities the shallower pH gradient will result under similar chromatographic conditions with the resin of higher capacity. The small ion capacities of different ion exchangers can be used to assess which resin will exhibit the more favourable distribution ratio for multi-component buffer eluents of low ionic strength and hence form the more appropriate pH gradient shape. Besides the influence of resin characteristics, the slope of the pH gradient can also be manipulated by changing the column bed volume. For example, an increase in column dimensions using the same resin and elution conditions resulted in a more shallow pH gradient. Finally, titration of the anion-exchange resins to lower initial pH values caused more shallow gradients to form under otherwise identical chromatographic conditions. However, it has been our experience that resin titration is not always appropriate in protein separations, *e.g.* when the resin pH and protein *pI* values are similar.

Protein separations using multicomponent buffer systems

The separation of two proteins, P_1 and P_2 with isoelectric points at pH 9.0 and pH 7.0, respectively, on an anion exchanger initially equilibrated to pH 10.0 and eluted with a multicomponent buffer system at pH 4.0 can be considered in terms of the respective distribution equilibria. Due to the Donnan effect, the pH inside the pores of the matrix will always be slightly higher than the pH of the surrounding mobile phase environment. When the pH of the resin falls to pH 9.0 and the charge on P_1 becomes zero, P_1 will diffuse away from the charged surface of the pore into a mobile phase environment which has a pH value slightly lower than the *pI* value of P_1 . As a consequence, P_1 will be protonated and move with a mobile phase zone at a pH slightly lower than its *pI* value. The migration of P_2 will follow in a similar fashion when the resin pH reaches 7.0. Selectivity under buffer focusing chromatographic conditions will thus arise due to differences between the participating equilibrium distribution processes for P_1 and P_2 , which for each protein can be represented by a equilibrium distribution constant. In the general case, the equilibrium distribution constant will take the form explicit to eqn. 4. Resolution will thus depend, *inter alia*, on the slope of the pH gradient (dpH/dx) and the rate of change of charge on the protein with pH, (dQ/dpH). The involvement of the latter term, which reflects the ionisation rate of a protein as the pH of the environment is varied, has important ramifications in both the buffer focusing chromatographic and electrophoretic separation modes. For examples, if the two proteins P_1 and P_2 have the same *pI* value but different values for dQ/dpH , that is different titration curves, it may be possible to resolve them under certain experimental conditions. Proteins with steep dQ/dpH slopes are expected to show narrower band widths than proteins with flatter dependencies of charge on pH.

Since the dpH/dx term in eqn. 4 is dependent on the concentration of buffer species, resolution is anticipated to decrease as the buffer concentration increases. Fig. 5 illustrates an example of this effect obtained with a crude myoglobin preparation using two different concentrations of the Buffalyte WR 3-10 system with a DEAE-cellulose column. Similar concentration-dependent changes in resolution have been described⁴ for proteins eluted from anion-exchange columns with mobile phases containing Ampholine systems.

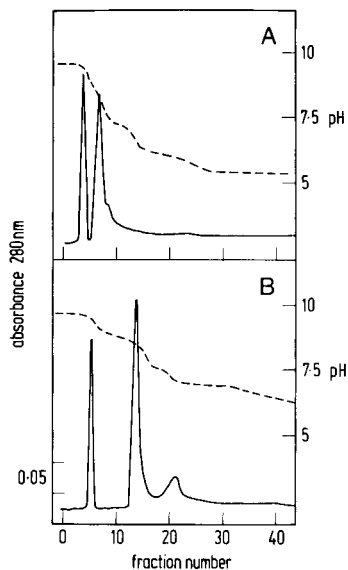


Fig. 5. Elution profiles for a crude myoglobin preparation on a column (25×1.6 cm) of DEAE-cellulose adjusted to pH 9.8. The elution buffers for A and B were respectively the 10 mM and the 2 mM multicomponent buffer systems, pH 5.3. Flow-rate 40 ml/h.

In Fig. 6A is shown the pH gradient and elution profile for a mixture of standard proteins (lysozyme, myoglobin, haemoglobin and human serum albumin) on a DEAE-cellulose column using a 5 mM Buffalyte WR 3-10 system at pH 3.0. In each case the proteins eluted in order of their isoelectric points at a pH value slightly lower than the pI value as measured by buffer electrofocusing⁶. Examination of the recovered fractions by SDS-polyacrylamide gel electrophoresis on 10% slab gels (Fig. 7), immunodiffusion, against specific antisera and by analytical buffer electrofocusing on 5% polyacrylamide slab gels¹⁵, confirmed that the individual proteins can be recovered with a high degree of purity. The elution profile obtained with the same protein mixture on a TETA-cellulose column eluted with the same buffer eluent at pH 5.5 is shown in Fig. 6B. With the buffer system at this terminating pH a 0-1 M NaCl gradient was required to elute the human serum albumin. In subsequent studies, similar buffer focusing chromatographic methods have been utilised in the purification of human transferrin, complement component C_3 and human thyroid auto-antibodies. Compared to existing ion-exchange methods for the fractionation of these

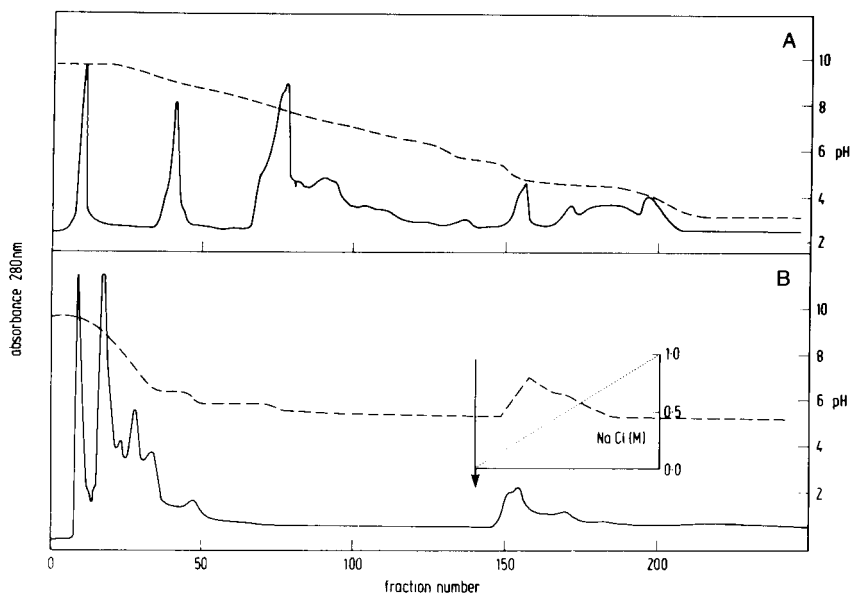


Fig. 6. A. Separation of protein mixture containing 50 mg each of chick lysozyme, sperm whale myoglobin, haemoglobin and human serum albumin on a DEAE-cellulose column (40×2.6 cm) eluted with the 5 mM Buffalyte WR 3-10 system, pH 3.0. The column was adjusted to pH 9.8 before application of the proteins. Flow-rate 40 ml/h. B. Separation of the same protein mixture on a TETA-cellulose column (40×2.6 cm) eluted with the same buffer system at pH 5.5. A salt gradient (0-1 M NaCl) was commenced at the point indicated.

proteins from suitable human sera, these buffer focusing chromatographic techniques permitted excellent resolution under preparative conditions, *i.e.* sample loadings greater than 500 mg.

In summary, this study has shown that internally generated pH gradients can be formed on ion-exchange resins with multicomponent buffer systems. Under these conditions proteins are resolved essentially according to their pI values. The separation mode bears close physicochemical similarities to the resolution of proteins under buffer electrofocusing conditions on granulated polysaccharide gels. These chromatographic procedures lend themselves to relatively large sample sizes because of the focusing effect to which solutes are subjected during their migration. In contrast to some synthetic polymeric ampholyte systems, the amphoteric and non-amphoteric components of the Buffalyte WR 3-10 system typically do not bind to proteins undergoing purification. In addition the buffer species can be easily removed from resolved proteins by ultrafiltration or dialysis, gel filtration or other appropriate chromatographic methods^{6,7}. From the array of low molecular weight buffers now available, clearly a large variety of multicomponent systems could be prepared for use in the generation of internal pH gradients on ion-exchange resins. Their selection will depend on further studies which establish the most appropriate combination of components of defined chemical composition for a particular application. With optimal pH gradient slope and precise control over the extent of solute ionisation, these buffer systems should find wide application in the separation of complex mixtures of pro-

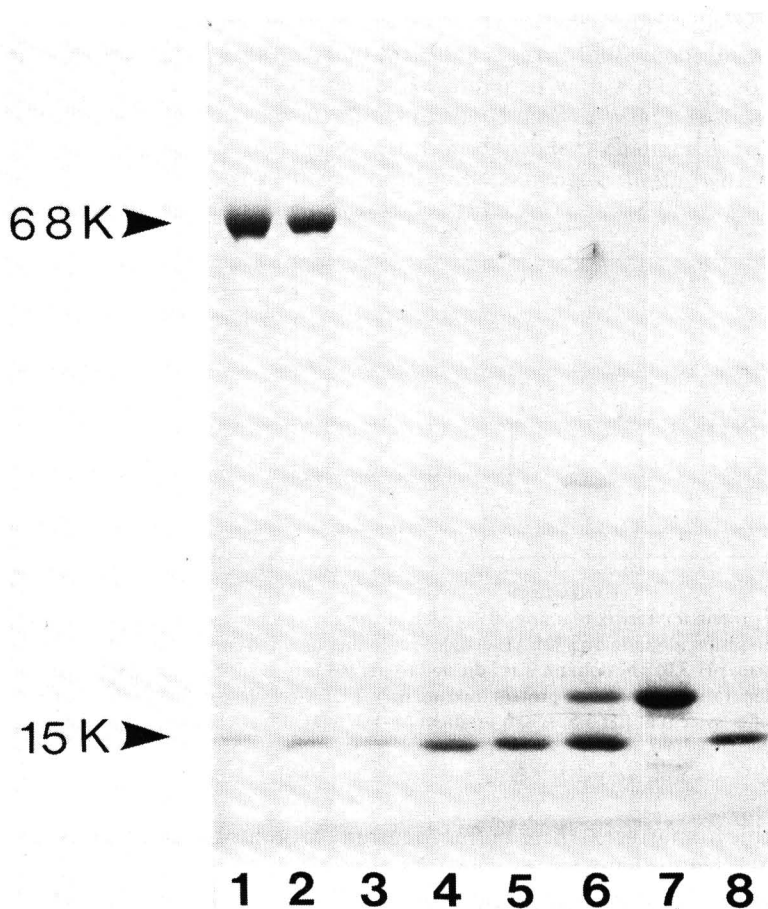


Fig. 7. Sodium dodecylsulphate-polyacrylamide slab gel electrophoresis of the recovered pooled fractions from the separation shown in Fig. 6A. The concentration of acrylamide and sodium dodecylsulphate in the gel were 10 and 0.1 %, respectively. The slab well numbers corresponding to the following pooled chromatographic fractions from the DEAE-cellulose separation: 1, 161-175; 2, 146-160; 3, 121-145; 4, 101-120; 5, 86-100; 6, 81-85; 7, 66-80; 8, 37-43. Under the electrophoretic conditions used, haemoglobin exhibits an apparent molecular weight of 15,500. The predominant protein as assessed by immunodiffusion in the pooled fractions was: 1, albumin; 2, albumin; 3-5, haemoglobin; 6, haemoglobin-myoglobin; 7, myoglobin and 8, lysozyme. Pooled chromatographic fractions 8-15 also contained only lysozyme.

teins and other biological polyelectrolytes. These aspects together with further potentials of this method, including its extension to high performance ion-exchange chromatographic systems, are under investigation.

REFERENCES

- 1 J. L. Young and B. A. Webb, *Anal. Biochem.*, 88 (1978) 619.
- 2 D. H. Leaback and H. K. Robinson, *Biochem. Biophys. Res. Comm.*, 67 (1975) 248.
- 3 L. A. Æ. Sluyterman and O. Elgersma, *J. Chromatogr.*, 150 (1978) 17.
- 4 L. A. Æ. Sluyterman and J. Wijdenes, *J. Chromatogr.*, 150 (1978) 31.

- 5 J. P. Emond and M. Pagé, *J. Chromatogr.*, 200 (1980) 57.
- 6 R. L. Prestidge and M. T. W. Hearn, *Anal. Biochem.*, 97 (1979) 95.
- 7 R. L. Prestidge and M. T. W. Hearn, *Sep. Purif. Methods*, 10, in press.
- 8 M. T. W. Hearn, R. L. Prestidge, J. F. T. Griffin and G. W. Mhlanga, *Prep. Biochem.*, 11 (1981) 191.
- 9 N. Y. Nguyen and A. Chrambach, *Electrophoresis*, 1 (1980) 23.
- 10 A. Chrambach, L. Hjelmeland, N. Y. Nguyen and B. An der Lan, in B. J. Radola (Editor), *Electrophoresis '79*, W. de Gruyter, Berlin, New York, 1980, pp. 3-23.
- 11 M. Bier, N. B. Egen, T. T. Allgyer, G. E. Twitty and R. A. Mosher, in E. Gross and J. Meienhofer (Editors), *Peptides, Structure and Biological Function*, Pierce Chemical Co., Rockford, 1979, pp. 79-89.
- 12 M. M. Bradford, *Anal. Chem.*, 72 (1976) 248.
- 13 R. Consden, A. H. Gordon and A. J. P. Martin, *Biochem. J.*, 38 (1944) 224.
- 14 P. G. Righetti and T. Caravaggio, *J. Chromatogr.*, 127 (1976) 1.
- 15 M. T. W. Hearn and E. J. Harris, unpublished results.

CHROM. 14,076

HIGH-PERFORMANCE LIQUID CHROMATOGRAPHY OF AMINO ACIDS, PEPTIDES AND PROTEINS

XXXVI*. ORGANIC SOLVENT MODIFIER EFFECTS IN THE SEPARATION OF UNPROTECTED PEPTIDES BY REVERSED-PHASE LIQUID CHROMATOGRAPHY

MILTON T. W. HEARN*** and BORIS GREGO

Immunopathology Research Unit, Medical Research Council of New Zealand, University of Otago Medical School, P.O. Box 913, Dunedin (New Zealand)

SUMMARY

The influence of the organic solvent modifier on peptide and polypeptide retention to octadecylsilica supports has been examined. Over a wide range of volume fractions of the organic solvent modifier, ψ_s , unprotected peptides do not show linear dependencies of their logarithmic capacity factors on the composition of binary hydro-organic solvent eluents. Instead, bimodal plots are observed with minima characteristic of the peptide and the organic solvent. The influence of acidic amine buffers on peptide retention behaviour to silica-bonded C_{18} hydrocarbonaceous stationary phases has also been further investigated. With mobile phases of low water content, it is possible to obtain on these alkylsilica supports, elution orders characteristic of a normal or polar phase elution mode. This irregular retention behaviour has been discussed in terms of the participation of multiple retention processes in the interaction of ionised peptides with chemically-bonded alkyl-silicas. The influence of flow-rate on column efficiencies for peptides separated under reversed-phase conditions has been studied. The results confirm that column efficiencies for small peptides decrease with increasing flow-rate and eluent viscosity. The significance of the dependence of $\ln k'$ on ψ_s for the isolation of peptides and polypeptides from biological sources is discussed.

INTRODUCTION

Because of its versatility and convenience, reversed-phase high-performance liquid chromatography (RP-HPLC) with chemically bonded hydrocarbonaceous silica supports has proved phenomenally successful for the separation of peptides^{1,2}. One of the special attributes of this technique when compared to other, more conven-

* For Part XXXV see ref. 6.

*** Present address: St Vincent's School of Medical Research, Victoria Parade, Melbourne, Victoria 3065, Australia.

tional chromatographic methods is the ease with which peptide selectivities can be manipulated by variation of the mobile phase composition. A number of specific mobile phase phenomena, including pH control over peptide ionisation levels, pairing ion complex formation and specific solvation effects can be readily exploited in order to modulate peptide retention and enhance selectivity of the reversed phase chromatographic systems. Although the elution of some very polar peptides from porous microparticulate alkylsilicas can be achieved with purely aqueous eluents, in most cases a hydro-organic solvent combination is required. It is a general experience that the retention of small peptides on reversed-phase silicas decreases as the volume fraction of the organic solvent, ψ_s , in the mobile phase is increased over the range *ca.* $0 < \psi_s < 0.4$. Under these elution conditions, the retention behaviour of small peptides tends to be regular, that is peptides elute in order of increasing hydrophobicities. However, with more hydrophobic peptides and some small proteins which require mobile phases of higher organic solvent content to affect elution from alkylsilicas, retention order reversals, indicative of a normal-phase separation mode, have been observed¹. Furthermore, the retention behaviour of polypeptides and proteins is particularly responsive to changes in the water content of the mobile phase. In many cases these larger solutes can only be efficiently chromatographed on chemically bonded alkylsilicas under isocratic conditions which encompass a very narrow range of organic solvent percentages. With mobile phases of high organic solvent content, *e.g.* when ψ_s is greater than 0.5, it has been noted³ that the relative selectivity factors for larger peptides separated on octyl- or octadecylsilicas tend to be lower than values obtained with mobile phases of lower solvent percentage. Despite the widespread use of organic solvent modifiers in RP-HPLC separations of peptides, few studies have systematically examined the physico-chemical basis of this modulation of selectivity as the volume fraction of the organic solvent is altered. The purpose of the present study was to compare the elution behaviour of a variety of unprotected peptides using mobile phases of widely differing organic solvent compositions. The results clearly implicate the involvement of multiple retention processes in the interaction of peptides with chemically bonded alkylsilicas.

EXPERIMENTAL

Chemicals and reagents

Acetonitrile, methanol and 2-propanol were all AnalaR or HPLC grade. Water was double distilled and deionised using a Milli-Q system (Millipore, Bedford, MA, U.S.A.). The peptides and polypeptides (Table I) used in this study were purchased from Sigma (St. Louis, MO, U.S.A.), Bachem (Torrance, CA, U.S.A.) or Research Plus Labs. (Denville, NY, U.S.A.). All amino acids except glycine were of the *L*-configuration. Orthophosphoric acid was obtained from May and Baker (Dagenham, Great Britain). Triethylamine was from BDH (Poole, Great Britain) and purified prior to use^{5,6}.

Apparatus

The chromatographic data were collected with one (isocratic) or two (gradient) Model M6000A solvent delivery pumps, a M660 solvent programmer, a U6K universal chromatographic injector, a Model M440 fixed wavelength (254 nm) or a

TABLE I

PEPTIDES AND POLYPEPTIDES USED IN THE PRESENT STUDY

The one letter code for the amino acids is used as given by M. O. Dayhoff in *Atlas of Protein Sequence and Structure*, National Biomedical Research Foundation, Silver Spring, MD, U.S.A., 1972.

No.	Peptide	No.	Peptide
1	F	9	RF
2	FF	10	RFA
3	FFF	11	DRVYIHPF (Angiotensin II)
4	FFFF	12	DRVYIHPFHL (Angiotensin I)
5	FFFFF	13	Bovine insulin B chain
6	LY	14	Bovine insulin
7	PY	15	Porcine glucagon
8	YYY		

Model M450 variable-wavelength UV detector, all from Waters Assoc. (Milford, MA, U.S.A.) coupled to a Rikadenki or Omniscrite dual channel recorder. Sample injections were made with Pressure Lok liquid syringes (0–25 μ l) from Precision Sampling (Baton Rouge, LA, U.S.A.). The pH measurements were performed with a Radiometer, PHM64 Research pH meter, equipped with a combination glass electrode.

Methods

All chromatograms were carried out at ambient temperatures. Bulk solvents and mobile phases were prepared and degassed by sonication as reported previously^{3,4}. This procedure ensures that no preferential evaporation of the organic solvent occurs from mobile phases of high organic solvent content. A single μ Bondapak C₁₈ column (particle diameter 10 μ m, 30 \times 0.4 cm I.D.) was used throughout this study. The column was equilibrated for at least 30 min (*ca.* 50–100 column volumes) with new mobile phases conditions. Sample sizes varied between 2 and 5 μ g of peptide material injected in volumes ranging between 2 and 5 μ l. The capacity factors were calculated in the usual way with NaNO₃ to calibrate the column. Column efficiencies in terms of theoretical plates (*N*) were determined under isocratic conditions from the retention time and peak width at the half height and are uncorrected for extra-column zone spreading effects. Apparent plate counts from gradient elution were also calculated in the same manner. The ionic strength and pH of the phosphate buffers were chosen on the basis of criteria established^{3,4,7–9} in earlier comparative studies to ensure adequate control over protic equilibria.

RESULTS AND DISCUSSION

The role of the organic solvent modifier in the manipulation of the retention of polar solutes in RP-HPLC has attracted considerable theoretical and experimental attention during the past few years^{10–22}. From a practical viewpoint, it is well recognised that both the molecular characteristics and the concentration of the organic solvent in binary hydro-organic solvent eluents have significant influences on the overall chromatographic distribution equilibria established by the solutes. For a

given separation temperature, linear relationships between the logarithmic capacity factors of neutral and anionic solutes and the volume fraction of the organic solvent modifier, ψ_s , in binary hydro-organic solvent eluents are frequently observed. Snyder and coworkers^{11,13} have proposed that such linear dependencies of $\ln k'$ on ψ_s are representative of regular retention behaviour in RP-HPLC with hydro-organic solvent eluents. Schoenmakers *et al.*¹⁴, have however argued that $\ln k'$ varies quadratically on solvent composition although over the narrow range in k' values of interest in chromatographic optimisation, *e.g.* $1 < k' < 20$, it has been concluded that linear relationships provide an adequate approximation. Assuming that the retention process in RP-HPLC was essentially determined by solvent effects, Horváth and coworkers^{17,19} adapted solvophobic theory to evaluate the role of the eluent in the retention behaviour of neutral and polar solutes on non-polar stationary phases. According to this comprehensive theoretical treatment, the chromatographic process can be viewed as a series of reversible hydrophobic interactions between the solute molecules and the alkyl ligands at the surface of the stationary phase with solute retention governed to a large extent by the bulk surface tension, γ , and the dielectric constant, ϵ , of the eluent. For water-rich eluents encompassing a narrow range of ψ_s values, *e.g.* $0.2 < \psi_s < 0.4$, the observed retention behaviour of neutral²⁰⁻²² and even some polar solutes including peptides^{3,19} has been in good agreement with the regular behaviour expected on the basis of the solvophobic effect. However, peptide retention in RP-HPLC does not always follow this regular behaviour and we now know that in many cases with these ionogenic solutes, the retention process is much more complex than simple hydrophobic expulsion of peptidic solutes from a mixed aqueous-organic solvent eluent. Anomalous retention behaviour for peptides separated on alkylsilicas, has been discussed¹⁻⁴ in terms of secondary chemical equilibria, notably solvation effects and ion-pairing phenomena. Most retention irregularities can be ascribed to peptide interaction with accessible silanol groups at the surface of the stationary phase. The heterogeneous nature of the surface of octyl- and octadecyl-silica stationary phases is well documented. Broad and asymmetric peaks have been observed²²⁻²⁵ when amino compounds and related cationic solutes have been chromatographed on alkylsilica supports under certain conditions. In addition, plots of $\ln k'$ versus ψ_s for such compounds may show minima^{3,26,27}. Horváth and coworkers^{15,16} recently evaluated retention of polar solutes on bonded stationary phases in terms of a dual solvophobic-silanophilic retention mechanism. Detailed investigations with cationic solutes, including protonated peptides, have led other workers to propose^{1-3,23} similar two site adsorption models with the surface silanol groups being implicated in peak tailing and regional selectivity changes. With this previous information in mind, we have investigated the retention behaviour of three series of peptides (Table I) using hydro-organic eluents containing different concentrations of methanol, acetonitrile or propan-2-ol.

The results obtained with the phenylalanine oligomers on a μ Bondapak/C₁₈ column with aqueous methanol, acetonitrile or propan-2-ol that contained 20 mM orthophosphoric acid, pH 2.25, are depicted in Fig. 1A, C and E. Shown in Fig. 1B, D and F are the results obtained under similar solvent compositions with mobile phases containing 15 mM triethylammonium phosphate, pH 2.95. For all cases it can be seen that plots of $\ln k'$ versus ψ_s are non-linear, and when acetonitrile or methanol was the organic modifier, the plots of $\ln k'$ versus ψ_s passed through minima. Further exami-

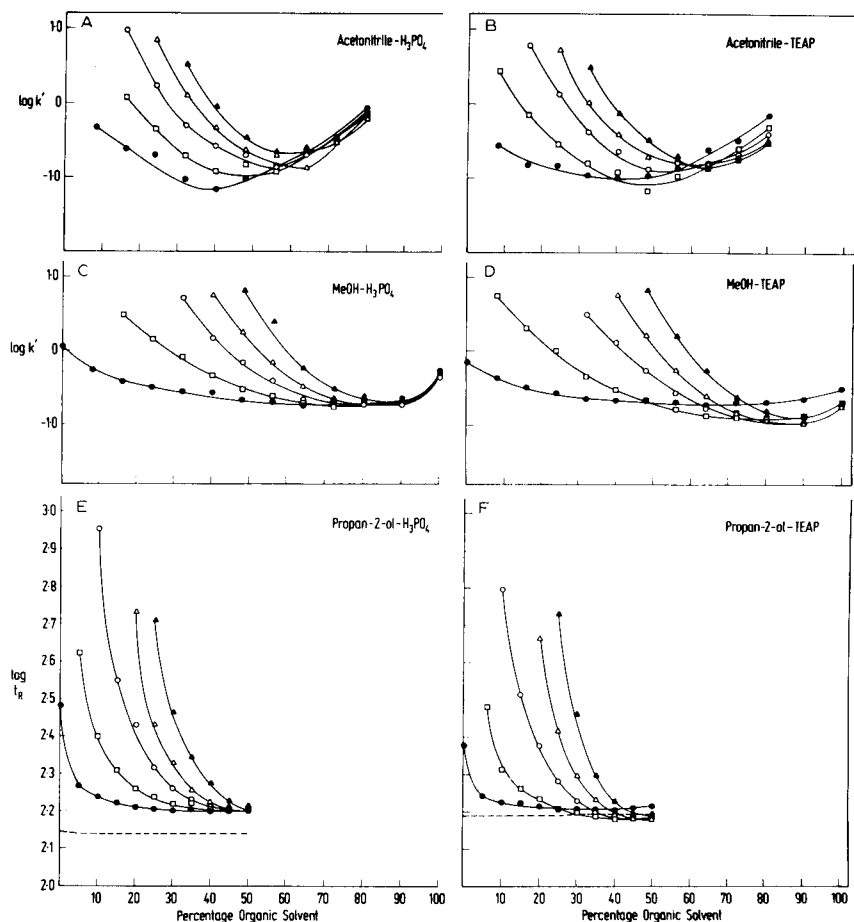


Fig. 1. Plots of the logarithmic retention factors of several phenylalanine oligomers (1-5) against the volume fraction of organic solvent in the aquo-organic solvent mixtures used as the eluent. In A, C and E are shown results obtained with the organic solvent modifiers acetonitrile, methanol or propan-2-ol, respectively with a primary mobile phase comprised of water-20 mM orthophosphoric acid. In B, D and F are shown the data for the corresponding experiments using a primary mobile phase of water-15 mM triethylammonium phosphate. The dashed lines in E and F represent the logarithmic retention time of a sodium nitrate peak. All the data for the propan-2-ol experiments are expressed in terms of retention times (sec). Column, μ Bondapak C_{18} ; flow-rate, 2.0 ml/min for the acetonitrile and methanol experiments, 1.2 ml/min for the propan-2-ol experiments. The phenylalanine oligomer key is: \bullet = F; \square = FF; \circ = FFF; \triangle = FFFF; \blacktriangle = FFFFF.

nation of the data reveals several important features germane to the role of the organic solvent modifier. Firstly, it can be readily seen that the capacity factors for the phenylalanine oligomers initially show progressive decreases with water rich eluents as ψ_s is increased. For all three solvents under conditions where $\psi_s < 0.4$, the peptide elution order follows the anticipated regular hydrophobic retention behaviour. Variation in the capacity factors for the different phenylalanine oligomers on changing from methanol to acetonitrile or propan-2-ol are in accord with differences in their respective solvent strengths. However, as ψ_s is increased further

above *ca.* 0.4 a progressive reversal in elution order becomes evident. Finally with water-lean or neat organic solvent eluents, *e.g.* $0.8 < \psi_s < 1$, these phenylalanine oligomers elute in an order characteristic of a normal phase separation mode. This data suggests that the interaction of peptides with alkylsilicas involves both a hydrophobic and a silanophilic component in the retention mechanism. The results obtained with the same eluents containing 15 mM triethylammonium phosphate are thus of special interest. The incorporation of aliphatic amines in the mobile phase has been used to mask peak tailing of cationic solutes^{1-3,16,23-25,28-30}. Appropriate concentrations of acidic amine buffers to ensure that silanol effects are negligible can be estimated from column efficiency or binding constant measurements. For peptide separations on alkylsilicas of low to intermediate carbon coverage, triethylammonium salts at concentrations ranging between 10–150 mM have been recommended^{1,2,6,29} to improve peak shape and reduce retention. Stein and coworkers^{31,32} have favoured 0.5–1 M pyridinium salts although under these conditions, post column fluorometric derivatisation and detection of the eluted peptides are required. With high coverage alkylsilica supports, the retention of basic peptides has been found^{1,25} to be practically independent of sample load when *ca.* 2 mM triethylammonium, and related trialkylammonium, buffers are added to the mobile phase. With bulky, amphiphatic alkylamines such as dodecylamine or N,N-dimethyldodecylamine, concentrations as low as 1 mM have been effective^{16,24}. Although a major effect of acidic alkylamine buffers is thought to involve the masking of accessible polar groups on the surface of the stationary phase, the ability of these buffer components to specifically modify the support into a dynamically coated weak anion exchanger must not be overlooked. Evidence for such an additional role has been presented previously³³⁻³⁶ and may explain several observations made in the present study, particularly with eluents containing propan-2-ol. For example, with the 15 mM triethylammonium phosphate–propan-2-ol mobile phases, the t_R of the nitrate anion, which was used to calibrate the column dead volume, was larger than the t_R of several of the protonated peptides. Furthermore, the t_R (nitrate) value was concentration dependent. For these reasons, the data for the propan-2-ol experiments are expressed as plots of $\ln t_R$ (observed) *versus* ψ_s . Several other small anions, including formate, and acetate, also exhibited enhanced t_R values under these 15 mM triethylammonium phosphate–propan-2-ol elution conditions. The role of such dynamic ion-exclusion and ion-exchange phenomena in the RP-HPLC of peptides with such eluents is, at this stage, poorly delineated and clearly warrants further attention. Evidence in favour of organic amines being extracted onto the stationary phase from the mobile phase appears however to be overwhelming.

Several studies have demonstrated^{12,18,36,37} that the organic solvent in a hydro-organic solvent eluent is also distributed between the mobile and stationary phases in RP-HPLC. Determination of the Langmuir adsorption isotherms of a number of organic solvent–water systems in contact with hydrocarbonaceous phases has revealed^{12,36} that a layer of solvent molecules form at the bonded-phase surface. The extent of this layer increases with solvent concentration and is inversely related to the dielectric constant, ϵ , and the elutropic value ϵ_0 (alumina), of the pure solvent. Specific adsorption of solvent molecules by the stationary phase will give rise to solvent-dependent changes in the surface characteristics of the non-polar support. As is evident from the data shown in Figs. 1–3 these effects have important sequelae as

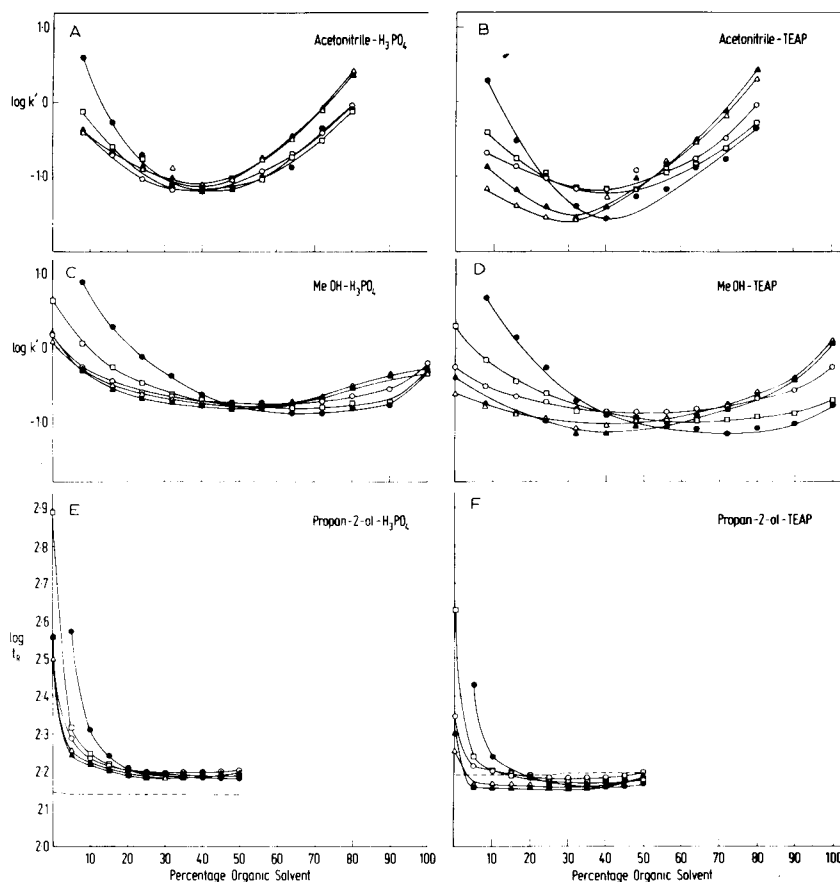


Fig. 2. Plots of the logarithmic retention factors for the peptides (6–10) against the volume fraction of the organic solvent in the water-organic solvent mixture used as the eluent. The chromatographic conditions are the same as in the legend to Fig. 1. The peptides key is: ● = YYY; □ = LY; ○ = PY; △ = RF; ▲ = RFA.

far as the hydrogen bonding processes which occur between peptide solutes and the stationary phase.

Peptides with ionogenic side chain groups also exhibit the concave binodal dependence of $\ln k'$ on ψ_s (Figs. 2 and 3). With water-rich eluents, the basic peptides tended to show lower retention than neutral or acidic peptides. However, at the other mobile phase extreme, the opposite pattern was generally seen. These observations, again, are compatible with dual or multiple retention processes being involved in the binding of the peptides to the stationary phase. In common with earlier observations^{1,2}, peptide retention with mobile phases where $\psi_s < 0.4$ appears independent of the number of amino acid residues. Selectivity was, however, responsive to pH changes which influence the extent of ionisation. It is noteworthy that the curvature of the $\ln k'$ dependence on ψ_s for the different small peptides examined in this study varied considerably between the three organic solvents. Many of the trends can be rationalised on the basis of specific solute interactions with the extracted modifier in the

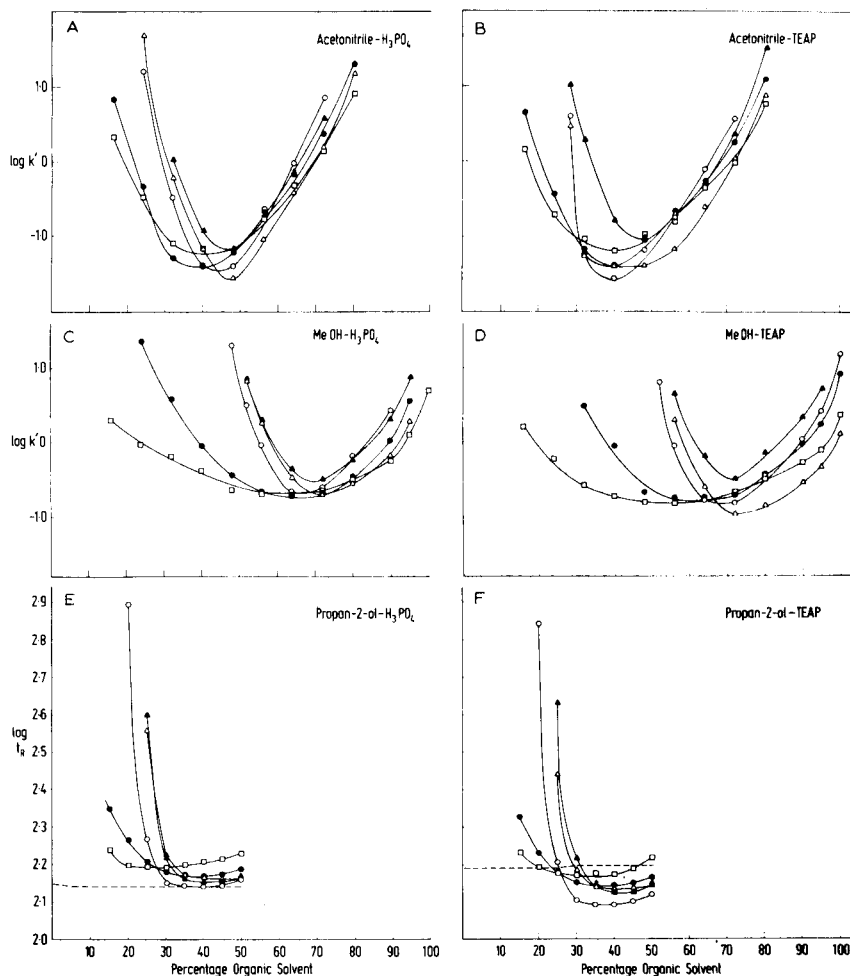


Fig. 3. Graphs illustrating the relationships of the retention factors of several polypeptide hormones (11–15) on octadecylsilica and the composition of the aquo-organic eluent. The chromatographic conditions were the same as given in the legend to Fig. 1. The polypeptides key is: ● = angiotensin I; □ = angiotensin II; ○ = bovine insulin; △ = bovine insulin B chain; ▲ = porcine glucagon.

stationary phase. Whereas methanol and 2-propanol are proton accepting solvents, *i.e.* in terms of Pearson's classification³⁸ these solvents are hard bases, acetonitrile is a weak dipolar base. One consequence of these solvent differences is their ability to manipulate the hydrogen bonding characteristics of the stationary phase. Such variations reflected in the dependence of $\ln k'$ on ψ_s could thus account for regional selectivity changes occasionally found when one solvent is substituted by another.

During these studies it was also apparent that column efficiencies were strongly influenced by alterations in the mobile phase composition. Broader peaks were generally observed for the smaller peptides using the more viscous propan-2-ol mobile phases than with the methanol- or acetonitrile-based eluents under otherwise identical conditions. Similar changes in theoretical plate numbers (N) for a given column

with increasing eluent viscosity have been noted^{17,39} previously in ion-pair RP-HPLC studies of simple amines and small peptides. Fig. 4 shows the influence of flow-rate on column efficiencies for several polypeptide hormones. The mobile phase compositions were chosen to give comparable capacity factors for these polypeptides eluted under isocratic conditions. In all cases a reduction in flow-rate improved the chromatographic efficiencies, with larger changes evident for the more hydrophobic polypeptides. When similar separations were carried out under gradient eluent conditions, the apparent plate counts were *ca.* 50–100 fold larger, that is the apparent heights equivalent to a theoretical plate (HETPs) were *ca.* 0.01 mm.

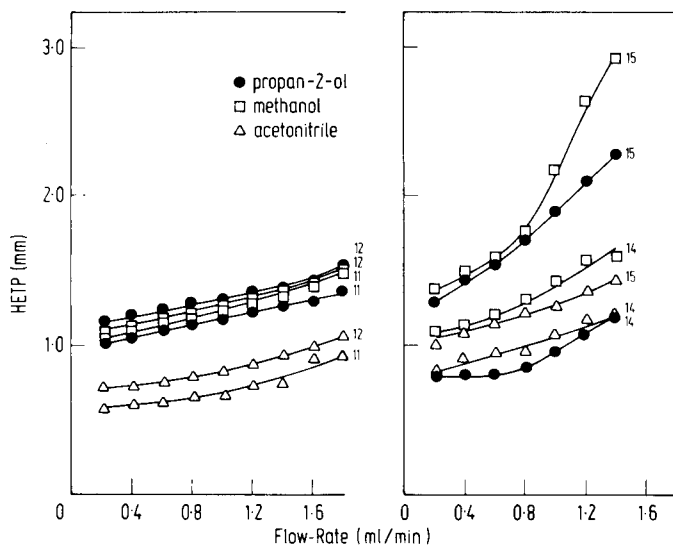


Fig. 4. Effects of mobile phase flow-rate and organic solvent composition on column efficiency for several polypeptides eluted under isocratic conditions. The aqueous 20 mM orthophosphoric acid mobile phases contained different percentages of the three organic solvents (acetonitrile, methanol and propan-2-ol) such that the polypeptides eluted with comparable capacity factors. The peptide key is: 11, angiotensin II; 12, angiotensin I; 14, bovine insulin; 15, porcine glucagon.

Knowledge of the dependence of $\ln k'$ on ψ_s has important consequences for the isolation of peptides and polypeptides from tissue sources. Since a given capacity factor can be obtained at two different eluent compositions, it should be possible to choose one organic solvent percentage which permits optimal resolution of a particular component. Although silanol effects are generally considered deleterious in peptide separation by RP-HPLC techniques, under appropriate conditions they permit additional control over selectivity. As we have demonstrated elsewhere^{1,6}, silanol effects may in fact prove advantageous for the preparative separation of hydrophobic polypeptides and proteins, including several pituitary protein hormones. Similar conclusions have been reached by Bij *et al.*¹⁶ from their studies on hydrophobic peptide fragments of glycophorin A. A very steep dependence of $\ln k'$ on ψ_s would imply that very little elution development occurs for a particular peptide–polypeptide during the separation. Although superficially, this could be considered undesirable, in reality such a dependence may be quite useful in obtaining adequate

selectivity for a separation of biological peptides, many of which are available in amounts less than 1 μg per g tissues. For example, the nature of the dependence of $\ln k'$ on ψ_s for peptides and polypeptides permits the reversed-phase support to be used for the concentration of peptides from very dilute solutions such as extracts or haemodialysates⁴⁰. Our experience has indicated that linear gradients for acetonitrile ($0 < \psi_s < 0.5$), and shallow convex gradients for methanol ($0 < \psi_s < 0.7$) and 2-propanol ($0 < \psi_s < 0.4$) are optimal gradient configurations for polypeptide resolution on surface modified hydrocarbonaceous silicas. Comparison of apparent column efficiencies reaffirms the value of gradient elution particularly in the initial stage of a micro or small scale RP-HPLC fractionation of a given component from a complex biological mixture. Batch elution methods using a window of organic solvent percentages chosen from $\ln k'$ versus ψ_s data, however, are currently more convenient for large scale preparative separations of peptides involving more than 1-g samples⁴¹. The use of ternary mobile phases provides an alternative approach to enhance polar selectivity effects and modulate retention. In this context low concentrations of a second organic solvent modifier, for example 1% *tert*-propanol or trifluoroethanol, have proved^{1,25} effective for the modulation of peptide retention to hydrocarbonaceous bonded silicas.

In conclusion, over a wide range of ψ_s values, minima are observed in the plots of $\ln k'$ versus ψ_s for peptides separated on octadecylsilica. With mobile phases of low water content, the elution order of unprotected peptides follows a normal-phase pattern. The curvature of the bimodal plots is influenced by the hydrophobicity of the peptide and the characteristics of the organic solvents. In accord with earlier observations¹⁻⁴, with water-rich eluents encompassing a narrow ψ_s range the regular retention behaviour exhibited by peptides can be approximated to linear dependencies of $\ln k'$ on ψ_s . Evaluation of the overall dependence of $\ln k'$ on ψ_s permits mobile phase compositions to be selected allowing optimal resolution of peptides on alkylsilica supports. Similar RP-HPLC methods can be extended to the separation and recovery of undegraded proteins. For example, on 50-nm pore diameter octylsilicas we have been able to resolve^{1,42} ovine thyrotrophins and human thyroglobulin 19S iodoproteins including the desialo-19S iodoprotein with preservation of native biological activity.

REFERENCES

- 1 M. T. W. Hearn, *Advan. Chromatogr.*, 20 (1981) in press.
- 2 M. T. W. Hearn, in Cs. Horváth (Editor), *High Performance Liquid Chromatography: Advances and Perspectives*, Vol. 3, Academic Press, New York, 1981, in press.
- 3 B. Grego and M. T. W. Hearn, *Chromatographia*, in press.
- 4 M. T. W. Hearn and B. Grego, *J. Chromatogr.*, 203 (1981) 349.
- 5 J. C. Sauer, *Org. Synth. Coll. Vol.*, 4 (1963) 560.
- 6 M. T. W. Hearn, B. Grego and C. A. Bishop, *J. Liquid Chromatogr.*, 4, in press.
- 7 E. P. Kroeft and D. J. Pietrzyk, *Anal. Chem.*, 50 (1978) 502.
- 8 I. Molnár and Cs. Horváth, *J. Chromatogr.*, 142 (1977) 623.
- 9 M. T. W. Hearn, B. Grego and W. S. Hancock, *J. Chromatogr.*, 185 (1979) 429.
- 10 W. R. Melander, A. Nahum and Cs. Horváth, *J. Chromatogr.*, 185 (1979) 129.
- 11 L. R. Snyder, J. W. Dolan and J. R. Gant, *J. Chromatogr.*, 165 (1979) 3.
- 12 R. M. McCormick and B. L. Karger, *J. Chromatogr.*, 199 (1980) 259.
- 13 L. R. Snyder, in Cs. Horváth (Editor), *High Performance Liquid Chromatography: Advances and Perspectives*, Vol. 1, Academic Press, New York, 1980, p. 208-315.

- 14 P. J. Schoenmakers, H. A. H. Billiet and L. de Galan, *J. Chromatogr.*, 185 (1979) 179.
- 15 A. Nahum and Cs. Horváth, *J. Chromatogr.*, 203 (1981) 53.
- 16 K. E. Bij, Cs. Horváth, W. R. Melander and A. Nahum, *J. Chromatogr.*, 203 (1981) 65.
- 17 W. R. Melander and Cs. Horváth, in Cs. Horváth (Editor), *High Performance Liquid Chromatography Advances and Perspectives*, Vol. 2, Academic Press, New York, 1980, p. 113-319.
- 18 H. Colin and G. Guiochon, *J. Chromatogr.*, 158 (1978) 183.
- 19 Cs. Horváth, W. Melander and I. Molnár, *J. Chromatogr.*, 125 (1976) 129.
- 20 K. Karch, I. Sebastian, I. Halász and H. Engelhardt, *J. Chromatogr.*, 122 (1976) 171.
- 21 B. L. Karger, J. R. Gant, A. Hartkopf and P. H. Weiner, *J. Chromatogr.*, 128 (1976) 65.
- 22 S. R. Abbott, J. R. Berg, P. Achener and R. L. Stevenson, *J. Chromatogr.*, 126 (1976) 421.
- 23 A. Sokolowski and K.-G. Wahlund, *J. Chromatogr.*, 189 (1980) 299.
- 24 W. S. Hancock, C. A. Bishop, R. L. Prestidge, D. R. K. Harding and M. T. W. Hearn, *J. Chromatogr.*, 153 (1978) 391.
- 25 W. S. Hancock, C. A. Bishop, L. J. Meyer, D. R. K. Harding and M. T. W. Hearn, *J. Chromatogr.*, 161 (1978) 291.
- 26 S. Eksborg, H. Ehrsson and V. Lönnroth, *J. Chromatogr.*, 185 (1979) 583.
- 27 K. Sugden, C. Hunter and J. G. Lloyd-Jones, *J. Chromatogr.*, 204 (1981) 195.
- 28 W. R. Melander, J. Stoveken and Cs. Horváth, *J. Chromatogr.*, 185 (1979) 111.
- 29 J. Rivier, *J. Liquid Chromatogr.*, 1 (1978) 347.
- 30 W. S. Hancock, C. A. Bishop, R. L. Prestidge, D. R. K. Harding and M. T. W. Hearn, *Science*, 200 (1978) 1168.
- 31 S. Stein, in E. Gross and J. Meienhofer (Editors), *Structure and Biological Function*, Pierce Chemical Co., Rockford, IL, 1979, p. 73-78.
- 32 S. Stein, C. Kenny, H. J. Friesen, J. Shively, U. D. Valle and S. Pestka, *Proc. Nat. Acad. Sci. U.S.*, 77, 5716, 1980.
- 33 M. T. W. Hearn, *Advan. Chromatogr.*, 18 (1981) 59-100.
- 34 M. T. W. Hearn, S. J. Su and B. Grego, *J. Liquid Chromatogr.*, 4, in press.
- 35 B. A. Bidlingmeyer, S. N. Deming, W. R. Price, Jr., B. Sachok and M. Petrusek, *J. Chromatogr.*, 186 (1979) 419.
- 36 R. P. W. Scott and P. Kucera, *J. Chromatogr.*, 175 (1979) 51.
- 37 J. H. Knox and A. Pryde, *J. Chromatogr.*, 112 (1975) 171.
- 38 R. G. Pearson and J. Songstad, *J. Amer. Chem. Soc.*, 89 (1967) 1827.
- 39 C. M. Riley, E. Tomlinson and T. M. Jefferies, *J. Chromatogr.*, 185 (1979) 197.
- 40 N. M. James and M. T. W. Hearn, *Amer. J. Psychiatry*, 137 (1980) 488.
- 41 C. A. Bishop, L. J. Meyer, D. R. K. Harding, W. S. Hancock and M. T. W. Hearn, *J. Liquid Chromatogr.*, 4 (1981) 661.
- 42 M. T. W. Hearn, B. Grego, P. S. Stanton and A. J. Paterson, unpublished observations.

CHROM. 14,077

APPLICATION OF 1,1'-CARBONYLDIIMIDAZOLE-ACTIVATED MATRICES FOR THE PURIFICATION OF PROTEINS

III. THE USE OF 1,1'-CARBONYLDIIMIDAZOLE-ACTIVATED AGAROSSES IN THE BIOSPECIFIC AFFINITY CHROMATOGRAPHIC ISOLATION OF SERUM ANTIBODIES

MILTON T. W. HEARN** and EUGENIE L. HARRIS

Autoimmunity Research Unit, Medical Research Council of New Zealand, University of Otago Medical School, P.O. Box 913, Dunedin (New Zealand)

and

G. S. BETHELL, W. S. HANCOCK and J. A. AYERS

Department of Chemistry, Biochemistry and Biophysics, Massey University, Palmerston North (New Zealand)

SUMMARY

The characteristics of ligands immobilised onto 1,1'-carbonyldiimidazole-treated cross-linked agarose have been further evaluated. Since the intermediate activated matrix (an imidazolyl carbamate-agarose) is susceptible to nucleophilic attack by free amino groups, but is relatively stable to oxygen nucleophiles, ligands ranging from simple organic primary amines, amino acids, proteins and other biological substances, which contain amino group functionality, can be bound to the agarose via a N-alkylcarbamate (urethane) linkage. This covalent linkage has been found to exhibit good chemical stability to mildly acidic and basic elution conditions. The use of 1,1'-carbonyldiimidazole-activated agarose in the biospecific affinity chromatography of immunoglobulins, present in normal and pathological sera, is described.

INTRODUCTION

Biospecific affinity chromatography is based on the ability of water-soluble biological substances to bind specifically and reversibly to complementary ligands which have been immobilised generally onto insoluble, inert polymers. As a technique for the specific isolation of a particular protein, biospecific affinity chromatography is probably the most powerful procedure currently available. The interaction of antibodies with specific antigens, enzymes with specific substrates, lectins with specific

* Present address: St. Vincent's School of Medical Research, Victoria Parade, Melbourne, Victoria 3065, Australia.

carbohydrates and hormones with specific receptors have all found expression in the numerous variants of this technique¹. The most popular form of ligand immobilisation is to covalently attach an appropriate ligand via its functional groups, such as amino, carboxylic or sulphhydryl groups, to a suitable support matrix which has been chemically modified by the incorporation of compatible reactive groups. Precise control over the degree of activation of the insoluble matrix and the multiplicity of site attachment of the ligand molecules are essential requirements for reliable affinity supports. To be fully effective in a chromatographic separation the ligand must be covalently attached to the support matrix, either directly or via a spacer, by a chemical linkage which does not restrict the physical accessibility or abolish the specific binding interactions between the ligand and the biological substances under investigation. In addition, the covalent linkage must be stable to the conditions required for the elution of the absorbed molecules.

The reaction of polysaccharide gels with cyanogen bromide (CNBr) at high pH has become the most widely used method for the activation of these insoluble supports. However, all ligand immobilisation procedures based on CNBr activation of polysaccharide gels suffer from the limited stability of the positively charged N-substituted isourea linkage formed between the ligand and the matrix, relatively low activation levels and difficulties in handling the CNBr reagent despite recent refinements in experimental technique²⁻⁴. These features of the CNBr method have prompted several groups to develop alternative methods of activation of polysaccharide gels, including the oxirane approach pioneered by Sundberg and Porath⁵, and the use of substituted *sec.*-triazines⁶, pyrimides⁷ and benzoquinones⁸ as activating reagents. Recently, we reported^{9,10} that 1,1'-carbonyldiimidazole (CDI) and related heterocyclic carbonylating reagents can be used to activate in an easily controlled manner, insoluble cross-linked polysaccharide gels, agarose-polyacrylamide copolymers and glycopase-controlled pore glasses. The intermediate activated matrix was found¹¹ to couple in good yields with N-nucleophiles to give a non-basic urethane linkage, devoid of additional charge groups due to the activation procedure in contrast to the CNBr approach^{12,13}. This paper reports additional studies on the characteristics of ligands immobilised onto cross-linked Sepharose CL-6B via the CDI procedure, including the use of affinity matrices for the purification of antibodies present in normal and pathological sera.

EXPERIMENTAL

Materials

Cross-linked agaroses (Sepharose CL-4B and CL-6B) were purchased from Pharmacia (Uppsala, Sweden) and the polyacrylamide-agarose copolymer Ultrogel AcA-44 was from LKB (Bromma, Sweden). CDI was obtained from Pierce (Rockford, IL, U.S.A.) as was CDI-activated 6% cross-linked agarose (Reacti-Gel (6X), activation level, 20–25 μ moles/ml gel). [U-¹⁴C]Glycine and ¹²⁵I (carrier-free) were obtained from The Radiochemical Centre (Amersham, Great Britain). Chloramine T was from May and Baker (Dagenham, Great Britain). All other chemicals were AnalaR reagent grade.

Human thyroglobulin was extracted from human thyroids by the method of Salvatore *et al.*¹⁴ and fractionated by gel filtration on Sepharose CL-4B using a 10

mM Tris-HCl-150 mM NaCl, pH 8.0, buffer as described previously¹⁵. Human and rabbit immunoglobulin preparations were obtained by ammonium sulphate fractionation of the appropriate sera, followed by DEAE-cellulose anion-exchange chromatography using established procedures. Specific antisera to the proteins used in this study were raised in this laboratory using New Zealand white rabbits or outbred strain guinea pigs and goats; other antisera were purchased from Hoechst-Behringwerke (Frankfurt, G.F.R.).

Methods

Sephacrose CL-6B and Ultrogel AcA-44 were activated with CDI in dioxan using the solvent exchange procedure as described elsewhere^{9,10}. The number of active groups present on the matrix was determined by titration analysis using a Radiometer pH titrator (TTT2). In a typical experiment treatment of the agarose matrix with CDI at the level of 300 μ moles reagent/g gel gave an activated matrix containing *ca.* 120–150 μ moles active groups/g gel. CNBr activation of Sepharose CL-6B was carried out using the procedure of March *et al.*². Proteins were generally immobilised onto the activated matrices at a solution concentration of 2–10 mg/ml using a 0.5 M sodium chloride–1 M sodium carbonate (pH 10.0) buffer for 12–18 h at 4 C. For protein couplings below pH 8.0 a 0.5 M sodium chloride–0.1 M sodium phosphate buffer was employed. Affinity chromatography was generally carried out at 18 C using 10–100 ml of the appropriate affinity adsorbent packed into glass columns of 12–20 mm I.D. The biospecific ligand–matrix supports were equilibrated in 150 mM NaCl–25 mM NaH₂PO₄, pH 7.2 or 20 mM Tris-HCl, pH 7.2, prior to an affinity separation. The sample proteins to be separated were pumped slowly onto the appropriate affinity column, over a period of 1–2 h, and the non-bound components eluted with the initial column equilibration buffer. Following desorption of the bound components, the eluates were immediately adjusted to pH 7.0 and desalted by gel filtration on short Sephadex G-25 columns, by rapid dialysis or by ultrafiltration through Millipore PM10 membranes (Millipore, Bedford, MA, U.S.A.). Lyophilisation of dialysed solutions containing affinity purified antithyroglobulin antibodies resulted in considerable loss of antibody binding capacity with some preparations. Protein concentrations in the eluates was monitored by the absorbance at 254 and 280 nm and in other samples by the Bradford assay¹⁶. Haemagglutination assays were carried out using the tanned red cell procedure¹⁷ and antibody binding capacity was evaluated from a specific double antibody “sandwich” technique¹⁸. Immunodiffusion and immunoelectrophoresis were carried out in 1% agarose in a barbital buffer. Protein iodinations with ¹²⁵I were carried out as described previously¹⁸.

RESULTS AND DISCUSSION

When the affinity between the interactive substances is high, as in the case with polypeptide hormone–receptor or antigen–antibody interactions, or when the abundance of a specific component under purification is very low, the major limitation of the use of biospecific affinity chromatography is the propensity of the coupled ligand to leak from the support under the eluting conditions. Our previous studies^{10,11} on the purification of trypsin and several other proteins using a CDI-activated matrix, led us to conclude that the N-alkylcarbamate linkage formed by the coupling reaction

was reasonably stable at room temperature over the pH range 2.5–10. In order to elucidate more closely the leakage of ligands coupled to agarose via the CDI activation procedure, the rate of release of [125 I]thyroglobulin and [U - 14 C]glycine from their respective specific sorbents was investigated at different times in buffers of different pH. Representative data obtained in these experiments are shown in Fig. 1. These and related experiments with immobilised labelled immunoglobulins, confirmed that the N-alkylcarbamate linkages, formed between the amino groups of amino acids or proteins and the CDI-activated Sepharose CL-6B, exhibit good stability over the pH range normally used in affinity chromatography. Extended periods of time at low or high pHs, *e.g.* treatment of the ligand-matrix with chaotropic eluents at pHs below 3.0 or above 11.0, result in enhanced ligand release and/or denaturation of the protein ligands examined in this study. A practical consequence of the low level of thyroglobulin release over the range pH 3–8.5 from the affinity supports prepared via CDI methods was that immunoadsorbents could be prepared in bulk and stored in neutral buffers containing an anti-microbial agent for more than six months prior to use. Tesser *et al.*^{19,20} have studied the liberation of a variety of ligands from sorbents prepared by means of the CNBr activation procedure and found, for example, that the rate of liberation of the ligand from a cAMP-spacer-agarose matrix (2–5 μ moles cAMP substituted/ml gel) in a 5 mM Tris-HCl–15 mM NaCl, pH 8.0, buffer was *ca.* 6 pmol/ml gel/min. Compared to the data reported in these and other studies^{21,22} on the ligand stability of the N-substituted isourea linkage formed by the reaction between amino groups and CNBr-activated agarose, ligands bound to agarose gels by the urethane linkage formed in the CDI procedure are detached more slowly, *i.e.* they are *ca.* 20 fold more stable at comparable pHs¹⁰. The urethane immobilised ligands

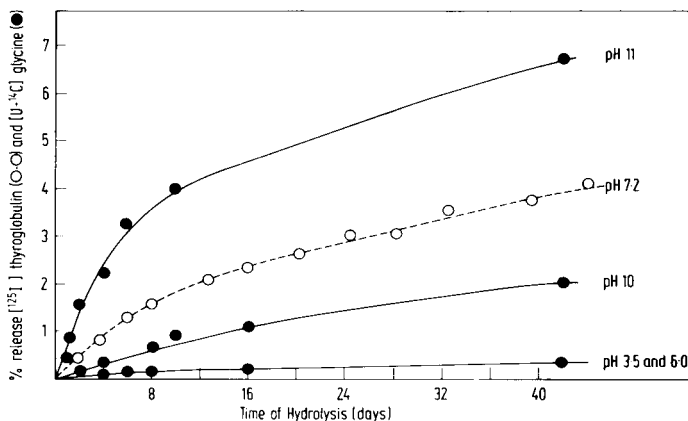


Fig. 1. Comparison of the rates of solvolytic detachment for [U - 14 C]glycine immobilised onto CDI-activated Sepharose CL-6B (*ca.* 100 μ moles active groups/g moist gel) and for human [125 I]thyroglobulin immobilised onto CDI-activated Sepharose CL-6B (*ca.* 300 μ moles active groups/g moist gel) as a function of pH and incubation time at 4 $^{\circ}$ C. The following 100 mM buffer solutions were employed: potassium hydrogen phthalate (pH 3.5); potassium hydrogen phosphate (pH 6.0); Tris HCl (pH 7.2); potassium carbonate (pH 10.0) and disodium hydrogen phosphate (pH 11.0). The residual ligand attached to the matrix at different time intervals was determined for the [U - 14 C]glycine matrix by digestion with 10 M HCl at 60 $^{\circ}$ C and measurement of the cpm of a neutralised 1:10 aliquot and for the human [125 I]thyroglobulin-matrix by direct measurement of the cpm of an aliquot, compensated for the spontaneous loss of 125 I.

TABLE I
COMPARATIVE COUPLING YIELDS FOR ACTIVATED SEPHAROSE CL-6B

<i>Protein</i>	<i>CNBr-activated matrix*</i>	<i>CDI-activated matrix**</i>
Human thyroglobulin	70	75
Human IgG	92	93
Human myeloma IgG	94	83
Rabbit anti-human serum immunoglobulins	—	98
Bovine thyrotrophin	89	67
Ovine thyroid binding proteins***	82	85
Human thyroid binding proteins***	82	80
Human serum proteins	64	40

* Activation level *ca.* 35 μ moles active groups/g moist gel.

** Activation level *ca.* 100 μ moles active groups/g moist gel.

*** A partially purified thyroid membrane glycoprotein fraction which exhibits binding activity for thyroid stimulating autoantibodies.

exhibit stabilities at intermediate pHs similar to ligands coupled to epoxy-activated agarose⁵ and hydrazine-activated polyacrylamide²⁰ gels.

In Tables I and II are shown comparative results for the coupling of human thyroglobulin and several other proteins to the CDI- and the CNBr-activated agarose matrices. These results demonstrate that this group of proteins can be coupled to CDI-activated cross-linked and copolymer polysaccharide gels with coupling yields similar to those found with CNBr-activated polysaccharides. Highly activated agaroses are known to lead to multiple point attachment of protein ligands to the gel support. This can result in impaired biological binding properties of the immobilised protein, attributed to induced conformational changes^{2,3}. However, with the thyroglobulin immunoabsorbent prepared by the CDI approach, no significant loss of binding activity of this antigen for its corresponding antibodies was apparent even with

TABLE II
COMPARATIVE COUPLING YIELDS FOR CDI-ACTIVATED POLYSACCHARIDE GELS

	<i>Sepharose CL-6B*</i>		<i>Ultrogel AcA-44**</i>	
	<i>Coupling yield (°o)***</i>	<i>Concentration of protein on matrix (μmoles/g) §</i>	<i>Coupling yield (°o)***</i>	<i>Concentration of protein on matrix (μmoles/g) §</i>
Human thyroglobulin	62	0.34	41	0.15
Human IgG	92	2.0	62	1.4
Bovine thyrotrophin	80	2.4	69	2.0
Ovine thyroid binding protein	91	3.6	52	2.0

* Activation level *ca.* 100 μ moles active groups/ml gel.

** Activation level *ca.* 60 μ moles active groups/ml gel.

*** Based on percentage of added substance.

§ Expressed as μ moles of coupled proteins per gram of dry polymer.

very highly activated (up to 300 μ moles active sites/ml gel) supports. In fact, when the coupling conditions were varied to favour a small number of binding sites per protein molecules, *e.g.* by using a slightly acidic coupling buffer and a gel with a low degree of activation, the protein ligand still coupled in satisfactory yield but the resultant support was not very effective as an affinity matrix. In this case, the corresponding antibodies bound very tightly to the immobilised thyroglobulin and this necessitated the application of more forcing elution conditions (3.5 *M* KCNS, pH 11.0). This in turn, resulted in deterioration of the affinity support due to enhanced leakage of the ligand as well as denaturation of the immobilised antigen molecules.

In order to study the binding capacity of the human thyroglobulin immunoadsorbent (CDI method), increasing amounts of a human serum from a patient, L1, with thyroid autoimmunity were added to a standard quantity of the immunoadsorbent. Antibody activity in the serum and the eluate was measured by passive haemagglutination using the tanned red cell procedure¹⁷ and by a double antibody capacity binding assay¹⁸. The results, summarised in Fig. 2, show that the maximal capacity of the immunoadsorbent was reached for this serum with a loading of *ca.* 900 μ l serum/ml gel, equivalent to an immunoadsorbent capacity of *ca.* 2.4 mg bound antibody/ml gel. The column binding capacity was similar when an immunoglobulin fraction purified on DEAE-cellulose, was used in place of whole serum.

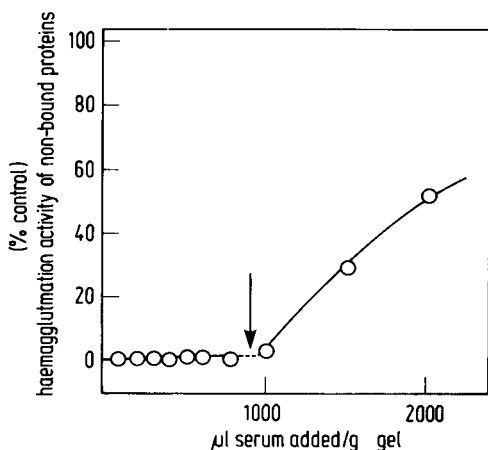


Fig. 2. Capacity of immobilised human thyroglobulin immunoadsorbent (*I*-thyroglobulin-Sephacrose CL-6B) in relationship to amount of serum antithyroglobulin autoantibodies applied. The serum in aliquots of 100 μ l was applied to equilibrated columns containing 2.75 g moist gel cake of the immunoadsorbent. The haemagglutination activity of the non-bound peak is expressed as a percentage of the activity for the control experiment using columns packed with Sephacrose CL-6B alone. The immunoadsorbent was prepared from CDI-activated Sephacrose CL-6B (*ca.* 180 μ moles active groups/g moist gel cake).

Rabbit anti-bovine thyroglobulin antibodies have been purified using conjugated polyaminopolystyrene or *p*-amino benzylcellulose matrices²⁴. More recently, human antithyroglobulin autoantibodies have been fractionated from other serum components using immunoadsorbents prepared from glutaraldehyde insolubilised supports²⁵ and CNBr-activated agarose^{26,27}. In the present study with CDI-activated matrices, it was found that desorption of the bound autologous or heterologous

antibodies from the *h*-thyroglobulin matrix could be achieved under a variety of conditions including 2 *M* sodium iodide and 2–3.5 *M* sodium thiocyanate, but most successfully with 200 *mM* glycine HCl, pH 2.8 (Fig. 3). Elution recovery of the binding activity of the antibodies purified by these affinity chromatographic procedures were evaluated by haemagglutination and double antibody techniques and compared to the binding capacity of the original serum. In several instances, very good recoveries of binding activities for autologous and heterologous antibodies were obtained *e.g.* serum L1 gave an elution recovery of specific autoantibodies greater than 80 %, although generally the recoveries were in the region of 30–50 % for the 200 *mM* glycine HCl (pH 2.8) or 2 *M* NaCNS (pH 9.0), desorption buffers and 10–20 % with 3 *M* NaCNS (pH 10.0) 5 *M* urea or 5 *M* guanidine hydrochloride (pH 3.0) desorption eluents. Similar results have been noted^{26,27} in earlier studies on anti-thyroglobulin antibodies purified by means of CNBr-activated gels.

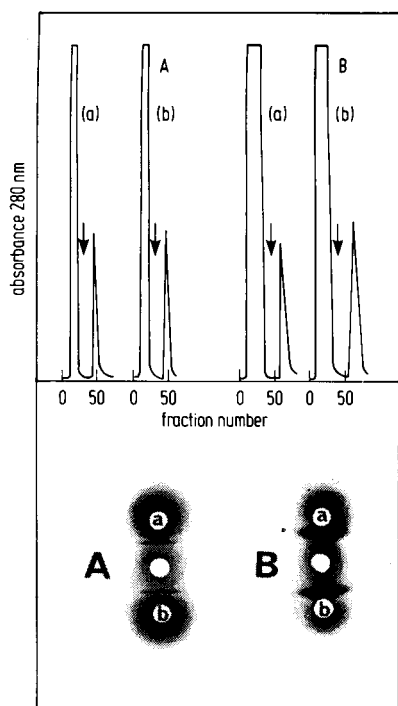


Fig. 3. A, Chromatography of human sera containing antithyroglobulin autoantibodies and B, chromatography of rabbit sera containing heterologous antithyroglobulin antibodies on columns containing a human thyroglobulin–Sepharose CL-6B immunoadsorbent, prepared by the CDI-activation procedure. The equilibration and washing buffer was 150 *mM* NaCl–20 *mM* Tris–HCl (pH 7.2). For the experiments shown in A and B the same columns were used for 10 consecutive affinity separations, runs 1 and 5 are shown in (a) and (b), respectively. Sample loadings: A, 1.5 ml serum; B, 5.0 ml serum. Specific desorption was performed with a 200 *mM* glycine–HCl (pH 2.8) buffer, added at the points indicated. Column size: A, 2.8 ml gel; B, 3.0 ml gel.

A further example of the use of a biospecific adsorbent derived from CDI-activated agaroses is shown in Fig. 4. Using a human IgG–Sepharose CL-6B conjugate, goat and rabbit anti-human IgG antibodies were fractionated from other

serum components using step elution conditions. The antibody capacity of the immunoabsorbent prepared for these experiments was *ca.* 6 mg goat/rabbit anti-human IgG antibodies/ml agarose gel. In Fig. 4A is shown the elution profile for the biospecific separation of goat antihuman IgG antibodies using different NaI concentrations (0.5, 2.0, 3.0 and 4.0 *M*) as the desorption reagent for the specific antibodies. Similar desorption patterns have been noted previously^{28,29} in the affinity chromatographic separation of mixed populations of antibodies with different affinities for a specific ligand.

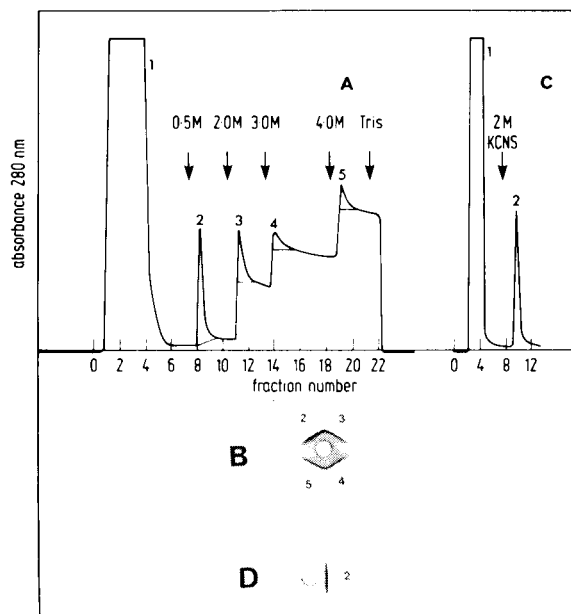


Fig. 4. Biospecific affinity chromatography of goat (A) and rabbit (C) anti-human IgG serum on human IgG-Sepharose CL-6B immunoabsorbents. The human IgG-gel conjugates were prepared from CDI-activated Sepharose CL-6B, 100 μ moles active groups/g moist gel cake. The equilibration and washing buffer was 150 mM NaCl 20 mM Tris-HCl (pH 7.2). For the experiment shown in A goat anti-human IgG serum (20 ml) was applied to the immunoabsorbent column (1.6 g gel, *ca.* 2 μ moles immobilised human IgG/g gel). After washing with 30 ml of buffer, elution of specific antibodies was affected with NaI at various concentrations (arrows). The elution profile is uncorrected for base-line absorbance changes due to the high NaI concentrations. Immunodiffusion patterns of the recovered fractions *versus* human IgG are shown in B. For the experiment shown in C, rabbit anti-human IgG serum (1 ml) was applied to the immunoabsorbent column (2.1 g gel, *ca.* 2 μ moles immobilised human IgG/g gel). After washing with 30 ml buffer, elution of specific antibodies was affected with 2 *M* KCNS (pH 9.5) (arrow). The immunodiffusion of the recovered fraction *versus* human IgG is shown in D.

In conclusion, the above experiments illustrate that the CDI-activation procedure can be used to produce effective immunoabsorbents for the fractionation of antibodies by biospecific affinity chromatography. Under suitable coupling conditions, the amounts of protein ligands which can be immobilised onto CDI-activated polysaccharide supports compare favourably with those obtained via the CNBr method. Under similar coupling conditions the CNBr-activated matrices appear to be more reactive than the corresponding CDI-activated gels. In view of the precise

control over the level of activation which can be achieved with the CDI reagent and the good stability of ligands immobilised onto insoluble gels activated by this method, CDI-activated agaroses provide a useful alternative to existing methods for the preparation of ligand-polysaccharide conjugates. With polysaccharide supports activated by CDI to very high substitution levels a decrease in the swollen bed volume of the ligand-matrix occurs, indicative of progressive cross-linking and a modified pore structure. Under high pH coupling conditions the ligand coverage on the matrix tends to approach limiting values with these highly activated supports, possibly due to steric restrictions. During the present study, immunoabsorbents prepared with polysaccharide gels, previously activated with CDI up to 300 μ moles active groups/ml gel, were found to be suitable in the purification of autologous and heterologous immunoglobulins with specificities directed against human thyroglobulin and human IgG. In studies involving the immobilisation of less robust protein ligands, lower levels of matrix activation may be required^{3,23,30}. In these cases, it should be possible to tailor the level of CDI activation to ensure that optimal binding activity of the ligand is preserved whilst still permitting a mode of interaction between the ligand and the substances under purification such that desorption can be achieved under mild elution conditions.

ACKNOWLEDGEMENT

This investigation was supported in part by a research award made to M.T.W.H. by the Development Finance Corporation of New Zealand.

REFERENCES

- 1 J. Turkova, *Affinity Chromatography*, Elsevier, Amsterdam, Oxford, New York, 1978.
- 2 S. C. March, I. Parikh and P. Cuatrecasas, *Anal. Biochem.*, 60 (1974) 149.
- 3 G. Kümel, H. Daus and H. Mauch, *J. Chromatogr.*, 172 (1979) 221.
- 4 A. H. Nishikawa and P. Bailon, *Anal. Biochem.*, 64 (1975) 268.
- 5 L. Sundberg and J. Porath, *J. Chromatogr.*, 90 (1974) 87.
- 6 T. Lang, C. J. Suckling and H. C. S. Wood, *J. Chem. Soc., Perkin Trans.*, 1 (1977) 2189.
- 7 T. C. J. Gribnau, in R. Epton and E. Horwood (Editors), *Chromatography of Synthetic and Biological Polymers*, Vol. 2, Chemical Society, London, 1978, p. 258-264.
- 8 J. Brandt, L. O. Anderson and J. Porath, *Biochim. Biophys. Acta*, 386 (1975) 196.
- 9 G. S. Bethell, J. S. Ayers, W. S. Hancock and M. T. W. Hearn, *J. Biol. Chem.*, 254 (1979) 1683.
- 10 G. S. Bethell, J. S. Ayers, W. S. Hancock and M. T. W. Hearn, *J. Chromatogr.*, in press.
- 11 M. T. W. Hearn, G. S. Bethell, J. S. Ayers and W. S. Hancock, *J. Chromatogr.*, 185 (1979) 463.
- 12 R. Jost, P. A. Myrin and M. Wilchek, *Biochim. Biophys. Acta*, 362 (1974) 75.
- 13 R. Axen, P. A. Myrin and J. C. Janson, *Biopolymers*, 9 (1970) 401.
- 14 G. Salvatore, M. Salvatore, H. J. Cahnmann and J. Robbins, *J. Biol. Chem.*, 254 (1979) 1683.
- 15 A. J. Paterson and M. T. W. Hearn, *Aust. J. Exp. Biol. Med. Sci.*, 57 (1979) 641.
- 16 M. M. Bradford, *Anal. Biochem.*, 72 (1976) 248.
- 17 A. J. Fulthorpe, I. M. Roitt, D. Doniach and K. G. Couchman, *J. Clin. Pathol.*, 14 (1961) 654.
- 18 A. J. Paterson and M. T. W. Hearn, *Proc. Univ. Otago Med. Sch.*, 56 (1978) 21.
- 19 G. I. Tesser, H. U. Fisch and R. Schwyzler, *FEBS Lett.*, 23 (1972) 56.
- 20 G. I. Tesser, H. U. Fisch and R. Schwyzler, *Helv. Chim. Acta*, 57 (1974) 1718.
- 21 I. Parikh, V. Sica, E. Nola, G. A. Puca and P. Cuatrecasas, *Methods Enzymol.*, 34 (1974) 670.
- 22 M. Wilchek, *FEBS Lett.*, 33 (1973) 70.
- 23 P. Cuatrecasas, *Advan. Enzymol.*, 36 (1972) 29.
- 24 M. Shimazaki, K. Hamba, C. Hiramane, N. Katsu, T. Mori and Y. Keno, *Wakayama Med. Reports*, 11 (1966) 59.

- 25 Y. Takeda, S. Thomas, G. Johnson and J. P. Kriss, *J. Clin. Endocr. Metab.*, 41 (1975) 738.
- 26 M. T. W. Hearn, A. J. Paterson, D. D. Adams, W. S. Hancock, P. K. Cashmore and K. M. Moriarty, *J. Mol. Med.*, 4 (1981) 279.
- 27 C. Davoli, G. B. Salabe and M. Andreoli, *Clin. Exp. Immunol.*, 31 (1978) 218.
- 28 P. Cuatrecasas, *Biochem. Biophys. Res. Commun.*, 35 (1969) 531.
- 29 R. F. Murphy, A. Imam, A. E. Hughes, M. J. McGucken, K. D. Buchanan, J. M. Conlon and D. T. Elmore, *Biochim. Biophys. Acta*, 420 (1976) 87.
- 30 H. Amneus, D. Gabel and V. Kasche, *J. Chromatogr.*, 120 (1976) 391.

CHROM. 14,234

ANALYSIS OF N-ACETYL-N,O,S-PERMETHYLATED PEPTIDES BY COMBINED LIQUID CHROMATOGRAPHY-MASS SPECTROMETRY

T. J. YU, H. SCHWARTZ, R. W. GIESE, B. L. KARGER and P. VOUIROS*

Institute of Chemical Analysis and Department of Chemistry, Northeastern University, Boston, MA (U.S.A.)

SUMMARY

Initial results are presented on the liquid chromatography-mass spectrometry (LC-MS) of N-acetyl-N,O,S-permethyated oligopeptides using a moving belt interface for the sequence analysis of the peptides. Using a quadrupole MS, it has been found that isobutane chemical ionization provides good intensity $[M + 1]^+$ ions, as well as well-defined N- and C-terminal fragment ions. It is shown that C-methylated peptides can be separated by LC and identified by MS. Examples are given on the LC-MS of N-acetyl-permethyated Leu-enkephalin as well as a mixture of derivatized peptides. In all cases sequence information is available by the LC-MS approach. Finally, initial and promising attempts at predicting chromatographic retention in a linear gradient condition in reversed-phase LC for the derivatized peptides are presented. These results establish that sequence analysis of permethylated peptides by LC-MS can be achieved.

INTRODUCTION

High-performance liquid chromatography (HPLC) using ultraviolet (UV) and fluorescence detection has emerged as a significant method for the separation of peptides¹⁻³ and more recently proteins⁴. The value of a powerful separation method is readily recognized considering the fact that there are 20 common amino acids which can yield 20ⁿ possible *n*-amino acid peptides, *e.g.*, 400 for dipeptides, 8000 for tripeptides and 160,000 for tetrapeptides. Along with separation, the problem of identification of individual peptides can also be very great.

Since the early days of paper chromatography⁵, attempts have been made to identify individual peptides from retention behavior. In this case, a Martin-type group additivity approach is tested, in which individual amino acids contribute a specific portion of the total-free-energy change in the distribution process. For example, the amino acid group contributions have been related to Rekker hydrophobic fragment constants in reversed-phase liquid chromatography (RPLC)⁶. In addition, empirically determined structural increments of retention have been used to obtain a rough estimate of total peptide retention in RPLC⁷. As these approaches are only approximations, the accurate identification of peptides based on retention often is not possible without some extra chromatographic information. Thus, there is need

for a more definitive structural identification of the species eluting from an HPLC column.

One approach is to collect individual peptide bands and to perform standard Edman degradation procedures⁸. This method works well in many cases, is conventionally employed and can indeed lead to low picomolar sequencing possibilities of intact oligopeptides⁹. Nevertheless, the procedure is relatively slow, cannot be used for peptides whose N-terminal sides do not contain a free amino group (*e.g.*, pyroglutamate) and has difficulty with uncommon amino acids. Thus, other approaches are necessary to complement the Edman procedure.

The value of mass spectrometry (MS) for elucidating the amino acid sequence of oligopeptides-proteins is now widely recognized¹⁰⁻¹². MS can provide valuable information on amino acid sequences from both the N- and C-terminals in one run, is relatively rapid, can handle unusual amino acids and end groups and is potentially highly sensitive. Because of the very large number of peptide possibilities, a desirable feature of MS analysis, in order to provide readily interpretable spectra, is the cleavage of the peptide at the amide bonds with little or no rearrangement. This has generally meant the need to employ derivatives for fragmentation purposes which at the same time enhance the volatility of the peptide. Generally, two types of MS analysis of peptides have commonly been employed: gas chromatography (GC)-MS and the direct insertion probe.

Analysis by GC-MS requires the formation of volatile derivatives of which the O-trimethylsilyl-polyamino alcohols, formed via a multi-step procedure, have proved to be the most developed for peptide sequencing thus far¹³. This approach has recently been combined with DNA sequencing procedures for the rapid sequencing of very-long-chain proteins¹⁴. Nevertheless, besides the complex and time consuming chemistry, a limitation of the GC-MS approach for oligopeptide sequencing is imposed by the low volatility of longer peptides. In general, the GC-MS analysis of peptides using O-trimethylsilyl ethers of polyamino alcohols is limited to chains containing not more than five or at best perhaps six amino acid residues¹⁵. It may also be noted that N-acetyl peptide esters generally work best for dipeptides in GC-MS¹⁶.

For peptide analysis using the direct insertion probe, the most commonly employed procedure involves the formation of N-acetylated-N,O,S-permethylated derivatives. Following the pioneering work of Das *et al.*¹⁷, the permethylation procedure, as modified by Morris¹⁸ and Leclercq and Desiderio¹⁹, involves N-acetylation and is followed by N,O,S-permethylation with methyl sulfinyl carbanion and methyl iodide. It has been reported that N,O,S-permethylation and sample introduction into the MS via the direct insertion probe can be satisfactory for the sequencing of peptides containing as many as fifteen amino acid residues using conventional ionization techniques [*i.e.*, electron impact (EI) or chemical ionization (CI)]²⁰. However, unlike GC-MS, analysis via the direct insertion probe is basically an off-line approach. While simple mixtures (two to five components) can be analyzed by fractional volatilization²¹, complex mixtures from peptide-protein hydrolysates could become a rather involved procedure. It is interesting to note in passing that the N-trifluoroacetyl-N,O,S-permethylated peptide derivative has also been employed in GC-MS for sequence determinations²².

Even though the most informative mass spectra of oligopeptides are obtained by formation of polyaminoalcohols or permethylated derivatives, as indicated above,

analysis of hydrolysates by GC-MS is limited to peptide mixtures containing relatively small peptides of, at the most, four to six amino acid residues. This limitation makes it more difficult to recognize overlapping sequences of peptides and ambiguities are likely. Since sample volatility is not an issue in HPLC, this procedure can, in principle, handle larger peptides than GC. Therefore, we sought to determine the applicability of combined HPLC-MS to peptide analysis. To this date, the technique of combined HPLC-MS for the analysis of peptide mixtures has been successfully utilized only in preliminary studies using N-acetyl peptide methyl ester derivatives²³. However, these derivatives are relatively non-volatile and their mass spectra not fully characterized, especially for peptides containing four or more amino acid residues. In order to ensure compatibility with MS, it was important to consider derivatives which could yield structurally informative mass spectra. In view of the analogy between the moving belt interface and the direct insertion probe as far as sample introduction is concerned, we decided to examine the utility of the permethylated derivatives for this purpose. The results of our preliminary studies towards meeting this goal are described in this manuscript.

EXPERIMENTAL

Materials

The peptides were purchased from Sigma (St. Louis, MO, U.S.A.) and Vega Biochemicals (Tucson, AZ, U.S.A.) and were used as received. The purities of these peptides were tested by HPLC when this seemed necessary. Pure peptides were collected by preparative HPLC where appropriate. Methyl sulfoxide (Mallinckrodt, St. Louis, MO, U.S.A.) and methyl iodide (Aldrich, Milwaukee, WI, U.S.A.) were freshly distilled before use. The sodium hydride was a 50% dispersion in oil and was obtained from J. T. Baker (Phillipsburg, NJ, U.S.A.). Other reagent grade chemicals and HPLC grade or spectrograde solvents were purchased commercially and were not purified further.

Acetylation and permethylation

The acetylation and permethylation procedures described by Leclercq and Desiderio¹⁹ were employed. Peptides containing arginine were treated with hydrazine to convert arginine to ornithine before acetylation, as described by Thomas *et al.*²⁴. The samples were refrigerated when not in use.

Mass spectrometry

Both CI and EI mass spectra were recorded on a Model 4000 quadrupole mass spectrometer (Finnigan, Palo Alto, CA, U.S.A.) with a Finnigan LC-MS interface and Incos data system. Approximately 100 ng of material dissolved in acetonitrile were used for each mass spectrum run. The conditions were set as follows: electron multiplier voltage, -1670 V; electron energy, 70 eV; ionizer temperature, 270°C; manifold temperature, 110°C; vaporizer temperature, 230°C; and ionizer pressure, 0.05 Torr for isobutane, 0.11 Torr for ammonia, 0.12 Torr for methane.

High-performance liquid chromatography

Two HPLC instruments were used: a Model 6000A pump (Waters Assoc.,

Milford, MA, U.S.A.) with a Model 770 variable-wavelength UV detector (Schoeffel, Westwood, NJ, U.S.A.) and an HP 3385A automation system (Hewlett-Packard, Avondale, PA, U.S.A.); and a Model 5000 high-performance liquid chromatograph (Varian, Walnut Creek, CA, U.S.A.) with a Varian UV-50 variable-wavelength detector. Detection was performed by UV absorption at 214 nm. A Supelcosil LC-8 column was used 150×4.6 mm I.D.) (Supelco, State College, PA, U.S.A.). Samples were introduced by using a microsyringe through a Model AH60 sample injector valve (Valco, Houston, TX, U.S.A.) actuated by air.

A standard linear gradient from 5 to 70 % acetonitrile in water in 20 min with a flow-rate of 1 ml/min was employed. These conditions were used to obtain the preliminary retention data for assessment of retention prediction of the permethylated peptides. Generally, the amount of sample injected was about 1 μ g in 5 μ l acetonitrile.

High-performance liquid chromatography-mass spectrometry

The HPLC-MS system consisted of a Varian 5000 high-performance liquid chromatograph and a Finnigan 4000 mass spectrometer equipped with a Finnigan LC-MS moving-belt interface. In order to accomodate reversed-phase eluents, the interface was modified according to the suggestions of Smith and Johnson²⁵. As shown in Fig. 1, a stream of hot nitrogen gas was passed through the HPLC effluent to create an aerosol spray for deposition of the effluent onto the belt. In addition, a block heater was placed under the belt just beneath the point of sample deposition to facilitate further the rate of solvent evaporation. The nitrogen gas heater was set from 140–170 °C and the block heater was maintained around 80 °C. The combination of heated nitrogen gas and the block heater allowed operation of the HPLC-MS interface at flow-rates as high as 0.5 ml/min for *ca.* 30 % acetonitrile in water. The conditions for CI mass spectra were the same as described above. A home-made 5- μ m octyl-silica bonded-phase column (150×2.8 mm I.D.) was used. The linear gradient system was the same as mentioned above with a flow-rate of 0.5 ml/min.

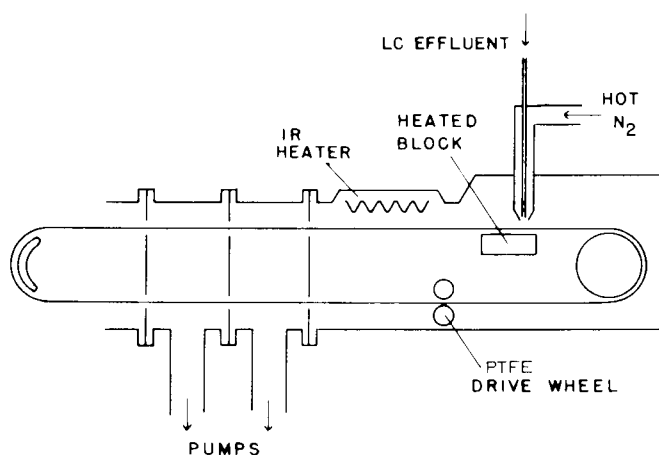


Fig. 1. Diagram of modification of moving belt interface to operate with aqueous-organic mobile phases. See text for description.

RESULTS AND DISCUSSION

Our investigation of the utility of N,O,S-permethylated derivatives of peptides for amino acid sequencing by HPLC-MS involved the following considerations: off-line evaluation of the mass spectral (EI and CI) properties of permethylated oligopeptides using the moving belt as the mode of sample introduction; and, examination of peptides and peptide mixtures by HPLC and on-line HPLC-MS.

Mass spectrometry

This portion of the work was necessary to establish the optimum conditions of our system, and in particular the moving belt interface (*e.g.*, interface vacuum and temperature for solvent removal, flash vaporizer temperature, etc.), for effective sample transfer and introduction into the mass spectrometer. Moreover, it was necessary to assess the relative merits of EI- and CI-MS for the sequencing of permethylated peptides in our specific system. This was particularly important because of the relative paucity of published spectral data in this area and previous observations to the effect that the overall signal-to-noise ratio was improved when the Finnigan 4000 HPLC-MS system was operated in the CI mode²⁶.

For this purpose, pure samples of permethylated peptides were dissolved in acetonitrile and aliquots containing *ca.* 100 ng of the solute were dripped onto the moving belt for transfer into the ion source. Typical mass spectra obtained are shown in Fig. 2a and b which compares the CI-isobutane spectrum and the EI spectrum of the permethylated derivative of the tripeptide Gly-Phe-Ala. Fig. 3 summarizes the observed fragmentation pattern under CI conditions and the "ideal" fragmentation expected from simple cleavages of the peptide bond under EI ionization conditions. Under CI conditions, two types of protonated ions are observed: the typical protonated molecular ion $[M + H]^+$ and the C-terminal ammonium ion [C-terminal fragment + 2H]⁺.

It is apparent that the CI-isobutane spectrum (Fig. 2a) gives a well-defined "molecular-ion" peak, characterized by the ion peaks at m/z 392, $[M + 1]^+$ and m/z 432, $[M + 41]^+$. "Molecular-ion" peaks, $[M + 41]^+$ and occasionally $[M + 57]^+$, are the adduct ions formed by combination of a solute molecule and the fragment ions of $C_3H_5^+$ and $C_4H_9^+$ of isobutane, respectively. In addition, sequence determining ions associated with both the N- (m/z 114, 247, 275, 332 and 360) and the C-terminals (m/z 118, 279 and 350) are for the most part easily discernible. These features should permit identification of the structure of the peptide. On the other hand, the EI mass spectrum of this peptide (Fig. 2b) yields a barely visible molecular-ion peak (m/z 391) and, aside from the C-terminal ion at m/z 116, it is dominated by N-terminal ions (m/z 86, 114, 247, 275, 332 and 360).

A second example of the advantages offered by CI-MS is given in Fig. 4, which shows the CI-isobutane mass spectrum of the permethylated derivative of the tetrapeptide Val-Ala-Ala-Phe. Sequence determining ions from both the N- and the C-terminals are again noted and, moreover, the molecular weight of the peptide is readily defined by the peaks at m/z 519, $[M + 1]^+$; m/z 559, $[M + 41]^+$; and m/z 575, $[M + 57]^+$. The peaks at m/z 86 and 134 are probably due to the formation of protonated imine ions of valine $[CH_3-\overset{+}{N}H=CH-CH(CH_3)_2]$ and phenyl alanine $[CH_3-\overset{+}{N}H=CH-CH_2-C_6H_5]$, respectively.

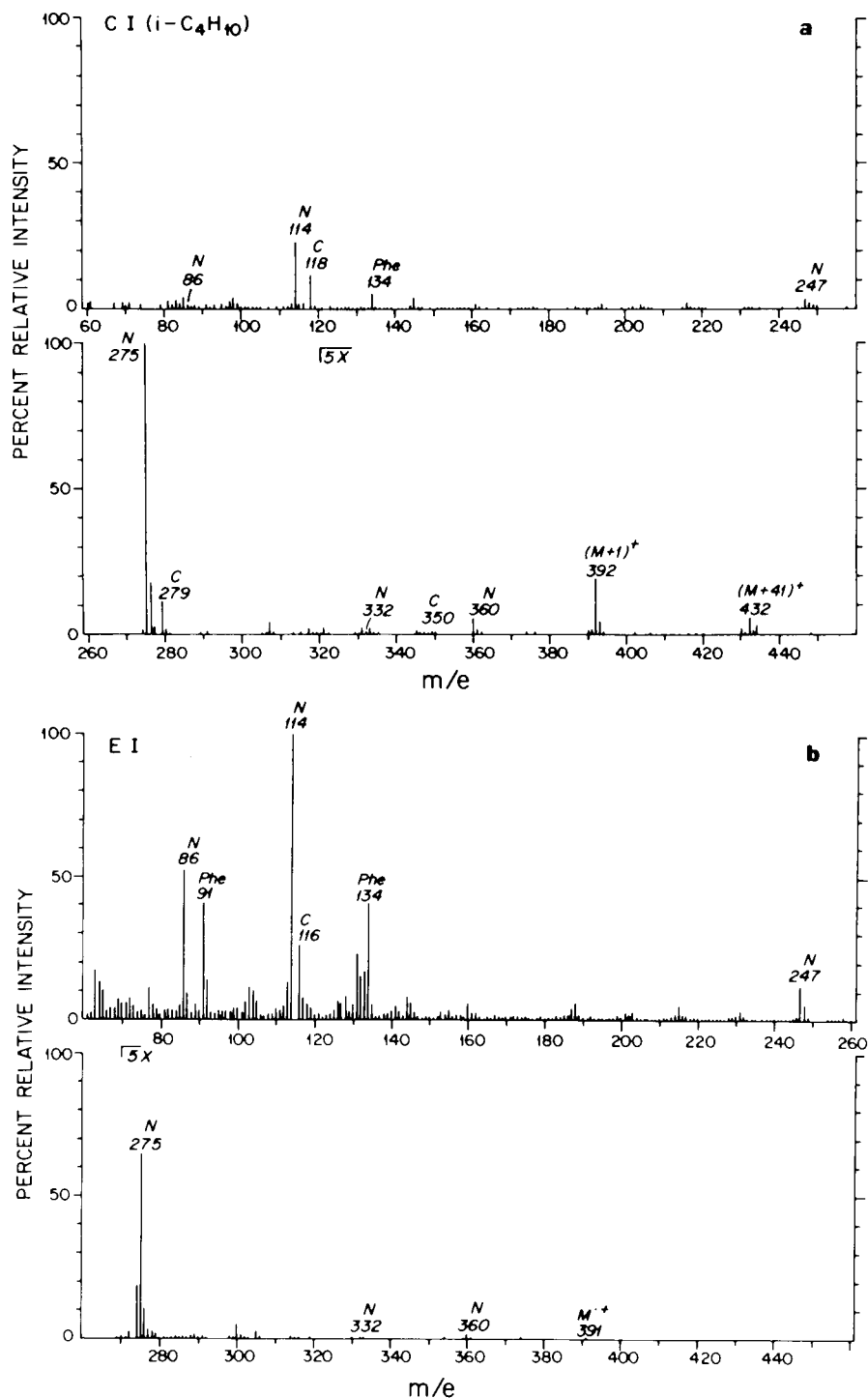


Fig. 2. a. Isobutane CI mass spectrum of Ac-Me-Gly-Me-Phe-Me-Ala-OMe. b. EI mass spectrum of Ac-Me-Gly-Me-Phe-Me-Ala-OMe. Ac = Acetyl; Me = methyl.

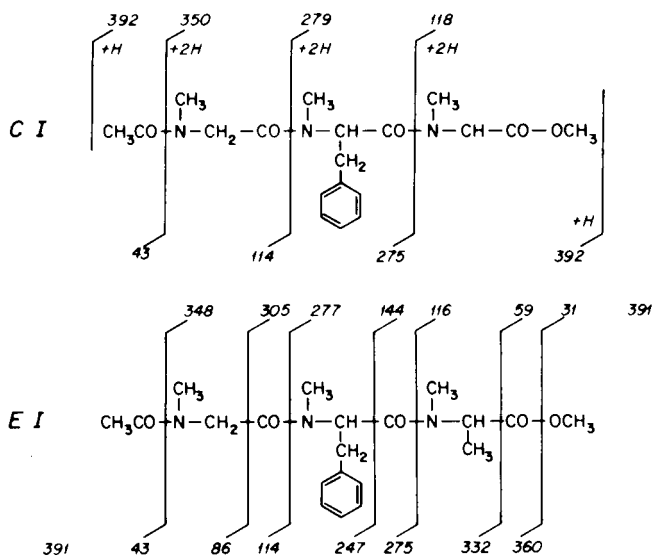


Fig. 3. Structure and fragmentation pattern of Ac-Me·Gly-Me·Phe-Me·Ala-OMe.

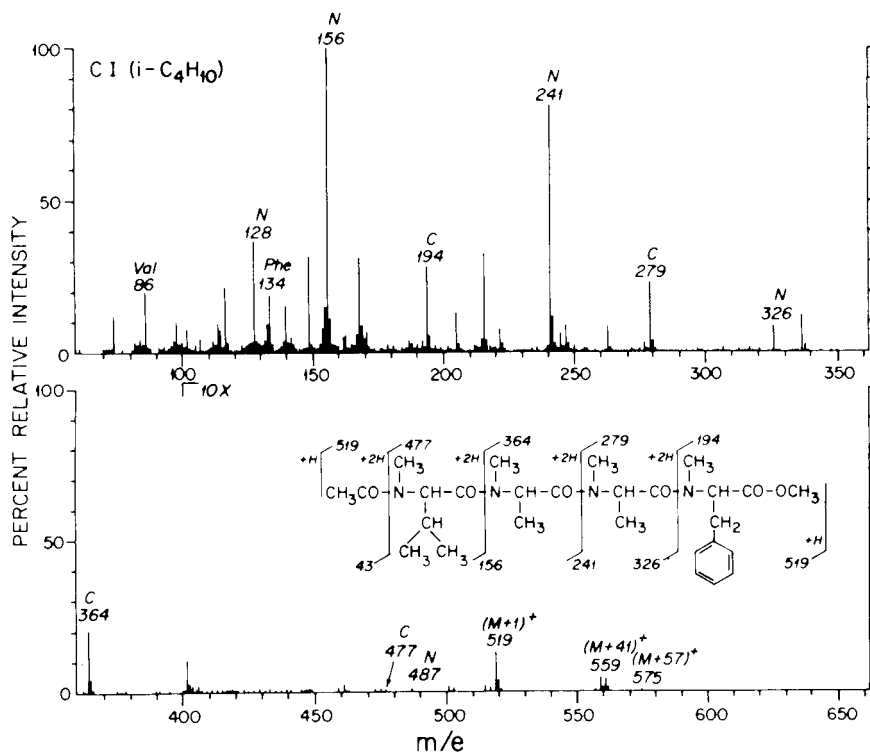


Fig. 4. Isobutane CI mass spectrum and fragmentation pattern of Ac-Me·Val-Me·Ala-Me·Ala-Me·Phe-OMe.

In general, we found that with our system the CI mass spectra of N-acetyl-N,O,S-permethylated peptides were more useful than the corresponding EI spectra. This is in agreement with the conclusions reached by Mudgett *et al.*²⁷ in their comparative study of the EI and CI spectra of a series of permethylated peptides. In our particular case, the advantages of CI over EI are realized not only in terms of the occurrence of both N- and C-terminal ions, but also because of the lower overall ion background level contributed by the polyimide belt under CI conditions. This increased signal-to-noise ratio permits a better definition of the "molecular-ion" peaks under CI rather than under EI conditions and, consequently, provides for more definitive structural identification of the peptides. It should be further noted that the CI-ammonia mass spectra of permethylated peptides were generally similar to those obtained with isobutane reagent gas. On the other hand, in agreement with the results of Mudgett *et al.*²⁷, use of methane instead of isobutane as the CI reagent gas resulted

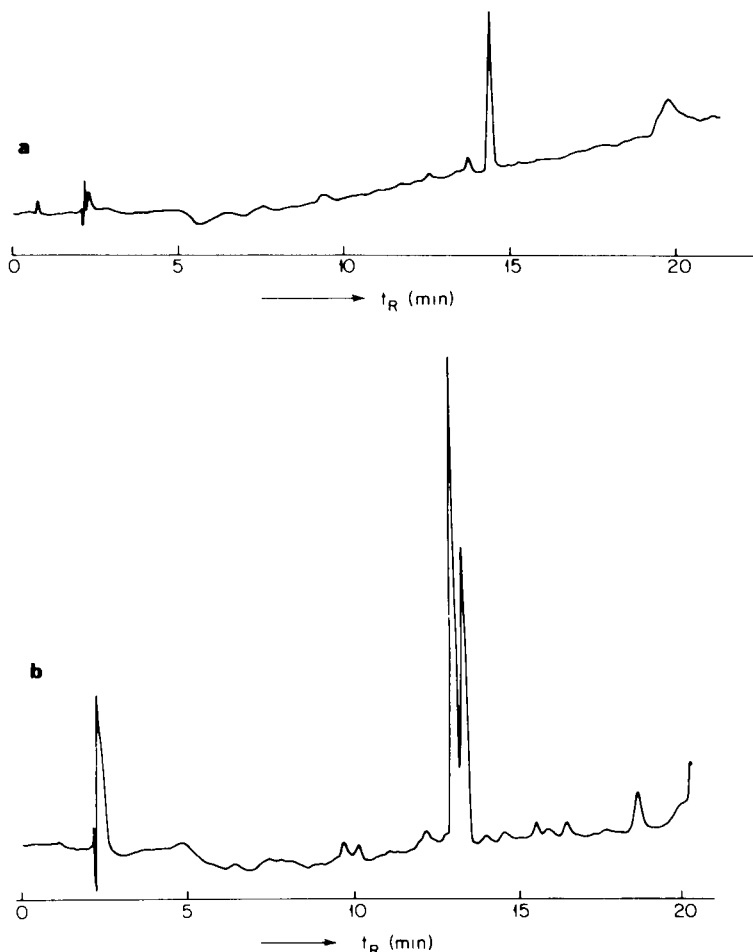


Fig. 5. a, HPLC chromatogram of Ac-Me·Phe-Pro-OMe. b, HPLC chromatogram of Ac-Me·Ala-Me·Val-OMe and the corresponding derivative C-methylated on the α -carbon of Val. Solvent A: water; solvent B: acetonitrile; gradient: from 5 to 70% acetonitrile in 20 min; flow-rate: 1 ml/min.

in spectra containing weaker molecular-ion peaks and relatively lower ion-peak intensities at the high mass region of the spectra.

High-performance liquid chromatography and high-performance liquid chromatography-mass spectrometry

The HPLC analyses of two N-acetyl-permethylated peptides, Phe-Pro and Ala-Val, are shown in Fig. 5 in order to illustrate the type of chromatograms observed. The gradient conditions and approximate sample sizes have been given in the Experimental section. In the case of Phe-Pro, a single chromatographic peak is observed, and the N- and C-terminal fragment ions as well as the protonated molecular-ion peak are readily recognized in the CI mass spectrum.

Of significance is the occurrence of a doublet in the chromatogram of the N-acetyl-permethylated derivative of Ala-Val (Fig. 5b). The mass spectra from the two peaks are shown in Fig. 6a and b. The CI spectrum from the first peak shown in Fig. 6a is easily identified as the expected permethylated derivative of the dipeptide. The CI spectrum from the second peak of this doublet is shown in Fig. 6b. The significant ion at 287, 14 mass units above the $[M + 1]^+$ ion of 273, strongly suggests an additional methyl group added to the molecule. The significant ions at 160 and 255 point to the methyl group being added to the α -carbon of valine. The chromatographic peak is thus identified as the C-methylated-N-acetyl-N,O,S-permethyl-Ala-Val, and its structure is shown in the figure. The major ions such as m/z at 146, 273 and 313 arise from the normal permethylated derivative which overlaps into the second peak and is in much higher quantity (see Fig. 5b).

C-Methylation is a well-known artifact in permethylation of peptides and has been studied specifically with peptides containing a glycine residue²⁸. It is significant that gradient elution HPLC can separate the C-methylated analogues from the principal chromatographic peaks of interest, namely those of the N-acetyl-N,O,S-permethylated derivatives. The exact identity of the C-methylated analogues, including the position(s) of C-methylation, can readily be identified from the mass spectra during HPLC-MS. The incidence of C-methylation and a discussion of the reaction conditions required to suppress the extent of its occurrence will be covered in more detail in a later paper²⁹.

It was noted in the Introduction that the ultimate advantage of HPLC-MS over GC-MS will be realized by its ability to handle longer chain peptides of low volatility which are difficult or impossible to analyze by GC-MS. Fig. 7a shows an HPLC chromatogram of the N-acetyl-permethylated leucine-enkephalin derivative. The small second peak in this chromatogram arises from C-methylation. This peptide contains five amino acid residues, *i.e.*, Tyr-Gly-Gly-Phe-Leu. In the analysis by GC-MS to form an O-trimethylsilyl-polyamino alcohol, the GC retention index, as calculated from retention index increments³⁰, is 3970. This value is at the upper retention range where elution through the GC is relatively difficult. As shown in Fig. 7b, a total ion chromatogram was readily obtained in which two distinct peaks are observed, indicative of reasonable band broadening characteristics in this region of the gradient (*ca.* 70%, acetonitrile). (Studies of band broadening with this LC-MS interface are in progress.) The corresponding mass spectrum of the derivatized peptide is shown in Fig. 7c with a $[M + 1]^+$ ion at 696. It is interesting to note that MS was originally used to aid in the identification of this peptide in brain samples³¹.

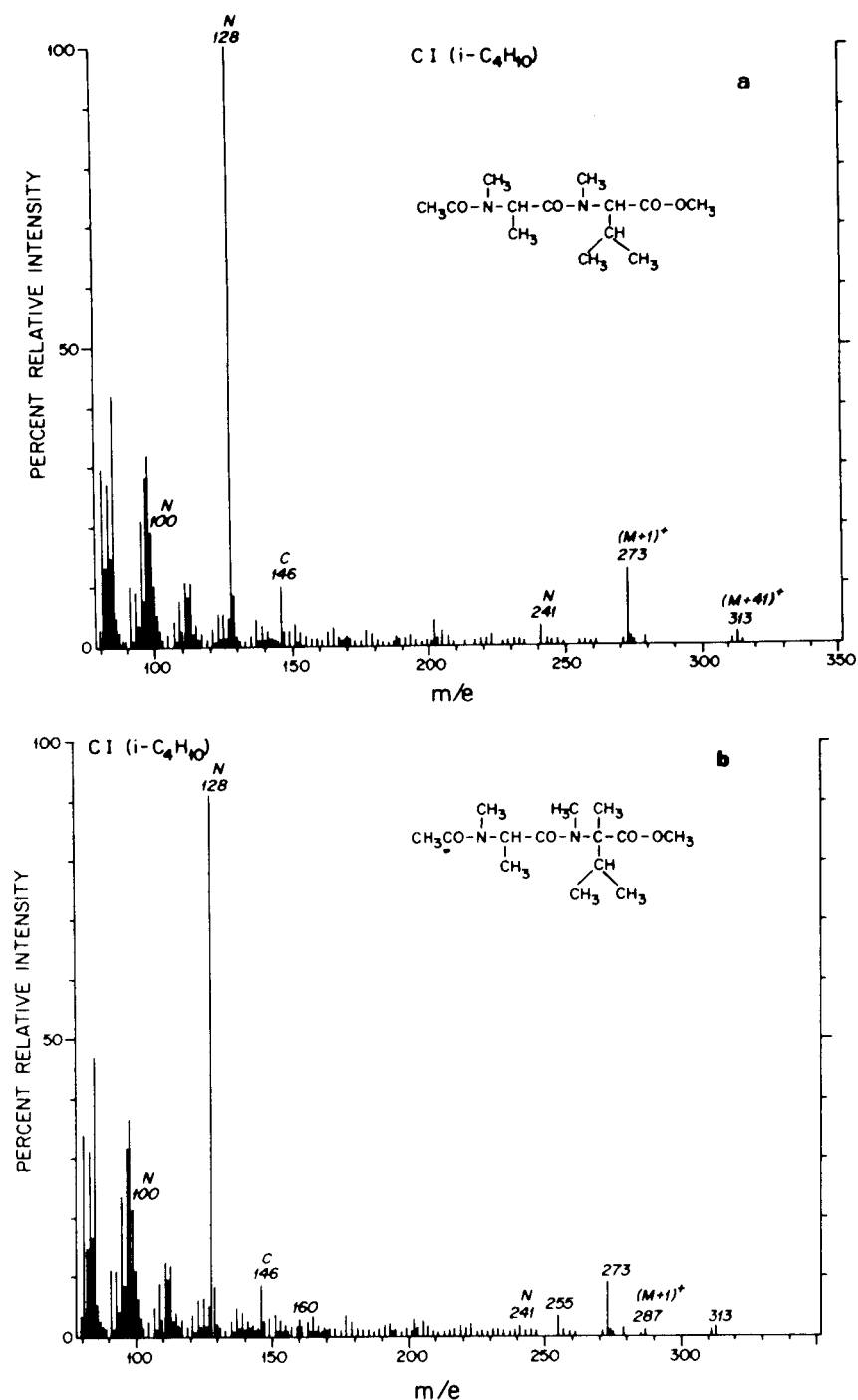


Fig. 6. a, Isobutane CI mass spectrum of the first peak of the Ala-Val chromatogram in Fig. 5b. The spectrum is readily interpreted as the expected permethylated derivative. b, Isobutane CI mass spectrum of the second peak of the Ala-Val chromatogram in Fig. 5b. The spectrum corresponds to the C-methylated derivative shown in the figure.

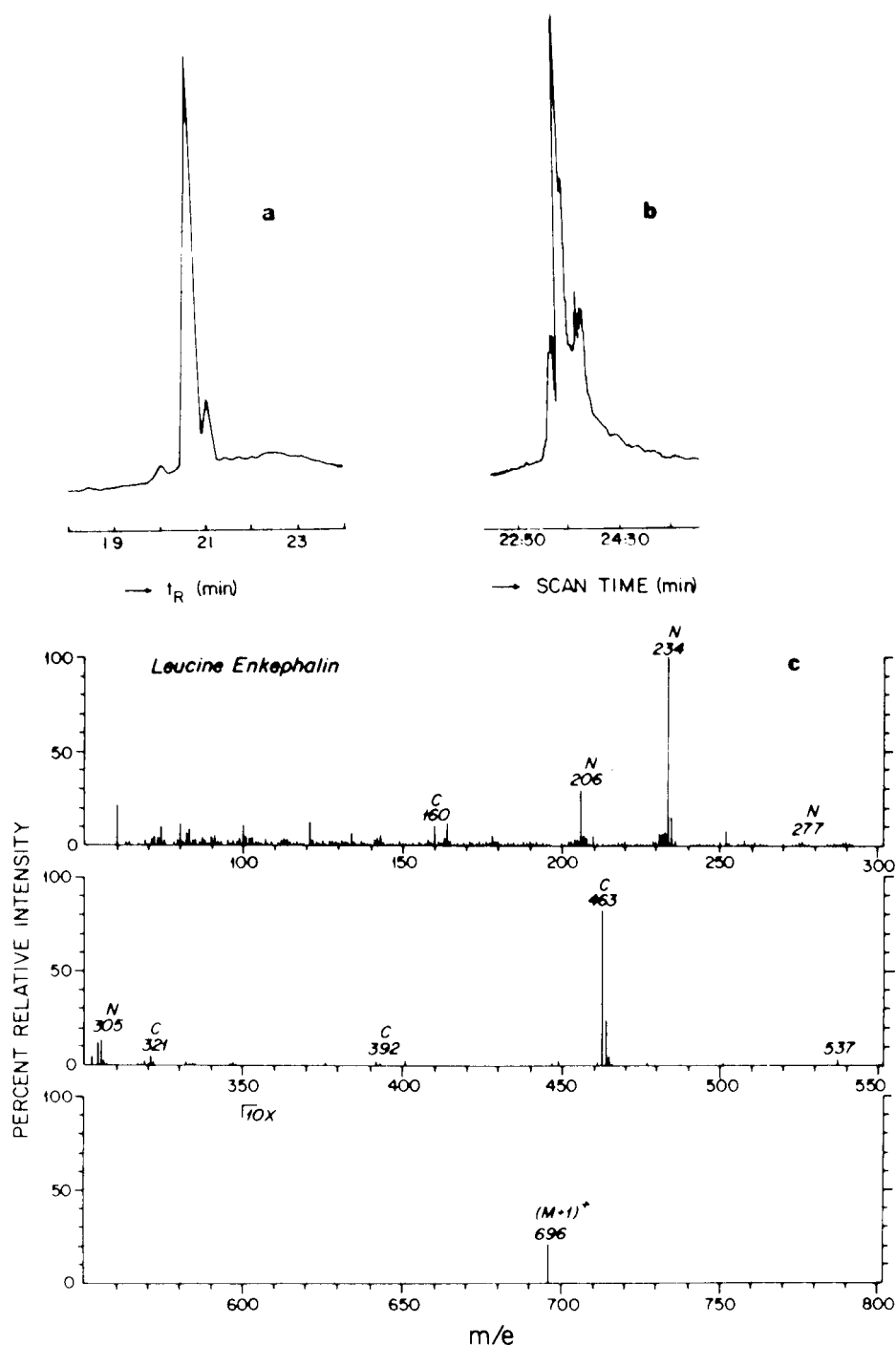


Fig. 7. a. HPLC chromatogram of N-acetyl-permethylated leucine-enkephalin. Gradient elution conditions given in the text. The second peak is a C-methylated derivative of the peptide. b. Total-ion chromatogram of N-acetyl-permethylated leucine-enkephalin obtained from moving belt system. c. Isobutane CI mass spectrum of N-acetyl-permethylated leucine-enkephalin obtained from the LC/MS system.

To assess whether or not HPLC–MS of permethylated peptides would be applicable to the analysis of peptide hydrolysates, we examined the HPLC–MS characteristics of a mixture of eight N-acetyl-permethylated peptides: tetra-Ala, Ala-Val, Gly-Phe-Ala, Phe-Pro, Trp-Gly, Gly-Phe-Phe, Leu-Phe and Val-Tyr-Val. The HPLC chromatogram of the mixture, using a UV detector, is shown in Fig. 8. The corresponding total ion chromatogram recorded during HPLC–MS and using the same HPLC conditions is shown in Fig. 9i. These chromatograms were obtained by injecting a mixture containing 5–10 nmol of each component into the HPLC. Mass chromatograms, utilizing the protonated molecular ions of the peptides are shown in Fig. 9a–h. All the peptides in the mixture could be further identified from their complete mass spectra. It can be seen that, as noted above, C-Methylation products are noticeable in Fig. 8 as well as in Fig. 9.

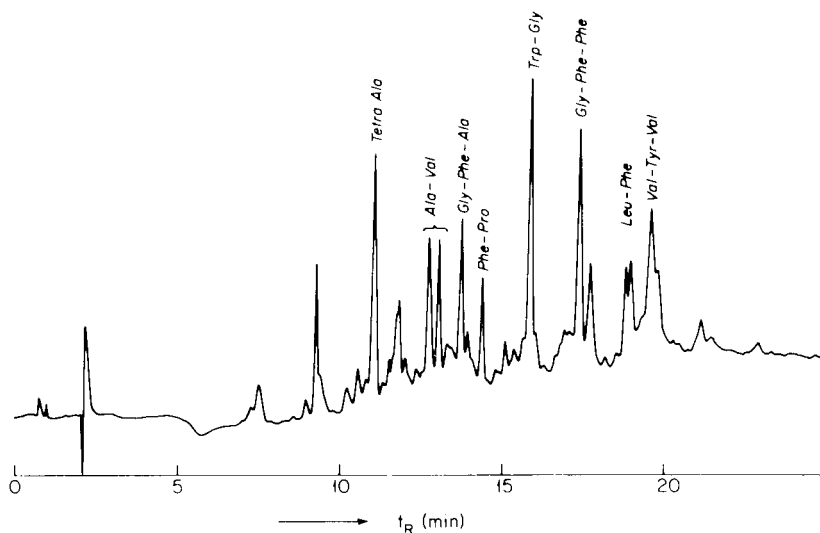


Fig. 8. HPLC separation of a mixture of eight N-acetyl N,O,5-permethylated peptides as indicated on the chromatogram. Gradient elution conditions given in the text.

It is apparent from the results of this preliminary study (Figs. 8 and 9) that detection of permethylated oligopeptides by HPLC–MS is greatly facilitated via the use of mass chromatograms or, if one is looking for a specific peptide(s), by selective ion monitoring. Obviously, this would be impractical when dealing with an unknown mixture. To overcome such difficulties in GC–MS, retention indices are calculated based on the summation of retention increments of individual amino acids³⁰. This greatly aids in the mass spectral search for specific peptides and in the cross-checking of peptides identified by MS. A retention increment scale for LC of the permethylated peptides is in principle possible. Using linear solvent strength (LSS) gradient conditions, it can be shown that the apparent solute capacity factor of the gradient, k'_{app} , is roughly proportional to $\log k'_0$ where k'_0 is the capacity factor of the solute under the starting mobile phase conditions³². Since the latter is a free energy term, it is possible to apply a Martin-type relationship to k'_{app} under LSS conditions.

As in the case of Nau and Biemann in GC³⁰ and Meek in LC⁷, our preliminary

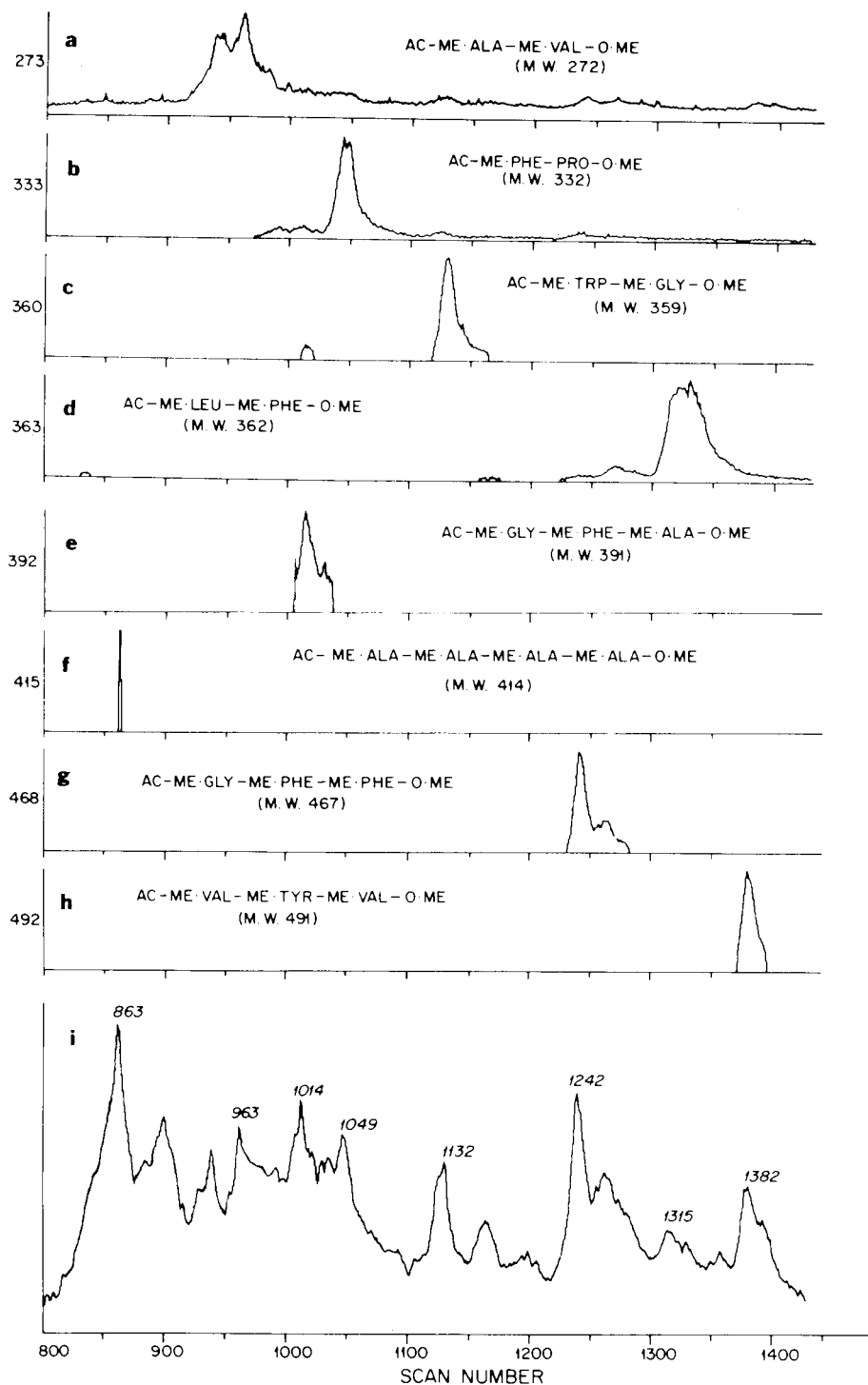


Fig. 9. a-h, Single ion monitoring $[M + 1]^+$ of the eight permethylated peptides eluting from the HPLC column (see Fig. 8). i, Total ion chromatogram of the coupled LC-MS analysis of the eight permethylated peptides. Sample size: *ca.* 5 nmol per peptide. AC = Acetyl; ME = methyl; M.W. = molecular weight.

approach has been to determine individual amino acid increments. We have obtained k'_{app} values by summing these increments for a specific peptide along with an end group contribution for the N-acetyl and $-OCH_3$ groups. Using a series of poly-alanines from $(Ala)_2$ to $(Ala)_5$ we have estimated the Ala contribution as 0.54 ± 0.12 and the end group contribution as 2.60 ± 0.50 . Other amino acid contributions have generally been calculated from dipeptides containing Ala, except where other homopeptides were available. We have examined predicted k'_{app} values vs. experimentally determined k'_{app} values for 40 di-, tri- and tetrapeptides, and some representative results are shown in Table I.

TABLE I

RETENTION PREDICTION OF PERMETHYLATED PEPTIDES USING A LINEAR SOLVENT STRENGTH GRADIENT

<i>Permethyated peptide</i>	k'_{app} , <i>exp.</i>	k'_{app} , <i>calc.</i>
Gly-Ser-Ala	3.72	3.61
Leu-Gly-Gly	5.05	4.99
Gly-Ala-Phe	6.47	6.40
Phe-Pro	6.82	6.98
Ser-Leu	6.99	6.60
Trp-Gly	7.79	7.61
Val-Ala-Ala-Phe	8.64	9.21
Leu-Phe	9.72	9.39
Val-Tyr-Val	10.22	9.71
Trp-Phe	10.48	10.65
Phe-Phe-Phe	11.13	13.52

In general, we find that k'_{app} calculated agrees with k'_{app} measured within 5–8%. This good agreement for a limited sample of peptides means that this approach is quite promising. Undoubtedly, the removal of a high degree of polarity in the peptide molecule upon derivatization aids in the additivity of the increments. We should also note that in a few cases, the difference in k'_{app} calculated vs. k'_{app} experimental can be as high as *ca.* 20%, as illustrated by Phe-Phe-Phe in Table I. This result may mean that steric correctional factors may at times be necessary to account for adjacent amino acids. Work is continuing to measure k'_{app} values for a wide variety of derivatized peptides in order to permit improved amino acid increment retention values for predictive purposes.

CONCLUSIONS

The data presented here demonstrate the feasibility of conducting on-line HPLC-MS of peptide mixtures using N-acetyl-permethyated derivatives. It is apparent that the moving belt interface can be used for the introduction of permethyated derivatives of peptides into the MS, in a manner analogous to the direct insertion probe. As a consequence, MS analysis of relatively long chain oligopeptides should in principle be possible. The combined use of MS data and chromatographic retention using HPLC-MS may thus augment the current state-of-the-art in the field of peptide

sequencing. Studies to optimize many of the parameters discussed in this paper *e.g.*, reaction conditions, chromatographic conditions, etc.) are currently in progress. In addition to these factors, our studies also include a consideration of other types of chemical derivatives and different interfacial designs, such as the direct liquid interface.

ACKNOWLEDGEMENTS

The authors wish to acknowledge NIH under grant numbers GM22787 (P.V.) and GM15847 (B.L.K.) for support of this work. Contribution number 101 from the Institute of Chemical Analysis.

REFERENCES

- 1 I. Molnár and Cs. Horváth, *J. Chromatogr.*, 142 (1977) 623.
- 2 J. E. Rivier, *J. Liquid Chromatogr.*, 1 (1978) 343.
- 3 W. S. Hancock, C. A. Bishop, R. L. Prestidge, D. R. K. Harding and M. T. W. Hearn, *Science*, 200 (1978) 1168.
- 4 F. E. Regnier and K. M. Gooding, *Anal. Biochem.*, 103 (1980) 1.
- 5 C. A. Knight, *J. Biol. Chem.*, 190 (1951) 753.
- 6 M. T. W. Hearn and B. Grego, *J. Chromatogr.*, 203 (1981) 349.
- 7 J. L. Meek, *Proc. Nat. Acad. Sci. U.S.*, 77 (1980) 1632.
- 8 P. Edman and G. Begg, *Eur. J. Biochem.*, 1 (1967) 80.
- 9 M. W. Hunkapiller and L. E. Hood, *Science*, 207 (1980) 523.
- 10 K. Biemann, *Pure Applied Chem.*, 50 (1978) 149.
- 11 P. J. Arpino and F. W. McLafferty, in F. C. Nachod, J. J. Zuckerman and E. W. Randall (Editors), *Determination of Organic Structures by Physical Methods*, Vol. 6, Academic Press, New York, 1976.
- 12 H. R. Morris, *Nature (London)*, 286 (1980) 447.
- 13 K. Biemann, *Chimia*, 14 (1960) 393.
- 14 W. C. Herlihy, N. J. Royal, K. Biemann, S. D. Putney and P. R. Schimmel, *Proc. Nat. Acad. Sci. U.S.*, 77 (1980) 6531.
- 15 H.-J. Förster, J. A. Kelley, H. Nau and K. Biemann, in E. Gross and J. Meienhofer (Editors), *Chemistry and Biology of Peptides*, Ann Arbor Sci. Publ., Ann Arbor, MI, 1972.
- 16 W. E. Siefert, Jr., R. E. McKee, C. F. Beckner and R. M. Caprioli, *Anal. Biochem.*, 88 (1978) 149.
- 17 B. C. Das, S. D. Gero and E. Lederer, *Biochem. Biophys. Res. Commun.*, 29 (1967) 211.
- 18 H. R. Morris, R. J. Dickinson and D. H. Williams, *Biochem. Biophys. Res. Commun.*, 51 (1973) 247.
- 19 P. A. Leclercq and D. M. Desiderio, *Anal. Lett.*, 4 (1971) 305.
- 20 D. W. Thomas, B. C. Das, S. D. Gero and E. Lederer, *Biochem. Biophys. Res. Commun.*, 32 (1968) 199.
- 21 H. R. Morris, D. H. Williams, G. G. Midwinter and B. S. Hartley, *Biochem. J.*, 141 (1974) 701.
- 22 K. Rose, J. D. Priddle, R. E. Offord and M. P. Esnouf, *Biochem. J.*, 187 (1980) 239.
- 23 B. G. Dawkins, P. J. Arpino and F. W. McLafferty, *Biomed. Mass Spectrom.*, 5 (1978) 1.
- 24 S. W. Thomas, B. C. Das, S. D. Gero and E. Lederer, *Biochem. Biophys. Res. Commun.*, 32 (1968) 519.
- 25 R. D. Smith and A. L. Johnson, *Anal. Chem.*, 53 (1981) 739.
- 26 B. L. Karger, D. P. Kirby, P. Vouros, R. L. Foltz and B. Hiby, *Anal. Chem.*, 51 (1979) 2324.
- 27 M. Mudgett, J. A. Sogan, D. V. Bowen and F. H. Field, *Advan. Mass Spectrom.*, 7 (1978) 1506.
- 28 M. Mudgett, D. V. Bowen, J. J. Kindt and F. H. Field, *Biomed. Mass Spectrom.*, 2 (1975) 254.
- 29 T. J. Yu, B. L. Karger and P. Vouros, in preparation.
- 30 H. Nau and K. Biemann, *Anal. Biochem.*, 73 (1976) 139.
- 31 J. Hughes, T. W. Smith, H. W. Kosterlitz, L. A. Fothergill, B. A. Morgan and H. R. Morris, *Nature (London)*, 258 (1975) 577.
- 32 L. R. Snyder, J. W. Dolan and J. R. Gant, *J. Chromatogr.*, 165 (1979) 3.

CHROM. 14,154

ASSESSMENT AND OPTIMIZATION OF SYSTEM PARAMETERS IN SIZE EXCLUSION SEPARATION OF PROTEINS ON DIOL-MODIFIED SILICA COLUMNS

P. ROUMELIOTIS and K. K. UNGER*

Institut für Anorganische Chemie und Analytische Chemie, Johannes-Gutenberg-Universität, 6500 Mainz (G.F.R.)

SUMMARY

On diol-modified silica columns the retention of proteins is governed by a size exclusion effect, but superimposed on this are some secondary effects, *i.e.*, ionic and diol-ligand interactions which can be controlled and adjusted reproducibly by varying the eluent composition. The eluent composition also affects the column efficiency and peak shape. Both dependences can be employed to obtain a better resolution of proteins than can be expected from size exclusion alone.

INTRODUCTION

The rapid separation of native biopolymers by high-performance liquid chromatography (HPLC) has attracted great interest as a means for both identification and isolation. Depending on the nature of the biopolymer and the purpose of the separation, three kinds of HPLC phase systems are commonly employed: reverse phase packings with ternary solvent mixtures, ion exchangers with buffers as eluents and size exclusion packings based on polar modified silicas with buffers¹. Of these size exclusion chromatography (SEC) is most frequently carried out prior to the other separation modes, *e.g.*, to isolate fractions of a certain molecular weight. For SEC of biopolymers a number of bulk materials and also prepacked columns were developed. These have recently been examined and compared for column selectivity and performance².

The molecular weight (MW) selectivity of these columns is expressed in terms of a calibration plot of log MW *vs.* elution volume, V_e , of solute, or by the distribution coefficient, K_D , of solute, taking values between 0 and 1 (ref. 3). Although the calibration curve is fairly linear for most columns investigated at a specific eluent composition, deviations are observed in some MW ranges when plotting all data in the log MW *vs.* V_e curve. This indicates that, in addition to size exclusion, other mechanisms are operating in the elution of biopolymers, and hence predictions of MW of unknown solutes based on V_e may be highly erroneous. This particular behaviour of biopolymeric solutes arises from the fact that variation of eluent composition has a significant influence on the charge and structure of solutes, as well as on the surface of the packing⁴.

The objective of this study was to elucidate the various contributions from non-size-exclusion effects to the elution volume of proteins on diol-modified silica columns. This enables an assessment of the most dominant mobile phase parameter controlling resolution and optimization of a separation. It will be demonstrated that the operation of several retention mechanisms in SEC of biopolymers may result in a resolution superior to that of pure SEC.

EXPERIMENTAL

Two packings were employed in this study: LiChrosorb® Diol, particle diameter, d_p , 5 μm (E. Merck, Darmstadt, G.F.R.), and a diol-silica prepared by ourselves. The latter was obtained by modifying a 5- μm angular silica (mean pore diameter 30 nm) with 1,2-epoxy-3-propoxypropyltrimethoxysilane (Dynamit Nobel, Köln, G.F.R.), followed by treatment in 0.1 *N* sulphuric acid at 80°C to convert the epoxy into diol groups. The surface concentration of bonded groups was $4.8 \pm 0.3 \mu\text{mol}/\text{m}^2$ for both products, assuming a bifunctional reaction. The monolayer capacity was calculated at $2.65 \mu\text{mol}/\text{m}^2$, and thus the values indicate some degree of polymerization of the bonded layer⁵.

Columns (250 \times 6 mm) were packed according to the high viscosity method using a 10% (w/w) slurry of paraffin-tetrachloromethane (50:50, v/v). The eluents were electrolytes and buffers, all of reagent grade (E. Merck). Standard proteins and dextrans were purchased from Boehringer (Mannheim, G.F.R.) and Serva (Heidelberg, G.F.R.). The chromatograph, a Hewlett-Packard Model 1084 A, was fitted with a UV photometer operated at a wavelength of 254 nm.

The electrophoretic velocities, v , of suspensions of the packing in various eluents were determined in a quartz cell (100 \times 470 \times 0.5 mm) using an Elphor VaP 11 (Bender & Hobein, München, G.F.R.). The zeta potential was calculated by the Helmholtz-Smoluchowski equation

$$\zeta = \eta v / \epsilon_e \epsilon_0 E$$

where η = viscosity, E = field strength, ϵ_e = dimensionless dielectric constant and $\epsilon_0 = 8.85 \cdot 10^{-12} \text{ cm}^{-1}$.

RESULTS AND DISCUSSION

Elution of proteins on diol-modified silica columns

Diol-modified silicas were chosen to examine the recovery, separation and isolation of proteins⁶⁻⁸ on account of their favourable surface properties. Most of the studies were carried out in eluents of around pH 7.0 and appropriate ionic strength. An optimum linear fit of the calibration curve could be achieved for particular eluent compositions. However, when plotting all the V_e values obtained at various eluent compositions on the log MW vs. V_e diagram a large scattering was observed. Fig. 1 exemplifies the situation on a LiChrosorb Diol column (250 \times 6 mm) with eluents of various pH ranging from 5.4 to 9.5 and almost constant ionic strength. Similar scattering occurs for the V_e values of proteins at different buffer and electrolyte concentrations and constant pH. Thus, the data demonstrate that the mechanism in this

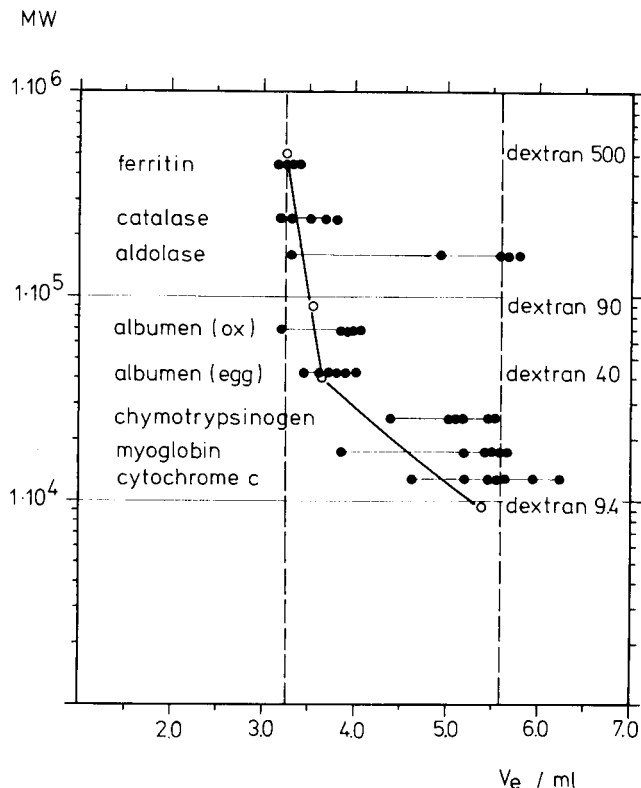


Fig. 1. Calibration curve for proteins and dextrans on a LiChrosorb Diol column (250 × 6 mm) with eluents of various pH (data taken from Table II).

particular phase system is not just pure size exclusion, additional effects being involved. Further, it is clear that all proteins are generally eluted between the interstitial volume, V_0 , of the column (= 3.2 ml) and $V_0 + V_i$ (= 5.7 ml), V_i being the internal column volume. This indicates that size exclusion is the controlling effect, while the other possible mechanisms contributing to V_e are second-order effects.

Pure size exclusion is basically an entropy controlled process³, giving a distribution coefficient $K_D \approx \exp(-\Delta S_0/R)$. Thus, peak retention may be expected to be temperature-independent. On the other hand, mechanisms based on solute-stationary phase interaction in liquid-solid chromatography (LSC) are enthalpy controlled processes. The distribution coefficient K_{LSC} is proportional to $\exp(-\Delta H/RT)$, ΔH is usually negative and K_{LSC} is dependent on temperature.

It is conceivable that solute-stationary phase interactions of biopolymers may take place when the solutes permeate the pore structure of the packing and hence gain access to the internal surface area. When the diol-modified silica surface is exposed to a buffered eluent two surface sites can be distinguished: ionic SiO^- groups and polar $-(\text{CH}_2)_3\text{OCH}_2\text{CHCH}_2$ groups which are undissociated. Deprotonation of silanol



groups, with $\text{p}K_a$ 6.8 (ref. 9), depends on the pH. The SiO^- groups thus formed are

simultaneously involved in ion-exchange reactions with cations of the electrolyte. Positively charged basic proteins are attracted to negative surfaces while negatively charged acidic proteins are repelled. As a first approximation, solute-surface interactions can be divided into two types: SiO^- -solute, *i.e.*, ionic, and diol-ligand-solute, which may be of a hydrophobic nature. Supposing that both interactions contribute independently to retention, the following assumption can be made:

$$V_e (\text{observed}) = V_{e(\text{SE})} + V_{e(\text{II})} + V_{e(\text{DL})}$$

Here V_e represents pure size exclusion, $V_{e(\text{II})}$ the ionic and $V_{e(\text{DL})}$ the diol-ligand interactions for a given solute.

The next problem to be solved is to find approaches which permit an estimation of the various contributions to V_e (observed). This can be done in the following ways:

(i) by studying the elution behaviour of those molecules which appear to be controlled mainly by one of the three mechanisms, *e.g.*, uncharged dextrans as reference substances for pure size exclusion effects, small monomeric ionic solutes for ionic interactions;

(ii) by systematically varying those parameters of the phase system which are assumed to affect one specific type of interaction, *i.e.*, column temperature, pH, type, valence and concentration of the eluent, etc.

Furthermore, changes in the surface charge of diol-modified silica particles suspended in the various eluents might be monitored by measuring the electrophoretic mobility, v , and the zeta potential, ζ .

Estimation of size exclusion effects in the elution of proteins on diol-modified silicas

Standard dextrans were applied in order to assess the extent of pure size exclusion relative to the other effects contributing to V_e (observed) of proteins, and the temperature dependence of V_e was examined both for proteins and dextrans. Three ionic test solutes, sulphanilic acid (pK 1, 3.25), phenylalanine (pK 2.58, 9.24) and benzoic acid (pK 4.20), were included in the study. The results for two diol packings and different eluent compositions are listed in Table I. V_e of proteins decreases slightly when the column temperature is raised from 25°C to 50°C, with the exception of aldolase and chymotrypsinogen, where the opposite takes place. This decrease may be understood in terms of weaker adsorption interactions between the solutes and the surface. The behaviour of aldolase and chymotrypsinogen is more difficult to interpret. These compounds either undergo conformational changes with temperature, or the adsorption interactions are associated with a positive enthalpy. The ionic solutes are eluted close to $V_i + V_0$ and hence may be considered as totally permeating solutes. The change in V_e with column temperature indicates that adsorption interactions are involved in the retention. It is of interest in this context that a so-called enthalpic exclusion of these solutes, as observed on reversed-phase columns¹⁰, does not appear to take place in this phase system.

Table I also shows that (i) the elution volumes of dextrans remains unaffected by variation in the column temperature, and (ii) the elution volumes of proteins of comparable molecular weight to dextrans, *e.g.*, albumen (egg) and dextran 40, are slightly higher. This demonstrates clearly that dextrans are eluted by a pure size

TABLE I

EFFECT OF COLUMN TEMPERATURE ON THE ELUTION VOLUMES OF PROTEINS, DEXTRANS AND IONIC SOLUTES

Solute	MW	LiChrosorb Diol, $d_p = 5 \mu\text{m}$				Diol-modified silica (30 nm), $d_p = 5 \mu\text{m}$.	
		Sörensen phosphate buffer, pH 7.4, + 0.02 m NaCl		Sörensen phosphate buffer, pH 7.4		Sörensen phosphate buffer, pH 7.4, + 0.02 m NaNO ₃	
		25°C	50°C	25°C	50°C	25°C	50°C
Ferritin	440,000	3.33	3.19	3.26	3.22	3.20	3.10
Catalase	240,000	3.40	3.30	3.38	3.32	3.60	3.54
Aldolase	158,000	3.44	4.00	3.46	5.42	3.78	5.32
Albumen (bovine)	68,000	3.56	3.40	3.52	3.49	—	—
Albumen (egg)	45,000	3.70	3.58	3.62	3.58	3.60	3.54
Chymotrypsinogen	25,000	5.30	5.70	5.74	6.14	—	—
Myoglobin	17,000	5.12	4.94	5.14	5.04	—	—
Sulphanilic acid	174	5.60	5.38	5.54	5.14	5.48	5.28
Phenylalanine	165	6.34	6.18	6.42	6.14	6.08	5.60
Benzoic acid	122	5.98	5.64	5.92	5.50	5.78	5.54
Dextran 500	500,000	3.23	3.20	3.25	3.20	2.84	2.80
Dextran 90	90,000	3.28	3.26	3.28	3.26	3.12	3.12
Dextran 40	40,000	3.50	3.45	3.46	3.50	3.32	3.28
Dextran 9.4	9400	5.40	5.30	5.40	5.30	5.28	5.28

exclusion mechanism while proteins undergo some additional interactions. The extent of the contribution of size exclusion to V_e of proteins may be quantitated by subtracting the V_e of dextrans with the same molecular weight, or more correctly the same hydrodynamic volume.

Ionic effects on the elution of proteins

It may be assumed that the small-size ionic substances used in this study are retarded only by ionic and possibly by additional ligand-solute interactions on diol-modified silicas. Furthermore, the strongest influence on solute retention due to ionic interactions in this phase system will arise from changes in the charge and charge distribution, respectively, of interacting entities, *i.e.*, through variation in pH and/or electrolyte concentration of the eluent. Table II lists the elution volumes of proteins and ionic reference substances measured over a wide range of eluent pH at almost constant ionic strength. For a meaningful discussion, Fig. 2 also needs to be considered, which, at the same eluent compositions as in Table II, presents the dependence of the zeta potential of suspensions of the LiChrosorb Diol packing on the pH of the eluent. It is seen that the negative charge on diol-silica particles increases with pH. The values are comparable to those obtained by Knox *et al.*¹⁰ on ODS-Hypersil, but are slightly lower than those measured by Kerner and Leiner¹¹ on Aerosil and phenylated Aerosil. It is somewhat surprising that, even when subjected to modification, the electrophoretic mobility of silica particles can still be monitored. Pre-

TABLE II

EFFECT OF ELUENT pH ON THE ELUTION (V_e IN ml) OF PROTEINS AND IONIC SOLUTES

The pH was adjusted by adding hydrochloric acid or ammonia to a 0.1 *M* solution of sodium acetate. Column: LiChrosorb Diol, $d_p = 5 \mu\text{m}$, $250 \times 6 \text{ mm}$.

Protein	pH of the eluent						
	9.49	7.56	6.48	6.08	5.89	5.67	5.42
Ferritin	3.16	3.24	3.26	3.34	3.34	3.35	3.38
Catalase	3.20	3.31	3.50	3.68	—	3.65	3.76
Aldolase	3.29	4.92	5.60	5.68	—	5.70	5.80
Albumen (bovine)	3.22	3.54	3.86	3.86	3.88	3.90	4.06
Albumen (egg)	3.42	3.62	3.78	3.84	3.86	3.90	4.00
Chymotrypsinogen	4.40	5.20	5.60	5.50	5.54	5.14	5.10
Myoglobin	3.86	4.94	5.58	5.54	5.62	5.46	5.50
Cytochrome c	4.74	5.20	5.48	5.94	6.24	5.64	5.54
Sulphanilic acid	5.00	5.32	5.46	5.64	5.64	5.68	5.70
Benzyltrimethyl-ammonium chloride	large	17.90	10.58	9.84	9.56	9.40	9.00
Phenylalanine	5.28	6.18	6.06	6.12	6.12	6.14	6.10
Benzoic acid	4.84	5.62	6.12	6.28	6.34	6.54	6.84

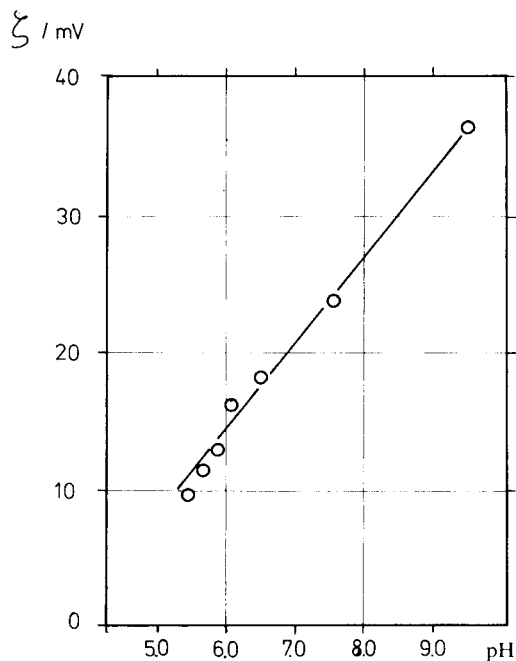


Fig. 2. Zeta potential of LiChrosorb Diol suspended in eluents of various pH (see Table II) as a function of the pH of the suspension.

sumably this should be attributed to the fact that a high population of silanols remains unaffected by surface reaction.

The data in Table II indicate that V_e of most proteins decreases steadily with increasing pH from 5.4 to 9.5. The last three basic proteins, chymotrypsinogen, myoglobin and cytochrome C, show a slight maximum in the V_e vs. pH dependence, but then V_e values in alkaline media are always lower than in weak acidic media. Depending on the isoelectric pH of the protein, the relative ratio of negative to positive charges will increase with eluent pH. The negative surface charges will also increase, so that ionic repulsion becomes dominant and V_e decreases. Ionic repulsion forces, however, are not strong enough to exclude all proteins totally from the internal pores. For all protein solutes, V_e is observed to vary within V_0 and $V_0 + V_i$, indicating that ionic interactions are of secondary importance. This does not hold for small-size ionic solutes, as the whole internal surface is accessible for interactions. For phenylalanine, sulphanilic acid and benzoic acid, V_e falls with increasing pH, the effect being most pronounced for benzoic acid. According to Knox *et al.*¹⁰ the retention of benzoic acid above $V_i + V_0$ ($k' > 0$) can be explained by considering the retentivities of both forms of the acid, HA and A^- . Of all the solutes, retardation is highest for benzyltrimethylammonium cation. A change from pH 5.4 to 7.6 leads to a doubling of V_e , mainly as a result of the increasing number of negative surface charges on the diol-modified silica (see Fig. 2).

Ionic interactions between charged species are known to be controlled by the type, valence and concentration of the electrolyte. By changing these parameters the properties of the silica surface and the solutes are affected in various ways: the configuration of proteins is sensitive to electrolyte concentration; metal ions may form complexes with proteins; adsorbed anions influence the degree of hydration of proteins according to the chaotropic series; depending on the electrolyte concentration, a double layer around the protein solute is built up, changing the charge and charge distribution. In the same way the properties of the silica surfaces varied according to the electrolyte, via deprotonation, ion exchange, adsorption, etc.

Schmidt *et al.*⁶ studied the effect of eluent ionic strength on the elution volume of proteins and found typical dependences for basic, acidic and neutral solutes. We believe that ionic strength is too simple a parameter to permit specification and elimination of single effects caused by the type of cation and anion, by the valence, etc. Assuming ionic strength, μ , to be the determining parameter, all V_e values of a given protein at the same level of μ should be equal. This, however, is not the case. Another feature is that at low ionic strength, $\mu < 0.1$, μ is adjusted by dilution of the buffer, while at $\mu > 0.1$ discrete μ values are obtained by adding a certain amount of electrolyte to the buffer. Table III lists the elution volumes of proteins at a wide range of electrolyte compositions. The eluent compositions are arranged in the order of decreasing zeta potential, which was measured in a suspension of the eluent with diol-modified silica. It is apparent that no correlation can be established between the zeta potential of silica particles and the retention of proteins at a constant pH of 7.4, leading to the interpretation that the observed deviations cannot be related to purely ionic interactions but also to other, *e.g.*, hydrophobic, interactions.

The data call for discussion of the relationship between V_e and the following quantities: type of cation (Li^+ , Na^+ , K^+ , Cs^+) at constant anion and concentration; type of anion (NO_3^- , ClO_4^- , Cl^-) at constant cation and concentration; the valence of

TABLE III

EFFECT OF IONIC TYPE, VALENCE, CONCENTRATION, IONIC STRENGTH AND ZETA POTENTIAL ON THE ELUTION VOLUME OF PROTEINS AND IONIC SOLUTES

Column: 250 × 6 mm, packed with LiChrosorb® Diol.

	V_e (ml) in Sörensen phosphate buffer, pH 7.4													
	$+0.02\text{ }m$	$+0.02\text{ }m$	$+0.08\text{ }m$	$+0.02\text{ }m$	$+0.02\text{ }m$	$+0.0067\text{ }m$	$+0.02\text{ }m$	$+0.0067\text{ }m$	$+0.02\text{ }m$	$+0.0267\text{ }m$	$+0.08\text{ }m$	$+0.02\text{ }m$		
μ	$LiCl$	$NaNO_3$	$NaClO_4$	$CsCl$	KCl	$MgCl_2$	$NaCl$	Na_2SO_4	$NaClO_4$	Na_2SO_4	$NaCl$	$MgCl_2$		
	0.1008	0.1008	0.1618	0.1008	0.1008	0.1008	0.1008	0.1008	0.1008	0.1608	0.1608	0.1408		
ξ (mV)	-35.53	-31.87	-30.17	-28.48	-28.41	-27.85	-27.85	-27.85	-26.44	-25.38	-22.07	-19.88		
Protein														
Ferritin	3.30	3.32	3.32	3.30	3.31	3.28	3.33	3.34	3.34	3.30	3.32	3.34		
Catalase	3.40	3.46	3.42	3.48	3.43	3.40	3.40	3.42	3.42	3.42	3.43	3.46		
Aldolase	3.58	3.60	—	3.58	3.59	3.58	3.44	3.52	3.54	—	—	3.60		
Albumen (bovine)	3.68	3.68	3.66	3.70	3.76	3.66	3.56	3.64	3.64	3.80	3.82	3.88		
Albumen (egg)	3.70	3.75	3.76	3.76	3.77	3.74	3.70	3.72	3.72	3.80	3.78	3.80		
Chymotrypsinogen	4.86	4.82	4.60	4.80	4.82	4.90	5.30	5.04	4.88	4.54	4.68	4.88		
Myoglobin	5.80	4.80	4.60	6.06	6.14	5.92	5.12	4.84	4.90	4.70	4.74	6.00		
Cytochrome <i>c</i>	6.20	6.00	5.10	5.84	6.00	6.10	—	5.40	6.00	5.14	5.26	5.58		

the cation (Mg^{2+} , Na^+) at given anion and constant concentration; the valence of anion (SO_4^{2-} , Cl^-) at given cation and constant ionic strength; the type of cation and anion at constant ionic strength (0.02 *m* LiCl, 0.02 *m* NaCl, 0.02 *m* KCl, 0.02 *m* CsCl, 0.0067 *m* MgCl_2 ; 0.02 *m* NaCl, 0.02 *m* NaClO_4 , 0.0067 *m* Na_2SO_4 ; 0.08 *m* NaCl, 0.08 *m* NaClO_4 , 0.08/3 *m* Na_2SO_4).

There appears to be no correlation between V_e and the ionic radius of the electrolyte cation in the eluent sequence 0.02 *m* LiCl, 0.02 *m* NaCl, 0.02 *m* KCl, 0.02 *m* CsCl. When the concentration and the type of cation are constant (0.02 *m* NaCl, 0.02 *m* NaNO_3 , 0.02 *m* NaClO_4), the variation of electrolyte anion results in small changes in V_e for aldolase, albumen (bovine), chymotrypsinogen and myoglobin. The substitution of Na^+ by Mg^{2+} at given anion and constant concentration (0.02 *m* NaCl, 0.02 *m* MgCl_2) causes a higher retention for most proteins in the fractionation range, except for chymotrypsinogen, even at constant ionic strength (0.02 *m* NaCl, 0.0067 *m* MgCl_2). At 0.02 *m* NaCl and 0.0067 *m* Na_2SO_4 changing the valence of the anion results in an increase, a decrease or no change in V_e , depending on the protein. At constant ionic strength and given anion, the type and valence of the cation appears to have no effect on V_e . This is not the case for a given cation, constant ionic strength but variable anion [0.02 *m* (0.08) NaCl, 0.02 *m* (0.08) NaClO_4 , 0.0067 *m* (0.0267) Na_2SO_4] at two ionic strength levels.

Unfortunately, the system behaves in such a complex way that the observed deviations of V_e cannot be treated on a rigorous physico-chemical basis. Furthermore, the effects are small compared to those caused by changing the pH of the eluent. It appears that no purely ionic effect is responsible for the changes in V_e .

Diol-ligand effects

Owing to its chemical structure, the bonded ligand has a hydrophilic as well as a hydrophobic character. It therefore appears questionable to determine the effect of the diol group on the retention of proteins alone. A possible way to estimate the relative magnitude of the two structural effects could be to synthesize and test a series of diol-modified silicas which differ in the length of the *n*-alkyl group at a given terminal position and in the number of OH groups per ligand at constant *n*-alkyl chain length. Such an examination, however, is extremely tedious and again harbours several sources of error when it comes to comparing the results.

The primary question is how great is the effect caused by the ligand in relation to size exclusion and ionic interaction. This can be established quite simply by a controlled change of the solvent strength of the eluent, *e.g.*, by addition of methanol to the buffer. Table IV presents the results of such a study. A small but distinct decrease in V_e of proteins is observed when the methanol content is increased stepwise from zero to 5% (v/v), with the exception of chymotrypsinogen. This decrease can be attributed to hydrophobic interactions arising from the hydrocarbon spacer groups. The opposite effect observed in the case of chymotrypsinogen indicates that the hydrophilic character of the diol group is dominant. The decreasing tendency of V_e is also observed for the small-size ionic solutes. However, the V_e of dextrans remains constant, in contrast to all other solutes. When comparing the elution volumes of proteins and dextrans of similar molecular weight, *e.g.*, albumen (egg) and dextran 40, the proteins are found to be retained more strongly. Hydrophobic interactions may also become dominant when the ionic interactions are suppressed, *i.e.*, at high ionic strength of the eluent, $\mu \gg 0.2$.

TABLE IV

ELUTION VOLUME (V_e IN ml) OF PROTEINS, DEXTRANS AND IONIC SOLUTES ON A LI-CHROSORB® DIOL COLUMN (250 × 6 mm) WHEN METHANOL IS ADDED TO THE ELUENT

Solute	Methanol (v/v) Sørensen phosphate buffer, pH 7.4				Methanol (v/v) Sørensen phosphate buffer, pH 7.4, +0.02 M NaCl	
	0	1	3	5	0	5
Ferritin	3.24	3.25	3.23	3.22	3.33	3.20
Catalase	3.38	3.34	3.34	3.30	3.40	3.30
Aldolase	3.46	3.44	3.42	3.38	3.44	3.38
Albumen (bovine)	3.48	3.48	3.46	3.38	3.56	3.48
Albumen (egg)	3.64	3.62	3.60	3.52	3.70	3.62
Chymotrypsinogen	5.74	5.80	5.80	5.78	5.30	5.43
Myoglobin	5.36	5.29	5.26	5.13	5.12	5.08
Sulphanilic acid	5.54	5.50	5.46	5.34	5.60	5.50
Phenylalanine	6.42	6.38	6.32	6.20	6.34	6.22
Benzoic acid	5.92	5.84	5.76	5.60	5.98	5.78
Dextran 500	3.25	3.26	3.24	3.20	3.23	3.24
Dextran 90	3.26	3.28	3.28	3.26	3.28	3.24
Dextran 40	3.46	3.40	3.50	3.45	3.50	3.45
Dextran 9.4	5.40	5.38	5.38	5.40	5.40	5.40

In conclusion, the diol ligand appears to have a minor but measurable effect on the elution behaviour of proteins and thus can be used for improving the selectivity.

Column efficiency and column lifetime

Unlike synthetic polymers^{1,2}, the pure proteins are monodisperse and therefore a relationship between the degree of polydispersity of the solute and the plate height does not exist, as is the case with the former. However, the plate height of the solute is still a function of the MW of the solute due to the increase of the diffusion coefficient with MW. For proteins of MW between 10,000 and 50,000 daltons, about 6000 theoretical plates per 250-mm column length could be achieved at optimum flow-rate. In addition to plate number, the peak symmetry of proteins is an important feature in separation. It was found that a change in the eluent composition dramatically affected the peak shape. For instance, peak symmetry was considerably improved at pH 8.0 compared to lower pH values. This may be due to the fact that the surface is covered more homogeneously with negative charges. A similar trend was observed when changing from high to low ionic strength. Peak efficiency and symmetry as well as recovery of proteins was found to be dependent on the type of electrolyte cation. For instance, K⁺ provided the most unfavourable results. However, the results are too fragmentary for a complete understanding. Nevertheless, they should be taken into account when optimizing a separation.

The lifetime of diol-modified silica columns, in particular LiChrosorb Diol, was found to be excellent; long-term stability using the same eluent, stability upon

frequent change of eluent composition and reproducibility of V_c when returning to the original eluent system (better than 2%) were exhibited. Prior to prolonged storage or when not in use, the buffer should be purged from the column first with water and thereafter by *n*-propanol. Saturation of the eluent with monosilicic acid was not necessarily required. For the examinations in this study the same LiChrosorb Diol column was used throughout without any noticeable changes in selectivity and performance, even with frequent alteration of eluent composition and using buffer up to pH 9.5.

CONCLUSIONS

It was demonstrated that:

- (i) the retention of proteins on diol-modified silica is based predominantly on a size exclusion mechanism;
- (ii) ionic interactions contribute to retention mainly through the variation of eluent pH;
- (iii) to some extent the diol-ligands also affect retention, depending on the solvent strength of the eluent.

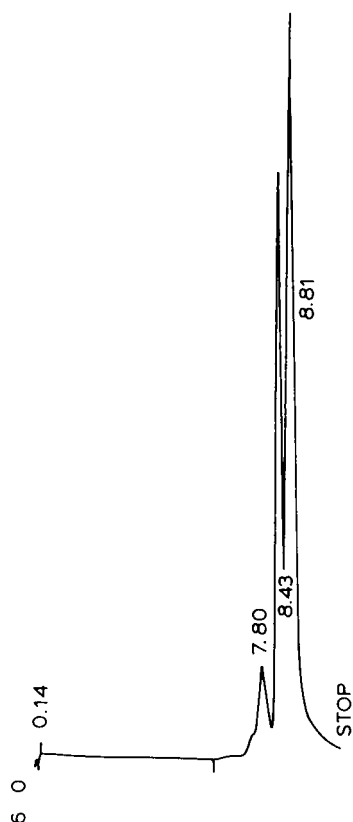


Fig. 3. Separation of two proteins, albumen (human) of MW 65,000 and transferrin of 80,000 daltons, on diol-modified silica (mean pore diameter 30 nm, $d_p = 5 \mu\text{m}$). Column: 250×6 mm. Eluent: phosphate buffer ($0.0645 \text{ m Na}_2\text{HPO}_4$, $0.002 \text{ m KH}_2\text{PO}_4$), pH 8.0.

Although the retention of proteins on diol-modified silicas has been treated here in a phenomenological rather than a profoundly theoretical manner, the various operating methods have provided in some, but not all, cases a higher resolution than might have been expected for a pure size exclusion mechanism. An example is given in Fig. 3, which shows a separation of two proteins having MW 65,000 [albumen (human)] and 80,000 (transferrin) daltons. Another advantage of this mode of HPLC is that it can readily be scaled-up for semi-preparative isolation of biopolymers.

ACKNOWLEDGEMENT

We gratefully acknowledge the assistance of Dr. von Steldern of the Institut für Immunologie, Johannes Gutenberg-Universität, Mainz.

REFERENCES

- 1 F. E. Regnier and K. M. Gooding, *Anal. Biochem.*, 103 (1980) 1-25.
- 2 E. Pfankoch, K. C. Lu, F. E. Regnier and H. G. Barth, *J. Chromatogr. Sci.*, 18 (1980) 430-441.
- 3 W. W. Yaw, J. J. Kirkland and D. D. Bly, *Modern Size Exclusion Chromatography*, Wiley-Interscience, New York, 1979.
- 4 P. Roumeliotis, K. K. Unger, J. Kinkel, G. Brunner, R. Wieser and G. Tschantz, in F. Lottspeich, A. Henschen and K. Hupe (Editors), *High Pressure Liquid Chromatography in Protein and Peptide Chemistry*, W. de Gruyter, Berlin, in press.
- 5 N. Becker and K. K. Unger, *Z. Anal. Chem.*, 304 (1980) 374-381.
- 6 D. E. Schmidt, R. W. Giese, D. Conron and B. L. Karger, *Anal. Chem.*, 52 (1980) 177-182.
- 7 N. Becker and K. Unger, *Chromatographia*, 12 (1979) 539.
- 8 P. Roumeliotis and K. K. Unger, *J. Chromatogr.*, 185 (1979) 445.
- 9 K. Unger, *Porous Silica (J. Chromatogr. Library, Vol. 15)*, Elsevier, Amsterdam, 1979.
- 10 J. H. Knox, R. Kaliszan and G. J. Kennedy, *Proc. Faraday Symp. No. 15, Brighton, Dec. 1980*, in press.
- 11 D. Kerner and W. Leiner, *Colloid Polym. Sci.*, 253 (1975) 960-968.
- 12 J. H. Knox and F. McLennan, *Chromatographia*, 10 (1977) 75.

CHROM. 13,994

LIGAND-EXCHANGE CHROMATOGRAPHY OF RACEMATES

XV*. RESOLUTION OF α -AMINO ACIDS ON REVERSED-PHASE SILICA GELS COATED WITH N-DECYL-L-HISTIDINE

V. A. DAVANKOV*, A. S. BOCHKOV and Yu. P. BELOV

Institute of Organo-Element Compounds, Academy of Sciences of the U.S.S.R., Moscow 117813 (U.S.S.R.)

SUMMARY

Zorbax ODS, Zorbax C₈ and LiChrosorb RP-18 columns were coated with N-decyl-L-histidine (C₁₀-L-His) and charged with copper(II) ions. The factors controlling the retention and resolution of racemic amino acids such as column temperature, pH and ionic strength of the eluent, concentration of copper ions and content and type of organic component in the eluent were examined. The best results were obtained with a 10⁻⁴ M copper(II) acetate solution in pure water. With the exception of aspartic acid, L-isomers of amino acids always eluted with smaller *k'* values than do the D-antipodes. The enantioselectivity (α) did not exceed 2, which is most convenient for analytical-scale separations. The possible nature of the interactions between the hydrophobic sorbent surface and the components of ternary sorption complexes is discussed.

INTRODUCTION

Chiral modification of commercially available high-performance liquid chromatographic (HPLC) columns by adsorption of appropriate chiral ligands² combines important advantages of the two approaches in resolving racemates by means of ligand-exchange chromatography, those of the "chiral eluent" method³⁻⁹ and the use of chiral stationary phases^{10,11}. Among these advantages are the possibility of using available chromatographic sorbents and applying desired chiral coating agents; the high stability of the chiral phase system; the unique possibility of eluting the modifier, thus regenerating both the column and the resolving agent; and, the possibility of preparative resolutions because of the absence of disturbing organic contaminants in the eluted fractions.

N-Alkyl-L-hydroxyproline² and -L-proline grafted to linear polyacrylamide¹² have been used to modify reversed-phase and normal-phase silica gels, respectively. L-Prolyl-N-dodecylamide was also found to adhere strongly enough to C₁₈ Hypersil to

* For Part XIV, see ref. 1.

render completely superfluous the addition of this chiral ligand to a water-rich eluent⁶.

In this work, *N*-decyl-*L*-histidine (C_{10} -*L*-His) has been used as a chiral coating on reversed-phase silica gels, and the resolution of unmodified amino acids in the presence of copper(II) ions has been examined.

EXPERIMENTAL

Commercially available columns (250×4.6 mm I.D.) were used, packed with Zorbax C_8 and Zorbax ODS ($10 \mu\text{m}$) reversed-phase sorbents. The packings were coated with C_{10} -*L*-His by passing a 1 % ethanolic solution of this compound through the columns followed by an aqueous solution of copper(II) acetate. The reproducibility of the parameters (retention and enantioselectivity) of columns that were coated in this manner is not very high, so that no systematic or significant difference between the behaviour of C_8 and C_{18} packings could be established.

The 250-mm columns were used in combination with a DuPont Model 850 liquid chromatograph, operated with an 8 mm^3 detection cell at 254 nm and a Rheodyne injection loop of 16 mm^3 volume. The elution rate was 2 ml/min.

With more strongly retained solutes, a shorter column was used (80 mm), which was packed with LiChrosorb RP-18 ($5 \mu\text{m}$) (E. Merck, Darmstadt, G.F.R.) by the usual slurry technique. This column was combined with a Tswett 304 liquid chromatograph (U.S.S.R.) with detection at 254 nm.

The retentions of *L*- and *D*-amino acid enantiomers (k'_L and k'_D) were calculated, based on a slightly modified eluent as a t_0 marker, the enantioselectivity was expressed as the ratio $\alpha = k'_D/k'_L$.

RESULTS AND DISCUSSION

General

Coating the reversed-phase columns by using a nearly saturated ethanolic solution of C_{10} -*L*-His results in adsorption of sufficient amounts of the chiral ligand on the hydrophobic sorbent surface.

As indicated in a previous paper², *n*-decyl groups of the chiral coating must be integrated in some way between the alkyl chains of the interface layer. This kind of arrangement seems to be attainable when ethanol is used as the medium during the coating procedure. However, water-rich eluents used in chromatography do not solvate the alkyl chains of the graft and coating, so that the hydrocarbonaceous interface layer must become more compact, thus entrapping the alkyl tail of the chiral ligand. The hydrophilic amino acid part of the latter should be oriented towards the polar eluent and should be accessible for the formation of ternary complexes with metal ions and mobile ligands.

It is interesting that the C_8 packing is generally as good as the C_{18} packing, although the C_{10} -alkyl chains of the coating can be fully embedded in the ODS layer alone (if a parallel orientation of alkyl chains is assumed). The higher efficiency of the Zorbax C_8 column and the higher capacity values (k') of the Zorbax ODS column are worth mentioning.

The main difference between the C_{10} -*L*-His coating studied here and the C_{10} -*L*-

hydroxyproline modification investigated previously² is the markedly lower enantioselectivity of the C₁₀-L-His system. However, this is not a disadvantage when the analysis of the enantiomeric composition of a certain solute is the purpose of the chromatography: an enantioselectivity exceeding $\alpha = 1.5$ leads to a decrease in the precision of evaluating the ratio of two chromatographic peaks. In contrast, for preparative resolutions one would prefer coatings with a higher enantioselectivity. Generally, the enantioselectivity of L-histidine-incorporated sorbents is lower than that of L-proline- or L-hydroxyproline-incorporated sorbents^{10,11}.

Considering analytical applications of enantioselective phase systems involving strong fixation (via chemical bonds or adsorption) of resolving chiral ligands on a sorbent matrix, we should emphasize their principal advantage over the "chiral eluent" method which was developed specially for analytical purposes. When a chiral agent is present in the eluent, the two enantiomers resolved in the column enter the detector cell in the form of ternary complexes with the resolving agent and metal ions. These two complexes are diastereomeric and therefore possess different molar absorptivities¹³. Direct spectrophotometric detection of the resolved enantiomers must be based on a special calibration for each racemate-chiral eluent pair. The correction coefficients may change with varying elution conditions because of the varying extent of formation of diastereomeric complexes in solution. This important property was overlooked in some publications^{5,7-9}. On the other hand, if the eluent is free of any chiral components, no diastereomeric species can form in solution and any type of detection would immediately produce the desired ratio of two enantiomers.

For the above reasons, the C₁₀-L-His-incorporated reversed-phase system is convenient for the enantiomeric analysis of most amino acids. Of 28 racemates examined, only basic amino acids (Arg, Lys, His), asparagine, glutamic acid and citrulline could not be resolved at the plate number of *ca.* 3000 achieved so far. It is also advantageous that pure water [containing trace amounts of Cu(II) ions] was found to be the best eluent in amino acid analysis.

TABLE I

RETENTION AND SEPARATION ENANTIOSELECTIVITY OF AMINO ACIDS ON ZORBAX C₈ AS A FUNCTION OF pH AND IONIC STRENGTH OF AQUEOUS ELUENTS CONTAINING 10⁻⁴ M COPPER(II) ACETATE AT 35°C

Substance	pH 6.18 (without NH ₄ Cl)			pH 4.85 (0.1 M NH ₄ Cl)		
	<i>k'</i> _L	<i>k'</i> _D	α	<i>k'</i> _L	<i>k'</i> _D	α
Asp	0.86	0.63	1.37	0.50	0.50	1.00
His	0.50	0.50	1.00	0.20	0.20	1.00
Arg	4.77	4.77	1.00	0.63	0.63	1.00
Thr	1.03	1.33	1.29	0.35	0.35	1.00
Pro	4.66	6.70	1.44	2.00	3.00	1.50
Abu	7.20	11.60	1.61	2.30	5.61	2.44
Val	19.33	35.33	1.83	7.41	9.26	1.25
Met	34.00	43.00	1.26	11.45	15.11	1.32
Tyr	31.78	44.21	1.39	9.17	13.29	1.45

Factors controlling retention and enantioselectivity

Several factors significantly influence the retention and resolution selectivity of amino acids on reversed-phase packings coated with C₁₀-L-His.

Addition of 0.1 M ammonium chloride to 10⁻⁴ M copper acetate solution leads to a decrease in pH from 6.18 to 4.85. As can be seen from the Table I, the capacity factors, k'_L and k'_D , decrease rapidly owing to the combined action of (i) increasing ionic strength, (ii) partial protonation of both fixed and mobile amino acid ligands and (iii) increasing concentration of ligands (NH₃) competing for coordination with Cu(II) ions. Hence hydrophilic amino acids leave the column with very small k' values with no resolution into isomers. For more hydrophobic solutes, the enantioselectivity remains nearly the same.

TABLE II

RETENTION AND SEPARATION ENANTIOSELECTIVITY OF RACEMIC AMINO ACIDS AS A FUNCTION OF COPPER ACETATE CONCENTRATION IN THE ELUENT (ETHANOL-WATER, 15:85; ZORBAX C₈; 35°C)

Substance	0.5 · 10 ⁻⁴ M			1 · 10 ⁻⁴ M			2 · 10 ⁻⁴ M		
	k'_L	k'_D	α	k'_L	k'_D	α	k'_L	k'_D	α
Orn	0.83	0.83	1.00	0.71	0.71	1.00	0.54	0.54	1.00
allo-Hyp	1.17	1.17	1.00	0.90	0.90	1.00	0.67	0.67	1.00
Ser	2.00	2.00	1.00	1.40	1.40	1.00	1.31	1.31	1.00
Asn	0.98	0.98	1.00	0.82	0.82	1.00	0.66	0.66	1.00
Glu	1.67	1.67	1.00	1.36	1.36	1.00	1.17	1.17	1.00
Thr	2.00	2.24	1.12	1.60	1.80	1.13	1.33	1.52	1.14
allo-Tyr	1.96	1.96	1.00	1.90	1.90	1.00	1.50	1.50	1.00
Cit	1.40	1.40	1.00	1.20	1.20	1.00	1.18	1.18	1.00
Pro	2.40	3.05	1.27	1.82	2.37	1.30	1.38	1.84	1.33
Asp	1.69	1.24	1.36	1.50	1.13	1.33	1.36	0.96	1.42
His	5.50	5.50	1.00	1.88	1.88	1.00	1.72	1.72	1.00
Aaa*	1.95	1.95	1.00	1.60	1.60	1.00	1.47	1.47	1.00
Ala	2.17	2.17	1.00	1.80	1.80	1.00	1.50	1.50	1.00
Abu**	3.40	3.40	1.00	2.76	2.76	1.00	2.57	2.57	1.00
Tyr	9.33	11.00	1.18	6.50	7.75	1.19	6.33	7.66	1.21
Lys	6.67	6.67	1.00	3.80	3.80	1.00	3.50	3.50	1.00
Ival	6.50	6.95	1.07	5.60	6.00	1.07	3.83	4.25	1.11
Val	7.60	9.35	1.23	5.30	6.70	1.26	4.67	6.02	1.29
Arg	8.20	8.20	1.00	5.70	5.70	1.00	4.17	4.17	1.00
Met	11.40	12.06	1.06	8.00	8.50	1.06	7.25	7.76	1.07

* α -Aminoadipic acid.

** Aminobutyric acid.

An increasing concentration of Cu(II) ions in the eluent produces a similar decrease in k' values (Table II). All the above factors control mainly the extent of formation of ternary sorption complexes, but do not affect the stereochemical interactions within these complexes which are responsible for enantioselectivity.

The type and amount of organic components in hydro-organic eluents strongly influence hydrophobic interactions in the system, including those within the sorption complex. The less organic solvent is present, the higher are the k' and α values (Table

III). Best results are obtained in pure water. This is especially important for small amino acids, which are weakly retained and are resolved only in the absence of organic solvents (Ala, *allo*-Thr). It is interesting that an increasing proportion of water in the eluent does not enhance the retention of highly hydrophilic solutes (Asp, Ser). Nevertheless, distinct improvements in column efficiency and enantioselectivity are observed even in this instance. The last column in Table III is the most important, as it gives the resolutions attainable in pure water for small and polar amino acids.

TABLE III

RETENTION AND RESOLUTION SELECTIVITY OF AMINO ACIDS WITH DIFFERENT RATIOS OF WATER TO ETHANOL IN THE ELUENT [10^{-4} M COPPER(II) ACETATE; ZORBAX C₈; 35°C]

Substance	Ratio (water-ethanol)											
	70:30			85:15			92.5:7.5			100		
	k'_L	k'_D	α	k'_L	k'_D	α	k'_L	k'_D	α	k'_L	k'_D	α
Ser	1.57	1.57	1.00	1.40	1.40	1.00	1.15	1.33	1.16	1.23	1.54	1.25
Asn	0.86	0.86	1.00	0.82	0.82	1.00	0.82	0.82	1.00	0.63	0.63	1.00
Glu	1.50	1.50	1.00	1.36	1.36	1.00	0.93	0.93	1.00	2.39	2.39	1.00
Thr	1.69	1.92	1.14	1.60	1.80	1.13	1.50	1.75	1.17	1.03	1.33	1.29
<i>allo</i> -Thr	2.29	2.29	1.00	1.90	1.90	1.00	1.88	1.88	1.00	3.31	4.00	1.21
Cit	1.29	1.29	1.00	1.20	1.20	1.00	1.83	1.83	1.00	2.00	2.00	1.00
Pro	1.71	2.21	1.29	1.82	2.37	1.30	2.00	2.66	1.33	4.66	6.70	1.44
Asp	1.71	1.29	1.33	1.50	1.13	1.33	1.47	1.09	1.35	0.86	0.63	1.37
His	1.67	1.67	1.00	1.88	1.88	1.00	1.88	1.88	1.00	0.50	0.50	1.00
Aaa*	1.47	1.47	1.00	1.60	1.60	1.00	2.00	2.00	1.00	5.46	6.43	1.18
Ala	1.86	1.86	1.00	1.80	1.80	1.00	1.71	1.71	1.00	2.48	3.35	1.35
Abu	2.79	2.79	1.00	2.76	2.76	1.00	3.25	3.88	1.19	7.20	11.60	1.61
Lys	3.07	3.07	1.00	3.80	3.80	1.00	7.33	7.33	1.00	3.29	3.29	1.00
Ival	1.71	1.71	1.00	5.60	6.00	1.07	6.88	7.63	1.11	19.57	24.33	1.24
Val	3.43	3.43	1.00	5.30	6.70	1.26	8.00	10.33	1.29	19.33	35.33	1.83
Arg	5.73	5.73	1.00	5.70	5.70	1.00	7.50	7.50	1.00	4.77	4.77	1.00
Met	4.00	4.24	1.06	8.00	8.50	1.06	10.25	11.38	1.11	34.00	43.00	1.26
Tyr	4.86	4.86	1.00	6.50	7.75	1.19	7.33	9.67	1.32	31.78	44.22	1.39

* α -Aminoadipic acid.

Different organic solvents were examined, namely acetonitrile (polarity $P' = 6.0$, viscosity $\eta = 0.34$), ethanol ($P' = 4.3$, $\eta = 1.08$) and methanol ($P' = 5.1$, $\eta = 0.54$); the retention of hydrophobic solutes gradually increased on passing from acetonitrile to methanol when mixed in equal proportions with water (Table IV).

An increase in the temperature of the column from 18 to 45°C reduces the elution time and slightly enhances the overall resolution (Table V). A drift of the detection baseline at temperatures above 45°C may result from partial desorption of fixed chiral C₁₀-L-His ligands.

Strongly retained hydrophobic amino acids were analysed on a short column. All of them can be resolved in the reversed-phase system (Table VI).

TABLE IV

RETENTION AND RESOLUTION SELECTIVITY OF AMINO ACIDS AS A FUNCTION OF THE ELUENT COMPOSITION [10^{-4} M COPPER(II) ACETATE; 35°C]

Substance	Water-acetonitrile (85:15)						Water-methanol (85:15)					
	Zorbax C ₈			Zorbax ODS			Zorbax C ₈			Zorbax ODS		
	k'_L	k'_D	α	k'_L	k'_D	α	k'_L	k'_D	α	k'_L	k'_D	α
allo-Hyp	0.71	0.71	1.00	1.00	1.00	1.00	0.82	0.82	1.00	0.93	0.93	1.00
Ser	0.74	0.74	1.00	1.75	1.75	1.00	1.12	1.12	1.00	1.23	1.23	1.00
Asn	0.43	0.43	1.00	1.40	1.40	1.00	0.61	0.61	1.00	0.75	0.75	1.00
Glu	0.57	0.57	1.00	0.88	0.88	1.00	0.81	0.81	1.00	0.96	0.96	1.00
Thr	0.59	0.59	1.00	1.75	1.75	1.00	1.66	1.91	1.15	2.31	2.59	1.12
allo-Thr	0.44	0.44	1.00	1.67	1.67	1.00	2.11	2.11	1.00	3.21	3.21	1.00
Cit	0.79	0.79	1.00	2.40	2.40	1.00	1.75	1.75	1.00	3.02	3.02	1.00
Pro	1.00	1.51	1.51	3.20	4.80	1.50	3.51	4.86	1.38	4.62	6.05	1.31
Asp	0.78	0.44	1.77	1.06	0.66	1.61	0.83	0.51	1.63	1.21	0.81	1.50
Aaa*	0.52	0.52	1.00	2.25	2.25	1.00	1.13	1.13	1.00	1.98	1.98	1.00
Ala	0.96	0.96	1.00	3.01	3.01	1.00	1.83	1.83	1.00	2.37	2.37	1.00
Abu	3.24	3.24	1.00	3.67	3.67	1.00	4.52	4.52	1.00	6.31	6.31	1.00
Lys	2.00	2.00	1.00	5.57	5.57	1.00	5.72	5.72	1.00	7.36	7.36	1.00
Ival	4.75	5.75	1.21	11.37	13.67	1.20	9.00	10.71	1.19	14.17	17.15	1.21
Val	3.58	5.84	1.63	10.60	16.85	1.59	8.27	10.67	1.29	13.92	16.98	1.22
Met	5.25	6.63	1.26	13.51	16.48	1.22	12.33	14.54	1.18	17.81	20.48	1.15
Tyr	4.67	5.88	1.26	6.68	8.41	1.26	12.33	15.33	1.24	15.02	17.72	1.18

* α -Aminoadipic acid.*Column efficiency*

The plate number of a 250-mm column calculated for the peak of L-proline in water ($k' \approx 5$) was 3000 and the reduced plate height was 8.3. This relatively low column efficiency cannot be ascribed to the ligand-exchange mechanism or to the influence of the chiral coating. On chromatography of a test mixture of benzene, nitrobenzene and naphthalene in methanol-water (85:15), the plate number was only 20–30% higher, which may well result from the difference in the eluent viscosity.

Also for L-proline, the peak asymmetry factor was calculated to be 1.6, skew 1.15. The column porosity (ϵ) was 68 and the Knox-Parcher ratio was 8.46. The sample loading capacity was 2 mg of L-proline.

As far as column stability is concerned, it can be stated that 500 analyses on each of the columns tested did not cause any change in their retention parameters, enantioselectivity or efficiency.

The reproducibility of results was within 1–2% and the detection limit was 10^{-8} – 10^{-9} g of amino acid (proline).

Mechanism of retention and chiral recognition of amino acids

Of all solutes examined, amino acids carrying large aliphatic or aromatic substituents at the α -carbon atom display the highest k' values. This indicates that hydrophobic interactions with the sorbent surface are mainly responsible for the retention of these solutes. Naturally, retention decreases with increasing content of organic

TABLE V

RETENTION AND RESOLUTION SELECTIVITY OF AMINO ACIDS AS A FUNCTION OF COLUMN TEMPERATURE [WATER-ETHANOL, 85:15; 10^{-4} M COPPER(II) ACETATE; ZORBAX C₈]

Substance	18°C			35°C			45°C		
	k'_L	k'_D	α	k'_L	k'_D	α	k'_L	k'_D	α
Orn · HCl	0.87	0.87	1.00	0.71	0.71	1.00	0.50	0.50	1.00
allo-Hyp	0.95	0.95	1.00	0.90	0.90	1.00	0.63	0.63	1.00
Ser	1.45	1.45	1.00	1.40	1.40	1.00	1.33	1.33	1.00
Asn	0.88	0.88	1.00	0.82	0.82	1.00	0.50	0.50	1.00
Glu	1.63	1.63	1.00	1.36	1.36	1.00	1.00	1.00	1.00
Thr	1.71	1.94	1.14	1.60	1.80	1.13	1.29	1.48	1.15
allo-Thr	2.27	2.27	1.00	1.90	1.90	1.00	1.36	1.36	1.00
Cit	1.33	1.33	1.00	1.20	1.20	1.00	0.88	0.88	1.00
Pro	2.01	2.54	1.27	1.82	2.37	1.30	1.72	2.27	1.32
Asp	2.07	1.50	1.38	1.50	1.13	1.33	1.39	0.98	1.42
His · HCl	2.40	2.40	1.00	1.88	1.88	1.00	1.77	1.77	1.00
Aaa*	1.80	1.80	1.00	1.60	1.60	1.00	1.36	1.36	1.00
Ala	1.85	1.85	1.00	1.80	1.80	1.00	1.38	1.38	1.00
Abu	3.13	3.13	1.00	2.76	2.76	1.00	2.70	2.70	1.00
Lys	4.47	4.47	1.00	3.80	3.80	1.00	2.88	2.88	1.00
Ival	6.33	6.64	1.05	5.60	6.00	1.07	4.00	4.36	1.09
Val	6.21	7.50	1.20	5.30	6.70	1.26	3.60	4.64	1.29
Arg	6.23	6.23	1.00	5.70	5.70	1.00	5.21	5.21	1.00
Met	10.80	11.34	1.05	8.00	8.50	1.06	6.43	6.94	1.08
Tyr	11.93	14.55	1.22	6.50	7.75	1.19	5.28	6.50	1.23

* α -Aminoadipic acid.

component in the eluent and with the replacement of methanol with acetonitrile. These regularities do not hold for hydrophilic amino acids, where the contribution from hydrophobic interactions to the total retention is small compared with the contribution from coordination interactions. The latter are especially evident on changing the concentration of copper(II) ions in the eluent or its pH and content of mineral salt. Thus, the retention of amino acids in the chromatographic column is governed by the formation of ternary sorption complexes [with Cu(II) ions and C₁₀-L-His] at the interface layer, hydrophobic interactions contributing considerably to the stability of these complexes.

The formation of ternary complexes is the only process responsible for the chiral recognition of mobile ligands. As the eluents used in the present work are free of any chiral agents, localization of the ternary complexes on the hydrophobic surface is a matter of course. In this respect, the system developed here is similar to the previously described enantioselective LiChrosorb RP-18 coating with N-alkyl-L-hydroxyproline². The main difference is the much lower overall enantioselectivity of the C₁₀-L-His-incorporated system. The highest α values observed for the C₇-L-Hyp and C₁₀-L-His coatings were 16.4 (ref. 2) and 1.83, respectively, so that the latter is more convenient for analytical separations and the former for preparative separations.

We explain the lower enantioselectivity of the histidine-type fixed ligand in terms of the structural ambiguity of its sorption complexes. Whereas in copper(II)

TABLE VI
RETENTION AND RESOLUTION SELECTIVITY OF STRONGLY RETAINED AMINO ACIDS ON A 80×4.6 mm I.D. COLUMN PACKED WITH LICHROSORB RP-18 ($5 \mu\text{m}$)

Amino acid	$10^{-4} M Cu^{2+}$; water-ethanol (85:15)						$10^{-4} M Cu^{2+}$; 18°C						Water-ethanol (85:15); 18°C					
	18°C			35°C			Water-ethanol (70:30)			Water-ethanol (92.5:7.5)			$5 \cdot 10^{-5} M Cu^{2+}$			$2 \cdot 10^{-4} M Cu^{2+}$		
	k'_L	k'_D	α	k'_L	k'_D	α	k'_L	k'_D	α	k'_L	k'_D	α	k'_L	k'_D	α	k'_L	k'_D	α
Ph-Ser	4.75	10.74	2.26	3.67	8.00	2.18	2.91	5.00	1.72	5.64	13.48	2.39	5.24	11.16	2.13	4.01	9.38	2.34
Leu	5.00	9.00	1.40	4.33	7.67	1.77	3.17	3.83	1.21	6.91	10.50	1.52	6.71	9.13	1.36	4.12	6.22	1.51
Norleu	8.25	13.78	1.67	6.33	10.30	1.62	5.29	6.29	1.19	10.39	18.80	1.81	11.31	17.98	1.59	6.11	10.88	1.78
Phe	25.00	40.00	1.60	13.70	21.65	1.58	14.30	17.73	1.24	43.60	75.43	1.73	29.06	45.04	1.55	21.10	36.29	1.72
Trp	40.50	51.00	1.26	33.00	42.60	1.29	17.10	18.63	1.09	85.90	113.38	1.32	48.20	59.77	1.24	35.30	46.24	1.31

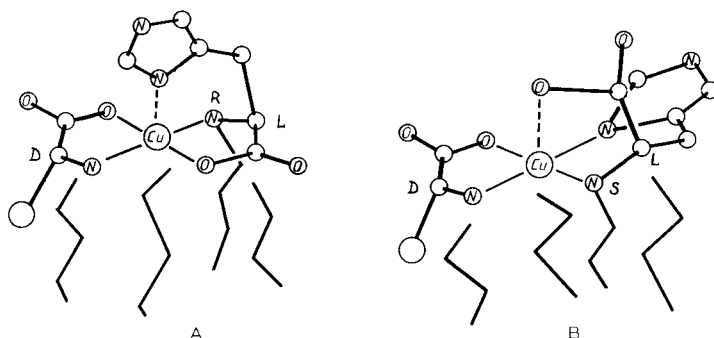


Fig. 1. "Glycine-type" (A) and "diamine-type" (B) ternary sorption complexes.

complexes of N-alkyl-L-proline, the configuration of the asymmetric nitrogen is always unique; in the primary amino group of L-His any of two hydrogen atoms can be replaced with an alkyl group, thus leading the way to two different configurations of the nitrogen, which can interchange even after coordination of a copper ion.

One of these configurations of nitrogen, (*R*), corresponds to a "glycine-type" coordination of copper where a carboxy group and an α -amino group are situated in the main coordination square of copper and the imidazole nitrogen occupies the axial position (Fig. 1A). In this case the ternary sorption complex is situated parallel to the hydrocarbonaceous interface layer and a mobile ligand of D-configuration has the possibility of additional hydrophobic interactions between its α -radical and the sorbent surface. We believe that this structure is responsible for the chiral recognition of mobile ligands with D-enantiomers forming stabler sorption complexes. The only exception is aspartic acid, which shows the opposite elution order of enantiomers. It is logical to suggest that the β -carboxy group of L-aspartic acid forms a hydrogen bond with the imidazole group of the fixed ligand, thus gaining an advantage over the D-isomer, for which only weak interactions with the hydrophobic surface are possible.

However, most fixed ligands seem to coordinate the copper ion according to a "diamine-type" interaction (Fig. 1B) with the carboxy group in the axial position. This situation corresponds to the (*S*)-configuration of the asymmetric α -nitrogen.

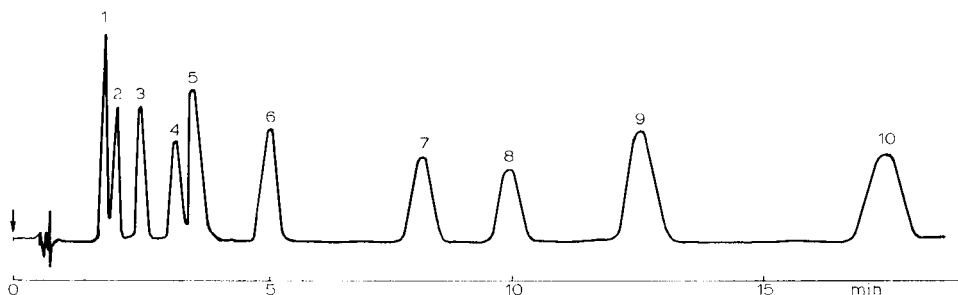


Fig. 2. Resolution of five racemic amino acids on Zorbax C_8 (10 μ m) coated with C_{10} -L-His. Column, 250 \times 4.6 mm I.D. Eluent, 10^{-4} M copper acetate in water. Flow-rate, 2 ml/min. 1 = L-Ala; 2 = D-Ala; 3 = L-Pro; 4 = D-Pro; 5 = L-Abu; 6 = D-Abu; 7 = L-Ival; 8 = D-Ival; 9 = L-Tyr; 10 = D-Tyr.

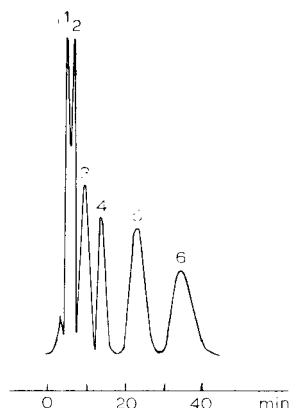


Fig. 3. Resolution of three racemic amino acids on LiChrosorb RP-18. Column, 80×4.6 mm I.D. Flow-rate, 0.5 ml/min. Other conditions as in Fig. 2. 1 = L-Abu; 2 = D-Abu; 3 = L-Val; 4 = D-Val; 5 and 6 = Ph-Ser.

Doubtless the diamine chelate contributes considerably to the retention of amino acid solutes (via ternary sorption complexes), but it does not enhance chiral recognition. α -Amino groups of the two amino acid ligands in such a ternary complex can occupy both the *cis*- and *trans*-positions in the copper coordination square because the carboxy group of the C_{10} -L-His ligand is no longer capable of directing into a *trans*-position the equally charged carboxy group of the mobile ligand, as was the case with the "glycine-type" complexes. At the *trans*-structure of the coordination square plane, hydrophobic interactions with the sorbent favour the binding of the L-solutes, and at the *cis*-structure the binding of D-isomers. Enantioselective effects in the "diamine-type" sorption complexes thus cannot be very high and, moreover, they may even display an opposite sign to the enantioselectivity of the above "glycine-type" sorption complexes.

Situation B possibly occurs more frequently than situation A (Fig. 1). In the

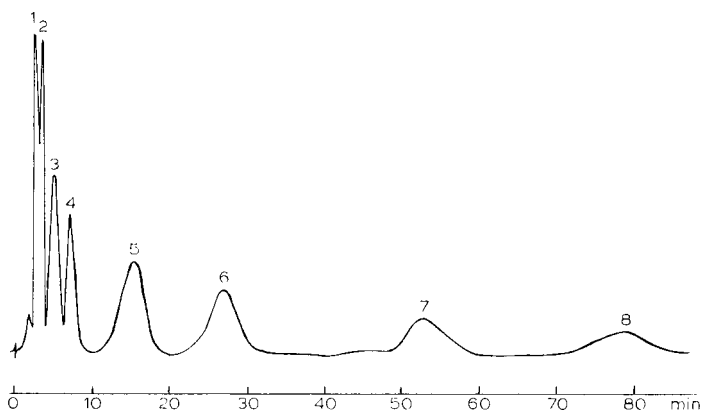


Fig. 4. Resolution of four racemic amino acids. Conditions as in Fig. 3. 1 = L-Abu; 2 = D-Abu; 3 = L-Val; 4 = D-Val; 5 = L-Nleu; 6 = D-Nleu; 7 = L-Phe; 8 = D-Phe.

former structure, both the six-membered chelate ring and the imidazole ring are situated nearly parallel to the surface of the sorbent.

A combination of the above two structures of sorption complexes may provide a basis for a sufficient retention of unmodified amino acids on a C₁₀-L-His-coated packing and for decreasing the enantioselectivity to a level most convenient for analytical separations (Figs. 2–4).

ACKNOWLEDGEMENTS

We are indebted to Drs. R. A. Eyre and J. A. Baxter of Scientific Glass Engineering for kindly supplying chromatographic columns.

REFERENCES

- 1 Yu. A. Zolotarev, N. F. Myasoedov, V. I. Penkina, O. R. Petrenik and V. A. Davankov, *J. Chromatogr.*, 207 (1981) 63.
- 2 V. A. Davankov, A. S. Bochkov, A. A. Kurganov, P. Roumeliotis and K. K. Unger, *Chromatographia*, 13 (1980) 677.
- 3 P. E. Hare and E. Gil-Av, *Science*, 204 (1979) 1226.
- 4 N. LePage, W. Lindner, G. Davies, D. E. Seitz and B. L. Karger, *Anal. Chem.*, 51 (1979) 433.
- 5 E. Oelrich, H. Preusch and E. Wilhelm, *J. High Resolut. Chromatogr. Chromatogr. Commun.*, 3 (1980) 269.
- 6 Y. Tapuhi, N. Miller and B. L. Karger, *J. Chromatogr.*, 205 (1981) 325.
- 7 C. Gilon, R. Leshem and E. Grushka, *J. Chromatogr.*, 203 (1981) 365.
- 8 C. Gilon, R. Leghem and E. Grushka, *Anal. Chem.*, 52 (1980) 1206.
- 9 C. Gilon, R. Leghem, J. Tapuhi and E. Grushka, *J. Amer. Chem. Soc.*, 101 (1979) 7612.
- 10 V. A. Davankov, *Advan. Chromatogr.*, 18 (1980) 139.
- 11 G. Gübitz, W. Jellenz and W. Santi, *J. Chromatogr.*, 203 (1981) 377.
- 12 J. Boué, R. Audebert and C. Quivoron, *J. Chromatogr.*, 204 (1981) 185.
- 13 V. A. Davankov, S. V. Rogozhin, A. A. Kurganov and L. Ya. Zuchkova, *J. Inorg. Nucl. Chem.*, 37 (1975) 369.

CHROM. 13,993

LIGAND-EXCHANGE CHROMATOGRAPHY OF RACEMATES

XVI. MICROBORE COLUMN CHROMATOGRAPHY OF AMINO ACID RACEMATES USING N,N,N',N'-TETRAMETHYL-(R)-PROPANEDIAMINE-1,2-COPPER(II) COMPLEXES AS CHIRAL ADDITIVES TO THE ELUENT

A. A. KURGANOV and V. A. DAVANKOV*

Institute of Organo-Element Compounds, Academy of Sciences, 117813 Moscow (U.S.S.R.)

SUMMARY

A $5 \cdot 10^{-4}$ M solution of $\text{Cu}_2(\text{tmpn})_2(\text{OH})_2(\text{ClO}_4)_2$ in water-acetonitrile (5:1) permits the direct resolution of racemates of aromatic amino acids on reversed-phase silica gel. D-Isomers are eluted after the corresponding L-antipodes. Almost all common racemic amino acids can be resolved in a normal-phase system with water-acetonitrile (1:9) containing the above complex and additional free (R)-tmpn as the eluent. In this instance the order of elution of the enantiomers is reversed (with the exception of Asp and Glu).

INTRODUCTION

In the chromatographic separation of optical isomers, there has recently been great interest in the proposal¹ to add the necessary resolving chiral agent to the eluent instead of grafting it to the stationary phase. Any chiral compound can be used as the resolving reagent if it forms two labile diastereomeric adducts with the racemate under resolution (with adducts that appear to be kinetically inert, their separation becomes trivial, like that of diastereomeric compounds).

As enantioselectivity in the formation of labile coordination compounds has proved to be a common phenomenon, thus providing a general base for ligand-exchange resolutions of complexing racemic compounds (for a review, see ref. 2), chiral complexes have been introduced as the resolving additives in to the eluent in high-performance liquid chromatography (HPLC)³⁻⁸. The use of a "chiral eluent" has the advantage over the classical "chiral stationary phase" method of making possible the use of commercially available HPLC columns. In most instances reversed-phase systems were used⁴⁻⁷, although ion-exchange resins³ and unmodified silica gel packings⁸ have also been tested. As far as the chiral resolving agent is concerned, much remains to be learned about the resolving power and efficiency of different chiral complexes.

This paper describes the use of copper(II)-N,N,N',N'-tetramethyl-(R)-propanediamine-1,2 (tmpn) complexes as chiral additives to the eluent for the resolu-

tion of unmodified α -amino acids on reversed-phase and normal-phase silica gel packings.

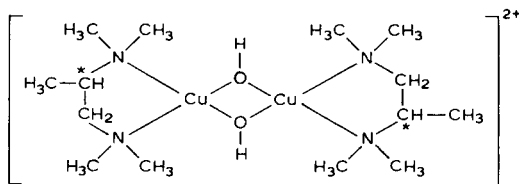
EXPERIMENTAL

N,N,N',N'-Tetramethyl-(*R*)-propanediamine-1,2 was prepared by methylation of (*R*)-propanediamine-1,2 according to Leuckart-Wallach⁹, $[\alpha]_D^{20} = +39.25^\circ$ (benzene, c 1.7). The complex $\text{Cu}_2(\text{tmpn})_2(\text{OH})_2(\text{ClO}_4)_2$ was obtained by mixing ethanolic solutions of (*R*)-tmpn and copper(II) perchlorate and crystallization from aqueous ethanol. For $\text{Cu}_2\text{C}_{14}\text{H}_{38}\text{N}_4\text{Cl}_2\text{O}_{10}$: calculated, Cu 20.48, N 9.03%; found, Cu 20.49, 20.19, N 8.53, 8.84%. Amino acids were purchased from Reanal (Budapest, Hungary), Merck (Darmstadt, G.F.R.) or Serva (Heidelberg, G.F.R.). LiChrosorb RP-18 (5 μm) and Si 100 (10 μm) were obtained from Merck.

The instrument used was a Model 1305 liquid chromatograph (PO "Nauchpribor", U.S.S.R.) equipped with a spectrophotometric detector operated at 254 nm. The detector cell volume was 1 μl . Home-made microbore glass columns (200 \times 1.3 and 100 \times 1.3 mm I.D.) were packed by the balanced-density slurry technique at 600 bar. The volume of the sample solution was 0.5–1.0 μl . The columns were operated at room temperature and a flow-rate of 1–8 ml/h.

RESULTS AND DISCUSSION

Tetramethylpropanediamine-1,2 reacts with Cu(II) ions to form binuclear hydroxo complexes with the structure¹⁰



These complexes are not very stable and are readily transformed into ternary mixed ligand structures if an appropriate amino acid ligand is present in the system:

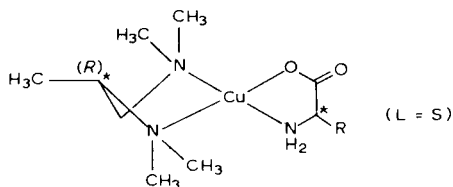


Table I shows the resolutions of a series of racemic amino acids using reversed-phase LiChrosorb RP-18 as the stationary phase and a solution of $\text{Cu}_2(\text{tmpn})_2(\text{OH})_2^{2+}$ in acetonitrile–water (15:85) as the chiral eluent. These results imply that a hydrophobic α -substituent in the amino acid molecule is an important prerequisite for the solute to be retained and chirally recognized in the above system. Hydrophilic amino acids display very low capacity factors, k' , which reflects the hydrophilic character of

TABLE I

RETENTION AND ENANTIOSELECTIVITY OF SEPARATION OF RACEMIC AMINO ACIDS AND MANDELIC ACID ON A LICHROSORB RP-18 (5 μ m) COLUMN (200 \times 1.3 mm I.D.) IN A $5 \cdot 10^{-4}$ M SOLUTION OF $\text{Cu}_2(\text{tmpn})_2(\text{OH})_2(\text{ClO}_4)_2$ IN ACETONITRILE-WATER (1:5)

<i>Racemate</i>	k'_D	k'_L	$\alpha = k'_D/k'_L$
Aspartic acid		0.18	1
Alanine		0.35	1
Isovaline		0.42	1
Valine		0.85	1
Norvaline		0.80	1
Leucine		1.10	1
Norleucine		1.70	1
Methionine		1.67	1
Serine		0.37	1
N,N-Dibenzylserine		3.90	1
Phenylserine*	7.33	6.81	1.08
Phenylglycine		2.00	1
Phenylalanine	5.96	5.75	1.04
Tyrosine	1.87	1.67	1.12
Dihydroxyphenylalanine	2.40	2.25	1.07
Tryptophan	10.30	9.00	1.14
Mandelic acid*	1.33	1.12	1.20

* Arbitrary assignment of enantiomers.

the resolving chiral reagent, $\text{Cu}_2(\text{tmpn})_2(\text{OH})_2^{2+}$, which is eluted within the void volume of the reversed-phase column.

Obviously, the amino acid (AA) itself has to be sufficiently hydrophobic in order to be retained on the sorbent surface and to promote adsorption of the ternary complex $\text{Cu}(\text{AA})(\text{tmpn})^+$. This particular case fits into the second or third of the three previously discussed¹¹ extreme situations in the "chiral eluent" technique, where the solute retention is governed by adsorption of (i) the resolving chiral ligand, (ii) the ternary complex or (iii) the racemate itself (the first and, occasionally, the third situations are accompanied by the ternary complex adsorption).

Two requirements should be met in order to achieve resolution of a racemic solute according to the "chiral eluent" method: (i) the solute should be retained on the sorbent (by one of the above retention mechanisms or their combination) and (ii) there should be enantioselectivity in the formation of ternary solute-metal-resolving ligand complexes. Apparently, there is no significant enantioselectivity in the case of Val, Norval, Leu, Norleu, Met, Ph-Gly and Bz₂-Ser which are retained but are not resolved. We cannot be certain about the absence of enantioselectivity in ternary complexes of Ala, Asp and Ser because these solutes are hardly retained in our system. Enantioselectivity, although relatively small, is certainly present in ternary tmpn-copper complexes of Tyr, DOPA, Phe, Ph-Ser and Trp, the L-enantiomers of which elute ahead of the D-isomers.

The nature of these enantioselectivity effects remains largely unknown. It is important to be aware that in the system discussed ternary complexes are formed both in the bulk solution and on the surface of the sorbent and that the stability and

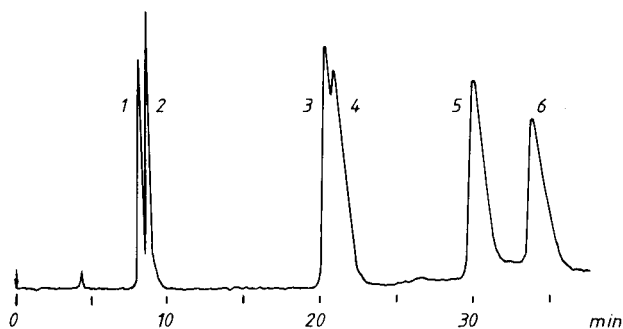


Fig. 1. Separation of three racemic amino acids on a LiChrosorb RP-18 ($5\ \mu\text{m}$) column ($200 \times 1.3\ \text{mm}$ I.D.). Eluent: acetonitrile–water (1:5) containing $5 \cdot 10^{-4}\ M\ \text{Cu}_2(\text{tmpn})_2(\text{OH})_2(\text{ClO}_4)_2$. Flow-rate, 1 ml/h. Detection, 254 nm. 1 = L-Tyr; 2 = D-Tyr; 3 = L-Phe; 4 = D-Phe; 5 = L-Trp; 6 = D-Trp.

enantioselectivity of these two species can be entirely different. We can assume that sorbent-bond complexes ("sorption complexes") are responsible for the resolution in our work, because only the more strongly retained amino acids are resolved in the reversed-phase system and because the k' values of these amino acids are significantly lower in the absence of Cu(II) or tmpn.

The fact that all of the solutes resolved happen to be aromatic amino acids (Fig. 1) suggests that the ternary sorption complexes of these solutes possess an unusual conformation, probably with the aromatic group axial to the copper ion. This conformation may result in an enhanced interaction of the diamine chelate ring with the hydrophobic surface of the sorbent, thus increasing the enantioselectivity of the ternary sorption complex.

Contrary to LiChrosorb RP-18, unmodified LiChrosorb Si 100 silica gel strongly retains the chiral resolving complex from its solution in aqueous acetonitrile, which is also shown by the intense blue colour of the sorbent. The interaction of Cu(II) ions or positively charged copper–diamine complexes with the silica gel surface is primarily of an electrostatic nature, so that decreasing the pH value of the eluent

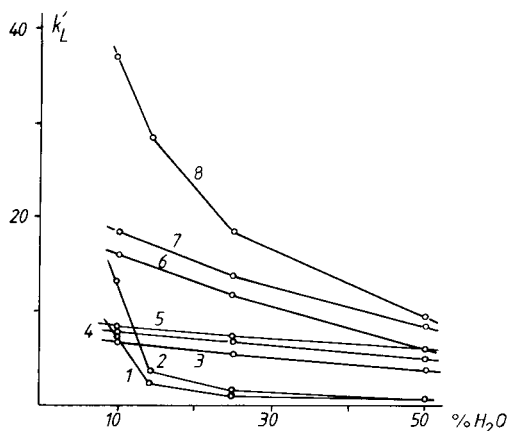


Fig. 2. Retention of L-amino acids as a function of water to acetonitrile ratio in the eluent. LiChrosorb Si 100 ($10\ \mu\text{m}$) column. Chiral additive to the eluent: $5 \cdot 10^{-4}\ M\ \text{Cu}_2(\text{tmpn})_2(\text{OH})_2(\text{ClO}_4)_2$ and $5 \cdot 10^{-3}\ M\ (R)\text{-tmpn}$. 1 = Asp; 2 = Glu; 3 = Ile; 4 = Met; 5 = Tyr; 6 = Pro; 7 = Thr; 8 = Ser.

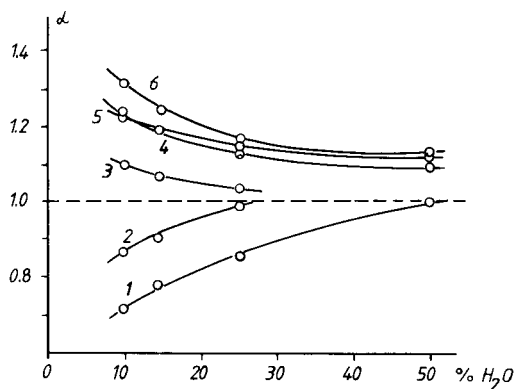


Fig. 3. Enantioselectivity as a function of water to acetonitrile ratio in the eluent. LiChrosorb Si 100 (10 μ m) column. Chiral additive to the eluent: $5 \cdot 10^{-4}$ M $\text{Cu}_2(\text{tmpn})_2(\text{OH})_2(\text{ClO}_4)_2$ and $5 \cdot 10^{-3}$ M (*R*)-tmpn. 1 = Asp; 2 = Glu; 3 = Val; 4 = Phe; 5 = Tyr; 6 = Trp.

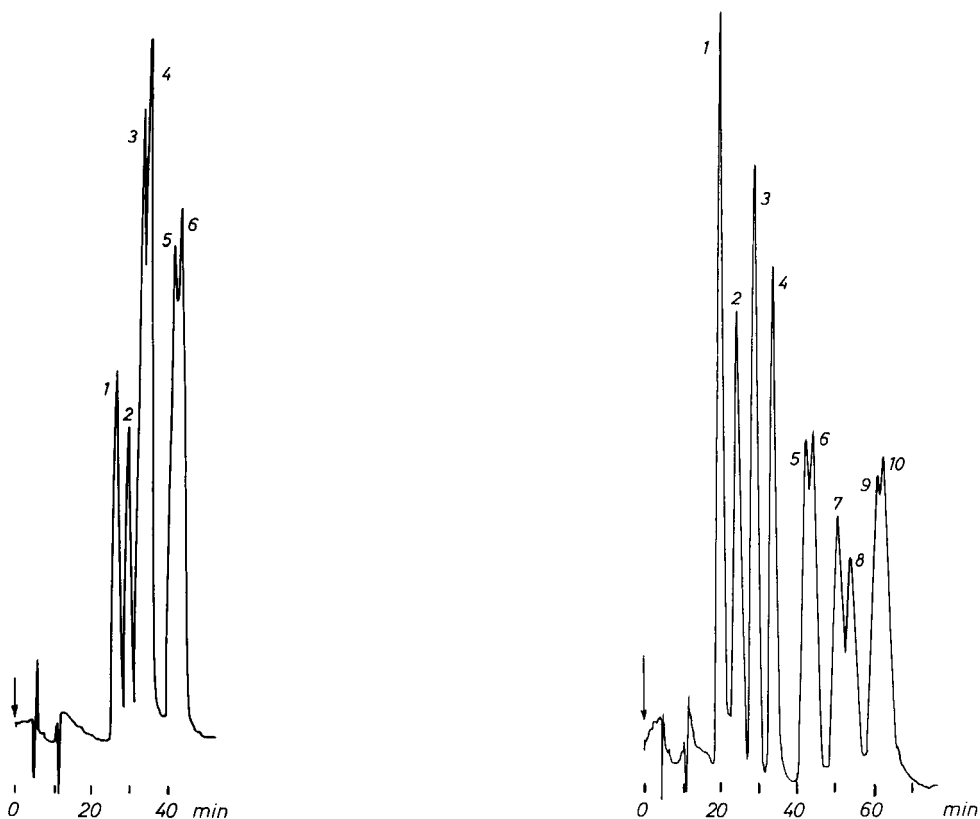


Fig. 4. Separation of three racemic amino acids on a LiChrosorb Si 100 (10 μ m) column (100 \times 1.3 mm I.D.). Eluent: acetonitrile–water (85:15) containing $5 \cdot 10^{-4}$ M $\text{Cu}_2(\text{tmpn})_2(\text{OH})_2(\text{ClO}_4)_2$ and $5 \cdot 10^{-3}$ M (*R*)-tmpn. Flow-rate, 2 ml/h. Detection, 254 nm. 1 = D-Phe; 2 = L-Phe; 3 = D-Val; 4 = L-Val; 5 = D-Abu; 6 = L-Abu.

Fig. 5. Separation of five racemic amino acids on LiChrosorb Si 100. Conditions as in Fig. 4. 1 = L-Asp; 2 = D-Asp; 3 = D-Trp; 4 = L-Trp; 5 = D-Abu; 6 = L-Abu; 7 = D-Pro; 8 = L-Pro; 9 = D-Thr; 10 = L-Thr.

TABLE II

RETENTION AND ENANTIOSELECTIVITY OF SEPARATION OF RACEMIC AMINO ACIDS ON A LICHROSORB Si 100 (10 μ m) COLUMN (100 \times 1.3 mm I.D.) IN A SOLUTION OF $5 \cdot 10^{-4}$ M $\text{Cu}_2(\text{tmpn})_2(\text{OH})_2(\text{ClO}_4)_2$ AND $5 \cdot 10^{-5}$ M (R)-tmpn IN DIFFERENT ACETONITRILE-WATER MIXTURES

Amino acid	90:10			85:15			75:25			50:50		
	k'_L	k'_D	α^*	k'_L	k'_D	α^*	k'_L	k'_D	α^*	k'_L	k'_D	α^*
Aspartic acid	7.44	10.5	0.72	3.40	4.30	0.79	1.28	1.50	0.85	0.55		1
Glutamic acid	15.1	17.4	0.87	6.66		1	1.72		1	0.55		1
Alanine		16.8	1	15.8		1	13.2		1	8.05		1
Aminobutyric acid (Abu)	12.1	11.2	1.07	8.77	8.33	1.05	7.33		1	6.77		1
Isovaline		13.7	1				9.83		1	5.89		1
Valine	8.83	8.05	1.10	7.87	7.37	1.07	7.00	6.80	1.03	5.78		1
Norvaline	8.16	7.61	1.07				6.72		1	5.00		1
Isoleucine	8.05	7.39	1.09	7.50	7.00	1.07	6.75	6.50	1.03	4.83		1
Leucine		6.78	1				5.83		1	4.61		1
Norleucine		7.23	1		6.25	1	5.00		1	4.05		1
Proline	16.1	14.4	1.12	11.0	10.2	1.08	9.30		1	6.11		1
Serine	37.3	35.4	1.05	25.7	24.7	1.04	18.3		1	9.61		1
Phenylserine**	6.10	5.15	1.12	4.89	4.55	1.07	4.28	3.89	1.10	3.94	3.78	1.04
Threonine	18.6	17.6	1.06	12.8	12.4	1.03	10.4		1	8.17		1
Methionine	7.89	7.22	1.09	6.11	5.77	1.06	5.43	5.17	1.05	4.94		1
Phenylglycine		7.17	1				4.66		1	4.28		1
Phenylalanine	6.11	5.00	1.22	5.67	4.89	1.20	5.14	4.66	1.10	4.77	4.38	1.09
Thyrosine	8.55	6.94	1.23	9.11	7.67	1.19	7.17	6.22	1.15	6.05	5.39	1.12
Tryptophan	6.80	5.40	1.31	6.33	5.33	1.16	5.50	4.85	1.13	4.88	4.33	1.13

* $\alpha = k'_L/k'_D$.

** Arbitrary assignment of enantiomers.

or increasing its ionic strength leads to rapid desorption of copper(II) ions. For this reason, it is impossible to keep the column capacity constant if the eluent (acetonitrile–water, 1:1) contains only $5 \cdot 10^{-4} M$ $\text{Cu}_2(\text{tmpn})_2(\text{OH})_2(\text{ClO}_4)_2$. To stabilize the system, an excess of chiral diamine has to be added to the eluent. In addition to stabilization of the column parameters, the excess of diamine ligand results in a decrease in the retention of amino acids.

It can be seen from Table II that the retention of amino acids in the normal-phase system differs considerably from that in the reversed-phase system: hydrophobic amino acids elute first, followed by hydrophilic amino acids. This observation agrees with results of Foucault *et al.*¹² for amino acid analysis using copper-modified silica gel columns. Aspartic acid and glutamic acid, although strongly hydrophilic, are negatively charged in the alkaline eluent and are expelled from the silica surface. However, they are strongly retained with a high content of acetonitrile in the eluent. Generally, the lower the water concentration in the eluent, the higher is the retention of hydrophilic amino acids (Fig. 2). Hence the retention of hydrophobic solutes increases insignificantly.

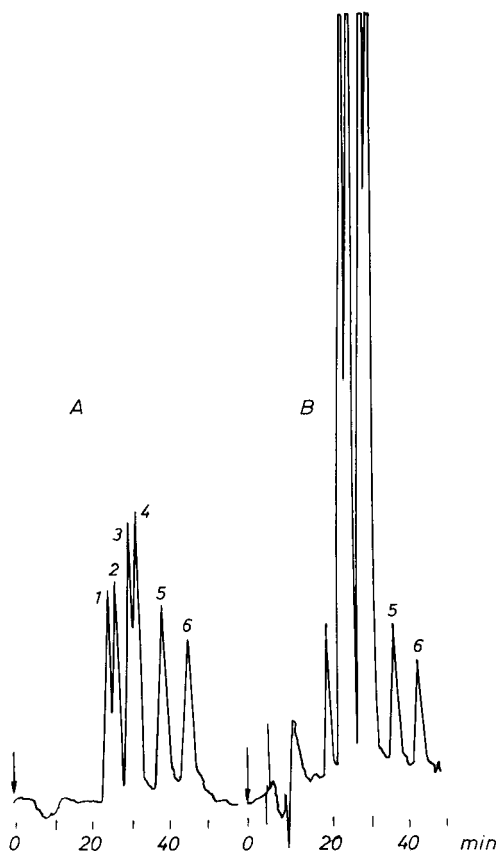


Fig. 6. Separation of three racemic amino acids on LiChrosorb Si 100. Conditions as in Fig. 4. 1 and 2 = Ph-Ser; 3 = D-Met; 4 = L-Met; 5 = D-Tyr; 6 = L-Tyr. A, Fresh solution of amino acids in the eluent; B, the same solution after 4 h.

Simultaneously, a decrease in the water content in the eluent leads to an increase in the separation enantioselectivity (Fig. 3), probably due to enhancement of the interaction of the ternary sorption complex with the silica surface. The mode of this interaction seems to be different from that on the reversed-phase sorbent, as the order of elution of the enantiomers is reversed, with the D-isomers eluting ahead of the L-isomers, except for aspartic acid and glutamic acid isomers.

The opposite directions of the net enantioselectivity effects in normal- and reversed-phase systems clearly demonstrate the difference in the properties of ternary sorption complexes that exist on the sorbent surface and those of the corresponding ternary complexes that exist in the bulk solution.

In both the reversed-phase and normal-phase systems, the enantioselectivity values (α) are not very high, but are still sufficient for the resolution of many amino acids and their mixtures (Figs. 4–6). The normal-phase system is especially useful for the rapid enantiomeric analysis of aromatic amino acids. Phenylalanine and tryptophan can be analysed within a few minutes (Fig. 7). An unexpected peculiarity of the eluent containing an excess of basic (*R*)-tmpn is the oxidation of phenolic groups: DOPA is rapidly oxidized and tyrosine disappears within 4 h (Fig. 6). It is interesting that a neutral solution of $\text{Cu}_2(\text{tmpn})_2(\text{OH})_2(\text{ClO}_4)_2$ is devoid of oxidizing properties (Fig. 1).

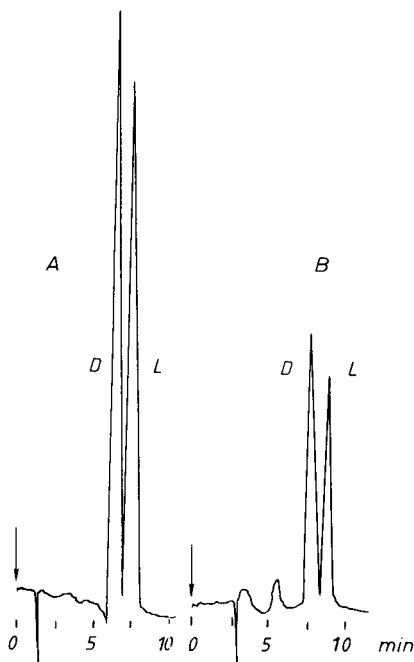


Fig. 7. Rapid analysis of racemic phenylalanine (A) and tryptophan (B) on a LiChrosorb Si 100 (10 μm) column (100 \times 1.3 mm I.D.). Eluent: acetonitrile-water (9:1) containing $5 \cdot 10^{-4}$ M $\text{Cu}_2(\text{tmpn})_2(\text{OH})_2(\text{ClO}_4)_2$ and $5 \cdot 10^{-3}$ M (*R*)-tmpn. Flow-rate, 8 ml/h. Detection, 254 nm.

REFERENCES

- 1 L. R. Sousa, D. H. Hoffman, L. Kaplan and D. J. Cram, *J. Amer. Chem. Soc.*, 96 (1974) 7100.
- 2 V. A. Davankov, *Advan. Chromatogr.*, 18 (1980) 139.
- 3 P. E. Hare and E. Gil-Av, *Science*, 204 (1979) 1226.
- 4 Y. Tapuhi, N. Miller and B. L. Karger, *J. Chromatogr.*, 205 (1981) 325.
- 5 C. Gilon, R. Leshem and E. Grushka, *J. Chromatogr.*, 203 (1981) 365.
- 6 S. Lam, F. Chow and A. Karmen, *J. Chromatogr.*, 199 (1980) 295.
- 7 E. Gil-Av, A. Tishbee and P. E. Hare, *J. Amer. Chem. Soc.*, 102 (1980) 5115.
- 8 E. Oelrich, H. Preusch and E. Wilhelm, *J. High Resolut. Chromatogr. Chromatogr. Commun.*, 3 (1980) 269.
- 9 G. Hilgetag and A. Martini, *Weigand-Hilgetag, Organisch-chemische Experimentierkunst*, J. A. Barth Verlag, Leipzig, 3rd ed., 1964.
- 10 C. Abcus, K. P. Fivizzani and S. Pavkovic, *J. Inorg. Nucl. Chem.*, 39 (1977) 285.
- 11 V. A. Davankov and A. A. Kurganov, *Chromatographia*, 13 (1980) 339.
- 12 A. Foucault, M. Caude and L. Oliveros, *J. Chromatogr.*, 185 (1979) 345.

CHROM. 14,096

COMPARISON OF SHORT AND ULTRASHORT-CHAIN ALKYL-SILANE-BONDED SILICAS FOR THE HIGH-PERFORMANCE LIQUID CHROMATOGRAPHY OF PROTEINS BY HYDROPHOBIC INTERACTION METHODS

E. C. NICE and M. W. CAPP

Ludwig Institute for Cancer Research (London Branch), Royal Marsden Hospital, Sutton, Surrey SM2 5PX (Great Britain)

N. COOKE

Altex Scientific Inc., Subsidiary of Beckman Instruments, 1780 Fourth Street, Berkeley, CA 94710, (U.S.A.)
and

M. J. O'HARE*

Ludwig Institute for Cancer Research (London Branch), Royal Marsden Hospital, Sutton, Surrey SM2 5PX (Great Britain)

SUMMARY

The optimization of the reversed-phase high-performance liquid chromatography of proteins has been examined using a series of maximum-coverage alkylsilane-bonded silica packings with different carbon chain-lengths (C_1 – C_{18}). The greatest range of individual compounds that could be successfully chromatographed was obtained with $< C_6$ chain-length packings. Optimum recoveries and efficiencies were noted with a C_3 material (Ultrasphere SAC). No loss of performance or changes in selectivity were observed during prolonged use (> 200 h) of these columns under acid (pH 2.1) conditions. This system has been used to separate prolactin and growth hormone (22 kD) from biological samples by employing a trace-enrichment step on 10- μ m tap-packed short alkyl-chain columns prior to gradient-elution chromatography on a 5- μ m particle-size (8 nm pore-size) Ultrasphere SAC column.

INTRODUCTION

One of the most powerful applications of high-performance liquid chromatography (HPLC) to emerge in recent years in respect of biological molecules has been the separation of peptides using alkylsilane-bonded and related reversed-phase (RP) type materials. Although these techniques have, for the most part, been used for the separation of relatively small molecules, larger polypeptides^{1,2} and indeed small proteins^{3,4} can be successfully chromatographed. As with the smaller polypeptides it appears that protein separations are dictated primarily by the interaction of their more accessible hydrophobic constituents or domains with the stationary phase.

TABLE I
SOURCES AND DETAILS OF POLYPEPTIDE AND PROTEIN STANDARDS USED

Compound	Supplier	Mol.wt. (kD)	Abbreviation used
Calcitonin (synthetic human)	Ciba (Basle, Switzerland)	3.4	hCT
Epidermal growth factor (mouse)	Collaborative Research (Waltham, MA, U.S.A.)	6.0	mEGF
Parathyroid hormone (bovine)	Dr. J. Zanelli (National Institute for Biological Standards and Control (NIBSC), Holly Hill, Hampstead, Great Britain)	9.5	bPTH
Cytochrome <i>c</i> (horse heart type III)	Sigma (Poole, Great Britain)	11.7	Cyt <i>c</i>
Ribonuclease A (bovine pancreas type IIIA)	Sigma	14.2	RNase
α -Lactalbumin (bovine)	Sigma	14.2	b α -Lact
α -Lactalbumin (rat)	Dr. K. E. Ebner (University of Kansas, Kansas City, U.S.A.)	14.2	r α -Lact
Lysozyme (hen eggwhite 3 \times recryst, A grade)	Calbiochem-Behring (Bishops Cleeve, Great Britain)	14.3	Lys
¹⁴ C-Methylated lysozyme*	Amersham International (Amersham, Great Britain)	14.3	
α -Hemoglobin (bovine)	Dr. J. Zanelli	15.1	α Hb
Myoglobin (whale muscle)	Calbiochem-Behring	17.2	Myo
β -Lactoglobulin A (bovine milk)	Sigma	18.3	Lactog A
β -Lactoglobulin B (bovine milk)	Sigma	18.3	Lactog B
Growth hormone (bovine GH-B-18)	National Institute of Arthritis, Metabolism and Digestive Diseases (NIAMDD), Pituitary Hormone Distribution Program (Bethesda, MD, U.S.A.)	22.0	bGH
Growth hormone (rat GH-B-6)	NIAMDD	22.0	rGH
Human placental lactogen	ICN Pharmaceuticals (Cleveland, OH, U.S.A.)	22.1	hPL
Prolactin (ovine P-S-13)	NIAMDD	22.6	oPRL
Prolactin (rat PRL-B-2)	NIAMDD	22.6	rPRL
Elastase (porcine pancreas type III)	Sigma	25.9	Elas
Carbonic anhydrase (bovine erythrocytes)	Sigma	29.0	CA
¹⁴ C-Methylated carbonic anhydrase*	Amersham International	30.0	
Ovalbumin (hen eggwhite, fraction V)	Sigma	45.0	Ovalb
Human serum albumin (fatty acid free)	Sigma	66.5	HSA
Bovine serum albumin (fraction V)	Sigma	68.0	BSA
¹⁴ C-Methylated bovine serum albumin*	Amersham International	69.0	

* Prepared by reductive alkylation with [¹⁴C]formaldehyde and sodium cyanoborohydride at pH 7.0 (ref. 10).

Experience in the optimization of such RP-systems specifically for protein chromatography is, however, still limited⁵. The majority of comparable studies with peptides and polypeptides have utilized long-chain packings of the C₁₈ (octadecylsilane) type. Some large polypeptides, such as, for example, bovine² and human⁶ parathyroid hormone (9.5 kD) can be successfully chromatographed with such supports, as can some even larger materials (< 69 kD)^{3,4}; it is, however, our experience that many small proteins well below the nominal exclusion limit of these mesoporous (6–10 nm) silica-based packings either cannot be eluted³, or give poor recoveries with these systems.

The use of C₈ (octylsilane) RP-packings and solvents such as propanol have both been shown to be advantageous for the separation of this type of compound⁷. The use of other shorter chain alkylsilane-bonded materials for protein chromatography by these "hydrophobic interaction" RP-HPLC methods has not, however, been systematically investigated. We report here such a study, and show that certain other short-chain alkylsilane-bonded silica packings afford additional advantages for protein HPLC. Not only can a larger number of individual compounds be chromatographed, but overall recoveries of proteins are also enhanced.

MATERIALS AND METHODS

Sources and details of individual protein standards used in this study are given in Table I. An explant culture of a pituitary gland from a lactating rat was used to generate a natural mixture of protein hormones. Nutrient medium from the culture was acidified (pH 2.1) and pumped through an 85 × 5 mm I.D. column containing tap-packed LiChrosorb RP-2 (as Table II except 10- μ m particle size) to trace-enrich the hormones therein. Adsorbed proteins were eluted using a step gradient of acetonitrile in pH 2.1 0.155 M NaCl solution, as described in previous studies of high molecular weight calcitonin-like materials⁸, and the organic modifier removed by evaporation under nitrogen prior to analytical chromatography of the fraction containing prolactin and growth hormone.

Analytical HPLC of these extracts and of protein standards was carried out with a series of 150 × 5 mm I.D. stainless-steel columns packed with each of the supports listed in Table II. Operating conditions were controlled using either a Spectra-Physics SP 8000, or an Altex Model 324-40 chromatograph. Dead volumes between the gradient former and column heads were different in these two instruments (low-pressure and high-pressure mixing, respectively), resulting in slight differences in absolute retention times of the proteins using the two systems, under gradient-elution conditions.

Separations were performed at 45 C and a constant flow of 1 ml/min, using continuous linear gradient elution between an aqueous primary solvent of 0.155 M NaCl solution adjusted to pH 2.1 with HCl, and a secondary solvent of either acetonitrile, or propan-2-ol (Rathburn Chemicals, Walkerburn, Great Britain). Eluted proteins were detected by UV-absorbance at 215 nm (acetonitrile gradients) or 280 nm (propan-2-ol gradients) (Schoeffel FS 770) and endogenous tryptophan fluorescence, 225 nm excitation, 340 nm emission filter (acetonitrile) or 280/370 nm (propan-2-ol) (Schoeffel FS 970). Radioactive ¹⁴C-proteins were detected on-line using a Packard 7500 HPLC monitor. Confirmation of the identity of eluted proteins was obtained

TABLE II
DETAILS OF RP-PACKINGS AND COLUMNS

<i>Packing</i>	<i>Carbon chain-length</i>	<i>Particle size (μm)</i>	<i>Pore diameter (nm)</i>	<i>Pore vol. (ml/g)</i>	<i>Specific surface area (m^2/g)</i>	<i>Shape*</i>	<i>Length (cm)</i>
Ultrasphere SAS	1	4-6	8	0.57	180	S	15
LiChrosorb RP-2	1	5-7	ND***	ND	500	I	15
Ultrasphere SAC	3	4-6	8	0.57	180	S	15
Spherisorb SSC6	6	3-7	8	0.57	200	S	15
LiChrosorb RP-8	8	4-7	ND	ND	>250	I	15
LiChrosorb RP-18	18	4.3 7.3	ND	ND	>100	I	15
Ultrasphere ODS	18	4-6	8	0.57	180	S	15
Hypersil ODS	18	5-7	10	0.7	200	S	15

* S = spherical, I = irregular.

** PP = packed by manufacturer, LP = packed in laboratory from methanol slurry.

*** ND = not divulged by manufacturer but probably 6-10 nm.

both by polyacrylamide gel electrophoresis of HPLC eluate fractions after evaporation of the organic modifier, and by determination of their retention times on a TSK SW 3000 size-exclusion column (600 \times 7.5 mm I.D.) with pH 7.0 phosphate buffer as eluent.

Recoveries of proteins obtained with the different columns tested (Table II) were estimated by one of three methods, depending on the types and quantities of the proteins involved. With standards available in large quantities the protein content of 1-ml eluate fractions was measured directly using a spectrophotometric Coomassie blue metachromatic method (Bio-Rad) with a detection limit, under the conditions used, of >20- μg fraction. The recovery of ^{14}C -methylated proteins was calculated directly from the radioactivity in peak fractions in eluate aliquots measured by liquid scintillation counting. For standards available in more limited amounts, or for which radioactive analogues were not available, an indirect method of estimating recovery was adopted. This was based on the relative areas of the protein peaks on the initial chromatogram, and of the corresponding "ghost" peaks, if any, seen on subsequent "blank" gradient-elution runs. These peaks of incompletely eluted protein diminished in size in sequential blank chromatograms and a linear regression analysis enabled the total amount of protein, and thus the recovery obtained from the initial chromatogram to be calculated. Good agreement ($\pm 5\%$) was obtained between recoveries calculated in this manner and measured directly using the Coomassie blue protein assay.

Recovery of biological activity was monitored in the case of lysozyme using a turbidimetric method⁸ and for elastase by the Congo red-elastin assay⁹.

RESULTS

Our initial series of experiments was aimed at establishing (1) which individual proteins could be chromatographed on the short and ultra-short alkylsilane-bonded

silica packings listed in Table II, and (2) whether practically useful selective effects could be obtained with individual packings of this type in respect of closely eluted proteins. For the purposes of this study, the results of which are given in Table III, acetonitrile was used as the organic modifier. In most cases between 5–20 μ g of each protein was injected. Although propanol affords significant advantages for protein

TABLE III

RETENTION TIMES (min) OF POLYPEPTIDE AND PROTEIN STANDARDS RELATIVE TO LYSOZYME

Short and ultra-short alkylsilane-bonded RP-packings were used under gradient-elution conditions (Spectra Physics SP8000 chromatograph, gradient profile as illustrated in Fig. 1) with acetonitrile as organic modifier and pH 2.1 0–0.155 *M* NaCl as primary solvent. See Table I for abbreviations used. NT = not tested; NR = not recovered using CH₃CN as organic modifier.

<i>Standards</i>	<i>C</i> ₁ [*]	<i>C</i> ₃ ^{**}	<i>C</i> ₆ ^{***}	<i>C</i> ₈ [§]
RNase	– 10.2	– 10.7	– 11.3	– 12.0
mEGF	NT	– 7.6	– 8.0	NT
hCT	– 4.1	– 4.4	– 4.1	– 5.0
Cyt <i>c</i>	– 2.5	– 3.1	– 2.3	– 3.8
bPTH	– 2.4	– 2.3	– 2.1	– 2.6
Lysozyme	0	0	0	0
BSA	3.2	3.3	5.8	7.2
HSA	3.8	3.5	NT	NT
b α -Lact	4.6	7.4	6.6	7.2
r α -Lact	4.9	NT	7.9	NT
Myoglobin	7.1	9.0	9.5	8.9
α Hb	8.2	9.2	9.6	11.3
CA	9.8	9.5	9.6	10.0
Lactog A	10.1	10.0	NT	8.8
Lactog B	10.1	10.0	NT	8.8
Elastase	11.1	10.0	11.7	NR
oPRL	13.1	16.7	16.6	16.6
hPL	14.3	20.2	17.6	18.5
rPRL	17.3	25.0	20.0	29.1
bGH	17.3	29.0	NT	39.4
Ovalbumin	NR	NR	NR	NR

* LiChrosorb RP-2.

** Ultrasphere SAC (experimental).

*** Spherisorb S5C6.

§ LiChrosorb RP-8.

HPLC⁷ its UV-absorbance limits the use of low-wavelength detection; consequently a number of high-purity proteins used in this study, and available in only limited quantities could not have been directly detected.

It is evident from Table III that a wide variety of proteins which cannot be chromatographed on *C*₁₈ packings can be successfully recovered from the short-chain materials. Furthermore, while most of the compounds tested could be eluted from,

albeit with varying recoveries, all short and ultrashort-chain packings, at least one protein tested (elastase) could only be recovered from C_6 or shorter-chain materials with acetonitrile as the organic modifier. The identity of the eluted peak was in this instance confirmed by both physical and biological methods (see Materials and methods). Thus, full biological activity was obtained from the protein eluted from the ultra-short chain packings after removal of the organic modifier from the eluent by evaporation.

Comparison of the retention times of these protein standards with that of lysozyme (Table III), under constant conditions of gradient elution with acetonitrile in acid (pH 2.1) saline, showed that while most increased with increasing chain-length (and carbon loading) of the packing, no reversals in retention order indicative of marked changes in selectivity were apparent. Thus by appropriate modification of the slope of the linear gradient profile (see Fig. 1) a virtually identical elution profile could be obtained with all the RP-supports tested. The separation of a series of such standards on a C_3 packing (Ultrasphere SAC) is illustrated in Fig. 1. Fig. 2 shows the UV-absorbance profile obtained with this column when a trace-enriched extract (see Materials and methods) of tissue culture medium from a lactating rat pituitary gland was chromatographed. The resolution of growth hormone and prolactin (both 22 kD) from this sample and their separation from other proteins was thus readily obtained by the use of RP-HPLC methods.

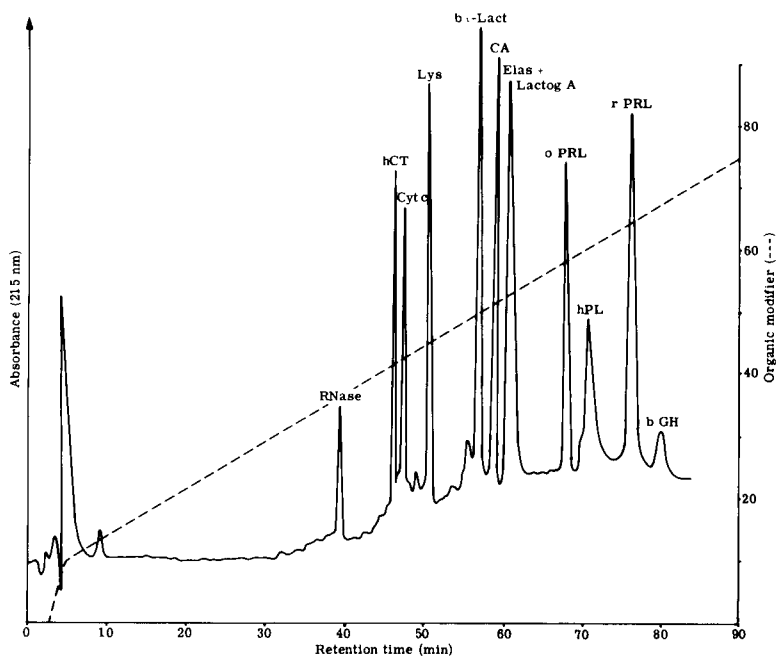


Fig. 1. Separation of protein standards (see Table I for abbreviations) on 150×5 mm I.D. Ultrasphere SAC column. Compounds were eluted with a linear gradient of acetonitrile (dotted line) in pH 2.1 0.155 *M* NaCl solution at 45 °C and a flow-rate of 1 ml/min (Spectra-Physics SP 8000). The identity of all protein peaks was confirmed by SDS-PAGE.

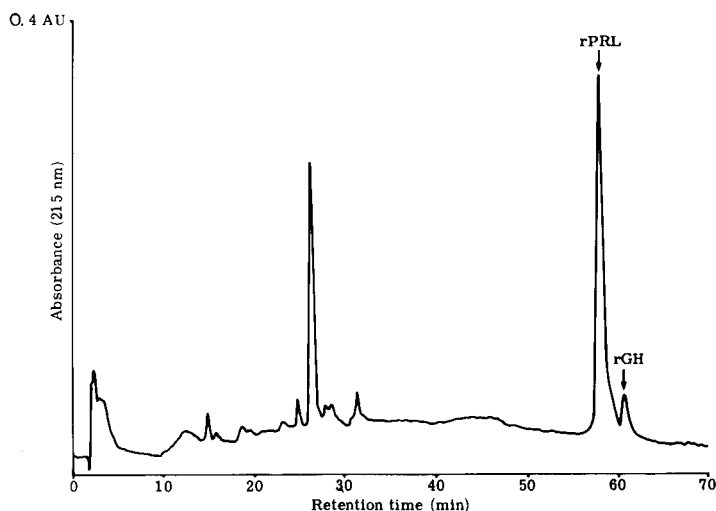


Fig. 2. Separation of hormones secreted by rat pituitary explant culture by RP-HPLC. Conditions of chromatography as Fig. 1, except using an Altex Model 324-40 chromatograph. Note resolution of prolactin (rPRL) and growth hormone (rGH) in this trace-enriched culture medium extract.

No significant loss of efficiency was noted with these packings when the elution volumes of a variety of proteins were compared. The only exception was the ultra-short chain materials (LiChrosorb RP-2, Hypersil SAS) on which the total elution volumes of typical proteins were increased by $<40\%$ compared with the other short-chain materials (C_3 – C_8). Preliminary experiments have noted further improvements in efficiency when large pore-size (30 nm) supports of the latter type were used.

The most notable advantage of the short-chain alkylsilane packings apparent from the present study was the improved recovery of many of the proteins tested. This was evident from the size of the "ghost" peaks seen with many compounds on the longer-chain materials, including C_8 packings, and their diminution or complete absence under identical conditions of gradient elution using the shorter chain (*i.e.* C_3) columns. This improvement in recovery is shown in quantitative form in respect of ovalbumin in Table IV. Although this 45 kD protein could not be eluted from any RP-packing tested when acetonitrile was used as the secondary solvent, it could be recovered, in varying yields, using propanol, a solvent which has been shown to have superior properties for protein RP-HPLC by other workers⁷. Recoveries on C_8 packings were, however, low (22%), while with C_{18} columns they were negligible (8%). Optimal recoveries of this protein (78%) were obtained when a C_3 packing (Ultrasphere SAC) was used. With even shorter alkylsilane-bonded phases recoveries were, however, somewhat reduced compared with the C_3 material. Optimal recoveries with the C_3 packing were also seen with a variety of other standards tested, and this stationary phase offered significant advantages in this respect over both C_8 and, to a lesser extent, C_6 -type packings.

As the recovery of individual proteins can pose problems with these RP-HPLC methods, the use of an internal standard in the form of a radiolabelled protein might seem of value when processing biological extracts. Examination of the elution profiles

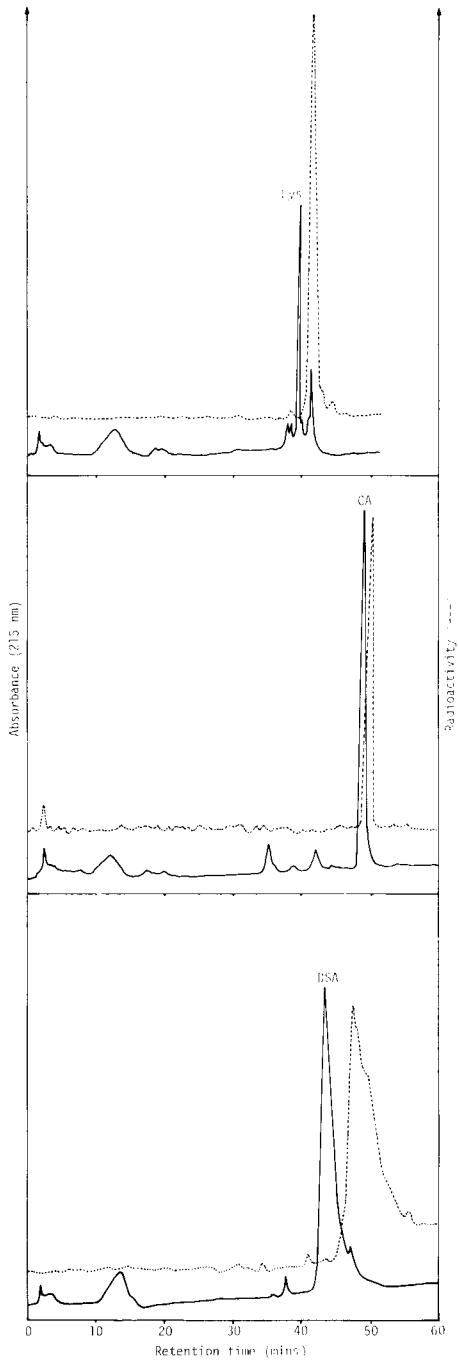


Fig. 3. RP-HPLC of ^{14}C -methylated proteins and their non-radioactive congeners. Simultaneous UV-absorbance and radioactivity profiles were determined with conditions of chromatography as in Fig. 1, except for the use of an Altex Model 324-40 chromatograph. Note separation of the radiolabelled proteins from their non-radioactive precursors.

TABLE IV

RECOVERY (%) OF PROTEIN STANDARDS FROM RP-PACKINGS

BSA (50 μ g) and ovalbumin (150 μ g) were separated on 150 \times 5 mm columns using a primary solvent of 0.155 *M* NaCl (pH 2.1) with propan-2-ol as organic modifier and a gradient of the form illustrated in Fig. 1. Recoveries were calculated from the respective peak heights on these chromatograms and those of ghost peaks due to incompletely eluted materials on subsequent blank runs.

<i>Packing</i>	<i>BSA (65 kD)</i>	<i>Ovalbumin (45 kD)</i>
LiChrosorb RP-2	100	35
Ultrasphere SAC	100	78
Spherisorb S5C6	100	57
LiChrosorb RP-8	100	22
LiChrosorb RP-18	100	8

of ^{14}C -methylated proteins tested (lysozyme, carbonic anhydrase and bovine serum albumin) revealed, however, that all were eluted at a slightly different place on the gradient from their respective unlabelled parent compounds (Fig. 3). Thus, their chromatographic properties differ from those of their parent molecules. They do not, therefore, constitute entirely appropriate internal standards for RP-HPLC when prepared by reductive alkylation¹⁰. These separations, do, nevertheless, afford another example of the power of these "hydrophobic interaction" methods using optimized RP-HPLC supports for resolving closely related proteins.

DISCUSSION

Although it is now some time since it was first reported^{11,12} that proteins could be chromatographed on RP-HPLC systems, it is only recently that attempts have been made to optimize these methods. The results presented here illustrate the wide range of small proteins which can be successfully separated with the use of optimized carbon chain-lengths of the alkylsilane-bonded silica packings and organic modifiers such as propanol⁷ which favour the continued solubility of such molecules at relatively high concentrations of secondary solvent necessary to elute proteins under gradient elution conditions. This is, however, unlikely to be a universal method for protein HPLC. Thus, many proteins will still probably be too hydrophobic or too insoluble in the eluting solvents to be successfully chromatographed. Nevertheless, such techniques provide a very useful adjunct to the size-exclusion and ion-exchange HPLC (and "medium" performance) methods recently developed for proteins⁵.

The RP-HPLC procedures provide in certain cases a very selective method of both trace-enriching such molecules and separating them from congeners of similar size and charge. A comparison of the elution order of the proteins we have tested with their net hydrophobicity (Table V) shows that as with polypeptides³ a general correlation exists, but that numerous individual anomalies occur. These are probably due to conformational differences including the clustering of hydrophobic aminoacid residues as hydrophobic domains¹³; net hydrophobicity does, nevertheless, afford a general guide as to the probability of an individual protein being successfully chromatographed.

TABLE V

THE CORRELATION BETWEEN HYDROPHOBICITY AND ELUTION ORDER OF PROTEINS ON ULTRASPHERE SAC (C₃) UNDER GRADIENT ELUTION CONDITIONS

<i>Protein</i>	<i>MW (kD)</i>	<i>Mole % hydrophobicity*</i>	<i>Elution order</i>
Ribonuclease A	13.7	21.8	1
Cytochrome <i>c</i>	11.7	25.0	2
Lysozyme	14.3	26.4	3
Human serum albumin	66.5	28.37	4
α -Haemoglobin	15.1	31.20	8
Myoglobin	17.2	31.37	8
Carbonic anhydrase	29.0	31.49	7
Bovine serum albumin	69.0	32.0	5
Elastase [†] **	25.9	32.5	10
α -Lactalbumin (bovine)**	14.2	32.5	6
Prolactin (ovine)**	22.6	32.8	12
Human placental lactogen**	22.1	33.7	13
Growth hormone (bovine)**	22.0	34.0	14
β -Lactoglobulin**	18.3	34.6	10

* Mole % hydrophobicity is calculated with respect to the following amino acids: Trp, Phe, Leu, Ile, Tyr, Val, Met.

** None of these proteins can be chromatographed on C₁₈ packings, using acetonitrile as the organic modifier with pH 2.1 0.155 *M* NaCl as the primary solvent. Elastase[†] was not recovered from either C₁₈ or C₈ packings tested, under these conditions.

The practical use of these methods is evident from the separations of prolactin and growth hormone that we have obtained (Fig. 2). Preparative separation of these hormones has traditionally posed several problems, not the least of which is the difficulty of obtaining high yields of pure pyrogen-free materials when using time-consuming conventional methods of size-exclusion and ion-exchange chromatography¹⁴. Hydrophobic HPLC methods would appear to offer significant advantages as they have in the case of parathyroid hormone^{2,6}.

Carbon chain-length (and carbon loading) are not, of course, the only factors of importance in optimizing RP-HPLC methods for protein chromatography. While all of the packings that we have used here have been capped (where appropriate) or reacted to minimal levels of residual accessible silanol groups^{15,16}, the possibility of some degree of "mixed mode" chromatography contributing to the differences we have noted between the different packings cannot be entirely excluded. Thus recent studies¹⁷ have shown that low carbon loading, low coverage octadecylsilane packings provide some selective effects with peptide and protein chromatography, although reduced efficiencies were noted unless residual silanol groups were suppressed. However, despite the prolonged exposure of our columns to unbuffered acid conditions, all have afforded useful column lives of > 200 h, with highly reproducible chromatography and no changes of selectivity. We believe, therefore, that residual silanols, if any, are probably not responsible for the differences in performance that we have observed.

The use of mobile-phase additives in protein RP-HPLC is complicated by problems in removing them from the eluted compounds after chromatography. Ion-pairing reagents such as the higher perfluoroalkanoic acids^{18,19} increase peptide retention; this may afford useful selective effects with smaller compounds but will militate against the successful elution of the more hydrophobic proteins. The use of more polar bonded phases, *e.g.* cyanoalkyl or phenylalkyl-type materials, may assist in the elution of proteins²⁰ but efficiencies are significantly reduced with at least some of these packings⁴. Another means of reducing the strength of the binding between proteins and alkylsilane phase and thus favouring elution of more hydrophobic molecules is by reducing the temperature, a consequence of the entropic properties of hydrophobic bonds and preliminary studies with sub-ambient temperatures have been encouraging in this respect.

Low flow-rates (≈ 0.3 ml/min) have been reported to enhance the resolution of proteins, increasing efficiency by compensating for the lower diffusion rates of the larger compounds²¹; preliminary results indicate, however, that similar improvements in efficiency may be obtained with larger pore-size silicas (30 nm) without loss of analysis time.

Large pore-size packings also, of course, enable larger proteins to potentially interact with the bulk of the stationary phase. Several recent reports^{7,20,22,23} have demonstrated that RP-chromatography of proteins such as collagens (< 300 kD) are possible with such materials. It remains to be seen, however, how many other large molecules, or mixtures thereof, can be chromatographed; results to date²⁰ indicate that parameters of the eluting solvent such as pH, may have to be tailored specifically to suit individual proteins. On the basis of the results obtained here ultra-short (C_3) alkylsilane-phases on large pore-size silica may prove suited to such methods.

ACKNOWLEDGEMENTS

We are grateful to Dr. J. Smith for supplying us with pituitary culture medium and identifying the secreted hormones by polyacrylamide gel electrophoresis, Mr. P. Davy for bioassay of lysozyme and elastase, Dr. B. G. Archer for helpful discussions and Professor A. Munro Neville for continued interest and support.

REFERENCES

- 1 E. C. Nice and M. J. O'Hare, *J. Chromatogr.*, 162 (1979) 401.
- 2 J. M. Zanelli, M. J. O'Hare, E. C. Nice and P. H. Corran, *J. Chromatogr.*, 223 (1981) 59.
- 3 M. J. O'Hare and E. C. Nice, *J. Chromatogr.*, 171 (1979) 209.
- 4 E. C. Nice, M. Capp and M. J. O'Hare, *J. Chromatogr.*, 185 (1979) 413.
- 5 F. E. Regnier and K. M. Gooding, *Anal. Biochem.*, 103 (1980) 1.
- 6 H. P. J. Bennett, S. Solomon and D. Goltzman, *Biochem. J.*, 197 (1981) 391.
- 7 M. Rubinstein, *Anal. Biochem.*, 98 (1979) 1.
- 8 A. N. Smolelis and S. E. Hartsell, *J. Bact.*, 58 (1949) 731.
- 9 M. A. Naughton and E. Sanger, *Biochem. J.*, 78 (1961) 156.
- 10 D. Dottavio-Martin and J. M. Ravel, *Anal. Biochem.*, 87 (1978) 562.
- 11 J. Rivier, *J. Liquid Chromatogr.*, 1 (1978) 343.
- 12 W. Mönch and W. Dehnen, *J. Chromatogr.*, 147 (1978) 415.
- 13 R. J. P. Williams, *Biol. Rev.*, 54 (1979) 389.
- 14 R. L. Jones, G. Benker, P. R. Salacinski, T. J. Lloyd and P. J. Lowry, *J. Endocr.*, 82 (1979) 77.
- 15 N. H. C. Cooke and K. Olsen, *J. Chromatogr. Sci.*, 18 (1980) 512.

- 16 R. E. Majors, *J. Chromatogr. Sci.*, 18 (1980) 488.
- 17 W. S. Hancock and J. T. Sparrow, *J. Chromatogr.*, 206 (1981) 71.
- 18 H. J. P. Bennett, C. A. Browne and S. Solomon, *J. Liquid Chromatogr.*, 3 (1980) 1353.
- 19 W. M. M. Schaaper, D. Voskamp and C. Olieman, *J. Chromatogr.*, 195 (1980) 181.
- 20 R. V. Lewis, A. Fallon, S. Stein, K. D. Gibson and S. Udenfriend, *Anal. Biochem.*, 104 (1980) 153.
- 21 B. N. Jones, R. V. Lewis, S. Pääbo, S. Kozima, S. Kimura and S. Stein, *J. Liquid Chromatogr.*, 3 (1980) 1373.
- 22 A. Fallon, R. V. Lewis and K. D. Gibson, *Anal. Biochem.*, 110 (1981) 318.
- 23 J. D. Pearson, W. C. Mahoney, M. A. Hermodson and F. E. Regnier, *J. Chromatogr.*, 207 (1981) 325.

CHROM. 14,068

ANALYSIS OF GLYCOPROTEIN HORMONES AND OTHER MEDICALLY IMPORTANT PROTEINS BY HIGH-PERFORMANCE GEL FILTRATION CHROMATOGRAPHY

DEREK H. CALAM* and JANICE DAVIDSON

National Institute for Biological Standards and Control, Holly Hill, Hampstead, London NW3 6RB (Great Britain)

SUMMARY

Glycoprotein hormones and growth hormone of human origin, and allergen extracts of plant and animal origin have been examined by high-performance liquid chromatography using size exclusion on TSK SW supports. The short times required for elution, compared with low-pressure systems, minimize changes such as aggregation and dissociation. Analysis can be performed with amounts of material too small for examination by conventional gel filtration. The elution behaviour of the glycoproteins is intermediate between those of globular proteins and of dextrans of the same molecular weight. Native luteinizing hormone and follicle stimulating hormone are well separated from their sub-units. Aggregates and sub-units detected in samples of these hormones are not chromatographic artifacts. Differences in the chromatographic profiles of preparations of follicle stimulating hormone are associated in differences in biological and immunological properties. Commercial samples of chorionic gonadotrophin manufactured to official specification contain varying amounts of protein and differ in composition. Analysis on TSK supports confirms that the composition of growth hormone preparations depends on the procedure by which they are obtained, and the main fractions have been examined by electrophoresis. A major peak found in an extract of house dust mite *Dermatophagoides pteronyssinus* is attributed to the P₁ allergen. Other mite species give distinctive elution profiles on chromatography. An extract of pollen from the grass *Dactylis glomerata* was fractionated and the components correlated with proteins in the whole extract separable by electrophoresis. Biological and immunological studies are in progress on the fractions.

INTRODUCTION

Chromatographic supports for separation by molecular size using aqueous media ("gel filtration") were introduced over 20 years ago¹. Since then, they have been employed extensively for purification and analysis of biological macromolecules such as proteins, polysaccharides and nucleic acids. They permit separation under very mild conditions, suitable for sensitive compounds, and recovery of components

for further investigation. They are, however, unsuitable for use under conditions employed for high-performance liquid chromatography (HPLC) because of the fragility of the gel matrices. Efforts to develop size-exclusion supports suitable for HPLC resulted in the preparation of porous glass beads to which a hydrophilic coat was bonded² and, later, other supports which are commercially available³⁻⁶. The desired characteristics of such supports, approaches to their preparation, and the properties of some of them have been summarized⁷. Much experimental work has been reported using the TSK series of chemically modified silicas (*inter alia* refs. 3 and 7-10) which give efficient separations of a number of proteins without significant adsorption or denaturation. Toste⁹ has pointed out that the next stage in evaluation of size-exclusion HPLC is to apply it to biologically important proteins. We now report the use of TSK size-exclusion supports for analysis of preparations of glycoprotein hormones and growth hormone of human origin, and of plant and animal extracts containing allergens. All these materials are medically important but are available in limited amounts, their preparations are usually heterogeneous, and their chemical structure and specific biological activities are not fully characterised.

EXPERIMENTAL

Chromatography

Separations were carried out at ambient temperature (about 20°C) on Toyo Soda TSK G3000SW and G2000SW columns (300 × 7.5 mm), obtained pre-packed. The chromatograph consisted of an Altex 110A pump, Cecil 212A variable wavelength UV detector, Tekman TE 200 recorder operating at 10 mV and Rheodyne 7125 loop injector. 0.1 M sodium phosphate buffer pH 7.0 and 0.1 M sodium acetate buffer pH 7.0 were used as solvents and a filter was fitted in-line between the solvent reservoir and column. The flow-rate was 0.5 ml/min. Samples up to 100 µl in volume were injected. Fractions (100-500 µl) were collected manually on the basis of the UV traces. The columns were calibrated with protein and dextran standards of known molecular weight in the usual way⁹. Separations on Sephadex G-100 (Pharmacia) were performed on a column, 600 × 10 mm, previously equilibrated with buffer, using 0.1 M sodium phosphate buffer pH 7.0 containing 0.02% (w/v) sodium azide, supplied at 0.1 ml/min through an LKB Perplex pump. The Cecil UV detector and Tekman recorder were used.

Electrophoresis

Polyacrylamide gel electrophoresis was used essentially as described by Davis¹¹ with the spacer and sample gels omitted. The running gels (60 × 5 mm) were stained with 1% (w/v) amido black in 7% (v/v) acetic acid and destained with 7% acetic acid.

Materials

Details of the samples examined are given in Table I. The columns were calibrated with a protein standard kit (Boehringer, Mannheim, G.F.R.), ranging from cytochrome *c* (mol.wt. 12,500) to ferritin (mol.wt. 450,000), and procion-dyed dextran standards (mean mol.wt. 40,000 to 150,000) from Dr. E. A. Johnson (this Institute). All other chemicals were of analytical grade or of the highest grade commercially available.

TABLE I

MATERIALS EXAMINED BY HIGH-PERFORMANCE SIZE-EXCLUSION CHROMATOGRAPHY

Material	Code/batch number	Content per ampoule, or unitage*
<i>Hormones</i>		
FSH	71/270	5.2 μ g FSH + 100 μ g mannitol
	71/333	4.38 μ g FSH + 100 μ g mannitol
	76/566	10 μ g FSH + 1 mg lactose
	73/519	4.4 μ g FSH + 200 μ g mannitol
LH	76/569	10 μ g LH + 1 mg lactose
	72/20	5 μ g LH α sub-unit + 100 μ g mannitol
HCG	75/533	2 μ g HCG + 100 μ g mannitol
	76/508	2 μ g HCG α sub-unit + 100 μ g mannitol
	75/535	2 μ g HCG β sub-unit + 100 μ g mannitol
	107	Manufacturer A 2000 units/vial
	0730	Manufacturer B 5000 units/vial
Growth hormone	HWP 40	From acetone preserved glands ¹² ; approx. 1 unit/mg
	FL 3	From frozen glands ¹³ ; approx. 2.5 units/mg
<i>Allergens</i>		
<i>Dermatophagoides pteronyssinus</i>		
	77/622	1.19 mg lyophilized mite extract
<i>Acarus siro</i>		
	77/662	0.96 mg lyophilized mite extract
<i>Dactylis glomerata</i>		
pollen extract	75/506	6.44 mg lyophilized pollen extract

* Samples obtained within this Institute unless other indicated.

RESULTS AND DISCUSSION

Glycoprotein hormones

Luteinizing hormone (LH) and follicle stimulating hormone (FSH) are glycoprotein hormones produced by the pituitary gland and play a role in sexual development and function. Human chorionic gonadotrophin (HCG) has properties similar to those of LH but is obtained from the urine of pregnant women. All three substances consist of two non-identical protein sub-units to which carbohydrate is attached, and have molecular weights in the range 30,000–40,000. The protein structure of the α sub-unit may be common to all three substances¹⁴. Methods of isolation are based on chromatographic separation¹⁵. Purified preparations of the hormones are used for standardizing and calibrating biological and immunological assay systems. HCG is also administered clinically, and its measurement is the basis of diagnostic tests for pregnancy. Because of the small amounts of hormone available, interpretation of bioassays has been complicated by doubts about the homogeneity of reference materials, and the importance of accurate analysis of such preparations is emphasized by problems in radioimmunoassay of LH¹⁶ and by known differences in types of activity¹⁷. The complete primary structures of the hormones are not yet established because of difficulties in extracting small amounts of hormone from a limited source of supply, in separating the individual substances and the structural heterogeneity of the hormones either through genetic factors or degradation.

A number of potential reference preparations of FSH have been examined using a TSK G3000SW column with the results shown in Fig. 1. These preparations (Table I) are highly purified but differences are apparent in their individual degrees of heterogeneity. The position of the main peak corresponds to that of a globular protein of molecular weight 46,000. Since dextrans of a given weight elute from the column in the position of larger proteins, the hormone behaves as might be predicted for a glycoprotein, assuming a correct molecular weight in the region of 36,000. Peaks eluting after about 20 min are attributable to inert bulking agent in the sample and preservatives. Despite the large amount of carrier, up to 100 times by weight that of the hormone, no interference in the separation is observed. During isolation of FSH, some dissociation into subunits or aggregation may occur. There is chromatographic evidence of aggregated material, in particular, in 71/333 (Fig. 1b) and 76/566 (Fig. 1c), and possibly of sub-units in 76/566 and 73/519 (Fig. 1d). The sample size is of the order of 100 pmoles. Evidence from a variety of biological and immunological assays¹⁸ suggests that the behaviour of 71/720 and 73/519 is similar in such systems but that the other two preparations possess somewhat different properties. Only limited deduction can be made from the chromatographic profiles and it is not possible to make any firm statement about the relationship between composition and activity. It is known, however, that carbohydrate is essential for biological but not for immunological activity. The resolution obtained on the G3000SW column would probably be insufficient to detect whether the carbohydrate is intact or partially degraded.

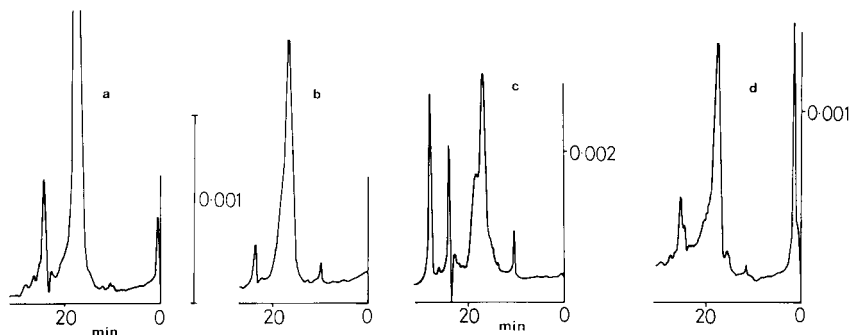


Fig. 1. High-performance size-exclusion chromatography of preparations of FSH from human pituitary glands. Conditions: TSK G3000SW column (300 \times 7.5 mm); mobile phase 0.1 *M* sodium acetate buffer pH 7.0; flow-rate 0.5 ml/min; ambient temperature; UV detection at 216 nm. a. Preparation 71/270; b. preparation 71/333; c. preparation 73/519; d. preparation 76/566. For details see Table I. Sample size 5 μ g (about 100 pmoles).

Fig. 2 shows the chromatograms obtained with preparations of LH and its α sub-unit. The position of elution of LH is also consistent with its approximate molecular weight. Fig. 2b suggests the presence in the sub-unit preparation of a small amount of material that behaves like the intact hormone on the column. Both preparations appear to contain high-molecular-weight (aggregated) material which is unlikely to be a chromatographic artifact.

Although HCG is available, from urinary sources, in greater amounts than LH or FSH, its isolation presents problems and there is still doubt about the sequence of



Fig. 2. High-performance size-exclusion chromatography of a, LH obtained from human pituitary glands and b, LH α sub-unit. Conditions as Fig. 1. Sample size 5 μ g.

Fig. 3. High-performance size-exclusion chromatography of a, HCG from the urine of pregnant women; b, HCG α sub-unit and c, HCG β sub-unit. Conditions as Fig. 1. Sample size 2 μ g.

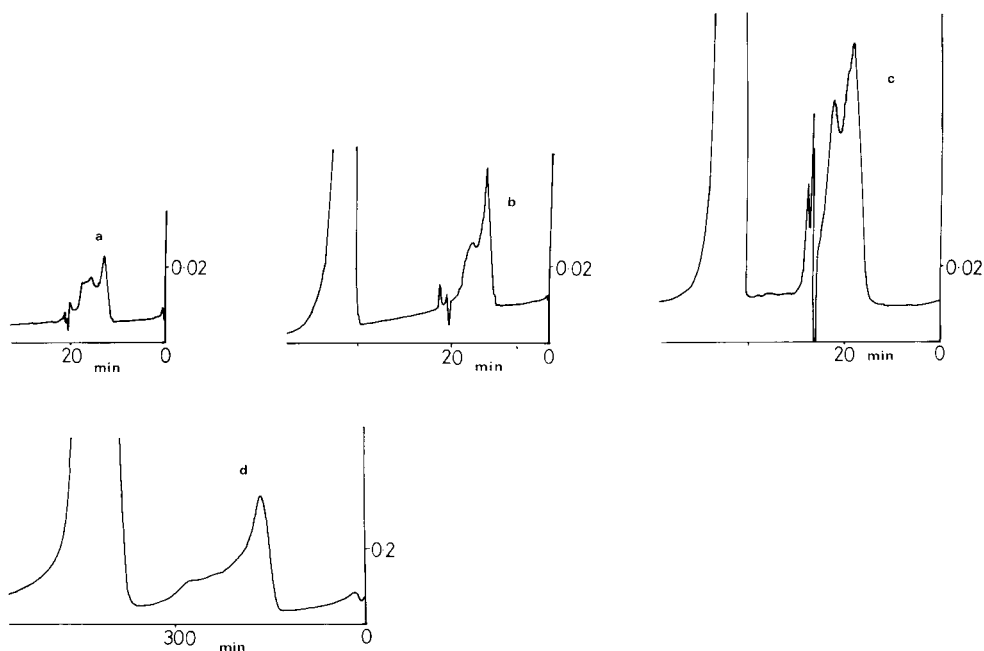


Fig. 4. Chromatography of commercial samples of HCG. a, Manufacturer A. Conditions: TSK G2000SW column (300 \times 7.5 mm), mobile phase 0.1 M sodium phosphate buffer pH 7.0; flow-rate 0.5 ml/min ambient temperature, UV detection at 280 nm; sample size 400 I.U.; b, as a but manufacturer B; c, as b but 1600 I.U. applied to TSK G3000 SW column; d, manufacturer B. Conditions: Sephadex G-100 column (600 \times 10 mm); mobile phase 0.1 M sodium phosphate pH 7.0 + 0.02% (w/v) sodium azide; flow-rate 0.1 ml/min, ambient temperature, UV detection at 280 nm, sample size 15000 I.U.

the sub-units¹⁹⁻²¹. The isolated material displays microheterogeneity within the sequence of the α sub-unit. Highly purified preparations of the intact hormone (50 pmoles) and of its two sub-units were chromatographed (Fig. 3). The hormones and the α sub-unit both appear to contain high-molecular-weight material (Figs. 3a and b). Comparison of the traces show that the β sub-unit elutes (Fig. 3c) before the α sub-unit (Fig. 3b) as would be expected since it contains 53 more amino acid residues²¹, representing a difference of about 6000 in molecular weight. A mixture of the hormone and both sub-units would be predicted to resolve on the column and this may be the case since peaks are present in the hormone preparation in positions corresponding to those of the two sub-units. The chromatographic behaviour of preparations of HCG manufactured to current pharmaceutical specifications is shown in Fig. 4. Figs. 4a and b are the traces obtained from the two preparations on the G2000SW column. Since highly purified material is not used, the traces are more complex than those in Fig. 3. There is also some difference in composition between the two samples. Loss of resolution on other supports is apparent when Fig. 4b is compared with Fig. 4c, obtained using the same sample but chromatographed on TSK G3000SW, and Fig. 4d where the analysis was carried out on Sephadex G-100.

Growth hormone

Growth hormone is extracted from human pituitaries which are obtained at autopsy and stored either frozen or in acetone until processed. It consists of a single protein chain of 190 amino acid residues and has a molecular weight of 21,500. It can undergo limited degradation without loss of activity and can form aggregates which are biologically inactive. Activity is measured by a number of complex bioassays. Of the various extraction procedures, material obtained by two^{12,13} has been administered clinically to stimulate growth of children. These two procedures are known to yield material of somewhat different composition. Figs. 5 and 6 show chromatograms of both types of growth hormone preparation obtained using TSK G2000SW and



Fig. 5. High-performance size-exclusion chromatography of preparations of human growth hormone. Conditions as Fig. 4a but detection at 210 nm. a, Sample isolated from acetone dried pituitary glands¹²; b, sample isolated from frozen glands¹³. The positions of fractions taken for electrophoretic examination (Fig. 7) are marked. Sample size 10 μ g.

Fig. 6. High-performance size-exclusion chromatography of growth hormone. Samples and conditions as Fig. 5a and b, respectively but using TSK G3000SW column.

TSK G3000SW columns, respectively. These figures confirm that the G2000SW column has higher resolving power for substances in this weight range than the G3000SW column. Differences in gross composition are apparent, in particular in the relative amounts of material of larger or smaller size compared with the main peak attributable to growth hormone itself. It is possible that the smaller peak eluting before the main one is due to aggregated material. Comparison of electrophoretic composition of the whole preparations with the main fractions (Fig. 7) shows recovery of hormone without background components although the fractions are not themselves homogeneous, producing one major and one minor band of protein. No evidence of change in composition is obtained when the hormone is rechromatographed so that the other constituents observed in the preparations are not chromatographic artifacts.

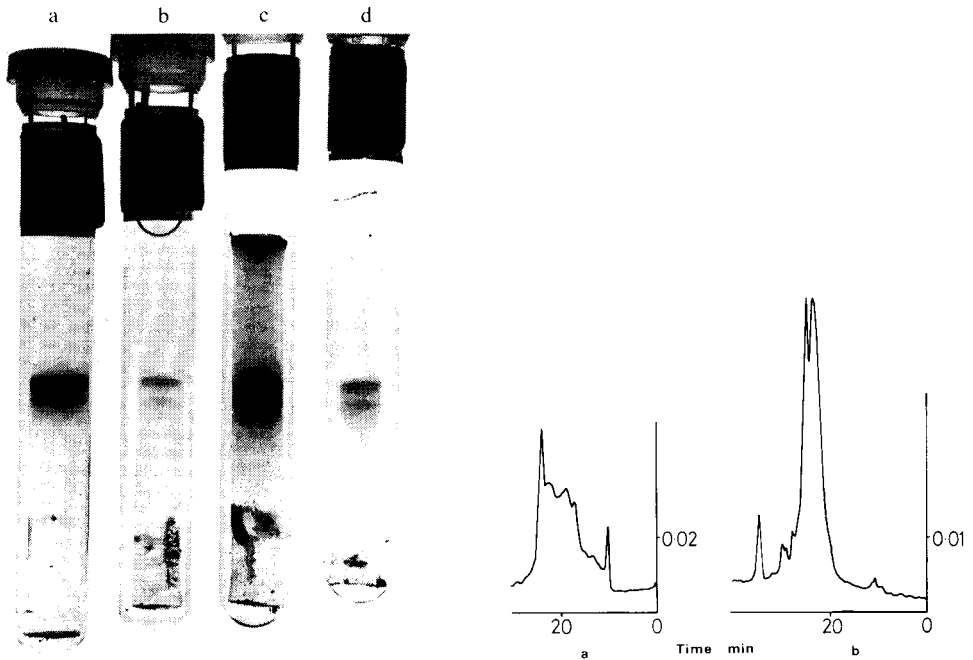


Fig. 7. Polyacrylamide gel electrophoresis of growth hormone preparations and of fractions isolated by chromatography (Fig. 5). Conditions: gels run at pH 8.3 and stained with amido black. Key: a, whole preparation applied in Fig. 5a; b, isolated fraction as marked; c, whole preparation applied in Fig. 5b; d, isolated fraction as marked.

Fig. 8. High-performance size-exclusion chromatography of mite extracts. Conditions as Fig. 5. a, Lyophilized aqueous extract of *Dermatophagoides pteronyssinus* (238 μ g); b, lyophilized aqueous extract of *Acarus siro* (96 μ g).

Allergens

An allergic response is provoked in man by a variety of natural and artificial substances, termed allergens, which are often protein in character. Although the cause of an allergy can be determined, few allergens themselves have been isolated or fully characterized. However, allergen extracts can be used to desensitize patients, preventing reactions that are often severe and debilitating. We have chromatograph-

ed allergen extracts, prepared from a number of materials, on TSK columns, first to compare their behaviour with their known properties and second, with the aim of recovering purified components for further investigation. Renck and Einarsson⁶ have reported the analysis of insect venoms by a similar technique using Shodex OHpak columns under low-pressure conditions.

It is known that the major allergen P_1 in house dust is associated with the presence in the dust of the mite *Dermatophagoides pteronyssinus* and is a glycoprotein of molecular weight about 24,000²². Chromatography of a house dust mite extract gave the separation shown in Fig. 8a with a series of peaks. One of these (indicated) elutes at a position expected for a protein of molecular weight about 25,000, as assessed from calibration of the column, but a considerable amount of higher molecular weight material is present. The main component P_1 of the mite fraction F_4P_1 described by Chapman and Platts-Mills²³ elutes in a comparable position. Several other extracts of mite species have been investigated using the TSK columns and patterns characteristic of each have been observed. Fractions have been collected for further investigation by immunological methods and the results will be reported elsewhere. However, the chromatographic profile obtained from *Acarus siro* extract (Fig. 8b) is illustrative of them and can clearly be distinguished from that of *D. pteronyssinus*.

Recent evidence²⁴ from skin testing suggests that common allergens may be present in certain groups of pollen extracts since many patients cross-react to different species within a group *e.g.* grass pollens. We have applied the size exclusion HPLC procedure to extracts of pollen from *Dactylis glomerata*, a common allergenic grass. Fig. 9a shows the separation obtained and Fig. 10 compares the electrophoretic pattern from the whole extract with those of the fractions collected from the column. Not only are the various components eluted to a considerable extent as discrete peaks on the column, but the electrophoretic examination confirms that there has been no significant loss of any component on the column. These fractions are currently under biological assessment. Unlike a previous method for fractionation²⁵ of the *D. glomerata* extracts, involving recovery of material after preparative isoelectric focussing, where the presence of extraneous components from the gel could influence subsequent *in vivo* testing, fractions from the TSK column can be examined directly. The improvements in resolution and speed of analysis, and smaller sample size associated with use of the TSK column are seen by comparing Fig. 9a with Fig. 9b

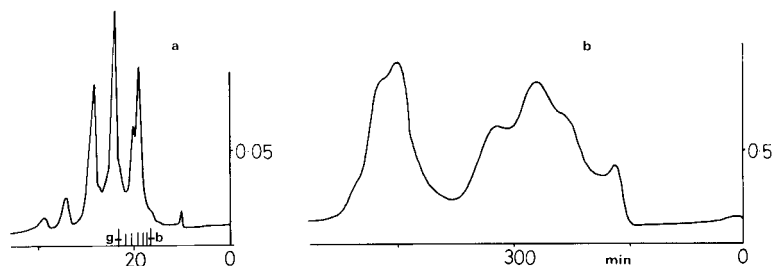


Fig. 9. Chromatography of a pollen extract from the grass *Dactylis glomerata*. a, 300 μ g applied to TSK G2000SW. Conditions as in Fig. 4b. Positions of fractions examined in Fig. 10 are indicated; b, 25.7 mg applied to Sephadex G-100. Conditions as in Fig. 4d.

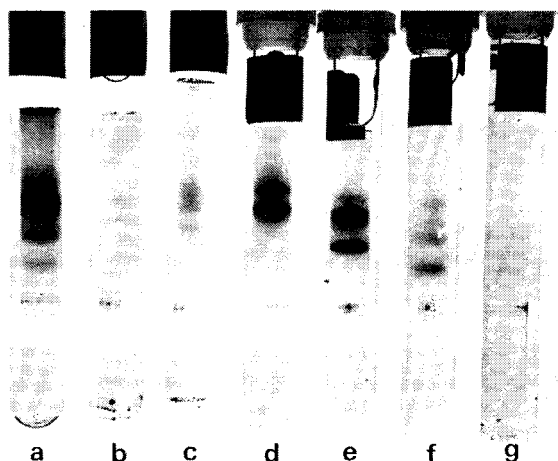


Fig. 10. Polyacrylamide gel electrophoresis of a, pollen extract from *D. glomerata* examined in Fig. 9 and b-g, of fractions isolated from it as shown in Fig. 9. Gels run at pH 4.3 and stained with amido black.

which shows the separation achieved on Sephadex G-100 with the same extract of *D. glomerata*.

CONCLUSION

Results obtained from examination of a variety of protein and glycoprotein preparations by size-exclusion chromatography on TSK columns under HPLC conditions show this to be a powerful addition to the techniques of biochemical analysis. Complex mixtures can be chromatographed rapidly under mild conditions and fractionated material recovered easily for further examination with little or no treatment. The use of simple aqueous media facilitates biological and immunological study of isolated components. Amounts difficult to analyse by previous chromatographic procedures can be studied. The speed of analysis suggest applications to studies on aggregation and dissociation and on binding equilibria. We conclude that this technique should play a valuable role in the identification and study of biologically important molecules.

ACKNOWLEDGEMENTS

We thank Mrs. A. W. Ford and Drs. E. A. Johnson, G. Limbrey and P. L. Storrington for providing many of the samples examined and for helpful discussion.

REFERENCES

- 1 J. Porath and P. Flodin, *Nature (London)*, 198 (1959) 1657.
- 2 F. E. Regnier and R. Noel, *J. Chromatogr. Sci.*, 14 (1976) 316.
- 3 S. Rokushika, T. Ohkawa and H. Hatano, *J. Chromatogr.*, 176 (1979) 456.
- 4 K. A. Gruber, J. M. Whitaker and M. Morris, *Anal. Biochem.*, 97 (1979) 176.
- 5 P. Roumeliotis and K. K. Unger, *J. Chromatogr.*, 185 (1979) 445.
- 6 B. Renck and R. Einarsson, *J. Chromatogr.*, 197 (1980) 278.

- 7 Y. Kato, K. Komiya, Y. Sawada, H. Sasaki and T. Hashimoto, *J. Chromatogr.*, 190 (1980) 305.
- 8 C. T. Wehr and S. R. Abbott, *J. Chromatogr.*, 185 (1979) 453.
- 9 A. P. Toste, *J. Chromatogr.*, 197 (1980) 207.
- 10 Y. Kato, K. Komiya, H. Sasaki and T. Hashimoto, *J. Chromatogr.*, 190 (1980) 297.
- 11 B. J. Davis, *Ann. N.Y. Acad. Sci.*, 121 (1964) 404.
- 12 A. S. Hartree, *Biochem. J.*, 100 (1966) 754.
- 13 R. Lumley-Jones, A. Benker, P. R. Salacinski, T. G. Lloyd and P. J. Lowry, *J. Endocrinol.*, 82 (1979) 77.
- 14 J. G. Pierce, in S. A. Berson and R. S. Yalow (Editors), *Methods in Investigative and Diagnostic Endocrinology*, Vol. 2A, North-Holland, Amsterdam, New York, 1973, p. 433.
- 15 A. S. Hartree, *Methods Enzymol.*, 37 (1975) 380.
- 16 J. E. Hammond, J. C. Phillips, C. B. Straight and M. G. Hammond, *Clin. Chem.*, 26 (1980) 772.
- 17 D. M. Robertson, B. Frøysa and E. Diczfalussy, *Mol. Cell. Endocrinol.*, 11 (1978) 91.
- 18 P. L. Storrington, A. A. Zaidi, Y. G. Mistry, B. Frøysa, B. E. Stenning and E. Diczfalussy, *J. Endocrinol.*, in press.
- 19 R. Bellisario, R. B. Carlsen and O. P. Bahl, *J. Biol. Chem.*, 248 (1973) 6796.
- 20 R. B. Carlsen, O. P. Bahl and N. Swaminathan, *J. Biol. Chem.*, 248 (1973) 6810.
- 21 F. J. Morgan, S. Birken and R. E. Canfield, *J. Biol. Chem.*, 250 (1975) 5247.
- 22 M. D. Chapman and T. A. E. Platts-Mills, *J. Immunol.*, 125 (1980) 587.
- 23 M. D. Chapman and T. A. E. Platts-Mills, *Clin. Exp. Immunol.*, 34 (1978) 126.
- 24 A. Dirksen and O. Østerballe, *Allergy*, 35 (1980) 611.
- 25 M. D. Topping, W. D. Brighton, M. Stokell and J. M. Patterson, *J. Immunol. Methods*, 19 (1978) 61.

CHROM. 14,044

HIGH-PERFORMANCE LIQUID CHROMATOGRAPHY OF ^{125}I -LABELLED PROTEINS WITH ON-LINE DETECTION

O. VON STETTEN* and R. SCHLETT

L. Merckle GmbH & Co., Blaubeuren (G.F.R.)

SUMMARY

Microgram amounts of ^{125}I -labelled proteins were chromatographed using hydrophilic molecular exclusion columns (Waters μ Bondapak-protein I125). A sodium iodide crystal was used as an on-line detector. Inherent hydrophobic properties of the column were overcome with a mobile phase containing 0.36 mol/l pyridinium formate-*n*-propanol (75:25), yielding recoveries in the range 90–95% of injected material. The resolution increased with increasing column length. Two columns (30 \times 0.8 cm) in series seem to be optimal. Compared with Sephadex chromatography of microgram amounts, high-performance liquid chromatography is superior with regard to resolution and operating time.

INTRODUCTION

^{125}I -labelled proteins are generally purified by gel filtration, *e.g.*, crude reaction mixtures containing labelled protein, chloramine-T, salts, etc.¹, are applied to appropriate Sephadex columns. In recent years, however, hydrophilic molecular exclusion columns for high-performance liquid chromatography (HPLC) have become available for the separation of proteins with molecular weights in the range 2000–80,000 daltons. These columns were expected to yield high resolutions and improved speed of chromatography. The aim of this study was to establish conditions for the HPLC of microgram amounts of ^{125}I -labelled proteins and to compare the results with those obtained by Sephadex chromatography.

EXPERIMENTAL

A Waters liquid chromatograph was used (Fig. 1).

Purified samples were collected at the Waters 6000A pump and evaluated by immunological methods. For the γ -detector (Fig. 2) a PTFE capillary was inserted in steel tubing, and passed through a drilled 2-in. sodium iodide crystal (Laboratorium Prof. Berthold). The radioactivity was recorded with a photomultiplier and rate meter.

Between 5 and 20 μg of proteins were labelled with ^{125}I according to Hunter and Greenwood¹. The crude mixtures were injected directly and chromatographed.

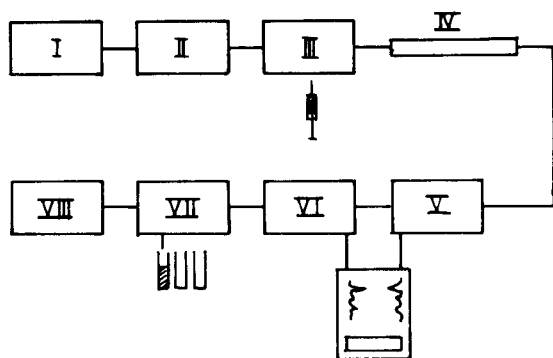


Fig. 1. Flow diagram of the chromatograph. I, Mobile phase; II, Waters 6000A pump; III, Waters U6K injection system; IV, Waters μ Bondapak-protein I125 column; V, γ -detector; VI, Waters 440 UV detector; VII, Waters 6000A sample collector; VIII, waste.

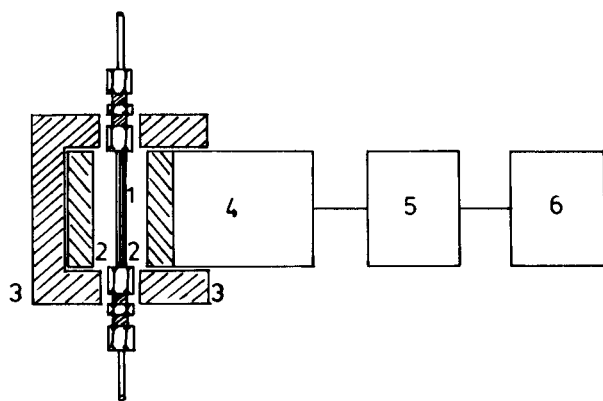


Fig. 2. γ -Detector. 1, PTFE capillary; 2, 2-in. sodium iodide crystal (Laboratorium Prof. Berthold); 3, lead shielding; 4, photomultiplier; 5, rate meter (Laboratorium Prof. Berthold); 6, recorder.

RESULTS

Recovery

In order to assess the hydrophobic properties of the column, five consecutive injections of 20 μ g of hPL* in 100 μ l of mobile phase were made. As Fig. 3 (I–V) demonstrates, the recovery of injected material increases with apparent saturation of the column, thus indicating the occurrence of hydrophobic interactions between the column and the protein.

The recovery could be further increased by co-chromatographing bovine serum albumin (BSA) (VI) or pre-saturation of the column with BSA. This was found, however, only for a limited number of proteins, including hPL and hFSH. The recovery of other labelled proteins, including hTSH and hLH, was unsatisfactory.

* Abbreviations: hPL = human placental lactogen; hFSH = human follicle-stimulating hormone; hTSH = human thyrotrophin; hLH = human luteinising hormone.

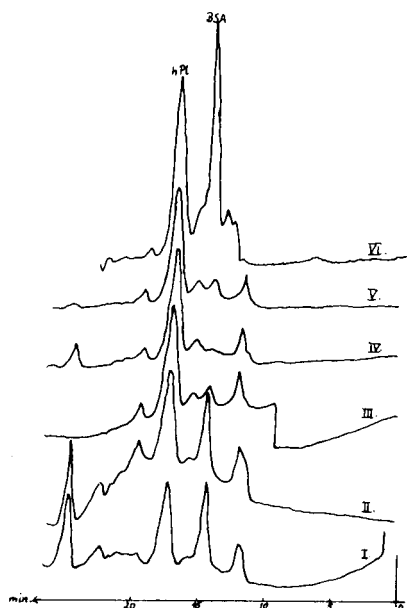


Fig. 3. HPLC of hPL. Columns, two 30×0.8 cm I.D. μ Bondapak-protein I125; mobile phase, 0.05 mol/l phosphate-buffered saline (pH 7.2); flow-rate, 1.0 ml/min; detection, UV (254 nm), 0.01 a.u.f.s. I–V = consecutive injections of 20 μg of hPL in 100 μl of mobile phase each; VI = injection of 20 μg of hPL and 50 μg of BSA in 100 μl mobile phase.

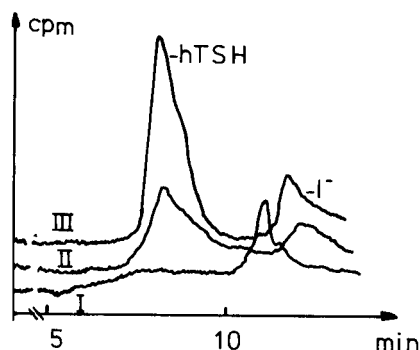


Fig. 4. HPLC of [^{125}I]hTSH using different mobile phases. Column, 30×0.8 cm I.D. μ Bondapak-protein I125; flow-rate, 1.0 ml/min; detection, γ -detector; injection, 8 μg of [^{125}I]hTSH. Mobile phase: I, 0.01 mol/l phosphate-buffered saline (pH 7.2); II, 8% acetic acid-*n*-propanol (95:5); III, 0.36 mol/l pyridinium formate (pH 3.0)-*n*-propanol (75:25).

Hydrophobic properties were overcome with the use of mobile phases containing organic solvents (Fig. 4).

Thus, on going from buffer to acetic acid-*n*-propanol the recovery increased, although there was still tailing of peaks and equilibration of the column took a long time. With pyridinium formate-*n*-propanol the recovery was 90–95% of injected material, with acceptable separation. Changes in the *n*-propanol content, *e.g.*, 22% instead of 25%, altered the chromatograms significantly. Using this mobile phase, UV detection at 254 nm is impossible owing to the pyridinium content.

Resolution

Influence of column length. In the process of labelling hTSH with ^{125}I and purification, aggregation or breakdown of molecules was sometimes observed, so the influence of column length on resolution with this system was investigated (Fig. 5).

With two 30-cm columns in series satisfactory resolution was obtained, but with one column the separation was not satisfactory. The consequent peak broadening and the increase in the time required for chromatography time were well within acceptable limits.

Influence of pH of mobile phase. In order to increase the resolution further and

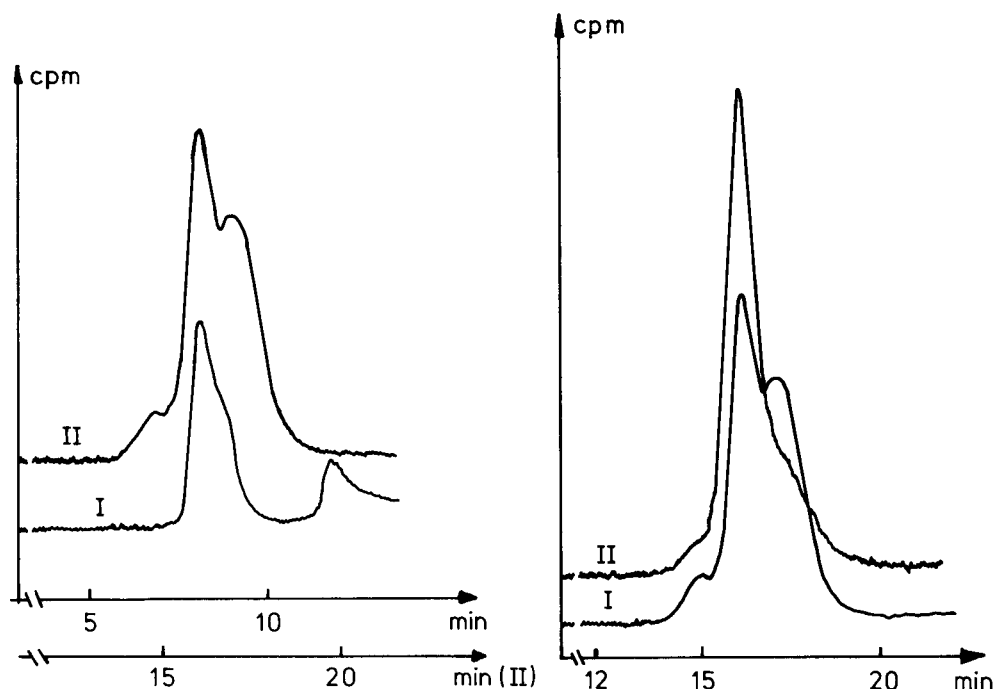


Fig. 5. Influence of column length on resolution. Columns: I, one μ Bondapak-protein I125 (30×0.8 cm I.D.); II, two μ Bondapak-protein I125 in series (30×0.8 cm I.D.). Flow-rate, 1.0 ml/min; detection, γ -detector; mobile phase, 0.36 mol/l pyridinium formate (pH 3.0)-*n*-propanol (75:25); injection, 8 μ g of [125 I]hTSH.

Fig. 6. Influence of pH on resolution. Columns, two 30×0.8 cm I.D. μ Bondapak-protein I125; flow-rate, 1.0 ml/min; detection, γ -detector; injection, 8 μ g of [125 I]hTSH. Mobile phase: I, 0.36 mol/l pyridinium formate (pH 3.0)-*n*-propanol (75:25); II, 0.36 mol/l pyridinium formate (pH 5.0)-*n*-propanol (75:25).

at the same time to chromatograph under milder conditions with regard to proteins, the pH of the mobile phase was changed to more neutral conditions while keeping its composition constant (Fig. 6).

Although the resolution remained unchanged the formation of by-products was reduced considerably. Thus, the use of pyridinium formate (pH 5.0)-*n*-propanol (75:25) as the mobile phase gave recoveries of 90–95 % of injected material, acceptable separation of the product and by-products and reduced aggregation of proteins during chromatography.

Comparison of HPLC and gel filtration

To compare HPLC with gel filtration, labelled mixtures were chromatographed using HPLC (two 30×0.8 cm I.D. columns) and Sephadex G-75 (60×0.9 cm I.D. column), respectively. Fig. 7 shows the results obtained when 5 μ g of [125 I]hLH were applied to each column.

HPLC gave much better separations of all products. In addition, the analysis time, including the time for column preparation and equilibration, was reduced by nearly 2 h (from 2–2.5 h to 30–45 min). As in HPLC all of the recovered material

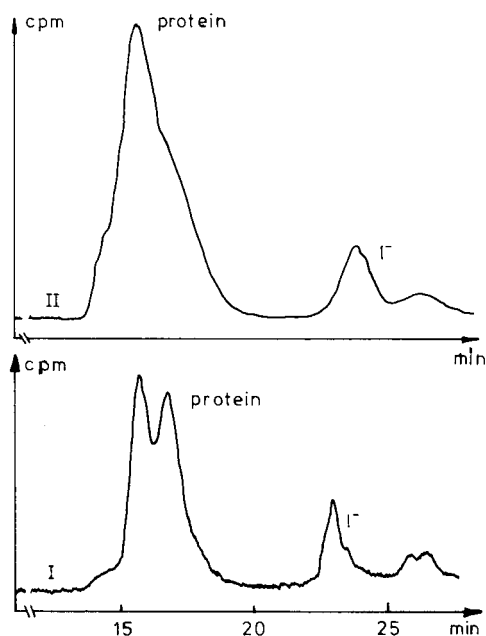


Fig. 7. Chromatography of $[^{125}\text{I}]\text{hLH}$ using different techniques. Columns: I, two $30\text{ cm} \times 0.8\text{ cm}$ I.D. $\mu\text{Bondapak}$ protein 1125 (HPLC); II, $60 \times 0.9\text{ cm}$ I.D. Sephadex G-75 (gel filtration). Mobile phase: I, 0.36 mol/l pyridinium formate (pH 5.0) n -propanol (75:25); II, 0.01 mol/l phosphate-buffered saline (pH 7.2). Detection, γ -detector.

retained its biological activity in immunological tests and behaved similarly to the material purified by gel filtration, HPLC of proteins using hydrophilic molecular exclusion columns and a pyridinium formate- n -propanol buffer is preferred for the purification of ^{125}I -labelled proteins. Results obtained so far are summarized in Table I, which compares the resolution, recovery and analysis times using HPLC and Sephadex chromatography.

TABLE I

COMPARISON OF HPLC AND SEPHADEX CHROMATOGRAPHY

Substance	Resolution*		Recovery (%)		Analysis time	
	HPLC	Sephadex	HPLC	Sephadex	HPLC	Sephadex
$[^{125}\text{I}]\text{hTSH}$	+	0	95	95	45 min	2.5 h
$[^{125}\text{I}]\text{hFSH}$	+	0	93	95	45 min	2.5 h
$[^{125}\text{I}]\text{hLH}$	+	—	90	93	45 min	2.5 h
$[^{125}\text{I}]\text{hPL}$	+	0	95	95	45 min	2.5 h

* +, Good; 0, satisfactory; —, not satisfactory.

CONCLUSIONS

1. HPLC using hydrophilic molecular exclusion columns is a fast and convenient technique for purifying microgram amounts of ^{125}I -labelled proteins.

2. Inherent hydrophobic properties of the columns causing reduced recovery of injected material are overcome by a proper choice of the mobile phase; 0.36 mol/l pyridinium formate (pH 5.0)-*n*-propanol (75:25) is suitable.

3. The resolution is improved considerably by using two 30-cm columns in series instead of one. The consequent peak broadening and increased analysis time are within acceptable limits.

4. For the purification of microgram amounts of ^{125}I -labelled proteins, HPLC compares favourably with Sephadex chromatography with regard to resolution and analysis time. Thus it is possible to purify proteins in 30–45 min by HPLC compared with 2–2.5 h by Sephadex chromatography.

REFERENCE

- 1 W. M. Hunter and F. C. Greenwood, *Nature (London)*, 194 (1962) 495.

CHROM. 14,101

IMPROVED HIGH-PERFORMANCE LIQUID CHROMATOGRAPHIC METHOD FOR THE ANALYSIS OF INSULINS AND RELATED COMPOUNDS

G. SZEPESI* and M. GAZDAG

Chemical Works of Gedeon Richter, Ltd., Budapest (Hungary)

SUMMARY

A new method has been developed for the separation and determination of insulins and related polypeptides. Octadecylsilica was used as stationary phase and a mixture of water and organic solvents (methanol, acetonitrile and isopropanol) containing a relatively high amount of inorganic salt (sodium sulphate and sodium perchlorate) for controlling the degree of ionization as eluent. By this method the separation of bovine and porcine insulins, desamidoinsulins and proinsulins as well as that of intermediates can be achieved.

INTRODUCTION

Recently, there has been considerable interest in sensitive and specific analytical methods for monitoring the purity of insulins. In the past, disc electrophoresis¹⁻⁴ and gel chromatography⁵⁻¹⁰ have been applied for this purpose. However, these methods are time-consuming and their accuracy, precision and efficiency are unsatisfactory. High-performance liquid chromatography (HPLC) has since been investigated for the separation of different insulins and related compounds, and great efforts have been made to find the most suitable system. Both reversed-phase partition chromatography¹¹⁻¹⁷ and reversed-phase ion-pair chromatography¹⁷⁻²⁰ have been studied in detail, however the separation of proinsulins, intermediates and degradation products of insulins has not been achieved.

In this paper we summarize our results in the field of insulin analysis. This work is a part of experiments aimed at the HPLC separation of large polypeptides. The explanation of the possible retention mechanism and discussion of the solvent and salt effects will be reported elsewhere²¹.

EXPERIMENTAL

A Hewlett-Packard 1081/A liquid chromatograph equipped with a loop injector and a variable-wavelength UV-detector (Schoeffel Model 770) was used. The separations were performed on a Nucleosil 10 C₁₈ column, 250 × 4.6 mm I.D. (Chrompack, Middelburg, The Netherlands).

All solvents used were of HPLC grade and were obtained from E. Merck (Darmstadt, G.F.R.). The chemicals were of analytical grade (Reanal, Budapest, Hungary). The insulin samples were from different sources; the bovine and porcine proinsulin were obtained from NOVO (Copenhagen, Denmark).

RESULTS AND DISCUSSION

Two different types of HPLC separation have previously been used for the analysis of insulins. In reversed-phase partition chromatography the ionization of the insulin molecule is controlled by the pH and salt concentration of the eluent and methanol or acetonitrile is used as organic modifier¹¹⁻¹⁶. The compounds are sep-

TABLE 1

CAPACITY RATIOS, k' , FOR INSULINS AND RELATED COMPOUNDS

Column: Nucleosil 10 C₁₈, 250 × 4.6 mm I.D. Flow-rate: 1 ml/min. Detection: UV at 215 nm. Eluents: A, methanol acetonitrile-aqueous 0.01 M phosphate buffer, pH 2.2 (5:1:4), containing 0.1 M sodium sulphate; B, organic modifier-aqueous 0.01 M phosphate buffer, pH 2.2 (4:6), containing 0.1 M sodium perchlorate. The organic modifier contained 33.3% isopropanol in acetonitrile.

	k'	
	Eluent A	Eluent B
Bovine insulin	5.25	2.53
Bovine desamidoinsulin	6.00	2.90
Porcine insulin	7.75	3.61
Porcine desamidoinsulin	9.50	8.12
Bovine proinsulin	15.40	4.45
Porcine proinsulin	—	12.90

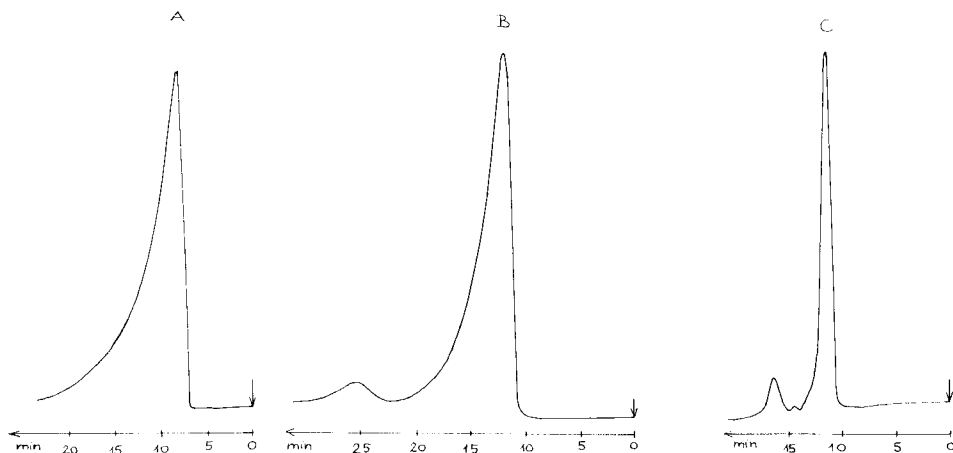


Fig. 1. Effect of the salt concentration on the separation of bovine and porcine insulins. Column: Nucleosil 10 C₁₈, 250 × 4.6 mm I.D. Flow-rate: 1 ml/min. Detection at 215 nm. Eluents: A, methanol-acetonitrile-buffered water, pH 2.2 (5:1:4); B, as A but buffer contained 0.01 M Na₂SO₄; C, as A but buffer contained 0.1 M Na₂SO₄.

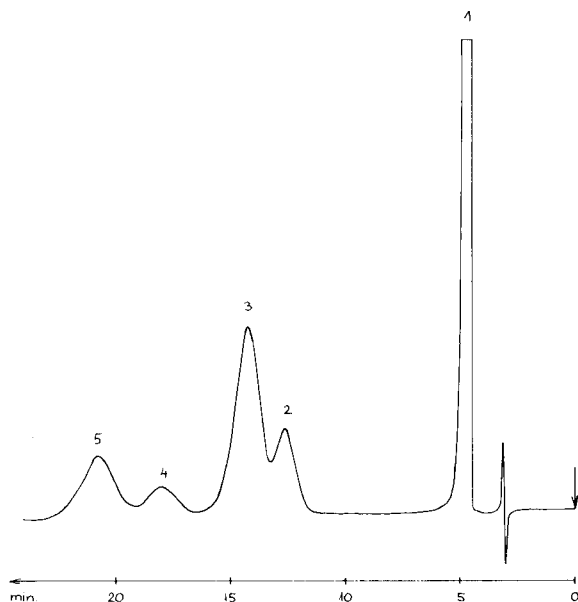


Fig. 2. Chromatogram of insulin injection decomposed by heat loading. Conditions as in Fig. 1, with eluent C. Compounds: 1 = ingredients; 2 = bovine insulin; 3 = bovine desamidoinsulin; 4 = porcine insulin; 5 = porcine desamidoinsulin.

arated on the basis of their different hydrophobicities. In reversed-phase ion-pair chromatography using anionic or cationic ion-pairing reagents¹⁷⁻²⁰, the compounds are separated as their ion pairs.

The first separation mode was chosen for our experiments, with octadecylsilica as stationary phase and a mixture of organic modifier and buffered water, pH 2.2, containing 0.1 *M* of an inorganic salt as eluent. The capacity ratios, k' , measured for the compounds in two different eluent systems are collected in Table I.

Fig. 1 shows the separation of bovine and porcine insulins using an optimal mixture of methanol, acetonitrile and buffered water containing different amounts of sodium sulphate as eluent. The presence of the inorganic salt has a favourable effect

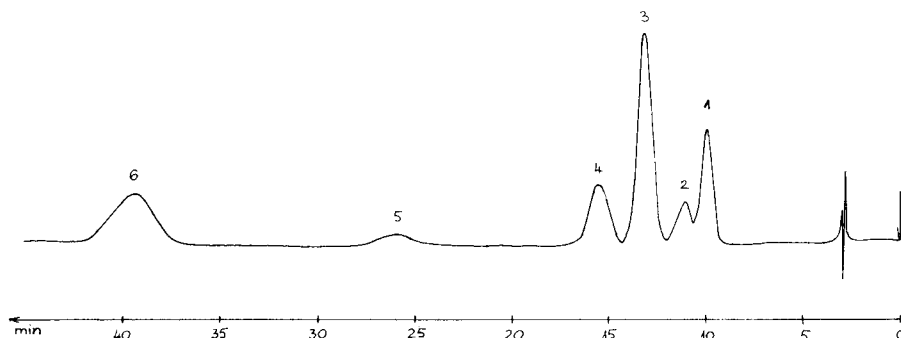


Fig. 3. Separation of bovine and porcine insulins and proinsulins. Eluent: B in Table I. Other conditions as in Fig. 1. Compounds: 1 = bovine insulin; 2 = bovine desamidoinsulin; 3 = porcine insulin; 4 = bovine proinsulin; 5 = porcine desamidoinsulin; 6 = porcine proinsulin.

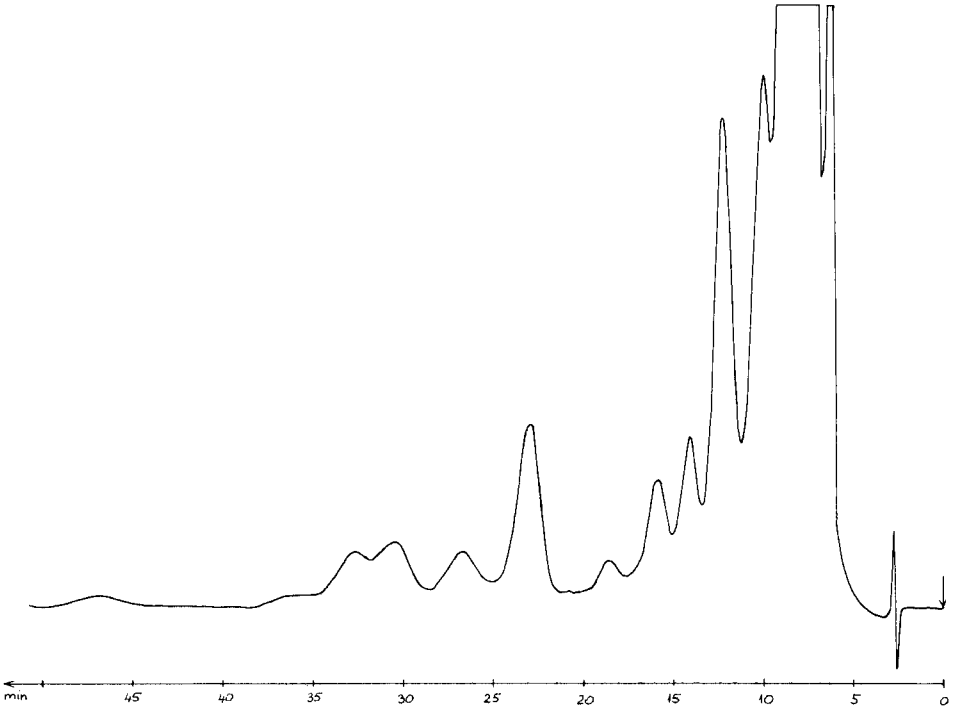


Fig. 4. Chromatogram of a commercial bovine insulin sample. Conditions: as in Fig. 3. Concentration: 500 μg per 20 μl .

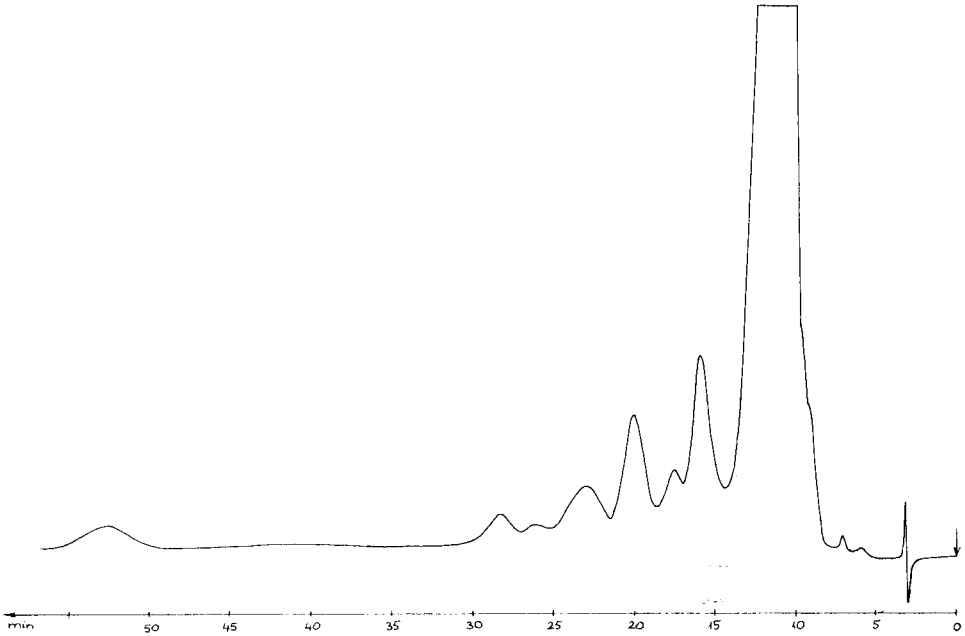


Fig. 5. Chromatogram of "so-called" proinsulin-free porcine insulin. Conditions as in Fig. 4.

on the separation efficiency, the peak shape being significantly improved. Fig. 2 demonstrates the applicability of this eluent to the investigation of a decomposed insulin injection (the decomposition was done by heat loading of the ampoules at 100 °C for 5 h). A satisfactory separation of bovine and porcine insulins as well as their decomposition products (desamidinsulins) was achieved.

When acetonitrile and isopropanol are used as organic modifier and the sodium sulphate is replaced with sodium perchlorate the efficiency of the separation can be increased further. This type of the eluent system facilitates the separation and identification of porcine and bovine insulins, desamidinsulins and proinsulins, as shown in Fig. 3.

The number of theoretical plates for the compounds was calculated to be more than 5000, which suggests that this system may be more effective in the separation of impurities from insulins compared to previously published systems. This is illustrated in Figs. 4–6, when 500- μ g insulin samples were injected. Fig. 4 shows the chromatogram of a commercial insulin satisfying the requirements of the British Pharmacopocia 1980 Edition, while Fig. 5 illustrates the chromatogram of a "so-called" proinsulin-free purified insulin sample. For estimation of the quantities of impurities present in the samples 0.5 μ g insulin were injected into the column, the resulting chromatogram can be seen in Fig. 6.

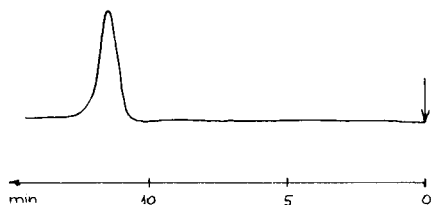


Fig. 6. Chromatogram of external standard solution. Concentration of insulin: 0.5 μ g per 20 μ l. Conditions as in Fig. 3.

CONCLUSION

On the basis of the above results it can be concluded that the types and concentration of organic modifier used in the eluent are important in the separation of insulins and related compounds. A mixture of acetonitrile, isopropanol and buffered water, pH 2.2, containing 0.1 M sodium perchlorate has been found to be optimal for the separation and analysis of insulins.

ACKNOWLEDGEMENT

We are grateful for the assistance given by Miss V. Windbrechtinger.

REFERENCES

1. F. Sundby, *J. Biol. Chem.*, 237 (1962) 3406.
2. H. Zühleke, H. G. Lippmann, W. Wilke, R. Menzel and R. Hildmann, *FEBS Lett.*, 6 (1970) 155.
3. U. Krause and J. Beyer, *Deut. Med. Wochenschr.*, 100 (1975) 238.
4. T. Kasama and Y. Iwata, *Jap. J. Pharmacol.*, 30 (1980) 293.
5. K. Gruber, A. Whitaker and M. Morris, *Anal. Biochem.*, 97 (1979) 176.

- 6 T. Imamura and K. Konishi, *J. Biochem. (Tokyo)*, 86 (1979) 639.
- 7 S. Rokushika, T. Ohkawa and H. Hatano, *J. Chromatogr.*, 176 (1979) 456.
- 8 N. Ui, *Anal. Biochem.*, 97 (1979) 65.
- 9 L. J. Fischer, R. L. Thies and G. Charkowski, *Anal. Chem.*, 50 (1978) 2143.
- 10 J. Schechter, *Anal. Biochem.*, 58 (1974) 30.
- 11 W. S. Hancock, C. A. Bishop, R. L. Prestidge and M. T. W. Hearn, *Anal. Biochem.*, 89 (1978) 203.
- 12 W. S. Hancock, C. A. Bishop, R. L. Prestidge and D. R. K. Harding, *Science*, 200 (1978) 1168.
- 13 M. T. W. Hearn, W. S. Hancock, J. G. R. Hunnell, R. J. Fleming and B. Kemp, *J. Liquid Chromatogr.*, 2 (1979) 919.
- 14 M. T. W. Hearn and W. S. Hancock, *Trends Biochem. Sci.*, 4 (1979) 58.
- 15 A. Dinner and L. Lorenz, *Anal. Chem.*, 51 (1979) 1872.
- 16 M. J. O'Hare and E. C. Nice, *J. Chromatogr.*, 171 (1979) 209.
- 17 M. E. F. Biemond, W. A. Sipman and J. Olivie, *J. Liquid Chromatogr.*, 2 (1979) 1407.
- 18 J. E. River, *J. Liquid Chromatogr.*, 1 (1979) 343.
- 19 V. Damgaard and J. Markussen, *Horm. Metab. Res.*, 11 (1979) 580.
- 20 S. Terabe, R. Konaka and K. Inouye, *J. Chromatogr.*, 172 (1979) 163.
- 21 M. Gazdag and G. Szepesi, *J. Chromatogr.*, 218 (1981) 603.

CHROM. 14,102

SEPARATION OF LARGE POLYPEPTIDES BY HIGH-PERFORMANCE LIQUID CHROMATOGRAPHY

M. GAZDAG* and G. SZEPESI

Chemical Works of Gedeon Richter, Ltd., Budapest (Hungary)

SUMMARY

The separation of polypeptides of biological interest has been investigated by hydrophobic chromatography. It was found that both the eluent composition and the salinity of the eluent have a profound influence on the efficiency and selectivity of the separation, and the use of isopropanol as organic modifier in the eluent improved the selectivity. The expected retention times were calculated for ACTH derivatives and a good correlation between the predicted and found capacity factors was obtained. The applicability of the method is demonstrated for samples of oxytocin, ACTH_{1–32}, aprotinine and insulins.

INTRODUCTION

In the last few years great efforts have been made to improve the efficiency and selectivity of the high-performance liquid chromatography (HPLC) methods used for the separation of proteins and polypeptides. Increasing numbers of individual polypeptide separations are now being published^{1–13} (for a comprehensive review see ref. 14). Most of the methods published so far can be divided into two groups.

In the first group, the separation mechanism proceeds according to liquid–liquid partition and the retention is mainly dependent on the hydrophobic nature of the compounds investigated^{15–17}. The hydrophobicity of polypeptides can be controlled by the pH or the salt and organic modifier concentrations of the eluent. In most cases, a gradient elution technique was for the most hydrophobic compounds, by increasing the organic solvent concentration in the mobile phase. A very elegant gradient elution system has been described by O'Hare and Nice¹² for the separation of proteins and polypeptides. On the basis of their retention data, the retention coefficients of amino acid residues were calculated by Meek¹³, enabling the prediction of retention times of different polypeptides.

The second group comprises reversed-phase ion-pair chromatographic methods, which employ a chemically bonded non-polar stationary phase and a mixture of organic solvent (mainly acetonitrile or methanol) and buffered water containing a small amount of an anionic or cationic ion-pairing reagent as eluent. Although a wide variety of such methods have been reported for polypeptide separation^{4,5,8,10,11},

sometimes the ion-pair formation seems to be questionable, identical retentions being obtained for the same compounds in the presence and in the absence of ion-pair reagents¹⁰.

The main aim of our work was to find an isocratic separation system for some polypeptides manufactured at Gedeon Richter (Budapest, Hungary), as well as to study the effects of the type and concentration of the organic modifier and that of salt concentration on the efficiency and selectivity of the separation.

EXPERIMENTAL

A Hewlett-Packard 1081/A liquid chromatograph equipped with a loop injector and variable-wavelength UV-detector (Schoeffel Model 770) was used. The separations were performed on a prepacked Nucleosil 10 C₁₈ column, 250 × 4,6 mm I.D. (Chrompack, Middelburg, The Netherlands) using the following eluent systems with a flow-rate of 1 ml/min (only the eluents found to be optimal are listed):

Eluent A: solutions 1 and 2 (4:6). Solution 1 contains 16,7% acetonitrile in methanol; solution 2 contains 0.1 *M* sodium sulphate in 0,01 *M* aqueous phosphate buffer, pH 2.2.

Eluent B: solutions 1 and 2 (35:65).

Eluent C: solutions 1 and 2 (6:4).

Eluent D: solutions 1 and 3 (3:7). Solution 3 contains 0,05 *M* sodium sulphate in 0,01 *M* aqueous phosphate buffer, pH 6.5.

Eluent E: solutions 4 and 5 (35:65). Solution 4 contains 16.7% isopropanol in methanol; solution 5 contains 0.1 *M* sodium perchlorate in 0.01 *M* aqueous phosphate buffer, pH 2.2.

Eluent F: solutions 6 and 5 (4:6). Solution 6 contains 33.3% isopropanol in acetonitrile.

All solvents used were of HPLC grade and were obtained from E. Merck (Darmstadt, G.F.R.). The chemicals were of analytical grade (Reanal, Budapest, Hungary). Most of the compounds investigated were prepared at Gedeon Richter and their quality was monitored by HPLC and other analytical methods.

RESULTS AND DISCUSSION

From the separation possibilities mentioned above, hydrophobic chromatography according to Molnár and Horváth¹⁶ was chosen for our experiments. In this case the retention can be controlled by ionization of the solutes. To suppress the dissociation of the ionizable functional groups of polypeptides, a high salt concentration and low pH in the eluent are employed, resulting in good peak shape and reproducible retention.

The capacity ratios, *k*, of polypeptides are generally very sensitive to the concentration of the organic modifier. However, only a small difference in selectivity can be achieved by changing the organic solvents^{12,18}. For this reason, methanol and acetonitrile are generally accepted solvents in the HPLC analysis of polypeptides.

In order to develop an isocratic chromatographic method for some polypeptides of biological interest, various eluent compositions containing relatively high amounts of inorganic salts (sodium sulphate and sodium perchlorate) were studied. It

was found that the use of 0.1 *M* salt concentrations in the eluent gave a good peak shape and better resolution compared to eluents which do not contain salts. This is illustrated in Fig. 1 for the separation of bovine and porcine insulins and desamido-insulins in the presence and in the absence of sodium sulphate.

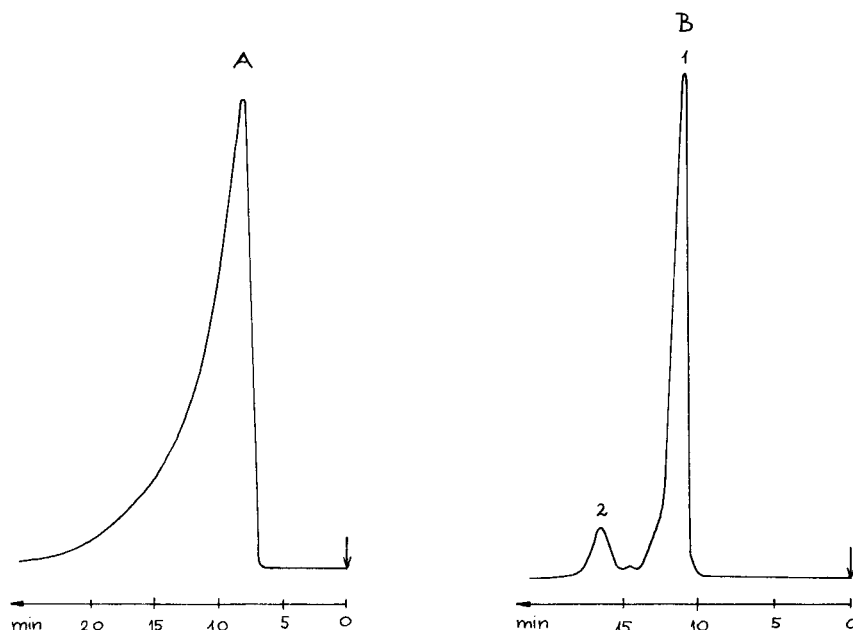


Fig. 1. Effect of salt concentration on the separation of bovine and porcine insulins. Column: Nucleosil 10 C_{18} , 250×4.6 mm I.D. Flow-rate: 1 ml/min. Detection: UV at 215 nm. Eluents: A, methanol-acetonitrile-buffered water, pH 2.2 (5:1:4); B, as A but buffer contained 0.1 *M* Na_2SO_4 . Compounds: 1 = bovine insulin; 2 = porcine insulin.

Fig. 2 demonstrates the increased selectivity obtained by the change of the organic modifier in the eluent, for the separation of oxytocin raw product. The elution order was found to change when acetonitrile was replaced with isopropanol in the eluent.

From the experimental data obtained on the solvent effect on the efficiency and selectivity of the isocratic separation of polypeptides, it can be concluded that on the one hand the use of mixed solvents as organic modifier in the eluent can increase the efficiency of the separation, whereas on the other the type of organic solvent has a significant effect upon the k' values of polypeptides, changing the selectivity of the separation.

Table I lists the capacity ratios measured for insulins using different organic solvents. Somewhat unexpectedly, the capacity ratios increased in the order isopropanol, tetrahydrofuran, acetonitrile, methanol.

Two types of eluent systems were found to be promising for the separation of polypeptides under isocratic conditions. The first system was a mixture of methanol, acetonitrile and buffered water containing 0.1 *M* sodium sulphate (see Experimental for eluents A–D) and this has proved to be suitable for the analysis of oxytocin,

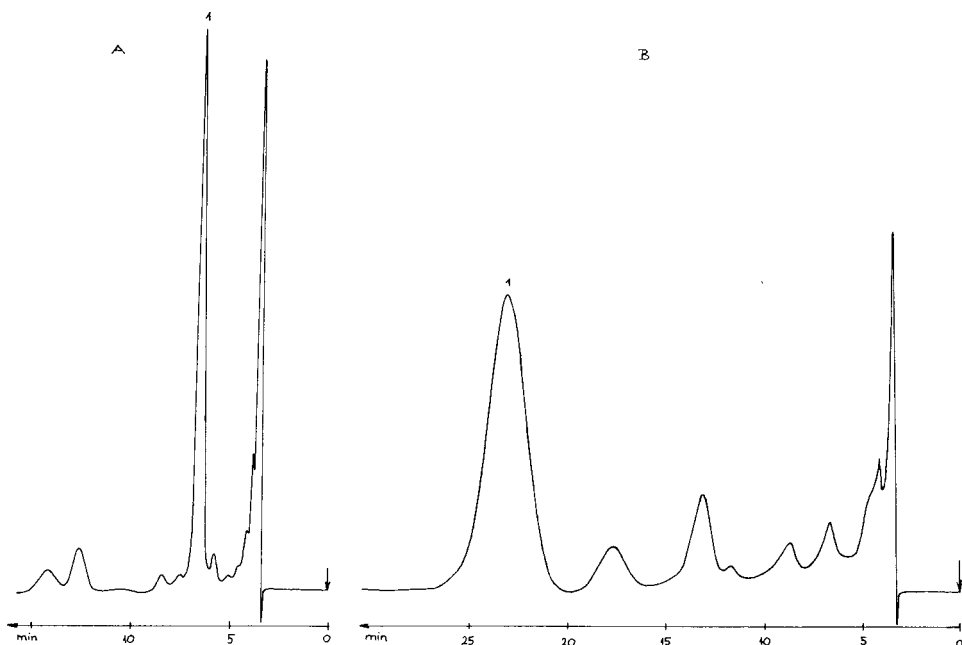


Fig. 2. Chromatograms of oxytocin raw product. A, Eluent A (see Experimental); B, Eluent E. Other conditions as in Fig. 1. Compounds: 1 = oxytocin; other peaks were not identified.

TABLE I

DEPENDENCE OF CAPACITY RATIOS, k' , ON THE ORGANIC SOLVENT USED FOR PREPARATION OF ELUENT

Eluent: methanol-X-0.1 M NaClO_4 , pH 2.2 (5:1:4), X_1 = Isopropanol; X_2 = tetrahydrofuran; X_3 = acetonitrile; X_4 = methanol.

	k'			
	X_1	X_2	X_3	X_4
Bovine insulin	0.17	1.01	2.69	4.23
Porcine insulin	0.18	1.95	4.10	9.10

ACTH_{1-32} and aprotinine. The second system, comprising acetonitrile, isopropanol and buffered water containing 0.1 M sodium perchlorate (eluent F), can be used for the separation of insulins.

As regards, the pH of the eluent, all polypeptides except aprotinine can be separated at a pH of 2.2; aprotinine can be investigated at a pH 6.5.

O'Hare and Nice¹² described a very good gradient elution system for the separation of proteins and polypeptides. They used a Hypersil ODS column and an acetonitrile gradient at pH 2.1. On the basis of their retention data, Meek¹³ calculated the retention coefficients of amino acid residues. He could then predict the retention

TABLE II

COMPARISON OF PREDICTED AND FOUND CAPACITY RATIOS OF ACTH DERIVATIVES

The predicted ratios were based on the retention times obtained by summing retention coefficients for each polypeptide. A retention time of 2.0 min was assumed for unretained compounds. See Experimental for eluents B and E.

	No. of residues	k'		
		Predicted pH 2.1	Found	
			Eluent B	Eluent E
ACTH ₁₅₋₃₂	18	2.15	1.5	0
ACTH ₁₋₃₂	32	13.8	7.5	4.7
ACTH ₁₋₁₄	14	20.15	10.1	9.1
ACTH ₁₋₂₄	24	26.25	13.9	17.7
ACTH ₁₋₂₈	28	20.8	10.6	10.0

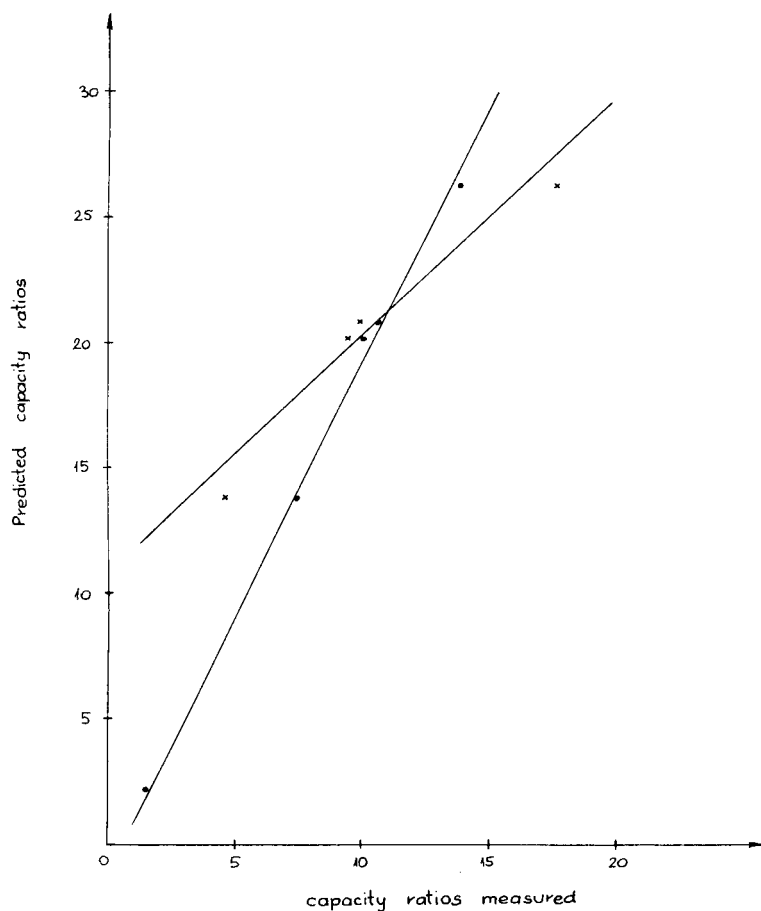


Fig. 3. Correlation of measured capacity ratios, k' , vs. capacity ratios predicted by summing retention coefficients for the amino acids and end groups present in ACTH derivatives. Eluents: \times , B; +, E.

times of different polypeptides. By summing the retention coefficients for each polypeptide; a good correlation was obtained between the predicted and found retention times.

We have examined the applicability of Meek's prediction method for isocratic elution with different eluents. Table II lists the predicted and found capacity factors obtained for ACTH derivatives. In Fig. 3 the predicted capacity factors are plotted against the capacity factors measured for ACTH derivatives using two different eluent systems. As is seen, a roughly linear relationship was obtained.

The predicted capacity ratios were calculated for the other polypeptides investigated and compared with the found values (Table III). The good correlation between estimated and found elution order indicates that the data calculated according to Meek can be transformed to isocratic conditions and different eluent systems. Thus the data in Table III can be used to select suitable chromatographic systems for the separation of polypeptides.

TABLE III

COMPARISON OF PREDICTED AND FOUND CAPACITY RATIOS FOR OXYTOCIN, APRO-TININE AND INSULINS

See Experimental for eluents A, D, E and F.

	<i>k'</i>					
	<i>Predicted</i>		<i>Found</i>			
	<i>pH 2.1</i>	<i>pH 7.4</i>	<i>Eluent A</i>	<i>D</i>	<i>E</i>	<i>F</i>
Oxytocin	13.3		1.31*		6.50	
Oxytocin			2.14		5.12	
Aprotinine		42.5		4.55		
Bovine	62.0					2.53
Insulin						
Porcine	71.9					3.61
insulin						
Bovine	87.0					4.45
proinsulin						
Porcine	95.9					12.90
Proinsulin						

Some applications of the method are now described. Fig. 4 shows the chromatogram of an oxytocin injection solution (10 I.U./ml). The relative standard deviation of the determination of oxytocin in formulations calculated for seven parallel runs was found to be 0.8% and a linear calibration curve was obtained within the concentration range 2–20 I.U./ml. When oxytocin concentrate (about 250 I.U./ml) was analysed the sample was diluted to about 10 I.U./ml.

Fig. 5 correlates the results obtained by HPLC and bioassay methods. Similar experiments were made by Krummen and Frei^{18,19} who found that the regression values were within the range of variation expected for bioassay tests. Our data support their observation that more reliable results can be obtained by HPLC. The very good correlation between the results obtained by the two methods suggests the use of

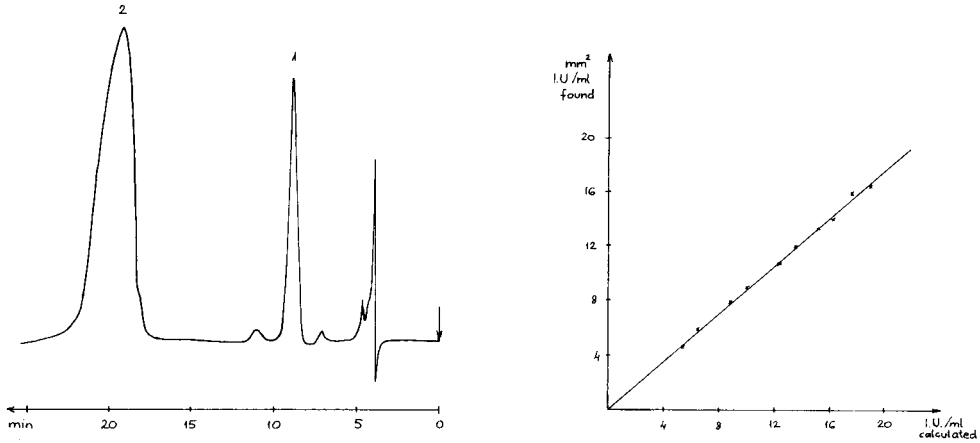


Fig. 4. Chromatogram of oxytocin injection solution (10 I.U./ml) and calibration curve for oxytocin. Eluent: A. Other conditions as in Fig. 2. Compounds: 1 = oxytocin; 2 = 4-trichlorobutanol-1.

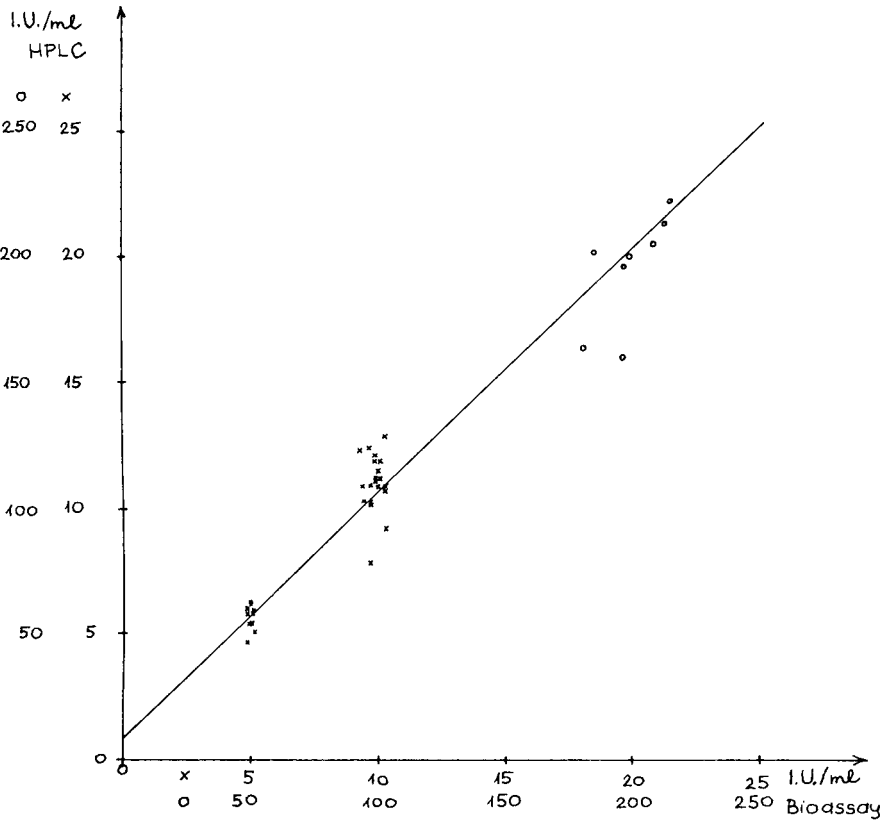


Fig. 5. Correlation between HPLC and bioassay results. Regression line (y = HPLC, x = bioassay): $y = 0.99x + 0.81$.

HPLC for the determination of oxytocin in pharmaceutical dosage forms and concentrates.

Fig. 6 shows the separation of aprotinine from Gordox® (Gedeon Richter) injection. In the case of aprotinine, satisfactory separation can be achieved only when the concentration of the organic modifier differs by less than $\pm 5\%$ compared to the optimal eluent system, because the separation efficiency is highly dependent on the concentration of the organic modifier.

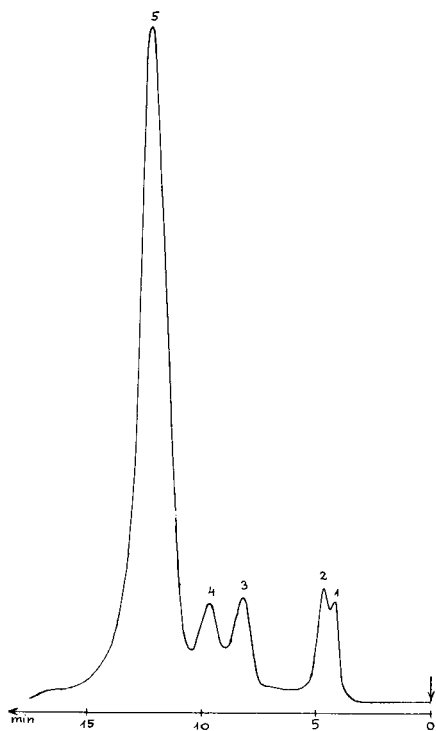


Fig. 6. Chromatograms of Gordox® injection. Eluent: D. Detection: 280 nm. Other conditions as in Fig. 1. Compounds: 1-4 = unknown; 5 = aprotinine.

The separation of insulins and related compounds by HPLC is a very important analytical task. We have reported our results elsewhere²⁰. However, the optimization of the separation system was not considered. The importance of the choice of solvent can be demonstrated for insulin separation, Fig. 7 (see also Fig. 2 for oxytocin). The best separation was achieved by using eluent F. The separation of bovine and porcine insulins, desamidinsulins and proinsulins is described elsewhere²⁰.

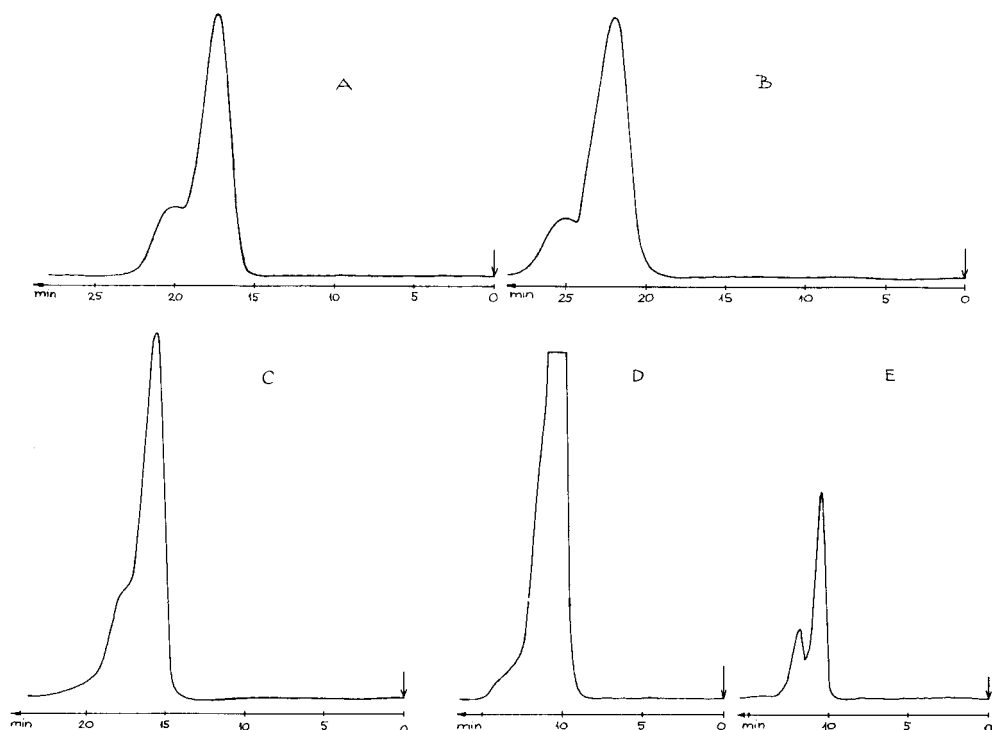


Fig. 7. Dependence of the separation of bovine insulin and desamidoinsulin on the eluent composition. Eluent: organic modifier aqueous 0.01 *M* phosphate buffer containing 0.1 *M* NaClO₄ (4:6). Organic modifier: A, methanol-isopropanol (4:2); B, methanol-isopropanol-acetonitrile (3:2:1); C, methanol-isopropanol-acetonitrile (2:2:2); D, methanol-isopropanol-acetonitrile (1:2:3); E, isopropanol-acetonitrile (2:4). Other conditions as in Fig. 1.

CONCLUSIONS

In the separation of polypeptides by hydrophobic chromatography it was found that both the type and concentration of the organic modifier as well as the salinity of the eluent have a significant influence on the selectivity and efficiency of the separation. The use of isopropanol as organic modifier in the eluent results in improved separations. It was also found that Meek's method of predicting retention times can be employed for isocratic elution with different eluent systems. The usefulness of this prediction method has been demonstrated for some polypeptides of biological interest.

ACKNOWLEDGEMENTS

The authors thank Miss V. Windbrechtinger for her technical assistance. The valuable discussions with Dr. M. Löw, Dr. I. Schön and T. Überhard are gratefully acknowledged.

REFERENCES

- 1 H. P. J. Bennett, A. M. Hudson, C. McMartin and G. E. Purdon, *Biochem. J.*, 168 (1977) 9.
- 2 N. Ling, *Biochem. Biophys. Res. Commun.*, 74 (1977) 248.
- 3 C. McMartin and G. E. Purdon, *J. Endocrinol.*, 77 (1978) 67.
- 4 W. S. Hancock, C. A. Bishop, R. L. Prestidge, D. R. K. Harding and M. T. W. Hearn, *Science*, 200 (1978) 1168.
- 5 W. S. Hancock, C. A. Bishop, R. L. Prestidge, D. R. K. Harding and M. T. W. Hearn, *J. Chromatogr.*, 153 (1978) 391.
- 6 W. Mönch and W. Dehnen, *J. Chromatogr.*, 147 (1978) 415.
- 7 J. A. Glasel, *J. Chromatogr.*, 145 (1978) 469.
- 8 J. Revier, *J. Liquid Chromatogr.*, 1 (1978) 343.
- 9 R. C. Nice and M. J. O'Hare, *J. Chromatogr.*, 162 (1979) 401.
- 10 M. E. F. Biemond, W. A. Sipman and J. Olivie, *J. Liquid Chromatogr.*, 2 (1979) 1407.
- 11 U. Damgaard and J. Markussen, *Horm. Metab. Res.*, 11 (1979) 580.
- 12 M. J. O'Hare and R. C. Nice, *J. Chromatogr.*, 171 (1979) 209.
- 13 J. L. Meek, *Proc. Natl. Acad. Sci. U.S.*, 77 (1980) 1632.
- 14 F. E. Regnier and K. M. Gooding, *Anal. Biochem.*, 103 (1980) 1.
- 15 Cs. Horváth, W. Melander and I. Molnár, *J. Chromatogr.*, 125 (1976) 129.
- 16 I. Molnár and Cs. Horváth, *J. Chromatogr.*, 142 (1977) 623.
- 17 W. R. Melander, J. Stoveken and Cs. Horváth, *J. Chromatogr.*, 185 (1979) 111.
- 18 K. Krummen and R. W. Frei, *J. Chromatogr.*, 132 (1977) 27.
- 19 K. Krummen and R. W. Frei, *J. Chromatogr.*, 132 (1977) 429.
- 20 G. Szepesi and M. Gazdag, *J. Chromatogr.*, 218 (1981) 597.

APPLICATIONS OF LIQUID CHROMATOGRAPHY IN THE ANALYSIS OF DRUGS

CHROM. 13,758

RAPID AUTOMATED DETERMINATION OF D-PENICILLAMINE IN PLASMA AND URINE BY ION-EXCHANGE HIGH-PERFORMANCE LIQUID CHROMATOGRAPHY WITH ELECTROCHEMICAL DETECTION USING A GOLD ELECTRODE

F. KREUZIG*

Research and Development, Biochemie GmbH, A-6250 Kundl (Austria)

and

J. FRANK

Metrohm AG, CH-9100 Herisau (Switzerland)

SUMMARY

A high-performance liquid chromatographic method for the determination of D-penicillamine in plasma and urine has been developed, based on separation on a cation-exchange resin followed by an amperometric detection of the SH group of D-penicillamine oxidized on a gold electrode. The method has been automated and separations from plasma and urine take 7 and 9 min, respectively. The detection limits are 0.05 µg/ml in plasma and 0.2 µg/ml in urine, with a coefficient of variation of 2.9% ($n = 10$).

INTRODUCTION

D-Penicillamine (D-2-amino-3-mercapto-3-methylbutanic acid) is administered for the treatment of Morbus Wilson, metal intoxications, cystinuria and rheumatoid arthritis, its therapeutic effect being due to the SH group, for example via the formation of metal chelates, the participation in redox reactions or SH and SS exchange. Further possible mechanisms of reactions have been discussed¹. Because of the high toxicity of L-penicillamine^{2,3} only the D-isomer is used for therapeutic administration.

For the specific determination of D-penicillamine in plasma and urine photometric methods with SH-specific reagents^{4,5} cannot be used, because other metabolites, such as cysteine and glutathione, also contain SH groups.

Only chromatographic methods are suitable for this determination, and in the absence of a chromophore in the molecule low concentrations cannot be detected in the UV region. Methods based on amino acid analysers^{6–9} and subsequent derivatization, for example with ninhydrin, taking at least 100 min per sample, are not suitable for routine application. The thin-layer chromatographic method of Pongor¹⁰ allows a quicker measurement, but it cannot distinguish between D-penicillamine and D-penicillamine disulphide and requires a lengthy sample preparation.

A sensitive and specific method has been published by Saetre and co-workers^{11,12} based on separation on a cation-exchange resin (Zipax SCX, 30 μm) with a pre-column, and detection with a mercury electrode, installed in a self-made flow-through cell. Eggli and Asper¹³ described the determination of cysteine and related compounds with a similar method. Both methods^{11,13} involve reduction of D-penicillamine disulphide to D-penicillamine to obtain information about the concentrations of these metabolites, when it could be demonstrated that these substances (and also mixed disulphides, such as cysteine-D-penicillamine disulphide) can be present in amounts 3–100-fold that of D-penicillamine in urine or plasma.

SH compounds can be oxidized on a mercury or on a gold electrode¹⁴. This allows the use of an amperometric detector, which is frequently applied in high-performance liquid chromatography (HPLC) for the selective detection of easily oxidizable compounds (phenols, indoles, aromatic amines, etc.)¹⁵. Solid-state electrodes (for example, glassy carbon) in these detectors permit optimal cell construction, a wide anodic range (up to 1200 mV), a small basic current and low noise¹⁶.

EXPERIMENTAL

Chemicals

The following substances were used: D-penicillamine (Biochemie, Kundl, Austria), D-penicillamine disulphide (Fluka, Buchs, Switzerland), L-cysteine (Fluka), L-glutathione, reduced (Fluka), titriplex III (Merck, Darmstadt, G.F.R.), diammonium hydrogen citrate (Fluka), metaphosphoric acid (Merck) and phosphoric acid (Merck).

Sample preparation

D-Penicillamine in solution is unstable at pH above 6 and is oxidized by trace amounts of iron(III), especially in the neutral region. Therefore, iron(III) must be masked and a low pH is necessary.

Plasma. To 1 ml of blood are added 100 μl of 10% Titriplex III solution. The mixture is shaken, centrifuged and 1 volume of the supernatant is mixed with 2 volumes of a solution prepared by dissolving 4.39 g of diammonium hydrogen citrate in *ca.* 900 ml of water, adding 100 g of metaphosphoric acid and to 1 l with water. The precipitated protein is centrifuged and the supernatant is analysed. If stored for later analysis, the samples are frozen in liquid nitrogen.

Urine. To 1 ml of urine are added 100 μl of 10% Titriplex III solution and 1 volume of this sample is mixed with 2 volumes of the solution described above for plasma. If turbidity the solution is treated as for plasma. If necessary, the above-mentioned disulphides can be reduced at a mercury cathode.

Standard solutions

Standard solutions are prepared so as to contain 1.0 and 5.0 μg of D-penicillamine plus 100 μg of Titriplex III per millilitre of eluent for plasma and urine, respectively.

HPLC method

The eluent (0.02 M diammonium hydrogen citrate solution for plasma or a

0.01 *M* solution for urine, the pH being decreased to 2.2 by means of phosphoric acid, followed by filtration through a 0.5- μ m Millipore filter and degassing) is pumped by means of an Orlita DMPAE 10.4 pump over a cation-exchange column (Nucleosil 5 SA 200/6/4, No. 715 300, Macherey, Nagel & Co., Düren, G.F.R., 150 bar, 1.5 ml/min) and the eluate is fed to a Metrohm EA 1096/2 flow-through cell. This cell is equipped with a three-electrode system (working electrode gold, EA 286/3; reference electrode silver-silver chloride with 3 *M* potassium chloride solution, EA 442; auxiliary electrode glassy carbon, EA 286/1), leading the signals to a Metrohm EA 611 amperometric detector. The polarization voltage is adjusted to +800 mV, the signal sensitivity is $12.5 \cdot 10^{-7}$ A for urine samples and $12.5 \cdot 10^{-8}$ A for plasma samples, and there is no need to damp the signal. A Servogor RE 511 recorder of sensitivity 1 V and paper advance speed 0.5 cm/min is used. For injecting the samples and standards a Hewlett-Packard 7671 A sampler, modified for HPLC, with a 20- μ l loop, is used¹⁷. After five samples a standard is injected. The control of the analysis programme and the evaluation is performed with a laboratory data system (Hewlett-Packard 3353), the dilution factor of 3.3 for the samples being taken into account.

RESULTS AND DISCUSSION

Under the conditions used the retention times of D-penicillamine are 6 and 7.4 min and the detection limits are 0.05 μ g/ml and 0.2 μ g/ml for plasma and urine, respectively.

The coefficient of variation ($n = 10$) is 2.9%. The correlation between peak height and concentration of standard solutions, obtained without changing the sensitivity of the current measurement, is given in Table I.

TABLE I
RELATIONSHIP BETWEEN CONCENTRATION AND SIGNAL

Concentration (μ g/ml)	Peak height (mm) (average of 3 measurements)
0.1	12
0.5	63
1.0	124
$r = 0.9999$	

Although the D-penicillamine in the plasma and urine samples prepared for analysis is stable for 8 h at 20°C (see Table II), the concentration decreases in native plasma in spite of the addition of 1% of Titriplex III (Table III).

The yield in the reduction of D-penicillamine disulphide to D-penicillamine¹¹ at a mercury electrode is 75–77% within 12 min.

The high selectivity and high sensitivity of the electrochemical detection of the SH group of D-penicillamine, separated chromatographically, permits its very rapid, automated determination without derivatization (Figs. 1 and 2).

It can be seen that urine samples contain larger amounts of detectable by-products than do deproteinized plasma samples, which is why for urine samples the

TABLE II

STABILITY OF D-PENICILLAMINE IN SAMPLES PREPARED FOR ANALYSIS

Time (h)	D-Penicillamine ($\mu\text{g/ml}$)	
	Plasma	Urine
0	0.70	1.14
1	0.70	1.14
2	0.68	1.11
3	0.69	1.16
4	0.72	1.17
5	0.70	1.14
6	0.72	1.14
7	0.71	1.14
8	0.70	1.12

TABLE III

STABILITY OF D-PENICILLAMINE IN PLASMA CONTAINING 1% OF TITRIPLEX III

Time (min)	D-Penicillamine ($\mu\text{g/ml}$)
0	2.9
5	2.7
10	2.5
20	2.3
30	2.1
60	1.7
120	1.1

eluent has been modified slightly to secure a better separation of different metabolites from D-penicillamine. Reduced glutathione and cysteine elute before D-penicillamine (Fig. 3).

It is essential to use a solute similar to the eluent in order to avoid changing the milieu of the gold electrode. If deproteinization is effected by means of ethanol, the conversion at the electrode for D-penicillamine in the injected sample is reduced to 60%, so that this method of deproteinization consequently cannot be applied. During the analytical run a small decrease in conversion at the gold electrode and a reduction of signal is observed, but this decrease can be accounted for mathematically by injecting standards in a certain sequence. If the intensity of the signals decreases too much, the gold electrode must be polished with alumina (Metrohm). It is not necessary to polish the auxiliary electrode.

The detection limits of this method are equal to those of the method of Sætre and Rabenstein¹¹. Increasing the injection volume to 100 μl reduces the detection limit by a factor of 4, but this can cause the accelerated formation of a film on the gold electrode with urine samples, which cannot be prevented by using a pre-column. Such a pre-column has proved not to be necessary, because even after the analysis of 1000

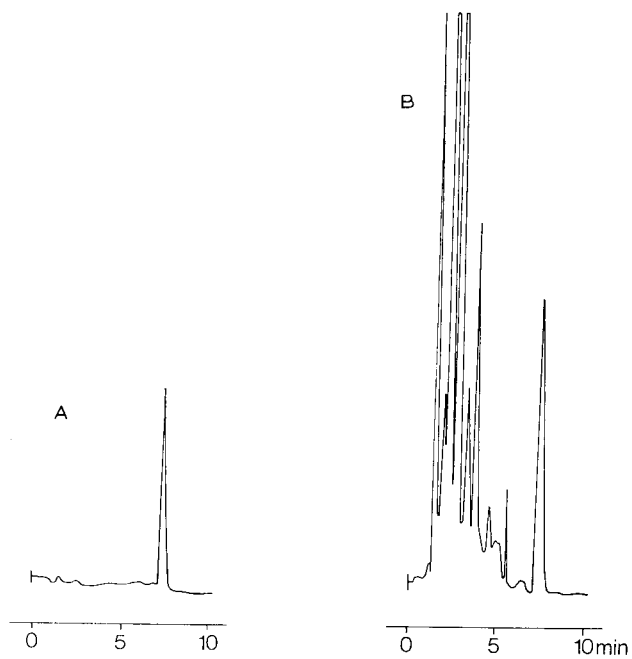


Fig. 1. Determination of D-penicillamine in urine. A, Standard (5 µg/ml); B, sample.

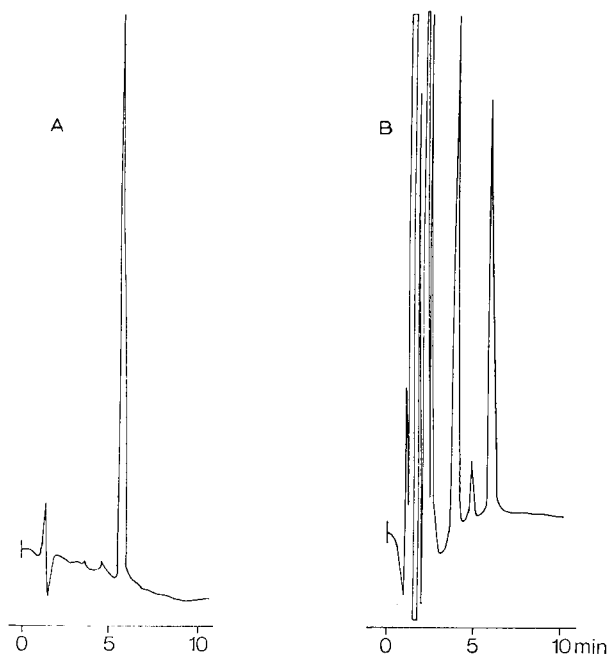


Fig. 2. Determination of D-penicillamine in plasma. A, Standard (1 µg/ml); B, sample.

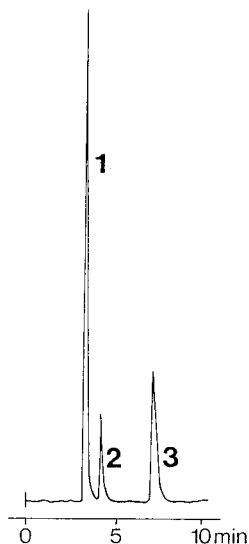


Fig. 3. Separation of L-cysteine (1), L-glutathione (2) and D-penicillamine (3), 1 $\mu\text{g/ml}$ each; sensitivity $12.5 \cdot 10^{-8}$ A.

samples the column shows an unchanged separation power for the samples prepared in the manner described above.

Adjusting the detector to a higher sensitivity ($5 \cdot 10^{-8}$ A) results in baseline drift after a short equilibration time of the electrode, and high-frequency disturbances may also occur. For an automated run, for example overnight, it is advisable not to set a high sensitivity. It is recommended that the flow-through cell is screened.

ACKNOWLEDGEMENTS

One of the authors (F.K.) is indebted to Miss Inge Auer, Miss Angelika Gaisbacher and Ing. Johann Patka for their valuable cooperation.

REFERENCES

- 1 M. Friedmann, *Protein Crosslinking*, Plenum Press, New York, London, 1977, p. 649.
- 2 A. Wacker, E. Heyl and P. Chandra, *Arzneim.-Forsch.*, 7 (1971) 971.
- 3 G. Kienel, *D-Penicillamin bei der chronischen Polyarthritits*, Biochemie, Vienna, 1972, p. 17.
- 4 J. Mann and P. D. Mitchell, *J. Pharm. Pharmacol.*, 31 (1979) 420.
- 5 P. R. Pal, *J. Biol. Chem.*, 234 (1959) 618.
- 6 M. Friedman, A. T. Noma and J. R. Wagner, *Anal. Biochem.*, 98 (1979) 293.
- 7 M. Hsiung, Y. Y. Yeo, K. Itiaba and J. C. Crawhall, *Biochem. Med.*, 19 (1978) 305.
- 8 D. Perrett, W. Sneddon and A. D. Stephens, *Biochem. Pharmacol.*, 25 (1976) 259.
- 9 A. O. Muijsers, R. J. Van de Stadt, A. M. A. Henrichs and J. K. Van der Korst, *Clin. Chim. Acta*, 94 (1979) 173.
- 10 S. Pongor, J. Kovács, P. Kiss and T. Dévényi, *Acta Biochem. Biophys. Acad. Sci. Hung.*, 13 (1978) 123.
- 11 R. Saetre and D. L. Rabenstein, *Anal. Chem.*, 50 (1978) 276.
- 12 A. S. Russell, R. Saetre, P. Davis and R. L. Rabenstein, *J. Rheumatol.*, 6 (1979) 15.
- 13 R. Eggli and R. Asper, *Anal. Chim. Acta*, 101 (1978) 253.
- 14 P. Bruttel, personal communication.
- 15 J. Frank, *Chimia*, 35 (1981) 24.
- 16 B. Fleet and C. J. Little, *J. Chromatogr. Sci.*, 12 (1974) 747.
- 17 F. Erni and H. Bosshard, *Chromatographia*, 12 (1979) 365.

CHROM. 13,852

RAPID HIGH-PERFORMANCE LIQUID CHROMATOGRAPHIC METHOD FOR THE MEASUREMENT OF VERAPAMIL AND NORVERAPAMIL IN BLOOD PLASMA OR SERUM

S. C. J. COLE and R. J. FLANAGAN

Poisons Unit, Guy's Hospital, St. Thomas' Street, London SE1 9RT (Great Britain)

A. JOHNSTON

Department of Clinical Pharmacology, St. Bartholomew's Hospital, West Smithfield, London EC1A 7BE (Great Britain)

and

D. W. HOLT*

Poisons Unit, Guy's Hospital, St. Thomas' Street, London SE1 9RT (Great Britain)

SUMMARY

A simple high-performance liquid chromatographic method for the simultaneous measurement of plasma verapamil and norverapamil concentrations has been developed. The sample (100 μ l) is vortex-mixed for 30 sec with 4 *M* sodium hydroxide solution, pH 13 (50 μ l), internal standard solution (aqueous 5,6-benzoquinoline, 0.20 mg/l) (50 μ l) and methyl *tert.*-butyl ether (200 μ l). After centrifugation at $9950 \times g$ for 2 min, a portion (100 μ l) of the resulting extract is analysed on a microparticulate (5 μ m) silica column using a methanolic solution of potassium bromide (3.0 *mM*) and perchloric acid (0.37 *mM*) as the mobile phase, and the column effluent is monitored by fluorescence detection using an excitation wavelength of 203 nm. A specimen, together with a quality control sample, can be analysed, in duplicate, within 30 min. The limit of accurate measurement of the assay is 2 μ g/l, and no potential sources of interference have been identified. The method has advantages of speed, small sample requirement and complete resolution of the three major metabolites of verapamil.

INTRODUCTION

Verapamil (DL-2-(3,4-dimethoxyphenyl)-2-isopropyl-5-(N-methyl, N- β (3,4-dimethoxyphenyl)ethylamino)valeronitrile; Fig. 1) has anti-anginal, anti-hypertensive and anti-arrhythmic properties¹. This compound is extensively metabolised by both N-demethylation and N-dealkylation (Fig. 1), and the N-demethylated metabolite (norverapamil) is pharmacologically active and can accumulate to plasma concentrations equal to or greater than those of verapamil itself^{2,3}.

Previously published techniques for the measurement of plasma verapamil concentrations have either measured metabolites together with the parent com-

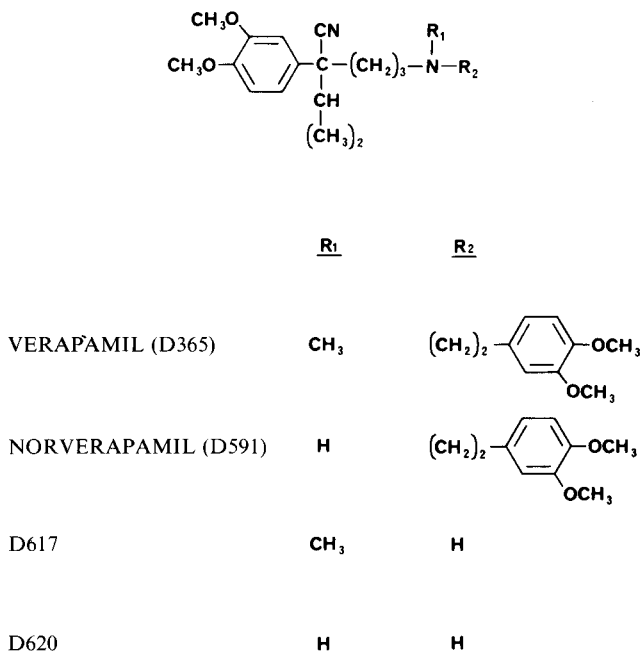


Fig. 1. Structural formulae of verapamil, norverapamil and two other metabolites.

pound⁴ or required relatively large sample volumes, long extract preparation times or the formation of derivatives prior to chromatographic analysis⁵⁻⁹. The method presented here is based on the direct high-performance liquid chromatographic (HPLC) analysis of an extract of a relatively small sample volume, and permits the simultaneous measurement of verapamil and norverapamil in the presence of the two remaining principal metabolites (Fig. 1).

EXPERIMENTAL

Materials and reagents

Verapamil and norverapamil hydrochlorides and the additional metabolites D617 and D620 (Fig. 1) were obtained from Abbott Labs. (Queenborough, Great Britain). The internal standard, 5,6-benzoquinoline, was obtained from Aldrich (Gillingham, Great Britain) and was used as a 0.20 mg/l solution in glass-distilled water. (This latter solution was prepared by dilution from a 1.00 g/l solution of 5,6-benzoquinoline in water-methanol, 80:20.) Methanol and methyl *tert.*-butyl ether were HPLC grade (Rathburn, Walkburn, Great Britain), and perchloric acid (70%), sodium hydroxide and potassium bromide were all analytical-reagent grade (BDH, Poole, Great Britain). Sodium hydroxide was used as a 4 *M* solution in glass-distilled water.

High-performance liquid chromatography

The solvent delivery system was a constant-flow reciprocating pump (Applied

Chromatography Systems, Model 750/04) and sample injection was performed using a Rheodyne Model 7125 syringe-loading valve fitted with a 100- μ l sample loop. Stainless-steel tubing (0.25 mm I.D.) was used to connect the outlet port of the valve to the analytical column, a stainless-steel tube 125 \times 5 mm I.D. packed with Spherisorb 5 silica (Hichrom, Woodley, Great Britain), which was used at ambient temperature (normally 22°C). The column effluent was monitored using a Schoeffel Model FS 970 fluorescence detector, with an excitation wavelength of 203 nm, no emission filter and a time constant of 0.5 sec. The mobile phase was a solution of potassium bromide (3 mM) and perchloric acid (0.37 mM, equivalent to 0.004%, v/v) in methanol, and was helium-degassed before use. The flow-rate was 2.0 ml/min, maintained by a pressure of approximately 60 bar.

The chromatography on this system of a methanolic solution containing verapamil and the three metabolites under study, together with the internal standard, is illustrated in Fig. 2. The retention times, measured relative to the internal standard, of verapamil, the metabolites under study and some additional compounds are given in Table I.

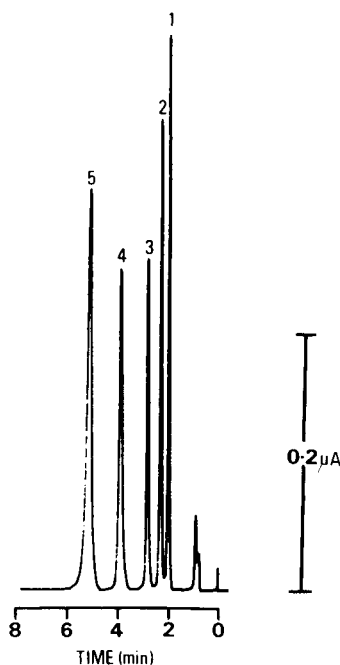


Fig. 2. Chromatogram obtained on analysis of a methanolic solution of D620 (1), norverapamil (2), D617 (3), verapamil (4) (all 0.10 mg/l) and 5,6-benzoquinoline (5) (0.20 mg/l); 100 μ l injection. For chromatographic conditions, see text.

Sample preparation

Plasma or serum (100 μ l) was pipetted into a small (Dreyer) test-tube (Poulton, Selfe and Lee, Wickford, Great Britain). Internal standard solution (50 μ l), sodium hydroxide solution (50 μ l) and methyl *tert.*-butyl ether (200 μ l) were added using Hamilton repeating mechanisms fitted with Hamilton gas-tight luer-fitting glass sy-

TABLE 1

RETENTION TIMES RELATIVE TO 5,6-BENZOQUINOLINE OF VERAPAMIL, NORVERAPAMIL AND SOME OTHER COMPOUNDS

See text for chromatographic conditions.

<i>Compound</i>	<i>Relative retention time</i>
Desalkylflurazepam	0.30
Mexiletine	0.31
Ajmaline	0.32
Nitrazepam	0.32
D620	0.37
Propranolol	0.42
4-Hydroxypropranolol	0.42
Nortriptyline	0.43
Norverapamil	0.45
D617	0.55
Doxepin	0.59
Desipramine	0.62
Amitriptyline	0.65
Dothiepin	0.69
Trimipramine	0.69
Atenolol	0.73
Verapamil	0.75
Orphenadrine	0.78
Imipramine	0.81
Chlorpromazine	0.83
Flurazepam	0.60–0.68*
Mianserin	0.85
Prajalium	0.86
5,6-Benzoquinoline	1.00
Quinidine	4.60
Quinine	4.73

* Tailing peak: retention times measured at 100 mg/l and 1.00 g/l.

ringes and stainless steel needles. The contents of the tube were vortex-mixed for 30 sec and centrifuged at 9950 g for 2 min in an Eppendorf centrifuge 5412 (Anderman, East Molesey, Great Britain). Subsequently, a portion (approximately 110 μ l) of the extract was taken and used to fill the sample loop of the injection valve.

Duplicate sample analyses were performed, and the mean result taken.

Instrument calibration

Standard solutions containing both verapamil and norverapamil at concentrations equivalent to 100, 200, 300, 500, 750 and 1000 μ g/l of analyte free-base were prepared in heparinised human plasma by serial dilution of solutions of the appropriate hydrochlorides in methanol at concentrations equivalent to 1.00 g/l free-base. These standards were stable for at least 3 months if stored in small aliquots at -20°C in the absence of light. On analysis of these solutions, the ratio of the peak height of the analyte to the peak height of the internal standard, when plotted against analyte concentration, was linear and passed through the origin of the graph in each case

(Fig. 3). The calibration gradients (peak height ratio/analyte concentration) normally obtained were 0.0108 and 0.0126 l/ μ g for verapamil and norverapamil, respectively.

A further set of solutions prepared in heparinised human plasma containing verapamil and norverapamil at concentrations of 5, 10, 20 and 50 μ g/l were available for use when indicated. The calibration obtained on analysis of these solutions was again linear and passed through the origin of the graph in each case. The calibration gradients obtained were the same as those quoted above.

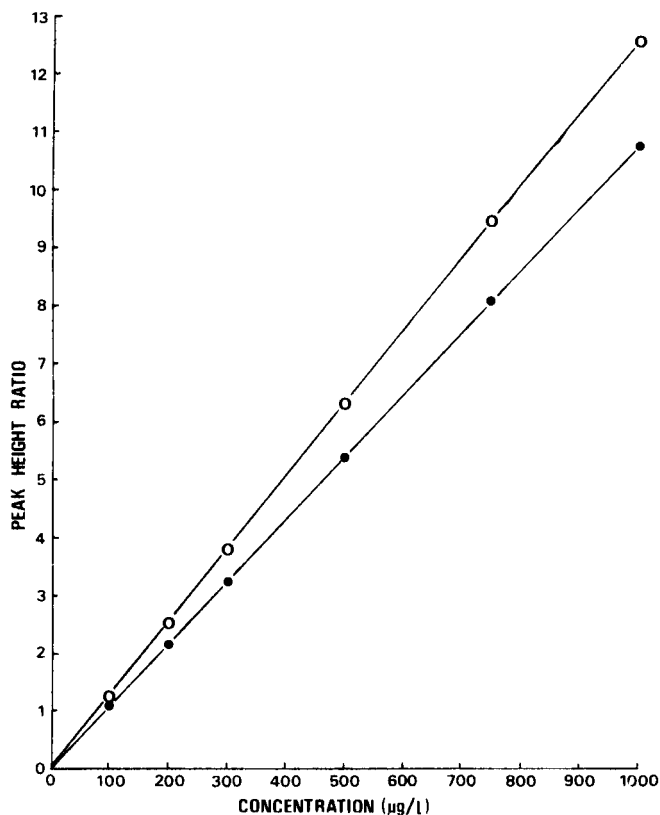


Fig. 3. Calibration graph of peak height ratio of verapamil (●) and norverapamil (○) against analyte concentration.

RESULTS AND DISCUSSION

Choice of chromatographic conditions

The use of inorganic anions such as bromide or perchlorate to promote the elution of basic and neutral drugs from silica columns has been described previously^{10,11}. In this case, the use of perchlorate alone at a concentration of 1.85 mM (0.02%, v/v, perchloric acid) in methanol did not achieve complete resolution of metabolite D620 (Fig. 1) from norverapamil, even if a 250 × 5 mm I.D. column packed with Spherisorb 5 silica was used. On the other hand, the use of

bromide as counter-ion at a concentration of 3.0 mM gave complete resolution of verapamil and the metabolites under study, but did not promote the elution of the internal standard selected on the basis of the work with perchlorate, 5,6-benzoquinoline. However, the combination of both bromide and perchlorate used not only maintained the separation of verapamil and the metabolites studied but also promoted the elution of the internal standard at a satisfactory retention time (Fig. 2).

The system was found to be both stable and reproducible, and during routine use the relative retention times of the compounds under study (Table I) varied by ± 0.01 , although the absolute retention times did vary up to 15%. Any deterioration in resolution or peak shape which did occur, however, was normally attributable to contamination of the chromatographic system with water or other compounds, or accumulation of insoluble material at the top of the column or in the microbore tubing from the injection port. Flushing with diethyl ether (approximately 50 ml) was often successful in removing soluble contaminants from the column, while simple cleaning and/or repacking of the top 2–3 mm of the column using a slurry of Spherisorb 5 silica in methanol was usually effective in prolonging the life of the column.

Selectivity

No endogenous sources of interference have been observed. The chromatogram obtained on analysis of a specimen of drug-free human plasma is illustrated in Fig. 4, and the chromatogram obtained from a plasma specimen from a patient treated chronically with verapamil is given in Fig. 5. Analyses of these and other specimens performed without the addition of 5,6-benzoquinoline have not revealed the presence of interfering compounds.

Compounds which were extracted under the conditions of the assay were studied further as potential sources of interference (Table I). Mexiletine, propranolol, orphenadrine, quinidine and quinine were detectable if present at concentrations similar to those attained during normal therapy, *i.e.* 5 mg/l or less, but were at least partially resolved from the compounds of interest on the chromatographic system (Table I). Other cardio-active drugs studied (amiodarone, disopyramide, lignocaine, lorcaïnide, metoprolol, procainamide, oxprenolol and tocainide) were not detected on this system. The relative responses of the remaining compounds studied (Table I) were generally much lower than those of verapamil and its metabolites, and so serious interference is unlikely to occur except following overdose.

Detection conditions

The use of an emission cut-off filter was not thought to be necessary in view of the high selectivity shown by the system in normal use. This had the advantage of giving enhanced sensitivity (increased signal to noise ratio), and directly facilitated the measurement of very low verapamil concentrations. The lowest-attainable detector time-constant (0.5 sec) was used in view of the very rapid elution of the compounds of interest (Fig. 2) and also to minimise problems such as that reported with propranolol¹² where analyte peak area was reported to be inversely proportional to eluent flow-rates up to 1.4 ml/min using a time-constant of 6 sec.

Recovery studies

Standard solutions containing verapamil and norverapamil at concentrations

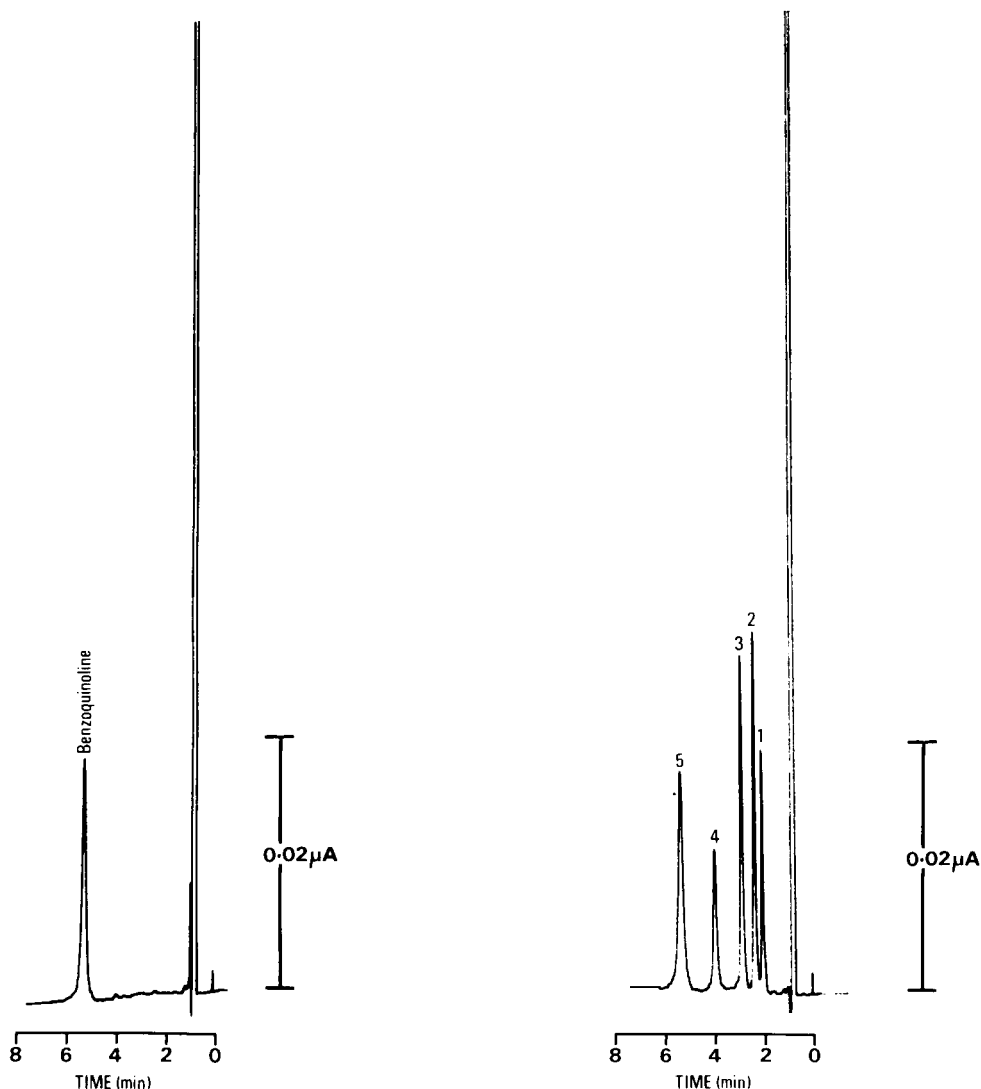


Fig. 4. Chromatogram obtained on analysis of a specimen of drug-free human plasma; 100 μ l injection. The initial 5,6-benzoquinoline concentration was 0.20 mg/l.

Fig. 5. Chromatogram obtained on analysis of a plasma specimen obtained from a patient treated chronically with verapamil (3×120 mg/day); 100- μ l injection. The initial 5,6-benzoquinoline (5) concentration was 0.20 mg/l, and the plasma verapamil (4) and norverapamil (2) concentrations were found to be 60 and 135 μ g/l, respectively. (1 and 3 were D620 and D617, respectively; cf. Fig. 1.)

of 25, 50 and 100 μ g/l were prepared in methanol by dilution from the 1.00 g/l stock methanolic solutions. The recovery of analyte from the corresponding plasma standards, *i.e.* 50, 100 and 200 μ g/l, was calculated by comparison of the peak heights of verapamil and norverapamil obtained on analysis of 100 μ l portions of the methanolic standards to those obtained from freshly-prepared sample extracts, and the

TABLE II

RECOVERY OF VERAPAMIL AND NORVERAPAMIL FROM HEPARINISED HUMAN PLASMA

n = 10 at each concentration.

Concentration ($\mu\text{g/l}$)	Recovery (%; mean \pm S.D.)	
	Verapamil	Norverapamil
50	97.7 \pm 2.9	94.5 \pm 3.2
100	96.6 \pm 3.4	88.7 \pm 3.8
200	94.3 \pm 3.0	89.4 \pm 3.6

results are presented in Table II. The recovery of 5,6-benzoquinoline was only approximately 60 % under the conditions of the assay.

Reproducibility

The intra-assay coefficients of variation (C.V.) measured from replicate analyses (*n* = 10) of standard solutions prepared in heparinised human plasma containing verapamil and norverapamil at concentrations of 5, 20, 50, 100 and 200 $\mu\text{g/l}$ are presented in Table III. The inter-assay C.V. at 100 $\mu\text{g/l}$ for verapamil was 2.98 % and for norverapamil was 2.80 % (*n* = 10 in both cases).

TABLE III

INTRA-ASSAY REPRODUCIBILITY OF THE ASSAY

n = 10 at each concentration.

Concentration ($\mu\text{g/l}$)	Coefficient of variation (%)	
	Verapamil	Norverapamil
5	4.4	4.8
20	3.1	4.0
50	2.9	3.0
100	1.3	2.8
200	1.2	2.2

Limit of sensitivity

The limit of accurate measurement of the assay was 2 $\mu\text{g/l}$ using a 100 μl sample; the intra-assay C.V. at this concentration was 6.2 % (*n* = 10). The use of larger sample sizes (*e.g.* 250 μl) could enable accurate measurements to be made down to concentrations of the order of 1 $\mu\text{g/l}$, should this be indicated.

CONCLUSIONS

The method described here has been used for the measurement of the plasma concentrations of both verapamil and norverapamil attained during therapy, and also

for the measurement of verapamil following single intravenous doses. Only 200 μ l of specimen are required for a duplicate analysis, which can be completed, together with the analysis of a quality control specimen, within 30 min. No potential sources of interference have been identified, and it should prove possible to measure additional metabolites of verapamil if this was indicated.

ACKNOWLEDGEMENTS

We thank Abbott Labs. for supplying verapamil and its metabolites and Dr. Brian Widdop, Poisons Unit, Guy's Hospital, for his criticism of the manuscript. A.J. received financial support from Abbott Labs.

REFERENCES

- 1 B. N. Singh, G. Ellrodt and C. T. Peter, *Drugs*, 15 (1978) 169.
- 2 M. Schomerus, B. Spiegelhalter, B. Dieren and M. Eichelbaum, *Cardiovasc. Res.*, 10 (1976) 605.
- 3 G. Neugebauer, *Cardiovasc. Res.*, 12 (1978) 247.
- 4 R. G. McAllister and S. M. Howell, *J. Pharm. Sci.*, 65 (1976) 431.
- 5 B. Spiegelhalter and M. Eichelbaum, *Drug Res.*, 27 (1977) 94.
- 6 R. G. McAllister, Jr., T. G. Tan and D. W. A. Bourne, *J. Pharm. Sci.*, 68 (1979) 574.
- 7 S. R. Harapat and R. E. Kates, *J. Chromatogr.*, 170 (1979) 385.
- 8 S. R. Harapat and R. E. Kates, *J. Chromatogr.*, 181 (1980) 484.
- 9 T. M. Jaouni, M. B. Leon, D. R. Rosing and H. M. Fales, *J. Chromatogr.*, 182 (1980) 473.
- 10 J. E. Greving, H. Bouman, J. H. G. Jonkman, H. G. M. Westenberg and R. A. de Zeeuw, *J. Chromatogr.*, 186 (1979) 683.
- 11 R. J. Flanagan, G. C. A. Storey and D. W. Holt, *J. Chromatogr.*, 187 (1980) 391.
- 12 M. Simon and M. Babich-Armstrong, *J. Anal. Toxicol.*, 3 (1979) 246.

CHROM. 14,021

AUTOMATED MEASUREMENT OF CATECHOLAMINES IN URINE, PLASMA AND TISSUE HOMOGENATES BY HIGH-PERFORMANCE LIQUID CHROMATOGRAPHY WITH FLUOROMETRIC DETECTION

KAZUKO MORI

National Institute of Industrial Health, 6-Chome, Naga-o, Tama-ku, Kawasaki 213 (Japan)

SUMMARY

An automated catecholamine analyzer was assembled from a high-performance liquid chromatograph, an autosampler and an air segmented reactor equipped with a sensitive fluorometer. The trihydroxyindole technique was applied to the fluorometric reactor. Urine, plasma and brain homogenate were usually purified on an alumina column prior to high-performance liquid chromatography (HPLC). Centrifuged urine and a supernatant of brain homogenate can, however, be injected onto the HPLC column without further pre-treatment. The measurement of noradrenaline and adrenaline in plasma of a man at rest required 0.5–1 ml samples. Approximately 100 alumina eluates from urine can be treated per day when the analyzer is operated continuously.

INTRODUCTION

In 1974, a new liquid chromatographic method for measuring catecholamines (CAs), based on the use of high-performance liquid chromatography (HPLC) with fluorometric detection, was presented¹. Since then, routine procedures have been developed and implemented for determination of urinary CAs^{2–6,14}, metanephrines in urine⁷ and CAs in plasma, cerebrospinal fluid and tissue homogenates⁸, utilizing the trihydroxyindole (THI)^{1–4,6–8} and ethylenediamine⁵ methods. An automatic HPLC system for the measurement of urinary CAs was also assembled by means of an autosampler in combination with an AutoAnalyzer equipped with a fluorometer⁹.

In this paper I describe the assay of urinary CAs with and without prepurification by the automated CA analyzer, and the application of the technique to measurements of CAs in plasma and brain homogenate.

EXPERIMENTAL

Reagents

CAs and alumina (neutral, Brockman activity grade I) were obtained from Sigma (St. Louis, MO, U.S.A.), sodium octyl sulphate from Eastman (Rochester, NY, U.S.A.) and sodium 1-heptanesulphonate from Regis (Morton Grove, IL,

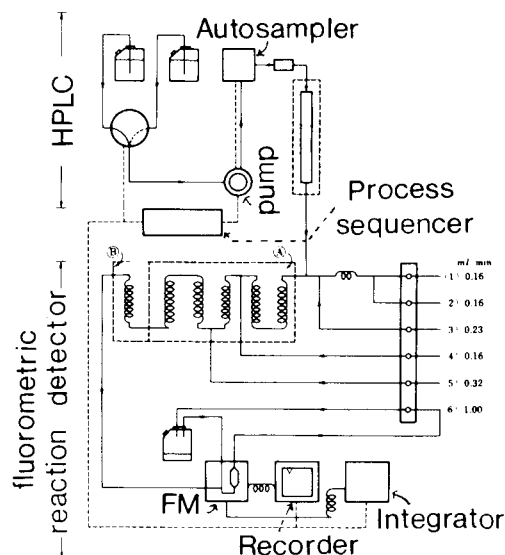


Fig. 1. Automated CA analyzer (THI method). Heating bath temperature: A, 30 °C; B, 15 °C (both 15 °C for plasma). Reagents: 1 = 1 M phosphate buffer; 2 = 0.1 % $\text{K}_3\text{Fe}(\text{CN})_6$; 3 = air; 4 = 0.1 % ascorbic acid; 5 = 4 M NaOH. FM = fluorometer.

U.S.A.). Other chemicals were reagent grade commercial materials. All chemicals were used without further purification.

Apparatus

Fig. 1 is a schematic presentation of the automated CA analyzer. It is comprised of a high-performance liquid chromatograph, an autosampler and an air segmented reactor equipped with a sensitive fluorometer. Unless otherwise stated, pumps, autosamplers, process sequencers, valves, gauges, dampers, connectors, etc., were from Kyowa-seimitsu (Tokyo, Japan) and proportioning pumps, glass coils, fittings, connectors, all tubing etc., were from Technicon (Chauncey, NY, U.S.A.). A Model 6000A solvent delivery system and a Model 710A WISP (Waters Assoc., Milford, MA, U.S.A.) were also used. Fluorometric measurements were made with a Model RF-510-LCA Shimadzu spectrofluorophotometer (excitation 420 nm, slit width 20 nm; emission 520 nm, slit width 40 nm). The fluorometer was equipped with a xenon lamp and a mirrored rectangular solid 120- μl flow cell. DuPont Zipax SCX, Hitachi gel 3011-C, Yanapak ODS-T and Waters $\mu\text{Bondapak C}_{18}$ were used as packing materials. Chromatographic conditions are described in the figure legends.

Procedure

Upon collection, urine was acidified to pH 3 with 6 M HCl and stored frozen at -20°C prior to analysis. To 10 ml of the acidified urine was added 1 ml of a 0.2 M solution of the disodium salt of EDTA. The pH was then adjusted to 8.5 by addition of 1 M NaOH. The solution was poured onto a column prepared from 0.5 g alumina and allowed to drain completely. The column was washed twice with 10 ml of distilled

water. The CAs were then eluted into a 10-ml test-tube using 5 ml of 0.5 *M* acetic acid. 10–200 μ l of the eluent were injected onto the chromatographic column. Total CAs were determined by addition of 2 *M* HCl (5 ml) to 5 ml of the acidified urine in a 20-ml test-tube. After heating for 20 min on a water-bath at 85°C, the hydrolyzed urine was treated in the manner described above for the unhydrolyzed urine.

Blood was collected by antecubital venipuncture in a centrifuge tube containing the disodium salt of EDTA (1 mg per 1 ml blood). The plasma separated by centrifugation at 6000 *g* at 2°C for 30 min can either be analyzed immediately or stored frozen at –80°C. A 1-ml volume of the plasma was placed in a centrifuge tube and 20 μ l glutathione-SH (60 mg/ml) and 500 μ l of 1.5 *M* perchloric acid were added. The tube was shaken vigorously for 1 min, and the contents centrifuged at 18,000 *g* at 2°C for 30 min. The supernatant was then transferred to a centrifugal microfiltration device⁹ and the pH of the deproteinized sample adjusted to 8.5 with 4 *M* and 1 *M* ammonium hydroxide. Fifty milligrams of alumina were added and the device was shaken for 10 min. The contents were filtered centrifugally at 3000 *g* for 10 min and the alumina was washed twice with 2.5 ml distilled water. The CAs were eluted into a 300- μ l microvial for WISP using 100 μ l of 1 *M* acetic acid. The wash and desorption steps are most conveniently carried out using the filtration device. A 90- μ l volume of the eluate was injected onto the chromatographic column.

RESULTS AND DISCUSSION

Automated measurement of CAs in human urine by HPLC with fluorometric detection using a Zipax SCX column

The chromatograms of urinary free and total (conjugated and free) CAs separated by two-stepwise elution are shown in Fig. 2. The calibration curves for CAs were linear over the range of 0.5–50 ng for noradrenaline (NA) and adrenaline (A), and 0.02–0.5 μ g for dopamine (DA). The coefficient of variation for each CA in intra-assay of an identical standard solution and of an identical alumina eluate from urine was 2.1% for NA, 0.7% for A, 2.2% for DA (*n* = 5) and 1.3% for NA, 2.2% for A,

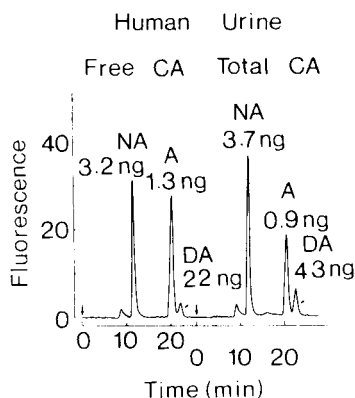


Fig. 2. Chromatograms of free and total CAs in human urine on a Zipax SCX column. Column: 1 m \times 2.1 mm; temperature, 40°C. Mobile phase: 0.03 *M* NaH₂PO₄ to 0.1 *M* NaH₂PO₄ (pH 4.3) (two-stepwise elution); flow-rate, 0.8 ml/min. Samples: alumina eluates from urine specimens excreted for 0.3 min (free CAs) and 0.15 min (total CAs).

1.5% for DA ($n = 5$), respectively. The overall precision of the method was evaluated from multiple analyses on an identical specimen of urine. The coefficient of variation for each CA in five analyses was 0.5% for NA, 0.4% for A and 4.8% for DA. The overall recoveries of CAs added to urine were $95.8 \pm 2.0\%$ for NA, $97.5 \pm 2.8\%$ for A and $99.6 \pm 2.6\%$ for DA (mean \pm S.D., $n = 10$). The sensitivity, reproducibility, precision and recovery were sufficient for the analysis of urinary CAs. If the automated CA analyzer is operated continuously, 70–100 samples per day can be treated by two-stepwise elution.

Assay of urinary CAs without prepurification by the automated CA analyzer equipped with an Hitachi gel 3011-C column

In the analyses of serotonin and 5-hydroxyindoleacetic acid in urine¹⁰ and concentrated CAs in tissue homogenate¹¹ the centrifuged urine or the diluted supernatant can be injected on the HPLC column without further pretreatment, but not in the analysis of CAs, especially NA, in urine. CAs in urine can be now measured, without alumina extraction, by HPLC using an Hitachi gel 3011-C column. Fig. 3 shows the chromatograms (with and without alumina extraction) of free CAs in the urine of a man after playing tennis. In the latter direct method it is necessary to clean up the column with 0.075 *M* citrate buffer (pH 4.0) containing 10% acetonitrile for 15 min after each measurement to eliminate the materials which are retained on the column. The fluorescence of CAs under the same operating conditions was linear at least in the range of 1–20 ng for NA and 0.5–10 ng for A. The coefficient of variation for each CA in intra-assay of an identical standard solution was 1.1% for NA and 0.8% for A ($n = 5$).

The two methods with and without alumina extraction were run in parallel on ten human urine samples. The results are plotted in Fig. 4a for NA and in Fig. 4b for A. Plots of NA and A values (ng/ml) obtained by the indirect method *vs.* those obtained by the direct method fitted the straight lines $y = 1.12x + 0.24$ with a

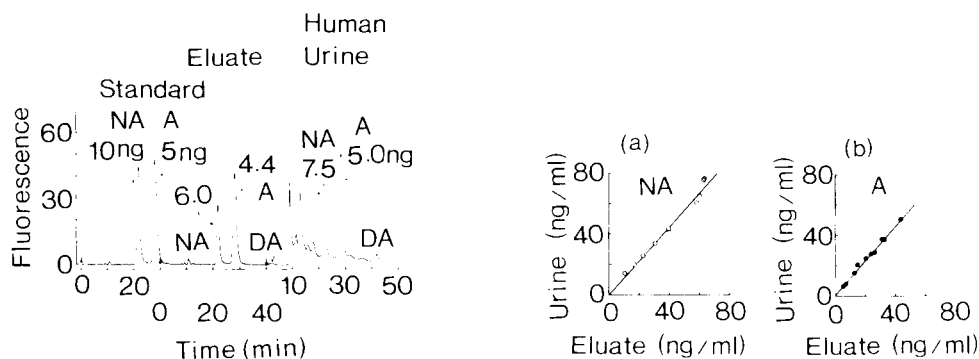


Fig. 3. Chromatograms of free CAs in human urine with and without alumina extraction on a Hitachi gel 3011-C column. Column: 20 cm \times 4 mm; temperature, 55°C. Mobile phase: 0.044 *M* citric acid-0.031 *M* sodium citrate (pH 4.0); flow-rate, 0.8 ml/min. Sample size: 100 μ l.

Fig. 4. Correlation of free CAs in human urine with and without alumina extraction on a Hitachi gel 3011-C column. Operating condition as in Fig. 3.

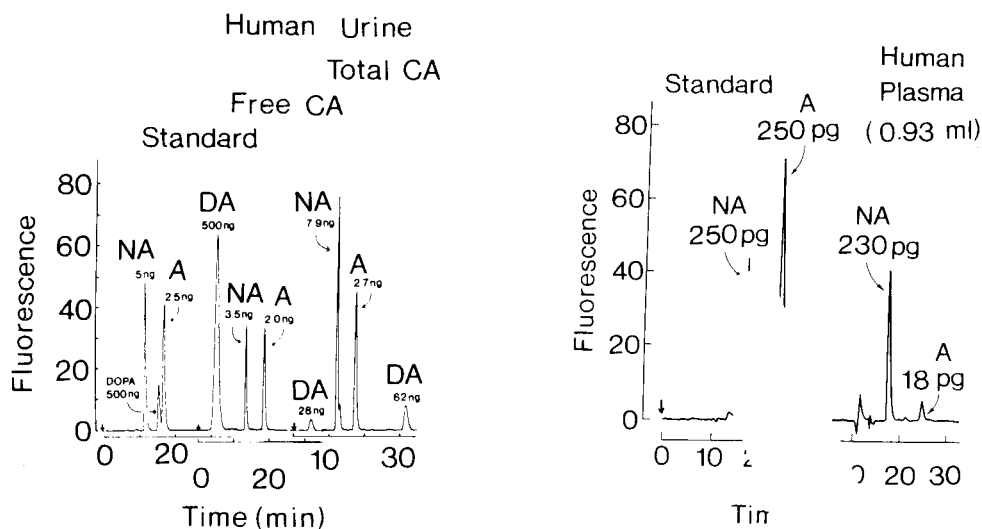


Fig. 5. Chromatograms of free and total CAs in human urine on a μ Bondapak C_{18} column. Column: 30 cm \times 4 mm; temperature, 20°C. Mobile phase: 0.065 M citric acid–0.035 M Na_2HPO_4 –10 mg/l sodium octyl sulphate (pH 3.0); flow-rate, 1.2 ml/min. Samples: alumina eluate from urine specimens excreted for 0.3 min (free CAs) and 0.15 min (total CAs).

Fig. 6. Chromatograms of CAs in plasma on a Yanapak ODS-T column. Column: 25 cm \times 4 mm; temperature, 20°C. Mobile phase: 0.1 M KH_2PO_4 + 100 mg/l sodium 1-heptanesulphonate (pH 3.1)–methanol (98:2); flow-rate, 0.6 ml/min. Sample: alumina eluate from plasma.

correlation coefficient of 0.983 and $y = 1.14x + 0.26$ with a correlation coefficient of 0.998, respectively. There are highly significant correlations between the values from the two methods ($p < 0.01$). The values for CAs in the alumina eluates are $88.6 \pm 6.9\%$ for NA and $87.0 \pm 2.4\%$ for A (mean \pm S.D.) of those obtained directly from the urine samples. About 30 centrifuged urine samples per day can be measured by the direct method.

Assay of CAs in human urine using μ Bondapak C_{18}

Over the past years reversed-phase HPLC with chemically bonded octadecyl and octyl chains has become popular. The separation of CAs and related compounds has been carried out by soap chromatography or hydrophobic chromatography using these columns. Riggins and Kissinger¹² recently reported a highly effective procedure for simultaneous assay of urinary CAs by soap chromatography with electrochemical detection. It is necessary to use two-step extraction as sample preparation, *i.e.*, cation-exchange column extraction followed by an alumina column to eliminate acidic and neutral catechols which are retained on the C_{18} column. Fig. 5 shows the chromatograms on a μ Bondapak C_{18} column of free and total CAs in daytime urine from a woman. These samples were prepurified using only the alumina column. In the case of fluorometric detection using the THI method, the sample preparation is easier than in the case of electrochemical detection. Approximately 60 samples per day can be analyzed by the automated CA analyzer.

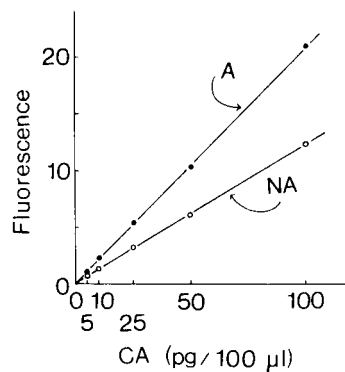
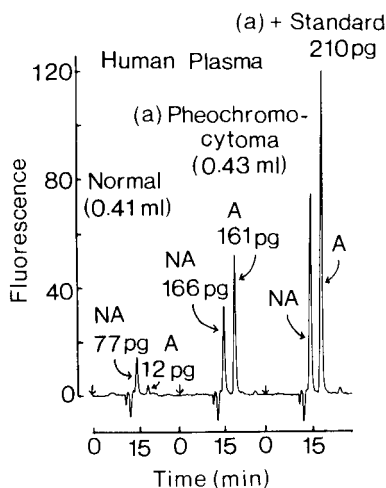


Fig. 7. Chromatograms of CAs in plasma on a Yanapak ODS-T column. Column as in Fig. 6. Mobile phase: 0.1 M KH_2PO_4 + 100 mg/l sodium 1-heptanesulphonate (pH 3.1)-methanol (97:3); flow-rate, 0.7 ml/min. Samples: alumina eluates from plasma.

Fig. 8. Calibration curves for CAs on a Yanapak ODS-T column. Operating conditions, as in Fig. 6.

Analysis of CAs in human plasma by use of Yanapak ODS-T

CAs in human plasma were determined by ion-pair chromatography with a Yanapak ODS-T column as shown in Figs. 6 and 7. The calibration curves for CAs were linear over the range of 5–1000 pg for NA and A (Fig. 8). The coefficient of variation for each CA in intra-assay of an identical standard solution was 0.5% for NA and 0.8% for A ($n = 10$), respectively. The recoveries of CAs added to the supernatant were about 80% for NA and A. The measurement of NA and A in plasma of

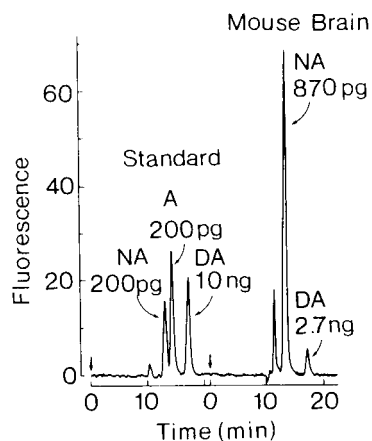


Fig. 9. Chromatograms of CAs in whole mouse brain on a Hitachi gel 3011-C column. Column: 15 cm \times 4 mm; temperature, 55°C. Mobile phase: 0.15 M KH_2PO_4 –0.15 M acetic acid (pH 3.3); flow-rate, 0.6 ml/min. Sample: supernatant from homogenate with 0.1 N HClO_4 .

a man at rest was achieved for 0.5–1 ml samples. The measurement of only NA requires 0.1–0.3 ml plasma. Fig. 7 shows the chromatogram of CAs in plasma of a pheochromocytoma patient at rest. The CAs values in her plasma were 0.57 ng/ml for NA and 0.55 ng/ml for A. The CAs in the plasma of a healthy subject at rest (Fig. 7) were 0.27 ng/ml for NA and 42 pg/ml for A. At least 90 μ l from the 100- μ l alumina eluate in a vial can be injected in HPLC by use of an automatic sample injector (WISP 710A; Waters). About 70 samples per day can be analyzed by the automated CA analyzer equipped with the autosampler.

Assay of CAs in mouse brain using Hitachi gel 3011-C

The chromatograms of CAs in whole mouse brain are shown in Fig. 9. A 20- μ l volume of the supernatant obtained from brain homogenate with 0.1 M perchloric acid was injected on the HPLC column. An alumina extraction procedure is necessary in order to detect the small amount of A in cerebral tissue. For the measurement of DA in plasma and brain parts, the chemical reactor based on ethylenediamine condensation or the *o*-phthalaldehyde method is preferable to that based on the THI method because of the stronger fluorescence obtained with the former reactor.

The use of air segmented reactors in HPLC has been reviewed by Frei and Scholten¹³. The automated CA analyzer with an air segmented reactor described here is useful for routine measurements of CAs in biological fluids and tissue homogenates.

REFERENCES

- 1 K. Mori, *Folia Endocrinol. Jap.*, 50 (1974) 637.
- 2 K. Mori, *Jap. J. Ind. Health*, 16 (1974) 490.
- 3 K. Mori, *Jap. J. Ind. Health*, 16 (1974) 494.
- 4 K. Mori, *Industr. Health*, 12 (1974) 171.
- 5 K. Mori, *Jap. J. Ind. Health*, 17 (1975) 170.
- 6 K. Mori, *Industr. Health*, 16 (1978) 41.
- 7 K. Mori, *Jap. J. Ind. Health*, 17 (1975) 116.
- 8 K. Mori, S. Saito, Y. Tak, H. Suzuki and S. Sato, *Folia Endocrinol. Jap.*, 52 (1976) 523.
- 9 K. Mori and T. Tezuka, *Proc. 24th Ann. Conf. Jap. LC Res. Assoc.*, 22 (1981) 67.
- 10 K. Mori, *Folia Endocrinol. Jap.*, 53 (1977) 529.
- 11 H. Matsuda, A. Iwata, T. Mogami, S. Sato and K. Mori, *Proc. 19th Ann. Conf. Jap. LC Res. Assoc.*, 17 (1976) 85.
- 12 R. M. Riggan and P. T. Kissinger, *Anal. Chem.*, 49 (1977) 2109.
- 13 R. W. Frei and A. H. M. T. Scholten, *J. Chromatogr. Sci.*, 17 (1979) 152.
- 14 K. Mori, in Z. Tamura, N. Ishibashi, Y. Ohkura, T. Tanimura and A. Tsuji (Editors), *LC-Keiko Bunseki* (*Analysis by Liquid Chromatography with Fluorometric Detection*), Kohdansha, Tokyo, 1978, p. 139.

CHROM. 14,103

GROUP-CONTRIBUTION APPROACH TO THE BEHAVIOUR OF 2-PHENYLETHYLAMINES IN REVERSED-PHASE HIGH-PERFORMANCE LIQUID CHROMATOGRAPHY

R. GILL*, S. P. ALEXANDER and A. C. MOFFAT

Home Office Central Research Establishment, Aldermaston, Reading, Berks. RG7 4PN (Great Britain)

SUMMARY

High-performance liquid chromatography retention data are reported for 2-phenylethylamine and 30 of its derivatives, including examples of CH₃, OH, OCH₃, COOH, NH₂ and N-oxide substitution. An octadecyl-silica column was used with an eluent of 10% methanol containing an amine-phosphate buffer (pH 3.15) to limit the interference of the silica support with chromatographic retention. The effects of individual substituents on retention are quantified by using group-contribution values (τ) and are discussed with reference to the position of substitution and the intramolecular interactions with other groups.

INTRODUCTION

2-Phenylethylamine can be regarded as the parent compound of a large group of drugs known as the sympathomimetic amines. The structure is modified by substitution of the aromatic ring, the α - and β -carbon atoms and the terminal amino group to yield compounds with a wide range of pharmacological activity¹. Many of the drugs undergo extensive modification *in vivo*. These reactions can include dealkylation of the amino group, hydroxylation of the aromatic ring or β -carbon or nitrogen atom and methylation of aromatic hydroxyl groups. Thus, there are a vast number of 2-phenylethylamine drugs and metabolites with closely related structures, which pose an enormous separation challenge to pharmaceutical, clinical and forensic laboratories. High-performance liquid chromatography (HPLC) offers an attractive approach to this problem, as all these compounds can be chromatographed without derivatization.

Chromatographic analysis can sometimes be limited by the absence of an authentic sample of the drug or metabolite for comparison of retention data. Many metabolites of 2-phenylethylamine drugs are difficult to obtain and in such instances, the prediction of retention data from molecular structure can be particularly valuable. The identification of unknown chromatographic peaks obtained during metabolic studies of new drugs or in toxicological studies may therefore be facilitated by the use of such data.

A group-contribution approach has been suggested for the prediction of

HPLC retention data of compounds having a common parent structure (Tomlinson and co-workers²⁻⁵; Horváth and co-workers^{6,7}). The chromatographic retention of a compound is described in terms of the retention of the parent structure with modifications for each of the substituents. Experimental data for a series of model compounds are required such that the group-contribution value (τ) for each substituent can be measured. Various factors can influence the magnitude of τ for a given substituent including temperature, eluent composition and stationary phase²⁻⁷. Further, the position of substitution within a molecule can also be important⁶. Nevertheless, for a given stationary phase and eluent, previous studies have indicated that this approach has potential for predicting chromatographic data.

Surprisingly, there have been few studies that have explored the effects of simple substituents on the chromatographic properties of a given structure. The present study seeks to expand our knowledge on the chromatographic behaviour of 2-phenylethylamine derivatives and contains data for 31 compounds on octadecyl-silica (ODS-silica). The effects of various substituents are discussed with reference to the positions of substitution and intra-molecular interactions with other substituents. Molnár and Horváth⁶ have considered some substituent effects within a group of hydrophilic phenylethylamines, but no data were presented for hydrophobic compounds of this type.

EXPERIMENTAL

Apparatus

HPLC was performed with a Waters M6000 pump, a Rheodyne 7120 injection valve (fitted with a 20- μ l loop) and a Perkin-Elmer LC-75 variable-wavelength UV detector operated at 250 nm. The column (25 cm \times 5 mm I.D.) was of stainless steel and packed with 5- μ m ODS-Hypersil (Shandon Southern Products, Runcorn, Great Britain) by a slurry procedure using isopropanol for dispersing the packing material and hexane as the pressurising solvent.

Materials

Methanol, sodium hydroxide and orthophosphoric acid were AnalaR grade (BDH, Poole, Great Britain). Diethylamine was puriss grade obtained from Fluka (Fluorochem, Glossop, Great Britain).

N,N-Dimethylphenylethylamine was prepared by reductive amination of phenylacetaldehyde with dimethylamine, using sodium cyanoborohydride following the method of Lane⁸. N,N-Dimethylphenylethylamine N-oxide was prepared by oxidation of N,N-dimethylphenylethylamine in 30% hydrogen peroxide at room temperature. N-Hydroxymethylamphetamine was prepared as the oxalate salt by the reaction of benzylmethylketone with N-hydroxymethylamine in the presence of sodium cyanoborohydride following the procedures of Morgan and Beckett⁹.

Eluent

Orthophosphoric acid (25.5 ml; 87%; 0.40 mole) was added to distilled water (1700 ml), and diethylamine (21.0 ml; 0.20 mole) was added. The pH was adjusted to 2.9 with concentrated sodium hydroxide solution and the total volume was adjusted to 1800 ml. Methanol (200 ml) was then added to give an eluent that had a pH of 3.15.

A flow-rate of 2.5 ml/min was used, and the eluent was recycled through the HPLC column for at least 1 h before retention measurements were made. All measurements were made at a temperature of $23^{\circ} \pm 2^{\circ} \text{C}$.

Evaluation of substituent effects

Retention data were expressed as capacity ratios, k' , which are defined by

$$k' = (t_R - t_0)/t_0$$

where t_R and t_0 are the retention times of the substance under investigation and a non-retained compound, respectively.

The effects of individual substituents on retention were quantified by using group-contribution values, τ , defined by

$$\tau = \log k'_1 - \log k'_2$$

where k'_1 and k'_2 are the capacity ratios of two compounds that differ by a single substituent (k'_2 is the capacity ratio of the unsubstituted compound). Hence, a positive value indicates that an increase in retention occurs on substitution.

RESULTS AND DISCUSSION

The eluent in this study contained diethylamine to ensure that chromatographic retention was not influenced by the silica matrix of the packing material. Without the addition of such masking agents, basic compounds often give broad and asymmetric peaks arising from a dual mechanism of hydrophobic interactions with bonded hydrocarbonaceous ligands and polar interactions with accessible silanol groups on the silica support¹⁰⁻¹⁴. The masking agent must show strong binding to the silanol groups and must be present at a concentration sufficient to compete with the solute. Previous studies on substituent effects using the group-contribution approach have not attempted to mask the silanophilic interactions of packing materials.

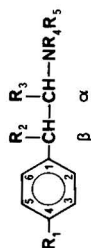
Table I lists the 2-phenylethylamine derivatives considered in this study, together with details of their structures and measured capacity ratios (k'). All compounds showed satisfactory peak shapes with the chosen eluent. It is envisaged that, at the pH of the eluent, the terminal amino groups of 2-phenylethylamines will be protonated. Further, the aromatic hydroxyl substituents will be non-ionised and the carboxyl groups of phenylalanine and tyrosine will be partially ionised (pK_a values 2.16 and 2.20, respectively)¹⁵.

Table I contains two pairs of compounds that have identical molecular formulae (*viz.*, ephedrine and pseudoephedrine, and phenylpropanolamine and norpseudoephedrine). The data show that both pairs can be separated on the present HPLC system. Each structural formula has two non-identical asymmetric carbon atoms, and hence diastereoisomers can exist¹⁶. Fig. 1 gives Newman projections indicating the stereochemical structures of the four compounds. The chromatographic data show that the "A" isomers have the shorter retention times (*i.e.*, ephedrine is eluted before pseudoephedrine, and phenylpropanolamine before norpseudoephedrine). The explanation probably rests with the intra-molecular hydrogen bonding that

TABLE I

HPLC RETENTION DATA FOR 31 2-PHENYLETHYLAMINES

Eluent: diethylamine (0.1 *M*) and orthophosphoric acid (0.2 *M*) in 10% (v/v) methanol adjusted to pH 3.15 with sodium hydroxide. Column: Hypersil-ODS; 25 cm \times 5 mm I.D.



Compound	Substituents						HPLC capacity ratio (<i>k'</i>)
	<i>R</i> ₁	<i>R</i> ₂	<i>R</i> ₃	<i>R</i> ₄	<i>R</i> ₅	Other	
Amphetamine	H	H	CH ₃	H	H		8.48
<i>N,N</i> -Dimethylamphetamine	H	H	CH ₃	CH ₃	CH ₃		11.08
<i>N,N'</i> -Dimethylphenylethylamine	H	H	H	CH ₃	CH ₃		4.82
<i>N,N</i> -Dimethylphenylethylamine N-oxide	H	H	H	CH ₃	CH ₃	N-oxide	10.78
Ephedrine	H	OH	CH ₃	CH ₃	H		5.68
Hordenine	OH	H	H	CH ₃	CH ₃		2.00
<i>p</i> -Hydroxyamphetamine	OH	H	CH ₃	H	H		2.24

5-Hydroxydopamine	OH	H	H	H	3-OH, 5-OH	0.05
<i>p</i> -Hydroxyephedrine	OH	OH	CH ₃	H		0.73
N-Hydroxymethylamphetamine	H	H	CH ₃	OH		33.53
Mescaline	OCH ₃	H	H	H	3-OCH ₃ , 5-OCH ₃	16.82
<i>p</i> -Methoxyamphetamine	OCH ₃	H	CH ₃	H		14.95
<i>o</i> -Methoxyphenamine	H	H	CH ₃	H	2-OCH ₃	32.17
<i>p</i> -Methoxyphenylethylamine	OCH ₃	H	H	H		5.55
Methylamphetamine	H	H	CH ₃	H		10.52
β -Methylphenylethylamine	H	CH ₃	H	H		8.55
N-Methylphenylethylamine	H	H	CH ₃	H		4.23
Noradrenaline	OH	OH	H	H	3-OH	0.10
Norpseudoephedrine	H	OH	CH ₃	H		4.39
Octopamine	OH	OH	H	H		0.18
Oxedrine	OH	OH	H	H		0.27
Phenelzine	H	H	CH ₃	H		5.91
Phentermine	H	H	NH ₂	H		19.46
Phenylalanine	H	H	H	H	α -CH ₃	2.46
Phenylethanamine	H	OH	H	H		1.63
Phenylethylamine	H	H	H	H		3.64
Phenylpropanolamine	H	OH	H	H		3.87
Pseudoephedrine	H	OH	CH ₃	H		5.90
<i>p</i> -Tolylethylamine	CH ₃	H	CH ₃	H		12.68
Tyramine	OH	H	H	H		0.81
Tyrosine	OH	H	COOH	H		0.74

TABLE II
EFFECT OF SUBSTITUENTS ON THE CHROMATOGRAPHIC RETENTION OF 2-PHENYLETHYLAMINES

<i>Substituent</i>	<i>Position</i>	<i>Parent compound</i>	<i>Substituted compound</i>	<i>τ value</i>
Methyl	α	Oxedrine	<i>p</i> -Hydroxyephedrine	+0.43
	α	Tyramine	<i>p</i> -Hydroxyamphetamine	+0.44
	α	<i>p</i> -Methoxyphenylethylamine	<i>p</i> -Methoxyamphetamine	+0.43
	α	Phenylethanamine	Phenylpropanolamine/norpseudoephedrine	+0.38/+0.43
	α	N-Methylphenylethylamine	Methylamphetamine	+0.40
	α	Phenylethylamine	Amphetamine	+0.37
	α	N,N-Dimethylphenylethylamine	N,N-Dimethylamphetamine	+0.36
	α	Amphetamine	Phentermine	+0.36
	β	Phenylethylamine	β -Methylphenylethylamine	+0.37
	<i>p</i> -Ar	Phenylethylamine	<i>p</i> -Tolylethylamine	+0.54
	N	Phenylpropanolamine	Ephedrine	+0.17
	N	Norpseudoephedrine	Pseudoephedrine	+0.13
	N	Amphetamine	Methylamphetamine	+0.09
	N	Phenylethylamine	N-Methylphenylethylamine	+0.07
Hydroxyl	N	N-Methylphenylethylamine	N,N-Dimethylphenylethylamine	+0.06
	N	Methylamphetamine	N,N-Dimethylamphetamine	+0.02
	β	Phenylethylamine	Phenylethanamine	-0.35
	β	Amphetamine	Phenylpropanolamine/norpseudoephedrine	-0.34/-0.29
	β	Methylamphetamine	Ephedrine/pseudoephedrine	-0.27/-0.25
	<i>p</i> -Ar	Ephedrine	<i>p</i> -Hydroxyephedrine	-0.89
	<i>p</i> -Ar	Phenylethylamine	<i>p</i> -Tyramine	-0.65
	<i>p</i> -Ar	Amphetamine	<i>p</i> -Hydroxyamphetamine	-0.58
	<i>p</i> -Ar	Phenylalanine	Tyrosine	-0.52
	<i>p</i> -Ar	N,N-Dimethylphenylethylamine	Hordenine	-0.38
	N	Methylamphetamine	N-Hydroxymethylamphetamine	+0.50
	<i>p</i> -Ar	Phenylethylamine	<i>p</i> -Methoxyphenylethylamine	+0.18
	<i>p</i> -Ar	Amphetamine	<i>p</i> -Methoxyamphetamine	+0.25
	<i>o</i> -Ar	Methylamphetamine	<i>o</i> -Methoxyphenamine	+0.49
Carboxyl	α	Tyramine	Tyrosine	-0.04
	α	Phenylethylamine	Phenylalanine	-0.17
Amino	N	Phenylethylamine	Phenelzine	+0.21
	N	N,N-Dimethylphenylethylamine	N,N-Dimethylphenylethylamine N-oxide	+0.35

can occur between the terminal amino group and the β -hydroxyl group. Models show that this hydrogen bonding is destabilised in the "A" isomers as a result of steric interactions between the methyl group on the α -carbon atom and the phenyl group of the β -carbon atom (see Fig. 1). In contrast, the "B" isomers show no steric crowding and can form strong hydrogen bonds. Thus, the polar groups of the "B" isomers are less accessible for interaction with the eluent and so increase retention. These examples emphasise the limitations of the group-contribution approach for predicting chromatographic retention and the need to consider intra-molecular interactions between substituents.

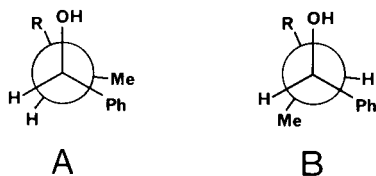


Fig. 1. Stereochemical structures of phenylpropanolamine (A, R = NH₂), norpseudoephedrine (B, R = NH₂), ephedrine (A, R = NHMe) and pseudoephedrine (B, R = NHMe). Me = Methyl; Ph = phenyl.

The data in Table I have been used to assess the quantitative effects of substituents. Table II contains τ values calculated for pairs of compounds that differ by a single substituent. Those compounds with $k' < 0.25$ (*i.e.*, 5-hydroxydopamine, noradrenaline and octopamine) have not been used, as the accuracy of such small capacity ratios is not expected to be high. Values of τ shown in Table II represent the replacement of a hydrogen atom on the phenylethylamine "core" by the given substituent. However, the N-oxide substitution is of a different type, the oxygen atom being added without replacement of hydrogen. Where substitution can produce two alternative diastereoisomers (*e.g.*, α -methylation of phenylethanolamine), both τ values are included in Table II. Values of τ for further substitution of diastereoisomers (*e.g.*, N-methylation of phenylpropanolamine; *p*-hydroxylation of ephedrine) are only included when the substituted compound has the same stereochemistry at the asymmetric carbon atoms.

The attachment of a methyl group to the molecule causes an increase in retention (τ positive) irrespective of the position of substitution. The values for α -carbon substitution are in the range +0.36 to +0.44, and the one example of β -carbon substitution also lies in this range. Methyl substitution on the aromatic ring causes a larger change (+0.54), whereas substitution on the nitrogen atom has a smaller effect than elsewhere. Further, it appears that the effect of the first methyl substitution on nitrogen is greater than the second.

Hydroxyl substitution on carbon leads to a decrease in retention (τ negative) in all instances. Values for β -carbon substitution fall in the range -0.25 to -0.35, and *p*-aromatic substitution causes larger decreases in retention (range -0.38 to -0.89). The low values for β -carbon substitution probably reflect the hydrogen bonding that can occur with the terminal amino group.

In contrast, hydroxyl substitution on nitrogen causes an increase in retention ($\tau = +0.50$). It is interesting to compare this result with that from the other example of N-oxidation included in this study (*i.e.*, N-oxide formation) where again an increase

in retention is observed ($\tau = +0.35$). This observation is supported by literature data for other N-oxides. Jensen¹⁷ records that the N-oxides of amitriptyline and imipramine are more strongly retained than the free bases (ODS-silica; 60% acetonitrile; pH 3). Under acidic conditions, both hydroxylamines and N-oxides protonate to give cations. Nitrogen-protonation of a hydroxylamine and oxygen-protonation of a N-oxide give species with equivalent cationic centres (*i.e.*, tetracoordinate nitrogen bearing one hydroxyl group). Thus, when the protonated forms of "parent" and "substituted" compounds are compared, it can be seen that a N-H bond is replaced by a N-OH bond for both hydroxylamine formation and N-oxide formation. The results indicate that cations bearing the N-OH group are more hydrophobic than the protonated parent amines. The attachment of an amino group to nitrogen also gives an increase in retention (see Table II).

Table II shows that the substitution of methoxyl groups on the aromatic ring increases chromatographic retention. Substitution at the 2-position gives the larger effect and again this probably indicates hydrogen bonding between the terminal amino group and the introduced substituent. A τ value of +0.66 is calculated for the simultaneous introduction of three methoxyl groups into phenylethylamine to give mescaline (see Table I). This is about three times the value for the substitution of one methoxyl group in the *p*-position (Table II) and suggests that the τ values for methoxyl groups in the *m*- and *p*-positions are equivalent and independent. The small changes in retention observed for substitution with a carboxyl group at the α -carbon atom are in agreement with the results of Molnár and Horváth⁶.

The present data provide a useful framework for understanding the behaviour of 2-phenylethylamine derivatives in reversed-phase HPLC. Further, the group-contribution values, τ , could prove valuable as an aid to the prediction of chromatographic data for the metabolites of sympathomimetic drugs.

REFERENCES

- 1 L. S. Goodman and A. Gilman (Editors), *The Pharmacological Basis of Therapeutics*, Macmillan, New York, 5th ed., 1975, chapter 24.
- 2 E. Tomlinson, *Proc. Anal. Div. Chem. Soc.*, 14 (1977) 294.
- 3 E. Tomlinson, H. Poppe and J. C. Kraak, *Methodol. Surv. Biochem.*, 7 (1978) 207.
- 4 C. M. Riley, E. Tomlinson and T. M. Jefferies, *J. Chromatogr.*, 185 (1979) 197.
- 5 C. M. Riley and E. Tomlinson, *Anal. Proc.*, 17 (1980) 528.
- 6 I. Molnár and Cs. Horváth, *J. Chromatogr.*, 145 (1978) 371.
- 7 B.-K. Chen and Cs. Horváth, *J. Chromatogr.*, 171 (1979) 15.
- 8 C. F. Lane, *Synthesis*, (1975) 135.
- 9 P. H. Morgan and A. H. Beckett, *Tetrahedron*, 31 (1975) 2595.
- 10 I. M. Johansson, K.-G. Wahlund and G. Schill, *J. Chromatogr.*, 149 (1978) 281.
- 11 K.-G. Wahlund and A. Sokolowski, *J. Chromatogr.*, 151 (1978) 299.
- 12 A. Sokolowski and K.-G. Wahlund, *J. Chromatogr.*, 189 (1980) 299.
- 13 A. Nahum and Cs. Horváth, *J. Chromatogr.*, 203 (1981) 53.
- 14 K. E. Bij, Cs. Horváth, W. R. Melander and A. Nahum, *J. Chromatogr.*, 203 (1981) 65.
- 15 R. M. C. Dawson, D. C. Elliott, W. H. Elliott and K. M. Jones (Editors), *Data for Biochemical Research*, Oxford University Press, Oxford, 2nd ed., 1969.
- 16 J. B. Stenlake, *Foundations of Molecular Pharmacology*, Vol. 1, Athlone Press, London, 1979, p. 377.
- 17 K. M. Jensen, *J. Chromatogr.*, 183 (1980) 321.

CHROM. 14,118

HIGH-PERFORMANCE LIQUID CHROMATOGRAPHY OF BILE PIGMENTS: SEPARATION AND CHARACTERIZATION OF THE UROBILINOIDS

ROSALIND V. A. BULL, C. K. LIM* and C. H. GRAY

Division of Clinical Chemistry, MRC Clinical Research Centre, Harrow, Middlesex HA1 3UJ (Great Britain)

SUMMARY

The detailed analysis of faecal bile pigments by high-performance liquid chromatography is described. Non-aqueous reversed-phase systems with acetonitrile-dimethyl sulphoxide or acetonitrile-dimethyl sulphoxide-methanol as the mobile phase on C_1 , C_8 or C_{18} -bonded silica are used for the group separation of verdinoids, violinoids and urobilinoids. A silica column, with acetonitrile-water-tetraethylene-pentamine as mobile phase, separates the laevorotatory stercobilin ($C_{33}H_{46}N_4O_6$) and half-stercobilin ($C_{33}H_{44}N_4O_6$) from the optically inactive urobilin ($C_{33}H_{42}N_4O_6$). The diastereoisomers are resolved by converting the urobilinoids into their dimethyl esters before chromatography on a silica column with *n*-heptane-methyl acetate-methanol containing 1% of diethylamine as the solvent system.

INTRODUCTION

The urobilinoids are naturally occurring bile pigments formed from bilirubin by bacterial reduction in the intestine. The colourless "urobilinogens" formed are usually completely oxidised to the orange "urobilins" during extraction from faeces.

"Urobilins" can be classified into three groups: dipyrrolidones (stercobilin), pyrrolinone-pyrrolidone (half-stercobilin) and dipyrrolinones (urobilin). Each may exist as pairs of enantiomorphs, the 2'- and 7'-positions of the molecules being chiral centres (see Fig. 1). Half-stercobilin and urobilin can be readily oxidised to half-stercoviolin and mesobiliviolin, respectively, while stercobilin is stable; mesobiliviolin can be further oxidised to mesobiliverdin (glucobilin) (Fig. 1).

The determination of the daily excretion of faecal bile pigments has been used as an index of the severity of haemolysis in diseases in which there is an abnormally high turn-over of haem, such as sickle cell and other haemolytic anaemias and congenital porphyria. However, due to the instability and, therefore, the complexity of the bile pigments and the lack of specific methods for their determination, they are now rarely measured.

The analysis of faecal bile pigments, especially the urobilinoids, by high-performance liquid chromatography (HPLC) has not been reported before. This paper

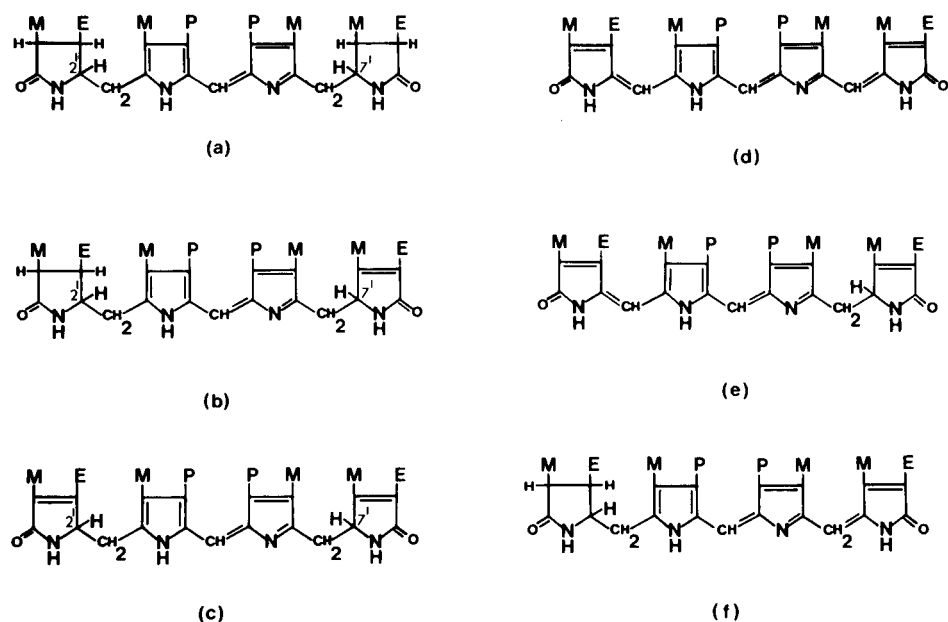


Fig. 1. Structures of bile pigments: (a), stercobilin; (b), half-stercobilin; (c), urobilin; (d), glaucobilin; (e), mesobiliviolin; and (f) half-stercoviolin. E = ethyl, M = methyl, P = propionic acid.

describes the detailed analysis of the urobilinoids by HPLC. Non-aqueous reversed-phase systems with acetonitrile–dimethyl sulphoxide (50:50) or acetonitrile–dimethyl sulphoxide–methanol (25:25:50) as solvents have been developed for the separation of the urobilinoids from the verdins and violins. The urobilinoids were separated into stercobilin, half-stercobilin and i-urobilin on a silica column (Hypersil) with acetonitrile–water–tetraethylenepentamine (85:15:0.05) as mobile phase. The diastereoisomers were resolved by converting the urobilinoids into their dimethyl esters, followed by separation on a silica column (Hypersil), with *n*-heptane–methyl acetate–methanol containing 1% of diethylamine (75:25:2) as eluent.

This efficient separation by HPLC will improve quantitation of the bile pigments, which might be important in assessing haem catabolism in clinical work.

EXPERIMENTAL

Materials

Acetonitrile (CH_3CN) was HPLC grade from Rathburn Chemicals (Walkerburn, Great Britain). Iodine was analytical grade from May and Baker (Dagenham, Great Britain). AnalaR-grade ethanol was from James Burrough (London, Great Britain). Reagent-grade anhydrous ferric chloride was from Hopkin and Williams (Chadwell Heath, Great Britain). Bilirubin was from Sigma (London). The following chemicals were from BDH (Poole, Great Britain): tetraethylenepentamine (TEPA), dimethyl sulphoxide (DMSO), *n*-heptane, methyl acetate, diethylamine (DEA), boron trifluoride in methanol (14%, w/v) and 5% palladium on charcoal were all reagent grade; glacial acetic acid, diethyl ether, hydrochloric acid, sodium acetate,

sodium hydrogen carbonate, chloroform, petroleum spirit (b.p. 60°–80°C), methanol, sodium hydroxide and mercury were all AnalaR grade.

Apparatus

Hypersil (spherical silica), SAS-Hypersil (C_1), MOS-Hypersil (C_8) and ODS-Hypersil (C_{18}), from Shandon Southern Products, Runcorn, Great Britain, were slurry packed. The column dimensions were 100 mm \times 5 mm I.D., except for the Hypersil column, which was 250 \times 5 mm I.D. A Pye Unicam (Cambridge, Great Britain) LC3-XP liquid chromatograph with a LC3-UV detector was used. Injection was via a loop-valve injector (Rheodyne 7125) fitted with a 20- μ l loop.

Preparation and isolation of bile pigments

The urobilinoids were extracted by the method of Watson¹ from a six-day collection of faeces from a patient with haemolytic anaemia. The final extract was precipitated from petroleum spirit, but not crystallised. A portion of the product was esterified by refluxing for 10 min in methanol (3 ml) and boron trifluoride in methanol (1 ml, 14% w/v). The mixture was diluted with water after cooling and extracted into chloroform. After successive washings with sodium hydrogen carbonate solution and water, the chloroform layer was filtered and dried.

Mesobiliverdin (glucobilin) was prepared from mesobilirubin, synthesised from bilirubin by the method of Fischer and Haberland². Mesobilirubin (50 mg) was dissolved in 10 ml of DMSO and quickly added, with continuous stirring, to a solution of 2,3-dichloro-5,6-dicyano-*p*-benzoquinone (41 mg) in DMSO (10 ml). After 5 min, 0.5% acetic acid (60 ml) was added to precipitate the mesobiliverdin formed. After centrifugation, the precipitate was washed once with 0.5% acetic acid then repeatedly with water until the supernatant liquid was clear. The final product was dried in a vacuum desiccator.

Mesobiliviolin was prepared by oxidation of mesobilirubinogen³ obtained by reduction of bilirubin⁴.

i-Urobilin was prepared from bilirubin as described by Watson⁴.

High-performance liquid chromatography

All HPLC solvents were made up by volume per cent. The free urobilinoids extracted from faeces were separated on a Hypersil column by elution with $CH_3CN-H_2O-TEPA$ (85:15:0.05) at a flow-rate of 1 ml/min; the samples were dissolved in chloroform for injection, and detection was at 450 nm.

The urobilinoid dimethyl esters were resolved on a Hypersil column with *n*-heptane–methyl acetate–methanol containing 1% of DEA (75:25:2) as mobile phase; other HPLC conditions were as described above.

SAS-Hypersil, MOS-Hypersil and ODS-Hypersil were used for the separation of glucobilin, mesobiliviolin and i-urobilin, with $CH_3CN-DMSO$ (50:50) and $CH_3CN-DMSO-CH_3OH$ (25:25:50) as mobile phases. The flow-rate was 1 ml/min; the samples were injected in DMSO. The detector was set at 340 nm for the detection of glucobilin and mesobiliviolin and at 450 nm for the detection of urobilin. Other verdinoids (biliverdin), violinoids (half-stercoviolin) and urobilinoids (stercobilin and half-stercobilin) were similarly chromatographed.

RESULTS AND DISCUSSION

The separation of mesobiliverdin, mesobiliviolin and i-urobilin on SAS-Hypersil with CH_3CN -DMSO (50:50) and with CH_3CN -DMSO- CH_3OH (25:25:50) as eluents is shown in Fig. 2. The presence of DMSO is essential for resolution; the pigments were not eluted by CH_3CN , CH_3OH or a mixture of CH_3CN - CH_3OH suggesting that DMSO may be preferentially extracted into the stationary phase, modifying the column selectivity. The chain length of the bonded phases had little influence on the capacity ratios (k') of the bile pigments, and similar results were obtained using SAS-Hypersil (C_1), MOS-Hypersil (C_8) and ODS-Hypersil (C_{18}), probably because DMSO was extracted similarly into the stationary phases, resulting in columns with virtually identical selectivities. To achieve reproducible results with non-aqueous reversed-phase systems, the column needs to be thoroughly equilibrated for at least 2 h with the mobile phase.

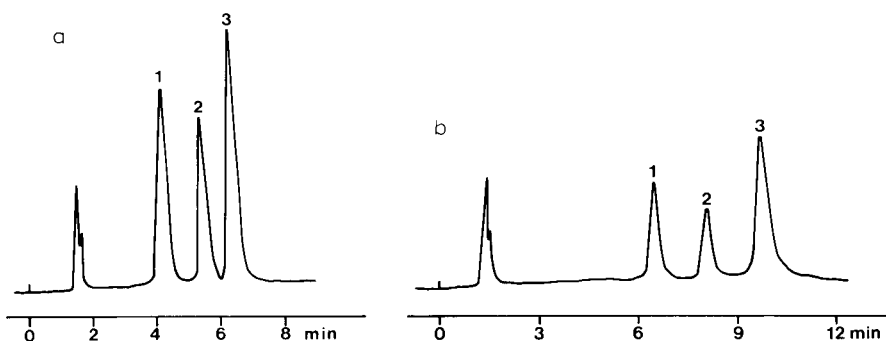


Fig. 2. Separation of bile pigments by non-aqueous reversed-phase HPLC with (a) CH_3CN -DMSO (50:50) and (b) CH_3CN -DMSO- CH_3OH (25:25:50) as mobile phase. Column: SAS-Hypersil; flow-rate, 1 ml/min; detection, 340 nm for glaucobilin (1) and mesobiliviolin (2), and 450 nm for urobilin (3).

The separation of these ionizable bile pigments by reversed-phase chromatography without the need for buffer solutions or ion-pairing reagents is attributed to the ability of DMSO to associate strongly with both the $-\text{NH}$ and $-\text{COOH}$ groups of the bile-pigment molecules rendering them "neutral". This explains the reversal of the elution order from that expected for reversed-phase chromatography, because mesobiliverdin is the least and i-urobilin the most polar molecule. Such a molecular association between solutes and DMSO would lead to changes in the polarity of the former.

Although non-aqueous reversed-phase systems do not separate biliverdin from mesobiliverdin, half-stercoviolin from mesobiliviolin and stercobilin from half-stercobilin and i-urobilin, the group separation is useful for the estimation of total faecal bile pigments and for the preparative isolation of bile pigments in haem turn-over studies using labelled precursors.

Stercobilin, half-stercobilin and i-urobilin were completely resolved (Fig. 3) on a silica column (Hypersil) with CH_3CN - H_2O -TEPA (85:15:0.05) as eluent. Verdinoids and violinoids were also separated in this system, but their separation from urobilinoids within a reasonable time required gradient elution. Similar systems developed for the separation of oligosaccharides have been shown to operate by the

HPLC OF BILE PIGMENTS

normal-phase mechanism^{5,6}, and the elution order of verdins, violins and "urobilins" was that expected for normal-phase chromatography. However, although amino-group bonded silica columns are satisfactory for the separation of oligosaccharides⁷⁻¹⁰, urobilinoids were not separated on aminopropylsilica (APS-Hypersil). Normal-phase ion-pair chromatography cannot be excluded, because the bile pigments can form ion-pairs with TEPA.

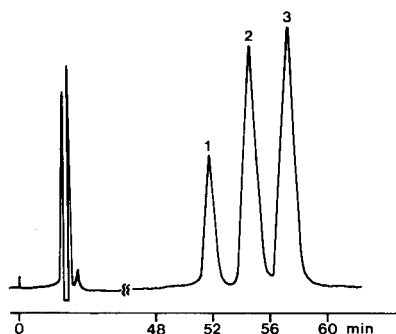


Fig. 3. Separation of stercobilin (1), half-stercobilin (2) and urobilin (3). Column, Hypersil; mobile phase, $\text{CH}_3\text{CN}-\text{H}_2\text{O}-\text{TEPA}$ (85:15:0.05); flow-rate, 1 ml/min; detection, 450 nm.

The compounds were identified by their characteristic chemical reactions with ferric chloride–hydrochloric acid as described by Watson *et al.*¹¹. Stercobilin is stable to this reagent; half-stercobilin is largely oxidised to the stable half-stercoviolin and i-urobilin is converted via mesobiliviolin into mesobiliverdin (glucobilin).

The urobilinoids can exist as (*RR,SS*) and (*RS,SR*) diastereoisomers, since the inner α -carbon atoms (2' and 7') of the end ring are chiral centres (Fig. 1)¹². They must be converted into their dimethyl esters in order to resolve the diastereoisomers (Fig. 4). Adsorption chromatography on Hypersil with *n*-heptane–methyl acetate–methanol containing 1% of DEA (75:25:2) as mobile phase was used for the separation, a small amount of DEA in the mobile phase being essential to eliminate poor resolution due to peak tailing.

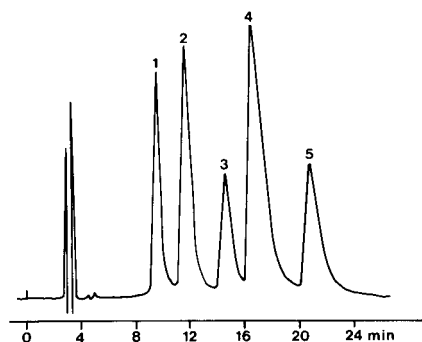


Fig. 4. Separation of dimethyl esters of (*SS*)-stercobilin (1), (*RR,SS*)-half-stercobilin (2), (*RR,SS*)-urobilin (3), (*RS,SR*)-half-stercobilin (4), and (*RS,SR*)-urobilin (5). Column, Hypersil; mobile phase, *n*-heptane–methyl acetate–methanol containing 1% of DEA (75:25:2); detection, 450 nm.

Naturally occurring stercobilin is in the *SS* configuration¹². Thus, only one peak corresponding to (*SS*)-stercobilin was observed. Both half-stercobilin and i-urobilin were resolved into two peaks corresponding to the *RR,SS* and *RS,SR* forms. The peaks were identified by chromatography of the dimethyl esters prepared from pure stercobilin, half-stercobilin and i-urobilin isolated by HPLC. The *RR,SS* isomers are eluted before the *RS,SR* isomers^{13,14}.

The analysis of faecal specimens by HPLC has shown that the urobilinoids are mixtures of stercobilin, half-stercobilin and i-urobilin in various proportions. Stercobilin and i-urobilin are formed from stercobilinogen and i-urobilinogen, respectively. The origin of half-stercobilin, however, is uncertain, because it could be formed artifactually by rearrangement from stercobilinogen and i-urobilinogen¹³.

The resolution of the urobilinoids into diastereoisomers allows the isolation of the bile pigments suitable for detailed characterization by physico-chemical methods such as mass spectrometry, nuclear magnetic resonance spectrometry and circular dichroism.

ACKNOWLEDGEMENT

R. V. A. Bull was supported by a grant from the Medical Research Council to C.H.G.

REFERENCES

- 1 C. J. Watson, *J. Biol. Chem.*, 105 (1934) 469.
- 2 H. Fischer and H. W. Haberland, *Hoppe-Seyler's Z. Physiol. Chem.*, 232 (1935) 236.
- 3 C. H. Gray, A. Kulczycka and D. C. Nicholson, *J. Chem. Soc.*, (1961) 2276.
- 4 C. J. Watson, *J. Biol. Chem.*, 200 (1953) 691.
- 5 K. Aitzetmüller, *J. Chromatogr.*, 156 (1978) 354.
- 6 B. B. Wheals and P. C. White, *J. Chromatogr.*, 176 (1979) 421.
- 7 J. C. Linden and C. L. Lawhead, *J. Chromatogr.*, 105 (1975) 125.
- 8 R. B. Maegher S.J. and A. Furst, *J. Chromatogr.*, 117 (1976) 211.
- 9 R. Schwarzenbach, *J. Chromatogr.*, 117 (1976) 206.
- 10 F. M. Rabel, A. G. Caputo and E. T. Butts, *J. Chromatogr.*, 126 (1976) 731.
- 11 C. J. Watson, J. W. Hall, III and M. Weimer, *Biochem. Med.*, 2 (1969) 461.
- 12 H. Brockmann, Jr., G. Knoblock, H. Plieninger, K. Ehl, J. Ruppert, A. Moscovitz and C. J. Watson, *Proc. Nat. Acad. Sci., U.S.*, 68 (1971) 2141.
- 13 M. S. Stoll, C. K. Lim and C. H. Gray, in P. D. Berk and N. I. Berlin (Editors), *Chemistry and Physiology of Bile Pigments*, U.S. Department of Health, Education and Welfare, 1977, p. 483.
- 14 C. H. Gray, C. K. Lim, J. M. Rideout, P. O. Skacel and M. S. Stoll, in A. M. Lawson, C. K. Lim and W. Richmond (Editors), *Current Developments in the Clinical Applications of HPLC, GC and MS*, Academic Press, London, New York, Toronto, Sydney, San Francisco, 1980, p. 75.

CHROM. 14,144

ISOLATION AND CHARACTERIZATION OF THREE NEW POLYMYXINS IN POLYMYXINS B AND E BY HIGH-PERFORMANCE LIQUID CHROMATOGRAPHY

INGELISE ELVERDAM*

Antibiotic Division, R & D Section, Dumex A/S (Dumex Ltd.), Prags Boulevard 37, DK-2300 Copenhagen S (Denmark)

and

PER LARSEN and ERIK LUND

The Danish Institute of Protein Chemistry, Venlighedsvej 4, DK-2970 Horsholm (Denmark)

SUMMARY

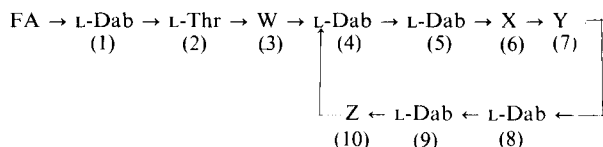
Two polymyxin antibiotics, polymyxins B and E (colistin), have been separated analytically into ten to thirteen components on a commercial reversed-phase material by isocratic elution with a mixture of acetonitrile, phosphate/formate and acetate buffer containing sodium sulphate and triethylamine. The analytical system was transferred to a preparative system, using a C₁₈-bonded stationary phase, without extensive impairing of the selectivity. The major components of each product were isolated and characterized by high-performance liquid chromatography, amino acid analysis and identification of the fatty acid. Three components were isolated and characterized for the first time. The fatty acid was also identified in some of the minor components.

INTRODUCTION

Polymyxin is the generic name of a group of chemically related fatty acyl decapeptide antibiotics, produced by *Bacillus polymyxa* and related species¹. The general structure (Table I) comprises a cyclic heptapeptide moiety with a straight tripeptide side chain. The N-terminal amino-group in the side chain is acylated.

Polymyxin B was discovered in 1948 and colistin in 1950. Following the elucidation of the corresponding structures in the mid-sixties¹, and the establishment of the identity of polymyxin E and colistin in 1965⁵, many attempts have been made to characterize further the commercial products polymyxin B sulphate and colistin sulphate. The complex composition of these products has been demonstrated by thin-layer chromatography (TLC), on silanized silica gel by Thomas and Holloway⁶ and on cellulose by Junge⁷. Junge separated polymyxin B sulphate into ten fractions, five of which were microbiologically active. High-performance liquid chromatography (HPLC) has also been used for this purpose^{8–11}. Thus, Tsuji and Robertson⁸ separated polymyxins B₁ and B₂ and E₁ and E₂ by reversed-phase chromatography with

TABLE I

STRUCTURES OF CYCLIC DECAPEPTIDES OF THE POLYMYXIN GROUP OF ANTI-BIOTICS²⁻⁴

Numerical suffix division of the polymyxins by fatty acyl radical (FA): 1, (+)-6-methyloctanoyl (MOA); 2, 6-methylheptanoyl (isooctanoyl, IOA); 3, octanoyl (OA); 4, heptanoyl (HA). Dab = α,γ -Diaminobutyric acid.

Compound	W	X	Y	Z
Circulin	L-Dab	D-Leu	L-Ile	L-Thr
Polymyxin A (M)	L-Dab	D-Leu	L-Thr	L-Thr
Polymyxin B	L-Dab	D-Phe	L-Leu	L-Thr
Polymyxin C (or P)	Dab	Phe	Thr	Thr
Polymyxin D	D-Ser	D-Leu	L-Thr	L-Thr
Polymyxin E (colistin)	L-Dab	D-Leu	L-Leu	L-Thr
Polymyxin S	D-Ser	D-Phe	L-Thr	L-Thr
Polymyxin T	L-Dab	D-Phe	L-Leu	L-Leu
Polymyxin F: Dab (5), Thr (1), Ser (1), Ile (1), Leu(2)				

a linear gradient elution. Terabe *et al.*⁹ developed an isocratic ion-pair reversed-phase chromatography method which was applied by Thomas *et al.*⁴ to separate polymyxin B sulphate into eleven components and colistin into thirteen components. Recently, Kimura *et al.*¹¹ separated the polymyxins into two or three components, both analytically and preparatively, using a porous styrene-divinylbenzene copolymer packing.

This paper describes an analytical (A-HPLC) and preparative (P-HPLC) isocratic reversed-phase chromatography method, by which polymyxin E sulphate can be separated into ten or eleven components and polymyxin B sulphate into twelve or thirteen components. The capacity ratios of the major components are shown to be dependent on the concentration of acetonitrile in the mobile phase. The relationships between the order of elution and the amino acid and fatty acid compositions are discussed. Differences in the compositions of commercial products of polymyxin B sulphate and colistin sulphate are reported.

EXPERIMENTAL

Reagents

Acetonitrile (HPLC S grade) was obtained from Rathburn (Walkerburn, Great Britain) and triethylamine (zur Synthese) from Merck-Schuchardt (Darmstadt, G.F.R.). All other solvents, except water, and reagents were obtained in analytical grade from E. Merck (Darmstadt, G.F.R.). Water was purified by using an ion-exchange column and by redistillation. The polymyxins investigated were obtained as follows: A, colistin sulphate, Lot No. 162107 (Dumex, Copenhagen, Denmark); B, colistin sulphate, Japanese source; C, polymyxin B sulphate, Lot No. 136307 (Dumex); D, polymyxin B sulphate, American source.

Apparatus

For the analytical work a DuPont Model 830 liquid chromatograph equipped with a Model 837 spectrophotometer was used. The extinction was recorded by means of a Hewlett-Packard Model HP 3380 A integrator. The column (15 cm \times 4.6 mm I.D.) was packed with 5- μ m Nucleosil 5 C₁₈ (Macherey, Nagel & Co., Düren, G.F.R.) by a slurry technique.

The preparative work was carried out on a Jobin-Yvon column (25 \times 4 cm I.D.), with a modified column-head, fitted with a six-port injection valve, Whitey SS-43Y6FS2, and a PTFE loop of 25 ml. The solvent was delivered by a Lewa FD pump, connected to a pressure transducer for pressure recording. A polarimeter, Perkin-Elmer 141, fitted with a recorder outlet, was used as detector. Recordings were made on a WW-recorder Series 316 (W & W Electronics, Basle, Switzerland). The packing material consisted of 125 g LiChrosorb Si 100 (10 μ m), substituted with octadecyldimethylchlorosilane, carbon content 16.62%, corresponding to a coverage of 3.16 μ mol/m².

Procedure

The polymyxins were dissolved in distilled water at a concentration of 0.4–5 mg/ml for analytical work and 100 mg/ml for preparative work. The amounts of sample injected were 20 μ l (8–100 μ g) and 5–10 ml (500–1000 mg) respectively.

For the analytical column the flow-rate was 0.9 ml/min and the inlet pressure was about 83 bar. UV detection at 220 nm was used. For the preparative column the flow-rate was about 20 ml/min and the inlet pressure 4–5 bar. Optical rotation detection at 365 nm was employed.

The mobile phase was prepared by mixing acetonitrile with a buffer: 0.023 *M* in phosphoric acid, 0.01 *M* in acetic acid, 0.05 *M* in sodium sulphate and triethylamine, pH 2.5. In the preparative rechromatographing of the components the phosphoric acid was replaced by 0.07 *M* formic acid. Acetonitrile and buffer were filtered through a membrane filter (0.45 μ m) before mixing. The acetonitrile content in the mobile phase is indicated in the legends to the figures.

After the first preparative elution, the acetonitrile in the collected fractions was removed by evaporation, and the purity was checked by A-HPLC. In order to concentrate the fractions, the aqueous buffer solutions of the components were pumped on to the preparative column and then rechromatographed. The resulting fractions were concentrated by evaporation, freeze-dried and desalted by methanol extraction and the components were analysed as follows.

The samples were hydrolyzed in 6 *N* hydrochloric acid in evacuated, sealed vials for 24 h at 110°C. The acid was then removed under reduced pressure. The hydrolysates were redissolved in 0.1 *N* hydrochloric acid. Part of the hydrolysates was extracted with dichloromethane, and the fatty acid content in the organic phase was analyzed with a Pye 104 gas chromatograph equipped with a flame-ionization detector and a Hewlett-Packard Model 3380 A integrator. The column (1.8 m \times 4 mm I.D., glass) was packed with OV-351 (10%) on Chromosorb W AW DMCS, 80–100 mesh (Ohio Valley Specialty Chemical Inc., OH, U.S.A.), and nitrogen was used as carrier gas. The remainder of the hydrolysates was used for amino acid analysis, carried out on a Kontron Liquimat III, using a standard procedure for protein hydrolysates. Finally, the chromatographic purity was checked by A-HPLC.

RESULTS AND DISCUSSION

Polymyxin B sulphate and polymyxin E sulphate are mixtures of several fatty acyl decapeptides, and the composition of the commercial products differs from one producer to another, as seen in Figs. 1–4. This may be the reason for the well known problems with the microbiological assay of potency. In order further to elucidate these problems, we isolated as many of the major components of each polymyxin as possible. For the subsequent tests of the biological characteristics of these components, it was necessary to use a mobile phase containing anions which do not interfere with these tests. Our method uses only hydrophilic anions, and provides a resolution at least as good as that Terabe *et al.*⁹ obtained using tartrate buffer and sodium 1-butanedisulphonate. The separation was strongly dependent on the concentration of acetonitrile in the mobile phase, as seen in Table II.

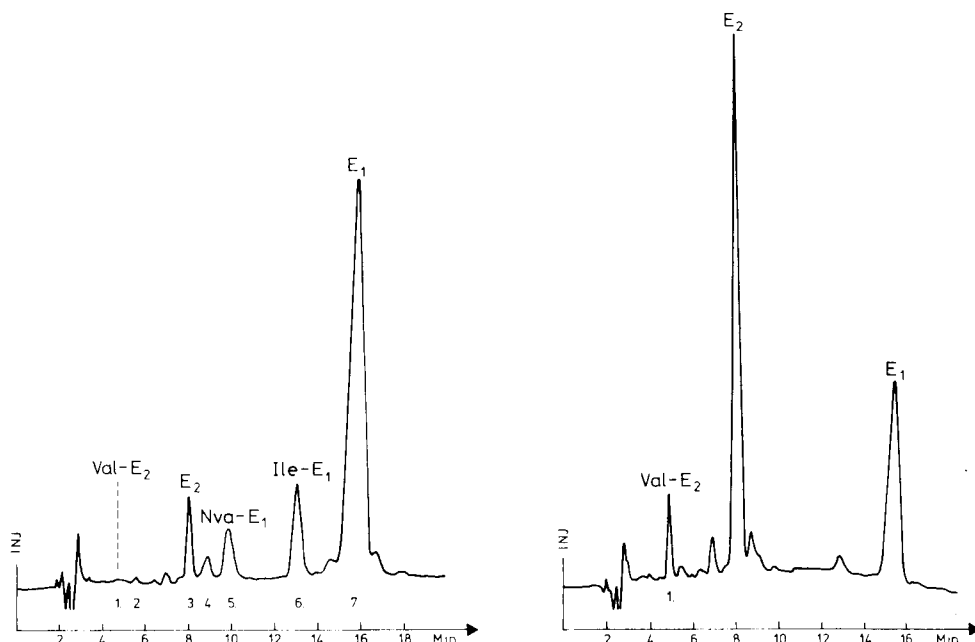


Fig. 1. Chromatogram from an analytical run of 100 μ g colistin sulphate (product A) on a 150×4.6 mm column containing Nucleosil 5 C₁₈. Mobile phase: 22% acetonitrile in 0.023 M phosphoric acid, 0.01 M acetic acid, 0.05 M sodium sulphate buffer adjusted to pH 2.5 by means of triethylamine; flow-rate 0.9 ml/min. Detection: UV, 220 nm.

Fig. 2. Chromatogram from an analytical run of 100 μ g colistin sulphate (product B). Conditions as in Fig. 1.

Transfer of the analytical system to a 25×4 cm I.D. column, chromatographing 1 g of the products, was accomplished without any problems, and no change of the mobile phase was necessary. Figs. 5 and 6 show chromatograms of 1.12 g colistin sulphate and 0.56 g of polymyxin B sulphate, respectively. The selectivity of the prepared C₁₈ phase is illustrated in Fig. 7, which shows the first part of a preparative chromatogram of 1 g of polymyxin B sulphate.

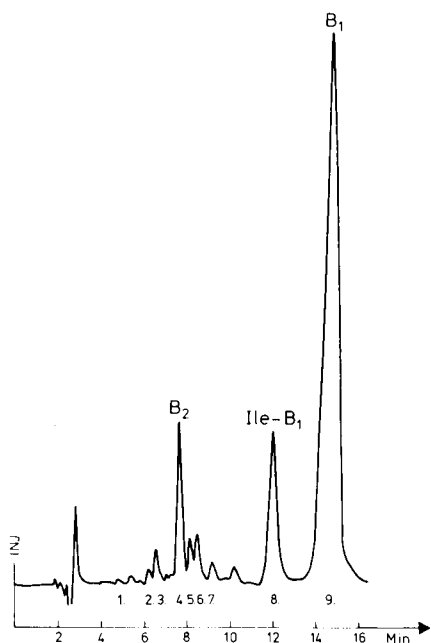


Fig. 3. Chromatogram of an analytical run of 100 μ g polymyxin B sulphate (product C) on a 150 \times 4.6 mm column containing Nucleosil 5 C₁₈. Mobile phase: 23% acetonitrile in 0.023 *M* phosphoric acid, 0.01 *M* acetic acid, 0.05 *M* sodium sulphate buffer adjusted to pH 2.5 by means of triethylamine; flow-rate 0.9 ml/min. Detection: UV, 220 nm.

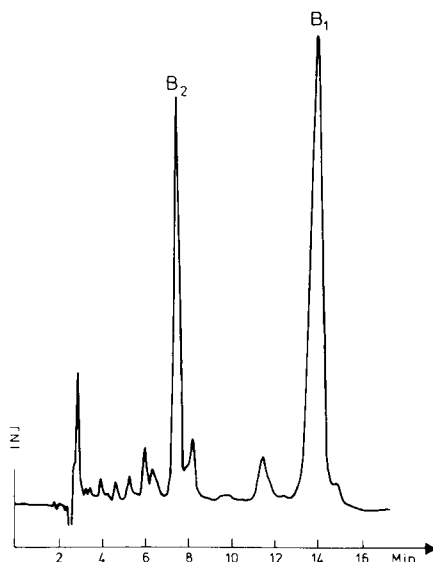


Fig. 4. Chromatogram from an analytical run of 100 μ g polymyxin B sulphate (product D). Conditions as in Fig. 3.

The effect of overloading on the capacity ratios is shown in Table II. This effect is relatively small at low capacity ratios, because the components have been separated in a non-overloaded state, whereas the effect on the major components is very large.

The amino acid and fatty acid compositions are listed in Tables III and IV, and it is seen that all the isolated components are fatty acyl decapeptides. The numbering corresponds to that in Figs. 1–3.

In the case of α,γ -diaminobutyric acid (Dab) the error in the estimation is relatively large since the peak of Dab coincides with a buffer change in the chromatogram.

TABLE II

CAPACITY RATIOS OF POLYMYXIN E COMPONENTS AS A FUNCTION OF THE ACETONITRILE CONTENT IN THE MOBILE PHASE

% Acetonitrile	Pol. E ₂	Ile-pol. E ₁	Pol. E ₁
22 (A-HPLC)	1.92	3.84	4.94
23 (A-HPLC)	1.37	2.78	3.48
23 (P-HPLC, 0.56 g)	1.70	3.50	5.86
23 (P-HPLC, 1.12 g)	1.78	3.68	7.18

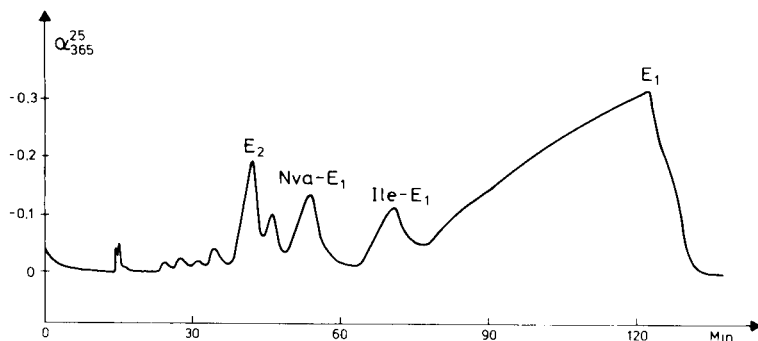


Fig. 5. Chromatogram from a preparative run of 1.12 g colistin sulphate (product A) on a 25×4 cm column containing octadecyldimethylsilyl substituted LiChrosorb Si 100, $10 \mu\text{m}$. Mobile phase: 23% acetonitrile in 0.023 *M* phosphoric acid, 0.01 *M* acetic acid, 0.05 *M* sodium sulphate buffer adjusted to pH 2.5 by means of triethylamine; flow-rate 20 ml/min. Detection: optical rotation measured in a 10-cm cell at 365 nm.

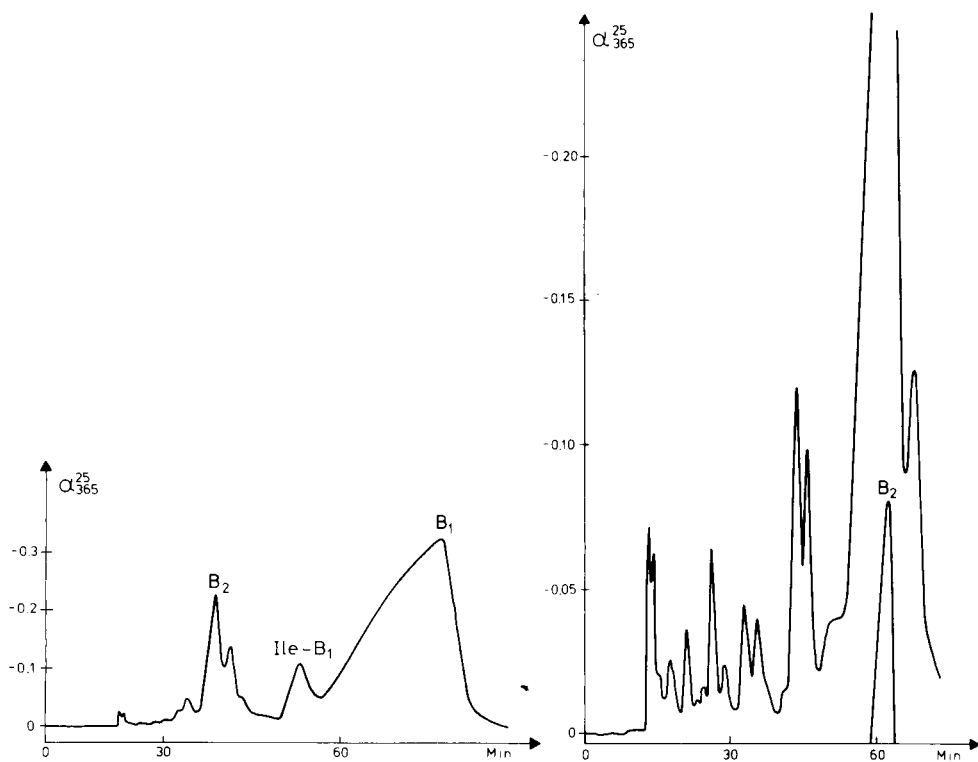


Fig. 6. Chromatogram from a preparative run of 0.56 g polymyxin B sulphate (product C) on a 25×4 cm column containing octadecyldimethylsilyl substituted LiChrosorb Si 100, $10 \mu\text{m}$. Mobile phase: 25% acetonitrile in 0.023 *M* phosphoric acid, 0.01 *M* acetic acid, 0.05 *M* sodium sulphate buffer adjusted to pH 2.5 by means of triethylamine; flow-rate 20 ml/min. Detection: optical rotation measured in a 10-cm cell at 365 nm.

Fig. 7. Chromatogram from a preparative run of 1.0 g polymyxin B sulphate (product D). Conditions as in Fig. 5. The chromatography was interrupted after the component B_2 was obtained.

TABLE III

AMINO ACID AND FATTY ACID ANALYSES ON SEPARATED POLYMYXIN B COMPONENTS

The peaks are numbered in elution order, compare Fig. 3. ID = Identified without quantitation.

Peak	Amino acid found (ratio)					Fatty acid	Identification
	Dab	Thr	Phe	Leu	Ile		
1.						IOA	
2.						IOA	
3.						IOA	
4.	5.92 (6)	1.89 (2)	1.01 (1)	1		IOA	Pol. B ₂
5.	ID	ID	ID	ID		OA	Pol. B ₃
6.						MOA	
7.						MOA	
8.	5.77 (6)	1.98 (2)	1		0.88 (1)	MOA	Ile-Pol. B ₁ *
9.	5.54 (6)	1.73 (2)	0.98 (1)	1		MOA	Pol. B ₁

* New polymyxin.

Initially norvaline was identified as methionine due to the closeness of the peaks of these amino acids. However, a control analysis was carried out after performic acid oxidation prior to hydrolysis. This showed only trace amounts of methionine sulphone in the sample, and left the "methionine peak" unchanged in the chromatogram. The retention time of a norvaline standard was identical with that of the unknown amino acid appearing in the sample. We ascribe the "methionine peak" to norvaline, on account of these results and the fact that differences in amino acid composition are often found among the non-polar amino acids.

The composition of Ile-pol. E₁ is the same as for circulin A, but the identity of these two compounds has to be demonstrated by sequence analysis. Three of the components, Ile-pol. B₁, Nva-pol. E₁ and Val-pol. E₂, have not been isolated before. The chromatographic purity of the components is shown in Figs. 8 and 9.

TABLE IV

AMINO ACID AND FATTY ACID ANALYSES ON SEPARATED POLYMYXIN E COMPONENTS

Peaks are numbered in elution order, compare Figs. 1 and 2. Nva = Norvaline.

Peak	Amino acid found (ratio)						Fatty acid	Identification
	Dab	Thr	Leu	Ile	Val	Nva		
1.	5.78 (6)	1.81 (2)	1		0.84 (1)		IOA	Val-pol. E ₂ *
2.							IOA	
3.	5.96 (6)	2.00 (2)	2				IOA	Pol. E ₂
4.	ID	ID	ID				OA	Pol. E ₃
5.	6.01 (6)	1.83 (2)	1			0.86 (1)	MOA	Nva-pol. E ₁ *
6.	5.48 (6)	1.64 (2)	1	0.85 (1)			MOA	Ile-pol. E ₁
7.	5.85 (6)	1.60 (2)	2				MOA	Pol. E ₁

* New polymyxin.

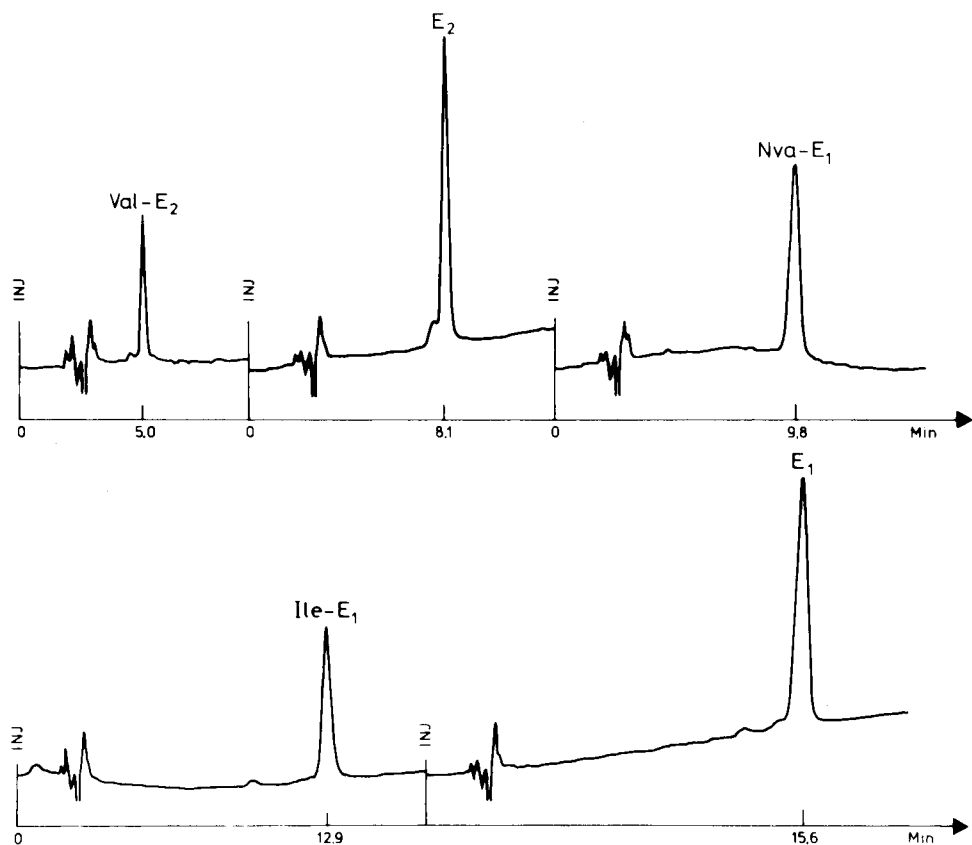


Fig. 8. Chromatograms from analytical runs of 8–50 μ g of pure components of colistin sulphate. Conditions as in Figs. 1 and 2.

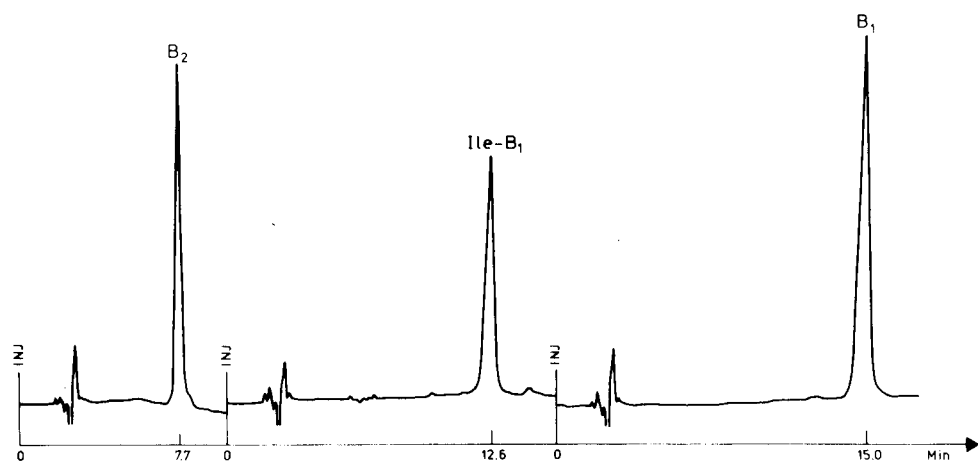


Fig. 9. Chromatograms from analytical runs of 8–50 μ g of pure components of polymyxin B sulphate. Conditions as in Figs. 3 and 4.

The fatty acid analyses (Tables III and IV) revealed that several components have the same fatty acid residue. Consequently, the test for colistin sulphate composition given in ref. 12 is a test for the relative distribution of the fatty acid residues in the compound rather than for the fatty acyl decapeptide composition.

By comparing Figs. 1–3 with Tables III and IV, it is seen that the elution order of the components is primarily dependent on the fatty acid residue, less obviously so on the amino acid composition. The retention time increases in the order isooctanoyl (IOA) < octanoyl (OA) < (+)-6-methyloctanoyl (MOA). Regarding the amino acid composition, the retention time increases in the order Nva < Ile < Leu in fatty acyl decapeptides with the fatty acid residue MOA, and Val < Leu in those with the fatty acid residue IOA.

The structures of the polymyxins are shown in Table I. Four variable positions in the molecules have been found, but at the present time it is not known how the amino acid position affects the elution order.

CONCLUSIONS

It has been shown that polymyxins B and E can each be successfully separated, both analytically and preparatively, into ten to thirteen components using a chemically bonded C₁₈ stationary phase and a mobile phase consisting of a mixture of acetonitrile and phosphate/formate and acetate buffer, containing sodium sulphate and triethylamine. The major components were isolated and identified by HPLC and analyses of the amino acids and fatty acids. None of them appeared to be degradation products. Three of the components represent new polymyxins, which have not been isolated before. We suggest the names polymyxin I₁ (= Ile-pol. B₁), O₁ (= Nva-pol. E₁) and L₂ (= Val-pol. E₂). The fatty acid analysis revealed that several components have the same fatty acid residue.

ACKNOWLEDGEMENT

We are grateful to Dr. P. Lading, Dumex Analytical Research Department, for details of the gas chromatographic method and for her kind assistance in the performance of the fatty acid analysis.

REFERENCES

- 1 K. Vogler and R. O. Studer, *Experientia*, 22 (1966) 345.
- 2 W. L. Parker, M. L. Rathnum, L. D. Dean, M. W. Nimeck, W. E. Brown and E. Meyers, *J. Antibiot.*, 30 (1977) 767.
- 3 J. Shoji, T. Kato and H. Hino, *J. Antibiot.*, 30 (1977) 1042.
- 4 A. H. Thomas, J. M. Thomas and I. Holloway, *Analyst (London)*, 105 (1980) 1068.
- 5 S. Wilkinson and L. A. Lowe, *Nature (London)*, 204 (1965) 993.
- 6 A. H. Thomas and I. Holloway, *J. Chromatogr.*, 161 (1978) 417.
- 7 O. Junge, *Int. J. Clin. Pharmacol.*, 61 (1972) 67.
- 8 K. Tsuji and J. H. Robertson, *J. Chromatogr.*, 112 (1975) 663.
- 9 S. Terabe, R. Konaka and J. Shoji, *J. Chromatogr.*, 173 (1979) 313.
- 10 G. W. K. Fong and B. T. Kho, *J. Liquid Chromatogr.*, 2 (1979) 957.
- 11 Y. Kimura, H. Kitamura, T. Araki, K. Noguchi, M. Baba and M. Hori, *J. Chromatogr.*, 206 (1981) 563.
- 12 *British Pharmacopoeia*, Vol. I, Her Majesty's Stationery Office, London, 1980, p. 125.

CHROM. 14,198

DETERMINATION OF 5-HYDROXYTRYPTOPHAN, SEROTONIN AND 5-HYDROXYINDOLEACETIC ACID IN RAT AND HUMAN BRAIN AND BIOLOGICAL FLUIDS BY REVERSED-PHASE HIGH-PERFORMANCE LIQUID CHROMATOGRAPHY WITH ELECTROCHEMICAL DETECTION

L. SEMERDJIAN-ROQUIER*

Synthélabo-L.E.R.S., 31 Avenue Paul-Vaillant Couturier, 92220 Bagneux (France)

L. BOSSI

Synthélabo, Clinical Research Department, 58 Rue de la Glacière, 75013 Paris (France)

and

B. SCATTON

Synthélabo-L.E.R.S., 31 Avenue Paul-Vaillant Couturier, 92220 Bagneux (France)

SUMMARY

A rapid and sensitive method for the concurrent determination of 5-hydroxytryptophan, serotonin and 5-hydroxyindole acetic acid by reversed-phase high-performance liquid chromatography with electrochemical detection has been developed. The separation of the indolic compounds was achieved using a phosphate-citric acid eluent containing 5% methanol. Detection limits in the low picogram range were found. The method has been applied to the determination of the indolic compounds in rat and human brain tissues, as well as in human plasma and cerebrospinal fluid. Tissue and plasma preparation required only deproteinization before chromatography, while cerebrospinal fluid was directly applied to the column.

INTRODUCTION

Owing to the role played by serotonin (5-HT)-containing neurons in a variety of physiological functions (*e.g.*, sleep regulation and sexual behaviour) and pathological states (*e.g.*, depression), a large number of methods for the determination of serotonin, its amino acid precursors and metabolites in biological samples have been developed over the past two decades. Fluorometric^{1,2}, gas chromatographic-mass spectrometric (GC-MS)^{3,4}, radioenzymatic^{5,6} and radioimmunological⁷ methods have been successfully employed to measure indolic compounds in brain and biological fluids. However, these techniques either lack adequate sensitivity (*e.g.*, fluorometry) or are expensive, time consuming and require complicated extraction and derivatization procedures (*e.g.*, GC-MS). Moreover, they do not allow the simultaneous detection and quantitation of indolic compounds.

Recently, high-performance liquid chromatography (HPLC) with fluorescence

or electrochemical detection has been successfully applied to the determination of 5-HT and its major metabolite 5-hydroxyindoleacetic acid (5-HIAA) in biological samples (see refs. 8–10). However, most of these methods required ion-exchange sample prepurification prior to the HPLC analysis and did not allow the simultaneous determination of serotonin and its amino acid precursors and metabolites.

We have developed a method for the concurrent measurement of 5-HT, 5-hydroxytryptophan (5-HTP) and 5-HIAA using reversed-phase HPLC with electrochemical detection which is rapid, sensitive, easy to perform and which does not require prepurification of the indolic compounds. This method has been applied to the determination of indolic compounds in rat and human brain areas as well as in human cerebrospinal fluid (CSF) and plasma.

MATERIALS AND METHODS

Reagents and solvents

The standards 5-HT creatinine sulphate, 5-HIAA, 5-HTP, homovanillic acid (HVA), 3,4-dihydroxyphenylethylene glycol (DOPEG), dihydroxyphenylacetic acid (DOPAC), 3,4-dihydroxyphenylalanine (DOPA), 3-methoxy-4-hydroxyphenylethylene glycol (MOPEG), norepinephrine hydrochloride (NE), epinephrine (E) and dopamine (DA) were purchased from Sigma (St. Louis, MO, U.S.A.) and the aromatic L-amino acid decarboxylase inhibitor, *m*-hydroxybenzylhydrazine (NSD 1015), from Aldrich (Beerse, Belgium). Standard solutions (100 µg/ml) were prepared in distilled water and stored at 4 °C (stock solutions). They were diluted to appropriate concentrations in the eluent immediately before use. NSD 1015 was dissolved in a few drops of 1 M hydrochloric acid and made up to the desired volume with water.

Water with resistivity greater than 10 MΩ/cm was obtained by double distillation. Methanol, spectroscopic grade, was from Rhône-Poulenc (France). All other chemicals were reagent grade from E. Merck (Darmstadt, G.F.R.). The mobile phase consisted of a 0.1 M K₂HPO₄-citric acid buffer (1:0.60, v/v; pH 4.7) containing 5% methanol and the disodium salt of ethylenediaminetetraacetic acid (EDTA) (0.1 mM). The solvent mixture was filtered under vacuum through a 0.22-µm Millipore GS type filter before use. The temperature of the solvent mixture was maintained at 30 °C by use of a constant-temperature water-bath.

Chromatography

Chromatography was performed using a Micromeritics (Model 750) pump, an automatic sample injection system WISP (Model 710 B, Waters Assoc.) and a stainless-steel column (15 cm × 4.6 mm I.D.) packed with C₁₈ reversed-phase, Spherisorb ODS (5 µm). The flow-rate was usually 1 ml/min and the column was operated at 30 °C. Electrochemical detection was accomplished using a Model LC-4 amperometric detector from Bio-analytical Systems (West Lafayette, IN, U.S.A.) and a carbon paste (silicone oil/graphite) electrode maintained at +0.6 V *versus* a silver-silver chloride reference electrode. The signal was recorded and the peak areas determined with a SP 4100 computing integrator from Spectra-Physics (Santa Clara, CA, U.S.A.). Quantitations were made automatically by comparison of the peak areas of the samples with those given by known concentrations of standards.

Sample preparation

Rat brain samples. Male Sprague Dawley rats (COBS CD strain; Charles River, France) weighing 140–160 g were used. They were maintained on a 12-h light/dark cycle with free access to food and water.

Animals were sacrificed by decapitation and the brain was immediately removed. Brain regions were dissected out in the cold, immediately frozen on solid carbon dioxide and kept at -80°C until analysis. For 5-HT and 5-HIAA measurements, tissues were homogenized in 0.1 M perchloric acid (1:10 w/v); after centrifugation, 100 μl of the supernatant were applied to the HPLC column. For 5-HTP measurements, rats received NSD 1015 (100 mg/kg i.p.) and were sacrificed 30 min thereafter. The tissues were homogenized in ten volumes of 0.1 M perchloric acid and after centrifugation (28,000 g for 10 min) the supernatant was directly applied to the HPLC column. In some cases, catechol compounds were removed as follows: the supernatant was adjusted to pH 8.4 with 2.8 M Tris (pH 9.6) and 50 mg of acid-washed alumina were added. The vials were shaken for 10 min, centrifuged and 150 μl of the supernatants were then transferred into minivials of the automatic injector for 5-HTP determination.

Human brain samples. Post-mortem human brain samples were collected from subjects with no history of psychiatric or neurological disorders, then frozen and dissected as described by Gaspar *et al.*¹¹. Tissues were homogenized in ten volumes of 0.1 M perchloric acid and centrifuged; 100 μl of the supernatant were used for chromatographic analysis.

Plasma samples. Plasma samples (500 μl) were deproteinized by adding 10 μl of 70% perchloric acid. After centrifugation, 50 μl of the supernatant were removed and diluted twelve-fold in the running buffer before chromatographic analysis (injection volume 50 μl).

CSF samples. Human CSF was obtained via lumbar puncture from schizophrenic patients and immediately stored at -80°C in polypropylene tubes. Chromatographic analysis was performed by direct injection of 100 μl CSF.

Recoveries

Recovery of 5-HT and 5-HIAA was determined by adding a known amount of the indolic compounds to duplicate samples of homogenates. Recovery of 5-HTP was estimated by adding 1 nCi (brain tissue) or 5 nCi (plasma) of [$U\text{-}^3\text{H}$]-L-5-HTP (specific activity 12.1 Ci/mmol, New England Nuclear) to the samples prior to deproteinization. Radioactivity was measured by liquid scintillation. The 5-HTP recoveries (mean \pm S.E.M.) were 85 ± 1 and $78 \pm 2\%$ for brain tissue and plasma samples, respectively.

RESULTS AND DISCUSSION

Chromatographic conditions

The optimal separation of 5-HT, 5-HTP and 5-HIAA was achieved using a K_2HPO_4 -citric acid (0.1 M, pH 4.7) buffer containing 5% methanol and 0.1 mM EDTA.

The separation of indolic compounds on the C_{18} reversed-phase column depended on the pH, the ionic strength and the amount of methanol in the mobile phase. As expected from the pK_a of 5-HIAA (4.7), the retention time of the acid

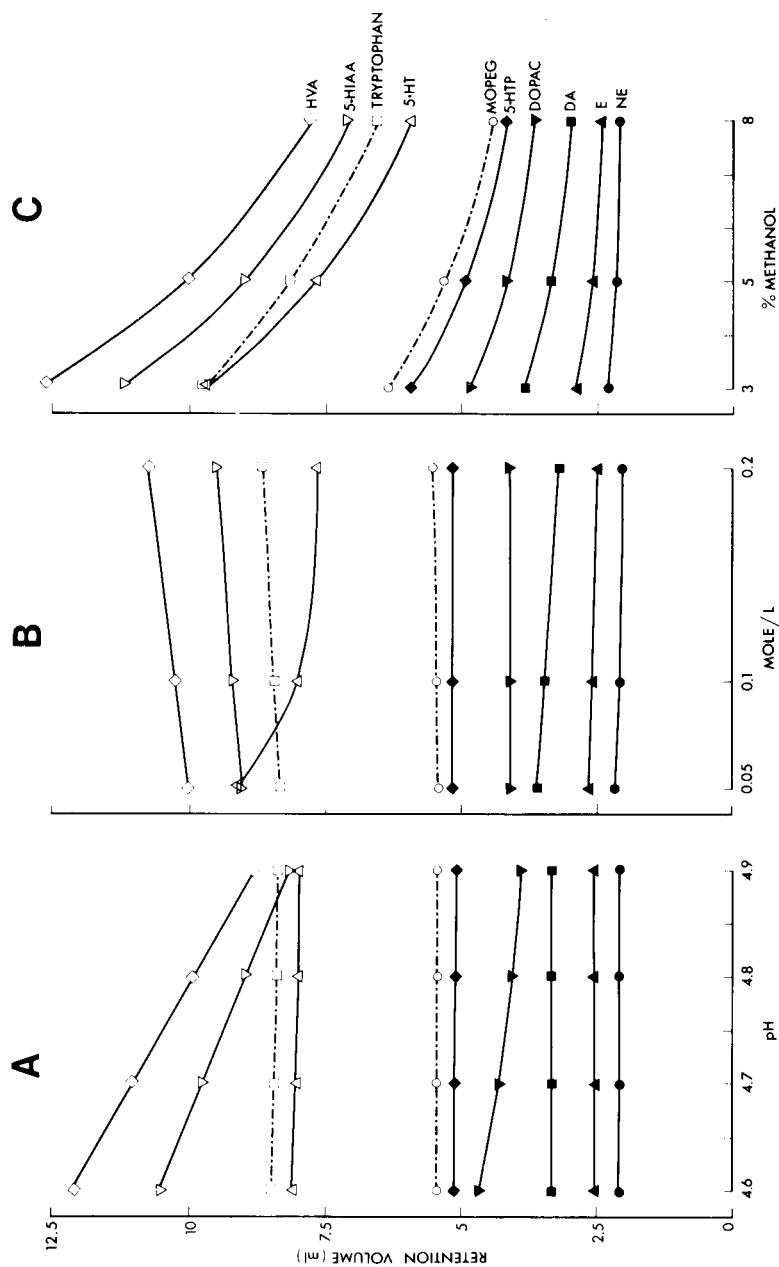


Fig. 1. Relationship between retention time and pH (A), ionic strength (B) and methanol concentration (C). Stationary phase: C_{18} Spherisorb ODS ($5\ \mu\text{m}$); Flow-rate $1\ \text{ml/min}$; temperature 30°C . Electrode potential: $+0.6\ \text{V}$ (straight line); $+0.88\ \text{V}$ (dotted line). Mobile phase: K_2HPO_4 -citrate containing methanol and $0.1\ \text{mM}$ EDTA; ionic strength $0.1\ \text{M}$, 5% methanol (A); pH 4.7 , 5% methanol (B); ionic strength $0.1\ \text{M}$, pH 4.7 (C).

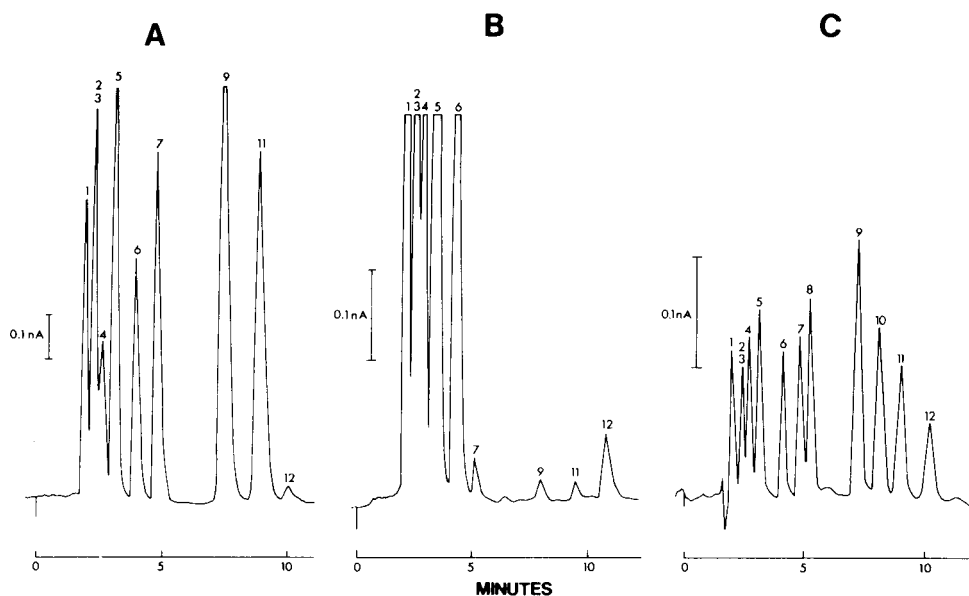


Fig. 2. Chromatogram of a standard mixture of indolic compounds and catechol derivatives. Peaks: 1 = NE; 2 = E; 3 = DOPA; 4 = DOPEG; 5 = DA; 6 = DOPAC; 7 = 5-HTP; 8 = MOPEG; 9 = 5-HT; 10 = tryptophan; 11 = 5-HIAA; 12 = HVA. Chromatographic conditions; column C_{18} Spherisorb ODS (5 μ m); flow-rate 1 ml/min; temperature 30°C. A and B, Eluent 0.1 M K_2HPO_4 -citrate, pH 4.73, containing 5% methanol and 0.1 mM EDTA; electrode potential +0.6 V. C, eluent 0.2 M K_2HPO_4 -citrate, pH 4.73, containing 5% methanol and 0.1 mM EDTA; electrode potential +0.88 V. Traces A and C correspond to 20 ng of compound 10 and 1 ng of the other compounds. B corresponds to 2.5 ng of compounds 1, 2, 3, 4, 5, 6, 8 and 12, 50 pg of 7, 15 pg of 9 and 25 pg of 11.

metabolite on the column increased with decreasing pH (Fig. 1A). In contrast, the retention times of 5-HT and 5-HTP were independent of the pH of the eluent in the range 4.6–5, probably due to the fact that in this pH range the amino groups are completely protonated. An increase in the ionic strength of the running buffer decreased the retention time of 5-HT but left unaffected those of 5-HTP and 5-HIAA (Fig. 1B). As indoles are relatively non-polar compounds, the addition of methanol to the buffer was necessary to reduce elution times. In our system, 5% methanol was found to be sufficient to achieve adequate resolution of the indolic compounds without unduly prolonging the retention of HVA, the last compound to be eluted (Fig. 1C). Addition of a small amount of EDTA, which strongly complexes metal ions, improved the baseline stability.

Fig. 2A shows that, under the conditions outlined above, the three indolic compounds (1 ng of each) could be resolved within less than 10 min. At a flow-rate of 1 ml/min the retention times for 5-HTP, 5-HT and 5-HIAA were 4.8, 7.6 and 8.9 min, respectively. A constant column temperature (30°C) was found to be necessary in order to obtain constant retention times. The detector response was linear over the range 0.01–50 ng for each of the indoles. The detection limits (signal-to-noise ratio of 2) were found to be 15, 10 and 20 pg for 5-HTP, 5-HT and 5-HIAA, respectively (see Fig. 2B), which are comparable to or even better than those obtained with existing GC-MS^{3,4}, HPLC with fluorescence^{12–14} or electrochemical^{10,15–19} detection or

radioenzymatic techniques^{5,6}. No variation of the detector response was found over (at least) 24 h, making unnecessary the use of internal standards.

The chromatographic behaviour of a variety of monoamines and their metabolites which may coexist with the indoles in brain tissue or biological fluids has also been examined (Figs. 1 and 2). A large number of these metabolites could be resolved with the present system (Fig. 2). However, DOPEG, NE, E and DOPA eluted close to the solvent front and could not be reliably assessed. As expected from its oxidation potential (+0.88 V), tryptophan was not detectable at the usual working potential (Fig. 2A). However, it could easily be detected using a higher potential (Fig. 2C), although the detection limits were worse than for the other indolic compounds due to the increase in baseline noise. Also, at this potential, tryptophan was found to slightly interfere with the detection of 5-HT, but this could easily be resolved by increasing the ionic strength of the running buffer to 0.2 M (Figs. 1B and 2C). An increase in the oxidation potential resulted in an increase in the electrochemical response and improved the detection limits for HVA and MOPEG (compare Fig. 2A and C). This was expected as O-methylated catechols are known to be less susceptible to oxidation than free catechols.

Applications

The chromatographic conditions described have been applied to the determination of 5-HT, 5-HTP and 5-HIAA in rat and human brain tissue and human lumbar CSF and plasma with only minimal sample pre-treatment. Representative chromatograms are shown in Fig. 3.

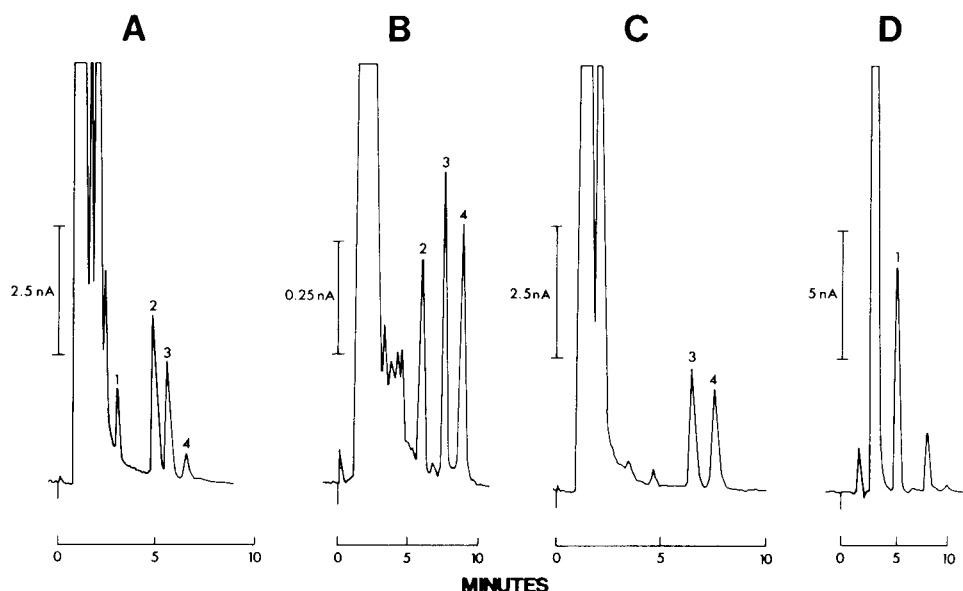


Fig. 3. Chromatograms from rat striatum (after injection of NSD 1015) (A), human hippocampus (B), human CSF (C) and human plasma (D). Peaks: 1 = 5-HTP; 2 = 5-HT; 3 = 5-HIAA; 4 = HVA. Chromatographic conditions: column C_{18} Spherisorb ODS ($5\ \mu\text{m}$); flow-rate 1.5 ml/min (A and C), 1 ml/min (B and D); temperature 30°C . Eluent: 0.1 M K_2HPO_4 -citrate, pH 4.7, containing 5% methanol and 0.1 mM EDTA. Electrode potential: +0.6 V.

TABLE I
5-HT AND 5-HIAA LEVELS IN HUMAN BRAIN

Values are means \pm S.E.M. for 6-12 determinations. N.D. = Not detectable.

Brain area	5-HT (ng/g)	5-HIAA (ng/g)
Frontal cortex	N.D.	104 \pm 16
Cingulate cortex	52 \pm 6	275 \pm 30
Entorhinal cortex	53 \pm 8	171 \pm 42
Hippocampus	55 \pm 8	197 \pm 43
Caudate nucleus	624 \pm 62	410 \pm 83

5-HT and 5-HIAA in brain tissues and CSF. For these determinations, tissue preparation required only homogenization in 0.1 M perchloric acid followed by centrifugation prior to application, while CSF samples were directly applied to the HPLC column.

The concentrations of 5-HT and 5-HIAA found in discrete regions of human brain (Table I) using this method are in agreement with those recently reported by other investigators¹⁹. 5-HIAA levels measured in the lumbar CSF of schizophrenic patients not treated with neuroleptics (16.7 ± 2.0 ng/ml, $n = 6$) are also in the range previously reported²⁰. Under the same experimental conditions, HVA could also be simultaneously quantitated (21 ± 5 ng/ml, $n = 6$).

5-HTP in rat brain tissues and human plasma. 5-HT is formed in the brain via hydroxylation of tryptophan into 5-HTP by tryptophan hydroxylase and subsequent decarboxylation of 5-HTP by aromatic L-amino acid decarboxylase. 5-HTP is not present in brain tissue under normal conditions owing to the high activity of the decarboxylase. However, after inhibition of this enzyme by NSD 1015, large amounts of 5-HTP could be detected in rat brain (Fig. 3A). The concentrations of 5-HTP were 187 ± 6 , 104 ± 8 and 205 ± 13 ng/g in the striatum, cerebral cortex and limbic areas respectively, in good agreement with previously published results obtained by a conventional fluorescence technique²¹. For most of the brain regions studied, sample preparation required only deproteinization by 0.1 M perchloric acid followed by centrifugation, but for some dopamine-rich brain areas, such as the striatum, it was preferable to remove catechol compounds by alumina adsorption (see Materials and methods) before chromatographic analysis in order to obtain more accurate determinations.

L-5-HTP levels were also measured in plasma from myoclonic patients upon oral administration of 100 mg carbidopa, an aromatic amino acid decarboxylase inhibitor, followed by intravenous infusion of L-5-HTP (100 mg). The plasma preparation prior to analysis required only deproteinization by perchloric acid. Fig. 3D shows a typical chromatogram. The plasma levels of L-5-HTP in these patients were previously undetectable, but amounted to 1.0 ± 0.2 , 2.1 ± 0.2 and 1.3 ± 0.1 μ g/ml at 30, 60 and 120 min, respectively, after drug administration (mean \pm S.E.M. for data obtained with five patients).

The present method for the separation and quantification of indoles has several advantages over previously published methods:

It requires only minimal sample handling and preparation (direct injection of perchloric acid extracts) as opposed to the more complicated and time-consuming

sample preparations (ion-exchange chromatography or organic extraction) previously described^{9,21}.

In spite of its simplicity, the detection limits are better than or comparable to those of previous HPLC with fluorescence or electrochemical detection techniques^{8-10,22}.

The rapidity (less than 10 min for the separation of all compounds), and resolution of the indoles (particularly 5-HTP), are superior to those of previously published methods^{8,10}.

To our knowledge, no previously reported method allows the simultaneous detection of indoles (including tryptophan and 5-HTP) and the major metabolites of dopamine and noradrenaline without interference.

Finally, it has been found to be practical and reliable in the measurement of indoles, not only in brain tissue but also in a variety of biological fluids.

In conclusion, the present method appears to be rapid, sensitive, reliable and requires minimal sample handling and preparation. By using an automatic injector and a digital peak integrator, 50 samples could be analyzed per day. This method has been successfully applied to the determination of 5-HT, 5-HIAA and 5-HTP in brain tissue and body fluids. The major metabolites of dopamine and norepinephrine can be measured concurrently.

ACKNOWLEDGEMENTS

We thank Professor G. Avanzini and S. Franceschetti, The Neurological Institute Besta, Milan, for the human plasma samples, Dr. D. Kemali, The University of Naples, for the human lumbar CSF and Drs. F. Javoy-Agid and Y. Agid for the human brain samples.

REFERENCES

- 1 G. Curzon and A. R. Green, *Brit. J. Pharmacol.*, 39 (1970) 653.
- 2 S. Udenfriend, *Fluorescence Assay in Biology and Medicine*, Academic Press, New York, 1969.
- 3 F. Artigas and E. Gelpi, *Anal. Biochem.*, 92 (1979) 233.
- 4 F. Cattabeni, S. H. Koslow and E. Costa, *Science*, 178 (1972) 166.
- 5 A. Boireau, J. P. Ternaux, S. Bourgoïn, F. Hery, J. Glowinski and M. Hamon, *J. Neurochem.*, 26 (1976) 201.
- 6 M. Tappaz and J. F. Pujol, *J. Neurochem.*, 34 (1980) 933.
- 7 S. F. Pang, G. M. Brown, L. J. Grotta, J. W. Chambers and R. L. Rodman, *Neuroendocrinology*, 23 (1977) 1.
- 8 G. M. Anderson, J. G. Young, D. K. Batter, S. N. Young, D. J. Cohen and B. A. Shaywitz, *J. Chromatogr.*, 223 (1981) 315.
- 9 D. D. Koch and P. T. Kissinger, *J. Chromatogr.*, 164 (1979) 441.
- 10 I. N. Mefford and J. D. Barchas, *J. Chromatogr.*, 181 (1980) 187.
- 11 P. Gaspar, F. Javoy-Agid, A. Ploska and Y. Agid, *J. Neurochem.*, 34 (1980) 278.
- 12 G. M. Anderson and W. C. Purdy, *Anal. Chem.*, 51 (1979) 283.
- 13 J. L. Meek, *Anal. Chem.*, 48 (1976) 375.
- 14 T. Flatmark, S. W. Jacobsen and J. Haavik, *Anal. Biochem.*, 107 (1980) 71.
- 15 C. Hansson and E. Rosengren, *Anal. Lett.*, B11 (1978) 901.
- 16 A. J. Cross and M. H. Joseph, *Life Sci.*, 28 (1981) 499.
- 17 J. F. Reinhard, Jr., M. A. Moskowitz, A. F. Sved and J. D. Fernstrom, *Life Sci.*, 27 (1980) 905.
- 18 D. D. Koch and P. T. Kissinger, *Life Sci.*, 26 (1980) 1099.
- 19 W. H. Lyness, N. M. Friedle and K. E. Moore, *Life Sci.*, 26 (1980) 1109.
- 20 A. Spissu, S. Congia, M. P. Piccardi, F. Fadda, A. Mangoni and G. L. Gessa, *Psychopharmacology*, 71 (1980) 7.
- 21 B. Biswas and A. Carlsson, *Naunyn-Schmiedeberg's Arch. Pharmacol.*, 299 (1977) 47.
- 22 G. P. Jackman, V. J. Carson, A. Bobik and H. Skews, *J. Chromatogr.*, 182 (1980) 277.

CHROM. 14,254

SEPARATION OF ACIDIC DRUGS IN THE $\mu\text{g/ml}$ RANGE IN UNTREATED BLOOD PLASMA BY DIRECT INJECTION ON LIQUID CHROMATOGRAPHIC COLUMNS

K.-G. WAHLUND

Department of Analytical Pharmaceutical Chemistry, Biomedical Center, Box 574, S-751 23 Uppsala (Sweden)

SUMMARY

Conditions are described that enable the injection of untreated, non-diluted blood plasma on liquid chromatographic columns for the determination of two acidic drugs. The mobile phase is chosen so that the plasma proteins are kept in solution. The influence of the number of plasma injections on the column back-pressure and retention time have been studied. Quantitations could be made without sample losses.

INTRODUCTION

The determination of drugs in complex mixtures such as body fluids usually involves a number of procedures, *e.g.*, extraction, evaporation, etc., that can contribute considerably to the total analysis time and work. There is an obvious need to reduce the number of working steps or to automate the total procedure. Liquid chromatography with aqueous mobile phases permits direct application of aqueous samples onto the separation column which means that extraction with organic solvents can be avoided.

The direct injection of blood plasma samples can be complicated by several factors. Aqueous mobile phases containing polar organic solvents will in many cases cause precipitation of the plasma proteins. Therefore plasma samples have often been equilibrated with the mobile phase solvent and the clear supernatant obtained after such a denaturing procedure then injected on the chromatographic column, *e.g.*, as in ref. 1. Alternatively, the proteins are removed by more efficient denaturing agents such as perchloric acid or ammonium sulphate² or acetonitrile³. However, denaturing can result in serious errors due to losses of the determined compound in the protein precipitate², especially for relatively hydrophobic compounds⁴, and therefore it may be an advantage to make direct injections of the untreated plasma samples.

Some work has already been done in which untreated plasma samples have been fed to liquid chromatographic columns. Thus, attempts to separate serum proteins were made on size exclusion columns⁵ or on ion-exchange columns⁶ with buffers as the eluent. For the determination of low-molecular-weight compounds, like many drugs, the conditions are chosen such that the compound to be determined is com-

pletely retained when the eluent is water. The compound is then rapidly eluted by switching to an aqueous eluent containing a suitable concentration of a polar organic solvent. This preconcentration technique has been performed on separate precolumns⁷ or on an automated system where the precolumn was coupled on-line to the separation column⁸. Preconcentration is of particular advantage in trace analysis when a large plasma sample is required.

There are many cases, however, where a drug or a similar compound is present in blood plasma in such high concentrations that a relatively small sample volume (e.g., 10 μ l) can be applied to the separation system in order to detect the compound. It should be possible in those cases to apply plasma samples without a previous precipitation of the proteins and without preconcentration steps that involve a change of the eluting solvent. Thus, N-acetyl-*p*-aminophenol has been determined in 1.5 μ l serum samples (after dilution 1:1 with buffer) on a 13- μ m cation-exchange resin protected by an exchangeable precolumn and with a buffer as eluent, but the separation time was rather long⁹. Recently¹⁰, the same drug was determined on a reversed-phase μ Bondapak C₁₈ column from 2- μ l plasma samples (diluted 1:1 with buffer) and with acetonitrile-buffer (7:93) as the eluent, without any precolumn. The same conditions were used for the determination of theophylline and no problems with the column back-pressure occurred¹¹.

In this paper, a study of the separation conditions for two carboxylic acids from blood plasma by direct injection of the untreated, non-diluted, plasma samples (10 or 20 μ l) on reversed-phase liquid chromatographic columns is described. Several of the experimental parameters which influence the performance of such a procedure have been examined. The choice of chromatographic phase system is discussed, as well as the stability of the system with respect to the back-pressure and retention time. Some results on quantitation are also presented.

EXPERIMENTAL

Chemicals

Salicylic acid and naproxen, (+)-2-(6-methoxy-2-naphthyl)propionic acid, were of pharmacopoeial grade. All other chemicals were of analytical grade.

LiChrosorb SI 60 (silica) and RP-2, RP-8 and RP-18 (alkyl-modified silicas) were obtained from E. Merck (Darmstadt, G.F.R.). They had particle diameters between 5 and 10 μ m.

Equipment

An LDC Solvent Delivery System 711-46 or 711-26 (Milton-Roy Minipumps with LDC pulse dampener; LDC, Riviera Beach, FL, U.S.A.), a Rheodyne Syringe Loading Injector 7120 equipped with 10-, 20- or 50- μ l loops and a SpectroMonitor III (LDC) variable-wavelength detector or a Schoeffel FS 970 fluorescence detector were used. The separation columns were LiChroma tubes (316 stainless steel, Handy and Harman), 100 \times 4.6 I.D. They were equipped with Swagelok end fittings containing Altex 250-21 bed supports with 2- μ m steel frits. The precolumns (5 \times 3.2 mm I.D.) were constructed from similar materials as the separation column after modification. Altex bed supports were placed in both ends. The precolumns were connected to the separation column by 1/16 in. I.D. tubing via a Swagelok zero dead volume union.

Procedures

All experiments were performed at 25.0°C, with buffers having an ionic strength of 0.1. The liquid–liquid chromatographic system was prepared as described previously¹². The support was LiChrosorb RP-18, 5 μm .

The separation columns were slurry packed with a high pressure pump. The precolumns were also slurry packed, either with the high pressure pump or by suction with a water pump. In the latter case the slurry was made up in methanol–dichloromethane (5:95).

Plasma samples were carefully centrifuged. Spiking with salicylic acid or naproxen was achieved by mixing 5 μl of concentrated aqueous solutions of these compounds with 500 μl centrifuged plasma. External standards were prepared in the same way except that the eluent solvent was used instead of the plasma.

RESULTS AND DISCUSSION

Solubility of plasma proteins

The success of a procedure to determine a drug in plasma by direct injection on a liquid chromatographic column depends to a great extent on the influence of the normal constituents of the plasma, especially those that are present in high concentrations, *e.g.*, proteins, normally having a total concentration of *ca.* 8% (w/v).

In this study the conditions are such that the plasma proteins are prevented from precipitating when they come in contact with the chromatographic eluent. It is known that water-miscible organic solvents, like those often used as the eluent of reversed-phase liquid chromatographic systems, are amongst the more efficient precipitants for proteins. Some simple experiments showed that concentrations of methanol and acetonitrile exceeding 50% in water gave pronounced precipitation of plasma proteins, whereas at lower concentrations the precipitation effect was much weaker and hardly noticeable below 10%. The results presented were obtained either without any organic solvent in the eluent or with 10% methanol in the eluent, but it is possible that even higher concentrations of organic solvent can be used.

Test compounds

Two carboxylic acids, salicylic acid and naproxen, have been used as test compounds. Salicylic acid is formed in the body after administration of the drug acetylsalicylic acid, whereas naproxen is used as a drug. Both compounds are present in rather high concentrations (well above 1 $\mu\text{g/ml}$) in blood plasma after administration. They have high molar absorptivities and are highly fluorescent, and can therefore easily be detected by an UV detector or a fluorescence detector. Thus, the conditions are favourable for direct injection of plasma samples of these compounds.

Phase systems

The phase systems tested are summarized in Table I. They represent both liquid–liquid and liquid–solid reversed-phase systems. The liquid–liquid system has been shown to be useful for the separation of carboxylic acids¹². The liquid–solid systems were prepared with eluents free from organic solvents, which means that the retention can only be regulated by the type of solid stationary phase and the concentration of salts in the eluent.

TABLE I
PHASE SYSTEMS

System	Mobile phase	Stationary phase
I* (liquid-solid)	Phosphate buffer, pH 7.5	LiChrosorb SI 60, 5 and 10 μ m
II* (liquid-solid)	Phosphate buffer, pH 7.5	LiChrosorb RP-18, 5 and 10 μ m
III (liquid-liquid)	Methanol + citrate buffer, pH 5.4 (1:9)	Tributyl phosphate
IV (liquid-solid)	Phosphate buffer + sodium octyl sulphate	LiChrosorb RP-18, 5 and 7 μ m
V (liquid-solid)	Phosphate buffer + sodium octyl sulphate	LiChrosorb RP-2, 6 μ m

* Precolumns only.

Normally the retention of a carboxylic acid should decrease with increasing pH of the mobile phase (above the pK_a value of the acid). Thus, in the liquid-liquid phase system the retention can be regulated in a predictable way and within wide limits¹². In the liquid-solid phase systems the retention often tends to level off even though the pH is increased. This may be due to the retention of the anions of the carboxylic acids, e.g., as ion pairs with sodium in the buffer¹³. In such cases it can be shown that the addition of a competitor to the mobile phase further decreases the retention. The competitor should compete with the sample anion for the solid stationary phase. For salicylic acid and naproxen it was necessary to add sodium octyl sulphate to the mobile phase as a competitor. The competition effect can be regulated by the concentration of the competitor and its hydrophobicity. Lauryl sulphate will be a more effective competitor than octyl sulphate since the former is more hydrophobic.

Effect of plasma injections on the back-pressure and retention time

In all experiments when plasma was injected the separation column was preceded by a short precolumn in order to protect the separation column from possible deterioration. The volume of the precolumn has not been optimized with respect to the number of plasma injections that can be made, and therefore the precolumns were in most cases routinely changed after about ten plasma injections or when they gave an excessive back-pressure.

TABLE II

EFFECT OF PLASMA INJECTIONS ON BACK-PRESSURE AND RETENTION TIME WITHOUT CHANGE OF THE PRECOLUMN

Phase system	Flow-rate (ml/min)	Plasma injections		Average increase of back-pressure (bar per injection)	Retention time (min)		
		Vol. (μ l)	No.		Mean	Relative S.D. $\times 100$	Range
I, II*	1.4	10	25	0.09-0.6			
III	0.8	20	8	1.5	—	—	3.7-3.9
IV	1.0	10	17	0.6	5.55	0.3	
V	1.0	10	15	0.9	6.42	1.2	
V	1.0	10	24**	2.2	6.47	1.5	

* Precolumns only.

** Precolumn changed twice.

It was essential to obtain a clear plasma solution otherwise the frits of the bed supports soon became blocked.

A possible effect of the injection of plasma is the enrichment of the stationary phase by substances like fats and proteins. This can decrease the porosity of the column which leads to an increase in the resistance to flow. Depending on the type of pump used, this can result in a decreased flow-rate and an increased retention time.

Table II summarizes the effects on back-pressure and retention time by plasma injections in some different systems. There was no clear difference between the ordinary silica (LiChrosorb SI 60) and hydrophobic silica (LiChrosorb RP-18) with respect to the increases in back-pressure over the precolumns, and only slightly better performance was seen with the larger particle sizes (10 μm). In many cases the back-pressure increased stepwise, which means that in one case fourteen injections could be made without any change of the back-pressure. The restrictions to flow were often localized to the frits of the bed supports in the precolumns.

In the liquid-liquid phase system (III) the increases in back-pressure and retention time were somewhat higher than in the other phase systems, which may be a result of the denaturing effect of methanol and tributyl phosphate on the proteins. In the liquid-solid systems (IV and V) the retention time was constant despite a gradual increase of the back-pressure, but the retention time at injection of a plasma sample was always 1 % lower than for an external standard.

The constancy of the retention time obtained with the relatively simple pumping system used in this study indicates that quantitations will be possible if the precolumns are changed at suitable intervals. With a more advanced pumping system the possibilities will be even greater.

On injecting a large number of plasma samples (60 samples, phase system V) the back-pressure occasionally increased drastically. It could always be restored by change of the precolumn and the retention time was always constant. This indicates that the retention properties of the separation system were unaffected by the plasma injections.

A study of the changes of back-pressure during the elution of a plasma sample shows that the viscous plasma components migrate with the solvent front. It is possible that the drastic increases of the back-pressure after many injections of plasma is related to this. The presence of the concentrated plasma plug may have increased the blocking of the pores. Therefore, injection of slightly more dilute plasma samples may result in improved performance.

Separation of salicylic acid

Phase system III. The buffer pH in the eluent was chosen as 5.4 in order to give salicylic acid a capacity ratio of close to 4. A comparison of the peak heights from a few plasma samples with those obtained from external standards indicated a recovery of close to 100 % at a concentration level of 40 $\mu\text{g/ml}$ salicylic acid.

When the plasma sample volume exceeded 20 μl the salicylic acid peak became skewed and for a 40- μl sample was divided into two peaks with the new peak occurring at a shorter retention time than the original. It could be shown that both peaks contained the salicylic acid. The effect seemed to depend on the amount of plasma injected, since if the plasma samples were diluted and a correspondingly larger volume was injected the effect remained. It was suspected that the peak splitting effect

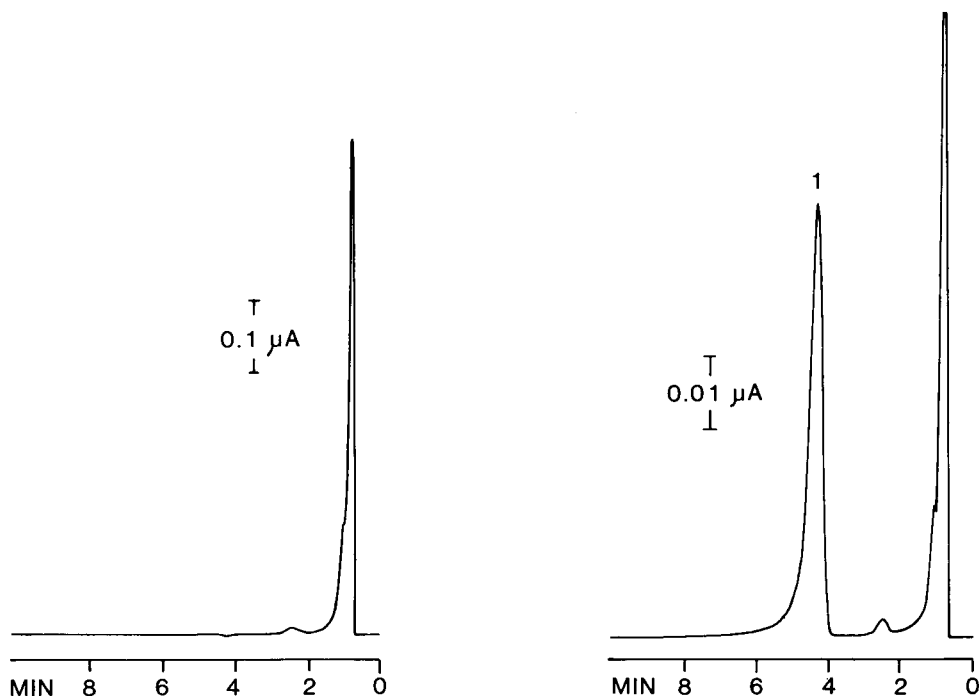


Fig. 1. Chromatograms of plasma. Left, 20 μ l plasma; right, 3 μ l plasma spiked with 40 μ g/ml salicylic acid (1). Separation column: LiChrosorb RP-18, 5 μ m, coated with tributyl phosphate. Precolumn: LiChrosorb RP-18, 5 μ m. Eluent: methanol-citrate buffer, pH 5.4 (1:9); 0.8 ml/min. Fluorescence detection: excitation at 295 nm, emission at > 370 nm.

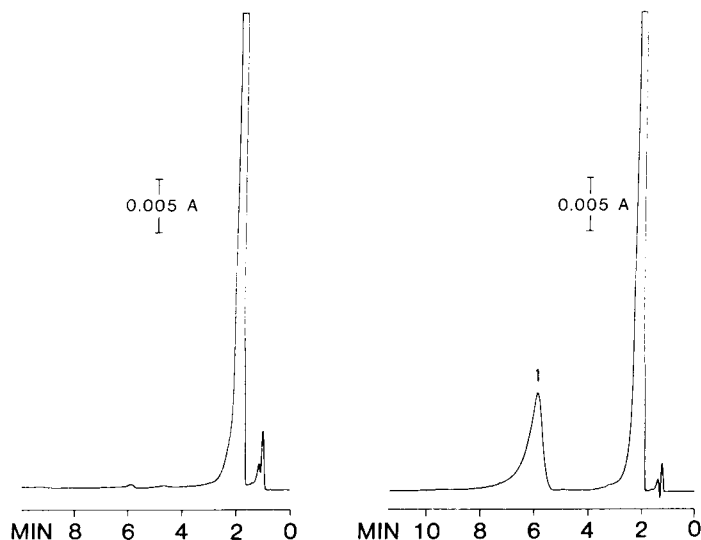


Fig. 2. Chromatogram of plasma. Left, 10 μ l plasma; right, 10 μ l plasma spiked with 27 μ g/ml salicylic acid (1). Separation column: LiChrosorb RP-18, 5 μ m. Precolumn: LiChrosorb 18, 10 μ m. Eluent: phosphate buffer, pH 5.90-1.02 $\cdot 10^{-4}$ M sodium octyl sulphate; 1 ml/min. Detection: UV at 296 nm.

could be due to the strong binding of salicylic acid to plasma albumin (as is also the case for naproxen), but the addition to the plasma sample of a substance (flurbiprofen), which would displace salicylic acid from albumin¹⁴, did not eliminate the effect. It is possible that the injection of plasma changed the properties of the stationary phase. Further studies are necessary to explain this problem.

Fig. 1 gives typical chromatograms from plasma, without and with addition of salicylic acid, obtained with fluorescence detection. Spectrophotometric detection at 296 nm could also be used and gave as good resolution from the leading peak even though this peak was much higher than the salicylic acid peak.

Phase system IV. In this case the separation column contained LiChrosorb RP-18, 5 or 7 μm , and the precolumn the same type of particles but of 10 μm . The eluent was of pH 5.9 and contained sodium octylsulphate, $1.0 \cdot 10^{-4} M$ or $3.1 \cdot 10^{-5} M$, which gave salicylic acid a capacity ratio of 4.7 or 3.6.

Quantitation was only briefly studied and a few comparisons with external standards indicated a recovery close to 100% at the 30- $\mu\text{g}/\text{ml}$ level. Fig. 2 shows a chromatogram of 10 μl plasma, before and after spiking with 27 $\mu\text{g}/\text{ml}$ salicylic acid, with spectrophotometric detection at 296 nm. The peak is well resolved.

Separation of naproxen in plasma with phase system V

The more hydrophobic compound naproxen required a less hydrophobic sta-

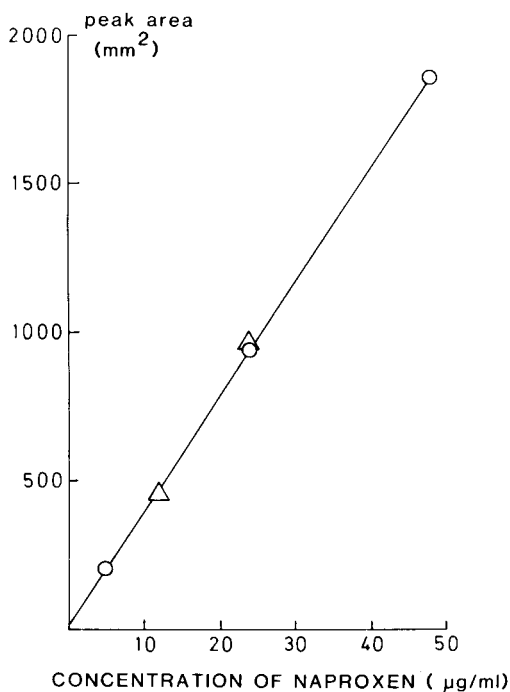


Fig. 3. Quantitation of naproxen in plasma. ○, External standards dissolved in the eluent (the mean of two or three values); △, plasma samples (single values). For conditions see Fig. 4.

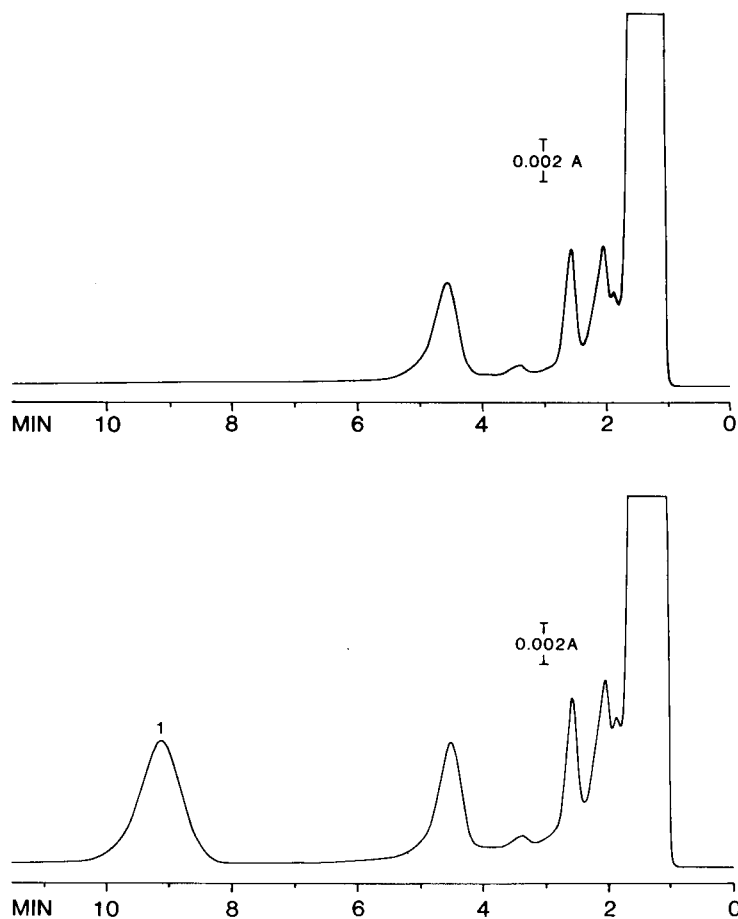


Fig. 4. Chromatograms of plasma. Top, 10 μ l plasma; bottom, 10 μ l plasma spiked with 24 μ g/ml naproxen (1). Separation column: LiChrosorb RP-2, 6 μ m. Precolumn: LiChrosorb RP-2, 6 μ m. Eluent: phosphate buffer, pH 7.6–0.01 *M* octyl sulphate; 0.8 ml/min. Detection: UV at 261 nm.

tionary phase (LiChrosorb RP-2) than salicylic acid. The capacity ratio was adjusted to 6. The precolumns contained either the same material as the separation column or LiChrosorb RP-8, 10 μ m. The latter gave a somewhat better performance with respect to the number of plasma injections that could be made until the back-pressure started to increase drastically.

The possibilities for quantitation were tested by comparing peak heights and peak areas from spiked plasma samples with those from external standards. Some results are given in Fig. 3 and they indicate that quantitation can be achieved with no loss of substance in the studied concentration range. These results were obtained with plasma samples and standards intermittently injected at close time intervals, and showed a quite normal dispersion. Over a longer time period the relative standard deviation of peak heights or peak areas was around 5% for both plasma and standards. This dispersion seemed to be random and could not be correlated to, *e.g.*,

changes in back-pressure. The fluctuations in the column efficiency that were observed might, however, have contributed to the dispersion.

Fig. 4 shows illustrative chromatograms of the separation of naproxen.

CONCLUSIONS

The chromatograms of plasma samples are surprisingly free from interfering peaks, which makes possible consecutive injection of plasma samples. There are some indications that most of the plasma proteins are unretained in the liquid-solid phase systems. A chromatogram of albumin gives support to this conclusion.

The column efficiency for salicylic acid and naproxen was rather low in the liquid-solid systems under the conditions used, the reduced plate height being around 20. This was not caused by the plasma injections.

The phase systems described have been optimized for the chromatography of salicylic acid and naproxen. The conditions can of course be changed to suit compounds of a different nature such as bases, anions, cations or uncharged aprotic compounds, but the requirement for a low concentration of organic solvent in the eluent can restrict the applicability of the technique. Since little knowledge of the retention properties of the endogenous compounds in plasma is available there is always a risk that they will cause interference if a new phase system is used.

ACKNOWLEDGEMENTS

I. Beijersten and T. Arvidson are thanked for having carried out most of the experiments. My thanks are also due to Professor G. Schill for his criticism of the manuscript.

REFERENCES

- 1 K.-G. Wahlund and U. Lund, *J. Chromatogr.*, 122 (1976) 269.
- 2 B. Henke and D. Westerlund, *J. Chromatogr.*, 187 (1980) 189.
- 3 B. E. Cham, D. Johns, F. Bochner, D. M. Imhoff and M. Rowland, *Clin. Chem.*, 25 (1979) 1420.
- 4 D. Westerlund and K. H. Karset, *Anal. Chim. Acta*, 67 (1973) 99.
- 5 L. R. Snyder and J. J. Kirkland, *Introduction to Modern Liquid Chromatography*, Wiley, New York, 2nd ed., 1979, p. 503.
- 6 A. J. Alpert and F. E. Regnier, *J. Chromatogr.*, 185 (1979) 375.
- 7 J. X. de Vries, W. Günther and R. Ding, *J. Chromatogr.*, 221 (1980) 161.
- 8 W. Roth, K. Beschke, R. Jauch, A. Zimmer and F. W. Koss, *J. Chromatogr.*, 222 (1981) 13.
- 9 D. Blair and B. H. Rumack, *Clin. Chem.*, 23 (1977) 743.
- 10 B. R. Manno, J. E. Manno, C. A. Dempsey and M. A. Wood, *J. Anal. Toxicol.*, 5 (1981) 24.
- 11 B. R. Manno, J. E. Manno and B. Hilman, *J. Anal. Toxicol.*, 3 (1979) 81.
- 12 K.-G. Wahlund and B. Edlén, *J. Liquid Chromatogr.*, 4 (1981) 309.
- 13 A. Tilly-Melin, Y. Askemark, K.-G. Wahlund and G. Schill, *Anal. Chem.*, 51 (1979) 976.
- 14 I. Sjöholm, B. Ekman, A. Kober, I. Ljungstedt-Pählman, B. Seiving and T. Sjödin, *Mol. Pharmacol.*, 16 (1979) 767.

OTHER APPLICATIONS

CHROM. 14,161

HIGH-PERFORMANCE LIQUID CHROMATOGRAPHY OF FLAVONOIDS IN BARLEY AND HOPS

I. McMURROUGH

Arthur Guinness Son & Co. (Dublin) Ltd., St. James's Gate, Dublin 8 (Ireland)

SUMMARY

Gradient elution from a reversed-phase high-performance liquid chromatography column was used to separate and quantitate the flavonol glycosides and simple flavanol oligomers extracted from hops and barley. Whereas flavonol monoglycosides, diglycosides and triglycosides, and flavanol monomers, dimers and trimers were readily separated, polymeric flavanols were not resolved. A column temperature of 30°C was found optimal for the separation of flavonol aglycones by isocratic elution.

INTRODUCTION

Flavonoids are very widely distributed in the plant world and a great diversity of chemical structures has been encountered¹. Most of these polyphenols contain catechol and phloroglucinol units within their structures, which confer on them an important range of chemical reactivities. Notably, flavonoids are very susceptible to oxidation and may also undergo both intramolecular and intermolecular hydrogen bonding, and most show a capacity to chelate metals². Unfortunately, the reactivity of flavonoid materials present in barley and hops can cause problems at several stages in the brewing process³. Most important of the problems known to be associated with flavonoids is the formation of unacceptable hazes and undesirable flavours in beer^{4,5}. For these reasons the measurement of flavonoids in brewing materials and in beers is a prominent feature of judicious quality control. Until recently, the standard methods for measuring polyphenols have suffered from shortcomings in specificity, speed or precision⁶. The advent of high-performance liquid chromatographic (HPLC) techniques has greatly enhanced the measurement of a variety of simple phenolic constituents⁷⁻¹⁰, including flavonoids from a number of plant sources¹¹⁻¹⁶, but the applications in brewing science have been relatively few¹⁷⁻²¹. In this study, HPLC on reversed-phase columns was used to measure the contents of specific components in grains of barley (*Hordeum vulgare*) and in flower cones of hops (*Humulus lupulus*). The flavonoids of interest were flavonol glycosides, e.g. rutin (Fig. 1) and simple flavanol oligomers, e.g. procyanidin B-3 (Fig. 2). The results obtained indicated that reversed-phase HPLC has wide applicability for the measurement of flavonoids in the raw materials of brewing.

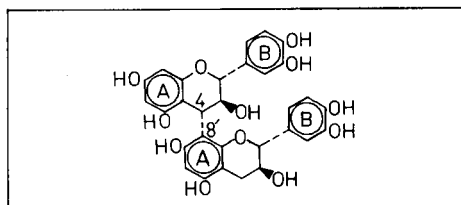
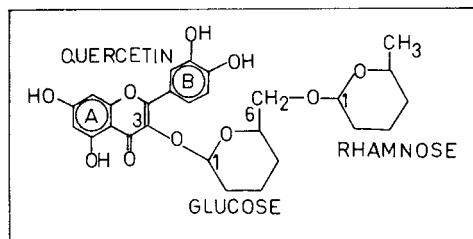


Fig. 1. Structure of rutin as an example of a flavonol glycoside. Other flavonol glycosides may differ in the number of B-ring hydroxyl groups in the flavonol aglycone (*e.g.* myricetin has three, quercetin two, kaempferol one, and galangin none) or in the glycosidic units.

Fig. 2. Structure of procyanidin B-3, a dimer of (+)-catechin as an example of a simple flavanol oligomer. Other oligomers may be derived from combination of (–)-epicatechin (two B-ring hydroxyl groups) or (+)-gallocatechin (three B-ring hydroxyl groups).

EXPERIMENTAL

Chemicals and equipment

Kaempferol, (–)-epicatechin, and diphenyl boric acid 2-aminoethyl ester were obtained from Sigma (Poole, Great Britain). Galangin and pelargonidin chloride were obtained from Fluorochem (Glossop, Great Britain). Rutin and (±)-catechin were obtained from Koch-Light Labs. (Colnbrook, Great Britain). Delphinidin chloride was obtained from Apin (Cardiff, Great Britain). Quercetin, quercitrin, cyanidin chloride and myricetin were obtained from ICN (Plainview, NY, U.S.A.). Apart from HPLC-grade solvents, all other chemicals were obtained from BDH (Poole, Great Britain).

HPLC was performed on a Waters Assoc. (Milford, MA, U.S.A.) liquid chromatograph equipped with two Model 6000 solvent delivery systems, a Model 660 solvent programmer, a Model U6K injector, a Model 440 absorbance detector and a Model 730 data module. The pre-packed reversed-phase column (30 cm × 3.9 mm I.D.) contained μ Bondapak C_{18} (Waters Assoc.) and was eluted with degassed and filtered mixtures of 2.5% (v/v) analytical grade acetic acid (BDH) in water containing organic modifiers²². For different purposes, the organic modifier used (HPLC grade) was either methanol (Rathburn, Walkerburn, Great Britain), acetonitrile (Rathburn) or tetrahydrofuran (Fisons, Loughborough, Great Britain), and was included either at a fixed concentration (isocratic elution) or automatically increased in concentration (gradient elution) during chromatographic development. A mobile phase flow-rate of 2.0 ml/min was used throughout this study, and a standard column temperature of 30°C was maintained by a glass water-jacket connected to a circulating system. Detection was carried out at either 254 nm, 280 nm, 365 nm or 546 nm as required, with a detector sensitivity of 0.1 a.u.f.s. Samples (5–50 μ l) were injected through a Microliter 810 syringe (Hamilton, Reno, NV, U.S.A.).

Extraction of flavonoids from plant material

Extracts were prepared from ground hops or barley grains in acetone–water (75:25, v/v) as described previously²³. The extracts so prepared were either used directly for HPLC analysis or fractionated further when necessary. As a first frac-

tionating step, an acetone-water extract was saturated with sodium chloride and then allowed to separate into two liquid phases. The upper liquid phase was then mixed with an equal volume of hexane, and phase separation was allowed for a second time. The lower liquid phase obtained by the second separation contained the bulk of the simple flavanols and flavonol glycosides, and was termed the flavonoid extract. The procedure not only accomplished a four-fold concentration of the simple flavonoids present in the acetone-water extract but also removed unwanted phenolic acids, depsides and polymeric flavanols.

Preparative chromatography of flavonoids

Flavonoid extracts from hops (100 g) or barley (500 g) were evaporated to dryness under vacuum at 30°C and then dissolved in ethanol (50 ml). The ethanol solutions were then applied to columns (100 cm × 2.5 cm I.D.) of Sephadex LH-20²⁴ (Pharmacia, Uppsala, Sweden) and eluted for 5 days with ethanol (50 ml/h). The distribution of flavonols and flavanols in the fractions collected (15 ml) was determined respectively by absorption measurements at 350 nm and reactivity with dimethylaminocinnamaldehyde²³. Pooled fractions were then concentrated and chromatographed on columns (30 cm × 1.5 cm I.D.) of Sephadex G-25 Superfine (Pharmacia) eluted with increasing concentration of methanol in water²⁵. Whereas this procedure was sufficient to purify most flavonoids, certain flavonol glycosides required final purification by preparative paper chromatography²⁶. Identities^{24,25} were assigned to the recovered flavonoids from the results of two-dimensional cellulose thin-layer chromatography (TLC), and examination of the products formed on hydrolysis with acid, alkali or enzymes.

Simultaneous extraction and hydrolysis of hop flavonoids

Each sample (10 g) of finely ground hops was refluxed in 150 ml of methanol-4 N HCl (75:25, v/v) for 2 h. After cooling, the hop debris was removed by filtration and washed twice with methanol (75 ml). Filtrate and washings were then combined and made up to 400 ml with water. The combined filtrate was then shaken with hexane, (100 ml) and, after the separated hexane phase had been discarded, the red filtrate was adjusted to 500 ml with methanol. A sample (10 ml) of the filtrate was centrifuged (15,000 g for 30 min) clear and examined by HPLC for flavonol aglycones and anthocyanidins²⁷ (flavylium ions).

Thin-layer chromatography

Two-dimensional chromatography on thin layers (20 cm × 20 cm) of cellulose (Eastman-Kodak, Rochester, NY, U.S.A.) was used for the identification of flavonoids and their products. Chromatograms were developed in the first dimension with isoamyl alcohol-acetic acid-water (2:1:1, v/v/v) and in the second dimension with acetic acid-water (6:94, v/v). For detection of flavonoids the three different spray reagents used contained either ferric chloride-potassium ferricyanide²⁶, diphenylboric acid 2-aminoethyl ester²⁵, or 4-dimethylaminocinnamaldehyde²³.

Raw materials

The samples of the hops used were from the varieties; Brewer's Gold, Bullion, Challenger, Comet, Fuggles, Hallertau, Northern Brewer, Pride of Ringwood, Talis-

man and Wye Target. The barley varieties examined were; Ackermann 253, *ant*-13, Aramir, Ark Royal, Arkil, Athos, Emma and Roland.

Procyanidins

Samples of procyanidins B-1, B-2, B-3 and B-4 were kindly given by Dr. E. Haslam of the University of Sheffield, Great Britain. Procyanidin B-3 was also synthesised by the method of Eastmond²⁸.

RESULTS AND DISCUSSION

Flavonol glycosides in hops

Samples (5–25 μ l) of the unfractionated acetone–water (75:25, v/v) extracts of hops were injected directly on to the HPLC column. Owing to the complex composition of these extracts, gradient elution was required to achieve adequate resolution of the constituent flavonol glycosides. Three organic modifiers were tested in conjunction with acetic acid–water (2.5:97.5, v/v) as eluents, and were ranked according to the separations obtained. Accordingly, in order of decreasing separating efficacy the solvents were graded (i) tetrahydrofuran (THF), (ii) acetonitrile, (iii) methanol.

An example of the separation of flavonol glycosides obtained from Challenger hops, which was representative of the ten varieties of hops that were examined, is shown in Fig. 3. Typically the chromatographic profile of hop flavonols consisted of four peaks and numerous incompletely resolved minor peaks. The identities of the major flavonol components were assigned on the results of co-chromatography with standards, obtained by isolation from hops²⁵ when not available commercially. Sixteen substances that displayed the properties of flavonol glycosides were isolated from hop extracts by chromatography on either Sephadex LH-20 or Sephadex G-25. Whereas complete chemical characterisation of only six of these substances was accomplished, tentative designations were assigned to the remainder. Quantitatively the predominant glycosides present in hops were monoglycosides and diglycosides of both kaempferol and quercetin. The most numerous group of glycosides present consisted of members that displayed the chromatographic mobilities of triglycosides on cellulose TLC and on dextran gels. A separation of selected glycosides of quercetin is shown in Fig. 4. With unfractionated hop extracts, the presence of many minor components slightly obscured the HPLC separation of the four major components, which were the β -3-rutinosides and β -3-glucosides of quercetin and kaempferol. Nonetheless, any large differences seen between the chromatographic profiles of extracts obtained from different varieties of hops were invariably in their relative contents of these four glycosides. A comparison of the HPLC profiles of extracts prepared under standard conditions provided, therefore, estimates of variability in the contents of flavonol glycosides in hops. For greater precision in the measurement of differences in the contents of flavonols in different hop varieties, a less complex separation was required.

Hydrolysis of flavonol glycosides

To simplify analysis, flavonols were simultaneously extracted from ground hops and hydrolysed in methanolic HCl to release their aglycones. Although the

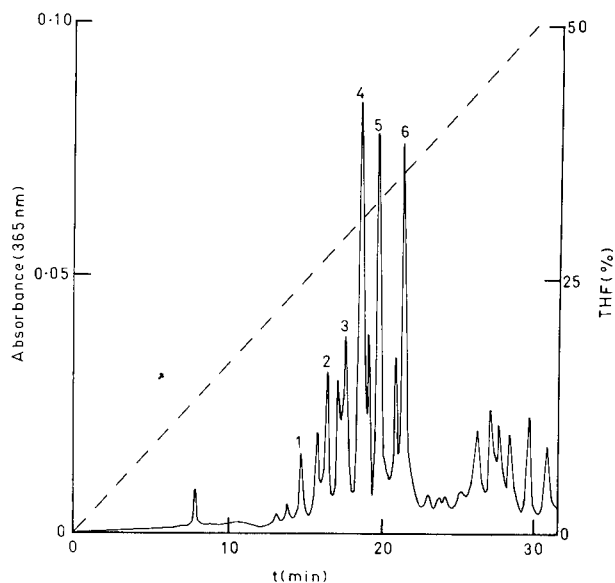


Fig. 3. Separation of flavonol glycosides from hops by gradient elution on μ Bondapak C_{18} . Peaks: 1 = quercetin triglycoside; 2 = quercetin neohesperidoside; 3 = quercetin rutinoside; 4 = quercetin glucoside; 5 = kaempferol rutinoside; 6 = kaempferol glucoside. The broken line is the percentage of THF in the mobile phase.

hydrolysis rates of isolated flavonol 3-glycosides is rapid¹, a reaction time of 2 h was required to ensure maximum recoveries of aglycones from the ground hop material, suggesting that rate of extraction determined the overall yields. Prolonged (4 h) or

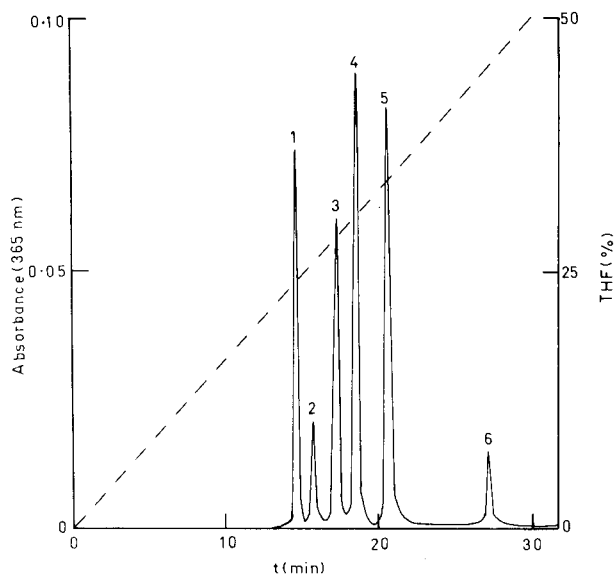


Fig. 4. Separation of quercetin glycosides by gradient elution on μ Bondapak C_{18} . Peaks: 1 = quercetin triglycoside; 2 = quercetin neohesperidoside; 3 = quercetin rutinoside; 4 = quercetin glucoside; 5 = quercetin rhamnoside; 6 = quercetin. The broken line is the percentage of THF in the mobile phase.

repeated (2 h) extraction cycles increased the overall yields by no more than 5%, total and were considered unnecessary. Precautions to minimise autoxidation²⁹ were judged effective, since rutin yielded 98% of the theoretical yield of quercetin, and neither myricetin, quercetin nor kaempferol were denaturated significantly, when these were included as controls in experiment. When samples of hops were hydrolysed in triplicate, the coefficients of variation (C.V.) for measurements of kaempferol and quercetin were never greater than 2.5%.

The amounts of aglycones recovered from hydrolysed hop cones were measured by HPLC using isocratic elution, which facilitated rapid repetitive analysis. Hydrolysates from hops contained kaempferol and quercetin as the predominant flavonol aglycones and traces of another substance similar in chromatographic behaviour to myricetin. Accordingly, the chromatographic system was calibrated with these three aglycones for measurements of peak areas.

Separation and quantitation of flavonol aglycones

Gradient elution was not required for satisfactory resolution of the three flavonol aglycones and, using a solvent containing equal volumes of methanol and acetic acid–water (5:95, v/v), the analysis was completed in 15 min with a column temperature of 30 °C. With the appropriate integration parameters, peak area measurements of aglycone standards were reproducible (C.V. = 2.5%, $n = 10$) and linearly related to sample loadings in the range 0–1 µg. Since it has been claimed¹⁴ that elevated temperatures improve the separation of flavonols on reversed-phase columns, the effect of changes in the range 10–60 °C on the separation of mixtures of four aglycones was investigated. Components of this mixture were well separated and eluted in the order myricetin: quercetin: kaempferol: galangin.

Van 't Hoff plots of retention data for the four flavonol aglycones showed the classical dependence of $\log k'$ and $1/T$ (where k' = capacity ratio and T = temperature)³⁰. Linear regression analysis of the data gave values for the slopes and intercepts of the four straight lines obtained. From the slopes the enthalpies of transition (stationary to mobile phase) for each aglycone were calculated to be: 6.54, 6.42, 6.31 and 6.20 kcal/mol, for myricetin (myr), quercetin (que), kaempferol (kae) and galangin (gal), respectively, and increased slightly with increasing retention. This result signifies that temperature variations had only a small effect on column selectivity. Selectivity, however, depends both on the enthalpies and entropies of transition of solutes³⁰. Calculation of the standard entropies of transition from intercept values of –4.278, –4.014, –3.710, and –3.296 for myricetin, quercetin, kaempferol and galangin was not possible since the phase ratio of the column³⁰ was not known. Nevertheless, the differences in the intercept values obtained from the Van 't Hoff plots (*cf.* ref. 31) suggested a marked dependence of column selectivity on the entropies of transfer for these solutes, which may differ in the contiguity of their orientations on the stationary surface³⁰.

Although temperature variations had little effect on column selectivity an optimum temperature of 30 °C for separation was found. Peak skewness³⁰ progressively increased as the temperature of the column was decreased below 30 °C, presumably owing to non-linearity of the absorption isotherm at low temperatures. Moreover, maximum values for the resolution of neighbouring pairs of aglycones (myr/que = 4.26, que/kae = 4.76, kae/gal = 8.5) in the chromatograms and measurements of

plate numbers (*ca.* 6000 plates/m) were obtained for separations performed at 30° C. These changes in column efficiency may be explained by the effects of temperature on solvent viscosity and swelling of the stationary phase³⁰.

The contents of flavonols, measured as aglycones, did not differ greatly in samples of ten varieties of hops harvested in 1980. Contents of kaempferol ranged from 0.82 to 1.63 mg/g and averaged 1.20 mg/g, while contents of quercetin ranged from 0.32 to 1.44 mg/g and averaged 0.92 mg/g. The contents of the four major flavanol glycosides and of their parent aglycones found in three varieties of hops are given in Table I.

TABLE I

CONTENTS OF MAJOR FLAVONOL GLYCOSIDES AND TOTAL FLAVONOL AGLYCONES IN THREE VARIETIES OF HOPS

Hop variety	Flavonol glycosides (mg/g)				Total flavanol* aglycones (mg/g)	
	Kaempferol (kac)		Quercetin (que)		Kac	Que
	Glucoside	Rutinoside	Glucoside	Rutinoside		
Bullion	0.62	0.68	0.08	0.13	0.82	0.52
Challenger	0.44	0.60	0.37	0.26	0.89	0.85
Talisman	0.31	1.16	1.04	0.91	0.87	1.32

* Measured after hydrolysis of total glycosides.

Flavanols in barley

The acetone water extract of barley contained many UV-absorbing substances, which interfered grossly with the chromatography of simple flavanols. The problem of separation was ameliorated greatly by prefractionation of the acetone-water extract so that the simple flavanols were freed largely from contaminating phenolic acids and polymeric tannins. Preparative-scale chromatography of flavanol extracts on dextran gels yielded catechin, three flavanol dimers, four flavanol trimers and polymeric material. The HPLC separation of a mixture of the isolated propelargonidin, procyanidin B-3 and prodelphinidin B-3 dimers is shown in Fig. 5. The superior selectivity of reversed-phase HPLC permitted the resolution of two minor trimeric components, which were not well separated from the two major trimeric³² components of barley by chromatography on dextran gels. Moreover, HPLC of the hydrolysis products²⁷ of the trimers revealed that two of the trimeric flavanols yielded either cyanidin or delphinidin exclusively. In contrast, the other two trimers yielded mixtures of cyanidin and delphinidin, although one or other of these anthocyanidins clearly predominated. These findings are entirely consistent with proposals made recently for the structures of flavanol trimers in barley³³.

All the simple flavanol components were identified by their retention times in HPLC profiles of flavanol extracts of barley, even though some were present in relatively small amounts. The failure of the prefractionating procedure to eliminate polymeric material completely from the flavanol extract, however, diminished the resolution of the smaller molecules. When recovered flavanol polymers were chromatographed on μ Bondapak C₁₈ they were eluted as a broad band that extended through-

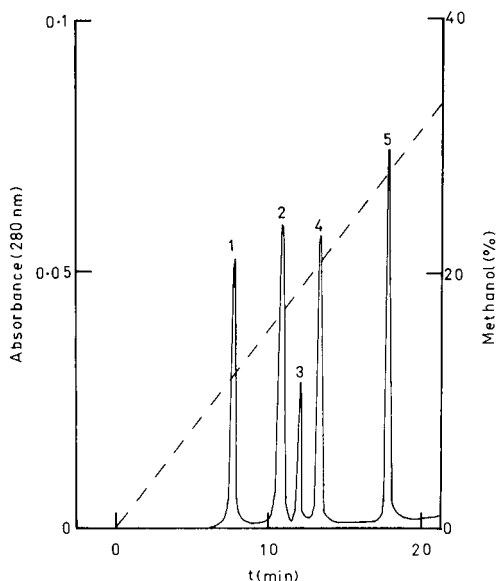


Fig. 5. Separation of flavanol dimers and monomers by gradient elution on μ Bondapak C_{18} . Peaks: 1 = prodelphinidin B-3; 2 = procyanidin B-3; 3 = propelargonidin; 4 = (+)-catechin; 5 = (-)-epicatechin. The broken line is the percentage of methanol in the mobile phase.

out the chromatogram. Despite this interference, the major flavanols were sufficiently resolved (Fig. 6) to permit their recognition and measurement. Extracts obtained from seven varieties of malting barley all contained measurable amounts of catechin, prodelphinidin B-3 and procyanidin B-3 (Table II). In contrast, none of these was detected in the mutant barley *ant-13*, which is blocked in the biosynthesis of flavanols³⁴.

Flavanols in hops

Unlike barley, hops contained a preponderance of polymeric material that was not separated sufficiently from the simple flavanols in the prefractionating stage to permit satisfactory HPLC of the flavonoid extract. To separate the simple and polymeric flavanols, the flavonoid extract of hops was fractionated on a column of Sephadex LH-20 eluted with ethanol. During elution with 1–1.5 l of ethanol, both catechin and epicatechin were eluted in a single peak. Flavanol dimers were recovered from a peak that was eluted during the passage of 2.75–3.25 l of ethanol. Four dimeric procyanidins were present, though in different amounts, and these were separated preparatively by chromatography on Sephadex G-25. The identities of the isolated dimers were assigned on the basis of thin-layer and high-performance liquid co-chromatography with authentic samples. The four procyanidin dimers were resolved well by HPLC when mixtures containing approximately equal amounts of each were chromatographed (Fig. 7). In Challenger hops the relative amounts present of the dimers B-1, B-2, B-3 and B-4 were 3:0.5:10:5. Although all these dimers are procyanidins, both delphinidin and cyanidin were detected by HPLC in the hydrolysates of whole hops. Most strikingly the ratio of cyanidin to delphinidin measured depended on the hop variety and varied from 1.2 (Northern Brewer) to 6.2 (Talisman)

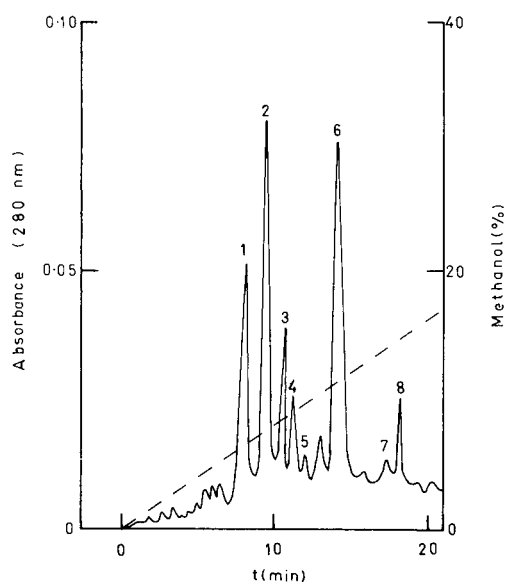


Fig. 6. Separation of flavanol trimers, dimers and monomer from barley by gradient elution on μ Bondapak C_{18} . Peaks: 1, 3, 4, 7 = trimers; 2 = prodelphinidin B-3; 5 = oxidised flavanol; 6 = procyanidin B-3; 8 = catechin. The broken line is the percentage of methanol in the mobile phase.

and averaged 2.5. The source of the delphinidin of hops is possibly the polymeric flavanol fraction. Five flavanols, tentatively identified as trimers, were resolved by HPLC and measured but collectively amounted to only 7.0 mg per 100 g of hops. The B-series procyanidin dimers amounted to 17.0 mg per 100 g of hops, whereas the contents of (–)-epicatechin and (+)-catechin were 19.4 mg and 26 mg, respectively, per 100 g of Challenger hops.

CONCLUSIONS

HPLC in the reversed-phase mode was suitable for the analysis of flavanol glycosides and simple flavanols in barley and hops. Doubtless, the presence in plant extracts of polymeric flavanols, which were not resolved by the column used, complicated otherwise facile separations. Even so, complex mixtures of flavanol oligo-

TABLE II

CONTENTS OF FLAVANOL MONOMER (CATECHIN) AND FLAVANOL DIMERS IN SEVEN VARIETIES OF MALTING BARLEY

Flavanol	Content (mg/kg)	
	Range	Mean
Catechin	30–95	51
Procyanidin B-3	65–350	191
Prodelphinidin B-3	108–450	230

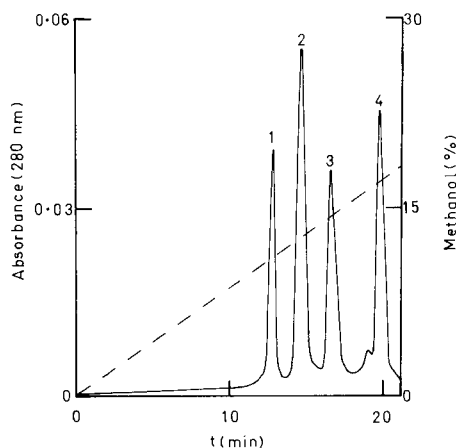


Fig. 7. Separation of procyanidin dimers present in hops by gradient elution on μ Bondapak C_{18} . Peaks: 1 = procyanidin B-3; 2 = procyanidin B-1; 3 = procyanidin B-4; 4 = procyanidin B-2. The broken line is the percentage of methanol in the mobile phase.

mers and flavonol glycosides were separable using gradient elution. The methods described can be used for measuring specific flavonoids in brewing materials as a useful supplement to existing quality controls.

ACKNOWLEDGEMENTS

Thanks are due to the Directors of Arthur Guinness Son & Co. (Dublin) Ltd. for permission to publish this work, to Miss J. M. Delaney, Mr. M. J. Loughrey and Mr. G. P. Hennigan for their technical assistance and to Miss E. de Foubert for preparing the manuscript.

REFERENCES

- 1 J. B. Harborne, *Comparative Biochemistry of the Flavonoids*, Academic Press, London, 1967.
- 2 J. B. Harborne, in E. A. Bell and B. V. Charlwood (Editors), *Secondary Plant Products*, Springer-Verlag, Berlin, Heidelberg, 1980, pp. 329-402.
- 3 J. S. Hough, D. E. Briggs and R. Stevens (Editors), *Malting and Brewing Science*, Chapman and Hall, London, 1971, pp. 599-648.
- 4 G. Harris and R. W. Ricketts, *European Brewing Convention, Proceedings of the Seventh Congress, Rome, 1959*, Elsevier, Amsterdam, pp. 290-301.
- 5 M. Dadic and G. Belleau, *Amer. Soc. Brew. Chem. Proc.*, (1973) 107.
- 6 R. J. Gardner and J. D. McGuinness, *Tech. Quart., Mast. Brew. Assoc. Amer.*, 14 (1977) 250.
- 7 L. W. Wulf and C. W. Nagel, *J. Chromatogr.*, 116 (1976) 271.
- 8 W. A. Court, *J. Chromatogr.*, 130 (1977) 287.
- 9 R. Schuster, *Chromatographia*, 13 (1980) 379.
- 10 A. G. H. Lea, *J. Sci. Food Agric.*, 30 (1979) 833.
- 11 S. Asen, *Hort. Sci.*, 12 (1977) 447.
- 12 R. Galensa and K. Herrmann, *J. Chromatogr.*, 189 (1980) 217.
- 13 S. V. Ting, R. L. Rouseff, M. H. Dougherty and J. A. Attaway, *J. Food Sci.*, 44 (1979) 69.
- 14 G. J. Niemann and J. W. Koerselman-Kooy, *Planta medica*, 31 (1977) 297.
- 15 J. F. Fisher and T. A. Wheaton, *J. Agr. Food Chem.*, 24 (1976) 898.
- 16 G. J. Niemann and J. van Brederode, *J. Chromatogr.*, 152 (1978) 523.

- 17 G. Charalambous, K. J. Bruckner, W. A. Hardwick and A. Linnebach, *Tech. Quart., Mast. Brew. Assoc. Amer.*, 10 (1973) 74.
- 18 W. Kirby and R. E. Wheeler, *J. Inst. Brew.*, 86 (1980) 15.
- 19 A. A. Qureshi, W. C. Burger and N. Prentice, *Amer. Soc. Brew. Chem. J.*, 37 (1979) 161.
- 20 J. Jerumanis, *European Brewers Convention, Proceedings of the 17th Congress, West Berlin, 1979*, European Brewery Convention, Zoetwoude, pp. 309–319.
- 21 P. Mulkay, R. Touillaux and J. Jerumanis, *J. Chromatogr.*, 208 (1981) 419.
- 22 S. R. Udupa and A. V. Patankar, *J. Chromatogr.*, 205 (1981) 470.
- 23 I. McMurrough and J. McDowell, *Anal. Biochem.*, 91 (1978) 92.
- 24 R. S. Thompson, D. Jacques, E. Haslam and R. J. N. Tanner, *J. Chem. Soc., Perkin Trans. I*, (1972) 1387.
- 25 R. Vancraenenbroeck, W. Callewort, H. Gorissen and R. Lontic, *European Brewers Convention, Proceedings of the 12th Congress, Interlaken, 1969*, Elsevier, Amsterdam, pp. 29–43.
- 26 G. Harris, *J. Inst. Brew.*, 62 (1956) 390.
- 27 M. Wilkinson, J. G. Sweeny and G. A. Iacobucci, *J. Chromatogr.*, 132 (1977) 349.
- 28 R. Eastmond, *J. Inst. Brew.*, 80 (1974) 188.
- 29 G. J. Niemann, *J. Chromatogr.*, 74 (1972) 155.
- 30 J. H. Knox and G. Vasvari, *J. Chromatogr.*, 83 (1973) 181.
- 31 G. Vigh and Z. Varga-Puchony, *J. Chromatogr.*, 196 (1980) 1.
- 32 I. McMurrough, *European Brewers Convention, Proceedings of the 17th Congress, West Berlin, 1979*, European Brewery Convention, Zoetwoude, pp. 321–334.
- 33 H. Outtrup and K. Schaumburg, *Carlsberg Res. Commun.*, 46 (1981) 43.
- 34 D. von Wettstein, B. Jende-Strid, B. Ahrenst-Larsen and J. A. Sørensen, *Carlsberg Res. Commun.*, 42 (1977) 341.

CHROM. 14.210

SEPARATION AND DETERMINATION OF SOME ORGANIC ACIDS AND THEIR SODIUM SALTS BY HIGH-PERFORMANCE LIQUID CHROMATOGRAPHY

EERO RAJAKYLÄ

Finnish Sugar Co. Ltd., Research Center, SF-02460 Kantvik (Finland)

SUMMARY

A liquid chromatographic method for the determination of gluconic acid is presented. The method has been used for the determination of gluconic acid and sodium gluconate as well as other acids formed in biochemical or catalytic oxidations of glucose. The acids are separated on a column of cation-exchange resin and eluted with dilute sulphuric acid. The effluent is monitored by an ultraviolet detector at 210 nm. The only pretreatment necessary is filtration of the samples through a membrane in order to prolong column life. Other column materials such as amino and hexyl phases have also been tested. The amino column is suitable for the determination of gluconates. The properties of the hexyl phase column make it especially useful for the separation of citric acid cycle acids.

INTRODUCTION

Gluconic acid as well as its salts and lactones are mild non-corrosive, non-toxic organic compounds. They have important industrial uses primarily due to their ability to form chelates with metal ions in caustic solutions. They are physiologically compatible and can therefore be used in foodstuffs without risk.

The oxidation of carbohydrates has been widely studied, but quantitative and even qualitative analytical data are often lacking^{1–3}. However, some analytical methods for the separation of organic acids have been reported. Many of these are related to the determination of the acids of the citric cycle. Samuelson and co-workers^{4–8} have reported the analysis of aldonic acids by chromatography on a strong basic anion-exchange resin. Recently, other workers^{9–12} have used a high-performance liquid chromatographic (HPLC) procedure which is based on the principle of ion exclusion and partition. Gas chromatography has also been used for the determination of organic acids. However, since most organic acids are not sufficiently volatile, the preparation of suitable volatile derivatives is required. The most frequently used derivatives involve the conversion of carboxyl groups into methyl esters or trimethylsilyl esters and of hydroxyl groups into trimethylsilyl ethers^{12–15}.

In this paper is described a liquid chromatographic procedure which separates gluconic acid from the other acids which are formed in the biochemical conversion of glucose into gluconic acid. This method has also been used for the determination of

arabinonic and formic acids which are formed in the chemical oxidation of glucose in alkaline media.

The method is based on ion exclusion and partition chromatography with UV monitoring of the column effluent at 210 nm. The acids are separated on a column packed with a strong cation-exchange resin (sulphonated polystyrene-divinylbenzene copolymer, H^+) using dilute sulphuric acid as eluent. Some alternative column materials for organic acid analysis are also presented.

EXPERIMENTAL

Apparatus

A Varian 5000 Series liquid chromatograph (Varian Aerograph, Walnut Creek, CA, U.S.A.) was used together with a Perkin-Elmer LC 75 variable-wave-

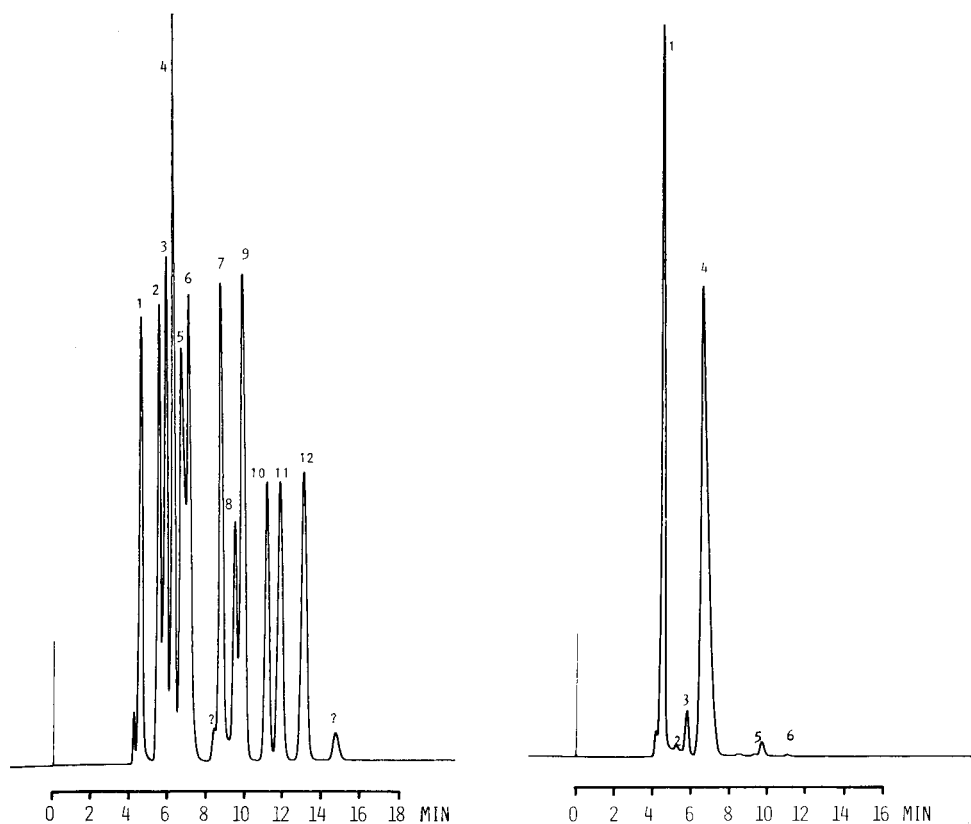


Fig. 1. Separation of standard acid mixture. Chromatographic conditions: column, Aminex HPX-87, 9 μm , 300 \times 7.8 mm I.D., temperature 65°C; UV monitoring at 210 nm, 0.16 absorbance units full scale; eluent, 0.006 $N H_2SO_4$ at flow-rate 0.8 ml/min. Peaks: 1 = oxalic; 2 = maleic; 3 = citric; 4 = tartaric; 5 = gluconic; 6 = malic; 7 = succinic; 8 = lactic; 9 = glutaric; 10 = acetic; 11 = levulinic; 12 = propionic acid.

Fig. 2. Chromatogram of the products formed in biochemical oxidation of D-glucose. Conditions as in Fig. 1. 1 = oxalic; 2 = maleic; 3 = citric; 4 = gluconic; 5 = unknown; 6 = acetic acid.

length spectrophotometric detector (Perkin-Elmer, Norwalk, CT, U.S.A.) and a Goerz Servogor 321 recorder (Goerz Electro, Vienna, Austria). The columns were as follows: self-packed Hamilton HC-X8.00 strong cation-exchange resin column, H^+ (particle size 10–15 μm , 500 \times 9 mm I.D.); Aminex HPX-87 strong cation-exchange resin column, H^+ (particle size 9 μm , 300 \times 7.8 mm I.D.) (Bio-Rad Labs, Richmond, CA, U.S.A.); self-packed Nucleosil 10 NH_2 , particle size 10 μm (250 \times 4.6 mm I.D.) and self-packed Spherisorb hexyl (5 μm , 170 \times 6.2 mm I.D.). The Rheodyne 7125 injector was provided with 20- μl loop (Rheodyne, Cotati, CA, U.S.A.).

Reagents

Dilute sulphuric acid solutions were prepared by making appropriate dilutions of reagent grade sulphuric acid (Läaketehtas Orion, Espoo, Finland) in ultra pure water. Acetonitrile (Art. 30) was obtained from E. Merck (Darmstadt, G.F.R.) and the analytical grade acids (minimum purity 99%) were obtained from Fluka (Buchs, Switzerland), BDH (Poole, Great Britain) and E. Merck.

Liquid chromatographic separation and quantitation

Standards of the acids were prepared individually in ultra pure water and chromatographed separately in order to determine the retention time for each acid. The acids were then chromatographed as a mixture (Fig. 1).

The samples were diluted to about 1 g/100 ml and filtered through a 0.22- μm membrane. This solution was injected into the chromatographic system. Three different columns were used for the analysis of oxidation products of D-glucose. Two of

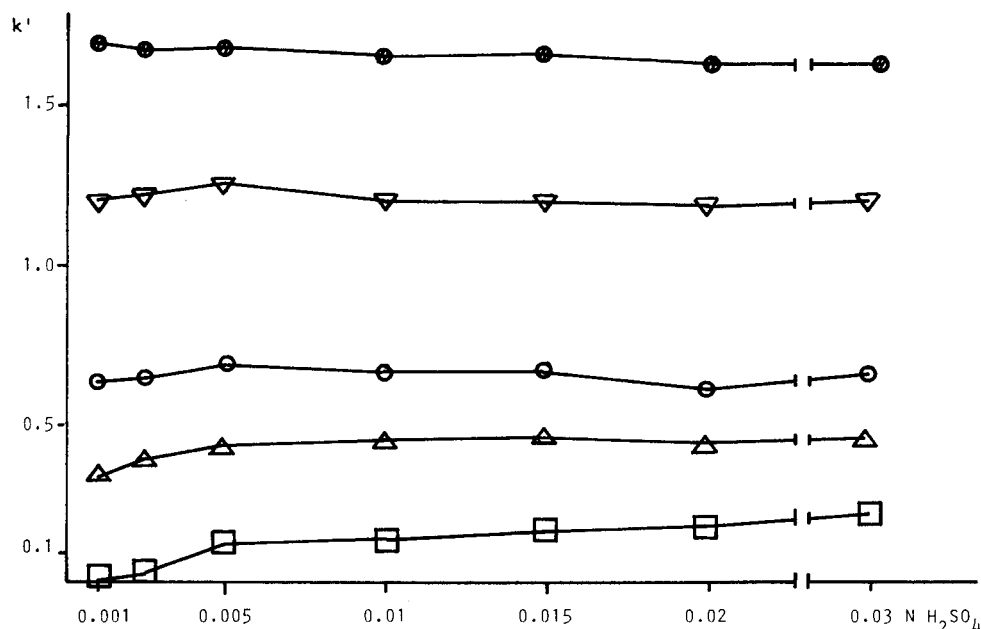


Fig. 3. Effect of sulphuric acid concentration on retention of some organic acids. Column: Aminex HPX-87. Flow-rate: 1.0 ml/min. Temperature: 75 $^{\circ}C$. Acids: \square , oxalic; \triangle , citric; \circ , gluconic; ∇ , glycolic; \bullet , acetic.

these were packed with strong cation-exchange resins (Hamilton HC-X8.00 and Aminex HPX-87, both H^+) and operated at elevated temperatures (338–353°K) using dilute sulphuric acid as eluent at flow-rates of 0.8–1.5 ml/min (see Fig. 2). The amino column (Nucleosil 10 NH_2), with phosphate buffer–acetonitrile (75:25) as eluent at a flow-rate of 2 ml/min, was operated at room temperature.

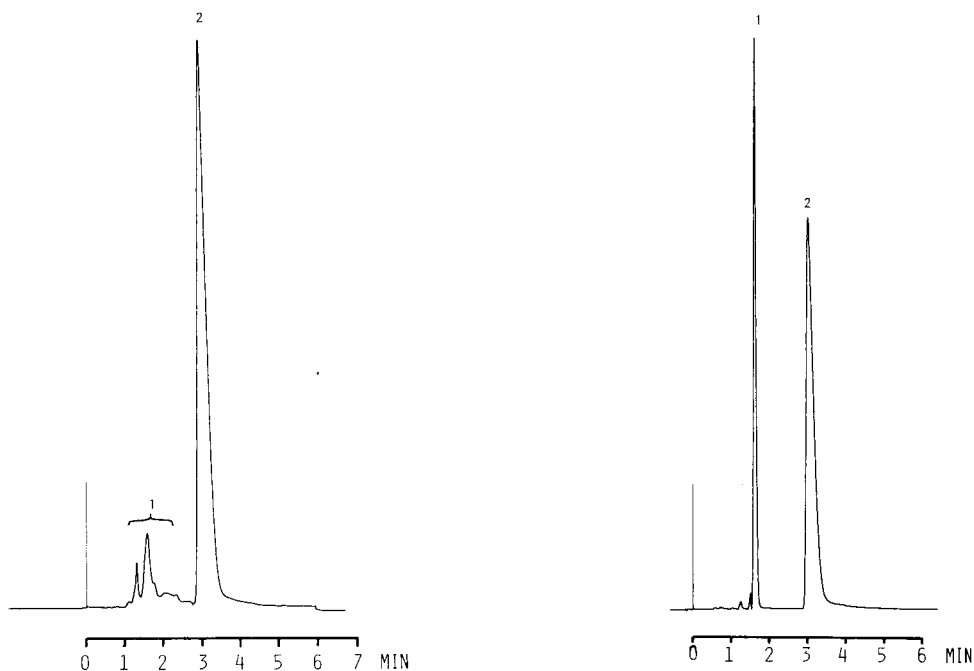


Fig. 4. Determination of sodium gluconate formed in biochemical oxidation of D-glucose. Chromatographic conditions: column, Nucleosil 10 NH_2 , 10 μm , 250 \times 4.6 mm I.D., ambient temperature; eluent, 0.01 M KH_2PO_4 (pH 2.5)–acetonitrile (75:25), flow-rate 2 ml/min; UV detection at 210 nm, 0.16 a.u.f.s. Peaks: 1 = unknowns; 2 = sodium gluconate.

Fig. 5. Separation of glucono delta lactone (1) and gluconic acid (2). Chromatographic conditions as in Fig. 4.

For the separation of organic acids, a hexyl phase column (Spherisorb hexyl) was also tested. The eluent was dilute phosphoric acid at a flow-rate of 1 ml/min.

In all cases the column effluents were monitored by an UV spectrophotometric detector at 210 nm. Peak height measurements with an external standard were used for quantitation.

RESULTS AND DISCUSSION

Effect of eluent concentration on capacity factors of some acids

The concentration of the eluent (sulphuric acid) seems to have only a slight

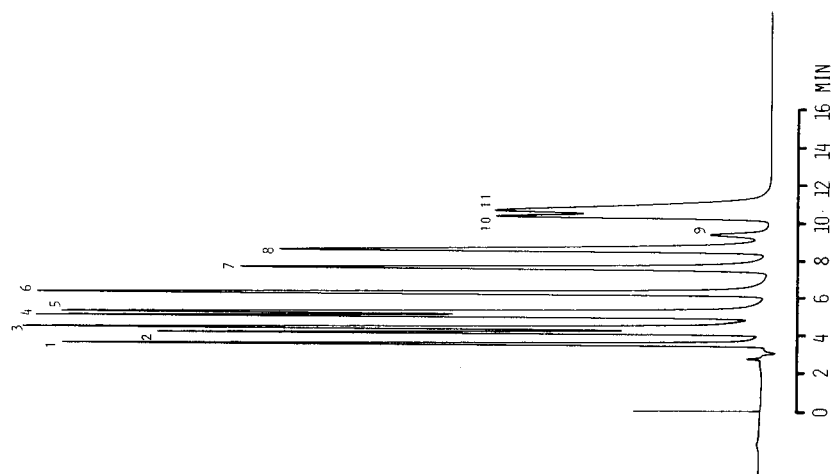


Fig. 6. Separation of standard acid mixture. Chromatographic conditions: column, $5\text{ }\mu\text{m}$ Spherisorb hexyl, $170 \times 6.2\text{ mm}$ I.D., ambient temperature; eluent, 0.01 N H_3PO_4 , flow-rate 1.0 ml/min ; UV detection at 210 nm , 0.16 a.u.s. Peaks: 1 = tartaric; 2 = malic; 3 = maleic; 4 = acetic; 5 = citric; 6 = succinic; 7 = unknown; 8 = propionic; 9 = unknown; 10 = glutaric; 11 = levulinic acid.

Fig. 7. Linearity curve for sodium gluconate. Column: Aminex HPX-87, temperature 65°C . Eluent: 0.015 N H_2SO_4 , flow-rate 1.0 ml/min . Detection: UV at 210 nm .

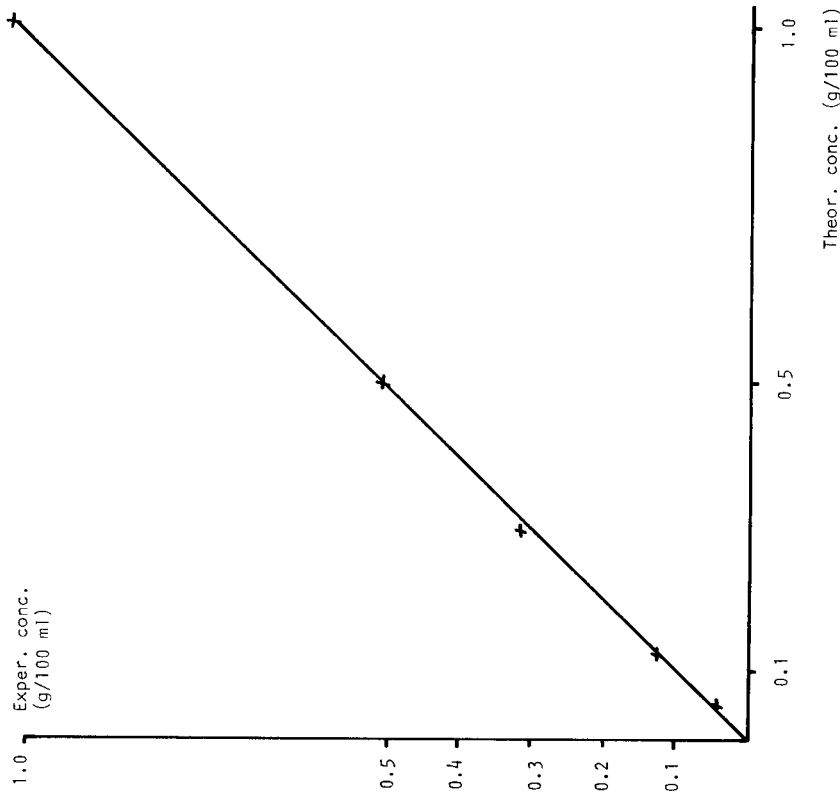


TABLE I

DETERMINATION OF SODIUM GLUCONATE IN FERMENTATION SAMPLES USING THREE DIFFERENT COLUMNS

Sample	Sodium gluconate content (%) on dry substance		
	Aminex HPX-87	Hamilton HC-X8.00	Nucleosil 10 NH ₂
1	94.4	94.0	94.5
2	91.9	91.2	91.5
3	87.2	87.0	86.8
4	92.0	91.8	91.3
5	88.6	88.3	88.3

effect on the retention time of gluconic acid sodium salt (see Fig. 3) on a column of strong cation-exchange resin. The effect of eluent composition on the resolution and retention times of the acids on NH₂ or hexyl columns has not yet been fully investigated (see Figs. 4-5). However, these silica-based materials offer different selectivities from that of styrene-based strong cation-exchange resins.



Fig. 8. Separation of oxygen-oxidation products of D-glucose (alkaline solution). Conditions: column, Hamilton HC-X8.00, 10–15 μ m, 500 \times 9 mm I.D., temperature 80°C; eluent, 0.003 N H₂SO₄, flow-rate 1.5 ml/min; UV detection at 210 nm. Peaks: 1 = oxalic; 2 = unknown; 3 = arabinonic; 4 = ribonic; 5 = glycolic; 6 = formic acid.

Detection limits and linearity

The detectable amount of gluconic acid sodium salt is 0.3–0.5 μg at 210 nm, but 0.1–0.2 μg at 210 nm.

The quantitation and linearity of the method were tested by means of a series of standard sodium gluconate solutions. Glycolic acid was used as internal standard (Fig. 7). The results for three different columns are shown in Table I.

Column life

The Hamilton HC-X8.00 column is very durable. It has been used for routine analysis of sodium gluconate, gluconic acid and arabinonic acid samples for 14 months without any noticeable deterioration of the column performance (see Fig. 8).

ACKNOWLEDGEMENTS

I thank Mrs. Pirkko Vehanen and Miss Merja Paloposki for technical assistance, Ms. Christine Lindqvist for assistance with the presentation and Mrs. Terhikki Elovaara for typewriting.

REFERENCES

- 1 R. H. Blom, V. F. Pfeifer, A. J. Moyer, D. H. Traufler and H. F. Conway, *Ind. Eng. Chem.*, 44 (1952) 435–438.
- 2 K. Heyns and H. Paulsen, *Advan. Carbohydr. Chem.*, 17 (1962) 169–221.
- 3 K. Heyns, H. Paulsen, G. Rudiger and J. Weyer, *Fortschr. Chem. Forsch.*, 11 (1968/1969), 285–374.
- 4 O. Samuelson and L. O. Wallenius, *J. Chromatogr.*, 12 (1963) 236–241.
- 5 U.-B. Larsson, T. Isaksson and O. Samuelson, *Acta Chem. Scand.*, 20 (1966) 1965–1969.
- 6 S. Johnson and O. Samuelson, *Anal. Chim. Acta*, 36 (1966) 1–11.
- 7 B. Carlsson, T. Isaksson and O. Samuelson, *Anal. Chim. Acta*, 43 (1968) 47–52.
- 8 B. Carlsson and O. Samuelson, *Anal. Chim. Acta*, 49 (1970) 247–254.
- 9 J. M. H. Dirkx and L. A. Th. Verhaar, *Carbohydr. Res.*, 73 (1979) 287–292.
- 10 V. M. Turkelson and M. Richards, *Anal. Chem.*, 50 (1978) 1420–1423.
- 11 B. H. Gump and S. A. Kupina, *Liquid Chromatographic Analysis of Food and Beverages*, Honolulu, April 1–6, 1979, Vol. 2, 1979, pp. 331–352.
- 12 N. Alcock, *Methods Enzymol.*, 13 (1969) 397.
- 13 C. E. Dalgleish, E. C. Horning, M. G. Horning, K. L. Knox and K. Yarger, *J. Biochem.*, 101 (1966) 792.
- 14 M. A. Harmon and H. W. Doelle, *J. Chromatogr.*, 42 (1969) 157.
- 15 M. G. Horning, E. A. Boucher, A. M. Muss and E. C. Horning, *Anal. Lett.*, 1 (1968) 713.

CHROM. 14,094

ANALYSIS OF ADDITIVES IN PLASTICS BY HIGH-PERFORMANCE SIZE-EXCLUSION CHROMATOGRAPHY

M. J. SHEPHERD* and J. GILBERT

Ministry of Agriculture, Fisheries and Food, Food Science Laboratories, Haldin House, Old Bank of England Court, Queen Street, Norwich NR2 4SX (Great Britain)

SUMMARY

The application of high-performance size-exclusion chromatography is described for the analysis, in plastics, of low-molecular-weight additives and their decomposition products. The limitation on maximum attainable sensitivity of the method due to sample size has been established by an examination of the relationship between column loading and resolution for a simple additive-polymer mixture. The effects of sample volume and concentration are described in terms of peak broadening, and the results are discussed in relation to mechanisms of solute dispersal. The advantages of this type of approach over other techniques for the analysis of non-volatile yet unstable components of plastics are discussed, and the use of the method is illustrated with examples of studies of the fates of phosphite and epoxidised oil stabilisers in heat-treated poly(vinyl chloride) sheets.

INTRODUCTION

Analysis or identification of low-molecular-weight components in plastics is severely restricted by the polymer matrix. *In situ* spectroscopic methods are sometimes possible¹, but it is usually necessary to perform a preliminary separation of the species of interest. This has commonly been achieved by selective solvent extraction or repeated fractional precipitation. Size-exclusion chromatography (SEC—we have now adopted the ASTM recommended term² in preference to “steric” exclusion chromatography) offers some advantages as an alternative or complement to the traditional methods, both because of the simplicity of SEC and also the possible uncertainties about the efficiency of selective techniques.

SEC has been used widely for the analysis of surface coatings, but its applications to the separation from polymers of small amounts of low-molecular-weight compounds have been limited. We have reported the use of open-column SEC in the analysis of plastics additives³, and residual isocyanates in urethane adhesives have been determined by SEC⁴ and high-performance SEC (HP-SEC)⁵. Styrene has been quantified in copolymers by HP-SEC⁶, and the same authors similarly measured low levels of polychlorinated biphenyls in polystyrene⁷. Other applications of SEC in this area have included the measurement of high levels of plasticiser in polystyrene⁸ and of

oil in extended elastomers⁹, whereas qualitative analysis of additives has been performed by stopped-flow SEC with IR detection¹⁰. Generally, however, only HP-SEC methods permit direct analysis, although the relatively low cost and much higher sample-loading capacity of open-column SEC ensure that this technique will be complementary to, rather than displaced by, HP-SEC.

Our requirement for the analysis of low-molecular-weight compounds in plastics has occurred in the course of work on the possible migration into food of such species from plastic food-packaging materials. Although the major area of concern has been perceived as being due to residual monomers¹¹⁻¹⁴, other constituents of packaging are also potential migrants. These include many of the additives incorporated into packaging for technological reasons of manufacture and use, and also decomposition products of these additives, residues of ingredients from the polymerisation process and oligomers.

Analysis of such specific migrants in food samples poses formidable problems, and consequently our approach has been that of characterising additive transformation products in the plastic, with the intension of subsequently carrying out migration studies on identified compounds, as exemplified by our studies of the poly(vinyl chloride) (PVC)-epoxidised oil stabiliser system¹⁵⁻¹⁷.

In this paper we describe an evaluation of the column-loading capacity of HP-SEC for the analysis of additives, their degradation products and any other low-molecular-weight compounds present in plastics and give some examples of applications of the method.

EXPERIMENTAL

Materials

PLgel HP-SEC columns (30 × 0.77 cm) packed with 10 µm poly(styrene-divinylbenzene) of pore sizes 50, 100 and 500 Å were obtained from Polymer Laboratories Ltd. (Church Stretton, Salop, Great Britain). Sephadex LH-60 and SR100/25 columns were from Pharmacia (Uppsala, Sweden). The 5-µm Techsphere ODS column (25 × 0.42 cm) was from HPLC Technology Ltd. (Macclesfield, Great Britain).

Polystyrene (PS; molecular weight *ca.* 100,000) was from BDH (Poole, Dorset, Great Britain), and PVC base resin "Corvic S57/116", a bottle-blowing grade of weight-average molecular weight between 75,000 and 100,000 with a *K* value of 56-57, from ICI Plastics Division (Welwyn Garden City, Great Britain). Tris(nonylphenyl) phosphite (TNPP, "Phosclere P315") was from Akzo Chemie (Liverpool, Great Britain) and *p*-nonylphenol (NP) from Pfaltz and Bauer (Stamford, CT, U.S.A.); 2-(2-hydroxy-5-methylphenyl)benzotriazole (HMBT, "Tinuvin P") was from Ciba Geigy (Basle, Switzerland); all solvents were of HPLC grade from Rathburn Chemicals Ltd. (Walkerburn, Great Britain). Glyceryl tri-[1-¹⁴C]epoxyoleate (TETO) and its trichlorohydrin were synthesised as before¹⁶. The PVC and polystyrene were reprecipitated from tetrahydrofuran-methanol when required for HP-SEC standard solutions.

Methods

HP-SEC. The chromatographic system consisted of a model 6000A pump

(Waters Assoc.); Rheodyne 7125 or Altex 210 valve injectors, fitted with 20- μ l loops unless otherwise indicated; and a Pye LC-UV detector followed in-line by an Optilab Multiref 902 differential refractometer thermostatically controlled at $30.00 \pm 0.01^\circ\text{C}$ with a Colara WK4 thermocirculator. The following column sets were used:

Set A, $2 \times 100 \text{ \AA}$ PLgel

Set B, 500 \AA , $2 \times 100 \text{ \AA}$, 50 \AA PLgel

All HP-SEC was performed in tetrahydrofuran (THF) medium at a flow-rate of 1.0 ml/min except where otherwise stated.

Column-loading experiments. Column set A was used. Series A injections were made by overfill of a 20- μ l loop. Series B and C injections were made by partial fill of a 100- μ l loop with the exception of injection mode 22, in which the loop was over-filled. The term injection mode is used (with reference to Table I) to describe the particular combination of parameters (sample volume, concentration of PS and loop size) under discussion.

Applications

Phosphite stabiliser analysis. Pressed sheets of PVC incorporating 1.00% of TNPP were prepared in a manner analogous to that reported for epoxidised stabilisers¹⁵; the sheet thickness was 0.08 cm. Sections of these sheets ($5 \times 1 \times 0.08$ cm) were heated in an air-circulating oven at 170°C for various times. The strips were then individually cut into pieces of *ca.* 1 mm², and these pieces were randomised before sampling to prepare 2-ml aliquots of 2% solutions in THF. These solutions were analysed by HP-SEC (column set A) at a flow-rate of 1.5 ml/min. Standard solutions of TNPP and NP contained 2% of precipitated PVC. Linear calibration graphs were obtained for 0–5 μg of NP and 0–10 μg of TNPP in 20- μ l injections.

Epoxide stabiliser analysis. PVC sheets incorporating 2.92% of [$1\text{-}^{14}\text{C}$]-labelled TETO were prepared as before¹⁶, giving material of specific activity 0.864 $\mu\text{Ci/g}$; the sheet thickness was 0.08 cm. Strips ($5 \times 1 \times 0.08$ cm) were heated at 170° in an air-circulating oven for 40 min, then cut into pieces of *ca.* 2 mm² and randomised. A sample of this polymer (0.305 g) was chromatographed in two portions on a Sephadex LH-60 column (74×2.4 cm), with THF as mobile phase, as described previously¹⁶.

The low-molecular-weight fraction from the Sephadex column was evaporated to dryness, the residue was dissolved in 200 μ l of THF, and four 20- μ l aliquots were separated by HP-SEC on column set B. The combined TETO–chlorohydrin fractions were evaporated, the residue was dissolved in 50 μ l of acetonitrile–chloroform (75:25), and 10- μ l samples were chromatographed on a Techsphere ODS column. Elution was with the same solvent mixture delivered from a Waters 6000A pump, and detection was by liquid scintillation counting (Beckman LS-100C) of 250- μ l aliquots collected directly in vials and mixed with 10.0 ml of a solution (4 g/l) of PPO in toluene.

RESULTS AND DISCUSSION

Sensitivity is generally of considerable importance in this area of analysis, and

TABLE I

COLUMN EFFICIENCIES FOR A LOW-MOLECULAR-WEIGHT PLASTICS ADDITIVE WHEN CO-INJECTED WITH POLYSTYRENE

Injection mode No.	Concentration of PS (%)	Volume injected (μ l)	Mass of PS injected (μ g)	Replicate HMBT peak $W_{\frac{1}{2}}$ volumes (ml)	Value of N for HMBT peak (calculated* from average $W_{\frac{1}{2}}$)
<i>Series A injections**</i>					
1	0	20	0	0.37, 0.37	12,400
2	1	20	200	0.38	11,800
3	2	20	400	0.39, 0.40	10,900
4	3	20	600	0.425	9390
5	4	20	800	0.53	6040
6	5	20	1000	0.65, 0.66, 0.645, 0.66, 0.645, 0.66	3980
7	6	20	1200	0.90	2090
<i>Series B injections**</i>					
8	2	20	400	0.39, 0.395	11,000
9	3	20	600	0.495	6920
10	4	20	800	0.55, 0.53	5820
11	5	20	1000	0.61, 0.59, 0.62, 0.59, 0.61	4650
12	6	20	1200	0.60, 0.625	4520
13	2	10	200	0.37	12,400
***	2	20	400	0.39, 0.395	11,000
14	2	30	600	0.455, 0.445	8380
15	2	40	800	0.495, 0.52	6590
16	2	50	1000	0.565, 0.53, 0.55, 0.52, 0.57	5670
17	2	60	1200	0.645, 0.69	3810
18	2	70	1400	0.71, 0.735	3250
<i>Series C injections**</i>					
***	5	20	1000	0.61, 0.59, 0.62, 0.59, 0.61	4650
19	3.33	30	1000	0.59, 0.625	4600
20	2.5	40	1000	0.56, 0.615, 0.60	4850
***	2	50	1000	0.565, 0.53, 0.55, 0.52, 0.57	5670
21	1.33	75	1000	0.445, 0.475, 0.47	7900
22	1	100	1000	0.43, 0.44	8970

* Calculated from the equation $N = 5.54 (L/W_{\frac{1}{2}})^2$.

** See *Methods* for experimental details.

*** These entries duplicated for ease of comparison.

therefore a knowledge of the maximum permissible column loading is essential. Sample size is limited because of peak broadening due to viscosity effects, including viscous fingering^{18,20} and restricted diffusion of the low-molecular-weight solutes. Hence, the relationship between column loading and resolution was investigated by injecting solutions containing both PS and the plastics UV-stabiliser HMBT and

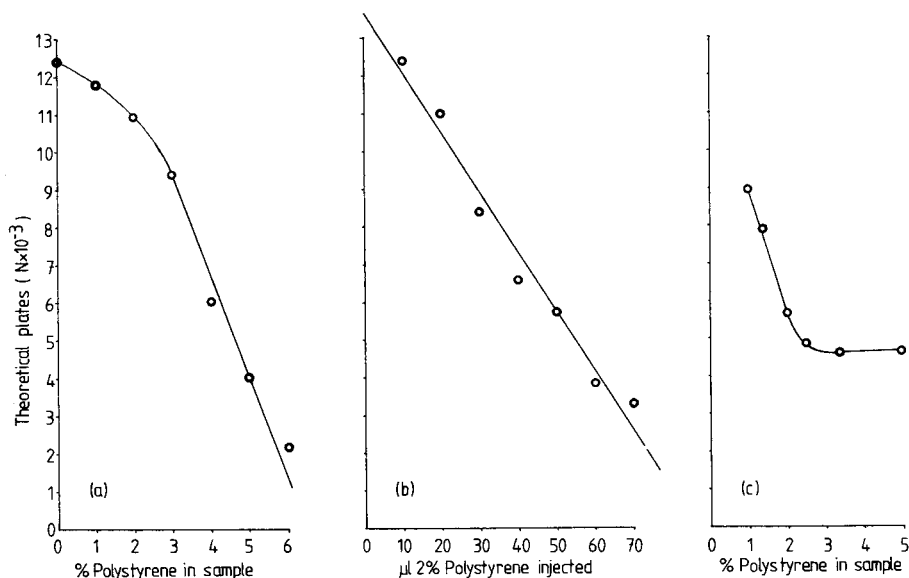


Fig. 1. Effect of sample volume and polymer concentration on chromatographic efficiency of a low-molecular-weight plastics additive when co-injected with polystyrene.

calculating theoretical plate numbers, N , for the additive peak (see *Methods*). The results are given in Table I, and the dependence of N on sample concentration and volume is shown graphically in Fig. 1. This indicates clearly that, when the total mass of injected polymer remains constant, higher efficiency arises from making larger injections of more dilute polymer solutions. This effect is well known in the SEC of polymers²⁰ and indicates that entrainment of low-molecular-weight additives by macromolecules is the major cause of peak broadening. This conclusion is confirmed by the observation that the retention time of the additive peak decreases progressively when the polymer loading is increased (without simultaneously reducing the concentration of the sample), as can be seen from Fig. 2.

The series C injections show that column efficiency was doubled when the same mass of polymer was injected as a 1% solution rather than as a 5% solution. Ultimately, maximum column loadings will be determined by the desired resolution, but for favourable separations 1 mg or more of polymer can be injected. It is of interest to compare injection modes 22 and 2. These indicate that the increase in injection volume from 20 to 100 μ l increases the $W_{1/2}$ value for the peak only by a similar amount. This is the result expected when chromatographing low-molecular-weight solutes by HP-SEC and thus indicates that, in this instance, the polymer is having little or no effect on the chromatography. Therefore, if a column efficiency of, for example, 4000 theoretical plates could be tolerated, which implies a peak half-width of approximately 0.65 ml, injection volumes of up to 300 μ l of a 1% polymer solution might be possible.

A comparison of the results from injection modes 1–7 and 8–12 of Table I indicates that there is little difference in column efficiency between the loop-overfill and loop-part-fill techniques of sample injection. Presumably, at the very highest

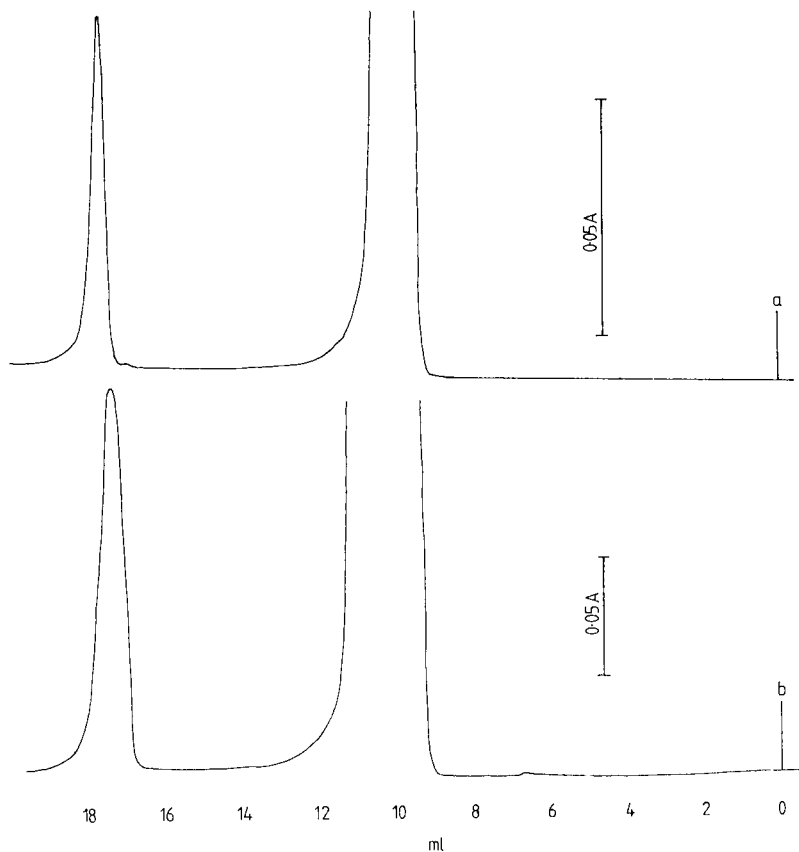


Fig. 2. Typical chromatograms of PS-HMBT mixtures. (a) Injection mode No. 8 (see Table I), UV detection, 0.16 A f.s.d. (b) Injection mode No. 18 (see Table I), UV detection, 0.32 A f.s.d.

polymer concentrations, some mixing is occurring in samples when the latter technique is used. Typical chromatograms from which the data of Table I were calculated are shown in Fig. 2. It can be seen that the major effect of an increase in polymer concentration on the additive peak is to broaden it, leaving the over-all peak profile unaltered. However, the effect of viscous fingering can be seen in the shape of the PS peaks in Fig. 3. Split peaks and other irregular shapes were usual at the higher PS concentrations (3% or more) and were not reproducible. Efficient SEC is dependent on rapid diffusion of solutes, and this too is reduced in viscous samples.

Although axial spreading of samples will occur in the valve loop and valve-column connection, this dispersal mechanism cannot be important. When the column set was removed and 20- μ l samples were injected directly into the detector, the trace width for a 6% PS solution was only 2.5 times that for a HMBT solution containing no PS. Thus, in the absence of additional on-column dispersal effects, the peak half-width for the 6% PS sample would have been no more than 150 μ l greater than that for the sample containing no polymer. As most of the peak broadening occurs on-column and additive-polymer mixtures may be widely separated by correct choice of columns, the results found here will apply to any set of columns (irrespective of their

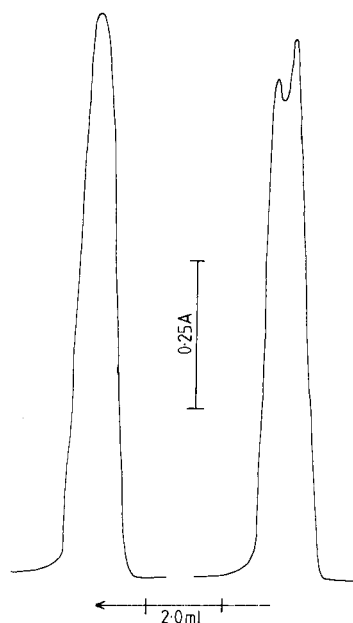


Fig. 3. Replicate PS peak profiles; injection mode No. 4 (see Table I), UV detection, 1.28 Å f.s.d.

number) packed with 10- μ m particles of porous polymer gels. Those with 5- μ m packings will probably perform better, as diffusion distances are shorter and viscous fingering should be reduced.

Hence, it has been shown that HP-SEC can be used to separate low-molecular-weight compounds from relatively large amounts of polymers without serious loss of resolution of the additives. The technique has been in routine use in this laboratory for a number of years, and the following applications illustrate the utility of HP-SEC

TABLE II

DEGRADATION OF TRIS(NONYLPHENYL) PHOSPHITE STABILISER (INCORPORATED IN PVC AT AN INITIAL CONCENTRATION OF 2% w/w) AS MEASURED BY DIRECT HP-SEC ANALYSIS

ND = not detectable (less than 2%).

Sample	Time sheet heated at 170°C (min)	Residual TNPP (%)	NP found as % of initial TNPP	Total TNPP accounted for (%)
Coated base resin	—	82.8	—	82.8+
Pressed sheet	0	39.3	18.9	58.2
Pressed sheet	5	4.1	51.8	55.9
Pressed sheet	10	ND	61.5	61.5
Pressed sheet	15	ND	56.5	56.5
Pressed sheet	20	ND	57.8	57.8
Pressed sheet	25	ND	53.7	53.7
Pressed sheet	30	ND	45.3	45.3

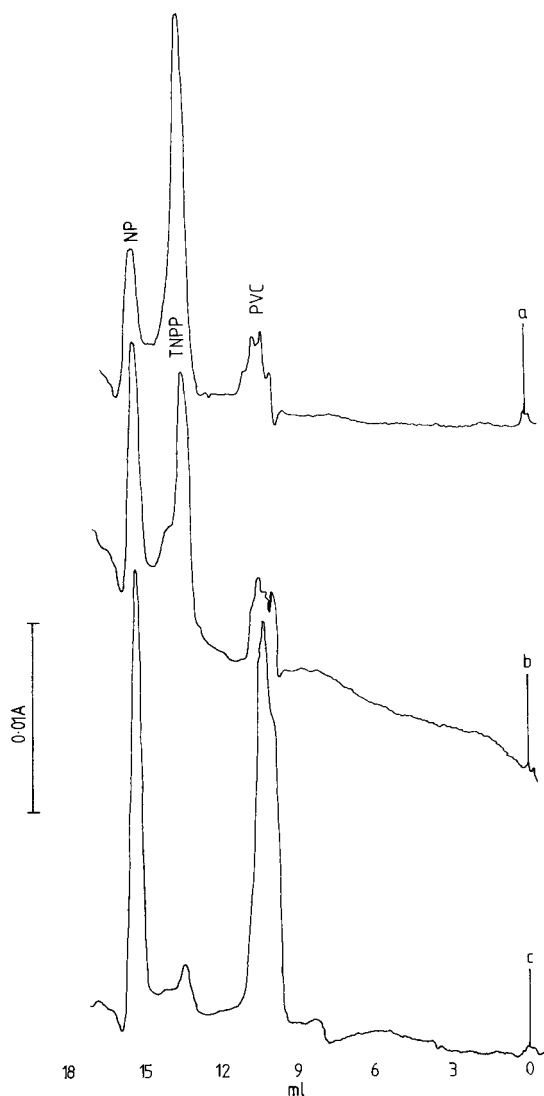


Fig. 4. HP-SEC chromatograms of TNPP-stabilised PVC: (a) Coated base resin powder. (b) Pressed sheet, no additional heat treatment. (c) Pressed sheet after 5 min at 170°C. UV detection, 0.04 A f.s.d. (See *Methods* for experimental details.)

in analysis and also the separation of components for further investigation by other techniques. Although in most instances the molecular-weight information gained has been valuable, it was usually of secondary benefit, the prime use of HP-SEC being as a physical method of separation.

Analysis of phosphite stabilisers

A pre-stabiliser is often added to PVC base resins during manufacture in order

to prevent discolouring of the resin during drying; phosphite esters may be used for this purpose. PVC sheets incorporating 1.0% of a typical stabiliser (TNPP) were analysed for TNPP and its degradation product nonylphenol (NP) after heating at 170° for various times to simulate heat processing during packaging fabrication. HP-SEC was the ideal technique for this analysis, as TNPP is both non-volatile and susceptible to hydrolysis. Thus, a liquid-chromatography method was necessary and it was important that stabiliser residues should be subjected to the minimum of handling. Analysis by HP-SEC required only that the sample be dissolved in THF. The results found are presented in Table II with chromatograms demonstrating progressive loss of TNPP shown in Fig. 4. It can be seen that most of the TNPP was consumed during the 30-sec pressing period and the remainder was lost during the first few minutes of subsequent heat treatment, with consequent formation of chromophores in the polymer (Fig. 4c). However, only about 60% of the additive is accounted for in Table II although there is evidence of partially degraded TNPP in Fig. 4b, which would increase the recovery of additive for the unheated sheet. The chro-

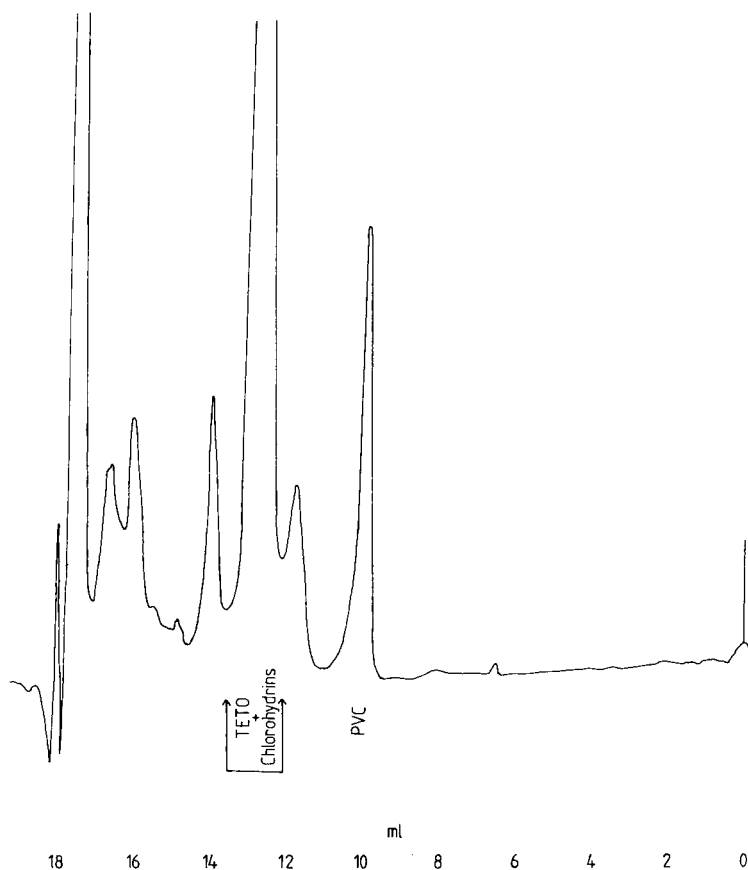


Fig. 5. HP-SEC chromatogram of low-molecular-weight fraction from TETO-stabilised PVC sheet. RI detection, "calibrate" setting. The chlorohydrins + TETO fraction indicated was collected for further analysis (see Fig. 6). (See *Methods* for experimental details.)

matograms in Fig. 4 indicated that no products of significantly lower molecular weight than NP were formed. All peaks later than NP were derived from the solvent. Thus, another advantage of HP-SEC was demonstrated, in that all components of the sample were eluted from the column in a defined time and therefore it can be deduced that the missing stabiliser-degradation products must have been associated with the polymer. The results of Table II were confirmed by both UV and RI studies, and it is unlikely that other products (derived, for example, by benzene ring cleavage) were not detected. However, although the degradation product is described here as NP, derivatives of NP of similar molecular weight would not have been resolved. The suggestion that the additive unaccounted for was lost by binding to the polymer requires confirmation, preferably by radio-tracer experiments.

Analysis of epoxide stabilisers

Epoxidised triglycerides, such as soya bean oil, are frequently used as PVC stabilisers. The use of HP-SEC for the analysis of chlorohydrin transformation products of the model compound glyceryl triepoxyoleate (TETO) has been described¹⁶. An estimate of total chlorohydrins was obtained by dissolving a sample of plastic in THF and derivatising the mixture with a bulky group. The derivatised chlorohydrins were then well separated from all other components of the mixture and, although partly resolved, could be measured as a group¹⁶. A complex mixture of chlorohydrins was expected, with various isomers of mono-, di- and tri-substituted TETO possible.

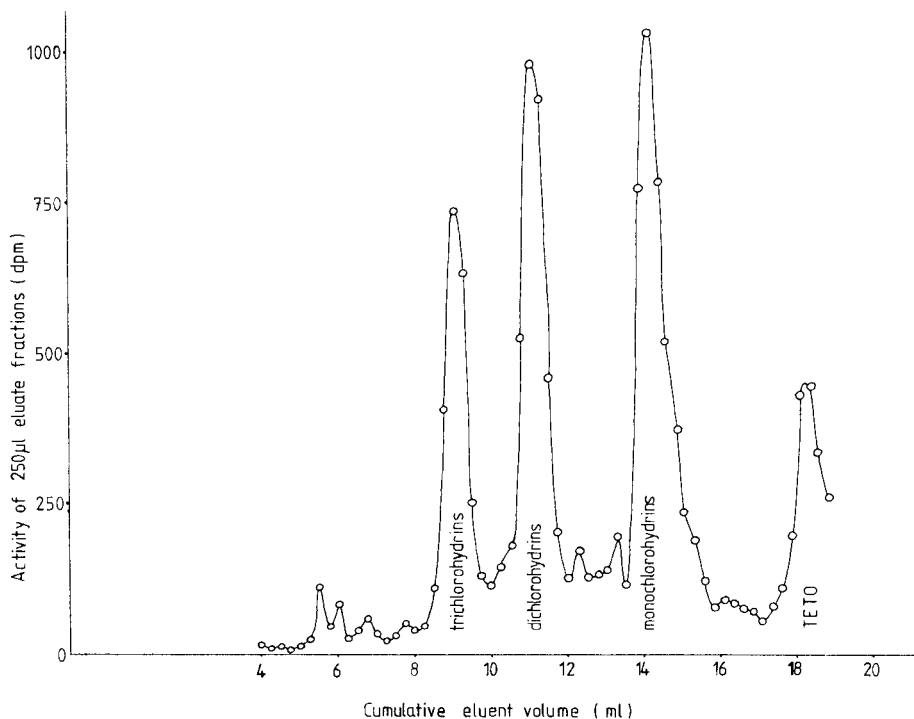


Fig. 6. Reversed-phase HPLC chromatogram of chlorohydrins + TETO fraction (Fig. 5) from TETO-stabilised PVC sheet. Radiochemical detection. (See *Methods* for experimental details.)

With the HP-SEC columns available, these components could not be resolved either from each other or from TETO itself, and recycle HP-SEC yielded only partial separation. Reversed-phase HPLC was suitable for the analysis of chlorohydrin mixtures, but not in the presence of polymer. Thus, SEC was used to separate material for subsequent examination by reversed-phase HPLC. Open-column SEC³ was performed in order to separate the additive and its transformation products from a 300-mg sample of heat-treated PVC stabilised with [1-¹⁴C]-TETO. However, the low-molecular-weight fraction still contained substantial amounts of PVC with molecular weights up to about 2000 (ref. 19). Consequently, HP-SEC was necessary in order to obtain a sample containing essentially only TETO and its derived chlorohydrins, as shown in Fig. 5. The indicated fraction was trapped and analysed by reversed-phase HPLC (see Fig. 6). A combination of chromatographic techniques were used here, but HP-SEC performed an essential function in obtaining a clean sample for reversed-phase HPLC; it is doubtful whether this could have been achieved in any other way.

Analysis of low-molecular-weight compounds in plastics by direct HP-SEC will not be suitable for all applications. Adequate sensitivity will often be a problem, as will the inherently limited resolving power of any SEC technique. Further, solubility limitations (of, for example, polyolefins) can rule out the use of SEC in this area. Nevertheless, for many analyses HP-SEC should be the method of choice because of its unique combination of simplicity and predictability with its additional advantage of generating information about molecular weight.

ACKNOWLEDGEMENTS

The authors wish to express their gratitude to ICI Ltd. (Plastics Division) for the gift of PVC base resin, and to Mr. M. Jumani of Southbank Polytechnic, London, and Mr. J. Bygrave for their assistance with the experimental work.

REFERENCES

- 1 D. A. Wheeler, *Talanta*, 15 (1968) 1315.
- 2 D. D. Bly, *J. Liquid Chromatogr.*, 3 (1980) 465.
- 3 M. J. Shepherd and J. Gilbert, *J. Chromatogr.*, 178 (1979) 435.
- 4 F. Spagnolo and W. M. Malone, *J. Chromatogr. Sci.*, 14 (1976) 52.
- 5 U. Lotz, *Farbe Lack*, 85 (1979) 172.
- 6 J. M. Pacco, A. K. Mukherji and D. L. Evans, *Sep. Sci. Technol.*, 13 (1978) 277.
- 7 J. M. Pacco and A. K. Mukherji, *J. Chromatogr.*, 144 (1977) 113.
- 8 D. F. Alliet and J. M. Pacco, *Sep. Sci.*, 6 (1971) 153.
- 9 R. D. Mate and H. S. Lundstrom, *J. Polym. Sci., C*, 21 (1968) 317.
- 10 F. M. Mirabella, E. M. Barrall and J. F. Johnson, *Polymer*, 17 (1976) 17.
- 11 L. Rossi, J. Waibel and C. G. vom Bruck, *Food Cosmet. Toxicol.*, 18 (1980) 527.
- 12 J. Gilbert and J. R. Startin, *Food Chem.*, (1982) in press.
- 13 J. Gilbert, M. J. Shepherd, J. R. Startin and D. J. McWeeny, *J. Chromatogr.*, 197 (1980) 71.
- 14 J. Gilbert and J. R. Startin, *J. Chromatogr.*, 205 (1981) 434.
- 15 J. Gilbert and J. R. Startin, *Eur. Polym. J.*, 16 (1980) 73.
- 16 M. J. Shepherd and J. Gilbert, *Eur. Polym. J.*, 17 (1981) 285.
- 17 J. Gilbert, M. J. Shepherd, J. R. Startin and J. Eagles, *Chem. Phys. Lipids*, 28 (1981) 61.
- 18 J. C. Moore, *Sep. Sci.*, 5 (1970) 723.
- 19 J. Gilbert, M. J. Shepherd and M. A. Wallwork, *J. Chromatogr.*, 193 (1980) 235.
- 20 J. Janča, *J. Liquid Chromatogr.*, 4 (1981) 181.

CHROM. 14,253

HIGH-PERFORMANCE LIQUID CHROMATOGRAPHIC COLUMN SWITCHING TECHNIQUES FOR RAPID HYDROCARBON GROUP-TYPE SEPARATIONS

THOMAS V. ALFREDSON

Varian Associates, 2700 Mitchell Drive, Walnut Creek, CA 94598 (U.S.A.)

SUMMARY

The application of high-performance liquid chromatographic column switching techniques for hydrocarbon group-type separations of petroleum samples was investigated. Model compounds were employed to study hydrocarbon class separations using normal bonded phase and silica gel columns. The use of a cyanopropyl column as the primary separation step coupled to a highly activated silica gel column as the secondary step allowed resolution of saturates, olefins, aromatics and polars (backflushed from cyanopropyl column). Saturates were further resolved into paraffin and naphthene classes through use of an experimental column packing. The entire operation was automatically controlled by a microprocessor-based liquid chromatograph with time-programmable events which allowed precise switching of high pressure pneumatically operated valves. Column switching techniques were applied to the isocratic analysis of gasolines, light and heavy gas oils and solvent refined coal.

INTRODUCTION

Characterization of natural and synthetic petroleum products has grown increasingly important because of the need to optimize feed stock use and evaluate product performance as a function of chemical composition. The performance and specifications of many petroleum fuels and lubricants are inherently dependent upon the types of hydrocarbons present. Group-type analysis is a widely used procedure for obtaining the information needed to evaluate feedstocks and products in the petroleum industry.

A general method of hydrocarbon group-type analysis is the fluorescent indicator adsorption (FIA) procedure which covers the determination of saturates, non-aromatic olefins and aromatics in petroleum products¹. Limitations of this technique such as time required for analysis (3–4 h), poor precision and the fact that most polar compounds are determined as aromatics have led to development of chromatographic methods for hydrocarbon class analysis. High-performance liquid chromatographic (HPLC) techniques are particularly well suited to group-type analysis due to separation speed and the ability to fingerprint most hydrocarbon classes of interest.

HPLC techniques utilizing normal phase packings have been widely applied to

TABLE I

SELECTED APPLICATIONS OF HPLC TECHNIQUES FOR SEPARATION OF PETROLEUM PRODUCTS

THF = Tetrahydrofuran.

<i>Petroleum sample type</i>	<i>Column type</i>	<i>Mobile phase</i>	<i>Refs.</i>
1. Gasoline and gasoline-range materials (b.p. 60–215°C)	Cyano (10 μm)	<i>n</i> -Hexane	6, 22
	Silica (5 μm)	<i>n</i> -Hexane	6, 22
	Silica (20–44 μm)	2,2,4-Trimethylpentane	2
	Silica (10 μm)	Fluorinert	13
	Silica (10 μm)	<i>n</i> -Heptane	17
	Silica (10 μm)	<i>n</i> -Hexane	18
2. Petroleum fractions (b.p. 190–360°C) and middle distillates	Silica (10 μm)	Hexane	3, 14
3. Heavy petroleum products and crude oils	Silica (10 μm)	<i>n</i> -Hexane	3
	Silica (20–44 μm)	<i>n</i> -Hexane	21
	Amino (10 μm)	<i>n</i> -Hexane	20
	Silica (5 μm)	<i>n</i> -Hexane	20
	Alumina (5 μm)	<i>n</i> -Hexane	20
	PAC (10 μm) (amino and nitrile functional groups)	<i>n</i> -Hexane	20
4. Coal liquefaction products and coal	μ -Styragel (GPC)	THF	15
	Amino (10 μm)	<i>n</i> -Heptane	15
	Phenyl (10 μm)	Water-methanol (1:1)	15
	Silica (10 μm)	<i>n</i> -Hexane	3, 4
	Amino (10 μm)	<i>n</i> -Hexane	19
	Silica (20–44 μm)	<i>n</i> -Hexane	21
5. Light virgin (LVN) and heavy virgin (HVN) naphthas	Silica (10 μm)	<i>n</i> -Heptane	17
6. Residues and distillates of shale oil	Silica (0.1–37 μm)	Cyclohexane	5
	Silica-AgNO ₃ (0.1–37 μm)	Cyclohexane	5
	Silica (20–44 μm)	<i>n</i> -Hexane	21
7. Tar sands	Silica (10 μm)	<i>n</i> -Hexane	4
8. Asphalts	Amino (10 μm)	<i>n</i> -Heptane	16
	μ -Styragel (GPC)	THF	16
9. Lubricant base oils and petroleum products	Alumina	Hexane-methylene chloride	24, 25
	Silica	Hexane	24, 25
	Polystyrene gel	Hexane	24, 25
	Amino	Hexane-methylene chloride	25
	Nitro	Hexane-methylene chloride	25
	Cyano	Hexane-methylene chloride	25

hydrocarbon group-type separations of petroleum samples. Stevenson² demonstrated the viability of HPLC for rapid group-type separations using silica columns coated with 10% Carbowax 600 for petroleum fuel and solvent analysis. Suatoni and Swab³ demonstrated the ability of microparticulate silica columns to separate saturates,

aromatics (backflushed from column) and polar compounds (determined by difference) for quantitative analysis of petroleum samples. Calibration factors for a refractive index detector were used for quantitation of different group types based upon standards isolated from petroleum fractions under investigation. Although detailed coverage of HPLC group-type analytical applications is beyond the scope of this paper, Table I lists a number of selected publications illustrating the use of the technique for analysis of petroleum products.

HPLC switching techniques utilizing normal phase supports have been primarily limited to backflushing techniques or dual column techniques. Dark *et al.*⁴ employed a backflushing technique for the analysis of polar hydrocarbons using an amino bonded phase column. McKay and Latham⁵ have used a dual column technique employing a silica column and silver impregnated silica column in series for the separation of olefins from saturates in shale oil samples. Recently, a column switching technique employing three columns (silica, cyano and silica impregnated with AgNO₃) has been developed by Apffel *et al.*⁶ for separation of saturate, olefin, aromatic and polar hydrocarbon classes in gasoline. Katz and Ogan⁷ have reported a coupled column technique utilizing a reverse phase column and a size exclusion column for sample preparation of petroleum and coal liquid samples for the separation of polynuclear aromatic hydrocarbons (PAHs).

The purpose of this work is two-fold: To investigate a variety of normal phase supports in terms of their utility for hydrocarbon group-type separations and to develop column switching methods employing these supports for rapid hydrocarbon class separations of petroleum samples.

EXPERIMENTAL

Instrumentation and columns

Fig. 1 is a schematic diagram of the multidimensional column switching system employed. This system is similar to one utilized for column switching techniques involving the cleanup and analysis of water-soluble samples previously reported from this laboratory⁸. The chromatograph is a Varian Model 5060, which has a single pump with three-solvent capability. It was equipped with a manual six-port sampling valve (Rheodyne) for injection of the sample onto the first analytical column (MicroPak CN-5 in all cases). In addition, two other six-port, two-position automatic

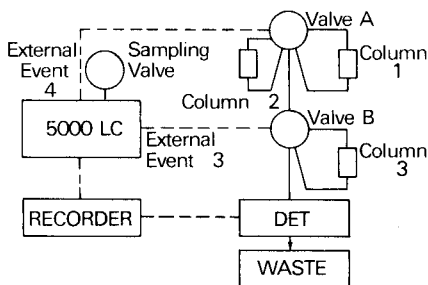


Fig. 1. System configuration for automated column switching using Model 5000 LC external events. DET = Detector.

switching valves (Valco) were employed. All valves could be controlled by time-programmable external events (powered contact closures) from the chromatograph. They could be automatically switched either off or on at predetermined times by single keyboard programming.

Microparticulate supports investigated in the normal phase mode were a MicroPak TSK 2000SW (250-Å diol-like bonded phase), MicroPak CN-5 (cyanopropyl bonded phase), MicroPak NH₂-5 (aminopropyl bonded phase), MicroPak AX-5 (diamino bonded phase), MicroPak Si-5 (60-Å porous silica) and an experimental support investigated for the separation of saturated hydrocarbon classes. All columns were 15 cm × 4 mm I.D. except the TSK 2000SW column (30 cm × 8 mm I.D.). Such short columns employing small d_p (d_p = particle diameter) packings (5 μ m) have been shown to be of high utility for rapid (<15 min) LC separations⁹. All of these columns are available from Varian Assoc. (Walnut Creek, CA, U.S.A.).

A Varian UV-50 variable wavelength detector and a Varian refractive index detector were employed.

Valving configurations

By appropriate configurations of the switching valves, a number of flow options were available. Fig. 2 depicts the normal configuration employing two switching valves. Such a configuration allows a variety of hydrocarbon group-type separations to be carried out with no plumbing changes. By using external events 3 and 4 from the Model 5000, valve A or valve B can be switched at different times in order to achieve different flow paths. The heavy lines represent the flow path for the normal configuration at time zero. In all cases, a MicroPak CN-5 column was employed as column 1, a MicroPak Si-5 column activated at 130–150°C overnight as column 2 and an experimental column packing as column 3 in the switching routines.

Solvents and chemicals

n-Hexane was distilled-in-glass solvent obtained from Burdick & Jackson

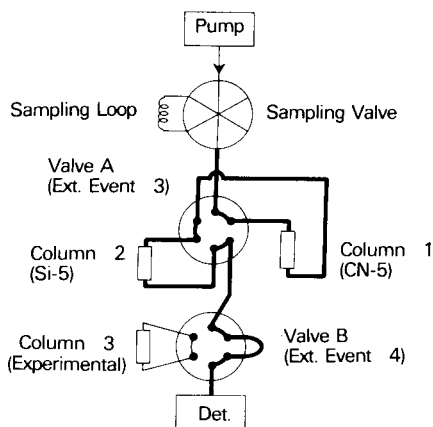


Fig. 2. Column switching flow diagram: normal flow path. Note that solid black line indicates path of flow. Det. = Detector; Ext. = external.

TABLE II
MODEL COMPOUNDS FOR COLUMN SELECTIVITY STUDY

<i>Saturates</i>		<i>Olefins</i>	
<i>Paraffins (I)</i>	<i>Naphthenes (Ia)</i>	<i>Monoolefins (II)</i>	<i>Diolefins (IIa)</i>
<i>n</i> -Heptane	Cyclohexane	2,4,4-Trimethyl-1-pentene	2-Methyl-1-butadiene
<i>n</i> -Octane	Methylcyclohexane	2,4,4-Trimethyl-2-pentene	2,2-Dimethyl-3,4-pentadiene
<i>n</i> -Nonane	1,1-Dimethylcyclohexane	1-Nonene	2,5-Dimethyl-2,4-hexadiene
<i>n</i> -Decane	1,3-Dimethylcyclohexane	4-Nonane	1,3-Cyclooctadiene
<i>n</i> -Undecane	Cyclooctane	3,5,5-Trimethyl-1-hexene	
<i>n</i> -Dodecane		1-Decene	
<i>n</i> -Tridecane		1-Undecene	
<i>n</i> -Tetradecane		1-Dodecene	
<i>n</i> -Pentadecane		1-Tridecene	
<i>n</i> -Hexadecane		1-Tetradecene	
<i>n</i> -Heptadecane		Cyclohexene	
<i>n</i> -Octadecane			
<i>n</i> -Nonadecane			
<i>Aromatics</i>		<i>Polars (V)</i>	
<i>Alkylbenzenes (III)</i>	<i>Polynuclear aromatic hydrocarbons (PAHs) (IV)</i>		
Benzene (B)	Naphthalene (NAP)	Methyl benzoate	
Toluene (T)	Anthracene (ANTHRA)	Phenol	
Ethylbenzene	Chrysene (CHY)	Chlorophenol	
<i>o</i> - <i>m</i> - <i>p</i> -Xylenes	Benzo[<i>a</i>]pyrene (B α P)	Nitrophenol	
Cumene	Benzo[<i>ghi</i>]perylene (BghiP)		
<i>n</i> -Propylbenzene	Acenaphthalene		
Mesitylene	Phenanthrene		
<i>p</i> -Cymene	Pyrene		
<i>n</i> -Butylbenzene	Benzo[<i>e</i>]pyrene		
<i>n</i> -Hexylbenzene	Benzo[<i>k</i>]fluoranthene		
<i>n</i> -Octylbenzene	Perylene		
<i>n</i> -Decylbenzene			

Labs. (Muskegon, MI, U.S.A.). The solvent was dried using a 4-Å molecular sieve to remove trace amounts of water. A drying column (Alltech Associates, Los Altos, CA, U.S.A.) was installed prior to the sampling valve to ensure removal of trace water from the mobile phase.

Samples of hydrocarbon standards used in this report were obtained from Varian (Palo Alto, CA, U.S.A.), Aldrich (Milwaukee, WI, U.S.A.) and Polysciences Inc. (Warrington, PA, U.S.A.). Hydrocarbon standards chosen as model compounds for paraffins (class I), naphthenes (class Ia), monoolefins (class II), diolefins (class IIa), aromatics (alkylbenzenes, class III), polynuclear aromatic hydrocarbons (PAHs, class IV) and polar (class V) hydrocarbon group-types are listed in Table II.

Samples of light and heavy gas oils were obtained from local refineries. The sample of AMAX solvent refined coal (SRC) was obtained from experimental studies

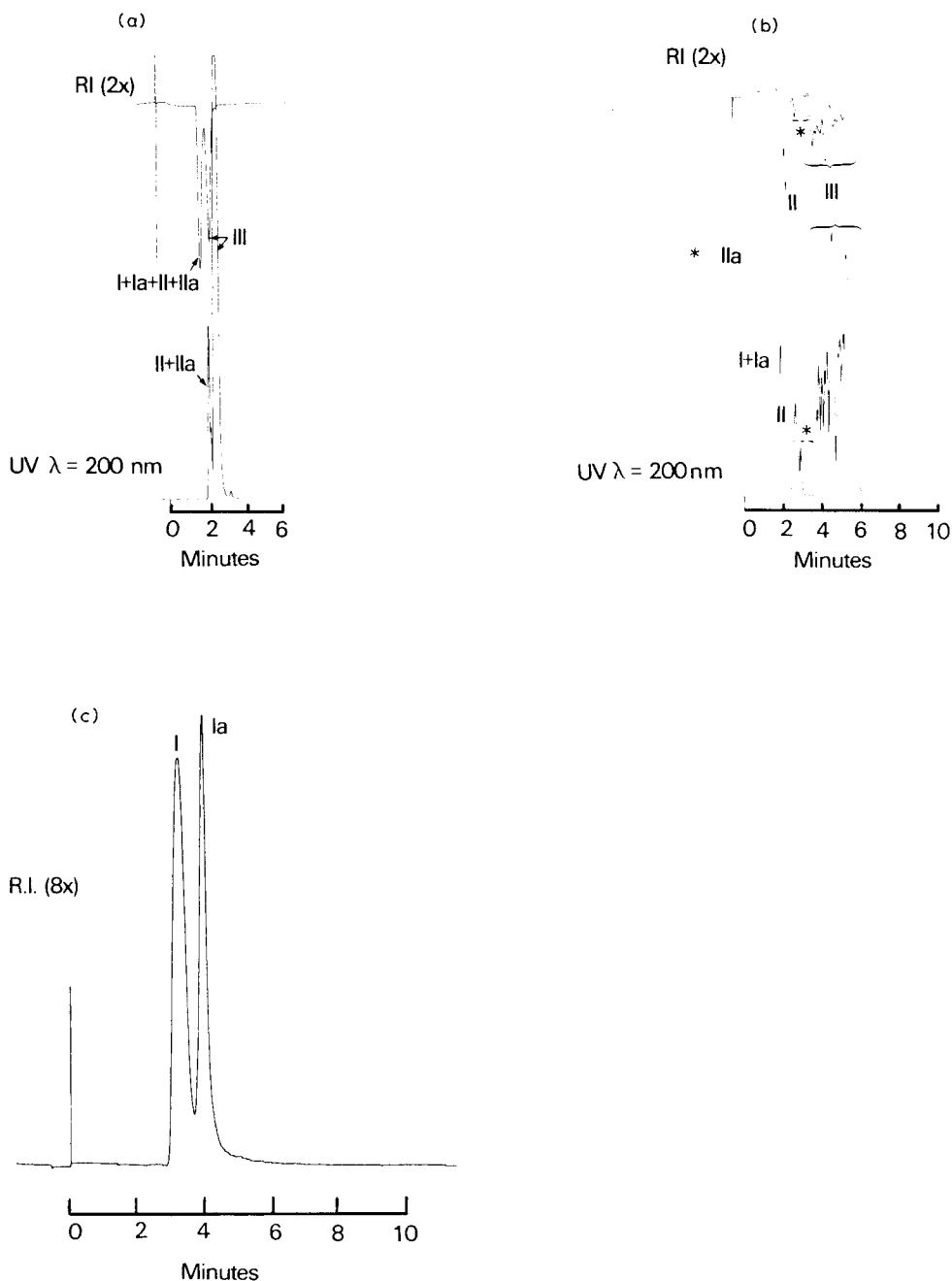


Fig. 3. Selectivity of normal-phase packings for various hydrocarbon classes: saturates-paraffins (class I), plus naphthenes (class Ia), mono- and diolefins (classes II and IIa) and aromatics (class III, alkylbenzenes). a, MicroPak CN-5 column; b, MicroPak Si-5 column; c, experimental column; all columns 15 cm \times 4 mm. Conditions: mobile phase, dry *n*-hexane at 0.7 ml/min. Detectors: UV at 200 nm (1.0 a.u.f.s.) and RI (2 \times) except c (8 \times).

conducted at Virginia Polytechnic Institute (Blacksburg, VA, U.S.A.). Gasoline samples were commercial samples purchased locally.

Preparation of samples

All samples were dissolved in hot *n*-hexane, allowed to cool and filtered through an 0.45- μ m membrane filter prior to injection. Asphaltene components are not soluble in hexane and thus were not chromatographically analyzed but could be determined by weighing. The SRC sample was prepared at a concentration of 50:1 in hexane and diluted to an appropriate level for chromatography. Samples of light and heavy gas oil were prepared at an 0.2% (w/w) level and subsequently diluted. Gasoline samples were 0.1% (w/w) and further diluted. Standard samples were dissolved in *n*-hexane at a level of 1 mg/ml and diluted at the appropriate concentration and then chromatographed.

Chromatography

The basic chromatographic procedures were carried out in a similar manner. The filtered sample was injected manually onto the analytical column and isocratically chromatographed using the Model 5060 pump. A mobile phase of dry *n*-hexane was used in all cases. Injection volume was held at 10 μ l and sample concentrations varied. Detection was performed at a wavelength of 200 nm with a UV detector. At this wavelength, mono- and diolefins can be detected as well as aromatics and PAHs. For investigation of PAH separations using model compounds, a wavelength of 254 nm was employed. A refractive index (RI) detector was also used in series with the UV detector.

RESULTS

Investigation of column support selectivity for hydrocarbon classes

Separation of saturate, olefin and aromatic (alkylbenzene) hydrocarbon group-types was studied using several column packings in the normal phase mode. Mixtures of the model compounds were prepared and chromatographed using dry *n*-hexane as eluent at a flow-rate of 0.7 ml/min. Detection was accomplished by use of a UV detector at 200 nm and a refractive index detector. MicroPak CN-5, NH₂-5 and AX-5 columns separated aromatics from other hydrocarbon classes (saturates plus olefins) which coelute. Fig. 3a shows the analysis of these hydrocarbon classes on a CN-5 column. Model compound classes I and II (saturates and olefins) coelute. Model class III (alkylbenzenes) are resolved from the other classes. Using hexane as the mobile phase, polar hydrocarbon compounds elute very slowly and can be backflushed off the column after elution of the aromatics. Separation of saturate, olefin and aromatic group-types was achieved with a MicroPak Si-5 column, as shown in Fig. 3b. Activated silica gel offers a high degree of resolution among aromatics as modeled by alkylbenzenes (class III). Separation of monoolefins (class II) and diolefins (class IIa) was also achieved; however, incomplete resolution was obtained between saturate (class I) and monoolefin model compounds. Resolution of these classes could be improved by further activation of the silica packing but at the expense of total analysis time for elution of the aromatic envelope.

In the analysis of gasoline-range petroleum products, information is required

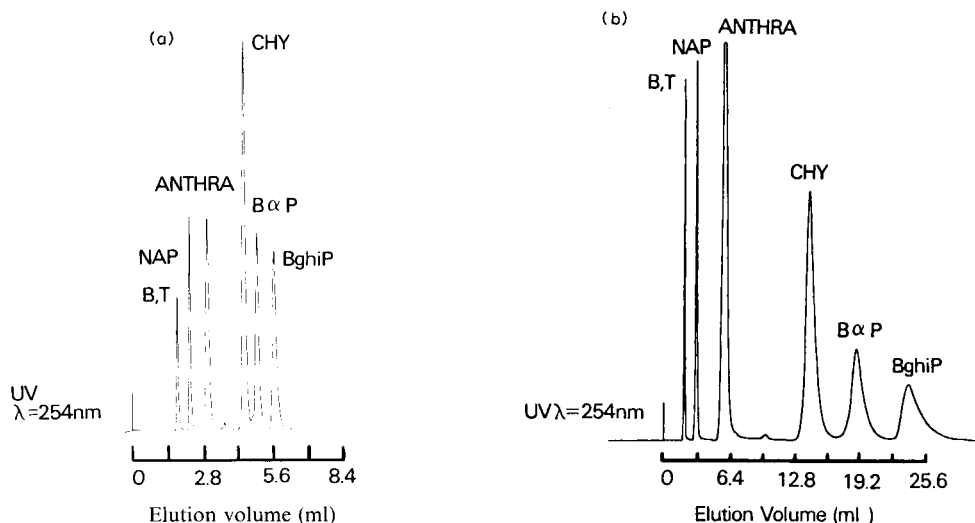


Fig. 4. Selectivity of normal phase packings for polynuclear aromatic hydrocarbons (PAHs). a, MicroPak CN-5 column; b, MicroPak NH₂-5 column; both columns 15 cm \times 4 mm. Conditions: mobile phase, dry *n*-hexane at 0.7 ml/min (a) and 1.6 ml/min (b). Detector: UV at 254 nm (0.5 a.u.f.s.). Model compounds: B = benzene; T = toluene; NAP = naphthalene; ANTHRA = anthracene; CHY = chrysene; B α P = benzo[a]pyrene; BghiP = benzo[ghi]perylene.

on both paraffin and naphthene (cycloalkane) saturated hydrocarbon classes. Selectivity to saturated hydrocarbon classes was achieved through the use of an experimental support, as shown in Fig. 3c. Using an experimental column with an eluent of dry hexane, paraffins (class I) elute first, followed by the naphthenes (class Ia). The compounds used to model the paraffin class contained only normal hydrocarbons. The effect of branching on saturate class resolution is currently under study. The support material is of a proprietary nature.

Several polar bonded phase and silica gel columns used in the normal phase mode were examined for separation of polynuclear aromatic hydrocarbons (PAHs). A mobile phase of dry *n*-hexane was used in conjunction with a UV detector at 254 nm for analysis of PAH model compounds. Capacity increased with condensed ring number of the PAH compound for MicroPak TSK 2000SW, CN-5, NH₂-5 and AX-5 columns with the most polar bonded phase (AX) displaying highest retention volume and the least polar bonded phase (SW) displaying lowest retention volume. Separation of model PAH compounds on MicroPak CN-5 and NH₂-5 columns is displayed in Fig. 4a and 4b respectively. These chromatograms illustrate the increase in retention of PAHs obtained with the NH₂-5 packing (high polarity) compared to the retention obtained with the CN-5 packing (medium polarity).

Fig. 5 displays a graph of capacity ratios (k') versus number of rings in the PAH model compounds. Such a graph serves as a summary of results from investigation of normal phase packings for PAH separations. Capacity appears to be a function of bonded phase polarity (diol-like SW giving lowest capacity and NH₂-5 and AX-5 greatest capacity). The poor resolution shown between chrysene and pyrene (four rings), benzo[a]pyrene and benzo[e]pyrene (five rings) and benzo[ghi]perylene (six rings) for the Si-5 column is due in part to the fact that benzo[a]pyrene,

benzo[*e*]pyrene, pyrene and benzo[*ghi*]perylene are pericondensed PAHs while benzene, naphthalene, anthracene, phenanthrene and chrysene are catacondensed. Popl *et al.*¹⁰ have found silica gel employing a paraffinic eluent to give lower adsorptivity to pericondensed aromatic hydrocarbons.

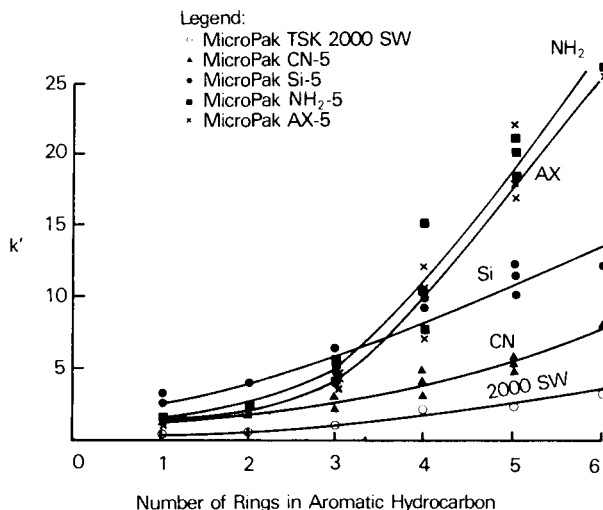


Fig. 5. Plot of PAH ring number versus capacity ratio (k') for MicroPak TSK 2000SW, CN-5, Si-5, NH₂-5 and AX-5 columns. Mobile phase: dry *n*-hexane.

The difference between the Si-5 and the NH₂-5 and AX-5 bonded phases (all polar stationary phases) displayed on the graph may be partly explained by the lower adsorptivity of the silica gel to pericondensed PAHs and may also partly arise from differences between the adsorption (silica) and partitioning (NH₂ and AX bonded phases) separation processes. Additionally, the level of activation of the silica gel column has a significant effect upon PAH capacity.

Column switching techniques for hydrocarbon class separations

Three normal phase column supports were chosen for incorporation into column switching schemes for hydrocarbon group-type separations. A MicroPak CN-5 column was chosen as column 1 (see Fig. 2) due to superior chemical stability compared to normal phase supports which contain primary amine functional groups such as the NH₂-5 column. Due to their reactivity with primary amine groups, aldehyde and ketone solutes should be avoided with an NH₂ bonded phase, thus limiting the utility of such supports¹¹. The CN-5 column is placed as the primary column to ensure that polar compounds are trapped on this packing (and subsequently backflushed) and not irreversibly adsorbed on the silica column¹² which was chosen as column 2 in the switching scheme.

Utilizing a single switching valve with a MicroPak CN-5 and Si-5 column in series, saturate, olefin and aromatic hydrocarbon classes were resolved. This is illustrated by the analysis of hydrocarbon model compounds as shown in Fig. 6a. An eluent of dry hexane at a flow-rate of 0.7 ml/min was used for analysis with a UV detector at 200 nm and RI detector in series. Saturates (classes I and Ia) elute first,

followed by monoolefine (class II), diolefins (class IIa) and aromatics (class III). Polars can be subsequently backflushed from the CN-5 column (column 1) by appropriate valve actuation after elution of the aromatics. Note that when column 1 is backflushed, column 2 is isolated from the flow path to preserve the integrity of the activated silica column (see Fig. 2).

Selectivity to saturates displayed by the experimental column packing was utilized in the present switching scheme by addition of a second switching valve. The employment of such a column in the switching technique allows separation of paraffin (class I), olefin (classes II and IIa), naphthene (class Ia) and aromatic hydrocarbon classes (P.O.N.A. separations) as depicted in Fig. 6b using hydrocarbon standards. Chromatographic conditions were identical to those used in Fig. 6a.

To obtain such a separation, saturates were loaded onto the head of the experimental column, at which time (corresponding to an elution volume of 4.5 ml—the point at which the olefins begin to elute) valve B is actuated (first switching point in Fig. 6b) so that elution of olefins (classes II and IIa) and aromatics (class III) occurs from the CN-5 and Si-5 columns (columns 1 and 2) in series. After elution of the aromatics, valves A and B were again actuated (second switching point in Fig. 6b) to allow elution of paraffins (class I) and naphthenes (class Ia) from the experimental column (column 3). Since saturate and olefinic classes were not totally resolved (see Fig. 6a), olefins which coelute with the saturates are detected as saturates in the elution profile of column 3.

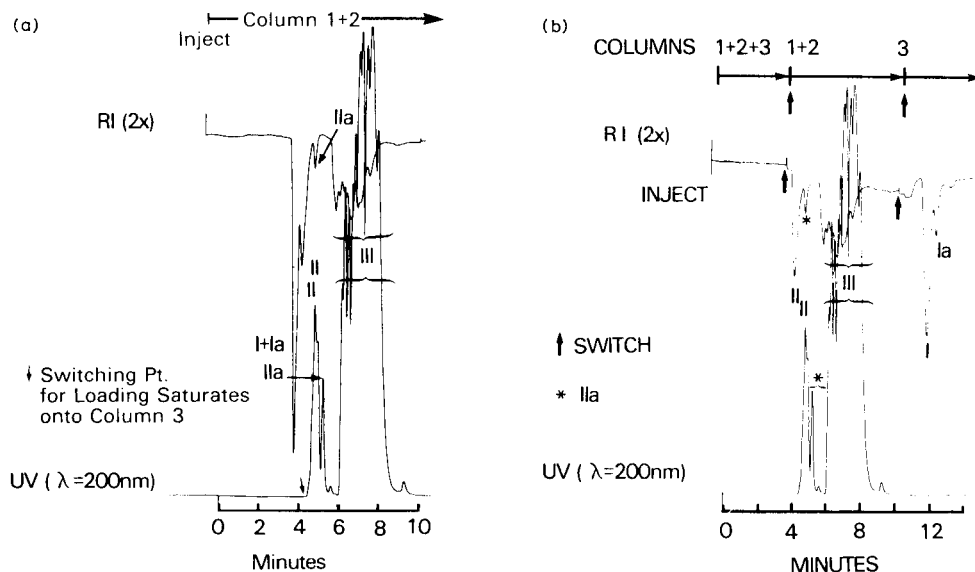


Fig. 6. Column switching scheme separations using two columns and one switching valve (a) and three columns and two switching valves (b) to obtain hydrocarbon group-type separations. a, Columns: MicroPak CN-5 (1); MicroPak Si-5 (2); both 15 cm × 4 mm. Mobile phase: dry-*n*-hexane at 0.7 ml/min. Detectors: UV at 200 nm (1.0 a.u.f.s) and RI (2×). Model compounds: I = paraffins; Ia = naphthenes; II = monoolefins; IIa = diolefins; III = aromatics (alkylbenzenes). Note that point for switching saturates onto head of column 3 corresponds to point at which olefins begin to elute (4.5 ml). b, Columns: MicroPak CN-5 (1); MicroPak Si-5 (2); experimental column (3); all columns 15 cm × 4 mm. Conditions as in a. Note first switching point for loading saturates onto head of column 3 and second switching point for analysis of saturate classes.

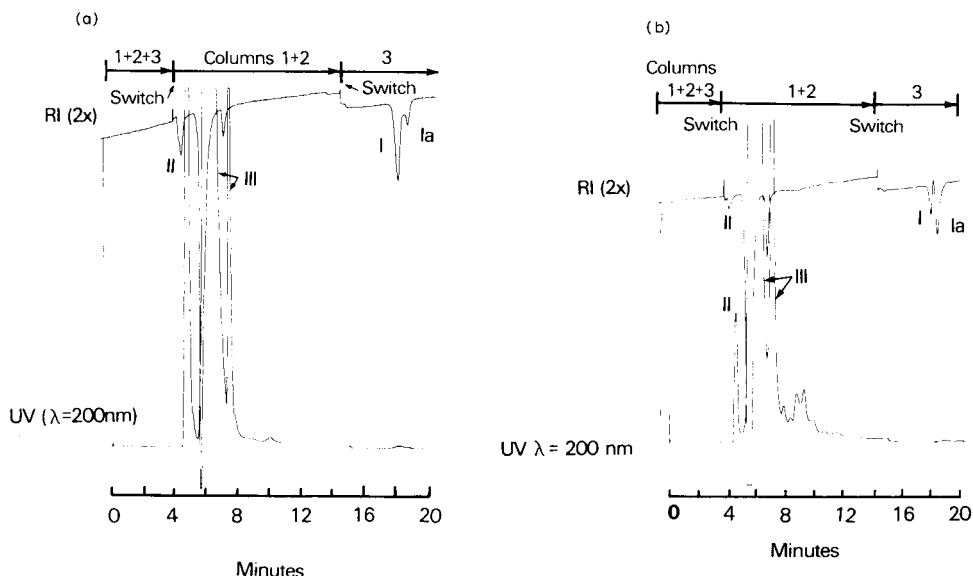


Fig. 7. P.O.N.A. type separations of gasoline samples (a, b). Columns: MicroPak CN-5 (1); MicroPak Si-5 (2); experimental column (3); all columns 15 cm \times 4 mm. Mobile phase: dry *n*-hexane at 0.7 ml/min. Detectors: UV at 200 nm (1.0 a.u.f.s) and RI (2 \times). I = Paraffins; Ia = naphthenes; II = olefins; III = aromatics.

Applications of column switching to hydrocarbon class separations of petroleum samples

P.O.N.A. type separations achieved by column switching methods have been applied to the analysis of gasoline samples as shown in Fig. 7a and 7b. Isocratic analyses of the gasoline samples employed dry *n*-hexane as a mobile phase at 0.7 ml/min flow. Both UV at 200 nm and RI detection were used for analysis of olefins (class II), aromatics (class III), paraffins (class I) and naphthenes (class Ia) in the gasoline samples. Sample B (Fig. 7b) appears to contain some paraffinic constituents with a refractive index less than hexane as evidenced by a slight negative response prior to elution of the naphthenes. In comparing the two gasoline samples, differences not only in naphthene content but also olefin and aromatic class content is apparent.

Hydrocarbon group-type separations were also performed on samples of light and heavy gas oils as shown in Fig. 8a and 8b respectively. Both MicroPak CN-5 and Si-5 columns were used with a *n*-hexane mobile phase for analysis of the gas oils. UV detection at 200 nm and RI detection were employed for separation of saturates (I), olefins (II), aromatics (alkylbenzenes, III), PAHs (IV) and polars (V) which were backflushed from the CN-5 column. Good resolution is obtained among the aromatic components of the light gas oil sample using a MicroPak CN-5 and Si-5 column in series. However, in comparing the light gas oil to heavy gas oil analysis, there is an apparent loss in resolution with the heavier sample. The loss in resolution with heavier petroleum samples seems to be a common characteristic with such samples as, for example, in the analysis of crude oils. Fig. 9 depicts the analysis of a solvent refined coal (SRC) sample for saturate, olefin, aromatic and polar hydrocarbon classes. MicroPak CN-5 plus Si-5 columns were used in series for this analysis.

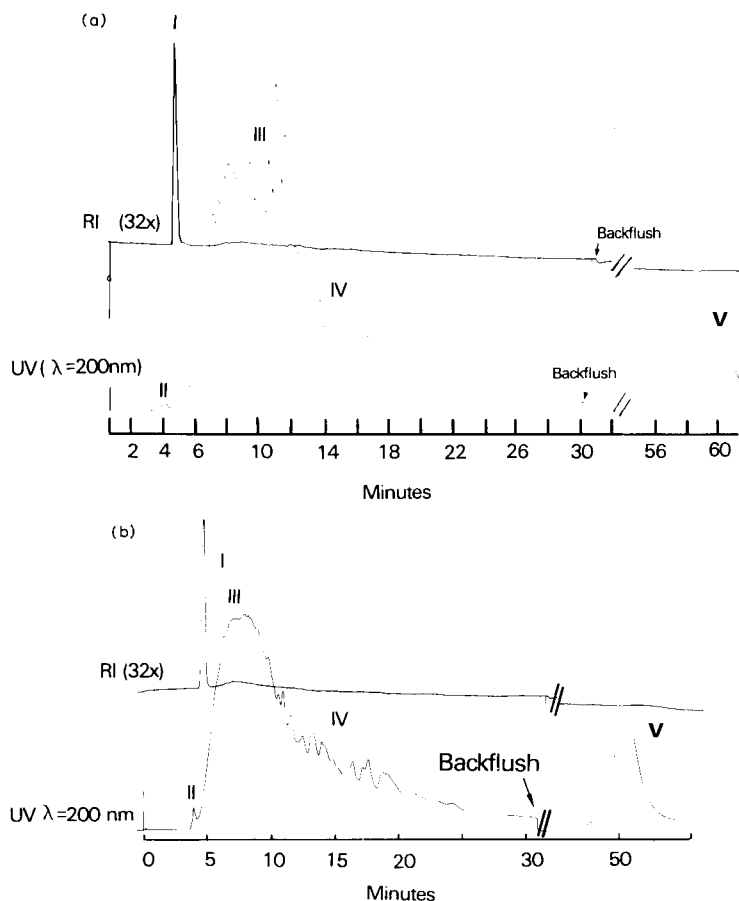


Fig. 8. Hydrocarbon group-type separations of light (a) and heavy gas oil (b). Columns: MicroPak CN-5 plus Si-5 in series. Mobile phase: dry *n*-hexane at 0.8 ml/min. Detectors: UV at 200 nm (1.0 a.u.f.s.) and RI (32 ×). I = Saturates; II = olefins; III = aromatics (alkylbenzenes); IV = PAHs; V = polars.

Through use of a time programmable flow change, elution of polar compounds is speeded up, thereby reducing analysis time. Separation speed is increased by almost a factor of two by flow programming backflush of the polar constituents. This can be seen by comparing the total analysis time for the gas oil samples in Fig. 8 with the analysis time of the SRC sample in Fig. 9.

DISCUSSION

For petroleum samples, LC column switching techniques have proven to be useful when normal phase packings are utilized to obtain hydrocarbon group-type separations. The wide selectivity available with a range of stationary phases can be exploited to achieve resolution among several hydrocarbon classes employing an isocratic elution profile^{2,3}. Isocratic analysis is advantageous when using silica gel columns due to elimination of time consuming re-equilibration steps which are necessary

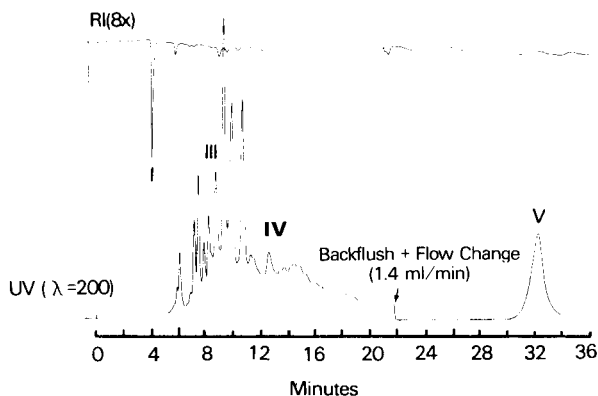


Fig. 9. Hydrocarbon group-type separation of SRC (solvent refined coal). Columns: MicroPak CN-5 plus Si-5 in series. Mobile phase: dry *n*-hexane at 0.7 ml/min with flow change to 1.4 ml/min upon backflushing. Detectors: UV at 200 nm (1.0 a.u.f.s.) and RI (8 ×). I = Saturates; III = aromatics (alkylbenzenes); IV = PAHs; V = polars.

in gradient elution. Alternately, by appropriate valve actuation, the silica column can be isolated from the rest of the switching system to allow gradient analysis with other columns.

Separation of saturates into paraffin and naphthene classes allows characterization of gasoline-range hydrocarbon samples by so-called P.O.N.A. analyses. One typical problem of such separations is maintaining activation of the silica column to obtain adequate resolution of saturate and olefin classes. Apffel *et al.*⁶ have applied silica columns impregnated with silver nitrate in column switching schemes to achieve adequate resolution of saturates and olefins without the necessity of maintaining a highly activated silica column and attendant trace water removal from the mobile phase. Such an approach eliminates a major source of retention time variance in such switching techniques—that arising from changes in silica activation due to trace water contamination. Although examples shown in this study are of a qualitative nature, quantitation of hydrocarbon classes can be achieved in switching schemes. Due to the wide variation of extinction coefficients for hydrocarbons in any one class, UV detection at 200 nm is not always useful and quantitation with an appropriately calibrated RI detector is preferable.

As evidenced by the elution profile of the heavy gas oil sample, another problem that frequently occurs with heavier petroleum samples is loss of resolution of the aromatic envelope. Comparison of light and heavy gas oil chromatograms (see Fig. 8) illustrates the difference in resolution that is achieved with such petroleum samples using the same analytical fingerprinting technique. Resolution for these sample types, however, may be increased by incorporation of a second CN-5 or Si-5 column employed as column 3 in the switching scheme.

Although two six-port switching valves were used in this work, use of a ten-port, two-position switching valve may eliminate the need for the second six-port valve in these types of switching schemes. Harvey and Stearns²⁶ have shown that such a valve can be used for both injection and sequence reversal with backflushing without need of an additional switching valve.

CONCLUSION

Column switching techniques utilizing normal-phase packings can separate saturate, olefin, aromatic and polar hydrocarbon classes using a single switching valve and a MicroPak CN-5 plus Si-5 column. Use of a second switching valve and an experimental column packing allow further resolution of saturates into paraffin and naphthene classes for P.O.N.A.-type separations of gasoline-range materials.

In column switching schemes for hydrocarbon group-type separations, MicroPak Si-5 packing is useful for separation of saturates, olefins and aromatics (alkyl-benzenes), offering high selectivity for these hydrocarbon classes upon activation at temperatures of 130–150°C. MicroPak NH₂-5 and AX-5 bonded phase columns exhibit large capacity (k') for PAHs. Normal phase supports offer a wide range of selectivity useful in fingerprinting petroleum samples when employed in column switching techniques.

ACKNOWLEDGEMENTS

Appreciation is given to G. A. Mangogna, Alex Appfel and A. Matsunaga for many helpful discussions. Special thanks are due to Sally Bird for preparation of this manuscript.

REFERENCES

- 1 ASTM Standard Test Method D1319, *Hydrocarbon Types in Liquid Petroleum Products by Fluorescent Indicator Adsorption*, Part 17, 1973, p. 476.
- 2 R. Stevenson, *J. Chromatogr. Sci.*, 9 (1971) 257–262.
- 3 J. C. Suatoni and R. E. Swab, *J. Chromatogr. Sci.*, 13 (1975) 361–366.
- 4 W. A. Dark, W. H. McFadden and D. L. Bradford, *J. Chromatogr. Sci.*, 15 (1977) 454–460.
- 5 J. F. McKay and D. R. Latham, *Anal. Chem.*, 52 (1980) 1618–1621.
- 6 A. Appfel, H. M. McNair, T. Alfredson and R. E. Majors, *Pittsburgh Conference on Analytical Chemistry and Applied Spectroscopy*, Atlantic City, NJ, March 1981.
- 7 E. Katz and K. Ogan, *5th International Symposium on PAHs*, Battelle Institute, Columbus, OH, October 1980.
- 8 J. A. Appfel, T. V. Alfredson and R. E. Majors, *J. Chromatogr.*, 206 (1981) 43–57.
- 9 T. V. Alfredson, R. L. Stevenson and L. Tallman, *Pittsburgh Conference on Analytical Chemistry and Applied Spectroscopy*, Atlantic City, NJ, March 1981.
- 10 M. Popl, V. Dolanský and J. Mostecký, *J. Chromatogr.*, 117 (1976) 117–127.
- 11 A. Streitwieser and C. H. Heathcock, *Introduction to Organic Chemistry*, Macmillan, New York, 1976, p. 378.
- 12 J. C. Suatoni and R. E. Swab, *J. Chromatogr. Sci.*, 14 (1976) 535–537.
- 13 J. C. Suatoni, H. R. Garber and B. E. Davis, *J. Chromatogr. Sci.*, 13 (1975) 367–371.
- 14 J. C. Suatoni and H. R. Garber, *J. Chromatogr. Sci.*, 14 (1976) 546–548.
- 15 W. A. Dark, *J. Chromatogr. Sci.*, 16 (1978) 289–293.
- 16 W. D. Dark and R. R. McGough, *J. Chromatogr. Sci.*, 16 (1978) 610–615.
- 17 M. L. Selucky, T. C. S. Ruo and O. Strausz, *Fuel*, 57 (1978) 585–591.
- 18 K. Jinno, H. Nomura and Y. Hirata, *J. High Resolut. Chromatogr. Chromatogr. Commun.*, 3 (1980) 503–506.
- 19 K. G. Liphard, *Chromatographia*, 13 (1980) 603–606.
- 20 C. Bollet, J.-C. Escalier, C. Souteyrand, M. Caude and R. Rosset, *J. Chromatogr.*, 206 (1981) 289–300.
- 21 L. G. Galya and J. C. Suatoni, *J. Liquid Chromatogr.*, 3 (1980) 229–242.
- 22 S. R. Abbott, *J. Chromatogr. Sci.*, 18 (1980) 540–549.
- 23 J. F. K. Huber, I. Fogy and C. Fioresi, *Chromatographia*, 13 (1980) 408–412.
- 24 A. Matsunaga and M. Yagi, *Anal. Chem.*, 50 (1978) 753–756.
- 25 A. Matsunaga and S. Kusayanagi, *Mid-Atlantic ACS Meeting*, Atlanta, GA, March 1981.
- 26 M. C. Harvey and S. D. Stearns, *Amer. Lab.*, 13 (1981) 151–157.

CHROM. 14,165

THIN-LAYER CHROMATOGRAPHY AS A PILOT TECHNIQUE FOR THE OPTIMIZATION OF PREPARATIVE COLUMN CHROMATOGRAPHY

EDWARD SOCZEWIŃSKI* and TERESA WAWRZYNOWICZ

Department of Inorganic and Analytical Chemistry, Medical Academy, 20-081 Lublin (Poland)

SUMMARY

Thin-layer chromatography can be used as a convenient small-scale model of preparative liquid chromatography in the same adsorbent–eluent system. Large volumes of sample solution should be introduced from the edge of the thin-layer and then eluted continuously; these conditions, similar to column chromatography, can be secured using a horizontal sandwich tank with a glass distributor. The formation and separation of zones can be frequently observed under UV light. Specific chromogenic reagents can also be used to obtain preliminary information about the qualitative and quantitative composition of the partly separated mixture. A modified thin-layer chromatographic technique for two-dimensional preparative separations is described.

INTRODUCTION

Preparative liquid chromatography, owing to the large amounts of adsorbents and solvents used, requires preliminary optimization of the adsorbent–eluent system; analytical separations usually precede preparative runs, the sample size being gradually increased to estimate the effect of overloading on the separation^{1–3}. Thin-layer chromatography (TLC) can also be used for the optimization of eluent composition⁴; the use of continuous elution and elimination of solvent demixing and preadsorption effects permits comparability of retention parameters in TLC and high-performance liquid chromatography (HPLC)^{4–8}.

It is also possible to produce in thin layers of adsorbent similar overloading to that occurring in preparative columns; in this way, the advantages of TLC (minimal loss of materials, rapidity, application of selective reagents) can be utilized for the choice of optimal systems for preparative separations.

The delivery of large volumes of sample solution to the thin layer cannot be carried out in the usual way, spotting (Fig. 1a) or streaking (Fig. 1b), owing to the formation of complex starting chromatograms. The sample should be introduced from the edge of the chromatographic bed as in column chromatography (Fig. 1c) so that the first stage of the process is equivalent to frontal chromatography, during which partial separation of the mixture is obtained⁹. This is followed by elution, which under favourable conditions results in full separation of the zones. The two

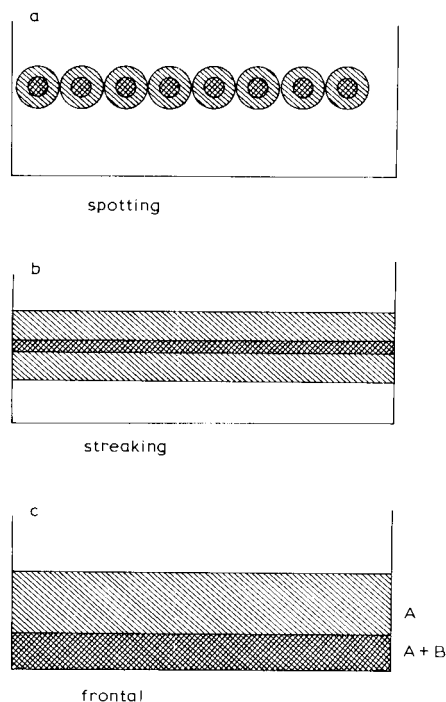


Fig. 1. Starting bands of large volumes of a binary sample (A + B) introduced by spotting, streaking and from the edge of the thin layer.

stages, frontal and elution chromatography, can also be performed using a modified sandwich tank of the Brenner–Niederwieser (BN) type with a glass distributor^{9–11} which permits ready change of the solution delivered to the layer.

The separation of components in the overloaded zone can be observed by inspection under UV light or by use of several selective spraying reagents on narrow strips of the chromatogram. In this way the main components of the mixture can be established and information obtained on their molecular structures (*e.g.*, presence of functional groups). Irreversible adsorption of some sample components, which would lead to the destruction of the preparative column, can also be detected.

To investigate in more detail the formation and separation of zones during the frontal and elution steps¹¹, a modified sandwich tank has been constructed which permits elution of the zone at right angles to the first elution direction.

EXPERIMENTAL

A sandwich tank^{10,11} with a modified glass distributor was used which permitted delivery of a 1 cm long zone of sample solution (dissolved in eluent), the remaining length of the plate being eluted with pure eluent. For 100 × 100 mm and 200 × 100 mm plates, the distributors were made from 1.2-mm glass (74 × 5 and 10 × 5 mm) attached with cyanoacrylic glue to the lower surface of the cover plate^{10,11}. The sample solution and the eluent were delivered from separate 5-ml containers by si-

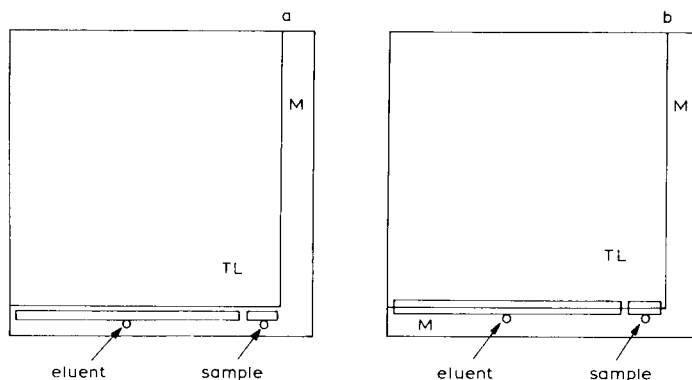


Fig. 2. Sandwich tank with two distributors for delivery of a 1 cm wide sample zone. M = Margin of the carrier plate cleaned of the adsorbent; TL = thin layer.

phones made of stainless steel capillaries (0.7 mm I.D.), the initial levels of the eluent being slightly lower than the thin layer¹⁰. The 2-mm gap between the two distributors prevents mixing of the sample and eluent. In model experiments the behaviour of coloured compounds was investigated. The flows of the two liquids were parallel and the boundary of the coloured zone was well defined and parallel to the edge of the plate. Only slight edge effects were observed.

Along two adjacent sides, 1-cm margins of the plate were cleaned of adsorbent. (It is essential that the edges of the layer are even and smooth.) The plate was activated, cooled in a desiccator and put in the horizontal tank with the distributors lying over the margin (Fig. 2a). By a slight temporary overpressure, the two siphons and the spaces under the short and long distributors were filled with sample solution and eluent, respectively. The cover plate was then moved along the carrier plate until the distributors lay partly over the adsorbent layer (Fig. 2b) and the two solutions were simultaneously delivered to the layer. After the formation of a sufficiently wide perpendicular starting zone, the container with the sample was replaced by another one containing pure eluent. Elution in the second dimension was carried out by placing another plate with a single distributor over the second, perpendicular, margin.

RESULTS AND DISCUSSION

A model mixture of dyes was investigated: azobenzene, dimethylaminoazobenzene, Sudan IV and Disperse Red 73. The solutes were dissolved in the eluent (1% each). The three stages of the run, formation of a wide starting zone (frontal chromatography), elution in the first direction and elution in the second direction, are illustrated in Fig. 3.

As illustrated previously⁹, the movement of the zones in the sandwich tank with continuous elution is regular and permits estimation of the retention volumes of the wide zones leaving the chromatographic bed. Considering the analogy between equilibrium-sandwich TLC in BN chambers and in column HPLC, the behaviour of the zones in preparative column chromatography can be predicted taking into account the weight of adsorbent, column length and differences in the surface areas of the adsorbents, if any.

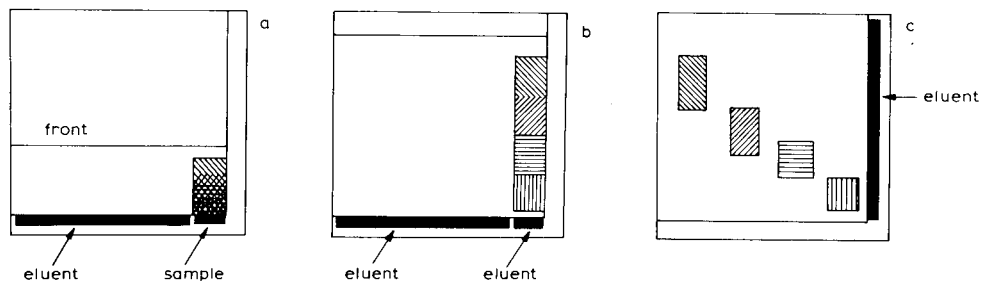


Fig. 3. Two-dimensional elution of a large sample volume: a, delivery of 25 μ l of sample solution (3% solution of azobenzene, dimethylaminoazobenzene, Sudan IV and Disperse Red 73 in the eluent 50% benzene-heptane); b, elution in the first direction; c, elution in the perpendicular direction.

The pilot TLC experiments, which can also be carried out on narrow strips of TLC plates (e.g., 10 \times 1 cm), can provide information about essential parameters of the process, such as eluent strength and qualitative composition required to secure good selectivity, maximal concentration and sample loading (capacity of the adsorbent), irreversible adsorption and whether gradient elution is necessary. The loss of materials in these rapid preliminary experiments is minimal.

Sometimes the formation and separation of zones in the adsorbent layer can be observed directly (coloured solutes) or intermittently under UV light (which, however, may cause decomposition of certain solutes). This is difficult to achieve in column chromatography—even in glass columns the zones at the walls are distorted owing to the wall effect.

The pilot experiments may be especially useful in the separation of complex samples such as plant extracts. Preliminary equilibration of the layer with the eluent may be necessary for low-percentage solvent systems¹².

REFERENCES

- 1 J. J. DeStefano and J. J. Kirkland, *Anal. Chem.*, **47** (1975) 1193A.
- 2 J. H. Knox, *Course Manual of the Chemical Society Residential School*, London, 1980, p. 61.
- 3 L. R. Snyder and J. J. Kirkland, *Introduction to Modern Liquid Chromatography*, Wiley-Interscience, New York, 2nd ed., 1979, p. 615.
- 4 S. Hara, *J. Chromatogr.*, **137** (1977) 41.
- 5 S. Hara and K. Mibe, *J. Chromatogr.*, **66** (1972) 75.
- 6 D. Jaenchen, in A. Zlatkis and R. E. Kaiser (Editors), *HPTLC —High Performance Thin-Layer Chromatography*, Elsevier, Amsterdam, 1977, p. 141.
- 7 R. E. Kaiser and E. Oelrich, *Optimierung in der HPLC*, Hüthig, Heidelberg, 1979, p. 149.
- 8 E. Soczewiński and J. Kuczmierczyk, *J. Chromatogr.*, **150** (1978) 53.
- 9 E. Soczewiński, J. Kuczmierczyk and B. Psionka, *J. Liquid Chromatogr.*, **3** (1980) 1829.
- 10 E. Soczewiński and T. Wawrzynowicz, *Chromatographia*, **11** (1978) 466.
- 11 E. Soczewiński and W. Maciejewicz, *J. Chromatogr.*, **176** (1979) 247.
- 12 T. Wawrzynowicz and E. Soczewiński, *J. Chromatogr.*, **169** (1979) 191.

Author Index

- Abbott, S.
 —, Achener, P., Simpson, R. and Klink, F.
 Effect of radial thermal gradients in elevated temperature high-performance liquid chromatography 123
- Achener, P., see Abbott, S. 123
- Alexander, S. P., see Gill, R. 639
- Alfredson, T. V.
 High-performance liquid chromatographic column switching techniques for rapid hydrocarbon group-type separations 715
- Atwood, J. G.
 — and Golay, M. J. E.
 Dispersion of peaks by short straight open tubes in liquid chromatography systems 97
- Ayers, J. A., see Hearn, M. T. W. 509
- Belov, Yu. P., see Davankov, V. A. 547
- Berg, J. H. M. van den, see Deelder, R. S. 327
- Bethell, G. S., see Hearn, M. T. W. 509
- Billiet, H. A. H., see Laurent, C. 83
 —, see Schoenmakers, P. J. 261
 —, Schoenmakers, P. J. and De Galan, L.
 Retention and selectivity characteristics of a non-polar perfluorinated stationary phase for liquid chromatography 443
- Björqvist, B.
 Separation and determination of phenyl isocyanate-derivatized carbohydrates and sugar alcohols by high-performance liquid chromatography with ultraviolet detection 65
- Bleumer, J. P. A., see Tijssen, R. 137
- Bochkov, A. S., see Davankov, V. A. 547
- Bodor, G., see Samay, G. 473
- Bossi, L., see Semerdjian-Rouquier, L. 663
- Brinkman, U. A. Th., see Scholten, A. H. M. T. 3
- Brugman, W. J. Th.
 —, Heemstra, S. and Kraak, J. C.
 High-performance liquid chromatography of organic acids on bare silica 285
- Bull, R. V. A.
 —, Lim, C. K. and Gray, C. H.
 High-performance liquid chromatography of bile pigments: Separation and characterization of the urobilinoids 647
- Buytenhuys, F. A.
 Ion chromatography of inorganic and organic ionic species using refractive index detection 57
- Calam, D. H.
 — and Davidson, J.
 Analysis of glycoprotein hormones and other medically important proteins by high-performance gel filtration chromatography 581
- Capp, M. W., see Nice, E. C. 569
- Chen, T., see Fenselau, C. 21
- Cole, S. C. J.
 —, Flanagan, R. J., Johnston, A. and Holt, D. W.
 Rapid high-performance liquid chromatographic method for the measurement of verapamil and norverapamil in blood plasma or serum 621
- Cooke, N., see Nice, E. C. 569
- Cotter, R., see Fenselau, C. 21
- Cser, F., see Samay, G. 473
- Davankov, V. A.
 —, Bochkov, A. S. and Belov, Yu. P.
 Ligand-exchange chromatography of racemates. XV. Resolution of α -amino acids on reversed-phase silica gels coated with N-decyl-L-histidine 547
 —, see Kurganov, A. A. 559
- Davidson, J., see Calam, D. H. 581
- DeArman Lukacs, K., see Jorgenson, J. W. 209
- Dębowski, J., see Kutner, W. 45
- Deelder, R. S.
 — and Van den Berg, J. H. M.
 Study on the retention of amines in reversed-phase ion-pair chromatography on bonded phases 327
- De Galan, L., see Billiet, H. A. H. 443
 —, see Laurent, C. 83
 —, see Schoenmakers, P. J. 261
- Denkert, M.
 —, Hackzell, L., Schill, G. and Sjögren, E.
 Reversed-phase ion-pair chromatography with UV-absorbing ions in the mobile phase 31
- Elverdam, I.
 —, Larsen, P. and Lund, E.
 Isolation and characterization of three new polymyxins in polymyxins B and E by high-performance liquid chromatography 653
- Engelhardt, H.
 — and Müller, H.
 Chromatographic characterization of silica surfaces 395
- Fenselau, C.
 —, Cotter, R., Hansen, G., Chen, T. and Heller, D.
 Middle molecule mass spectrometry (a review) 21

- Flanagan, R. J., see Cole, S. C. J. 621
- Frank, J., see Kreuzig, F. 615
- Frei, R. W., see Scholten, A. H. M. T. 3
- Frenz, J. H., see Horváth, Cs. 365
- Füzes, L., see Samay, G. 473
- Galan, L. de, see Billiet, H. A. H. 443
- , see Laurent, C. 83
- , see Schoenmakers, P. J. 261
- Gazdag, M., see Szepesi, G. 597
- and Szepesi, G.
Separation of large polypeptides by high-performance liquid chromatography 603
- Giese, R. W., see Yu, T. J. 519
- Gilbert, J., see Shepherd, M. J. 703
- Gill, R.
—, Alexander, S. P. and Moffat, A. C.
Group-contribution approach to the behaviour of 2-phenylethylamines in reversed-phase high-performance liquid chromatography 639
- Glajch, J. L., see Snyder, L. R. 299
- Golay, M. J. E., see Atwood, J. G. 97
- Gray, C. H., see Bull, R. V. A. 647
- Grego, B., see Hearn, M. T. W. 497
- Gübitz, G.
—, Wintersteiger, R. and Hartinger, A.
Fluorescence derivatization of tertiary amines with 2-naphthyl chloroformate 51
- Hackzell, L., see Denkert, M. 31
- Haefelfinger, P.
Limits of the internal standard technique in chromatography 73
- Hafkenschied, T. L., see Riley, C. M. 427
- Hafkenschied, T. L.
— and Tomlinson, E.
Estimation of aqueous solubilities of organic non-electrolytes using liquid chromatographic retention data 409
- Hancock, W. S., see Hearn, M. T. W. 509
- Hansen, G., see Fenselau, C. 21
- Harris, E. L., see Hearn, M. T. W. 509
- Harris, J. M., see Leach, R. A. 15
- Hartinger, A., see Gübitz, G. 51
- Hearn, M. T. W.
— and Grego, B.
High-performance liquid chromatography of amino acids, peptides and proteins. XXXVI. Organic solvent modifier effects in the separation of unprotected peptides by reversed-phase liquid chromatography 497
- , Harris, E. L., Bethell, G. S., Hancock, W. S. and Ayers, J. A.
Application of 1,1'-carbonyldiimidazole-activated matrices for the purification of proteins. III. The use of 1,1'-carbonyldiimidazole-activated agaroses in the biospecific affinity chromatographic isolation of serum antibodies 509
- and Lyttle, D. J.
Buffer-focusing chromatography using multi-component electrolyte elution systems 483
- Heemstra, S., see Brugman, W. J. Th. 285
- Heller, D., see Fenselau, C. 21
- Holt, D. W., see Cole, S. C. J. 621
- Horváth, Cs.
—, Nahum, A. and Frenz, J. H.
High-performance displacement chromatography 365
- Ishii, D.
— and Takeuchi, T.
Study of the performance of cation-exchange columns in open-tubular microcapillary liquid chromatography 189
- , see Takeuchi, T. 199
- Johnston, A., see Cole, S. C. J. 621
- Jorgenson, J. W.
— and DeArman Lukacs, K.
High-resolution separations based on electrophoresis and electroosmosis 209
- Jurand, J., see Knox, J. H. 341, 355
- Karger, B. L., see Yu, T. J. 519
- Kemula, W., see Kutner, W. 45
- , Sybilska, D. and Lipkowski, J.
Selectivity and efficiency of separation of isomers of organic acids by clathrate chromatography 465
- Kirkland, J. J., see Snyder, L. R. 299
- , see Yau, W. W. 217
- Klink, F., see Abbott, S. 123
- Knox, J. H.
— and Jurand, J.
Mechanism of zwitterion-pair chromatography. I. Nucleotides 341
- and Jurand, J.
Mechanism of zwitterion-pair chromatography. II. Ampicilline, lysergic acid, tryptophan and other solutes 355
- Kraak, J. C., see Brugman, W. J. Th. 285
- Krejčí, M.
—, Tesařík, K., Rusek, M. and Pajurek, J.
Flow characteristics and technology of capillary columns with inner diameters less than 15 μm in liquid chromatography 167

- Kreuzig, F.
— and Frank, J.
Rapid automated determination of D-penicillamine in plasma and urine by ion-exchange high-performance liquid chromatography with electrochemical detection using a gold electrode 615
- Kurganov, A. A.
— and Davankov, V. A.
Ligand-exchange chromatography of racemates. XVI. Microbore column chromatography of amino acid racemates using N,N,N',N'-tetramethyl-(*R*)-propanediamine-1,2-copper(II) complexes as chiral additives to the eluent 559
- Kutner, W.
—, Dębowski, J. and Kemula, W.
Extra-column effects in polarographic *versus* UV detection in high-performance liquid chromatography 45
- Larsen, P., see Elverdam, I. 653
- Laurent, C.
—, Billiet, H. A. H., Van Dam, H. C. and De Galan, L.
Computer-controlled single-pump solvent programmer for high-performance liquid chromatography 83
- Leach, R. A.
— and Harris, J. M.
Thermal lens calorimetry. Application to chromatographic detection 15
- Lim, C. K., see Bull, R. V. A. 647
- Lipkowski, J., see Kemula, W. 465
- Lund, E., see Elverdam, I. 653
- Lyttle, D. J., see Hearn, M. T. W. 483
- McGuffin, V. L.
— and Novotný, M.
Micro-column high-performance liquid chromatography and flame-based detection principles 179
- McMurrough, I.
High-performance liquid chromatography of flavonoids in barley and hops 683
- Moffat, A. C., see Gill, R. 639
- Mori, K.
Automated measurement of catecholamines in urine, plasma and tissue homogenates by high-performance liquid chromatography with fluorometric detection 631
- Müller, H., see Engelhardt, H. 395
- Nahum, A., see Horváth, Cs. 365
- Nice, E. C.
—, Capp, M. W., Cooke, N. and O'Hare, M. J.
Comparison of short and ultrashort-chain alkylsilane-bonded silicas for the high-performance liquid chromatography of proteins by hydrophobic interaction methods 569
- Novotný, M., see McGuffin, V. L. 179
- O'Hare, M. J., see Nice, E. C. 569
- Pajurek, J., see Krejčí, M. 167
- Porath, J.
Development of modern bioaffinity chromatography (a review) 241
- Rajakylä, E.
Separation and determination of some organic acids and their sodium salts by high-performance liquid chromatography 695
- Riley, C. M.
—, Tomlinson, E. and Hafkenschied, T. L.
Structural effects in enthalpy/entropy compensated and non-compensated behaviour in ion-pair reversed-phase high-performance liquid-solid chromatography 427
- Roumeliotis, P.
— and Unger, K. K.
Assessment and optimization of system parameters in size exclusion separation of proteins on diol-modified silica columns 535
- Rusek, M., see Krejčí, M. 167
- Samay, G.
—, Füzes, L., Cser, F. and Bodor, G.
Comparison of dimensions obtained by size-exclusion chromatography and X-ray diffraction of rigid molecules 473
- Scatton, B., see Semerdjian-Rouquier, L. 663
- Schill, G., see Denkert, M. 31
- Schlett, R., see Von Stetten, O. 591
- Schoenmakers, P. J.
—, Billiet, H. A. H. and De Galan, L.
Systematic study of ternary solvent behaviour in reversed-phase liquid chromatography 261
—, see Billiet, H. A. H. 443
- Scholten, A. H. M. T.
—, Brinkman, U. A. Th. and Frei, R. W.
Fluorescence detection of chloroanilines in liquid chromatography using a post-column reaction with fluorescamine. Comparison of reactor types and mixing tees 3
- Schwartz, H., see Yu, T. J. 519
- Semerdjian-Rouquier, L.
—, Bossi, L. and Scatton, B.
Determination of 5-hydroxytryptophan, serotonin and 5-hydroxyindoleacetic acid in rat and human brain and biological fluids by reversed-phase high-performance liquid chromatography with electrochemical detection 663
- Shepherd, M. J.
— and Gilbert, J.
Analysis of additives in plastics by high-performance size-exclusion chromatography 703

- Simpson, R., see Abbott, S. 123
- Sjögren, E., see Denkert, M. 31
- Smit, A. L. C., see Tijssen, R. 137
- Snyder, L. R.
- , Glajch, J. L. and Kirkland, J. J.
Theoretical basis for systematic optimization of mobile phase selectivity in liquid-solid chromatography. Solvent-solute localization effects 299
- Soczewiński, E.
- and Wawrzynowicz, T.
Thin-layer chromatography as a pilot technique for the optimization of preparative column chromatography 729
- Stetten, O. von, see Von Stetten, O. 591
- Stuurman, H. W.
- and Wahlund, K.-G.
Separation of proton-donating solutes by liquid chromatography with a strong proton acceptor, tri-*n*-octylphosphine oxide, in the liquid stationary phase 455
- Sybiliska, D., see Kemula, W. 465
- Szepesi, G.
- and Gazdag, M.
Improved high-performance liquid chromatographic method for the analysis of insuline and related compounds 597
- Szepesi, G., see Gazdag, M. 603
- Takeuchi, T.
- and Ishii, D.
Application of ultra-micro high-performance liquid chromatography to trace analysis 199
- , see Ishii, D. 189
- Tesařík, K., see Krejčí, M. 167
- Tijssen, R.
- , Bleumer, J. P. A. and Van Kreveld, M. E.
Microcapillary liquid chromatography in open tubular columns with diameters of 10–50 μm . Potential application to chemical ionization mass spectrometric detection 137
- Tomlinson, E., see Hafkenscheid, T. L. 409
- , see Riley, C. M. 427
- Unger, K. K., see Roumeliotis, P. 535
- Van Dam, H. C., see Laurent, C. 83
- Van den Berg, J. H. M., see Deelder, R. S. 327
- Van Kreveld, M. E., see Tijssen, R. 137
- Von Stetten, O.
- and Schlett, R.
High-performance liquid chromatography of ^{125}I -labelled proteins with on-line detection 591
- Vouros, P., see Yu, T. J. 519
- Wahlund, K.-G.
Separation of acidic drugs in the $\mu\text{g/ml}$ range in untreated blood plasma by direct injection on liquid chromatographic columns 671
- , see Stuurman, H. W. 455
- Wawrzynowicz, T., see Soczewiński, E. 729
- Wintersteiger, R., see Gübitz, G. 51
- Yau, W. W.
- and Kirkland, J. J.
Comparison of sedimentation field flow fractionation with chromatographic methods for particulate and high-molecular-weight macromolecular characterizations 217
- Yu, T. J.
, Schwartz, H., Giese, R. W., Karger, B. L. and Vouros, P.
Analysis of N-acetyl-N,O,S-permethylated peptides by combined liquid chromatography-mass spectrometry 519

PUBLICATION SCHEDULE FOR 1981

Journal of Chromatography (incorporating *Chromatographic Reviews*) and *Journal of Chromatography, Biomedical Applications*

MONTH	N 1980	D 1980	J	F	M	A	M	J	J	A	S	O	N	D
Journal of Chromatography			203 204 205/1 205/2	206/1 206/2 206/3	207/1 207/2 207/3	208/1 208/2 209/1	209/2 209/3 210/1	210/2 210/3 211/1	211/2 211/3 212/1 212/2	212/3 213/1 213/2	213/3 214/1 214/2	214/3 215 216	217 218 219/1	219/2 219/3
Chromatographic Reviews							220/1					220/2		220/3
Biomedical Applications	221/1	221/2	222/1	222/2	222/3	223/1	223/2	224/1	224/2	224/3	225/1	225/2	226/1	226/2

INFORMATION FOR AUTHORS

(Detailed *Instructions to Authors* were published in Vol. 209, No. 3, pp. 501–504. A free reprint can be obtained by application to the publisher.)

Types of Contributions. The following types of papers are published in the *Journal of Chromatography* and the section on *Biomedical Applications*: Regular research papers (Full-length papers), Short communications and Notes. Short communications are preliminary announcements of important new developments and will, whenever possible, be published with maximum speed. Notes are usually descriptions of short investigations and reflect the same quality of research as Full-length papers, but should preferably not exceed four printed pages. For reviews, see page 2 of cover under Submission of Papers.

Submission. Every paper must be accompanied by a letter from the senior author, stating that he is submitting the paper for publication in the *Journal of Chromatography*. Please do not send a letter signed by the director of the institute or the professor unless he is one of the authors.

Manuscripts. Manuscripts should be typed in double spacing on consecutively numbered pages of uniform size. The manuscript should be preceded by a sheet of manuscript paper carrying the title of the paper and the name and full postal address of the person to whom the proofs are to be sent. Authors of papers in French or German are requested to supply an English translation of the title of the paper. As a rule, papers should be divided into sections, headed by a caption (e.g., Summary, Introduction, Experimental, Results, Discussion, etc.). All illustrations, photographs, tables, etc., should be on separate sheets.

Introduction. Every paper must have a concise introduction mentioning what has been done before on the topic described, and stating clearly what is new in the paper now submitted.

Summary. Full-length papers and Review articles should have a summary of 50–100 words which clearly and briefly indicates what is new, different and significant. In the case of French or German articles an additional summary in English, headed by an English translation of the title, should also be provided. (Short communications and Notes are published without a summary.)

Illustrations. The figures should be submitted in a form suitable for reproduction, drawn in Indian ink on drawing or tracing paper. Each illustration should have a legend, all the legends being typed (with double spacing) together on a separate sheet. If structures are given in the text, the original drawings should be supplied. Coloured illustrations are reproduced at the author's expense, the cost being determined by the number of pages and by the number of colours needed. The written permission of the author and publisher must be obtained for the use of any figure already published. Its source must be indicated in the legend.

References. References should be numbered in the order in which they are cited in the text, and listed in numerical sequence on a separate sheet at the end of the article. Please check a recent issue for the lay-out of the reference list. Abbreviations for the titles of journals should follow the system used by *Chemical Abstracts*. Articles not yet published should be given as "in press", "submitted for publication", "in preparation" or "personal communication".

Proofs. One set of proofs will be sent to the author to be carefully checked for printer's errors. Corrections must be restricted to instances in which the proof is at variance with the manuscript. "Extra corrections" will be inserted at the author's expense.

Reprints. Fifty reprints of Full-length papers, Short communications and Notes will be supplied free of charge. Additional reprints can be ordered by the authors. An order form containing price quotations will be sent to the authors together with the proofs of their article.

News. News releases of new products and developments, and information leaflets of meetings should be addressed to: The Editor of the News Section, *Journal of Chromatography*/*Journal of Chromatography, Biomedical Applications*, Elsevier Scientific Publishing Company, P.O. Box 330, 1000 AH Amsterdam, The Netherlands.

Advertisements. Advertisement rates are available from the publisher on request. The Editors of the journal accept no responsibility for the contents of the advertisements.

Structural Analysis of Organic Compounds

by Combined Application of Spectroscopic Methods

J. T. Clerc, E. Pretsch and J. Seibl, Zürich, Switzerland.

Studies in Analytical Chemistry, 1

Spectroscopic methods have certainly captured the lion's share of organic analysis with at least one such method in current use in all chemical laboratories. Now at last a concise and logically structured reference work details how their combined application substantially increases overall effectiveness. By giving examples which demonstrate different methods of approach and reasoning, and supplementing these with comments and hints on previously neglected analytical aspects, the authors have produced a work to cover the widest possible variety of chemical structures and spectroscopic capabilities.

1981 280 pages
0-444-99748-2

US \$66.00/Dfl. 135.00

Evaluation and Optimization of Laboratory Methods and Analytical Procedures

D. L. Massart, L. Kaufman and A. Dijkstra

Techniques and Instrumentation in Analytical Chemistry, 1

Acclaimed as "... a valuable addition to the analytical literature" by *Analytical Chemistry*, "a comprehensive and practical handbook... all as-

from ELSEVIER your partner in successful CHEMICAL ANALYSIS

pects of optimization are discussed" by *Laboratory Equipment* and "... a real aid to postgraduate students following taught courses" by *Chromatographia*. The authors provide in a single volume, a discussion of all aspects of optimization from the simple evaluation of procedures to the organization of laboratories and the selection of optimal complex analytical programmes. No laboratory or library can afford to be without this book.

1978. 1st reprint 1980
612 pages 0-444-41743-5
US \$68.25/Dfl. 140.00

Chemical Derivatization in Gas Chromatography

J. Drozd, Brno, Czechoslovakia.

Journal of Chromatography Library, 19.

The novice will find here explanatory coverage of the entire range of problems, will become acquainted with all types of derivatives and methods, and will be able to apply the information without re-

course to original sources. For proficient workers it will be a valuable information source, a guide to the most recent research results and an indication of future trends.

1981 244 pages
0-444-41917-9
US \$58.50/Dfl. 120.00

Analytical Isotachophoresis

Proceedings of the 2nd International Symposium on Isotachophoresis, Eindhoven, September 9-11, 1980

F. M. Everaerts, Eindhoven The Netherlands (Editor)

Analytical Chemistry Symposia Series, 6

"A new twig on the tree of differential separation methods": Thus has isotachophoresis been described.

It is proving a valuable technique in clinical (bio)chemistry, pharmacy, physical and inorganic chemistry, as well as in the industrial and environmental field.

Theoretical and practical aspects of the method, new developments in isotachopheric equipment and applications are presented clearly.

1981 246 pages
0-444-41957-8
US \$58.50/Dfl. 120.00

Send your order with your payment to one of the addresses below and receive the book(s) ordered postfree.

For further details on these titles and our Spring list of analytical chemistry publications check number 3 on the reader enquiry card.

ELSEVIER

P.O. Box 211
1000 AE Amsterdam
The Netherlands

52 Vanderbilt Ave
New York, N.Y. 10017
U.S.A.



*The Book of the Tree of Life
The Book of the Tree of Life
The Book of the Tree of Life*

74/2

4009